*KAPL, Inc.*
*Knolls Atomic Power Laboratory*
*P.O. Box 1072*
*Schenectady, NY 12301-1072*

*Bechtel Bettis, Inc.*
*Bettis Atomic Power Laboratory*
*P. O. Box 79*
*West Mifflin, PA 15122-0079*

SPP-67210-0010
B-SE(SPS)-001

January 27, 2006

The Manager
Schenectady Naval Reactors Office
United States Department of Energy
Schenectady, New York

The Manager
Pittsburgh Naval Reactors Office
United States Department of Energy
West Mifflin, Pennsylvania

Subject: **Space Nuclear Power Plant Pre-Conceptual Design Report; for Information**

References: See Page 6

Enclosure: (1) Space Nuclear Power Plant Pre-Conceptual Design Report

Dear Sirs:

This letter transmits, for information, the Project Prometheus Space Nuclear Power Plant (SNPP) Pre-Conceptual Design Report completed by the Naval Reactors Prime Contractor Team (NRPCT). This report documents the work pertaining to the Reactor Module, which includes integration of the space nuclear reactor with the reactor radiation shield, energy conversion, and instrumentation and control segments. This document also describes integration of the Reactor Module with the Heat Rejection segment, the Power Conditioning and Distribution sub-system (which comprise the SNPP), and the remainder of the Prometheus spaceship.

## BACKGROUND

Project Prometheus was established in 2003 and included the goal of developing the first reactor-powered spaceship and demonstrating that it can be operated safely and reliably on long duration, deep-space missions for civilian space exploration. NASA's Jet Propulsion Laboratory (JPL) had overall lead for the project. The initial application of space fission power being evaluated was for the Jupiter Icy Moons Orbiter (JIMO), a nuclear electric propulsion spaceship intended to perform deep-space scientific research.



Pre Decisional – For Planning and Discussion Purposes Only

In March 2004, the Naval Reactors Program was assigned responsibility for design and delivery of the Reactor Module for Project Prometheus. The spaceship is comprised of a multi-mission Deep Space System coupled with a mission specific Mission Module. The Deep Space System consists of two modules:

1. The Reactor Module, which includes the nuclear reactor and the energy conversion equipment to produce electric power.
2. The Spaceship Module, which includes the spaceship structure, radiator panels (heat rejection segment), electric power conditioning and distribution equipment (PCAD), and the ion propulsion system.

In accordance with Reference (a), design responsibility for the Reactor Module (with the exception of the Aeroshell reentry protection cover) was assigned to the NRPCT, and the approval responsibility was assigned to DOE-Naval Reactors (NR).

The NRPCT design strategy was to first assess potential reactor and energy conversion system concepts and to identify those that may be feasible to support the JIMO mission. This assessment, documented in Reference (b), identified the following reactor/energy system concepts as having sufficient design space and feasibility for further evaluation to support the JIMO mission and launch schedule:

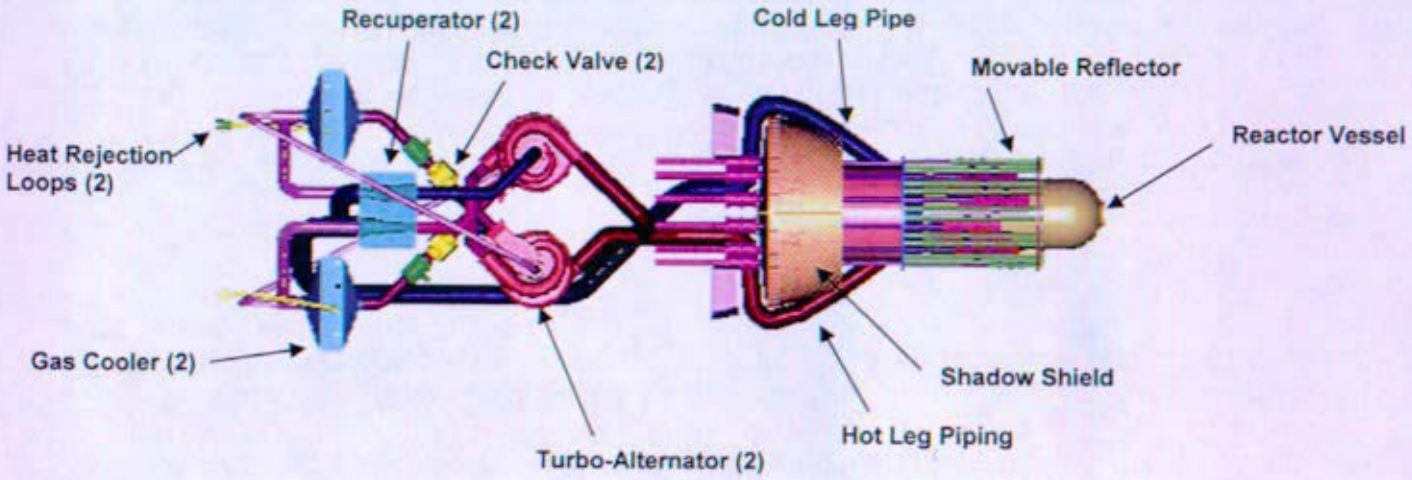
- A direct cycle, gas cooled reactor with a Brayton energy conversion system
- A heat pipe cooled reactor with a Brayton energy conversion system
- A liquid lithium cooled reactor with a Brayton energy conversion system
- A liquid lithium cooled reactor with a thermoelectric energy conversion system
- A lower temperature, liquid metal (e.g., sodium, potassium) cooled reactor with a Stirling energy conversion system

The next step in the design process was to assess these potential concepts in greater detail, and to select one reactor/energy conversion system concept for continued design development. In March 2005, the NRPCT recommended in Reference (c) that a gas cooled reactor with a directly coupled Brayton turbine energy conversion system be designed for Project Prometheus (see Figure 1). This system is likely capable of fulfilling the requirements for the envisioned missions, simplifies engineering development and testing, offers the fewest hurdles to development, and is extensible to surface missions. NR approved that recommendation in Reference (d). In September 2005, NASA priorities changed and NR Program participation in Project Prometheus was terminated. Closeout activities were initiated, including generation of this report.

Enclosure (1) describes the pre-conceptual design work performed on the Reactor Module since the concept selection recommendation. Included are preliminary conclusions and technical perspectives. This report complements other significant reports, primarily:

Reference (e) - spaceship design
Reference (f) - the space reactor pre-conceptual design
Reference (g) - the radiation shield design
Reference (h) - the Instrumentation and Control architecture
Reference (i) - structural materials

**Figure 1: Reactor Module**




## DISCUSSION

Since selection of the gas reactor Brayton concept, several primary aspects of pre-conceptual power plant design work were pursued that are detailed in this report:

- System steady-state heat balance analysis
- Transient system response analysis
- Component design options and performance evaluations
- Reactor Module arrangements
- Mass estimates
- Redundancy and reliability evaluations
- Operational strategies
- Integrated testing plans

Because the work performed to date was focused on initial plant architecture decisions, system performance optimization had not been performed. In addition to JIMO spaceship evaluations, a perspective is provided about the extensibility of the selected gas-Brayton system to other deep space and Lunar/Mars surface missions.

## SIGNIFICANT CONCLUSIONS

Based on the evaluations of the gas Brayton system done to date, NRPCT continues to view this nuclear powered deep space mission as feasible. The primary Reactor Module concerns are design of the reactor for a safe landing in the event of an inadvertent re-entry accident and demonstrating reliable operation for the long duration of the deep space missions.

Impact of System Architecture on Reliability and Mass

Although spaceship mass allocations were not yet established, the spaceship conceptual design was being iterated toward a solution of mass, power, and duration for the JIMO mission. Based on recent evaluations of the initial sizes and arrangements for components within the Reactor

Module, preliminary mass predictions are higher than previous estimates for most parts of the plant. Preliminary reliability studies indicate that having one or two loops would likely provide a more reliable plant than having three or four loops. JPL had baselined the number of Brayton loops as four in prior spaceship studies. A decision on the appropriate number of Brayton loops was not made during this project closeout process. This decision would have had to involve JPL and the spaceship designer to include overall spaceship mass trades, evaluations of alternate methods to accommodate angular momentum, parameter optimizations for each arrangement, and other aspects of spaceship and mission integration which were not done prior to project termination.

Operating Power Levels

The option of operating at full rated power over life or at two distinct power levels was being evaluated for power plant operations. Full power of approximately 185 kWe would have been used when propulsion was required, and potentially a lower power level (~40 kWe or less) would have been used when the spaceship was coasting during transit (propulsion not required) and during periods of scientific data collection once the spaceship arrived on station. To operate at a reduced power level, the reactor coolant temperature and the Brayton turbo-machinery operating speed would be reduced. Operating at lower power during the years when propulsion is not required would reduce overall stress on the system and could maximize Reactor Module lifetime.

Design Space

Cycle analyses (heat balances) show that achieving system performance within the originally envisioned design space is challenging. Limiting the heat rejection area to 450 $m^2$, the maximum heat rejection heat pipe temperature to 500 K and the maximum reactor coolant temperature to 1150 K can be achieved in plant configurations where one Brayton normally provides the total electrical output. The gas Brayton system performance is extremely sensitive to pressure drop differences among the arrangement options. Further optimization of system piping arrangements, or relief from some constraints (radiator area, heat pipe operating temperature, or reactor coolant temperature) would be required for systems with two or more normally operating Brayton units. Transient analyses show that a closed cycle system with multiple Brayton units is feasible, with no apparent system instabilities. However, parallel operation of multiple Braytons in a closed loop has never been demonstrated, therefore integrated system testing would be needed to confirm feasibility. Allowances for off-nominal parameters (e.g. temperatures and pressures) would need to be allocated early in the project to ensure design margin for component degradation over service life, transient performance, casualty recovery, instrument error, manufacturing tolerance, operating strategy, and associated operating bands.

Technology Development

The designs for major plant components (recuperator, gas cooler, Brayton turboalternator, valves, and piping) are within the bounds of current technology. Designing these components to be leak tight for the long life of deep space missions remains a development item. A more significant development item is a material system, combining all parts of the Reactor Module in contact with each other that will be compatible for the long duration of the deep space mission.

Extensive developmental testing will be required early in the project to support system design decisions.

The capability and performance of the heat rejection system is intimately linked to that of the reactor system. High temperature water heat pipe performance and lifetime limits need to be fully characterized. These limits could have a significant impact on the ability to reach required mass goals and mission lifetime.

Space Environment

A reactor operating in space may generate a significant electrical charge buildup on the spaceship. Actions will need to be taken to characterize, test and mitigate this effect to ensure spaceship operations are not affected.

The Reactor Module will require a micrometeoroid protection covering to prevent impact damage and chemical contamination from the space environment. This covering will complicate the thermal design, so this should be considered from the inception of design activities.

Detailed information supporting these conclusions is contained in Enclosure (1). In addition, next actions required to pursue this design are included in each section of this enclosure.

**CONCURRENCES**

This report has been reviewed and concurred with by the KAPL Managers of Space Energy Conversion, Space Electrical Systems and Space Materials, and the Bettis Manager of Space Reactor Engineering.

Very truly yours,

Wayne D. Burdge

WD Burdge, Manager
Power Plant Design
SPACE POWER PROGRAM
KAPL

Brian Levine

BL Levine, Lead Engineer
Power Plant Design
SPACE POWER PROGRAM
KAPL

GM Brewer

GM Brewer, Manager
Space Fluid and Mechanical Systems Design
SPACE ENGINEERING
Bettis

Approved by:

H Schwartzman, Manager
Space Power Plant Systems
SPACE POWER PROGRAM
KAPL

References:

(a) Enclosure 1 of KAPL/Bettis letter, SPP-67510-0020/B-SE-0091, "Responsibility Assignment Matrix (RAM)", dated April 2, 2005
(b) SPP-67110-0004/B-SE-0037, "NR Program Assessment of the Design Space for the Prometheus 1 Project", dated November 2, 2004
(c) KAPL/Bettis letter, SPP-67110-0005/B-SE-0077, "Space Nuclear Power Plant Concept Selection, for NR Approval", dated March 4, 2005
(d) NR letter I#05-01228, "Space Nuclear Power - Reactor Coolant and Power Conversion System Concept - Approval of", dated April 20, 2005
(e) JPL Report 982-R120461, "Prometheus Project Final Report" , dated October 1, 2005
(f) KAPL/Bettis letter, SPP-67410-0013/B-SE(RE)-0003, "Space Reactor Preconceptual Design Report", dated January 27, 2006
(g) KAPL letter SPP-67210-0011, "Integrated Shield Design Summary", not yet issued
(h) KAPL letter SPP-67610-0008, "Space Power Program, Instrumentation and Control System Architecture, Preconceptual Design, for Information (U)", dated October 20, 2005
(i) KAPL letter MDO-723-0010, "Summary of Structural Materials Considered for the Prometheus Space Nuclear Power Plant (SNPP)", not yet issued

# *Summary of Design Checks Performed*

SPP-67210-0005 / B-SE(SPS)-001, "SNPP Plant Pre-Conceptual Design Report"

| Section | Authors | Peer Reviewer | Completed |
|---|---|---|---|
| 1: Introduction | W. Burdge, KAPL<br>J. Watson, KAPL | S. D'Amico | Stephen D'Amico |
| 2: Preliminary Plant Parameters | A. Klawitter, KAPL | B. Proctor | Beth Proctor 1/26/06 |
| 3: System Architecture | W. Burdge, KAPL<br>J. Martino, KAPL | G. Stasik | 1/26/06 |
| 4: Mass Estimates | G. Stasik, KAPL | J. Martino | |
| 5: Arrangements | J. Wells, Bettis<br>A. Zemo, Bettis<br>J. Watson, KAPL | J. Watson | 1/26/06 |
| 6: Heat Balances | J. Martino, KAPL<br>E. Clementoni, Bettis | S. Belanger | |
| 7: Reliability | B. Proctor, KAPL<br>K. Jensen, KAPL | S. Belanger | |
| 8: Operational Strategy | B. Levine, KAPL<br>E. Johnson, KAPL<br>D. Howard, Bettis | S. D'Amico | Stephen W. D'Amico |
| 9.1: Brayton TCA | S. Belanger, KAPL | R. Bechtel | |
| 9.2: Recuperator | M. Postlethwait, KAPL | B. Eckhardt | |
| 9.3: Gas Cooler | D. Vargo, Bettis<br>M. Haire, Bettis | S. Belanger | |
| 9.4: Piping | A. Gribik, Bettis | P. DiLorenzo | 1/26/06 |
| 9.5: Valves | K. Poczynek, BPMI | G. Stasik | 1/26/06 |
| 9.6: Heat Rejection System | S. Belanger, KAPL | A. Brooks | |
| 9.7: Piping Thermal Stress Analysis | P. DiLorenzo, KAPL | B. Levine | Brian Levine 1/25/06 |
| 10: Plant Support Structure and Environmental Protection | J. Watson, KAPL<br>J. Wells, Bettis<br>C. Dubovsky, Bettis<br>J. D'Antonio, Bettis<br>M. Moenssens, Bettis<br>J. Schuren, Bettis<br>A. Rice, KAPL | J. Watson | 1/27/06 |
| 11: Potential Plant Transients | B. Proctor, KAPL<br>D. Howard, Bettis | B. Levine | Brian Levine 1/25/06 |
| 12: Transient Analysis | M. Hexemer, KAPL<br>A. Brooks, KAPL<br>L. McCann, Bettis | M. Postlethwait | |
| 13: Testing | S. D'Amico, KAPL<br>M. Zavidny, Bettis | R. Bechtel | |
| 14: Plant Materials Summary | G. Stasik, KAPL | Y. Ballout | |
| 15: Structural Design Basis Summary | S. Sham, KAPL | B. Levine | Brian Levine 1/25/06 |
| 16: Extensibility to Other Missions | S. D'Amico, KAPL | J. Watson | 1/26/06 |

# Enclosure 1

# Plant Pre-Conceptual Design Report

(Intentionally Blank)

# Plant Pre-Conceptual Design Report

## Table of Contents

1 Introduction ..... 1-1
2 Plant Parameter List ..... 2-1
3 System Architecture ..... 3-1
4 Mass Estimates and Basis ..... 4-1
5 Arrangements ..... 5-1
6 Heat Balances – Design and Off-Design System Performance, Parameter Sensitivity Studies ..... 6-1
7 Reliability ..... 7-1
8 Operational Strategy ..... 8-1
9 Component Descriptions ..... 9-1
10 Plant Support Structure and Environmental Protection ..... 10-1
11 Potential Space Nuclear Power Plant Design Events ..... 11-1
12 Transient Modeling ..... 12-1
13 Testing ..... 13-1
14 Plant Materials Summary ..... 14-1
15 Structural Design Basis Summary ..... 15-1
16 Extensibility ..... 16-1

(Intentionally Blank)

# Section 1
# Introduction

(Intentionally Blank)

# Introduction

## Table of Contents

1 Introduction ..... 5
1.1 Background and Systems Overview ..... 5
1.2 Reactor Module Requirements ..... 8
1.2.1 Principal Requirements Development ..... 8
1.2.2 Requirements Allocation and Project Hierarchy ..... 12
1.3 Reactor Module Description ..... 14
1.3.1 Reactor Module Segments and Subsystems ..... 14
1.3.2 Reactor Module Interfaces ..... 19
1.4 Summary and Conclusions ..... 22

## List of Figures

Figure 1-1: Spaceship and Modules (Ref 1- 2) ..... 5
Figure 1-2: JPL Prometheus Systems Overview ..... 7
Figure 1-3: Project Document Hierarchy ..... 12
Figure 1-4: Two Brayton System Arrangement: Reactor Module Major Components ..... 14
Figure 1-5: Volume of Space Shielded by Shadow Shield ..... 16
Figure 1-6: Notional PCAD Schematic ..... 21
Figure 1-7 SNPP Reliability versus System Mass ..... 23

## List of Tables

Table 1-1: Key Level 2 Requirements, Impacts, and Implementations ..... 9
Table 1-2: Additional Key Requirements ..... 11
Table 1-3: NASA-JPL Prometheus Project Hierarchy Definitions ..... 13

(Intentionally Blank)

# 1 Introduction

This document describes the concept design work performed on the Space Nuclear Power Plant since the Concept Selection recommendation, submitted to NR on March 4, 2005 (Reference 1- 1). Included are preliminary conclusions, technical challenges, and the future actions envisioned to progress this design.

## 1.1 Background and Systems Overview

Project Prometheus was established in 2003 and included the goal of developing the first reactor-powered spaceship and demonstrating that it can be operated safely and reliably on long duration, deep-space missions for civilian space exploration. The NASA Jet Propulsion Laboratory (JPL) had overall lead for the project. The initial application of space fission power being evaluated was the Jupiter Icy Moons Orbiter (JIMO), a nuclear electric propulsion spacecraft intended to perform deep-space scientific research around three moons of Jupiter (Callisto, Ganymede, and Europa)

In March 2004, the Naval Reactors Program was assigned responsibility for design and delivery of the Reactor Module for Project Prometheus. The Reactor Module, the Spacecraft Module, and the Mission Module comprised the JIMO spaceship as described in Reference 1- 2. Figure 1-1 shows a pre-conceptual view of the spaceship. The three modules are indicated along with some of the prominent elements of the reactor and spacecraft modules. A description of the modules follows.

f

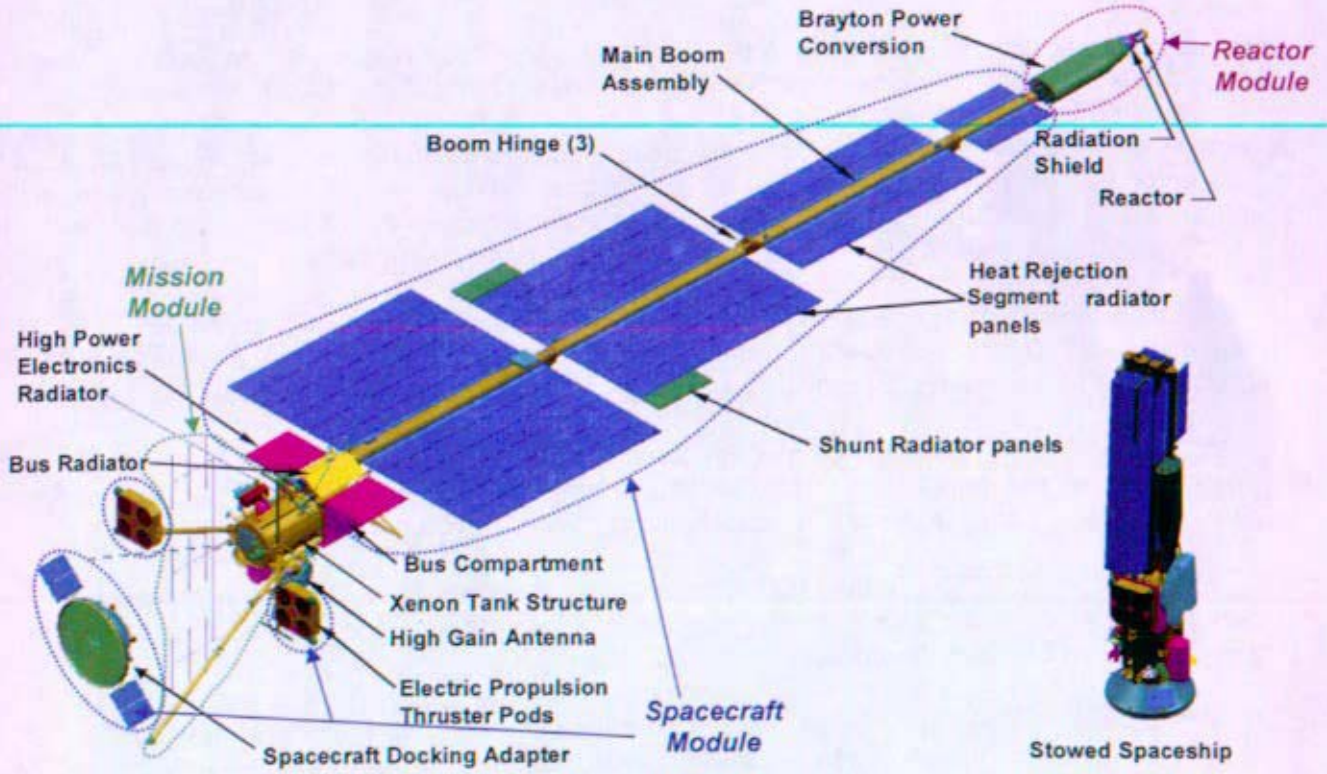



**Figure 1-1: Spaceship and Modules (Ref 1- 2)**

The Reactor Module includes the primary elements needed to deliver the required electrical power to the rest of the Spaceship. This includes the nuclear reactor, reactor coolant, energy conversion equipment, reactor shield, support structure, and other supporting equipment. The Reactor Instrumentation and Control segment is also part of the Reactor Module, with the sensors physically located in the Reactor Module and the electronics located with the bulk of the other electronics in the Bus Segment of the Spacecraft Module. In accordance with Reference 1- 10, the design responsibility for all parts of the Reactor Module was assigned to the Naval Reactors Prime Contractor Team (NRPCT) and the approval responsibility is assigned to NR, with the exception of the Aeroshell.

The set of elements needed to generate and manage, by distribution or rejection to space, the power created by the reactor, is frequently referred to as the Space Nuclear Power Plant (SNPP). The SNPP includes the Reactor Module, the Heat Rejection Segment, and the Power Conditioning and Distribution Subsystem.

The Spacecraft Module includes all the spaceship systems other than the Reactor Module or the Science System elements. This includes the power management and distribution subsystem, the ion propulsion system, the heat rejection segment (radiator panels and heat transport system), telecommunications, control, and spacecraft structure.

The Mission Module is mission specific and includes all science instruments and supporting equipment necessary to meet science requirements. The supporting equipment may have included the following: scan platform, turntable, associated electronics, booms, deployment devices, radiation shields, cabling, multi-layer insulation and thermal control devices, and flight software.

The Reactor Module and the Spacecraft Module comprise the Deep Space Vehicle (DSV). This is the vehicle which is designed for multiple missions and thus does not include the science system elements located in the Mission Module. It does include the Science Computer and its core software that support the Mission Module. A spacecraft docking adapter (Docking Segment) is also included in the Spacecraft Module to support early on-orbit operations and docking with the interplanetary transfer stages. The docking adapter provides power, communications, and attitude control functions for the DSV in the post-launch phases through deployment and commissioning.

A more complete view of the project system structure is depicted in Figure 1-2, taken from Reference 1- 3. All elements of the Prometheus Project fall within one of the four systems shown. A description of the four systems, as provided in Reference 1- 3, follows:

Launch System (LS) – The Launch System consists of the hardware, software, facilities, procedures, and personnel used to conduct launch operations. The Launch System includes the launch vehicle(s), transfer vehicle(s), launch site facilities, and launch services.

Deep Space System (DSS) – The Deep Space System consists of the hardware, software, facilities, procedures, and personnel used to design, integrate, and test the Deep Space Vehicle (See description of Deep Space Vehicle above).

Science System (SS) – The Science System consists of the hardware, software, facilities, procedures, and personnel used to design, integrate, test, and operate the Mission Module. The Mission Module includes the instruments, its support engineering hardware (e.g., turntables, scan platforms, booms etc.), and mission-unique software. The Science System also includes the

Science Operations Module, which consists of the personnel and science ground hardware and software that support the Ground System.

Ground System (GS) – The Ground System consists of the ground hardware, software, facilities, procedures, and personnel used to conduct flight operations. The Ground System for Prometheus consists of the trained personnel, their procedures, facilities, and computer and communication hardware and software required to operate the Spaceship as described in the Mission Plan. It interfaces with the Deep Space Network (DSN) and JPL's multi-mission operations services and tools.

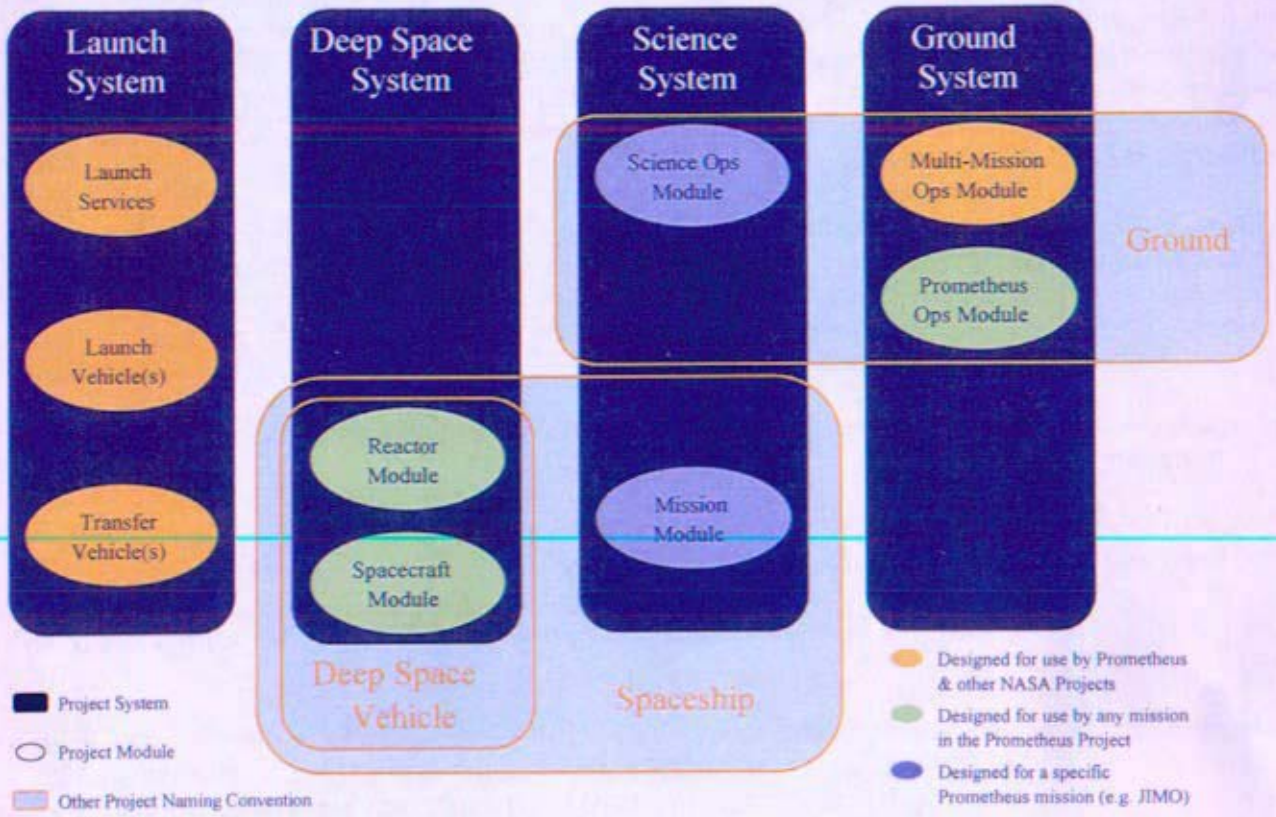



**Figure 1-2: JPL Prometheus Systems Overview**

## 1.2 Reactor Module Requirements

Described below are the primary, high level requirements for Project Prometheus. The Level 1 JIMO Requirements (Reference 1- 5) issued by NASA headquarters formed the basis for Level 2 Multi-mission (Deep Space Vehicle) and JIMO (Mission Module) requirements. These include the resulting key requirements for the Reactor. At this stage of mission and technology definition, all requirements are preliminary and not fully defined.

### 1.2.1 Principal Requirements Development

The ambitious mission of orbiting and exploring the icy moons of Jupiter was developed to meet the Exploration Requirements for NASA (Reference 1- 4) and to support the "goal of developing the first reactor-powered spacecraft capability and demonstrating that it can be operated safely and reliably in deep space on long-duration missions" (Ref 1- 4). The high level requirements for the JIMO mission were developed and documented in Level 1 Requirements (Reference 1- 5). Because some requirements presented in Reference 1- 5 were still preliminary, some items are indicated as *objectives or requiring further review.*

The Level 1 JIMO Requirements include the Development Technology requirements, which describe the primary technical goals required to enable a deep space mission, and the mission and science requirements, which describe delivery of the space vehicle to the Jovian system and operation during the science phase. The Level 1 requirements formed the central starting point for development of project requirements and conceptual design efforts.

The Level 1 Development Technology requirements which ultimately drive the key reactor module requirements are as follows:

> *The JIMO Project shall develop a Deep Space Vehicle for outer solar system robotic exploration missions that combines a safe, reliable, Space Nuclear Reactor with electric propulsion.*
>
> *The Deep Space Vehicle shall have a Payload Accommodation Envelope with a mass capability of no less than 1500 kg.*
>
> *The following Space Nuclear Reactor technologies shall be developed for Lunar and Mars surface power reactors: 1) Nuclear fuel, 2) Reactor core materials and coolants, and 3) Instrumentation and Control.* (This item was indicated as an objective – minimum requirement not yet defined.)

Multiple studies and analyses were performed to develop and evolve the conceptual spaceship design required to satisfy the Level 1 requirements. These studies resulted in the configuration described in Figure 1-1 and numerous Level 2 documents detailing mission requirements, environments, hardware and software selection and validation requirements, safety and security requirements, science requirements, and many other aspects covering the design and validation of the JIMO mission.

**Table 1-1: Key Level 2 Requirements, Impacts, and Implementations**

| *Key Level 2 Requirement* | Impact on Reactor Module | Implementation |
|---|---|---|
| *The Space Nuclear Reactor design shall utilize technologies that facilitate extensibility to surface operations.* | Drives selection of design and materials compatible with Lunar and Mars missions. | Must consider compatibility of pressure boundaries and external surfaces with surface environments. |
| *The Project shall use a Deep Space Vehicle that provides jet power greater than or equal to [130] kW of primary thrust during thrust periods.* | 200 kWe reactor module power output required to deliver net thruster power. | Plant Electrical Power ≈ 200 kW<br>Plant Thermal Power ~ 1 MW |
| *The Project shall design the Deep Space Vehicle to have an operating lifetime greater than or equal to [20] years.* | 20 year life is long term requirement for very deep space missions. The JIMO requirement is for 12 years. | Initial design efforts to support 15 year operational life.<br>Long term design goal is to satisfy 20 year life requirement. |
| *The Project shall use a Reactor Module that is capable of generating the maximum electrical power required by the Spaceship for cumulative minimum of [10] years, and is capable of generating the minimum required electrical power for the rest of the operating lifetime.* | This requirement permits the option of reducing power in order to conserve reactor energy or reduce pressure and temperature during non-thrust phases. This may maximize reactor module life for the most demanding follow-on missions to the outer solar system. | Trade studies would be required to determine if reduction of power would improve reactor module longevity. |
| *The Project shall comply with the Prometheus Single Point Failure Policy as documented in the Prometheus Project Policies Document 982-00057.* | Single point failure locations shall be avoided. Where this is not practical (e.g., reactor), must demonstrate that alternatives to single point failure are not available and show sufficient robustness to mitigate risk of failure. | Where possible, redundancy would be part of the reactor module design. |
| *The Project shall be able to autonomously detect and correct any single fault that prevents thrusting in less than or equal to [1 hour].* (Note: Missing thrust during many of the mission phases severely jeopardizes mission success, and therefore should be prevented or minimized.) | This requirement must be considered in the design of instrumentation and control for a self-regulating plant and design for recovery from transients for which the module would be designed. | Robust and redundant system architecture for instrumentation and control.<br>Automatic recovery from transients must be considered in system design. |
| *The Spaceship shall survive without Ground System commanding for at least [50] days in the presence of a single failure.* | Must consider this, with other autonomy and single point failure requirements, in design of the control system. | Design for redundancy and robustness wherever practical.<br>The spaceship cannot survive in deep space for more than a short time without reactor power. |
| *The Project shall assure that all Science System hardware in its deployed configuration, except approved science hardware, shall remain within the protected zone of the reactor radiation shield.* | Coordination between the shield and spaceship designs is required to assure that maximum dose levels are not exceeded. Shielding of local electronics will also be required. | Shielding sufficient to reduce payload neutron flux to 5E10 n/cm2 and payload gamma flux to 25 kRad Si damage and cover roughly a 12° by 6° cone angle. |
| *The Project shall obtain launch approval as specified in the Prometheus Launch Approval Plans.* | To meet this requirement, satisfaction of various governing safety requirements would have to be demonstrated by NRPCT and NASA. | Design features will be required to assure safety. Safety assurance must be considered during design of certain Reactor Module elements. |
| *The Spaceship total dry mass at launch shall not exceed [25,000] kg.* | Minimum module mass is a goal and a selection criteria for design. | High temperature reactor is required to minimize overall mass |

Note: Values in [brackets] were not firm and thus subject to review.

The primary set of non-JIMO specific Level 2 technical requirements was collected into the Multi-mission Project Derived Requirements, Reference 1- 6. The JIMO specific Level 2 technical requirements were given in Reference 1- 7. The Level 2 technical requirements which drive key aspects of the Reactor Module design are listed in Table 1-1. Accompanying each requirement is a statement of the impact on the Reactor Module. Also provided, where applicable, is a description of the implementation required to meet the requirement.

Electric power output of the reactor module is one of the most important requirements because it ultimately drives system mass and volume. While thrusting, the majority of electric power is used to drive the ion propulsion thrusters. Minimum acceptable thrust (and thus power) was determined to be driven by the complex gravity fields around the Jovian moons, where a minimum thrust level is required to achieve stable orbit and de-orbit of the moons. Due to the high mass of the JIMO vehicle, driven in part by the systems required to support the high voltage ion propulsion thrusters, the xenon propellant, the 1500 kg science payload, and the reactor module, an output power of 130 kWe for propulsion is required. The 200 kWe reactor module power output listed in Table 1-1 results after accounting for propulsion unit efficiency of 72%, conversion losses, transmission losses, and other vehicle power requirements. Explicitly stated, the required reactor output is estimated as follows: [(130 kWe thruster output / 0.72 Propulsion Power Units Efficiency) + 5 kWe Vehicle Operation] / 0.95 Power Conversion and Distribution (PCAD) efficiency = 195 kWe (~ 200 kWe).

In addition to the key requirements addressed above, many other important requirements must be considered in evaluating, selecting, and demonstrating design options. Some of these are listed in the JIMO Deep Space Vehicle Level 3 Key Driving Requirements, Reference 1- 8: some in Prometheus Project Environmental Requirements Document (ERD), Reference 1- 9: and others were still being developed. Some of the more important items for the Reactor Module are listed Table 1-2, with references as appropriate.

**Table 1-2: Additional Key Requirements**

| *Requirement* | Impact on Reactor Module |
|---|---|
| *The Spaceship launch configuration shall be compatible with a [5-m] launch vehicle payload fairing (dynamic envelope dimensions 4.5m diameter, 26m height), or smaller* (Ref 1- 8) | Arrangements and overall sizing must fit within allocated space inside the fairing. This mainly constrains the radiator area, which drives the heat balance design space of the Reactor Module. |
| *The Spaceship shall accommodate the solid particle mission environments defined in {ERD} with a probability of meeting end-of-mission (EOM) requirements greater than or equal to 0.99 ...*(Ref 1- 9) | Protection from orbital debris and micrometeoroids is required, especially of the crucial pressurized components and moving assemblies. |
| *The Spaceship shall be designed to accommodate the radiation environment specified in the Environmental Requirements Document (982-00029).* (Ref 1- 8) | Solar, galactic and Jovian radiation sources, coupled with reactor radiation, must be considered during electronics selection, shielding trades and material evaluation. |
| *The Spacecraft Module shall be capable of rejecting [682] kWt of heat from the Reactor Module.* (Ref 1- 8) | If radiator size is constrained, temperature and flow rate must be maximized to reject sufficient heat. This impacts the Reactor Module heat balance. |
| *The Prometheus flight hardware shall be designed and verified to meet applicable functional, performance, operation, and other design requirements without damage or degradation when exposed to the design environments specified herein {in ERD}.* (Ref 1- 9) | In addition to particle and radiation environments described above, the module must withstand launch loads and other space environments. Section 10 has more details about environments. |
| *During no-thrust periods of Science Orbits, the Deep Space System shall continuously point a Spaceship-fixed vector to commanded directions in the target-centric reference frame to within 20, 20, and 20 mrad (3 sigma) about the reference frame X, Y, and Z axes respectively...* (Ref 1- 8) | This requirement drives the need for positional stability of the spaceship. Counter-rotating Braytons, or alternate localized means to offset angular momentum, would be necessary to provide the needed stability. |

Note: Values in [brackets] were not firm and thus subject to review.

Limits for several parameters such as mass and volume were still being developed in parallel with other reactor and space ship design efforts. Although precise values were not defined, failure to address the limits indicated would result in a design which would overly burden the rest of the vehicle and could even make design of a viable spaceship untenable.

See Reference 1- 8 for a more complete listing of the driving requirements for the Deep Space Vehicle, which includes the reactor module.

### 1.2.2 Requirements Allocation and Project Hierarchy

As depicted in Figure 1-3, there were multiple levels of documents increasing in detail. Level 2 documents address five different categories as depicted below. The requirement allocation process that was planned for the JIMO project would have assigned requirements from each tier of documents, as well as interface requirements and other derived requirements, to the next lower level elements. In this way, requirements would have been assigned to the various modules and then to their constituent segments, sub-systems, etc. A tabular depiction of the project hierarchy, and description of the reactor module segments, follows.

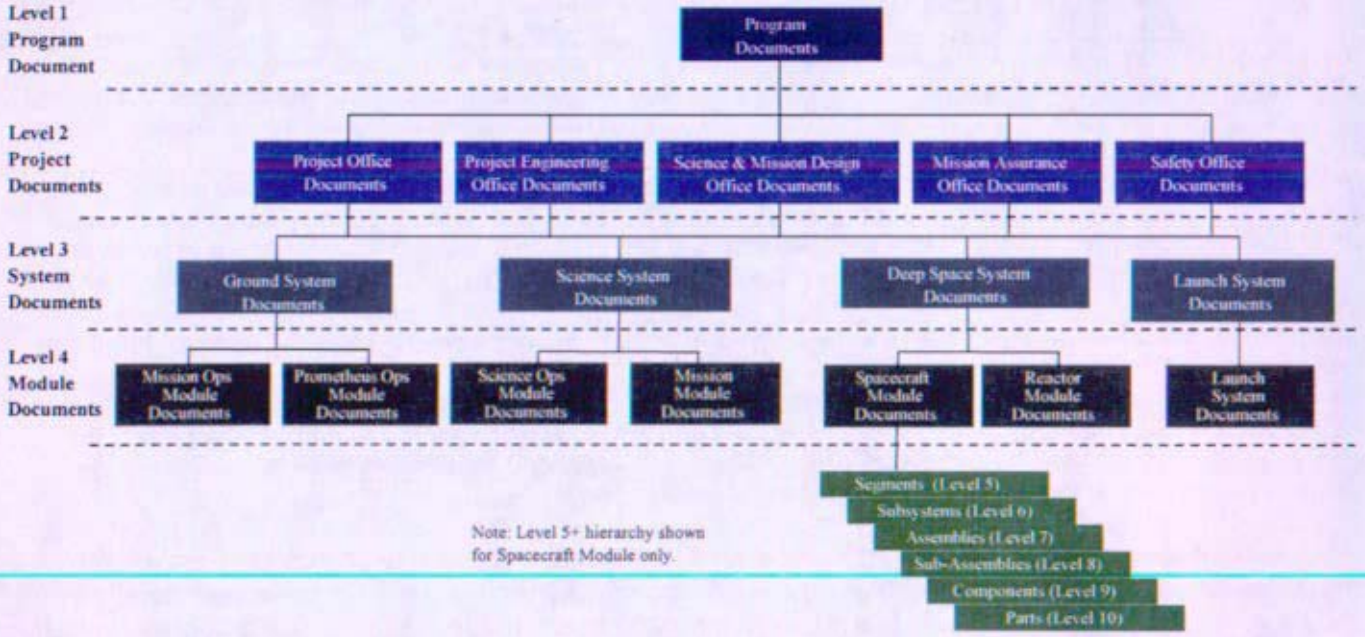



**Figure 1-3:** Project Document Hierarchy

Table 1-1 shows the hierarchical definitions established for Prometheus by JPL [Reference 1- 3]. As described in this table, each module is broken down into segments. Segments are functional hardware groupings typically referred to as systems in the NR Program. In order to develop a common vocabulary with JPL, the NRPCT recommended (Reference 1-11) applying this nomenclature and referring to module subgroups as segments which is a revision to the standard NR program terminology. Segments are further divided into subsystems.

## Table 1-3: NASA-JPL Prometheus Project Hierarchy Definitions

| Project Level | Name | Definition | Examples |
|---|---|---|---|
| 2 | Project | An integrated set of Systems that accomplish the Prometheus Program Objectives | Project Engineering<br>Science & Mission Design<br>Mission Assurance<br>Safety |
| 3 | System | An integrated set of modules that accomplish the Prometheus Project objectives. | Launch System<br>Deep Space System<br>Science System<br>Ground System |
| 4 | Module | A major product, service, or facility of the system. | Multi-Mission Operations Module<br>Prometheus Operations Module<br>Science Module<br>Mission Module<br>Spacecraft Module<br>Reactor Module |
| 5 | Segment | A major product, service, or facility of the module. | Heat Rejection Segment<br>Electric Propulsion Segment<br>Docking Adapter Segment |
| 6 | Subsystem | An integrated set of assemblies, components, and parts which performs a cleanly and clearly separated function, involving similar technical skills, or a separate supplier. | Power Conditioning and Distribution Subsystem<br>Telecommunications Subsystem<br>Bus Structure Subsystem<br>Command & Data Handling Subsystem |
| 7 | Assembly | An integrated set of components and/or subassemblies that comprise a defined part of a subsystem. | Battery<br>Power Conditioning Unit<br>Transponder<br>Deployment Assembly |
| 8 | Subassembly | An integrated set of components and/or parts that comprise a well-defined portion of an assembly. | Motor<br>CPU |
| 9 | Component | Comprised of multiple parts (a cleanly identified item). | Memory<br>Input/Output Devices<br>Structural beam |
| 10 | Part | The lowest level of separately identifiable items. | Bolt<br>Resistor<br>Diode |

## 1.3 Reactor Module Description

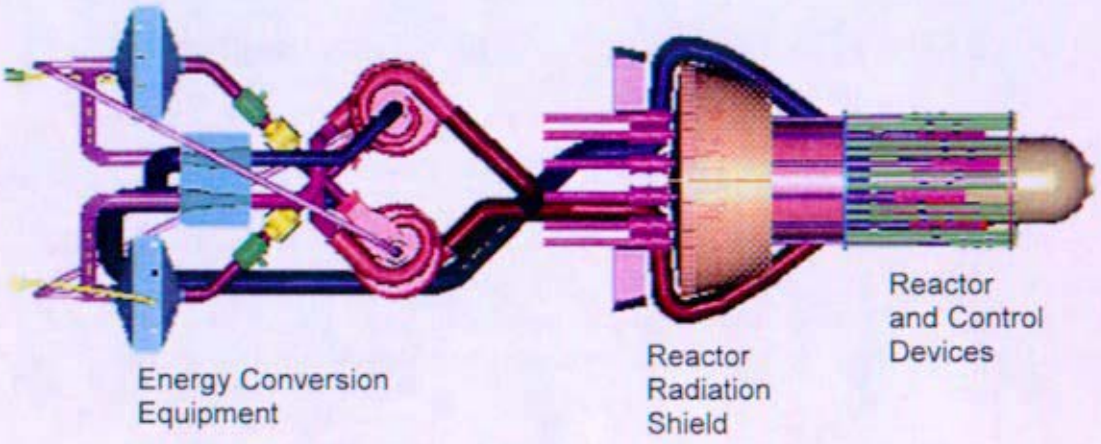



**Figure 1-4: Two Brayton System Arrangement: Reactor Module Major Components**

The Reactor Module (notionally shown in Figure 1-4) provides the thermal energy source for the generation of electrical power. After extensive studies to evaluate different energy conversion approaches, the NRPCT recommended, for NR approval, a gas-cooled reactor with a directly coupled Brayton energy conversion system (Reference 1- 1). Reference 1- 12 approved this recommendation and authorized work on further development of this concept.

The reactor is a helium/xenon (He/Xe) gas-cooled, fast neutron spectrum, fission reactor with an approximately 1 MWt uranium heat source directly coupled to a gas Brayton energy conversion equipment. The reactor requires a radiation shield to provide a shadow volume of diminished radiation to the rest of the Spaceship. The radiation shield concept is an elliptical cone which produces this shadow with half-angles of 12° and 6°. All major elements of the spacecraft and Mission Modules will be located within this shielded area.

### 1.3.1 Reactor Module Segments and Subsystems

The Reactor Module is portioned into six segments: Reactor Segment, Reactor Coolant Segment, Reactor Radiation Shield Segment, Plant Structure and Environmental Protection Segment, Reactor Instrumentation and Control (I&C) Segment, and Aerothermal Protection Segment. A brief description of each of these segments is listed below.

Also listed are the other space vehicle segments to which there would be key interfaces with the reactor module. Each segment will be discussed in more detail in the report sections which apply to the segments listed.

#### 1.3.1.1 Reactor Segment

The nuclear reactor generates heat by fissioning atoms of nuclear fuel and supplies this heat to the Brayton Energy Conversion Units by means of the reactor coolant piping. It is a fast-spectrum, gas-cooled reactor that is controlled by fixed and movable reflectors. A removable safety rod(s) is

installed to ensure that the reactor remains sub-critical prior to and during launch. A pressure vessel surrounds the reactor core and contains the cooling helium/xenon gas mixture. He/Xe gas is circulated through the reactor vessel and reactor coolant segment by the compressor located in the Energy Conversion Subsystem. The Reactor Segment consists of four subsystems:

1. Reactor Core Subsystem – Consists of the reactor core, cladding and internal structural supports.
2. Reactivity Control Subsystem – Consists of the fixed and movable reflectors, the associated alignment and support structures, shafts, and positioning motors.
3. Reactor Vessel Subsystem – Consists of the reactor vessel and support that attaches it to the shield.
4. Reactor Safety Subsystem – Consists of the safety rod(s) and associated removal mechanism(s) and mechanical features to preclude motion of movable reflectors prior to reactor operation.

Primary Functions:

1. Generate thermal energy from fissioning of nuclear fuel.
2. Transfer thermal energy to the reactor coolant.
3. Contain He/Xe gas.
4. Support the core.
5. Contain fission gases.
6. Control core reactivity.
7. Provide sufficient shutdown margin to prevent inadvertent criticality.

### 1.3.1.2 Reactor Radiation Shield Segment

Shielding requirements are based on the radiation tolerance of the electrical components, sensors, and other materials in the Reactor Module and in the remainder of the spacecraft. These sensitive components are subjected to radiation damage from both the space environment and the reactor. The space environment sources of radiation include charged particles (electrons, protons, heavy ions, and secondary particles, such as spallation neutrons) and gamma radiation. In general, the shielding associated with environmental sources surrounds the sensitive components and consists of aluminum plate shielding with a thickness of 300 mils or more. This space radiation shielding is not part of the reactor radiation shield but is an interface that will be considered in the shield design.

The reactor radiation shield segment shields spaceship components from radiation emitted by the reactor, such as direct neutron and gamma radiation, neutron capture, activation of coolant or structure, fission product release to the coolant, electrons leaving the reactor/reflector surface, etc.

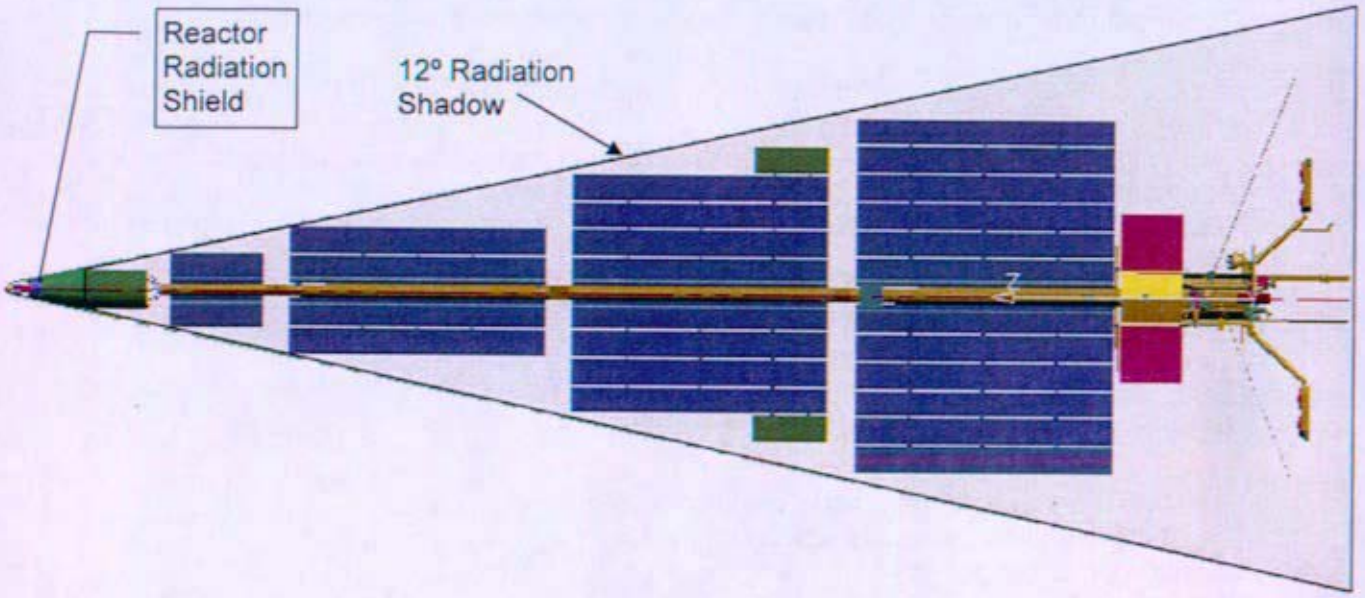



**Figure 1-5: Volume of Space Shielded by Shadow Shield**

Primary Functions:

1. Limit radiation dose from the reactor to the spacecraft and energy conversion and reactor control equipment.

Secondary Functions:

1. Provide a thermal neutron fluence, appropriate temperature environment, and a protective housing for the nuclear instrument detectors, if necessary.
2. Provide structural supports for the reactor vessel, control drive mechanisms (CDMs), and energy conversion system equipment structural supports.
3. Provide piping passage and thermal control between the reactor and energy conversion segment.

### 1.3.1.3 Reactor Coolant Segment

The Reactor Coolant Segment contains the reactor coolant piping and associated components needed to support energy transfer and conversion into useful electric power. It includes reactor coolant piping connecting the hot and cold leg reactor vessel nozzles to the Brayton turboalternator unit(s) and associated valves. This segment includes the Energy Conversion Subsystem The Energy Conversion Subsystem consists of a Brayton turboalternator (turbine, alternator, and compressor on a single rotating shaft) that converts the heat from the coolant into useful electrical energy. The Brayton turboalternator is a closed cycle unit that is integrally coupled to the reactor coolant piping.

A permanent magnet, rotary alternator converts the mechanical energy of the Brayton engine into electrical energy. The alternator is located within the gas pressure boundary and requires electrical feeds through the pressure boundary. These feed-throughs must be sealed to prevent leakage.

Primary Functions:

1. Remove heat from nuclear fission in the reactor core and transfer this heat to the Brayton Units.
2. Utilize heat from the reactor to generate electric power.
3. Circulate reactor coolant during initial reactor startup.
4. Contain the reactor coolant gas.

Secondary Functions

1. Provide cooling to the Energy Conversion Subsystem components.

In order to ensure long life of the turbo-machinery, a coolant purification and or filtering subsystem may be required. This would most likely make use of sharp piping bends and mechanical filters to centrifugally separate small potentially damaging particles out of the gas stream. Should a filtering subsystem be needed, care should be taken to minimize any pressure drops associated with it.

### 1.3.1.4 Plant Structure and Environmental Protection

The Plant Structure and Environmental Protection Segment provides structural support, micrometeoroid protection, and thermal management for the Space Nuclear Power Plant arrangement. It consists of three subsystems:

1. Structural Support Subsystem – Supplies structural load paths necessary to maintain physical support and alignment of equipment and to accommodate all anticipated static, dynamic and thermally-induced loads. The system includes the primary support structure that provides overall support and connection of the Reactor Module to the Spacecraft Module, including the module portions of the separable interfaces. The system also includes the secondary support structure that provides structural connections among Reactor Module components and the primary support structure.
2. Micrometeoroid Protection Subsystem – Consists of material barriers around critical elements to protect the Reactor Module against impact damage, erosion and chemical contamination from micrometeoroids. This protection comes, in part, from existing structural elements and thermal control elements supplemented by other materials to provide the degree of protection desired.
3. Thermal Management Subsystem – Provides the heat rejection, thermal isolation, and supplemental heating needed to keep the different Reactor Module elements within temperature limits. The thermal management subsystem would include insulating materials (insulation, multi-layer blankets, spacers), surface thermo-optical materials (paints, coatings, treatments, etc), conductive and isolating materials, and probably more active elements such as heaters, temperature sensors and heat pipes.

Primary Functions:

1. Provide structural alignment and support of the reactor, shield, piping and energy conversion components.
2. Provide structural attachment of the Reactor Module to the Spacecraft Module.
3. Provide structural mounting features to accommodate launch loads, flight loads, thermally-induced relative displacements, and deployment loads on Space Nuclear Power Plant equipment.
4. Provide support for the Micrometeorite Protection and Thermal Management Subystems.
5. Protect the Reactor Module components from micrometeoroid damage.
6. Provide thermal isolation or coupling between components to meet performance requirements.
7. Provide localized heat rejection from Reactor Module components.

Secondary Functions:

1. Provide a means for cable management and routing.
2. Assure that Reactor Module temperatures are within the required values prior to reactor startup.

### 1.3.1.5 Reactor Instrumentation and Control Segment

The Reactor I&C segment contains the sensors and control circuits needed to continuously monitor the state of the Reactor Module and control its functions throughout the mission. The sensors are placed in key locations in the Reactor Module at the forward end of the spaceship and are connected to signal processing circuits via spaceship cabling assemblies which extend the length of the boom. The Reactor I&C signal processing circuits, reactor controllers, and other hardware are located in the shielded Bus Compartment at the aft end of the spaceship where the sensitive electronics are protected from the space environment.

Primary Functions:

1. Monitor important reactor parameters. These include reactor coolant temperature, pressure, and flow; reactor power (neutron flux); position of the reflectors and safety rod(s); and position of the isolation valves (if used).
2. Monitor Brayton unit parameters. These signals would be obtained from data links with the PCAD subsystem and would include Brayton unit speed and output power.
3. Control the positioning of the movable reflectors. The reflectors are part of the reactivity control subsystem and are used to control reactor temperature and power by adding or subtracting reactivity.
4. Control the positioning of the reactor coolant isolation valves. These isolation valves prevent coolant flow through idle loop(s) in the configurations which use spare Brayton units.
5. Control Reactor Module heaters (if used).
6. Coordinate with the PCAD subsystem to control the speed of the Brayton units.
7. Communicate with the spaceship Command and Data Handling subsystem to send and receive reactor data and commands to and from Ground Control.

These functions will be performed autonomously through pre-programmed algorithms in the reactor controller software. Such autonomous operation is required because of the absence of continuous, real-time communication with the spaceship.

### 1.3.1.6 Aerothermal Protection Segment (APS)

Description

The APS, also known as the Aeroshell, is a physical structure that surrounds the reactor vessel and reflector and provides an aerodynamic envelope in the event of an accident that causes the reactor module to reenter the Earth's atmosphere. It is in place during launch and may be jettisoned prior to reactor criticality.

Primary Functions

1. Protect the reactor core from aerothermal heating during reentry into the Earth's atmosphere.
2. Keep the reactor essentially intact during an impact with the Earth to support recovery of the fuel.

## 1.3.2 Reactor Module Interfaces

The following is a list of other spaceship segments and subsystems with which the Reactor Module would interface:

1. Heat Rejection Segment – Removes heat from the energy conversion subsystem and radiates the heat to space. It also includes the Boom Assembly, which interfaces to the Reactor Module and controls the relative position of the Reactor Module and Bus Segment. This segment is described in Section 9.
2. Bus Segment – Receives electric power from the energy conversion subsystem and distributes it throughout the spacecraft. Provides the primary structural support for the space vehicle. It also contains the spacecraft control and communications subsystems.
    a. Power Conditioning and Distribution (PCAD) Subsystem – Conditions and distributes power to the spacecraft bus segment. To apply a controllable electrical load to the turbo-alternator, the PCAD subsystem utilizes independent (one per Brayton Channel) shunt regulators. It also includes the startup power from the solar array and power during launch from the battery.
    b. Figure 1-6 shows a notional schematic of the PCAD subsystem. It consists of four independent busses and equipment to support conditioning and distribution of power throughout the Spaceship.
    c. Command and Data Handling (C&DH) Subsystem – Provides two way communication between the spaceship and Ground Control.
    d. Bus Cabling Subsystem – Electrical cabling that allows electricity to be transferred from point to point.
    e. Environmental Monitoring Subsystem – Monitors the radiation environment and the health of the spacecraft.
    f. Structures and Mechanisms Subsystem – Provides the primary support interface for the reactor module.
3. Data Management Subsystem – Part of the Ground System that manages the data to the ground system operations stations.

4. Launch Vehicle Adapter Segment – Attaches the Spaceship (Reactor, Spacecraft, and Mission Modules) to the launch vehicle. It may also provide supplemental supports for the Reactor Module within the launch vehicle during liftoff.
5. System Level Software Segment – Spacecraft software that monitors and controls processes.

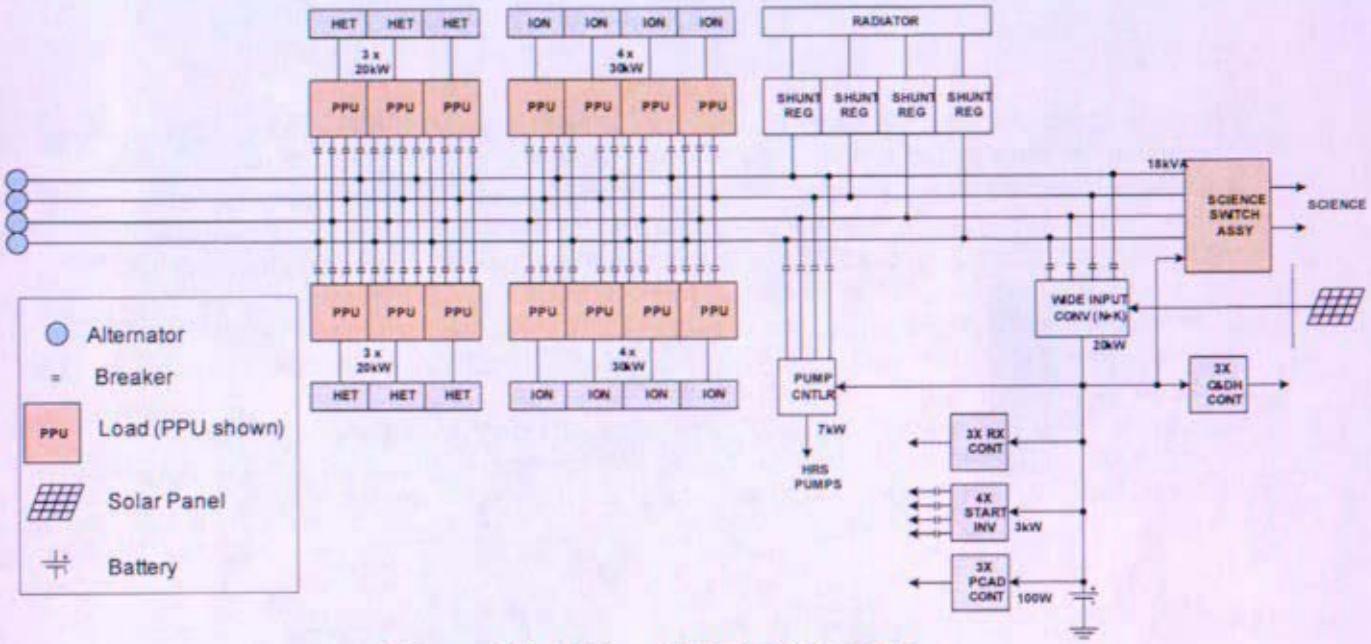



**Figure 1-6: Notional PCAD Schematic**

## 1.4 Summary and Conclusions

Since the previous NRPCT reports consisted of a comparison of many nuclear power plant concepts, this is the first in-depth evaluation of a single concept. NRPCT concludes that this nuclear powered deep space mission remains feasible, with the primary concerns being ensuring public safety in the event of an inadvertent re-entry accident, and demonstrating reliable operation for the long-duration of the deep space missions. Although spaceship mass allocations were not yet established, Project Prometheus was iterating toward a solution of mass, power, and time for the JIMO mission. Comparisons of the reliability of plants having from one to four Brayton loops indicate that having one or two loops would likely provide a more reliable plant than having three or four loops. (These reliability analyses are comparative at this stage and cannot be used to determine the absolute value of a given plant configuration.) Also, based on NRPCT recent evaluations of each component within the SNPP, the preliminary mass predictions are higher than NASA's for each part of the plant. (This would likely have been true for other reactor/energy conversion concepts besides the gas-Brayton system as well.) These findings would contribute to consideration of less redundancy (but potentially more reliability) among energy conversion loops, which NASA had baselined as four in prior spaceship studies (See Figure 1-7). The masses in this figure have been based on initial plant and piping arrangements using large diameter pipes for the single turbine and small diameter branch loop piping for the multiple turbine cases. These small diameters lead to unexpected high pressure drops, large penalties on system efficiency, and higher mass. No further studies to investigate arrangements with larger branch piping were completed but heat balance sensitivities to larger branch piping in Section 6 show significant improvement in efficiency for small increases in branch pipe diameter. A decision on the appropriate number of Brayton loops will not be made during this project closeout process. This decision would have involved NASA JPL and the spaceship designer to include overall

spaceship mass trades, evaluations of alternate methods to accommodate angular momentum, and other aspects of spaceship and mission integration.

The nomenclature (1-1-1) on Figure 1-7 relates to the system architecture. This nomenclature is explained in detail in Section 3. Additional summary conclusions are as follows:

Reliability and Mass

- Although spaceship mass allocations were not yet established, the spaceship conceptual design was being iterated toward a solution of mass, power, and duration for the JIMO mission. Based on recent evaluations of the initial sizes and arrangements for components within the Reactor Module, preliminary mass predictions are higher than previous estimates for most parts of the plant. Reliability studies indicate that having one or two loops would likely provide a more reliable plant than having three or four loops (See Figure 1). NASA had baselined the number of Brayton loops as four in prior spaceship studies. A decision on the appropriate number of Brayton loops was not made during this project closeout process. This decision would have had to involve NASA JPL and the spaceship designer to include overall spaceship mass trades, evaluations of alternate methods to accommodate angular momentum, parameter optimizations for each arrangement, and other aspects of spaceship and mission integration which were not done prior to project termination

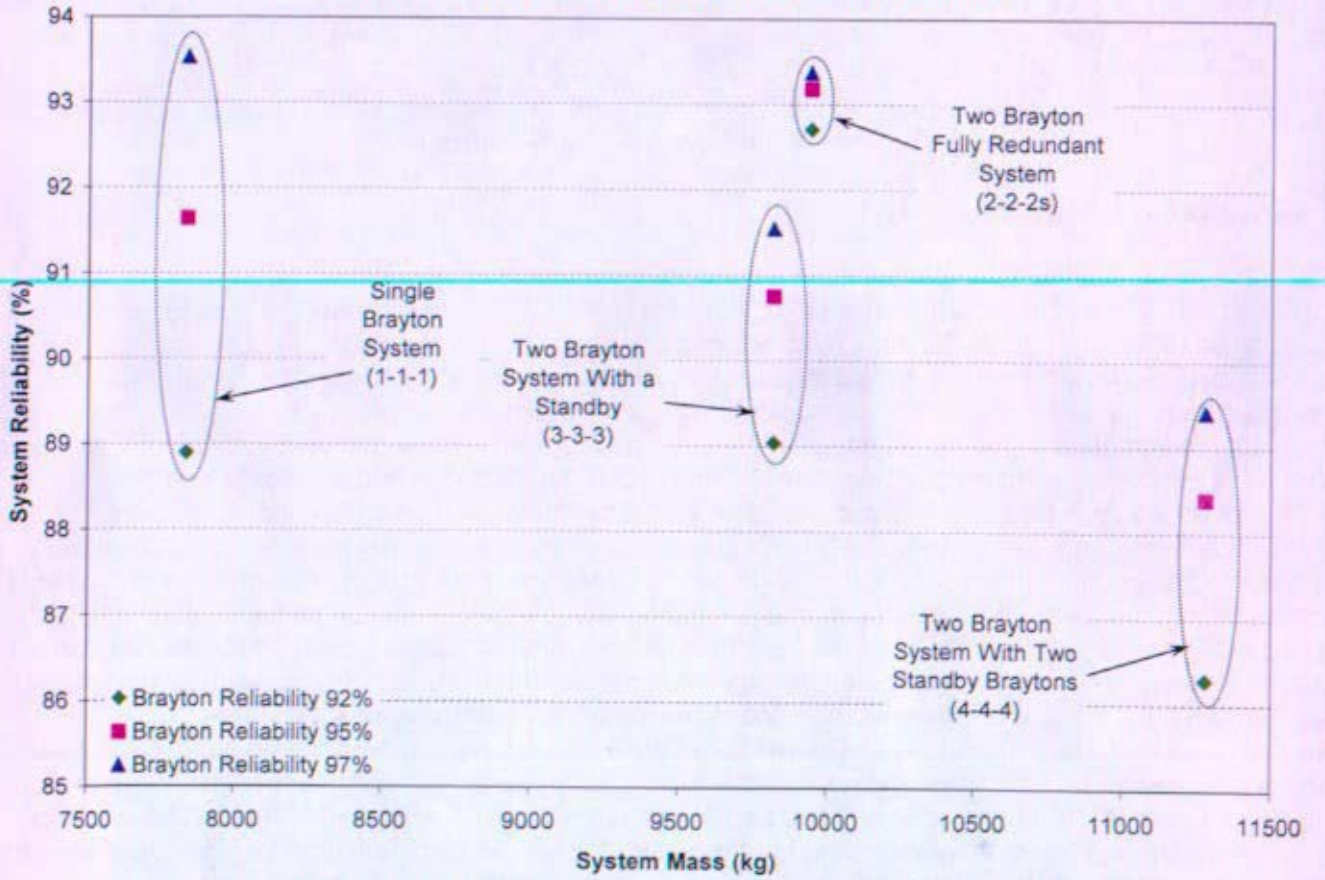



**Figure 1-7 SNPP Reliability versus System Mass**
[Both mass and reliability values are preliminary.]

System Architecture

- A single Brayton system offers the simplest design, the least required component development, and the simplest plant operation. The single Brayton system also has the lowest mass and the highest thermal efficiency. The extra capability could not be quantified until plant arrangements and parameter optimization studies were completed. Plant parameters that would be part of an optimization include coolant molecular weight, turbine speed, coolant temperatures at various heat exchangers, system pressure, and compressor pressure ratio. (Note that the current two Brayton system heat balance shows a higher efficiency. However, no conclusion should be drawn because the heat balances are based on current non-optimized configurations. The single Brayton system with no valves, fewer pipe fittings, etc., will have a lower pressure drop and higher system efficiency.) The single Brayton concept should be considered along with other system architectures despite NASA's single point failure tolerance criteria. An additional momentum compensation system would be required for any spacecraft architecture, including the single Brayton system, that does not have counter-rotating turbines.

- To meet the single failure tolerance criteria, multiple Brayton units would be required, resulting in a mass penalty and overall thermal efficiency decrement relative to a single Brayton system. It is noted that the approach to use multiple components is based on the Level 2 Prometheus Requirement to meet the NASA Single Point Failure Policy. NASA experience indicates the prudence of having redundant components, even if they have demonstrated reliability, to ensure that manufacturing defects, human error, or an unexpected event does not lead to a mission ending failure. This is also consistent with NRPCT practice. For those components where redundancy is considered impractical, exceptions to the single point failure avoidance requirement is provided. For the currently envisioned Prometheus spacecraft, the reactor, the reactor coolant loop, the boom, and the xenon propellant tank all require such exceptions. Some critical elements of a single Brayton system could have redundancy built in (e.g., alternators). Others, like turbine bearings, cannot have redundancy built in. Exceptions could be provided for a single Brayton system, but the desirability of operating high speed equipment over an extended lifetime must be considered.

- The determination of which system layout is most reliable depends on the reliability of the constituent components. A two Brayton system, in which both Braytons are normally running but each could, upon failure of one Brayton, supply full power to the spaceship (2-2-2s) would probably be the most reliable system. This system would have a mass of ~2,000 kg greater than the one Brayton system, although a 2-1-1s was not fully evaluated and may save several hundred kilograms of mass. Assuming Brayton components could be developed with acceptably high reliability (approximately 97% or greater for the Brayton assembly), the most reliable system would be the single Brayton system with one recuperator and one gas cooler (1-1-1). However, for systems with Brayton assembly reliability less than 97%, a second redundant Brayton results in a higher overall system reliability, offsetting the impact of additional components and increased complexity. System architectures with three or more Braytons (See Figure 1-4) had lower overall reliability. This reliability was reduced because of additional welds, valves, and surface area vulnerable to leaks to space and/or micrometeoroid impact. Because this system is significantly different than any other in existence, the decision on plant redundancy will have to be made without specific data on component reliability, and the envisioned test program will not be sufficient to establish a true statistical basis.

- The mass difference between the one Brayton (1-1-1) and two Brayton systems (2-2-2s) is ~2,000 kg based on these non-optimized results, which would be significant to the overall spaceship mass, although a 2-1-1s was not fully evaluated and may save several hundred kilograms of mass. The compilation of component masses for the SNPP was done recently, and actions to minimize mass had not yet been undertaken. As discussed in Section 4, these actions would have included optimization of the system arrangement and heat balance; trades on the reactor shield, mission module shield, and boom length; selection of the most appropriate reactor configuration; selection of materials and specification of their design bases; trimming of the reactor shadow shield configuration based on established spaceship configuration; etc.

Plant Operation and Plant Dynamics

- Reactor plant dynamic models were made using three different modeling tools (Simulink, RELAP5-3D, and TRACE). Model results show that a multiple closed Brayton unit system is feasible, with no apparent system instabilities. However, parallel operation of multiple Braytons in a closed loop has never been done before and substantial testing would be needed to further demonstrate feasibility and validate the models.

- Utilization of two distinct power levels may allow for the reduction of system temperature and/or reactor power for significant portions of the mission, extending spacecraft life. Two distinct power levels were envisioned for the JIMO mission: high power – thrusters operational, ~185 kWe load; low power – thrusters secured, lower voltage/lower frequency electrical power. Low power would include periods when science data is being collected and may require compensation for the angular momentum induced by the Brayton system on the spaceship. The simplest way to implement multiple operating modes would be to maintain speed and only reduce temperature (by reducing reactor power). However, this is most efficiently accomplished by a combination of speed control and temperature (power) reduction. Use of on/off control of Braytons and use of gas inventory control required increased system complexity and would not significantly improve performance. Reactor material performance may be affected by lowering of reactor temperatures and must also be considered.

- Reduced reliability results by adding spare Braytons in arrangements where 2 Braytons are already operating (3-3-3 and 4-4-4)

Design Space

- Cycle analysis shows that achieving a system performance within the originally envisioned design space is challenging. Limiting the heat rejection area to 450 $m^2$, while limiting maximum heat rejection heat pipe temperature to 500 K and the reactor coolant outlet temperature to 1150 K can only be achieved in plant configurations where one Brayton normally provides the total electrical output given the preliminary piping system arrangements and non-optimized plant conditions that have been developed thus far. Allowing some increase in converter loop piping diameter, radiator area, heat pipe temperature, or allowing less margin for reactor temperature uncertainty would be required for plant configurations where two or more Brayton units normally provide the total electrical output.

- A key driver to overall plant efficiency is the arrangement of the converter loop piping system and the resulting impact on piping system pressure drop. For plants with multiple converter

loops, flow splits in the reactor inlet and outlet headers and inclusion of valves become significant additions to the overall piping system pressure drop. Large diameter pipe, few valves, low pressure drops through components, simple pipe runs, and large gentle bend radii are required to minimize loop pressure drop. However, these considerations will need to be balanced against the need to make the plant sufficiently flexible to accommodate thermal transients and the need to make it fit within the available volume.

- Allowances for off-design parameters (e.g., temperatures and pressures) need to be allocated early in the conceptual phase of the project to account for component degradation over service life, transient performance, casualty recovery, instrument error, operating strategy, and associated operating bands.

Material Selection

- Use of refractory metal alloys for pressure boundary components were considered, but these alloys required substantial testing and development to mitigate inherent risks. Leading concerns included irradiation embrittlement, interstitial embrittlement from the absorption of working gas impurities and the integrity of dissimilar metal joints. Adequate protection from carbon and oxygen contamination would have required vacuum facilities exceeding those necessary for a nickel-base alloy pressure boundary. Similar complications would exist for extensibility to Lunar or Mars surface applications. Irradiation embrittlement would have made thermal cycling of a ground test unit difficult.

- Nickel-base superalloys were considered as leading candidate materials for the reactor vessel, loop piping, turbine, and heat exchangers. A large property, component manufacturing and performance database exists for Ni-base superalloys with the majority of the data obtained for air-breathing turbine engine applications. However, significant testing and development was required for the Prometheus design. Specific concerns were thermal creep, irradiation embrittlement for the pressure vessel, chemical interactions with the working gas and working gas impurities and the integrity of dissimilar metal joints.

- Demonstration of dissimilar metal joining feasibility, including cast to wrought nickel-base superalloys, wrought nickel-base superalloy to titanium alloys, wrought nickel-base superalloy to various refractory metal alloys, and possibly, stainless steel to titanium alloys will be required prior to the selection and specification of materials for all major system components. If dissimilar metal joints are required, development of a sound joint for the material pairs would be required.

- A thorough understanding of environmental degradation issues relevant to the application of all candidate material types in a common system, including the implications of the heat rejection system materials, must be obtained prior to selection and specification of materials for all major system components. Issues included potential degradation from the space vacuum, fission products, impurities in the working gas and the transport of impurities from one material to another in the common gas loop.

- Refractory metal and nickel-base alloys are not readily available in wrought forms such as seamless pipe and tubing. This may be critical to meeting schedule.

- To support the development and deployment of an SNPP, extensive material, component, and system testing had been planned. This testing would need to be a coordinated effort leading up to nuclear testing of a ground based prototype and non-nuclear testing integrated with the spaceship leading up to launch. The report for the Ground Test Reactor Facility (GTRF) for testing the prototype was transmitted by Reference 1-13. It should be noted that no final decision on the need for a GTRF or where it should be sited had been made; preliminary engineering work had started to support the NEPA process, establish scope, and meet the schedule. At the time of termination of NRPCT participation in Project Prometheus, the functional requirements for the facility were preliminary and had not yet been reviewed against federal requirements, peer reviewed, or approved by Naval Reactors.

Components

- The designs for major plant components (recuperator, gas cooler, Brayton turboalternator, valves, bearings, and piping) are within the bounds of current technology assuming non-refractory materials are used. Designing these components to be leak tight for the long life of the deep space missions remains a large development item.

- The largest turbine component design uncertainties are the scale-up of the turboalternator assembly for a single 200 kWe Brayton system and the ability of the turbine to operate for an extended lifetime in the service environment. Further rotor dynamic evaluations, bearing development and alternator cooling studies and testing would be needed.

- Reactor Module thermal management must be designed to reject sufficient heat from the hot components while maintaining other components at acceptable temperatures. This challenge is significantly complicated by the need to provide micrometeoroid protection and is somewhat complicated by the need to provide sufficient heat before start-up to maintain temperatures above low extremes. Identification and testing of materials, coatings, finishes, etc., will be needed to identify options that will satisfy requirements after prolonged exposure to radiation and temperature. Thermal management must be integrated with the power plant design and should be considered early in conceptual design.

- The interface of the heat transfer segment to the Reactor Module requires significant integration to resolve key tradeoffs for reducing mass, spacecraft size, and project risk. Key integration items include the heat transport loop coolant and ducting materials that interface with the gas cooler, start-up and normal operational strategy, radiator mass versus temperature capability, heat load capability, and size. Lifetime degradation in the radiator performance, due to changes in effective emissivity and isolated heat pipe failures will lead to a slow increase in radiator temperature. Continued research is required to understand high temperature water heat pipe performance (500 K) and life capability needed for this application operating at relatively high power throughput and evaporator surface heat flux (10 $W/cm^2$).

- A reactor operating in space may generate a significant electrical charge buildup on the spaceship. Actions will need to be taken to characterize, test and mitigate this effect to ensure spaceship operations aren't affected.

## References


**1- 1** NRPCT letter SPP-67110-0005, B-SE-0077 "Space Nuclear Power Plant (SNPP) Concept Recommendation for Prometheus 1 Space Craft for NR Action (U)", dated March 4, 2005

**1- 2** JPL Document 982-R120461, "Prometheus Project Final Report", dated October 1, 2005

**1- 3** JPL Document 982-00101, Rev. 0, "Prometheus Project Engineering Plan", dated July 15, 2005

**1- 4** NASA Document SA-0001, "Baseline, Level 0 Exploration Requirements for the National Aeronautics and Space Administration", dated May 4, 2004

**1- 5** NASA Document OExS-RQ-0-0003, "Baseline, Level 1 Jupiter Icy Moons Orbiter (JIMO) Requirements", dated May 18, 2004

**1- 6** JPL Document 982-00115, "Revision 2, Prometheus Project Multi-mission Project Derived Requirements", dated July 15, 2005

**1- 7** JPL Document 982-00116, "Revision 2, Prometheus Project JIMO Project Derived Requirements", dated July 15, 2005

**1- 8** JPL Document 982-00098, "Revision 0, Jupiter Icy Moons Orbiter Deep Space Vehicle Level 3 Key Driving Requirements", dated July 12, 2005

**1- 9** JPL Document 982-00029, "Revision 0, Prometheus Project Environmental Requirements Document", dated July 6, 2005

**1- 10** Enclosure 1 of KAPL/Bettis letter, SPP-67510-0020/B-SE-0091, "Responsibility Assignment Matrix (RAM)", dated April 2, 2005

**1- 11** KAPL letter SPP-67210-0008, "Space Nuclear Power Plant - List of Reactor Module Segments, for NR Approval", dated July 22, 2005

**1- 12** NR letter I#05-01228, "Space Nuclear Power - Reactor Coolant and Power Conversion System Concept - Approval of", dated April 20, 2005

**1- 13** Bettis letter B-SE(SPS)GT-005, "Space Nuclear Power Plant – Ground Test Reactor Facility Planning Closeout Report – For Information," dated December 13, 2005

# Section 2
# Plant Parameter List

(Intentionally Blank)

# Plant Parameter List

## Table of Contents

2 Plant Parameter List ..... 5
2.1 Introduction ..... 5
2.2 Overview – Prometheus Pre-Conceptual Plant Parameter List ..... 5
2.3 Overview – Instrumentation and Control Parameter List ..... 5

## List of Tables

Table 2-1: Prometheus Pre-Conceptual Plant Parameters ..... 8
Table 2-2: Parameter Justification and References ..... 11
Table 2-3: Prometheus Pre-Conceptual Instrumentation and Control Parameters ..... 14
Table 2-4: Prometheus Pre-Conceptual Instrumentation and Control Parameters References and Justifications ..... 16

(Intentionally Blank)

# 2 Plant Parameter List

## 2.1 Introduction

The purpose of the pre-conceptual plant parameter and instrumentation and control (I&C) parameter lists was to provide a common set of design parameters used by the Naval Reactors Prime Contractor Team (NRPCT) for preconceptual evaluation of Space Nuclear Power Plant (SNPP) concepts.

## 2.2 Overview – Prometheus Pre-Conceptual Plant Parameter List

The Prometheus Preconceptual Plant Parameter List, Table 2-1, contains a listing of basic parameters and a corresponding range of values, designated "Range/Options", to be considered in integrated plant trade studies and other preconceptual design efforts. Parameters are grouped by the component to which they pertain. The range of values identified for each parameter is considered to envelope the parameter's design space for full power operation. Additional information related to the parameters, reference documents, and bases of values is provided in Table 2-2.

The preliminary plant parameter list includes a column of values, designated "A set of common parameters", which, when taken together, satisfy a system heat balance. It should not be inferred that the values given in this column were identified as optimal values for any particular plant configuration. These values are provided only to illustrate the interrelationship of the parameters.

Values in the "Reduced Electrical Power Range/Options" column represent ranges of values to evaluate reduced power operations. One JIMO level 2 requirement, from JPL Document 982-00115, "Revision 2, Prometheus Project Multi-mission Project Derived Requirements", dated July 15, 2005, is the project shall use a nuclear reactor whose thermal power output is adjustable to allow long-term operation at any reactor level down to the minimum of full power output required to support the minimum required electrical power. A reduced power mode may be used when electrical demand is reduced for long periods of time. The period of reduced electric demand may allow reactor power and/or temperature to be reduced, which allows fuel and clad temperature reduction (increased creep life) and burn up reduction (increased core life). The reduced power options are further discussed in Section 8, "Operational Strategy".

All design values were notional and a range of values were being evaluated. These values were based on preliminary functional requirements and objectives provided by NASA-JPL. For all of the key driving requirements, future trade studies would have been performed to obtain reactor and reactor plant requirements and constraints.

## 2.3 Overview – Instrumentation and Control Parameter List

The Prometheus Preconceptual I&C Parameter List Table 2-3 presents the plant parameters being considered for operation of the space nuclear power plant (SNPP). These parameters would be measured by sensing elements of the I&C system and used in the monitoring, control, and calibration processes associated with the continuous operation of the plant. The tabulation evaluates each of the plant parameters selected for measurement and, based upon the best sensing technologies identified in B-SE(SPS)IC-008, NRPCT Closeout of Prometheus Sensor Development Work for NR Information,

dated December 21, 2005, identifies the fundamental requirements for these measurements. These criteria were developed to support the design and development of the SNPP and its components.

Reactor plant operations demand sufficient sensors and instrumentation to provide for the control and monitoring of the reactor for all the modes of plant operation. These modes include:

- Startup
- Constant power operation (steady state power operation)
- Power transitions
- Casualty Operations
- Maintenance and Testing Operations
- Shutdown

These operations must successfully function under nominal as well as off-nominal conditions. To provide for all these conceivable situations a sufficiently diverse set of reactor plant instrumentation is required to ensure the control actions taken by the instrumentation and control (I&C) system are consistent with the actual state of the plant.

For the space reactor plant in particular, the requirements and conditions are exceptionally severe and demanding, namely, the harsh temperature and radiation environment, ~15 year lifetime, and high accuracy. A minimum sensor suite consisting of a diverse set of sensor capabilities and failure modes is desirable at this stage of the program since it is not clear that sensors will be found for all the desired locations and functions. Moreover, a reactor plant final design has not yet been determined, including the number of turbo-alternators (1, 2, 3,or 4), reactor coolant makeup system, the method of reactor control (slider or drum), and the methods of plant control (Brayton speed, voltage, current, load). At the pre-conceptual phase the controls for the reactor plant could be based one or more of the following parameters:

- Reactor power, temperature, pressure, flux, and / or control element position
- Brayton speed, electrical load, coolant flow, alternator and / or parasitic load radiator power, voltage, current
- Heat rejection temperature, flow rate, or pressure
- Pressure or coolant inventory

All of these considerations suggest that at the pre-conceptual phase of the space reactor design effort *a diverse set of reactor primary sensors be pursued to ensure that the parameters necessary for all* the operations of the final plant are ultimately provided. The fundamental set of parameters considered necessary for reactor plant operation and monitoring are listed in Table 2-3. For each plant parameter, its nominal value and the characteristics of the sensor necessary to measure it are identified. The pre-conceptual nominal value is the parameter value identified in the four loop non-optimized Brayton system of Section 6. The sensor qualities represent the most capable technology for the measurement based on the sensor studies of B-SE(SPS)IC-008, NRPCT Closeout of Prometheus Sensor Development Work for NR Information, dated December 21, 2005. For example, the reactor outlet temperature measurement assumes the use of sapphire Fiber Bragg Grating (FBG) thermometry; the reactor coolant flow assumes an ultrasonic time-of-transit flowmeter. For these sensors, the typical accuracy, resolution, and time response of the technology are used to characterize the quality of the parameter measurement. The operational range considers all the various plant operations for which the sensor may be applied and identifies the range of values associated with these operations accordingly. The accuracy of a sensor measurement represents the

ability of the sensor output to match the absolute value of the actual parameter. The resolution represents the finest increment that the sensing system can differentiate. Both of these metrics are based on the range of parameter measurement unless otherwise indicated. The response time of the sensing system represents the time it requires to respond to a step change in the parameter and accurately represent its final value. The related reference information and justifications for the various criteria of the I&C parameters are provided in Table 2-4.

**Table 2-1: Prometheus Pre-Conceptual Plant Parameters**

| Section | Parameter | Range/Options | A Set of Common Parameters | Reduced Electric Power Range/Options |
|---|---|---|---|---|
| | Mission Duration | 10-20 years | 15 years | |
| **I. Reactor** | | | | |
| | Core Energy | 10-20 Full Power Years | 15 Full Power Years | |
| | Nominal Core Thermal Power | 0.5-1.5 MWt | 1000 kWt | |
| | Reactor Inlet Temperature | 810-935 K (998-1160°F) | 911 K (1144°F) | 685-935 K (773-1160°F) |
| | Reactor Outlet Temperature | 1050-1200 K (1430-1700°F) | 1150 K (1610°F) | 872-1200 K (1110-1700°F) |
| | Number of Reactor Inlet Nozzles | 1-2 | 1 | |
| | Number of Reactor Outlet Nozzles | 1-2 | 1 | |
| | Reactor Nozzle-to-Nozzle Pressure Drop (dP/P) | 2.0-4.0% | 2.5% | |
| | Gas Molecular Weight | 20-45 g/mol<br>(He mole fraction = 0.874 - 0.560) | 31.5 g/mol<br>(He mole fraction = 0.784) | |
| **II. Shield** | | | | |
| | Pipe Outer Diameter | TBD | 16 cm | |
| | Number of Shield Penetrations for Piping | 1-4 | 2 | |
| | Number of Shield Penetrations for CDM | 6-18 | 12 | |
| | Payload Rx Neutron (DDD) | TBD | 5E10 n/cm2 | |
| | Rx Gamma (TID) | TBD | 25 kRad Si Damage | |
| | Behind Shield Rx + Space Neutron (DDD) | TBD | TBD | |
| | Rx + Space Gamma (TID) | TBD | 0.5 GRad Si Damage | |
| **III. Braytons** | | | | |
| | Number of Braytons | 4 (2 op at 100% capacity, 2 spare)<br>3 (2 op at 100% capacity, 1 spare)<br>3 (3 op at 66% capacity)<br>2 (2 op at 50% capacity)<br>2 (1 op at 100% capacity, 1 spare)<br>1 (1 op at 100% capacity) | 4 (2 op at 100% capacity, 2 spare) | |
| | Brayton Shaft Speed | 30000-75000 rpm | 45000 rpm | 24000-75000 rpm |
| | Power delivered from alternator | 97.0 -110 kWe per Brayton for 3 & 4 loop systems<br>195-220 kWe per Brayton for 1 & 2 loop systems | 97.0 kWe per Brayton<br>193.9 kWe Total | 45-220 kWe |
| | Compressor Outlet Pressure | 1380-4000 kPa (200-580psi) | 2000 kPa (290psi) | 800-4000 kPa (58-580psi) |

| Section | Parameter | Range/Options | A Set of Common Parameters | Reduced Electric Power Range/Options |
|---|---|---|---|---|
| | Compressor Inlet Temperature | 350-450 K (170-350°F) | 390 K (242°F) | |
| | Compressor Pressure Ratio | 1.8-2.2 | 2.0 | |
| **III, Braytons continued** | Converter Loop Pipe Outer Diameter | 10-16 cm (3.9-6.3 in) | 10 cm (3.9 in) | |
| | Alternator Loop Pipe Outer Diameter | TBD | 5 cm (2 in) | |
| **IV. Valves** | | | | |
| | Isolation Valves | 1 at Turbine Outlet<br>1 at Compressor Inlet<br>1 at Compressor Outlet<br>1 at Low Pressure Recuperator Outlet 1 Alternator Bleed Flow Outlet | 1 at Compressor Outlet | |
| | Check Valves | 1 at Compressor Inlet<br>1 at Compressor Outlet<br>1 at Alternator Bleed Flow Outlet | 1 at Compressor Outlet | |
| **V. Recuperator** | | | | |
| | Number of Recuperators | 1-4 | 4 | |
| | High Pressure side of Recuperator dP/P | 0.5-1.5% | 0.8% | |
| | Low Pressure side of Recuperator dP/P | 1.0-3.0% | 1.5% | |
| | Recuperator effectiveness | 0.86-0.94 | 0.92 | |
| **VI. Gas Cooler** | | | | |
| | Number of Gas Coolers | 1-4 | 4 | |
| | Gas Side of Gas Cooler dP/P | 0.5-1.5% | 1.0% | |
| | Pressure Drop in HRS Side of Gas Cooler | | 25 kPa (3.6 psi) | |
| | Gas Cooler effectiveness | 0.90-0.96 | 0.94 | |
| **VII. Radiator** | | | | |
| | Heat Rejection System Fluid | Water, NaK | Water | |
| | Two-Sided Radiator Area with 14.5% Margin | 400-650 $m^2$ (4300 - 7000$ft^2$) | 450 $m^2$ (4840 $ft^2$) | |
| | Inlet Coolant Temperature | 485-530 K (413-494°F) | 505K (449°F) | |
| | Emissivity | 0.75-0.95 | 0.9 | |
| | HRS Operating Pressure | 5-11 MPa (725 - 1595 psi) | 7.8 MPa (1130 psi) | |
| | Pressure Drop in Loop | 100-400 kPa (15-58 psi) | 365 kPa (53 psi) | |
| | Number of Loops | 1-4 | 4 | |

| Section | Parameter | Range/Options | A Set of Common Parameters | Reduced Electric Power Range/Options |
|---|---|---|---|---|
| | Number of Pumps per Loop | 1-2 | 2 | |

**Table 2-2: Parameter Justification and References**

| Section | Parameter | Justification and References |
|---|---|---|
| | Mission Duration | Jupiter Icy Moons Orbiter (JIMO) mission duration is 12 years. The multi-mission duration is 20 years, and applies to subsequent missions. To meet these NASA requirements, the reactor should be designed to support an initial operating life of 12-15 years, with subsequent missions of increasing duration, up to 20 years. Based on JPL document 982-00116, revision 2, Prometheus Project JIMO Project Derived Requirements, dated July 15, 2005 and JPL document 982-00115, revision 2, Prometheus Project Multi-mission Project Derived Requirements, dated July 15, 2005. |
| **I. Reactor** | | |
| | Core Energy | 15 full power years is a simplifying assumption used for initial concept comparisons. It approximates to 10 years total thrust (full power) time and 10 years reduced power (~50% power) for a 20 year mission. Based on JPL Document 982-00115, "Revision 2, Prometheus Project Multi-mission Project Derived Requirements", dated July 15, 2005. |
| | Nominal Core Thermal Power | The Pre-Conceptual Base Case value does not include uncertainties associated with plant operating band. Based on 4 Brayton case SNPP Heat Balance Section 6. |
| | Reactor Inlet Temperature | Based on SNPP Heat Balance Section 6 and consistent with Reactor Pre-conceptual Design Report (SPP-67410-0013/B-SE(RE)-0003, dated January 27, 2006). |
| | Reactor Outlet Temperature | Consistent with industry practice for current materials used in turbine assembly. Based on SNPP Heat Balance Section 6 and consistent with Reactor Pre-conceptual Design Report (SPP-67410-0013/B-SE(RE)-0003, dated January 27, 2006). |
| | Number of Reactor Inlet Nozzles | Based on SNPP Heat Balance Section 6 and consistent with Reactor Pre-conceptual Design Report (SPP-67410-0013/B-SE(RE)-0003, dated January 27, 2006). |
| | Number of Reactor Outlet Nozzles | Based on SNPP Heat Balance Section 6 and consistent with Reactor Pre-conceptual Design Report (SPP-67410-0013/B-SE(RE)-0003, dated January 27, 2006). |
| | Reactor Nozzle-to-Nozzle Pressure Drop (dP/P) | Indicates fraction of inlet pressures. Based on an evaluation envelope to include many reactor pressure boundary designs from the SNPP Heat Balance Section 6. |
| | Gas Molecular Weight | Gas being assumed as coolant is a mixture of Helium Xenon. Considered a benign, single-phase coolant to achieve high efficient energy conversion with a low activation energy. Molecular weight based on past JIMO trade studies. Based on heat balance Section 6. |
| **II. Shield** | | |
| | Pipe Outer Diameter | Based on preliminary radiation study to decrease radiation streaming through the shield by turning or spiraling the pipe through the edge of a shield initially assumed to be 55 cm thick. Space Reactor Shield Design Summary (SPP-67210-0011). |
| | Number of Shield Penetrations for piping | Does not include control drive mechanism penetration or instrumentation wiring. Assumed one hot leg pipe and one cold leg pipe, for limiting shield penetration and radiation streaming. Space Reactor Shield Design Summary (SPP-67210-0011). |

| Section | Parameter | Justification and References |
|---|---|---|
| | Number of Shield Penetrations for CDM | Does not include piping penetration or instrumentation wiring. Reactor studies have used 12 as a base case for reactivity controls with sensitivities resulting in more reactivity controllers to decrease the space envelope of the reactor. Reactor Pre-conceptual Design Report (SPP-67410-0013/B-SE(RE)-0003, dated January 27, 2006), Shielding Pre-conceptual Design Report (SPP-67210-0011). |
| | Payload Rx Neutron (DDD) | Displacement Damage Dose (DDD) based on JPL document 982-00029, Prometheus Project Environmental Requirements Document, dated July 6, 2005. |
| | Rx Gamma (TID) | Total Ionizing Dose (TID) based on JPL document 982-00029, Prometheus Project Environmental Requirements Document, dated July 6, 2005. |
| | Behind Shield Rx + Space Neutron (DDD) | Displacement Damage Dose (DDD) based on the limiting radiation dose to materials just behind the shield. |
| | Rx + Space Gamma (TID) | Total Ionizing Dose (TID) based on the limiting radiation dose to materials just behind the shield by current standards; the most limiting dose was due to cabling and wiring. |
| **III. Braytons** | | |
| | Number of Braytons | Four converters were originally selected as a comparison basis when other concepts were being evaluated with a range of 1 to 4 converters. Based on SNPP Heat Balance Section 6 and System Architecture Section 3. |
| | Brayton Shaft Speed | Based on SNPP Heat Balance Section 6 and Brayton Turboalternator Section 9.1. |
| | Power delivered from alternator | Alternator output required to meet spaceship electrical power needs, including propulsion, engineering, and science loads. Based on [(130 kW thrusters output/0.72 Electric Propulsion efficiency) + 5 kWe (Vehicle operation)]/ 0.95 PMAD efficiency = 195 ~200 kWe and on JPL document 982-00115, revision 2, Prometheus Project Multi-mission Project Derived Requirements, dated July 15, 2005. |
| | Compressor Outlet Pressure | Originally set based on coolant selection and system optimization from past JIMO trade studies. Based on SNPP Heat Balance Section 6 and Brayton Turboalternator Section 9.1. |
| | Compressor Inlet Temperature | Decreasing compressor inlet temperature increases cycle efficiencies. Based on SNPP Heat Balance Section 6 and Brayton Turboalternator Section 9.1. |
| | Compressor Pressure Ratio | Based on SNPP Heat Balance Section 6 and Brayton Turboalternator Section 9.1. |
| | Converter Loop Pipe Outer Diameter | Based on SNPP Heat Balance Section 6 and Piping Section 9.4. |
| | Alternator Loop Pipe Outer Diameter | Based on SNPP Heat Balance Section 6 and Piping Section 9.4. |
| **IV. Valves** | | |
| | Isolation Valves | Based on minimizing pressure drops and temperatures; Heat Balance Section 6. |
| | Check Valves | Based on minimizing pressure drops and temperatures; Heat Balance Section 6. |
| **V. Recuperator** | | |
| | Number of Recuperators | Four converters were originally selected as a comparison basis when other concepts were |

| | | |
|---|---|---|
| | | being evaluated. Based on SNPP Heat Balance Section 6 and System Architecture Section 3. |
| **Section** | **Parameter** | **Justification and References** |
| | High Pressure side of Recuperator dP/P | Indicates fraction of inlet pressures. Based on heat balance in section 6 and Recuperator Section 9.2 |
| | Low Pressure side of Recuperator dP/P | Indicates fraction of inlet pressures. Based on heat balance in section 6 and Recuperator Section 9.2. |
| | Recuperator effectiveness | Based on heat balance in section 6 and Recuperator Section 9.2. |
| **VI. Gas Cooler** | | |
| | Number of Gas Coolers | Four converters were originally selected as a comparison basis when other concepts were being evaluated. Based on SNPP Heat Balance Section 6 and System Architecture Section 3. |
| | Gas Side of Gas Cooler dP/P | Indicated fraction of inlet pressure. Based on heat balance in section 6 and Gas Cooler section 9.3. |
| | Pressure Drop in HRS Side of Gas Cooler | Based on heat balance in section 6 and Gas Cooler section 9.3. |
| | Gas Cooler effectiveness | Based on heat balance in section 6 and Gas Cooler section 9.3. |
| **VII. Radiator** | | Northrop Grumman Space Technology (NGST) was the Heat Rejection System (HRS) design agent. |
| | Heat Rejection System Fluid | Based on SPP-67310-0009 and NGST Prometheus Spacecraft Module and Subcontractor-provided Reactor Module Segment Design Description Report, SDRL SE-002-001. |
| | Two-Sided Radiator Area with 14.5% Margin | This is an objective not a requirement. Further trades would be required for radiator area and temperature. Current heat balances (section 6) show radiator areas up to 626 $m^2$ for a 200kWe power system. Based on NGST Prometheus Spacecraft Module and Subcontractor-provided Reactor Module Segment Design Description Report, SDRL SE-002-001. |
| | Inlet Coolant Temperature | This is an objective not a requirement. Further trades would be required for radiator area and temperature. Based on Heat Balance Section 6, Heat Rejection System Section 9.6, and NGST Prometheus Spacecraft Module and Subcontractor-provided Reactor Module Segment Design Description Report, SDRL SE-002-001. |
| | Emissivity | Based on NGST Prometheus Spacecraft Module and Subcontractor-provided Reactor Module Segment Design Description Report, SDRL SE-002-001. |
| | HRS Operating Pressure | Assumes HRS coolant is water. Based on SPP-67310-0009. |
| | Pressure Drop in Loop | Based on Heat Balance Section 6 and NGST Prometheus Spacecraft Module and Sub-contractor-provided Reactor Module Segment Design Description Report, SDRL SE-002-001. |
| | Number of Loops | Based on HRS Section 9.6 and NGST Prometheus Spacecraft Module and Subcontractor-provided Reactor Module Segment Design Description Report, SDRL SE-002-001. |
| | Number of Pumps per Loop | Based on HRS Section 9.6 and NGST Prometheus Spacecraft Module and Subcontractor-provided Reactor Module Segment Design Description Report, SDRL SE-002-001. |

**Table 2-3: Prometheus Pre-Conceptual Instrumentation and Control Parameters**

| Section | Parameter | Nominal Value | Range | Accuracy | Resolution | Response Time |
|---|---|---|---|---|---|---|
| **I. Reactor** | | | | | | |
| | Outlet Temperature | 1150 K | 250-1280 K | ±5 K | 1 K | 10 sec. |
| | Inlet Temperature | 911 K | 250-1000 K | ±4 K | 1 K | 10 sec. |
| | Wide Range Flux Based Power | 100% | $10^{-9}$ - $2x10^{2}$ % | ±1% of point | 0.5% of point | 1 sec. |
| **II. Compressor** | Outlet Pressure | 2000 kPa | 0 kPa-2200 kPa | ±45 kPa | 9 kPa | 1 sec. |
| | Outlet Volumetric Flow | 0.15 $m^3$/sec | 0.01-1 $m^3$/sec | ±0.0025 $m^3$/sec | 0.0025 $m^3$/sec | 1 sec. |
| | Outlet Temperature | 538 K | 250-600 K | ±2 K | 1 K | 10 sec. |
| | Inlet Temperature | 390 K | 250-460 K | ±1 K | 1 K | 10 sec. |
| **III. Recuperator** | Inlet Temperature [Turbine Outlet] | 943 K | 250-1040 K | ±5 K | 1 K | 10 sec |
| **IV. Gas Cooler** | Inlet Temperature [Recupertor Outlet] | 559 K | 250-630 K | ±2 K | 1 K | 10 sec |
| **V. Alternator** | Bleed Temperature | 456 K | 250-510 K | ±1.2 K | 1 K | 10 sec |
| **VI. Reactor Control** | | | | | | |
| **Slider Position** | Continuous Position | Actual position | 0-45 cm | ±0.05 cm | 0.005 cm | 1 sec |
| | Discrete Position 1 | Stowed for Launch | Fixed: Full Out | ±0.05 cm of point | 0.005 cm of point | 0.001 sec |
| | Discrete Position 2 | Edge of Core Region | Fixed: Initial Position | ±0.05 cm of point | 0.005 cm of point | 0.001 sec |
| | Discrete Position 3 | Near Critical Position | Fixed: Mid-Position | ±0.05 of point | 0.005 of point | 0.001 sec |
| **Drum Position** | Continuous Position | Actual position | 0-360 deg | ±0.1 deg | 0.1 deg | 1 sec |
| | Discrete Position 1 | Stowed for Launch | Fixed: Full Out | ±0.1 deg of point | 0.1 deg of point | 0.001 sec |
| | Discrete Position 2 | Edge of Core Region | Fixed: Initial Position | ±0.1 deg of point | 0.1 deg of point | 0.001 sec |
| | Discrete Position 3 | Near Critical Position | Fixed: Mid-Position | ±0.1 deg of point | 0.1 deg of point | 0.001 sec |
| **Safety Rod** | Discrete Position | Full In | Full In - Full Out | ±0.05 cm of point | 0.005 cm of point | 0.001 sec |
| | Discrete Position | Full Out | Full In - Full Out | ±0.05 cm of point | 0.005 cm of point | 0.001 sec |
| **VII. Valves** | | | | | | |
| **Valve Position** | Sensor 1 | Assert: Valve open<br>Deassert: Valve shut | Open | 0.1% of point | 0.01% of point | 0.001 sec |
| | Sensor 2 | Deassert: Valve open<br>Assert: Valve shut | Shut | 0.1% of point | 0.01% of point | 0.001 sec |
| **VIII. PCAD** | | | | | | |
| **Alternator** | Voltage | 450 V RMS L-L | 0 – 500 V | ±0.5 V | 0.1 V | 1 sec |
| | Current | 128 A | 0 – 150 A | ±0.15 A | 0.03 A | 1 sec |
| | Frequency (Brayton Speed) | 2250 Hz (45000 RPM) | 450-2475 Hz (9000-50000 RPM) | ±0.225 Hz (±4.5 RPM) | 0.1 Hz (2.0 RPM) | 1 sec |
| | Power [Single Alternator] | 97.0 kWe | 0 - 110 kWe | ±0.2 kWe | 0.03 kWe | 1 sec |
| | Total Power [Two Alternators] | 193.9 kWe | 0 - 220 kWe | ±0.4 kWe | 0.06 kWe | 1 sec |

| Section | Parameter | Nominal Value | Range | Accuracy | Resolution | Response Time |
|---|---|---|---|---|---|---|
| Start Inverter | Voltage | 135 V RMS L-L | 0 – 150 V | ±0.15 V | 0.01 V | 1 sec |
| | Current | 13 A | 0 – 15 A | ±0.015 A | 0.003 A | 1 sec |
| | Frequency (Brayton Speed) | 675 Hz (13,500 RPM) | 125-750 Hz (2750-15000 RPM) | ±0.07 Hz (±1.5 RPM) | 0.03 Hz (0.75 RPM) | 1 sec |
| | Power | 2.7 kWe | 0 – 5 kWe | ±0.01 kWe | 0.001 kWe | 1 sec |
| Parasitic Load Radiator (PLR) | Voltage | 450 V RMS L-L | 0 – 500 V | ±0.5 V | 0.1 V | 1 sec |
| | Current | 135 A | 0 – 150 A | ±0.15 A | 0.03 A | 1 sec |
| | Power | 103 kWe | 0 – 110 kWe | ±0.2 kWe | 0.03 kWe | 1 sec |
| IX. Radiator | | | | | | |
| | Pump Speed (Multispeed) | TBD | TBD | NA | NA | NA |
| | Water Flow | 600 $cm^3/s$ | 10-1000 $cm^3/s$ | ±20 $cm^3/s$ | 10 $cm^3/s$ | 1 sec |
| | Inlet Temperature | 505 K | 250-570 K | ±3.0 K | 1.5 K | 10 sec |
| | Outlet Temperature | 379 K | 250- 430 K | ±2.0 K | 1.0 K | 10 sec |

**Table 2-4: Prometheus Pre-Conceptual Instrumentation and Control Parameters References and Justifications**

| Section | Parameter | Justification and References |
|---|---|---|
| I. Reactor | | |
| | Outlet Temperature | The reactor outlet temperature 1150 K is the nominal value for the four loop non-optimized Brayton system of Section 6. The range 250-1280 K assumes the plant maintains temperature not below 250 K, a ±10 K control band for reactor operation at full power, the stated accuracy of ±0.5% and a 10% uncertainty for transient performance due to casualty or maneuvering. The number is rounded.<br><br>The accuracy ±5K is ±0.5% of the baseline operating range. Accuracy value typifies high precision, high temperature FBG sensor with digital instrumentation.<br><br>The resolution of 1 K is a factor 5 times finer than the absolute accuracy. The sensor signal is continuous; the associated signal processing circuitry must be capable of resolving it sufficiently to achieve the resolution.<br><br>The time constant of 10 seconds typifies the response of a high precision sensor including its thermal and instrumentation response. |
| | Inlet Temperature | The reactor inlet temperature 911 K is the nominal value for the four loop non-optimized Brayton system of Section 6. The range 250-1000 K assumes the plant maintains temperature not below 250 K , a ±10 K control band for reactor operation at full power, the stated accuracy ±0.5% and 10% uncertainty for transient performance due to casualty or maneuvering. The number is rounded.<br><br>The accuracy ±4K is ±0.5% of the baseline operating range. Accuracy value typifies high precision, high temperature FBG sensor with digital instrumentation.<br><br>The resolution of 1 K is a factor 4 times finer than the absolute accuracy. The sensor signal is continuous; the associated signal processing circuitry must be capable of resolving it sufficiently to achieve the resolution.<br><br>The time constant of 10 seconds typifies the response of a high precision sensor including its thermal and instrumentation response. |
| | Wide Range<br>Flux Based Power | The single wide range nuclear detector has been pursued for the SNPP to minimize the number and types of detectors. It would cover a range of power from $1x10^{-9}$ % to $2x10^{2}$ %, ~11decades, to monitor reactor operations from initial startup to full power. Fission counter technology is capable of this wide range performance assuming it is located near the reactor fore of the shield and in the radiation shield nearest the reactor.<br><br>The nuclear instrumentation for the wide range detector must be a logarithmic instrument. For this reason its accuracy of ±1% is defined on a percent of point basis. Accuracy and resolution reflect the typical capabilities of a high precision, digital nuclear instrument.<br><br>The nuclear detector and its associated instrumentation is generally characterized by a rapid response time of the order of 1 second or less over most of the anticipated range. |

| Section | Parameter | Justification and References |
|---|---|---|
| **II. Compressor** | Outlet Pressure | The nominal compressor outlet pressure 2000kPa value for the four loop non-optimized Brayton system of Section 6 is assumed.<br><br>The range of the pressure detector 0-2200 assumes a detector technology capable of sensing 0 kPa and a maximum value approximately 110% of the nominal value allowing for uncertainty and transient plant performance.<br><br>The accuracy of ±45 kPa is based on a typical commercial pressure detector capability of 2% of the operating range. Assumes a 2% accuracy over operation range.<br><br>The resolution of 9 kPa is 5 times finer than the absolute accuracy.<br><br>The 1 second time response typifies a high precision pressure sensor with digital instrumentation. |
| | Outlet Volumetric Flow | The nominal volumetric flow of 0.15 $m^3$/sec (corresponding to a mass flow of 3.08 kg/sec) for the four loop non-optimized Brayton system of Section 6 is assumed.<br><br>The range 0.01-1 $m^3$/sec has been selected to cover a sufficiently wide range of operation to provide for plant startup at reduced flows, full power operation, and casualty performance.<br><br>The accuracy of ±0.0025 $m^3$/sec typifies the accuracy of 0.25% of point found in gas industry ultrasonic flow metering equipment.<br><br>The time constant of 1 second typifies high precision pressure sensor with digital instrumentation. |
| | Outlet Temperature | The nominal compressor outlet temperature 538 K for the four loop non-optimized Brayton system of Section 6 is assumed.<br><br>The range 250-600 K assumes the plant maintains temperature not below 250 K, a ±10 K control band for reactor operation at full power, the stated accuracy of ±0.5%, and a 10% uncertainty for transient performance due to casualty or maneuvering. The number is rounded.<br><br>The accuracy ±2 K is ±0.5% of the baseline operating range. Accuracy value typifies high precision, high temperature FBG or RTD sensor with digital instrumentation.<br><br>The resolution of 1 K is a factor 2 times finer than the absolute accuracy. The sensor signal is continuous; the associated signal processing circuitry must be capable of resolving it sufficiently to achieve the resolution.<br><br>The time constant of 10 seconds typifies the response of a high precision temperature sensor including its thermal and instrumentation response. |

| Section | Parameter | Justification and References |
|---|---|---|
| | Inlet Temperature | The nominal compressor inlet temperature 390 K for the four loop non-optimized Brayton system of Section 6 is assumed.<br><br>The range 250-460 K assumes the plant maintains temperature not below 250 K, a ±10 K control band for reactor operation at full power, the stated accuracy of ±0.5%, and a 10% uncertainty for transient performance due to casualty or maneuvering. The number is rounded.<br><br>The accuracy ±1 K is ±0.5% of the baseline operating range. Accuracy value typifies high precision, high temperature FBG or RTD sensor with digital instrumentation.<br><br>The resolution of 1 K equals the absolute accuracy. The sensor signal is continuous; the associated signal processing circuitry must be capable of resolving it sufficiently to achieve the resolution.<br><br>The time constant of 10 seconds typifies the response of a high precision temperature sensor including its thermal and instrumentation response. |
| **III. Recuperator** | Inlet Temperature | The nominal recuperator inlet temperature 943 K for the four loop non-optimized Brayton system of Section 6 is assumed.<br><br>The range 250-1040 K assumes the plant maintains temperature not below 250 K, a ±10 K control band for reactor operation at full power, the stated accuracy of ±0.5%, and a 10% uncertainty for transient performance due to casualty or maneuvering. The number is rounded.<br><br>The accuracy ±5 K is ±0.5% of the baseline operating range. Accuracy value typifies high precision, high temperature FBG or RTD sensor with digital instrumentation.<br><br>The resolution of 1 K is a factor of 5 times finer than the absolute accuracy. The sensor signal is continuous; the associated signal processing circuitry must be capable of resolving it sufficiently to achieve the resolution.<br><br>The time constant of 10 seconds typifies the response of a high precision temperature sensor including its thermal and instrumentation response. |
| **IV. Gas Cooler** | Inlet Temperature | The nominal gas cooler inlet temperature 559 K for the four loop non-optimized Brayton system of Section 6 is assumed.<br><br>The range 250-630 K assumes the plant maintains temperature not below 250 K, a ±10 K control band for reactor operation at full power, the stated accuracy of ±0.5%, and a 10% uncertainty for transient performance due to casualty or maneuvering. The number is rounded.<br><br>The accuracy ±2 K is ±0.5% of the baseline operating range. Accuracy value typifies high precision, high temperature FBG or RTD sensor with digital instrumentation. |

| Section | Parameter | Justification and References |
|---|---|---|
| | | The resolution of 1 K is a factor of 2 times finer than the absolute accuracy. The sensor signal is continuous; the associated signal processing circuitry must be capable of resolving it sufficiently to achieve the resolution.<br><br>The time constant of 10 seconds typifies the response of a high precision temperature sensor including its thermal and instrumentation response. |
| **V. Alternator** | Bleed Temperature | The nominal alternator bleed temperature 456 K for a non-optimized single loop Brayton architecture and heat balance is assumed.<br><br>The range 250-510 K assumes the plant maintains temperature not below 250 K, a ±10 K control band for reactor operation at full power, the stated accuracy of ±0.5%, and a 10% uncertainty for transient performance due to casualty or maneuvering. The number is rounded.<br>The accuracy ±1.2 K is ±0.5% of the baseline operating range. Accuracy value typifies high precision, high temperature FBG or RTD sensor with digital instrumentation.<br><br>The resolution of 1 K is a factor 1.2 times finer than the absolute accuracy. The sensor signal is continuous; the associated signal processing circuitry must be capable of resolving it sufficiently to achieve the resolution.<br><br>The time constant of 10 seconds typifies the response of a high precision temperature sensor including its thermal and instrumentation response. |
| **VI. Reactor Control** | | |
| **Slider Position** | Continuous Position | Each reactivity control slider will have a position sensing device that measures its actual realtime absolute location. The slider for the SNPP reactors is characterized by a linear movement over a range from 0 to 45 cm.<br><br>Based on the slider range and its step size of 0.1 cm, an accuracy of ±0.05 cm equal to 0.1% of range has been chosen. This accuracy is typical of position indication technologies such as LVDT and ultrasonic devices used for this application.<br><br>A resolution of 0.005 cm has been chosen, 10 times finer than the absolute accuracy to ensure any movement of the slider is identified. For continuous signal position detector technologies like LVDT and ultrasonic devices, the associated signal processing circuitry must be capable of resolving the signal sufficiently to achieve the resolution.<br><br>The time constant of 1 second typifies the response of a high precision position sensor including its sensor and instrumentation response. |

| Section | Parameter | Justification and References |
|---|---|---|
| | Discrete Position 1 | One discrete position sensor is considered required for monitoring the slider in its stowed position prior to launch and operation of the SNPP reactor. It is a fixed position sensor that confirms the slider in the fully withdrawn position. Photo, proximity, and microswitch technologies are typically applied as discrete position sensors. An accuracy of ±0.05 cm of point and resolution of 0.005 cm of point for the sensor equal to that of continuous position sensor is readily achievable. A response time of 0.001 seconds is common for these discrete position technologies. |
| | Discrete Position 2 | One discrete position sensor is considered required for monitoring the slider at the boundary of the active core region if this position is different from its stowed location. As initial critical operations commence, this sensor may be used as an interlock or confirmation of the continuous position. Photo, proximity, and microswitch technologies are typically applied as discrete position sensors. An accuracy of ±0.05 cm of point and resolution of 0.005 cm of point for the sensor equal to that of continuous position sensor is readily achievable. A response time of 0.001 seconds is common for these discrete position technologies.. |
| | Discrete Position 3 | One discrete position sensor is considered required for monitoring the slider near its expected critical position. This sensor may be used as an interlock or confirmation of the continuous position. Photo, proximity, and microswitch technologies are typically applied as discrete position sensors. An accuracy of ±0.05 cm of point and resolution of 0.005 cm of point for the sensor equal to that of continuous position sensor is readily achievable. A response time of 0.001 seconds is common for these discrete position technologies. |
| **Drum Position** | Continuous Position | Each reactivity control drum will have a position sensing device that measures its actual realtime absolute location. The drum for the SNPP reactors is characterized by a rotary movement over a range from 0 to 360 degrees.<br><br>An accuracy and resolution of ±0.1 degrees equal to 0.03% of range has been selected for this continuous position sensor. These values are typical of the rotary position sensor technologies such as resolver devices.<br><br>The time constant of 1 second typifies the response of a high precision position sensor including its sensor and instrumentation response. |
| | Discrete Position 1 | One discrete position sensor is considered required for monitoring the drum in its stowed position prior to launch and operation of the SNPP reactor. It is a fixed position sensor that confirms the drum in the fully withdrawn position. Photo, proximity, and microswitch technologies are typically applied as discrete position sensors. An accuracy of ±0.1degree of point and resolution of 0.1 degree of point for the sensor equal to that of continuous position sensor is readily achievable. A response time of 0.001 seconds is common for these discrete position technologies. |
| | Discrete Position 2 | One discrete position sensor is considered required for monitoring the drum at the boundary of the active core region. It is a fixed position sensor that confirms the drum in this position. Photo, proximity, and microswitch technologies are typically applied as discrete position sensors. An accuracy of ±0.1degree of point and a resolution of 0.1 degree of point for the sensor equal to that of continuous position sensor is readily achievable. A response time of 0.001 seconds is common for these discrete position technologies. |

| Section | Parameter | Justification and References |
|---|---|---|
| | Discrete Position 3 | One discrete position sensor is considered required for monitoring the drum near its expected critical position. It is a fixed position sensor that confirms the drum in this position. Photo, proximity, and microswitch technologies are typically applied as discrete position sensors. An accuracy of ±0.1degree of point and a resolution of 0.1 degree of point for the sensor equal to that of continuous position sensor is readily achievable. A response time of 0.001 seconds is common for these discrete position technologies. |
| **Safety Rod** | Discrete Position 1 | One discrete fixed position sensor is considered required for monitoring the safety rod in its fully inserted position prior to launch and operation of the SNPP reactor. Photo, proximity, and microswitch technologies are typically applied as discrete position sensors. An accuracy of ±0.05 cm of point and resolution of 0.005 cm of point for the sensor equal to that of continuous position sensor is readily achievable. A response time of 0.001 seconds is common for these discrete position technologies. |
| | Discrete Position 2 | One discrete fixed position sensor is considered required for monitoring the safety rod in its fully withdrawn position after launch and prior to initial critical operations of the SNPP reactor. Photo, proximity, and microswitch technologies are typically applied as discrete position sensors. An accuracy of ±0.05 cm of point and resolution of 0.005 cm of point for the sensor equal to that of continuous position sensor is readily achievable. A response time of 0.001 seconds is common for these discrete position technologies. |
| **VII. Valves** | | |
| **Valve Position** | Sensor 1 | In multiple-loop SNPP architectures with 2 or more Brayton machines, valves are used to direct coolant flow appropriately. Sensing of valve position is necessary for monitoring and control of these valves. For each valve a discrete fixed position sensor is required to be active (asserted) when the valve is in its OPEN position. Otherwise it is inactive (deasserted). Photo, proximity, and microswitch technologies are typically applied as discrete position sensors. Accuracy and resolution values for the sensor of 0.1% of point and 0.01% of point and a response of 0.001 seconds are typical of these technologies |
| | Sensor 2 | In multiple-loop SNPP architectures with 2 or more Brayton machines, valves are used to direct coolant flow appropriately. Sensing of valve position is necessary for monitoring and control of these valves. For each valve a discrete fixed position sensor is required to be active (asserted) when the valve is in its SHUT position. Otherwise it is inactive (deasserted). Photo, proximity, and microswitch technologies are typically applied as discrete position sensors. Accuracy and resolution values for the sensor of 0.1% of point and 0.01% of point and a response of 0.001 seconds are typical of these technologies. |

| Section | Parameter | Justification and References |
|---|---|---|
| **VIII. PCAD** | | |
| **Alternator** | Voltage | The line-to-line 3 phase alternating voltage output of each Brayton machine alternator is to be measured for monitoring and control of the alternator, the machine, and the power plant. A nominal line-to-line voltage of 450 volts at 2250 Hz is assumed at full power operation. To accommodate startup and steady state operations, the sensor would have a wide range capability of 0 – 500 volts with an accuracy of ±0.5 volts (0.1% FS), a resolution of 0.1 volts (0.01% FS), and a time constant of 1 second including sensor and instrumentation. These criteria represent typical capabilities of commercial sinusoidal voltage meters. |
| | Current | The 3 phase alternating current output of each Brayton machine alternator is to be measured for monitoring and control of the alternator, the machine, and the power plant. A nominal phase current of 128 A at 2250 Hz is assumed at full power operation. To accommodate startup and steady state operations, the sensor would have a wide range capability of 0 – 150 A with an accuracy of ±0.15 A, a resolution of 0.03 A, and a time constant of 1 second including sensor and instrumentation. These criteria represent typical capabilities of commercial sinusoidal current meters. |
| | Frequency (Brayton Speed) | The frequency of each Brayton machine alternator is to be measured for monitoring and control of the alternator, the machine, and the power plant. In this usage, the frequency of the alternator may be used as a measure of the speed of the Brayton machine and the coolant flow through the plant. A nominal frequency of 2250 Hz is assumed at full power operation. To accommodate startup, transitions in power level, steady state, and transient operations, the sensor would have a wide range capability of 450-2475 Hz corresponding to 9k to 50kRPM. Representing the typical capabilities of commercial metering equipment for sinusoidal frequency measurement, an accuracy of ±0.225 Hz (±0.01%FS, ±4.5 RPM), a resolution of 0.1 Hz (0.005%FS, 2.0 RPM), and a 1 second response time including sensor and instrumentation have been selected. |
| | Power [Single Alternator] | The power output of each Brayton machine alternator is to be measured for monitoring and control of the alternator, the machine, and the power plant. A nominal power of 97.0 kWe is assumed at full power operation based on a non-optimized four loop Brayton machine rated for 100 kWe operation. To accommodate startup, transitions in power level, steady state, and transient operations, the sensor would have a wide range capability of 0-110 kWe providing 10% margin to the nominal value. RMS evaluations of the alternator current and voltage uncertainties of ±0.2% are assumed to obtain a ±0.2 kWe accuracy. The resolution of 0.03 assumes voltage and current measurement resolutions of 0.2%. A 1 second response time including sensor and instrumentation typifies commercial electrical metering equipment. |
| | Total Power [Two Alternators] | The total power output from both 100 kWe Brayton machines is to be measured for monitoring and control of the power plant. A nominal power of 193.9 kWe is based on the non-optimized four loop Brayton system of Section 6. To accommodate startup, transitions in power level, steady state, and transient operations, the sensor would have a wide range capability of 0-220 kWe providing 10% margin to the nominal value. RMS evaluations of the alternator current and voltage uncertainties of ±0.2% are assumed to obtain a ±0.4 kWe accuracy. The resolution of 0.06 kWe assumes voltage and current measurement resolutions of 0.2%. A 1 second response time including sensor and instrumentation typifies commercial electrical metering equipment. |
| | | |

| Section | Parameter | Justification and References |
|---|---|---|
| Start Inverter | Voltage | The start inverter supplies 3 phase electrical power to the Brayton alternator to motor the machine during its startup. A nominal line-to-line voltage of 135 volts is assumed based on the anticipated speed of the machine for startup. A nominal range 0-150 volts provides 10% margin. An accuracy of ±0.15 volts (±0.1%FS), a resolution of 0.01 volts (0.01% FS), and a response of 1 second are typical values associated with commercial voltage metering equipment. |
| | Current | The start inverter supplies 3 phase electrical power to the Brayton alternator to motor the machine during its startup. A nominal phase current of 13 A is assumed based on the anticipated speed of the machine for startup. A nominal range 0-15 A provides 10% margin. An accuracy of ±0.015 A (±0.1%FS), a resolution of 0.003 A (0.02% FS), and a response of 1 second are typical values associated with commercial current metering equipment. |
| | Frequency (Brayton Speed) | The start inverter supplies 3 phase electrical power to the Brayton alternator to motor the machine during its startup. The nominal frequency of 675 Hz corresponds to the machine speed of 13500 RPM, the assumed motoring speed for machine startup. The range of 125-750 Hz provides 10% margin. The accuracy of ±0.07 Hz (±0.01%FS, 1.5 RPM), resolution of 0.03 Hz (0.005% FS, 0.75 RPM), and a response of 1 second are typical values associated with commercial frequency measurement equipment |
| | Power | The start inverter supplies 3 phase electrical power to the Brayton alternator to motor the machine during its startup. The nominal power of 2.7 kWe corresponding to the machine speed of 13500 RPM is assumed. A meter range of 0-5 kWe reflects the large potential variation in this value during startup. The accuracy of ±0.01 kWe assumes an RMS evaluation of voltage and current accuracies of 0.2%FS. The resolution of 0.001 kWe assumes an RMS evaluation of the voltage and current resolutions of 0.02%FS. These accuracies and resolution, and the 1 second response typify voltage and current metering equipment and the resulting power measure. |
| Parasitic Load Radiator (PLR) | Voltage | The PLR absorbs the output of the Brayton alternator up to its maximum output plus a few additional percent to accommodate speed regulation at full power conditions. Therefore, nominal line-to-line 3 phase alternating voltage output of each Brayton machine alternator is 450 volts at 2250 Hz. The voltage metering equipment for the PLR would be the same as the Brayton alternator voltage metering equipment and have the same accuracies, resolution, and response time. |
| | Current | The PLR absorbs the output of the Brayton alternator up to its maximum output plus a few additional percent to accommodate speed regulation at full power conditions. The nominal phase current of each PLR under full load conditions of 135 A has been selected. The current metering equipment for the PLR would be the same as the Brayton alternator current metering equipment and have the same accuracies, resolution, and response time. |
| | Power | The PLR absorbs the output of the Brayton alternator up to its maximum output plus a few additional percent to accommodate speed regulation at full power conditions. Therefore the PLR nominal value of 103 kWe has been selected for operation at full power conditions. The power metering equipment for the PLR would be the same as the Brayton alternator power metering equipment and have the same accuracies, resolution, and response time. |
| IX. Radiator | | |
| | Pump Speed (multispeed) | The method of pump speed measurement had not been determined. |

| Section | Parameter | Justification and References |
|---|---|---|
| IX. Radiator continued | Water Flow | The nominal water mass flow through the heat rejection is 0.70 kg/sec corresponding to a volumetric flow rate of approximately 600 $cm^3$/sec based on the four loop non-optimized Brayton system. Flowmeters are generally capable of measurement ratios of 1:100 providing a design range of 10-1000 for the HRS flow measure, Flowmeters typically have 2% (±20 $cm^3$/sec) accuracies, 1% (10 $cm^3$/sec) resolutions, and responses times of 1 second including instrumentation. |
| | Inlet Temperature | The nominal heat rejection system inlet temperature of 505 K is based on the four loop non-optimized Brayton system of Section 6. The range 250-570 K assumes the plant maintains temperature not below 250 K, a ±10 K control band for reactor operation at full power, the stated accuracy of ±1% and a 10% uncertainty for transient performance due to casualty or maneuvering. The number is rounded. The accuracy of ±3 K (1% of range) and the resolution of 1.5 K (0.5% of range) and the 10 second response typify the characteristics of quality commercial temperature sensors and instrumentation. |
| | Outlet Temperature | The nominal heat rejection system outlet temperature of 379 K is based on the four loop non-optimized Brayton system of Section 6. The range 250-430 K assumes the plant maintains temperature not below 250 K, a ±10 K control band for reactor operation at full power, the stated accuracy of ±1% and a 10% uncertainty for transient performance due to casualty or maneuvering. The number is rounded. The accuracy of ±2.0 K (1% of range) and the resolution of 1.0 K (0.5% of range) and the 10 second response typify the characteristics of quality commercial temperature sensors and instrumentation. |

# Section 3
# System Architecture

(Intentionally Blank)

# System Architecture

## Table of Contents

3 System Architecture ..... 5
3.1 Summary and Conclusions ..... 5
3.2 Plant Configuration Options ..... 7
3.3 Single Operating Brayton Unit (1-1-1 Arrangement) ..... 10
3.3.1 System Design ..... 10
3.3.2 Commissioning ..... 12
3.3.3 Normal Operation ..... 13
3.3.4 Abnormal Operation ..... 13
3.4 Single Operating Brayton Unit with Spare Brayton Unit (2-1-1 Arrangement) ..... 14
3.4.1 System Design ..... 14
3.4.2 Commissioning ..... 14
3.4.3 Normal Operation ..... 14
3.4.4 Abnormal Operation ..... 14
3.5 Dual Operating Brayton Units, Each Unit Capable of 50% of Rated System Power (2-2-2 Arrangement) ..... 15
3.5.1 System Design ..... 15
3.5.2 Commissioning ..... 16
3.5.3 Normal Operation ..... 17
3.5.4 Abnormal Operation ..... 17
3.6 Dual Operating Brayton Units, Each Unit Capable of 100% and 50% of Rated System Power (2-2-2s Arrangement) ..... 18
3.6.1 System Design ..... 18
3.6.2 Commissioning ..... 18
3.6.3 Normal Operation ..... 18
3.6.4 Abnormal Operation ..... 19
3.7 Three Operating Brayton Units, Each Unit Capable of 33% and 50% of Rated System Power (3-3-3s Arrangement) ..... 20
3.7.1 System Design ..... 20
3.7.2 Commissioning ..... 20
3.7.3 Normal Operation ..... 20
3.7.4 Abnormal Operation ..... 21
3.8 Dual Operating Brayton Units, Each Unit Capable of 50% of Rated System Power with Spare Brayton Unit (3-2-2 Arrangement) ..... 22
3.8.1 System Design ..... 22
3.8.2 Commissioning ..... 24
3.8.3 Normal Operation ..... 24
3.8.4 Abnormal Operation ..... 24
3.9 Dual Operating Brayton Units, with Two Spare Brayton Units (4-2-2 Arrangement) ..... 25
3.9.1 System Design ..... 25
3.9.2 Commissioning ..... 25
3.9.3 Normal Operation ..... 25
3.9.4 Abnormal Operation ..... 26
3.10 Dual Operating Brayton Units, with Two Spare Brayton Units (4-4-4 Arrangement) ..... 27
3.10.1 System Design ..... 27
3.10.2 Commissioning ..... 28

3.10.3 Normal Operation ..... 29
3.10.4 Abnormal Operation ..... 29

The 1-1-1 system is schematically depicted in Figure 3-4:

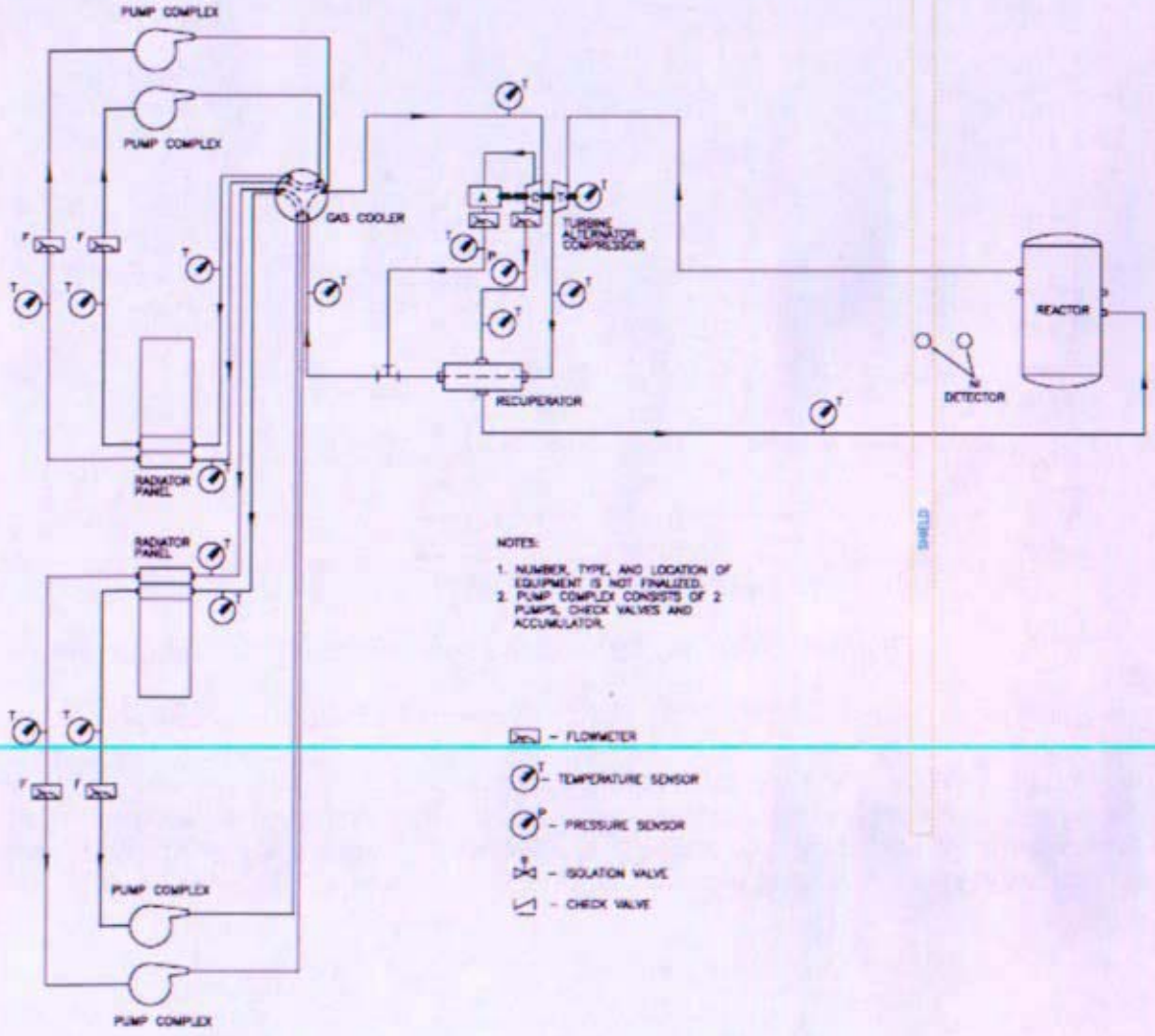



**Figure 3-4: Single Brayton Schematic**

### 3.3.2 Commissioning

- Motor the 200 kWe Brayton using solar electric power to provide coolant flow to the reactor
- Startup the reactor
- Bring the Brayton to self-sustaining power level
- Raise power as needed

### 3.3.3 Normal Operation

- Brayton unit is in service at all times
- During Propulsion mode: [1150] K, [45000] rpm [2] (temperature used to control Brayton cycle)
- Coast and Science mode: reduced temperature, reduced speed (temperature and/or speed used to control Brayton cycle)

### 3.3.4 Abnormal Operation

- On loss of the operating Brayton unit, compressor or alternator – End of Mission.

**Table 3-1:** System Pros and Cons; Single Operating Brayton Unit (1-1-1 Arrangement)

| Pros | Cons |
|---|---|
| Simplest system design and operation | Mission is lost if Brayton unit fails |
| Valves are not required | For spacecraft applications, momentum compensation system may be required |
| Lowest system mass | May be less able to accommodate any unforeseen casualties or alternate operating modes than other system architectures |
| Four gas cooler heat exchangers in a common pressure boundary – simplified piping | Commissioning power requirements to startup a 200 kWe Brayton unit may be greater than that required for a 100 kWe Brayton unit |
| Minimizes the potential for gas leakage from the system | If the energy conversion system fails in deep space, there may not be power to communicate the reason for failure |
| Highest thermal efficiency (potentially lowest reactor outlet temperature) | Dual alternator stator windings are required to simplify electrical system |
| Easiest arrangement within a space envelope | No component redundancy (except alternator stator windings) |
| Lowest required radiator area | |
| Straightforward Heat Rejection Segment (HRS) interface | |

[2] Bracketed values are estimated values which will be finalized as the design progresses. A single Brayton unit has the highest cycle efficiency. This efficiency can be traded for other design parameters such as lower operating temperatures, larger design margins and/or radiator area.

## 3.4 Single Operating Brayton Unit with Spare Brayton Unit (2-1-1 Arrangement)

### 3.4.1 System Design

- Two 200 kWe Brayton units, potentially with dual alternator stator windings
- One recuperator sized to service one 200 kWe Brayton
- One gas cooler sized to cool one 200 kWe Brayton (may be multiple independent flow paths housed within a common pressure boundary)
- Each Brayton has a set of turbine outlet valves, to isolate a Brayton unit and a check valve in each alternator cooling line
- Electrical power storage device (battery, flywheel, etc.) required to start standby Brayton unit
- *Means for momentum compensation may be required*

An isolation valve would be located at each turbine outlet to shutdown an over-speeding unit and to limit flow through a non-operating Brayton unit. This valve would be normally shut for a standby Brayton unit.

A check valve or isolation valve would be placed at the compressor outlet to prevent reverse flow through the compressor in a non-operating Brayton. The reverse flow would be driven by the differential pressure across the operating compressor. Reverse flow through the non-operating compressor could cause the Brayton to spin backwards and damage its bearings. If an isolation valve were employed, it would have to be normally shut for the standby Brayton.

A check or isolation/shutoff valve may be required at the alternator outlet to prevent reverse flow through the alternator. This flow would be driven by gas cooler differential pressure.

### 3.4.2 Commissioning

- Motor of one 200 kWe Brayton using solar electric power to provide coolant flow to the reactor
- Startup the reactor
- Bring the Brayton to self-sustaining power level
- Raise power as needed

### 3.4.3 Normal Operation

- One Brayton unit is in service at all times
- During Propulsion mode: [1150] K, [45000] rpm (temperature used to control Brayton cycle)
- Coast and Science mode: reduced temperature, reduced speed (temperature and/or speed used to control Brayton cycle)

### 3.4.4 Abnormal Operation

- Upon loss of a single Brayton unit, the reactor plant experiences a complete loss of coolant flow. Thus, reactor power must be expeditiously lowered to ensure core thermal limits are not exceeded.
- On loss of an operating Brayton unit (turbine, compressor or alternator) – utilize electrical power storage device to start the standby Brayton unit and restart the reactor

**Table 3-2:** System Pros and Cons; Single Operating Brayton Unit with a Standby Brayton Unit (2-1-1 Arrangement)

| Pros | Cons |
|---|---|
| Can tolerate a single Brayton unit failure | High temperature gas valves are required and must function to start standby Brayton unit |
| Recuperator and gas cooler configurations may reduce system mass and reduce potential for gas leakage from system | For spacecraft applications, momentum compensation system may be required |
| May be more able to accommodate unforeseen casualties or alternate operating modes than a single Brayton system | Commissioning power requirements to startup a 200 kWe Brayton unit may be greater than that required for a 100 kWe Brayton unit |
| The most limiting components from a gas leakage perspective (tubing and joints in heat exchangers) are not redundant (number minimized) – minimizing the potential for gas leakage from the system | On a loss of Brayton unit, all coolant flow through the reactor is lost |
| The most massive components (gas cooler and recuperator) are not redundant, minimizing the mass penalty for redundancy | Most severe reactor transients upon loss of a Brayton unit – reactor and plant must be able to handle this transient |
| | Electrical power storage device (battery, flywheel, etc.) required to start standby Brayton unit and the reactor |

## 3.5 Dual Operating Brayton Units, Each Unit Capable of 50% of Rated System Power (2-2-2 Arrangement)

### 3.5.1 System Design

- Two 100 kWe Brayton units, counter-rotational designs
- Two recuperators each sized to service one 100 kWe Brayton unit operating in parallel
- Two gas coolers sized to cool two 100 kWe Braytons (may be multiple independent flow paths housed within a common pressure boundary)

An isolation valve at the compressor outlet could be used in this arrangement to shut down an over-speeding Brayton.

The 2-2-2 system is schematically depicted in Figure 3-5. This schematic also applies to other 2-2-2 system options, including the option discussed in Section 3.6. The valves shown are consistent with the base arrangement stated in the Plant Parameter List (Section 2). The 'NO' associated with the isolation valve at each compressor outlet indicates that the valves are normally open when the system is operating. The bracketed 'NS' indicates the position of the isolation valve if the associated Brayton is no longer operating and is isolated.

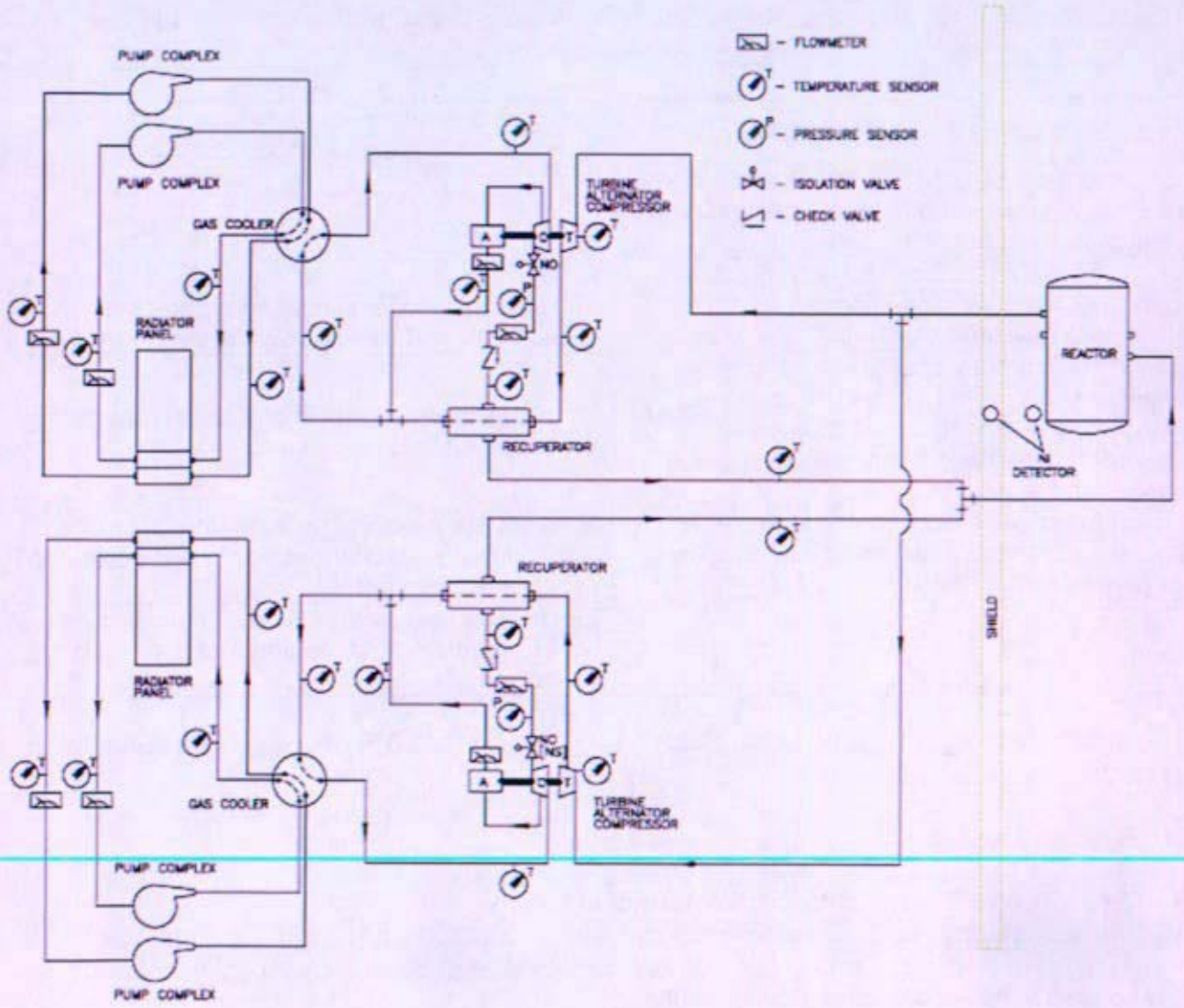



**Figure 3-5 Dual-Brayton Schematic**

### 3.5.2 Commissioning

- Motor one 100 kWe Brayton using solar electric power to provide coolant flow to the reactor
- Startup the reactor
- Bring the first Brayton to self-sustaining power level
- Startup of the second 100 kWe Brayton using electric power from the operating Brayton
- Raise power as needed

### 3.5.3 Normal Operation

- Two Brayton units in service at all times operating at 100% of rated power
- During Propulsion mode: [1150] K, [45000] rpm (temperature used to control Brayton cycle)
- Coast and Science mode: reduced temperature, reduced speed (temperature and/or speed used to control Brayton cycle)

### 3.5.4 Abnormal Operation

- On loss of an operating Brayton unit, insufficient electrical power to support the mission – may provide a minimum power to allow for communications and potential Brayton restart
- Upon loss of a single Brayton unit, the reactor plant experiences a reduction in coolant flow. Decay heat removal (DHR) capability is maintained; therefore a separate DHR system is not needed.

**Table 3-3:** System Pros and Cons; Dual Operating Brayton Units, Each Unit Capable of 50% of Rated System Power (2-2-2 Arrangement)

| Pros | Cons |
|---|---|
| On a loss of Brayton unit, coolant flow through the reactor is maintained | Mission is lost if one Brayton fails (cannot achieve full power) |
| No component redundancy, minimizing Brayton loop mass | High temperature gas valves may be required |
| For spacecraft applications, separate momentum compensation system is not required | |
| Commissioning power requirements to startup a 100 kWe Brayton unit may be less than that required for a 200 kWe Brayton unit | |
| Electrical power storage device (battery, flywheel, etc.) is not required to restart a shutdown Brayton unit | |
| Paired gas coolers simplifies the HRS interface | |
| May be more able to accommodate unforeseen casualties or alternate operating modes than a single Brayton system | |
| The most limiting components from a gas leakage perspective (tubing and joints in heat exchangers) are not redundant (number minimized) – minimizing the potential for gas leakage from the system | |
| The most massive components (gas cooler and recuperator) are not redundant, minimizing the mass penalty for redundancy | |

## 3.6 Dual Operating Brayton Units, Each Unit Capable of 100% and 50% of Rated System Power (2-2-2s Arrangement)

System architectures in which the PCAD system is designed to operate at full rated power at multiple frequencies are designated with an "s", e.g. 2-2-2s. Additional detail regarding this mode of operation is provided in Section 3.11.

### 3.6.1 System Design

- Two 200 kWe Brayton units, counter-rotational designs, designed to operate at two system state points: 50% rated system power and 100% rated system power
- Two recuperators each sized to service a 200 kWe Brayton (may be multiple independent flow paths housed within a common pressure boundary)
- Two gas coolers sized to service a 200 kWe Brayton unit (may be multiple independent flow paths housed within a common pressure boundary)
- Each Brayton has a set of valves at the compressor outlet to allow for isolation of a failed Brayton unit

An isolation valve or a combination of an isolation valve and a check valve at the compressor outlet could be used in this arrangement to shut down an over-speeding Brayton or to isolate an out of commission loop, minimizing backflow. The check valve would be used to prevent back flow through the standby Brayton. The isolation valve would be used to stop an over-speeding Brayton.

The 2-2-2s system is schematically depicted in Figure 3-5.

### 3.6.2 Commissioning

- Motor one 200 kWe Brayton using solar electric power to provide coolant flow to the reactor
- Startup the reactor
- Bring the first Brayton to self-sustaining power level
- Startup of the second 200 kWe Brayton using electric power from the operating Brayton
- Raise power as needed

### 3.6.3 Normal Operation

- Two Brayton units in service at all times operating at 50% of rated power, isolation valves open
- During Propulsion mode: [Reserved] K, [Reserved] rpm (temperature and speed used to control Brayton cycle)
- Coast and Science mode: reduce temperature further (temperature used to change operating state points)

### 3.6.4 Abnormal Operation

- On loss of an operating Brayton unit, electrical loads are transferred to the remaining Brayton unit by adjusting reactor outlet temperature and Brayton speed as discussed in Section 3.11.
- The compressor outlet isolation valves are shut in the loop with the damaged Brayton unit
- Upon loss of a single Brayton unit, the reactor plant experiences a reduction in coolant flow. Decay Heat Removal (DHR) capability is maintained; therefore a separate DHR system is not needed.
- Upon loss of a single Brayton unit, electrical power would continue to be available from the operating Brayton unit; therefore, an alternate power supply would not be needed.

**Table 3-4:** System Pros and Cons; Dual Operating Brayton Units, Each Unit Capable of 100% and 50% of Rated System Power (2-2-2s Arrangement)

| Pros | Cons |
|---|---|
| Valves are not required to function to maintain the operating components in-service | Valves are required to function to isolate a damaged Brayton unit |
| Mission not impacted by loss of a single Brayton unit | Two system state points results in cycle inefficiency at a minimum of one operating point, resulting in a mass penalty and a tighter design space |
| On a loss of Brayton unit, coolant flow through the reactor is maintained | For spacecraft applications, separate momentum compensation system may be required if a Brayton unit fails |
| Electrical power storage device (battery, flywheel, etc.) is not required to restart a shutdown Brayton unit | Mass impact on the electrical distribution system to accommodate two frequencies (Brayton unit speed) |
| Paired alternators simplifies electrical distribution system | Commissioning power requirements to startup a 200 kWe Brayton unit may be greater than that required for a 100 kWe Brayton unit |
| Paired gas coolers simplifies the HRS interface | The most limiting components from a gas leakage perspective (tubing and joints in heat exchangers) are redundant – increasing the potential for gas leakage from the system |
| May be more able to accommodate unforeseen casualties or alternate operating modes than a single Brayton system | The most massive components (gas cooler and recuperator) are redundant, increasing the mass penalty for redundancy |

## 3.7 Three Operating Brayton Units, Each Unit Capable of 33% and 50% of Rated System Power (3-3-3s Arrangement)

System architectures in which the PCAD system is designed to operate at full rated power at multiple frequencies are designated with an "s", e.g. 3-3-3s. Additional detail regarding this mode of operation is provided in Section 3.11.

### 3.7.1 System Design

- Three 100 kWe Brayton units, two of three co-rotational, designed to operate at two system state points: 33.3% rated system power and 50% rated system power
- Recuperators sized to support the operation of two 100 kWe Brayton units or three 66.7 kWe Brayton units operating in parallel (may be multiple independent flow paths housed within a common pressure boundary or may be three independent recuperators each sized to service a 100 kWe Brayton)
- Gas coolers sized to support the operation of two 100 kWe Brayton units or three 66.7 kWe Brayton units operating in parallel (may be multiple independent flow paths housed within a common pressure boundary or may be three independent gas coolers each sized to service a 100 kWe Brayton)
- Each Brayton has a set of compressor outlet valves to allow for isolation of the failed Brayton

An isolation valve at the compressor outlet could be used in this arrangement to shut down an over-speeding Brayton.

No schematic is provided for the 3-3-3s system. The only major differences in the 3-3-3s system compared to the 2-2-2 or 4-4-4 systems occur in the connection of the primary system to the heat rejection segment. Section 9 provides discussion of the heat rejection segment design. The heat rejection segment design and operation have not been evaluated for the dual operating mode 3-3-3s system.

### 3.7.2 Commissioning

- Motor one Brayton unit using solar electric power to provide coolant flow to the reactor
- Startup the reactor
- Bring the first Brayton to self-sustaining power level
- Startup of the second Brayton unit using electric power from the operating Brayton
- Startup of the third Brayton unit using electric power from the operating Brayton
- Raise power as needed

### 3.7.3 Normal Operation

- Three Brayton units in service at all times operating at 33.3% of rated power, isolation valves open
- During Propulsion mode: [Reserved] K, [Reserved] rpm (temperature and speed used to control Brayton cycle)
- Coast and Science mode: reduce temperature further (temperature used to change operating state points)

- Upon loss of a single Brayton unit, the reactor plant experiences a reduction in coolant flow. Decay Heat Removal (DHR) capability is maintained; therefore a separate DHR system is not needed
- Upon loss of a single Brayton unit, electrical power would continue to be available from the operating Brayton unit; therefore, an alternate power supply would not be needed.

### 3.7.4 Abnormal Operation

- On loss of an operating Brayton unit, electrical loads are transferred to the two remaining Brayton units by adjusting reactor outlet temperature and Brayton speed as discussed in Section 3.11.
- The compressor outlet isolation valves are shut in the loop with the damaged Brayton unit
- Upon loss of a single Brayton unit, the reactor plant experiences a reduction in coolant flow. Decay Heat Removal (DHR) capability is maintained; therefore a separate DHR system is not needed.
- Upon loss of a single Brayton unit, electrical power would continue to be available from the operating Brayton unit; therefore, an alternate power supply would not be needed.

**Table 3-5:** System Pros and Cons; Three Operating Brayton Units, Each Unit Capable of 33% and 50% of Rated System Power (3-3-3s Arrangement)

| Pros | Cons |
|---|---|
| Valves are not required to function to maintain the operating components in-service | High temperature gas valves are required to function to isolate a damaged Brayton unit |
| Mission not impacted by a single Brayton unit failure | Two system state points results in cycle inefficiency at a minimum of one operating point, resulting in a mass penalty and a tighter design space |
| On a loss of Brayton unit, coolant flow through the reactor is maintained | For spacecraft applications, separate momentum compensation system may be required |
| Commissioning power requirements to startup a 100 kWe Brayton unit may be less than that required for a 200 kWe Brayton unit | Mass impact on the electrical distribution system to accommodate two frequencies (Brayton unit speed) |
| The most massive components (gas cooler and recuperator) are not redundant, minimizing the mass penalty for redundancy | Interface with electrical system complicated by system with three operating converter loops |
| The most limiting components from a gas leakage perspective (tubing and joints in heat exchangers) are not redundant (number minimized) – minimizing the potential for gas leakage from the system | Interface with HRS system complicated by system with three operating converter loops |
| May be more able to accommodate unforeseen casualties or alternate operating modes than a single Brayton system | |

## 3.8 Dual Operating Brayton Units, Each Unit Capable of 50% of Rated System Power with Spare Brayton Unit (3-2-2 Arrangement)

### 3.8.1 System Design

- *Three 100 kWe Brayton units, two of three co-rotational*
- Two recuperators each sized to service a 100 kWe Brayton units (may be multiple independent flow paths housed within a common pressure boundary)
- Two gas coolers each sized to cool a 100 kWe Brayton (may be multiple independent flow paths housed within a common pressure boundary)
- The operating Brayton units share a common recuperator and set of gas coolers with the standby Brayton unit
- Four isolation valves per heat exchanger allow for isolation of the standby (failed) Brayton
- Each Brayton has a set of compressor outlet valves

An isolation valve or a combination of an isolation valve and a check valve at the compressor outlet could be used in this arrangement to shut down an over-speeding Brayton or to isolate an out of commission loop, minimizing backflow. The check valve would be used to prevent back flow through the standby Brayton. The isolation valve would be used to stop an over-speeding Brayton.

Figure 3-6 shows one conceptual layout for a 3-2-2 system. A key point of this concept is that the *third Brayton can replace either one of the other Braytons and use the corresponding recuperator and* gas cooler. Therefore, the third Brayton requires two isolation valves in the turbine outlet, the compressor inlet, and the alternator cooling outlet in order to direct gas flow to the appropriate components. The normally operating Brayton units have in addition to the isolation valve and the check valve in the compressor outlet (the base valve arrangement per Section 4) another isolation valve located in the turbine outlet to prevent flow from bypassing the standby Brayton when the standby is in use.

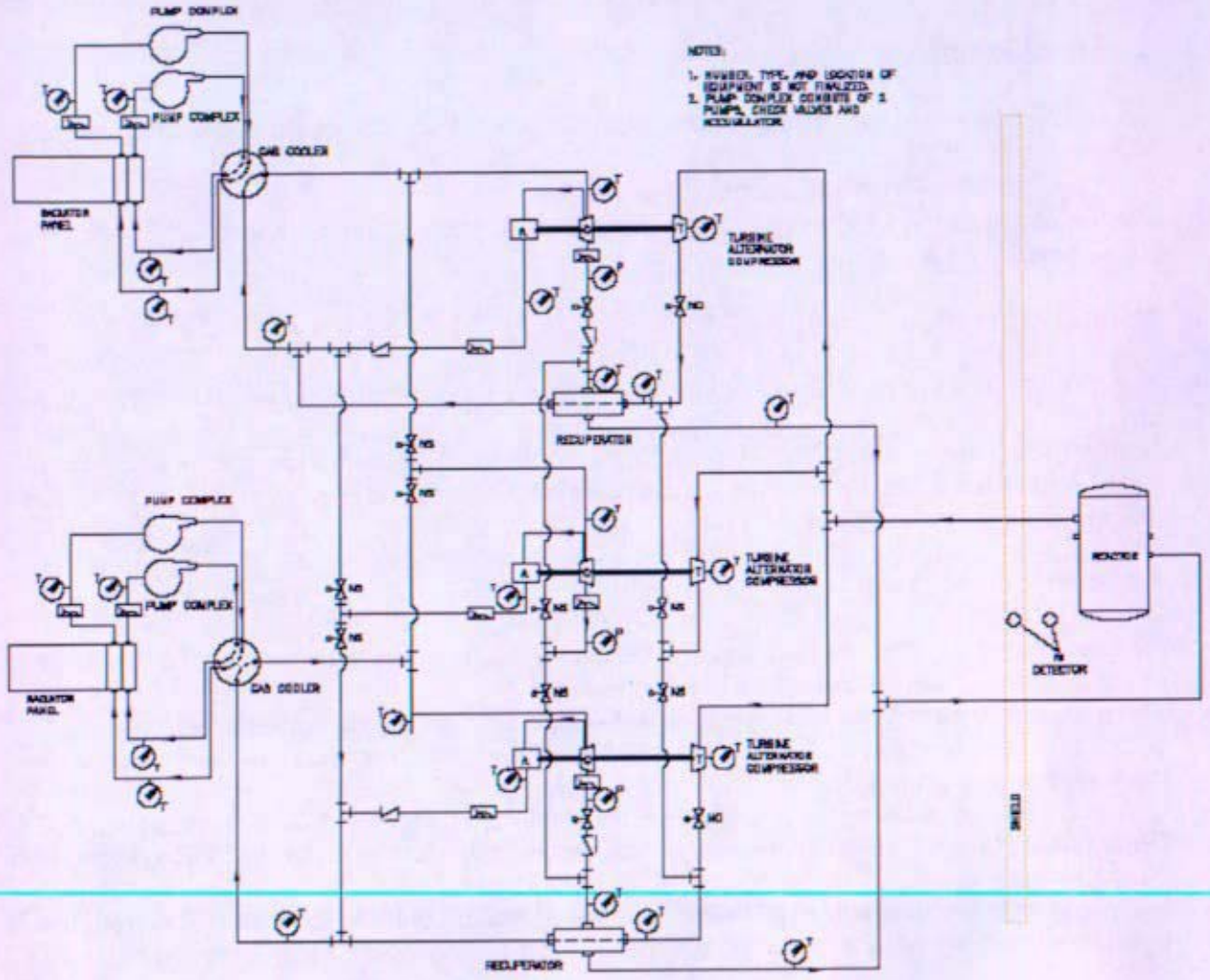



**Figure 3-6: Dual Brayton System with Spare Brayton Unit (3-2-2)**

### 3.8.2 Commissioning

- Motor one 100 kWe Brayton using solar electric power to provide coolant flow to the reactor
- Startup the reactor
- Bring the first Brayton to self-sustaining power level
- Startup of the second 100 kWe Brayton using electric power from the operating Brayton
- Raise power as needed

### 3.8.3 Normal Operation

- Two Brayton units in service at all times operating at 100% of rated power, isolation valves open
- During Propulsion mode: [1150] K, [45000] rpm (temperature used to control Brayton cycle)
- Coast and Science mode: reduced temperature, reduced speed (temperature and/or speed used to control Brayton cycle)

### 3.8.4 Abnormal Operation

- On loss of an operating Brayton unit, the remaining operating Brayton unit would supply the power needed to start the standby Brayton unit.
- The recuperator and gas cooler isolation valves are shut for the damaged Brayton, compressor or alternator and the isolation valves connecting this recuperator and gas cooler to the standby Brayton are opened.
- Upon loss of a single Brayton unit, the reactor plant experiences a reduction in coolant flow. Decay Heat Removal (DHR) capability is maintained; therefore a separate DHR system is not needed.
- Upon loss of a single Brayton unit, electrical power would continue to be available from the operating Brayton unit; therefore, an alternate power supply would not be needed.

**Table 3-6:** System Pros and Cons; Dual Operating Brayton Units, Each Unit Capable of 50% of Rated System Power with Spare Brayton Unit (3-2-2 Arrangement)

| Pros | Cons |
|---|---|
| On a loss of Brayton unit, coolant flow through the reactor is maintained | High temperature gas valves are required to function to isolate a damaged Brayton unit |
| The most massive components (gas cooler and recuperator) are not redundant, minimizing the mass penalty for redundancy | For spacecraft applications, separate momentum compensation system may be required if a Brayton unit fails |
| Mission not impacted by a single Brayton unit failure | Additional valves are required to allow sharing of components between converter loops |
| The most limiting components from a gas leakage perspective (tubing and joints in heat exchangers) are not redundant (number minimized) – minimizing the potential for gas leakage from the system | |

| | |
|---|---|
| Commissioning power requirements to startup a 100 kWe Brayton unit may be less than that required for a 200 kWe Brayton unit | |
| Electrical power storage device (battery, flywheel, etc.) is not required to restart a shutdown Brayton unit | |
| Paired alternators simplifies electrical distribution system | |
| Paired gas coolers simplifies the HRS interface | |
| May be more able to accommodate unforeseen casualties or alternate operating modes than a single Brayton system | |

## 3.9 Dual Operating Brayton Units, with Two Spare Brayton Units (4-2-2 Arrangement)

### 3.9.1 System Design

- Four 100 kWe Brayton units, two counter-rotational sets
- Two recuperators each sized to service one 100 kWe Brayton (may be multiple independent flow paths housed within a common pressure boundary).
- Two gas coolers each sized to cool one 100 kWe Brayton (may be multiple independent flow paths housed within a common pressure boundary).
- Two Braytons share a common recuperator and gas cooler
- Two of four of the Braytons are running at any given time (opposite rotations)
- Four isolation valves per recuperator allow for isolation of the failed Brayton
- Each Brayton unit has a set of compressor outlet valves.

An isolation valve or a combination of an isolation valve and a check valve at the compressor outlet could be used in this arrangement to shut down an over-speeding Brayton or to isolate an out of commission loop, minimizing backflow. The check valve would be used to prevent back flow through the standby Brayton. The isolation valve would be used to stop an over-speeding Brayton.

### 3.9.2 Commissioning

- Motor one 100 kWe Brayton using solar electric power to provide cooling flow to the reactor
- Startup the reactor
- Bring the first Brayton to self-sustaining power level
- Startup of the second 100 kWe Brayton using electric power from operating Brayton
- Raise power as needed

### 3.9.3 Normal Operation

- Two Brayton units in service at all times, isolation valves open
- During Propulsion mode: [1150] K, [45000] rpm (temperature used to control Brayton cycle)
- Coast and Science mode: reduced temperature, reduced speed (temperature and/or speed used to control Brayton cycle)

### 3.9.4 Abnormal Operation

- On loss of an operating Brayton unit, compressor or alternator, high voltage loads are shed
- The recuperator and gas cooler isolation valves are shut for the damaged Brayton, compressor or alternator
- The recuperator and gas cooler isolation valves are opened for the standby Brayton unit
- An emergency startup system is used to motor and startup the standby Brayton
- Upon loss of a single Brayton unit, the reactor plant experiences a reduction in coolant flow. Decay Heat Removal (DHR) capability is maintained; therefore a separate DHR system is not needed.
- Upon loss of a single Brayton unit, electrical power would continue to be available from the operating Brayton unit; therefore, an alternate power supply would not be needed.

**Table 3-7:** System Pros and Cons; Dual Operating Brayton Units, with Two Spare Brayton Units (4-2-2 Arrangement)

| Pros | Cons |
|---|---|
| Valves are not required to function to maintain the operating components in-service (i.e. if the valves failed to operate, system reliability is similar to a single Brayton) | Valves are required to function to startup a spare Brayton and to isolate a damaged Brayton |
| Redundant turbomachinery | |
| Mission not impacted by the loss of a single Brayton unit in each loop. | |
| The most massive components (gas cooler and recuperator) are not redundant, minimizing the mass penalty for redundancy | |
| The most limiting components from a gas leakage perspective (tubing and joints in heat exchangers) are not redundant (number minimized) – minimizing the potential for gas leakage from the system | |
| May be more able to accommodate unforeseen casualties or alternate operating modes than a single Brayton system | |
| Valves could be used to isolate the standby/failed components | |
| Commissioning power requirements to startup a 100 kWe Brayton unit may be less than that required for a 200 kWe Brayton unit | |
| On a loss of Brayton unit, coolant flow is maintained through the reactor | |
| Electrical power storage device (battery, flywheel, etc.) is not required to restart a shutdown Brayton unit | |
| Paired alternators simplifies electrical distribution system | |
| Paired gas coolers simplifies the HRS interface | |

## 3.10 Dual Operating Brayton Units, with Two Spare Brayton Units (4-4-4 Arrangement)

### 3.10.1 System Design

- Four 100 kWe Brayton units, two counter-rotational sets
- Four recuperators each sized to service one 100 kWe Brayton unit (may be multiple independent flow paths housed within a common pressure boundary)
- Four gas coolers each sized to cool one 100 kWe Brayton unit (may be multiple independent flow paths housed within a common pressure boundary)
- Each Brayton unit has a recuperator and set of gas coolers
- Two of four of the Braytons are running at any given time (opposite rotations)
- Each Brayton unit has a set of compressor outlet valves

An isolation valve or a combination of an isolation valve and a check valve at the compressor outlet could be used in this arrangement to shut down an over-speeding Brayton or to isolate an out of commission loop, minimizing backflow. The check valve would be used to prevent back flow through the standby Brayton. The isolation valve would be used to stop an over-speeding Brayton.

The 4-4-4 system is schematically depicted in Figure 3-7. The valves shown are consistent with the base arrangement stated in the Plant Parameter List (Section 2). Each Brayton loop is cooled by an independent HRS loop.

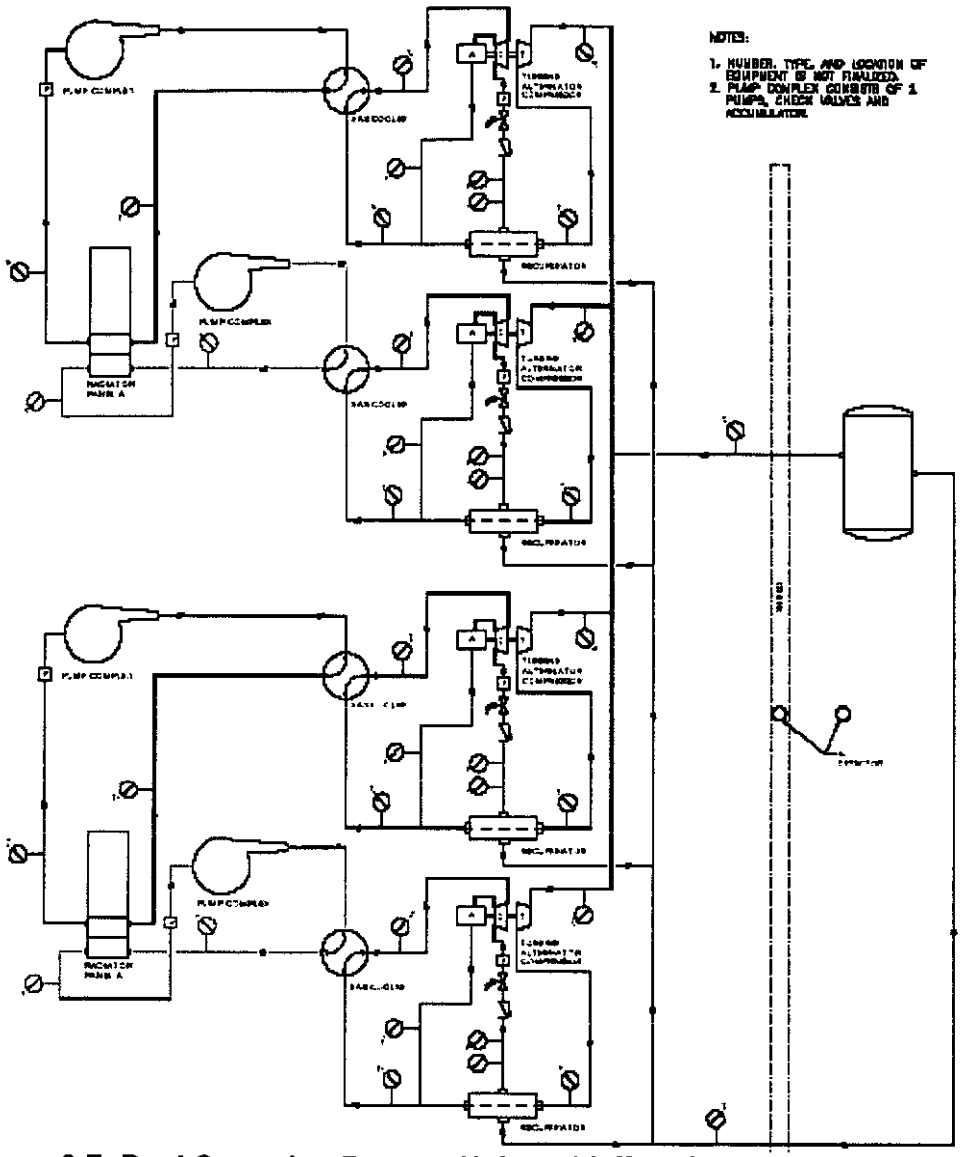



**Figure 3-7: Dual Operating Brayton Units, with Two Standby Brayton Units**

## 3.10.2 Commissioning

- Motor one 100 kWe Brayton using solar electric power to provide coolant flow to the reactor
- Startup the reactor
- Bring the first Brayton to self-sustaining power level
- Startup of the second 100 kWe Brayton using electric power from operating Brayton
- Raise power as needed

### 3.10.3 Normal Operation

- Two Brayton units in service at all times
- During Propulsion mode: [1150] K, [45000] rpm (temperature used to control Brayton cycle)
- Coast and Science mode: reduced temperature, reduced speed (temperature and/or speed used to control Brayton cycle)

### 3.10.4 Abnormal Operation

- On loss of an operating Brayton unit, compressor or alternator, high voltage loads are shed
- The compressor outlet isolation valves are shut in the loop with the damaged Brayton unit
- The compressor outlet isolation valves are opened for the standby Brayton unit
- An emergency startup system is used to motor and startup the standby Brayton
- Upon loss of a single Brayton unit, the reactor plant experiences a reduction in coolant flow. Decay Heat Removal (DHR) capability is maintained; therefore a separate DHR system is not needed.
- Upon loss of a single Brayton unit, electrical power would continue to be available from the operating Brayton unit; therefore, an alternate power supply would not be needed.

**Table 3-8:** System Pros and Cons; Dual Operating Brayton Units, with Two Spare Brayton Units (4-4-4 Arrangement)

| Pros | Cons |
|---|---|
| Valves are not required to function to maintain the operating components in-service (i.e. if the valves failed to operate, system reliability is similar to a single Brayton) | Valves are required to function to startup a spare Brayton and to isolate a damaged Brayton |
| All rotating equipment has a redundant/backup component | The most massive components (gas cooler and recuperator) are redundant, resulting in a mass penalty for redundancy |
| May be more able to accommodate unforeseen casualties or alternate operating modes than a single Brayton system | The most limiting components from a gas leakage perspective (tubing and joints in heat exchangers) are redundant – increasing the potential for gas leakage from the system |
| Mission not impacted by the loss of a single Brayton unit | |
| Commissioning power requirements to startup a 100 kWe Brayton unit may be less than that required for a 200 kWe Brayton unit | |
| On a loss of Brayton unit, coolant flow is maintained through the reactor | |
| Electrical power storage device (battery, flywheel, etc.) is not required to restart a shutdown Brayton unit | |
| Paired alternators simplifies electrical distribution system | |
| Paired gas coolers simplifies the HRS interface | |

## 3.11 Dual Brayton Operating State Points for Full Power Operation

System architectures in which the PCAD system is designed to operate at full rated power at multiple frequencies are designated with an "s", i.e. 2-2-2s and 3-3-3s systems. This capability permits a mode of operation where all turboalternators are normally operating at less than their rated capacity but jointly produce the full rated system power by reducing turbine inlet temperature and rotational speed. In the event of failure of one turboalternator, full rated system power is restored by increasing the turbine inlet temperature and rotational speed of the remaining unit(s) such that each turboalternator operates at its rated capacity. This mode of operation is desirable to mitigate concerns associated with material performance at elevated temperature. Analysis shows that operating the turboalternators at a reduced turbine inlet temperature and reduced rotational speed allows for significant plant sizing advantages (higher thermodynamic efficiency) over operating by only reducing turbine inlet temperature at a constant speed (see Figure 3-8).

Figure 3-8 presents a map of alternator load capability (solid lines) ranging from 25 to 200 kWe, reactor inlet temperature (dashed lines) with ranges from 740 to 970 K, and cycle efficiency (contour color map) with ranges from 0.08 to 0.259 for a 2-2-2s system architecture. The proposed reactor vessel material for Prometheus is a Ni-based superalloy, which is cooled by the reactor inlet flow. A design temperature of ~900K is the near the limit for acceptable creep allowance. Plant operation is envisioned to control the turbine inlet temperature, by reactor reflector motion, and Brayton speed to not exceed the blue line (constant reactor inlet temperature) on Figure 3-8.

Table 3-9 shows operating points that yield the highest cycle efficiencies for 2-2-2s and 3-3-3s plant architectures. Note that for a 2-2-2s plant architecture, a reduction of 18.5% in rotational speed, 45,000 to 36,668, and a reduction of reactor outlet temperature from 1150 to 1091 K is required to operate steady state at 50% alternator load capacity. Due to the cycle efficiency penalty of operating additional engines at lower speed, and lower turbine inlet temperature, the reactor and heat rejection system need to be sized larger to support full power operation. Additional detail regarding this mode of operation is provided in Reference 3-2.

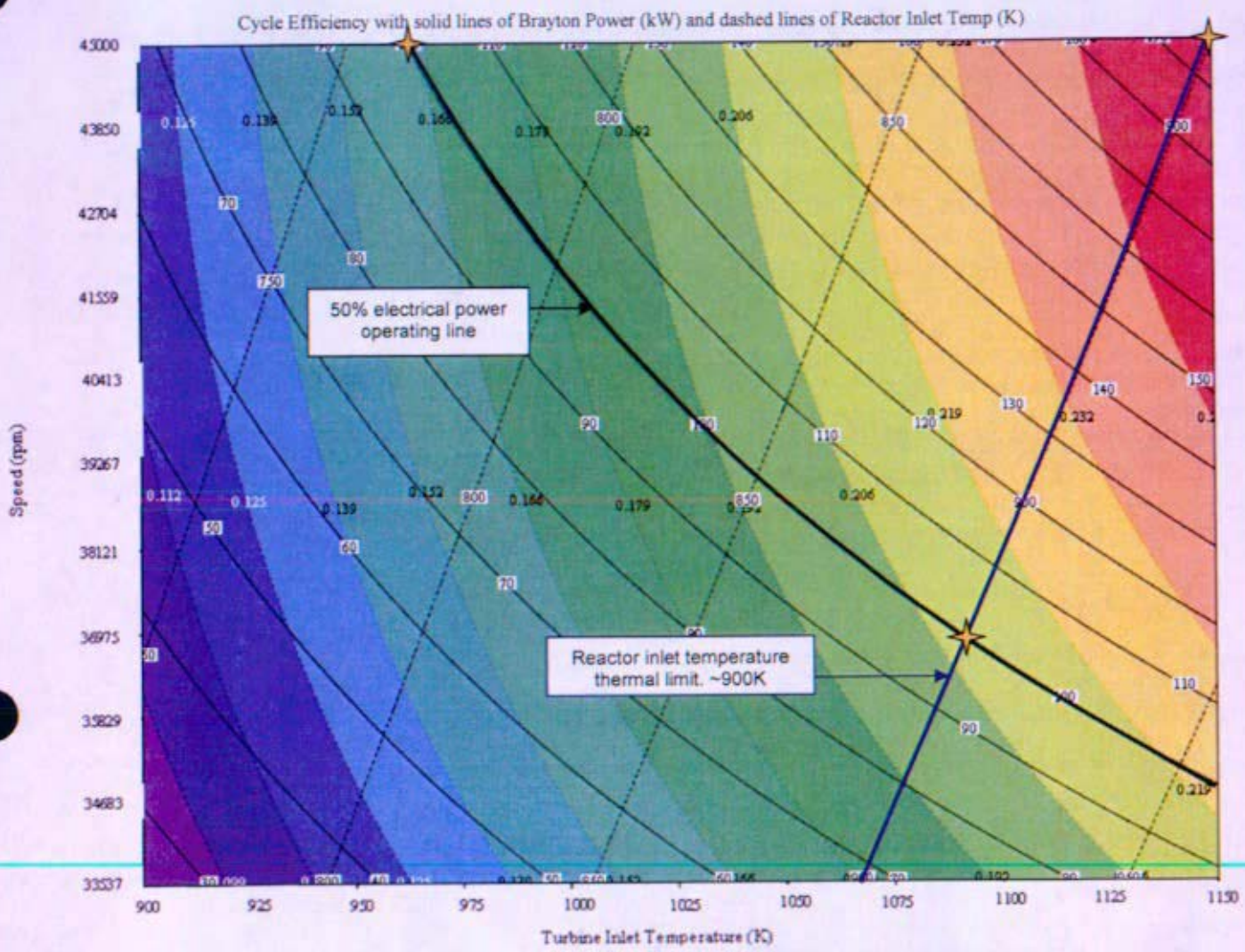



**Figure 3-8: Dual Brayton Operating State Points Map for 2-2-2s Architecture**

**Table 3-9: Dual Mode - Plant Architecture Performance**

| | **Mode 1** (2 or 3 engines operating) | | | | | **Mode 2** (1 or 2 engine(s) operating, one idle) | | | | |
|---|---|---|---|---|---|---|---|---|---|---|
| System Architecture | Turbine Inlet Temperature (K) | Rotational Speed (RPM) | Conversion Efficiency (%) | Reactor Power (kWth) | Heat Rejection Power (kWth) | Turbine Inlet Temperature (K) | Rotational Speed (RPM) | Conversion Efficiency (%) | Reactor Power (kWth) | Heat Rejection Power (kWth) |
| 2-2-2s | 1091 | 36668 | 20.8 | 970 | 750 | 1150 | 45000 | 25.9 | 783 | 559 |
| 3-3-3s | 1115 | 39840 | 19.3 | 1042 | 882 | 1150 | 45000 | 21.8 | 932 | 698 |

## 3.12 Number of Heat Exchangers

It may be desirable to house individual recuperators or gas cooler heat exchangers within a common pressure boundary to achieve certain design objectives; e.g. minimize mass, improve reliability, facilitate system arrangement. The potential for gas leakage increases with the pressure boundary surface area and the number of pressure boundary joints (welds). Therefore, pressure boundary area and number of pressure boundary joints should be minimized. Housing heat exchangers within a common pressure boundary, or sharing sides between two heat exchangers, would effectively minimize system pressure boundary surface area while retaining separation of converter loop flow paths.

Sharing heat exchangers between converter loops, where converter loop flow paths could combine, is another means of potentially achieving the design objectives listed above. However, plant configurations that utilize cross-strapped heat exchangers would require additional valves to properly isolate idle converter loops. The mass reductions obtained by eliminating redundant heat exchangers may be offset by the mass these additional valves and the resulting increased system pressure drop. Similarly, system reliability could be improved or degraded with the elimination of redundant heat exchangers associated additional valves.

## 3.13 Valve Operations

For any system with spare turboalternators, check valves or isolation valves would be required to minimize reverse flow through the idle loop(s). While these valves do not see high operating temperature (300-500 K), they do need to operate reliably after long periods in a fixed position. While gas valves can and have been used in previous space applications, gas valves of the size considered here (10-12 cm diameter) are considered to be developmental. Not all valve faults would result in mission ending failures. For example, if a check valve in an idle loop failed to function properly, reverse flow would be initiated in that loop. This would result in a reduction in reactor flow and could potentially damage turbomachinery bearings in the affected loop, rendering it inoperable. However, use of the remaining loops would still be possible. See Section 9.5 for additional discussion.

Configurations that incorporate shared heat exchangers require isolation valves in hotter portions of the loop. In order to share a recuperator and gas cooler, multiple valves are required to successfully switch from an operating Brayton unit to a spare unit. The number of valves is further increased in this case given the bearing and alternator cooling arrangement that draws cold gas from the compressor inlet. Some of these valves must operate at the turbine exit conditions (~900 K).

## 3.14 Number of Alternator Stator Windings or Alternators

In addition to the number of Braytons units, the number of alternator windings or alternators must also be considered. The addition of redundant alternators or stator windings within a Brayton unit provides a higher degree of fault tolerance at the expense of additional mass, volume, and rotor-dynamic complexity. Plant configurations where one Brayton unit is normally providing the full plant output (1-1-1 and 2-1-1) require dual alternators or dual stator windings to maintain single point failure tolerance of some electrical system faults. Furthermore, electrical systems are subject to a large number of temporary faults which may make dual alternators or dual stator windings necessary for a sufficiently reliable system. A complete explanation of alternator failure modes is provided in Section 9.1.8.

The mass penalty associated with redundant alternators is ~10 kg for a 100 kWe alternator and ~20 kg for a 200 kWe alternator. The additional mass for a second set of stator windings is less than the mass of an additional alternator. Most of the failure modes that are made survivable with redundant alternators are made survivable when dual stator windings are utilized. The increased mass and changes in rotor geometry that would result from the use of dual alternators would require additional study and analysis of the Brayton rotor dynamics.

## 3.15 Alternate Means for Momentum Compensation – Use of Reaction Wheels

In the PB1 spaceship configuration, every effort was made to reduce the need to compensate for momentum developed by the rotating turbomachinery. For example, counter-rotating units are preferred and the orientation of the Brayton units is such that the axis of rotation is perpendicular to the long axis of the spaceship. Any spaceship architecture that does not incorporate counter-rotating turbines may require some other means of momentum compensation to counteract Brayton unit momentum and to compensate for torque developed during Brayton speed changes. The initial mass estimate for an appropriately sized reaction wheel is ~25 kg. This mass penalty is considered small relative to the increase in mass and system complexity associated with the addition of a counter-rotating Brayton unit. Momentum compensation wheels are a standard spacecraft technology and have been designed and used by the space industry. The PB1 spaceship configuration incorporates reaction wheels in the mission module for spaceship orientation control. Due to their location, these reaction wheels may not be able to adequately compensate for angular momentum vectors developed by operation of turbomachinery at the opposite end of the boom during periods when spaceship orientation control is particularly critical. An additional spaceship study is required to probe the validity of this concern.

## 3.16 Impact on Interface Systems

### 3.16.1 PCAD Subsystem

Spacecraft electrical power systems have traditionally employed multiple distribution buses for fault tolerance. This allows for continued operation of spacecraft functions with one or more failures in the electrical buses, the switches connecting loads to the buses, or the load circuits themselves. The same was true for the Prometheus spaceship. The PB 1 PCAD architecture called for a separate electrical bus for each Brayton unit, with each load capable of receiving power from any electrical source. The same approach must also be used in considering PCAD arrangements for the system architectures described above, including the 1-1-1 configuration with dual alternator windings (i.e. a separate bus for each alternator winding).

The largest impact on the PCAD subsystem posed by the system architectures described above is the desire to operate the spaceship electrical buses at multiple frequencies and voltages (the result of operating the Brayton units at multiple speeds). Typically, power electronic circuits are designed for a specified input voltage and frequency in order to provide optimum performance and power quality. Some latitude in their input may be allowable, but an input variation of greater than 10-15% in voltage and frequency may require additional hardware (e.g. special transformers, larger filter circuits and rectifiers). The mass impact of the additional hardware would be most significant in the configurations where multiple Brayton speeds are used during thrusting phases of the mission, as the largest amount of power is consumed by the power processing units (PPUs). The HRS pump power supplies, some of the science loads, and the power downconverter for the spaceship computers are also powered

from the Brayton units' electrical buses and would likewise be affected, but the mass impact of alternate circuit designs with these loads would be less because of the small percentage of power they consume.

If the desired speed variation is large, or if more than two operating speeds are required, a DC electrical system with rectifiers connected to the Brayton outputs should be considered. A DC electrical system would make all of the spaceship loads immune to the changing Brayton speeds, but the added rectifier circuits would make it heavier than a comparable AC plant.

### 3.16.2 Heat Rejection Segment

A block diagram schematic of the interface of the converter loops with the HRS for a system architecture using four Brayton energy conversion loops that are each capable of generating 50% electrical power (4-4-4) is given in Section 9.6. The ability to integrate two HRS fluid loops to each radiator panel is desirable for any system architecture. This redundancy is considered a key design element as it allows for full power operation in the event of failure of one HRS loop or energy conversion loop. The interface of converter gas loops to the heat rejection segment loops for several other plant architectures is described in Section 9.3. The 3-3-3s system architecture presents a challenge with regards to achieving the desired redundancy and fault tolerance features in a way that does not result in the potential for an unbalanced flow condition between the three converter loops.

## 3.17 References

**3-1** KAPL letter SPP-67110-0005, Bettis letter B-SE-0077, "Space Nuclear Power Plant Concept Selection, For NR Approval", dated 3/4/05.

**3-2** KAPL letter SPP-SEC-0035, "Brayton Cycle Off-Design Performance", dated 1/25/06.

# Section 4
# Mass Estimates and Basis

(Intentionally Blank)

# Mass Estimates and Basis

## Table of Contents

4 Mass Estimates and Basis ..... 5
4.1 Purpose ..... 5
4.2 Background ..... 5
4.3 Summary and Conclusions ..... 5
4.4 Overall SNPP Mass ..... 6
4.5 Mass Discussion ..... 7
4.5.1 Reactor Segment ..... 7
4.5.2 Reactor Radiation Shield Segment ..... 8
4.5.3 Reactor Coolant Segment ..... 9
4.5.4 Heat Rejection Segment ..... 12
4.5.5 Reactor I&C Segment ..... 13
4.5.6 Plant Structure and Environmental Protection Segment ..... 14
4.5.7 Aerothermal Protection Segment ..... 14
4.5.8 Power Conditioning and Distribution (PCAD) ..... 14
4.5.9 Mass Variation from Concept Selection ..... 15
4.6 Mass Comparison with JPL Final Report ..... 18
4.7 References: ..... 20

## List of Figures

Figure 4-1: Mass Comparison for Key System Architectures ..... 7
Figure 4-2: Current 4-4-4 Best Estimate Mass Compared to Concept Selection ..... 15
Figure 4-3: Mass Differences between Current 4-4-4 Architecture and Concept Selection Mass Estimate ..... 16
Figure 4-4: JPL Mass Estimate Comparison ..... 19

## List of Tables

Table 4-1: System Architecture Mass Summary ..... 9
Table 4-2 Reactor Coolant Segment Mass Calculation ..... 12
Table 4-3: PCAD Mass summary ..... 15
Table 4-4: Reactor Module Mass Estimate from JPL Final Report ..... 18

(Intentionally Blank)

# 4 Mass Estimates and Basis

## 4.1 Purpose

The purpose of this section is to summarize the component mass estimates presented in the other sections of this report and to develop system mass estimates for the Space Nuclear Power Plant (SNPP) pre-conceptual design cases. The masses presented herein are best estimates and do not include margins or uncertainty allowances.

## 4.2 Background

Mass is a significant concern in spacecraft design due to the capability of the available launch vehicle and the propulsion/trajectory solutions. In Reference 4-1, mass was used as a discriminator in concept selection. Mass allocations must be assigned early in the design process and carefully tracked throughout the project. The NRPCT has been developing the methodology for estimating the mass of reactor module components. Mass estimates for the Reactor, Reactor Radiation Shield, Plant and Structural segments have been developed and, while still in the early stages, have been documented in this report so that future refinement of the reactor module concept will have a basis for better mass estimates. While the Heat Rejection Segment (HRS) and the Power Control and Distribution (PCAD) subsystem were not part of the NRPCT portion of the spacecraft, the masses associated with them must be included in the overall SNPP mass to get a complete and accurate representation of how the power plant mass changes for different system architectures.

## 4.3 Summary and Conclusions

The SNPP mass depends on the specific reactor design, materials of construction and the number of energy conversion components chosen. The number of components and how they are operated affect the efficiency of the conversion process and thus the thermal ratings (and therefore the masses) of the Reactor and the Heat Rejection Segments. The Reactor Segment mass is also affected by the material of construction and core geometry. Because the details of the reactor design have not been selected, a range of SNPP masses is possible. Bounding estimates of the reactor module mass were calculated based on the 1-1-1 and 4-4-4 energy conversion equipment system architectures described in Sections 3.3 and 3.10 respectively. All mass estimates provided herein assume the use of a fast spectrum, unmoderated, MoRe reactor core using $UO_2$ as a fuel. Since no specific reactor geometry or material has been selected, an average reactor and shield mass was calculated based on information in Reference 4-5. The mass variation associated with reactor core geometry and material options is discussed in detail in Reference 4-5.

Several conclusions can be drawn from the mass estimating that was done. They are:

- The 1-1-1, 2-1-1 and 2-2-2 system architectures are within the JPL/NGST Reactor Module mass estimates for the Prometheus Baseline 1 (PB1) concept (see Section 4.6).
- Thermal power rating has the single largest influence on SNPP mass. For example, if the system efficiency is 20%, a 10 kWe reduction would result in a 50 kWt reduction in thermal power and associated reductions in reactor mass, reactor radiation shield mass, and HRS mass. A rough order of magnitude mass reduction of 350 kg would result.
- All mass estimates could potentially be reduced by:

  - Optimizing the physical arrangement to minimize pressure drops and piping lengths. This would lower reactor thermal power by raising cycle efficiency.
  - Optimizing the operating parameters using the sensitivity studies that are documented in Section 6.
  - Coupling the plant with one of the lighter reactor geometry/material concepts.
  - Optimizing the trade of HRS radiator area versus reactor thermal rating.
  - Trimming the reactor radiation shadow shield for a more specific spaceship configuration (eliminate shielding in zones having no equipment).
  - Optimize the spaceship shield mass trade among reactor shielding, mission module shielding and boom length.
  - Using lightweight materials such as carbon-carbon composite, and titanium alloys in heat exchangers vice the nickel-base superalloys that were assumed
  - Coupling the recuperator with the gas cooler within the same housing and no connecting piping.
  - Use aluminum cabling in the PCAD subsystem instead of heavier copper cabling.
  - Relaxation of the radiation hardening requirements for the spacecraft electronics to reduce shield mass.
  - For the range of parameters analyzed herein, an increase in launch vehicle capability that would allow an increased radiator area may allow operating the HRS at a lower temperature and may result in a reduced mass.
- The 1-1-1 SNPP mass is the lowest and substantially lower (~2000 kg) than a fully redundant system (2-2-2s).
- The mass savings that would be gained by sharing a recuperator, in some cases, would be essentially offset by the mass of the added piping and valves that would be required for cross strapping.
- The mass of the reactor and reactor radiation shield combination is very sensitive to the overall dimensions of each reactor concept (diameter, length), the configuration of the fixed reflectors and control devices (drums vs. sliders) and the proximity of the core to the shield.

---

## 4.4 Overall SNPP Mass

The estimated overall SNPP masses for various system architectures, which include the estimated Heat Rejection Segment and PCAD subsystem masses, are shown in Figure 4-1. The reactor thermal power estimate for each system architecture is shown above the applicable bar. The system architectures marked by the letter 's' are dual speed cases (i.e. 2-2-2s would be two, 200 kWe Braytons operating at reduced temperature and speed together at 100 kWe each to produce a total of 200 kWe). The changes in Brayton loading would be accomplished by a means of both speed and temperature control. Additional detail regarding this mode of operation is provided in Section 3.11. The mass of the 2-2-2s case was estimated using Reference 4-7 estimates for thermal power. Specific reactor mass calculations were done for the 1-1-1 and 4-4-4 system architectures. The remaining reactor mass estimates are interpolations (based on thermal power) using these two calculated reactor masses. Summaries of the bases for the estimates are provided in Section 4.5.

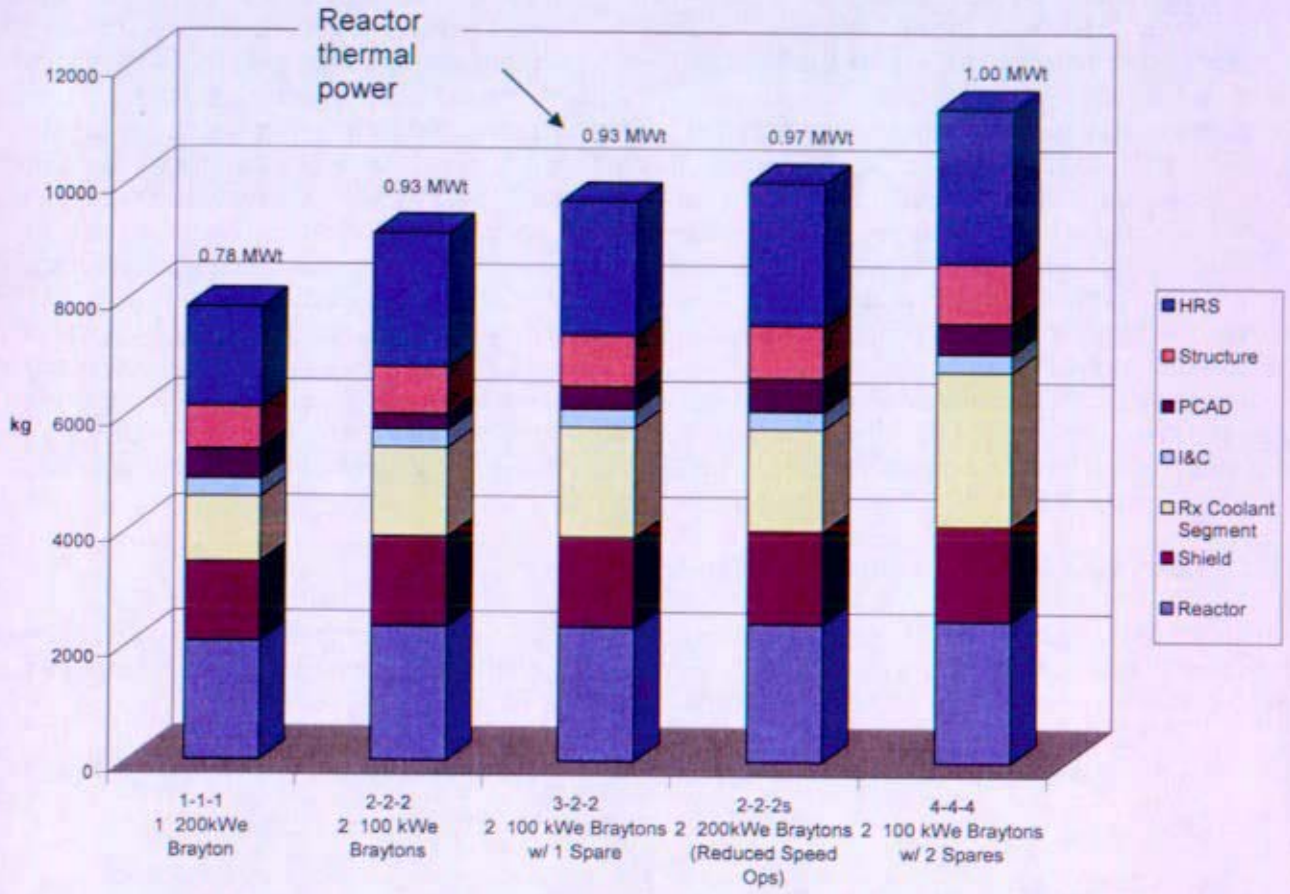



**Figure 4-1: Mass Comparison for Key System Architectures**

Notes:

1. 's' designates partial load control using a combination of speed and temperature control.
2. Mass estimates do not include the Aerothermal Protection Segment or Thermal Management Subsystem masses
3. Best-estimate mass values do not include uncertainty or design growth allocations

## 4.5 Mass Discussion

### 4.5.1 Reactor Segment

#### 4.5.1.1 Nuclear Reactor

Cores were sized for both the 1-1-1 and the 4-4-4 systems. The 1-1-1 and 4-4-4 system architectures were chosen as bounding cases and the reactor masses were calculated based on the thermal power associated with them. Both reactor designs incorporate solid ceramic $UO_2$ fuel pellets, a multi-micron coating molybdenum liner on a Mo47.5Re cladding. These modular annular flow block designs also make use of a Mo47.5Re modular block that provides annular flow guides to cool the fuel pins. All designs use a helium-xenon coolant with an average molecular weight of 31.5 g/mol at the plant design conditions identified on the heat balances described in Section 4.5.3. These reactors have been designed using the consistent methods and procedures as discussed in Reference 4-5 which are in accordance with both the Nuclear and Thermal/Hydraulic Design Bases of References 4-8

and 4-9, respectively. The reactor masses quoted for both designs were obtained from the Monte Carlo nuclear models for the specific design concepts. These nuclear models include the active radial reflector and its canning, as well as the reactor vessel (represented as a right circular cylinder). Within the core, the fuel, liner, clad, block, barrel, vessel thimble and axial BeO reflector pellets are included. Components that were not modeled include the control drive mechanisms, pressure vessel support skirt, and slider guide rails or drum drive axles. It has been identified that these additional components could increase the reactor mass calculated from the nuclear model by 40%, which has already been added to the masses as displayed in this section. A more complete description of reactor mass calculations is provided in Reference 4-6. Each energy conversion architecture described above results in a slightly different reactor thermal power rating. Reference 4-5 evaluated the impact on the reactor mass with the use of various core materials and core geometries. Of these design variations, the $UO_2$ fuel/molybdenum coated liner on a Mo47.5Re cladding refractory alloy annular flow block and open lattice designs were used to obtain a representative reactor mass. Since the reactor concept masses varied, an average reactor mass was calculated for these two cases and used herein for the comparison of different plant architectures. See Reference 4-5, for a more detailed explanation of how reactor masses vary for the different designs and material cases.

### 4.5.1.2 Movable Reflector Control Drive Mechanism

The Movable Reflector Control Drive Mechanism (CDM) System mass estimate of 221 kg was based on twelve CDMs each having a mass of approximately 18.4 kg. The preliminary mass estimate was based on a slider design and includes the following components:

- Position transducer
- Ball screw
- Ball nut
- Driveline
- Cover
- Flanges
- Motor
- Brake

The mass of the CDM system as well as the control material is included in the nuclear reactor mass estimate. Cabling to the twelve CDM motors was included in the Reactor I&C Segment. Reference 4-5 contains details of the CDM.

## 4.5.2 Reactor Radiation Shield Segment

The best-estimate value for Reactor Shielding mass was obtained using the Quick Mass Analysis for Reactor Shields Program (QMARS v2.0) developed by Oak Ridge National Laboratory and modified for NRPCT application and normalized to agree with Reference 4-3 mass estimates. Shield mass and dimensions are sized to limit the neutron fluence at the payload to no more than $5 \times 10^{10}$ n/cm$^2$ and the gamma dose at the payload to no more than $2.5 \times 10^4$ rads. Other areas of the propulsion plant forward of the payload will experience doses greater than this. Each reactor case of Reference 4-5 has a unique shield mass. This mass depends on parameters specific to the reactor design and the material composition of the shield. The parameters for the specific reactor designs of Section 4.5.1.1 were used to size a beryllium/$B_4C$ shield and estimate its mass.

The resulting QMARS output for the 1-1-1 and 4-4-4 architectures is shown below:

| Parameter | 1-1-1 Value | 4-4-4 Value |
|---|---|---|
| Shield Mass (kg) | 1502 | 1672 |
| $R_{6°}$ (cm) | 49.56 | 51.74 |
| $R_{12°}$ (cm) | 61.5 | 64.35 |
| $L_{shield}$ (cm) | 65.47 | 66.19 |

The above shield masses were used as a basis for estimating shields for system architectures other than 1-1-1 and 4-4-4. This estimation was a simple linear interpolation based on reactor thermal power. Reference 4-4 discusses the shield in more detail and how its mass depends on the materials of construction.

### 4.5.3 Reactor Coolant Segment

Details of the Reactor Coolant Segment component masses are given in the respective sections of this report. These individual masses were used in calculating a combined mass of each energy conversion architecture outlined in Section 6.

Table 4-2 shows how the masses for the components were combined to obtain the resultant total mass. The thermal rating for each component was calculated using a heat balance with the following common parameters:

Reactor Outlet Temperature = 1150 K

Compressor Outlet Pressure = 2.0 MPa

Compressor Pressure Ratio = 2.0

He-Xe Coolant Molecular Weight = 31.5 g/mol

Electrical Power Rating = 185 kWe

Maximum Radiator Water Temperature = 505 K

Assumed one isolation valve and one check valve on the compressor outlet (except for the 1-1-1 case which requires no valves)

For each of the possible plant configurations, it was determined that, for mass estimating purposes, the individual energy conversion component thermal ratings could be approximated by one of four heat balances. Section 6 discusses the heat balances in more detail. Table 4-1 gives a summary of which heat balance and arrangement was used for each mass estimate.

**Table 4-1: System Architecture Mass Summary**

| Architecture | Heat Balance[1] | Thermal Power | Arrangement | Comments |
|---|---|---|---|---|
| 1-1-1 | Figure 6-1 | 780 kWt | Figure 5-26 | None |
| 2-1-1 | Figure 6-1 | 780 kWt | Figure 5-33 | None |
| 2-2-2 | Figure 6-3 | 930 kWt | Figure 5-23 | None |

| Architecture | Heat Balance[1] | Thermal Power | Arrangement | Comments |
|---|---|---|---|---|
| 2-2-2s | Figure 6-2/ Reference 4-7 | 970 kWt | Figure 5-23 | Heat balance used for energy conversion components, Rx, shield and HRS from reference |
| 3-3-3s | Figure 6-3/ Reference 4-7 | 1,040 kWt | Figure 5 24 | Heat balance used for energy conversion components, Rx, shield and HRS from reference |
| 3-2-2 | Figure 6-3 | 930 kWt | N/A | Piping mass was estimated using the 2-2-2 architecture |
| 4-2-2 | Figure 6-4 | 1,000 kWt | N/A | Piping mass was estimated using the 2-1-1 architecture |
| 4-4-4 | Figure 6-4 | 1,000 kWt | Figure 5-21 | None |

[1]The 4-Brayton heat balance used for the mass estimate was slightly modified (compressor inlet temperature) from Figure 6-4 so that full electric power could be generated.

It should be noted that the heat balances used for each system architecture had not been optimized. In particular, the 4-4-4 arrangement was found to need larger piping diameters to reduce reactor coolant pressure drops in the reactor coolant loop piping. This arrangement had not been optimized to incorporate the increased piping diameters, due to project termination. Hence, it is recognized that the 4-4-4 heat balance and associated mass presented herein is higher than expected and could be better optimized following revision of the 4-4-4 arrangement and determination of associated new piping pressure drops. Section 6 presents a partially optimized 4-4-4 heat balance. A preliminary mass assessment of this heat balance shows that the mass of the 4-4-4 arrangement could be reduced by as much as 1,500 kg.

The mass estimating techniques for the turbine are discussed in Section 9.1.2, the gas cooler in Section 9.3.5 and the recuperator in Section 9.2.2.6. Where arrangements were developed, the piping mass was calculated by taking the piping lengths and diameters directly from the associated arrangement (see Section 9.4.5) and using the following information to calculate piping masses.

Piping material: Inconel 617 with density of 8360 kg/m$^3$
Insulation material: Inconel 617 hollow spheres with density of 710 kg/m$^3$
Pipe wall thickness: per Section 9.4.3

Since all cases did not have a specific arrangements developed, the piping masses for the 3-2-2 and 4-2-2 were estimated using the other arrangements as a guide.

A description of the valve requirements and the vendor base that was being considered is given in Section 9.5. A rough estimate of valve masses was obtained using the Section 9.5 information and the following assumptions:

- Industry Check Valve masses based on information available for Enertech Nozzle Check Valves. These masses were estimated shipping weights for flanged carbon steel or AISI 316 or AISI 321 stainless steel valves.
- It was assumed that with the elimination of the flanges (space valves will be butt welded) and with design enhancements that a 50% reduction in check valve mass could be achieved for the space check valve applications.
- Industry Isolation Valve masses based on information available for VALTEK Shear Stream ball valves with butt weld connections and a pneumatic/spring operator.

- It was assumed that with design enhancements for the valve and operator that a 50% reduction in isolation valve mass could be achieved for the space isolation valve applications.

The resulting estimates for valve masses are:

| | |
|---|---|
| Isolation valve: | 18 kg/valve |
| 5 cm Check valve: | 4.5 kg/valve |
| 10 cm Check valve: | 17.5 kg/valve |

Table 4-2 shows the results of combining the masses in the 'Total' column. Each set of rows corresponds to one of the system architectures described in Section 6. Each component has a column that shows the rating of that component, the number required for the specific architecture, how much one component weighs and the total mass of that specific component.

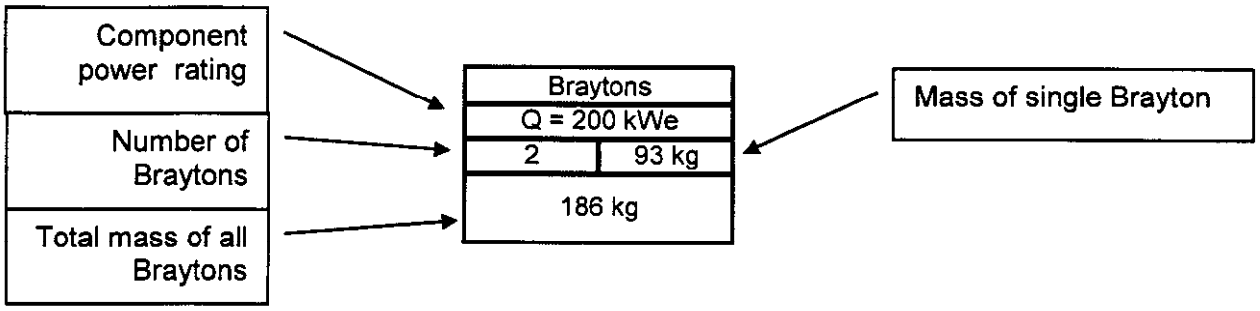


**Table 4-2 Reactor Coolant Segment Mass Calculation**

| Architecture | Braytons | Recuperators | Gas Coolers | Piping | Valves[1] | Total |
|---|---|---|---|---|---|---|
| 1-1-1 see Section 3.3 | Q = 200 kWe | Q = 1074 kWt | Q = 559 kWt | | | 1126 kg |
| | 1 @ 93 kg | 1 @ 299 kg | 1 @ 411 kg | | 0 | |
| | 93 kg | 299 kg | 411 kg | 323 kg | 0 kg | |
| 2-1-1 see Section 3.4 | Q = 200 kWe | Q = 1074 kWt | Q = 559 kWt | | | 1528 kg |
| | 2 @ 93 kg | 1 @ 299 kg | 1 @ 411 kg | | 4 + 4 | |
| | 186 kg | 299 kg | 411 kg | 516 kg | 116 kg | |
| 2-2-2 see Section 3.5 | Q = 100 kW | Q = 681 kW | Q = 349 kW | | | 1546 kg |
| | 2 @ 81 kg | 2 @ 193 kg | 2 @ 262 kg | | 2 + 2 | |
| | 162 kg | 386 kg | 524 kg | 403 kg | 71 kg | |
| 2-2-2 see Section 3.6 | Q = 200 kWe | Q = 1064 kWt | Q = 554 kWt | | | 1764 kg |
| | 2 @ 93 kg | 2 @ 296 kg | 2 @ 205 kg | | 2 + 2 | |
| | 186 kg | 592 kg | 410 kg | 505 kg | 71 kg | |
| 3-3-3 see Section 3.7 | Q = 100 kWe | Q = 681 kWt | Q = 349 kWt | | | 2025 kg |
| | 3 @ 81 kg | 3 @ 193 kg | 3 @ 175 kg | | 3 + 3 | |
| | 243 kg | 579 kg | 524 kg | 573 kg | 106 kg | |
| 3-2-2 see Section 3.8 | Q = 100 kWe | Q = 681 kWt | Q = 349 kWt | | | 1901 kg |
| | 3 @ 81 kg | 2 @ 193 kg | 2 @ 262 kg | | 12 + 4 | |
| | 243 kg | 386 kg | 524 kg | 488 kg | 260 kg | |
| 4-2-2 see Section 3.9 | Q = 100 kW | Q = 761 kW | Q = 397 kW | | | 2426 kg |
| | 4 @ 81 kg | 2 @ 214 kg | 2 @ 284 kg | | 8 + 8 | |
| | 324 kg | 428 kg | 568 kg | 874 kg | 232 kg | |
| 4-4-4 see Section 3.10 | Q = 100 kW | Q = 761 kW | Q = 397 kW | | | 2666 kg |
| | 4 @ 81 kg | 4 @ 214 kg | 4 @ 142 kg | | 4 + 4 | |
| | 324 kg | 856 kg | 568 kg | 776 kg | 142 kg | |
| Architecture | Braytons | Recuperators | Gas Coolers | Piping | Valves[1] | Total |

[1]Valves list the estimated number of isolation valves + check valves

### 4.5.4 Heat Rejection Segment

The Heat Rejection Segment was not an NRPCT cognizant segment. The mass estimates were done using the heat balances of Section 6 as an input to a NASA Glenn mass estimating tool (SRPS Opt) and the following assumptions:

- Working fluid is water
- Maximum inlet temperature of 505K
- Materials consist of titanium pressure boundary and carbon-carbon facesheet panel fins
- Four transport loops each with two pumps and accumulator
- Titanium heat pipes with water working fluid

- Includes micrometeoroid shield, survival heaters, clamps, insulation for the transport loops
- No deployment system or panel support structure mass has been included

Additional detail of the geometry of the radiator panels and heat exchanger connection to the transport loops are shown in Section 9.6.

### 4.5.5 Reactor I&C Segment

The current best-estimate value for Reactor Instrumentation and Control segment, 321 kg, is based on projected Reactor Module I&C needs for the JIMO mission.

The following assumptions for the Reactor I&C system were made to provide a basis for this mass estimate:

a. The reactor system design is assumed to be as documented in Reference 4-1. It is assumed that 12 sliders are utilized for reactivity control, and one safety rod is withdrawn at plant startup and not used. It is also assumed that there are between one and four loops with one Brayton Generator per loop (and two valves per loop, unless there is only one loop). The reactor system design is extensible to control drums if required.

b. There are four independent control channels and independent sensors are used for each channel (e.g. there are four independent sensors measuring the same parameter – one connects to each channel) with the following exceptions: continuous slider position indication (one sensor per slider), discrete slider position, discrete valve and safety rod position, and fission product level (one sensor overall not used for control but only for information-gathering).

c. Assuming 12-slot card racks are used; this architecture can be implemented using six card racks, 10 unique card types, and 45 total cards (41 if analog circuitry is combined onto another card).

d. The alternator is designed to produce 440 volt AC electrical power to operate the spacecraft systems and provide propulsion power.

e. All Reactor I&C circuits will be located at the aft end of the spacecraft inside the same shielded compartment as the Power Conditioning and Distribution (PCAD) controller and electronics, and the Command & Data Handling (C&DH) subsystem.

f. All reactor functions will be controlled directly by the Reactor I&C segment, and not by other spacecraft subsystems.

g. A direct communication link with the spacecraft PCAD controller will be provided.

The Reactor Controllers control the reactor and maintain continuity of electrical power to the spacecraft based on sensor inputs. The reactor sensors include, but are not limited to, hot leg temperature, cold leg temperature, pressure, flow, neutron flux, fission products, continuous control device assembly position, and discrete valve and control device assembly positions. Details of the mass for circuit cards, sensors and cabling are contained in Reference 4-2 and are summarized below.

| I&C System Mass | Total mass 4-4-4 (kg) |
|---|---|
| Circuit Cards & Card Racks (with Analog Interface cards) | 106 |
| Sensors and Actuators | 25 |
| Cabling | 190 |
| **Total** | **321** |

A similar analysis was done for the single Brayton system that resulted in a mass of 305 kg

### 4.5.6 Plant Structure and Environmental Protection Segment

The design of the Reactor Module structure has not progressed to the point of having a mass estimate based on a specific design. Based on discussions with NASA JPL, it was estimated that 12% of the reactor module mass would be the supporting structure. This includes the shielding structure and the primary support structure but does not include HRS structure or spacecraft boom.

The Thermal Management and Micrometeoroid Protection Subsystem masses are not yet known and are not included in the overall Reactor Module mass. Reference 4-10 estimates the Thermal Management Subsystem mass at 75 kg.

### 4.5.7 Aerothermal Protection Segment

No mass estimates were done on the Aerothermal Protection Segment (or Aeroshell). Thus, mass of this segment has not been included in the overall Reactor Module mass. It is anticipated that the aeroshell would be separated from the Reactor Module prior to reactor startup. Therefore, its mass is important for launch vehicle capacity, but not for interplanetary trajectory calculations. Reference 4-10 estimates the aeroshell mass at 143 kg.

### 4.5.8 Power Conditioning and Distribution (PCAD)

The PCAD Subsystem is not an NRPCT cognizant subsystem. Thus, a complete mass evaluation of PCAD mass has not been performed by the NRPCT. However, PCAD mass depends heavily on the number of energy conversion units and how they are controlled, so some evaluation of this subsystem has been performed.

PCAD mass is dominated by the cabling from the alternators to the spacecraft bus. Table 4-3 shows estimates of the PCAD cabling for the various system architectures. In each case, the cabling mass was calculated assuming a 3% electrical loss. Conductors are copper and the mass excludes insulation. Use of aluminum conductors is estimated to reduce these conductor masses to approximately 41% of the mass shown in Table 4-3.

For the 1-1-1 case, two full rated cables have been included, assuming that the alternator has two independent stator windings. This configuration is required to maintain single fault tolerance in the PCAD subsystem.

For the 2-2-2s and 3-3-3s cases, 50 kg additional mass has been added for tap-changing transformers in the PPUs. These additional components may be needed to maintain constant PPU operating voltage at the partial speed conditions of these two cases.

**Table 4-3: PCAD Mass summary**

| System name[1] | Number of Braytons | Full Load Speed (RPM) | Brayton Power (kWe) | Mass (kg) |
|---|---|---|---|---|
| 1-1-1 | 1 | 45000 | 200 | 520 |
| 2-2-2 | 2 | 45000 | 200 | 260 |
| 2-2-2s | 2 | 45000 | 200 | 570 |
| 3-3-3 | 3 | 45000 | 100 | 390 |
| 3-3-3s | 3 | 45000 | 100 | 440 |
| 4-4-4 | 4 | 45000 | 100 | 520 |

[1]s designates partial load control using a combination of speed and temperature control.

### 4.5.9 Mass Variation from Concept Selection

Reference 4-1 included a best estimate mass of approximately 6,500 kg for the 4-4-4 system. This mass was calculated by NRPCT using an extrapolation from a NASA Glenn mass estimating tool (SRPS Opt) substituting a gas reactor for the liquid lithium reactor used by NASA. This compares with a current best estimate mass for a 4-4-4 system of 11,300 kg. This is an increase in estimated mass of 4,750 kg. Figure 4-2 shows a graphical representation of the masses of the current 4-4-4 system and the mass reported in the concept selection report for the same system.

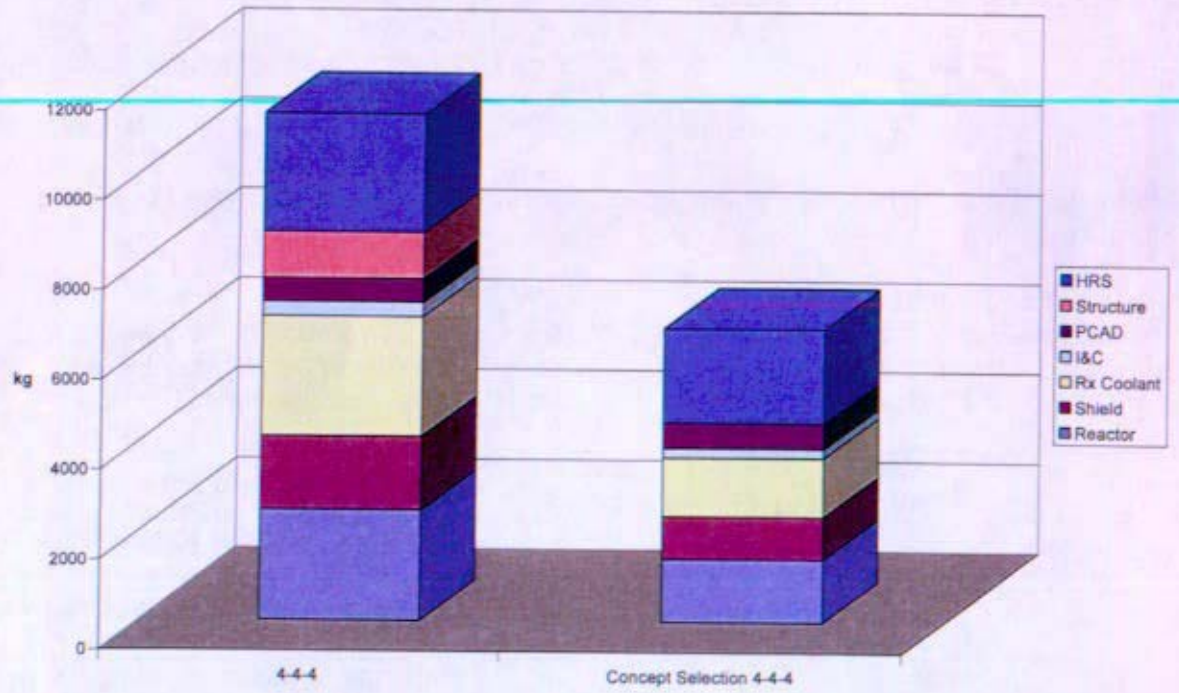



**Figure 4-2: Current 4-4-4 Best Estimate Mass Compared to Concept Selection**

Each portion of the total mass increased as shown in Figure 4-3 below. The following sections explain why the mass has increased from the Reference 4-1 values.

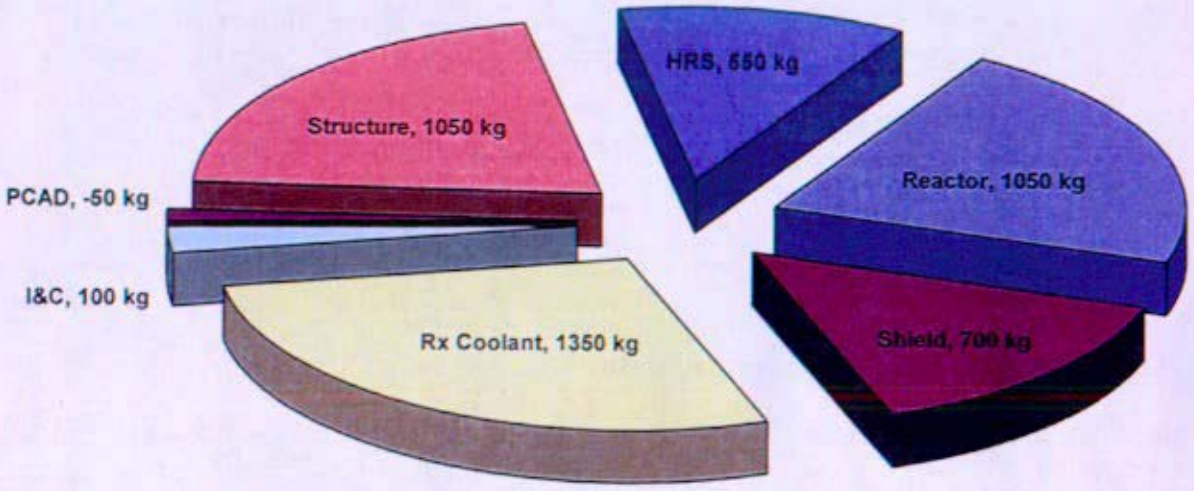



**Figure 4-3: Mass Differences between Current 4-4-4 Architecture and Concept Selection Mass Estimate**

**Reactor Segment Mass**

The reactor mass increase resulted from the following differences:

- Power level increase from 810 kWt to 1000 kWt
- Change in reactor mass factor from 1.1 to 1.4 to account for portions of the reactor not explicitly modeled (Reference 4-6)
- Core material changes from Nb1Zr to Mo47.5Re and fuel from UN to $UO_2$

More information on the changes in the reactor design that resulted in the mass increase can be found in Reference 4-5.

**Reactor Coolant Segment Mass**

The total reactor coolant mass, which includes the energy conversion equipment, increased by 1,235 kg. Each component in the reactor coolant system experienced a mass increase from that stated in the concept selection report. These differences are discussed below.

| Component | Mass Difference (kg) | Percent Increase | Comments |
|---|---|---|---|
| Turboalternator | 110 | 50% | 30 kg per unit due to heat balance differences |
| Recuperator | 320 | 60% | 80 kg per unit due to heat balance differences |
| Gas Cooler | 260 | 85% | 65 kg per unit due to change of heat rejection segment working fluid to water and minor heat balance differences |

| Component | Mass Difference (kg) | Percent Increase | Comments |
|---|---|---|---|
| Piping | 630 | 360% | Increase in piping diameter, wall thickness and inclusion of internal insulation; detailed arrangements used to determine lengths |
| Valves | 140 | 100% | No valves included in concept selection |

**Primary Support Structure**

The structure mass increase resulted from the following differences:

- Minimal mass of structural support was included in the Concept Selection process
- The current concept estimated that 12% of the total reactor module mass would be from the structure
- The spacecraft boom was not included in either estimate

**Reactor Shield Mass**

The reactor shield mass increase resulted from the following differences:

- Reactor size changes due to power increase
- Power level increase effect on shielding effectiveness
- Normalization of the QMARS mass estimating tool to NRPCT design goals

More information on the changes in the reactor shield that resulted in the mass increase can be found in Reference 4-4.

**Heat Rejection Segment**

The heat rejection segment mass increase resulted from the following differences:

- Increased thermal load due to power increase (mass increase)
- Change of working fluid from NaK to water (mass decrease)

**PCAD and I&C**

A minor increase in the Reactor I&C segment was seen. The PCAD mass decreased slightly (52 kg) because the NRPCT estimate only includes conductors.

## 4.6 Mass Comparison with JPL Final Report

Reference 4-10 discussed the mass summary for the entire spaceship. In the Reference 4-10 summary, details of the reactor module were given. These masses are shown in Table 4-4.

**Table 4-4: Reactor Module Mass Estimate from JPL Final Report**

| Segment of SNPP | JPL Final Report Reactor Module Mass Estimate[1] [kg] | Notes |
|---|---|---|
| **Reactor Segment** | 2,823 | |
| **Reactor Radiation Shield Segment** | 807 | Unknown materials of construction |
| **Reactor I&C Segment** | 373 | |
| **Reactor Coolant Segment** | 1,954 | 4-4-4 system architecture |
| **Heat Rejection Segment** | 2,019 | |
| **PCAD Segment** | 958 | |
| **Structure** | 940 | Not specified in JPL report. This 940 kg has been added by NRPCT for comparison purposes |
| **Total:** | ~9,850 | |

[1]Includes an 80% uncertainty allowance and a 250 kg design growth allowance

Comparing these JPL masses with the NRPCT estimates shows that the NRPCT 1-1-1, 2-2-2 and 3-2-2 plant configurations all fall below the JPL estimate. The 1-1-1 NRPCT estimate has a margin of 2,050 kg to the JPL mass. The NRPCT 4-4-4 plant configuration comes in 1,400 kg over the JPL estimate. This is shown graphically in Figure 4-4.

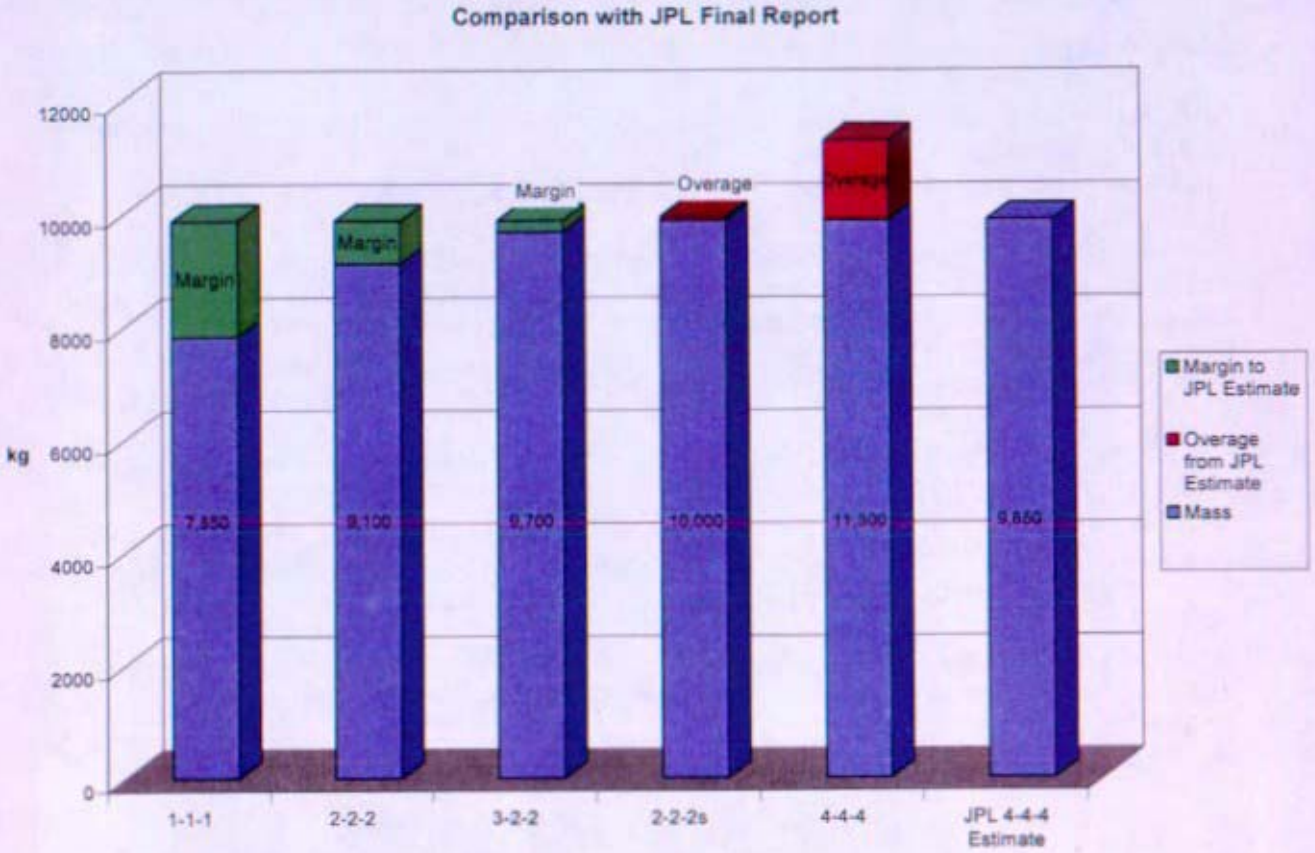



**Figure 4-4: JPL Mass Estimate Comparison**

Because these mass comparisons have been done using non-optimized heat balances and preliminary piping system arrangements, improvements in the masses from that estimated above is expected. These mass reductions would come from improved cycle efficiency resulting in lower thermal energy requirements. These efficiency gains would come from improvements in the piping arrangement and minor changes in the compressor outlet pressure, compressor pressure ratio, compressor inlet temperature and heat rejection water temperature. A first iteration on optimization of these parameters for the 4-4-4 heat balance, using the same preliminary piping system arrangement, is described in Section 6.3.6.8. This optimization resulted in a thermal power reduction from 1.00 MWt to 0.80 MWt for the 4-4-4 system. A rough mass estimate for this optimized 4-4-4 arrangement shows that the 4-4-4 SNPP mass could drop by 1,500 kg. Other system architecture masses could also drop but by a lesser amount. System efficiencies would continue to improve with additional piping system optimization and further refinement of operating parameter assumptions resulting in lower mass estimates for each of the architectures described in Figure 4-4. It should be noted that the NRPCT mass estimates do not include any explicit margin for uncertainty or design growth as the JPL estimate does.

The current designs do not account for implementation of control bands, degradation over time or micrometeoroid/environmental protection. Each of these factors will result in higher masses for each of the arrangements described above.

## 4.7 References:

4-1 KAPL/Bettis letter, SPP-67110-0005/B-SE-0077, "Space Nuclear Power Plant Concept Selection", dated 03/04/2005
4-2 Enclosure (1) to SPP-67610-0008, "Preconceptual I&C System Architecture", dated 10/20/2005
4-3 "Reactor Shield Optimization in Support of the Prometheus 1 Project Preconceptual Design Analyses", JA Bucholz, ED Blakeman, JO Johnson, Oak Ridge National Laboratory dated October 2005 ORNL/LTR/NR-PROM1/05-27
4-4 KAPL letter SPP-67210-0011, "Integrated Shield Design Summary", dated TBI
4-5 KAPL/Bettis letter, SPP-67410-0013/B-SE(RE)-0003, "Space Reactor Preconceptual Design Report", dated 01/27/2006
4-6 Bettis letter, B-SE(RE)CMD-0010 , "A Study of the Nuclear Model Mass and the Reactor Mass multiplier", dated 12/7/2005
4-7 KAPL letter SPP-SEC-0035, "Brayton Cycle Off-Design Performance", dated 01/25/2006
4-8 Joint KAPL/Bettis letter SPP-67410-0008/B-SE(RE)NE-0003, "Space Reactor Program, Pre-Conceptual Prometheus Space Reactor Nuclear Design Basis, for NR Information", dated 06/30/2005
4-9 Joint KAPL/Bettis letter B-SE(RE)THD-0010/SPP-67410-0011,"Space Power Program, Revision 1 of Preconceptual Thermal-Hydraulic Design Basis, for NR Information", dated 12/9/2005
4-10 JPL Report 982-R120461 "Prometheus Project Final Report ", dated 10/01/2005

# Section 5
# Arrangements

(Intentionally Blank)

# Arrangements

## Table of Contents

5 Arrangements ..... 6
5.1 Summary and Conclusions: ..... 6
5.2 Technical Observations ..... 9
5.3 Design Considerations ..... 10
5.4 Model Development ..... 12
5.4.1 3-3-3 System Architecture - Revision 1 ..... 12
5.4.2 3-3-2 with a Shared Gas Cooler System Architecture - Revision 1 ..... 17
5.4.3 3-3-3 System Architecture - Revision 2a and 2b ..... 19
5.4.4 4-4-4 System Architecture - Revision 1 ..... 21
5.4.5 3-3-3 System Architecture - Revision 3 ..... 23
5.4.6 4-4-4 System Architecture - Revision 2a, 2b, 2c ..... 24
5.5 Four Brayton Piping Sensitivity Study ..... 26
5.6 Trade Study ..... 27
5.6.1 Arrangement Concepts involved in Trade Study ..... 27
5.6.1.1 1-1-1 System- Revision 1 ..... 27
5.6.1.2 2-2-2 System Architecture - Revision 1 ..... 28
5.6.1.3 3-3-3 System Architecture - Revision 4 ..... 29
5.6.1.4 4-4-4 System Architecture - Revision 2b ..... 29
5.6.2 Trade Study Results ..... 29
5.6.3 Additional Trade Study and Results ..... 31
5.7 Arrangement Concepts with Shared Components ..... 32
5.7.1 2-1-1 System Architecture ..... 32
5.7.1.1 2-1-1 System Architecture - Version 1 ..... 33
5.7.1.2 2-1-1 System Architecture - Version 2 ..... 34
5.7.1.3 2-1-1 System Architecture - Version 3 ..... 35
5.7.1.4 2-1-1 System Architecture - Version 4 ..... 36
5.7.1.5 2-1-1 System Architecture - Version 5 ..... 37
5.8 Future Actions ..... 37
5.9 References ..... 38

## List of Figures

Figure 5-1. Prometheus Baseline 1 ..... 7
Figure 5-2. Spaceship Stowed Within 5 Meter Diameter Fairing ..... 8
Figure 5-3. Original Reactor Module Space Envelope Provided by JPL/ NGST ..... 9
Figure 5-4. 3-3-3 System Architecture - Revision 1 ..... 13
Figure 5-5. Base case Brayton design ..... 14
Figure 5-6. Two dimensional schematic for basic plant configuration ..... 15
Figure 5-7. Hamilton Sundstrand initial gas cooler concept ..... 15
Figure 5-8. Recuperator in Power Conversion System (PCS) ..... 16
Figure 5-9. 3:3:2 with a Shared Gas Cooler System Architecture - Revision 1 ..... 17
Figure 5-10. Brayton engine ..... 18
Figure 5-11. 3:3:3 System – Revision 2a ..... 19
Figure 5-12. 3:3:3 System – Revision 2b ..... 19
Figure 5-13. Various valve concepts in Revision 2 ..... 20

Figure 5-14. Revision 2a exceeds space envelope ..... 21
Figure 5-15. Two Brayton PCS module ..... 22
Figure 5-16. 4-4-4 System Architecture - Revision 1 ..... 22
Figure 5-17. 3-3-3 System Architecture - Revision 3a ..... 23
Figure 5-18. 3-3-3 System Architecture - Revision 3b ..... 24
Figure 5-19. 4-4-4 System Architecture - Revision 2a Piping around both the shield and the CDMs . 25
Figure 5-20. 4-4-4 System Architecture - Revision 2b Piping around the Shield ..... 25
Figure 5-21. 4-4-4 System Architecture - Revision 2c Piping through the shield ..... 26
Figure 5-22. 1-1-1 System Architecture - Revision 1 ..... 28
Figure 5-23. 2-2-2 System Architecture - Revision 1 ..... 29
Figure 5-24. 3-3-3 System Architecture - Revision 4b ..... 29
Figure 5-25. Trade Study of 4 PCS Configurations ..... 30
Figure 5-26. 1-1-1 System Architecture ..... 31
Figure 5-27. 2-2-2 System Architecture ..... 31
Figure 5-28. Piping Modification Comparison for 1-1-1 and 2-2-2 System Architectures ..... 32
Figure 5-29. 2-1-1 System Architecture - Version 1 ..... 33
Figure 5-30. 2-1-1 System Architecture - Version 2 ..... 34
Figure 5-31. 2-1-1 System Architecture - Version 3 ..... 35
Figure 5-32. 2-1-1 System Architecture - Version 4 ..... 36
Figure 5-33. 2-1-1 System Architecture - Version 5 ..... 37

## List of Tables

Table 5-1. List of Design Considerations for Arrangement Models ..... 11
Table 5-2. 4-4-4 System Architecture - Comparison Three Version of Piping ..... 27

(Intentionally Blank)

# 5 Arrangements

## 5.1 Summary and Conclusions:

Several arrangements and associated trade studies were evaluated by the NRPCT based on estimates available for each component and the overall spaceship envelope. Spaceship constraints, which led to reactor module envelope targets, and individual component constraints, and system pressure drop were the primary influences for the arrangement models. It was anticipated that accommodation of thermal expansion and thermal management objectives would have heavily influenced future efforts. Although no specific arrangements were selected, the process of developing alternate arrangements was informative.

Numerous design considerations affected the size, orientation, and positioning of the components and subsequent assemblies. Design information and constraints were gathered by area of expertise from NRPCT members, from vendors, and from primary members of the Prometheus Project, (i.e., JPL and NGST). Some of the considerations are collected in Section 5.3.

The overall process is described in Section 5.4, followed by a discussion of trade studies and a view of future actions that would have been pursued.

Key conclusions are

- Adhering to the space envelope design constraint coupled with other design constraints, such as minimizing pressure drop, would be a challenge for configuration options having more primary components than a system with one Brayton, one recuperator, and one gas cooler.
- It would be difficult to configure more than two Brayton loops within the baseline design envelope (See Figure 5-3) without compromising system pressure drop or other performance characteristics. Changes in the baseline design envelope, which is driven by the shield shadow size and by packaging constraints within the fairing, would need to be considered in parallel with arrangement development efforts.
- Control of system angular momentum, in order to avoid interference with the science mission, could be a significant driver for arrangement of the Reactor Coolant Segment. Orientation of the Brayton units so that the momentum axis is orthogonal to the orbit plane limits the design space. Angular momentum of the primary coolant would also need to be considered. Placement of a momentum offload system (e.g., reaction wheel assembly), if necessary, should be considered part of early design trades.
- Advantages were identified for both functional and modular grouping of the components. Thermal management, piping, or structural concerns may be simplified by grouping components according to function (e.g., all coolers together). Modular placement, in which complete loops (Brayton, cooler, recuperator) are assembled and tested prior to installation may offer advantages such as more complete testing prior to installation and greater ease of installation. The reactor radiation shielding value of the component arrangements also will need to be considered.

- Routing of the pipes around the shield and CDMs would pose a significant arrangement challenge. Constraints for this routing, especially where and how the piping exits the shield and how to thermally isolate the CDMs from the piping, would need to be definitized early in the design process.

---

The initial layout of the spaceship was provided by Jet Propulsion Laboratory and Northrop Grumman Space Technology, and it formed a starting point for the NRPCT arrangements. The reactor module was located at the forward end of the spaceship as seen in Figure 5-1 below. In this configuration, the reactor module space envelope was influenced by the shield cone angle and the ability to stow the spaceship within an assumed five meter diameter launch vehicle fairing. Keeping within the cone angle of the shield protects the reactor module elements from reactor radiation and minimizes radiation exposure to other spaceship components, especially electronic equipment located in the mission module.

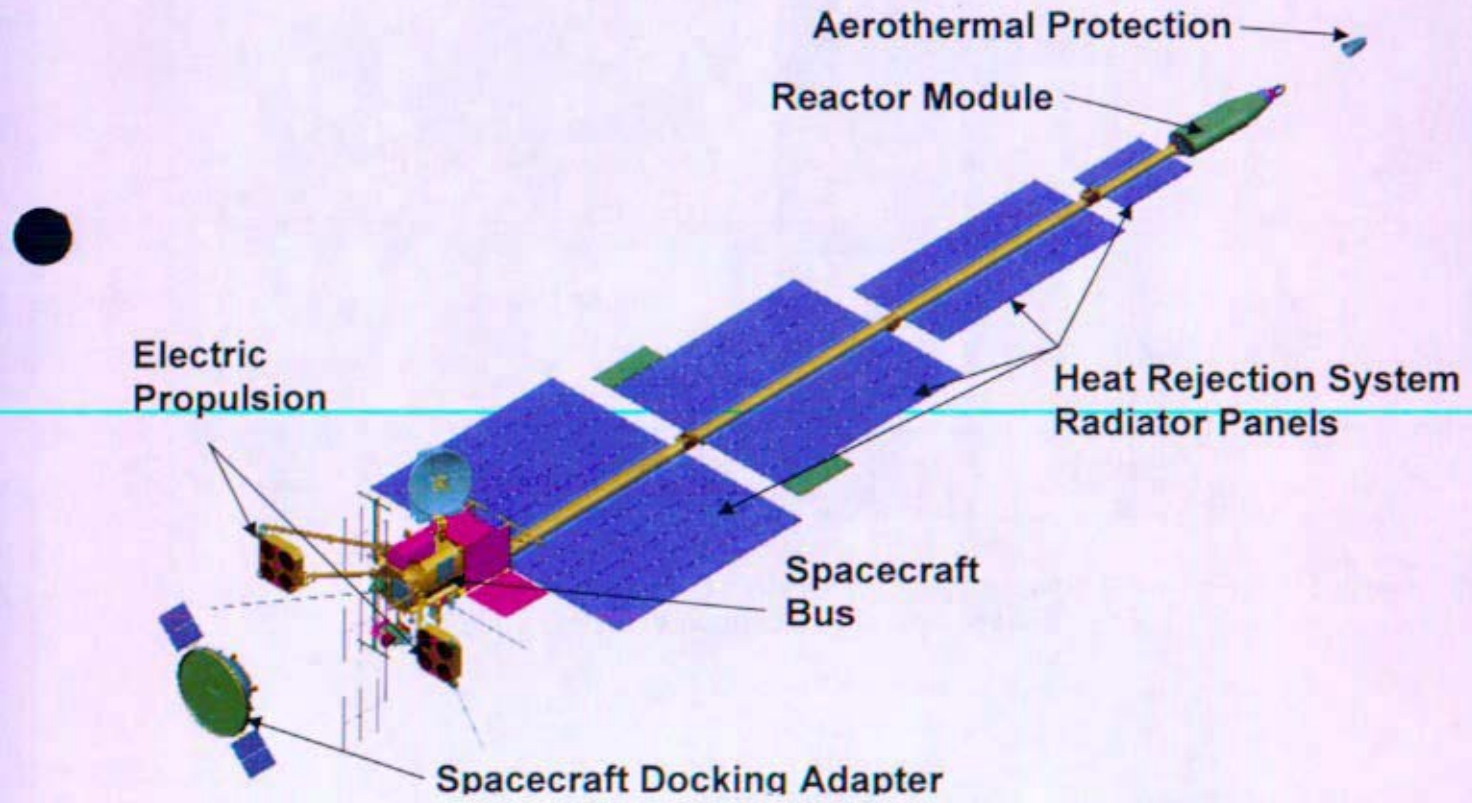



**Figure 5-1. Prometheus Baseline 1**

The folded configuration of the spaceship within the launch vehicle fairing limits the allotted design volume for the reactor module, as shown in Figure 5-2 The design volume, on the other hand, could be modified if either a larger launch vehicle is used, the stowed configuration of the spaceship is altered, or the shield cone angles are changed. The original dimensions of the reactor module space envelope can be seen in Figure 5-3 below.

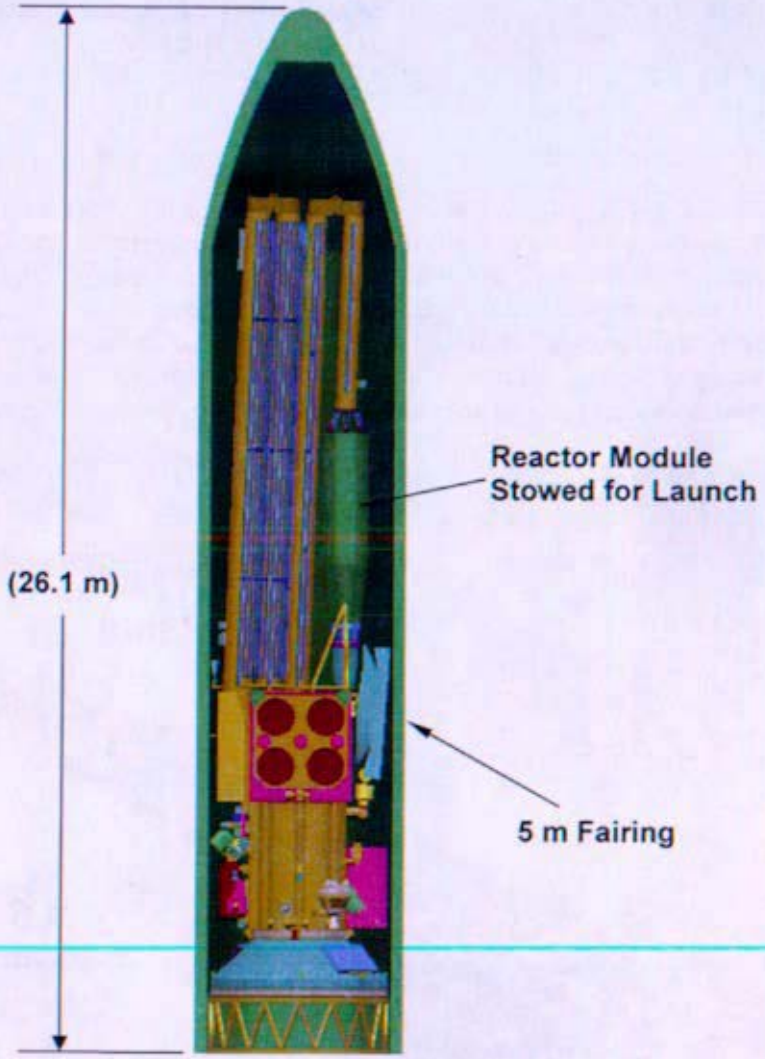



**Figure 5-2. Spaceship Stowed Within 5 Meter Diameter Fairing (Based on Delta IV Launch Vehicle)**

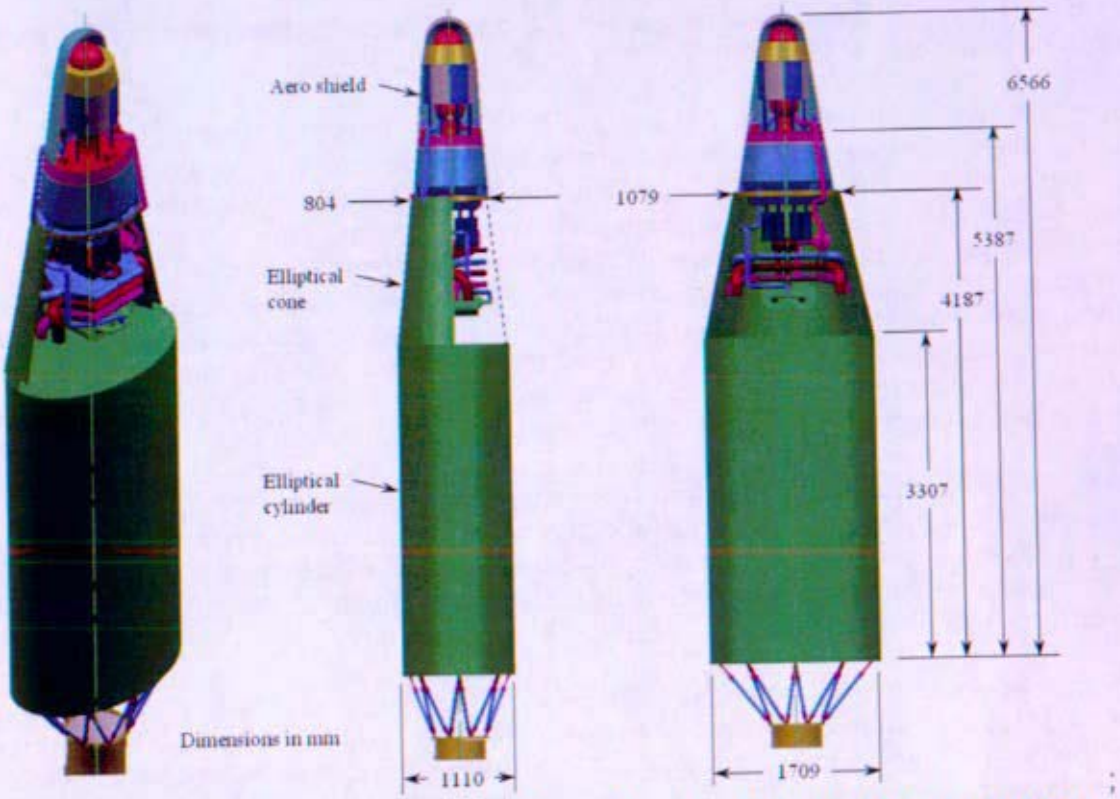



**Figure 5-3. Original Reactor Module Space Envelope Provided by JPL/ NGST**

## 5.2 Technical Observations

The layout concepts and arrangements of the reactor module yielded many valuable lessons and design constraints, including design envelope options, pipe routing and sizing effects, advantages and disadvantages of shared components among multiple energy conversion loops, and individual component design variations. Adhering to the space envelope design constraint coupled with other design constraints, such as minimizing pressure drop, became a challenge for configuration options having more primary components than a system with one Brayton, one recuperator, and one gas cooler. While remaining within the design envelope was difficult, the systems primarily exceeded the space envelope only in length so as to remain within the cone angle of the shield. Striking a balance between the volume required for the piping system and an appropriate size and bend radii of the actual piping for operational performance yielded different layout options for reactor modules with different numbers of components.

A trade study of four different energy conversion systems was performed and concluded that all systems were viable considering pressure drop, relative reactor module size, and total number of joints and welds in the piping, although none were optimized for system performance. The path of the piping was also affected by the number of independent and shared components. By decreasing the number of components, the size of the system within the design envelope was generally decreased. Design layout symmetry proved to be a successful method to decrease overall reactor module system size and allow straighter lengths of piping with larger diameters. Symmetry of Energy Conversion loops required additional component design, such as right and left hand rotating Brayton units, since the Brayton design itself is not symmetrical. The arrangement process was intended to study different

arrangements with varying numbers of components and various configurations to capture constraint and decision drivers during and after each arrangement study.

Six arrangement layouts (1-1-1, 2-1-1, 2-2-2, 3-3-2, 3-3-3, 4-4-4) were generated. The layouts vary by the number of main components referenced by "x-y-z" nomenclature. The designation of 1-1-1 or B-R-G is B is the number of Brayton units, R is the number of recuperators each sized to support the operation of one Brayton unit at its rated power and G is the number of gas coolers each sized to support the operation of one Brayton unit at its rated power. It does not indicate the number of individual recuperators or gas coolers. For example a 2-2-2 for a 200 kWe system with both Braytons running (no spares) would be two 100 kWe Brayton units with two recuperators and gas coolers, each sized to support a 100 kWe Brayton unit. Additional reactor module components that were modeled include reactor and associated components, piping, valves, heat rejection system components, such as pumps and accumulators, shielding, and the primary support structure.

A significant highlight in the arrangement modeling effort was a quantitative comparison of the 1-1-1, 2-2-2, 3-3-3, and 4-4-4 systems based on a list of metrics. The metrics encompassed the primary drivers for the system, including pressure drop, manufacturability, simplicity, and redundancy, among others. The quantitative comparison provided additional information to support the selection of the number of Braytons for Prometheus.

In addition, concepts with varying degrees of component redundancy, such as the 2-1-1 and the 3-3-2 with a shared gas cooler, were considered to evaluate reliability, extensibility, and other arrangement dependent metrics such as pressure drop. The 2-1-1 arrangement studies intentionally neglected mission specific space envelope constraints for a deep space mission to the Jupiter Icy Moons in order to explore pros and cons to arrangement options outside of our prior design space. Mission specific constraints, such as the space envelope or Brayton orientation, were lifted to assess all potential component geometric arrangements for clear solutions to arrangements issues or to obtain advantages for the system. Though mission specific constraints were lifted, individual component constraints were still incorporated into the possible layout. Constraint removal did not yield clear advantages over the other systems upon first review, but further trade studies would be needed to more fully explore the alternatives. The 3-3-2 with a shared gas cooler study maintained spaceship and individual component constraints. Both studies demonstrate the ability to arrange alternate concepts and understand advantages and disadvantages of these systems.

All revisions of the arrangement models afforded the NRPCT technical insight into the relationship between components, piping effects on pressure drop, component orientation, thermal concerns, manufacturability issues, and effects of mission on reactor and plant layout. Several other subsystems were to be incorporated, such as the Primary Support Structure, micrometeoroid protection, and aeroshell, which would lead to additional iterations and trade studies.

## 5.3 Design Considerations

One of the important outcomes of the arrangement efforts was the identification of design considerations. These considerations promoted the natural evolution of the arrangements process and are discussed throughout the descriptions of the individual arrangements. Table 5-1 lists some of the significant design considerations identified, with an accompanying explanation of the consideration or the impact as appropriate. Some of the items listed are also constraints, but are grouped together with considerations for simplicity.

**Table 5-1. List of Design Considerations for Arrangement Models**

| Design Consideration | Explanation / Impact |
|---|---|
| Configuration Considerations | |
| Reactor Module Envelope Dimensions are based on the spaceship stowed configuration within a five meter fairing and the requirement to remain within the cone angle of the shield. | These considerations were captured in the envelope defined by NGST and described in Figure 5-3. |
| Support structure components forward of the shield must be minimized to avoid interference with core reactivity, e.g. neutronics. | This was not yet a factor in the efforts to date. It would have become a constraint for design of the launch supports and other structures. |
| The shield and its supporting structure must not interfere with aero shell performance. | This guideline was preliminary, and did not have an effect on efforts to date. It was anticipated that special consideration would be needed to assure that the shield and its supports would have to separate cleanly from the aeroshell, in order to maximize the beneficial effects of the aeroshell. |
| The angular momentum of the Braytons must not interfere with the momentum of the space ship when the space ship is orbiting with no thrust. | This requirement reflects the need for pointing stability during the science operations. Counter-rotating braytons or other forms of momentum compensation may be necessary to offset Brayton or gas flow momentum. |
| Piping Considerations | |
| To minimize pressure drop, piping must be modified in length, diameter, number of bends, and general routing. Increasing the ratio of pipe bend radius to pipe diameter will decrease pressure drop through the system. (See Section 9 Component Descriptions) | This is a trade which must be performed in order to meet the competing requirements of packaging, minimum pressure drop, and acceptable thermal expansion stresses. |
| To avoid large velocity gradients at the compressor inlet, a de-swirler arrangement or 2 to 4 diameters in length of straight piping is currently required before the compressor. Velocity and pressure gradient avoidance is less critical for the turbine, because flow enters a vortex. (See Section 9 Component Descriptions) | Compressor inlet is much more sensitive to straight piping than turbine inlet piping. Flow characteristics in the inlet to the compressor affect surge and efficiency. |
| For reliability, surface area of pressure boundaries should be minimized. This is to include the recuperator and gas cooler. Arrangement and orientation may help protect the system against external impacts, such as from micrometeoroids. (See Section 7 Reliability) | As arrangement efforts progressed, one consideration for placement of components would have been shielding of the more vulnerable components by more robust elements and orientation of components so that the more vulnerable surfaces face away from higher particle flux directions. |
| Thermal coupling between hot leg piping and plant components must be accounted for when evaluating thermal expansion issues, structural issues, and operational performance issues (see Section 10). | This constraint reflects the thermal management internal to the reactor module See Section 10. |
| CDM Related Considerations | |
| The control drive mechanisms for the sliders for the reactor require clearance behind the shield nearly equal to their length due to the translational motion with respect to the reactor necessary for operation. | This forces the Energy Conversion elements to be placed further away from the shield to keep clear of the sliders. Use of drums would reduce the offset form the shield. |

| Design Consideration | Explanation / Impact |
|---|---|
| Shield Related Considerations: | |
| Piping arrangements must consider streaming through the reactor shadow shield. Routing the piping through the shield with a 90 to 180 degree spiral provides good neutron attenuation and was a leading candidate (see Reference 5- 1). | How piping routes through the shield and then around the CDM's is a significant driver in the piping configuration. This would need to be addressed early in future work. |
| Where possible, consideration should be given to placement of components in a manner which provides extra shielding for local components (e.g., alternator) or for the space vehicle bus | For example, aligning the axis of the Brayton with the axis of the space ship and placing the turbine and compressor closer to the shield than the alternator may provide added shielding for the alternator. Also, placement of equipment of substantial mass closest to the back side of the shield with respect to the rest of the plant components provides additional gamma shielding for plant components. |

## 5.4 Model Development

A valuable part of the arrangement studies effort was the development and evolution of the different configuration models. The evolution of the arrangement models described herein details the logic trail based on the best estimates available at the time each model was created. Insight into the process and where future efforts might lead can be gained by understanding the different evolutions and the overall approach to updates and evaluation of the different arrangements.

With each model description, component best estimates are revised and, in some cases, completely altered from previous revision descriptions. Since the arrangement process evolved using best estimates and resulted in several revisions, there is not yet a single preferred arrangement. The component dimensions used in the models are based on operational conditions of the system and its components to achieve rated power level and minimize pressure drop.

### 5.4.1 3-3-3 System Architecture - Revision 1

The NRPCT evaluated options for an initial base case arrangement. The options ranged from a one to a four Brayton system, all sized to produce 200 kWe with the normally operating components in-service, which were all completely redundant systems with exception to the 1-1-1 system. A completely redundant system is redundant from a component perspective such that there are no shared components for the energy conversion loops. These systems require the additional complexity of valves and potentially cross strapping. In order to capture some of the challenge of packaging many components and in keeping with the goal to pursue a redundant system, the team selected a completely redundant three Brayton system to serve as the first iteration of a multi-Brayton system arranged in the pre-determined space envelope. The 3-3-3 system Revision 1 is shown in Figure 5-4.

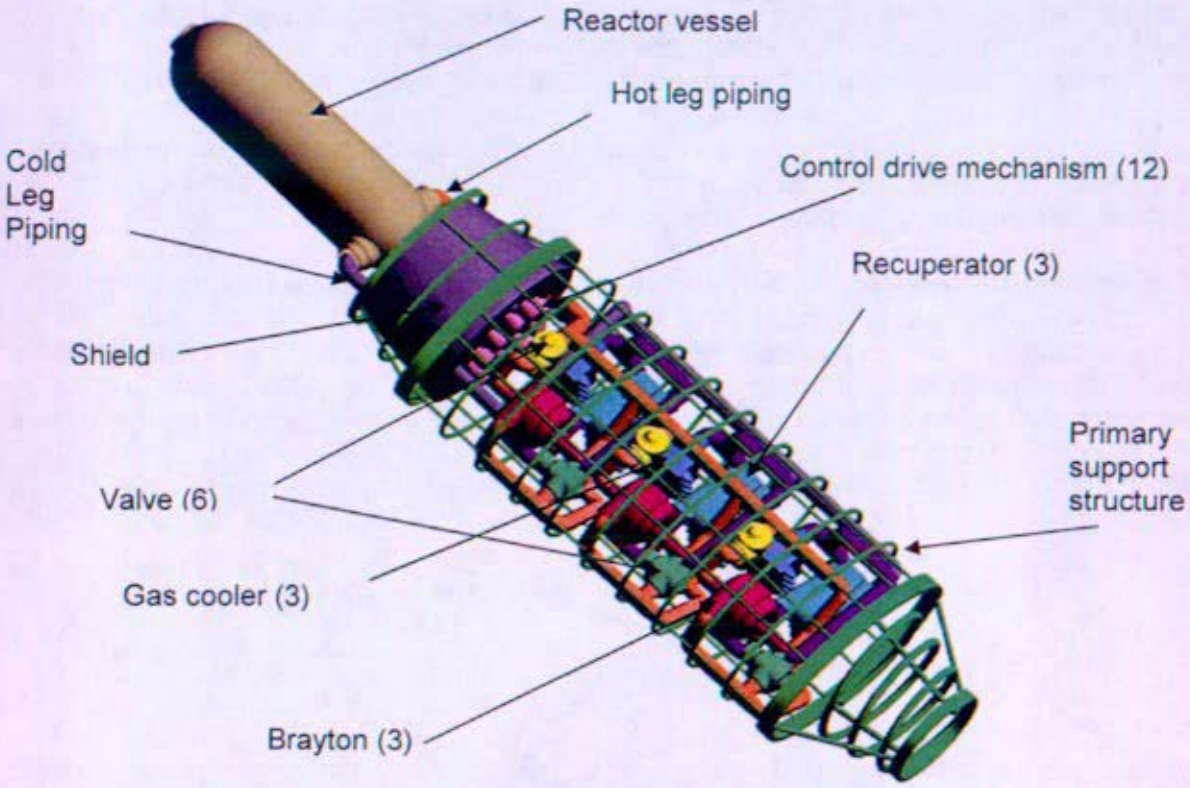



**Figure 5-4. 3-3-3 System Architecture - Revision 1**

The reactor is located at the forward end of the reactor and plant assembly and is shown in this revision with only the reactor pressure vessel. Reactor components, such as the control rods and reflectors, are not included in this revision, as these models were not available at the time the model was generated. Sizing for the reactor in this revision was generated by the reactor design community for a 1MWt reactor with a vessel height of 168cm, an outer diameter of 56cm, and a thickness of 0.76cm.

The shield is positioned closest to the reactor relative to the other components to minimize shield mass and provide maximum radiation protection to the components aft of the shield. The cross section of the shield is an ellipse with a minor axis diameter of 95.6 cm and a major axis diameter of 129 cm on the back side of the shield. The shield forms a six to twelve degree cone angle in which the plant, radiators and associated heat pipes and plumbing, electronics packages, and science packages avoid irradiation effects. As various concepts were being evaluated, no structural components were added in this revision to support either the shield or other components, i.e. the structural shield plates.

The preliminary outer piping diameter (17 cm) for the hot and cold legs was based on temperature and stress dependent estimations for three different materials: Inconel 617, Haynes 230, and Hastelloy X. The pipe is crudely routed through the shield without bending before, within, or after the shield. The hot and cold leg piping is arranged on opposite sides of the plant for simplicity only.

The primary power conversion subsystem (PCS) components: Brayton, recuperator, and gas cooler, were arranged in sets. The effect of PCS sets on thermal management of the reactor module would need to be considered (see Section 10). PCS sets would be more fabricable and testable than grouping components individually. Severe structural distortion, large stresses, and potential operational deficiencies are potential effects which must be avoided due to the extreme temperature differences between components. Thus, the PCS sets are aligned along the axis of the space craft to avoid large temperature differences throughout the plant.

The Brayton dimensions are sized for a 100kWe Brayton, since two Braytons are operating at full capacity and one Brayton is a spare. The Braytons are oriented with the axis of the alternator parallel to the axis of the space ship boom to provide additional protection of the alternator's electrical sensors from reactor radiation. The Braytons are also oriented to avoid turbulent flow in the turbine to protect the thrust bearings and maintain efficiency. Figure 5-5 shows the base case Brayton design. The label numbers from Figure 5-5 correspond directly to the label numbers in Figure 5-6, a two dimensional schematic, which shows the path of the primary coolant through the primary components only.

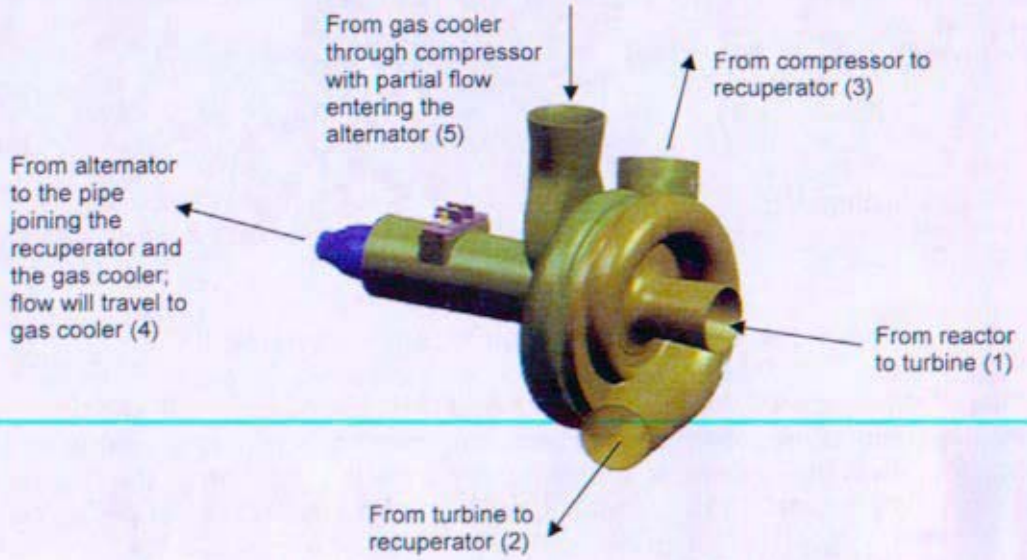



**Figure 5-5. Base case Brayton design**

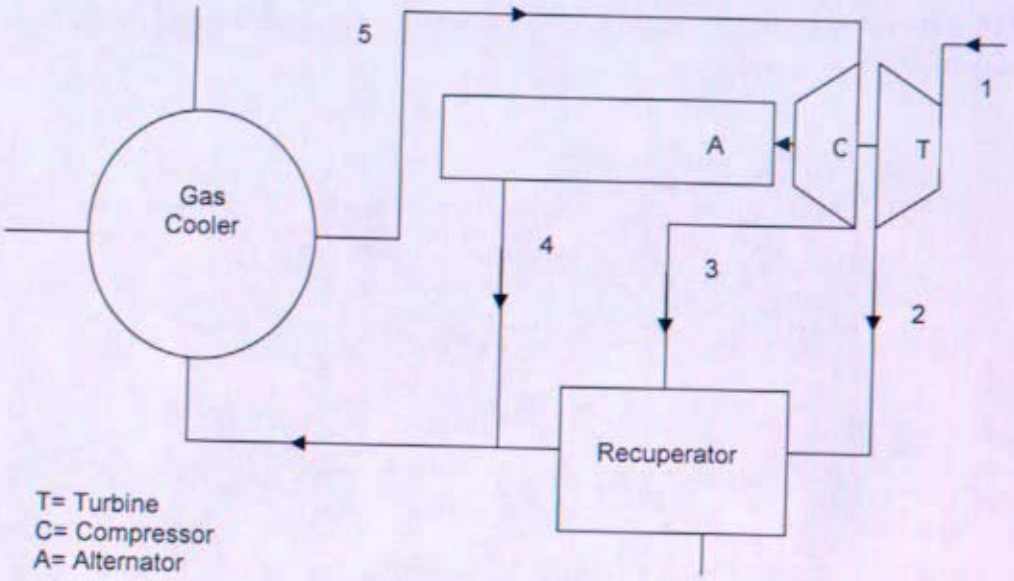



**Figure 5-6. Two dimensional schematic for basic plant configuration**

Several gas cooler concepts were considered, but since multiple designs and data were unavailable, the PB1 Gas Cooler model designed by Hamilton Sundstrand was selected for the first arrangement model. Figure 5-7 shows the initial concept for a gas cooler, which has a fin and plate heat exchanger design. The gas cooler was positioned with the secondary coolant nozzle axes parallel to the axis of the boom to simplify the expected routing of the heat rejection system piping (not included in this version due to incomplete information).

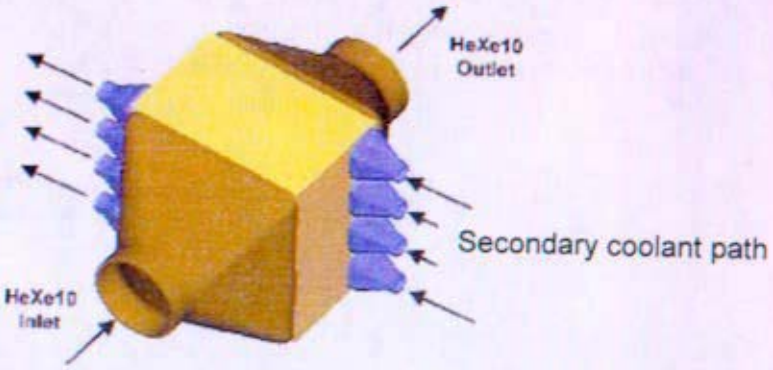



**Figure 5-7. Hamilton Sundstrand initial gas cooler concept**

The recuperator concept was also based on the initial Hamilton Sundstrand model including baseline dimensions and operating capabilities. The recuperator is placed such that the long axis of the

recuperator is oriented perpendicular to the axis of the boom. Figure 5-8 displays the recuperator in the primary PCS module configuration.

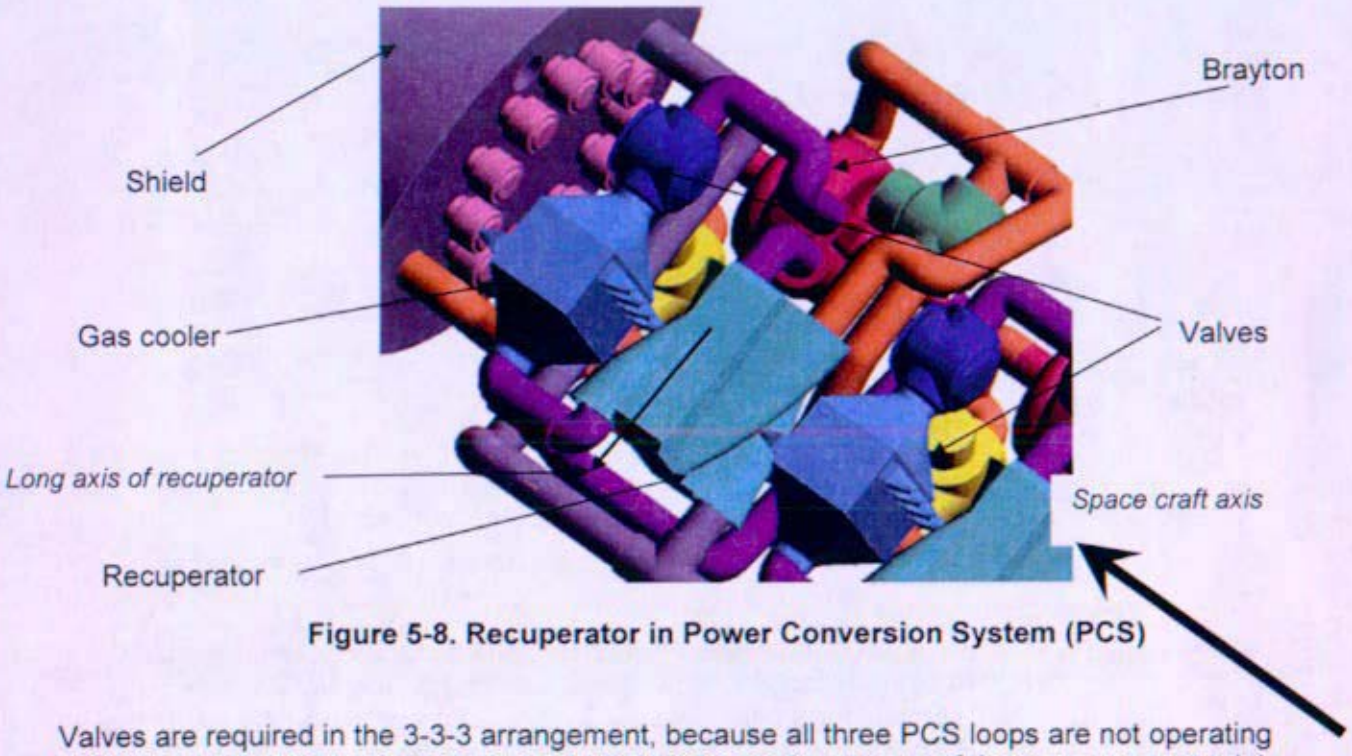



**Figure 5-8. Recuperator in Power Conversion System (PCS)**

Valves are required in the 3-3-3 arrangement, because all three PCS loops are not operating simultaneously. In this revision, a check valve is located upstream of the compressor, and the isolation valves are located upstream of the turbine. These two locations are intended to isolate flow through a PCS loop and prevent reverse flow through the turbine to protect the thrust bearings.

Finally, the Primary Support Structure (PSS) serves as the primary means to support all reactor and plant components and also support this system as it relates to the rest of the space craft. The concept displayed in this arrangement was based on the JPL/ NGST concept as a base case place holder for this layout.

### 5.4.2 3-3-2 with a Shared Gas Cooler System Architecture - Revision 1

As the 3-3-3 system served as the first completely component redundant NRPCT arrangement model, the next concept evolved by varying the number of components. The 3-3-2 with a shared gas cooler system architecture has the same number of Braytons and recuperators as the 3:3:3 system but has one shared gas cooler with single pass flow for the primary coolant sized to support the operation of two 100 kWe Brayton units. In addition to the PCS component quantity variations, as more information was made available, all component constraints were re-evaluated.

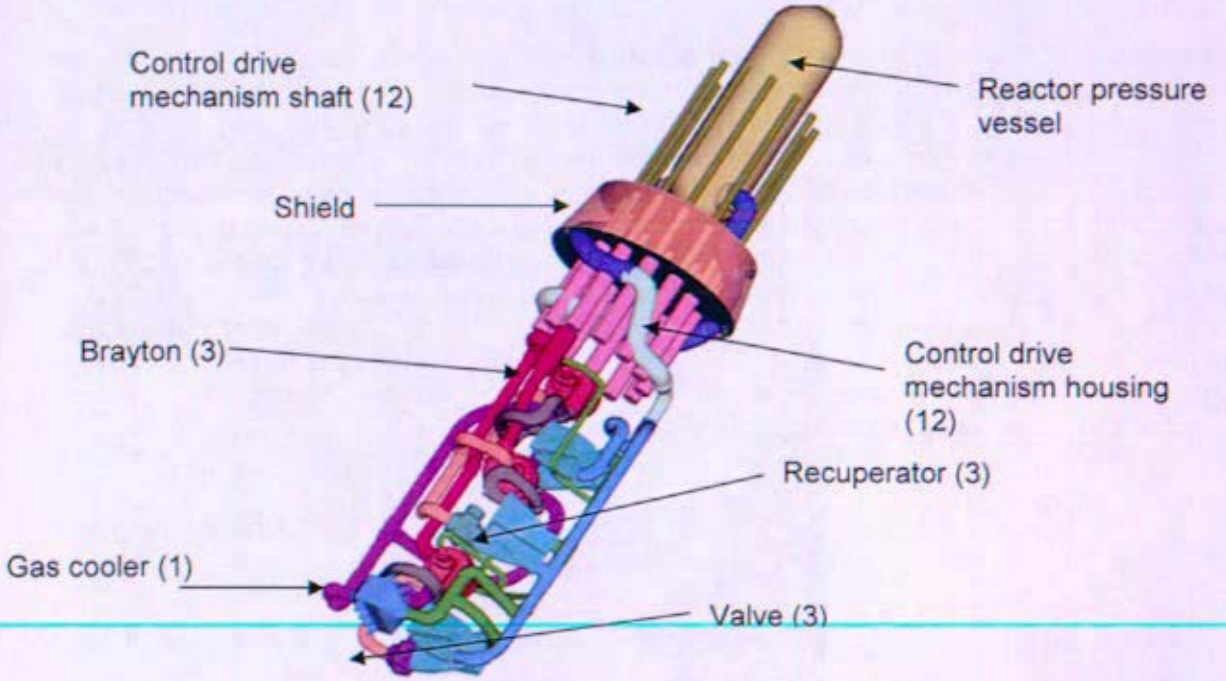



**Figure 5-9. 3:3:2 with a Shared Gas Cooler System Architecture - Revision 1**

The reactor components are updated in this revision as Control Drive Mechanism (CDM) shafts were added. They were added to the model so that their position could be observed relative to the hot and cold leg piping for potential geometric issues. Interference between the CDM shafts and the piping was a concern from a structural, thermal, and operational standpoint. The hot and cold leg pipes do not interfere with the CDM shafts between reactor nozzle and shield penetration.

Different shield requirements were introduced, which resulted in piping through the shield exiting parallel to the back of the shield. Pipes aft of the shield are bent 90 degrees in effort to avoid excess radiation exposure to the rest of the plant. Straight pipes through the shield provide a direct path for radiation to reach components aft of the shield. Though the pipes must bend aft of the shield, the pipe routing and CDM housings and placement cause gross interference between these two components.

Pipe routing and sizing is dramatically different in this revision as estimated bend radii are satisfied for increased accuracy of the model. The suggested minimum bend radius is three times the outer diameter due to manufacturability concerns, ovalization issues, and cold working the pipe and to reduce head losses in the pipe. (Standard short radii used in this revision are equal to the outer

diameter of the pipe, and long radii are one and one half times the outer diameter of the pipe.) The constraints affected the diameters of all piping in the primary system. The hot and cold leg piping was decreased from seventeen centimeters to sixteen centimeters because of the difficulty to maintain bend radii while remaining within the space envelope. Alternator bleed flow was independently affected in order to balance the pressure drop through the sections of PCS piping. Since pressure drop is a function of the density and the square of the velocity, if the density is changed the velocity must be changed as well to compensate and minimize the pressure drop. Changing the velocity is accomplished by altering pipe diameter. Thus, the alternator bleed flow piping was reduced from the ten centimeter outer diameter consistent with the rest of the PCS loop piping to five centimeters outer diameter.

The orientation of the Braytons was changed in this revision. In order for the Brayton momentum vectors to be aligned with the other momentum vectors which act on the vehicle during gravity stabilized science orbit, the axis of the alternator must be oriented perpendicular to the plane of the radiators. The first and third Braytons are oriented in one direction, and the second Brayton was oriented in the opposite direction so that this Brayton would, in normal operation, counter the momentum in one of the other Braytons. In this model, adjacent Braytons are simultaneously operational. Additional momentum compensation might be necessary if a spare Brayton that is oriented the same way as the operating Brayton must also become operational. In addition, the turbine inlet and outlet piping was corrected from the first revision. Low pressure coolant exits the turbo-machinery parallel to the shaft, and high pressure coolant enters the turbo-machinery normal to the shaft. Figure 5-10 shows the proper inlets and outlets of a Brayton. Figure 5-10 now correctly corresponds to the schematic for the primary coolant in Figure 5-6.

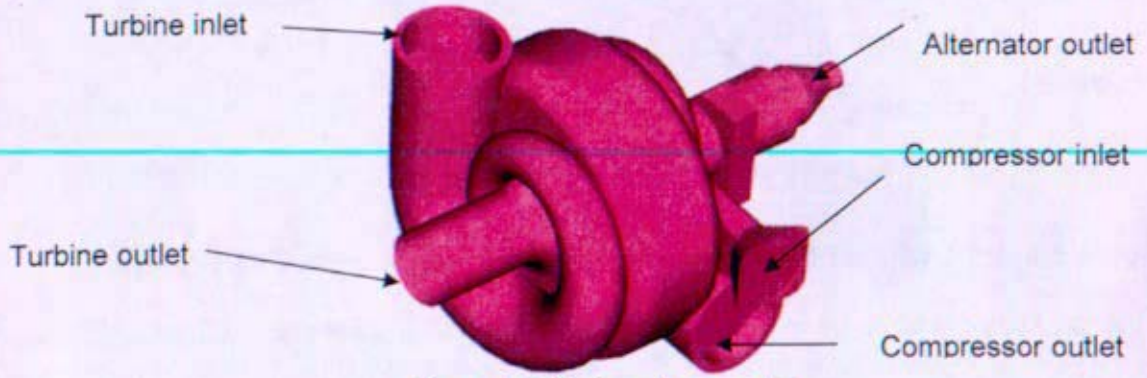



**Figure 5-10. Brayton engine**

One gas cooler from the 3-3-3 system Revision 1 was eliminated, and the resulting two gas coolers were combined within one pressure boundary with single pass flow from two parallel operating Brayton loops. The gas cooler was placed at the furthest position in the plant from the reactor in order to be closest to the Heat Rejection System (HRS) components for piping simplicity. The single gas cooler boundary was included in this revision to decrease the overall size of the plant assembly and simplify the piping.

The recuperator dimensions and orientation were not changed in this revision.

Valve locations were reviewed and revised. The isolation valve from Revision 1 was moved from the hot leg piping to between the turbine and the recuperator. It is a lower temperature location, which is more beneficial for operation and life of the valve.

The primary support structure did not change from the last revision.

### 5.4.3 3-3-3 System Architecture - Revision 2a and 2b

The second revision of the 3-3-3 system has two versions, which differ in the pipe routing with respect to the shield (see Reference 5- 1 for shielding studies related to piping penetrations through the reactor shadow shield). [Note that the angle of the pipes exiting the pressure vessel had not been optimized in these studies.] Both versions have identical reactor and plant components. Revision 2a routes piping through the shield, whereas revision 2b routes piping around the shield with shield caps to prevent streaming. In creating two versions, it was feasible to study different techniques for routing piping to address the key shielding and piping issues, e.g. irradiation doses aft of the shield, pressure drop associated with pipe routing, and thermal management. Figure 5-11 shows Revision 2a, and Figure 5-12 shows Revision 2b.

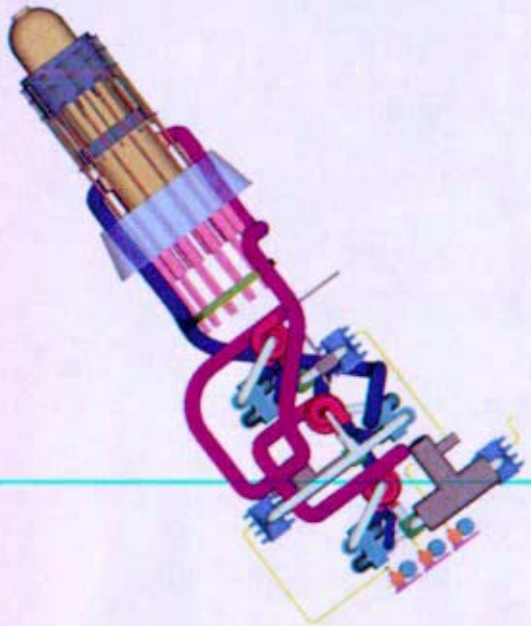


**Figure 5-11. 3:3:3 System – Revision 2a**

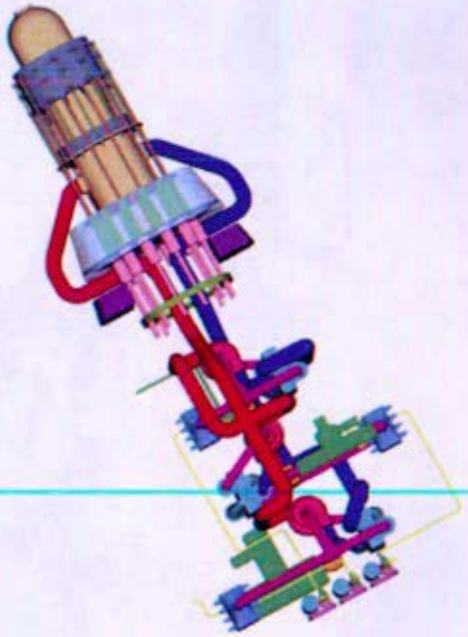


**Figure 5-12. 3:3:3 System – Revision 2b**

Reactor components, such as the translational sliders (reflectors), the fixed reflector, and the Control Drive Mechanism (CDM) shafts, are incorporated. The dimensions of the CDM housings were altered in order to accommodate piping concerns, specifically pressure drop. Only the housing for the shaft was reduced in diameter for this revision, as the housing for the motor and hysterisis brake could not be altered. A support structure was also added to the CDM shafts to provide in and out of plane stiffness. A revolved tee, which formed a ring, was used as a placeholder at the end of the CDM shafts.

Piping lengths were straightened as much as possible to reduce pressure drop throughout the system. Piping lengths were also reconfigured to make hot leg piping to each module (from the main manifold to each Brayton) nearly equal for thermal management, consistency in pressure drop, and Brayton efficiency. Brayton efficiency also depends on the type of flow entering each section. Since

the flow enters a scroll in the turbine inlet, laminar flow is not necessary. It is actually the compressor that requires a length of straight pipe or a mechanism, such as a de-swirler arrangement or annulus to avoid turbulent flow, which affects surge and component efficiency.

The bypass loop, a feature to rapidly shutdown a Brayton unit in case of loss of Parasitic Load Resistor (PLR), was eliminated because it would not provide sufficient benefit and added other complexities. In addition, the Brayton orientation remains unchanged from the first revision, as the axis of the alternator must be perpendicular to the plane of the radiator to not preclude the angular momentum of the space ship while in science orbit with no thrust. Though the recuperator remains unchanged from the previous revision, the number of gas to liquid loop coolers was increased to three as in revision 1, so that the ratio of Braytons to Gas Coolers is 1:1.

Three vastly different valve concepts were considered for this revision. For detailed valve information, see Section 9 Component Descriptions. Figure 5-13 shows three different valve concepts.

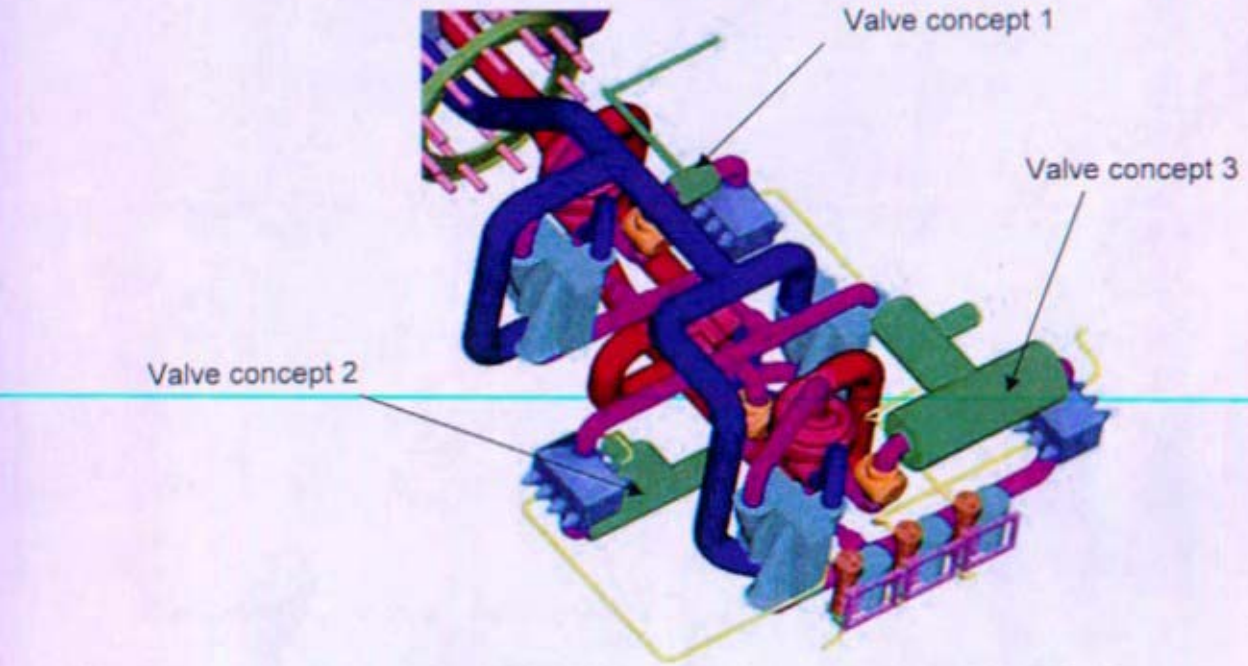



**Figure 5-13. Various valve concepts in Revision 2**

The Heat Rejection System (HRS) components were incorporated into Revision 2. Space envelopes for the components are those received from NGST based on their calculations for NaK. According to their calculations, the accumulator space envelope may change based on required storage volume if incorporated into the arrangement models. The pump assembly space envelope will not change noticeably based on the coolant (water or NaK). Based on the assumptions made by NGST for a 1:1 gas cooler liquid loop flow, a single loop of liquid coolant will pass through each gas cooler and flow through the pump accumulator assembly to the radiator panels.

The original space envelope provided by NGST was exceeded in all dimensions as needed to reduce system pressure drop, accommodate thermal issues, orientation requirements, and number of components. On the other hand, the cone angle was not exceeded so as not to adversely affect the

shield dimensions or radiation exposure to components. Though both revisions exceed the space envelope, Revision 2a is shown in Figure 5-14 to demonstrate this result. The red shaded area represents the original NGST space envelope.

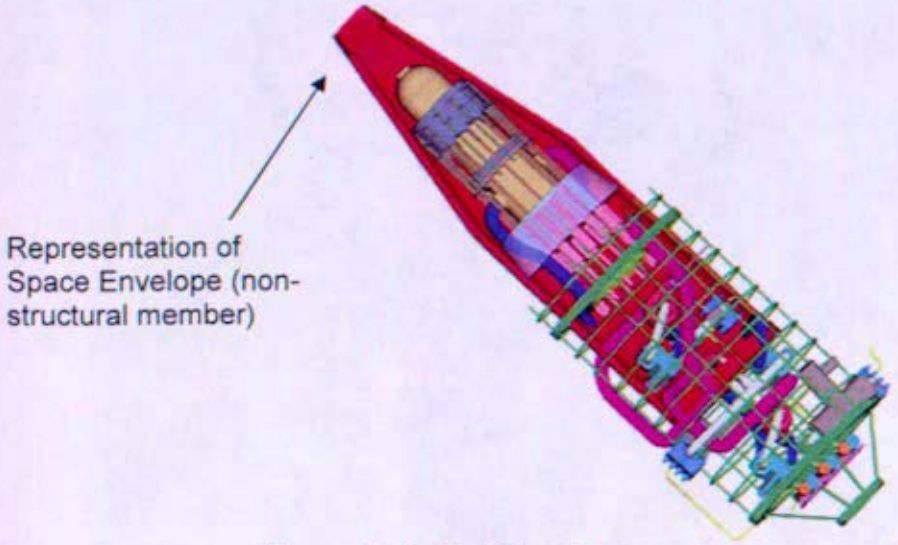



**Figure 5-14. Revision 2a exceeds space envelope**

### 5.4.4 4-4-4 System Architecture - Revision 1

As the arrangement concepts continued to evolve, multiple models with different quantities of Braytons were generated, including the 4-4-4 system. The 4-4-4 System is significantly different than previous 3-3-3 systems. Due to the additional components, a new configuration was required, since the provided space envelope was still considered a design constraint. The Braytons are grouped in pairs to form nearly symmetrical PCS modules. A two Brayton PCS module is shown in Figure 5-15. Two Brayton PCS module
. For the 4-4-4 systems, the two PCS modules are aligned along the axis of the space craft, and hot and cold leg piping are routed accordingly. Figure 5-16 shows the 4-4-4 system with two PCS modules.

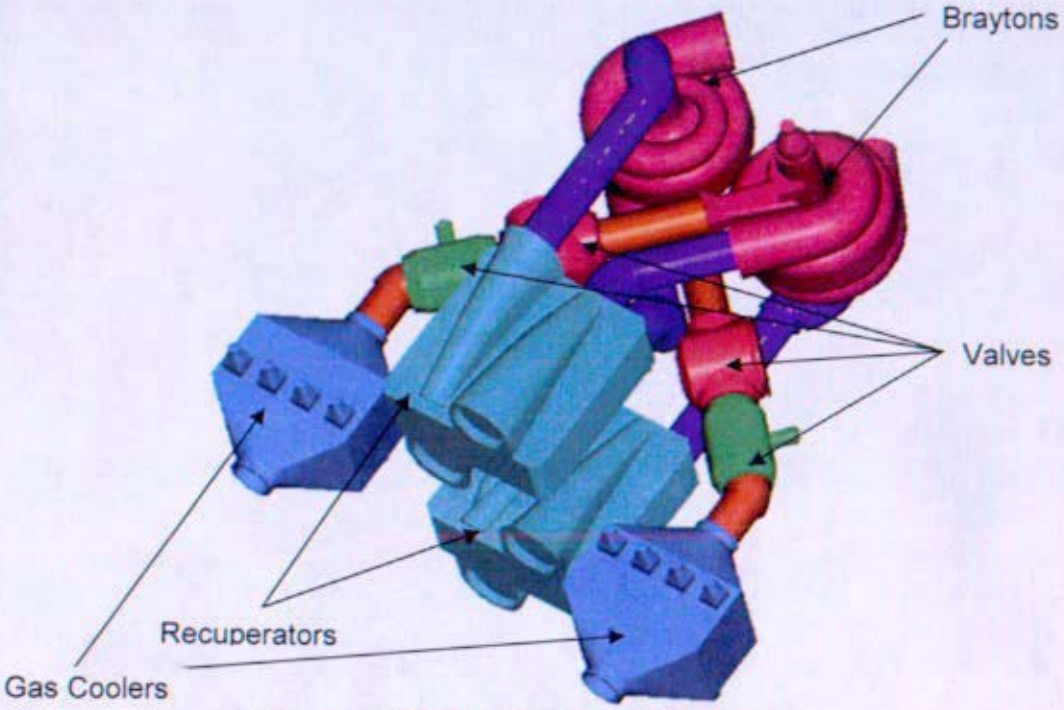



**Figure 5-15. Two Brayton PCS module**

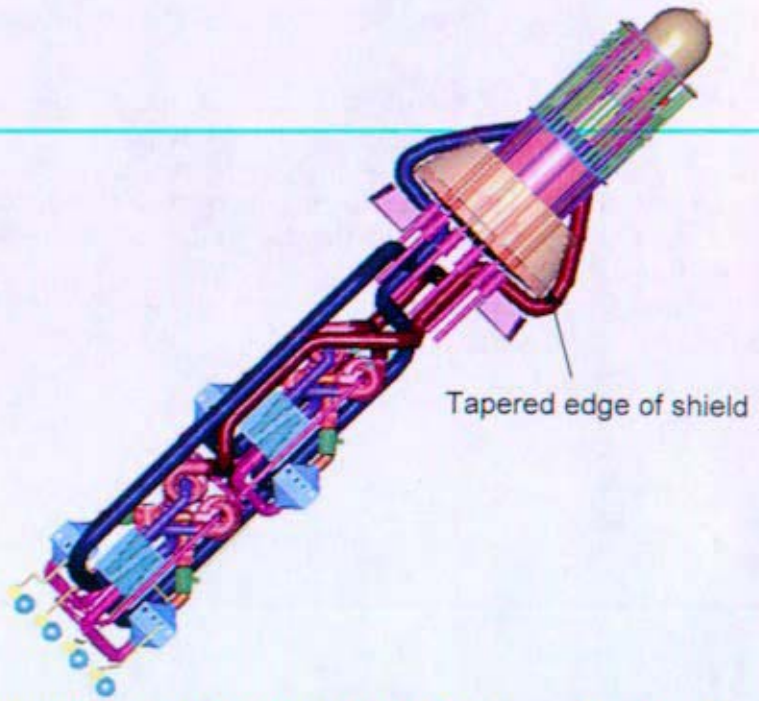



**Figure 5-16. 4-4-4 System Architecture - Revision 1**

The reactor vessel and associated components were not altered for this revision. The shield, however, has been redesigned with tapered edges to reduce the bend angle of the piping as it rounds the back of the shield. The large pipe bend increases the hot and cold leg piping pressure drops. Nevertheless, the shield still retains the twelve degree cone angle. The thickness of the shield is also larger due to the penetrations in the shield from the hot and cold leg piping.

The hot and cold leg piping in this revision has less severe bends than the previous revision (3-3-3 2a), which routes the pipes through the shield. The requirement remains, though, that the piping must be parallel to the shield plate immediately aft of the shield to prevent streaming. The piping is then routed to the center of the CDMs due to space availability, where it turns ninety degrees and divides flow to the PCS modules. The PCS module piping was routed as compactly as possible while adhering to bend radii requirements.

Plant component sizes were unaffected from the 3-3-3 system to the 4-4-4 system. In each system, two Braytons are operating, but different numbers of spares are available. One spare Brayton unit is available in the 3-3-3 system, and two spare Brayton units are available in the 4-4-4 system. Therefore, though the quantity of components was altered, both primary and auxiliary component sizes were unchanged.

### 5.4.5 3-3-3 System Architecture - Revision 3

Revision 3 incorporated design characteristics from the 3-3-3 System Revision 2 and the 4-4-4 system Revision 1. Two versions of Revision 3 were generated with identical plant layouts but different pipe routing with respect to the shield. Revision 3a routed the piping through the shield, and Revision 3b routed the piping around the shield and through the CDMs. Figure 5-17 and Figure 5-18 display Revisions 3a and 3b, respectively.

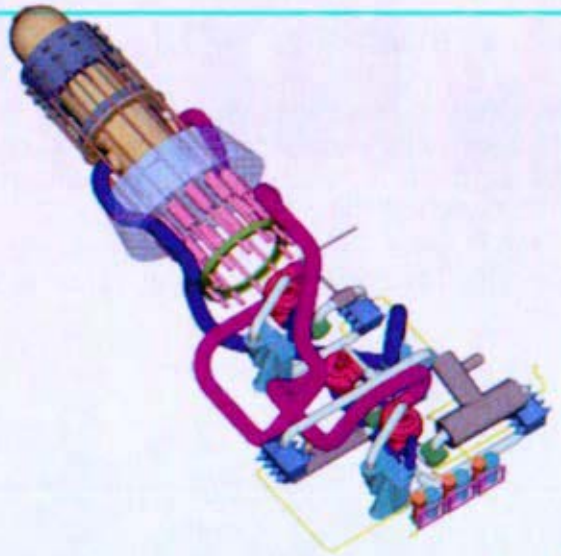


**Figure 5-17. 3-3-3 System Architecture - Revision 3a**

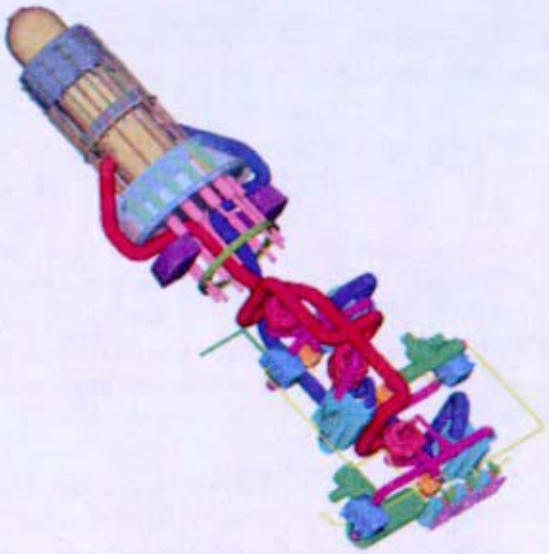


**Figure 5-18. 3-3-3 System Architecture - Revision 3b**

The CDM shaft dimensions were modified slightly to provide additional space for the piping. Due to the thermal concerns for the CDM motor and hysterisis brake, the location between the shield and the ball nut was increased to accommodate the hot leg piping. This prevents the hot and cold leg piping from being routed adjacent to the brake and motor.

Though the PCS piping was altered slightly to further straighten piping lengths, the plant components were not altered significantly in this revision. The revision was intended to demonstrate additional pipe routing with respect to the shield.

### 5.4.6 4-4-4 System Architecture - Revision 2a, 2b, 2c

Similar to the 3-3-3 system, a 4-4-4 system was generated with different versions of piping with respect to the shield. A total of three versions were generated for the 4-4-4 system. Revision 2a of the 4-4-4 system routes the piping around the shield and around the CDMs. The 4-4-4 2b routes piping around the shield and through the CDMs, and 4-4-4 System Revision 2c routes piping through the shield. Figure 5-19, Figure 5-20, and Figure 5-21 show the completely redundant four Brayton systems, where Figure 5-19 represents Revision 2a, Figure 5-20 represents Revision 2b, and Figure 5-21 represents Revision 2c.



**Figure 5-19. 4-4-4 System Architecture - Revision 2a Piping around both the shield and the CDMs**



**Figure 5-20. 4-4-4 System Architecture - Revision 2b Piping around the Shield**

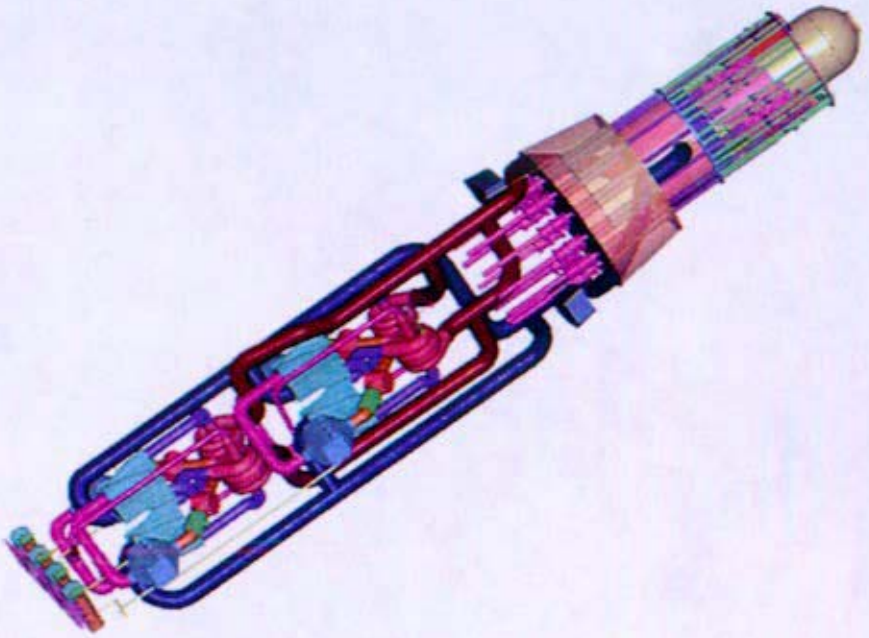


**Figure 5-21. 4-4-4 System Architecture - Revision 2c Piping through the shield**

Estimates for component sizing and placement remain the same from the previous 4-4-4 System, but the space envelope is still exceeded in axial length only. The module arrangement from the first revision of the 4-4-4 system has been adopted for the three versions of the second revision. The modules were adopted based on functionality and extensibility to alternate missions. Modules provide a compact and symmetrical design, which would also be beneficial for missions permitting maintenance.

## 5.5 Four Brayton Piping Sensitivity Study

A relative quantitative comparison was performed on each of the three versions of the 4-4-4 System Revision 2 for certain metrics, including pressure drop comparisons, total system % delta P/P, number of welds, weld length, surface area of pressure boundary, number of tees in the hot and cold legs only, and the number of bends in the hot and cold legs only. Calculations involving pressure drop did not include losses due to primary components other than the piping. The number of welds, weld length, and number of tees were the same for all three versions, and the remaining comparisons were so similar that any piping configuration with respect to the shield could be accommodated. Table 5-2 shows the results of this comparison. Based on the results, despite their minimal numeric differences, Revision 2b was chosen as a reference pipe routing for the subsequent trade study configurations due primarily to the lower pressure drop and fewer bends.

**Table 5-2. 4-4-4 System Architecture - Comparison Three Version of Piping**

| | Total System Pressure Drop (kPa) | Total System %ΔP/P | Number of Welds | Weld Length (m) | Surface Area of Pressure Boundary (Pipes only) ($m^2$) | Number of Ts (Hot and Cold Leg only) | Numbers of Bends (Hot and Cold Leg only |
|---|---|---|---|---|---|---|---|
| 2a - Piping around Shield and around CDMs | 63.3 | 5.4 | 28 | 14.1 | 7.4 | 6 | 29 |
| 2b - Piping around Shield and through CDMs | 62.2 | 5.3 | 28 | 14.1 | 7.9 | 6 | 27 |
| 2c - Piping through Shield | 72.6 | 5.8 | 28 | 14.1 | 8.2 | 6 | 32 |

## 5.6 Trade Study

A global comparison was performed to quantitatively compare systems with different numbers of components.

### 5.6.1 Arrangement Concepts involved in Trade Study

As numerous concepts had been generated, a relative comparison of the systems was necessary to determine if any unexpected differences existed between the models. The systems involved in the trade study include the 1-1-1 system Revision 1, the 2-2-2 system Revision 1, the 3-3-3 system Revision 4, and the 4-4-4 system Revision 2b.

#### 5.6.1.1 1-1-1 System- Revision 1

The one Brayton system consists of three primary components: one Brayton, one recuperator, and one gas cooler. It is arranged with the piping routed around the shield, which was chosen from the sensitivity study that was performed on the 4-4-4 system described in Section 5.5. This system has no valves, because loop isolation is not necessary when there are no spare Braytons. Figure 5-22 shows the 1-1-1 system. This system shows the heat rejection system components, which are located at the rear of the plant and are consistent with previous revisions having a 1:1 primary gas loop to HRS cooling loop.

To determine the dimensions of the recuperator and gas cooler for a 200 kWe Brayton loop, the length was held constant to the length of the 100 kWe heat exchanger, while the height and width were multiplied by the square root of two. This was done to keep the pressure drop approximately constant by keeping the length and velocity constant. The flow within a 200 kWe Brayton loop is approximately double the flow within a 100 kWe Brayton loop, meaning that the heat exchanger flow areas would need to be a factor of two larger.

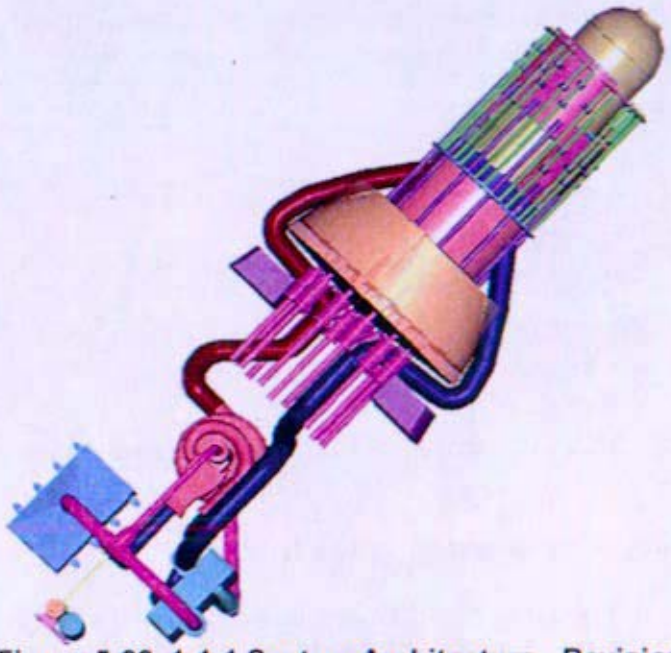


**Figure 5-22. 1-1-1 System Architecture - Revision 1**

### 5.6.1.2 2-2-2 System Architecture - Revision 1

This two Brayton system arrangement is completely redundant such that one Brayton loop is operating with one spare idle loop. Valves are required in this system to isolate the idle loop. The arrangement is based on the two Brayton module originally conceived for 4-4-4 system. Each Brayton was sized for a 200 kWe capacity, and the recuperator and gas cooler sizes are same as for 1:1:1 configuration.

The modular design provides a compact and symmetrical system, which satisfies system requirements, such as Brayton orientation and remaining within the cone angle and space envelope. It maintains equal lengths of hot leg piping to each Brayton and satisfies straight pipe inlet requirements for the compressor. The 2-2-2 system includes the heat rejection system components at the aft end of the plant, which is arranged with a 1:1 liquid to gas loop configuration. Figure 5-23 shows a conceptual arrangement for the system.

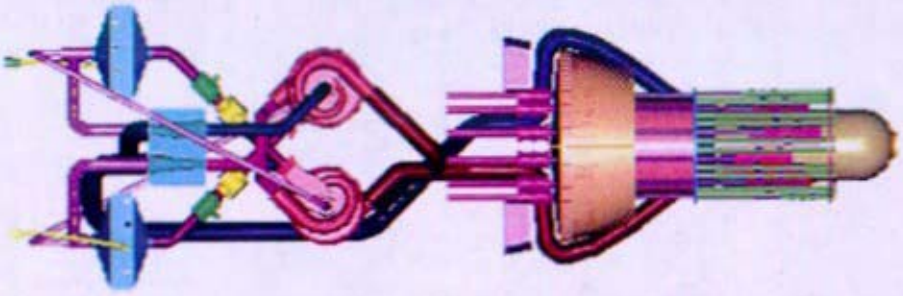


**Figure 5-23. 2-2-2 System Architecture - Revision 1**

### 5.6.1.3 3-3-3 System Architecture - Revision 4

The three Brayton system is a redundant system with two operating Direct Gas Brayton loops and one spare idle loop. This three Brayton system is the combination of the single Brayton PCS loop and the two Brayton PCS module. It is arranged in a triad with the one Brayton PCS loop immediately aft of the shield and the two Brayton PCS module aft of the single Brayton spare loop. This configuration is more compact with simplified piping as compared to the 3-3-3 System- Revision 3. All three piping configurations with respect to the shield were arranged, but Figure 8-22 shows the 3-3-3 System-Revision 4b with piping routed around the shield, which matches the 2b piping configuration from the 4-4-4 Trade Study discussed in Section 5.5.



**Figure 5-24. 3-3-3 System Architecture - Revision 4b**

### 5.6.1.4 4-4-4 System Architecture - Revision 2b

The four Brayton system in this comparison was chosen from the four Brayton Trade Study discussion in Section 5.5. This version can be seen in Figure 5-20.

## 5.6.2 Trade Study Results

The four systems described in section 5.6.1 were compared based only on metrics for the primary coolant piping and flow through the primary coolant piping. The primary coolant piping was solely involved in the trade study to control the number of variables in the study. The metrics include total system pressure drop, total system % delta P/P, total piping length, number of joints, weld length, and surface area of piping pressure boundary. Internal component losses and HRS piping were excluded

from this study. Figure 5-25 shows a graphical representation of the different metrics and their quantitative values for each of the four systems. An explanation for the artificially high delta pressure drop for the one and two Brayton configurations follows.

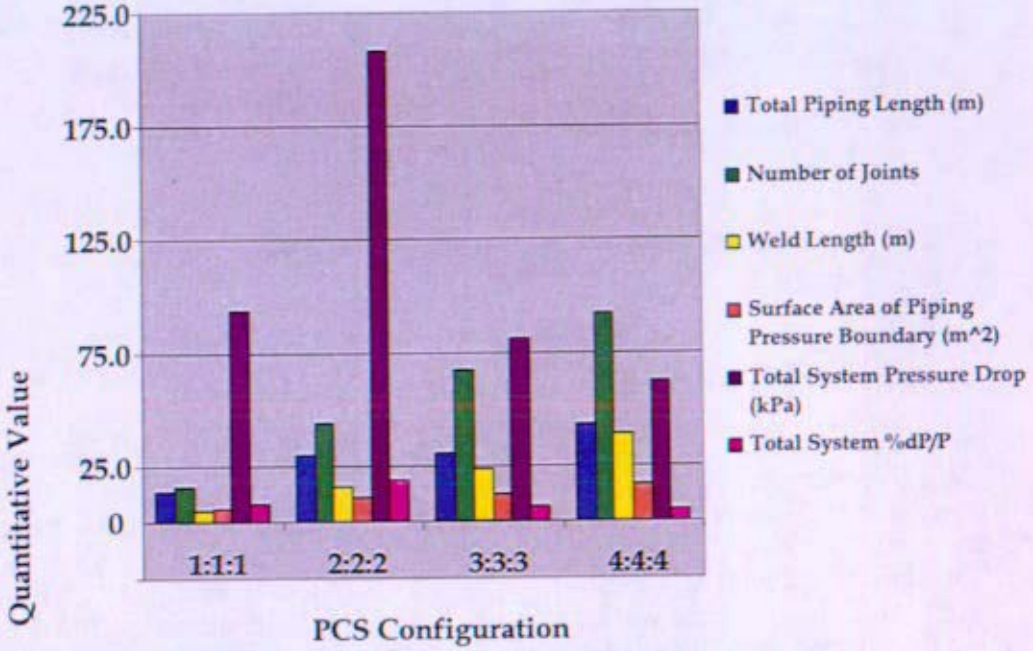



**Figure 5-25. Trade Study of 4 PCS Configurations**

The delta pressure results reflect the effect of keeping piping diameter constant for each configuration in the piping segments from the turbine to recuperator, the recuperator to gas cooler, the gas cooler to compressor and the compressor to recuperator. This resulted in high pressure drops for single operating brayton configurations because the piping in these segments was carrying 100% of the flow instead of 50% flow present in the two operating Brayton configurations. Further trade study effort to assess changing the segment piping diameters is presented in the next section.

The results shown in Figure 5-25 should be reviewed with the results in Figure 5-26 in order to better identify the overall pressure dependence on arrangement. The absolute values are not definitive because optimizations on diameter and configurations were not performed. The two trades do indicate that pressure drop is highly sensitive to piping diameter and layout. More effort would be needed to optimize each of the configurations.

### 5.6.3 Additional Trade Study and Results

Due to the large pressure drop through the one and two Brayton systems, the piping was increased in the PCS loop to accommodate the different flow characteristics. The main PCS loop piping was increased from ten centimeters to sixteen centimeters, which is equal to the hot and cold leg piping outer diameter. The alternator bleed flow was increased from five centimeters to eight centimeters. Figure 5-26 and Figure 5-27 show the modified one and two Brayton system arrangements, respectively.

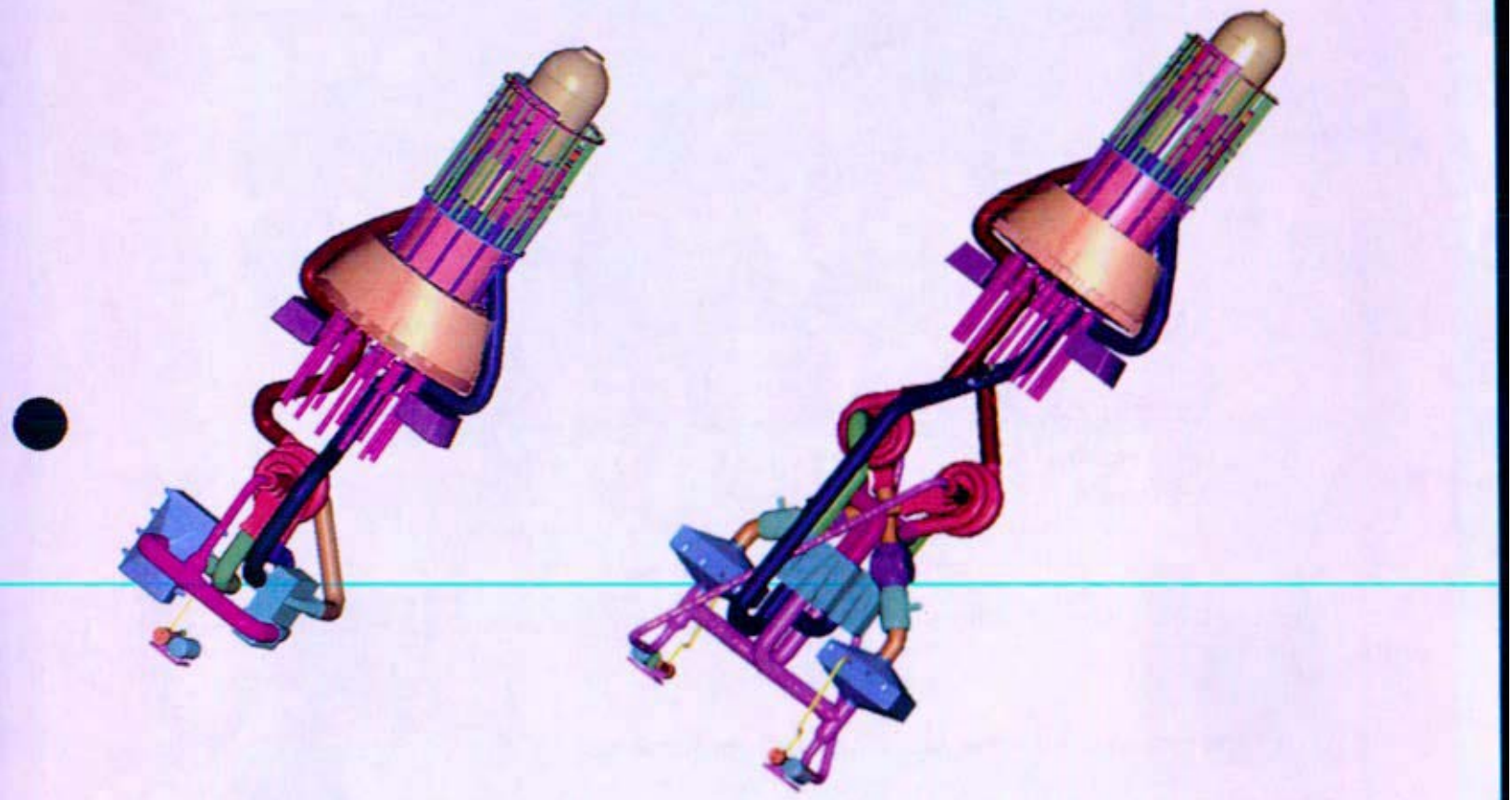


**Figure 5-26. 1-1-1 System Architecture**
**Revision 2b**

**Figure 5-27. 2-2-2 System Architecture**
**Revision 2b**

The metrics were recalculated and compared to the one and two Brayton system values from the original trade study. By increasing the pipe diameters, the pressure drop decreased by almost 75%. Figure 5-28 shows the results graphically with all metrics clearly compared.

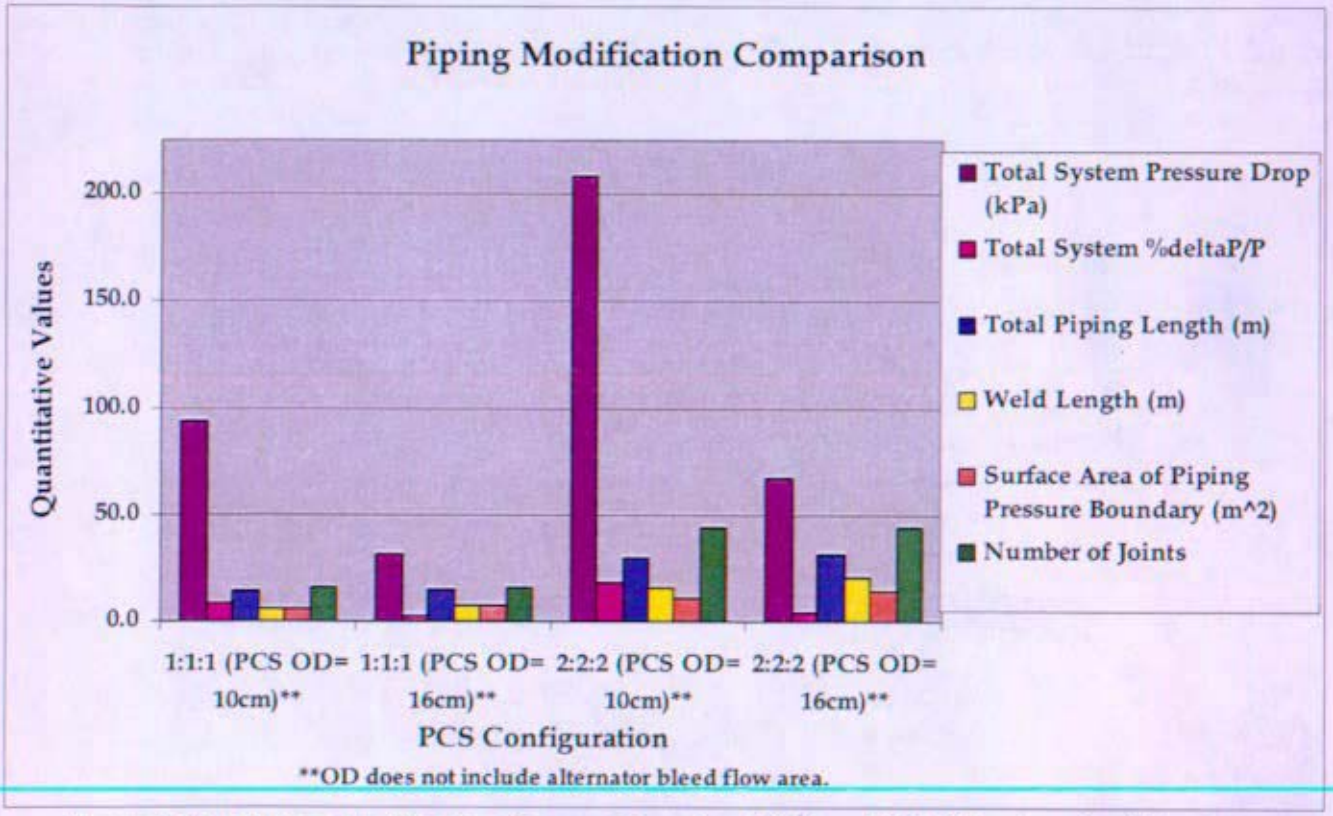



**Figure 5-28. Piping Modification Comparison for 1-1-1 and 2-2-2 System Architectures**

## 5.7 Arrangement Concepts with Shared Components

Additional arrangements were generated to investigate redundant systems with shared components.

### 5.7.1 2-1-1 System Architecture

Alternate arrangement concepts were necessary to show the geometric feasibility of arranging a redundant system with shared components. The 2-1-1 layouts also neglected all spaceship constraints, including the space envelope provided by the spacecraft vendor and the Brayton orientation requirements, in order to determine if evaluation of unconstrained arrangements would reveal valuable perspectives. Though the spaceship constraints were lifted, the individual component constraints were still imparted on the arrangement.

The piping was routed through the shield, because it is better from a neutronics perspective; however, manufacturability concerns were not considered and could affect piping arrangement in subsequent revisions. The piping was sized to provide acceptable flow characteristics such that the system

% delta P/P for piping only was between one and two percent to be consistent with the values from other arrangement drawings. The hot, cold, and PCS piping is 16cm outer diameter, and the alternator bleed flow is 8cm outer diameter.

Individual component constraints were maintained for all versions of the 2-1-1 system. All components, including the gas cooler, recuperator, and piping were sized for the conditions, where one 200 kWe Brayton is operating with one spare idle Brayton. The orientation and location of PCS components were drastically altered from previous revisions and are the distinguishing features of the various versions of the 2-1-1 system.

### 5.7.1.1 2-1-1 System Architecture - Version 1

The first version included only main components: the Braytons, recuperator, and gas cooler with associated piping. The Braytons were oriented to provide maximum protection for the alternators by placing the alternators behind other components such as the other subassemblies of the Brayton, including the turbine and compressor. The recuperator was positioned horizontally along the centerline and closest to the shield to provide additional shielding to components behind it from gamma radiation. The current design of the recuperator does not provide the length required for the component to extend the entire width of the shield. There is no change to the gas cooler size, and the positioning remains at the rear of the plant.

Figure 5-29 shows the first version of the 2-1-1 system. This system is relatively symmetrical and is within the cone angle of the shield. The piping is simply routed with as few bends as possible but does not include valves.

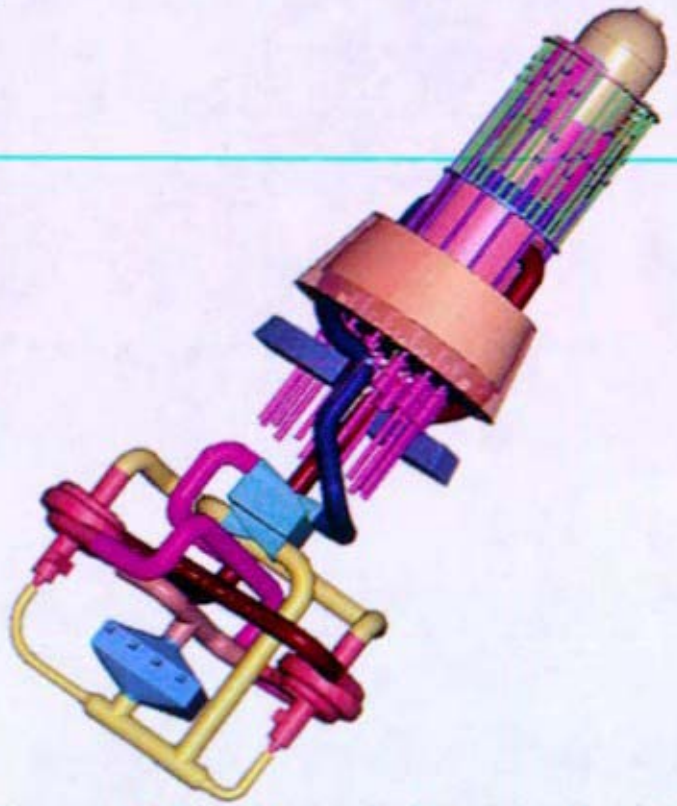


**Figure 5-29. 2-1-1 System Architecture - Version 1**

### 5.7.1.2 2-1-1 System Architecture - Version 2

The second version of the 2-1-1 system is shown in Figure 5-30. It is an iteration of Version 1 by adding the necessary valves to the system. It is clear that, by adding valves, the system increases in size. In this version, the valves are added mainly to the horizontal legs of the system, which, in turn, expands the system perpendicular to the axis of the space ship. If the valves are added to the vertical sections of pipe in Version 1, the system would expand axially.

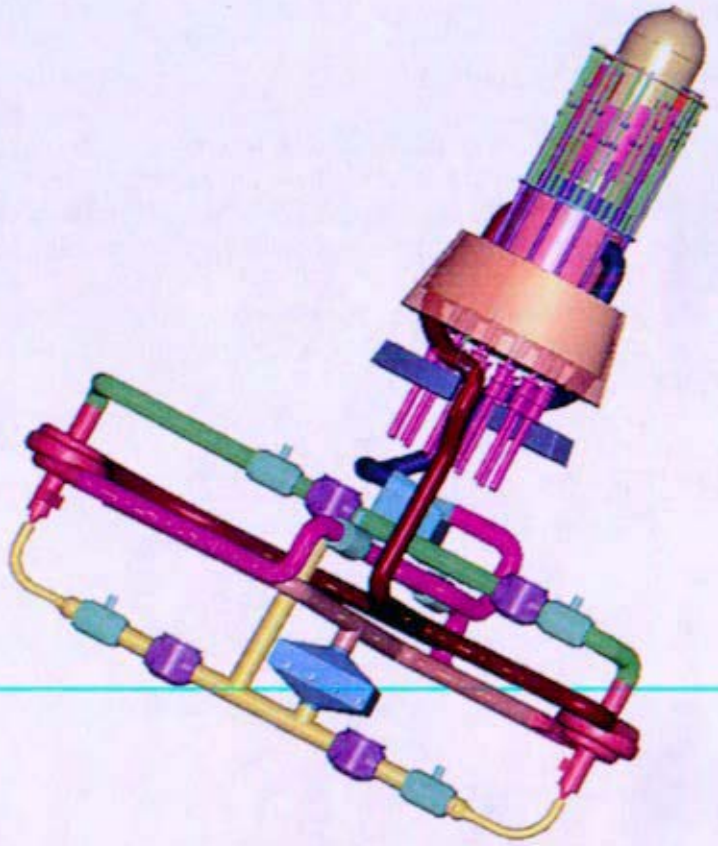


**Figure 5-30. 2-1-1 System Architecture - Version 2**

### 5.7.1.3 2-1-1 System Architecture - Version 3

Version 3 further revises Version 2 by increasing the bend radii such that the piping r/D ratio, where r is the bend radius and D is the pipe diameter, is between one and three to reduce the pressure drop. Figure 5-31 shows the third version of the 2-1-1 system.

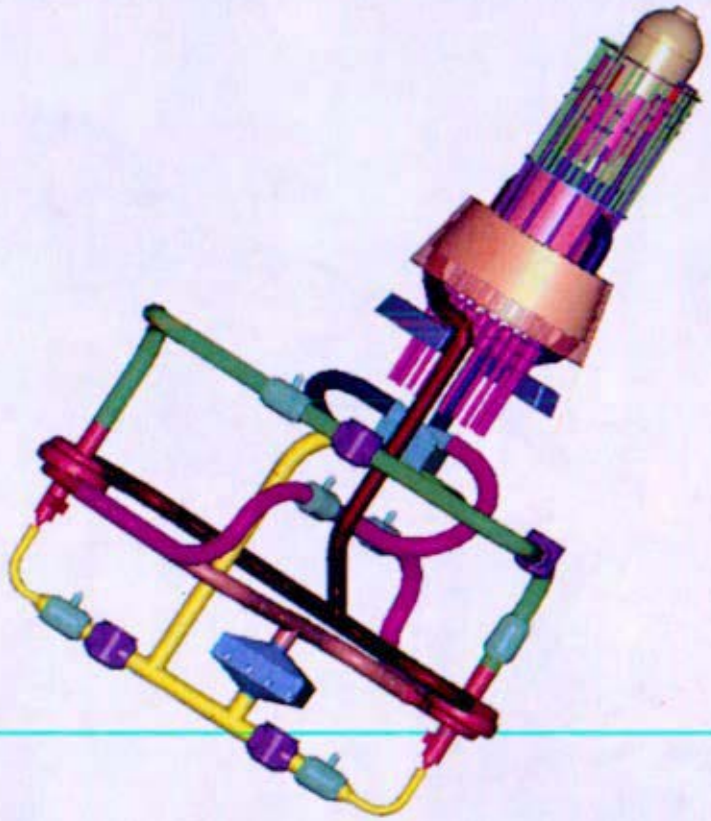


**Figure 5-31. 2-1-1 System Architecture - Version 3**

### 5.7.1.4 2-1-1 System Architecture - Version 4

Since the first three versions are not geometrically favorable from an assembly standpoint, a completely separate model was generated. In Version 4, the Braytons are reoriented and rotated such that the axis of the alternator is perpendicular to the plane of the radiator panels. Piping lengths are dissimilar between the two loops and do not satisfy suggested bend radii. Other component orientations require sharp piping bends. Figure 5-32 shows Version 4 of the 2-1-1 System.

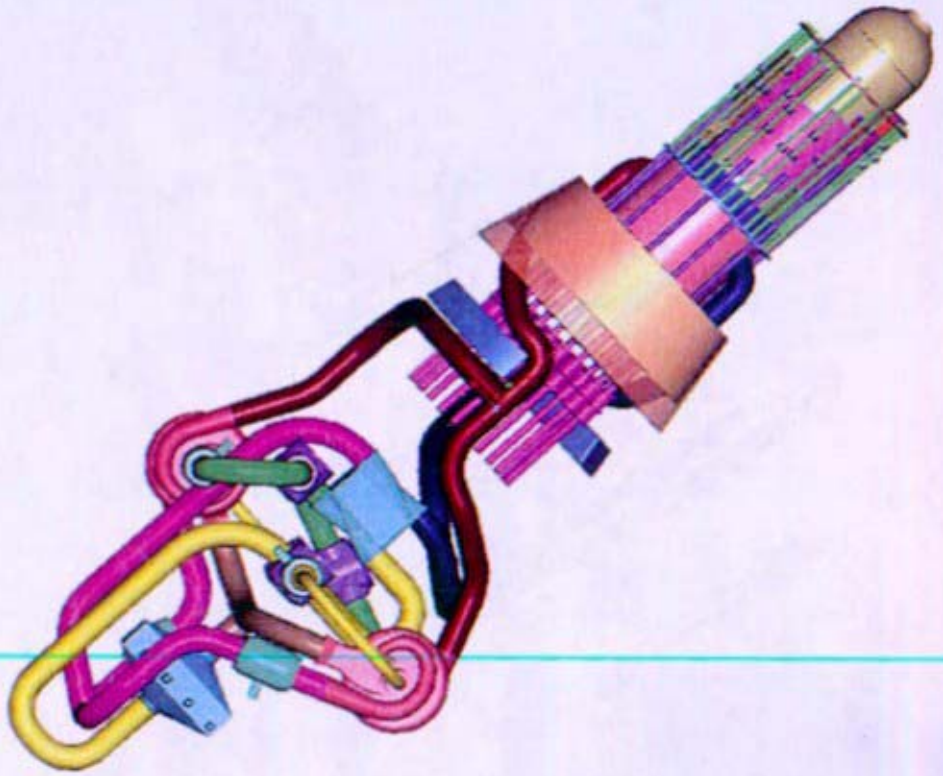


**Figure 5-32. 2-1-1 System Architecture - Version 4**

### 5.7.1.5 2-1-1 System Architecture - Version 5

Version 5 is the next evolution of the 2-1-1 arrangement. By reorienting the gas cooler, the overall piping lengths were decreased and provided other piping benefits. This can be seen in Figure 5-33. All of the components with exception of the Braytons are aligned along the centerline, which benefits the payload. It is also advantageous to thermally couple the hot leg piping to the outside of the plant from a reactor module thermal management standpoint.

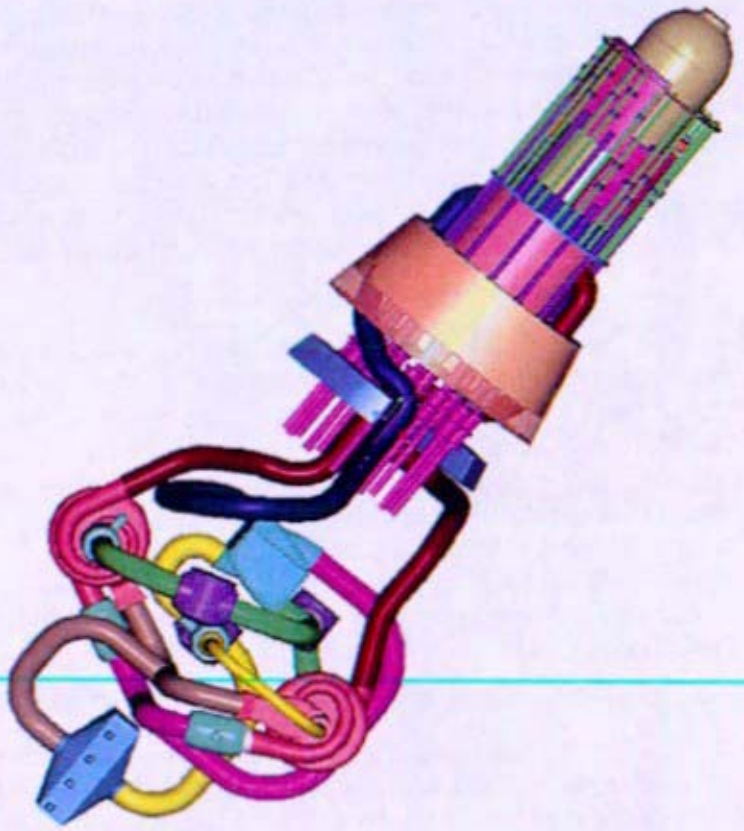


**Figure 5-33. 2-1-1 System Architecture - Version 5**

## 5.8 Future Actions

As the arrangement models evolved, design drivers and constraints were being identified. This iterative process of developing arrangements, evaluating them against design objectives and revising arrangements to better optimize them from a system performance perspective would have continued. The results of these studies would be incorporated into the system architecture selection decision. The process of identifying the reactor module functional requirements and performing spacecraft trade studies would be a joint effort with the spaceship integrator and others involved with the spacecraft design.

Following the system architecture selection decision (number of components), efforts would have shifted to define and evaluate fully the ability of arrangements to satisfy all reactor module functional

requirements and design objectives. These issues include structural, thermal, and operational effects on arrangements, component size and orientation, and additional arrangements with various levels of component redundancy. The following paragraphs describe some of the anticipated challenges.

Structural considerations, thermal management, and operational effects would all affect arrangements of components. With the incorporation of structural systems, such as an aeroshell and the Primary Support Structure as well as auxiliary components, such as micrometeoroid protection, the locations and orientations of all components would be affected. Aspects such as flexibility within the design space, accessibility for equipment support points, and physical geometry of all system components, would impose layout challenges. Thermal concerns would affect placement and orientation of components for heat rejection, and thermal isolation would be required to provide moderate temperature zones and avoid excessive heating of plant and structure components. Additional features would be required to accommodate thermal movement of components relative to each other as temperature changed. Finally, operational effects would affect arrangements, because pipe routing and valve locations are directly coupled with pressure drop, which, in turn, affects system efficiency. Additional information would be required to further investigate these concerns and their effects on the system.

As with the layout of components, the component sizes depend on many factors. The power requirements, number of operating components, pressure drop through the system, and heat balance requirements all affect the dimensions of components by varying the heat transfer area, inlet and outlet ducts, and structural support area. It is also necessary to refine metrics, such as pressure drop, to include component specific values as they become available. Not only are the component dimensions dependent on these metrics, but they are dependent on each other. For example, operational component pressure losses and the pipe diameter and routing affects pressure drop, which affects system efficiency. System efficiency, then, affects the size of the reactor, which also determines the size of the shield and the need for shield caps. Thus, all components, especially the reactor, shield, and primary PCS components would require re-evaluation to both continuously update the individual dimensions and promote the individual design optimizations as well.

Design optimization and re-evaluation is also dependent on mission requirements. The mission dictates module functional requirements and influences design constraints for the arrangement and individual components. Various configurations would have been investigated for feasibility for manned or unmanned missions, different destinations for varying lengths of time, and for missions where levels of maintenance were available.

Lastly, based on the various levels of component redundancy and cross strapping, additional iterations could be performed to assess arrangements with different numbers of components. These systems would be arranged such that the PCS loops would share different components. The 3-3-2 system and the various iterations of the 2-1-1 system are examples of these types of systems.

## 5.9 References

5- 1: KAPL letter SPP-67210-0011, "Space Reactor Shield Design Summary, for Information", to be issued

# Section 6
# Heat Balances – Design and Off-Design System Performance, Parameter Sensitivity Studies

*PRE-DECISIONAL - For planning and discussion purposes only*

(Intentionally Blank)

# Heat Balances – Design and Off-Design System Performance, Parameter Sensitivity Studies

## Table of Contents

6 Heat Balances – Design and Off-Design System Performance, Parameter Sensitivity Studies .... 5
6.1 Summary and Conclusions .... 5
6.2 Heat Balance Model .... 5
6.3 Preliminary Design Heat Balances and Parameter Sensitivity Studies .... 6
6.3.1 Heat Balance for Single Brayton Arrangement .... 9
6.3.2 Heat Balance for Two Brayton Arrangement .... 10
6.3.3 Heat Balance for Three Brayton Arrangement .... 12
6.3.4 Heat Balance for Four Brayton Arrangement .... 14
6.3.5 System Comparison .... 15
6.3.6 Parameter Sensitivity Studies .... 15
6.3.6.1 Converter Loop Piping Diameter Sensitivity – Design Case .... 17
6.3.6.2 Reactor Outlet Temperature Sensitivity – Design Case .... 19
6.3.6.3 Compressor Inlet Temperature Sensitivity – Design Case .... 20
6.3.6.4 Compressor Outlet Pressure Sensitivity – Design Case .... 21
6.3.6.5 Compressor Pressure Ratio Sensitivity – Design Case .... 23
6.3.6.6 Brayton Turbomachinery Efficiency Sensitivity – Design Case .... 24
6.3.6.7 Radiator Heat Pipe Operating Temperature Sensitivity – Design Case .... 25
6.3.6.8 Conclusions – Design Heat Balances .... 26
6.4 Preliminary Off-Design Heat Balances and Parameter Sensitivity Studies .... 27
6.4.1 Reactor Outlet Temperature Sensitivity – Off-Design Case .... 30
6.4.2 Loss of Radiator Area Margin – Off-Design Case .... 31
6.4.3 Gas Leakage – Off-Design Case .... 32
6.4.4 Turbomachinery Efficiency Degradation – Off-Design Case .... 33
6.4.5 Effective Sink Temperature – Off-Design Case .... 34
6.4.6 Conclusions – Off-Design Heat Balances .... 35
6.5 References .... 36

## List of Figures

Figure 6-1: Single Brayton System Heat Balance (Non-optimized) ..... 9
Figure 6-2: Two Brayton System Heat Balance (Non-optimized) ..... 10
Figure 6-3: Three Brayton System Heat Balance (Non-optimized) ..... 12
Figure 6-4: Four Brayton System Heat Balance (Non-optimized) ..... 14
Figure 6-5: Reactor Mass Sensitivity to HeXe Coolant Composition ..... 16
Figure 6-6: Converter Loop Piping Diameter Sensitivity ..... 18
Figure 6-7: Reactor Outlet Temperature Sensitivity ..... 19
Figure 6-8: Compressor Inlet Temperature Sensitivity ..... 20
Figure 6-9: Compressor Outlet Pressure Sensitivity ..... 22
Figure 6-10: Compressor Pressure Ratio Sensitivity ..... 23
Figure 6-11: Brayton Turbomachinery Efficiency Sensitivity ..... 24
Figure 6-12: Radiator Heat Pipe Operating Temperature Sensitivity ..... 25
Figure 6-13: Four Brayton System Heat Balance (1st Iteration of Parameter Optimization) ..... 27
Figure 6-14: Design Heat Balance used as Basis for Off-Design Studies ..... 28
Figure 6-15: Baseline Off-Design Heat Balance ..... 29
Figure 6-16: Reactor Outlet Temperature Sensitivity ..... 30
Figure 6-17: Loss of Radiator Area Margin Sensitivity ..... 31
Figure 6-18: Gas Leakage Sensitivity ..... 32
Figure 6-19: Turbomachinery Efficiency Degradation Sensitivity ..... 33
Figure 6-20: Effective Sink Temperature Sensitivity ..... 34

## List of Tables

Table 6-1: Comparison of Non-optimized Design Heat Balances ..... 15
Table 6-2: Reference Pipe Sizing for Four Brayton Arrangement ..... 17
Table 6-3: Assumed Pipe Sizes for Compressor Outlet Pressure Sensitivity Study ..... 21
Table 6-4: Assumed Turbomachinery Efficiencies ..... 21
Table 6-5: Brayton Turbomachinery Efficiency Sensitivity Study Parameters ..... 24

# 6 Heat Balances – Design and Off-Design System Performance, Parameter Sensitivity Studies

## 6.1 Summary and Conclusions

This section describes the results of system heat balance studies and parameter sensitivity studies that were performed for the Prometheus Space Nuclear Power Plant (SNPP). These evaluations were performed to establish the range of plant operating parameters needed to satisfy the requirements described in Section 1. The results of these studies are used to establish SNPP component sizing and operating conditions, enable comparison of candidate system architectures, and initiate trade studies. A few key observations regarding these preliminary heat balances and parameter sensitivity studies are:

---

- A key driver for the overall plant efficiency is the relative complexity of the piping system and the resulting impact on piping system pressure drop. Without optimization, both the single Brayton and two Brayton system arrangements are able to produce ~185 kWe while meeting the 450 $m^2$ heat rejection segment radiator area objective.
- Relatively minor improvements in assumed heat pipe capability (heat flux vs. operating temperature and service life) and Brayton turbomachinery performance (turbine and compressor efficiency) were found to provide significant system benefits. Conversely, relatively small reductions in turbine and compressor efficiencies were shown to significantly degrade overall system performance. Thus, Brayton turbomachinery should continue to be a key area of development.
- Design heat balance sensitivity studies suggest that fundamental design concerns (material performance at elevated operating temperatures, manageable mass and radiator area) may be alleviated with a modest reduction in the spaceship electrical requirement. Conversely, spaceship electric requirements greater than the 185 kWe assumed in these studies would make satisfying all design constraints progressively more difficult and would require increased reactor thermal output and increased heat rejection segment radiator area.
- Additional effort must be directed toward identification of material temperature limits, operating strategy, temperature band, instrumentation accuracy, and plant transient response prior to establishing an operating temperature band that will ensure design limits are not exceeded.
- For the four Brayton system, increasing pipe diameter and decreasing compressor inlet temperature were found to have larger impacts on system performance for small changes than the other parameters studied.

---

## 6.2 Heat Balance Model

Heat balance studies were performed using a spreadsheet model created by the NRPCT to calculate operating conditions for the direct gas Brayton system. The model uses the plant arrangements described in Section 5 which have one reactor providing heat to one, two, three, or four parallel Brayton conversion loops. Each energy conversion loop incorporates one Brayton turboalternator, one recuperator, one gas cooler, and associated piping. One converter loop is normally operating for the one and two loop cases and two loops are normally operating for the three and four loop cases.

The model has the ability to determine both design state points and off-design operating points for a fixed sized system. The design portion of the model determines the state points for a system designed to produce a net 185 kWe to be supplied to the spaceship. The off-design portion of the model uses fixed sized components, as determined in the design portion of the model, to predict off-design operating conditions for the system. A more detailed description of the model can be found in Reference 6-1.

## 6.3 Preliminary Design Heat Balances and Parameter Sensitivity Studies

The key driver for the heat balance is to produce the 185 kWe required by the spaceship. In order to achieve this output from the Power Conditioning and Distribution (PCAD) system, ~200 kWe must be output from the operating converter loop(s). The total electrical output of a converter is the turbine power minus the compressor power, shaft mounted fan power, bearing losses, windage losses, and alternator efficiency losses.

$$Power_{alt} = \dot{W}_{Turb} - \dot{W}_{Comp} - \sum \dot{W}_{Losses}$$

Plant parameters can be varied to optimize the system to achieve desired objectives. Key design objectives include:

- Maximize converter loop and overall system efficiency
- Minimize mass
- Maximize reliability
- Minimize required heat rejection segment radiator area; a limit of ~450 $m^2$ had been assumed for concept downselection trade studies documented in Reference 6-7
- Minimize reactor fuel load
- Maximize operational flexibility
- Minimize operating temperatures of reactor vessel and reactor outlet piping to mitigate concerns associated with material performance at elevated temperature
- Maximize extensibility to missions with other power requirements and/or operating environments

While many of these objectives are complementary, variation of parameters can sometimes result in competing effects. For example, a set of plant parameters that may tend to maximize efficiency, minimize mass, minimize fuel load, and minimize radiator area may lack sufficient operational flexibility, degrade system reliability, result in unsatisfactory material performance, or preclude operation in other environments. Ultimately, a set of parameters must be identified which satisfactorily balances all the design objectives.

Converter and system efficiencies may be increased by increasing the turbine inlet temperature and/or decreasing the compressor inlet temperature. Increasing turbine inlet temperature increases turbine power by creating a larger temperature drop across the turbine. Decreasing compressor inlet temperature decreases the compressor and fan power requirements by creating a smaller temperature rise across the compressor and fan. Decreasing compressor inlet temperature also effectively increases system efficiency and decreases the heat rejection segment temperature. These competing factors combine to create an optimal value for compressor inlet temperature for which required radiator area is minimized and heat rejection segment operating temperature is maximized but within operational limits.

Piping and component pressure drops also impact the converter and system efficiencies. The turbine pressure ratio is set by the pressure rise across the compressor minus the pressure losses in the components and piping. The larger the pressure drop within the system, the smaller the turbine pressure ratio. Decreasing the turbine pressure ratio decreases the turbine temperature ratio and therefore the turbine temperature drop. This decreases the amount of useful work extracted from the fluid and results in a less efficient system.

The following assumptions apply to the design heat balances and sensitivity studies described in Section 6.3:

- ~185 kWe total to bus and electric plant loads
- Piping system arrangements as described in Section 5 which incorporate internally insulated reactor outlet piping as described in Reference 6-2
  - Reactor Outlet Piping
    12.4 cm ID flow diameter (internally insulated)/16.0 cm OD
  - Reactor Inlet Piping
    15.2 cm ID flow diameter/16.0 cm OD
  - Converter Loop Piping
    15.2 cm ID flow diameter/16.0 cm OD – for single and two Brayton arrangements (Sections 6.3.1 and 6.3.2)
  - Converter Loop Piping
    9.4 cm ID flow diameter/10.0 cm OD – for three and four Brayton arrangements (Sections 6.3.3 and 6.3.4) [1]
  - Piping wall thickness as calculated by methods described in Attachment B of Reference 6-2
  - Hydraulically smooth piping
- 1150K reactor outlet temperature [1]
- 390K compressor inlet temperature [1]
- 2.00 MPa compressor outlet pressure [1]
- 2.00 compressor pressure ratio [1]
- 500K maximum radiator heat pipe operating temperature [1]
- 31.5 g/gmol HeXe mixture reactor coolant/working fluid [78.4% He (atomic)]
- 2.9% of the reactor thermal output is lost to the environment
- Brayton turbine efficiency (see Section 9.1.3)
  - 90.0% – for single and two Brayton arrangements (Sections 6.3.1 and 6.3.2)
  - 88.4% – for three and four Brayton arrangements (Sections 6.3.3 and 6.3.4) [1]
- Brayton compressor efficiency (see Section 9.1.4)
  - 84.7% – for single and two Brayton arrangements (Sections 6.3.1 and 6.3.2)
  - 84.0% – for three and four Brayton arrangements (Sections 6.3.3 and 6.3.4) [1]
- Brayton turbomachinery operating at constant speed of 45,000 RPM

[1] Except when evaluating the sensitivity of these parameters in Section 6.3.6

- Pressure drop across components are assumed to be independent of flow parameters; e.g. temperature, pressure, flowrate
  - 50 kPa reactor
  - 15 kPa low pressure side of recuperator
  - 15 kPa high pressure side of recuperator
  - 20 kPa gas cooler (gas side) – for single and two Brayton arrangements (Sections 6.3.1 and 6.3.2)
  - 10 kPa gas cooler (gas side) – for three and four Brayton arrangements (Sections 6.3.3 and 6.3.4)
- 20% margin applied to calculated piping system pressure drop values
- 92% effective recuperator
- 94% effective gas cooler
- 30% efficient heat rejection segment pumps
- 95% alternator electromagnetic efficiency
- 99% efficient cabling from converter to PCAD system
- 97% efficient Power Management and Distribution (PMAD) electronics
- 99% efficient cabling from PCAD system to loads
- 500 W PMAD controller load
- 200K radiator sink temperature
- 14.5% margin applied to calculated required heat rejection area

The heat balances given in Sections 6.3.1, 6.3.2, 6.3.3, and 6.3.4 are preliminary and are provided only for baseline comparisons. To enable comparison of the one, two, three, and four Brayton systems, the heat balances assume the same set of input parameters. The assumed operating parameters do not represent the optimal set of operating conditions for any particular configuration. Each of the heat balances incorporate piping system pressure losses based on the preliminary arrangements described in Section 5 of this report which have not been optimized for pressure drop, mass, or thermal management concerns.

Without optimization, both the single Brayton and two Brayton system arrangements are able to produce ~185 kWe while meeting the 450 $m^2$ heat rejection segment radiator area objective. The two Brayton system also meets the single fault tolerance requirement. Further optimization of operating parameters and arrangements of piping and components is required. Trade studies with the spaceship must be performed to optimize reactor module and spaceship design in areas such as heat rejection radiator area and boom length.

System heat balances determine component heat loads and operating conditions and, thus, provide the basis of system mass estimates. Section 4.5.3 describes the heat balances and piping arrangements that were assumed for mass estimating purposes.

### 6.3.1 Heat Balance for Single Brayton Arrangement

The plant arrangement assumed for the single Brayton system heat balance is illustrated in Figure 5-26. This system has one turboalternator, recuperator, and gas cooler. The turboalternator is sized to produce the entire ~200 kWe required for full power. The recuperator and gas cooler are appropriately sized to meet this power requirement. No valves are required in this system since there is only one energy conversion loop.

The reactor thermal rating for this case is 783 kWt with a reactor inlet temperature of 896 K. The converter is 25.9% efficient and the system efficiency is 23.6%. The required radiator area, with 14.5% margin, is 453 $m^2$ to reject 560 kWt.

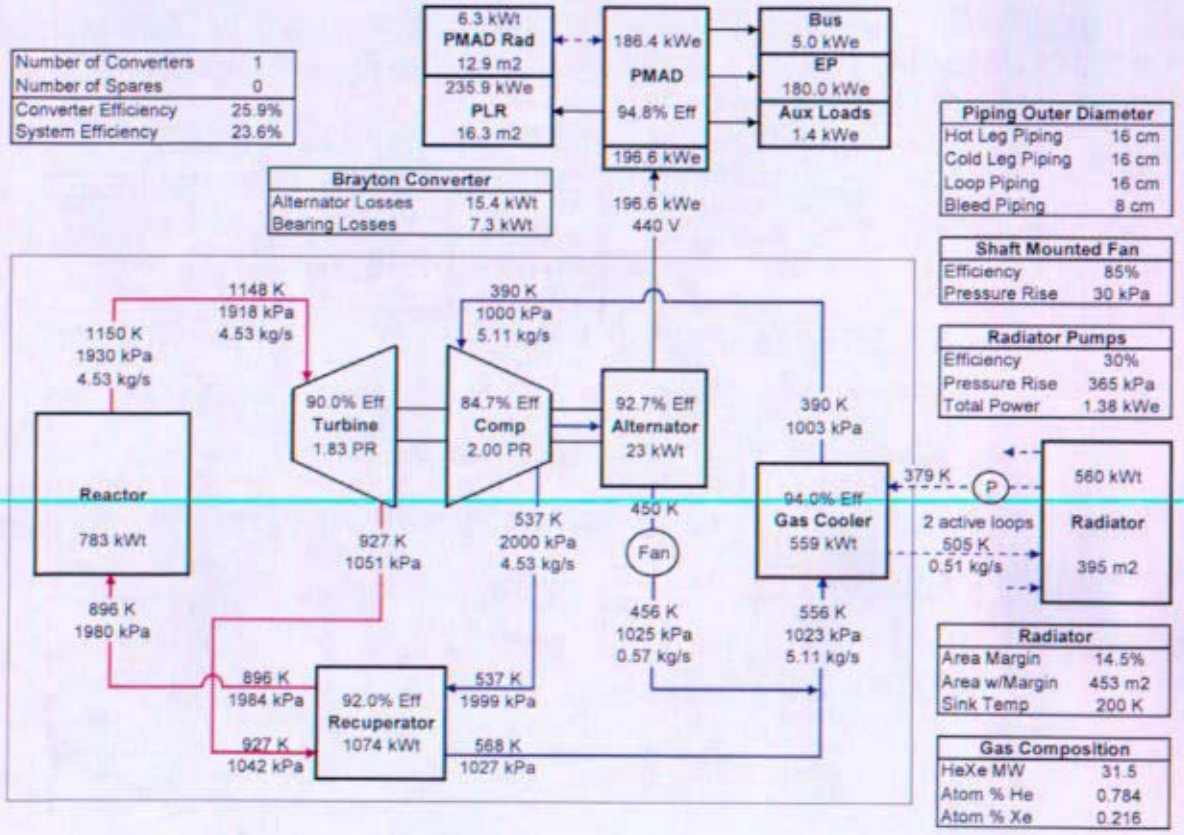



**Figure 6-1: Single Brayton System Heat Balance (Non-optimized)**

### 6.3.2 Heat Balance for Two Brayton Arrangement

The plant arrangement assumed for the two Brayton system heat balance is illustrated in Figure 5-27. This system has two converter loops each with one turboalternator, recuperator, and gas cooler. No cross-strapping of converter loop components is assumed. Each turboalternator is sized to produce the entire ~200 kWe required for full power. The recuperator and gas cooler are appropriately sized to meet this power requirement. One converter loop is normally operating while the other is an idle spare. A check valve is located at the outlet of each compressor to prevent backflow through the idle loop to maximize system efficiency, minimize bypass cooling flow around the reactor, and prevent potential damage to turbomachinery due to reverse rotation. An isolation valve installed the outlet of each compressor enables loop shutdown and startup evolutions and provides Brayton overspeed protection for certain electric plant casualties.

The reactor thermal rating for this case is 779 kWt with a reactor inlet temperature of 895 K. The converter is 26.0% efficient and the system efficiency is 23.8%. The required radiator area, with 14.5% margin, is 449 $m^2$ to reject 556 kWt.

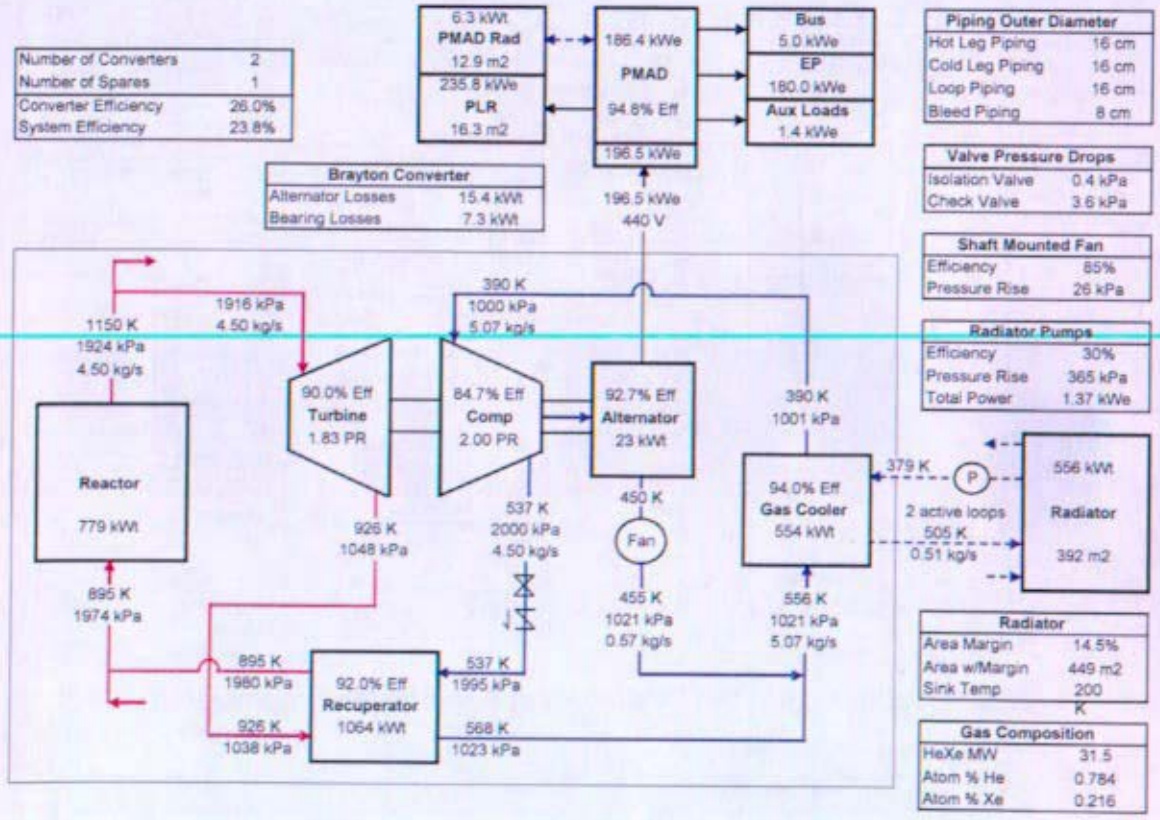



**Figure 6-2: Two Brayton System Heat Balance (Non-optimized)**

As discussed in Section 3.6, an alternative two Brayton system architecture was evaluated where both turboalternators would normally operate at less than their rated capacity but jointly produce the full rated system power by reducing turbine inlet temperature and rotational speed. In the event of failure of one turboalternator, full rated system power is restored by increasing the turbine inlet temperature and rotational speed of the remaining unit such that each turboalternator operates at its rated capacity. This mode of operation is desirable to mitigate concerns associated with material performance at elevated temperature and is expected to perform comparably to the system described in Figure 6-2.

The two Brayton system architecture discussed in Section 3.5 includes two Brayton units each rated for approximately 100 kWe. Since both Brayton units would be operated in parallel to produce the required electrical output, the heat balance would be similar to that generated for the three Brayton arrangement (Figure 6-3).

### 6.3.3 Heat Balance for Three Brayton Arrangement

The plant arrangement assumed for the three Brayton system is illustrated in Figure 5-24. This system has three converter loops each with one turboalternator, recuperator, and gas cooler. No cross-strapping of converter loop components is assumed. Each turboalternator is sized to produce half of the required power or ~100 kWe. The recuperator and gas cooler are appropriately sized to meet this power requirement. Two converter loops are normally operating while the other is an idle spare. A check valve is located at the outlet of each compressor to prevent backflow through the idle loop to maximize system efficiency, minimize bypass cooling flow around the reactor, and prevent potential damage to turbomachinery due to reverse rotation. An isolation valve installed the outlet of each compressor enables loop shutdown and startup evolutions and provides Brayton overspeed protection for certain electric plant casualties.

The reactor thermal rating for this case is 932 kWt with a reactor inlet temperature of 906 K. The converter is 21.8% efficient and the system efficiency is 19.9%. The required radiator area, with 14.5% margin, is 566 $m^2$ to reject 700 kWt.

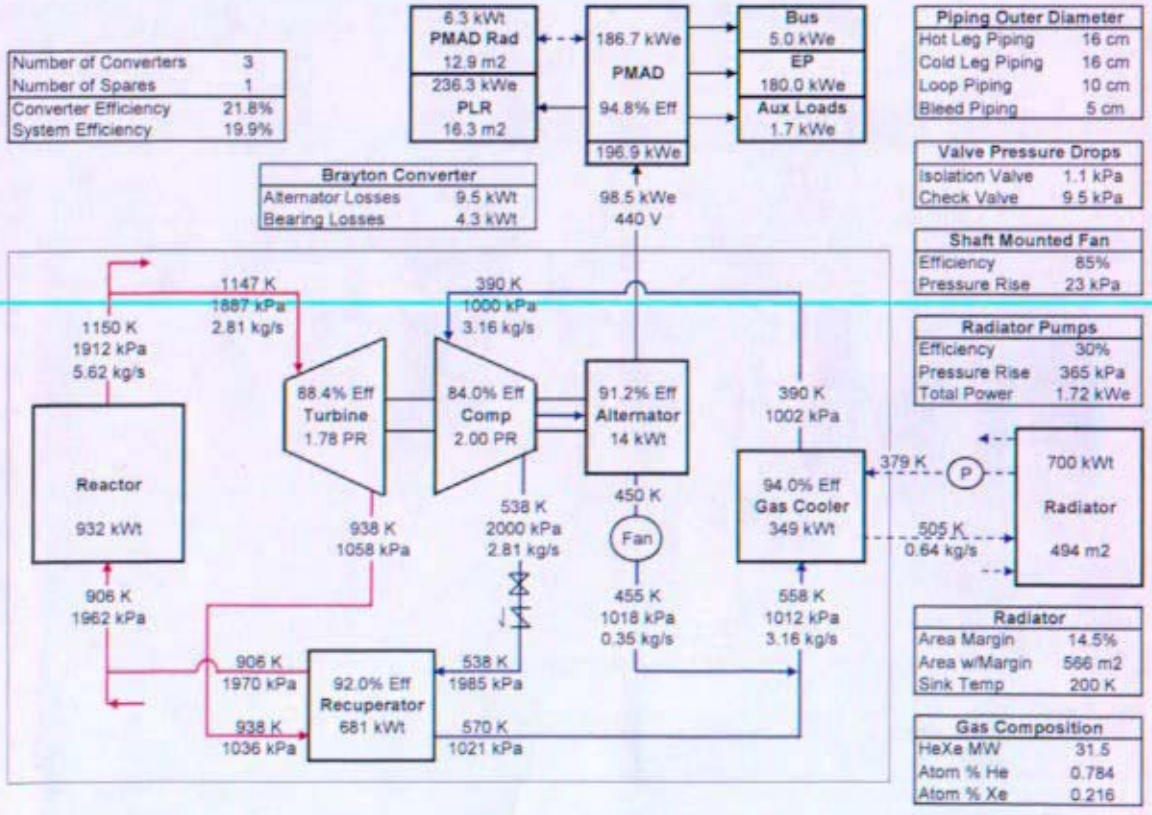



**Figure 6-3: Three Brayton System Heat Balance (Non-optimized)**

As discussed in Section 3.7, an alternative three Brayton system architecture was evaluated where all three turboalternators would normally operate at less than their rated capacity but jointly produce the full rated system power by reducing turbine inlet temperature and rotational speed. In the event of failure of one turboalternator, full rated system power is restored by increasing the turbine inlet temperature and rotational speed of the remaining units such that each turboalternator operates at its rated capacity. This mode of operation is desirable to mitigate concerns associated with material performance at elevated temperature and is expected to perform comparably to the system described in Figure 6-3.

### 6.3.4 Heat Balance for Four Brayton Arrangement

The plant arrangement assumed for the four Brayton system is illustrated in Figure 5-20. This system has four converter loops each with one turboalternator, recuperator, and gas cooler. No cross-strapping of converter loop components is assumed. Each turboalternator is sized to produce half of the required power or ~100 kWe. The recuperator and gas cooler are appropriately sized to meet this power requirement. Two converter loops are normally operating while the remaining two are idle spares. A check valve is located at the outlet of each compressor to prevent backflow through the idle loop to maximize system efficiency, minimize bypass cooling flow around the reactor, and prevent potential damage to turbomachinery due to reverse rotation. An isolation valve installed the outlet of each compressor enables loop shutdown and startup evolutions and provides Brayton overspeed protection for certain electric plant casualties.

The four Brayton system makes at most 182 kWe of the required 185 kWe with the assumed piping arrangement and system parameters. Increasing the mass flow rate typically increases the power output but, in this case, the accompanying increase in piping pressure drop dominates and less power is produced as the mass flow rate increases above an optimal flow rate. The reactor thermal rating for this case is 1002 kWt with a reactor inlet temperature of 911 K. The converter is 19.9% efficient and the system efficiency is 18.2%. The required radiator area, with 14.5% margin, is 621 $m^2$ to reject 767 kWt.

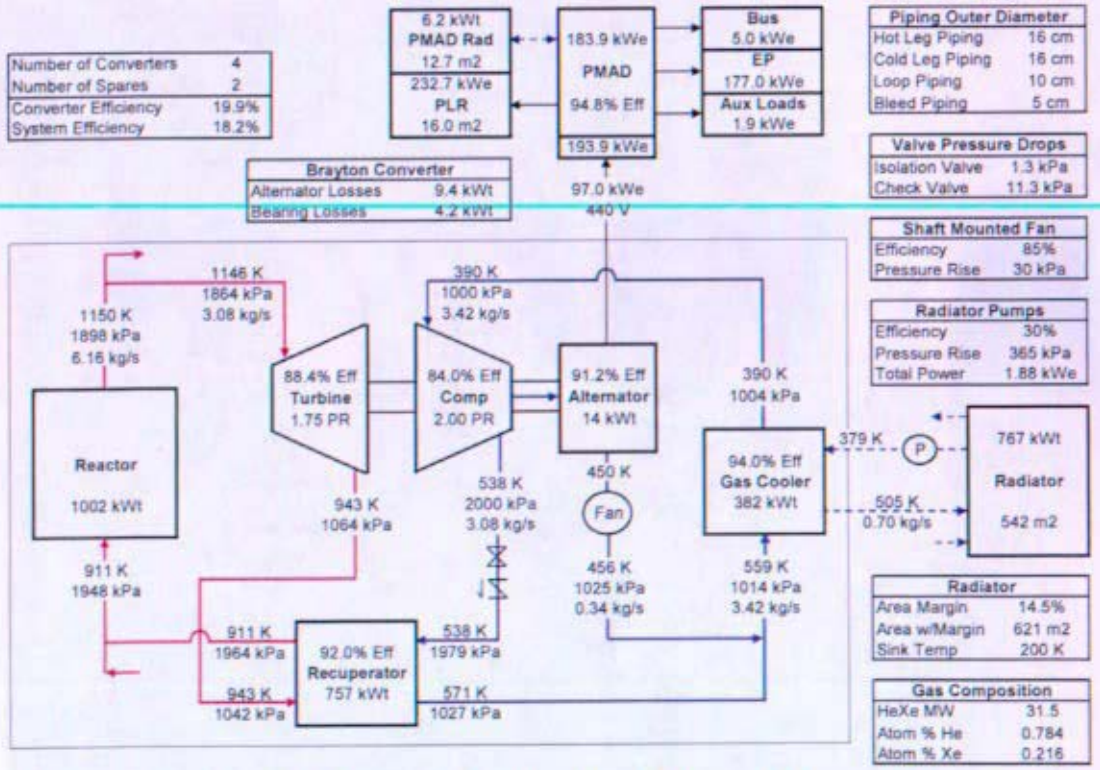



**Figure 6-4: Four Brayton System Heat Balance (Non-optimized)**

### 6.3.5 System Comparison

A summary of key outputs from the design heat balances for the non-optimized one, two, three, and four Brayton plant configurations (Figure 6-1 through Figure 6-4) is provided in Table 6-1.

**Table 6-1: Comparison of Non-optimized Design Heat Balances**

| Basic Plant Configuration | Electrical Output [kWe] | Reactor Thermal Power [kWt] | Required Radiator Area [$m^2$] | Reactor Inlet Temperature [K] | System Efficiency [%] |
|---|---|---|---|---|---|
| Single Brayton Section 6.3.1 | 185 | 783 | 453 | 896 | 23.6 |
| Two Brayton Section 6.3.2 | 185 | 779 | 449 | 895 | 23.8 |
| Three Brayton Section 6.3.3 | 185 | 932 | 566 | 906 | 19.9 |
| Four Brayton Section 6.3.4 | 182 | 1002 | 621 | 911 | 18.2 |

While it is assumed that the turbine and compressor efficiencies are slightly higher for the single Brayton and two Brayton systems, the key driver for the degradation in overall plant efficiency for the three and four Brayton systems is the relative complexity of the piping systems and the resulting impact on piping system pressure drop. For plants with multiple converter loops, flow splits in the reactor inlet and outlet headers and inclusion of valves become significant additions to the overall piping system pressure drop. Piping system complexity generally increases as more components are arranged into the prescribed space envelope. Notwithstanding these factors, it is noted that the two Brayton system is slightly more efficient than the single Brayton system. This is an artifact of the preliminary, non-optimized piping system arrangements used in the these heat balances where the single Brayton arrangement has slightly greater piping system pressure drop than the two Brayton system despite having no converter loop flow splits and no valves. The performance trends exhibited in Table 6-1 clearly demonstrate the need for continued piping system optimization to reduce piping system pressure drops.

As discussed in Section 6.3.4, the four Brayton system is able to produce only ~98% of the required 185 kWe given the assumed piping arrangement and system parameters. Parameter sensitivity studies (Section 6.3.6) indicate that the four Brayton system remains a viable plant configuration as very minor changes to the baseline assumptions utilized here result in a plant output of 185 kWe.

### 6.3.6 Parameter Sensitivity Studies

A number of sensitivity studies were performed to determine the effect of parameter variations on the plant's overall heat balance and other parameters of interest. Of particular interest was the effect of parameter variation on required reactor thermal output, required radiator area, and reactor inlet temperature. The overall mass of the SNPP is minimized when reactor thermal output and required radiator area are near minimum values as the mass of the reactor, the reactor radiation shield, and the heat rejection segment dominate the overall SNPP mass. Minimizing the required thermal output of the reactor has many benefits as the mass of the fuel load, reactor structure, and reactor radiation

shield decrease with required reactor thermal output. The effect of parameter variation on reactor inlet temperature was of interest since concerns associated with material performance at high temperatures are alleviated as reactor inlet temperature is reduced.

Sensitivity studies were performed for the following plant parameters:

- Converter Loop Piping Diameter
- Reactor Outlet Temperature
- Compressor Inlet Temperature
- Compressor Outlet Pressure
- Brayton Turbine and Compressor Efficiency
- Radiator Heat Pipe Operating Temperature

As stated in Section 6.3, all heat balances and sensitivity studies were performed assuming a HeXe mixture with a molecular weight of 31.5 g/gmol [78.4% He (atomic)]. Studies of the overall plant performance sensitivity to other HeXe compositions were not performed. Sensitivity studies described in References 6-3 and 6-4 indicate that a HeXe mixture with a molecular weight of ~40 g/gmol minimizes overall plant mass and provides adequate Brayton performance and heat transfer capability for closed loop, indirect gas Brayton systems operating at the power levels assumed here. Since the direct gas Brayton plant configuration utilizes the same fluid for the energy conversion working fluid and the reactor coolant, the competing effects of turbomachinery performance and heat transfer capability must be further evaluated. The sensitivity of reactor mass to HeXe coolant composition for several candidate reactor design concepts is shown in Figure 6-5 (from Reference 6-5).

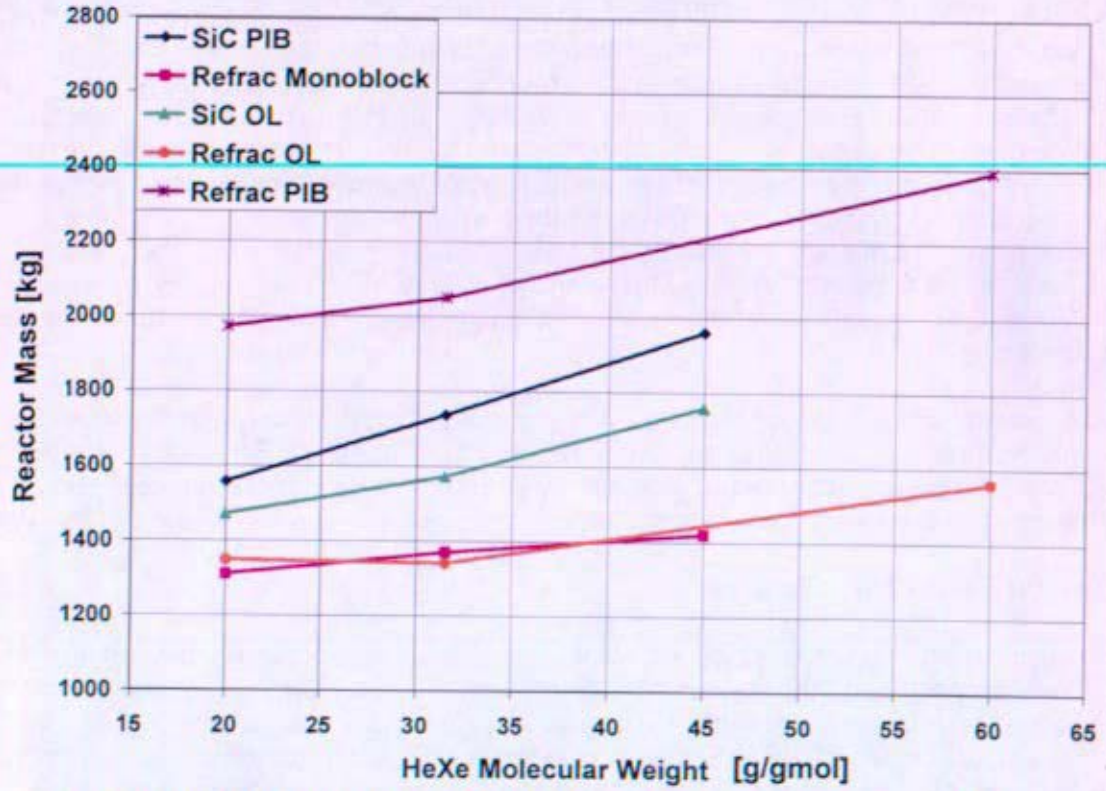



**Figure 6-5: Reactor Mass Sensitivity to HeXe Coolant Composition**

For each of the reactor concepts represented in Figure 6-5, reactor mass decreases as the concentration of He increases toward the lowest molecular weight mixture that was evaluated, 20.0 g/gmol. It is noted that reactor mass at a molecular weight of 31.5 g/gmol, the composition assumed here, is within 10% of the reactor mass evaluated at 20.0 g/gmol for each case. Heat exchanger and reactor mass and performance optimize toward lower molecular weight (better heat transfer) while turbomachinery performance optimizes toward higher molecular weight (higher specific speed). Integrated plant trade studies must be performed to identify the optimal composition of HeXe that balances turbomachinery performance with heat transfer capability for the direct gas system.

The plant parameter sensitivity studies described in this section demonstrate that significant improvements in system performance can be realized with advances in a few key technology areas. Relatively minor improvements in heat pipe capability (heat flux vs. operating temperature and service life) and Brayton turbomachinery performance (turbine and compressor efficiency) were found to provide significant system benefits. Piping system and component pressure losses were also found to have a significant impact on overall plant efficiency.

### 6.3.6.1 Converter Loop Piping Diameter Sensitivity – Design Case

Table 6-2 describes the piping sizes assumed in the four Brayton system arrangement (Figure 5-19) used as a baseline for these sensitivity studies.

**Table 6-2: Reference Pipe Sizing for Four Brayton Arrangement**

| | Outer Diameter [cm] | Inner Diameter [cm] | Wall Thickness [cm] |
|---|---|---|---|
| Reactor Outlet Piping | 16.0 | 12.4 (assumes 1.39 cm thick internal insulation and liner) | 0.4 |
| Reactor Inlet Piping | 16.0 | 15.2 | 0.4 |
| Converter Loop Piping | 10.0 | 9.4 | 0.3 |
| Alternator Cooling Piping | 5.0 | 4.6 | 0.2 |

Flow losses in converter loop piping were found to have a significant impact on the overall plant efficiency, particularly in the low pressure portions of the loops. The sensitivity of converter loop piping diameter to overall plant performance was examined for a range of converter loop piping sizes from 10.0 to 16.0 cm outer diameter. The wall thickness for the converter loop piping was assumed constant over the range of sizes evaluated.

It should not be inferred that piping arrangements were developed for four Brayton systems with converter loop piping greater than 10 cm OD. The piping lengths and bend locations used in the baseline four Brayton arrangement (Figure 5-19) are assumed in this sensitivity study. Converter loop piping diameter and bend radii were simply increased without regard for space envelope constraints or resultant changes to piping length and bend locations. The results of the converter loop piping diameter sensitivity study are shown in Figure 6-6.

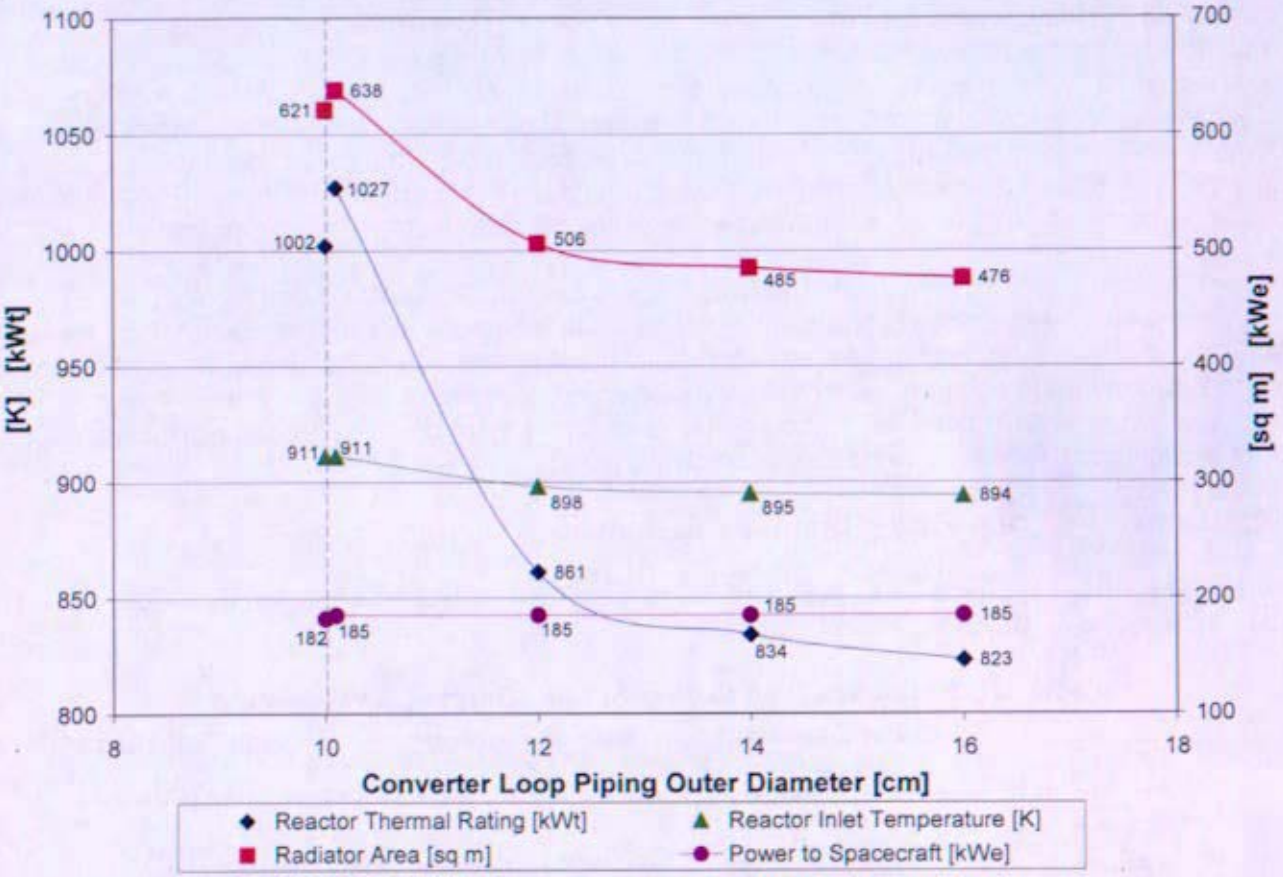



**Figure 6-6: Converter Loop Piping Diameter Sensitivity**

As discussed in Section 6.3.4, the baseline four Brayton system is able to produce only ~98% of the required 185 kWe given the assumed piping arrangement and system parameters. However, Figure 6-6 shows that 185 kWe may be achieved with a very small increase in the size of converter loop piping (9.5 cm ID/10.1 cm OD). It is also noted that other parameters of interest (reactor thermal rating, required radiator area, and reactor inlet temperature) significantly benefit if the diameter were further increased to 11.4 cm ID/12.0 cm OD. Increases in converter loop piping size beyond 11.4 cm ID/12.0 cm OD provide comparatively little additional benefit.

### 6.3.6.2 Reactor Outlet Temperature Sensitivity – Design Case

The sensitivity of reactor outlet temperature to overall plant performance was examined for a temperature range of 1100K to 1200K. Turbine isentropic efficiency is assumed to be constant over the range of temperatures evaluated. The results of the reactor outlet temperature sensitivity study are shown in Figure 6-7.

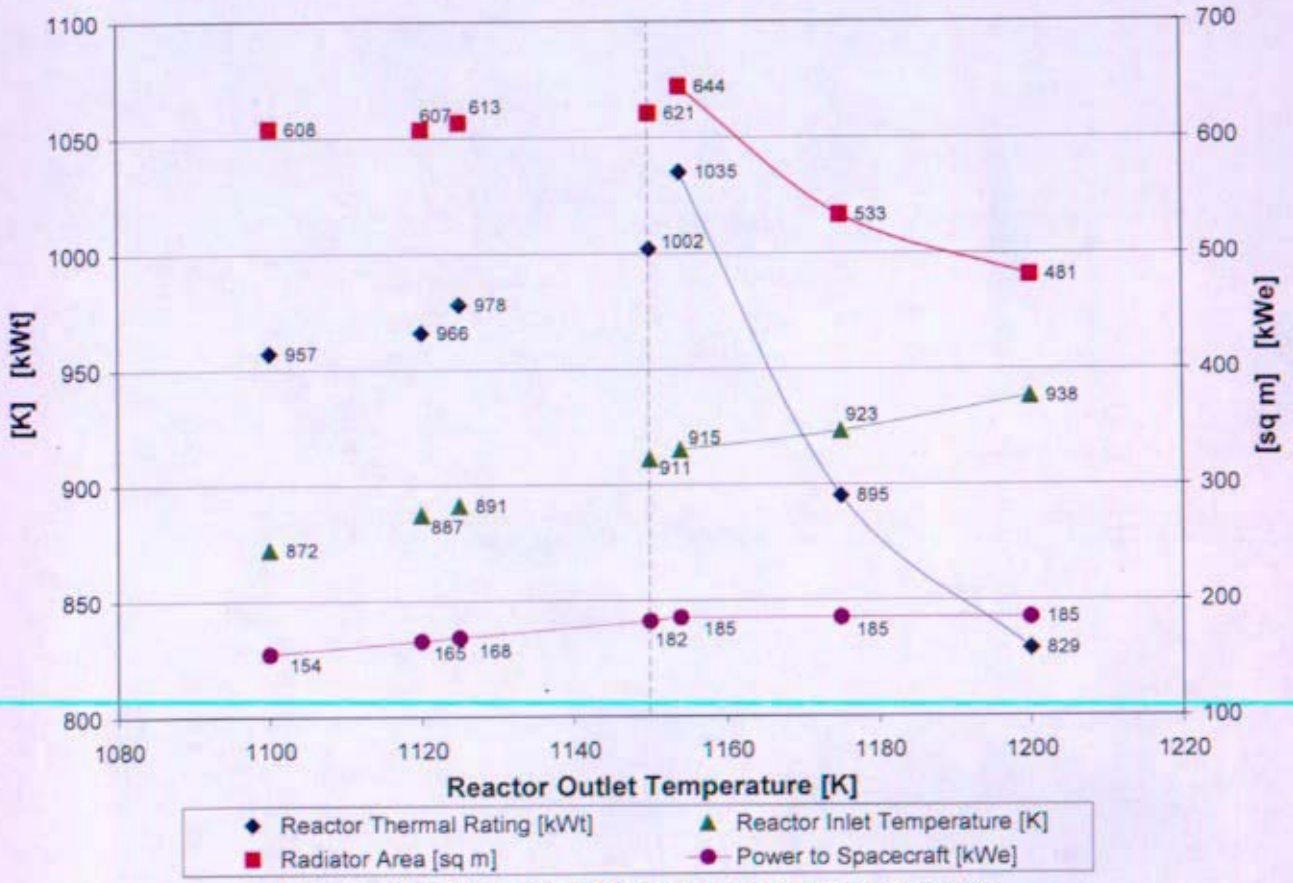



**Figure 6-7: Reactor Outlet Temperature Sensitivity**

As shown in Figure 6-7, the 185 kWe requirement may be achieved with a very small increase in the reactor outlet temperature (1154K). It is also noted that the reactor thermal rating and the required radiator area significantly benefit as reactor outlet temperature increases. However, it is noted that reactor inlet temperature increases as reactor outlet temperature increases. The benefits of increasing reactor outlet temperature (reduced system mass and fuel loading) must be weighed against issues associated with material performance at high temperatures.

### 6.3.6.3 Compressor Inlet Temperature Sensitivity – Design Case

The sensitivity of compressor inlet temperature to overall plant performance was examined for a temperature range of 350K to 400K. Compressor efficiency is assumed to be constant over the range of temperatures evaluated. The results of the compressor inlet temperature sensitivity study are shown in Figure 6-8.

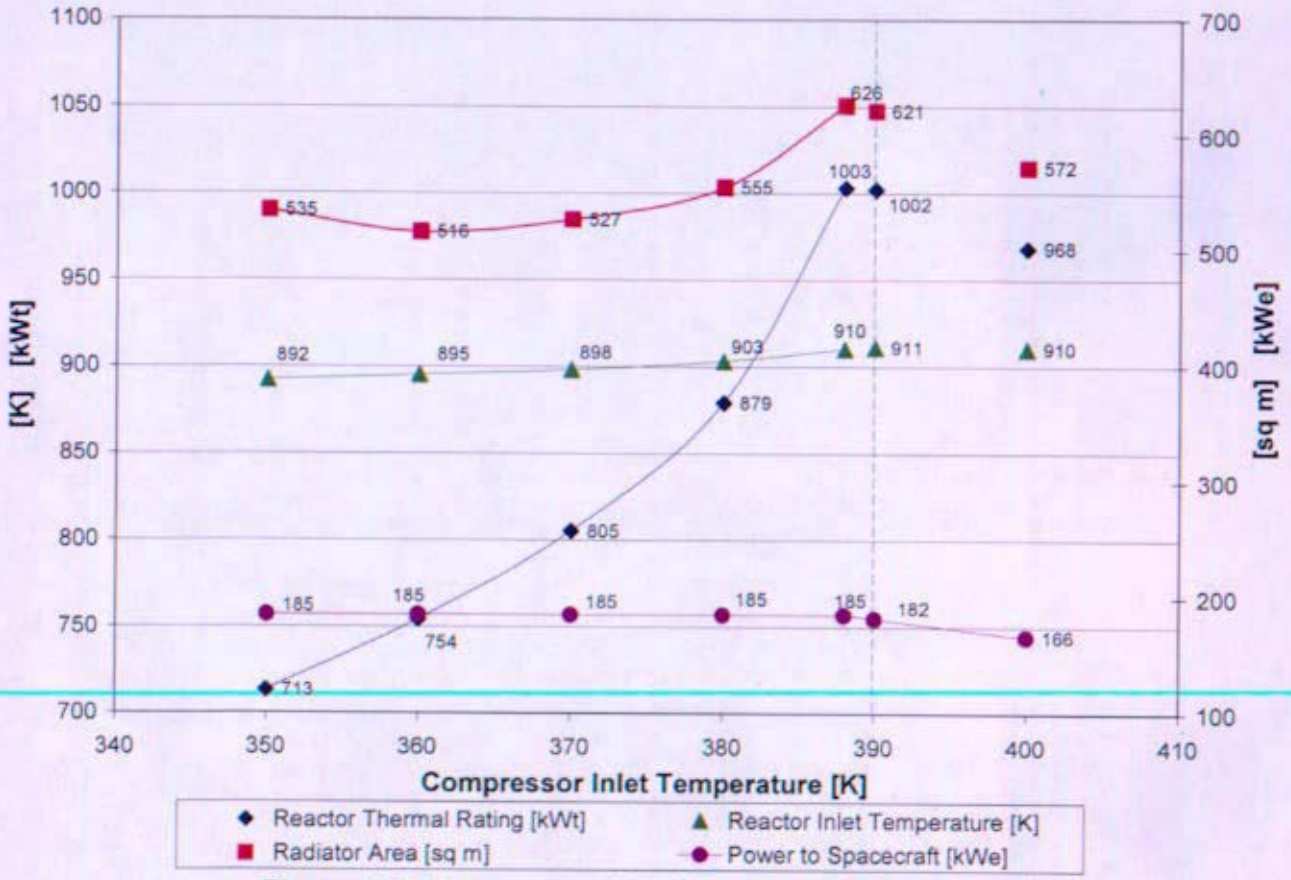



**Figure 6-8: Compressor Inlet Temperature Sensitivity**

As shown in Figure 6-8, the 185 kWe requirement may be achieved with a very small decrease in the compressor inlet temperature (388K). It is also noted that reactor thermal rating, required radiator area, and reactor inlet temperature benefit with decreasing compressor inlet temperature. However, gas cooler inlet temperature also decreases as compressor inlet temperature decreases. This reduces the temperature difference between the gas and the water streams and results in a larger required heat transfer area in the gas cooler. For example, decreasing compressor inlet temperature from 390K to 360K requires a 19% increase in the gas cooler heat transfer area. The benefits of lowering compressor inlet temperature must be balanced against increased gas cooler mass and a potential increase in the probability of failure of the gas cooler pressure boundary.

### 6.3.6.4 Compressor Outlet Pressure Sensitivity – Design Case

The sensitivity of compressor outlet pressure to overall plant performance was examined for a pressure range of 1.38 MPa to 4.00 MPa. Outer diameter of the reactor outlet piping, reactor inlet piping, converter loop piping, and alternator cooling piping were assumed to be constant as shown in Table 6-2. Thickness of insulation and liner in the reactor outlet piping was also assumed to be constant at 1.39 cm. Piping wall thickness is assumed to vary with compressor outlet pressure as shown in Table 6-3.

**Table 6-3: Assumed Pipe Sizes for Compressor Outlet Pressure Sensitivity Study**

| | Compressor Outlet Pressure [MPa] | | | | | |
|---|---|---|---|---|---|---|
| | ≤ 2.00 | 2.03 | 2.50 | 3.00 | 3.50 | 4.00 |
| Reactor Outlet Piping Wall Thickness [cm] | 0.40 | 0.41 | 0.50 | 0.60 | 0.70 | 0.80 |
| Reactor Inlet Piping Wall Thickness [cm] | 0.40 | 0.41 | 0.50 | 0.60 | 0.70 | 0.80 |
| Converter Loop Piping Wall Thickness [cm] | 0.30 | 0.30 | 0.38 | 0.45 | 0.53 | 0.60 |
| Alternator Cooling Piping Wall Thickness [cm] | 0.20 | 0.20 | 0.25 | 0.30 | 0.35 | 0.40 |

It should be noted that the inside diameter decreases with increasing pressure since outer diameter was held constant. This approach maintains consistency of the piping system arrangement but results in increased hydraulic resistance. Turbine and compressor isentropic efficiency were assumed to decrease with increasing pressure as shown in Table 6-4.

**Table 6-4: Assumed Turbomachinery Efficiencies for Compressor Outlet Pressure Sensitivity Study**

| | Compressor Outlet Pressure [MPa] | | | | | | | |
|---|---|---|---|---|---|---|---|---|
| | 1.38 | 1.50 | 2.00 | 2.03 | 2.50 | 3.00 | 3.50 | 4.00 |
| Turbine Efficiency [%] | 90.0 | 89.7 | 88.4 | 88.3 | 87.1 | 85.8 | 84.5 | 83.2 |
| Compressor Efficiency [%] | 84.5 | 84.4 | 84.0 | 84.0 | 83.6 | 83.2 | 82.8 | 82.4 |

The results of the compressor outlet pressure sensitivity study are shown in Figure 6-9.

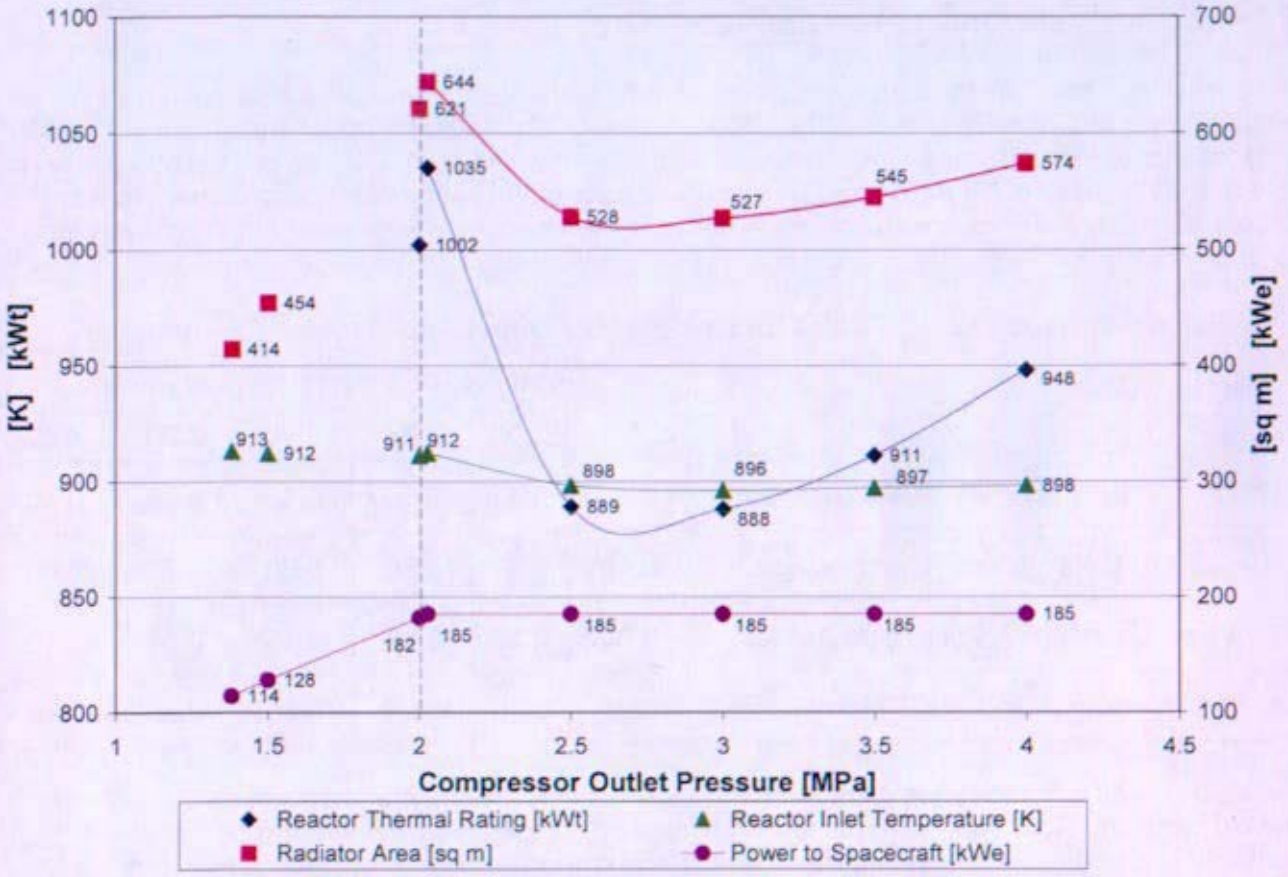



**Figure 6-9: Compressor Outlet Pressure Sensitivity**

The 185 kWe requirement may be achieved by slightly raising the compressor outlet pressure (2.03 MPa). Figure 6-9 shows that reactor thermal rating, required radiator area, and reactor inlet temperature significantly benefit if the compressor outlet pressure is increased further to ~2.6 MPa. As peak plant pressure increases, piping flow losses generally decrease for a constant mass flow rate (positive effect), turbomachinery bearing and windage losses increase (negative effects), and turbine pressure ratio increases (positive effect). Given the assumptions of this analysis, the negative effects of increasing peak pressure dominate the positive effects when compressor outlet pressure is increased above an optimal value above which the overall plant efficiency degrades. Sensitivity studies described in Reference 6-6 do not indicate an optimum value for compressor outlet pressure as suggested by Figure 6-9. This is most likely due to the fact that the analysis provided herein incorporates explicit modeling of a piping arrangement, albeit preliminary and not optimized, and associated piping system flow losses.

### 6.3.6.5 Compressor Pressure Ratio Sensitivity – Design Case

The sensitivity of compressor pressure ratio to overall plant performance was examined for a range of pressure ratios from 1.90 to 2.20. The results of the compressor pressure ratio sensitivity study are shown in Figure 6-10.

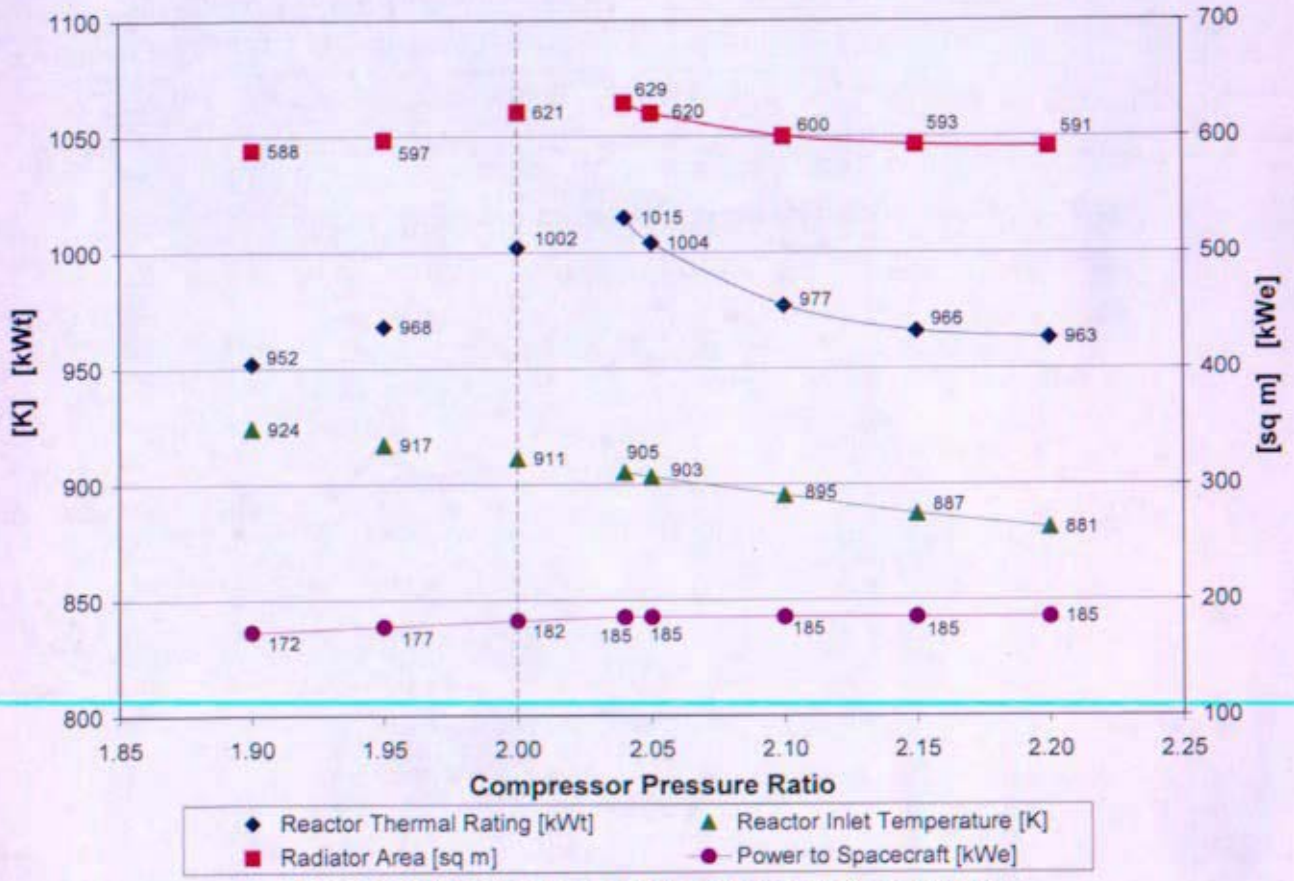



**Figure 6-10: Compressor Pressure Ratio Sensitivity**

As shown in Figure 6-10, the 185 kWe requirement may be achieved if the compressor pressure ratio is slightly increased (2.04). It is also noted that reactor thermal rating, required radiator area, and reactor inlet temperature continue to benefit as compressor pressure ratio increases within the range evaluated.

### 6.3.6.6 Brayton Turbomachinery Efficiency Sensitivity – Design Case

The sensitivity of Brayton turbine and compressor isentropic efficiency to overall plant performance was examined for a range of efficiencies ±2% from their baseline values. Turbine and compressor efficiencies were assumed to vary simultaneously as listed in Table 6-5.

**Table 6-5: Brayton Turbomachinery Efficiency Sensitivity Study Parameters**

| | $\eta_{baseline}$ - 2.0% | $\eta_{baseline}$ - 1.0% | $\eta_{baseline}$ | $\eta_{baseline}$ + 0.2% | $\eta_{baseline}$ + 1.0% | $\eta_{baseline}$ + 2.0% |
|---|---|---|---|---|---|---|
| $\eta_{turbine}$ | 86.4% | 87.4% | 88.4% | 88.6% | 89.4% | 90.4% |
| $\eta_{compressor}$ | 82.0% | 83.0% | 84.0% | 84.2% | 85.0% | 86.0% |

The results of the Brayton turbomachinery sensitivity study are shown in Figure 6-11.

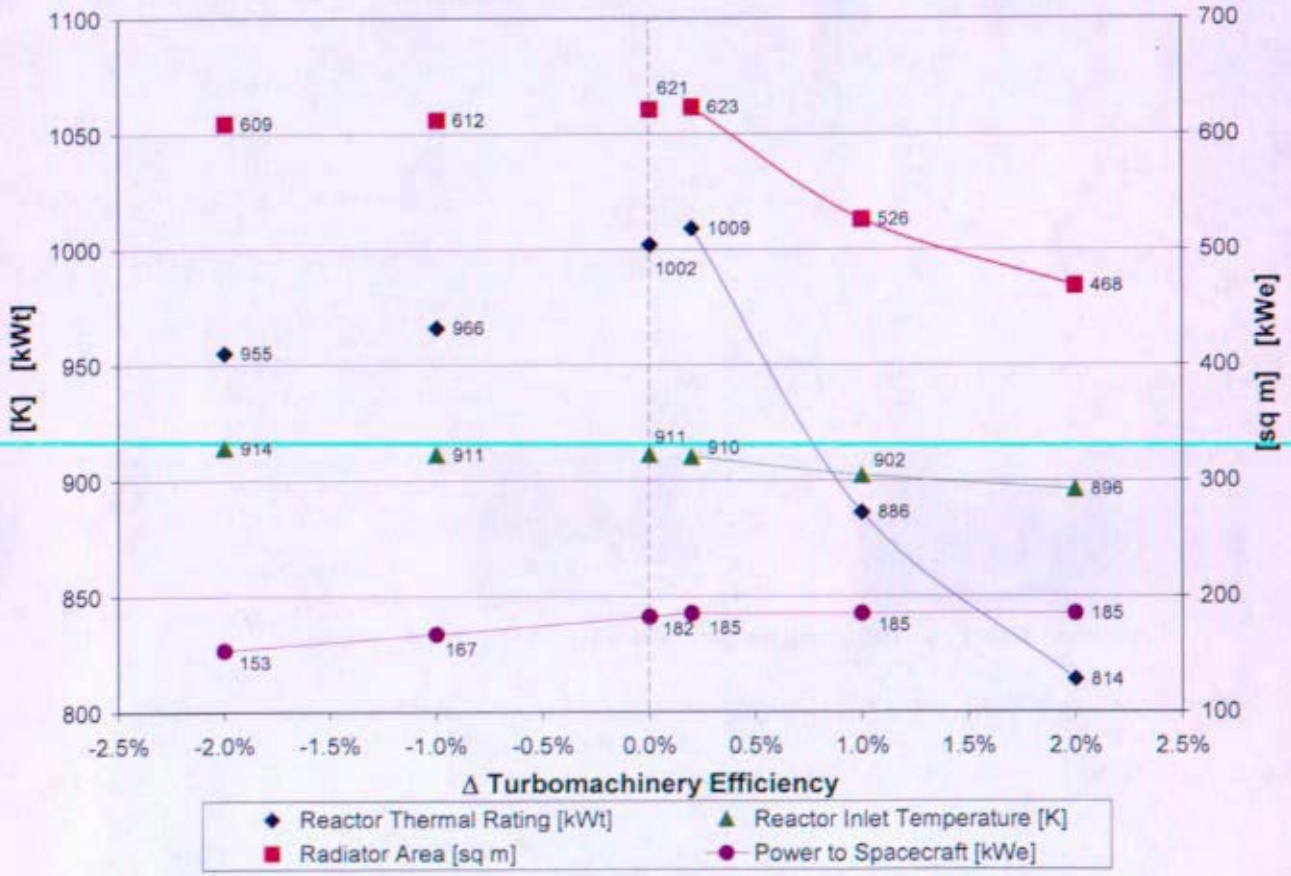



**Figure 6-11: Brayton Turbomachinery Efficiency Sensitivity**

The results shown in Figure 6-11 illustrate that the overall plant efficiency is extremely sensitive to the efficiency of the Brayton turbomachinery. Reactor thermal rating, required radiator area, and reactor inlet temperature decrease significantly as turbine and compressor efficiencies increase. Given the assumptions of this analysis, the 185 kWe requirement may be achieved if the turbine efficiency is increased to 88.6% and the compressor efficiency is simultaneously increased to 84.2%. Conversely, a relatively small reduction in Brayton efficiency is shown to significantly degrade overall system

performance. Thus, Brayton turbomachinery should continue to be a key area of development. Test programs should be implemented to verify actual performance of flight-unit hardware.

### 6.3.6.7 Radiator Heat Pipe Operating Temperature Sensitivity – Design Case

The sensitivity of radiator heat pipe operating temperature to overall plant performance was examined for a range of maximum heat pipe operating temperatures from 475K to 525K. In all cases, a temperature difference of 5K was assumed between the maximum heat rejection segment water temperature and the heat pipe. It should not be inferred that satisfactory heat pipe performance has been demonstrated over the range of temperatures evaluated in this study. Heat pipe operating temperature was simply increased without regard for evaporator heat flux limits or service life considerations. The results of the radiator heat pipe operating temperature sensitivity study are shown in Figure 6-12.

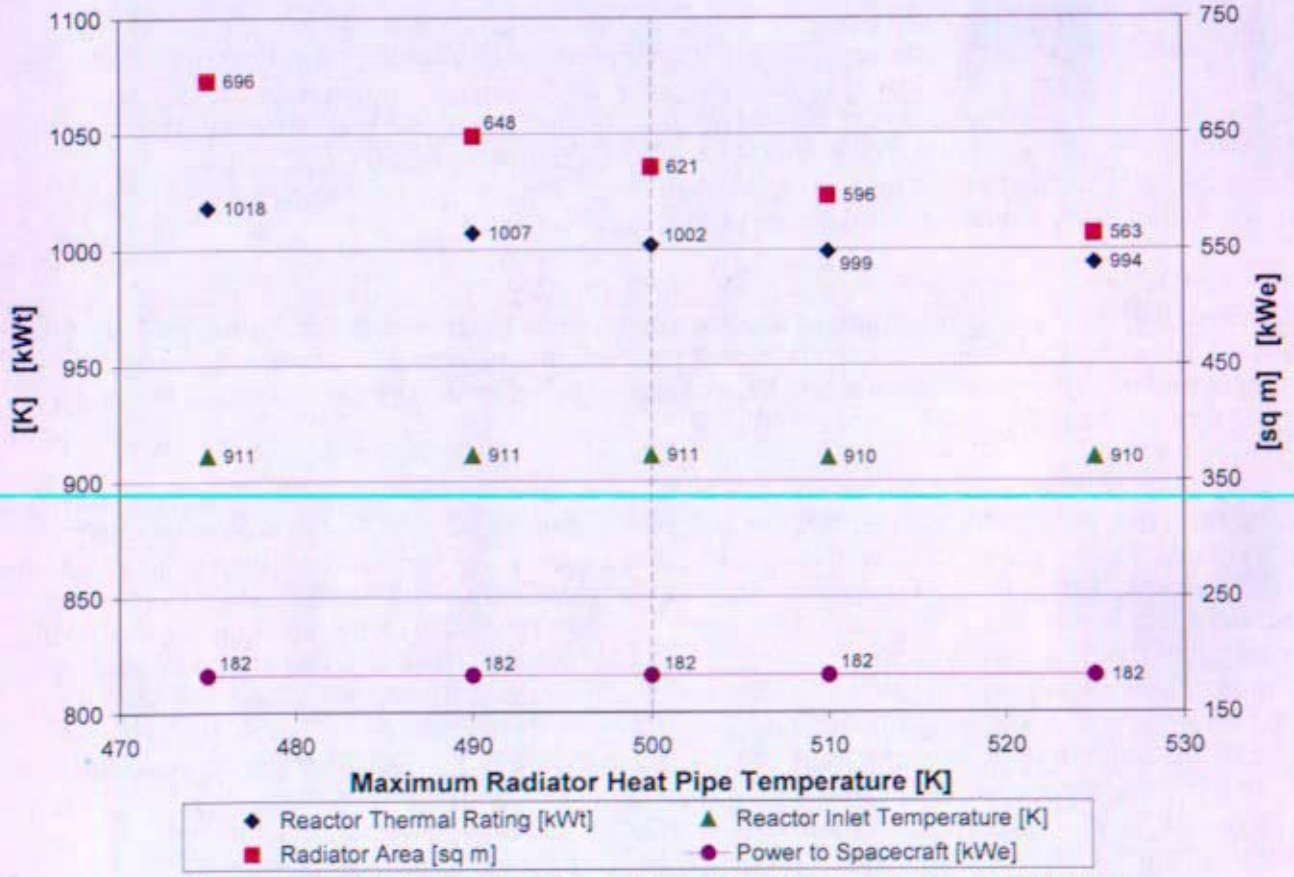



**Figure 6-12: Radiator Heat Pipe Operating Temperature Sensitivity**

Increasing maximum allowable heat pipe operating temperature is an effective means of reducing required radiator area. System efficiency and other key gas loop parameters are negligibly affected when heat pipe operating temperature is varied. As heat rejection segment water temperature increases, the required gas cooler heat transfer area increases to achieve the same gas temperature drop across the gas cooler. For example, increasing maximum heat pipe operating temperature from 500K to 525K reduces required radiator area by 9% (58 $m^2$) but requires a 19% increase in gas cooler heat transfer area. As the heat rejection segment water temperature increases, the operating pressure and mass of the heat rejection segment also increase. The benefits of increasing maximum

heat pipe temperature must be balanced against increased gas cooler mass and a potential increase in the probability of failure of the gas cooler pressure boundary. Also, heat pipe evaporator heat flux limits as a function of operating temperature and service life must be further evaluated and validated through test programs.

### 6.3.6.8 Conclusions – Design Heat Balances

A key driver for the overall plant efficiency is the relative complexity of the piping system and the resulting impact on piping system pressure drop. For plants with multiple converter loops, flow splits in the reactor inlet and outlet headers and inclusion of valves become significant additions to the overall piping system pressure drop. Piping system complexity generally increases as more components are arranged into the prescribed space envelope. The performance trends exhibited in Table 6-1 clearly demonstrate the need for continued piping system optimization to reduce piping system pressure drops.

For the four Brayton system, increasing pipe diameter and decreasing compressor inlet temperature were found to have larger impacts on system performance for small changes than the other parameters studied. Also, reactor thermal rating, required radiator area, and reactor inlet temperature decrease significantly as turbine and compressor efficiencies increase. Thus, Brayton turbomachinery should continue to be a key area of development. Test programs should be implemented to verify actual performance of flight-unit hardware.

Design heat balance sensitivity studies suggest that fundamental design concerns (material performance at elevated operating temperatures, manageable mass and radiator area) may be alleviated with a modest reduction in the spaceship electrical requirement. Conversely, spaceship electric requirements greater than the 185 kWe assumed in these studies would make satisfying all design constraints progressively more difficult.

While the baseline four Brayton system (Figure 6-4) makes at most 182 kWe of the required 185 kWe with the assumed piping arrangement and system parameters (Section 6.3), the preceding design heat balance sensitivity studies show this system can be significantly improved with minor adjustment to a few assumed parameters. Efficiency of this system significantly benefits from increased compressor outlet pressure, increased compressor pressure ratio, and decreased compressor inlet temperature. The increased system efficiency, combined with an increased heat rejection water temperature, results in a significant reduction in required radiator area. A first iteration on the four Brayton system heat balance, assuming the piping arrangement described Figure 5-19 and Table 6-2 and a reactor outlet temperature of 1150K, is provided in Figure 6-13. Note that the one, two, and three Brayton systems would optimize at parameters other than those shown in Figure 6-13 for the four Brayton system. This is primarily due to differences in assumed turbine and compressor efficiencies and the relative impact of hydraulic resistance on the overall heat balance.

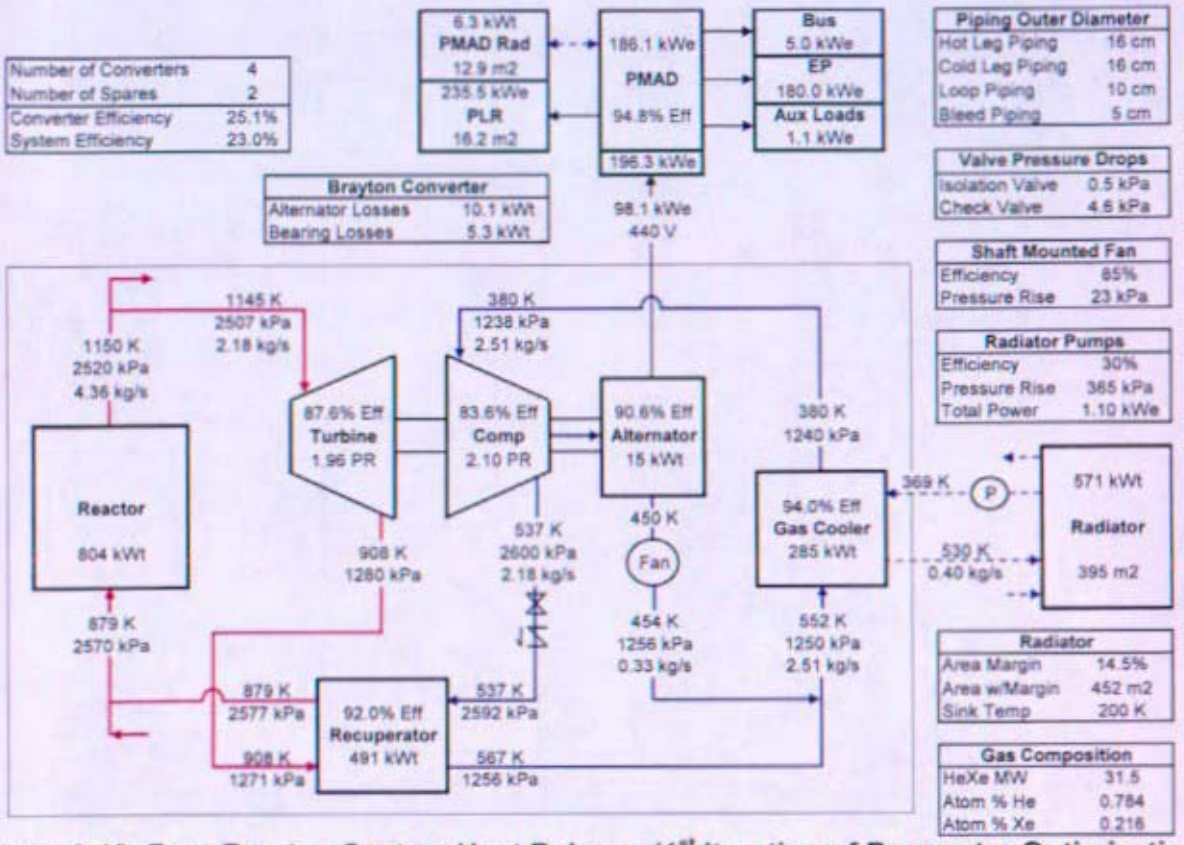



**Figure 6-13: Four Brayton System Heat Balance (1st Iteration of Parameter Optimization)**

The heat balance given in Figure 6-13 and the converter loop piping diameter sensitivity study (Section 6.3.6.1) suggest that the four Brayton system is a viable alternative and would continue to improve with additional piping system optimization and further refinement of operating parameter assumptions. This conclusion is also considered valid for the single, two, and three Brayton systems evaluated herein.

## 6.4 Preliminary Off-Design Heat Balances and Parameter Sensitivity Studies

Off-design heat balance sensitivity studies were performed using the single Brayton system with fixed component sizes based on the design heat balance shown in Figure 6-14. A reactor outlet temperature of 1120K was assumed based on the premise that the plant operating temperature must be less than a design limit to account for operating strategy and resulting operating band, instrument uncertainty, and transient response. It should not be inferred that the 1150K reactor outlet temperature assumed in the design heat balances was identified as the maximum allowed actual reactor outlet temperature or that a 30K offset from the design condition was specifically evaluated and found to be acceptable. Additional effort must be directed toward identification of material temperature limits, operating strategy, temperature band, instrumentation accuracy, and plant transient response prior to establishing an operating temperature band that will ensure design limits are not exceeded.

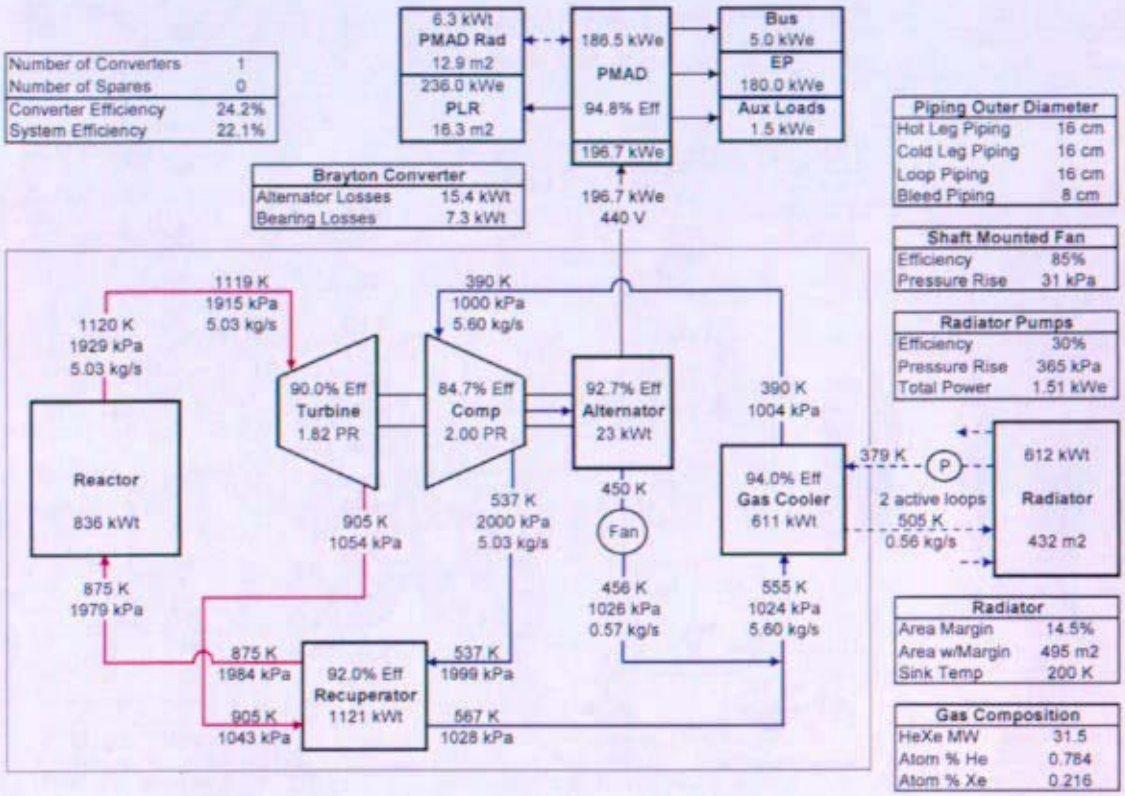



**Figure 6-14: Design Heat Balance used as Basis for Off-Design Studies**

The off-design heat balance resulting from the design heat balance shown in Figure 6-14 is shown in Figure 6-15. This is the heat balance used as a baseline for off-design sensitivity studies described in Sections 6.4.1 through 6.4.5.

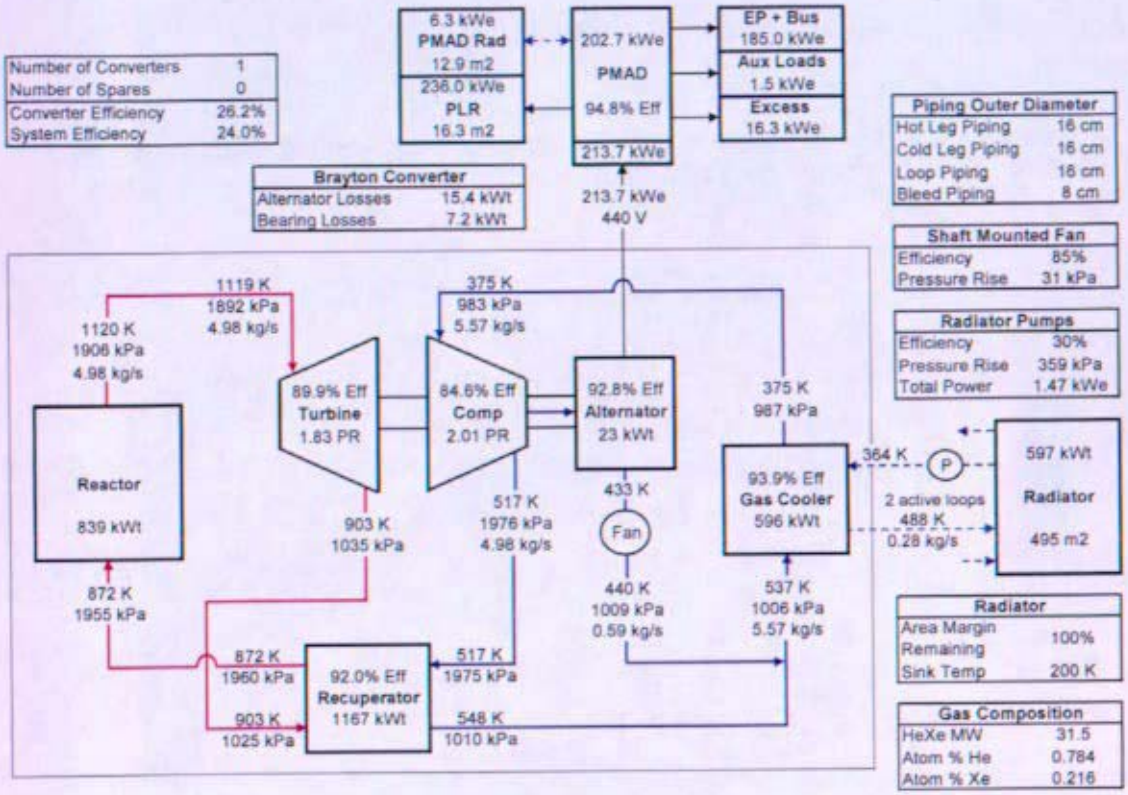



**Figure 6-15: Baseline Off-Design Heat Balance**

The radiator area with margin calculated in the design heat balance (495 $m^2$) is used in the off-design studies. Using this additional radiator area effectively reduces compressor inlet temperature which makes the system more efficient assuming that the heat rejection segment mass flow rate remains constant. This results in a net electrical power output in excess of the 185 kWe produced in the design heat balance; 16.3 kWe excess at beginning-of-life for the parameters and plant arrangement assumed here. This excess power could be utilized to achieve other design objectives. For example, the plant could be operated at a reduced reactor outlet temperature at beginning-of-life to alleviate time-at-temperature material concerns while achieving the full power required by the spaceship.

### 6.4.1 Reactor Outlet Temperature Sensitivity – Off-Design Case

Sensitivities to the reactor outlet temperature are shown in Figure 6-16 for the off-design case. Within the temperature range evaluated the net electrical output available for spaceship loads varies from 201.3 kWe to 219.8 kWe. Over this same range the reactor thermal power varies from 839 kWt to 874 kWt.

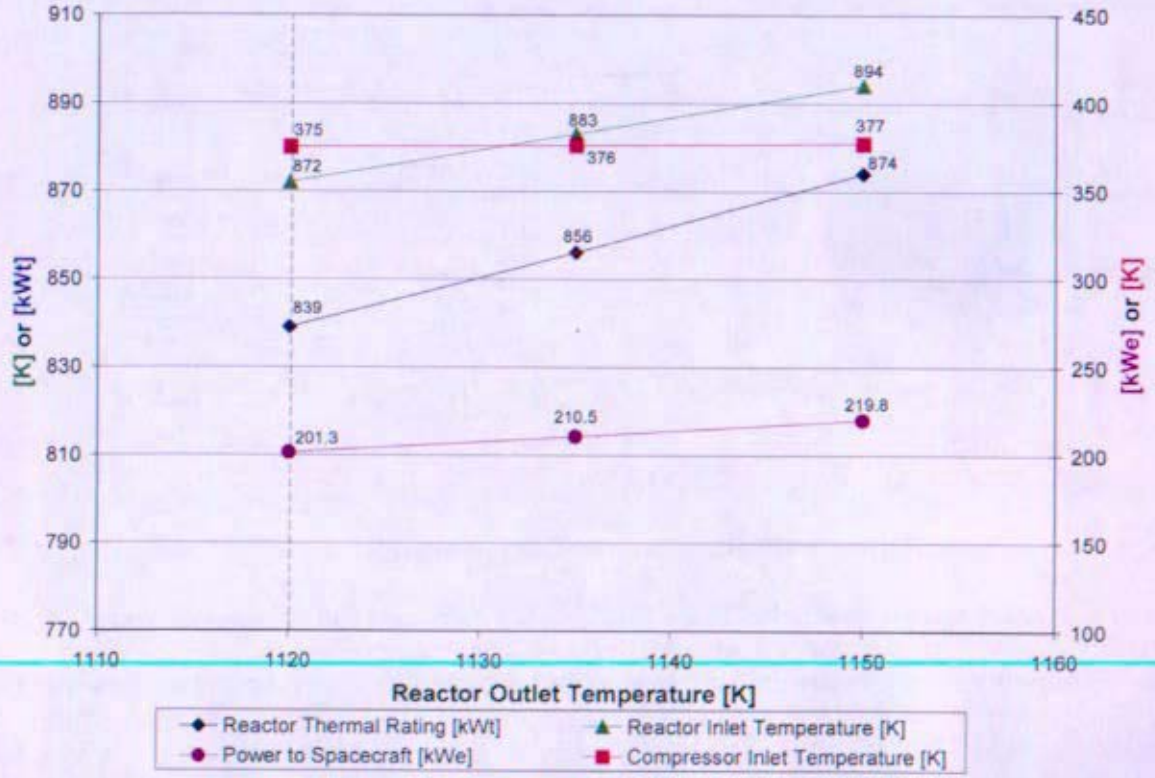



**Figure 6-16: Reactor Outlet Temperature Sensitivity**

### 6.4.2 Loss of Radiator Area Margin – Off-Design Case

A radiator area margin of 14.5% is built into the design to account for degradation of the radiator. This degradation covers loss of heat pipes, reduction in emissivity, and other potential changes to the radiator performance. All of this area margin is available for use at beginning of life and the available amount would degrade over time.

Sensitivities to the radiator degradation are shown in Figure 6-17. As the radiator area margin is lost, the net electrical output available for spaceship loads falls from 201.3 kWe to the required 185 kWe. Over this same range the reactor thermal power is reduced from 839 kWt to 835 kWt.

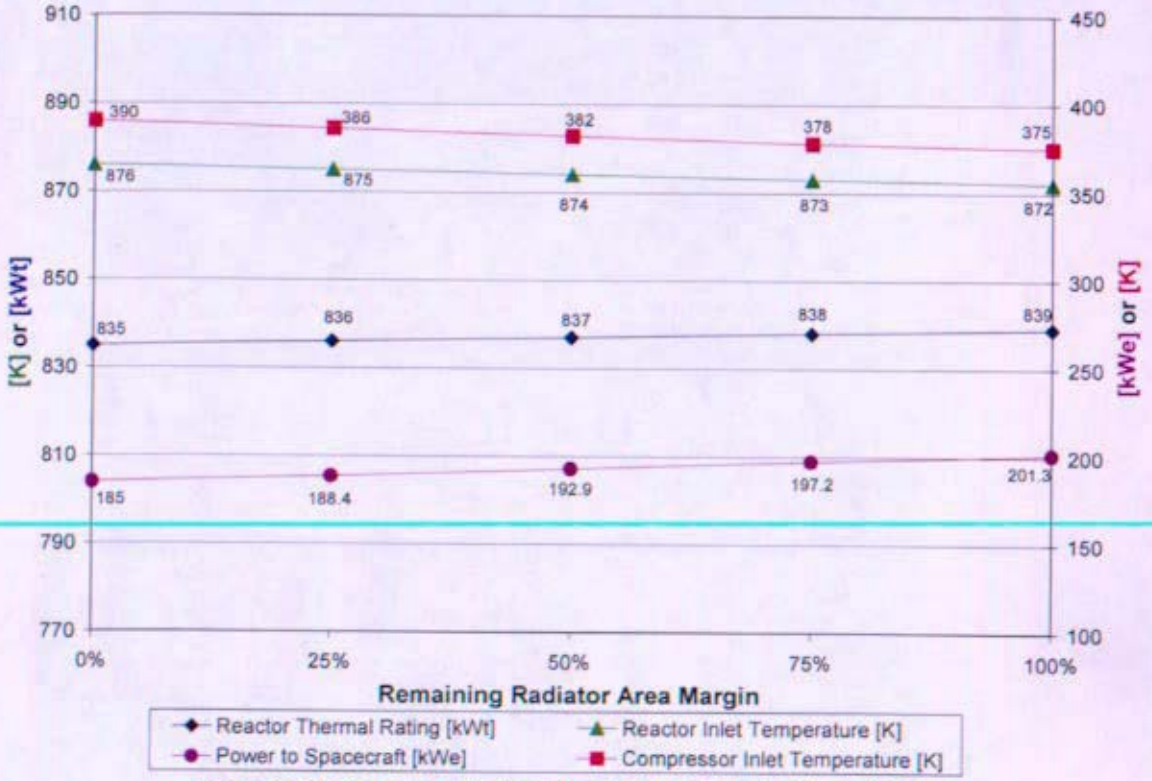



**Figure 6-17: Loss of Radiator Area Margin Sensitivity**

### 6.4.3 Gas Leakage – Off-Design Case

Some of the gas is expected to leak from the system over the life of the mission. Gas leakage leads to a reduction in system pressures as the system volume is fixed. This leads to a reduction in the amount of power that can be produced.

Sensitivities to gas leakage are shown in Figure 6-18. When 10% of the gas leaks from the system the net electrical output available for spaceship loads falls from 201.3 kWe to 190.7 kWe. Over this same range, the reactor thermal power is reduced from 839 kWt to 753 kWt. This large drop in reactor thermal power is caused by decreased gas density and the resulting reduction in mass flow rate.

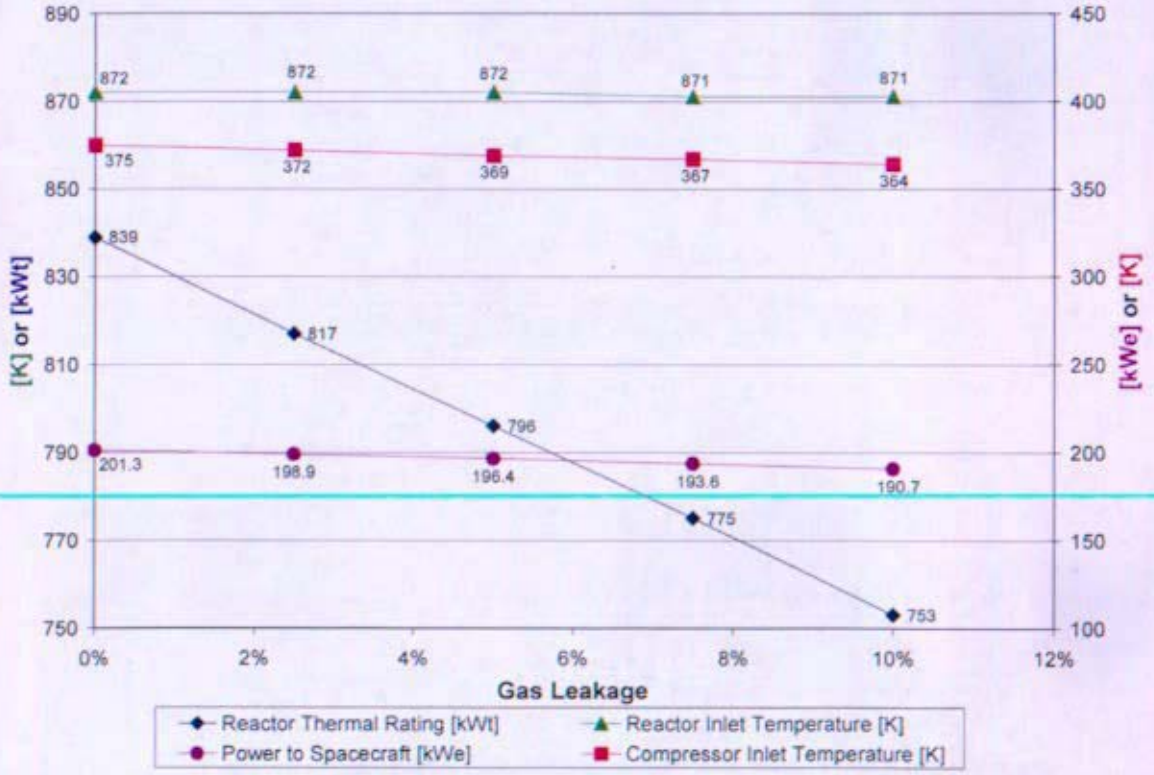



**Figure 6-18: Gas Leakage Sensitivity**

### 6.4.4 Turbomachinery Efficiency Degradation – Off-Design Case

The efficiency of the turbine and compressor may degrade over the life of the mission. As the efficiency degrades, the system will produce less electrical output. This study shows the effect of the turbine and compressor efficiency degrading equally.

Sensitivities to turbomachinery isentropic efficiency degradation are shown in Figure 6-19. As the turbomachinery efficiencies degrade by up to 5% the net electrical output available for spaceship loads falls from 201.3 to 139.8 kWe. The system no longer makes the required 185 kWe when the efficiency has degraded 1.3%. Over the same degradation range the reactor thermal power is reduced from 839 kWt to 807 kWt.

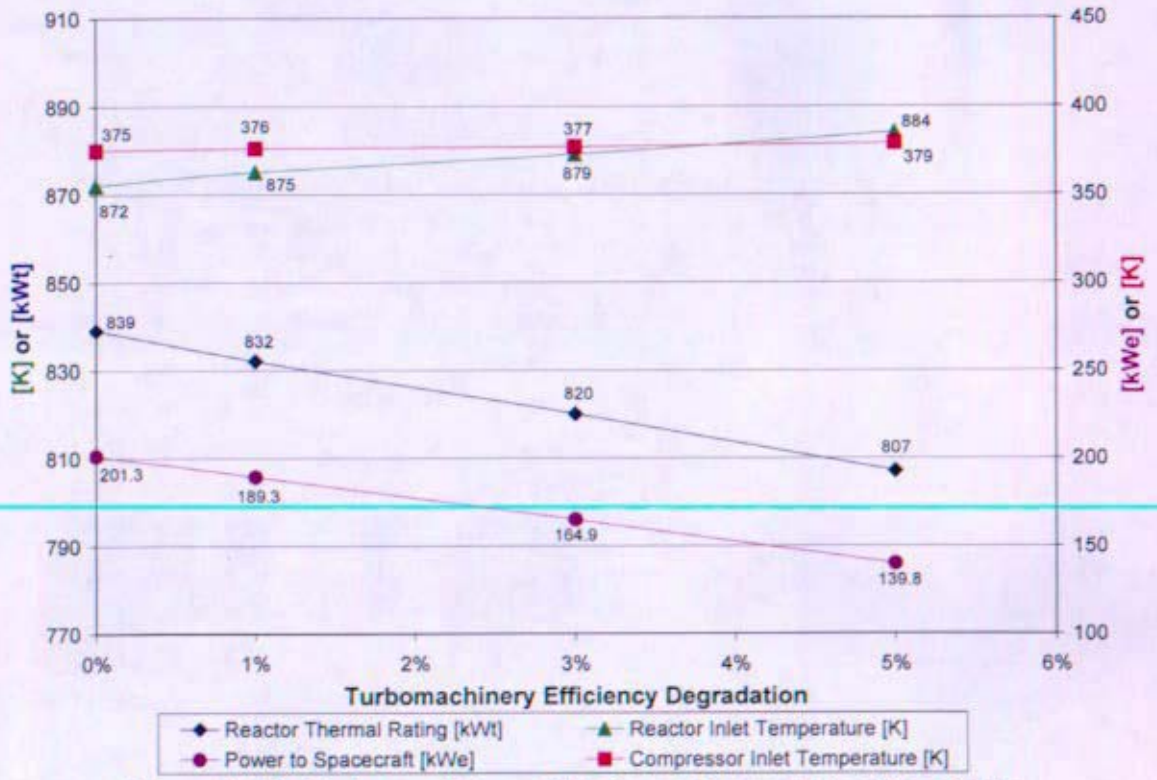



**Figure 6-19: Turbomachinery Efficiency Degradation Sensitivity**

### 6.4.5 Effective Sink Temperature – Off-Design Case

Throughout the mission, the effective sink temperature to which the waste heat is rejected may change. Deep space environments may have a sink temperature lower than the 200K that is being assumed for design. Conversely, if the radiator panels are not maintained parallel to the sun's rays the sink temperature may increase.

Sensitivities to the effective sink temperature are shown in Figure 6-20. Within the sink temperature range evaluated, 4K to 300K, the net electrical output available for spaceship loads varies from 217.4 kWe to 153.1 kWe. The system no longer makes the required 185 kWe when the sink temperature exceeds 225K. Over the same sink temperature range, the reactor thermal power varies from 841 kWt to 828 kWt.

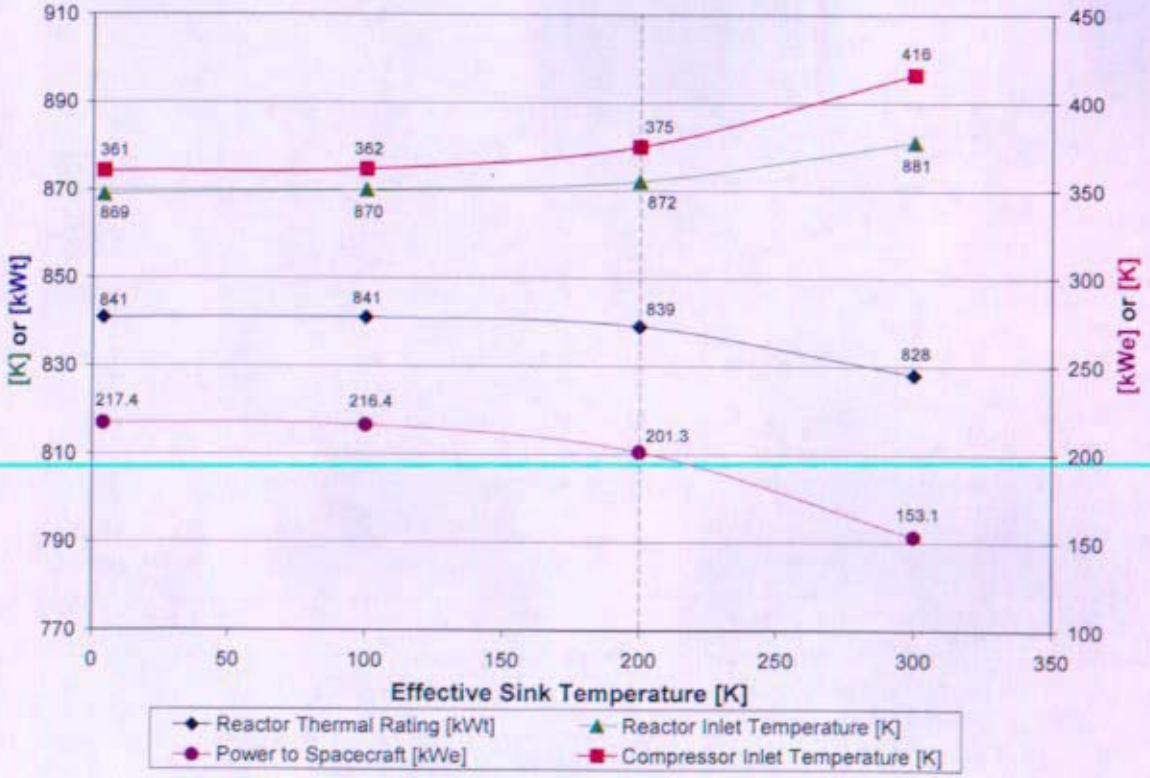



**Figure 6-20: Effective Sink Temperature Sensitivity**

### 6.4.6 Conclusions – Off-Design Heat Balances

Off-design studies indicate that system performance is highly sensitive to Brayton turbine and compressor efficiency. The system can sustain only a 1.3% degradation in turbine and compressor efficiency, when taken simultaneously, and still be able to produce the required 185 kWe at beginning-of-life. This result supports the conclusion obtained from the design sensitivity studies; i.e. Brayton turbomachinery should continue to be a key area of development. Test programs should be implemented to verify satisfactory turbine and compressor performance over component life.

System performance was shown to degrade significantly as effective sink temperature increases above the assumed design value (Figure 6-20). This sensitivity study illustrates the need to ensure that radiator panels do not have a view to an effective sink temperature greater than design value when full electrical power is required. Effective sink temperatures less than the design value were shown to negligibly improve plant performance.

Off-design studies show that the plant can sustain a loss of 10% of the original gas inventory and still be able to produce the required 185 kWe (Figure 6-18). This preliminary conclusion confirms assumptions used in previous analyses related to Brayton system gas leakage which were based on acceptable system leak rate of $10^{-3}$ std cc/s giving a 10% reduction in system pressure over 15 years (Whitepaper B, Enclosure 7 to Attachment D of Reference 6-7).

## 6.5 References

6-1 KAPL letter SPP-SPPS-0032, Bettis letter B-SE(SPS)FMS-011, "Space Power Program; NRPCT Direct Gas Brayton Heat Balance Model Documentation; For Information", dated 12/14/05.

6-2 KAPL letter SPP-67210-0007, Bettis letter B-SE-0124, "Hot Leg Piping Concept for Further Development – For NR Approval", dated 6/30/05.

6-3 Barrett, M.J., and Reid, B.M., "System Mass Variation and Entropy Generation in 100-kWe Closed-Brayton-Cycle Space Power Systems," prepared for the Space Technology and Applications International Forum (STAIF-2004), NASA/TM-2004-212741, January 2004.

6-4 Kerwin, P.T., "Analysis of a 35- to 150-Kilowatt Brayton Power-Conversion Module for use with an Advanced Nuclear Reactor," NASA TN D-6525, September 1971.

6-5 KAPL letter SPP-67410-0013, Bettis letter B-SE(RE)-0003, "Space Reactor Preconceptual Design Report", dated 1/27/06.

6-6 Johnson, P.K., and Mason, L.S., "Design and Off-Design Performance of 100 kWe-Class Brayton Power Conversion Systems," prepared for the Space Technology and Applications International Forum (STAIF-2005), NASA/TM-2005-213626, June 2005.

6-7 KAPL letter SPP-67110-0005, Bettis letter B-SE-0077, "Space Nuclear Power Plant Concept Selection, For NR Approval", dated 3/4/05.

# Section 7
# Reliability

*PRE-DECISIONAL - For planning and discussion purposes only*

(Intentionally Blank)

# Reliability

## Table of Contents

7 Reliability ..... 5
7.1 Summary and Conclusions ..... 5
7.2 Terminology ..... 8
7.3 Listing of Systems Evaluated ..... 8
7.3.1 Assumptions ..... 8
7.3.2 List of Systems Evaluated ..... 8
7.4 Component Reliability Values and Basis ..... 14
7.4.1 Background ..... 14
7.4.2 Component Reliability Values ..... 14
7.5 Reliability and Sensitivity Studies Results ..... 17
7.5.1 Reliability Study Results ..... 17
7.5.2 Sensitivity Studies Results ..... 22
7.5.3 SNPP Reliability Versus Mass ..... 27
7.6 Future Actions ..... 28
7.7 Methodology of Reliability Studies ..... 31
7.7.1 Identify system architectures to be evaluated ..... 31
7.7.2 Identify failure modes for each component ..... 31
7.7.2.1 Effect of Heat Rejection System Failures on Brayton Primary System ..... 31
7.7.3 Calculate reliability of each system ..... 35
7.7.4 Perform sensitivity study for each system based on individual component reliabilities ..... 40
7.8 System Fault Trees ..... 41
7.8.1 Background ..... 41
7.8.2 Example Fault Tree ..... 41
7.9 Documentation of software (BlockSimFTI, XFMEA) ..... 47
7.9.1 Description of software ..... 47
7.9.2 Justification for use of software ..... 47
7.10 Mathematical Models for Brayton, Valves and HRS ..... 48
7.11 Tables of Detailed Sensitivity Study Results By System Architecture ..... 51
7.12 References ..... 55

## List of Figures

Figure 7-1: Sensitivity of System Reliability to Brayton Reliability ..... 6
Figure 7-2 SNPP Reliability Versus Mass ..... 7
Figure 7-3: System Reliability Based on Brayton Assembly Reliability ..... 21
Figure 7-4: Similar Material Weld Reliability on System Reliability ..... 24
Figure 7-5: Cooler Reliability on System Reliability ..... 25
Figure 7-6: HRS Loop Reliability on System Reliability ..... 26
Figure 7-7: System Reliability Versus System Mass ..... 27
Figure 7-8: 1-1-1 Gas Cooler Concept ..... 32
Figure 7-9: 2-2-2 concept – Braytons rated at 200kWe (2 operating at reduced capacity) ..... 32
Figure 7-10: 2-2-2 concept – Braytons rated at 200kWe (1 on, 1 off) ..... 33
Figure 7-11: 3-3-3 Gas Cooler Concept (2 operating, 1 standby) ..... 34
Figure 7-12: 4-4-4 Gas Cooler Concept (2 operating, 2 standby) ..... 34

## List of Tables

Table 7-1 Component Input Reliability Values and Component Failure Modes ..... 14
Table 7-2 System Reliability Results for Turbine/Compressor Reliability of 97% ..... 18
Table 7-3 Reliability Results for Turbine/Compressor Reliability of 99% ..... 19
Table 7-4 Breakdown of Brayton Assembly Reliability ..... 22
Table 7-5: System Reliability Change Due to Doubling the Component Failure Rate ..... 23
Table 7-6: System Reliability Change Due to Removing the Component Failure Rate (component reliability goes to 1) ..... 23
Table 7-7 Reliability Data Databases and Resources ..... 29
Table 7-8 Impact of Isolation Valve Double Failure Mode on System Reliability ..... 39
Table 7-9 Component Reliability Sensitivity Ranges ..... 40
Table 7-10 One Brayton System Detailed Sensitivity Study Results ..... 51
Table 7-11 Two Brayton System (1 Running, 1 Standby) Detailed Sensitivity Study Results ..... 52
Table 7-12 Two Brayton System (2 Running) Detailed Sensitivity Study Results ..... 52
Table 7-13 Three Brayton System (2 Running, 1 Standby) Detailed Sensitivity Study Results ..... 53
Table 7-14 Three Brayton System (3 Running) Detailed Sensitivity Study Results ..... 53
Table 7-15 Four Brayton System (2 Running, 2 Standby) Detailed Sensitivity Study Results ..... 54
Table 7-16 Four Brayton System (4 Running) Detailed Sensitivity Study Results ..... 54

# 7 Reliability

## 7.1 Summary and Conclusions

Reliability values calculated in this study are based on individual component reliabilities estimated from limited research and engineering judgment; therefore conclusions made herein are based on the performance of each system studied relative to the other systems. No conclusions have been made, nor should be made, based on the absolute reliability values contained in this report. Comparison between system configurations can be made by understanding the impacts of different system architectures using estimates of relative component reliabilities.

This reliability study mainly focused on comparisons of potential system architectures of the energy conversion system (see Section 3). Variations in other systems, such as the heat rejection system or the electrical control system were not included in this study. A specific decision concerning the number of energy conversion loops was not made due to project termination. However, these studies reveal that a one or two Brayton system would probably be recommended over a three or four Brayton system because they would be more reliable.

---

- The most reliable systems have fewer components and less surface area (fewer opportunities to fail). For Brayton assemblies with high assumed reliabilities (approximately 97% or higher), the single Brayton system with one recuperator and one gas cooler (1-1-1) is the most reliable (See Figure 7-1). The fully redundant two Brayton (2-2-2s and 2-2-2 one operating, one standby) systems provide a reliability benefit assuming Brayton assembly reliabilities below 97%. These system architectures only require one Brayton unit to produce rated system power. The reliabilities of these two Brayton systems are also less sensitive to changes in assumed Brayton reliability. Future studies would need to determine whether the benefits of adding a second Brayton loop compensate for additional mass (shown in Figure 7-2).

- As shown in Figure 7-1, the 1 of 2 (2-2-2) Brayton system architecture will always be more reliable than either a 2 of 3 (3-3-3) or a 2 of 4 (4-4-4) Brayton configuration. The results are based on system architecture and are independent of component reliabilities. Three and four Brayton systems have a significant increase in the number of certain components, along with an increase in surface area for redundant components, which negatively impact the reliability of the overall system. The three and four Brayton systems require two Brayton units to be operable to produce rated system power.

- Components most affecting system reliability differ based on system architecture. For the system configurations studied, the four components having the largest reliability impact were the gas cooler, heat rejection system loops, electrical penetrations, and the turbine/compressor (part of the Brayton assembly). Bearings also have a strong impact on the reliability of a single Brayton system, while the considerable number of welds significantly impacts multiple Brayton system reliabilities.

- To achieve an overall system reliability of 95% for a one Brayton system, each individual component needs to have a minimum reliability of roughly 0.994 (If the average reliability of multiple components is 0.994, a system reliability of 95% can be obtained.); due to the increased number of components, the average reliability for multiple Brayton system components would need to be higher to achieve 95% reliability. To achieve system reliability

of 99%, every component needs to have an approximate reliability of 0.999. The Prometheus spacecraft would be launched without a statistically significant reliability history on most components. Design decisions will have to be made without empirical data; however databases exist for some similar components (Table 7-7) that could be used to develop more accurate overall reliability estimates.

- The details of these conclusions could be affected if future research or testing show significant differences from what was assumed in this study for failure modes and functions.

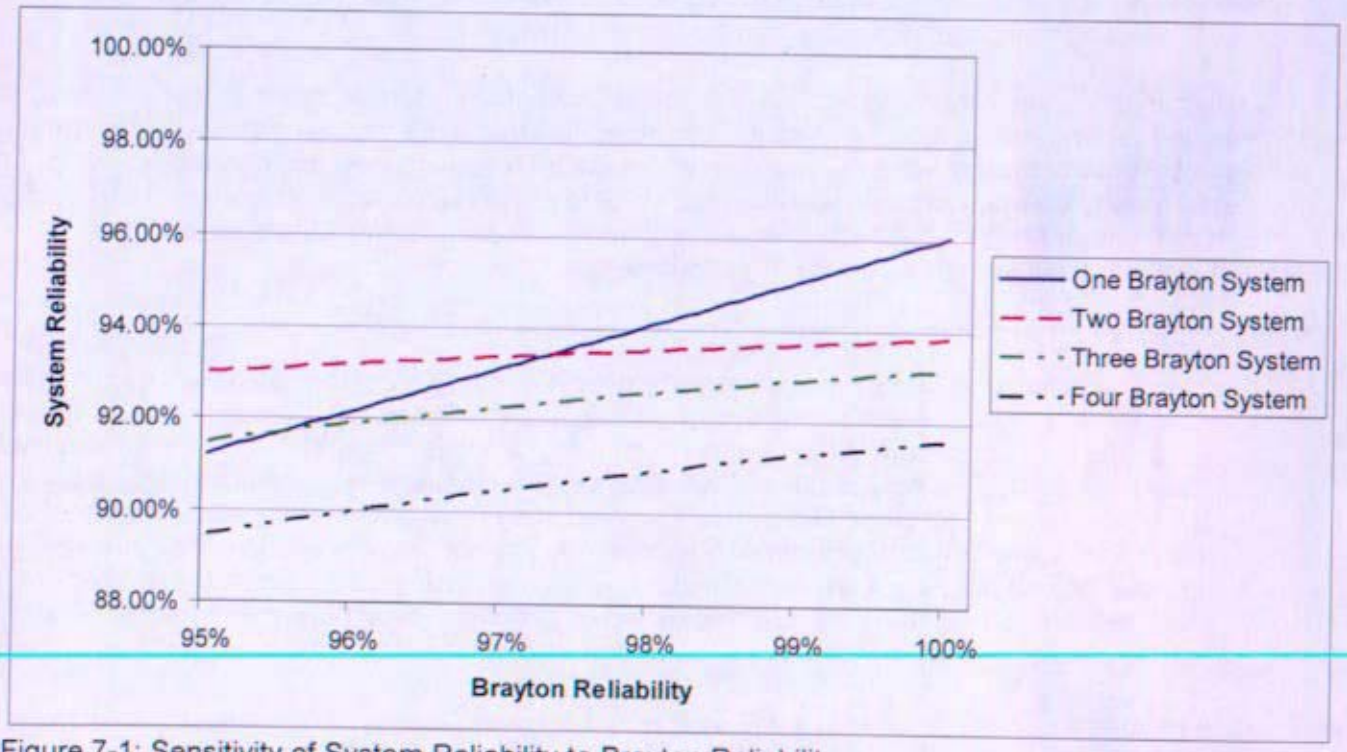



Figure 7-1: Sensitivity of System Reliability to Brayton Reliability

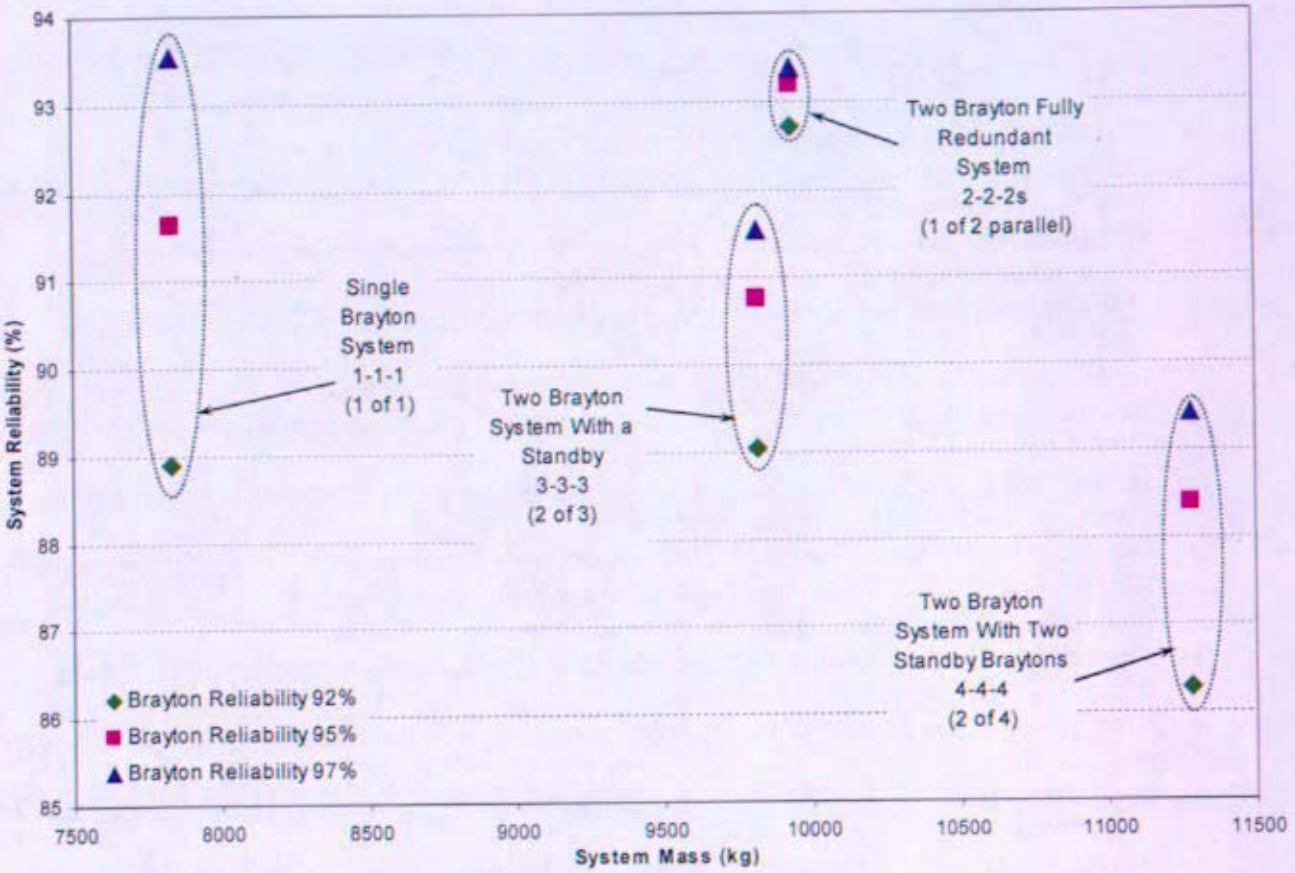



Figure 7-2 SNPP Reliability Versus Mass

**Background**

A key decision in the pre-conceptual design phase is the system architecture for the Space Nuclear Power Plant (SNPP) (see Section 3). The decision on system architecture involves determining the number of energy conversion loops, components and cross strapping to provide highly reliable electric power generation and low system mass, while also supporting all of the system operational requirements.

This section discusses the NRPCT reliability strategy and work to support the decision on the number of energy conversion loops and the number of individual components as well as longer-term decisions affecting the design of the system and its components.

Little reliability data is available for the components (many of which have not been designed yet) that will make up the SNPP. Component reliabilities were estimated based on NRPCT experience and assessed comparatively to ensure that relative reliability values were consistent with engineering experience. Limited commercial data was used to confirm these estimates. Sensitivity studies were performed to determine the impact of each component on overall system reliability.

## 7.2 Terminology

The following definitions are used in this report:

- **Reliability**: The probability of performing a required function in the desired manner under all relevant conditions and on the occasions or during the time intervals when it is required so to perform (Reference 7- 2).
- **Redundancy**: The ability to survive one or more equipment faults and continue with its intended operational function (Reference 7- 2).
- **Redundancy, active**: Redundancy wherein all redundant items are operating simultaneously (Reference 7- 3).
- **Redundancy, standby**: Redundancy wherein the alternative means of performing the function is not operating until it is activated upon failure of the primary means of performing the function (Reference 7- 3).
- **Robustness**: Ability of a system to successfully operate under more extreme conditions than those for which it was designed (Reference 7- 2).
- **Series Components**: Two (or more) components independent of one another where the failure of either (any) component will fail the system.
- **Parallel Components**: Also known as redundant components.
- **Total component reliability**: the combination of reliabilities of the parts that form a component
- **Brayton unit:** composed of turbine/compressor, alternator, housing, bearings, windings, rotor, shaft
- **Brayton assembly:** For the purposes of this study, this is defined as the Brayton unit plus recuperator internal area
- **Brayton loop:** all components in primary system from reactor outlet to reactor inlet
- **System architecture:** composed of Brayton loops.
- **Parallel System**: Term used to indicate a system architecture in which 100% power is supplied by all Brayton units operating at a reduced capacity, but in the event of failure(s), full power can be supplied by fewer Braytons.

## 7.3 Listing of Systems Evaluated

### 7.3.1 Assumptions

1. Multiple loop systems contain two valves per loop--one check valve and one isolation valve both in the compressor outlet.
2. Backup power (battery) is available for starting the standby Brayton when the operating Brayton is not available in the 2-2-2 (1 operating, 1 standby) system architecture. However, the backup power source is not included in the current reliability studies.
3. Brayton engines can be designed to have different operating power levels. Section 8 and Reference 7- 8 evaluate the feasibility of this assumption.

### 7.3.2 List of Systems Evaluated

The general system architecture evaluated includes piping, valves, turbine/compressor, alternator, and heat exchangers. Smaller piping and instrumentation such as alternator bleed flow piping and sensors were not included. The reactor was not included in the study (reliability set to 100%) because not enough information is available at this time to assign a reliability number or to show if the reactor reliability would change with different system architectures. Instrumentation and control (control of

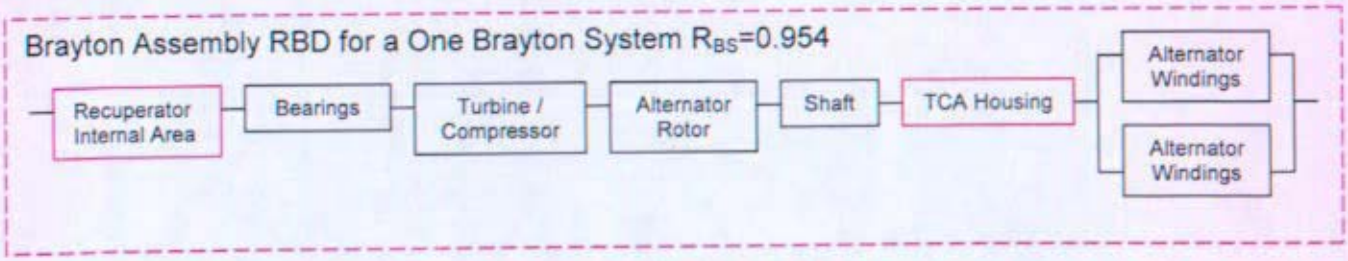
reactor functions) would have been included in reactor reliability. Electrical control system (control of Brayton units by the power conditioning and distribution system) was incorporated in the reliability studies as represented by a single reliability value because minimal information was available on system designs and reliability of electrical components. However, electrical control system reliability is not expected to be a major factor for Energy Conversion System (ECS) architecture since the electrical control system can be designed to be fault tolerant for all ECS architectures evaluated. Future reliability studies would have included more detail for the electrical control system.

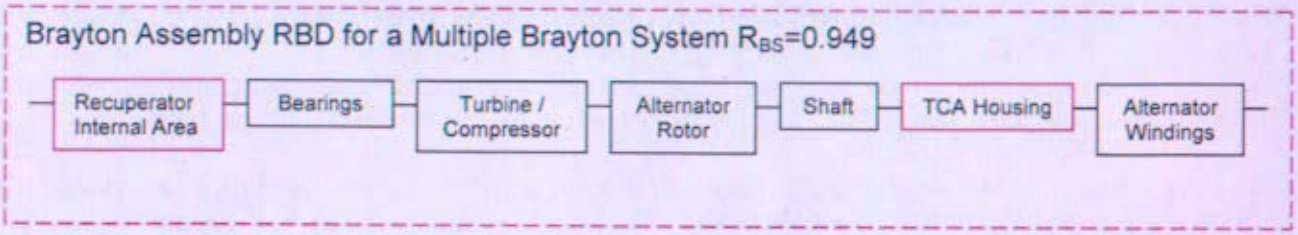
The heat rejection system was included to show the impact of the current heat rejection system (HRS) design on different system architectures. The reference HRS design uses four separate cooling loops (see Failure Modes, Section 7.7.2.1 below, and Section 9 for details). This design minimizes the effect of HRS failures on the one and two Brayton systems because a failure in the HRS does not necessarily cause the associated Brayton to be unusable. Failures in the HRS for three or four Brayton systems require switching to standby Brayton(s) to maintain full power capability.

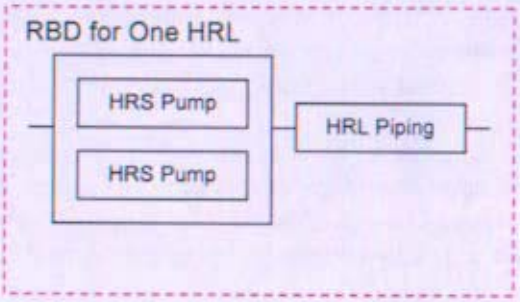
This study did not evaluate the effect of shared heat exchangers on overall system reliability. Different combinations of heat exchangers have varying mass, reliability, or operational advantages and disadvantages. Section 3 discusses the advantages and disadvantages of shared components and Section 4 presents comparisons of mass estimates for systems with and without shared heat exchangers.

Section 3 contains more detailed information on the systems evaluated. Schematics are provided in Section 3 for some of the systems evaluated in the reliability study.

Each system architecture evaluated is illustrated by a reliability block diagram (RBD). A RBD is used to identify operating characteristics of components with one another (Series, parallel, 'r' of 'N' defined in Section 7.7.3.) (Reference 7- 3 also discusses RBDs). Each RBD shows how the components are grouped or divided according to function. Each system RBD consists of individual elements, such as "Piping Area," "Cooler Area," and "Similar Material Welds," and two compound elements, "Brayton assembly" and "HRS Loop" (HRL). These compound elements are made of individual elements as shown below. The Brayton assembly is different depending on whether the Brayton assembly is part of a single Brayton system or a multiple Brayton system because the Brayton unit for a single Brayton system has two alternator windings operating in parallel. RBDs usually have reliability numbers associated with each block; however, the RBDs below are shown solely to illustrate the different system architectures studied. Multiple Brayton systems contain valves; however, due to the complex interaction of valves with failures in the system, discussed in Section 7.7.3, the valves cannot be shown easily in the RBDs. The heat rejection system (HRS) is comprised of four HRLs made up of two heat rejection pumps (HRP) running in parallel operating in series with the HRL piping. Operating configuration of the HRS is parallel for each of two HRLs for each radiator. The HRS is discussed more thoroughly in Section 7.7.2.1.

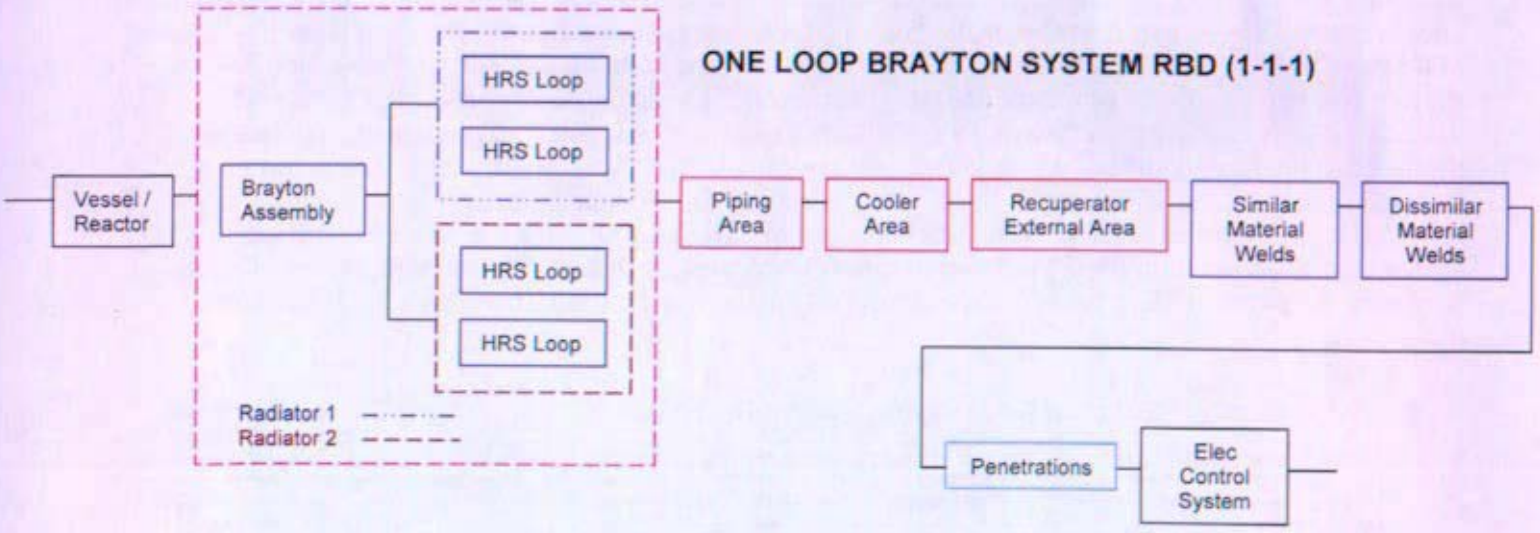





**1-1-1 System Architecture: One Brayton Loop with Two Alternator Windings**

- One 200 kWe Brayton unit, with dual alternator stator windings
- One recuperator sized to service one 200 kWe Brayton unit
- One gas cooler sized to reject heat from one 200 kWe Brayton
- No valves



**2-2-2 System Architecture, One Brayton Loop Operating, One Standby Loop**

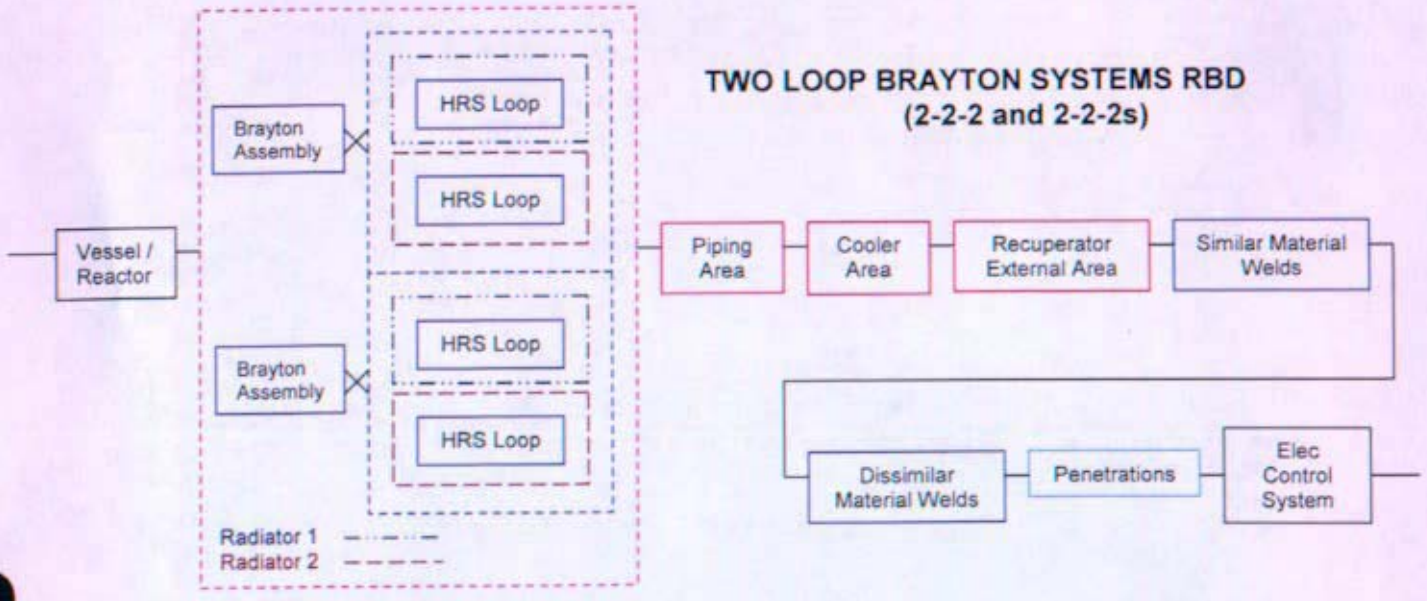
- Two 200 kWe Braytons
- Two recuperators each sized to service a 200 kWe Brayton.
- Two gas coolers each sized to service a 200 kWe Brayton.

**2-2-2s System Architecture**--Two Operating Brayton Loops, Each Unit Capable of 100% and 50% of Rated System Power

- Two 200 kWe Braytons – counter-rotational, each designed to operate at 50% rated system power and 100% rated system power.
- Two recuperators each sized to service a 200 kWe Brayton.
- Two gas coolers each sized to service a 200 kWe Brayton.

The RBD is the same for both operating configurations of a two Brayton system. System reliability differences are due to the isolation valves, check valves (RBD does not show valves) and configuration of the HRS. Both valves are included in the total reliability for the Brayton system due to the fact that they do not follow a conventional operating structure with the Brayton units; that is, a failure of a valve may or may not fail the system, depending on the situation. This is discussed further in Section 7.7.3. The different HRS configurations for each operating condition are taken into account in the mathematical models presented in Section 7.10 used to calculate system reliability.

The crossed lines in the following multiple Brayton system RBDs indicates that the Brayton uses either of the two HRS loops indicated (not at the same time), but it does not indicate valve functionality.

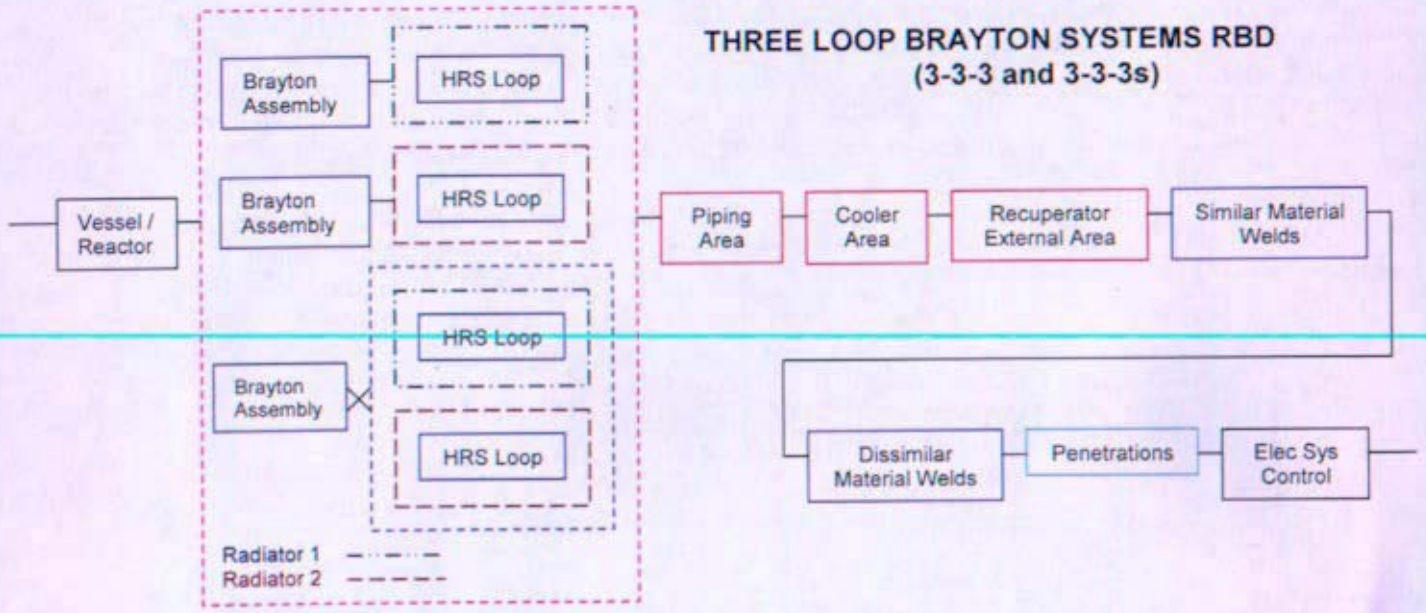


### 3-3-3 System Architecture—Two Brayton Loops Operating, One Standby Loop

- Three 100 kWe Braytons – two co-rotational.
- Three recuperators each sized to service a 100 kWe Brayton.
- Three gas coolers each sized to service a 100 kWe Brayton unit.

### 3-3-3s System Architecture--Three Brayton Loops operating with capability of any 2 covering full load.

- Three 100 kWe Braytons – two of three co-rotational, each one designed to operate at 33.3% rated system power and 50% rated system power.
- Recuperators each sized to support the operation of a 100 kWe Brayton unit..
- Gas coolers each sized to support the operation of a 100 kWe Brayton unit.



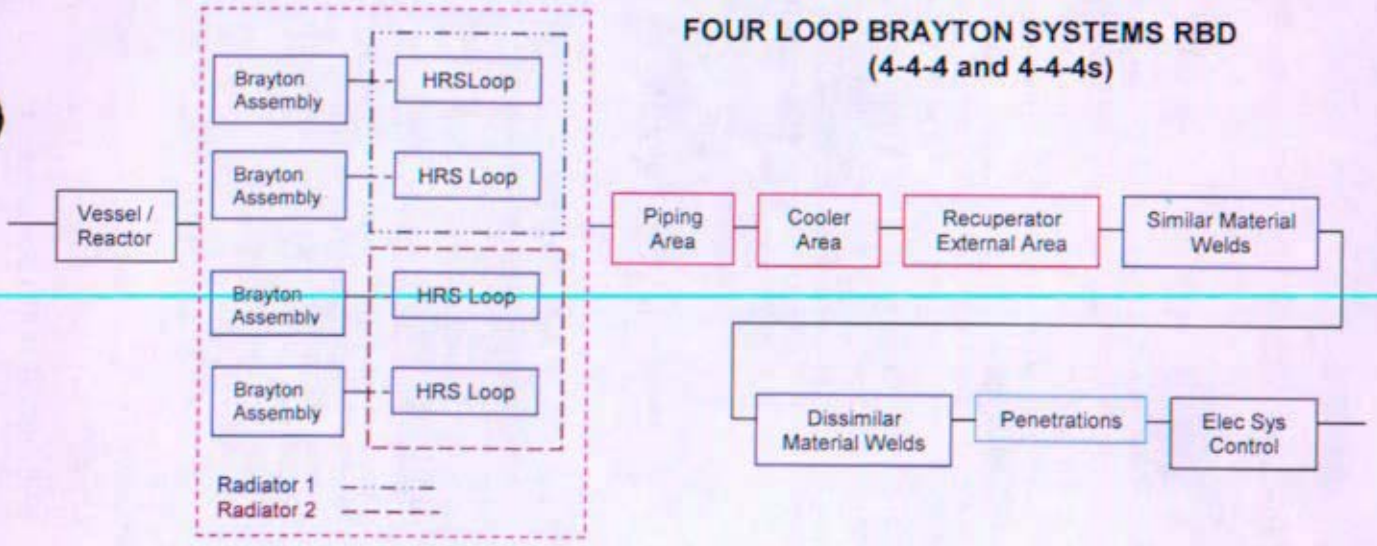

Like the two Brayton systems, the same RBD is given for both operating conditions. The complexity of the valves and configuration of the HRS is taken into account in the mathematical models used to calculate system reliability.

**4-4-4 System Architecture—Two Brayton Loops Operating, Two Standby Loops**

- Four 100 kWe Braytons; two counter-rotational sets
- Four recuperators each sized to service one 100 kWe Brayton unit.
- Four gas coolers each sized to cool one 100 kWe Brayton unit.

**4-4-4s System Architecture--Four Brayton Loops Operating at Reduced Capacity with Capability of Two Brayton Loops to Cover the Full Load**

- Four 100 kWe Braytons; two counter-rotational sets, designed to operate at 25% rated system power and 50% rated system power.
- Recuperators each sized to support the operation of a 100 kWe Brayton unit.
- Gas coolers each sized to support the operation of a 100 kWe Brayton unit.




The only difference in the system reliability between the two operating conditions for a four Brayton system are the failure criteria for the isolation and check valves, which is discussed in Section 7.7.3.

Further discussion of operating modes is included in Reference 7- 8 and Section 8.

## 7.4 Component Reliability Values and Basis

### 7.4.1 Background

Reliability values used in this study are shown in Table 7-1. Little reliability data is available for the components (many of which have not been designed yet) that will make up the SNPP. Component reliabilities were estimated based on NRPCT experience. Limited commercial data was used to confirm these approximations (as noted below). The values of some of the components were based on perceived reliability relative to other components. For example, the recuperator was perceived to have higher reliability than the gas cooler due to differences in functional requirements. Therefore, since a specific reliability value was given for the gas cooler, and a specific reliability value was not given for the recuperator, the constituents of the recuperator were assigned reliability values to ensure that the overall reliability value of the recuperator was higher than the gas cooler reliability for this study. The reliability of some of the components is based on either surface area or length of the critical dimension that is a pressure boundary. The general expression relating reliability to surface area or length takes the form $(1\text{-}1*10^{-j})^{k}$ , where "j" is a value given to achieve an estimated component reliability for a single Brayton system and then incremented as stated for multiple brayton systems. "k" is the surface area or the dimension (length) of the component vulnerable to the specified failure mode. Section 9 provides a detailed description of the component functional requirements, concept designs, failure modes, and review of available historical component benchmarks.

### 7.4.2 Component Reliability Values

**Table 7-1 Component Input Reliability Values and Component Failure Modes**

| System Component | Reliability | Basis and Remarks | Benchmark | Failure Mode | Reliability per unit or area |
|---|---|---|---|---|---|
| Reactor and Core | 1.0 | Not enough information is available at this time to assign a reliability number for the reactor or to show how the reactor reliability changes with different system configurations. | None | Leak to space, Control Rod/Mechanism failure, Stops producing heat | 100.00% |
| Piping Area per loop | $(1\text{-}1*10^{-8.4859})^{2\text{xmx8x(2436)}}$ | Piping length of 2436 cm for one Brayton loop from arrangement studies. Pipe radius of 8 cm from arrangements. Piping area is incremented by 50% for each additional Brayton | None | Leak to space | 99.96% |

| System Component | Reliability | Basis and Remarks | Benchmark | Failure Mode | Reliability per unit or area |
|---|---|---|---|---|---|
| Recuperator External Area | $(1-1*10^{-6.58})^{k}$ (k=recuperator external area) | Recuperator area derived from code (recuperator design team); Section 9. External area for recuperator is 14000 $cm^2$ & 18000 $cm^2$ for 100 kWe and 200 kWe recuperators, respectively | Approximately 97% - 99% total for internal and external areas combined--Commercial data from Hamilton Sundstrand and Garrett for similar type heat exchangers (Section 9) | Leak to space | 99.63% 100 kWe 99.53% 200 kWe |
| Recuperator Internal Area | $(1-(1*10^{-0.000959}))^{(N/1.44x10^6)}$ (N=recuperator internal area) | Internal area is 150000 $cm^2$ for a 100 kWe Brayton and 245000 $cm^2$ for a 200 kWe Brayton from recuperator design team; Section 9. Values adjusted to ensure higher reliability than for gas cooler. | Approximately 97% - 99% total for internal and external areas combined--Commercial data from Hamilton Sundstrand and Garrett for similar type heat exchangers (Section 9) | Internal leak (fails) | 99.99% 100 kWe 99.98% 200 kWe |
| Gas Cooler Area | 0.9813 | Estimate given based on a function of time (15 years). HRS architecture is assumed to be the same for any Brayton system configuration, Therefore, the gas cooler area will be the same for all systems. Information from Hamilton Sundstrand (see Reference 7- 10 and Section 9) | Vendor data for similar heat exchangers (same as above) | Leak to space. Both internal leaks and external leaks to space cause failure; however, the probability of leakage is likely different for internal versus external. This difference is not quantified in this study. | 98.13% |
| Similar Material Welds | 0.9996 | Joints at every pipe meeting and component interface. Value chosen to be higher than the reliability for dissimilar material welds. | None | Leak to space | 99.96% |
| Dissimilar Material Welds | 0.999 | Joints between gas cooler and gas piping; Two per gas loop. | None | Leak to space | 99.90% |
| Refractory to Non-refractory joints | 1 (current reliability models assume no such joints) | N/A | None | Crack/Leak to space | N/A |
| Turbo Alternator Housing | 0.996 | Research | None | Leak to space | 99.60% |
| Turbine/Compressor | 0.97 | Research (Hamilton Sundstrand) | Commercial data | Mechanical failure | 97.00% |

| System Component | | Reliability | Basis and Remarks | Benchmark | Failure Mode | Reliability per unit or area |
|---|---|---|---|---|---|---|
| (T/C) | | 0.99 | Research (Garrett) | Commercial data (Reference 7- 12) | | 99.00% |
| Alternator Rotor | | 0.998 | Research (Section 9, Garrett, Hamilton Sundstrand) | None | Mechanical failure | 99.80% |
| Shaft | | 0.999 | Educated Decision | None | Mechanical failure | 99.90% |
| Bearing (3) | | $0.997^3$ | Educated Decision (Garrett, Hamilton Sundstrand) | Commercial data—Reference 7- 12 | Seize | 99.10% |
| Stator | Alternator Winding (electrical bus) | 0.994 | A single Brayton system Brayton assembly has two alternator windings running in parallel. Multiple brayton system Brayton assemblies have one alternator winding per Brayton. | Research-- Hamilton Sundstrand | Loss of load/Cable short | 99.40% |
| | Total electrical penetration circumference | $(1\text{-}0.000478)^{(2\pi r)}$ (r= radius of penetration in cm) | The radius in cm is 1 for a 100 kWe Brayton and 2 for a 200 kWe Brayton. Based on estimated Brayton conductor size. Based on power rating of Brayton. Originally based on research, but value was adjusted relative to other components. | None | Leak to space | 99.70% 100 kWe 99.40% 200 kWe |
| Isolation Valves | | $0.99^2$ (two failure modes) | Educated Decision | 0.998 per demand to operate for a solenoid valve or 0.987 for solenoid to fail over 15 years (Reference 7- 11) | Electrical (incorrect signal to change valve position) Mechanical (unable to change position when required) | 98.01% |
| Check Valves | | 0.99 (one failure mode) | Educated Decision | 0.999-0.9999 per demand to shut or open, respectively. Commercial data—Reference 7- 11 | Mechanical (unable to change position when required) | 99% |
| Heat Rejection System Loop | | 0.97 | Educated Decision | None | Leak to space | 97.0% |
| Heat Rejection System Pump | | 0.99 | Educated Decision | None | Electrical and mechanical (not separated for this study) | 99.0% |
| Electrical Control System | | 0.998 0.996 (parallel systems) | Value chosen based on relative reliability compared to other components. | None | Loss of load control | 99.8% 99.6% |

None of the component reliabilities based on area reflect differences due to variations in system efficiency with system configuration. For example, although the three and four Brayton system recuperators are nominally the same size (100 kWe), differences in overall system efficiency would require the recuperators for the four Brayton system to have a larger heat transfer area, according to the system heat balances of Section 6.

System efficiency differences between the three and four Brayton systems results in approximately a 28% higher thermal rating for the four Brayton system recuperator, causing a lower reliability for the four Brayton system recuperator then the three Brayton system recuperator.

Although this reliability study does not relate reliability to the surface area of the gas cooler, the four Brayton system gas cooler would also require more heat transfer area compared to the three Brayton system gas cooler due to differences in system efficiency between the three and four Brayton systems. From Section 6 heat balances, the difference in system efficiency causes the four Brayton system gas cooler to require approximately a 25% higher thermal rating than the three Brayton system gas cooler. However, as noted in Section 6 Conclusions, optimization of the heat balances may lead to reduced differences in efficiency among the systems evaluated.

## 7.5 Reliability and Sensitivity Studies Results

### 7.5.1 Reliability Study Results

Two separate values for the turbine/compressor (T/C) component were given in Table 7-1. Reliability results for both component reliability values are presented in Table 7-2 and Table 7-3. The columns for "parallel" systems indicate systems where every Brayton is operating below rated capacity such that they could supply full power if a Brayton is lost. In the following tables, "CRP" refers to counter-rotating pairs, which indicates that each operating Brayton must rotate in the opposite direction from the other operating Brayton (usually to minimize angular momentum effects on a spacecraft). Originally, the reliability study included the variation in which any Brayton could operate with any other Brayton regardless of rotation direction; however, due to the connection between the Brayton loops and the HRS (discussed in Section 7.7.2.1), both of these variations are mathematically the same with respect to calculating reliability.

**Table 7-2 System Reliability Results for Turbine/Compressor Reliability of 97%**

| System Component T/C at 0.97 | Area | Number of Components | Component Reliability | 1 Brayton | 1 of 2 Braytons | 2 of 3 Braytons | 2 of 4 Braytons (CRP) | 1 of 2 parallel | 2 of 3 parallel | 2 of 4 parallel |
|---|---|---|---|---|---|---|---|---|---|---|
| 100 kWe Braytons/Valves/HRS | | | | | | 0.9762 | 0.9683 | | 0.9777 | 0.9711 |
| 1-200 kWe Brayton /HRS | | | | 0.9527 | | | | | | |
| 2-200 kWe Braytons/Valves/HRS | | | | | 0.9854 | | | 0.9944 | | |
| Recuperator Ext 100 kWe | 14000 $cm^2$ | | 0.9963 | | | 0.9890 | 0.9854 | | 0.9890 | 0.9854 |
| Recuperator Ext 200 kWe | 18000 $cm^2$ | | 0.9953 | 0.9953 | 0.9906 | | | 0.9906 | | |
| Piping Area | 122446.7 $cm^2$ | | 0.9996 | 0.9996 | 0.9994 | 0.9992 | 0.9990 | 0.9994 | 0.9992 | 0.9990 |
| Similar Welds (1 loop) | | 12 | 0.9996 | 0.9952 | | | | | | |
| Similar Welds (2 loops) | | 40 | | | 0.9841 | | | 0.9841 | | |
| Similar Welds (3 loops) | | 63 | | | | 0.9751 | | | 0.9751 | |
| Similar Welds (4 loops) | | 86 | | | | | 0.9662 | | | 0.9662 |
| Dissimilar Welds (1 loop) | | 2 | 0.999 | 0.9980 | | | | | | |
| Dissimilar Welds (2 loops) | | 4 | | | 0.9960 | | | 0.9960 | | |
| Dissimilar Welds (3 loops) | | 6 | | | | 0.9940 | | | 0.9940 | |
| Dissimilar Welds (4 loops) | | 8 | | | | | 0.9920 | | | 0.9920 |
| Penetrations 100 kWe | Radius - 1 cm | | 0.997 | | | 0.9910 | 0.9881 | | 0.9910 | 0.9881 |
| Penetration 200 kWe | Radius - 2 cm | | 0.9940 | 0.9940 | 0.9881 | | | 0.9881 | | |
| Cooler Area Leak | | | 0.9813 | 0.9813 | 0.9813 | 0.9813 | 0.9813 | 0.9813 | 0.9813 | 0.9813 |
| Electrical Control System | | | 0.9980 | 0.9980 | 0.9980 | 0.9980 | 0.9980 | 0.9960 | 0.9960 | 0.9960 |
| **Reliability of System** | | | | **0.9164** | **0.9253** | **0.9075** | **0.8840** | **0.9318** | **0.9071** | **0.8848** |
| **Reliability in Percent** | | | | **91.64%** | **92.53%** | **90.75%** | **88.40%** | **93.18%** | **90.71%** | **88.48%** |

**Table 7-3 Reliability Results for Turbine/Compressor Reliability of 99%**

| System Component T/C at 0.99 | Area | Number of Components | Component Reliability | 1 Brayton | 1 of 2 Braytons | 2 of 3 Braytons | 2 of 4 Braytons (CRP) | 1 of 2 parallel | 2 of 3 parallel | 2 of 4 parallel |
|---|---|---|---|---|---|---|---|---|---|---|
| 100 kWe Braytons/Valves/HRS | | | | | | 0.9847 | 0.9793 | | 0.9859 | 0.9817 |
| 1-200 kWe Brayton /HRS | | | | 0.9723 | 0.9895 | | | 0.9964 | | |
| 2-200 kWe Braytons/Valves/HRS | | | | | | | | | | |
| Recuperator Ext 100 kWe | 14000 $cm^2$ | | 0.9963 | | | 0.9890 | 0.9854 | | 0.9890 | 0.9854 |
| Recuperator Ext 200 kWe | 18000 $cm^2$ | | 0.9953 | 0.9953 | 0.9906 | | | 0.9906 | | |
| Piping Area | 122446.7 $cm^2$ | | 0.9996 | 0.9996 | 0.9994 | 0.9992 | 0.9990 | 0.9994 | 0.9992 | 0.9990 |
| Similar Welds (1 loop) | | 12 | 0.9996 | 0.9952 | | | | | | |
| Similar Welds (2 loops) | | 40 | | | 0.9841 | | | 0.9841 | | |
| Similar Welds (3 loops) | | 63 | | | | 0.9751 | | | 0.9751 | |
| Similar Welds (4 loops) | | 86 | | | | | 0.9662 | | | 0.9662 |
| Dissimilar Welds (1 loop) | | 2 | 0.9990 | 0.9980 | | | | | | |
| Dissimilar Welds (2 loops) | | 4 | | | 0.9960 | | | 0.9960 | | |
| Dissimilar Welds (3 loops) | | 6 | | | | 0.9940 | | | 0.9940 | |
| Dissimilar Welds (4 loops) | | 8 | | | | | 0.9920 | | | 0.9920 |
| Penetrations 100 kWe | Radius - 1 cm | | 0.9970 | | | 0.9910 | 0.9881 | | 0.9910 | 0.9881 |
| Penetration 200 kWe | Radius - 2 cm | | 0.9940 | 0.9940 | 0.9881 | | | 0.9881 | | |
| Cooler Area Leak | | | 0.9813 | 0.9813 | 0.9813 | 0.9813 | 0.9813 | 0.9813 | 0.9813 | 0.9813 |
| Electrical Control System | | | 0.9980 | 0.9980 | 0.9980 | 0.9980 | 0.9980 | 0.9960 | 0.9960 | 0.9960 |
| **Reliability of System** | | | | **0.9353** | **0.9291** | **0.9154** | **0.8941** | **0.9337** | **0.9147** | **0.8945** |
| **Reliability in Percent** | | | | **93.53%** | **92.91%** | **91.54%** | **89.41%** | **93.37%** | **91.47%** | **89.45%** |

From the previous tables it can be seen that the results for the different system configurations are very close in reliability.

Because the reliability of a Brayton assembly as a whole is lower than any of the other given components, the reliabilities of the system architectures were analyzed based on increases in Brayton assembly (turbine/compressor, alternator, housing, bearings, windings, rotor, shaft, and recuperator internal surfaces) reliability. Figure 7-3 illustrates the overall system reliability trend for each of four system architectures based on Brayton assembly reliability. Assuming that both a 100 kWe and 200 kWe Brayton assembly have the same reliability, it can be seen in Figure 7-3 that for a Brayton assembly reliability of 0.95, the two Brayton system is more reliable than the other systems. There is a crossover point where the single Brayton system becomes more favorable, given component reliabilities provided in Table 7-1, than any of the multiple Brayton systems. For Brayton assembly reliability below a certain crossover point, the single Brayton system is less reliable than the three Brayton system. In Figure 7-3, system reliability of 95% was only achieved for the one Brayton system when the Brayton assembly reliability reached nearly 100%. This indicates that the Brayton assembly reliability is critical in determining whether the system reliability could achieve 95%.

Because the same trend exists for both standby systems and systems with all Braytons running below rated capacity, the following figure contains the one Brayton system and only the standby systems for multiple Brayton configurations.

Given an increase in Brayton assembly reliability, the configuration of multiple Brayton systems does not produce as much of an increase in system reliability as for the single Brayton system. With increased redundancy in Braytons units, there is an increase in the number of redundant components in a series configuration. As the number of components operating in series increases the reliability of the system decreases. Therefore, the increase in Brayton redundancy is negated by the increase in units of components along with an increase in surface area.

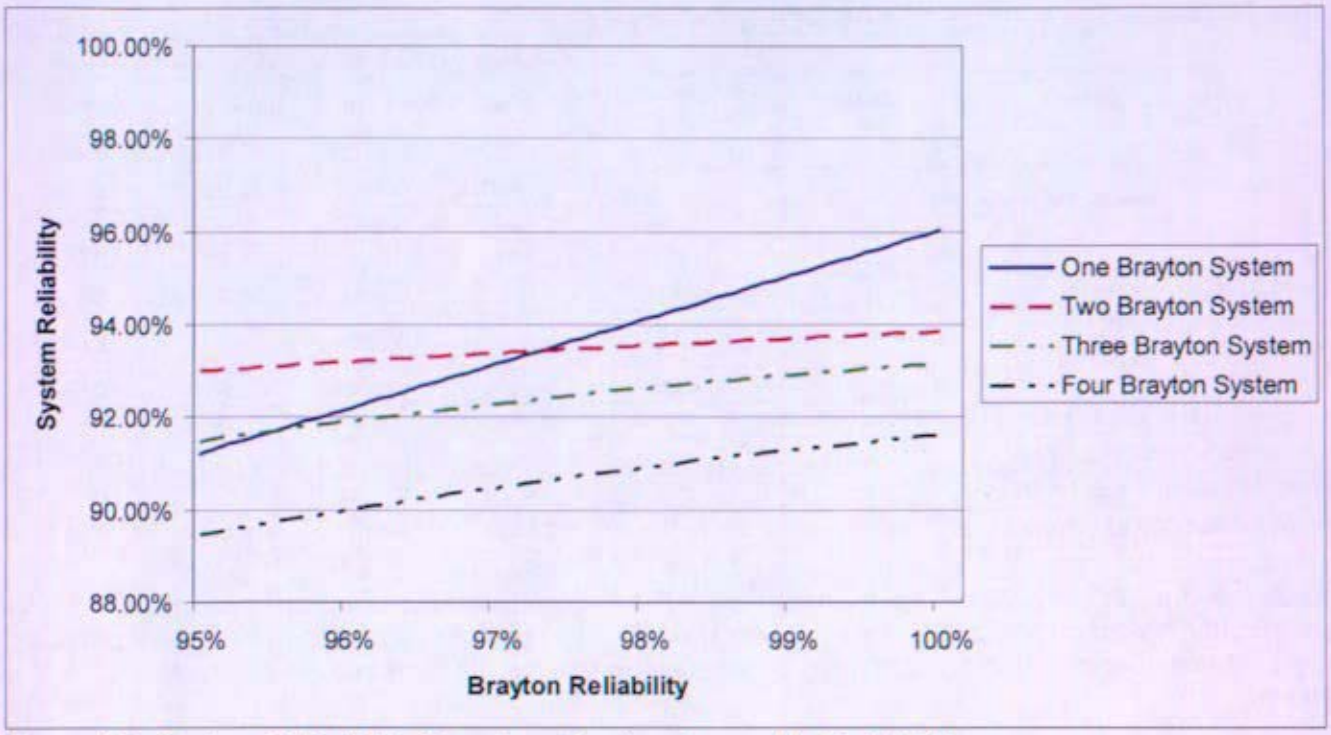



**Figure 7-3: System Reliability Based on Brayton Assembly Reliability**

In order to increase reliability for any system configuration, the reliability of the Brayton assembly components needs to be increased. As shown in Table 7-4, the Brayton assembly itself is a weak link in the system with a reliability ranging from 0.9487 to 0.9741 based on the reliability for the T/C of 0.97 and 0.99 respectively.

**Table 7-4 Breakdown of Brayton Assembly Reliability**

| | | | T/C Reliability at 0.97 | | T/C Reliability at 0.99 | |
|---|---|---|---|---|---|---|
| **Brayton Component** | **Area** | **Component Reliability** | **100 kWe** | **200 kWe** | **100 kWe** | **200 kWe** |
| Turbine Compressor | | 0.97 or 0.99 | 0.9700 | 0.9700 | 0.9900 | 0.9900 |
| Alternator Rotor | | 0.9980 | 0.9980 | 0.9980 | 0.9980 | 0.9980 |
| Shaft | | 0.9990 | 0.9990 | 0.9990 | 0.9990 | 0.9990 |
| Bearing (3) | | 0.9970 | 0.9910 | 0.9910 | 0.9910 | 0.9910 |
| TCA Housing | | 0.9960 | 0.9960 | 0.9960 | 0.9960 | 0.9960 |
| Alt Windings 1 Brayton system (two in parallel) | | 0.9940 | | 0.9999 | | 0.9999 |
| Alt Windings >1 Brayton system | | 0.9940 | 0.9940 | 0.9940 | 0.9940 | 0.9940 |
| Recuperator Internal 100 kWe | 150000 $cm^2$ | | 0.9999 | | 0.9999 | |
| Recuperator Internal 200 kWe | 245000 $cm^2$ | | | 0.9998 | | 0.99984 |
| **Brayton Reliability 1 Brayton** | | | | **0.9544** | | **0.9741** |
| **Brayton Reliability >1 Brayton** | | | **0.9488** | **0.9487** | **0.9683** | **0.9683** |

Due to the small differences between system reliabilities, a particular conclusion of system configuration based on reliability numbers is not meaningful. However, the sensitivity studies provide insight into components that need to have an increase in reliability to increase overall system reliability,

## 7.5.2 Sensitivity Studies Results

This section summarizes system reliability sensitivity studies based on varying the assumed reliability for a given component. Failure rates (1.0 minus the reliability value) were used as the sensitivity range for component reliabilities to test effects of component reliability changes on system reliability. Table 7-9 provides the ranges for the sensitivity study based on failure rates of one unit of each component. Each of the components in the analyzed systems proved to be a significant factor. Based on these results, components with the greatest impact on system reliability were identified. As component reliabilities either increased or decreased the components that affected the system the most changed. A listing of the five components that affected overall system reliabilities the most, given a decrease in component reliability (increase in failure rate), are given in Table 7-5. A listing of components that had the most significant impact on system reliabilities, given an increase in component reliabilities (decrease in failure rate) are given in Table 7-6. The ranking of the significance of the components is given followed by the percent increase or decrease in system reliability in parentheses. Complete component significance ratings for each system can be found in Section 7.11.

**Table 7-5: System Reliability Change Due to Doubling the Component Failure Rate**

| System Component (Percent decrease in System Reliability is given) | One Brayton | Two Brayton (standby) | Two Brayton (running) | Three Brayton (standby) | Three Brayton (running) | Four Brayton (standby) | Four Brayton (running) |
|---|---|---|---|---|---|---|---|
| | Data in these columns shows ranking (1-5) of component effect on system reliability followed by percent change in system reliability due to doubling the component failure rate. | | | | | | |
| Similar Material Weld | 5 (0.42%) | 3 (1.42%) | 2 (1.45%) | 1 (2.17%) | 1 (2.18%) | 1 (2.85%) | 1 (2.87%) |
| Bearing | 3 (0.79%) | | | | | | |
| Cooler Area Leak | 2 (1.68%) | 1 (1.71%) | 1 (1.74%) | 4 (1.65%) | 4 (1.66%) | 4 (1.59%) | 4 (1.60%) |
| HRSLoop | | 2 (1.67%) | 4 (0.53%) | 3 (1.72%) | 3 (1.68%) | 3 (2.12%) | 3 (2.05%) |
| Penetration | 4 (0.53%) | 4 (1.06%) | 3 (1.09%) | 5 (0.78%) | 5 (0.78%) | 5 (1.00%) | 5 (1.00%) |
| T/C | 1 (2.75%) | 5 (0.83%) | 5 (0.48%) | 2 (1.72%) | 2 (1.68%) | 2 (2.12%) | 2 (2.05%) |

**Table 7-6: System Reliability Change Due to Removing the Component Failure Rate (component reliability goes to 1)**

| System Component (Percent increase in System Reliability is given) | One Brayton | Two Brayton (standby) | Two Brayton (running) | Three Brayton (standby) | Three Brayton (running) | Four Brayton (standby) | Four Brayton (running) |
|---|---|---|---|---|---|---|---|
| | Data in these columns shows ranking (1-5) of component effect on system reliability followed by percent change in system reliability due to removing the component failure rate. | | | | | | |
| Dissimilar Material Weld | | | 5 (0.39%) | | | | |
| Similar Material Weld | | 2 (1.55%) | 2 (1.55%) | 1 (2.42%) | 1 (2.42%) | 1 (3.27%) | 1 (3.27%) |
| Bearing | 3 (0.86%) | | | | | | |
| Cooler Area Leak | 2 (1.80%) | 1 (1.82%) | 1 (1.83%) | 2 (1.81%) | 2 (1.81%) | 2 (1.80%) | 2 (1.80%) |
| HRSLoop | 5 (0.17%) | 4 (0.68%) | | 5 (0.74%) | 5 (0.72%) | 5 (0.97%) | 5 (0.93%) |
| Penetration | 4 (0.58%) | 3 (1.16%) | 3 (1.16%) | 3 (0.87%) | 3 (0.87%) | 3 (1.14%) | 3 (1.14%) |
| Recuperator External Area | | 5 (0.48%) | 4 (0.46%) | | | | |
| T/C | 1 (2.92%) | | | 4 (0.74%) | 4 (0.72%) | 4 (0.97%) | 4 (0.93%) |

Analysis of the components indicates that components with the largest failure rate and components that have multiple units running in series have the largest impact on system reliability. Components with items running in parallel may have a larger individual component reliability but do not have as much of an impact on system reliability due to the redundancy in system configuration. For system configurations with a failure rate increase in component reliability (component reliability – failure rate) the largest decrease in system reliability occurs when the failure rate of similar material welds decreases for both three (-2.18%) and four (-2.87%) Brayton configurations. This is due to the large number of similar welds in the three and four Brayton systems. It is assumed in this study that the single Brayton system only has 12 similar material welds, the two Brayton system has 40, the three Brayton system has 63, and the four Brayton system has 86 similar welds. Similar material welds are independent of one another and therefore function in series. As the number of like components required to function increases, the effect on a given system whether positive or negative also increases as illustrated in Figure 7-4. All the following figures showing sensitivity of the system reliability to changes in component reliability are based on T/C reliability of 0.97.

For the three and four Brayton systems, an increase in T/C reliability would increase overall system reliability by about 1%, while increasing the similar material welds would increase system reliability between 1.5% and 3.3%.

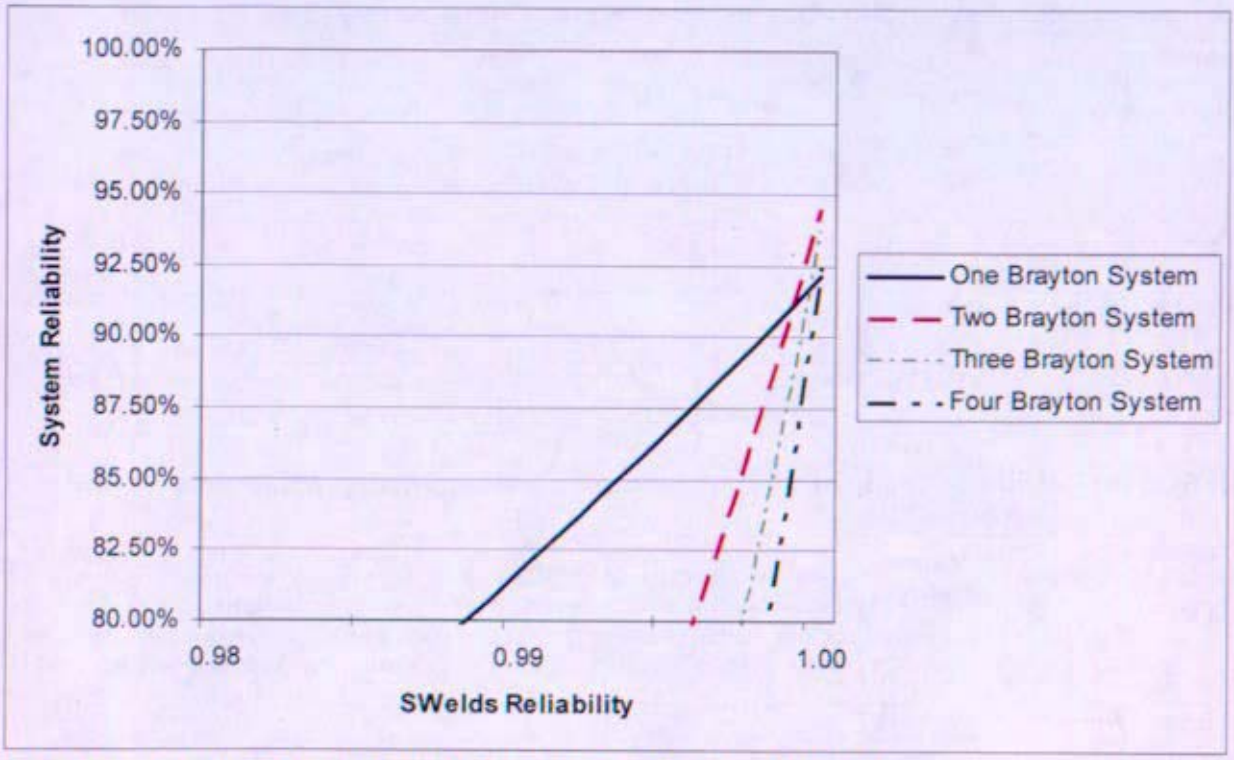



**Figure 7-4: Similar Material Weld Reliability on System Reliability**

For the two Brayton systems, a failure rate increase for gas cooler area decreases system reliability by 1.74% and a failure rate increase for T/C for the one Brayton system decreases system reliability by 2.75%. The T/C component has the largest failure rate along with the gas cooler, followed by the bearings. For a single Brayton configuration, the T/C does not have redundancy in the system. However, in multiple Brayton configurations there is redundancy in the T/C component. The gas cooler area does not have redundancy for any of the system configurations (due to any failure in the gas cooler causing a failure of the system) and thus contributes significantly to each system.

The gas cooler has a significant impact on system reliability for all of the systems evaluated. A decrease in reliability of 1.87% results in 1.59-1.74% decrease in overall system reliability, depending on the system. As discussed in Section 7.4.2, the gas cooler reliability number is not based on surface area and does not reflect any differences in reliability due to system efficiency differences (which would translate into a different amount of surface area). However, to investigate the effect of system efficiency on system reliability, assume that the gas cooler reliability is related to surface area by the following equation:

$(1-1*10^{-7.747})^{1052405.6} = 98.13\%$, where $1 \times 10^{-7.747}$ refers to a failure rate per area (derived to achieve the reliability value given for the gas cooler in Table 7-1) and 1052405.6 $cm^2$ is the total pressure boundary and heat transfer area of the gas cooler.

As discussed in Section 7.4.2, from the Section 6 heat balances, the four Brayton system would require approximately a 25% higher thermal rating for the gas cooler than the three Brayton gas cooler. If this corresponded directly to a 25% increase in gas cooler surface area (larger heat transfer area plus a larger pressure boundary), the reliability of the gas cooler would be 97.67%. Therefore, the difference in system efficiency could result in about a 0.4% decrease in overall system reliability

for the four Brayton system due to the increased area of the gas cooler. However, as discussed in Section 6 Conclusions—Design Heat Balances, optimization of the design may minimize efficiency differences among systems evaluated and thus mitigate any negative impact on reliability.

Figure 7-5 provides insight into the effects of increasing the reliability of the cooler area for all systems.

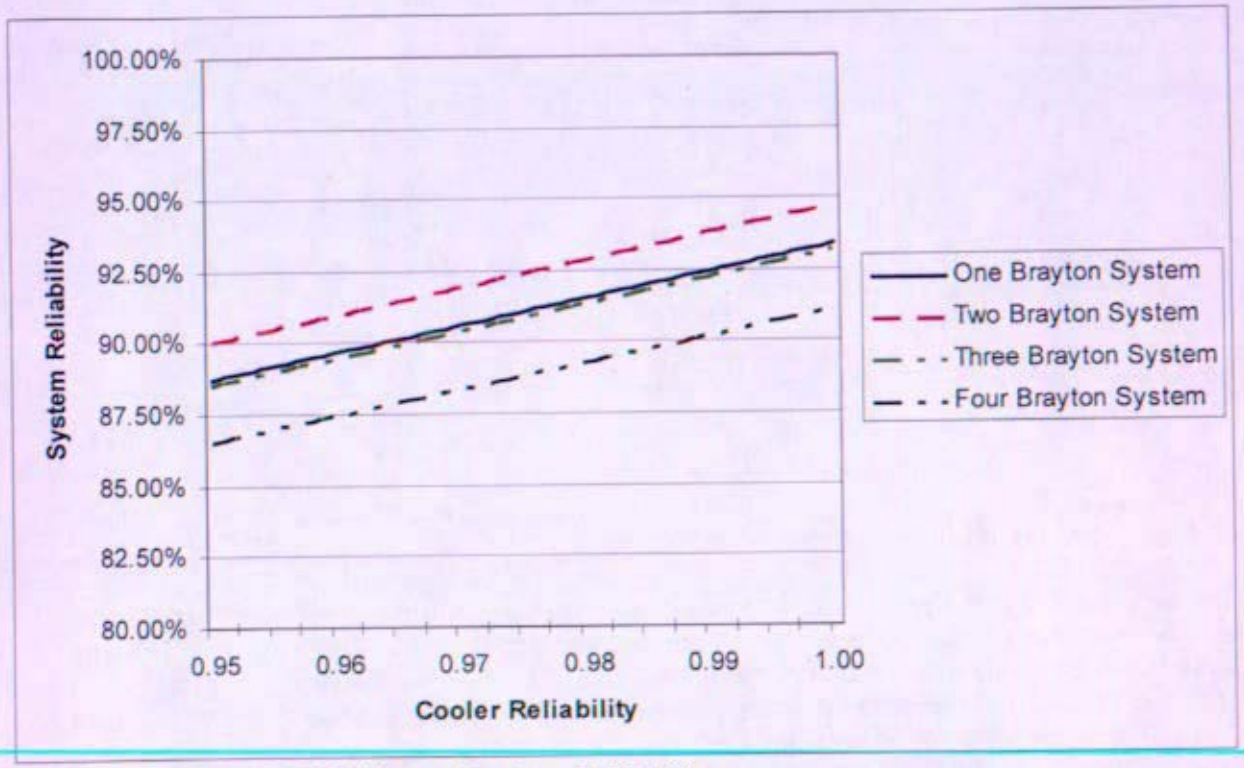



**Figure 7-5: Cooler Reliability on System Reliability**

In order to increase system reliability, the components that would need to be focused on differ based on the Brayton configuration. However, the top five components for each system are consistent with the exception of the one Brayton system, and the two brayton system with both braytons operating at reduced capacity, where an increase in bearing reliability to 1 could increase overall system reliability by 0.86%. The bearing component does not affect multiple Brayton configurations because the redundancy in the Braytons decreases the impact of the bearings on system reliability. For a one Brayton system an increase in the T/C component would affect system reliability the greatest by a potential of a 2.92% increase in system reliability when T/C reliability is 1. For a two Brayton system, the cooler area would provide the greatest system reliability improvement with an approximate increase of system reliability of 1.83%.

Figure 7-6 illustrates the effects of a HRS loop on overall system reliability. As the reliability for a HRL increases from 0.95 to 1, system reliability increases approximately 3% for a four Brayton system and increases about 1% for a one Brayton system. The difference in system reliability increases for different systems is due to the redundant nature of HRLs for one, two and three Brayton architectures. The four Brayton system does not have redundant HRLs for any Brayton unit.

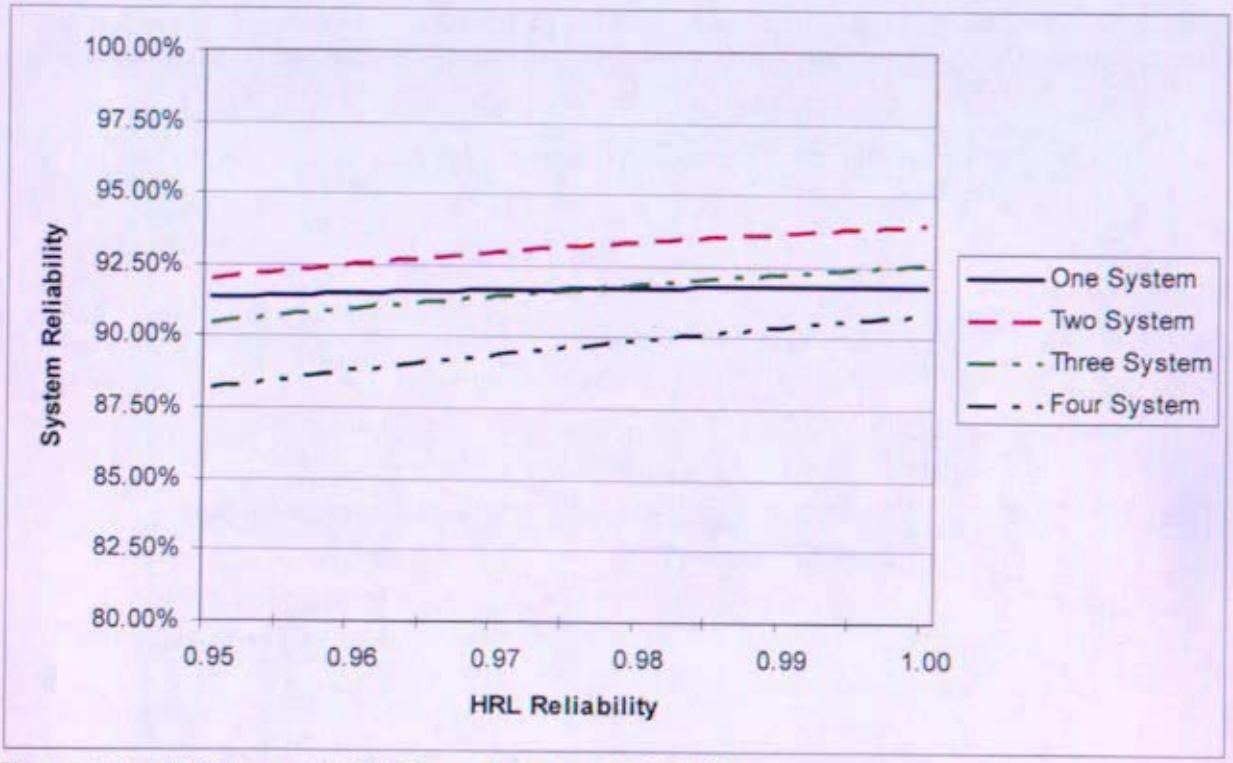



**Figure 7-6: HRS Loop Reliability on System Reliability**

For the three and four Brayton system architectures the same components affect overall system reliabilities. This is based on the fact that both systems are based on 100 kWe Braytons. The one and two Brayton system architectures do not have the same components affecting the system reliability (although similar). This is due to having Brayton redundancy in the two Brayton system and an increased number of similar material welds in the two Brayton system.

Even though the reliability of the Brayton needs to be increased, other system components are critical to increasing overall system reliability. Increasing the component reliability of the T/C increases system reliabilities by a range of 2.92% to 0.74% while increasing the component reliability for the gas cooler could increase system reliability by approximately 1.8% for any system. Of the five components that could increase system reliability by the largest amount, only the T/C is part of a Brayton unit with the exception of bearings which are only in the top five components for a one Brayton system.

Redundancy in Brayton units decreases the impact of Brayton components on the overall system reliability. However, despite this fact, the reliability for the T/C component is low with respect to the other Brayton components (failure rate of either 0.03 or 0.01) and thus significantly impacts overall system reliability for every Brayton system architecture. The isolation valve, check valve, and the HRS pump have the highest failure rates after the T/C and gas cooler, but these components do not affect overall system reliability as much as any other system components. This is due to the fact that two HRS pumps operate in parallel for each HRL and the valves function in parallel for an operating Brayton given the assumption that either the check valve or isolation valve has to close for mission success given another Brayton is able to come online or carry the full load.

### 7.5.3 SNPP Reliability Versus Mass

Rocketdyne presented in Reference 7- 6 a simple methodology for comparing the reliability versus mass to evaluate system architectures. The SP-100 study evaluated energy conversion system architectures for a lunar mission. NRPCT reviewed the methodology and decided to perform a similar study using the detailed reliability study results and the current mass estimates for each system architecture.

Section 4 provides the pre-conceptual mass estimates for several plant configurations, including the one Brayton (1-1-1), 1 of 2 parallel (2-2-2s), 2 of 3 (3-3-3), and 2 of 4 (4-4-4) Brayton system architectures. Figure 7-7 shows the results of system mass versus system reliability using mass estimates from Section 4 and using the system reliability values presented above in Table 7-2 and Table 7-3. The system masses include the reactor, shield, instrumentation and control, support structure, turbine, compressor, alternator (collectively called the turboalternator), recuperator, gas cooler, power conditioning and distribution (PCAD) system, system piping, valves, and the heat rejection system.

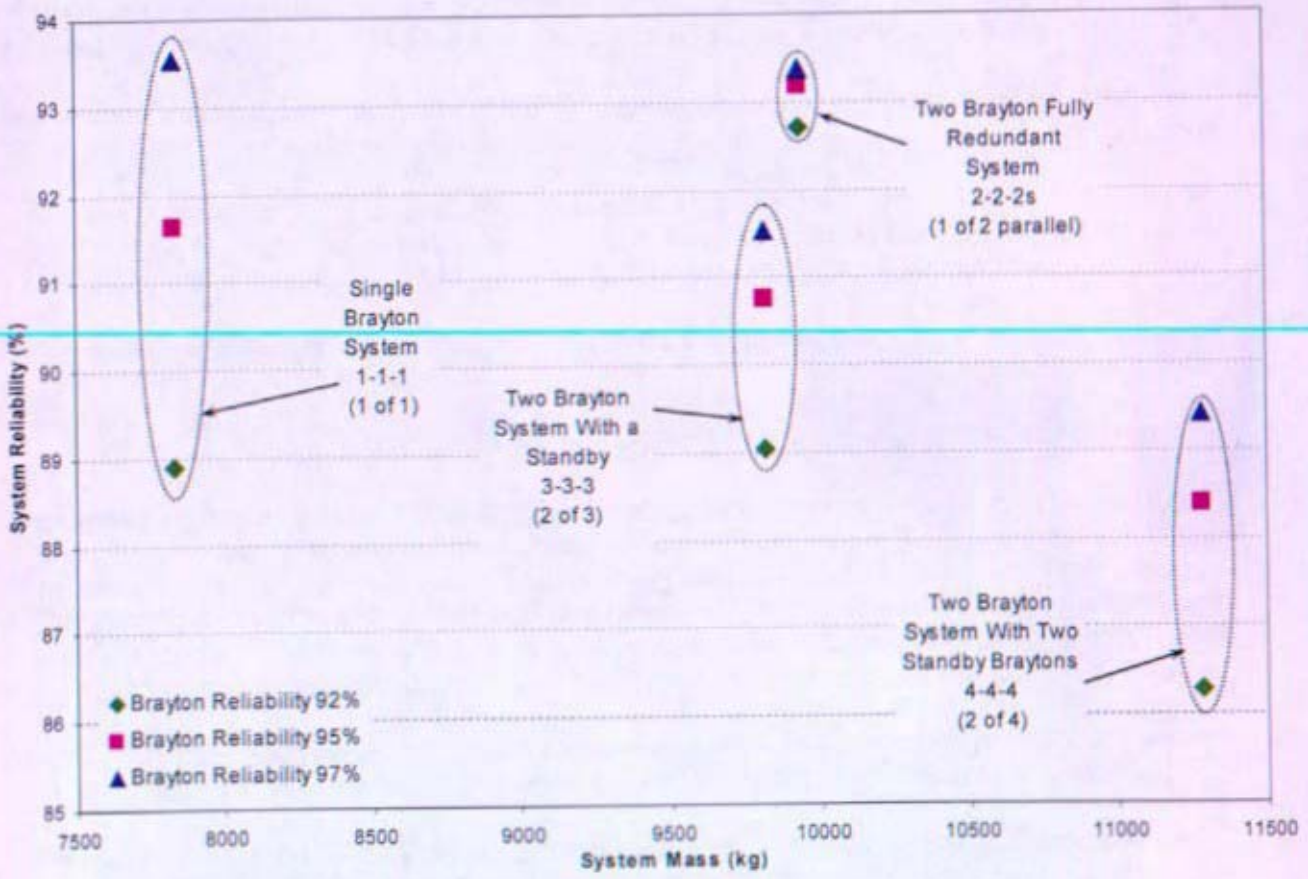



**Figure 7-7: System Reliability Versus System Mass**

Figure 7-7 shows that although the mass of the three 100kWe Brayton system is about the same as the system with two 200kWe Braytons, the reliability of the system drops sharply. This shows that the

addition of piping, valves, and other equipment beyond the two Brayton system reduces the overall system reliability.

## 7.6 Future Actions

Had the Prometheus project continued, the following actions would have been pursued concerning system reliability studies:

1. Work with the cognizant NASA Centers and aerospace contractors to select the most appropriate Reactor Module architecture, balancing the need to maximize reliability with the need to minimize mass.

2. Research space industry use of fault tree analysis and probabilistic risk assessments (PRAs) and evaluate their use for SNPP design.
    - Research how the NR Program has used fault tree analysis and apply as appropriate
    - Develop a fault tree for each system (See Section 7.8)
      Fault trees graphically represent a system and its functions and show relationships between component events and system level events. Fault trees created by NRPCT would be integrated with NASA overall system fault trees.

3. Integrate NRPCT reliability studies (including fault trees) with future project partners' reliability evaluations.

4. Add interfacing systems to the reliability evaluation, such as heat rejection system and electrical control systems (instrumentation and control and power conditioning and distribution), and evaluate potential system architectures of the interfacing systems.

5. Research options to increase reliability or to reduce consequences of failure, including engineered features.

6. Perform Failure Mode, Effects, and Criticality Analysis (FMECA)

   This analysis is performed to identify all system design failure modes to minimize catastrophic and critical failures. This tool ranks failures according to the potential impact on the overall system. For the analysis to be most effective, it must occur early in the design process so that problem areas in the design may be identified. Depending on the amount of component failure rate information available, either a qualitative or quantitative FMECA would be performed. Various resources such as Reference 7- 3 describe the FMECA process.

7. Refine and validate component reliability values and failure modes through testing of components and research of component failures, including understanding transient and age effects, etc.
    a. Assumptions of operating failures would need to be verified for both valves and the HRS. Given any modifications to these assumptions, system reliability models would need to be updated and applied to the analysis. Changes in assumptions for the valves or particularly the HRS based on system configuration could substantially alter conclusions made herein.

b. Develop baseline reliability levels for comparison (using NNPP components)

This task would research reliability values for Naval Nuclear Propulsion Program (NNPP) components to benchmark and understand the magnitude of reliability for the SNPP components.

c. Identify component testing required to support improvements in reliability

d. Study effects of steady state conditions, including temperature effects due to plant arrangement.

e. Study transient and casualty effects on reliability

f. Research and estimate reliabilities of components utilizing commercial and Naval experience

Potential resources include Naval component databases, Reactor Safety organization knowledge, and the following commercial or government nuclear and non-nuclear component failure databases and reliability resources:

**Table 7-7 Reliability Data Databases and Resources**

| **Reliability Databases** | |
|---|---|
| Reliability Data for Nuclear Power Plant Components - VGB PowerTech Germany (ZEDB centralized Reliability and Events Database) | |
| Japanese data base from CRIEPI | |
| NRC database CCFDB (Common-cause failures data base) | |
| RADS (Reliability and Availability Data System - NRC) | |
| British and French Gas Cooled Power reactors Databases | |
| | |
| **Data Source:** | **Equipment Covered:** |
| MIL-HDBK-217F - Reliability Prediction of Electronic Equipment | Electronic components |
| EPRD - Electronic Parts Reliability Data (RAC) | Electronic components |

| | |
|---|---|
| NPRD-95 Non-electronic Parts Reliability Data (RAC) | Mechanical and electro-mechanical components |
| NONOP-1 Nonoperating Reliability Data (RAC) | Mechanical and electro-mechanical components |
| FMD-97 Failure Mode/Mechanism Distributions (RAC) | Electronic, electrical, mechanical and electro-mechanical components |
| SR-332 Reliability Prediction for Electronic Equipment (Telcordia Technologies) | Electronic components |
| EiReDA - European Industry Reliability Data | Mainly components in nuclear power plants |
| OREDA - Offshore Reliability Data | Topside and subsea equipment for offshore oil and gas production |
| MechRel - Handbook of Reliability Prediction for Mechanical Equipment | Mechanical equipment - military applications |
| T-Book (Reliability Data of Components in Nordic Nuclear Power Plants (ISBN 91-631-0426-1) | Components in nuclear power plants |
| Reliability Data for Control and Safety Systems - PDS Data Handbook | Sensors, detectors, valves & control logic |
| Safety Equipment Reliability Handbook (exida) | Safety equipment (sensors, logic units, actuators) |
| WellMaster (ExproSoft) | Components in oil wells |
| SubseaMaster (ExproSoft) | Components in subsea oil/gas production systems |
| PERD - Process Equipment Reliability Data (AIChE) | Process equipment |
| GIDEP (Government-Industry Data Exchange Program) | |
| CCPS Guidelines for Process Equipment Reliability Data, AIChE, 1989 | Process equipment |
| PERD - Process Equipment Reliability Data (AIChE) | Process equipment |
| FARADIP | Electronic, electrical, mechanical, pneumatic equipment |
| IEEE Std. 500-1984: IEEE Guide to the Collection and Presentation of Electrical, Electronic, Sensing Component, and Mechanical Equipment Reliability | See title |

| Data for Nuclear Power Generating Stations | |
|---|---|
| FASIT (Feil og avbrudd i kraftsysteme) | Failure in the electro-power supply system (in Norwegian) |

## 7.7 Methodology of Reliability Studies

### Objectives

- To support pre-conceptual design of a space nuclear power plant system: Perform reliability studies to identify relative system configuration reliabilities and reliability drivers for number of Brayton units and other components.
- Identify design features and actions to mitigate failures.
- Identify components that have a significant effect on system reliability.

### Assumptions

- Mission parameters and requirements are as stated in Section 2, Preconceptual Plant Parameter Report
- Turbomachinery may be designed to operate at two separate operating points.

### Methodology

### 7.7.1 Identify system architectures to be evaluated

Refer to Section 7.3.2 for a list of system architectures. In general, the system architectures included the reactor, piping, varying numbers of turbomachinery components (including the alternator and heat exchangers), and any required valves. Smaller piping and instrumentation, such as alternator bleed flow piping and temperature sensors, were not included. The heat rejection system (HRS) was included to investigate how the HRS design can affect the reliability of the energy conversion system. The electrical control system (PCAD control of Brayton units) was incorporated in the reliability studies as represented by a single reliability value because minimal information was available on system designs and reliability of electrical components. Future reliability studies would include more detail for the electrical control system.

### 7.7.2 Identify failure modes for each component

Component failure modes would be collected and the information would be used to develop fault trees and identify potential component failure issues relative to overall system reliability. Ultimately, a failure rate (the probability a given failure of a component will occur within a given period of time) is determined from component reliabilities and used in calculating overall system reliability.

A few simple failure modes were initially identified for the components included in the reliability studies. Failure mode information is included in Table 7-1 in Section 7.4.

#### 7.7.2.1 Effect of Heat Rejection System Failures on Brayton Primary System

The way the HRS connects to the primary system through the gas cooler affects how failures in the HRS impact the primary system. Detailed descriptions of HRS system and gas cooler configurations are included in Section 9.3. Figure 7-8 through Figure 7-12 are from Section 9.3.

### 1-1-1 System Architecture

Because there is only one Brayton loop and only one gas cooler in this system, HRS failures would not affect the primary system unless heat rejection capability is significantly reduced. One back-up (redundant) HRS loop exists for each radiator. Corrective actions would occur in the HRS system (such as switching to a back up HRS cooling loop), but no action would be necessary in the primary system.

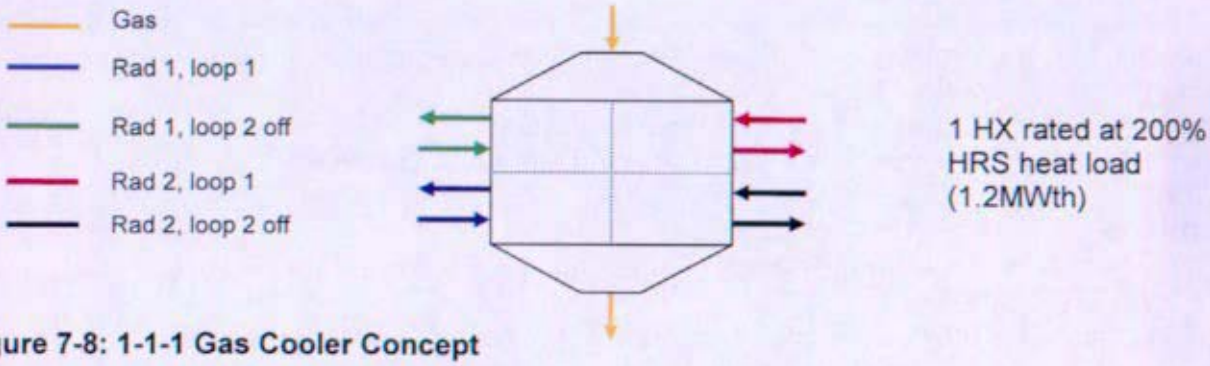



**Figure 7-8: 1-1-1 Gas Cooler Concept**

### 2-2-2 System Architectures

HRS system failures have different effects on a two-Brayton system depending on the mode of Brayton operation. For a two Brayton system each Brayton is connected to two heat rejection loops where each loop is connected to one of the two radiators. One loop per radiator is needed for mission success.

#### Two Braytons Operating at Reduced Capacity

In the two-Brayton system where both Braytons are running at reduced capacity, but one can carry the full load, a failure in one HRS loop would require switching to the other HRL associated with the gas cooler. A second failure affecting the same Brayton (failure in the HRS loop associated with the opposite radiator) would require bringing the unaffected Brayton to full capacity and increasing flow in the second HRL associated with the unaffected Brayton. A second failure associated with an individual radiator would result in loss of full heat rejection capability.

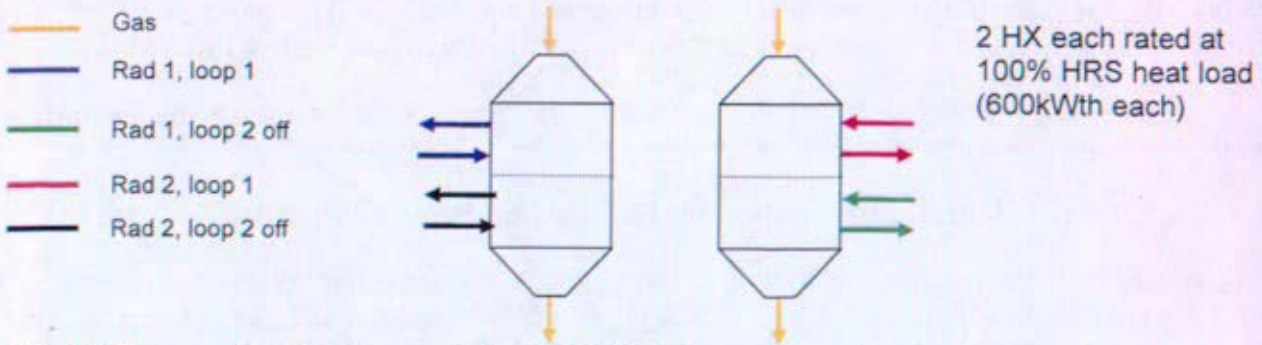



**Figure 7-9: 2-2-2 concept – Braytons rated at 200kWe (2 operating at reduced capacity)**

**One Operating Brayton, One Standby Brayton**

In the two-Brayton system with one Brayton in standby, a failure in an HRS loop associated with the operating Brayton would require switching to the other Brayton because each gas cooler is cooled by both sides of the radiator to reject the full heat load. Since the HRS loops are independent, a failure in a loop would decrease the cooling of the associated gas cooler.

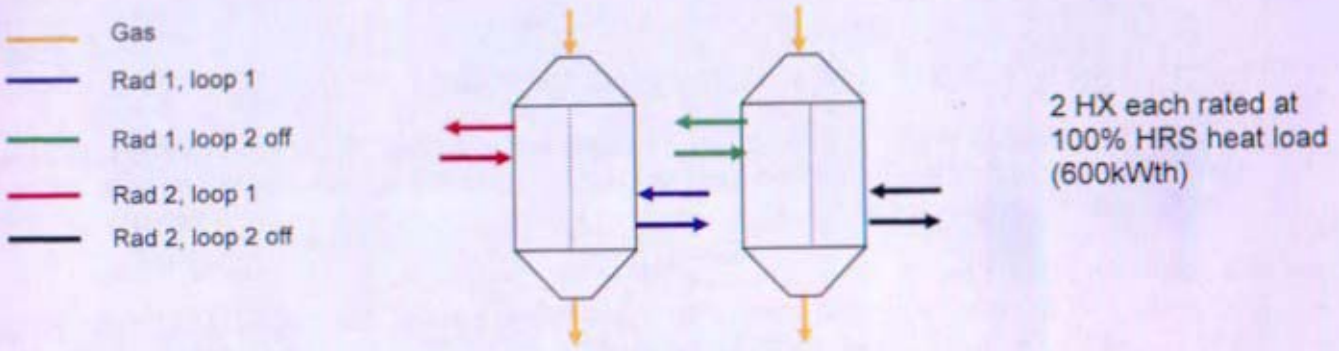



**Figure 7-10: 2-2-2 concept – Braytons rated at 200kWe (1 on, 1 off)**

**3-3-3 System Architectures (Three Braytons Operating at Reduced Capacity or Two Running with One Spare)**

For three Brayton systems, two Braytons are connected to one HRL while the third Brayton is connected to two HRLs. The two Braytons associated with one HRL are connected to one radiator while the third Brayton connected to two HRLs is connected to both radiators.

**Three Braytons Operating at Reduced Capacity**

If one of the HRLs associated with either Brayton connected to one radiator fails both remaining operational Braytons will need to be ramped up to full capacity to handle the load. If either one of the Braytons connected to a single HRL becomes non-operational, the Brayton associated with the two HRLs could use the HRL associated with the non-operational Brayton as a back-up if either of its HRLs becomes non-operational. The system is not currently designed to have this function; however, it is expected that this feature would be incorporated to allow operational flexibility. This reliability study takes credit for this function, but since details of this design feature are not available, the additional necessary valves and piping are not included in this study.

**Two Operating Braytons, One Standby Brayton**

The Braytons connected to a single radiator would initially be operating while the third Brayton connected to two radiators would be the standby unit. If either a Brayton or a HRL fails the standby Brayton will be brought online. For a secured failed Brayton the HRL associated with that Brayton would not be available for use by the standby Brayton unit.

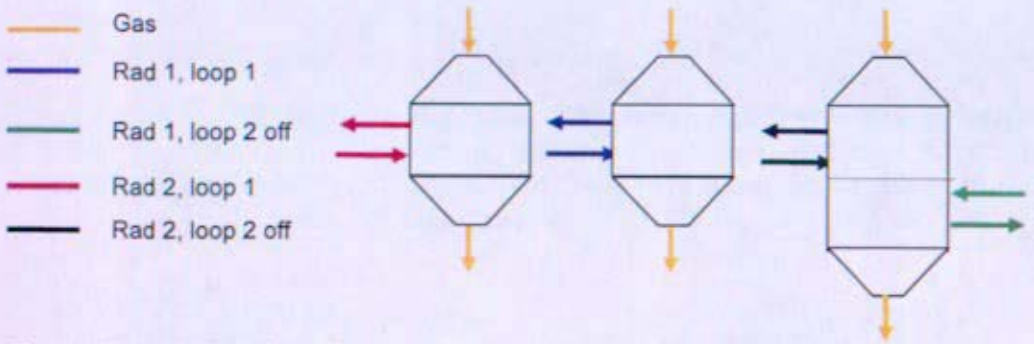



**Figure 7-11: 3-3-3 Gas Cooler Concept (2 operating, 1 standby)**

System configuration for the three brayton HRS is still tentative. Because the HRS system is still under question the HRS for the three brayton configurations were based on functionalities of the two brayton systems.

### 4-4-4 System Architectures

For the four Brayton system where four units are running at reduced capacity or the condition where two units are operational and two in standby (four 100 kW Braytons), each Brayton is connected to one HRL and each radiator has two HRLs. An operational Brayton associated with a failed HRL is not able to access another Brayton's HRL regardless of whether the Brayton is operational or idle.

A failure in a HRL associated with an operating Brayton would necessitate stopping the operational Brayton loop and either bringing the standby Brayton unit associated with the same radiator online (for the 2 operating, 2 standby system) or bringing the running Brayton associated with the same radiator to full capacity (for the system with four Braytons running at reduced capacity) At least one Brayton and HRL associated with each radiator must operate for mission success.

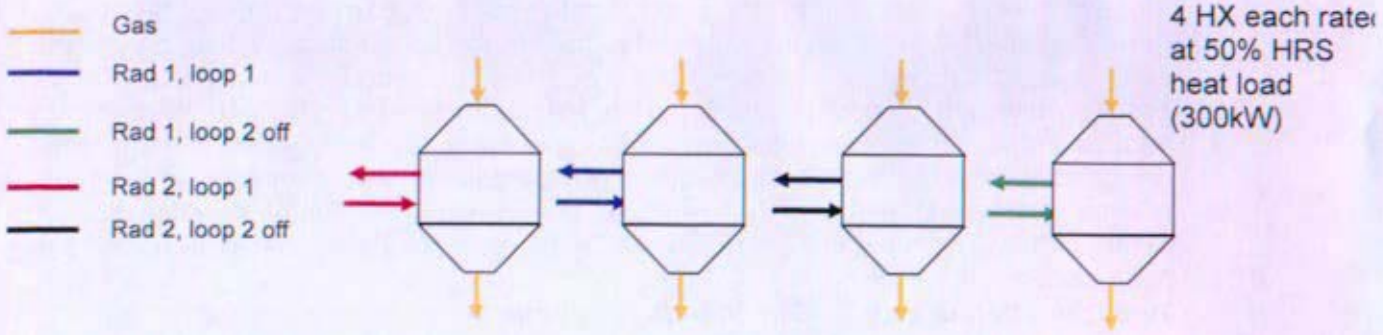


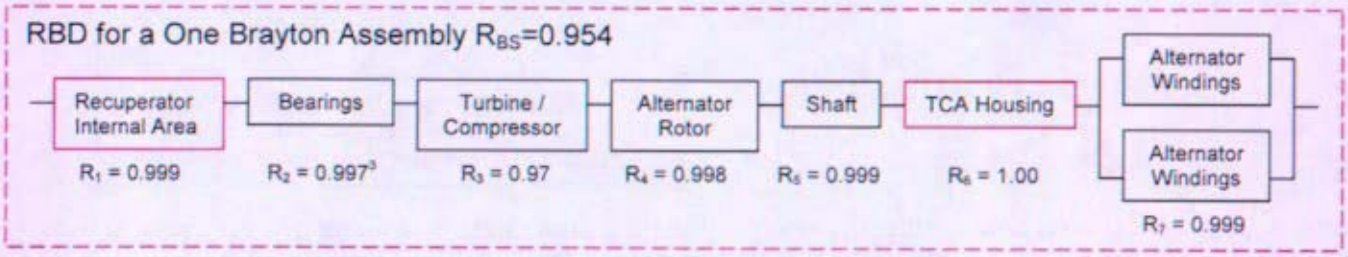

**Figure 7-12: 4-4-4 Gas Cooler Concept (2 operating, 2 standby)**

### 7.7.3 Calculate reliability of each system

In order to determine reliability for a given system, component reliabilities and system configurations were obtained. Component reliabilities were either based on a mathematical formula (e.g., relating a failure rate to the amount of surface area in a component) or an educated decision. Due to the time-frame (lack of life data) in which these data were obtained it is important to note that these reliabilities are solely estimates. Where commercial or research data was available, the numbers were applied for components. Where no information was available, components were ranked based on perceived relative reliability and assigned a reliability value accordingly. The majority of component reliabilities are based on engineering intuition.

Component reliabilities and estimate sources are presented in Table 7-1 in Section 7.4.

To calculate system reliabilities, it was necessary to identify whether a component functioned in series or in parallel with other components. Various system configurations were identified, some of which have associated schematics (see Section 3 for schematics). RBDs of system configurations were given in Section 7.3.2. The RBD for the one Brayton assembly for a one Brayton system is presented below.




**Components functioning in series**: Two components independent of one another where the failure of either component will fail the system. In the RBD presented above for a single Brayton assembly for a one Brayton system the Recuperator Internal Area, Bearings (which in turn have three in series), Alternator Rotor, Shaft and TCA Housing operating in series. To illustrate the calculation of system reliability for components operating in series assume two components exist with the following reliabilities.

Reliability of Component 1 ($R_{c1}$)=0.95
Reliability of Component 2 ($R_{c2}$)=0.97

For a system consisting of only Components 1 and 2 the reliability of the system succeeding would be:

System Reliability = ($R_{c1}$)* ($R_{c2}$)
0.9215 = 0.95 * 0.97

The system would have a 92.15% chance of successfully completing a mission for a given duration of time. For a system containing multiple components of one type (e.g., welds) each one of the like components is operating in series. For a system with N number of welds, where any weld failure would end in system failure, the calculation for weld reliability would be (weld reliability)$^N$.

**Components functioning in parallel**: Parallel components are also known as redundant components. Redundant components are used to avoid single point failures. Parallel components

exist when two components are operating or one component is operating and one is in standby and mission success is dependent on only one component operating. For a single Brayton assembly in a one Brayton system only one alternator winding needs to operate for mission success. The mathematical computation of components in parallel given the component reliabilities in the previous example is:

$$\text{System Reliability} = (1-(1-R_{c1})(1-R_{c2}))$$
$$0.9985 = (1-(1-0.95)(1-0.97))$$

Thus, components in parallel can provide a higher probability of success for a given mission.

Complexity of systems arise when a specific combination of components do not function entirely in series or parallel, or a specified number of components needs to operate for mission success (r of N components). For component configurations where 'r' of 'N' components needs to operate the component reliability can be quantified using the Binomial model. An example of needing 'r' of 'N' components is seen in the structure of the HRS for a single Brayton system where one of two HRLs associated with a given radiator needs to operate for mission success. The binomial model is as follows:

$$\text{Binomial model} = \binom{N}{r} p^r (1-p)^{(N-r)}$$

$R_4 = 0.998$
N = number of components
r = number of components (success/failure)
p = reliability of one component (either reliability of failure or success)

For a system with three components, the reliability of no components operating, one component, two components, or three components operating should sum to 1. This is illustrated as follows where the reliability of a component is 0.95:

$$\binom{3}{0} 0.95^0 (1-0.95)^{(3-0)} = 0.0125\%$$ probability of none succeeding

$$\binom{3}{1} 0.95^1 (1-0.95)^{(3-1)} = 0.7125\%$$ probability of one succeeding

$$\binom{3}{2} 0.95^2 (1-0.95)^{(3-2)} = 13.5375\%$$ probability of two succeeding

$$\binom{3}{3} 0.95^3 (1-0.95)^{(3-3)} = 85.7375\%$$ probability of three succeeding

Total Probability = 0.01% + 0.71 % + 13.54 % + 85.74%= 100%

To determine the reliability for two of three components operating for mission success (at least two; lower bound), the probabilities of two and three components operating are needed. The probabilities

of two and three components operating are summed to give the reliability of a system configuration where two out of three components are needed to operate for mission success. In the example above the reliability of at least two components operating is 99.28%.

A failure set is used when a configuration of components does not operate in parallel, series, or have a redundant set of components where a specified number have to operate for mission success, as is the case with the isolation valves mechanical and electrical failure modes. A failure set is a combination of all possible combinations of components failing. For example, given that '1' represents a success and '0' represents a failure, the following shows a failure set for a system containing three components:

| Component 1 | Component 2 | Component 3 |
|---|---|---|
| 1 | 1 | 1 |
| 1 | 1 | 0 |
| 1 | 0 | 1 |
| 1 | 0 | 0 |
| 0 | 1 | 1 |
| 0 | 1 | 0 |
| 0 | 0 | 1 |
| 0 | 0 | 0 |

To calculate the reliability of a given system or combination of components based on a failure set, combinations of successes and failures that allow a system to still operate need to be determined. For the three given components, if component 1 is needed to work and either component 2 or component 3 is needed to operate, the first three combinations of successes and failures would end in mission success. Given Component 1 has a reliability of 0.97, Component 2 has a reliability of 0.96 and Component 3 has a reliability of 0.99, a model can be formulated by putting in the reliability of each component for a '1' and (1- component reliability) for '0'.

| System Status | Component 1 | Component 2 | Component 3 |
|---|---|---|---|
| Success | $R_1 = 0.97$ | $R_2 = 0.96$ | $R_3 = 0.99$ |
| Success | $R_1 = 0.97$ | $R_2 = 0.96$ | $(1- R_3) = (1-0.99)$ |
| Success | $R_1 = 0.97$ | $(1- R_2) = (1-0.96)$ | $R_3 = 0.99$ |
| Failure | $R_1 = 0.97$ | $(1- R_2) = (1-0.96)$ | $(1- R_3) = (1-0.99)$ |
| Failure | $(1- R_1) = (1-0.97)$ | $R_2 = 0.96$ | $R_3 = 0.99$ |
| Failure | $(1- R_1) = (1-0.97)$ | $R_2 = 0.96$ | $(1- R_3) = (1-0.99)$ |
| Failure | $(1- R_1) = (1-0.97)$ | $(1- R_2) = (1-0.96)$ | $R_3 = 0.99$ |
| Failure | $(1- R_1) = (1-0.97)$ | $(1- R_2) = (1-0.96)$ | $(1- R_3) = (1-0.99)$ |

For each combination that ends in a success multiply the reliability of the components whether it is a success or a failure and sum up the products of all combinations ending in a success.

For success combination 1 the mathematical model is: $R_1*R_2*R_3$
For success combination 2 the mathematical model is: $R_1* R_2*(1-R_3)$
For success combination 3 the mathematical model is: $R_1*(1- R_2)*R_3$

Combining the models into one model you have:

Reliability of System Success = $(R_1)x(R_2)x(R_3) + (R_1)x(R_2) + (R_1)x(R_3) - (2x((R_1)x (R_2)x(R_3))$.

Check valves, isolation valves and HRS loops for multiple Brayton systems did not function in either parallel or series with the Braytons themselves. Because of this complexity, a failure set was created for each system and mathematical models were formulated. In determining success combinations, assumptions were made regarding valves and HRS loops. Assumptions for valves were the same regardless of system configuration. Assumptions for the HRS were determined on a per-system basis.

Valve assumptions are based on an operational system with all valves in their correct positions for system operation.

Assumptions associated with valves:

1. There is one check valve and one isolation valve for each Brayton loop.
2. A check valve is controlled based on pressure and stays in its correct position until the compressor which it is adjacent to starts (or stops, if already running).
3. A valve failure is when the valve does not perform its intended function (all failures will occur at the same point in time, creating non-time dependent results: time dependency is with standby Braytons only.).
4. For a running Brayton, if the isolation valve has an electrical failure and is unable to close because of a mechanical failure, the Brayton remains running (i.e., the isolation valve is sent a message to close but is unable to.).
5. Once a valve fails it does not recover.

Assumptions for Braytons in parallel:

1. If one Brayton fails and the remaining survives, either the check valve (1) or the isolation valve (1) has to close for the system to survive (the system will not operate with a non-secured dead Brayton).
2. For a loop to remain operational, the isolation valve has to remain open, and the Brayton has to be working.
3. For an isolation valve to fail on an operational Brayton, the mechanical portion of the valve has to be operational and the electrical portion has to fail.
4. The electrical failure of the isolation valve is the electrical control commanding the valve to move to the opposite of the position required to maintain the system operating.
5. Failure of the check valve is when the disc is welded in place at the time that system changes require the check valve disc to move.

Assumptions for Braytons in standby:

1. If the standby Brayton(s) has at least one shut valve, the system survives.
2. Limitation of the study is recognized because there is a case where the isolation valve on a standby Brayton unit opens and remains open until the time where it is required to open to bring the standby loop into operation. This case is not considered in this study because time dependency is not included in the study; i.e., all failures occur at the same time.
3. Valves associated with a standby Brayton are in their original positions when called upon from an operating Brayton failing.

Braytons, check valves and isolation valves are analyzed separately to determine the Brayton condition based on a combination of failures from a failure set. The conditions of a running Brayton are 1) Running, 2) Secured (whether by failure or not), and 3) non-operational and non-secured. Conditions for a standby Brayton are 1) able to start and operate, 2) secured. For the operational Brayton the condition of "running" includes when the isolation valve fails electrically and mechanically

(valve assumption #4). This condition is not applicable for a standby Brayton. Impact of the isolation valve on system reliability is minimal. The increase in overall system reliability from the double failure mode of the isolation valve is presented in Table 7-8. The double failure mode is seen most commonly in systems where multiple Braytons are running at reduced capacity. However, the double failure of the isolation valve does not impact system reliability by even a 1% increase.

**Table 7-8 Impact of Isolation Valve Double Failure Mode on System Reliability**

| System Architecture | Operational Configuration | Possible Failure Combinations | Isolation Valve Failures Ending in Mission Success | System Reliability Contribution |
|---|---|---|---|---|
| 2-2-2s | Both running | 256 | 60 = 24.44% | 0.0199 % |
| 2-2-2 | 1 standby unit | 256 | 34 = 13.28% | $9.959 * e^{-5}$ % |
| 3-3-3s | All running | 4096 | 680 = 16.60% | 0.0297 % |
| 3-3-3 | 1 standby unit | 4096 | 400 = 9.77% | 0.0198 % |
| 4-4-4s | All running | 65536 | 15280 = 23.32% | 0.9930 % |
| 4-4-4 | 2 standby units | 65536 | 6460 = 9.86% | 0.0198 % |

Assumptions for the HRS are broken down for each system configuration. Each system has a two radiator configuration with four heat rejection loops (HRL). Two HRLs are associated with each radiator. The failure modes for the HRS are discussed in Section 7.7.2.1.

Using component reliability values shown in Table 7-1, the reliability calculation for a single Brayton given a turbine/compressor (T/C) reliability of 0.97 is

200 kWe Brayton =(T/C: 0.97) * (Alternator Rotor: 0.998) * (Shaft: 0.999) * (Bearings: $0.997^3$) * (Turbine/Compressor/Alternator (TCA) Housing: 0.996) * (Alternator Windings: (1-(1-0.994)^2)) *(Recuperator Internal Area: 0.9998)

Reliability of a 200 kWe Brayton = 0.95439 or 95.44%

System = (Recuperator External Area: 0.9952) * (Piping Area: 0.9996) * (Similar Material Welds: 0.9952) * (Dissimilar Material Welds: 0.998) * (Electrical Penetrations: 0.994) * (Cooler Area: 0.9813) * (Electrical control system: 0.998) * (Brayton: 0.9544)

Reliability of a Single 200 kWe Brayton System = 91.64%

Analysis for the multiple Brayton systems was built upon the foundations set by the given assumptions. Mathematical models for conditions of the Brayton and valves were determined and used to develop models including the HRS that calculate the reliability of success for a given system configuration. The mathematical models for reliability values for the combination of Brayton assembly(ies), valves and HRS can be found in Section 7.10. Results are discussed in Section 7.5.

### 7.7.4 Perform sensitivity study for each system based on individual component reliabilities

Since absolute reliability values are not credible at this stage of the design, the reliability study focuses on determining the relative reliability of various systems and the impact individual components have on overall system reliability. Sensitivity studies allow design teams to determine which components need to be further developed to increase system reliability and which components a given system is robust to, allowing for developers to focus on components needing improvement.

A Designed Computer Experiment (DCE) was developed to perform sensitivity studies on the given system configurations. Sensitivity studies help, identify which factors contribute significantly to system reliability and to which factors a system is robust. A system is said to be robust to a given component if the reliability of the system does not change significantly with changes in component reliability. The DCE changes component reliabilities based on a given range to identify how the system changes with increases or decreases in component reliabilities. The range for the sensitivity studies was based on the failure rate for each component. Failure rates were used instead of a common range (e.g., 95%-99% reliability for each component) to prevent components that would not have an impact on system reliabilities from being identified as such (e.g., a similar material weld would not in practicality have a failure rate of 5%). The values used in the sensitivity studies are given in Table 7-9

**Table 7-9 Component Reliability Sensitivity Ranges**

| Component | Area | Reliability | Failure Rate | Sensitivity Range |
|---|---|---|---|---|
| 1 Dissimilar Weld | | 0.9990 | 0.0010 | (0.9980, 1.00) |
| 1 Similar Weld | | 0.9996 | 0.0004 | (0.9992, 1.00) |
| Alt Windings | | 0.9940 | 0.0060 | (0.9880, 1.00) |
| Alternator Rotor | | 0.9980 | 0.0020 | (0.9960, 1.00) |
| Bearing | | 0.9970 | 0.0030 | (0.9940, 1.00) |
| Check Valve | | 0.9900 | 0.0100 | (0.9800, 1.00) |
| Cooler Area Leak | | 0.9813 | 0.0187 | (0.9626, 1.00) |
| Electrical Control Sys Parallel | | 0.9960 | 0.0040 | (0.9920, 1.00) |
| Electrical Control System | | 0.9980 | 0.0020 | (0.9960, 1.00) |
| HRSLoop | | 0.9700 | 0.0300 | (0.9400, 1.00) |
| HRSPump | | 0.9900 | 0.0100 | (0.9800, 1.00) |
| Isolation Valve Electric | | 0.9900 | 0.0100 | (0.9800, 1.00) |
| *Isolation Valve Mechanical* | | *0.9900* | *0.0100* | *(0.9800, 1.00)* |
| Penetrations 100 kWe | 1 cm | 0.9970 | 0.0030 | (0.9940, 1.00) |
| Penetration 200 kWe | 2 cm | 0.9940 | 0.0060 | (0.9880, 1.00) |
| Piping Area | 122446.72 $cm^2$ | 0.9996 | 0.0004 | (0.9992, 1.00) |
| Recuperator Ext 100 kWe | 14000 $cm^2$ | 0.9963 | 0.0037 | (0.9926, 1.00) |
| Recuperator Ext 200 kWe | 18000 $cm^2$ | 0.9953 | 0.0047 | (0.9906, 1.00) |
| Recuperator Internal Area 100 kWe | 150000 $cm^2$ | 0.9999 | 0.0001 | (0.9998, 1.00) |
| Recuperator Internal Area 200 kWe | 245000 $cm^2$ | 0.9998 | 0.0002 | (0.9996, 1.00) |
| Shaft | | 0.9990 | 0.0010 | (0.9980, 1.00) |
| T/C | | 0.9700 | 0.0300 | (0.9400, 1.00) |
| TCA Housing | | 0.9960 | 0.0040 | (0.9920, 1.00) |

The DCE was performed in MATLAB and was analyzed using JMP software. Because of the non-linear response, two DCEs were performed; one for decreases in component reliability and one for increases in component reliability. This provided the exact percentage increases in system reliability based on an increase or decrease in failure rate.

## 7.8 System Fault Trees

### 7.8.1 Background

Fault trees are typically used to identify how component failures can cause system level failures.

The fault tree shown in this section is generic. Future fault trees would have more detail for each component and have probabilities of either success or failure for each box. The top tier box would have an overall probability of success or failure for the whole fault tree.

JPL requested NRPCT to provide input on reactor plant faults for the Prometheus fault tree to support presentations for the Project Mission and Systems Review (PMSR). NRPCT generated a fault tree organized by start up operations and post-start up operations, but the final form of NRPCT input to JPL included markups of existing JPL fault trees instead of providing the newly created fault tree.

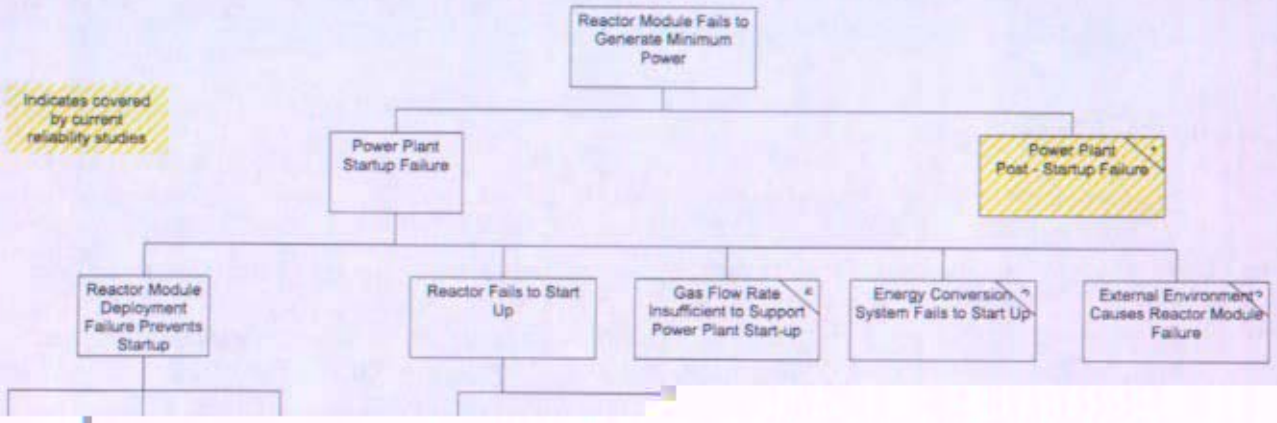
Future work would have included fault trees for different system layouts and included more detailed events.

### 7.8.2 Example Fault Tree

The following fault tree was originally developed to support the Project Mission and Systems Review (PMSR), which is a milestone for each NASA project.

Startup failures were not included in the initial reliability study because the startup procedure was not complete and it was assumed that pre-startup testing would minimize startup failures. External environment effects due to micrometeoroids and orbital debris are implied in the leak to space failure mode and probabilities assumed for pressure boundaries. Reactor failures were included in the fault tree, but the specific failure modes and probabilities were not included.

# Start Up Fault Tree



## 7.11 Tables of Detailed Sensitivity Study Results By System Architecture

**Table 7-10 One Brayton System Detailed Sensitivity Study Results**

| One Brayton System | Failure Rate | % change in System Reliability due to an increase in component reliability by the failure rate | % change in System Reliability due to a decrease in component reliability by the failure rate |
|---|---|---|---|
| 1 Dissimilar Weld | 0.0010 | 0.1916 % | 0.1753 % |
| 1 Similar Weld | 0.0004 | 0.4597 % | 0.4203 % |
| Alt Windings | 0.0060 | 0.0034 % | 0.0095 % |
| Alternator Rotor | 0.0020 | 0.1917 % | 0.1756 % |
| Bearing | 0.0030 | 0.8630 % | 0.7912 % |
| Check Valve | 0.0100 | N/A | N/A |
| Cooler Area Leak | 0.0187 | 1.8073 % | 1.6838 % |
| Electrical Control System | 0.0020 | 0.1917 % | 0.1756 % |
| HRSLoop | 0.0300 | 0.1730 % | 0.4761 % |
| HRSPump | 0.0100 | 0.0006 % | 0.0045 % |
| Isolation Valve Electric | 0.0100 | N/A | N/A |
| Isolation Valve Mechanical | 0.0100 | N/A | N/A |
| Penetration 200 KW | 0.0060 | 0.5753 % | 0.5261 % |
| Piping Area | 0.0004 | 0.0383 % | 0.0350 % |
| Recuperator External Area 200 kW | 0.0047 | 0.4533 % | 0.4159 % |
| Recuperator Internal Area 200 KW | 0.0002 | 0.0156 % | 0.0142 % |
| Shaft | 0.0010 | 0.0958 % | 0.0877 % |
| T/C | 0.0300 | 2.9161 % | 2.7492 % |
| TCA Housing | 0.0040 | 0.3838 % | 0.3522 % |

**Table 7-11 Two Brayton System (1 Running, 1 Standby) Detailed Sensitivity Study Results**

| Two Brayton System (1 Running 1 standby) | Failure Rate | % change in System Reliability due to an increase in component reliability by the failure rate | % change in System Reliability due to a decrease in component reliability by the failure rate |
|---|---|---|---|
| 1 Dissimilar Weld | 0.0010 | 0.3869 % | 0.3553 % |
| 1 Similar Weld | 0.0004 | 1.5470 % | 1.4199 % |
| Alt Windings | 0.0060 | 0.0666 % | 0.1605 % |
| Alternator Rotor | 0.0020 | 0.0222 % | 0.0532 % |
| Bearing | 0.0030 | 0.0998 % | 0.2396 % |
| Check Valve | 0.0100 | 0.0534 % | 0.1294 % |
| Cooler Area Leak | 0.0187 | 1.8247 % | 1.7065 % |
| Electrical Control System | 0.0020 | 0.1935 % | 0.1779 % |
| HRSLoop | 0.0300 | 0.6833 % | 1.6715 % |
| HRSPump | 0.0100 | 0.0022 % | 0.0159 % |
| Isolation Valve Electric | 0.0100 | 0.0576 % | 0.1382 % |
| Isolation Valve Mechanical | 0.0100 | 0.0531 % | 0.1273 % |
| Penetration 200 KW | 0.0060 | 1.1616 % | 1.0663 % |
| Piping Area | 0.0004 | 0.0580 % | 0.0532 % |
| Recuperator External Area 200 kW | 0.0047 | 0.4577 % | 0.4215 % |
| Recuperator Internal Area 200 KW | 0.0002 | 0.0018 % | 0.0043 % |
| Shaft | 0.0010 | 0.0111 % | 0.0265 % |
| T/C | 0.0300 | 0.3382 % | 0.8336 % |
| TCA Housing | 0.0040 | 0.0443 % | 0.1067 % |

**Table 7-12 Two Brayton System (2 Running) Detailed Sensitivity Study Results**

| Two Brayton System (2 Running) | Failure Rate | % change in System Reliability due to an increase in component reliability by the failure rate | % change in System Reliability due to a decrease in component reliability by the failure rate |
|---|---|---|---|
| 1 Dissimilar Weld | 0.0010 | 0.3879 % | 0.3622 % |
| 1 Similar Weld | 0.0004 | 1.5512 % | 1.4475 % |
| Alt Windings | 0.0060 | 0.0349 % | 0.0920 % |
| Alternator Rotor | 0.0020 | 0.0116 % | 0.0305 % |
| Bearing | 0.0030 | 0.0523 % | 0.1374 % |
| Check Valve | 0.0100 | 0.0002 % | 0.0019 % |
| Cooler Area Leak | 0.0187 | 1.8297 % | 1.7396 % |
| Electrical Control System | 0.0020 | 0.1941 % | 0.1814 % |
| HRSLoop | 0.0300 | 0.1800 % | 0.5271 % |
| HRSPump | 0.0100 | 0.0006 % | 0.0050 % |
| Isolation Valve Electric | 0.0100 | 0.0580 % | 0.1516 % |
| Isolation Valve Mechanical | 0.0100 | 0.0000 % | 0.0005 % |
| Penetration 200 KW | 0.0060 | 1.1647 % | 1.0870 % |
| Piping Area | 0.0004 | 0.0582 % | 0.0542 % |
| Recuperator External Area 200 kW | 0.0047 | 0.4589 % | 0.4297 % |
| Recuperator Internal Area 200 KW | 0.0002 | 0.0009 % | 0.0025 % |
| Shaft | 0.0010 | 0.0058 % | 0.0152 % |
| T/C | 0.0300 | 0.1780 % | 0.4786 % |
| TCA Housing | 0.0040 | 0.0233 % | 0.0612 % |

Table 7-13 Three Brayton System (2 Running, 1 Standby) Detailed Sensitivity Study Results

| Three Brayton System (2 Running 1 standby) | Failure Rate | % change in System Reliability due to an increase in component reliability by the failure rate | % change in System Reliability due to a decrease in component reliability by the failure rate |
|---|---|---|---|
| 1 Dissimilar Weld | 0.0010 | 0.5766 % | 0.5168 % |
| 1 Similar Weld | 0.0004 | 2.4208 % | 2.1686 % |
| Alt Windings | 0.0060 | 0.1459 % | 0.3315 % |
| Alternator Rotor | 0.0020 | 0.0485 % | 0.1098 % |
| Bearing | 0.0030 | 0.2186 % | 0.4950 % |
| Check Valve | 0.0100 | 0.0784 % | 0.1796 % |
| Cooler Area Leak | 0.0187 | 1.8131 % | 1.6548 % |
| Electrical Control System | 0.0020 | 0.1923 % | 0.1725 % |
| HRSLoop | 0.0300 | 0.7437 % | 1.7223 % |
| HRSPump | 0.0100 | 0.0024 % | 0.0164 % |
| Isolation Valve Electric | 0.0100 | 0.1645 % | 0.3717 % |
| Isolation Valve Mechanical | 0.0100 | 0.0775 % | 0.1739 % |
| Penetrations 100 KW | 0.0030 | 0.8656 % | 0.7755 % |
| Piping Area | 0.0004 | 0.0768 % | 0.0688 % |
| Recuperator External Area 100 kW | 0.0037 | 0.3537 % | 0.3179 % |
| Recuperator Internal Area 100 KW | 0.0001 | 0.0024 % | 0.0054 % |
| Shaft | 0.0010 | 0.0242 % | 0.0548 % |
| T/C | 0.0300 | 0.7438 % | 1.7238 % |
| TCA Housing | 0.0040 | 0.0971 % | 0.2203 % |

Table 7-14 Three Brayton System (3 Running) Detailed Sensitivity Study Results

| Three Brayton System (3 Running) | Failure Rate | % change in System Reliability due to an increase in component reliability by the failure rate | % change in System Reliability due to a decrease in component reliability by the failure rate |
|---|---|---|---|
| 1 Disimilar Weld | 0.0010 | 0.5768 % | 0.5184 % |
| 1 Similar Weld | 0.0004 | 2.4217 % | 2.1754 % |
| Alt Windings | 0.0060 | 0.1412 % | 0.3238 % |
| Alternator Rotor | 0.0020 | 0.0469 % | 0.1073 % |
| Bearing | 0.0030 | 0.2115 % | 0.4835 % |
| Check Valve | 0.0100 | 0.0003 % | 0.0023 % |
| Cooler Area Leak | 0.0187 | 1.8137 % | 1.6600 % |
| Electrical Control System | 0.0020 | 0.1924 % | 0.1731 % |
| HRSLoop | 0.0300 | 0.7198 % | 1.6827 % |
| HRSPump | 0.0100 | 0.0023 % | 0.0160 % |
| Isolation Valve Electric | 0.0100 | 0.2346 % | 0.5343 % |
| Isolation Valve Mechanical | 0.0100 | - 0.00096 % | 0.0059 % |
| Penetrations 100 KW | 0.0030 | 0.8659 % | 0.7779 % |
| Piping Area | 0.0004 | 0.0769 % | 0.0690 % |
| Recuperator External Area 100 kW | 0.0037 | 0.3538 % | 0.3189 % |
| Recuperator Internal Area 100 KW | 0.0001 | 0.0023 % | 0.0053 % |
| Shaft | 0.0010 | 0.0235 % | 0.0536 % |
| T/C | 0.0300 | 0.7200 % | 1.6840 % |
| TCA Housing | 0.0040 | 0.0940 % | 0.2152 % |

Table 7-15 Four Brayton System (2 Running, 2 Standby) Detailed Sensitivity Study Results

| Four Brayton System (2 running 2 standby) | Failure Rate | % change in System Reliability due to an increase in component reliability by the failure rate | % change in System Reliability due to a decrease in component reliability by the failure rate |
|---|---|---|---|
| 1 Disimilar Weld | 0.0010 | 0.7613 % | 0.6633 % |
| 1 Similar Weld | 0.0004 | 3.2725 % | 2.8495 % |
| Alt Windings | 0.0060 | 0.1906 % | 0.4070 % |
| Alternator Rotor | 0.0020 | 0.0634 % | 0.1348 % |
| Bearing | 0.0030 | 0.2857 % | 0.6078 % |
| Check Valve | 0.0100 | 0.1505 % | 0.3219 % |
| Cooler Area Leak | 0.0187 | 1.7956 % | 1.5929 % |
| Electrical Control System | 0.0020 | 0.1904 % | 0.1661 % |
| HRSLoop | 0.0300 | 0.9731 % | 2.1160 % |
| HRSPump | 0.0100 | 0.0032 % | 0.0202 % |
| Isolation Valve Electric | 0.0100 | 0.1670 % | 0.3560 % |
| Isolation Valve Mechanical | 0.0100 | 0.1497 % | 0.3165 % |
| Penetrations 100 KW | 0.0030 | 1.1430 % | 0.9953 % |
| Piping Area | 0.0004 | 0.0951 % | 0.0827 % |
| Recuperator External Area 100 kW | 0.0037 | 0.3503 % | 0.3060 % |
| Recuperator Internal Area 100 kW | 0.0001 | 0.0032 % | 0.0067 % |
| Shaft | 0.0010 | 0.0317 % | 0.0673 % |
| T/C | 0.0300 | 0.9732 % | 2.1169 % |
| TCA Housing | 0.0040 | 0.1269 % | 0.2705 % |

**Table 7-16 Four Brayton System (4 Running) Detailed Sensitivity Study Results**

| Four Brayton System (4 running) | Failure Rate | % change in System Reliability due to an increase in component reliability by the failure rate | % change in System Reliability due to a decrease in component reliability by the failure rate |
|---|---|---|---|
| 1 Disimilar Weld | 0.0010 | 0.7619 % | 0.6672 % |
| 1 Similar Weld | 0.0004 | 3.2748 % | 2.8662 % |
| Alt Windings | 0.0060 | 0.1817 % | 0.3944 % |
| Alternator Rotor | 0.0020 | 0.0604 % | 0.1307 % |
| Bearing | 0.0030 | 0.2723 % | 0.5890 % |
| Check Valve | 0.0100 | 0.0004 % | 0.0030 % |
| Cooler Area Leak | 0.0187 | 1.7968 % | 1.6022 % |
| Electrical Control System | 0.0020 | 0.1906 % | 0.1672 % |
| HRSLoop | 0.0300 | 0.9280 % | 2.0501 % |
| HRSPump | 0.0100 | 0.0030 % | 0.0195 % |
| Isolation Valve Electric | 0.0100 | 0.3021 % | 0.6508 % |
| Isolation Valve Mechanical | 0.0100 | - 0.0012 % | 0.0070 % |
| Penetrations 100 KW | 0.0030 | 1.1438 % | 1.0011 % |
| Piping Area | 0.0004 | 0.0952 % | 0.0832 % |
| Recuperator External Area 100 kW | 0.0037 | 0.3505 % | 0.3078 % |
| Recuperator Internal Area 100 KW | 0.0001 | 0.0030 % | 0.0065 % |
| Shaft | 0.0010 | 0.0302 % | 0.0652 % |
| T/C | 0.0300 | 0.9283 % | 2.0518 % |
| TCA Housing | 0.0040 | 0.1210 % | 0.2621 % |

## 7.12 References

7- 1: KAPL/Bettis letter SPP-67110-0005, B-SE-0077, "Space Nuclear Power Plant Concept Selection, For NR Approval," dated March 4, 2005

7- 2: Green, AE and AJ Bourne, 1972. Reliability Technology. London: Wiley—Interscience.

7- 3: Dodson, B and D Nolan 2002. Reliability Engineering Handbook, Tucson: QA Publishing, LLC

7- 4: Not used

7- 5: Not used

7- 6: NASA Contractor Report CR-191023, dated March 1993

7- 7: Not used

7- 8: KAPL letter SPP-SEC-0025, "The Effect of Reducing Turbine Inlet Temperature (TTI) to Achieve Brayton Part Capacity Operation on Reactor Thermal Power for Multiple Brayton Configurations," dated August 18, 2005

7- 9: Not used

7- 10: Hamilton Sundstrand, Windsor Locks, CT. "Evaluation of Gas Cooler Materials of Construction and Reliability, Scoping Phase Final Report." Bechtel Bettis Purchase Order #3007352, August 30, 2005

7- 11: NUREG/CR-4550, Volume 1, Revision 1, "Analysis of Core Damage Frequency: Internal Events Methodology," dated January 1990

7- 12: Allied Signal, Garrett Fluid Systems Division, "Space Power 1991 and Beyond" p.49, 1991

(Intentionally Blank)

# Section 8
# Operational Strategy

(Intentionally Blank)

# Operational Strategy

## Table of Contents

8 Operational Strategy ..... 7
8.1 Summary ..... 7
8.2 Operating Assumptions ..... 8
8.3 Plant and Reactor Controls ..... 8
8.3.1 Reactor Outlet Temperature (Reactivity) Control ..... 9
8.3.2 Brayton Unit Shaft Speed (Electrical Load) Control ..... 10
8.3.3 Heat Rejection System (HRS) Flow Rate Control ..... 13
8.3.4 Primary Coolant Pressure Control ..... 14
8.4 Operation and Control Band ..... 14
8.5 Plant Configuration Options ..... 15
8.5.1 The 1-1-1 System Architecture ..... 16
8.5.2 The 2-2-2 System Architecture ..... 17
8.5.2.1 One 200 kWe Operating Brayton Unit with One 200 kWe Idle Spare (2-2-2) ..... 18
8.5.2.2 Two 100 kWe Brayton Units Operating at 100% Capacity (2-2-2) ..... 19
8.5.2.3 Two 200 kWe Brayton Units Operating at 50% Capacity (2-2-2s) ..... 19
8.5.3 The 3-3-3 System Architecture ..... 19
8.5.3.1 Two 100 kWe Operating Brayton Units with One 100 kWe Idle Spare (3-3-3) ..... 20
8.5.3.2 Three 100 kWe Brayton Units Operating at 50% Capacity (3-3-3s) ..... 20
8.5.4 The 4-4-4 System Architecture ..... 20
8.5.4.1 Two 100 kWe Operating Brayton Units with Two 100 kWe Spares (4-4-4) ..... 22
8.6 Normal Operation and Control Strategies ..... 22
8.6.1 Reactor Startup and Power Production Sequence ..... 22
8.6.1.1 Reactor Startup Procedure and Principles ..... 23
8.6.2 Startup of a Second Brayton Unit During Plant Startup ..... 37
8.6.3 Steady State Operation ..... 38
8.6.4 Reduced Power Operation ..... 39
8.6.4.1 Reduce the Number of Operating Brayton units ..... 39
8.6.4.2 Reduce Reactor Outlet Temperature ..... 40
8.6.4.3 Reduce Brayton Unit Speed ..... 40
8.6.4.4 Reduce Reactor Outlet Temperature and Brayton Unit Speed ..... 41
8.6.5 Reactor Shutdown ..... 42
8.6.5.1 Flight Unit Shutdown ..... 42
8.6.5.2 Ground Test Reactor Shutdown ..... 43
8.7 Abnormal Operations and Casualties ..... 43
8.7.1 Inadvertent Valve Closure ..... 43
8.7.1.1 Turbine or Compressor Isolation Valve ..... 44
8.7.1.2 Alternator Cooling Isolation Valve ..... 45
8.7.2 Loss of Brayton unit Speed Control ..... 45
8.7.2.1 Indications ..... 46
8.7.2.2 Desired Plant Response ..... 46
8.7.2.3 Required Plant Instrumentation ..... 46
8.7.3 Mechanical Loss of Brayton unit ..... 46
8.7.3.1 Bearing/Wheel Rub ..... 47
8.7.3.2 Brayton Unit Shaft Shear ..... 47

8.7.4 Gas Leaks - Flight Unit ..... 48
8.7.4.1 Indications ..... 49
8.7.4.2 Desired Plant Response ..... 49
8.7.4.3 Required Plant Instrumentation ..... 50
8.7.5 Stuck Open Valve in Idle Loop (Partial Loss of Flow) ..... 50
8.7.5.1 Indications ..... 50
8.7.5.2 Desired Plant Response ..... 51
8.7.5.3 Required Plant Instrumentation ..... 51
8.7.6 Partially Shut Valve in Operating Loop ..... 51
8.7.6.1 Indications ..... 51
8.7.6.2 Desired Plant Response ..... 51
8.7.6.3 Required Plant Instrumentation ..... 51
8.7.7 Loss of HRS Radiator Area ..... 52
8.7.7.1 Indications ..... 52
8.7.7.2 Desired Plant Response ..... 52
8.7.7.3 Required Plant Instrumentation ..... 52
8.7.8 Loss of Flow in a HRS Loop ..... 52
8.7.8.1 Indications ..... 52
8.7.8.2 Desired Plant Response ..... 52
8.7.8.3 Required Plant Instrumentation ..... 52
8.7.9 Inadvertent Slider Motion ..... 52
8.7.9.1 Indications ..... 52
8.7.9.2 Desired Plant Response ..... 53
8.7.9.3 Required Plant Instrumentation ..... 53
8.8 References ..... 53

## List of Figures

Figure 8-1: Net Brayton unit work versus speed with no electrical loading $(W_E = 0)$ ..... 11
Figure 8-2: Net Brayton unit work versus speed with a constant electrical loading $(W_E \neq 0)$ ..... 12
Figure 8-3: Net Brayton unit work versus speed with spaceship electrical and PLR loads ..... 12
Figure 8-4: Reactor power, electrical power, reactor outlet temperature, and compressor inlet temperature versus percent HRS mass flow rate (Simulink model) ..... 14
Figure 8-5: 1-1-1 System Architecture ..... 17
Figure 8-6: 2-2-2 System Architecture ..... 18
Figure 8-7: Typical 4-4-4 System Architecture ..... 21
Figure 8-8: JIMO Power Conditioning & Distribution Subsystem (PCAD) ..... 34
Figure 8-9: 104 kW Brayton Unit Motoring Power. ..... 35
Figure 8-10: Typical Power / Low Speed Curves for a Brayton Unit Turbo-Compressor-Alternator Operating at Various Turbine Inlet Temperatures. ..... 36
Figure 8-11: Typical Power / Speed Curves for a Brayton Unit TCA Operating at Various Turbine Inlet Temperatures. ..... 37
Figure 8-12: Example of a Space Brayton Unit Turboalternator Conceptual Design (Hamilton-Sundstrand) ..... 48

## List of Tables

Table 8-1: Reactor Startup Procedure and Principles ..... 23
Table 8-2: System parameters using reactor outlet temperature to reduce reactor power. ..... 40
Table 8-3: System Parameters using Brayton Unit Speed to Reduce Reactor Power ..... 41
Table 8-4: System parameters using reactor outlet temperature and Brayton unit speed to reduce reactor power. ..... 42

(Intentionally Blank)

# 8 Operational Strategy

This section develops an operational strategy for the Direct Gas Brayton space nuclear power plant. General methods of plant operation and control that will allow it to most effectively meet its mission requirements within the constraints of the space application are identified. The most significant conclusions regarding operational strategy include:

- Space Nuclear Power Plant (SNPP) electric power output could be controlled on reactor outlet temperature and Brayton speed. Mass inventory control (system pressure) was not pursued based on increased complexity and the additional risks to spaceship performance introduced by such a system (e.g., inadvertent coolant addition, additional leak paths).
- SNPP operations during startup, initial criticality evolutions, and during abnormal conditions require integrated operations of the reactor, the energy conversion system, and the power distribution system using other controls from those applied at constant power.
- A reduced reactor power and temperature mode may be used when electric power demand is reduced for long periods of time, i.e., coasting during interplanetary transfer and during science orbits. This mode would result in fuel and plant temperature reductions, fuel burn up reductions, lower turbo-compressor speed and could maximize plant lifetime.
- An autonomous control system for the plant (including the reactor) would be required. Some events require action to occur in less time than a signal could be sent to and from the spacecraft, or during communication blackout periods (of several weeks).
- Instrumentation uncertainty, the coarseness of reactor and Brayton speed control actions, other control band allowances, allowances for transients, casualties and age effects all impact the efficiency of the thermal cycle and therefore the sizing of all components. These uncertainties have a significant impact on the SNPP design and the necessary margin to accommodate these uncertainties. Developing an autonomous control scheme that minimizes operating bands and error will be necessary to minimize system mass.

## 8.1 Summary

The development of an operational control scheme for the SNPP was at an early stage when project cancellation occurred. The choice of methods for reactor control, energy conversion system control, and power distribution system control, and the integration of their operation by the instrumentation and control (I&C) system to meet all the operational requirements and conditions of the plant have significant effects on complexity, size, and robustness of the plant design. This section considers these effects and develops operational strategies to best accommodate them.

This operational strategy also provides an assessment of the various options and issues associated with reactor operations for the flight unit and includes some discussion of the differences that would be required for the Ground Test Reactor (GTR).

The operational strategies discussed herein are developed from a power plant perspective. Sections 8.2 and 8.3 discuss operating assumptions and reactor and plant control. A number of control options have been assessed. Section 8.5 discusses the impact of different plant configurations (system

architecture) on plant operations. Sections 8.6 and 8.7 assess normal operations and potential system casualties and the instrumentation and controls needed to identify and recover from these potential events. These evaluations were used to identify instrumentation needs and operational methods. A complementary discussion, focused on the reactor is in Reference 8- 1, Section 5.1.

## 8.2 Operating Assumptions

1. The reactor and plant are required to produce ~200 kWe during portions of the mission when full power is required (i.e., thrusting).
2. After commissioning (Reactor Module and spaceship startup), a reactor shutdown would result in a loss of the spaceship (due to planned ejection of the solar panels following startup).
3. Reactivity will normally be added using one method at a time (e.g., HRS flow would not be increased while inserting reflectors, although reflector position may be changed to accommodate a change in HRS flow or to minimize the subsequent transient).
4. A low power operating mode may be used to maximize the service life of the Reactor Module.
5. A range of operating parameters (e.g., pressure and temperature) will need to be established early in the design, taking into consideration measurement uncertainty, minimum slider movement, minimum Brayton speed increment, operating bands, slider (or drum) sensitivity, component performance decrement over life, overall cycle thermal efficiency, and transients during normal operations and recoverable casualties.

## 8.3 Plant and Reactor Controls

The operating state of the SNPP is defined by a specific set of parameters (e.g., pressure, temperatures, flow rates, electrical power, reactor power, etc.). This operating state may be changed by adjusting one of the four following plant control parameters:

1. **Reactor Outlet Temperature (Reactivity)**
   Reactor outlet temperature is controlled by adding or removing reactivity via the reactivity control devices (sliders or drums) to increase or decrease reactor power. Changes in alternator output, Brayton speed (and therefore primary gas flow rate) and HRS performance (flow, heat transfer efficiency) also impact this parameter.

2. **Brayton Unit Shaft Speed (Electrical Load)**
   Brayton unit shaft speed is controlled by adding or removing electrical load(s) to the alternator using the Parasitic Load Radiator (PLR). Primary system gas flow is directly coupled to Brayton shaft speed.

3. **Heat Rejection System (HRS) Flow Rate (HRS Pump Speed)**
   Heat Rejection System flow rate is changed by changing the HRS pump speed therefore changing the cooling water flow through the gas cooler and the radiators. Changes in HRS performance (flow, heat transfer efficiency) impact primary system Brayton unit compressor inlet gas temperature.

4. **Primary Coolant Pressure (Mass inventory)**
   Primary coolant pressure could be controlled by adjusting the coolant gas inventory or via bypass flow schemes around the compressor.

These are discussed in more detail in the following sections.

Reactor coolant temperature, nuclear power, and alternator electric power output at constant Brayton machine speed, are parameters commonly considered for control of reactor operation. Regardless of which parameter(s) is chosen for steady-state reactor control, the same physical principles apply. Inserting reflectors (or rotating drums to increase reactivity) adds reactivity, which increases reactor power. Increased reactor power increases fuel temperature and reactor coolant outlet temperature ($T_{hot}$), which in turn increases the power delivered to the Brayton unit and the HRS. The Brayton machine is held to a constant speed by the Parasitic Load Radiator which absorbs the additional output electrical power and moves to a more efficient operating point governed by its improved thermodynamic performance at the higher temperature. The parameters are all interrelated allowing some flexibility as to which ones are monitored and which are controlled.

One advantage of having several control parameters for reactivity control available is that the system can cross-check its results or respond to potential sensor failures. If electric power is the control parameter, for example, and the signals for electric power are lost, then the reactivity controller could switch to $T_{hot}$ for reactor control.

Although some of the preceding control parameters have a strong influence over a single monitored parameter, manipulation of any one of the control parameters would influence monitored parameters throughout the system. Due to the interdependent nature of the system parameters, it may be necessary to control the plant based on certain parameters or combination of parameters (a derived control signal, potentially allowing for anticipatory control), while allowing others to vary within predetermined bands.

### 8.3.1 Reactor Outlet Temperature (Reactivity) Control

*Summary*

Reactor outlet temperature ($T_{hot}$) is directly affected by core reactivity. Positive or negative reactivity is added through movement of the reactivity control devices (sliders or drums). In general, adding positive reactivity will increase reactor outlet temperature; adding negative reactivity will decrease reactor outlet temperature. Reactivity changes needed for plant transient response and to account for the normal burnup of fuel will be controlled by the Reactor Instrumentation and Control (I&C) segment. This controller will be required to operate autonomously for periods in the mission when communication with Earth is not possible (up to 50 days), and for periods in the mission when communication with Earth has a long delay or is not possible. It is envisioned that ground control intervention from an SNPP perspective will be limited to commissioning, periodic monitoring, performance enhancements (software uploads), and long term corrective actions to recover from unforeseen casualties or equipment degradation.

Present Control Drive Mechanism (CDM) concepts use stepper motors which will provide discrete positioning steps of the reflector segments (sliders) or drums. Presently each step motion is assumed to be one millimeter, although this would need to be optimized after a complete control scheme, including all aspects of the overall plant is developed. Moving one reflector segment a millimeter changes reactor temperature by about 2 K based on currently assumed reflector segment worths and temperature coefficients. Additional detail is contained in Section 5 of Reference 8- 1.

*Reactivity Control for Startup*

The general reactor startup sequence is discussed in Section 8.6.1. After pre-critical checks and establishing reactor flow by motoring a Brayton unit using solar power, the reflectors are inserted (or drums positioned) to a position estimated to be 2% from critical conditions. The critical position will be known from previous ground testing of the actual flight unit but uncertainties exist due to temperature changes and other unexpected changes due to effects of shipping or launch loads.

From the 2% from critical position, the approach to criticality is made by inserting reactivity at a slower rate and monitoring the reactor's neutron level. Such a procedure most likely would consist of a series of steps initiated from ground control and autonomously executed by the reactor controller because there is no guarantee of continuous communications with the spaceship. Once criticality has been reached, a brief check of reactor conditions will be performed by ground control.

The next phase of the reactor startup is to bring reactor power low into the power range (approximately 1% power) and use reactor power to perform a plant heat-up at a specified rate, (notionally 0.5 K/min). Achieving this heat up rate should require roughly moving one reflector segment 1 mm about every 3 to 5 minutes. As the plant temperature increases, the amount of electrical power required to motor the Brayton unit will decrease as the turbo-compressor starts to extract power from the primary coolant. The Brayton unit will require an electric load controller for motoring at a fixed speed as plant temperature increases. When plant temperature is high enough, the Brayton unit produces sufficient electric power to become self-sustaining. The speed controller must be able to adapt to this change of state. Electric power produced by the Brayton unit continues to increase as the plant heat-up continues. When sufficient power is being produced a second Brayton unit can be motored and brought on line.

### 8.3.2 Brayton Unit Shaft Speed (Electrical Load) Control

*Summary*

In this concept, a variable load is imposed on the Brayton unit by the PLR which can be adjusted if electrical demand changes to maintain constant Brayton unit loading and shaft speed. The PLR always maintains load on the Brayton above the required spaceship electrical demand. If the electrical demand on the SNPP increases, the PLR decreases its load the same amount to maintain a constant load on the Brayton unit and thus maintain constant speed. If the electrical demand on the SNPP decreases, the PLR increases its load the same amount, again maintaining a constant load on the Brayton unit and thus a constant speed. This has the advantage of allowing the plant to operate at maximum efficiency.

*Brayton Unit Speed Control*

Brayton unit shaft speed is fundamentally controlled by the balance of work produced by the turbine minus the work required by the compressor, electrical work removed, and losses. The Brayton unit will only operate at a constant speed when the sum of these terms is zero. That is:

$$W_T - (W_C + Losses) - W_E = 0$$

where $W_T$ is the work produced by the turbine, $W_C$ is the work required by the compressor, $W_E$ is the electrical work removed, and $Losses$ account for losses in the turbomachinery and alternator. The net work generated by the Brayton unit follows a roughly parabolic shape, as shown qualitatively in Figure 8-1. When the net Brayton unit work is positive the Brayton unit is producing electrical power; when the net Brayton unit work is negative electrical power must be supplied to maintain Brayton unit speed ("motoring" the Brayton unit). Motoring is used to maintain or increase speed when the turbine work is not great enough to offset compressor work plus losses, and is used to start a Brayton unit from rest.

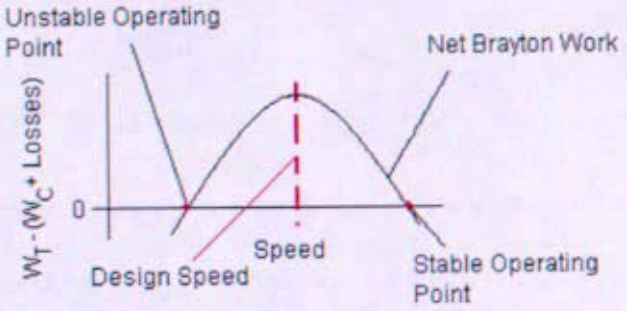



**Figure 8-1: Net Brayton unit work versus speed with no electrical loading $(W_E = 0)$**

Figure 8-1 shows qualitative net Brayton unit work as a function of Brayton unit speed at constant turbine inlet and compressor inlet temperatures. Two constant speed operating points exist for a Brayton unit under these conditions; a low speed unstable operating point, and a high speed stable operating point. The low speed point is called the "self-sustaining point," and represents the transition point between motoring the Brayton unit and the Brayton unit producing useable power.

The low speed operating point Figure 8-1 is unstable because any perturbation in speed will cause the Brayton unit to come to a new steady state speed, unless control actions are taken. A decrease in speed will cause the net Brayton unit work to go negative, indicating that the turbine can no longer supply enough power to offset the compressor needs and losses. This imparts a negative torque to the Brayton unit shaft and will slow the Brayton unit down and eventually stop the Brayton unit if it is not motored to bring the speed back up. An increase in speed will cause the net Brayton unit work to go positive, indicating that the turbine is supplying more work than the compressor and losses are consuming. As long as the net Brayton unit work is positive, a positive torque will be applied to the shaft and the Brayton unit speed will continue to increase, eventually reaching the stable operating point speed.

The high speed operating point in Figure 8-1 is stable because perturbations tend to damp out and speed returns to the stable operating point speed. An increase in speed will cause the net Brayton unit work to go negative, imparting a negative torque to the shaft and slowing the Brayton unit back near to the stable operating point. A decrease in speed will cause the net Brayton unit work to go positive, imparting a positive torque to the shaft and increase Brayton unit speed back near to the stable operating point.

The speed of the two operating points can be changed by adding an electrical load to the system, as shown in Figure 8-2. By adding an electrical load, the new constant speed operating points are shifted to the intersection of the electrical work removed line and the net Brayton unit work curve. The

electrical load effectively shifts the x-axis upward, drawing the two constant speed operating points closer together. The operating points in Figure 8-2 are unstable and stable, respectively, for the same reasons as in Figure 8-1.

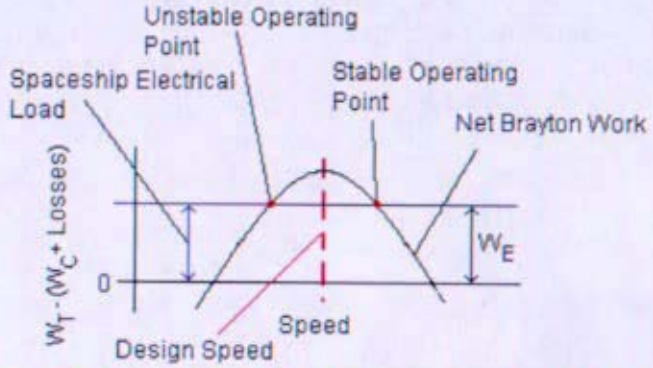



**Figure 8-2: Net Brayton unit work versus speed with a constant electrical loading $(W_E \neq 0)$**

The difference between the net Brayton unit work line and the zero work line in Figure 8-2 is the useable work that can be removed from the system. The current Brayton unit design generates maximum useable work and is most efficient at the design speed; if the unit is operated at any speed different than the design speed, less electrical work is being removed than could be removed. In order to maintain speed at the design speed, another electrical load must be added through the PLR. The PLR removes a variable amount of electrical work from the Brayton unit to maintain speed at the design point. If the electrical demand on the SNPP increases, the PLR decreases its load the same amount to maintain a constant load on the Brayton unit and thus maintain constant speed. If the electrical demand on the SNPP decreases, the PLR increases its load the same amount, again maintaining a constant load on the Brayton unit and thus a constant speed. Figure 8-3 shows the PLR loading in combination with the electrical demand.

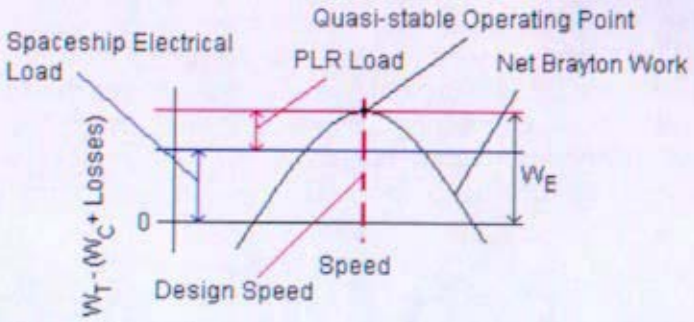



**Figure 8-3: Net Brayton unit work versus speed with spaceship electrical and PLR loads**

Figure 8-3 shows a single, quasi-stable operating point at the design speed. This point is quasi-stable because a slight decrease in speed puts a negative torque on the shaft, slowing it to rest if no action is taken. An increase in speed also puts a negative torque on the shaft, slowing it back to the quasi-stable operating point speed.

At the quasi-stable point no action is needed to correct an increase in speed because the negative torque will slow the Brayton unit back to the quasi-stable operating point. However, if the speed decreases, the total electrical load must be reduced below the net Brayton unit work at the reduced speed. This is done by decreasing the electrical work removed by the PLR. The net Brayton unit work will now be positive, resulting in a positive torque on the Brayton unit shaft and increasing Brayton unit speed. The PLR load must be increased again as the Brayton unit approaches the quasi-stable point. In a similar manner the PLR can be used to operate the Brayton unit at the unstable point. Because the PLR is an electrical system and can respond much faster than the mechanical Brayton unit system, it is possible to operate at the quasi-stable and unstable points.

To operate at the unstable point, a Brayton unit speed increase is countered by an increase in PLR loading, putting a negative torque on the shaft and slowing it back to the desired speed. A decrease in speed is countered by a reduction in PLR loading, putting a positive torque on the shaft and increasing speed back to the desired speed. It is desirable to operate the Brayton unit at a speed near the quasi-stable operating point to maximize efficiency.

### 8.3.3 Heat Rejection System (HRS) Flow Rate Control

*Summary*

The Brayton unit compressor inlet temperature (CIT) is affected by varying the HRS flow rate (pump speed). Changes in the compressor inlet temperature influence reactor power and thus reactor outlet temperature and Brayton unit electric power output. This change in reactor power is caused by the change in reactor inlet temperature (Tcold) coming from the compressor and the resultant change in reactivity due to the reactivity temperature coefficient. It is desirable to operate at the lowest compressor inlet temperature for maximum plant efficiency. Control of the plant based on HRS flow rate thus prevents the system from operating at maximum efficiency. As such, this control scheme is not envisioned for use for normal operation.

*System Operation*

The HRS mass flow rate would be controlled by changing HRS pump speed. Changes in the HRS mass flow rate influence the CIT and radiator coolant temperatures. Figure 8-4 demonstrates the sensitivity of reactor power, electrical power, reactor outlet temperature, and compressor inlet temperature to changes in HRS flow rate.

Decreasing CIT increases system efficiency, making it desirable to operate at the lowest CIT attainable. This will be achieved when the gas cooler is operating near the design point, as shown in Figure 8-4. Operating at a different HRS mass flow rate increases CIT, which decreases system efficiency. Decreasing HRS mass flow rate reduces the heat transfer between the gas and the HRS fluid in the gas cooler, increasing CIT. Increasing HRS mass flow rate also increases CIT for the fixed size system. Increasing the HRS mass flow rate will transiently increase the heat transfer in the gas cooler; however, because the HRS fluid system spends less time in the radiator and because the radiator is near its limit, the increased heat is not able to be rejected and the HRS fluid returns to the gas cooler hotter, increasing CIT. Control of the HRS mass flow rate may also be needed to keep the HRS from freezing or overheating, limiting its ability to fluctuate and control CIT

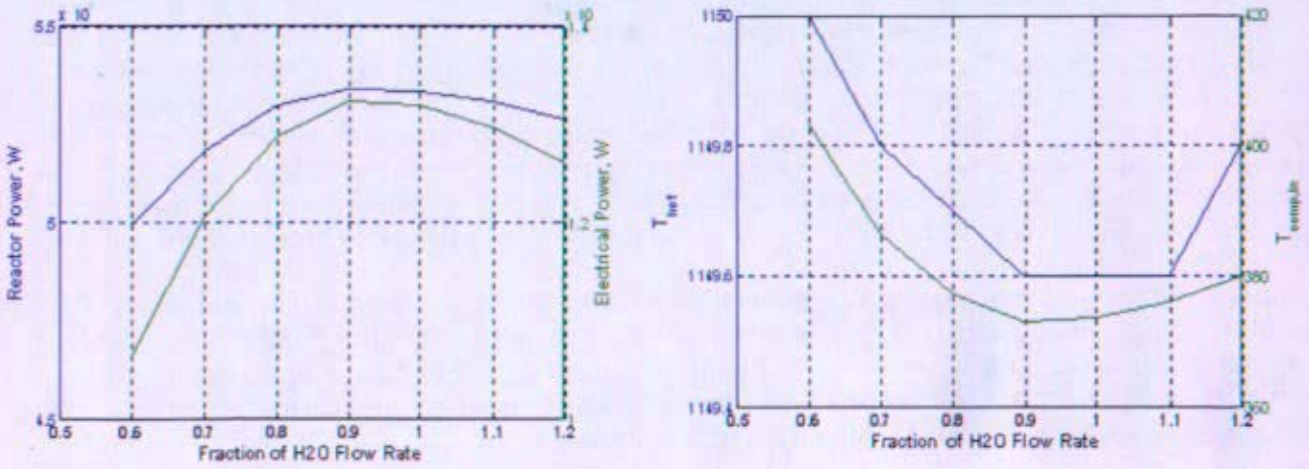



**Figure 8-4: Reactor power, electrical power, reactor outlet temperature, and compressor inlet temperature versus percent HRS mass flow rate (Simulink model)**

Since changing flow rate from the design condition impacts system efficiency and the potential need to use HRS mass flow rate to keep HRS temperatures in an acceptable range, this control would not be used for normal operation. HRS mass flow rate control may be used during startup or casualty evolutions if analysis showed a need or benefit.

### 8.3.4 Primary Coolant Pressure Control

Primary coolant inventory control requires an auxiliary system to remove and add coolant (gas). This could be a bypass line and accumulation tank, a more complex dual chamber system, or a system using a compressor. Means to effect gas flow in and out of the accumulation tank would also require development. Any gas inventory control system would add mass, volume, additional potential leakage locations, and significant complexity. The envisioned control strategy did not need gas inventory control to operate the plant. Therefore, an active gas inventory control scheme was not envisioned for use.

## 8.4 Operation and Control Band

The previous section described several plant parameters which might be used to control the operating point of the SNPP. The choice of which plant parameter or combination of parameters to use and how to use them has not been optimized. Models of the plant were under development at the time of project termination, and their completion would have provided a better understanding of the plant behavior and system interactions. These would have in turn led to the development of initial algorithms to define the control actions needed to change or maintain the state of the plant. Model development and preliminary transient analyses are discussed in Section 12.

The modeling studies to date have demonstrated that measurement errors associated with a control parameter, the size of the discrete control actions, and the width of the control band both have an impact on the overall sizing of major plant components. The measurement error is the uncertainty

associated with a given parameter (i.e., the difference between the "indicated" and actual values) and is determined by physical effects such as material degradation of the sensing element and by the sensor's signal conditioning circuitry. The reactor sliders and the load changes of the PLR are characterized by discrete fixed movements or changes in resistance. The control band is the amount of deviation allowed in the indicated control parameter before an action is taken to change it. The size of the control band is determined predominately by the uncertainty in the control parameter and the minimum change in that parameter in response to the discrete control actions (e.g., the minimum reactor temperature change in response to a slider step, or the minimum change in Brayton unit electrical load (and hence operating speed) in response to the minimum PLR resistance change). The size of the control band will increase as either of these factors increase in size.

The incentive to minimize the size of the control band is to maximize plant operating efficiency and minimize the potential impact on component ratings, required core power, and overall plant mass. The upper limit of the control band for temperature is fixed at the maximum allowable (actual) plant temperature (because of material limitations). Therefore with a fixed maximum temperature, a larger control band implies a lower minimum control band temperature. The minimum control band temperature is associated with a lower operating efficiency, which in turn increases the sizing of the plant. The reduced efficiency drives the size of each component larger, from the reactor through the Brayton unit system to the heat rejection panels. Because of these issues, there is a strong incentive to minimize the size of the control band through small sensor and control errors and through small discrete actuator actions. The benefits of a small control band in reduced reactor power and component sizes and ratings, are potentially limited by the more frequent shims of the slider mechanisms which could lead to excessive mechanical wear, or result in increased complexity of the PLR. These drivers would have to be balanced to determine an appropriately sized control band.

## 8.5 Plant Configuration Options

This section describes the operation of different plant configuration options. It is assumed that all configurations are required to produce approximately 200 kWe. Heat balances for the various configurations can be found in Section 6 and detailed arrangements can be found in Section 5.

The system architecture is described by three numbers separated by dashes. For example, the designation 1-1-1 uses a convention of B-R-G, where B is the number of Brayton units, R is the number of recuperators sized to support the operation of one Brayton unit at 100% of its rated power, and G is the number of gas coolers sized to support the operation of one Brayton unit at 100% of its rated power. It does not indicate the number of individual recuperators or gas cooler assemblies as more than one unit may be housed within a common pressure boundary to achieve design objectives; e.g., minimize mass, improve reliability, facilitate system arrangement. For example a 2-2-2 for a 200 kWe system with both Brayton units running (no spares) would incorporate two 100 kWe Brayton units with two recuperators and two gas coolers, each sized to support a 100 kWe Brayton unit. The gas cooler and/or recuperator may be physically one unit with multiple flow paths or independent flow paths or multiple units.

Also noted in each system architecture discussion is the number of frequencies at which the Power Conditioning & Distribution (PCAD) system is designed to operate (systems architectures designed to operate at full rated power at multiple (two) frequency and temperature points are designated with an "s", e.g., 2-2-2s). This operation at a second state point is discussed in detail in Section 3.12. The conceptual PCAD design accepted a single frequency and converted it to the required bus voltages

and frequencies. Increasing the number of acceptable frequencies increases the PCAD system complexity and mass, see Section 4.

### 8.5.1 The 1-1-1 System Architecture

The 1-1-1 system architecture has one Brayton unit running at full capacity to produce the required 200 kWe. This configuration does not require any valves, nor does it carry any spare Brayton units, recuperators, or gas coolers, making it the simplest configuration. Refer to Figure 8-5. Failure of any major component in the Reactor Module would be mission ending. The PCAD system is simplest because the AC bus operates on only a single voltage during full power operation. This concept may require addition of an angular momentum compensation device (flywheel) to ensure adequate spaceship control during science orbits.

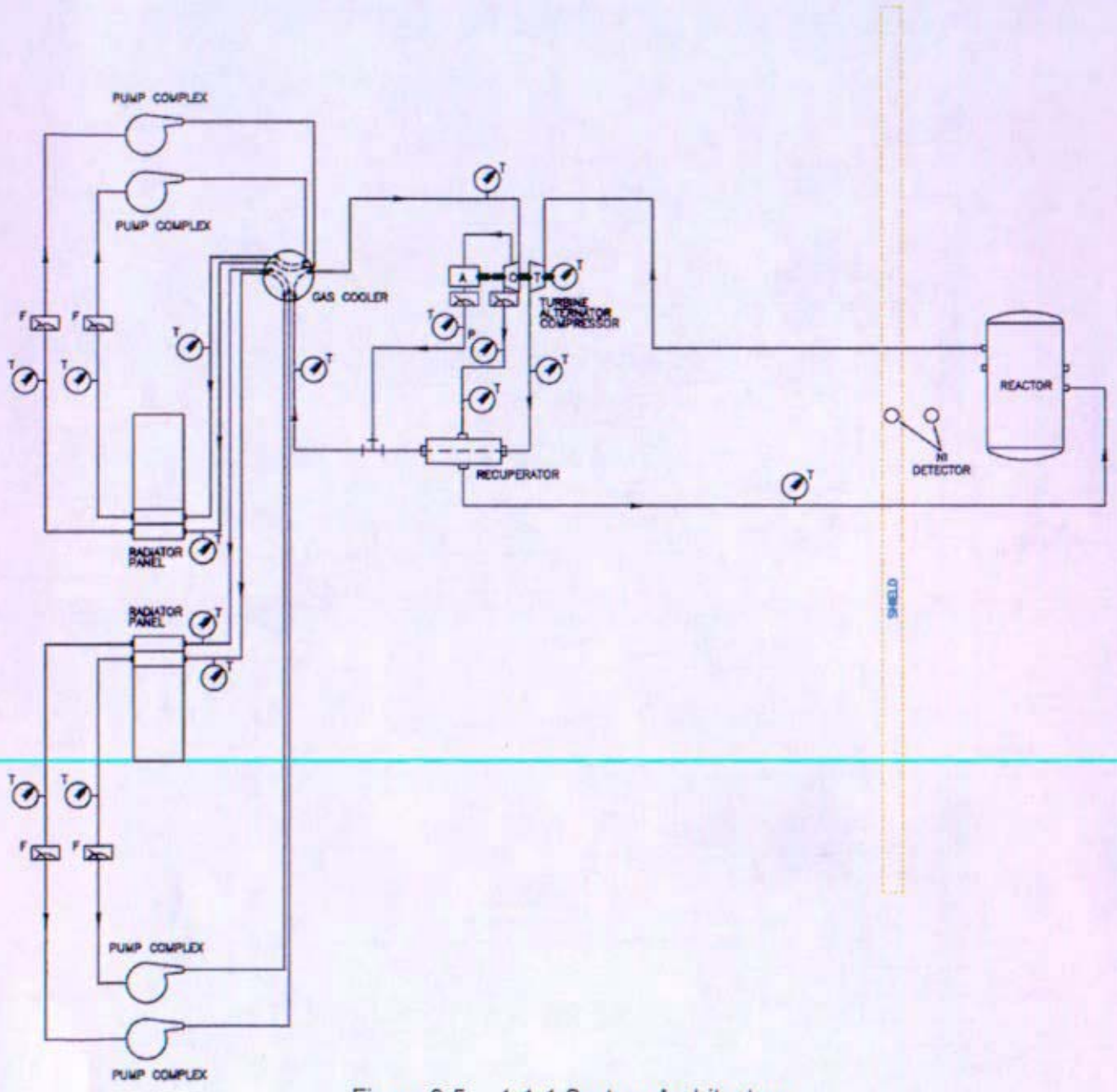



Figure 8-5: 1-1-1 System Architecture

### 8.5.2 The 2-2-2 System Architecture

The 2-2-2 system architecture has three possible system configurations: two 200 kWe Brayton units with the associated recuperators and coolers (fully redundant) with one Brayton unit operating at a time, two 100 kWe Brayton units with the associated recuperators and coolers (no redundancy), and two Brayton units designed to operate at both 100 kWe each (normal operation) and 200 kWe (with the loss of a Brayton unit) by raising temperature and Brayton unit shaft speed with the associated

recuperators and coolers (fully redundant). Only one of these operational modes would be used on the spaceship. A typical configuration is shown in Figure 8-6.

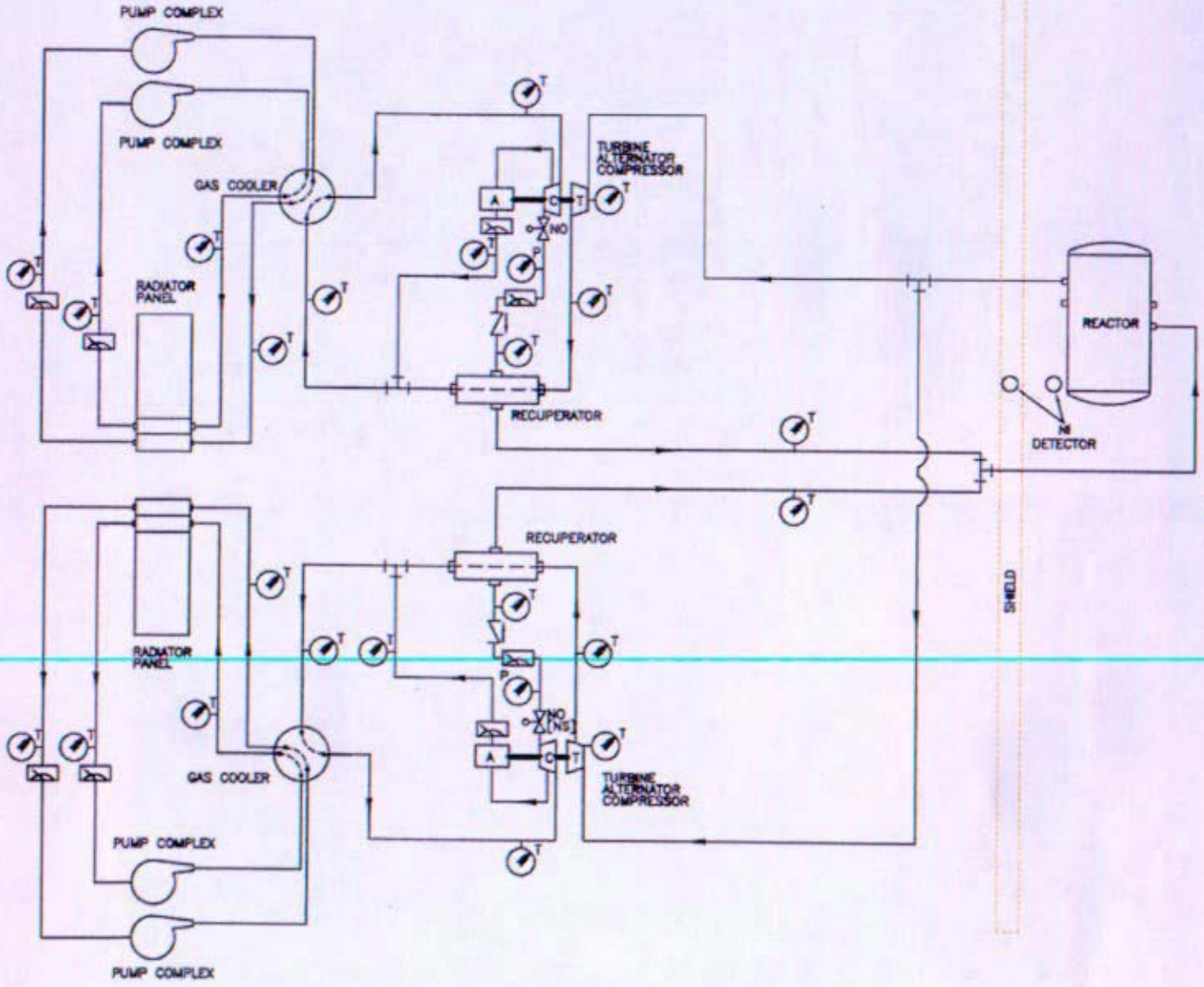



**Figure 8-6: 2-2-2 System Architecture**

### 8.5.2.1 One 200 kWe Operating Brayton Unit with One 200 kWe Idle Spare (2-2-2)

A 2-2-2 configuration with one operating Brayton unit has two 200 kWe Brayton units; one operating and the other as an idle spare. This arrangement requires valves and a backup power supply. If the operating Brayton unit fails, the spare Brayton unit is started and used to produce power. Since the operating Brayton unit is the only planned source of power on the spaceship once the solar panels are

ejected after initial startup, a long term energy storage system would be required to start the spare Brayton unit if the operating Brayton unit fails. The PCAD system would be simpler because the AC bus operates on only a single voltage and frequency during full power operation as opposed to configurations such as the 2-2-2s that involve Braytons operating at multiple speeds, resulting in multiple electrical bus voltages and frequencies.

### 8.5.2.2 Two 100 kWe Brayton Units Operating at 100% Capacity (2-2-2)

This 2-2-2 configuration has two Brayton units, each rated at 100 kWe, running at full capacity to produce the required electrical power. This configuration requires valves. Failure of a Brayton unit would be mission-impacting, since full power could no longer be generated. Although this configuration does not provide redundancy for full power operation in the event of a failure, it would allow the option of securing a Brayton for troubleshooting or to react to an unusual circumstance. Also, even if one Brayton were lost, the spaceship would continue to be operational indefinitely and a reduced scope mission may be an option. Reasons for choosing this option are: (1) if the development of Brayton unit machinery of the 200kWe size proves to be undeliverable (which is unlikely – see section 9.1) or (2) there is a significant advantage to the spaceship having angular momentum compensation provided by counter-rotating Brayton units as opposed to a flywheel system, and/or the Reactor Module mass allowance allows this as an acceptable alternative that has some level of redundancy. The PCAD system is only required to accept a single voltage during full power operation.

### 8.5.2.3 Two 200 kWe Brayton Units Operating at 50% Capacity (2-2-2s)

This 2-2-2s system architecture has two Brayton units, each rated at 200 kWe, normally running at half capacity (100 kWe) through reduced temperature and speed to produce the required spaceship power. This configuration requires valves. In the event an operating Brayton unit fails, the remaining operating Brayton unit is brought up to full capacity to supply the spaceship power demand. Operating State Points for the 2-2-2s configuration are shown in Section 3.11.

This configuration provides additional operational flexibility and relatively high reliability with an overall mass that is only about 2000 kg greater than for a single Brayton unit (1-1-1) option. However, it requires a PCAD system that is capable of supplying the spaceship with full power at two frequency and voltage points. This adds some mass to the power conditioning circuits. System efficiency will be reduced because the turbomachinery can only be optimized for one of the two sets of parameters (speed and temperature) or optimized for some midpoint, increasing the required radiator area and reactor power rating. The difference in overall system mass is primarily driven by the mass of added mechanical components, the loss of system thermal efficiency operating at non-optimized parameters, and the mass penalty associated with system pressure drop due to the more complex arrangements. Additional information for this configuration is contained in Section 3.7 and 3.12.

### 8.5.3 The 3-3-3 System Architecture

Similar to the 2-2-2 system architecture, there are many options for the 3-3-3 configuration. Several of these options are discussed below that provide different levels of redundancy.

### 8.5.3.1 Two 100 kWe Operating Brayton Units with One 100 kWe Idle Spare (3-3-3)

This 3-3-3 configuration has two Brayton units, each rated at 100 kWe, running at full capacity to produce the required electrical power, and a 100 kWe idle spare. This configuration requires valves. Failure of a Brayton unit requires starting the spare in order to produce full spaceship demand. The power to start the spare is supplied by the remaining operating Brayton unit. The PCAD system is simpler because the AC bus operates on only a single voltage and frequency during full power operation.

### 8.5.3.2 Three 100 kWe Brayton Units Operating at 50% Capacity (3-3-3s)

This 3-3-3s system architecture has three Brayton units, each rated at 100 kWe, running at two-thirds capacity (67 kWe) through reduced temperature and speed to produce the required spaceship power. This configuration requires valves. In the event an operating Brayton unit fails, the remaining two operating Brayton units are brought up to full capacity to supply the spaceship power demand.

This configuration provides additional operational flexibility and relatively high reliability with an overall mass that is only about 2000 kg greater than for a single Brayton unit (1-1-1) option. However, it requires a PCAD system that is capable of supplying the spaceship with full power at two sets of frequency and voltages. This adds some mass to the power conditioning circuits. System efficiency will be reduced because the turbomachinery can only be optimized for one of the two sets of parameters (speed and temperature) or optimized for some midpoint, increasing the required radiator area and reactor power rating. The difference in overall system mass is primarily driven by the mass of added mechanical components, the loss of system thermal efficiency operating at non-optimized parameters, and the mass penalty associated with system pressure drop due to the more complex arrangements. Additional information for this configuration is contained in Section 3.8 and 3.12.

### 8.5.4 The 4-4-4 System Architecture

Similar to 2-2-2 and 3-3-3 system architectures, there are many options for the 4-4-4 configuration. A typical configuration is shown in Figure 8-7.

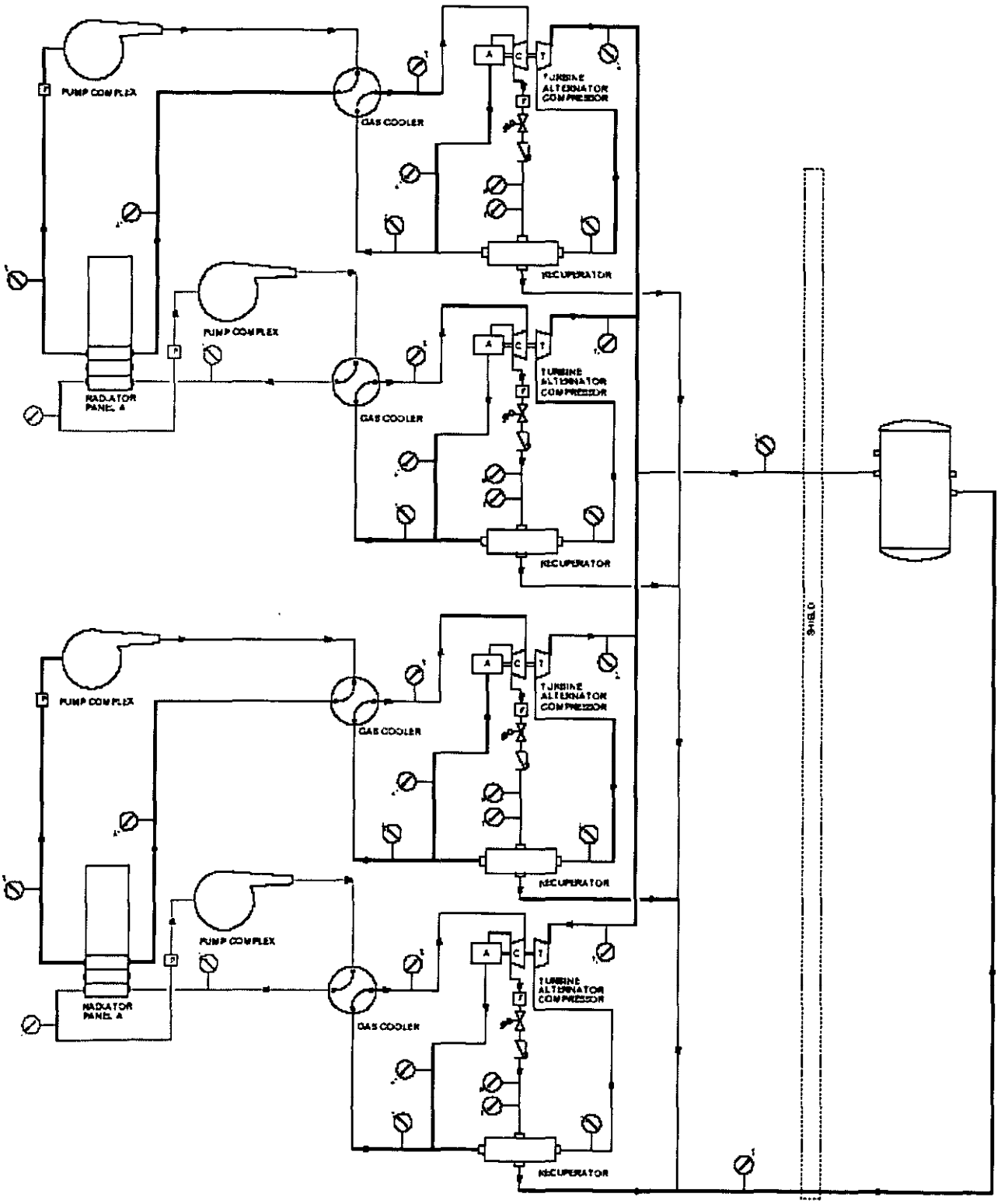



**Figure 8-7: Typical 4-4-4 System Architecture**

### 8.5.4.1 Two 100 kWe Operating Brayton Units with Two 100 kWe Spares (4-4-4)

This 4-4-4 configuration has two Brayton units, each rated at 100 kWe, running at full capacity to produce the required electrical power with two idle spares. This configuration requires valves. Failure of a Brayton unit requires starting the spare in order to produce full spaceship electrical demand. The power to start the spare is supplied by the remaining operating Brayton unit. The PCAD system is only required to accept a single voltage during full power operation.

## 8.6 Normal Operation and Control Strategies

### 8.6.1 Reactor Startup and Power Production Sequence

Table 8-1 provides the steps for the initial commissioning of the SNPP for the JIMO spaceship. It includes the startup (approach to criticality) of the reactor, the startup of the Brayton unit(s), heatup of the SNPP, and the production of full electrical power for the spaceship. The conclusion of this sequence supports supplying electrical power and checkout of the remaining spacecraft systems and the eventual transition to the thrusting phase.

This startup scenario is based on the mission plan utilizing transfer stages to boost the spacecraft out of earth orbit and into the interplanetary trajectory before full spacecraft deployment is achieved and the reactor startup is begun. The following is also assumed within the procedure:

- The PCAD architecture assumed (Figure 8-8) is the Northrop Grumman Space Technology arrangement at the time of Project Mission Systems Review (PMSR). A PCAD controller is assumed to control the lineup of the spacecraft electrical buses and to coordinate the operation of the Brayton unit Start Inverter and PLR.
- A reflector made up of twelve segments (sliders) is assumed for reactivity control. Each segment is controlled individually by a stepper motor. Only one segment is moved at a time. The assumed increment of movement is one millimeter per step.
- Physics testing will have been performed on the flight unit reactor prior to launch. This will provide confirmation of the core design and manufacture, and will support an accurate determination of the reactor's estimated critical position (ECP) for the plant startup in space.
- Valve operation is not addressed in this procedure.
- Mission Control will not be in direct control of each step of the startup sequence. Time delays in the communication path between Mission Control and the spacecraft preclude real time monitoring and control of plant functions. Also, continuous communication with the spacecraft is not assured during the deployment and startup phases (Level 2 Requirements are 92%). It is therefore assumed that the control architecture for the Reactor Module would be designed such that an entire series of steps or phase of the startup would be initiated by a command from Mission Control and controlled autonomously from the spacecraft. Mission Control would wait for satisfactory indications that the sequence steps had been completed before proceeding with the next phase of the sequence. How the steps in the following startup sequence would be accomplished within the respective spacecraft controllers (Reactor Module and PCAD) has not been determined.
- The assumed plant arrangement requires two Brayton at 45,000 rpm to produce full electrical power.

### 8.6.1.1 Reactor Startup Procedure and Principles

**Table 8-1: Reactor Startup Procedure and Principles**

| Procedure | Principles |
|---|---|
| **1.1 Initial Conditions** | |
| 1. The PCAD subsystem is operational. | *The PCAD subsystem provides the electrical power to operate the Command and Data Handling subsystem, the Reactor I&C segment, and to motor the Brayton unit to produce reactor coolant flow.* |
| 2. The solar arrays are sun pointing and are providing electrical power during the reactor startup. | *The solar arrays (located on the docking adapter in the PB1 arrangement) provide the primary source of electrical power for all functions on the spacecraft. The reactor startup requires an established flow of gas through the reactor to provide cooling when heat is produced. This gas flow is provided by motoring the first Brayton unit from the spacecraft electrical bus. Since the Brayton unit imposes the largest single load on the spacecraft electrical bus during the startup, the solar arrays must be pointed to generate maximum electrical power.* |
| 3. The telecom link to Mission Control is operational. | *The telecom link provides a communication path for commands to activate the Reactor I&C segment and control phases of the reactor startup. Once reactor specific commands are received on the spacecraft, they are processed by the Command and Data Handling subsystem's flight computer and passed to the Reactor I&C segment.* |
| 4. The reactor module aeroshell has been jettisoned. | *The aeroshell must be absent when the reactor is operational in order to allow adequate heat dissipation from the reactor and energy converters. It must be jettisoned prior to the startup of the reactor to preclude any undesired interference with the operational reactor.* |

| Procedure | Principles |
|---|---|
| 5. Heat Rejection Segment (HRS) is deployed.<br>a. HRS trace heaters are energized to preclude freezing in the piping to the radiators.<br>b. HRS pumps are in a low flow mode to preclude freezing in the piping to the radiators. | *The Heat Rejection Segment provides the heat sink necessary for operation of the Brayton unit cycle. Full deployment of the radiator panels is required prior to reactor startup and the raising of the power system's temperature. Spacecraft operational planning assumes that trace heaters and a minimum ("survival") flow will be utilized to prevent HRS fluids from freezing from launch until operation of the power system.* |
| 6. Reactor I&C segment is energized. | *Initial planning has assumed that the reactor I&C segment would be launched in a deenergized state to conserve battery power. The initial architecture of the reactor I&C segment does not provide for partial energization during launch to monitor limited reactor plant parameters. This is considered acceptable because the sliders would be launched in their least reactive position with no means to energize them, and shutdown safety rod(s) with locking mechanisms would be in the reactor core to provide additional shutdown margin.*<br><br>*Energization of the reactor I&C segment would be initiated from Mission Control. The command would be received by the spacecraft Command and Data Handling subsystem's flight computer and passed to the Reactor I&C segment's supervisor controller. Energization of the Reactor I&C segment could occur anytime after deployment of the spacecraft solar arrays, but does not have to occur until the full deployment of the spacecraft is complete.* |
| 7. The reactor is shutdown. | *Except for a single ground test to confirm criticality of the flight unit core, this reactor will not have been operated previously, and will never have been operated at power. The reactor will have been launched in a safe/shutdown condition and will not be taken critical until the spacecraft is on the interplanetary trajectory.* |

| Procedure | Principles |
|---|---|
| 8. All sliders are in their least reactive position (launch condition). | *The safety position for launch of the reactor is with all sliders in their least reactive position, and the safety rod(s) fully inserted. All devices are deenergized until the systems power up prior to reactor startup.* |
| 9. Reactor vessel, piping, and Brayton unit Turbo-Compressor Alternator are at a temperature of approximately 250-300 K. | *The preliminary plant design assumes a thermal management subsystem which maintains the temperature of the plant components at 250-300 K from launch until startup of the power plant.* |
| 10. Reactor I&C segment pre-critical checks have been performed satisfactorily. | *Once energized, the reactor I&C circuits would perform self checks to verify proper operation. Additionally, checks would be performed to confirm correct operating constants and gain factors. Additional checks would be identified as the detailed circuit designs are completed. The purpose of these checks is to confirm that all of the reactor I&C circuits survived launch, are properly aligned to support the reactor startup, and will perform their assigned functions during the subsequent reactor operation. Confirmation of satisfactory completion of the pre-critical checks would be required before Mission Control could initiate the reactor startup.* |
| 11. Permission has been received from the Director, Naval Nuclear Propulsion to commence the startup of the JIMO reactor. | |
| **1.2 Precautions** | |
| 1. From the start of slider motion until reactor power is greater than [1.0%] power, the following shall not occur:<br>a. Brayton unit speed shall not be changed.<br>b. Heat Rejection subsystem pump speed / lineup shall not be changed. | *Slider motion (direct reactor reactivity control), Brayton unit speed (reactor coolant flow rate), and HRS flow all represent independent methods of affecting reactivity and are controlled by separate control systems on the spacecraft. To avoid power swings and control oscillations caused by interactions from the respective controllers, only one factor affecting reactivity may be changed at a time. Communication between the respective controllers is imperative.* |

| Procedure | Principles |
|---|---|
| 2. Following the reactor startup (reactor power greater than [1.0%]), no combination of slider motion, Brayton unit speed change, and HRS pump speed / lineup change shall occur simultaneously. | *The primary justification for this concern is to preclude multiple, independent additions of reactivity to the reactor core at the same time. While modeling efforts may eventually demonstrate that this is not an issue, this precaution should remain until later in the design phase because the reactor's sliders, the Brayton unit speed, and the HRS pump speed are controlled by different portions of the spacecraft. Effective coordination between the control functions on the various segments of the spacecraft needs to be established.* |
| **2.1 Reactor Startup** | |
| 1. Perform operational checks on the reactor slider drive mechanisms. | *Each slider is inserted one or two steps and then withdrawn to its least reactive position to confirm the integrity of the slider drive motor circuits and the operability of the slider mechanism.*<br><br>*Each slider check is commanded from Mission Control and proper operation is verified before completion of the step.* |
| 2. Withdraw the safety rod(s) to the full out position. | *Once the slider drive mechanism checks have been completed, the safety rod(s) are withdrawn from the reactor. This allows normal reactivity control with the sliders.* |
| 3. Secure the thermal management heaters in the reactor module. | *The thermal management heaters (estimated power demand: 1 -2 kWe) represent a competing electrical load for the power needed for the Brayton unit Start Inverter. This power is now required for the reactor startup phase. Insulation and micrometeorite protection coverings will need to maintain residual heat until the reactor is producing thermal energy.* |
| 4. Start Brayton unit #1. The initial frequency setpoint shall be [675 Hz (equivalent to a Brayton unit speed of 13,500 rpm)]. | *The command is sent from Mission Control to the spacecraft flight computer which then passes it to the PCAD controller. The PCAD controller energizes the Brayton unit Start Inverter (see Figure 1) to apply AC electrical power to rotate the Brayton unit, using its alternator as a motor. The Brayton unit Start* |

| Procedure | Principles |
|---|---|
| | *Inverter converts DC electrical power (source) to variable frequency AC power. (This represents the largest single load on the DC distribution bus during the startup and drives the sizing of the solar array.) (See Figure 2).* |
| | *For the first phase of the reactor startup, the frequency of the Start Inverter would notionally be set to 675 Hz – corresponding to a Brayton unit speed of 13,500 rpm (30% of 45,000 rpm). (This speed would likely be in the range of 20-30%. Less than 20%, and the speed would be too close to the Brayton unit's low end critical rotor speeds, and additionally, the speed would be so low that the turbine wheel would not begin producing work at any attainable temperature from the reactor. Greater than 30% speed, and the Start Inverter power demand would increase solar array sizing unnecessarily.) This speed is controlled by the Start Inverter, and is likely a frequency control on its output. Brayton unit speed and voltage will be ramped up to minimize the peak power demand on the electrical bus. At this point, the PLR is not providing load on the AC bus.* |
| 5. Commence slider insertion to the ECP-0.02 position ( 2% sub-critical). | *These programmed sequences for the reactor startup will be initiated from Mission Control and will be executed autonomously by the Reactor I&C segment. Continuous downlinks from the spacecraft will provide status information to Mission Control on the progress of the startup. Mission Control would be able to stop the startup sequence at any point.* |
| | *The slider control program will insert one slider at a time, moving each slider in succession around the reactor vessel in order to keep the relative position of all sliders approximately equal. The slider motion interval for the first phase of reactivity addition is assumed to be one slider step every second, or a total of 60 mm of slider motion per minute.* |
| | *When the ECP-0.02 position is reached, slider motion will cease until the next command is* |

| Procedure | Principles |
|---|---|
| | *received from Mission Control.* |
| 6. Commence slider insertion to reach criticality. | *This slider control program will begin by inserting one slider at a time at an interval of one slider step every 10 sec.*<br><br>*Startup rate (as derived from the nuclear instrument outputs) will be continuously monitored. Startup rate in excess of [0.5 DPM] will cause slider motion to be suspended until the startup rate has decreased to [0 DPM]. Slider motion will cease completely when the startup rate remains positive.*<br><br>*Mission Control will confirm the slider positions, power level, and coolant temperature when criticality is achieved.* |
| **2.2 Raise Plant Temperature to Set Brayton unit #1 Power Positive** | *Adding reactivity to slowly heat the plant from a cold condition while motoring a Brayton unit to maintain a constant reactor coolant flow rate is potentially the most challenging part of the startup sequence. As the turbine inlet temperature slowly increases from reactor heat, the turbine will begin to produce work and the power drawn from the start inverter will decrease.*<br><br>*The following method needs to be modeled and tested to determine the speed stability of the Brayton unit as its alternator phase currents approach zero, and also to assess the sensitivity of the reactor core to variations in Brayton unit speed (coolant flow rate) at this temperature.* |
| 1. Insert sliders to raise turbine inlet temperature.<br><br>a. Control the interval of slider insertions to limit the rate of temperature increase to [0.5 K/min].<br><br>b. Continue to hold Start Inverter frequency setpoint at [675 Hz | *A heatup rate of [0.5 K/min] is expected to require slider motion of approximately 1 slider step every 3-5 minutes. The heatup rate of [0.5 K/min] was conservatively chosen to allow for gradual thermal growth of the power system components. After final material selections and detailed design and analysis of the components, a more aggressive heatup rate may be permissible.* |

| Procedure | Principles |
|---|---|
| (Brayton unit speed: 13,500 rpm)]. | *As the plant temperature increases, the Brayton unit will begin to produce electrical energy and eventually become power positive (self-sustaining). As this happens, the PCAD controller will secure the start inverter and transition speed control of the Brayton unit to the PLR such that its speed remains constant.* |
| 2. Secure slider motion when the turbine inlet temperature reaches [950 K]. | *Increasing the plant temperature to a point above that where the Brayton unit becomes power positive places the power plant in a state where the Brayton unit can support small changes in plant loads without risk of stalling.*<br><br>*The [950 K] stopping point needs to be confirmed with modeling and prototype testing to ensure that sufficient power is available to support the plant load changes in the following steps.* |
| **3.1 Raise Plant Power** | |
| 1. Increase the HRS Loop 1 pump speed to [intermediate]. | *The HRS pump speed needs to be increased from the minimum flow value to support higher power plant operation. The setting of the HRS pump speeds needs to be verified with accurate models of the final plant design.* |
| 2. Increase the PLR speed setpoint to [35,000 rpm]. Limit the rate of change of the speed setpoint to approximately [TBD rpm/min]. | *The approach being used to transition from the Brayton unit power positive point to the full power state is to "stair-step" upwards in increments of temperature and then power. With temperature being raised in the step above, the Brayton unit speed (and load) can now be increased to the value consistent with the new temperature. The optimum rate of change of speed needs to be chosen based on thermal considerations for plant components and to limit the overshoot of speed and reactor power. It must also be verified based on an accurate model of the final plant design. Refer to Figure 4 for the typical family of curves relating temperature, electrical output power, and Brayton unit speed.* |

| Procedure | Principles |
|---|---|
| 3. Increase the HRS Loop 1 pump speed to [fast]. | *The HRS pump speed needs to be increased to the full flow value to support Brayton unit full power operation. The setting of the HRS pump speeds needs to be verified with accurate models of the final plant design.* |
| 4. Insert sliders to raise turbine inlet temperature to [1,000 K].<br>a. Control the interval of slider insertions to limit the rate of temperature increase to [0.5 K / min.]<br>b. Continue to hold the Brayton unit speed setpoint at [35,000 rpm].<br>c. Secure slider motion when the turbine inlet temperature reaches [1,000 K]. | *1,000 K represents an intermediate temperature point which will support an increased Brayton unit speed.* |
| 5. Increase the PLR speed setpoint to [40,000 rpm]. Limit the rate of change of the speed setpoint to approximately [TBD rpm/ min]. | *As above, the rate of change of Brayton unit speed needs to be determined to limit the overshoot of speed and reactor power and with considerations for the thermal limits of plant components.* |
| 6. Insert sliders to raise turbine inlet temperature to [1,150 K].<br>a. Control the interval of slider insertions to limit the rate of temperature increase to [0.5 K / min.]<br>b. Continue to hold the speed setpoint at [40,000 rpm].<br>c. Secure slider motion when the turbine inlet temperature reaches [1,150 K]. | *[1,150 K] is the final operating temperature for the plant, and will support full speed operation of the Brayton unit.* |

| Procedure | Principles |
|---|---|
| 7. Increase the PLR speed setpoint to [45,000 rpm]. Limit the rate of change of the speed setpoint to approximately [TBD rpm/ min]. | *45,000 rpm is the design operating speed of the Brayton unit. At this speed, the frequency of the electrical output is the PCAD design value of 2250 Hz.* |
| **3.2 Perform the Intermediate Heat Balance** | *The purpose of this step is to provide an in-situ calibration of the nuclear instruments monitoring reactor flux. The details will be developed as the plant design is finalized.*<br><br>*An in-situ calibration is required as the correlation between actual reactor power and the flux measured by the nuclear instruments is affected by their location relative to the reactor and by structures and geometry of the sensor locations.*<br><br>*It is anticipated that steady state plant conditions will be established and maintained. During this steady state period, measurements will be made of the pressures, temperatures, and flows in the primary coolant loop and the HRS loops. From these measurements and adjustments made to account for thermal losses to the space environment, a calculation may be made to determine the total energy (and therefore the power level) being produced by the reactor. This value will then be used to adjust the gain on the nuclear instruments.*<br><br>*Performance of this calibration at this power point (~50%) provides an intermediate adjustment on the nuclear instrument gains, thereby improving the accuracy of the level and rate measurements during the remainder of the increase to full plant power.* |

| Procedure | Principles |
|---|---|
| **4.1 Start Brayton unit #2** | *This approach starts the second Brayton unit when the plant has reached full operating temperature. It is acknowledged that this represents a temperature transient on plant components and the reactor, and that a more gentle approach may be to start Brayton unit #2 at a lower temperature and bring both units up to full speed together.*<br><br>*However, should a plant configuration with spare Brayton units be developed, and a spare unit be called upon to replace a failed unit during the mission, a procedure similar to the following may be required to restore full power to the spacecraft.*<br><br>*If the following approach is used, pre-heaters on colder components may be required.* |
| 1. Set the HRS Loop 2 pump speed to [intermediate]. | *The HRS pump speed needs to be increased from the minimum flow value to support higher power plant operation. The setting of the HRS pump speeds needs to be verified with accurate models of the final plant design.* |
| 2. Energize Brayton unit Start Inverter #2. Set the frequency setpoint to [675 Hz. Equivalent Brayton unit speed: 13,500 rpm]. | *This will start Brayton unit #2 rotating. Power for the Start Inverter will come from the solar arrays (still connected in the initial startup) or from the High Voltage AC bus through the wide input down-converter to the 28 vdc bus.* |
| 3. As Brayton unit #2 speed increases, limit speed to [13,500 rpm] with the PLR. | *With the plant at normal operating temperature, Brayton unit #2 will rapidly increase in speed and begin to produce electrical energy to become power positive (self-sustaining). As this happens, the PCAD controller will secure the start inverter and transition speed control of the Brayton unit to the PLR such that its speed remains constant.*<br><br>*The approach considered here is to limit the speed of Brayton unit #2 to a modest value and then control its ramp up rate by adjusting load.* |

| Procedure | Principles |
|---|---|
| 4. Set the HRS Loop 2 pump speed to [fast]. | *The HRS pump speed needs to be increased from the intermediate flow value to support higher power plant operation. The setting of the HRS pump speeds needs to be verified with accurate models of the final plant design.* |
| 5. Increase Brayton unit #2 speed from 13,550 rpm to 45,000 rpm at a rate of [TBD rpm/ min]. | *The optimum rate of change of speed needs to be chosen based on thermal considerations for plant components and to limit the overshoot of speed and reactor power. It must also be verified based on an accurate model of the final plant design.* |
| **5.1 Perform the Final Heat Balance** | *The purpose of this step is to provide a final in-situ calibration of the nuclear instruments monitoring reactor flux at full power conditions. The details will be developed as the plant design is finalized.* |
| | *As discussed in step 3.2, this procedure is required to correlate the output of the nuclear instrument circuits with the actual flux produced by the reactor. This procedure must be repeated at full power to adjust this calibration to the full power operating conditions of the reactor and power plant.* |

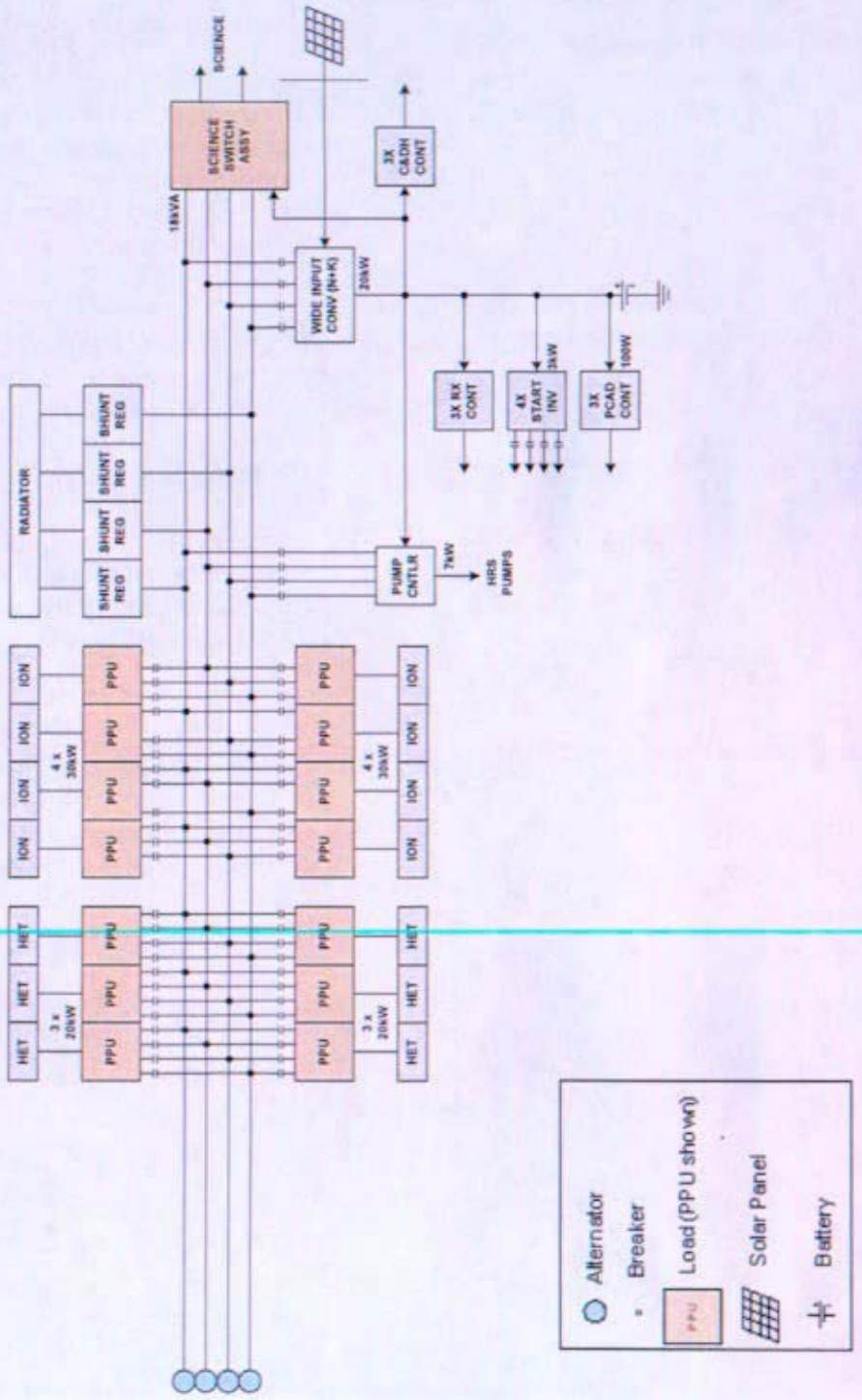



**Figure 8-8: JIMO Power Conditioning & Distribution Subsystem (PCAD)**
This is the architecture for the power distribution system at the conclusion of the Northrup Grumman Space Technology's Phase A JIMO contract (PMSR).

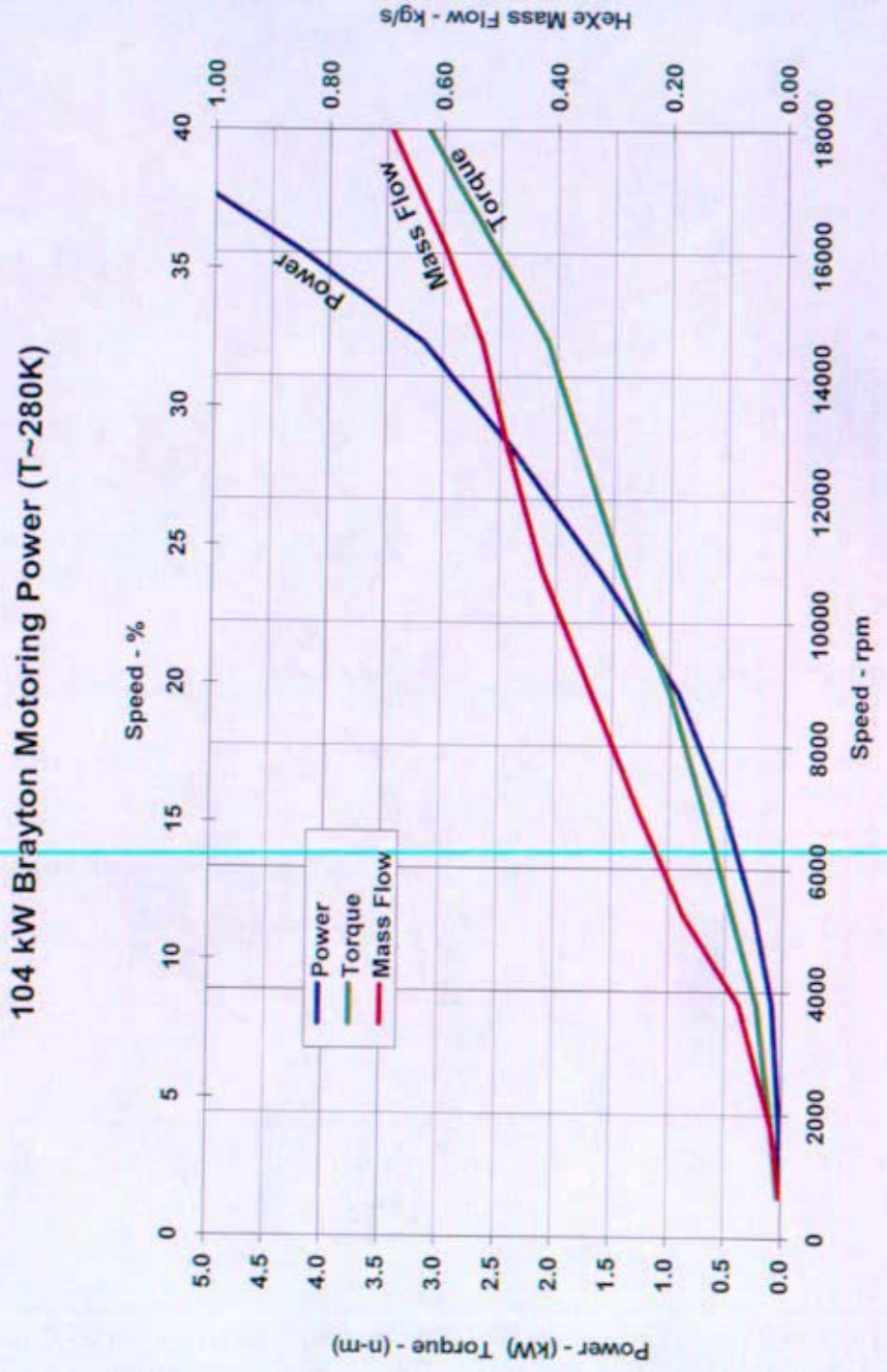



**Figure 8-9: 104 kW Brayton Unit Motoring Power.**
Source: Hamilton Sundstrand sizing studies for Brayton unit development.

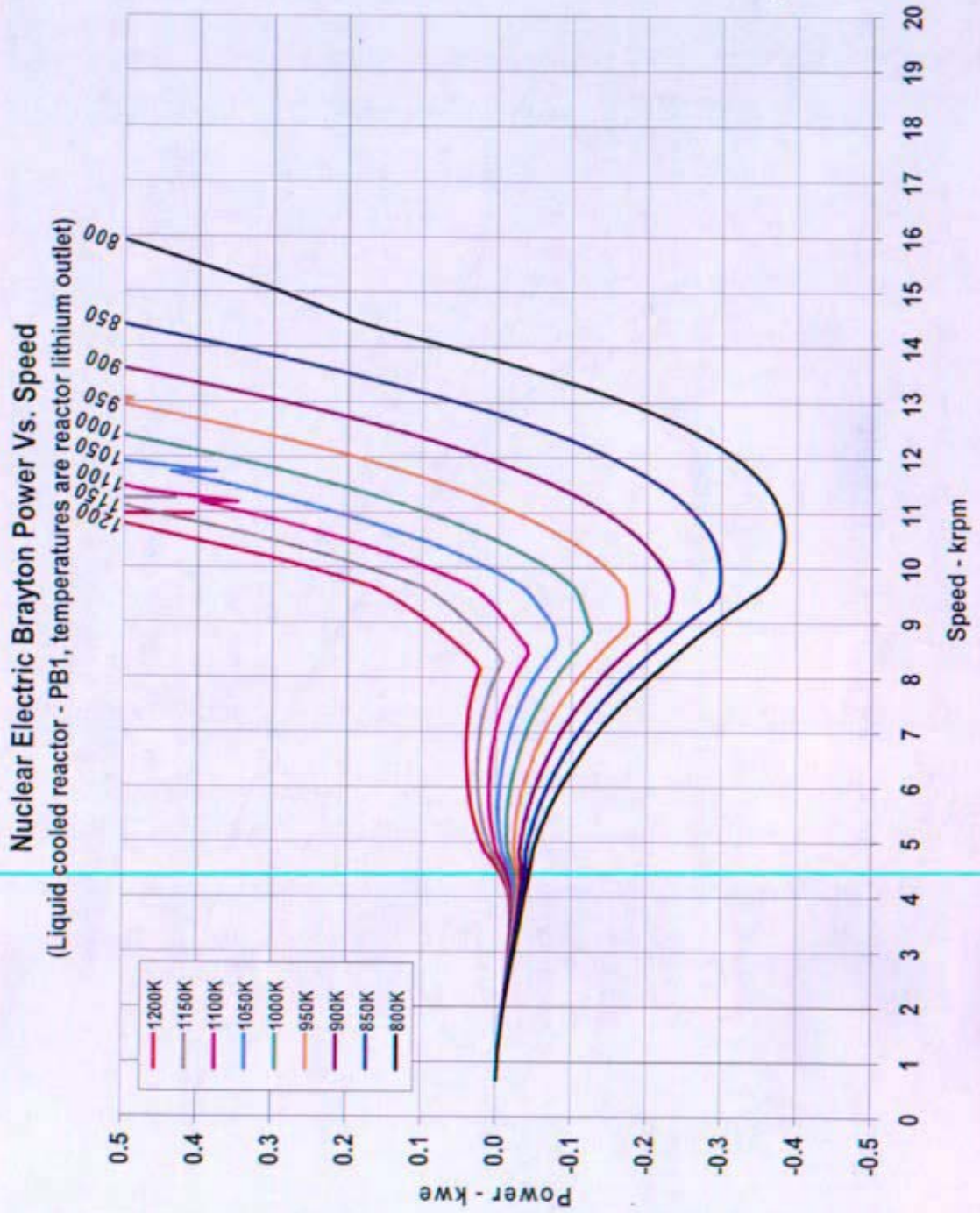



**Figure 8-10: Typical Power / Low Speed Curves for a Brayton Unit Turbo-Compressor-Alternator Operating at Various Turbine Inlet Temperatures.**

Source: Hamilton Sundstrand sizing studies for Brayton unit development. Note: these curves were developed for a 95 kWe unit in the Government reference case liquid metal cooled reactor plant. For a direct gas cooled reactor plant, the curves are expected to be similar with the power levels being slightly higher for a 100 kWe Brayton unit, and the family of temperature curves expanding to include temperatures below the 800 K shown here.

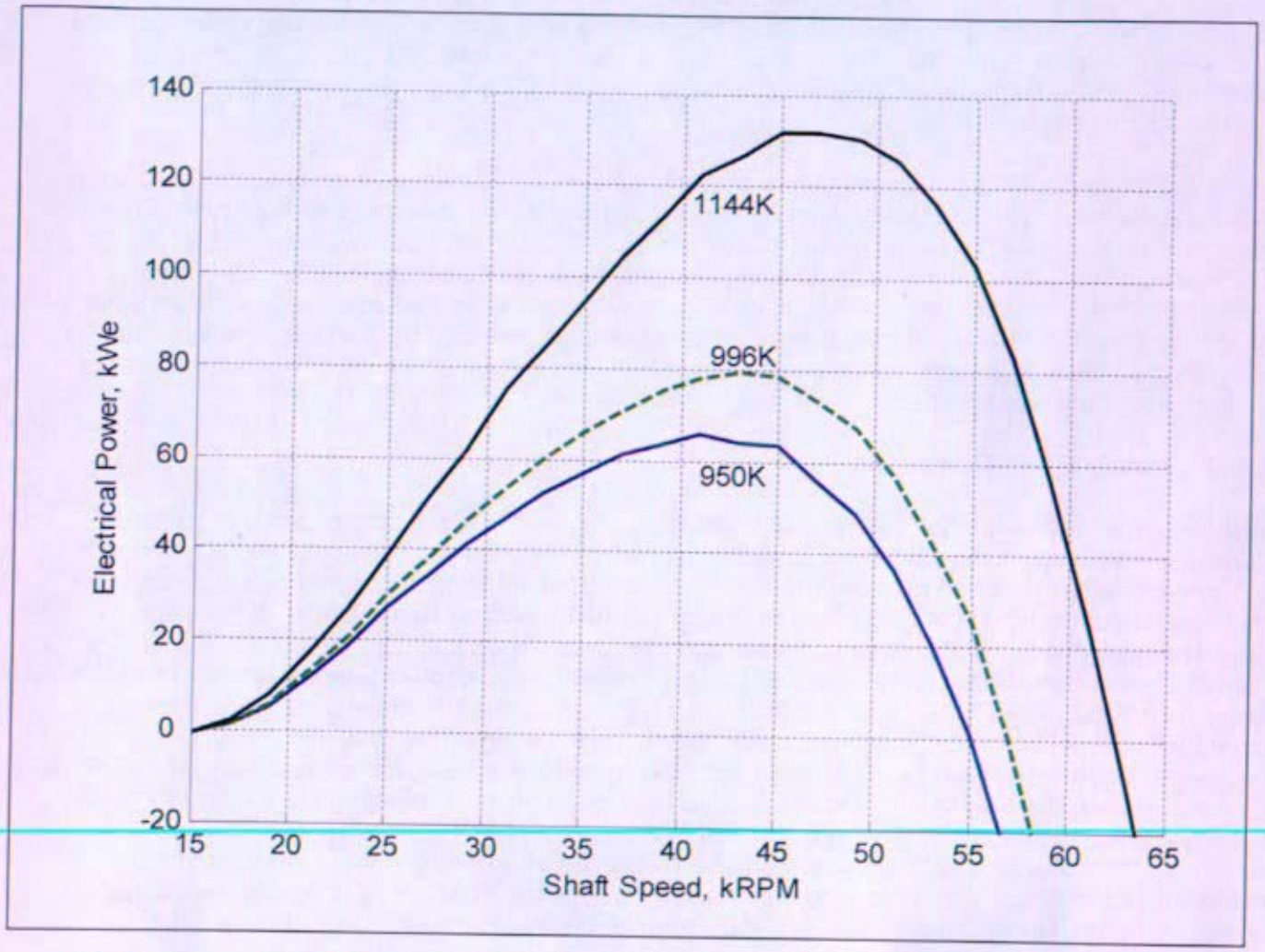



**Figure 8-11: Typical Power / Speed Curves for a Brayton Unit TCA Operating at Various Turbine Inlet Temperatures.**

Source: KAPL Simulink Model of the Direct Gas Brayton unit. Note: These curves depict total electrical output from two Brayton units operating at 65 kWe each. The performance of a single Brayton unit operating during the startup phase is expected to be similar, with the total electrical output reduced by half.

### 8.6.2 Startup of a Second Brayton Unit During Plant Startup

Motoring both Brayton units simultaneously in the initial startup may not be feasible due to the additional power required. The power demand to motor just one Brayton unit represents about two thirds of the total power supplied by the solar arrays (as currently envisioned), and is the main driver for their sizing on the spacecraft. Adding the power required to motor a second Brayton unit simultaneously would increase the solar array sizing even more. The spaceship battery is not sufficient to start a Brayton unit. The power demand and length of time required for the startup would deplete it. Therefore all electrical power for the startup will come from the solar arrays. An alternative

would be to start Brayton unit #1, startup the reactor, heatup the plant to the point where Brayton unit #1 goes power positive (self-sustaining), and then use the solar array's "Brayton unit power budget" to start Brayton unit #2. This would occur at an intermediate temperature (800 - 900 K), and might lessen the thermal transient on the plant compared to starting Brayton unit #2 when the plant was at normal operating temperature.

While it may be possible to shim reflectors and change Brayton unit speed simultaneously in theory, it would be difficult to execute this on the spacecraft. In the current spacecraft architecture, the two functions are controlled by separate controllers (Reactor I&C and PCAD) which would require continuous coordination and unnecessarily complicate the control algorithms. It is thus likely that these functions would be performed sequentially. Brayton unit speed would be held constant while shimming reflectors to raise temperature, then reflector position would be held constant while raising Brayton unit speed. This sequence would be repeated until normal Brayton unit operating speed and plant temperature was reached.

### 8.6.3 Steady State Operation

Once the reactor and Brayton unit startup is complete, the SNPP is in a configuration to support continuous, unlimited operation of the spaceship. This would place the reactor at 100% power and the Brayton units producing full power (185 kWe total). Until thrusting is commenced, the power demand for spaceship loads would be on the order of 10-20 kWe. The remainder of the electrical power being produced would be absorbed by the PLR sections on each electrical bus. As with the startup phase, the reactor controller would act to maintain reactor coolant temperature within its prescribed band. The PCAD controller (through the PLR) would act to maintain the Brayton unit speed (or voltage) within its prescribed band. When the thrusting phase is commenced, the necessary electrical power would be made available by reducing the power consumed by the PLR, thus maintaining the Brayton units at their desired operating point. If desired, this steady state operating lineup could continue for the duration of the mission with no significant actions by the respective controllers except the occasional reactivity addition (reflector shim) to the reactor to compensate for fuel burnup, or to respond to an anomaly in the plant. In the thrusting mode, full power would be required to provide thrust capability for the interplanetary transfer or for orbit maintenance at the mission's target.

Certain phases of the mission do not require full power capability for thrusting. During the interplanetary transfer, there are coast periods where the spaceship thrusters are secured and the actual power demand is reduced significantly. In addition, thrusting would not typically be required during periods of science observation. In both cases, the power demand would be reduced to 40 kWe or less. This affords the opportunity to lower the operating point of the Brayton units (temperature and speed) and thereby reduce the necessary operating temperature of the reactor and extend its operational lifetime, as well as reducing temperatures and stresses in the Reactor Coolant/Energy Conversion components. These options are discussed in more detail below.

Evaluations of the control methods for the reactor and Brayton units were not complete at the time of project cancellation. Some initial conclusions on control approaches and plant responses are provided in Section 12.

### 8.6.4 Reduced Power Operation

The JIMO Level 2 requirements (Reference 8- 3) state:

> **PRD_18 - Reactor Throttle Capability**
>
> The Project shall use a nuclear reactor whose thermal power output is adjustable to allow long-term operation at any reactor power level down to [30%] of full power output

The 30% reactor power level is a tentative number that would be determined as the project progressed. Utilization of a low power operating mode may allow for the reduction of system temperature and/or reactor power for significant portions of the mission, maximizing Reactor Module lifetime. This low power mode may also represent a state in which to place the Reactor Module while recovering from a casualty transient. Two power levels were envisioned for power plant operations. A higher power level of approximately 185 kWe would have been utilized when propulsion was required, and a low power level (~40 kWe or less) would have been utilized when the spaceship was coasting (i.e., propulsion not required) and during periods of scientific data once the spaceship arrived on station. Increased plant and core life allow follow-on missions of longer duration than the first JIMO mission. JPL estimates that non-thrusting periods could range from 3 years for the JIMO mission to 10 years for the longest envisioned (20 year) Prometheus mission.

Several methods using the plant controls listed in Section 8.3 were explored to achieve a distinct low power level. The methods of reducing power considered were:

1. Reduce the number of operating Brayton units
2. Reduce reactor outlet temperature
3. Reduce Brayton unit speed
4. Reduce reactor outlet temperature and Brayton unit speed

Options 2, 3, and 4 were analyzed using a version of the Simulink model for a 132 kWe plant (Reference 8- 4) with a NaK secondary loop (an earlier conceptual design iteration). This model does not take into account the degradation of heat pipe performance with reduction in HRS temperatures. Below ~340°K the heat pipe heat transfer begins to decrease and below ~310°K the heat pipes cease to transfer heat. Cases where these temperature limitations are exceeded would have decreased efficiencies relative to the efficiencies reported by the Simulink model.

#### 8.6.4.1 Reduce the Number of Operating Brayton units

If the plant utilizes multiple Brayton units, one or more Brayton unit(s) could be shut down to reduce reactor power. Plant and core temperatures would remain fairly constant, with reactor flow reduced by the amount attributable to the secured Brayton unit. The percentage of reactor power reduction will nearly follow the percentage of flow reduction. System efficiency will stay near design efficiency, and may increase slightly due to reduced pressure drop in common flow paths. This method could be used in conjunction with temperature reduction to increase creep life.

A disadvantage of this method is that shutting down an operating Brayton unit makes the system less tolerant of an operating Brayton unit failing. In a plant where only two Brayton units normally operate, shutting one down for a reduced power mode requires an energy storage device to restart the

shutdown Brayton unit in the event the operating Brayton unit fails. Another disadvantage is that the operating Brayton doesn't experience any temperature or stress advantages in the reduced power mode.

### 8.6.4.2 Reduce Reactor Outlet Temperature

Table 8-2 shows system parameters when reactor outlet temperature is used to reduce reactor power. This method reduces reactor power and plant and core temperatures, which decreases burn up and increases creep life. System efficiency decreases sharply with decreasing temperature, so reducing electrical power 75% only reduces reactor power by 35%. The allowable temperature reduction may be limited by low temperature limits in the core and/or plant.

**Table 8-2: System parameters using reactor outlet temperature to reduce reactor power.**

| Electrical Power Level | 100% | 50% | 25% |
|---|---|---|---|
| Reactor and Plant Temps | | | |
| Compressor Inlet | 374 K | 365 K | 361 K |
| Compressor Outlet | 515 K | 504 K | 499 K |
| Reactor Inlet | 880 K | 745 K | 685 K |
| Reactor Outlet | 1145 K | 960 K | 872 K |
| Turbine Outlet | 920 K | 773 K | 705 K |
| Gas Cooler Inlet | 564 K | 535 K | 523 K |
| Shaft Speed | 45000 RPM | 45000 RPM | 45000 RPM |
| Electrical Power | 132 kWe | 66 kWe | 33 kWe |
| HRS Temps | | | |
| Radiator Inlet | 522 K | 494 K | 481 K |
| Radiator Outlet | 363 K | 358 K | 355 K |
| Reactor | | | |
| HeXe mass flow rate | 3.77 kg/s | 3.58 kg/s | 3.46 kg/s |
| Average Fuel Temperature | 1157 K | 969 K | 880 K |
| Power | 533 kWt | 407 kWt | 344 kWt |
| Cycle Efficiency | 24.7% | 16.2% | 9.6% |

### 8.6.4.3 Reduce Brayton Unit Speed

Table 8-3 shows resulting system parameters when reduced Brayton unit speed is used to reduce reactor power. With this method system efficiency stays relatively high, allowing a reduction of 50% and 75% electric power to reduce reactor power 48% and 68%, respectively. A disadvantage of this method is that hot plant and core temperatures increase as Brayton unit speed is decreased. The temperature increases decrease creep life and violate temperature limits at the reactor inlet.

The PCAD subsystem is normally optimized to operate within a narrow band of frequency and voltage. While some deviation might be allowable, speed changes as large as those shown in Table 8-3 would produce voltage and frequency values that would require alternate designs for any power

supplies that are energized during the period of lower speed operation. These designs may contribute small increases in PCAD mass.

**Table 8-3: System Parameters using Brayton Unit Speed to Reduce Reactor Power**

| Electrical Power Level | 100% | 50% | 25% |
|---|---|---|---|
| Brayton unit System "A"* | | | |
| Compressor Inlet | 374 K | 340 K | 320 K |
| Compressor Outlet | 515 K | 403 K | 358 K |
| Reactor Inlet | 880 K | 967 K | 1005 K |
| Reactor Outlet | 1145 K | 1150 K | 1153 K |
| Turbine Outlet | 920 K | 1030 K | 1076 K |
| Gas Cooler Inlet | 564 K | 479 K | 444 K |
| Shaft Speed | 45000 RPM | 29580 RPM | 24020 RPM |
| Electrical Power | 132kWe | 66 kWe | 33 kWe |
| Heat Rejection System | | | |
| Radiator Inlet | 522 K | 421 K | 376 K |
| Radiator Outlet | 363 K | 339 K | 320 K |
| Reactor | | | |
| HeXe mass flow rate | 3.77 kg/s | 2.75 kg/s | 2.09 kg/s |
| Average Fuel Temperature | 1157 K | 1153 K | 1152 K |
| Power | 533 kWt | 275 kWt. | 172Wt |
| Cycle Efficiency | 24.7% | 24% | 19.3% |

### 8.6.4.4 Reduce Reactor Outlet Temperature and Brayton Unit Speed

Table 8-4 shows system parameters when a combination of reactor outlet temperature and Brayton unit speed reductions are used to reduce reactor power. Reducing reactor outlet temperature reduces reactor power and increases creep life in the core and plant. Reducing Brayton unit speed further reduces reactor power, and because temperature reductions are more modest than in Section 8.6.4.2, cycle efficiency is higher. Reducing Brayton unit speed also reduces mechanical stresses on the turbomachinery. This is discussed further in Section 3.

This is the preferred low power mode because it reduces core and plant temperatures, Turbomachinery stresses, and achieves a significant reduction in reactor power. The actual low power setpoint had not been determined and may be limited by material temperature limitations in certain plant locations, turbomachinery performance considerations, and/or PCAD subsystem design considerations.

**Table 8-4: System parameters using reactor outlet temperature and Brayton unit speed to reduce reactor power.**

| Electrical Power Level | 100% | 50% | 25% |
|---|---|---|---|
| Brayton unit System "A"* | | | |
| Compressor Inlet | 374 K | 342 K | 319 K |
| Compressor Outlet | 515 K | 415 K | 366 K |
| Reactor Inlet | 880 K | 877 K | 855 K |
| Reactor Outlet | 1145 K | 1057 K | 991 K |
| Turbine Outlet | 920 K | 929 K | 908 K |
| Gas Cooler Inlet | 564 K | 477 K | 431 K |
| Shaft Speed | 45000 RPM | 32115 RPM | 25982 RPM |
| Electrical Power | 132kWe | 66 kWe | 33 kWe |
| Heat Rejection System | | | |
| 7 – Radiator Inlet | 522 K | 425 K | 374 K |
| 8 – Radiator Outlet | 363 K | 340 K | 319 K |
| Reactor | | | |
| HeXe mass flow rate | 3.77 kg/s | 2.9 kg/s | 2.28 kg/s |
| Average Fuel Temperature | 1157 K | 1061 K | 992 K |
| Power | 533 kWt | 282 kWt | 171 kWt |
| Cycle Efficiency | 24.7% | 23.4 % | 19.3% |

### 8.6.5 Reactor Shutdown

Shutdown assumptions for the flight unit and the GTR are significantly different and are discussed separately. Flight unit shutdown procedures would be required to address problems noted during initial startup. The Ground Test Reactor requires shutdown procedures commensurate with the need to test, maintain and protect this power plant.

#### 8.6.5.1 Flight Unit Shutdown

If a reactor start-up is halted during commissioning (prior to ejection of the solar panels), the solar panels may be used to provide electrical power to resume the startup, or for a complete restart if necessary. However, following commissioning (after ejection of the solar panels), a reactor shutdown would result in a loss of the spaceship. Current plans do not include a provision for a scram (rapid shutdown) mechanism on the slider drives because scram capability is not needed for the deep space mission. Therefore, a shutdown (if performed) would be accomplished by withdrawing the reflectors using the stepper motor drives (or rotating drums) to remove reactivity from the core. As soon as the reflector segments start to withdraw, the coolant temperature will begin to drop. As temperature drops, PLR load will decrease in order to maintain speed until there is no more PLR load to shed. At that point, Brayton unit speed and voltage will decrease until the power converters that feed the 28 Vdc bus and the reactor controllers drop out. When that occurs, outward slider motion would stop unless battery power or solar panels were still available to complete the withdrawal. It is noted that there was no mission requirement to shutdown the reactor, and thus there were no plans for this sequence at the time of project cancellation.

### 8.6.5.2 Ground Test Reactor Shutdown

The Ground Test Reactor would have to be designed with normal shutdown, emergency shutdown, and restart capabilities. These would be required for normal test and maintenance evolutions, as well as for reactor protection from potential casualties and engineered safeguards for a potential reactor accident condition.

Normal shutdown of the GTR could be accomplished by withdrawing the moveable reflectors and/or inserting the safety rod(s). The GTR will likely also need a rapid shutdown function for reactor emergencies. The form of this shutdown function has not yet been determined and requires consideration of such aspects as public safety requirements, single-failure criteria and the desire for the reactor module to be as prototypical as possible to the flight unit.

Shutdown would cause a reduction in the turbine inlet temperature of the Brayton unit energy converters. This would reduce their power output, and require that power be supplied from the test facility to motor their alternators for decay heat removal (similar to the beginning of the reactor startup sequence). The Brayton units could be continuously motored to provide decay heat removal, or a separate circulator could be added to the prototype support facility to provide the function and allow the Brayton units to be secured. The prototype support facility would also need to provide a continuous source of power to the 28 Vdc bus for uninterrupted power to the reactor controllers to completely withdraw the sliders and allow for continuous reactor monitoring after the shutdown.

## 8.7 Abnormal Operations and Casualties

This section qualitatively identifies indications the plant might use to identify abnormal or casualty events along with the desired plant response. Instrumentation that may be necessary for control or monitoring of plant parameters during these events is also identified.

### 8.7.1 Inadvertent Valve Closure

It is extremely unlikely for a solenoid operated valve to inadvertently close. The most likely cause would be failure of the solenoid coil or the control circuitry. However, the valve could be designed so that it would fail as is. Other actions to minimize failure could also be taken, such as redundancy in the control circuitry. Although there is an extremely low probability of inadvertent valve closure, closure of a valve in an operating loop potentially would have serious plant ramifications. If valve closure causes loss of a Brayton unit, electrical loads may be lost if the subject valve cannot be re-opened, or another Brayton unit started.

Indications and plant response will vary depending on whether the affected valve is associated with a Brayton unit turbine/compressor, or alternator cooling line (for multiple Brayton unit configurations). Closure of an inlet or outlet valve to a Brayton unit turbine or compressor causes loss of loop flow and consequent loss of the Brayton unit. Closure of a valve in the alternator cooling line will cause overheating of the alternator and potential loss of delivered electrical power. Evaluations have been performed for a two loop plant with one loop operating and the other is an installed spare, and for a three loop plant with two operating and one spare loops.

### 8.7.1.1 Turbine or Compressor Isolation Valve

#### 8.7.1.1.1 Initial Indications

For a two loop plant with one operating Brayton unit, the following initial indications are expected to signify closure of a turbine or compressor isolation valve. Subsequent indications that might occur if this event were to continue are not listed.

- Valve position indication for the affected valve indicates shut or does not indicate open
- Loop flow rate reduction or complete loss of flow
- Brayton unit speed decreasing due to loop mass flow rate below the capability of the Brayton unit speed controller
- Alternator output reduction due to reduced Brayton unit speed
- Primary temperature increasing due to reduced coolant mass flow rate though the core

Inadvertent closure of a Brayton unit turbine or compressor isolation valve is less severe for a three loop plant with two operating Brayton units than for a two loop plant with only one operating Brayton unit. With two Brayton units initially operating, loss of one Brayton unit does not cause a potentially mission ending complete loss of electrical power. The following initial indications are expected for this scenario.

- Valve position indication indicates shut or does not indicate open
- Primary flow rate reduction to 50% flow
- Brayton unit speed decreasing in affected loop due to loop mass flow rate below the capability of the Brayton unit speed controller
- Alternator output reduction due to reduced Brayton unit speed; combined output 50% of rated
- Primary temperature increasing due to reduced coolant mass flow rate though the core

#### 8.7.1.1.2 Desired Plant Response

An attempt should be made to re-open the valve as soon as it no longer indicates fully open. If the affected valve can be successfully re-opened prior to loss of the Brayton unit, no further immediate actions may be required. If the valve cannot be re-opened, then the following plant response would be desired regardless of whether one or two Brayton units were initially operating.

- Reduce plant electrical loads to those within the capacity of the remaining Brayton unit(s)
- Open the isolation valve associated with the idle (spare) Brayton unit
- Motor spare Brayton unit, observing heat-up rate limitations
- Transition spare Brayton unit to self-sustaining, switch to PLR voltage control
- Secure the affected Brayton unit

#### 8.7.1.1.3 Required Plant Instrumentation

The following instrumentation is desired to support implementation of the preceding strategy.

- Valve position or loop flow indication
- Alternator output voltage and current or Brayton unit shaft speed
- Coolant temperature leaving the core (entering the Brayton unit)
- Electrical bus voltage indication

### 8.7.1.2 Alternator Cooling Isolation Valve

Inadvertent closure of a Brayton unit alternator cooling isolation valve is serious because of the potential loss of electrical output due to alternator overheating and damage. However, this transient is less severe than loss of a Brayton unit turbine or compressor isolation valve as more time is available to take action. This transient does not affect Brayton unit turbine or compressor performance, but causes overheating of the associated alternator and eventual alternator damage if the overheating is not corrected.

#### 8.7.1.2.1 Initial indications

The following initial conditions are expected regardless of whether a two loop plant with one operating Brayton unit or a three loop plant with two operating Brayton units is chosen.

- Valve position indication indicates shut or does not indicate open
- Alternator stator temperature increasing

#### 8.7.1.2.2 Desired plant response

An attempt should be made to re-open the alternator cooling line isolation valve as soon as it no longer indicates fully open. If the affected valve can be successfully opened prior to alternator damage, no further immediate actions will be required. If the valve cannot be opened, then the alternator will likely fail, causing a loss of electrical power from that unit. An idle (spare) Brayton unit, if available, will need to be started and electrical loads shifted to maintain electrical power continuity to the Plant. The following plant response would thus be desired if the subject valve cannot be opened regardless of whether one or two Brayton units were initially operating.

- Open the isolation valve associated with the idle (spare) Brayton unit
- Motor spare Brayton unit, observing heat-up rate limitations
- Transition spare Brayton unit to self-sustaining, pick up electrical load
- Secure the affected Brayton unit

#### 8.7.1.2.3 Required Plant Instrumentation

The following instrumentation is desired to support implementation of the preceding strategy.

- Valve position indication
- Alternator stator temperature
- Loop flow indication
- Alternator output voltage and current
- Brayton unit shaft speed
- Coolant temperature leaving the core (entering the Brayton unit) to verify proper loop flow rate

### 8.7.2 Loss of Brayton unit Speed Control

A controller is required to maintain Brayton unit shaft speed constant as load varies. Constant Brayton unit speed is desirable to maintain maximum Plant efficiency. Without a speed controller, a reduction in load could cause a significant increase in Brayton unit speed, possibly to the point of overspeed and damage. Similarly, an increase in load could cause a significant reduction in Brayton unit speed, possibly to below self-sustaining. Loss of Brayton unit speed control must be identified

and responded to promptly to prevent potentially catastrophic equipment damage or loss of electric power.

### 8.7.2.1 Indications

- Brayton unit speed outside of the established normal band and moving away from normal limits
- Brayton unit speed rate of change exceeding established normal limit

### 8.7.2.2 Desired Plant Response

It is necessary to secure the Brayton as soon as practicable to preclude loss of the Brayton unit, reduction in core cooling, and loss of associated electrical power. A spare Brayton unit, if available, should be started and electrical loads transferred accordingly. The following steps are thus required.

- Open the isolation valve associated with the idle (spare) Brayton unit
- Motor spare Brayton unit, observing heat-up rate limitations
- Transition spare Brayton unit to self-sustaining, switch to PLR voltage control
- Secure the affected Brayton unit

### 8.7.2.3 Required Plant Instrumentation

The following instrumentation is desired to support implementation of the preceding strategy.

- Brayton unit shaft speed
- Valve position indication
- Loop flow indication
- Alternator output voltage and current
- Coolant temperature leaving the core (entering the Brayton unit) to verify proper loop flow rate

### 8.7.3 Mechanical Loss of Brayton unit

There are potentially serious plant ramifications associated with a loss of a Brayton unit. There are a number of ways in which a Brayton unit fail, such as inadvertent valve closure, overspeed due to loss of load, electrical failure, gas leakage, etc. This section focuses only on Brayton unit failure due to mechanical causes.

Brayton unit failure results in loss of alternator electrical output, reduced loop flow and reduction in core cooling. Initial Indications may vary depending on the specific cause of Brayton unit failure. For a single Brayton unit plant, this event is mission ending. For multiple Brayton unit plants, this event still represents a significant plant transient. To maintain continuity of electrical power to Plant loads, the loads must be rapidly transferred to another operating Brayton unit or loads shed until plant capacity is restored (either by starting an idle Brayton unit or raising the capacity of the operating Brayton unit). For plant configurations such as the 3-3-3 or 4-4-4 that have spare Brayton units, the spare Brayton unit is started and electrically loaded. For plant configurations such as the 2-2-2s that have alternate state points, increase the speed and temperature of the operating Brayton unit until the higher power operating state point is obtained, and then supply plant electrical loads.

Evaluations have been performed assuming a two loop plant with one loop operating and the other is an installed spare, and a three loop plant with two operating and one spare loop. Indication trends are

generally the same regardless of the number of Brayton units running. However, the casualty is more severe if fewer Brayton units are initially operating because a greater percentage of total loop flow is lost.

### 8.7.3.1 Bearing/Wheel Rub

#### 8.7.3.1.1 Indications

- Rapid Brayton unit shaft speed reduction with associated loss of loop flow rate
- Loss of Brayton unit alternator output
- System pressure decrease due to loss of Brayton unit compressor
- Primary temperature increasing due to reduced coolant mass flow rate though the core
- Autonomous control action (if the autonomous reactor control system provides action for a complete loss of flow)

#### 8.7.3.1.2 Desired Plant Response

- Reduce reactor power by inserting negative reactivity (if necessary)
- Secure affected Brayton unit by closing any valves required in failed Brayton unit loop
- Open the isolation valve associated with the idle (spare) Brayton unit
- Motor spare Brayton unit, observing heat-up rate limitations
- Transition spare Brayton unit to self-sustaining, pick up electrical load
- Increase reactor power by inserting positive reactivity (as required)

#### 8.7.3.1.3 Required Plant Instrumentation

The following instrumentation is desired to support implementation of the preceding strategy.

- Brayton unit speed
- Loop flow indication
- Alternator output voltage and current
- Coolant temperature leaving the core (entering the Brayton unit) to verify proper loop flow rate
- Reactor power
- Valve position indication

### 8.7.3.2 Brayton Unit Shaft Shear

Shaft shear represents a total and immediate failure of the Brayton unit regardless of whether the shear occurs between the turbine and compressor wheels, or between the compressor and the alternator. Figure 8-12 shows an example of a conceptual design of a Brayton unit turboalternator (Hamilton Sundstrand concept design, Reference 8- 2).

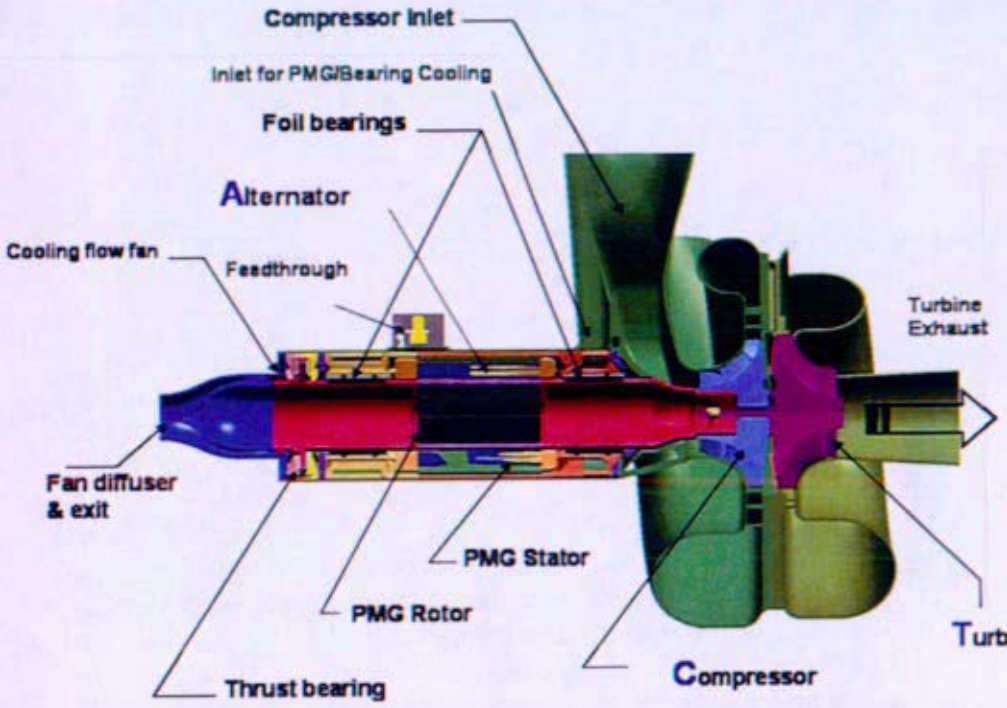



**Figure 8-12: Example of a Space Brayton Unit Turboalternator Conceptual Design (Hamilton-Sundstrand)**

Structural support for the shaft is provided by the thrust bearing and the two foil bearings. The Brayton unit operates at approximately 45000 rpm. The unit must therefore be precisely balanced. Clearances in the unit must be very small to maintain high efficiency. The clearance between the turbine/compressor wheels and the casing is approximately 5-8 mils. Similarly, the clearance between the shaft and the foil bearing during operation is approximately 1 mil. Shaft shear significantly changes the balance of the Brayton unit, and causes moment loads on the bearings. There will be significant contact between the turbine/compressor wheels and the casing, and between the shaft and the bearings.

Indications, desired plant response and required instrumentation is thus the same as for Section 8.7.3.1, Bearing/Wheel Rub.

### 8.7.4 Gas Leaks - Flight Unit

Gas leaks to ambient are potentially mission ending casualties. A slight loss of gas, perhaps associated with a very small leak or gas migration, will result in reduced plant efficiency. However, a more significant loss of gas will render the Brayton unit(s) inoperable, resulting in a loss of electrical power, core cooling and a loss of spaceship. It is thus imperative that all reasonable precautions and design features be implemented to preclude gas leakage.

If a leak were to occur, it is more likely to occur in components with high thermal stress that can lead to cracking, such as the recuperator or gas cooler. Leaks are also more likely to develop at locations with seals, such as valves, and at areas of discontinuity, such as weld joints, especially bimetallic weld joints. The probability that a leak will develop can thus be greatly minimized by utilization of welded caps on valves, seamless piping, minimizing the number of pipe joints and bi-metallic joints, and a carefully developed, and thoroughly implemented inspection program.

Currently there are no valves designed for gas service at the operating temperatures of a space reactor that will have zero seat leakage over any significant length of time. While it may be possible to reduce the leakage rate in a multi-Brayton unit plant by shutting an isolation valve, it is currently not be possible to completely arrest a leak if it should develop. In general, any small leak that develops will initially reduce plant efficiency, and over time will become mission ending. A gas reservoir could be used to prolong plant life in case of a leak. However, the reservoir would add mass and volume to the plant along with additional complexity.

### 8.7.4.1 Indications

The following initial conditions are expected regardless of whether a two loop plant with one operating Brayton unit or a three loop plant with two operating Brayton units is chosen.

- Primary pressure decreasing due to loss of gas mass
- Primary plant temperature increasing due to less mass of gas available to cool the core
- PLR load on the Brayton unit decreasing

As primary plant temperature drops and less gas inventory exists in the system, the Brayton unit will not be able to keep up with the applied electrical load, and so the tendency will be for it to slow down. The PLR load on the Brayton unit is thus expected to be decreasing to maintain Brayton unit speed. At some point however, there will be no more PLR load on the Brayton unit to reduce, and at that point, Brayton unit speed and voltage will decrease. The Brayton unit speed and voltage decrease will continue until the power converters drop out that feed the 28 Vdc bus and the reactor controllers, resulting in loss of electrical power.

### 8.7.4.2 Desired Plant Response

Currently, the NRPCT does not believe it is practical to implement a leak isolation procedure for a gas cooled space nuclear reactor.

The following strategy closes isolation valves in an attempt to reduce the gas leakage rate, extending plant life. A spare Brayton unit would be started if available, and electrical loads would be shifted to it for continuity of electrical power. If a gas makeup system was provided, it would be utilized to restore gas mass and pressure within the Plant. However, the ability to successfully execute such a strategy requires three assumptions:

- Small leak rate
- Ability to quickly identify the leak
- Ability to quickly isolate the leak

It becomes increasingly difficult to identify a leak as its leak rate decreases. Thus, this strategy also requires instrumentation of sufficient sensitivity and response time.

For a two loop plant with one operating Brayton unit, the following would be the desired plant response.

- Reduce reactor power to prevent exceeding thermal limits due to reduced coolant flow
- Open the isolation valve associated with the idle (spare) Brayton unit
- Start the idle Brayton unit in the spare loop
- Shift electrical loads to the second Brayton unit
- Restore normal reactor thermal power level
- Isolate the first Brayton unit loop by closing the Brayton unit turbine inlet and compressor outlet isolation valves
- Observe pressure changes in the isolated loop for indications of a gas leak

For a three loop plant with two operating Brayton units, the following would be the desired plant response.

- Reduce reactor power to preclude thermal limits from being exceeded due to reduced coolant flow
- Open the isolation valve associated with the idle (spare) Brayton unit
- Start the idle Brayton unit in the spare loop using the power supply provided for that purpose
- Shift electrical loads to the started Brayton unit
- Sequentially isolate loops while monitoring parameters until the affected loop is identified and isolated (these parameters need to be distinguished from normal changes in system pressure due to temperature changes)
- Restore normal reactor thermal power level

### 8.7.4.3 Required Plant Instrumentation

The following instrumentation will be required to implement the preceding strategies.

- Loop pressure instruments
- Reactor power indication
- Valve position indication
- Alternator output voltage and current
- Coolant temperature leaving the core (entering the Brayton unit) to verify proper loop flow rate

## 8.7.5 Stuck Open Valve in Idle Loop (Partial Loss of Flow)

### 8.7.5.1 Indications

- Reverse flow in idle loop caused by pressure drop across the reactor
- Decrease in reactor coolant flow since some is reverse flowing through the idle loop
- Rise in TCO, CIT, and other temperatures if the idle loop is cold
- Increase in temperature rise across reactor due to reduced reactor coolant flow
- Operating compressor outlet pressure decreasing due to lower overall system resistance

### 8.7.5.2 Desired Plant Response

- Attempt to shut the stuck open isolation valve. If this is not possible, shut an alternate valve to preclude reverse flow through the idle loop.
- The preceding should be performed rapidly to minimize potential Brayton unit damage from backflow, and to prevent exceeding reactor core thermal limits

### 8.7.5.3 Required Plant Instrumentation

- Loop flow sensors
- Loop temperature sensors (TCO, CIT, others)
- Reactor inlet and outlet temperature sensors
- Loop pressure sensors (compressor outlet)

## 8.7.6 Partially Shut Valve in Operating Loop

### 8.7.6.1 Indications

- Large pressure drop in affected loop due to flow restriction
- Reduced load on PLR or Brayton unit speed decrease due to flow restriction
- Reduced alternator output
- Unbalanced loop flow rates due to equalization of pressure drops in each loop
- Higher steady state pressure drop in both loops
- Mismatched temperature change across loop components due to unbalanced loop flow rates affecting heat exchanger performance

### 8.7.6.2 Desired Plant Response

- Attempt to open the partially shut valve
- If the valve can't be fully opened, start a spare Brayton unit if available and supply electrical power.
- The preceding should be performed rapidly to avoid exceeding reactor core thermal limits

### 8.7.6.3 Required Plant Instrumentation

- Multiple pressure sensor locations per loop
- PLR load reporting
- Alternator power output sensors
- Loop flow sensors
- Loop temperature sensors

### 8.7.7 Loss of HRS Radiator Area

#### 8.7.7.1 Indications

- Higher water temperatures in the gas cooler due to less heat rejection in the radiator
- Increased CIT due to hotter water temperature at the outlet of the gas cooler
- Increased alternator temperature due to hotter water temperature at the outlet of the gas cooler

#### 8.7.7.2 Desired Plant Response

- Increase $T_{hot}$ consistent with temperature limits to make up for loss of radiator area.
- Do not exceed $T_{cold}$ and/or $T_{hot}$ limits
- Do not exceed alternator or bearing temperature limits

#### 8.7.7.3 Required Plant Instrumentation

- CIT sensor
- HRS loop temperature sensors
- Alternator temperature sensors

### 8.7.8 Loss of Flow in a HRS Loop

#### 8.7.8.1 Indications

- Loss of flow indication in HRS loop
- Increase in CIT and other loop temperatures due to loss of gas cooler heat transfer
- Increase in gas cooler water temperatures

#### 8.7.8.2 Desired Plant Response

- Do not exceed temperature limits
- Ability to continue using Brayton unit, if pump failure (carry a spare pump)
- Ability start a spare Brayton unit and continue mission (if leak)

#### 8.7.8.3 Required Plant Instrumentation

- HRS loop flow meters
- Loop temperature sensors
- HRS loop temperature sensors

### 8.7.9 Inadvertent Slider Motion

#### 8.7.9.1 Indications

- Increase or decrease in reactor power (if within the range of detectors).

- Increase or decrease in startup rate (unless detectors are saturated).
- Change in slider segment position indication.
- Change in coolant temperature (if above the POAH).
- Change in plant pressure (if above the POAH). This effect may be detectable only if all Brayton units are idle; i.e., during reactor startup.
- Change in PLR loading. This effect is due to the change in plant efficiency as the control system restores a steady operating state at a higher or lower turbine inlet temperature.
- Change in voltage or current to slider segment controllers or motors.

### 8.7.9.2 Desired Plant Response

- The reactor control system senses the accident from one or more of the above indications and takes action to stop or reverse reflector motion as needed.

### 8.7.9.3 Required Plant Instrumentation

- Reactor power indication
- Slider segment position indication
- Loop pressure instruments
- Loop coolant temperature
- Alternator output voltage and current

## 8.8 References

**8- 1:** SPP-67410-0013 / B-SE(RE)-0003, "Prometheus Reactor Preconceptual Design Report", dated 01/27/2006

**8- 2:** NGST Report 04.1F102.JM.006, "Task 2 Conceptual Design Summary Report, Jupiter Icy Moons Orbiter (JIMO) Phase A Study, JPL Contract N. 120530" dated 8/13/04.

**8- 3:** Prometheus Project, Project Requirements Document, Preliminary; JPL Document 982-00056, Rev. 1, dated 12/16/04

**8- 4:** SPP-SPPS-0031,"Transmittal of the Prometheus Space Nuclear Power Plant Simulink Dynamic Model Description and Analysis", to be issued

(Intentionally Blank)

# Section 9
# Component Descriptions

(Intentionally Blank)

# Component Descriptions

## Table of Contents

9 Component Descriptions ..... 10
9.1 Brayton Turboalternator ..... 14
9.1.1 Summary and Conclusions ..... 14
9.1.2 Introduction ..... 15
9.1.3 Turbine Assembly ..... 20
9.1.3.1 Turbine Efficiency ..... 21
9.1.3.2 Turbine Assembly Materials ..... 24
9.1.4 Compressor Assembly ..... 29
9.1.4.1 Compressor Efficiency ..... 30
9.1.4.2 Compressor Assembly Materials ..... 31
9.1.5 Alternator Assembly ..... 32
9.1.5.1 Alternator Description ..... 32
9.1.5.2 High Speed Alternator Design Challenges ..... 33
9.1.5.3 Dual Alternator Design Option ..... 33
9.1.6 Bearing Assembly ..... 34
9.1.7 Component & System Integration ..... 36
9.1.7.1 Shaft Speed Control ..... 36
9.1.7.2 Rotordynamic Stability ..... 37
9.1.8 Failure Modes ..... 38
9.1.8.1 Turbomachinery Failure Modes ..... 39
9.1.8.2 Alternator Failure Modes ..... 41
9.1.8.3 Bearing Failure Modes ..... 43
9.1.9 Future Development Needs ..... 45
9.1.9.1 Turbomachinery Development ..... 45
9.1.9.2 Alternator Development ..... 45
9.1.9.3 Bearing Development ..... 45
9.2 Recuperator ..... 47
9.2.1 Summary and Conclusions ..... 47
9.2.2 Introduction ..... 47
9.2.2.1 General Configuration ..... 47
9.2.2.2 Recuperator Benefits in a Closed Brayton Cycle ..... 51
9.2.2.3 Recuperator Component Requirements ..... 53
9.2.2.4 Design/Fabrication Considerations ..... 53
9.2.2.5 Potential Materials of Construction ..... 55
9.2.2.6 Recuperator Sizing Evaluations ..... 58
9.2.3 Design Tradeoffs/Performance Estimates ..... 62
9.2.3.1 Heat Transfer Coefficient Uncertainty Effects ..... 62
9.2.3.2 Flow Maldistribution Effects ..... 66
9.2.4 Failure Modes ..... 81
9.2.4.1 Leakage to Space ..... 81
9.2.4.2 Interchannel Leakage ..... 82
9.2.5 Future Development Needs ..... 86
9.3 Gas Cooler ..... 87
9.3.1 Summary and Conclusions ..... 87

9.3.2 Component Description ..... 88
9.3.3 Development Program ..... 91
9.3.4 Design Configuration ..... 92
9.3.4.1 Compact Heat Exchangers ..... 92
9.3.4.2 Shell and Tube ..... 94
9.3.5 Materials ..... 95
9.3.6 Heat Rejection System Fluid – Impacts of Using NaK-55 Instead of Water ..... 97
9.3.7 Reliability ..... 99
9.3.8 Gas Cooler Sizing ..... 100
9.3.8.1 1-1-1 Brayton rated at 200 kWe ..... 101
9.3.8.2 2-2-2 Braytons rated at 100kWe (2 on at full capacity) ..... 101
9.3.8.3 2-2-2 Braytons rated at 200kWe (1 on, 1 off) ..... 102
9.3.8.4 2-2-2s Braytons rated at 200kWe (2 on at reduced capability) ..... 102
9.3.8.5 3-3-3 Braytons rated at 100kWe (2 on, 1 off) ..... 103
9.3.8.6 4-4-4 Braytons rated at 100kWe (2 on, 2 off) ..... 103
9.3.8.7 2-1-1 100 kWe Braytons (2 on) – Same gas cooler as 1-1-1 ..... 104
9.3.8.8 2-1-1 200 kWe Braytons (1 on, 1 off) – Same gas cooler as 1-1-1 ..... 104
9.3.8.9 2-1-1s Braytons rated at 200kWe (2 on at reduced capability) ..... 105
9.3.8.10 3-1-1 Braytons rated at 100kWe (2 on, 1 off) - Same as 1-1-1 ..... 105
9.3.9 Mass Summary ..... 106
9.3.10 Future Work ..... 108
9.4 Piping ..... 109
9.4.1 Summary and Conclusions ..... 109
9.4.2 Background ..... 109
9.4.3 Pipe Sizing Calculations ..... 111
9.4.4 Pressure Drop Calculations ..... 113
9.4.4.1 Pressure Losses Due to Friction ..... 113
9.4.4.2 Pressure Losses Due to Dividing Flow Junctions ..... 114
9.4.4.3 Pressure Losses Due to Combining Flow Junctions ..... 115
9.4.4.4 Pressure Losses Due to Pipe Bends ..... 116
9.4.4.5 Pressure Losses Due to Valves ..... 117
9.4.4.6 Percentage ΔP/P Calculation ..... 117
9.4.5 Piping Mass Estimates ..... 118
9.4.5.1 Hydraulic Analysis and Mass Estimate – Results ..... 119
9.4.5.2 Hydraulic Analysis and Mass Estimates – Diameter Sensitivity ..... 119
9.4.6 Hot Leg Piping ..... 120
9.4.6.1 Hot Leg Piping Requirements ..... 120
9.4.6.2 Baseline - Internally Insulated Hot Leg Piping Concept ..... 121
9.4.6.3 Hot Leg Piping Development ..... 122
9.4.7 Future Development Needs ..... 135
9.5 Valves ..... 137
9.5.1 Summary and Key Conclusions ..... 137
9.5.2 Valve Locations ..... 137
9.5.3 Valve Function ..... 138
9.5.4 Functional Requirements and Design Challenges ..... 139
9.5.4.1 Key Design Goals ..... 139
9.5.4.2 Service Life ..... 140
9.5.4.3 Valve Operational Pressure Drop ..... 140

9.5.4.4 Fluid Leakage to Ambient ..... 143
9.5.4.5 Valve Seat Leakage ..... 143
9.5.4.6 Operational Conditions/Environment ..... 144
9.5.4.7 Environmental/Ambient Conditions ..... 144
9.5.4.8 Valve Operators ..... 145
9.5.4.9 Materials of Construction ..... 145
9.5.4.10 Design Basis ..... 145
9.5.4.11 Pipe Diameter ..... 146
9.5.4.12 Operational Cycles ..... 146
9.5.4.13 Thermal Cycles ..... 146
9.5.4.14 Launch and Operating Loads ..... 146
9.5.4.15 Position Indication ..... 147
9.5.5 Potential Failure Modes ..... 147
9.5.5.1 Seat Leakage ..... 147
9.5.5.2 Leakage to Ambient ..... 147
9.5.5.3 Sticking in the Shut Position/Failure to Open ..... 147
9.5.5.4 Sticking in the Open Position/Failure to Close or Partial Closure ..... 148
9.5.5.5 Wear Particles/Material Introduction to the Fluid ..... 148
9.5.5.6 Electromechanical Operation ..... 148
9.5.6 Summary ..... 148
9.6 Heat Rejection Segment ..... 151
9.6.1 Summary and Conclusions ..... 151
9.6.2 Segment Description ..... 152
9.6.2.1 Heat Transport Loop Assembly ..... 155
9.6.2.2 Radiator Panel Assembly ..... 156
9.6.3 Failure Modes ..... 160
9.6.3.1 Launch / Deployment Failure Modes ..... 160
9.6.3.2 Normal Operation Failure Modes ..... 160
9.6.4 Future Development Needs ..... 161
9.7 Thermal Stress Analysis of Hot Leg Piping ..... 163
9.7.1 Summary and Conclusions ..... 163
9.7.2 Analysis Results ..... 164
9.7.3 Thermal Stress Model ..... 168
9.7.3.1 Model Geometry ..... 168
9.7.3.2 Assumptions ..... 170
9.7.3.3 Loads and Boundary Conditions ..... 171
9.7.3.4 Material Properties ..... 173
9.7.3.5 Section Moment Calculation ..... 174
9.7.3.6 Method to Evaluate Piping Stress Limits ..... 174
9.7.4 Piping Modal Analysis ..... 176
9.7.5 Checks ..... 176
9.8 References ..... 177

## List of Figures

Figure 9-1: Energy Conversion Cycle and Components ..... 11
Figure 9-2: Example of a Space Brayton Turboalternator Conceptual Design ..... 16
Figure 9-3: Turboalternator Mass vs. Electrical Power ..... 19
Figure 9-4: Inward Flow Radial Turbine Schematic ..... 20
Figure 9-5: IFR Turbine Geometry Variation versus Specific Speed ($\Omega_S$) for Maximum Static Efficiency (Reference 9- 13) ..... 22
Figure 9-6: Representative IFR Turbine Distribution of Losses versus Specific Speed for Maximum Total-to-Total Efficiency (Reference 9- 13) ..... 23
Figure 9-7: IFR Turbine Static Efficiency ..... 24
Figure 9-8: Turbine Wheel Allowable Creep Strength ..... 26
Figure 9-9: Hot leg to Turbine Casing Joint ..... 26
Figure 9-10: NASA Glenn Turbine Creep Analysis ..... 27
Figure 9-11: Centrifugal Compressor Schematic ..... 29
Figure 9-12: Compressor Static efficiency vs. Specific Speed and Corrected Mass Flow ..... 31
Figure 9-13: Alternator detailed picture ..... 32
Figure 9-14: Gas foil bearing diagram ..... 35
Figure 9-15: Power Loss versus Percent Load Capacity (Reference 9- 30) ..... 36
Figure 9-16: Typical plate fin structure of a recuperator. ..... 49
Figure 9-17: Examples of compact heat exchanger fin configurations ..... 50
Figure 9-18: Simplified temperature entropy diagram illustrating the effects of increased compressor pressure ratio on recuperated energy (assumes 100% effective recuperator designs). ..... 52
Figure 9-19: Hamilton Sundstrand recuperator assembly (from Reference 9- 54). ..... 60
Figure 9-20: The effects of reductions in the overall heat transfer coefficient on the effectiveness of the recuperator for various baseline thermal ratings. ..... 64
Figure 9-21: The effects of reducing the overall heat transfer coefficient on the heat transfer rate of the recuperator for various thermal ratings. ..... 65
Figure 9-22: System efficiency and power output as a function of recuperator effectiveness. ..... 66
Figure 9-23: Velocity and dynamic pressure at the inlet pipe conditions as a function of inlet pipe inner diameter for the high and low pressure sides of the recuperator. ..... 70
Figure 9-24: As-built Mini_BRU recuperator (from Reference 9- 49). ..... 70
Figure 9-25: Mini-BRU recuperator internal flow configuration (from Reference 9- 49) ..... 71
Figure 9-26: Exit temperature map for the high pressure side of the Mini-BRU recuperator (based on a 1 dimensional, counter flow TRACE model with air as the working fluid). ..... 72
Figure 9-27: Exit temperature map for the low pressure side of the Mini-BRU recuperator (based on a 1 dimensional, counter flow TRACE model with air as the working fluid). ..... 72
Figure 9-28: Recuperator effectiveness as a function of various flow distribution maps (see Table 9-13 for corresponding flow distribution maps). ..... 74
Figure 9-29: (a) Mini-BRU core geometry generated with Pro-Engineer, (b)corresponding FLUENT model geometry for the low pressure side of the recuperator. ..... 76
Figure 9-30: Inlet flow path lines for the (a) low pressure side and (b) high pressure side of the recuperator. ..... 77
Figure 9-31: Horizontal cross sections of velocity magnitude for the (a) low pressure side and (b) high pressure side of the recuperator ..... 78
Figure 9-32: Velocity magnitudes at the recuperator core inlet and exit faces for the (a) low pressure side and (b) high pressure side of the recuperator. ..... 79

Figure 9-33: Mass flow fraction plot of the high pressure and low pressure sides of the recuperator. ....80
Figure 9-34: Estimated effects of recuperator interchannel leak size on Brayton cycle performance. (Modeling Assumptions for Symbols: (1) Single unit Brayton generating 100 kWe (2) Turbine inlet temperature is fixed at 1150K (3) Leakage does not impact turbine flow (4) Reduced compressor/turbine efficiencies are not considered in the impact on power output (5) Changes in pressure losses are not considered in the impact on power output.)....83
Figure 9-35 Initial Development Program Heat Balance....89
Figure 9-36 Baseline Gas Cooler Concept (Hamilton Sundstrand, Reference 9- 37) ....90
Figure 9-37: Nominal Direct Gas Concept System Schematic with Operating Conditions ....110
Figure 9-38: Dividing Y-Junction Schematic....114
Figure 9-39: Dividing Angled-Junction Schematic ....114
Figure 9-40: Combining Y-Junction Schematic ....115
Figure 9-41: Combining Angled-Junction Schematic....115
Figure 9-42: %ΔP/P and Piping Mass Sensitivity to Pipe Outer Diameter ....120
Figure 9-43: Internally Insulated Concept....122
Figure 9-44: Inconel 617 Hollow Sphere Foam ....123
Figure 9-45: Internally Insulated Piping Concept with End Caps at the Reactor Interface ....126
Figure 9-46: Internally Insulated Piping Concept with End Caps at the Brayton Interface....127
Figure 9-47: Sensor in Gas Stream....129
Figure 9-48: Sensor in Well Concept ....130
Figure 9-49: Sensor Embedded in Insulation ....131
Figure 9-50: Pipe Wall Attachment Concept....131
Figure 9-51: Through Inlet Transmission of Ultrasonic Signal ....133
Figure 9-52: Hot Leg Piping Transient Temperature Response ....134
Figure 9-53: Typical Location of isolation and Check Valves....138
Figure 9-54: Prometheus Baseline 1 Spacecraft (NGST drawing)....152
Figure 9-55: Heat Rejection Segment Schematic (NGST drawing) ....153
Figure 9-56: Boom Length vs. Heat Rejection Radiator Area ....155
Figure 9-57: Heat Transport Loop Assembly Layout (NGST drawing)....156
Figure 9-58: Heat Pipe to Heat Transport Loop Assembly (NASA Glenn drawing)....158
Figure 9-59: Side View of the Heat Pipe to Heat Transport Loop Assembly (NASA Glenn drawing)....158
Figure 9-60: NGST Heat Pipe Geometry....159
Figure 9-61: H20 Heat Pipe Performance Capability for NGST Heat Pipe Design ....159
Figure 9-62: Wall Thickness Sensitivity: Primary Stress Intensity....165
Figure 9-63: Wall Thickness Sensitivity: Primary + Secondary Stress Intensity Range ....166
Figure 9-64: Structure Temperature Sensitivity (Titanium): Primary + Secondary Stress Intensity Range....167
Figure 9-65: Structure Temperature Sensitivity (Aluminum): Primary + Secondary Stress Intensity Range....167
Figure 9-66: Secondary Support Stiffness Sensitivity: Primary + Secondary Stress Intensity Range....168
Figure 9-67: CAD Representation of Hot Leg Piping with Reactor and Four Brayton units (Side View)....169
Figure 9-68: CAD Representation of Hot Leg Piping with Reactor and Four Brayton units (Top View)....169

Figure 9-69: ABAQUS Beam element Model with Primary Structure (Top View).....170
Figure 9-70: Equivalent Representation of Cross Section of Primary Structure in ABAQUS Model.....170
Figure 9-71: ABAQUS Beam element Model: Secondary Support to Primary Structure Results .....171

## List of Tables

Table 9-1: Summary of Component Development Needs .....12
Table 9-2: Notional Brayton Turboalternator Specifications .....17
Table 9-3: Turbine Assembly Sections.....21
Table 9-4: Compressor Assembly Sections .....30
Table 9-5: Reliability Study from Garrett Fluid Systems (Reference 9- 27) .....38
Table 9-6: Relevant Brayton Operating Experience *.....39
Table 9-7: Gas foil bearing commercial experience relative to Prometheus concept.....44
Table 9-8: Summary of recuperator operating conditions for a four Brayton/Recuperator configuration as described in Section 6. .....53
Table 9-9: Approximate initial stress (MPa) to produce creep for selected Ni-base superalloys at a temperature of 922K.....56
Table 9-10: Brazes identified for potential use in the recuperator. Nominal compositions, along with melting points are provided.....57
Table 9-11: Vapor pressures of the braze constituents at 922 K. The value for Si has been extrapolated from higher temperatures (from Reference 9- 53). .....57
Table 9-12: Comparison of geometry and operating parameters for the proposed Hamilton Sundstrand recuperator design (from Reference 9- 54) to the mass models being used by NRPCT.....61
Table 9-13: Recuperator flow distribution maps generated to assess the sensitivity of recuperator effectiveness to maldistribution.....73
Table 9-14: Recuperator data for ground based gas turbine units (from Reference 9- 66).....85
Table 9-15: Reliability study form Garrett Fluid Systems (see Reference 9- 67).....86
Table 9-16 Mass Summary for a Water Coolant Design (Total Gas Cooler Dry Mass in kg) ...106
Table 9-17: Gas Cooler Mass Estimates Scaled from a Titanium Shell and Tube Design.....107
Table 9-18: Gas Cooler Mass Estimates Scaled from a Titanium Plate-fin/chemically etched Hybrid Design without a Barrier Layer .....107
Table 9-19: Gas Cooler Mass Estimates Scaled from a Titanium Plate-fin/chemically etched Hybrid Design with a Barrier Layer .....107
Table 9-20: Gas Cooler Mass Estimates Scaled from an Inconel Shell and Tube Design .....107
Table 9-21: Gas Cooler Mass Estimates Scaled from an Inconel Plate-fin/chemically etched Hybrid Design without a Barrier Layer .....108
Table 9-22: Gas Cooler Mass Estimates Scaled from an Inconel Plate-fin/chemically etched Hybrid Design with a Barrier Layer .....108
Table 9-23 – Nominal Piping Operating Parameters .....110
Table 9-24 – Minimum Wall Thickness as a Function of .....113
Table 9-25- Hydraulic Results.....119
Table 9-26: Ball, Butterfly and Check Valve K and L/D Evaluation for Space.....142
Table 9-27: Failure Mode Summary.....149
Table 9-28: Heat Rejection Segment Parameter List for Non-Optimized System Arrangements/Heat Balances .....154
Table 9-29: Wall Thickness Sensitivity: Stress Intensity Results .....165

Table 9-30: Structure Material & Temperature Sensitivity: Primary + Secondary Stress Intensity Results ..... 166
Table 9-31: Secondary Support Stiffness Sensitivity: Primary + Secondary Stress Intensity Results ..... 168
Table 9-32: Analysis Case Summary ..... 172
Table 9-33: Curved Pipe or Elbows Calculated Stress Indices ..... 175
Table 9-34: Moment of Inertia for Pipe Sections ..... 176

# 9 Component Descriptions

This enclosure summarizes the main primary plant components of the direct gas Brayton system envisioned for Prometheus excluding the reactor and shield and also describes the heat rejection system. A simplified diagram of the direct gas Brayton system is provided in Figure 9-1. As illustrated in the figure, the working gas (potentially HeXe) is heated in the reactor. The gas then enters the turbine and expands extracting work from the gas. The gas then enters the low pressure side of the recuperator. In this component, heat from the high temperature gas exiting the turbine is exchanged with the lower temperature gas exiting the compressor. The exiting gas from the low pressure side of the recuperator passes through the gas cooler. As the gas passes through the gas cooler it is cooled by exchanging heat with the working fluid of the heat rejection system which radiates this waste heat to space. The exiting gas from the gas cooler then enters the compressor and the helium xenon is compressed. The gas exiting the compressor then enters the high pressure side of the recuperator where it is heated by exchanging heat with the high temperature gas exiting the turbine. The gas exiting the high pressure side of the recuperator then enters the core where it is heated prior to entering the gas turbine.

The components addressed in this enclosure have been studied to a conceptual level by NRPCT. The component sections specifically addressed include:

Section 9.1 Brayton Turboalternator
Section 9.2 Recuperator
Section 9.3 Gas Cooler
Section 9.4 Piping
Section 9.5 Valves
Section 9.6 Heat Rejection System
Section 9.7 Hot Leg Piping Thermal Stress Analysis

The following component sections provide a description of the component requirements, materials selection, technology maturity, failure modes, and development plan/needs. Table 9-1 provides a summary of the main future development needs identified by NRPCT for each of the component areas.

Based on the conceptual development of Brayton cycle components during the Prometheus project, NRPCT concludes that the envisioned energy conversion components have a strong industrial base, and limited technology development to allow the delivery of highly efficient, reliable deep space hardware. The established plan for component development had testing of a near prototypic energy conversion system occurring in ~3 yrs. from concept selection.

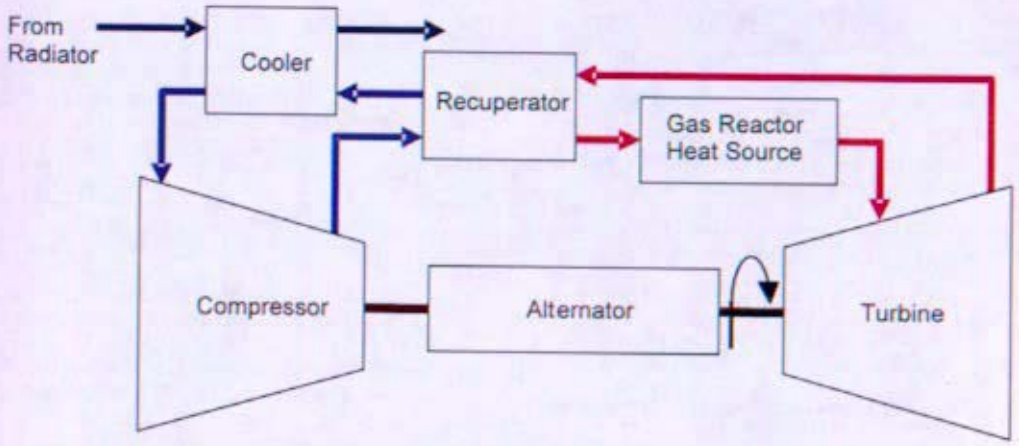
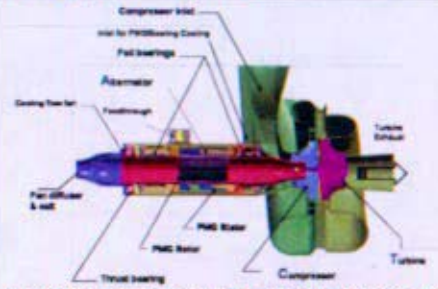
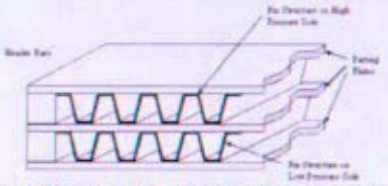
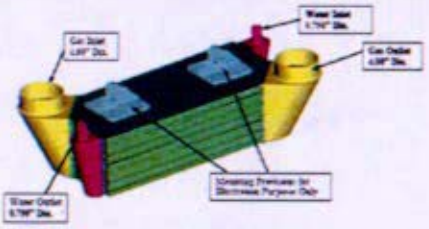



**Figure 9-1: Energy Conversion Cycle and Components**

**Table 9-1: Summary of Component Development Needs**

| Component/System | | Development Needs |
|---|---|---|
| Brayton Turboalternator |  Hamilton Sundstrand Turbine/Alternator/Compressor concept (from Reference 9- 1) | Design of the turbine scroll, turbine wheel, and turbine stator for creep over mission life<br><br>Further evaluation of the compressor efficiency performance and arrangement to the power unit<br><br>Further evaluation of gas foil bearing operation in a HeXe environment<br><br>Further assessment of alternator electrical winding and magnet tolerance to temperature/irradiation |
| Recuperator |  Typical Recuperator Internal Fin Structure | Design of a superalloy compact heat exchanger for creep and creep fatigue over the life of the mission<br><br>Accelerated testing of braze materials for structural integrity and chemical compatibility over mission life<br><br>Further evaluation of flow maldistribution effects on designs specific to the Prometheus mission |
| Gas Cooler |  Hamilton Sundstrand Gas Cooler Concept Design | Development and extensive testing to ensure no leakage from the high pressure water heat rejection system to the primary gas loop over mission life<br><br>Further evaluation and accelerated testing of proposed fabrication techniques for both printed circuit and shell and tube designs<br><br>Development of designs and inspection techniques to ensure 100% inspection of all gas/water and gas/space structural joints |
| Piping |  CAD Representation of Hot Leg Piping with Reactor and Four Brayton units (Top View) | Further development and system testing of hot leg piping and insulation<br><br>Further development of hot leg piping penetrations for measuring turbine inlet temperature |
| Valves |   | Development and extensive testing of high temperature, large diameter, long life gas valves<br><br>Development of high temperature, low pressure drop check valves |

(Intentionally Blank)

## 9.1 Brayton Turboalternator

### 9.1.1 Summary and Conclusions

The Brayton turboalternator component has been studied to a conceptual level to establish the technology design space, determine supplier capabilities, establish key system interfaces impacting the design, failure modes, and future development steps to enhance performance and increase reliability.

The Brayton turboalternator component requires some development, though the base technologies exist and have demonstrated reliable service life in aircraft and distributed power generation applications. There are four critically important future developments that would need to be completed prior to, or in parallel with, the design and test of a prototypic Prometheus Brayton turboalternator. These four development efforts include:

---

- Turbine scroll, turbine wheel, and turbine stator creep life- The turbine inlet stagnation temperature of 1150K has been an established parameter from heat balance development to allow for sufficient thermodynamic efficiency performance. Thermal management (blade conduction, "aerodynamic cooling") of the turbine wheel is needed to obtain the analyzed maximum turbine metal temperature of ~1030K for an inlet stagnation temperature of 1150K. The turbine scroll and stator blades are proposed to operate at near stagnation temperature though have lower stresses and higher allowable total creep strain. Cast Ni-based superalloys have advanced over the past thirty years and are currently envisioned to be suitable. Other material options include ceramic turbines and stator blades (SiN), and refractory turbine scrolls or internally insulated scrolls.

- Compressor efficiency performance and arrangement to the power unit – The currently envisioned compressor design isentropic efficiency is 84-85%. This efficiency greatly affects the power system efficiency and should be a focus for detailed design and potentially sub component independent testing prior to integration into a power unit. The location of the compressor on the turboalternator shaft can greatly affect the inlet diameter and fluid conditions depending whether the machine is designed as an overhung "single" disk or designed by separating the compressor from the turbine on either end of the shaft. Thermal management, rotor dynamic stability, and compressor performance would all need to be evaluated prior to making this fundamental design decision.

- Helium/Xenon gas bearing performance –The current data (load capacity, stiffness, damping, and power loss) being used in the analysis of the rotor dynamic stability, component thermal management, and power conversion efficiency is based on data obtained for air. Some models have been developed to scale this data to the high pressure He/Xe fluid, though these models differ dramatically. Future testing using high pressure bearing test rigs needs to be completed prior to development of a reference bearing/shaft design.

- Alternator electrical winding and magnets temperature/irradiation tolerance – The Prometheus Brayton alternator would have needed to operate at an ambient fluid temperature near the thermal limit of many of typical winding insulation materials. Many of the more conventional materials temperature capabilities may have not been sufficient and the higher temperature electrical insulation materials have unknown irradiation tolerances. Increased irradiation dose from fission product release or buildup of corrosion/erosion products is a driving concern for the closed loop alternator windings. An alternative is to add a supplemental cooler for the alternator cooling bleed flow or an independent cooling loop, both of which add complexity and mass to the system.

---

Other development issues included a cast to wrought Ni-base superalloy pressure boundary joint, an electrical pressure boundary penetration seal, and corrosion due to interactions between the alternator and bearing coating materials with other materials in the closed gas loop.

### 9.1.2 Introduction

The Brayton Turboalternator, also referred to as a Brayton rotating unit (BRU) or Brayton unit, is a component containing many complex, highly integrated sub-components. The major sub-components include the turbine assembly (turbine wheel, scroll, diffuser), the compressor assembly (compressor wheel, volute, diffuser), the bearing assembly (journal and thrust bearings, shaft, & thrust disk), and the alternator assembly (alternator rotor, stator windings, electrical feedthrough, and alternator pressure boundary housing). The main function of the turboalternator is to convert thermal-hydraulic energy to mechanical shaft energy, and then to electrical energy. This energy conversion process is obtained by expanding a high temperature gas through a turbine, extracting energy from the fluid and transferring this energy to mechanical energy of shaft rotation. This shaft energy is used to drive both the alternator and the compressor. The alternator is a permanent magnet generator (PMG) which uses Lorentz forces to induce current from the rotating permanent magnets located on the components rotating shaft. A significant amount of energy from the turbine (~2/3) is used to drive the compressor that raises the fluid pressure prior to being heated by the recuperator and the reactor. During startup the alternator also operates as a starter motor until the energy conversion systems temperature ratio is high enough to allow for self sustaining rotation. Figure 9-2 shows an example of a conceptual design of a Brayton turboalternator (Hamilton Sundstrand concept design, Reference 9- 1) completed as part of the JIMO spacecraft concept study.

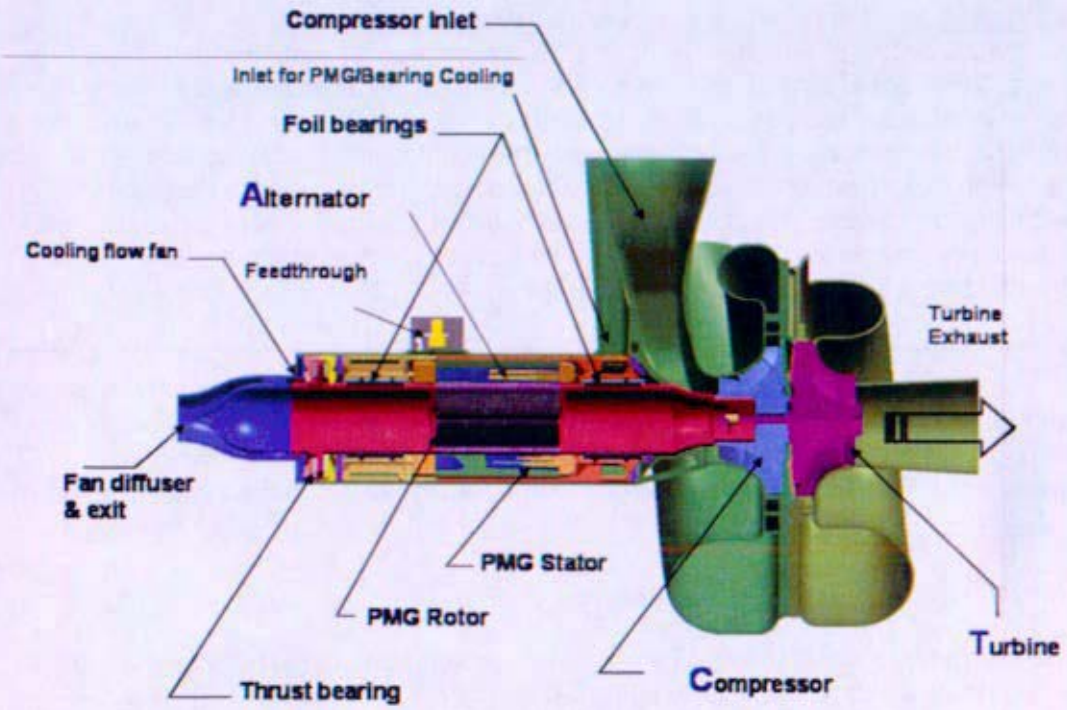



**Figure 9-2: Example of a Space Brayton Turboalternator Conceptual Design**

The NR program's role in Brayton component development was to lead in the technical specification, procurement, technical oversight, and design validation of a selected vendor's design and manufacturing processes. This responsibility was planned to be closely integrated with NASA Glenn Research Center's role in sub-component technology development and transfer to industry. The NRPCT would also be leading the component and system test programs (Section 13) which were also planned to use NASA Glenn's facilities and expertise.

Functional requirements for the component design were not fully established because the system design requirements had not yet been developed. Table 9-2 presents notional component requirements for the proposed JIMO mission using one or two Brayton unit operating at 100% power capacity to support full mission lifetime. Other proposed system architectures have operating layouts using two or three Brayton units operating at 50% or 66% power capacity with one or more combinations of part load techniques (variable speed, temperature, or gas inventory), and in the event that one Brayton unit failed, the operating unit(s) would be brought to its 100% power capacity. Operating layouts needing part load control techniques would need to balance the efficiency optimization for both the part load and full load operating conditions.

**Table 9-2: Notional Brayton Turboalternator Specifications**

| | 1 Turboalternator | 2 Turboalternators |
|---|---|---|
| Alternator Power | 196.6 kWe | 97.7 kWe |
| Alternator Frequency | 2250 Hz | 2250 Hz |
| Alternator Voltage | 440 VAC rms L-L | 440 VAC rms L-L |
| Poles | 6 | 6 |
| Alternator efficiency | 95% | 95% |
| Rotational Speed | 45,000 RPM | 45,000 RPM |
| | | |
| Coolant | HeXe with molecular weight of 31.5 gm/mol | |
| Lifetime | 20 years (10 years for JIMO) | |
| Neutron Radiation | $3 \times 10^{14}$ n/cm $^2$ | |
| Gamma Radiation [1] | 500 Mrad | |
| | | |
| Compressor Outlet Pressure | 2 MPa | 2 MPa |
| Compressor Pressure Ratio | 2.0 | 2.0 |
| Compressor Inlet Temperature | 390K | 390 K |
| Compressor efficiency | 84.7% | 84.0% |
| | | |
| Turbine Pressure Ratio | 1.83 | 1.75 |
| Turbine Outlet Pressure | 1.051 | 1.064 |
| Turbine Inlet Temperature | 1150K | 1150 K |
| Turbine efficiency | 90.0% | 88.4% |
| | | |
| Bearings | Gas Foil Bearings | |

[1] Space radiation will also provide up to 1 Grad of gamma radiation near Europa.

Past space BRU development programs (1960's – 70's) have been completed to understand the closed Brayton cycle and component performance for space nuclear & non-nuclear applications. These programs were led by NASA Glenn and were successful in achieving the component technical specifications. No closed Brayton power cycle has been operated in space, though a significant amount of turbomachinery has been operated for cooling spacecraft hardware.

Differences in the Prometheus BRU over previous space designs include an increase in power capability, lifetime, and compressor and alternator temperatures. However, since these development programs, a significant amount of additional development has occurred in aircraft industry on Brayton technology. A more comprehensive historical view of the space BRU engines and aircraft applications of small Brayton hardware can be found by researching the following development programs and applications below:

- **Brayton Rotating Unit** (BRU) (References 9- 3, 9- 4, 9- 5) – Space designed closed cycle turbine, compressor, alternator (10.5 kWe) with gas foil bearings
- **Mini-Brayton Rotating Unit** (Mini-BRU) (Reference 9- 6) – Space designed closed cycle turbine, compressor, alternator (2kWe) with gas foil bearings
- **Integrated Power Unit** (IPU) (Reference 9- 8) – Development program for an open cycle advanced APU (200kWe) with magnetic bearings.
- **Capstone Microturbine** (Reference 9- 7) – Open cycle turbine, compressor, alternator (30-200 kWe) with gas foil bearings for high efficiency distributed power generation.
- **Auxiliary Power Units** (APU) (Reference 9- 2) – Open cycle turbine, compressor, alternator (up to ~40kWe)
- **Air Cycle Machines** (ACM) – Open cycle turbine, compressor, starter motor which use gas foil bearings

Two Brayton vendors were involved in the Prometheus spacecraft project proposals, teamed with bidding aerospace contractors. These vendors were Hamilton Sundstrand in Rockford IL and Honeywell (formerly Allied Signal, AiResearch, Garett) in Tempe AZ. These two suppliers teamed with other leading vendors in the fields of gas foil bearings and turbomachinery design to generate closed cycle conceptual designs for use with a liquid metal reactor. Honeywell had also been the lead subcontractor for the NASA-built space BRU and mini-BRU engines. Hamilton Sundstrand competed and won a NASA Glenn contract during the Prometheus project to build a 100 kWe high speed alternator named the Alternator Test Unit (ATU). Both vendors had competed and won different phases of the recent IPU Air Force development program (1994-2004). Requirements for the IPU machine were similar to the Prometheus project in power, speed, and turbine temperature, though different to the Prometheus requirements in shock loads, compressor inlet temperature and pressure, working fluid (air vs. HeXe), and lifetime. Reference 9- 8 describes the recent IPU progress made by Hamilton Sundstrand.

Plans were developed for involving the vendor base to establish a conceptual design for use with a direct gas reactor (Reference 9- 9), along with the phased approach to build the first generation development hardware, termed the Thermal Test Model (TTM) (Reference 9- 10), also further described in Section 13.

Performance, mass and efficiency estimates for the Brayton turboalternator have been made based on historical data, and recently developed conceptual designs (Figure 9-3). The turboalternator component is not envisioned to be a very significant source of mass within the space nuclear power plant, though the components efficiency affects the system mass substantially. The current mass estimate model for system tradeoff studies is a simple model that provides mass as a function of component electrical power output and compressor pressure ratio (see equation below). Component mass increases with increasing compressor pressure ratio due to the higher power needed by the turbine and compressor compared to the alternator at higher pressure ratios. This component mass relationship was developed by

NASA Glenn by curve fiting a logarithmic relationship based on the BRU and Mini-BRU previously built designs, and the space station freedom (SSF) conceptual design as shown on Figure 9-3.

$$Mass = A * \sqrt{\frac{CPR}{B}} * \left(C * LN(P_{elec}) + D\right)$$

Where: A – Constant (0.6)
B – Constant (2)
C – Constant (30.522)
D – Constant (-5.7178)
CPR – Compressor Design Point Pressure Ratio
$P_{elec}$ – Electrical Power (kWe)
Mass – Mass in kg

All of these Brayton turboalternators were designed in a Turbine-Alternator-Compressor (TAC) arrangement by Honeywell. The Hamilton Sundstrand Turbine-Compressor-Alternator (TCA) concept design for Prometheus is also plotted on this figure, which had a mass of 40% of the developed curve fit. This unit was much lighter than past hardware per kWe due to its higher operating speed, advanced materials used, and advanced alternator design. The NRPCT recommends the use of this curve fit with a 0.6 (60%) factor which is based on the more recent TCA design arrangement, design speed, and the higher power-density permanent magnet generator (PMG), which all help reduce the component mass. The HS-BRU design was developed to be coupled to a liquid metal reactor and had a lower internal coolant pressure inside the unit (1.28MPa max) compared to current gas reactor concept (2MPa). Due to increases in the internal pressure and the elimination of titanium and aluminum as pressure boundary materials for the compressor and alternator, the component mass is estimated to increase from their baseline design 40% of the curve fit to an estimated 60%. This mass model has significant uncertainty which would have been decreased with additional conceptual design for the current component specifications and hardware development.

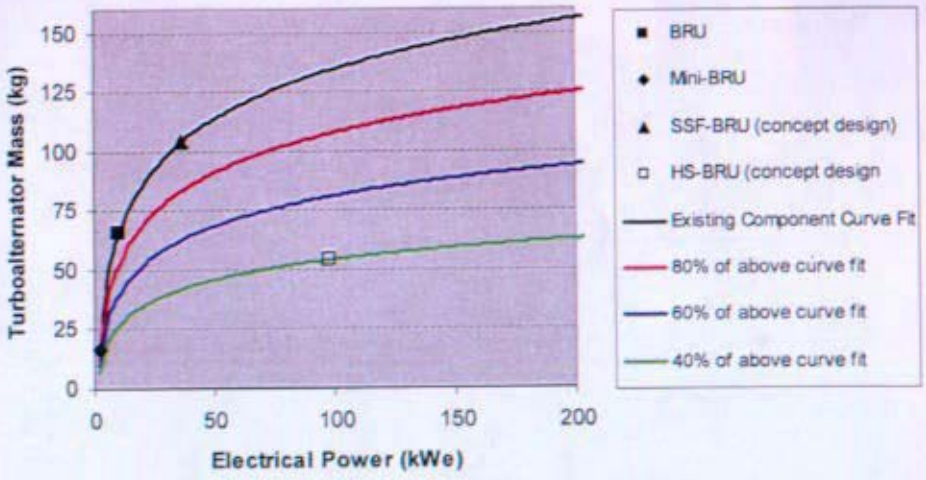



**Figure 9-3: Turboalternator Mass vs. Electrical Power**

The turboalternator has many characteristics that determine the operational efficiency of the Brayton power cycle. Irreversibilities in the component which affect the system efficiency include the turbine and compressor isentropic efficiency, bearing power losses, windage losses, EM & $I^2R$ alternator losses, thermal management power losses (pump), and ambient heat loss to space. These losses will be described in more detail in the sub-component sections below. Reference 9- 11 describes the significance of these parasitic losses to the overall power system efficiency.

Sensitivities to the main Brayton cycle design power operating parameters including compressor inlet pressure, compressor pressure ratio, compressor inlet temperature, turbine inlet temperature, recuperator and gas cooler effectiveness, and total $\Delta P$ of loop are discussed in Section 5.0. The following design constraints have been used to guide the current design state points:

- Turbine inlet stagnation temperature ≤ 1150K, based on historical hardware ranges & concern for turbine wheel / scroll creep
- Compressor inlet temperature ≤ 400K, based on a need for adequate HRS average temperature, and alternator and bearing material temperature limits
- Compressor pressure ratio ≤ 4
- Turbine/Compressor Specific Speed 0.3 <SS< 0.8 (defined in Section 9.1.3)
- Turbine Tip Speed ≤ 400m/s, based on maximum centrifugal stress of the superalloy rotor

### 9.1.3 Turbine Assembly

The turbine assembly consists of a pressure boundary housing and turbine. The housing consists of many sections that are either formed together or welded. These sections are shown on Figure 9-4, and their function is described in Table 9-3.

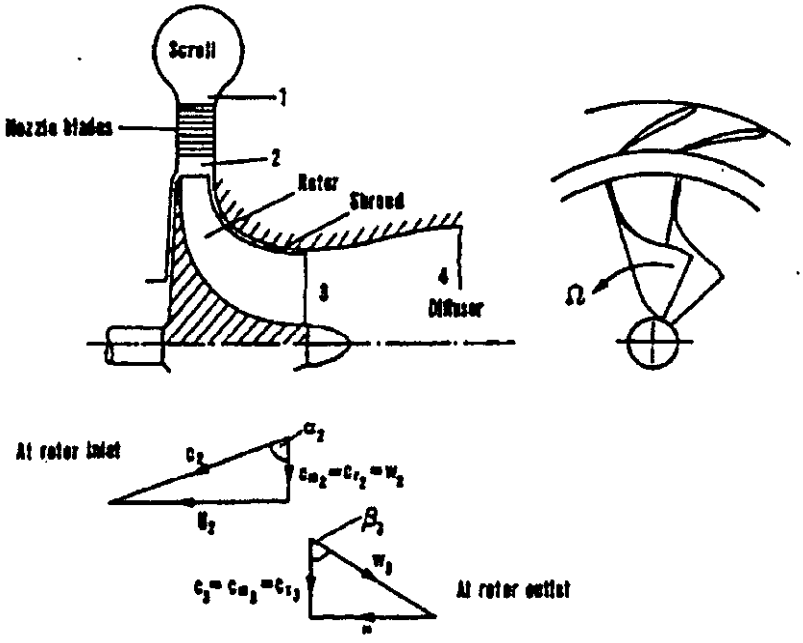



**Figure 9-4: Inward Flow Radial Turbine Schematic**

**Table 9-3: Turbine Assembly Sections**

| Section | Function |
|---|---|
| Inlet duct | Circular duct to be joined to the hot leg pipe and allows flow to enter the scroll |
| Scroll | Radial housing that accelerates the flow into a centrifugal motion to have good flow distribution into the stator blades |
| Nozzle blades | These blades increase the gas velocity and establish the angle at which the flow impinges on the turbine rotor inlet to establish the optimum velocity triangle. These are the stationary blades also referred to as the turbine stator |
| Shroud | Provides tight clearance to the rotor prohibiting leakage |
| Diffuser | Diffuses the kinetic energy into recovered pressure |
| Turbine Wheel | Power producing rotating turbomachine, converting hydraulic power to shaft power |

The turbine, as shown conceptually in Figure 9-4, is a single stage 90° inward flow radial (IFR) turbine. This turbine configuration has been applied to this application due to the extensive experience of using the 90° IFR in many other small power, high speed applications with high efficiency. New methods of fabrication enable the blades of small axial-flow turbines to be cast integrally with the rotor so that both types of turbines can operate at about the same blade tip speed. Reference 9- 12 has compared the relative merits of axial and radial gas turbines at some length. Based on proven hardware in this power range, the IFR is the base case.

The interaction between the fluid and the machine is primarily fluid-dynamic lift with some drag forces also present. Lift and drag forces are normally defined with reference to airfoils. Airfoils very similar to airplane wings are used in axial-flow compressors and turbines. However, the IFR radial turbine employs shaped channels rather than airfoils. Lift and drag forces must then be defined with reference to the normal and tangential directions of the channel walls. The IFR turbine rotor blades extend from a radially inward inlet to an axial outlet. The exit part of the blades is curved to remove most (if not all of) the absolute tangential component of velocity, maximizing the achievable power extracted from the fluid. This curved section of blading is known as the exducer. The 90° IFR turbine is also known as a centripetal turbine, and is very similar in appearance to the centrifugal compressor, but with the flow direction and blade motion reversed.

Radial flow gas-turbines use radial inward flow because the increase in the volume flow is relatively small and can easily be accommodated in the flow path near the axis, and because there are advantages in locating the interaction of the nozzle exit flow in a region of high and constant rotor-blade velocity.

### 9.1.3.1 Turbine Efficiency

The turbine assembly has many losses that combine to produce significant frictional work through frictional torques exerted by the casing. These include the fluid scrubbing on the back of the disk and on the back of the rotating shroud, if used, stator blade fluid frictional losses, and rotor blade frictional losses. Other losses include leakage from clearances between the rotor

and shroud, and the loss of recovering the exit kinetic energy of the fluid back to near the stagnation enthalpy for duct flow. An axial diffuser is used on the turbine exhaust to recover a fraction of this exit kinetic energy. Reference 9- 12 describes an analytical approach for establishing the appropriate geometry for IFR turbines. This report discusses the effects of optimizing geometry (nozzle exit flow angle,$\alpha_2$ , rotor diameter ratio $D_2/D_{3avg}$, and rotor blade entry height to exit diameter ratio $b_2/D_{3avg}$) to maximize efficiency. Figure 9-5 and Figure 9-6 from Reference 9- 13 show how the relative geometry and efficiency vary for this non-dimensional turbine specific speed. Turbine specific speed, $\Omega_S$, (see equation below) is a function of the volumetric flow, rotational speed, and the isentropic total–to-total enthalpy drop ($\Delta h_{0S}=1/2*c_0^2$). Specific speed is a dimensionless parameter.

$$\Omega_S = \frac{N * Q_3^{\frac{1}{2}}}{\Delta h_{0S}^{\frac{3}{4}}} = \left(\frac{\sqrt{2}}{\pi}\right)^{\frac{3}{2}} \left(\frac{U_2}{c_0}\right)^{\frac{3}{2}} \left(\frac{Q_3}{N * D_2^3}\right)^{\frac{1}{2}}$$

Where: N – Rotational speed
$Q_3$ – Volumetric Flow (turbine exhaust)
$\Delta h_{0S}$ – Isentropic total-to-total enthalpy drop
$D_2$ – Diameter of turbine wheel
$U_2$ – Blade tip speed = $\pi*N*D_2$
$c_o$ – Spouting fluid velocity (nozzle outlet)

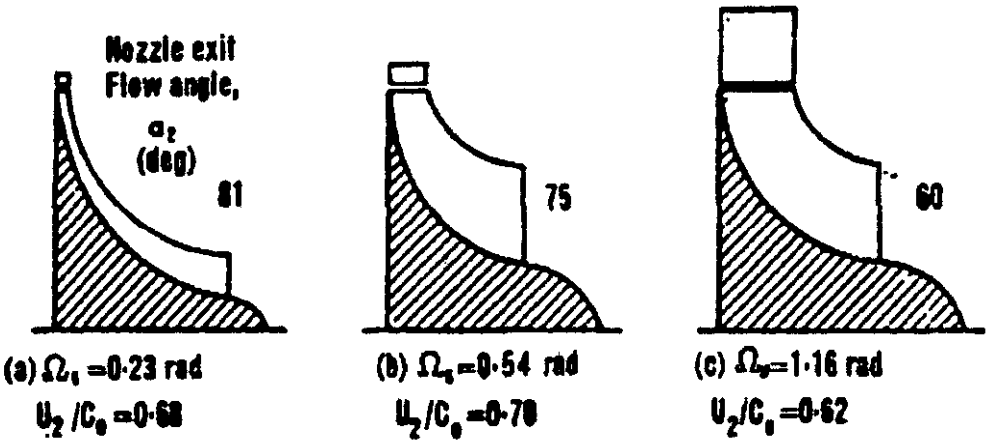



**Figure 9-5: IFR Turbine Geometry Variation versus Specific Speed ($\Omega_S$) for Maximum Static Efficiency (Reference 9- 13)**

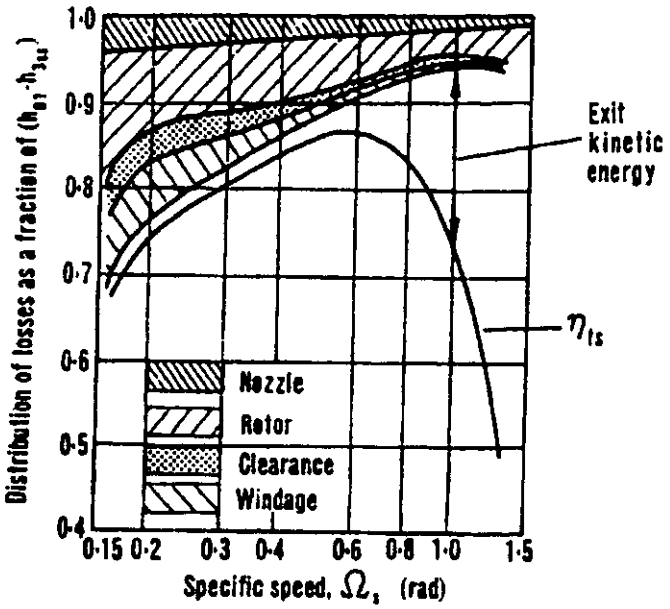



**Figure 9-6: Representative IFR Turbine Distribution of Losses versus Specific Speed for Maximum Total-to-Total Efficiency (Reference 9- 13)**

The Hamilton Sundstrand conceptual design of Figure 9-2 was designed to a specific speed of 0.56 which is consistent to the peak of Figure 9-6. Many of the current NRPCT heat balances have selected to trade some of the turbomachinery efficiency to allow for better heat transport/transfer coolants to be used in the power system to reduce duct, reactor, recuperator, & gas cooler volume and mass. Either increasing design pressure or reducing molecular weight (more Helium) lowers the specific speed. The ability to increase design rotational speed would be studied further to evaluate whether the turbomachinery efficiency can be increased while obtaining an acceptable mechanical design with acceptable damping for dynamic stability. The current NRPCT heat balances have turbine specific speeds in the range from 0.4 to 0.6. Figure 9-6 is a representative total-to-total efficiency curve. Based on new optimization methods since the late 60's, increases to these achievable turbine efficiencies have been obtained. The current estimates used by the NRPCT for plant design trade studies is shown on Figure 9-7. The shaded area on Figure 9-7 represents where various design point heat balance sensitivity studies have been focused.

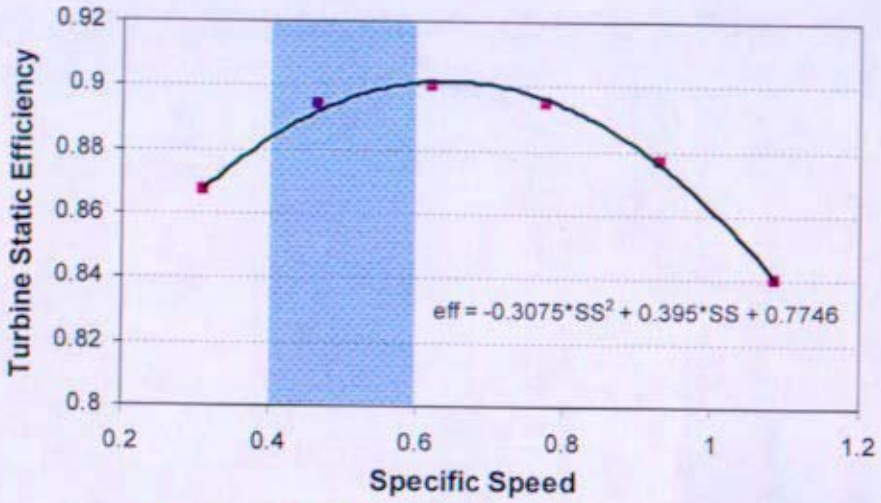



**Figure 9-7: IFR Turbine Static Efficiency**

### 9.1.3.2 Turbine Assembly Materials

Material options envisioned for the turbine assembly consist of cast Ni-base superalloys because they display superior creep strength over their wrought Ni-base counterparts. After evaluating various material options, NASA and Hamilton Sundstrand had considered two candidate materials, equiaxed Ni-base superalloys MAR-M-247LC and IN 792(5A). NRPCT has adopted these choices for preliminary evaluation. MAR-M-247LC is a well established turbine blade material used for applications requiring high strength at elevated temperatures up to approximately 1300 K for 20,000 hours (References 9- 14 & 9- 15). Mar-M-247LC has good castability, an important characteristic for the production of integral wheel/blade configurations. A database of material properties is available in the Aerospace Handbook (Reference 9- 14). Available creep data are primarily in air environments with limited inert gas data. Two helium tests have recently been performed with MAR-M-247LC by NASA Glenn (Reference 9- 16) and have measured a 70% improvement in reducing creep strain for the high temperature test (1200 K) and a 3.5 times lower creep rate for the lower temperature test (1090 K). More testing in prototypical environments is obviously needed. Hamilton Sundstrand had previous experience with IN 792 in the microcast condition (very refined grains) for use in their auxiliary power units (APUs) due to its superior fatigue resistance. When cast conventionally, IN 792 has properties similar to those of MAR-M-247, i.e. good creep capability. Compositionally, one of the major differences in the two alloys is that MAR-M-247 contains Hf, an undesirable addition when fatigue issues dominate, but desirable for creep resistance. Limited creep rate data was gathered for IN792(5A) alloy and showed that MAR-M-247LC was a more creep resistant alloy for the low creep strains tested, though had higher ductitility.

The base case configuration casts the turbine scroll, stator, and inlet duct as one part that would be joined to both the hot leg piping from the reactor outlet, and to the compressor housing. Materials being considered for the piping and compressor housing are wrought Ni-base superalloys (PE16, Haynes 230, Alloy 617). Cast alloys are not being considered for the piping because they have limited ductility due to a high volume fraction of strengthening precipitates. There is very limited information for cast-to-wrought Ni-base superalloy joining, but fusion

joining methods are not recommended due to extensive reheat and solidification cracking and other weld defects. Concerns for these pressure boundary joints include cracking and thermally induced stresses due to different coefficients of thermal expansion between the cast and wrought materials. There is precedence in industry for developing cast-to-wrought Ni-base superalloy joints by hot-isostatic-pressing (HIPing), coextrusion, inertia (friction) welding, or brazing, but further investigation is needed due to the limited amount of information available. Additional joining development was scheduled to occur in FY06 with NASA Glenn to select the most appropriate joining procedure. For detailed information on cast to wrought Ni-base superalloy joining, please refer to References 9- 17 and 9- 18.

The temperature capability of MAR-M-247LC or IN 792(5A) materials operating for 20 years is limited by either thermal creep or creep fatigue, depending on the number and severity of transient cycles. Figure 9-8 shows the current MAR-M-247 creep test data in air from Reference 9- 16. Depending on the structural requirements of the application of this material (allowable growth), the useful lifetime of the material, or the allowable stress will vary. Very limited rupture data exists, but what is available has shown creep strains of >3% before rupture. The data below shows the potential capability for this material to operate for 20 years (175,000 hours) at 1090 K with a stress of 100 MPa (15 ksi) while reaching a creep strain of 2%. The basis for allowable creep strains for each component is not well established at this point, though 2% creep strain may be acceptable for the turbine housing. A detailed structural analysis of this turbine housing has not been performed, though a 15 ksi allowable stress should be acceptable design strength for this pressure boundary. Raising the temperature up to 1150K would reduce the allowable stress or life. Extrapolations of these curves show that increasing the temperature to 1150 K would reduce the operating lifetime at 100 MPa by an order of magnitude, down to 2 years from 20. Careful consideration needs to be taken to determine the change in location of the stator blades in relation to the turbine due to creep deformation.

This cast superalloy turbine scroll is currently envisioned to be insulated externally over the majority of the area, placing this material at maximum operating gas temperature through life. More complex arrangements for thermally managing the pressure boundary either by internally insulating or other means has been considered, though the manufacturing complexity and reliability of this construction has not been researched. Figure 9-9 shows a schematic of the hot leg to turbine housing joint. This joint would allow for a wrought alloy to maintain a steady state temperature of ~900 K with no significant thermal stress present due to the transition of the cast alloy being internally and externally insulated.

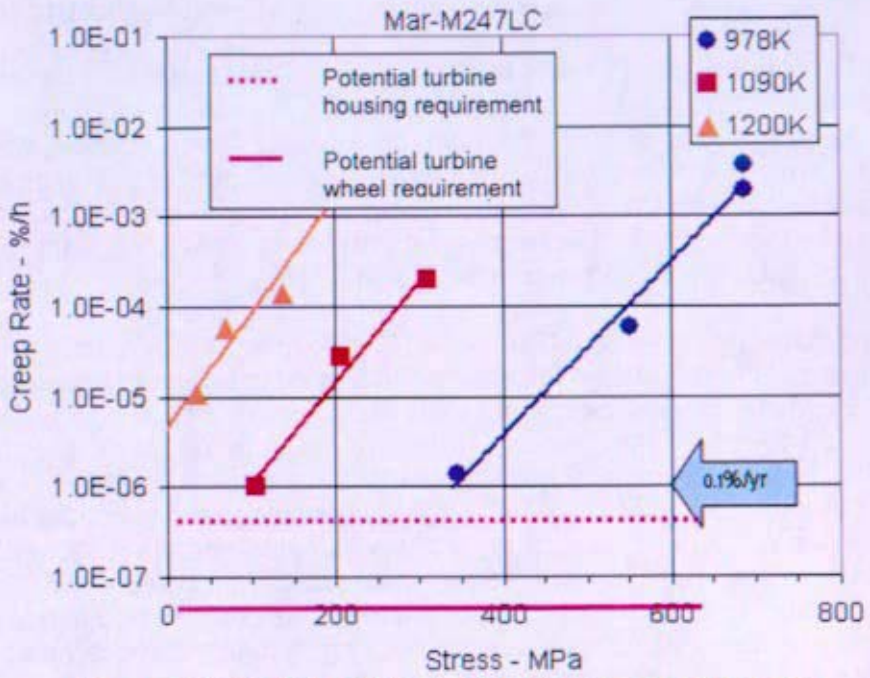



**Figure 9-8: Turbine Wheel Allowable Creep Strength**




**Figure 9-9: Hot leg to Turbine Casing Joint**

The turbine wheel is a complex mechanically designed component that operates over a wide range of both temperature and material stress. The temperature distribution of the material is governed by the pressure ratio, gas compressibility, inlet temperature, velocity of the gas, coupling of the turbine to the shaft or compressor, and the hydraulic and heat transfer losses of the fluid through the machine. The primary stress is governed by the centrifugal loads from the turbine itself. Thermal stress loads will relax and will not contribute significantly to the overall creep deformation. The design basis for allowable creep values will need to be carefully evaluated, and the experience from the turbine vendors is considered key input. For the preliminary Hamilton Sundstrand concept design of Figure 9-2, the blade radius is 7.6 cm with a tip clearance of 0.2mm. The allowable creep rate for the proposed machine would be ~0.26% diferential creep strain before the machine would generate a blade rub. Typical commercial design basis value of creep for turbo-machinery is 0.2% (Reference 9- 19), and NASA Glenn had targeted 0.5% for the built BRU design for a 50,000 hr mission life (Reference 9- 20).

Conceptual turbine mechanical analyses have been completed to evaluate the capability of MAR-M-247LC and IN 792(5A) to meet mission requirements. These analyses have been performed by NASA Glenn and Hamilton Sundstrand. The analysis performed by Hamilton Sundstrand showed a mean lifetime before rupture of 338 years for an IN 792(5A) turbine. This design was limited to a stress of 370 MPa (56 ksi) near the root of the turbine with a calculated operating temperature of 943 K. The NRPCT does not currently have a material database for IN 792(5A) and performed no review of this analysis. The proposed design basis took this material to its creep rupture, rather than having a more constraining limit on creep rate (0.2%) due to functional criteria (tip rubs).

NASA Glenn analyzed a representative turbine (Reference 9- 21) and found the allowable material strength margin for MAR-M-247LC was very small (within the level of uncertainty in the analysis methods and assumptions). Figure 9-10 shows results from the NASA Glenn analysis. This analysis showed creep growth for 10 years of operation was small compared to the elastic and thermal growth of the wheel, and the difference in creep growth between the maximum blade temperature of 1033 K (1400 °F) vs. 1089 K (1500 °F) was 0.25% (acceptable) vs. 7.5% (failure) respectively. Therefore boundary condition information on turbine wheel temperatures are crucial for determining an acceptable design lifetime.

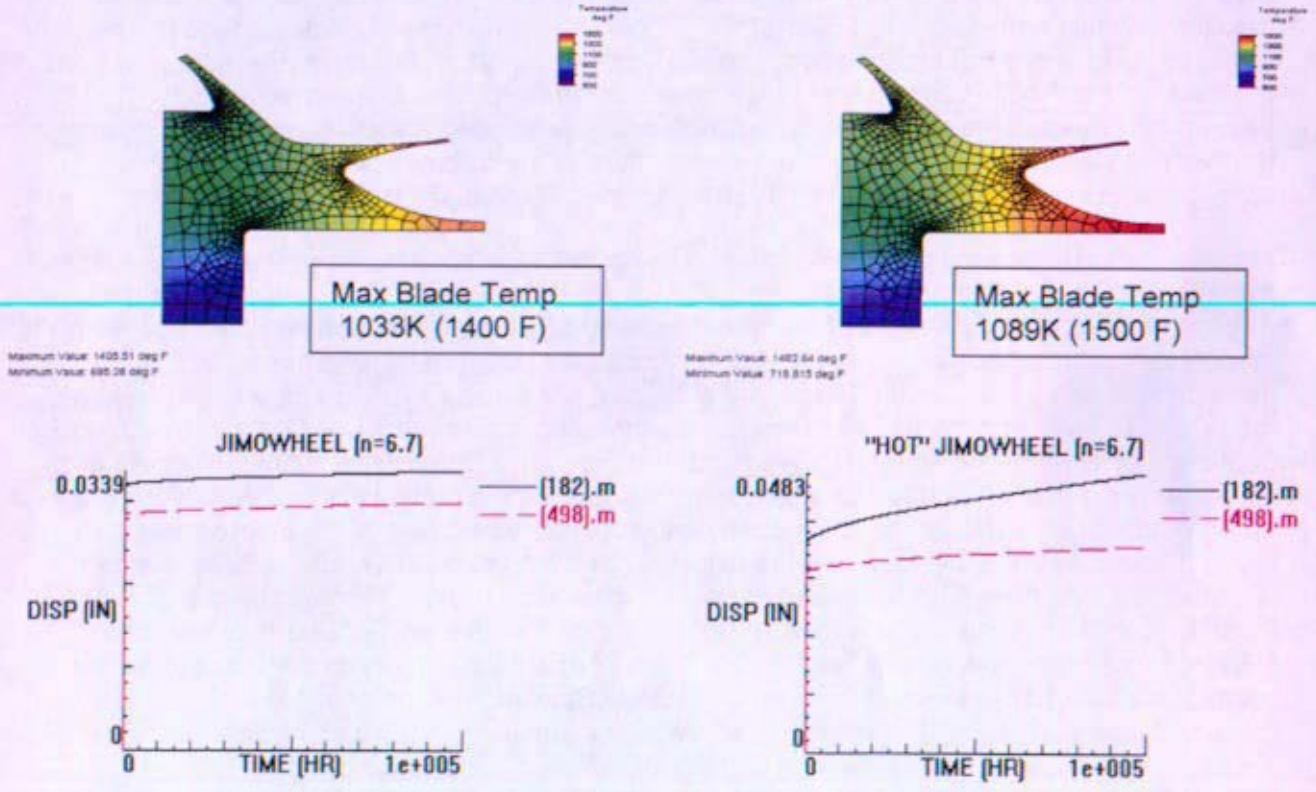



**Figure 9-10: NASA Glenn Turbine Creep Analysis**

As the gas enters a radial inflow turbine, the fluid is accelerated to a velocity higher than the turbine tip speed termed the spouting velocity. This acceleration transfers enthalpy of the fluid to kinetic energy. The combination of these two energies is called the stagnation enthalpy. Helium/Xenon mixtures behave close to a perfect gas, allowing the equation below to be valid to relate how the total temperature of the gas varies from its static temperature when the gas has a high kinetic energy.

$$Cp * T_O = Cp * T + \frac{V_{gas}^2}{2}$$

Where: Cp – Fluid Heat Capacity
$T_O$ – Stagnation Temperature
T – Static Temperature
$V_{gas}$ – Fluid velocity entering turbine

This high spouting velocity decreases the static temperature of the gas as it enters the turbine. An example of this is for a turbine wheel rotating at a tip speed of 400 m/s. The spouting velocity at the design point for IFR turbines typically ranges between 30-40% higher than the turbine wheel tip speed. This places the gas at a velocity of 520 m/s or 0.36 M for a He/Xe fluid with a molecular weight of 31.5 gm/mole. At this speed, the 1150 K stagnation temperature of the He/Xe would correspond to 950 K static temperature. The turbine blade surface temperature would operate at stagnation conditions (no slip), though would have convective heat flow from the blade to the fluid lowering the blade surface temperature. This phenomenon has been termed "aerodynamic cooling" which helps reduce needed material capabilities. Hamilton Sundstrand's estimate for the maximum temperature of the turbine blade in Figure 9-2 conceptual design was 1031 K for an 1150 K gas inlet stagnation temperature.

Another method that reduces turbine material temperature includes coating the turbine with an oxide that has a low thermal conductivity, allowing for reduced heat flow through the turbine wheel reducing the temperature of the wheel itself by conducting this reduced heat flow to the compressor more effectively. Thermal barrier coatings (TBCs) have long been used in the aerospace industry to lower the temperature seen by the turbine wheel in jet engines. State-of-the-art TBCs are comprised of ~8-10 mil thick, yttria-stabilized zirconia ($ZrO_2$-8 wt.%$Y_2O_3$) (YSZ) deposited by electron-beam physical vapor deposition. This deposition technique results in a columnar grain microstructure (carpetlike) with a low thermal conductivity (~2 $Wm^{-1}K^{-1}$). Dense YSZ would quickly spall off from a Ni-base base superalloy because of the differences in thermal coefficient of expansion, but the columnar microstructure allows the YSZ to expand without cracking. After long times at elevated temperatures the columnar grains will sinter together and the coating will lose its elastic compliance and eventually fail due to spallation. TBCs are generally re-applied after 20-30,000 hrs of operation. After this period of time, the coating has very little resistance to thermal cycling. Spallation of the coating within the Brayton gas could lead to particle erosion effects elsewhere in the loop. TBC's should be evaluated as a means to reduce turbine metal as long as their use does not introduce other material interactions or compatibility issues. Previous operating experience with the BRU closed-cycle machines (Reference 9- 20) suggests that coatings were not needed.

For Prometheus, the turbine wheel stress and temperature values are not exact until a detailed turbine design is available. Therefore, a definitive view of the creep stresses and allowable temperatures is not possible at this phase in the conceptual design. However, these estimates point to a need for careful thermal management of the turbine blade and possibly the need for an alternative blade material if MAR-M-247LC or IN 792(5A) is not adequate. NASA Glenn has identified silicon nitride ($Si_3N_4$) as a possible alternative but no specific developmental plans are in place at this point since MAR-M-247LC is believed to be the best candidate. Turbine wheel creep is believed to be a key potential component life limiting failure mode, discussed in Section 9.1.8.

### 9.1.4 Compressor Assembly

The compressor assembly consists of a pressure boundary housing and compressor wheel. The housing consists of many sections that are either formed together or welded. These sections are shown on Figure 9-11, and their function is described in Table 9-4.

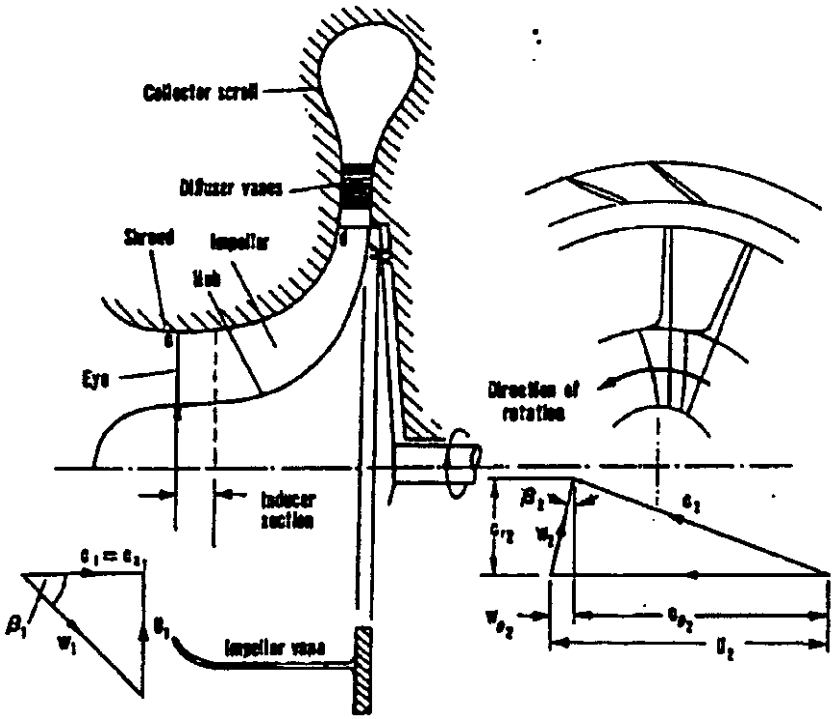



**Figure 9-11: Centrifugal Compressor Schematic**

**Table 9-4: Compressor Assembly Sections**

| Section | Function |
|---|---|
| Inlet duct | Circular duct to be joined to the compressor shroud allowing the flow to enter the inlet with an appropriate velocity distribution and swirl. |
| Inducer | Section of the impeller that draws the flow smoothly and efficiently or without disruptions into the main stage |
| Compressor Wheel (Impeller) | Rotating turbomachine that transfers shaft power to hydraulic power by increasing gas pressure |
| Shroud | Provides tight clearance to the rotor prohibiting leakage |
| Diffuser | Diffuses the kinetic energy into recovered pressure at the outlet of the stage. |
| Collector Scroll | Radial housing that is connected to the diffuser that collects the fluid to near static conditions and transfers this flow to the compressor outlet duct |

The compressor assembly, as shown conceptually in Figure 9-4, is a single stage centrifugal gas compressor designed for maximum efficiency, low mass, with a moderate pressure ratio ranging between (1.8 to 2.4). The sensitivity of performance (efficiency) for this application is highly sensitive, as shown in Section 6, to meeting required electrical power for a given heat rejection size. Compressor efficiency of the preliminary design heat balances range between 84 to 85%, and are envisioned to be achieved with limited turbomachinery development. This development would have followed the three step process as described in Reference 9- 22. The third level of the process uses comprehensive models, and utilizing them systematically to develop new optimum configurations based on the basic flow phenomena for each section of the compressor stage.

Key areas of study to maximize the performance of a compressor design includes the entrance and inducer design, the angle of the blades inclined backwards to the direction of rotation, number of blades and height, and the shape and configuration of the diffuser. The term specific speed (non-dimensional) as discussed in the turbine assembly section above is also used in compressor design to help characterize the overall geometry (blade height to diameter). Clearance from the shroud to the impeller blades has an effect on efficiency and is more important for a low specific speed design (<0.5) due to the increasing clearance to blade height fraction.

### 9.1.4.1 Compressor Efficiency

Hamilton Sundstrand had worked with Concepts NREC to develop a compressor conceptual design. This design had a 55° backswept blade angle, Ns = 0.68, blade tip speed of 368 m/s, CPR=1.85, Tin=400K, Pin=0.69MPa, $\eta$=84.5%, and a low solidity airfoil diffuser plus volute and conical diffuser. The current heat balances from Section 6 includes a slightly higher pressure ratio, higher inlet pressure, lower inlet temperature, which all lower the impeller specific speed for a constant rotational speed and coolant MW. The mass flow per unit electrical power of the system was higher for the current heat balances than the Hamilton Sundstrand concept due to

increased parasitic losses (piping ΔP, bearing, and windage) which increases specific speed. The vendor chosen specific speed of 0.68 is where most texts show maximum efficiency. The current baseline heat balances shown in Section 6 have compressor specific speeds of 0.52 for a four Brayton system architecture (2-100kWe operating units, 2 spares units), and 0.66 for the single 200kWe Brayton system architecture. He/Xe molecular weight or shaft operating speed would be the key parameters to change if the turbomachinery needed to increase the specific speed to maximize system efficiency. Figure 9-12 presents a range of optimized compressor static stage efficiencies for a pressure ratio of 2.0 and for a range of corrected flow ($P_{ref}$=101.3kPa, $T_{ref}$=288.2K).

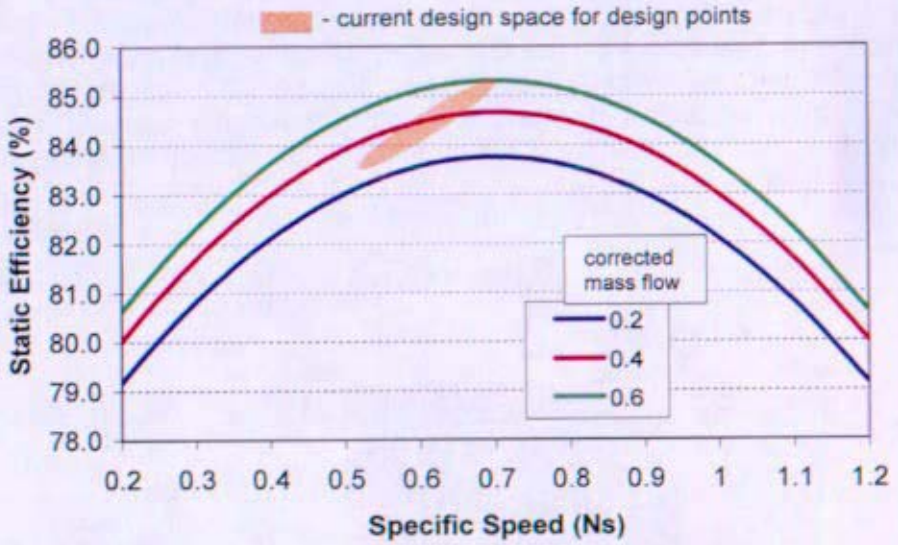



**Figure 9-12: Compressor Static efficiency vs. Specific Speed and Corrected Mass Flow**

### 9.1.4.2 Compressor Assembly Materials

The compressor materials considered include Ni-base, Ti-base, and stainless steel alloys. Historically, NASA BRU designs used S41000 stainless steel for the impeller due to its good strength and thermal conductivity. 17-7PH stainless steel was used for the compressor diffuser and collector because it maintained good corrosion resistance, fabricability, and high strength. Hamilton Sundstrand had proposed using Ti6Al4V alloy for the compressor impeller, diffuser, and collector because of its favorable strength-to-mass ratio, but the mechanical, physical and metallurgical differences between titanium and Ni-base alloys would have made joining these two materials extremely challenging. For example, fusion welding of nickel to titanium leads to formation of brittle intermetalllic phases at the interface, compromising joint integrity. Use of a wrought Ni-base alloy for the compressor collector would have made this transition more reliable, but joining a wrought alloy to the cast alloys considered for the turbine casing would have required design studies for use of unconventional joining techniques. Design studies would need to be performed to understand the ability to thermally manage the compressor collector when joined to the hot turbine scroll for the various classes of materials before selection.

### 9.1.5 Alternator Assembly

The alternator assembly is an integral part of the Brayton Turboalternator and is used to convert rotating mechanical energy into electrical energy. The electrical energy is then transferred through the primary pressure boundary to the spaceship power distribution cabling. Three key components are needed to accomplish this within the alternator. These components are shown in Figure 9-13 and described below.

#### 9.1.5.1 Alternator Description

The alternator rotor contains permanent magnet segments which are attached to the common shaft containing the turbine and compressor wheels. These magnets create a magnetic flux field which crosses the gap between the rotor and stator and penetrates the wire coils of the stator. As the turboalternator shaft rotates from the flow of hot gas through the turbine and compressor sections, this magnetic field moves through the stator coils inducing the flow of electrical current in the coils. The permanent magnets of the rotor assembly are held in place by mechanical restraints or metallic canning.

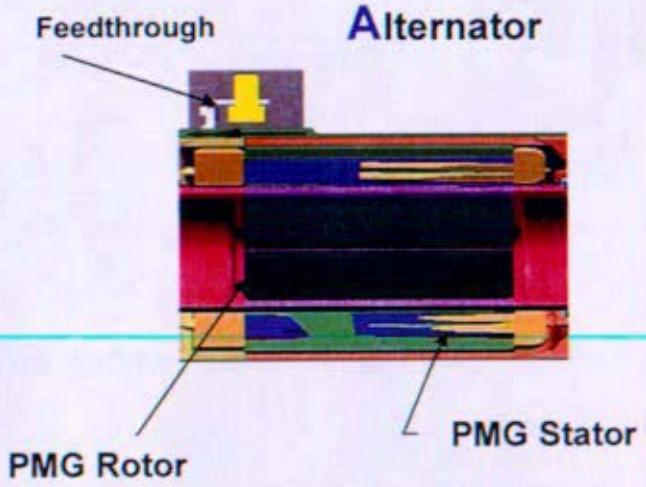



**Figure 9-13: Alternator detailed picture**

The stator is a stationary assembly containing electrical coils which surround the rotor. These coils are placed in slots formed by stacking thin laminations of metal which provide a path for the magnetic flux field and mechanical support for the coils. The coils are placed such that uniform three phase electrical power is produced as the Brayton rotor spins. The coils are ultimately connected to the spaceship's electrical distribution system where the electrical power is used to operate the spaceship. The coils are electrically insulated from the stator laminations and are contained within the pressure boundary of the alternator housing.

The electrical feedthrough provides a non-conducting path for the electrical circuit to penetrate the housing of the alternator, thus transferring the electrical power produced within the alternator's stator coils to the electrical loads in the spaceship without compromising the

integrity of the pressure boundary. The feedthrough is comprised primarily of an outer shell which is bonded to the alternator housing, an electrical conductor, and an insulator which is bonded or otherwise sealed to both the outer shell and the conductor. The electrical conductor connects internally to a stator coil, and externally to the power system cabling. The bonds between the outer housing and the pressure vessel, the outer housing and the insulator, and the insulator and the conductor must all be hermetic. Careful attention must be paid to the selection of the feedthrough device, as it is the sole through-penetration in the Brayton energy converter and represents a potential source of leakage. The feedthrough must remain hermetic through the entire life of the SNPP. The NRPCT evaluation of potential electrical feedthrough options is contained in Reference 9- 26.

### 9.1.5.2 High Speed Alternator Design Challenges

The high operating speed of the Brayton unit allows a reduction in overall mass compared to larger, slower electrical generators, but also brings several challenges with respect to the alternator design. First, rotor dynamics and balance become more difficult at higher speeds where the light rotor contains significant rotational energy and where more vibration modes are excited. (Critical vibration modes can also place limits on the operating envelope of the Brayton unit such as the minimum allowable motoring speed assumed in the reactor startup sequence described in Section 8. The low end critical rotor modes required a higher motoring speed than might be needed for the reactor coolant demand and therefore drove the sizing of the spaceship solar arrays.) The higher rotational speeds also place more stress on the permanent magnet structure on the rotor, as centrifugal forces tend to close the gap between the rotor and the stator assemblies. The size of this gap is critical and must reach a balance between a small gap to increase the magnetic flux density and a larger gap to allow expansion of the permanent magnet structure due to thermal effects and centrifugal force at the highest operating speed.

The higher operating speed also produces a higher frequency electrical output. While a higher frequency alternator requires less iron in the stator laminations (less penetration of the magnetic flux) and therefore less mass, the higher frequency magnetic field produces more losses in the stator laminations which result in additional heating of the stator. Thermal management thus becomes more important.

### 9.1.5.3 Dual Alternator Design Option

One three phase alternator per Brayton unit has been the base case Prometheus concept design considered thus far. However, an independent dual winding system has recently been considered and could be used in the Brayton design to enable electrical system redundancy without adding mechanical complexity to the rest of the system. There are several ways to implement a double winding. These concepts are preliminary and require further evaluation.

One method is to employ a double alternator with two sets of magnets and two stator assemblies. This approach provides redundancy in the magnets, complete electrical isolation of the windings, and is the most fault tolerant approach. However, this approach results in lengthening of the machine and carries the largest mass penalty. Also, providing redundant magnets yields little reliability gain, as the most plausible magnet failure mode is degradation from excessive temperature and would affect both sets of magnets equally.

Another approach is to provide a double winding with a single magnet assembly and stator structure. Utilizing a single magnet structure maintains the length of the alternator and minimizes the mass impact. The methods considered include:

- A sectored winding in which alternate poles are electrically connected to form two independent 3 phase circuits. This is potentially the best method as the slot count can be retained and the winding reactances will be nearly equal. Additionally, the windings can be loaded arbitrarily without adversely affecting the magnetic field in the alternator and causing undesirable vibrations.
- An interleaved winding in which conductors are placed in adjacent slots. This approach requires doubling the number of slots in the stator and may not be achievable due to the small stator diameter of the proposed machine.
- A six phase winding in which two independent 3 phase sets are used for the two circuits. Again, this approach requires doubling of the slot number and may not be achievable.
- A double layer winding in which the two sets of coils are stacked in the slots and separated by an insulator. This technique requires Roebelled conductors to achieve balance of reactances for the two windings. Since this stator winding is more complicated than the sectored approach, this method is probably less preferable.

It should be noted that any of these methods require approximately a doubling of the conductor mass in the alternator. If the length of the machine is held constant then slot depth must be nearly doubled, and will increase the diameter of the stator. Back iron thickness of the laminations would not be affected. A final selection of winding type would require a series of optimization studies for the alternator. During normal operation with both windings running at 100 kWe, temperatures within the stator will be quite low as the windings would be designed for continuous 200 kWe service.

Use of a second winding provides partial protection against single point failures of the alternator windings. However, some winding failures are catastrophic and will not be mitigated by a second winding. For example, a phase to phase short in a winding is likely to result in severe over-temperature, melting of the copper conductors, and possible ejection of the winding into the air gap and complete failure of the alternator.

### 9.1.6 Bearing Assembly

Due to the closed-loop environment, foil bearings are the proposed method of supporting the rotating shaft due to their ability to use the process gas as a lubricant, while exhibiting long life and high reliability under extreme temperatures. Gas foil bearings are self-acting, compliant surface hydrodynamic bearings. A diagram of the main parts of these bearings is shown in Figure 9-14 below. Traditional oil lubricated bearings are not practical in closed loop systems because oil can enter the process flow causing downstream coking problems, and also would contaminate refractory metal alloys if selected as reactor materials. The use of magnetic bearings was considered, however it was determined that the technology was more complex and potentially less reliable for long deep space mission duration.

Gas foil bearing technology has improved over the years and is often described in three evolutions, or generations. Generation I bearings have stiffness characteristics that are uniform in the axial and circumferential directions. In Generation II bearings, the stiffness characteristics are tailored in either the axial or circumferential direction, but not both. Generation III bearings take this a step further by tailoring the stiffness in the axial, circumferential and radial directions. The ability to tailor the stiffness characteristics in different directions was considered important for successful operation in a zero gravity environment. In addition to these improvements, gas foil bearings have also increased their load capacity as the technology has matured.

Even though a foil bearing relies on a thin layer of fluid to separate it from the shaft, use of a lubricant is preferred to insure against failure. NASA has demonstrated a solid coating system that provides bearing lubrication from 300-773 K. The system, PS304, is a mixture of Ag and $BaF_2/CaF_2$ for low and high-temperature lubrication, respectively (Reference 9- 29). All of the coating constituents are stable at 550 K, as none have a vapor pressure higher than $10^{-18}$ Torr. As oil-free turbomachinery is still in early developmental stages, the coating system would need to be tested within the impure-He environment envisioned for the Prometheus reactor.

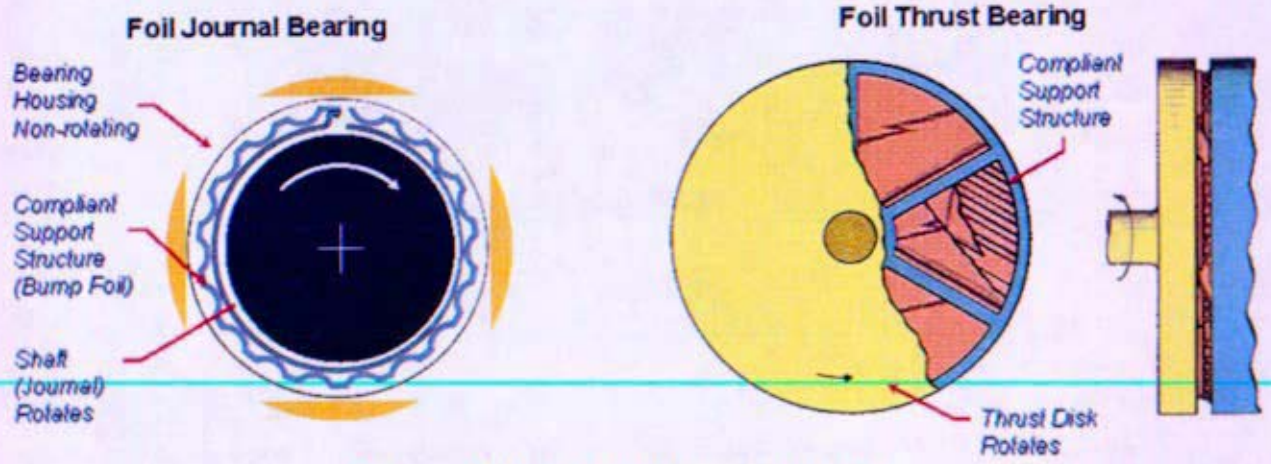



**Figure 9-14: Gas foil bearing diagram**

In order to facilitate the integration of gas foil bearings into Brayton systems, NASA Glenn developed a 4 step development process. The steps are: 1) rotordynamic feasibility analysis, 2) bearing development and testing, 3) experimental rotordynamic simulation and stability verification tests and 4) turbomachinery testing. This process is described in detail in Reference 9- 30. At the time of the cancellation of the project, work had been ongoing in steps 1 and 2. Additionally, work was planned in FY06 to design and procure the test rigs required for step 3 as well as develop the Thermal Test Model that would eventually serve as the turbomachinery testing platform (step 4).

Gas foil bearing performance is typically described in terms of power loss, lift-off speed, thermal management needs and load capacity. The performance parameters are functions of operating gas pressure, temperature and composition. Because there are a large number of factors affecting these performance measures, some of which are not yet fully understood, NASA Glenn has developed a rule-of-thumb to provide a quick indicator of the expected bearing performance. NASA's rule-of-thumb approach is as follows: "a pound of load per inch of

bearing diameter per square inch of bearing projected area per thousand rpm." The development of this rule of thumb approach is described in Reference 9- 31. This rule of thumb holds true for gas foil bearings operating in air at ambient pressure. In alternate gases and at higher pressures, however, the bearing performance varies. Understanding this change was to be the focus of testing at NASA Glenn in FY06, however some preliminary testing was conducted in 2005 for low pressure and low speed performance. The results of this testing, described in Reference 9- 30, showed the bearing load capacity improved with increasing pressure. This was exhibited in Air, Helium and Argon although the effect was more pronounced in Air. It was also shown that increasing pressure resulted in less power loss at a given load, implying that the increase gas pressure caused the foil bearings to perform with less friction. Finally, it was shown that plotting (Figure 9-15) the power loss data from all three gases against their respective normalized load capacity revealed very similar behavior.

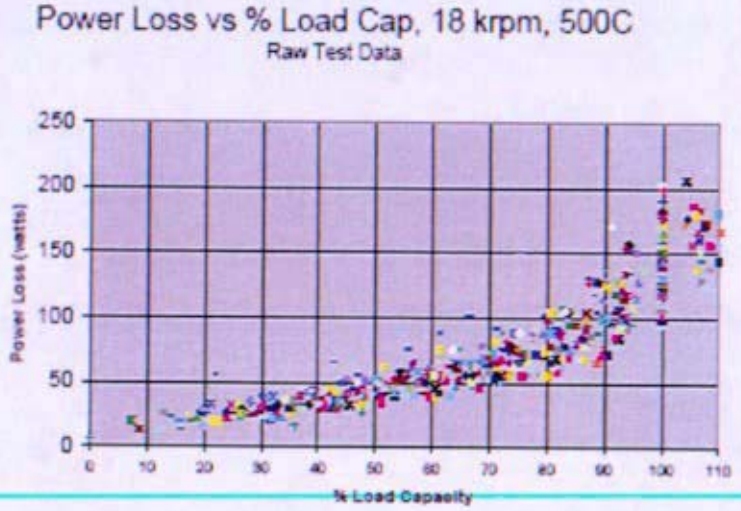



**Figure 9-15: Power Loss versus Percent Load Capacity (Reference 9- 30)**

### 9.1.7 Component & System Integration

#### 9.1.7.1 Shaft Speed Control

Brayton unit speed is affected primarily by the combination of turbine inlet temperature and the electrical load on the alternator. The approach considered for the Prometheus spaceship was to maintain a constant Brayton unit speed by establishing nearly constant conditions for both the inlet temperature and the electrical load. (Constant Brayton unit speed was desired to provide a constant voltage and frequency on the electrical bus.) The turbine inlet temperature is determined by the reactor coolant temperature, which is in turn controlled by the position of the reflectors surrounding the reactor vessel. The reflector positions will remain essentially constant except for minor changes to account for fuel depletion over the life of the mission and to make major adjustments in temperature for reduced power operation (if used). The electrical load on the alternator is a combination of the spaceship loads (e.g. thrusters, science packages, flight computers, etc.) and the PLR (a parasitic load). The PLR load is continuously adjustable to

accommodate for changes in the spaceship loads, thus maintaining a constant Brayton unit speed that is independent of spaceship operating requirements.

The control architecture being planned for the Prometheus spaceship had the reflector position (and temperature control) being provided by the Reactor Controller, and Brayton unit speed being controlled by the PCAD controller. Coordination between these two controllers was expected in order to achieve integrated control of the SNPP.

### 9.1.7.2 Rotordynamic Stability

The turboalternator rotor design couples all of the subassemblies together into an integrated unit. An iterative design process occurs to meet both the allowable bearing performance parameters (load capacity, damping, stiffness) along with meeting the rotors structural design. The current shaft design uses a large diameter hollow shaft that provides high rigidity with low mass. This allows the shaft to operate at the design operating speed (~45,000 RPM) with sufficient margin below the first bending critical speed (67,000 RPM). The large diameter allows for high shaft surface velocity, which improves the load capacity of gas foil bearings.

Preliminary analyses were performed by KAPL and NASA Glenn on the Hamilton Sundstrand conceptual design using a broad set of analysis methods. These methods include DyRoBeS (NASA Glenn), RotorLab (KAPL), and ABAQUS (KAPL) computer simulation programs. All simulations were used to predict the rigid and bending critical speeds and mode shapes. These comparisons showed that all three methods with slightly different modeling techniques predicted similar mode shapes and speeds for the proposed rotor as further described in Reference 9- 32. Assumptions that were neglected in these analyses, though are considered important second order effects, include the side load forces from the alternator magnetic field and the thrust bearing loads.

When performing damped rotor simulations with unbalanced forces, there were differences in the magnitude and location of the largest displacement of the shaft. The NASA Glenn DyRoBeS analysis had shown the largest displacement of 0.8 mils at design speed at the turbine wheel. This displacement is an acceptable magnitude. The KAPL RotorLab analysis predicted smaller maximum displacements, between 0.8 and 0.3 mils, depending on how the model was constructed.

A stability analysis was performed by NASA-GRC and KAPL. Rotor stability is determined by calculating the log decrement of forward whirling undamped modes. A negative log decrement suggests vibration amplitudes that tend to increase in time. Forward whirling undamped modes can be self-exciting, leading to instability if they have a negative log decrement. NASA-GRC calculated the threshold speed of stability, the rotor speed at which the log decrement of any forward whirling damped mode becomes negative, for varying bearing damping. The KAPL RotorLab results agree with the NASA-GRC conclusions, that the rotor system is stable for bearing damping above 10 lb-in/s. This level of damping is believed to be attainable for gas foil bearings.

These rotor design analyses assume the known bearing properties with atmospheric air as the working fluid at atmospheric pressure. A primary focus is needed to understand how these

bearings and rotor designs would be modified from changes in the fluid operating pressure, temperature, and composition. Some early results show that increasing pressure allows for higher bearing load capacity, or a lower power loss for a constant load capacity, when gas pressure is increased and when using alternate gases (He, Ar). The bearing stiffness and damping are less well known bearing parameters, and are very important to the shaft design.

Future work is needed to confirm that the gas bearings can be designed with the appropriate damping and stiffness with high pressure He/Xe fluid and that more refined second order forces are considered in follow on scoping analyses.

### 9.1.8 Failure Modes

In general, Prometheus is no more demanding than the current Brayton Turboalternator units in terms of tip speeds and turbine inlet temperatures and it is much less demanding in terms of start/stop cycles. The key difference is that with the exception of BRU/Mini-BRU and Hubble cryo-cooler, they are open cycle machines and have regular maintenance performed so direct comparison is difficult.

Gas bearing history is very positive and provides high reliability in Capstone and air cycle machines. Mean time between failure has exceeded 100,000 hours in some Boeing machines. Similarly, the robustness of gas foil bearings for the Hubble Space Telescope cryocooler designed and manufactured by CREARE has shown exceptional performance for long periods (14 years on life testing and 3 years to-date in space). While at low operating temperature and much smaller, these cryo-coolers operate at over 100,000 rpm.

A Garett (now Honeywell) study estimated failure rates for space Brayton systems. The estimated failure rates for relevant components of a Prometheus mission are shown in Table 9-5. Based upon their values, a reliability rate of ~99.6% for a 3 year mission and ~97% for a 20 year mission are inferred. While these values are only rough estimates based upon open cycle experience not directly related to the Prometheus design/mission, it indicates that high reliability rates are believed achievable, even for longer life missions.

Hamilton Sundstrand study of Brayton failure probability resulted in similar reliability numbers as the Garrett study (~97% for a 20 year mission); however, their results used a 10x factor on some of the reliability numbers to account for what are considered favorable conditions for our program versus land based units. This may be true but it is hard to substantiate such a factor at this point due to the lack of hard data from space based units.

**Table 9-5: Reliability Study from Garrett Fluid Systems (Reference 9- 27)**

| Component | Failure Rate | |
|---|---|---|
| | (per hour) | (per year) |
| Foil Bearings | $3 \times 10^{-8}$ | $3 \times 10^{-4}$ |
| Turbine | $1 \times 10^{-8}$ | $1 \times 10^{-4}$ |
| Compressor | $6 \times 10^{-8}$ | $6 \times 10^{-4}$ |
| Alternator | $5 \times 10^{-8}$ | $5 \times 10^{-4}$ |

Sections 9.1.8.1, 9.1.8.2, and 9.1.8.3 list individual failure modes and risk mitigation methods. There are several alternator failure modes common to all electric machines which are not discussed here, though can be found in Reference 9- 28.

**Table 9-6: Relevant Brayton Operating Experience ***

Capstone Turbines (Since 1998)
- 30 and 60 kW units
- 6 million total operating hours
- 44,000 hours on high time unit
- 14,000 start/stop on high unit
- 2600 units produced since 1998
- Max bearing temp: 727 K
- TIT=1100 K, Tip Speed 550 mps

NASA BRU Testing*
- 10 kW
- 38,000 hours on high time unit
- TIT=1144 K, Tip Speed~300 mps

HS APU/GPU
- 21,000 units produced
- 70 million operating hours

JIMO Reference Design
- 92.5 kW
- 100,000 hour life
- 100 start/stops?
- Max bearing temp: 450K
- TIT=1150 K, Tip Speed=384 mps

HS Air Cycle Machines (Since 1984)
- 40 million total operating hours
- 50,000 hours on high time unit
- 18,000 start/stop on high unit
- 4600 units in service
- Max bearing temp: 560 K

Honeywell Air Cycle Machines (Since 1968)
- 300 million total operating hours
- 80,000 hours on high time unit
- 20,000 start/stop on high unit
- 25000 units in service
- Max bearing temp: 572 K

* Note: With exception of JIMO, NASA BRU and Creare Cryocooler units, all other operating experience is with open cycle machines.

CREARE Hubble Space Telescope Cryocooler
- 14 year (120,000 hours) life testing w/o failure
- 3 years (25,000 hours) in space without failure
- Cold temperatures (30-70 K)
- ~100,000 rpm operating speed
- Demonstrated ability to reliably seal He system

### 9.1.8.1 Turbomachinery Failure Modes

**Turbine Creep**

A high temperature gas turbine (1150 K) has never operated for 20 years continuously. Excessive turbine creep would cause blade rubbing which would decrease net shaft power and lead to material ablation from the blade tips and stators eventually causing increased friction and binding. Turbine wheel creep may also lead to bearing failure by generating an increased shaft imbalance from anisotropic creep growth. A discussion of turbine creep analyses is discussed above in Section 9.1.3. The concern for turbine creep is due to the high material stresses and limited allowable creep strain (order of magnitude less than rupture) due to the tight clearances needed to keep tip bypass losses to a minimum.

Thermal management of the turbine to keep highly stressed areas at low temperature is very important. Large conduction area to the shaft or compressor is needed to allow for good thermal management.

Turbine creep is considered one of more likely life limiting failure modes and should be continually studied through the conceptual design process.

**Turbine Scroll Creep**

In the base case design, the turbine scroll is the maximum operating temperature pressure boundary in the entire reactor power system. Creep failure of the turbine scroll could end in a breech of the pressure boundary, or lead to significant deformation in the turbine stator to degrade or fail turbine performance/operation. Risk mitigation of this failure mode includes designing the turbine scroll with a refractory metal alloy, which was researched as part of the Mini BRU program (Reference 9- 6), or internally insulating the pressure boundary as is planned for the base case hot leg pipe design. A scroll based on a refractory metal alloy was not seriously considered due to concerns over a bimetallic pressure joint. This is also why a Ni-base superalloy pressure vessel was advocated over one made from a refractory metal alloy. Section 9.1.3 discusses details as to the structural materials capabilities for the cast Ni-base superalloy materials (Figure 9-8) currently being envisioned. From this figure, the turbine scroll may be as limiting as the turbine due to the material operating at a high temperature (1150 K max vs. ~1031 K max).

**Pressure boundary breech**

If catastrophic failure can lead to breach of the pressure boundary and loss of coolant, there are methods to capture the turbine wheel and prevent such failure. However, mass penalty and possibility of debris from a "blade catcher" may make such options unattractive. Most likely the design will need to be of high enough reliability to reasonably prevent catastrophic failure without a blade catcher device. Options also exist relative to bearing design to cause the unit to shutdown and self-weld to bearing prior to contact with shroud to prevent catastrophic failure. Recent communications from NASA Glenn and earlier discussions with vendors have indicated that passive failure modes where a unit shuts down but does not cause catastrophic failure to the loop or other components has been demonstrated to occur in operation, and is a requirement for APU on aircraft (Reference 9- 33).

**Erosion from debris**

Issue of debris in a closed loop is also a concern due to possible long term erosion effects if not removed from the main flow. Short term tolerance of debris has been shown to be acceptable and it is part of the design basis for aircraft units that must be reasonably tolerant of dust and sand ingestion during takeoff and landing. Debris can be from failure of a unit or corrosion/erosion (see section (c) of Attachment D of Enclosure 7 of Reference 9- 23)). While some Brayton failures could release debris into loop, the amount and size of debris is not clearly known and the tendency for this material to remain in the flow (vs. settling out in low flow regions) is not characterized. NASA Glenn is reviewing this issue in more detail but experience with gas foil bearings has shown the damage and debris tend to be contained in the bearing cavity due to the rapid deceleration experienced following failure and the tortuous path that must be taken to exit the bearing cavity. Erosion from particulate matter smaller than 20 μm in diameter has been shown to not be an issue but this is very dependent upon the flow and material. Large debris from the Brayton (> 1mm) would be trapped by recuperator but small

debris (< 1mm and > 20 μm) could cause long term erosion if not removed. Separators or filters may have been needed with further test and analysis of erosion.

**Compressor Failure**
The compressor within this closed cycle is envisioned to have a much lower failure rate than an open cycle due to the nature of not being the first component in the path of ingested debris. The compressor is a highly stressed material, though operates at low temperature. Thermal creep is not considered a failure mode at this low temperature (<550 K). Compressor stability through transients is known to cause imbalanced blade loading, causing the compressor to potentially rub the shroud. Erosion wear from potential high velocity particulate flow on the diffuser vanes could also reduce compressor performance.

### 9.1.8.2 Alternator Failure Modes

**Electrical Feedthrough Failure (gas leakage, single point failure)**

Gas leakage through the feedthrough was identified to occur from four principal modes. The first is baseline molecular diffusion. This was not determined to be a feedthrough specific failure mode. The second is through-sealant leakage from induced microcracks in the sealant material. The third is an imperfect bond between the sealant and conductor. The fourth is an imperfect bond between the sealant material and the body or outer housing of the feedthrough. The mechanisms by which these failure modes can occur are detailed below.

**Alternator material failure from irradiation**
The two primary failure modes expected from irradiation are insulation system failure which would lead to a short, as described below, or magnet heating from irradiation.

**Open circuit on Alternator**
The event of a three phase open circuit at the feedthrough, cable or inside the alternator windings would result in the loss of load on the alternator. Since the Brayton TCA shaft speed is based on the torque balance between the alternator, turbine and compressor, the loss of load would lead to an acceleration of the rotor shaft until some mechanical failure occurred, or a new stable operating speed was reached. For a single phase open circuit on the alternator a similar acceleration to the point of stability or mechanical destruction would occur, but the rate of acceleration would be much slower.

It should be noted that a double wound stator prevents a single failure from removing load from an operating Brayton and causing turbine runaway.

**Electrical faults on Alternator**
There are many different faults that can occur in a stator winding:

- Turn to turn faults are most common and result from an insulation breakdown between adjacent conductors. They can occur in the end turns or within the slots. A turn to turn fault results in a localized hot spot which can later develop into a ground fault or phase to phase fault.
- Phase to ground faults occur when both coil insulation and the slot liner have been compromised. For the spacecraft (which has an ungrounded power system) a single

phase to ground fault will not necessarily fail the stator. However if multiple ground faults develop then large circulating currents resulting in total stator failure are possible.
- Phase to phase faults can arise in the slots or the end turns and result in potentially large short circuit currents and stator failure.
- Conductive contaminants can fail a stator since the insulation system is not perfectly sealed. Conduction through small holes in the insulation occurs and burns small "tracks" on the insulation surface.

Many of these faults could be detected at an incipient stage through the use of a ground detector, and the affected Brayton unit (or winding if a dual alternator approach is used) removed from service. This approach may prevent further degradation of the winding, but in some cases may not be sufficient. Early detection of insulation system grounds is important for this approach to be successful. Other advanced methods of detecting stator defects are possible as well and could either be implemented on the spacecraft or on the ground using telemetry data.

**Rotor Can Rupture**

Rotor can rupture is one means of mechanical destruction of the Brayton shaft which can occur in the over speed condition. In this scenario the hoop stress on the rotor can by the mass of the spinning magnets and the magnetic forces pulling the magnets to the stator, rupture the rotor can allowing the magnets to travel across the small (~50 mm) gap to the stator surface. Once on the stator, the magnets exert a normal force of about 10 kN which is expected to cause the shaft to stop. The kinetic energy from the shaft is then transferred to the housing through the alternator. Further analysis will need to be done to determine if the torque that is placed on the housing by this fault is sufficient to cause pipe leakage.

**Loss of Alternator Thermal Management**

Loss of alternator coolant resulting from a blockage in the alternator and bearing coolant channel or damage to the shaft fan, leads to over heating of the alternator components and bearings. Thermal management analyses of a proposed Turboalternator can be found in References 9- 24 and 9- 25.

***Magnet overheating***

As the alternator magnets heat, the field produced in the gap will decrease, and consequently the EMF on the stator will decrease. The EMF on the stator is proportional to the field strength and the shaft speed. If the control on the PLR is set up for constant voltage then the alternator will accelerate until the new EMF matches the design EMF. If the control on the PLR is setup for current control, the alternator may maintain a steady speed if there is enough reserve PLR capacity available or accelerate to a new steady state speed. A temporary demagnetization would be fine, but a permanent demagnetizing to a large extent would lead to loss of capability on the alternator and ultimately mission failure.

***Winding overheating***

The heating of the winding insulation will lead to the outgassing of the organic materials which make up the insulation. Since the coolant in the alternator is in thermodynamic contact with all the other components in the primary loop, it is important that the alternator does not outgas any material which can lead to material damage of other components. For example, Nb- and Ta-base alloys cannot be exposed to sources of carbon and oxygen as they suffer from rapid

interstitial embrittlement. This rapid loss of ductility can occur at contamination levels of around a few hundred wppm of C and O. There is currently a preliminary mass transport model completed that would have advanced to quantify an acceptable outgassing rate of these constituents for various reactor materials.

**Material Transport to Alternator Materials**
Fission product release, which is not yet fully characterized, can also lead to beta radiation from the decay of fission products in the coolant. The fission products also will tend to plate on surfaces which match the materials temperature limits. Since the alternator coolant flow path is near the low temperature for the system, a difficult flow path, and has a large magnetic field there is a high probability of the alternator acting as a getter for fission products.

### 9.1.8.3 Bearing Failure Modes

The requirement for the bearing system to support the rotating machinery for a mission length on the order of 20 years makes the gas foil bearings a possible area of concern. Additionally, many of the spacecraft concepts envisioned multiple or back-up Brayton units in order to increase the overall system reliability. These concepts therefore require that a failure of one of the Brayton units would not compromise the other units or the rest of the spacecraft and allow the mission to continue, perhaps at some lower capability. This places an additional requirement on the bearings that if failure does occur, it is contained in the bearing assembly. The primary failure modes identified were particle ingestion, poor thermal management, high cycle faitigue, overloading, and excessive wear.

***Particle Ingestion***
Particle ingestion failure is of minimal concern for the envisioned spacecraft because it is a closed loop system, as discussed above in the section on debris from erosion. However, there is some concern that particles emerging from within the loop could potentially damage the gas foil bearings. In fact the gas foil bearings themselves produce submicron particulate due to rubbing that occurs during start-up and shutdown. It is believed, however, that gas foil bearings are tolerant of particles less than 25 micron in size and greater than 100 microns (Reference 9-34). This is due to the fact that the larger particles are to big to enter the bearings and the smaller particles simply flow through them. If a large particle were to block the cooling flow path for the bearing cavity, it could result in thermal management problems. Over-heating of the bearings could lead to creep problems or if heating was excessive, to melting of the gas foils themselves.

***Reverse flow of idle units***
If idle units are present in system for redundancy, then the current foil thrust bearing design does not allow for reverse rotation of the unit without damage to the bearing. Reverse rotation would need to be prevented by either use of check valves or electrically locking the rotor. Both options would be acceptable, and the key unknown is the amount of backflow needed to cause reverse rotation. This would dictate how leak resistant the valves would have to be and whether electronic locking would be required in addition to or in place of valves.

***Launch loads***
Overloading of the bearings could be a concern during the launch of the spacecraft. This damage would occur due to excessive displacements from launch vibrations causing plastic

deformation of the foil structure. This damage would perhaps go unnoticed until operation of the Brayton units began, and problems would arise during startup. This scenario may necessitate that a temporary support structure is designed to prevent turboalternator shaft deflections during launch. This support structure would then be removed prior to initial start-up of the Brayton unit.

***Wear***

The majority of wear in current gas foil bearing applications occurs during start-ups and shutdowns, when the shaft is rotating at too low of a speed for a gas film to develop therefore causing the shaft to be in direct contact with the bearing surface. Since the envisioned mission profiles contained relatively few start-up and shut-down cycles, this type of wear was not considered to be a major concern. However, during normal operation, there is some small amount of contact between the shaft and bearing surface during transients. Over a long period of time, this could cause concern for failure. Fortunately, testing has shown that gas foil bearings exhibit what can be called a soft failure mode. This means that failure of the bearings would not trigger a catastrophic event within the Brayton unit.

***Over-Loading***

The most common failure mode in a gas foil bearing is a breakdown of the compliant support structure either by over-loading the bearing or running at too high a temperature. This breakdown causes the bearing to no longer be able to support the shaft and the rotor will quickly stop spinning. However it has been shown in that this quick stopping does not cause the Brayton unit to come apart and compromise the rest of the spacecraft (Reference 9- 34).

***Foil Attachement Failure***

The foil layer and compliant support is attached to the structure by a spot welded attachment joint. High cycle fatigue (HCF) has been shown to cause failure of this joint. More advanced assembly methods may be required to reduce the likelihood of this failure.

Despite the potential failure modes discussed above, reliable gas foil bearing experience has been demonstrated in the aircraft and power generation industry. Table 9-7 shows the commercial experience for various metrics, and compares them to the projected Prometheus concept. Although the Prometheus spacecraft would be unique in that no maintenance would be possible, it is evident from the table that the planned design fits within the operational experience of current state-of-the-art gas foil bearings.

**Table 9-7: Gas foil bearing commercial experience relative to Prometheus concept**

| Gas foil bearing experience | Capstone | Hamilton Sundstrand | Honeywell | Prometheus concept |
|---|---|---|---|---|
| | Microturbines | Air Cycle Machines | Air Cycle Machines | |
| total operating hours (all units) | 6 million | 40 million | 300 million | |
| hours on high time unit | 44,000 | 50,000 | 80,000 | 175,000 |
| start/stops on high cycle unit | 14,000 | 18,000 | 20,000 | << 100 |
| units produced / in service | 2,600 | 4,600 | 25,000 | - |
| max temperature | 727 K | 560 K | 572 K | 450 K |
| surface speed | 480 - 600 ft/sec | 500 ft/sec | 500 ft/sec | 519 ft/sec |

### 9.1.9 Future Development Needs

#### 9.1.9.1 Turbomachinery Development

The turbine assembly structural design needs further development in evaluating:

- The turbine wheel, turbine scroll, and turbine stator blades allowable creep deformation (% creep strain),
- More comprehensive set of creep property data for the proposed materials in a prototypic He/Xe environment,
- Further development of creep mitigation techniques (scroll internal insulation, and advanced materials).

The current shaft conceptual design of an overhung "single disk" layout with a large shaft diameter has a difficult entrance of the flow to the compressor making the stability and efficiency of this machine less than ideal. Future study should focus on the requirements of the compressor inlet flow area and hub diameter needed to understand if the overhung "single disk" layout is an acceptable layout with a single rigid shaft for the needed high performance compressor stage. Other shaft layout options should be explored including the capstone microturbines flexible shaft coupling from the compressor to the alternator, and the more traditional shaft layout with the turbine and compressor on either end of the shaft. More detailed analysis of the rotor dynamic stability of these various shaft layouts, the hydrodynamic performance of the compressor, and the thermal management of the machine would be needed before one option is carried forward.

#### 9.1.9.2 Alternator Development

The primary future developments needed for alternators in a Brayton unit is an insulation system able to withstand the necessary temperatures along with being chemically compatible with the rest of the materials in the loop, and the development of a high power electrical feedthrough with acceptable hermiticity for retaining the gas inventory. The design and build of this component appears to be an engineering challenge at this time, but it is possible.

#### 9.1.9.3 Bearing Development

In the NRPCT Feasibility Report (Reference 9- 35), gas foil bearings were identified as one of the key issues requiring special consideration in the development of Brayton technology. Specifically, concerns were raised on the ability of the gas foil bearings to perform without failure and with no maintenance for a period of 20 years. Although the report indicates this concern was partially alleviated due to the reliable experience gas bearings have demonstrated in the aircraft industry (See Table 9-7), it was still understood that further testing and development would be required prior to launch to minimize the risk of a bearing failure. This testing and development was to have occurred primarily at NASA Glenn with input from the NRPCT. The planned focus of the testing was to occur in the following areas: high speed and high pressure testing, imbalance and misalignment sensitivity, alternate gas performance, and solid coating development. The details of this work can be found in the NASA Glenn Research

Center FY06 Workscope (Reference 9- 36). Additionally, the existing NASA Glenn facilities are described in Reference 9- 30.

In addition to the bearing development work conducted at NASA Glenn, a smaller effort was to be focused specifically on the rotor dynamics of the proposed concepts. A preliminary effort was completed in this area and reported in Reference 9- 32. This paper focused on the conceptual design proposed by Hamilton Sundstrand. This study concluded that the conceptual design was feasible from a rotor dynamic standpoint. This preliminary study was to be followed in FY06 by a more rigorous study of new conceptual designs and more prototypic bearing properties for the high pressure He/Xe fluid. Later in FY06, a simulated rotor was to be created and rig tested to characterize the stability of the system.

## 9.2 Recuperator

### 9.2.1 Summary and Conclusions

The recovered heat in the recuperator significantly improves cycle efficiency for the relatively low pressure ratios (~2) of the turbomachinery. This component has been evaluated on a conceptual level in this report. The following provides a summary of the main conclusions:

---

- Based on vendor discussions, resizing a single recuperator to handle 100% of the envisioned recuperated thermal load for a 200 kW electric plant is expected to be feasible. In the current recuperator sizing assumptions two recuperators are assumed to share the recuperated thermal load.

- Initial studies indicate that for the high effectiveness designs being considered (> 0.9), the recuperator performance may be influenced more by flow maldistribution than by uncertainties in heat transfer coefficients. Further studies to quantify flow maldistribution would need to be performed as more detailed designs progressed.

- Based on constructed units under similar operating conditions, component reliabilities of greater than 0.95 are expected to be achievable with development and testing.

- The largest material challenges for this component are the braze performance and creep/creep fatigue tolerance of the hot end of the unit over mission life. The mechanical design basis for this component will need to be further developed to minimize mass while providing a robust design over mission life.

---

### 9.2.2 Introduction

#### 9.2.2.1 General Configuration

The recuperator designs being considered for Prometheus are based on compact plate fin designs. Compact plate fin designs provide compact, lightweight and highly effective heat exchanger configurations. The importance of mass in space applications makes the plate fin configuration an attractive alternative to more conventional, bulkier shell and tube heat exchanger designs. The basic geometry of a plate fin design is provided in Figure 9-16. Typically the fin geometry is configured to break up the thermal boundary layer of the working gas. Figure 9-17 provides an example of two standard fin configurations, the offset fin design and wavy fin design. The offset fin configuration and the wavy fin configuration improve heat transfer characteristics relative to fully developed flow conditions at the expense of pressure drop through the heat exchanger core.

Typically, a recuperator can be subdivided into the following regions: (1) the heat exchanger core, (2) the headers and (3) the inlet manifolds or plenums. Figure 9-16 provides a simple schematic illustrating the various regions of a recuperator. For a highly effective recuperator

design, a counter flow arrangement is desired for the heat exchanger core. A counter flow arrangement minimizes the required heat transfer surface area for a given thermal load relative to parallel or cross flow configurations. In order to deliver the gas flow to the counter flow core region of the recuperator, header regions are required as shown in Figure 9-16. Due to geometry constraints the flow configuration in the header regions is typically cross flow. Because of the lower heat transfer performance associated with the cross flow configuration relative to the counter flow configuration it is desirable to minimize the fraction of cross flow heat exchanger area.

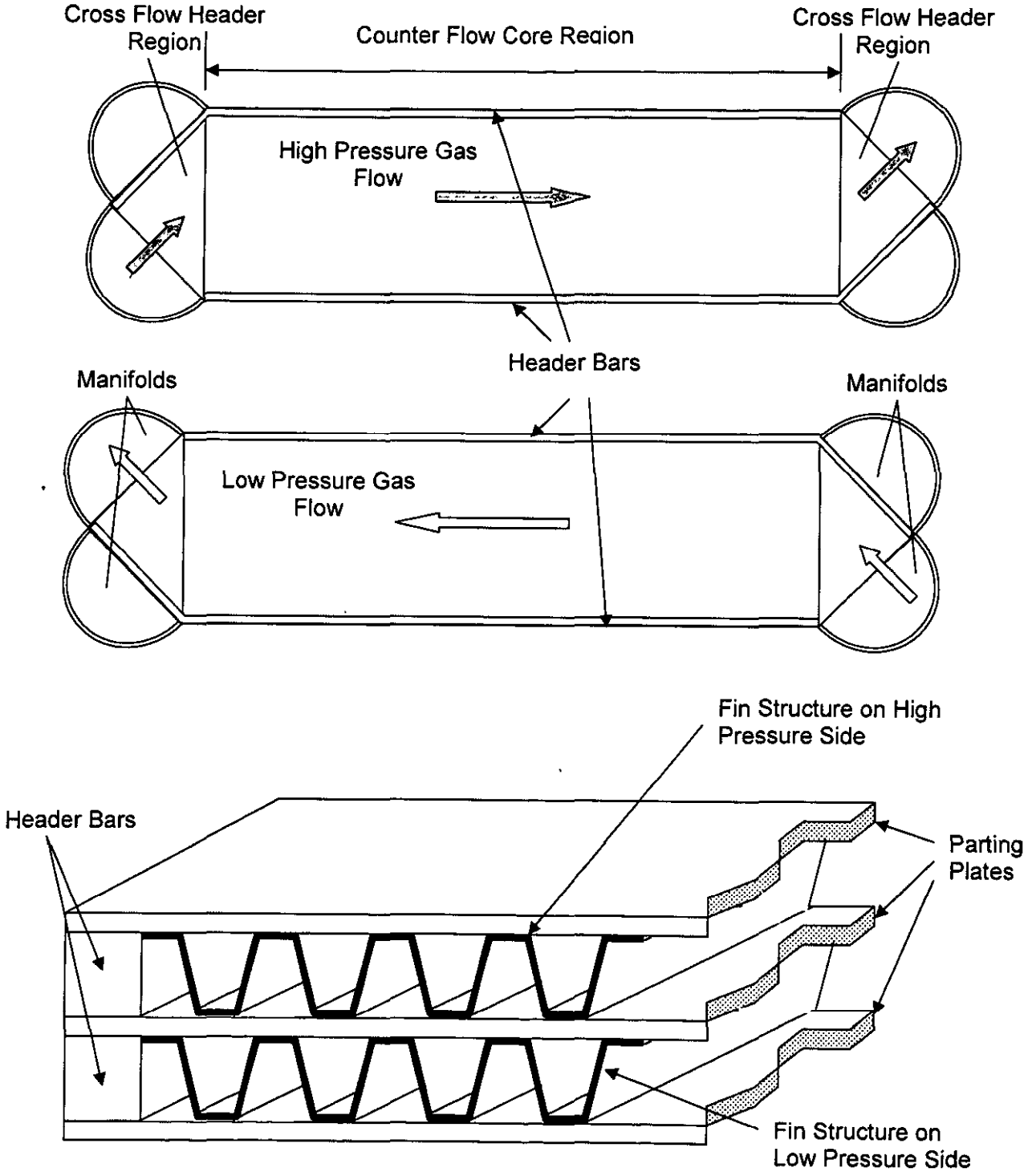
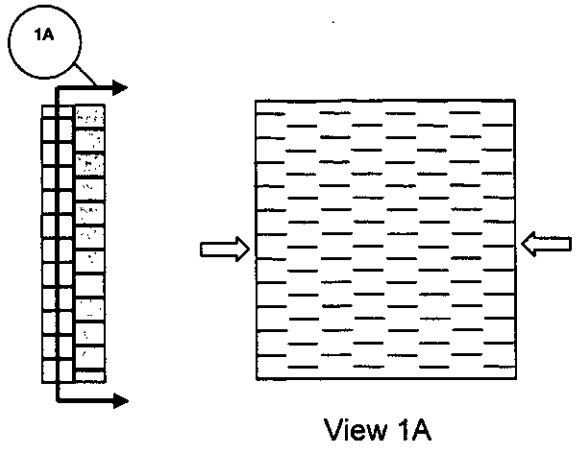
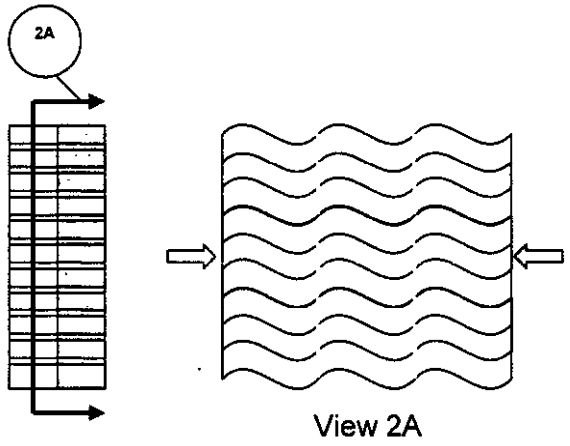



**Figure 9-16: Typical plate fin structure of a recuperator.**




**Offset Fin Geometry**




**Wavy Fin Geometry**

**Figure 9-17: Examples of compact heat exchanger fin configurations.**

### 9.2.2.2 Recuperator Benefits in a Closed Brayton Cycle

The recuperator is an essential component in the closed direct cycle Brayton system being considered for Prometheus. For the compressor pressure ratios being considered (~ 2.0) for Prometheus applications the thermal load of the recuperator is a significant fraction of the coolant enthalpy rise from the compressor exit to the turbine inlet and enthalpy reduction from the turbine exit to compressor inlet.

Figure 9-18 provides a simplified temperature entropy diagram of the Brayton cycle illustrating the effects of compressor pressure ratio on the thermodynamic cycle (the heat transfer in the recuperator is larger than the heat transferred in the reactor). The recovered heat in the recuperator increases efficiency for Brayton cycles with relatively low compressor pressure ratios by increasing the temperature difference between the high temperature expansion in the turbine and low temperature compression in the compressor for a fixed reactor thermal rating. For the direct Brayton systems being considered for Prometheus, the turbine inlet temperature is expected to be limited to approximately 1150K due to material limitations and the compressor inlet temperature is limited to approximately 400K due to the increased size of the heat rejection system at lower compressor inlet temperatures. In this scenario where the temperatures are constrained the recovered heat in the recuperator reduces the thermal load needed from the reactor.

At higher pressure ratios the enthalpy increase across the compressor becomes a significant fraction of the total fluid enthalpy rise. When the compressor exit enthalpy is greater than the turbine exit enthalpy, the presence of a recuperator in the system reduces cycle performance. For the power ratings being considered for Prometheus, low pressure ratio, radial turbomachinery designs provide the best design options; and therefore, require a recuperator for system efficiency improvements.

Designing the recuperator to transfer heat in a configuration providing a large heat transfer area per unit volume is a primary design consideration for space applications. Another consideration in recuperator designs is the effect of pressure drop on overall system performance. For a desired electrical output, an increase in the nonrecoverable pressure drop in a recuperator is a system irreversibility that must be compensated for by an increase in turbine work and system mass flow. The typical parameter for assessing pressure drop is to ratio the stagnation pressure drop across a component to the inlet pressure of that component ($\Delta P/P$).

Another approach in assessing the effects of pressure drop on system performance is to express the pressure drop in terms of system entropy as discussed in Reference 9- 44. This Reference also compares various recuperator designs and evaluates their performance from both a pressure drop and entropy increase perspective.

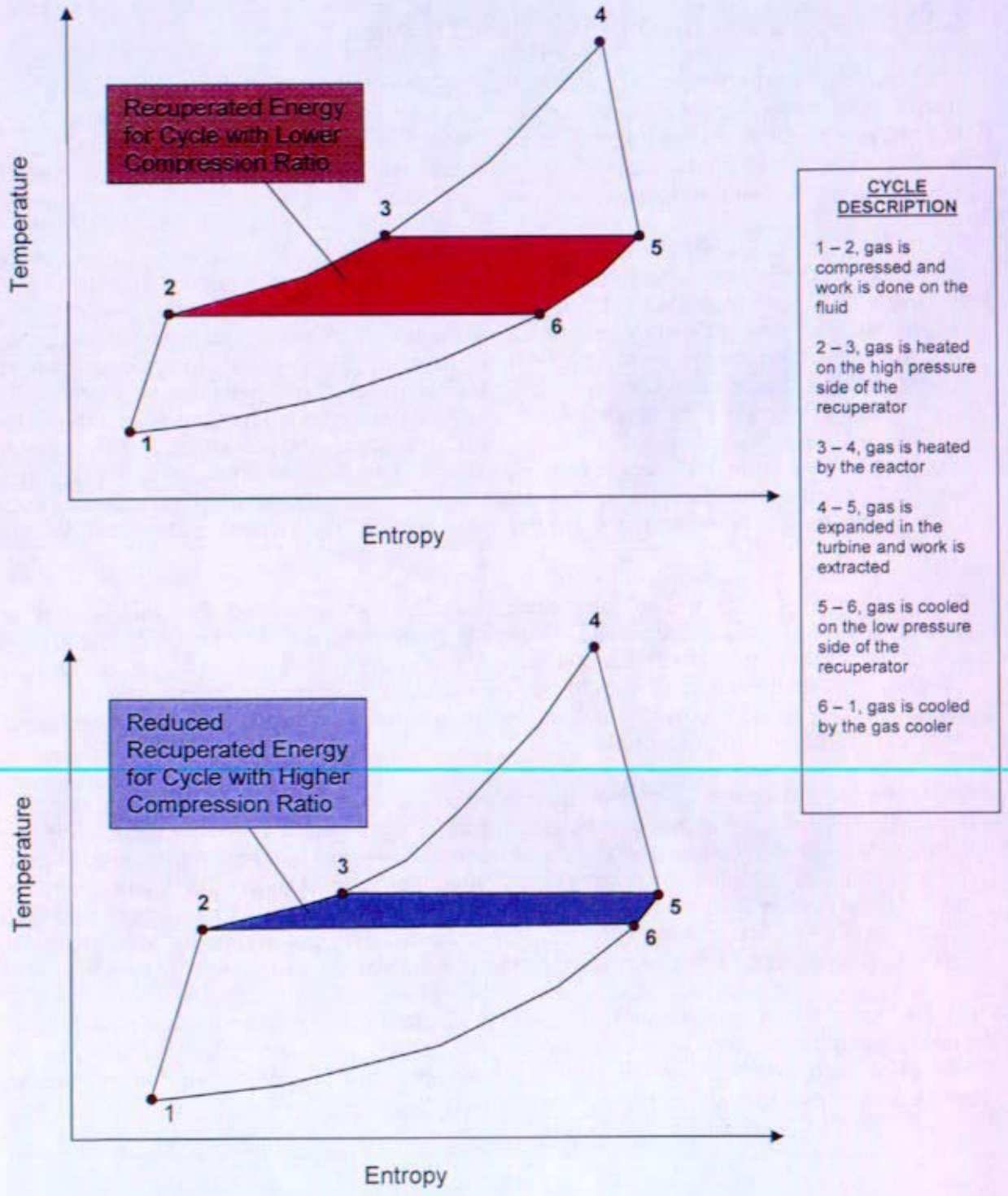



**Figure 9-18: Simplified temperature entropy diagram illustrating the effects of increased compressor pressure ratio on recuperated energy (assumes 100% effective recuperator designs).**

### 9.2.2.3 Recuperator Component Requirements

Final functional requirements for the component design have not been established. Table 9-8 presents notional component operating conditions assuming two engines operating at 100% of designed power capacity to support full mission lifetime with two spare units available for backup. These operating conditions are consistent with the four Brayton configuration discussed in Section 6. As indicated in the table the recuperator heat transfer results in a significant temperature difference in the working gas. The heat transfer rate in a single recuperator (~757kW) is almost twice as large as the gas cooler (~382kW) and for two operating recuperators the thermal rating of the recuperators (~1514 kW) is larger than the thermal rating of the reactor (~1002 kW).

**Table 9-8**: Summary of recuperator operating conditions for a four Brayton/Recuperator configuration as described in Section 6.

| Parameter | High Pressure Side | Low Pressure Side |
|---|---|---|
| Inlet Temperature (K) | 538 | 943 |
| Exit Temperature (K) | 911 | 571 |
| Inlet Pressure (MPa) | 1.98 | 1.04 |
| Pressure Drop (MPa) | 0.015 | 0.015 |
| Thermal Rating (kWt) | 757 | |
| Effectiveness (-) | 0.92 | |
| Mass Flow (kg/s) | 3.08 | |
| Single Brayton Electrical Load (kWe) | ~100 | |

### 9.2.2.4 Design/Fabrication Considerations

The ability to join the loop piping to the inlet plenum piping of the recuperator is a critical aspect of the plant design. Various material options have been considered for loop piping. For the titanium based piping materials, joining to a Ni base recuperator material will require development. Reference 9- 45 provides a summary of joining issues and potential design solutions for various dissimilar metal joints being considered in the direct Brayton plant.

The fin structures in a recuperator are typically structurally more limiting than the braze joints for the primary pressure loads. As described in Reference 9- 46, the governing equation for evaluating fin tensile stress is given by the following equation:

$$\sigma_{fin} = \frac{P}{f} \cdot \left( \frac{b_{fin} - t_{fin}}{t_{fin}} \right)$$

Where: P = internal pressure (Pa)
$b_{fin}$ = fin spacing (m)
$t_{fin}$ = fin thickness (m)
f = fin strength efficiency factor

An excerpt from Reference 9- 46 provides more details on the fin strength efficiency factor:

"Fin strength efficiency factors have been found to range from 0.33 to 0.60 based upon actual test results on a wide variety of plate and fin configurations. The 0.33 factor is used in creep designs and 0.60 is used in short time load situations. The strength efficiency factor is defined as the ratio of actual burst pressure to burst pressure as calculated from ultimate stress properties. The apparent reduction in strength is attributable to non-uniform load distribution across the fins that arises due to inequality in fin height. The taller fins actually buckle during the braze operation and, as a consequence, the shorter fins carry the bulk of the pressure containment forces. Since the fins are never perfectly straight, pressure loads will also cause fin bending stresses. Finally, the fins can not be formed with perfectly square corners, and stress concentrations will actually occur at the fin-to-plate braze fillet joints. This strength reduction factor is based upon the performance of successfully brazed heat exchangers, i.e., the failure mode at burst is tensile rupture of the fins. For poorly brazed heat exchangers, (incomplete braze joining of the fins and plates), the pressure containment capability of the plate-fin structure is drastically reduced. For this reason, all heat exchangers are subjected to a proof pressure test at 150 percent of working pressure. This proof test is expected to cause a failure in defective cores, and conversely, a unit that passes the proof test is expected to achieve the required pressure capability."

In fin design, fin uniformity must not only be maintained for structural reasons as discussed above, but also for thermal hydraulic reasons as well. Variations in fin dimensions within a heat exchanger core can result in flow maldistribution which impacts recuperator performance as discussed in Section 9.2.3.2. The fin material must be capable of withstanding the maximum turbine exit temperature and lifetime requirements (~ 20 years) for proposed Prometheus missions. The header bars, parting plates, plenum/manifold structure and braze materials must be designed to meet the temperature and lifetime requirements. For the hot end temperatures and lifetimes of proposed Prometheus missions, creep fatigue is a critical design consideration for the recuperator. The creep characteristics of potential recuperator materials are discussed further in Section 9.2.2.5. Any cyclic transients would need to be considered in conjunction with the creep characteristics in assessing the long term reliability of a recuperator unit. Although transients were expected to be minimal during the Prometheus mission, for other nuclear space missions thermal transients may be significant and low cycle creep fatigue would be of even greater importance.

For the direct cycle Brayton system being considered, appropriate structural design criteria will need to be developed for the various components in the primary coolant path. Reference 9- 47 provides an initial NRPCT assessment of necessary structural design requirements for the various primary system components. As stated in Reference 9- 47:

"Since mass is one of the critical challenges for the SNPP design, structural design methodologies employed in various weight/mass critical applications such as aircrafts and space vehicles will be assessed to explore ways to reduce the design factors that are applied to land-based nuclear reactors and yet to enable a safe, capable, reliable and deliverable SNPP design. Pending this review, basing the SNPP structural requirements on the ASME Code for high temperature nuclear components is appropriate."

The recuperator designs for an envisioned Prometheus application have been based on standards established for the aircraft/space industry. At the hot end temperatures of the recuperator, some of the materials under consideration are not qualified for nuclear applications in the ASME Code. Brazing is also not recognized as a typical joining method for a pressure boundary in the nuclear section of the ASME code. To assist in meeting mass goals for a launch application, standards similar to the aerospace industry will need to be explored. For a ground based prototype, the level of risk associated with the aerospace standards may not be acceptable from a safety perspective and additional structural containment may need to be considered for the design.

Initial criteria were established in Reference 9- 47 for the structural boundaries in the primary loop of the plant. The structural boundary of the recuperator to space would need to be assessed based on these criteria. If the project were to proceed, more detailed criteria would need to be established for assessing structural boundary integrity as a function of lifetime and temperature to meet mass goals of a space application while providing adequate safety margin for a nuclear application.

### 9.2.2.5 Potential Materials of Construction

Recuperator vendor contracts were not established prior to the termination of the project and specific materials were not defined for the construction of the recuperator. NRPCT was planning to competitively bid the Brayton/recuperator design and fabrication as described in Reference 9- 48. Possible materials of construction included various Ni-base superalloys. In a previous design in Reference 9- 49, Hastelloy X was selected as the base material for the recuperator core. Hamilton Sundstrand was considering alloy 625 as a potential candidate material. Other possible materials included alloy 617 and Haynes 230. The biggest material challenge for the recuperator materials was the proposed long term operation at elevated temperatures. The combination of the hot end inlet temperature of 922K in combination with a 20 year lifetime make creep fatigue, microstructural phase stability and long term material compatibility potential issues for the recuperator.

**Creep**

High temperature creep data is presented in Table 9-9 for alloys 625, 617, Haynes 230 and Hastelloy X. Initial strain in Alloy 617 will be due to yielding rather than creep due to its low yield stress at 922 K. Haynes 230 and Alloy 625 have fairly comparable creep properties, both of which are better than Hastelloy X. Alloy 625 is not recommended for long term service at elevated temperatures (>868K) due to the formation of a deleterious $Ni_3Nb$ phase that impairs both tensile ductility and impact strength. Haynes International recommends the use of Haynes 230 for situations where thermal stability is an issue.

**Table 9-9: Approximate initial stress (MPa) to produce creep for selected Ni-base superalloys at a temperature of 922K.**

| Creep % | 0.5 % | | | 1.0% | | | Rupture | | |
|---|---|---|---|---|---|---|---|---|---|
| Time (hrs) | 10 | 100 | 1000 | 10 | 100 | 1000 | 10 | 100 | 1000 |
| | | | | | | | | | |
| Haynes 230[a] | 330 | 220 | 150 | 350 | 250 | 170 | 460 | 330 | 250 |
| Alloy 625[a] | 350 | 250 | 160 | 400 | 275 | 170 | - | 530 | 380 |
| Alloy 617[b] | * | * | * | * | * | * | 480 | 390 | 310 |
| Hastelloy X[a] | 276 | 186 | 121 | 303 | 207 | 145 | 462 | 331 | 170 |

[a]Haynes International, Inc.
[b]Special Metals, Inc.
*At 922K, 617 will plastically deform with a 0.2% yield stress of ~250 MPa.

**Microstructural Phase Stability**

All four of the above Ni-base superalloys contain about 0.1 wt.% carbon. At a temperature of 922 K, it is expected that the kinetics for carbon release from the superalloys would be very slow. A number of references (References 9- 50 and 9- 51 ) have shown decarburization of superalloys only becomes a concern above ~1073 K. It is currently unknown if the kinetics are slow enough to be safely ignored for a period of 120,000 hrs. The acquisition of experimental data to determine the rate of impurity release from candidate superalloy materials was planned as part of the compatibility testing effort to support the SNPP (Space Nuclear Power Plant).

**Long Term Braze/Base Metal Material Compatibility**

In choosing a braze compound, it is important to select a material that demonstrates metallurgical stability with the materials to be joined, as well as low volatility to preclude contamination of the HeXe gas loop. Table 9-10 lists the braze materials identified for potential use in the recuperator and Table 9-11 lists the vapor pressures of the elements found in these brazes. Based on the vapor pressure data (elements with higher vapor pressures are more volatile), caution is warranted in the use of BNi-8 because of the danger of Mn preferentially evaporating from the braze and entering the He gas stream. The other components of the various braze materials have vapor pressures on the same order of the superalloys and should pose no difficulty. Under high neutron flux, the use of BNi-2 or Palnicro 36M raises concerns due to the transmutation of boron to helium under neutron irradiation. He will migrate to grain boundaries to form voids (bubbles) and subsequently decrease the ductility of the material. However, for the flux levels expected behind the shield, boron transmutation to helium is not expected to be a concern.

Testing and joining development should concentrate on BNi-5 and the eutectics Pd-Co and Pd-Ni. BNi-5 is promising because Haynes 230 already contains all of these elements, whereas Pd-Co and Pd-Ni are systems with complete solid solubility and should braze the materials well. Long-term testing should be conducted to identify any phase evolution between the braze materials and base superalloys. Pd does form an intermetallic phase with Mo, and at least 8 intermetallic phases with Al, both of which are alloying elements of Haynes 230 (see Reference

9- 52). Intermetallic phase formation between braze and base metal could compromise the joint integrity.

**Table 9-10: Brazes identified for potential use in the recuperator. Nominal compositions, along with melting points are provided.**

| Name | Chemical Composition | Melting Range (K) |
|---|---|---|
| BNi-8 | Ni-23Mn-7Si-4.5Cu | 1310-1340 |
| BNi-2 | Ni-7Cr-3Fe-3.1B-4.5Si | 1243-1273 |
| BNi-5 | Ni-19Cr-10.1Si | 1353-1408 |
| Palnicro 36M | Ni-36Pd-10.5Cr-3B-0.5Si | 1093-1233 |
| Pd-Co | 65Pd-35Co | 1492 (eutectic point) |
| Pd-Ni | 60Pd-40Ni | 1511 (eutectic point) |

**Table 9-11: Vapor pressures of the braze constituents at 922 K. The value for Si has been extrapolated from higher temperatures (from Reference 9- 53).**

| Element | $P_{Vap}$ @ 922 K (Torr) |
|---|---|
| Pd | $1.3\times10^{-12}$ |
| Ni | $2.2\times10^{-14}$ |
| Co | $3.3\times10^{-14}$ |
| Si* | $3.1\times10^{-14}$ |
| Cr | $1.8\times10^{-12}$ |
| Cu | $2.5\times10^{-10}$ |
| B | $3.1\times10^{-22}$ |
| Mn | $2.0\times10^{-06}$ |
| Fe | $4.8\times10^{-13}$ |

In addition to the Ni base materials being considered for recuperator construction, developmental work exploring carbon/carbon recuperators is ongoing at NASA Glenn with a contract through Allcomp. The feasibility of a carbon-carbon (C/C) recuperator for space systems has been assessed in Reference 9- 44. The excellent thermal properties, high-temperature capabilities, and low density of carbon-carbon materials make them attractive for use in the recuperator, but development issues such as compatibility, joining, and fabrication must be addressed.

Carbon-carbon materials provide high-strength at low weight and can withstand operational temperatures up to 2273 K in a non-oxidizing environment. Also, C/C composites present the opportunity to tailor their thermal or mechanical properties, which can be controlled by the different fiber, matrix, or processing options.

C/C composites present significant risks that can prohibit their adoption into the direct gas Brayton system. Foremost is the concern over corrosion. Incorporating a C/C composite into the primary working gas could yield gaseous C or CO leading to contamination of Nb- or Ta-base refractory metal alloys. Also, the corrosion of carbon produces impurities that can drive the coolant chemistry into a regime where superalloys carburize, decarburize, or oxidize depending on the specific chemistry of the coolant. Carbon/carbon composites are expected to be compatible with a SiC reactor; however, the previously mentioned compatibility issues with the remainder of the Ni base plant loop piping may still pose a concern.

Integrating a carbon-carbon composite into an otherwise all-metallic energy conversion system raises concerns over joining the composite to the metal structure of the recuperator. The coefficient of thermal expansion mismatch between C/C and metal interfaces may create excessive thermal stresses causing failure at the joint and catastrophic gas leakage. The joining technology between C/C and metal is underdeveloped and unproven for high-temperature joint reliability over a long mission lifetime. Fabrication of C/C recuperators must also overcome obstacles such as developing uniform fin heights, and properly joining plates to fins.

### 9.2.2.6 Recuperator Sizing Evaluations

Both fin configurations provided in Figure 9-17 were considered in recuperator designs for Prometheus. Figure 9-19 from Reference 9- 54 provides a conceptual design from Hamilton Sundstrand for a 514 kW thermal rating. The fin structure for this design is wavy fin. An offset strip fin design has also been considered for high temperature recuperator applications in the past as documented in References 9- 49 and 9- 55. For the recuperator, a sizing model based on a double stacked offset fin design has been used for mass estimates. This model was developed by NASA Glenn and independently verified through an NRPCT recuperator model. The mass estimates for this model are larger than the proposed Hamilton Sundstrand recuperator design by a factor of approximately 1.3. Table 9-12 compares various aspects of the offset fin design used for mass estimates to the Hamilton Sundstrand design for the thermal rating and design conditions assumed by Hamilton Sundstrand in Reference 9- 54.

Due to the large size differences between the offset strip fin design and the Hamilton Sundstrand design, an independent sizing assessment was also performed to confirm the sizing and pressure drop of the Hamilton Sundstrand design. Simple counter flow calculations were performed assuming the same thermal load and flow areas. The largest driver in the heat transfer area is the improved fin effectiveness of the Hamilton design relative to the double stacked offset strip fin design currently being used for mass estimates. The tighter fin pitch associated with the Hamilton design also results in reduced recuperator size. The independent NRPCT calculations did not attempt to capture the cross flow characteristics of the headers for the Hamilton Sundstrand design and assumed the same Reynolds Colburn and friction factor analogy currently being assumed for the offset fin model. The required heat transfer areas of the high pressure and low pressure sides of the recuperator core were estimated at 21.4 $m^2$ and 32 $m^2$ respectively. Assuming the offset fin friction analogy, the estimated pressure drop for this design was consistent with the Hamilton estimates of pressure drop after correcting for flow length differences.

At this point in the design process the more conservative offset fin mass estimates are being reported. The justification for using the more conservative mass estimate is based on the following:

1. The absolute system pressure is a factor of approximately 1.6 larger in the current plant concept (compressor exit pressure is 2.0 MPa vs 1.28 MPa in the Hamilton Sundstrand concept). The compressor pressure ratio is also larger in the current base case design resulting in a larger pressure difference between the high pressure and low pressure side of the recuperator. The high to low side pressure differential in the Hamilton Sundstrand design is approximately 0.56 MPa compared to 1 MPa in the current base case design. The higher pressure improves the thermal hydraulic performance of the recuperator but also requires additional structure to support the increased primary loads. Structural analysis and redesign has not been performed on either the Hamilton or the offset fin design to calculate the potential mass increase associated with the higher system pressure. The heavier mass estimate associated with the offset strip design provides margin to accommodate the increased pressure differentials.

2. The baseline recuperator effectiveness has been increased from 0.90 to 0.92 and the thermal load has been increased from 514 kW to 761 kW relative to the Hamilton Sundstrand recuperator configuration in Reference 9- 54.

3. Assessments of creep on the recuperator core fin configuration were considered by Hamilton in the design; however, detailed structural models assessing creep fatigue performance have not yet been performed for the Hamilton Sundstrand recuperator for a twenty year life which integrated the manifold structure and evaluated potential thermal transients. The higher mass estimates provide margin to absorb potential mass increases associated with creep fatigue design details.

4. Literature (Reference 9- 58) suggests that for the low Prandtl number HeXe fluid being considered for the direct Brayton cycle, the heat transfer coefficients may be lower resulting in larger heat transfer area requirements to meet the desired recuperator effectiveness.

5. The effects of flow maldistribution on recuperator performance have not been fully addressed. For highly effective recuperator designs with low pressure drop requirements, flow maldistribution in both the recuperator headers/core and the plenums/manifolds can adversely affect both effectiveness and pressure drop goals. Detailed assessments of flow maldistribution on specific recuperator designs for Prometheus have not been performed. In Reference 9- 54 the following concern was raised relative to flow maldistribution for the Hamilton Sundstrand design:

   "With respect to the many previous NASA Brayton system studies, the allowable pressure drop for the heat exchangers usually falls into the 2-3% range for $\Delta P/P$. At low percentage pressure drops, flow distribution in the headers and heat exchanger core is an issue that leads to over sizing the heat exchanger to account for such inefficiencies. Therefore, after subsequent discussions and assessments, it was agreed to establish 0.020 MPa as the allowable pressure drop for both sides of the

recuperator. This reduces cycle efficiency slightly, but yields a substantial weight and volume savings for the recuperator. The allowable range with the 0.020 MPa pressure drop for both gas loops is now approximately 2.8% for $\Delta P/P_{hot}$ and 1.5% for $\Delta P/P_{cold}$. Accordingly, with this modification, the recuperator design conditions were established from which a design effort was conducted. Higher allowable pressure drops provide good flow distribution within the headers and the core for the folded fin-plate compact heat exchanger design. Therefore, in order to obtain a useful and a high performance recuperator design, special consideration will be required in the design of the inlet gas ducting, the headers and the core. It may also require the addition of features within the headers to direct and distribute the flow across the face of the core and avoid distribution problems that could impact the allowable pressure drop budget."

Currently, the baseline pressure drop allotments ($\Delta P/P$) of 1.5% and 0.8% on the low pressure and high pressure side of the recuperator are approximately 20 - 25% lower than the 0.02 MPa guidance established by Hamilton Sundstrand.

Section 9.2.3.2 provides an initial assessment of flow maldistribution on the performance of the Mini-BRU recuperator.

6. The effects of microstructural phase stability and braze/base metal compatibility over a 20 year life on material properties has not been fully investigated or incorporated into the design for the Ni-base superalloy materials being considered for the recuperator. Hamilton Sundstrand had planned on long term braze sample tests to better address this issue.

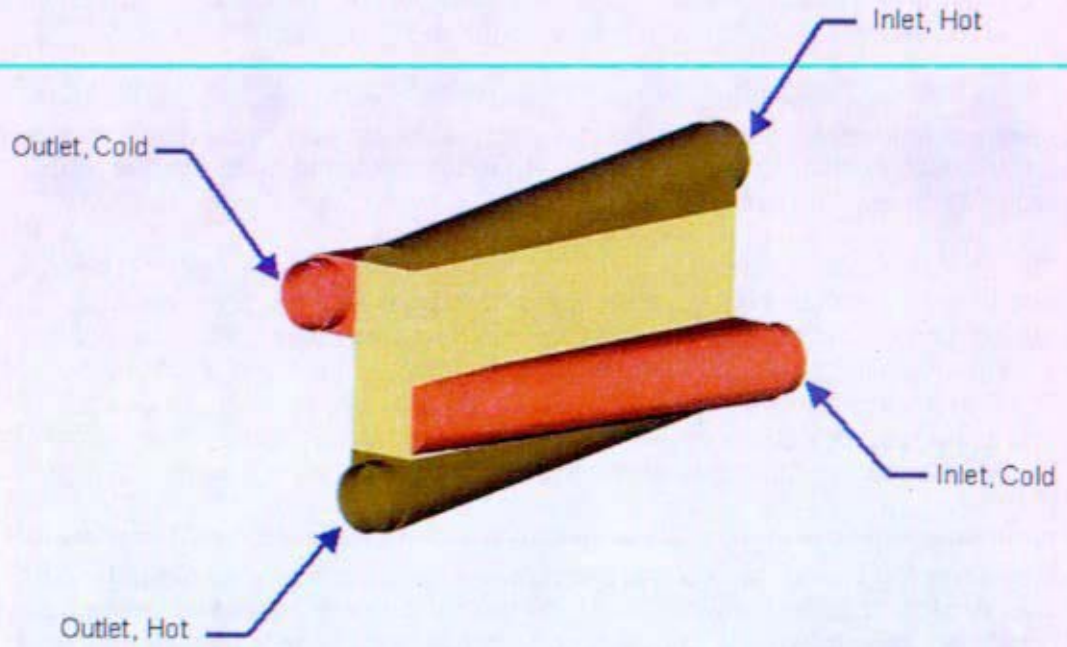



**Figure 9-19: Hamilton Sundstrand recuperator assembly (from Reference 9- 54).**

**Table 9-12: Comparison of geometry and operating parameters for the proposed Hamilton Sundstrand recuperator design (from Reference 9- 54) to the mass models being used by NRPCT.**

| | NRPCT/Glenn Recuperator Model Sized to Conditions Assumed by Hamilton Sundstrand | | Hamilton Sundstrand Design | | NRPCT/Glenn Recuperator Model Sized for NRPCT Baseline Plant Conditions | |
|---|---|---|---|---|---|---|
| | Low Pressure Side | High Pressure Side | Low Pressure Side | High Pressure Side | Low Pressure Side | High Pressure Side |
| Thermal Rating (kW) | 514 | | 514 | | 761 | |
| Effectiveness (%) | 90 | | 90 | | 92 | |
| Mass Flow Rate (kg/s) | 2.07 | | 2.07 | | 3.08 | |
| Inlet pressure (MPa) | 0.71 | 1.28 | 0.71 | 1.28 | 1.04 | 1.98 |
| Pressure drop (MPa) | 0.02 | 0.01 | 0.02 | 0.02 | 0.015 | 0.015 |
| Inlet temperature (K) | 947 | 531 | 947 | 531 | 943 | 536 |
| Outlet temperature | 573 | 905 | 573 | 904 | 568 | 910 |
| MW of working fluid (kg/kmol) | 31.37 | | 31.37 | | 31.5 | |
| Fin Spacing (mm) | 1.59 | 1.59 | 0.7943 | 1.058 | 1.59 | 1.59 |
| Fin Height (mm) | 3.139 | 3.139 | 2.540 | 1.905 | 3.139 | 3.139 |
| Fin Thickness (mm) | 0.1524 | 0.1524 | 0.076 | 0.076 | 0.1524 | 0.1524 |
| Total Surface Effectiveness - $\eta_o$ | 0.48 | 0.49 | 0.66** | 0.78** | 0.49 | 0.49 |
| Fin Effectiveness - $\eta_f$ | 0.39 | 0.39 | 0.57** | 0.67** | 0.40 | 0.40 |
| Heat Transfer Surface Area ($m^2$) | 49.3 | 49.3 | 32.0** | 21.4** | 99.2 | 99.2 |
| Recuperator Core Volume ($m^3$) | 0.056 | | 0.030 | | 0.113 | |
| Recuperator Core Mass (kg) | 84.3 | | 64.4 | | 169 | |
| Recuperator Total Mass (kg) | 112 | | 83.9 | | 214 | |

** NRPCT estimated values based on information provided in Reference 9- 54.

## 9.2.3 Design Tradeoffs/Performance Estimates

### 9.2.3.1 Heat Transfer Coefficient Uncertainty Effects

For the HeXe gas mixtures being considered as the working coolant, the Prandtl number of the mixture is approximately 0.2. Test data from Reference 9- 56 indicate that for fully developed turbulent flow, a significant decrease (as much as a 66% reduction relative to Dittus Boelter) in heat transfer coefficients has been observed for these low Prandtl number gas mixtures relative to the standard Dittus Boelter heat transfer correlation. For the heat transfer geometries being considered for the recuperator, the flow is typically in the undeveloped regime due to the interrupted surfaces used in these designs; and therefore, the fully developed turbulent results are not expected to be applicable. Typically for these interrupted surface geometries, the heat transfer and pressure drop correlations are based on test data for the specific geometry being considered. For offset fin geometries, Manglik and Bergles in Reference 9- 57 have provided geometry based correlations for calculating heat transfer coefficients and friction factors which are in good agreement with experimental results. However, these correlations were compared to heat exchanger test data in air and do not address the low Prandtl number effects associated with HeXe.

Reference 9- 58 provides a summary of open literature for heat transfer and pressure drop correlations/test data for offset strip and wavy fin surface geometries. Only one set of test data for a fixed offset strip geometry have been identified for HeXe gas mixtures in the Prandtl/Reynolds regime being considered for the recuperator. Reference 9- 59 provides a summary of test data for various gas mixtures of HeXe for an interrupted plate fin geometry. The authors from this reference recommended a 0.516 exponent (vs. 0.667) on the Prandtl number in the Colburn correlation. This difference results in a reduction of approximately 8% in heat transfer coefficient for a helium xenon gas mixture relative to the previous Colburn correlation being assumed. It should be noted that this is a limited set of data for a specific fin geometry and detailed descriptions of the surface geometry, materials and experimental apparatus/procedures were not provided.

Reference 9- 60 provides a summary of pressure drop and heat transfer test data for a variety of surface geometries tested in air or water. For the recuperator sizing evaluations provided in Section 9.2.2.6, a power fit to the experimental data from Reference 9- 60 was used to calculate the heat transfer coefficient for the design. Because of the limited information available in open literature, no corrections were made to compensate for the low Prandtl number associated with the HeXe mixture being investigated for the Prometheus mission (He mole fraction = 0.784, Xe mole fraction = 0.216).

For the recuperator designs being considered for Prometheus, a reduction in the overall heat transfer coefficient corresponds to a relatively small reduction in recuperator effectiveness due to the high effectiveness of the design. This result is illustrated in Figure 9-20 and Figure 9-21. In these figures the effectiveness and fraction of thermal load of the recuperator are plotted as a function of percent reduction in overall heat transfer for various recuperator thermal ratings. In these figures, the inlet temperatures on the high pressure and low pressure side of the recuperator are fixed at 538K and 922K respectively based on the system state point assessment for a direct gas Brayton system documented in Reference 9- 62. The mass flow rates for both the high and low pressure sides of the recuperator are also fixed at 2.31 kg/sec.

Fixing these parameters implies that for recuperator thermal ratings lower than the 539 kW load the gas cooler and reactor loads would need to increase to supply the same cycle compressor and turbine inlet temperatures relative to the 539 kW case.

The maximum theoretical heat transfer rate possible for a counter flow or cross flow design assuming infinite heat transfer is defined as:

$$Q_{\max} = C_{\min}(T_{lpin} - T_{hpin})$$

Where:

$C_{min}$ is defined as the minimum of the product of mass flow rate and working fluid specific heat for the high pressure and low pressure gas streams.

Because specific heat is independent of temperature and pressure at the conditions being considered for this application and the mass flow rate is equal for the high and low pressure sides of the recuperator, the maximum theoretical heat transfer rate for the conditions described above is:

$$Q_{\max} = 2.31\frac{kg}{\sec}\cdot 659.7\frac{J}{kg\cdot K}\cdot(922K - 538K) = 585.2kW$$

Since heat exchanger effectiveness is defined as :

$$\varepsilon = \frac{Q_{actual}}{Q_{\max}}$$

and $Q_{max}$ is fixed as defined above, the thermal rating of the recuperator establishes the effectiveness with the lower thermal ratings resulting in lower effectiveness as shown in Figure 9-20. As the overall heat transfer coefficient is reduced for the 539 kW base case, relatively large changes in the overall heat transfer coefficient result in smaller percent changes in the actual heat being transferred. This is driven by the large percent increase in the log mean temperature difference for a relatively small percent decrease in thermal load as shown in Figure 9-21. At the high effectiveness of the recuperator envisioned for the Prometheus mission (0.92), the log mean temperature difference is approximately 31K. This 31K temperature difference is a small fraction of the total temperature difference of 353K associated with the enthalpy change of the gas.

Figure 9-22 provides a plot of overall system efficiency and power output as a function of recuperator effectiveness. If after constructing a recuperator unexpected reductions in overall heat transfer coefficient result in reduced recuperator effectiveness, three options are available: (1) redesign the recuperator to add heat transfer area to accommodate the reduced heat transfer coefficient/effectiveness resulting in an increase in overall system mass, (2) redesign the remainder of the system to accommodate the reduced effectiveness resulting in an increase in system mass, (3) accept the overall reduction in system performance associated with the lower recuperator effectiveness. The selected option would be driven by the system margin in the as-built Brayton cycle.

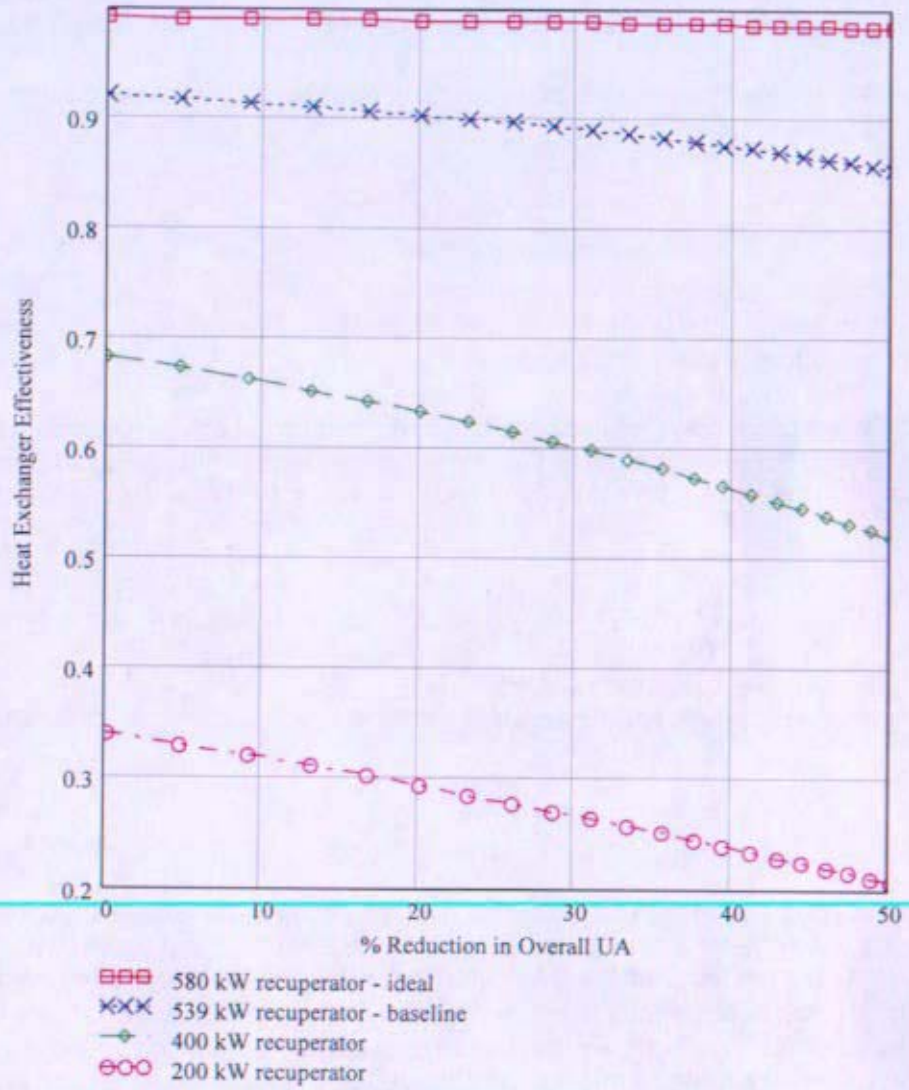



**Figure 9-20: The effects of reductions in the overall heat transfer coefficient on the effectiveness of the recuperator for various baseline thermal ratings.**

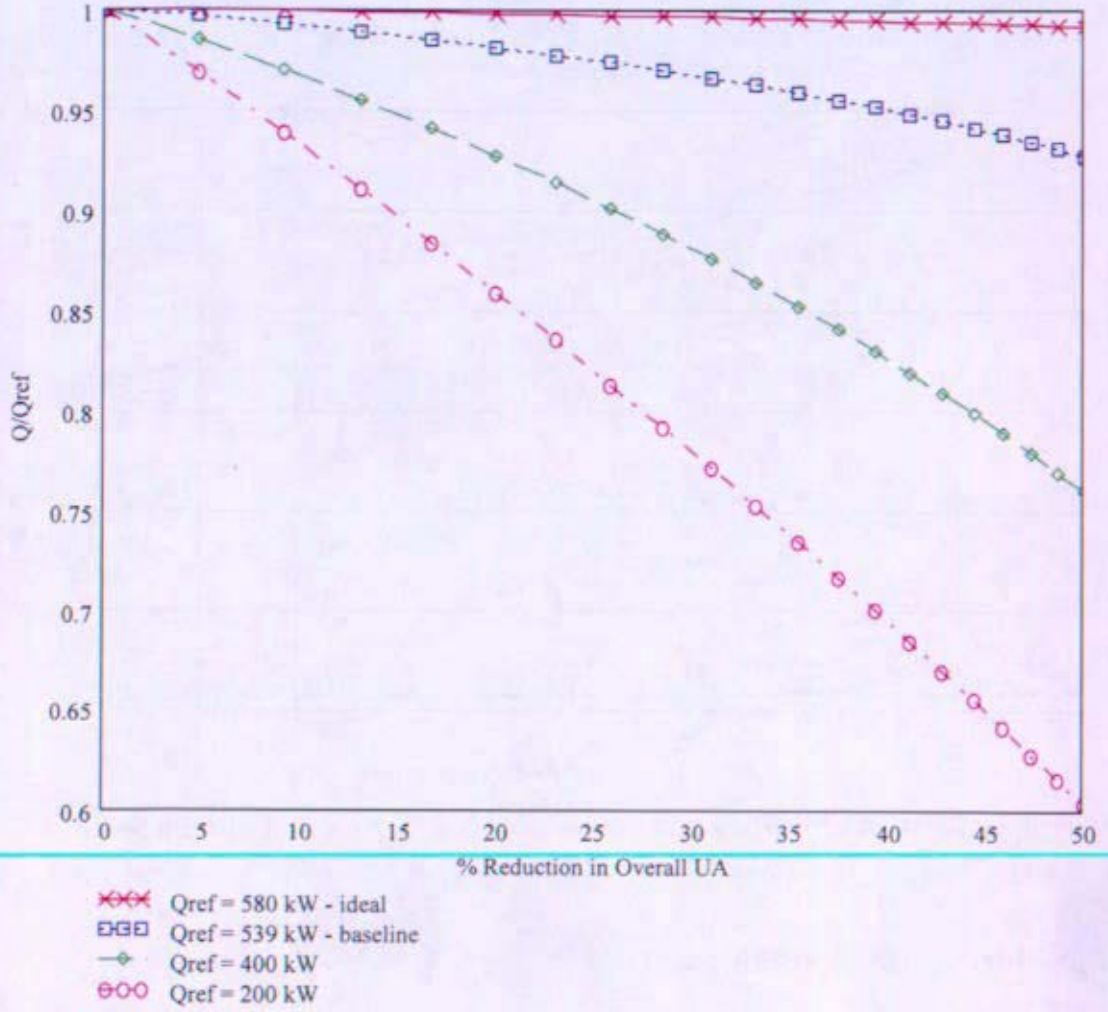



**Figure 9-21: The effects of reducing the overall heat transfer coefficient on the heat transfer rate of the recuperator for various thermal ratings.**

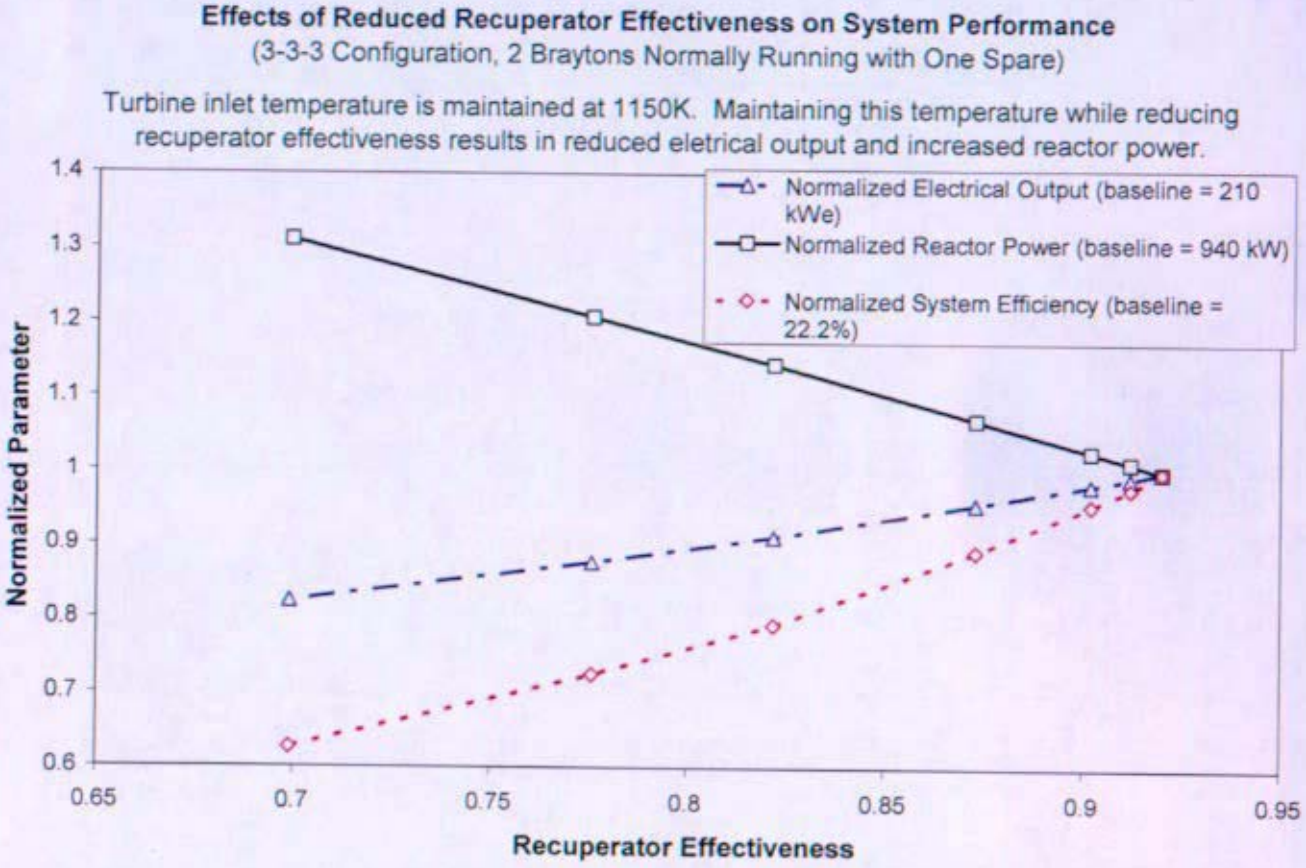



**Figure 9-22: System efficiency and power output as a function of recuperator effectiveness.**

### 9.2.3.2 Flow Maldistribution Effects

Flow maldistribution can have a negative impact on heat exchanger performance from both an effectiveness and pressure drop perspective. For the Brayton cycles being considered for Prometheus, system performance is a function of recuperator effectiveness as illustrated in Figure 9-22. The low stagnation pressure drop requirements ($\Delta P/P \sim 1.5\%$ for a 600kW thermal rating) and high inlet velocities associated with the Prometheus mission make flow maldistribution a design consideration for the recuperator. The inlet pipe velocities and associated dynamic pressure are plotted as a function of inlet pipe diameter for the high pressure and low pressure sides of the recuperator as shown in Figure 9-23. For the low pressure inlet side of the recuperator, the dynamic pressure associated with diameters smaller than 9.5 cm are larger than the total pressure drop of 15 kPa across the recuperator. Increases in heat exchanger core resistance will help to mitigate flow maldistribution effects at the expense of system pressure drop. If the level of flow maldistribution for the Prometheus recuperator can be quantified then system trades would need to be performed to compare the system sensitivities to flow maldistribution and recuperator hydraulic resistance.

As discussed in Reference 9- 63, flow maldistribution can be categorized in the following two areas: (1) flow maldistribution due to heat exchanger geometry, and (2) flow maldistribution due to heat exchanger operating conditions. Specifically, flow maldistribution due to the recuperator manifold geometry is being addressed in this write up to provide better design guidance when integrating the recuperator with the remaining loop piping. To assess the effects and level of flow maldistribution in a highly effective recuperator design, the recuperator from Reference 9- 49 was modeled. This recuperator is designed to operate in a closed Brayton cycle (Mini-BRU) with a thermal rating of approximately 24 kW and an effectiveness of 97.5%. Figure 9-25 provides a schematic of the mini-BRU recuperator design. A one dimensional model of the recuperator was constructed and coupled with flow distribution maps to assess the performance sensitivities to various levels of flow maldistribution. To evaluate the level of flow maldistribution expected in a highly effective recuperator application, a CFD model was developed based on geometry similar to the mini-BRU recuperator geometry described in Reference 9- 49.

**Modeling Assumptions**

To simplify modeling, counter flow geometry was assumed over the entire length of the recuperator for both the high pressure and low pressure flow streams. The cross flow regions at the entrance and exit of the recuperator core were modeled as counter flow regions. For the large inlet/outlet temperature differences associated with the recuperator designs for Prometheus, a significant variation in fluid properties is observed from the hot end to the cold end of the recuperator. The property differences coupled with the cross flow nature of the header regions can result in pressure drop differences from one side of the recuperator to the other. This difference was reported in Reference 9- 49 for the recuperator constructed for the Mini-BRU. The effects of fluid property variations in these cross flow regions and the associated variations in pressure drop and flow maldistribution were not considered in the cases considered.

The flow maldistribution evaluations on recuperator effectiveness assumed that the integrated mass flow rate of the uniform flow case was conserved for the nonuniform cases. Additional system performance reductions will result due to the larger recuperator pressure drops associated with the nonuniform flow conditions. The increased pressure drop for the nonuniform flow condition was not modeled. The effects of reduced effectiveness and increased pressure drop were also not iterated on in a system model to establish the reduced flow conditions for the nonuniform distribution cases relative to the uniformly distributed case.

For the CFD model the heat exchanger core is assumed to have a uniform hydraulic resistance for all of the sub passages making up the heat exchanger core. The recuperator is subdivided into 300 subunits for the low pressure side and 294 subunits for the high pressure side at the inlet and exit core faces. No fluid mixing between the subunits is assumed in the vertical direction, since each subunit is separated from its adjacent subunit in the vertical direction by a separation plate that divides the hot and cold side layers in the core. However, migration of flow from side to side in a given hot or cold side layer is not assumed negligible, especially in the headers. Although flow generally is assumed to stay within the channels of the split fin geometry, especially within the center region of the core, flow in the headers must migrate horizontally outside the split-fin channels due to the fact that the flow cross sectional area diverges at the inlet and converges at the exit header regions.

**Flow Maldistribution Performance Sensitivities**

In order to assess the effects of flow maldistribution on recuperator effectiveness an approach similar to the approach outlined in Reference 9- 63 was taken. In this approach the recuperator is subdivided into a matrix of M by N subunits. In Reference 9- 63 the effectiveness of each subunit was evaluated to obtain the total integrated effectiveness of the recuperator. The approach assumed uniform flow for one of the flow streams and nonuniform flow for the other stream. In the following approach nonuniform flow distributions can be assumed for both sides of recuperator. Each recuperator subunit has a flow rate assigned to the high pressure and low pressure sides based on the expected flow distribution for this region. A thermal hydraulic model of the recuperator was used to map the exit temperatures of both the high pressure and low pressure fluid streams assuming fixed inlet temperatures for a range of high pressure and low pressure flow combinations. The exit temperature maps were then coupled with flow distribution maps and double linear interpolation was used to determine the exit temperature of a particular subunit for a given high pressure side and low pressure side flow rate combination. The overall effectiveness of the recuperator was then calculated based on the following equations:

$$\varepsilon = \frac{Q_{actual}}{Q_{\max}}$$

The actual heat transfer rate in the expression above can be defined as:

$$Q_{actual} = \sum_{i=1}^{MxN} \dot{m}_{lp,i} \cdot c_{p,i} \cdot (T_{in,lp} - T_{exit,lp,i}) = \sum_{i=1}^{MxN} \dot{m}_{hp,i} \cdot c_{p,i} \cdot (T_{exit,hp,i} - T_{in,hp})$$

Where:

***i*** is the index denoting the $i^{th}$ subunit of the MxN matrix of "mini" heat exchangers
***lp*** denotes the low pressure side of the recuperator
***hp*** denotes the high pressure side of the recuperator
$c_p$ specific heat of the working fluid (J/kg/K)
$\dot{m}$ is the mass flow rate of the working fluid (kg/s)
$T_{in,lp}$ is the inlet temperature for the low pressure side of the recuperator (= 995K for the Mini-BRU recuperator being studied.)
$T_{in,hp}$ is the inlet temperature for the high pressure side of the recuperator (= 380K for the Mini-BRU recuperator being studied)

The maximum heat transfer rate in effectiveness definition can be expressed as:

$$Q_{\max} = C_{\min} \cdot (T_{lp,in} - T_{hp,in})$$

Where:

$C_{min}$ is the smaller of the following two expressions:

$$C_{lp} = \sum_{i=1}^{MxN} \dot{m}_{lp,i} \cdot c_{p,lp,i}$$

$$C_{hp} = \sum_{i=1}^{MxN} \dot{m}_{hp,i} \cdot c_{p,hp,i}$$

The minimum fluid capacity rate in the above effectiveness equation is not the minimum for each subunit, but is rather the minimum of the integrated high pressure and low pressure heat capacity rates. From an overall system perspective this provides an effectiveness which can be related to the mixed mean exit temperatures of the two recuperator fluid streams, and does not require knowledge of the effectiveness/flow distribution for the individual recuperator subunits.

To generate exit temperature maps for the mini-BRU recuperator a flow forced TRACE model was developed. This model assumes air as the working fluid for both sides of the recuperator. The air mass flow rates were established by matching the air Reynold's numbers at the entrance for both the high pressure and low pressure sides of the recuperator to the helium xenon mixture Reynolds numbers proposed for the Mini-BRU application (Helium/Xenon mole fraction of 0.373/0.627). The inlet temperatures for both flow streams for the air model were consistent with the helium xenon conditions (high pressure side inlet temperature = 380 K, low pressure side inlet temperature = 995 K). Figure 9-26 and Figure 9-27 provide the high pressure side and low pressure side exit temperature maps respectively.

To evaluate the sensitivity of recuperator effectiveness to flow distribution, four sets of flow fraction maps were generated. The four sets of flow maps are provided in Table 9-13. For each of the maps, the integrated flow of the uniformly distributed case was conserved. Figure 9-28 provides a comparison of the effectiveness for each of the four flow distribution combinations. From the figure one can see that the overall effectiveness is essentially unaffected for cases where the high pressure and low pressure flow distribution maps are balanced. As the difference between the flow fractions of the high pressure and low pressure sides for individual subunits increases, the overall effectiveness decreases. This trend is driven by the heat capacity rate differences between the high pressure and low pressure gas streams and the fact that the recuperator was designed for balanced heat capacity rates.

One technique to help balance the flow maldistribution effects is to maintain symmetry in the manifold designs for the high pressure and low pressure sides of the recuperator. In a recuperator design which is primarily counter flow, this symmetry helps to maintain similar flows for a given region of the recuperator for the low pressure and high pressure side flow paths.

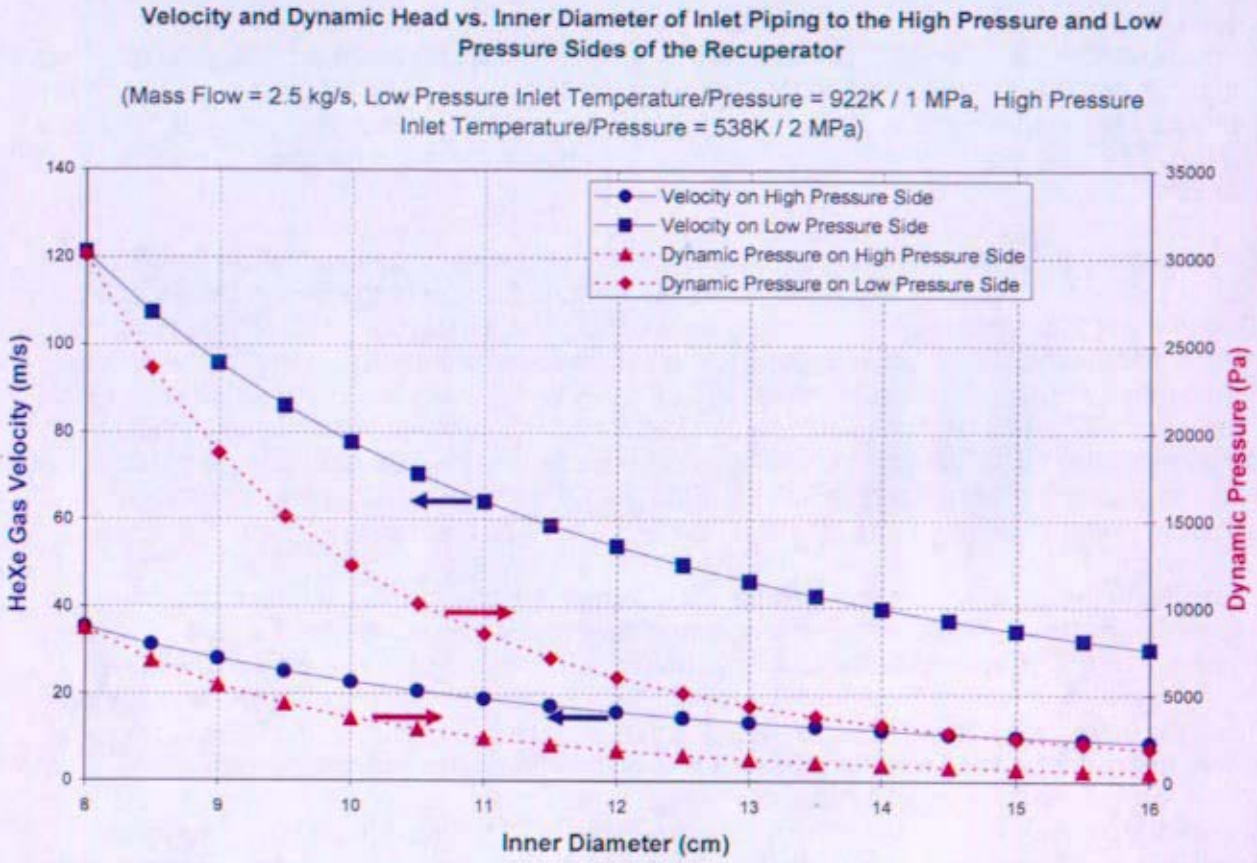



**Figure 9-23: Velocity and dynamic pressure at the inlet pipe conditions as a function of inlet pipe inner diameter for the high and low pressure sides of the recuperator.**

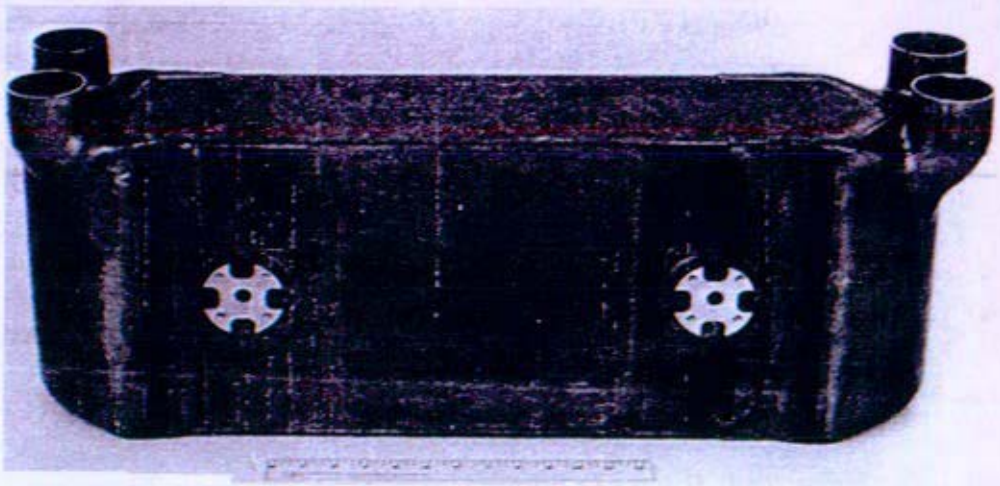
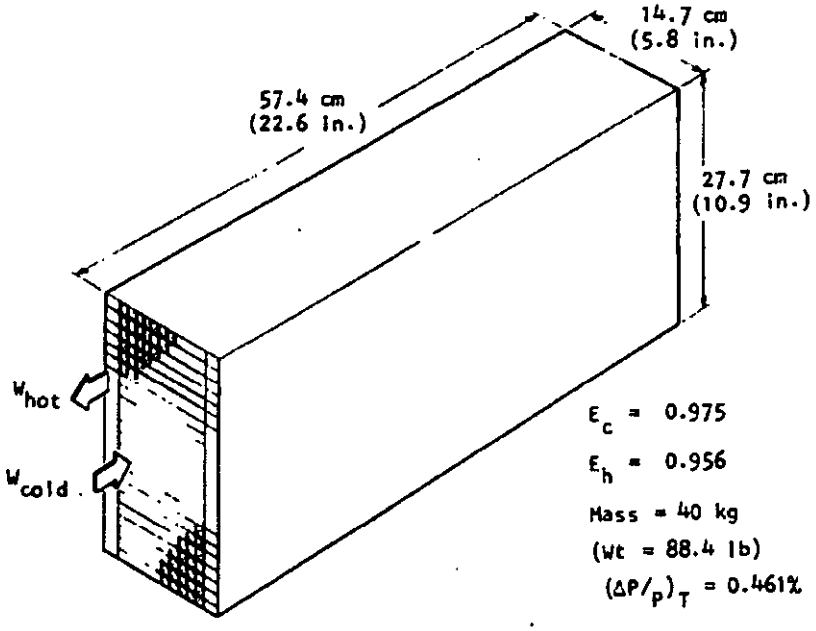
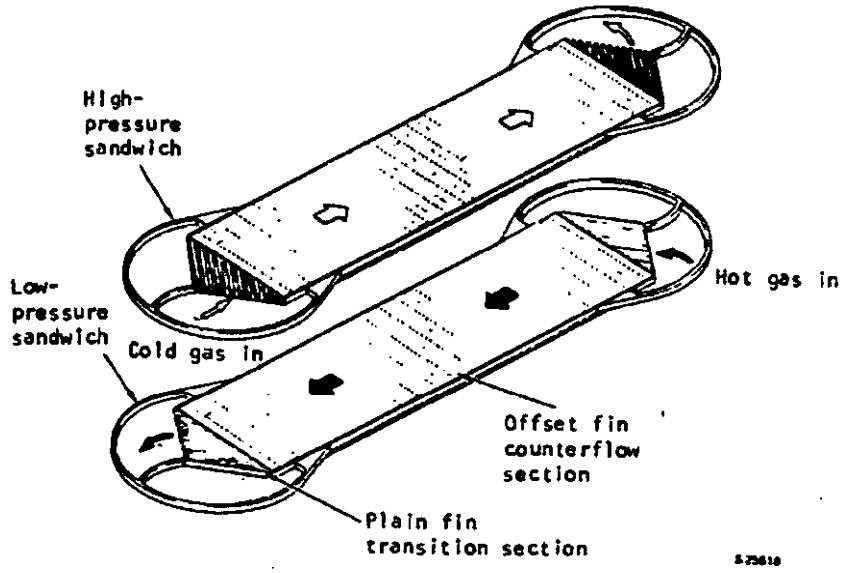


**Figure 9-24: As-built Mini_BRU recuperator (from Reference 9- 49).**




(a) Counterflow Section.




(b) Gas Flow Path and Fin Configuration

**Figure 9-25: Mini-BRU recuperator internal flow configuration (from Reference 9- 49).**

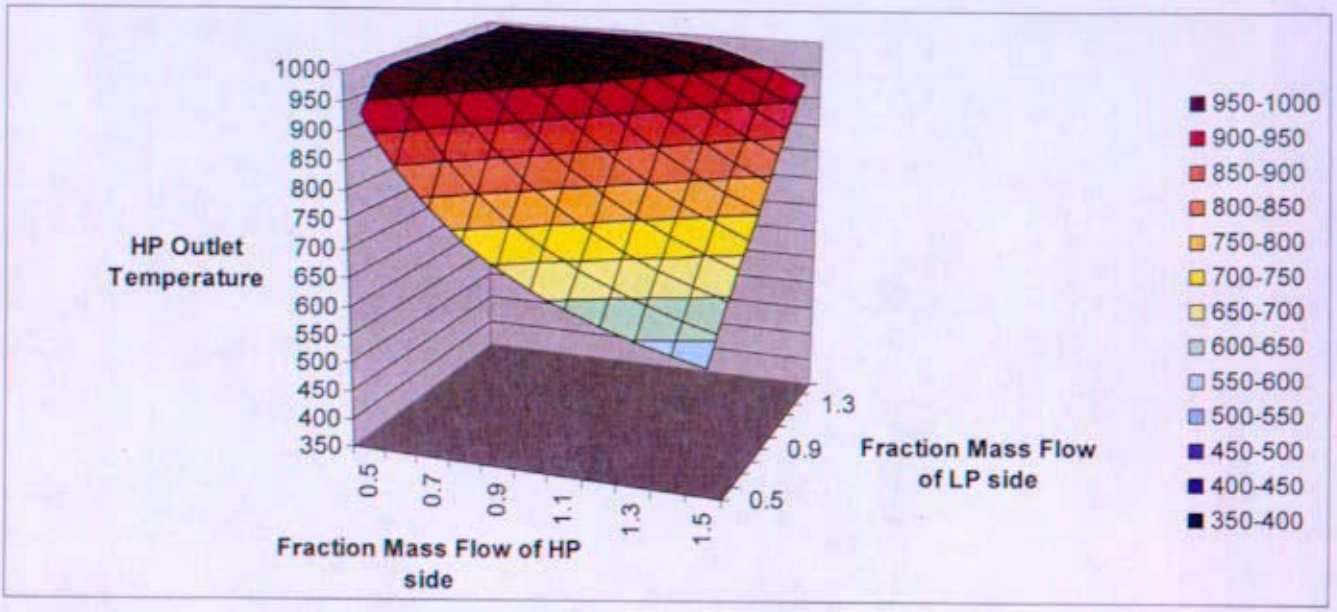



**Figure 9-26: Exit temperature map for the high pressure side of the Mini-BRU recuperator (based on a 1 dimensional, counter flow TRACE model with air as the working fluid).**

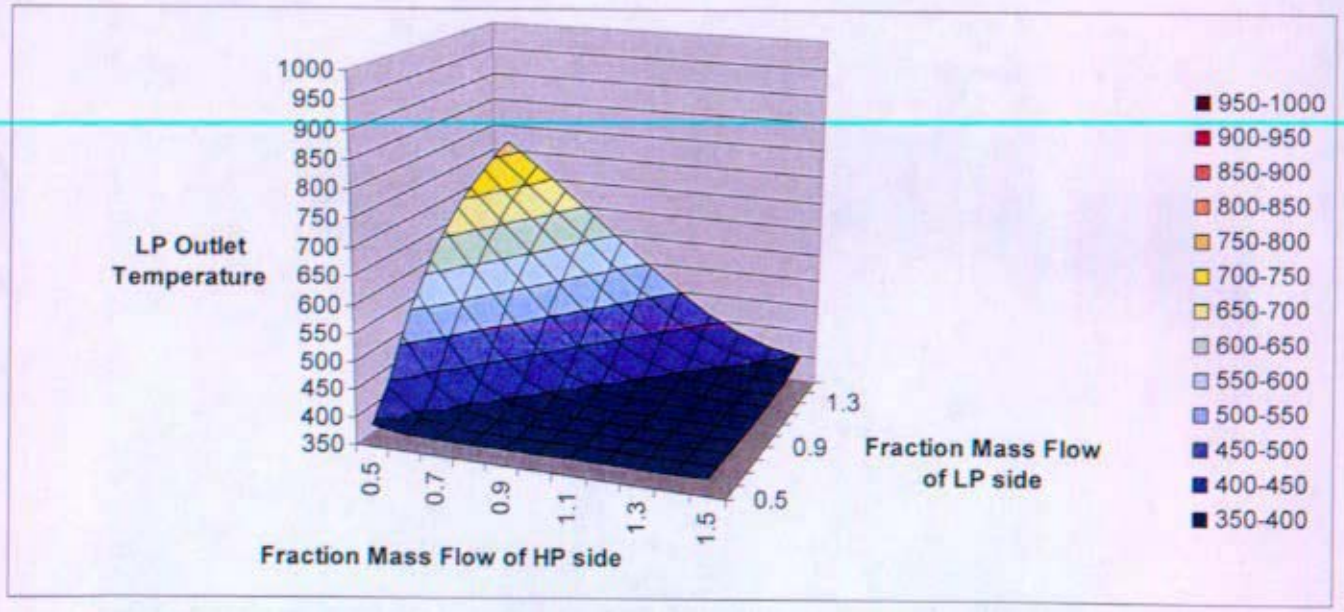



**Figure 9-27: Exit temperature map for the low pressure side of the Mini-BRU recuperator (based on a 1 dimensional, counter flow TRACE model with air as the working fluid).**

**Table 9-13: Recuperator flow distribution maps generated to assess the sensitivity of recuperator effectiveness to maldistribution.**

| | | Flow Fraction Map for High Pressure Side of the Recuperator | | | | | Flow Fraction Map for Low Pressure Side of the Recuperator | | | | |
|---|---|---|---|---|---|---|---|---|---|---|---|
| | | X coordinate | | | | | X coordinate | | | | |
| CASE 1: Uniform Flow | | 1.0 for all x and y coordinates | | | | | 1.0 for all x and y coordinates | | | | |
| CASE 2: Balanced Flow Maldistribution | Y coordinate | 0.51 | 0.51 | 0.51 | 0.51 | 0.51 | 0.51 | 0.51 | 0.51 | 0.51 | 0.51 |
| | | 0.51 | 0.51 | 0.51 | 0.51 | 0.51 | 0.51 | 0.51 | 0.51 | 0.51 | 0.51 |
| | | 0.51 | 0.51 | 1 | 1.49 | 1.49 | 0.51 | 0.51 | 1 | 1.49 | 1.49 |
| | | 1.49 | 1.49 | 1.49 | 1.49 | 1.49 | 1.49 | 1.49 | 1.49 | 1.49 | 1.49 |
| | | 1.49 | 1.49 | 1.49 | 1.49 | 1.49 | 1.49 | 1.49 | 1.49 | 1.49 | 1.49 |
| CASE 2: Unbalanced Flow Maldistribution | Y coordinate | 0.51 | 0.51 | 0.51 | 0.51 | 0.51 | 1.49 | 1.49 | 1.49 | 1.49 | 1.49 |
| | | 0.51 | 0.51 | 0.51 | 0.51 | 0.51 | 1.49 | 1.49 | 1.49 | 1.49 | 1.49 |
| | | 0.51 | 0.51 | 1 | 1.49 | 1.49 | 1.49 | 1.49 | 1 | 0.51 | 0.51 |
| | | 1.49 | 1.49 | 1.49 | 1.49 | 1.49 | 0.51 | 0.51 | 0.51 | 0.51 | 0.51 |
| | | 1.49 | 1.49 | 1.49 | 1.49 | 1.49 | 0.51 | 0.51 | 0.51 | 0.51 | 0.51 |
| CASE 3: Balanced Flow Maldistribution | Y coordinate | 1.25 | 1.25 | 1.25 | 1.25 | 1.25 | 1.25 | 1.25 | 1.25 | 1.25 | 1.25 |
| | | 1.25 | 1.25 | 1.25 | 1.25 | 1.25 | 1.25 | 1.25 | 1.25 | 1.25 | 1.25 |
| | | 1.25 | 1.25 | 1 | 0.75 | 0.75 | 1.25 | 1.25 | 1 | 0.75 | 0.75 |
| | | 0.75 | 0.75 | 0.75 | 0.75 | 0.75 | 0.75 | 0.75 | 0.75 | 0.75 | 0.75 |
| | | 0.75 | 0.75 | 0.75 | 0.75 | 0.75 | 0.75 | 0.75 | 0.75 | 0.75 | 0.75 |
| CASE 3: Unbalanced Flow Maldistribution | Y coordinate | 1.25 | 1.25 | 1.25 | 1.25 | 1.25 | 0.75 | 0.75 | 0.75 | 0.75 | 0.75 |
| | | 1.25 | 1.25 | 1.25 | 1.25 | 1.25 | 0.75 | 0.75 | 0.75 | 0.75 | 0.75 |
| | | 1.25 | 1.25 | 1 | 0.75 | 0.75 | 0.75 | 0.75 | 1 | 1.25 | 1.25 |
| | | 0.75 | 0.75 | 0.75 | 0.75 | 0.75 | 1.25 | 1.25 | 1.25 | 1.25 | 1.25 |
| | | 0.75 | 0.75 | 0.75 | 0.75 | 0.75 | 1.25 | 1.25 | 1.25 | 1.25 | 1.25 |
| CASE 4: Balanced Flow Maldistribution | Y coordinate | 1.1 | 1.1 | 1.1 | 1.1 | 1.1 | 1.1 | 1.1 | 1.1 | 1.1 | 1.1 |
| | | 1.1 | 1.1 | 1.1 | 1.1 | 1.1 | 1.1 | 1.1 | 1.1 | 1.1 | 1.1 |
| | | 1.1 | 1.1 | 1 | 0.9 | 0.9 | 1.1 | 1.1 | 1 | 0.9 | 0.9 |
| | | 0.9 | 0.9 | 0.9 | 0.9 | 0.9 | 0.9 | 0.9 | 0.9 | 0.9 | 0.9 |
| | | 0.9 | 0.9 | 0.9 | 0.9 | 0.9 | 0.9 | 0.9 | 0.9 | 0.9 | 0.9 |
| CASE 4: Unbalanced Flow Maldistribution | Y coordinate | 1.1 | 1.1 | 1.1 | 1.1 | 1.1 | 0.9 | 0.9 | 0.9 | 0.9 | 0.9 |
| | | 1.1 | 1.1 | 1.1 | 1.1 | 1.1 | 0.9 | 0.9 | 0.9 | 0.9 | 0.9 |
| | | 1.1 | 1.1 | 1 | 0.9 | 0.9 | 0.9 | 0.9 | 1 | 1.1 | 1.1 |
| | | 0.9 | 0.9 | 0.9 | 0.9 | 0.9 | 1.1 | 1.1 | 1.1 | 1.1 | 1.1 |
| | | 0.9 | 0.9 | 0.9 | 0.9 | 0.9 | 1.1 | 1.1 | 1.1 | 1.1 | 1.1 |
| CASE 5: HP Uniform Flow and LP Nonuniform Flow | Y coordinate | 1 | 1 | 1 | 1 | 1 | 1.1 | 1.1 | 1.1 | 1.1 | 1.1 |
| | | 1 | 1 | 1 | 1 | 1 | 1.1 | 1.1 | 1.1 | 1.1 | 1.1 |
| | | 1 | 1 | 1 | 1 | 1 | 1.1 | 1.1 | 1 | 0.9 | 0.9 |
| | | 1 | 1 | 1 | 1 | 1 | 0.9 | 0.9 | 0.9 | 0.9 | 0.9 |
| | | 1 | 1 | 1 | 1 | 1 | 0.9 | 0.9 | 0.9 | 0.9 | 0.9 |

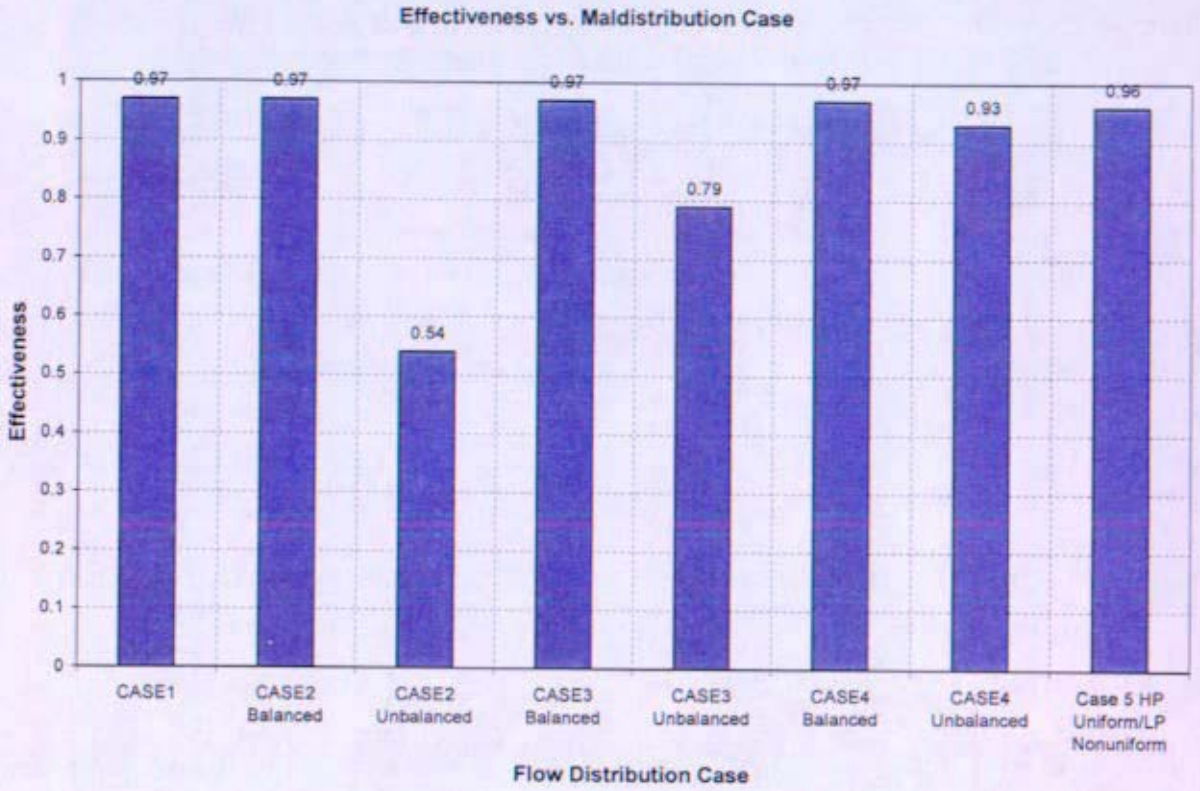


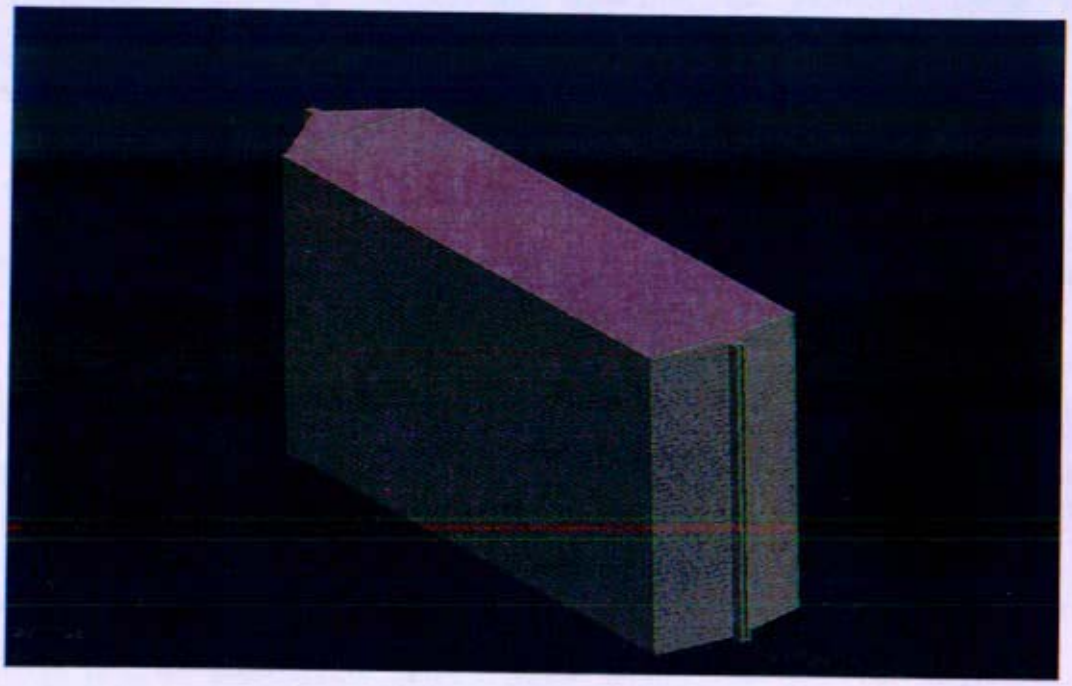

**Figure 9-28: Recuperator effectiveness as a function of various flow distribution maps (see Table 9-13 for corresponding flow distribution maps).**

## CFD Modeling

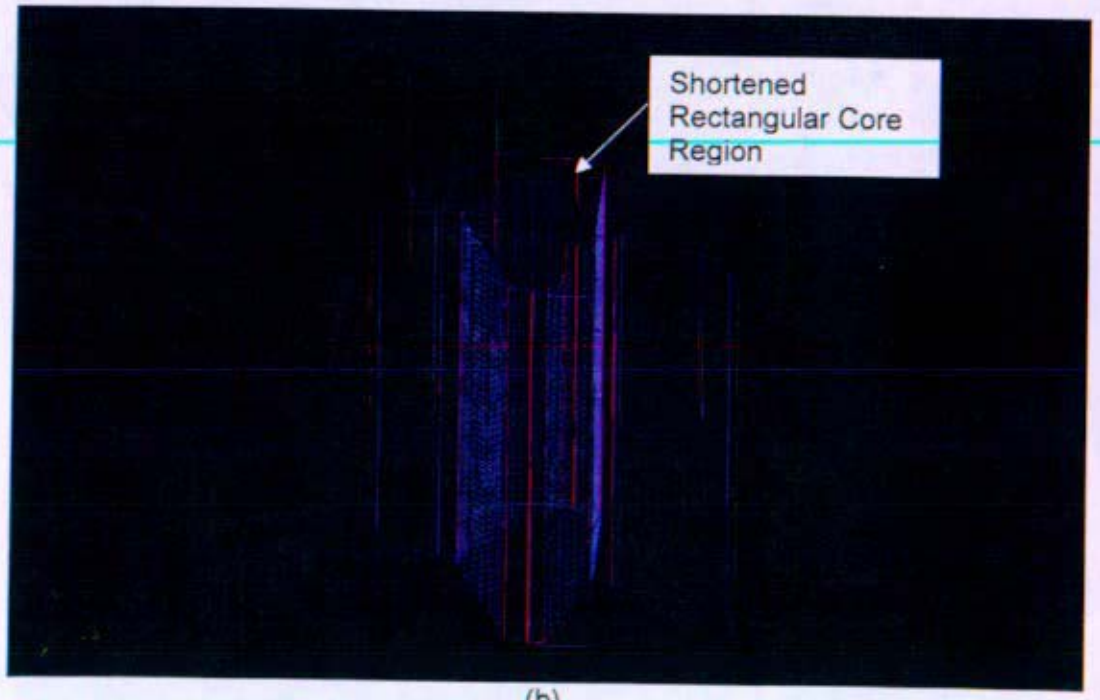
A Computational Fluid Dynamics model of the Brayton cycle (Mini-BRU) recuperator was developed using FLUENT, a finite-volume code. This model focused on evaluating the plenum effects on the flow distribution within the recuperator. The primary challenge in developing a CFD model of the (Mini-BRU) recuperator is modeling the flow through a complex core geometry, which includes a counter flow design with off-set fins. Since the purpose of this study is to assess plenum geometry effects on recuperator flow distribution, flow through the core may need to be considered only to the extent that it impacts flow at the inlet face of the recuperator core. Consequently a simplified approach using a porous media model to simulate flow through the core was adopted for this study. This approach avoids the need to model the fin geometry and hot and cold side passages within the core, which requires a much greater effort to develop a large mesh and would also require greater computational resources from a CFD solver (processors, memory, disk space, etc.). Figure 9-29(a) provides a CAD schematic of the recuperator core illustrating the hot and cold side passages of the core structure. Figure 9-29 (b) shows the FLUENT model and the simplification of the core geometry. The core in the FLUENT model has been shortened to reduce the volume mesh while maintaining the prototypic pressure drop through user defined loss factors in the porous media. For the purpose of this study, flow was assumed to follow the fin geometry in the core. FLUENT's porous media model includes features which allow the user to direct the flow through the media in a specific

orientation and to impose loss characteristics in order to achieve a required pressure drop through the media. Air was used as the fluid in the FLUENT model rather than the Helium-Xenon mixture used in the (Mini-BRU) recuperator to avoid the need to input property data in FLUENT. Recuperator core temperatures were fixed in a stepwise fashion in the direction of flow in order to approximate the fluid property changes.

Results form the hot and cold side cases indicate that flow is not uniform at the inlet core face for the hot side case to a much larger degree than for the cold side case. This is believed to be in large part due to the fact that although the flow rates for both the hot and cold side are similar (.1048 kg hot side vs .1156 kg/s cold side), the higher inlet temperatures for the hot side (995 K) produce an inlet plenum velocity of 22.34 m/s (73.3 ft/s), which is three times as great as the cold side inlet plenum velocity of 6.35 m/s (20.83 ft/s) at 380 K. The flow fields in both the high pressure and low pressure inlets are depicted in Figure 9-30 respectively showing the flow pathlines from the plenum inlet faces. Figure 9-31 illustrates the significantly increased inlet plenum velocities in the low pressure, high temperature side in comparison to the high pressure, low temperature side. Whereas the flow from the hot side inlet duct appears to "impinge" on the inlet face of the core due to it's higher velocity as shown in Figure 9-32(a), the lower velocity flow from the cold side inlet duct is "dispersed", and distributed more evenly across the inlet face as shown in Figure 9-32(b). The "side-to-side" or horizontal flow distribution in these figures is a function of the porous media assumptions within the core and may not accurately reflect the actual horizontal distribution in the core. Further work would be needed to evaluate and confirm the true horizontal distribution of flow within the recuperator core. Details of the modeling assumptions are documented in Reference 9- 61. Because the geometry in the vertical orientation is much less ambiguous (is based on the separating plates between the hot and cold sides) the flow distribution in this direction can be more accurately represented in the FLUENT model. Figure 9-33 provides a plot of the relative flow fractions for each flow channel in the vertical direction. This plot further emphasizes the vertical mismatch in flow in the low pressure side relative to the high pressure side. This "mismatch" of non-uniform flow between the hot and cold sides as discussed in the pre-ceding section promotes lower heat exchanger effectiveness.

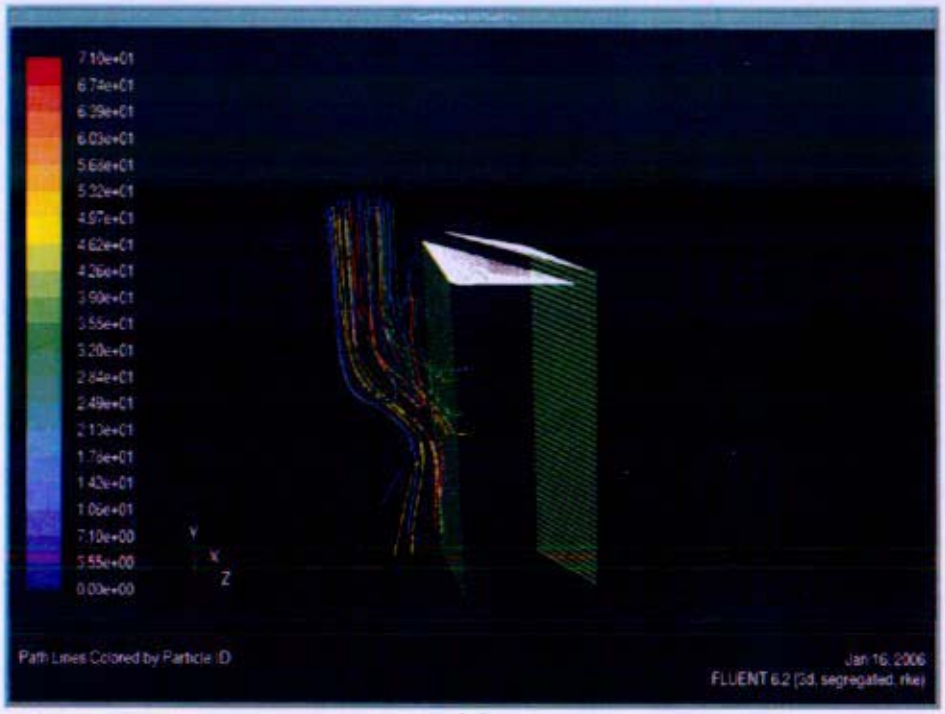


(a)

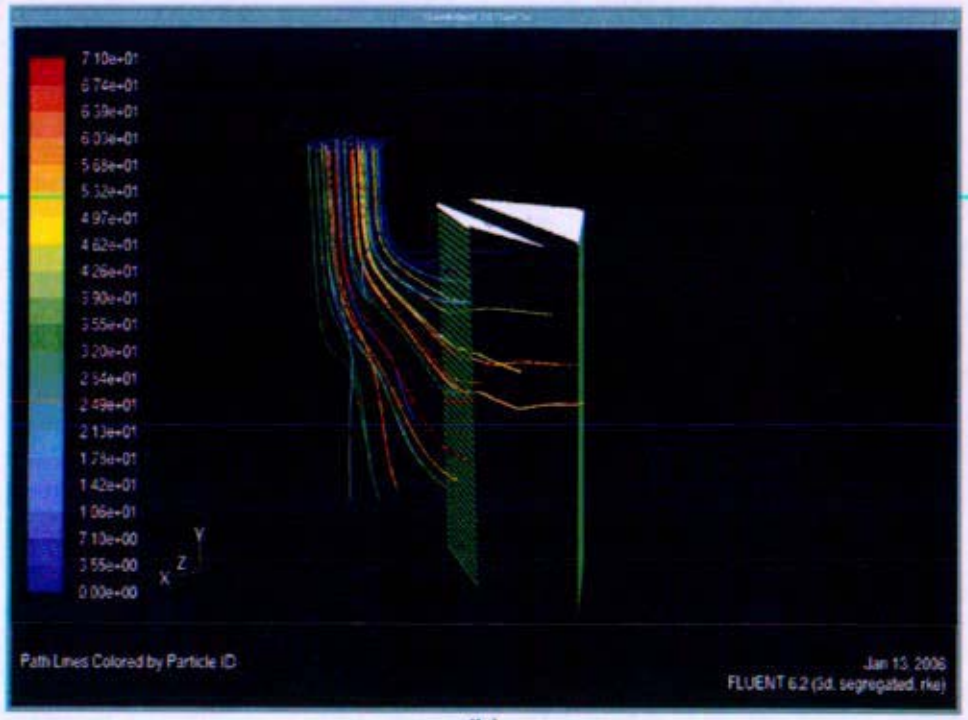



(b)

**Figure 9-29: (a) Mini-BRU core geometry generated with Pro-Engineer, (b)corresponding FLUENT model geometry for the low pressure side of the recuperator.**

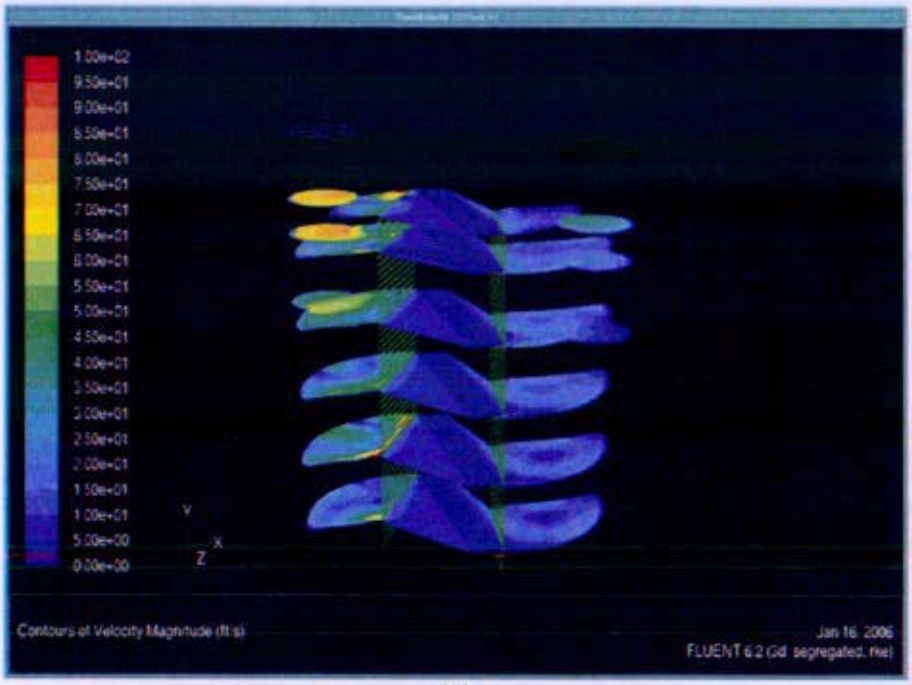



(a)

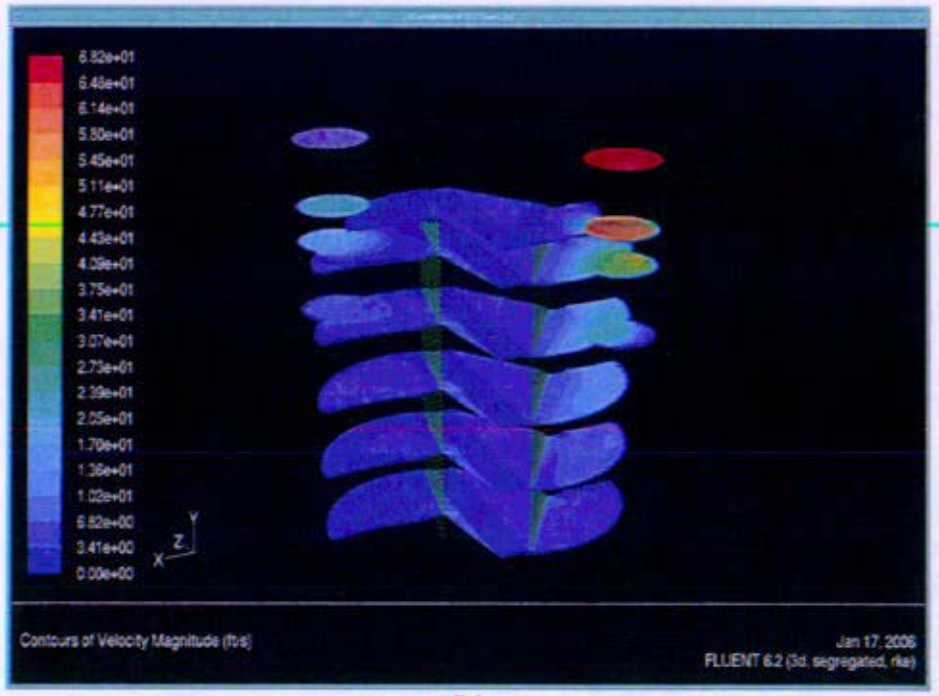



(b)

**Figure 9-30: Inlet flow path lines for the (a) low pressure side and (b) high pressure side of the recuperator.**

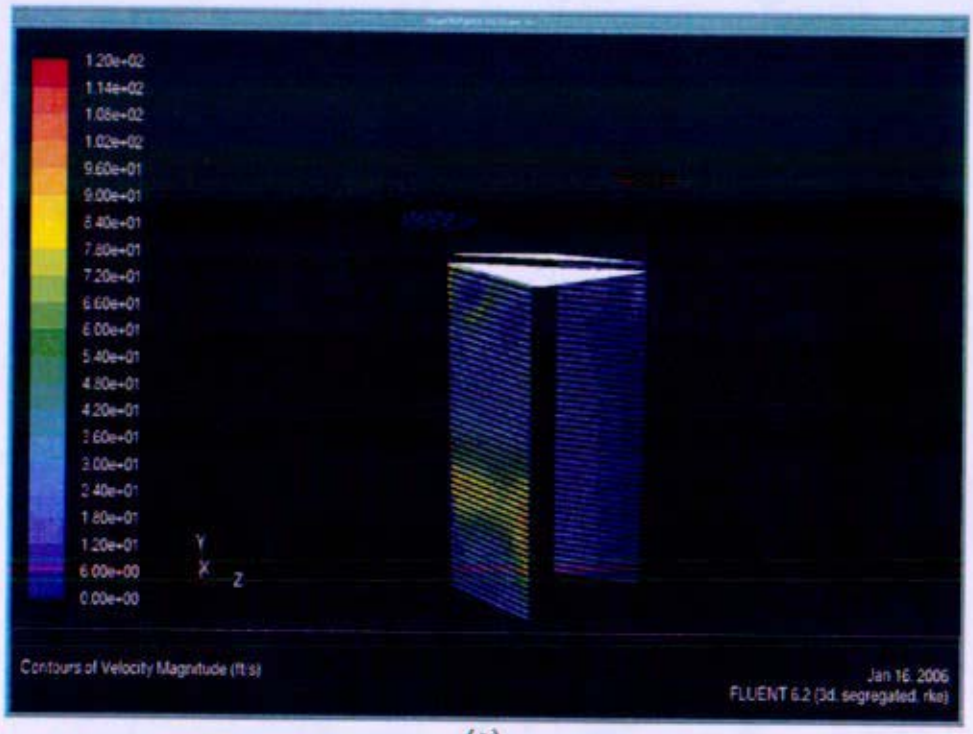



(a)

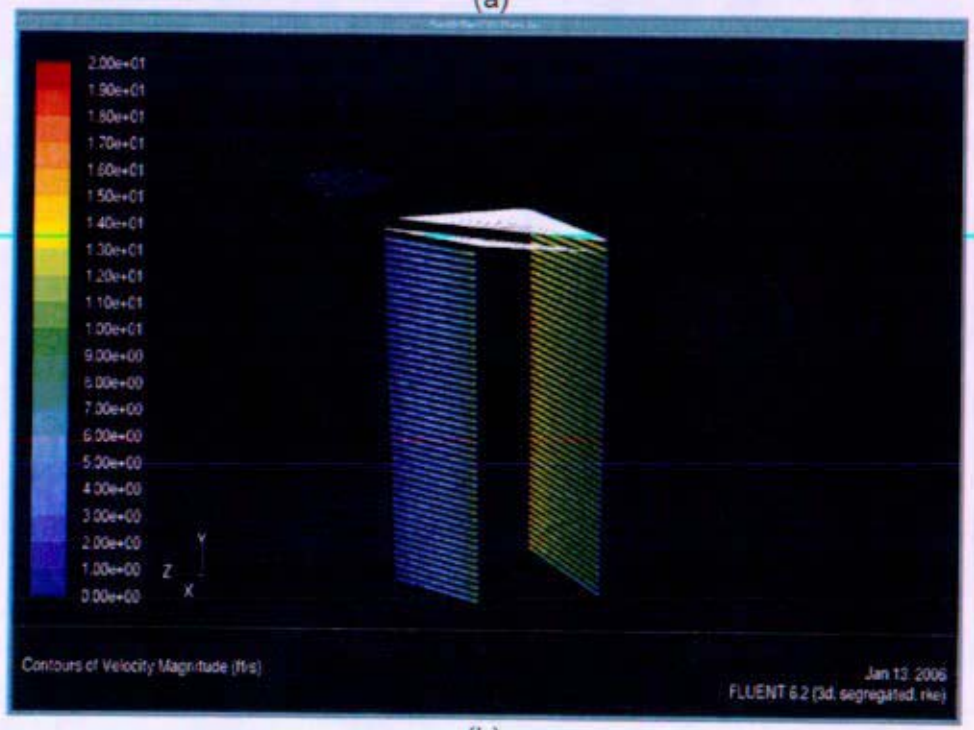



(b)

**Figure 9-31: Horizontal cross sections of velocity magnitude for the (a) low pressure side and (b) high pressure side of the recuperator.**




(a)




(b)

**Figure 9-32: Velocity magnitudes at the recuperator core inlet and exit faces for the (a) low pressure side and (b) high pressure side of the recuperator.**

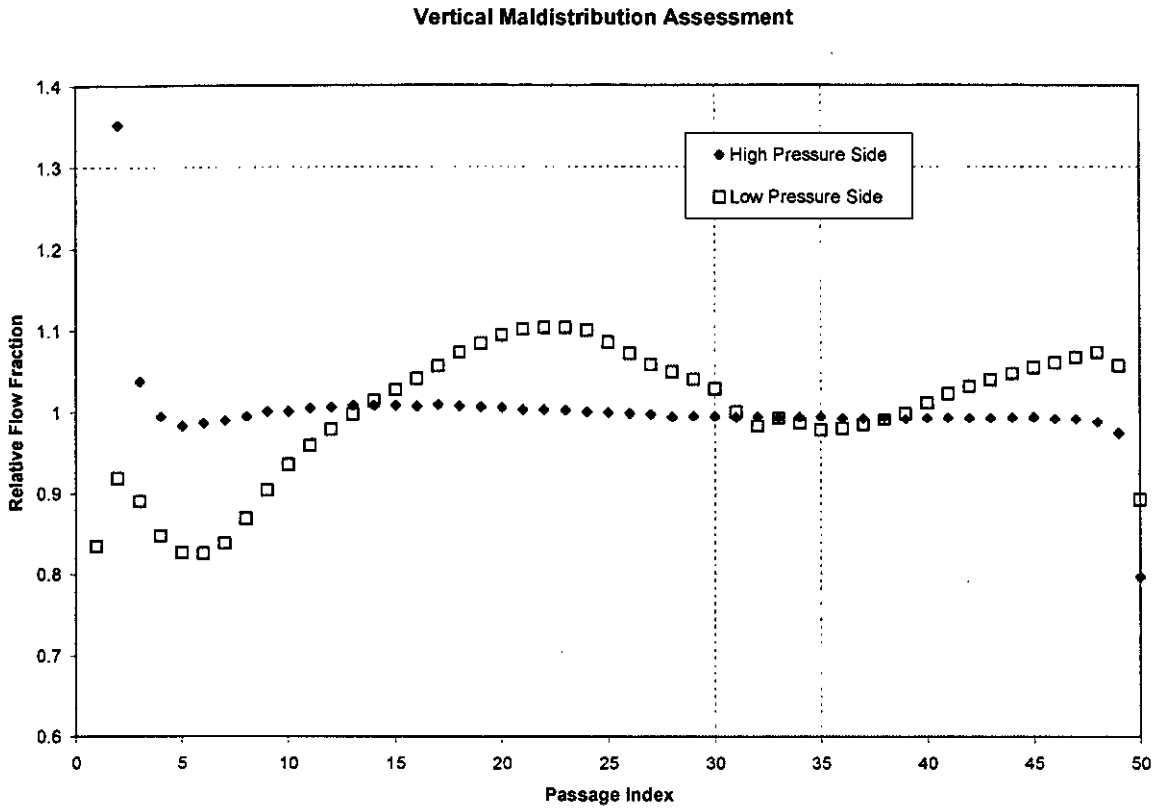



**Figure 9-33: Mass flow fraction plot of the high pressure and low pressure sides of the recuperator.**

### 9.2.4 Failure Modes

Two main failure modes are of concern for the recuperator. The first failure mode is a direct leak to space due to a containment structure failure. The second failure mode is interchannel leakage due to a failure of the pressure boundary between the high pressure side (compressor discharge side) of the recuperator and the low pressure side (turbine discharge side of the recuperator). Low cycle creep fatigue is the main design consideration for both of these failure modes. Due to the relatively high operating temperatures at the recuperator hot end (~890 - 940K nominally) creep is a concern for the structural materials. These structures include manifolds, parting plate structures, closure bars and fin structures as shown in Figure 9-16. For the plate fin designs envisioned for the recuperator, brazing is typically the joining method used to form the heat exchanger core structure. The braze joints must be capable of withstanding both the hot end and cold end recuperator temperatures and provide the necessary strength to survive any thermal cycles through life and vibratory/acceleration loads during launch. The Ni-base super-alloy materials currently being considered for recuperator construction are not considered susceptible to radiation exposure damage at the exposure levels expected behind the shield.

#### 9.2.4.1 Leakage to Space

Per Enclosure 7 of Reference 9- 62 an acceptable leak rate to space from the system was estimated at 1.27E-7 kg/min assuming a 10% reduction in system pressure could be tolerated at the end of a 15 year mission for a four Brayton direct gas reactor system. This leakage rate is the equivalent of a 1.13E-6 $mm^2$ hole size. Similar to the interchannel leakage evaluation, at the current stage of the design the actual probability of developing a recuperator leak to space is difficult to estimate. As mission requirements and design configurations of a specific recuperator design evolve, the probability of developing a space structural boundary leak will become better defined. Typically the most vulnerable areas for developing a leak to space are along brazed and welded joints in the design. The manifolds and manifold joints at the hot end of a counter flow recuperator are typically most susceptible to thermal fatigue failure. During a thermal transient, the differences in thermal mass and heat transfer characteristics between the heat exchanger core and the manifold structure produce thermal gradients with the thermal response of the manifold structure typically lagging in response relative to the header region of recuperator core. The fins in the header region of the recuperator provide improved heat transfer relative to the manifold structure; and therefore, the header region thermal response is more rapid than the manifold structure. These cyclic thermal gradients coupled with the high temperatures at the hot end of the recuperator make the brazed and welded joints in this portion of the recuperator more susceptible to failure. Due to the large number of brazed header joints along either side of the recuperator these are also susceptible to leakage to space. Recuperator designs in the past have incorporated plate overlays which are brazed to the sides of the recuperator and welded to the top/bottom plates and the manifold structures to minimize the number of exposed brazed joints to space. One example of this design approach is provided in Reference 9- 49. NRPCT recommends that a similar all-welded external structure (vs exposed brazed joints) be incorporated to minimize the likelihood of a recuperator mission-ending leak to space.

### 9.2.4.2 Interchannel Leakage

Recuperator interchannel leakage is defined as leakage from the high pressure side of the recuperator to the low pressure side due to unwanted leakage paths in the structure separating these flow paths. Interchannel leakage results in the loss of overall system performance due to the bypass effect of the leak on the system. This bypass flow path results in increased flow and work input from the compressor with no increase or a possible decrease in work output from the turbine depending on the control system in place. The most probable locations for interchannel leakage paths are at the braze joints along the header bars and at the manifold structure separating the high pressure and low pressure sides of the recuperator. An example of interchannel leakage due to cyclic fatigue is provided in Reference 1. In this reference, interchannel leaks developed in the recuperator during thermal cycle acceptance testing of the unit. Interchannel leak rates following 200 thermal cycles were estimated at 0.2% of the rated system flow. This leak rate had an insignificant impact on the overall performance of the Brayton system.

A preliminary, simple system state point evaluation was performed to estimate the system performance impacts for various leak sizes. This evaluation was non-conservative because the effects of reduced compressor efficiency and the increased pressure losses in the system were not considered in the evaluation. The effects of leak size on system performance are summarized in Figure 9-34. Included in this figure are the state point assumptions. Based on bypass control analysis performed in Reference 9- 64 an additional reduction in overall system performance is expected based on more detailed system models which capture the effects of system pressure, variations in component pressure drop and turbine/compressor efficiency variations. For a 10% bypass flow on the compressor side of the 100 kWe Brayton system in Reference 9- 64 a reduction in electrical output of approximately 37% was calculated compared to 24% predicted by the simpler state point model.

From a system reliability perspective, a much larger interchannel leak can be tolerated relative to a system leak to space. Assuming a 1% reduction in system performance can be tolerated, an interchannel leak area of approximately 3 $mm^2$ would be acceptable for a leak on the compressor side of the recuperator. The as-built system design margins and mission requirements will set the acceptable interchannel leak sizes. At the current stage of the design the actual probability of developing an interchannel leak of this size is difficult to estimate. As mission requirements, design configurations, structural design evaluations and testing of the recuperator evolve the probability of developing a leak of this size will need to be better defined.

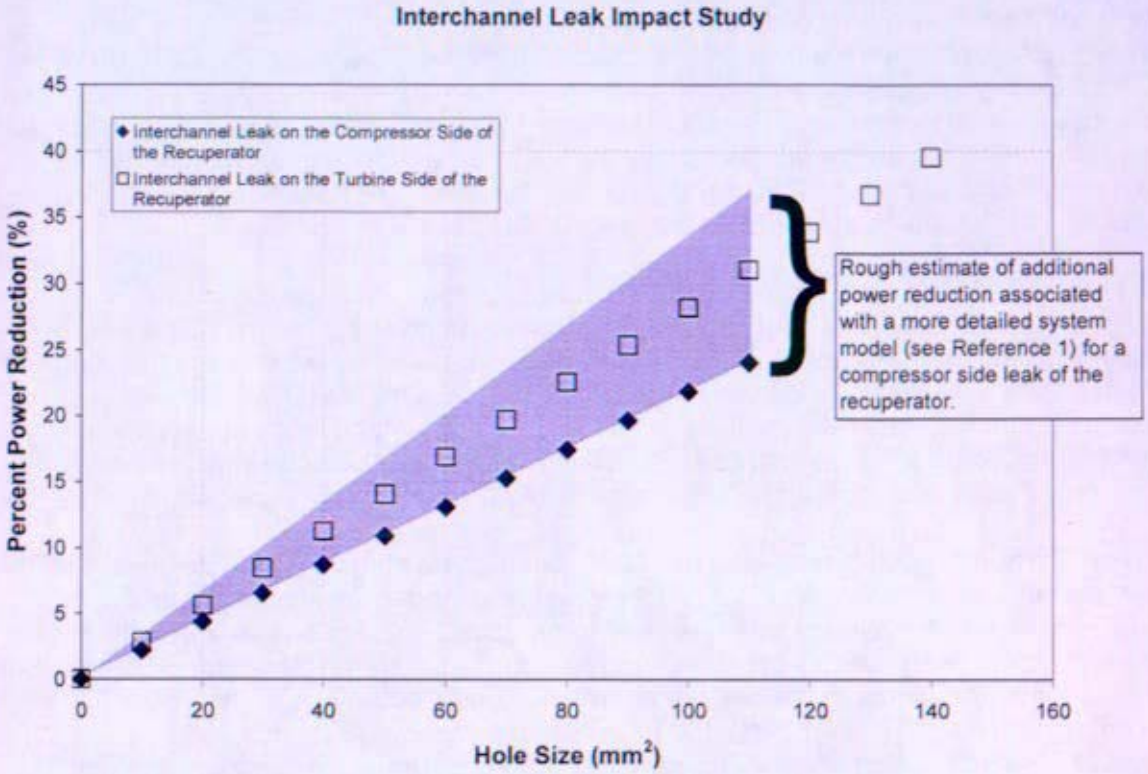



**Figure 9-34: Estimated effects of recuperator interchannel leak size on Brayton cycle performance.** (Modeling Assumptions for Symbols: (1) Single unit Brayton generating 100 kWe (2) Turbine inlet temperature is fixed at 1150K (3) Leakage does not impact turbine flow (4) Reduced compressor/turbine efficiencies are not considered in the impact on power output (5) Changes in pressure losses are not considered in the impact on power output.)

## Published Reliability Data for Recuperators

Hamilton Sundstrand has provided flight qualified heat exchanger life data for various heat exchangers for space applications. Reference 9- 65 provides a summary of the various heat exchangers designed and operated by Hamilton for both the Shuttle Orbiters and International Space Station (ISS). The working fluids for these heat exchangers include water, ammonia and Freon. To date there have been no recorded failures with over 6,950,000 hours of operation. The design methodology of these heat exchangers is similar to the approach Hamilton would take for a recuperator design. The operating temperatures of these units (381K maximum) and design life are significantly different than the hot end temperatures envisioned for a recuperator in a Prometheus mission (920 - 940K) with up to a 20 year life requirement. To better quantify the reliability of the recuperator, future efforts will need to focus on hardware lifetime data under similar operating temperatures and leakage restrictions which have been designed and built by the selected recuperator vendor. Vendor capabilities and experience with the specific materials of construction, creep fatigue design and joining methods will also need to be assessed. Additional important criteria in assessing the reliability of a recuperator design will be the ability to inspect structural boundaries following component fabrication.

Reference 9- 66 provides life data for recuperators designed by AiResearch, now part of Honeywell, and operated in a 15,000 horsepower gas turbine system. Table 9-14 summarizes the operating data for the various units. These recuperators were designed for a 140,000 hour lifetime and 5,200 cycles at an operating temperature of 866K. These units were ground based and were not designed to the same mass and leakage constraints imposed on a flight qualified unit; however, the lifetime and temperatures are fairly similar to those envisioned for the Prometheus mission. At the time Reference 9- 66 was issued these units had accumulated approximately 768,000 hours of operation and over 9,250 starts with no failures.

In Reference 9- 67 Garrett Corporation (now part of Honeywell) estimated the failure probabilities of various Brayton system components based on a variety of open cycle engine data. Table 9-15 summarizes the projected failure probabilities for the various Brayton system components. For the recuperator a failure probability rate of $3 \times 10^{-4}$ failures/year was estimated. This estimate is based on open cycle systems and is not directly applicable to a recuperator designed for a Prometheus based mission. However, the estimates provide confidence that a reliable recuperator can be constructed for a 15 to 20 year operational life.

Closed cycle Brayton system testing through NASA also has demonstrated single unit reliability at the temperatures expected in the actual application for extended periods of operation. In Reference 9- 55, a Brayton system was designed to produce 2 to 10 kilowatts of electric power for a minimum of five years. In this program four Brayton units were constructed. At the time of publication, over 21,000 hours of operating time was accumulated on one of the units. For a large fraction of test time (17,568 hours), the turbine inlet temperature for this unit was maintained at 1144K. Another unit was operated for 11,000 hours. Some leakage from the heat exchanger/recuperator units to the atmosphere was reported during testing. The extent of the leaks and the details of the leak paths to ambient were not clearly explained in the report.

Another closed cycle Brayton loop, the Mini-BRU, was tested at NASA Glenn as documented in Reference 9- 68. This Brayton system was sized for 1200 watts electric. This system was operated for over slightly over 1000 hours. For the first 700 hours the turbine inlet temperature was maintained at 1025K and for the last 300 hours the turbine inlet temperature was reduced to 866K. No system problems were reported during testing.

Table 9-14: Recuperator data for ground based gas turbine units (from Reference 9- 66)

| Name and Location | Regenerator Model | Operating Experience as of January 1985 | |
|---|---|---|---|
| | | Hours | Starts |
| **Pacific Gas and Electric Company** | | | |
| Delevan, California | ARG262H | 27400 | 303 |
| Delevan, California | ARG262H | To start first quarter 1985 | |
| **Canadian Pipeline** | | | |
| Cabri, Saskatchewan | ARG361V | 18300 | 60 |
| Herbert, Saskatchewan | ARG361V | 14382 | 144 |
| **Texas Eastern, Transmission Corporation** | | | |
| Danville, Kentucky | ARG260H | 17654 | 383 |
| Danville, Kentucky | ARG262V | 14915 | 371 |
| Athens, Ohio | ARG262V | 33358 | 150 |
| Athens, Ohio | ARG262V | 27759 | 135 |
| St. Francisville, Louisiana | ARG261V | 25712 | 101 |
| St. Francisville, Louisiana | ARG261V | 26705 | 123 |
| Clinton, Mississippi | ARG262V | 16848 | 96 |
| Clinton, Mississippi | ARG262V | 16928 | 111 |
| Yazoo City, Mississippi | ARG261V | 18868 | 216 |
| Grantville, Pennsylvania | ARG261V | 22835 | 283 |
| Grantville, Pennsylvania | ARG262V | 14897 | 96 |
| Athens, Ohio | ARG262V | 11519 | 138 |
| Athens, Ohio | ARG262V | 16162 | 63 |
| St. Francisville, Louisiana | ARG262V | 14614 | 53 |
| St. Francisville, Louisiana | ARG262V | 12431 | 67 |
| Clinton, Mississippi | ARG262V | 11518 | 46 |
| Owingsville, Kentucky | ARG262V | 3647 | 11 |
| Owingsville, Kentucky | ARG262V | 4032 | 18 |
| Glaveville, Tennessee | ARG462H | 394 | 9 |
| **Transwestern Pipeline (Division of Texas Eastern Transmission Corporation)** | | | |
| Corona, New Mexico | ARG261V | 29129 | 393 |
| **Chemical Plant** | | | |
| Louisiana | ARG461H | 31950 | 62 |
| Louisiana | ARG461H | 33278 | 71 |
| **El Paso Natural Gas Company** | | | |
| Caprock, New Mexico | ARG261V | 28627 | 113 |
| Leupp, Arizona | ARG262H | 17501 | 83 |
| Gallup, New Mexico | ARG262H | 15460 | 105 |
| **Tennessee Gas Pipeline** | | | |
| Leaville, Louisiana | ARG262H | 12671 | 53 |
| Port Sulphur, Louisiana | ARG262H | 15975 | 36 |
| Alexandria, Louisiana | ARG262V | 5497 | 68 |
| Collinwood, Tennessee | ARG262V | 17934 | 121 |
| Bay St. Louis, Mississippi | ARG261H | 12068 | 81 |
| Port Sulphur, Louisiana | ARG262H | 4461 | 33 |
| Hamilton, Alabama | ARG262V | 3229 | 98 |
| Morehead, Kentucky | ARG262V | 344 | 12 |
| Columbus, Mississippi | ARG262V | 11767 | 72 |
| Savannah, Tennessee | ARG262V | 0 | 2 |
| **Texas Gas Transmission Company** | | | |
| Columbus, Louisiana | ARG262V | 18245 | 33 |
| Greenville, Mississippi | ARG262V | 22751 | 31 |
| Slaughters, Kentucky | ARG262V | 8319 | 40 |
| Lake Cormorant, Louisiana | ARG262V | 15019 | 25 |
| Jeffersontown, Kentucky | ARG262V | 6780 | 92 |
| Clarksdale, Mississippi | ARG262V | 10447 | 55 |
| Kenton, Tennessee | ARG262V | 4366 | 17 |
| Hardingsburg, Kentucky | ARG262V | 3498 | 44 |
| **ANR Pipeline Company** | | | |
| Delhi, Louisiana | ARG262V | 8329 | 82 |
| Brownville, Tennessee | ARG262V | 16910 | 83 |
| **Great Lake Transmission Company** | | | |
| Crystal Falls, Michigan | ARG261H | 8084 | 76 |
| **Philadelphia Electric** | | | |
| Philadelphia, Pennsylvania | ARG286H | 3266 | 686 |
| Philadelphia, Pennsylvania | ARG286H | 3266 | 686 |
| Philadelphia, Pennsylvania | ARG286H | 2834 | 718 |
| Philadelphia, Pennsylvania | ARG286H | 2834 | 718 |
| Philadelphia, Pennsylvania | ARG286H | 3195 | 625 |
| Philadelphia, Pennsylvania | ARG286H | 3195 | 625 |
| **Foothills Pipeline** | | | |
| Piepot, Saskatchewan | ARG462H | 432 | 38 |
| **Arco-Parsons** | | | |
| Prudhoe Bay, Alaska | ARG461H | 8032 | 79 |
| **Natural Gas Pipeline Company** | | | |
| Glasco, Kansas | ARG262V | 7252 | 77 |
| **Independence Power and Light** | | | |
| Independence, Missouri | ARG286H | 59 | 22 |
| Independence, Missouri | ARG286H | 59 | 22 |
| **Trunkline Gas Company** | | | |
| Eppe, Louisiana | ARG262H | To start third quarter 1985 | |

**Table 9-15: Reliability study form Garrett Fluid Systems (see Reference 9- 67).**

| Component | Failure Rate | |
|---|---|---|
| | (per hour) | (per year) |
| Foil Bearings | $3 \times 10^{-8}$ | $3 \times 10^{-4}$ |
| Turbine | $1 \times 10^{-8}$ | $1 \times 10^{-4}$ |
| Compressor | $6 \times 10^{-8}$ | $6 \times 10^{-4}$ |
| Alternator | $5 \times 10^{-8}$ | $5 \times 10^{-4}$ |
| Recuperator | $3 \times 10^{-8}$ | $3 \times 10^{-4}$ |
| Bleed Cooler | $9 \times 10^{-8}$ | $9 \times 10^{-4}$ |
| Bellow/Ducts | $1 \times 10^{-8}$ | $1 \times 10^{-4}$ |

### 9.2.5 Future Development Needs

To deliver a reliable recuperator to meet the design needs of a Prometheus mission, the following near term development needs were identified:

- Establish competitive bid vendor contracts to identify conceptual designs and materials of construction and have vendors initiate small scale coupon fabrication and testing to identify fabrication and material compatibility issues with a focus on braze fin integrity. Identify accelerated testing to ensure braze base metal compatibility and fin and braze interface strength over mission life.

- Develop a more detailed structural design basis that addresses the operating temperatures, operating lifetimes and manufacturing practices for a recuperator design in the primary direct Brayton system envisioned for Prometheus. This work would need to address operational and safety issues in both the flight unit as well as any ground based prototypes.

- Develop a better definition of nominal and design operating conditions for the recuperator as mission requirements become better defined. This work would involve identifying temperature and pressure conditions as a function of time for normal plant conditions (including operating and uncertainty bands) and recoverable system failure scenarios. These temporal operating conditions would be supplied to perspective vendors to ensure that the structural design criteria for the recuperator were satisfied.

- Perform further flow maldistribution studies on the recuperator designs proposed for Prometheus. In conjunction with these studies, perform component design trades on recuperator mass, pressure drop and effectiveness to determine if the low pressure drop goals can be met with the current mass and effectiveness goals.

## 9.3 Gas Cooler

### 9.3.1 Summary and Conclusions

The gas cooler transfers heat from the primary HeXe coolant to the heat rejection system coolant, and lowers the compressor inlet temperature. The amount of heat transfer in the gas cooler must be weighed against the corresponding increases in mass and pressure drop across the component as well as the corresponding increase in heat rejection size due to the reduced average heat rejection temperature.

Initial scoping phase contracts with Hamilton Sundstrand, Heatric, Holtec International, Inc., and Honeywell International, Inc. assessed gas cooler material options, recommended design configurations and provided an initial reliability assessment. Various component configurations were recommended for water and NaK heat rejection coolants by each of the vendors. Heat rejection coolant selection ($H_20$ or NaK) impacts both the gas cooler material and configuration selection.

---

A chemically etched/brazed fin design offers the lightest configuration option while a shell and tube design is considered to be a more robust design (see Section 9.3.6 for a detailed mass comparison). A conventional plate/fin configuration is not considered suitable for use with the pressure requirements of water coolant, though could be considered for a NaK coolant design.

Ni-based alloys were identified as a more reliable material option for the water environment. Thorough evaluation and testing is required if it is decided to use dissimilar materials, e. g., titanium alloys and stainless steels, in common contact within either of the working fluids.

The main areas of development for this component include:

- Developing a reliable design over the projected 20 year life of the component. The largest reliability challenge is eliminating the potential of a mission ending leak from the high pressure water in the heat rejection system to the lower pressure primary coolant for the aggressive water side pressures and temperatures.

- Establishing design standards to provide an adequate structural design over a 20 year operating life while minimizing the overall component mass and volume.

- Selecting a material system which meets the component mass and reliability design goals.

Conceptual development of both the shell-and-tube and chemically etched/brazed fin design configurations were to be the focus in the next phase of development due to the competing design trades of reliability and mass with each of the design options. Ni- based and titanium based alloys were considered the leading material options.

---

### 9.3.2 Component Description

The gas cooler transfers heat from the HeXe working fluid in the gas reactor system to the heat rejection system. The gas cooler is located in the HeXe flow path between the recuperator discharge and the compressor inlet. The performance of the gas cooler has a significant impact on Brayton cycle efficiency because the HeXe flows from the gas cooler discharge to the compressor inlet and the compressor inlet temperature is a key determinant of cycle efficiency. A gas cooler development program (Section 9.3.3) was initiated to develop a fully qualified and operational heat exchanger for use in a space based nuclear electric power plant.

There are several issues associated with the gas cooler that make it a critical component. High operating pressure in the water heat rejection system, significant joints and joining issues, and large surface area combine to contribute to leakage concerns, with leakage considered mission ending. The high water pressure may shift the design from the lighter plate-fin style heat exchangers to heavier types such as shell and tube. Materials being considered for heat exchanger construction include titanium and titanium alloys, stainless steels, and Ni-base alloys. The gas cooler may include dissimilar material joints as the current Prometheus design uses Ni-base alloy primary piping and titanium Heat Rejection System (HRS) piping. Specific to the three main challenges associated with the gas cooler (leakage, material selection, and mass and volume minimization) the following are noted as potential challenges and vulnerabilities associated with the gas cooler:

- 20 year continuous operation with minimal degradation in performance
- Leakage
  - Gas/coolant cross contamination
  - Gas/coolant to space
- Material Selection
  - Bimetallic joining to other piping or components
  - Base metal joint integrity
  - Chemical incompatibility (NaK, Water)
  - Mass transport contaminates (Carbon, Nitrogen, Oxygen, Hydrogen, Nickel, Iron, Chromium)
  - Mechanical properties (creep, yield/tensile stress, ductility, fatigue)
- Mass minimization
- Volume minimization
  - Performance (efficiency versus size)
- Manufacturability/Inspectability

Initial plant operating parameters and design requirements were developed, based on the current heat balance (See Figure 9-35) at the initiation of the gas cooler development program. The heat balance described in Section 6 reflects work performed since the inception of the gas cooler development program. The next phase of the gas cooler design would use the more recent heat balances, although the differences are not envisioned to have an appreciable affect on the gas cooler configuration and materials selection.

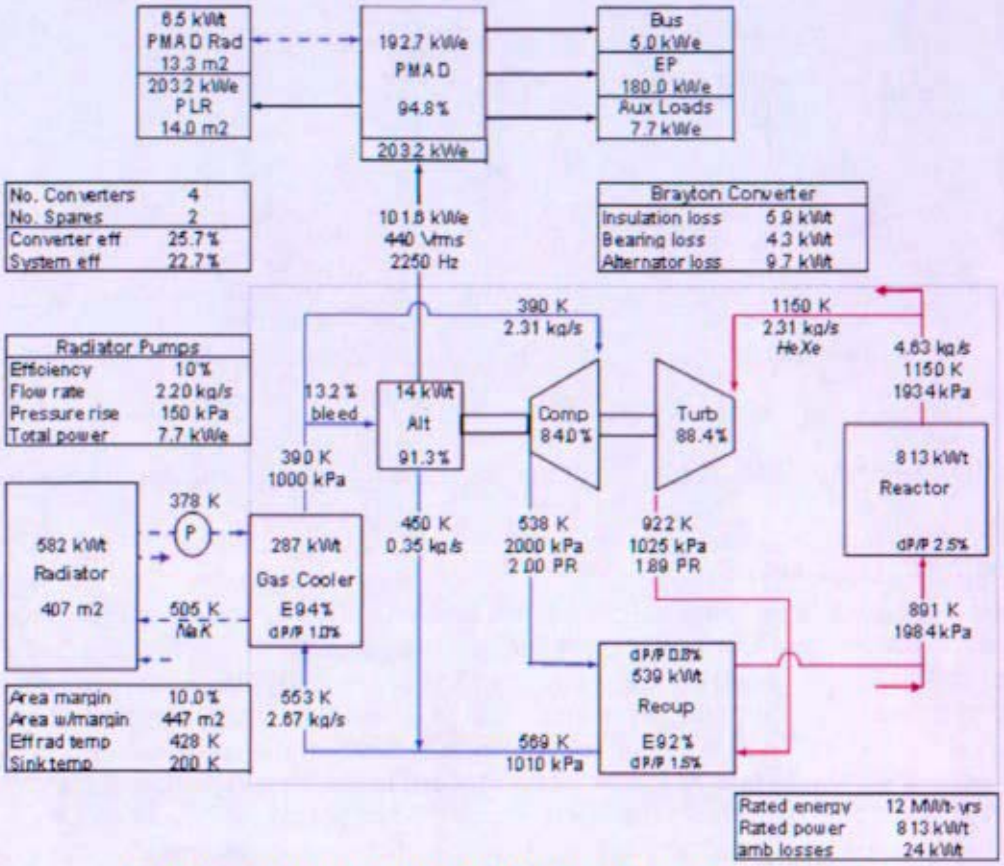



**Figure 9-35 Initial Development Program Heat Balance**

The heat balance was used to obtain gas cooler inlet and exit operating temperatures and pressures by optimizing system design. Water heat rejection loop design pressures were established through operating pressure plus system design margins outlined in Reference 9- 43, which addressed issues of changing from a NaK coolant to a high pressure water coolant. A baseline gas cooler configuration was established by Hamilton Sundstrand and submitted to NASA by Northrop Grumman as part of the Phase A studies for Prometheus, Reference 9- 37. For Phase A work, Hamilton Sundstrand proposed a compact, brazed, folded fin-plate construction with a three pass cross-counter flow liquid side (NaK) and single pass gas side (HeXe) configuration. The material of construction was CP2 titanium joined by brazing. The operation of this gas cooler sustained any combination of Brayton units by ducting each NaK loop to flow uniformly through the gas cooler of each operating Brayton unit. A pictorial representation of this design is shown in Figure 9-36. This concept was used as a baseline in determining plant operating, design and performance requirements for the development program. Although the Hamilton Sundstrand design is recognized as an extremely lightweight design, the NRPCT was interested in obtaining information from multiple vendors that would assess a variety of heat exchanger styles including plate-fin, shell and tube, and PCHE (printed circuit heat exchanger).

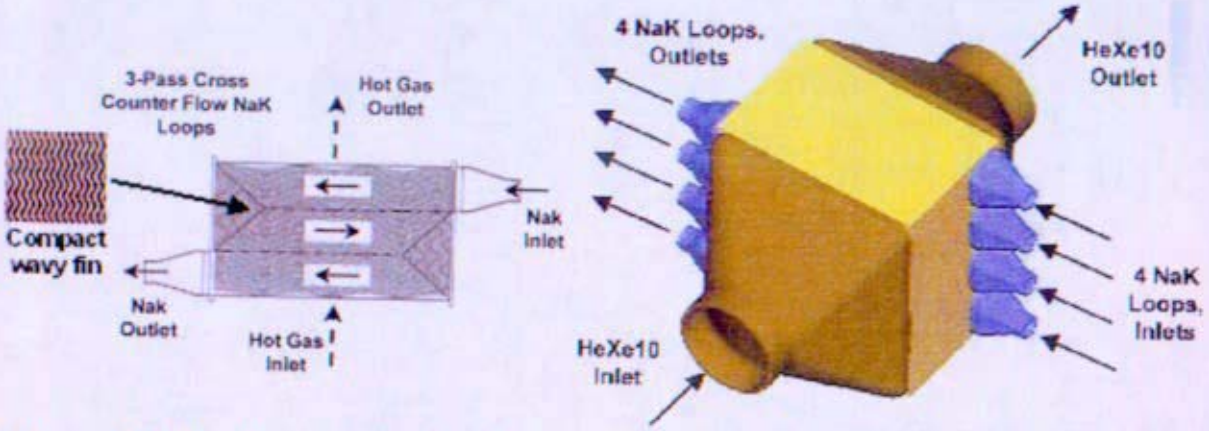



**Figure 9-36 Baseline Gas Cooler Concept (Hamilton Sundstrand, Reference 9- 37)**

### Plant Operating Parameters

Plant operating parameters were based on a 4-4-4 system configuration containing four Brayton loops, four recuperators, and four gas coolers for initial development. Each of the four Brayton units is rated at 100 kWe and normal operation consists of two operating Braytons with two idle Braytons for redundancy. The parameters listed below reflect this baseline assumption, requiring the gas cooler outlined in the Scoping Phase to dissipate approximately 300 kWt (waste heat corresponding to one 100 kWe Brayton loop) to the heat rejection system. More information on gas cooler interface to the HRS is provided in Section 9.3.8, as well as alternatives to the 4-4-4 configuration baseline. The plant operating parameters were as follows:

- Gas composition = 78.4 volume % helium and 21.6 volume % xenon (gas MW = 31.5)
- Gas inlet temperature = 553 K
- Gas outlet temperature = 390 K
- Gas outlet pressure while operating =1000 kPa absolute
- Maximum gas dP/P = 1% of operating pressure or dP = 10 kPa
- Gas mass flow rate = 2.67 kg/s (heat transfer calculated to be 287 $kW_t$)
- Gas pressure while idle (0 flow) = 2000 kPa absolute
- Chemically controlled water with final characteristics to be established at a later date
- Water inlet temperature = 378 K
- Water outlet temperature = 505 K
- Water inlet pressure = 5000-7800 kPa absolute
- Maximum water dP = 25 kPa
- Water flow rate to be calculated by seller based on gas side heat duty and specified water temperatures
- Component subjected to thermal and mechanical loads during transport, launch (axial launch loads approximately +/-9g and lateral launch loads approximately +/-6g), deployment, and operation (normal, transient, shock, vibration, thermal cycles)
- Component subjected to thermal stresses induced by a 200 K to 553 K heat up

**Design and Performance Requirements**

- 20 year maintenance free operation while achieving thermal performance and maintaining mechanical integrity
- No cross leakage of fluid or loss of fluid to space
- Minimum mass
- Minimum volume
- Maximum gas pressure = 3000 kPa absolute
- Maximum gas temperature = 600 K
- Maximum water pressure = 10500 kPa absolute
- Maximum water temperature = 559 K
- Maximum metal temperature = 600 K
- Minimum number of joints and joint length
- Corrosion allowance/fouling factor to be recommended by seller
- Assume no thermal losses to ambient
- 10% margin on heat transfer surface
- Titanium/titanium alloy as the material of construction
- Alternate alloy as the material of construction
- Final product that will be designed to the methods and limits of the ASME B&PV Code
- Gas cooler foundation/mounting arrangement to be determined

### 9.3.3 Development Program

The development program was envisioned to have multiple phases associated with vendor design input, NRPCT independent design, modeling, and testing, and component construction and integration. The initial phase, termed the Scoping Phase, was completed and investigated gas cooler materials of construction and heat exchanger styles that could potentially satisfy the parameters and requirements above. Subsequent design phases would produce a first cut at fabrication drawings for gas cooler manufacturing development and test hardware. Future phases of the proposed development plan are documented in Reference 9- 38.

**Scoping Phase Development**

Ten vendors were solicited for this initial scoping study. Vendor selection was based on a combination of experience, past performance, current capabilities, heat exchanger style experience, and cost. Hamilton Sundstrand, Heatric, Holtec International, Inc., and Honeywell International, Inc. were selected as the four vendors to receive Scoping Phase contracts. The contract report references are included (9- 39, 9- 40, 9- 41, 9- 42). The Heatric report was received concurrently with the issue of this closeout report. Information from this contract was not incorporated into the limited description of vendor evaluations.

The Scoping Phase included an evaluation of: gas cooler materials of construction, a preliminary gas cooler style and configuration analysis, and a reliability evaluation. The vendors were required to perform an evaluation of, at a minimum, two materials of construction for the gas cooler. As a base case the vendor was required to evaluate titanium/titanium alloys and a recommendation of the titanium/titanium alloy considered best suited for this application. In addition, the vendor was required to consider materials capable of meeting the design and operating parameters other than titanium and a recommendation of one of those materials as an

alternate. The vendor was to indicate if the alternate material was superior or inferior to the titanium/titanium alloy.

The vendors were required to recommend a style and configuration for a gas cooler that met the design operating and performance requirements. The vendors were to provide a summary of the alternative configurations considered and the evaluation of each with emphasis on reliability and mass. The vendors were to indicate the impact of material selection on style and configuration and to identify design pressure, temperature, and flow breakpoints that impact their selection. These evaluations were to include a description of the proposed gas cooler including materials of construction, unit construction, unit mass, and a pictorial representation.

A reliability assessment was to include potential failure modes, including procedures and features intended to mitigate failure, the potential for corrosion, and a summary of company historical data and past experience that supports component lifetime (20 years) expectations. Reference 9- 38 provides a detailed summary of the results of the Scoping Phase.

### 9.3.4 Design Configuration

A number of heat exchanger configurations were reviewed within the gas cooler scoping phase. These configurations consisted of a variety of compact heat exchangers (plate/fin, chemically etched, and hybrid designs), and shell-and-tube designs.

#### 9.3.4.1 Compact Heat Exchangers

Of the multiple configurations possible for heat exchangers, the highest performing provides a large heat transfer surface area with a high thermal efficiency. A "compact heat exchanger" is defined by AIChE to have a heat transfer area to volume greater then 400 $m^2/m^3$. This configuration assumes elimination of all configurations that do not satisfy this requirement based on achieving the gas cooler performance requirements at minimum mass and volume. As an example, a shell and tube configuration is not typically considered a compact heat exchanger because its heat transfer area to volume ratio is typically only 65-70 $m^2/m^3$. Several high performance compact heat exchangers were eliminated for reliability reasons. As an example a Primary Surface Recuperator (PSR) allows inter-path leakage, which is not acceptable for the gas cooler application.

It should be noted that while the compact heat exchanger minimizes mass and volume; it does not minimize the number of joints and joint length. This is a reliability issue that would need to be explored further prior to configuration selection.

Hamilton Sundstrand, Heatric, and Honeywell reviewed compact heat exchangers during the scoping phase. All vendors assessed this design configuration from a performance and reliability perspective. One example of a compact heat exchanger is described below. This example is a chemically etched/plate formed fin hybrid design reviewed by Hamilton Sundstrand.

**Example Compact Heat Exchanger: Chemically etched/Plate formed fin hybrid**

The hybrid chemically etched/plate formed fin configuration is a three pass cross counter flow design. The core is vacuum brazed and consists of chemically etched water layers, closure bars, formed gas fins, parting sheets, and end sheets. Headers and mounting brackets are welded onto the core. This design was evaluated for three materials, titanium CP-70, stainless steel 347, and nickel alloy 625.

The proposed design consists of a hybrid configuration comprised of a gas side heat exchanger formed from layers of very thin tightly spaced formed fins and the water side of the heat exchanger is a chemically etched plate to handle the high water pressure. The layers are separated by parting sheets and brazed together.

***Gas Side Design***

As with most gas to liquid heat exchangers the gas side drives the design since the thermal performance of the liquid is an order of magnitude higher. A counter flow heat exchanger would typically be the most effective solution. The density difference between the HeXe mixture and the water is rather large. This constrains the gas side pressure difference and increases the flow areas for both the water and gas. Increasing the flow area for the water decreases the velocity of the water, and the convective heat transfer coefficient, making a larger heat exchanger to account for this. This problem can be accommodated by using a multi-pass cross-flow design. The wavy fin proposed for the gas circuit prevents a uniform velocity profile by interrupting boundary layer formation. Other fin types are considered (ruffled, serrated, straight) and the selection is based on the heat exchanger application.

***Water Side Design***

The required water side pressure is too high for the traditional plate and fin design. As a result, the water side is designed with chemically etched mini-channel plates. The result is a heavier heat exchanger than the traditional plate fin, but one that can handle the high pressure of the water. The heat exchanger would be constructed of alternating layers of formed fins for the gas side and etched plates for the water side, which are all brazed together.

***Effect of Pressure on Core and Header Geometry***

A large duct diameter is needed for the gas side of the heat exchanger to meet pressure drop limitations. The water side is not an issue. There are two types of headers considered, domed and tapered conical parallel. Typically a domed header is used. It is a simple design for low pressure, low flow systems, and has a thin wall thickness that minimizes the mass. For the gas cooler, the gas side pressure and flow is high enough that an alternate header is needed. As a result, tapered conical parallel flow header may avoid load on the core and ensure effective flow distribution.

***Design Against Inter-path Leakage***

This design of heat exchangers typically exhibits leakage as low as $1.5 \times 10^{-9}$ scc/sec. The gas cooler specification outlined a zero leakage requirement, as the allowable leakage rate has not been defined. As an option, a "barrier layer" that can be vented to space could be used to ensure any leakage to not cross the boundary from the water side to the gas side. Leakage of any water to the gas side of the system could result in mission failure. This is an option that could be considered in a future design phase and was not outlined in detail for the Scoping Phase. The addition of the barrier would increase the reliability of the heat exchanger, but

increase its mass and volume by approximately 55-85% and 33% respectively, while maintaining the same heat transfer capability. Other potential leakage could occur at the headers where the closure bars are exposed to the other fluid. In this instance, a double closure bar could be added with a gap to vent any possible leakage.

***Impact of Material on Style/Configuration***

The impact of material choice on style and configuration is secondary to design temperature, pressure, flow rates and required effectiveness. The material fabrication factors and material properties will drive thickness and weight.

***Heat Exchanger Style Impact Due to Pressure, Temperature, and Flow Breakpoints***

With the exception of materials, the only definable breakpoint is pressure. At approximately 400-600 psig (2700-4100 kPa) a transition needs to be made from conventional plate and fin type heat exchanger to a chemically etched plate or shell-and-tube design to handle the water pressure, as the operating pressure far exceeded the 400-600 psig limit for plate and fin.

## 9.3.4.2 Shell and Tube

While the compact hybrid design provides a heat exchanger that is small and low mass, gas cooler reliability is a major factor (20 year maintenance free requirement). The shell-and-tube design is envisioned to have a higher reliability as compared to conventional compact heat exchanger designs for high pressure water gas coolers. Honeywell and Holtec reviewed the performance capability of shell-and-tube designs during the scoping phase. Material types reviewed for the shell-and-tube design included Ni-based alloys 617, 690, 625, stainless steel 304, 316, and titanium based alloys. One example (Honeywell configuration) of a shell-and-tube design is described below.

**Example Shell-and-Tube Heat Exchanger**

The hot gas side is two-pass cross-counterflow with the coolant side folded once in order to create a compact package. The gas flows down and across one-half of the tube bundle, and then flows back up and over the second half of the tube bundle before exiting. The water flows through half of the tube bundle in one direction, reverses directions in the manifold and then flows through the second half of tubes before exiting.

Both configurations utilize smooth tubes with turbulator inserts that disrupt the flow. The tubes are staggered and the number of tubes in the flow direction was adjusted to manage the gas side pressure drop.

***Impact of Material on Style/Configuration***

Titanium shell and tube design were found to be lower mass than the Inconel designs studied. The Inconel shell and tube design utilizes thinner walled tubes with slightly higher thermal conductivity, allowing reduction of the overall tube length.

***Pressure Drop***

To ensure that most of the allowable pressure drop is available in the heat transfer section, the inlet and outlet ducts and manifolds must have a large effective diameter. For the shell and tube gas cooler, two passes with a limited tube density limited pressure drop.

The pressure drop of the HeXe mixture is a significant design driver. Increasing the flange-to-flange pressure drop requirement would allow for a wider range of surfaces to be explored and would yield smaller gas duct sizes, reducing weight and volume.

## 9.3.5 Materials

In selecting candidate materials for their gas cooler design proposals, vendors chose from three classes of materials: titanium alloys (CP Gr. 2, CP Gr. 3, Ti-3Al-2.5V, Ti-6Al-6V-2Sn, TIMETAL, CP 70), stainless steels (SS304, SS316, SS347), and nickel alloys (617, 690, 625).

In making a final gas cooler material selection, the heat rejection system working fluid chemistry and materials of construction (e. g., piping, valves, heat pipes, etc.) must be considered. All three classes of materials are extremely susceptible to accelerated corrosion in the presence of chloride ions in aqueous media. Titanium cannot be exposed to fluorides since they readily attack and strip the protective oxide layer. Previous studies have shown that hydrogen absorption is significantly increased whenever titanium is contaminated by iron ions, hypothetically because the iron contamination provides convenient sites for hydrogen absorption into the oxide layer and metal. Thorough evaluation and testing is required if it is decided to use dissimilar materials, e. g., titanium alloys and stainless steels, in common contact with the working fluid.

***Fabricability, Strength & Mass Issues***

Given the complexity of heat exchanger fabrication, the necessity to accommodate formability requirements limits titanium alloy selection to those with higher fabricability and lower strengths. To tolerate proposed water coolant pressures, titanium walls would need to be thicker than initially envisioned when only higher strength titanium alloys were considered. If it had become necessary to use thicker wall material to meet minimum strength requirements, then any potential mass advantage gained by using titanium becomes marginal. Therefore, material reliability in terms of corrosion resistance, long-term mechanical properties, and compatibility (including the effects of possible mass transport and transfer of impurities) with other materials in the heat rejection system, as well as the potential impact on chemistry in the reactor plant gas system, were likely to have been decisive factors in material selection rather than any presumed mass advantage of titanium alloys.

***Corrosion***

*Water Working Fluid*

Because of the oxide layer ($TiO_2$) that forms instantaneously on its surface when exposed to $O_2$ or $H_2O$, titanium is generally considered resistant to aqueous corrosion up to 589 K. assuming that the oxide layer is present on the surface of titanium, absorption or release of impurities or interstitials, such as hydrogen, is unlikely.

Titanium alloys may have experienced crevice corrosion or pitting if the heat rejection system working fluid had become trapped in a stagnant area. Galvanic corrosion was also a concern. Materials that are considered "safe" to be coupled to titanium include the 300 series of stainless steels and Alloy 625, as long as titanium and the alloys in question maintain a passive oxide on their respective surfaces. However, titanium should not be coupled to alloys that have high contents of magnesium, zinc, aluminum, copper, or chromium. In addition, studies have shown that in certain environments, alloys with more than 20% chromium content also may create a galvanic couple with titanium.

Most studies have shown that there should be few corrosion concerns for stainless steels or nickel base alloys in water aside from stress corrosion cracking, crevice corrosion and pitting; however, the use of stainless steels and nickel alloys with NaK can present significant problems.

All three classes of materials are particularly susceptible to enhanced corrosion in aqueous environments containing small concentrations of chlorine ions. Assurance and maintenance of extremely low concentrations of chlorine (and, likely, other halides ions) would have been mandatory.

*NaK Working Fluid*

A literature search did not reveal any serious concerns with molten NaK – titanium systems. However, oxygen as an impurity can directly or indirectly contribute to corrosion of stainless steels and nickel alloys exposed to NaK. Oxygen impurity levels greater than 100 ppm in NaK accelerate intergranular infiltration in stainless steels and nickel alloys, and can promote mass transfer of impurities from other materials coupled to the system. If oxygen levels reach 200 ppm, corrosion rates in stainless steels increase substantially. If oxygen is present at concentrations greater than 1000 ppm, extensive, rapid intergranular corrosion is observed in stainless steels and nickel alloys. Extensive surface, intergranular, and grain boundary dissolution have been directly observed in Ni-based alloys 600 and 718, and is expected in similar nickel alloys. Oxygen will catalyze the mass transfer of Ni, Cr, Co, Mn, and Ta from stainless steels and of Fe and Cr from nickel alloys via the NaK, thus depleting these elements from the base materials. Ni-based braze alloys are also particularly susceptible to dissolution by NaK, especially when pure Ni phases are present. Depletion of the base materials and/or dissolution of the brazing alloys could increase the risk of various system failures, including failure of the pressure boundary between loops, thus allowing NaK to leak into the inert gas system loop.

***Hydrogen Embrittlement of Titanium***

Hydrogen embrittlement is a particular concern when using titanium. Whenever titanium absorbs hydrogen above a threshold of 30-150 ppm, hydrides can form and create stress fields which reduce ductility of titanium and induce brittle behavior. For hydrogen embrittlement to occur, three conditions must exist simultaneously:

1) the surface $TiO_2$ layer must be compromised as an effective barrier against hydrogen,
2) the temperature must be above 353 K,
3) a mechanism for generating hydrogen (such as dissociation of water, radiolysis of water or hydrogen impurity).

In addition to the hydrogen embrittlement issue, it is plausible that hydrogen would actually diffuse through the titanium and into the He-Xe working fluid of the reactor plant. This is hypothesized to be a particularly problematical issue since addition of hydrogen in the inert gas would upset the equilibrium of oxygen, carbon and hydrogen believed to be critical to maintenance of satisfactory chemistry in the gas system. The result could have been extremely detrimental, and potentially catastrophic, for Ni-base alloys and/or refractory metal alloys that were proposed for use in the reactor core and power conversion system. However, at the point of project restructuring, it was unclear whether hydrogen would pose any problem for the He coolant as it was likely to diffuse through hot structural materials and escape into the vacuum of space.

***Other Materials Compatibility Concerns***

Carburization of structural materials may occur if carbon is either present as a working fluid impurity or is transferred between dissimilar metals through the NaK working fluid. Carburization of stainless steel embrittles the metal surface through grain boundary diffusion. Solid metal exposed to carbon and oxygen impurities in the NaK may also undergo sensitization, which occurs when carbon forms chromium carbide precipitates at the grain boundaries. While this does not increase the likelihood of corrosive attack by the NaK, it can negatively impact the material's mechanical properties. While at the low proposed gas cooler operating temperatures carburization would not have been considered a major threat to stainless steels and nickel alloys, it still could have been a concern for titanium alloys and would have been addressed during the proposed environmental testing.

## 9.3.6 Heat Rejection System Fluid – Impacts of Using NaK-55 Instead of Water

***Design and Operating Pressures***

The use of NaK-55 (45 weight % sodium and 55 weight % potassium) instead of water as the heat rejection system fluid results in significant decreases in design and operating pressures (all pressures cited below are absolute). The specified water pressures proposed are 10,500 kPa (1523 psia) for design and 5,000 kPa (725 psia) to 7,800 kPa (1131 psia) in operation. The specified NaK-55 pressures proposed are 400 kPa (58 psia) for design and 276 kPa (40 psia) in operation. The reduced pressures with NaK may allow the use of compact plate-fin style heat exchangers rather than the larger and heavier alternatives (e.g. shell and tube or chemically etched plates) required to contain the higher water pressures and the use of reduced material thicknesses with resulting reductions in heat exchanger mass and volume.

The direction of the liquid to gas pressure gradient will be reversed with NaK. The specified gas pressures proposed are 3,000 kPa (435 psia) for design and 1,000 kPa (145 psia) to 2,000 kPa (290 psia) in operation. This means that gas side pressure will be lower than water pressure but higher than NaK pressure. This reverses the likely direction of fluid to fluid leakage.

***Fluid Properties***

The following are representative properties of water at gas cooler conditions:

- Density = 56 lb/ft3
- Specific Heat = 1.05 Btu/lb-F
- Absolute Viscosity = 0.4 lb/hr-ft
- Thermal Conductivity = 0.4 Btu/hr-ft-F
- Prandtl Number = 1.1

The following are representative properties of NaK-55 at gas cooler conditions:

- Density = 54 lb/ft3
- Specific Heat = 0.27 Btu/lb-F
- Absolute Viscosity = 1.0 lb/hr-ft
- Thermal Conductivity = 15.1 Btu/hr-ft-F
- Prandtl Number = 0.02

***Fluid Properties and Pump Power***

Pump power is equal to pump energy per unit mass of fluid multiplied by fluid mass flow rate. Pump energy per unit mass of fluid is equal to fluid specific volume times pump pressure rise divided by pump fractional efficiency. An increase in fluid mass flow rate results in a double penalty if system pressure drop increases due to the higher fluid mass flow rate.

The specific heat of water is approximately four times the specific heat of NaK-55 meaning that the mass flow rate of NaK will be approximately four times the mass flow rate of water for a fixed heat duty and fixed terminal fluid temperatures. The ratio of volumetric flow rates will be also be approximately four as water and NaK densities are similar. For a fixed flow area, NaK velocity will be approximately four times water velocity while the Reynolds Number with NaK will be approximately 1.6 to 1.7 times the Reynolds Number with water for a given equivalent diameter. While the higher Reynolds Number will reduce the friction factor with NaK, the higher NaK velocity will still result in increased pressure drop due to friction relative to water for a given equivalent diameter and flow path length.

These considerations may be more of an issue for the liquid piping external to the gas cooler where the liquid flow path length is relatively fixed and the primary means to reduce pressure drop is to increase pipe diameter. Increased pipe diameter carries a penalty of increased pipe mass and pipe volume while increased pressure drop carries a penalty of greater pump energy per unit mass of fluid. Even for a fixed system pressure drop, pump power will still increase by the ratio of mass flow rates. Pipe diameter would have to be further increased to reduce system pressure drop from the baseline value with water to fully offset the impact of greater mass flow of NaK.

The greater mass flow rate of NaK may have less of an adverse impact on heat exchanger pressure drop where a change in configuration to a more compact heat exchanger style could reduce flow path length or allow other modifications to mitigate the potential increase in pressure drop due to higher velocity. Pump power would still increase with NaK due to the increased mass flow rate unless pressure drop could be reduced from the baseline value with water to fully compensate.

***Fluid Properties and Heat Transfer***
The dominant resistance to heat transfer in the gas cooler is the gas side film. While the significantly higher thermal conductivity of NaK relative to water will result in a greater convective heat transfer coefficient with NaK than water, the magnitude of the overall heat transfer coefficient will not be greatly enhanced because of the relatively low gas side convective heat transfer coefficient controlling the magnitude of the overall heat transfer coefficient. Also, the higher thermal conductivity of NaK will increase axial conduction which, while probably not a very significant factor, will actually adversely impact heat exchanger effectiveness.

***Fluid Compatibility***
The subjects of fluid compatibility and potential for corrosion are addressed in the materials section. The use of reduced material thicknesses due to reduced operating pressure with NaK is subject to an assessment of corrosion potential with NaK relative to water and the possibility of additional thickness required as corrosion allowance.

### 9.3.7 Reliability

Gas cooler reliability was evaluated by each of the vendors during the scoping phase of the gas cooler contract. Internal leakage and external leakage were identified as two mission ending failure modes. Blocked passages were also identified as another potential failure mode resulting in reduced component performance and possible mission termination depending on the extent of blockage. Hamilton Sundstrand performed an initial assessment of heat exchangers designed and operated by the company in a space environment as documented in Reference 9- 39. Using a Mean Time Between Failure (MTBF) prediction in conjunction with the operating data for Space Shuttle and International Space Station (ISS) heat exchangers a gas cooler reliability over mission life was approximated at 97.5% for the chemically etched plate fin design proposed by Hamilton Sundstrand operating for 20 years. The operating temperatures for the Space Shuttle and ISS heat exchangers are significantly lower (~150 – 250 K lower) than the Prometheus gas cooler operating conditions and would need to be evaluated in any future reliability assessments.

A relative reliability comparison between various heat exchanger configurations and material options was provided by Holtec and Honeywell. In the Holtec comparisons mechanical properties and corrosion resistance were evaluated for stainless steel, titanium alloys and Ni-base alloys. If reliability is the main design consideration, Holtec identified the Ni-base shell-and-tube designs as the best material design option at the expense of mass.

Honeywell evaluated the relative reliability of both plate fin and shell-and-tube heat exchanger design configurations and Ni-base and titanium-base material options using a Failure Modes and Effects Analysis (FMEA). From a reliability perspective Honeywell identified a shell-and-tube configuration as the only acceptable configuration for a high temperature water-based HRS from their design experience. For a NaK- based HRS, a plate fin design was only considered due to the considerable mass savings of a plate fin configuration and lower operating pressures associated with NaK. They also evaluated both titanium-base and Ni-base material options from a reliability perspective. Corrosion, pressure overload and vibrations were identified as the three categories of failure mechanisms. A risk level was assigned to each of these failure

mechanisms for the material options, configuration and HRS coolant. A Ni-base shell-and-tube water design was identified as the design option with the greatest reliability/lowest risk and a NaK titanium plate fin design was identified as the option with lowest reliability/greatest risk.

In summary a shell and tube Ni-base design provides the best perceived overall reliability at the expense of mass. Chemically etched plate fin heat exchanger designs provide a substantial mass savings relative to shell-and-tube designs (see Section 9.3.9) and the mass benefits would merit further work in demonstrating reliability over the operating conditions envisioned for this component.

### 9.3.8 Gas Cooler Sizing

Gas cooler sizing is based on the number of Brayton loops and system operations. The number of Brayton loops range from one to four, while system operations include multiple possible combinations of operating Braytons. Brayton full load capacity may be 100 kWe or 200 kWe and Braytons may operate at full or partial load. Possible combinations of Brayton loops and the resulting gas cooler are discussed in the following sections. The Scoping Phase was based on the heat balance of Figure 9-35 for a 444 Brayton configuration.

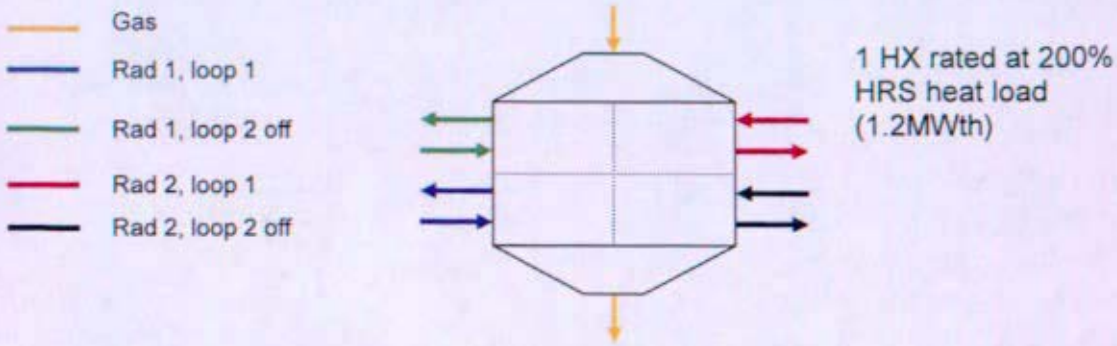
Since the inception of the Scoping Phase, Project Prometheus work has progressed. The gas cooler development program was setup as an evolutionary process to facilitate the modification of plant operating and design and performance requirements as a result of NRPCT work since the initiation of the Scoping Phase. Other configurations have since been proposed and are discussed below. The NRPCT would have evaluated these configurations and modified the plant operating and design and performance requirements from the Scoping Phase to reflect this work and incorporated it into the Phase I Statement of Work.

The following assumptions are made for the gas cooler configurations:

- 800 kWth generated by the reactor
- 200 kWe produced by the Brayton
- The gas cooler must reject the remaining 600 kWth to the Heat Rejection System (HRS)
- Redundant radiator loops are used – two pumped loops per radiator half
- The gas cooler may be over sized to accommodate the redundancy of radiator loops without using valves

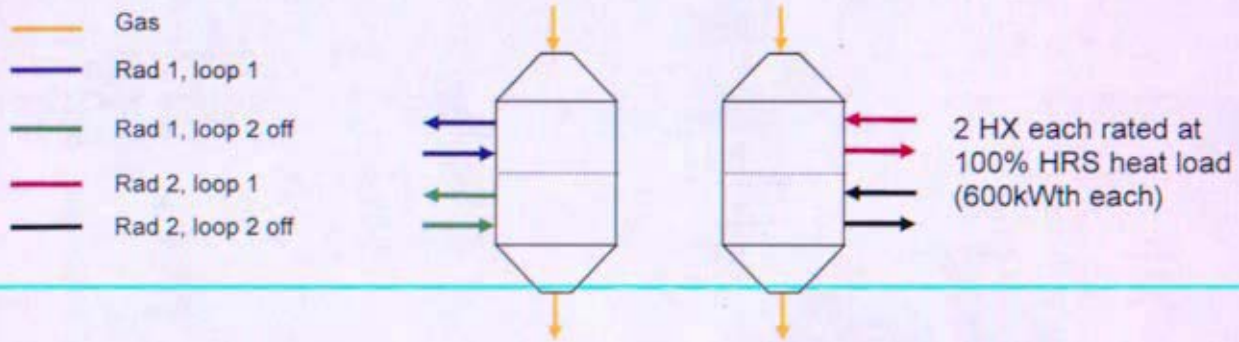
Normal operation requires the gas cooler to dissipate 600 kWth to the heat rejection system. If the gas cooler is not capable of dissipating 600 kWth, full power operation is not attainable. Reference 9- 38 reviews the redundancy of operation/failure scenarios (Brayton failures, heat rejection loop failures) for each system architecture described below.

### 9.3.8.1 1-1-1 Brayton rated at 200 kWe



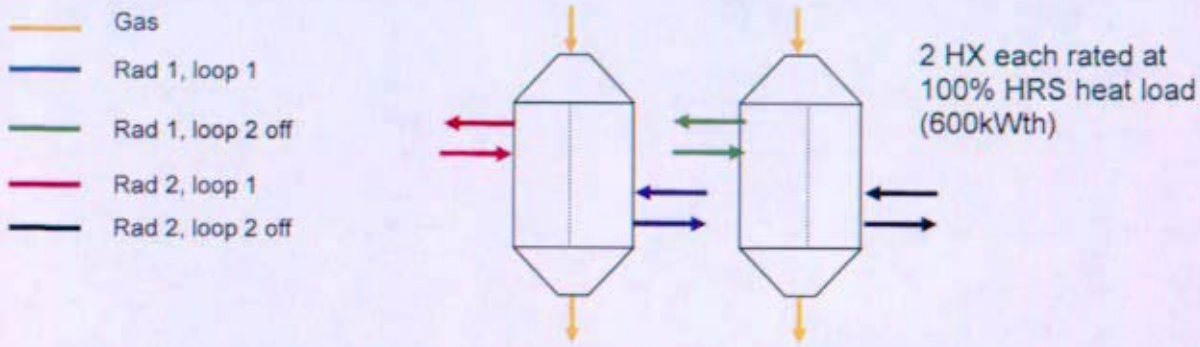

The 1-1-1 system architecture has one Brayton loop, one recuperator, and one gas cooler. Two of the radiator loops would operate, with two off for redundancy. Therefore, each radiator loop would be capable of dissipating 300 kWth, resulting in a 1.2 MWth gas cooler.

### 9.3.8.2 2-2-2 Braytons rated at 100kWe (2 on at full capacity)



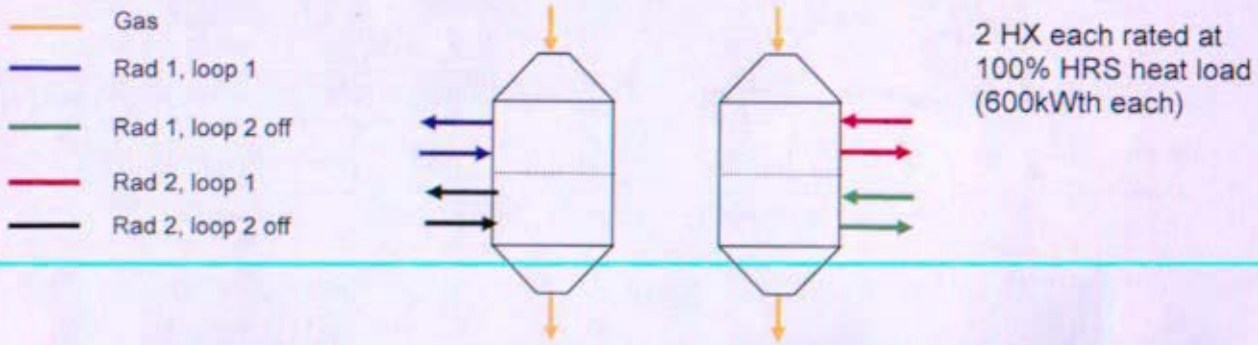

The 2-2-2 system architecture has two Brayton loops, two recuperators, and two gas coolers. Each Brayton would operate at full capacity (100 kWe) for a total of 200 kWe. Therefore, each gas cooler would be responsible for dissipating half of the heat load (300 kWth). For redundancy, two radiator loops would run through each gas cooler with one on and one off. Each radiator loop would then have to be capable of dissipating the 300 kWth, for a gas cooler rating of 600 kWth.

### 9.3.8.3 2-2-2 Braytons rated at 200kWe (1 on, 1 off)



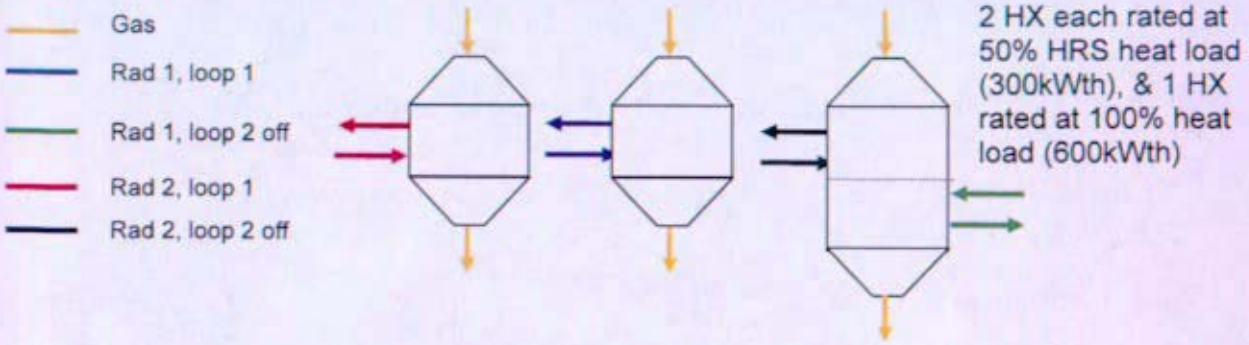

This 2-2-2 system architecture has two Brayton loops rated at 200 kWe with one on and one off for normal operation. Each gas cooler would then be responsible for dissipating 600 kWth, with both radiator loops on. Each radiator loop is capable of dissipating 300 kWth. Redundancy is provided by multiple Brayton loops and multiple radiator loops.

### 9.3.8.4 2-2-2s Braytons rated at 200kWe (2 on at reduced capability)



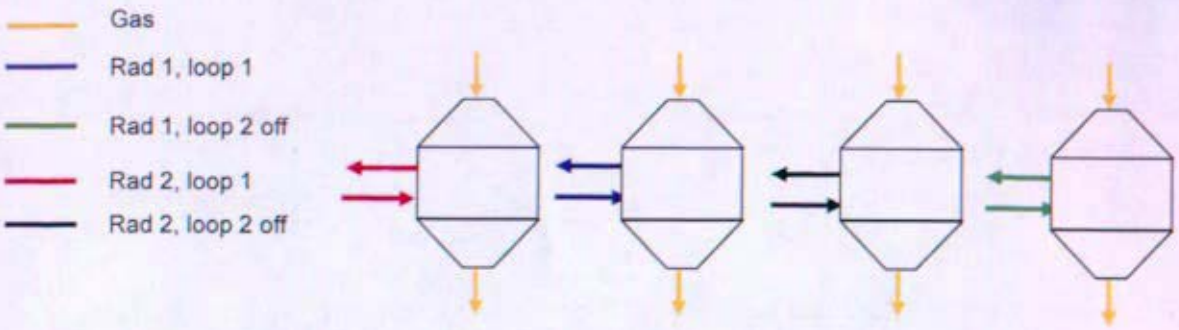

This 2-2-2s system architecture has two Brayton loops, two recuperators, and two gas coolers. Normal operation would run both Brayton loops (rated at 200 kWe) at reduced capacity (100 kWe). Therefore, each gas cooler would be responsible for dissipating half of the heat load, 300 kWth for a total of 600 kWth. Redundancy of radiator loops is provided. Each radiator loop must be capable of dissipating the 300 kWth, so each gas cooler is rated at 600 kWth.

### 9.3.8.5 3-3-3 Braytons rated at 100kWe (2 on, 1 off)




The 3-3-3 system architecture has three Brayton loops, three recuperators, and three gas coolers. Normal operation would run two of the three Brayton loops (rated at 100 kWe) at full capacity. Therefore, each gas cooler would be responsible for dissipating half of the heat load (300 kWth) for a total of 600 kWth. There are four radiator loops, two for each radiator. Therefore, redundancy of radiator loops is provided in the third Brayton loop. Each radiator loop must be capable of dissipating the 300 kWth. Each gas cooler that has one radiator loop (gas cooler 1 and 2) is rated at 300 kWth. Gas cooler one goes to one radiator and gas cooler two goes to the other radiator to maximize redundancy options to maintain 600 kWth dissipated heat. The third Brayton has a gas cooler rated at 600 kWth, and two radiator loops (one for each radiator). A potential drawback to this configuration is the third Brayton loop. There is a greater pressure drop in this gas loop and may lead to unbalanced flow. This would need to be investigated if this configuration became a contender.

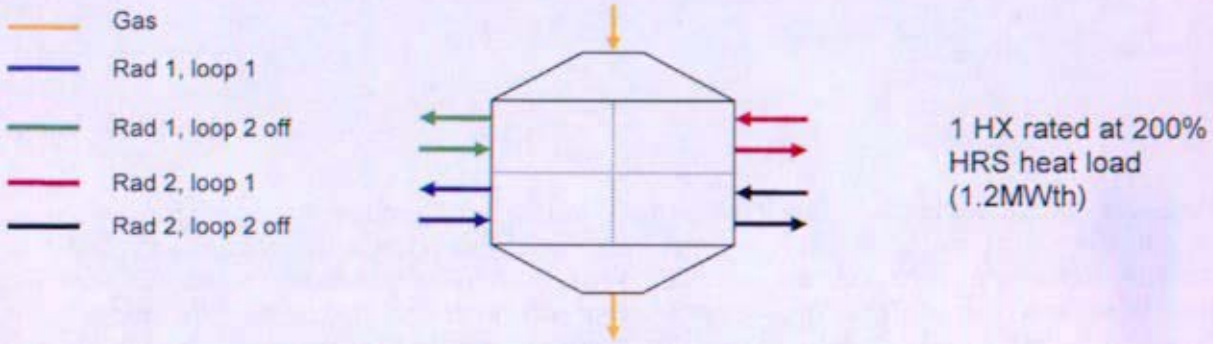
### 9.3.8.6 4-4-4 Braytons rated at 100kWe (2 on, 2 off)




The 4-4-4 system architecture has four Brayton loops, four recuperators, and four gas coolers. Normal operation would run two of the four Brayton loops (rated at 100 kWe) at full capacity. Therefore, each gas cooler would be responsible for dissipating half of the heat load, 300 kWth for a total of 600 kWth. There are four radiator loops, two for each radiator. Therefore, redundancy of radiator loops is provided through redundancy in Brayton loops for this configuration. A failed radiator loop would bring down a Brayton loop, but there are four Brayton loops and two need to be operational for normal operation. A failed Brayton in this situation will

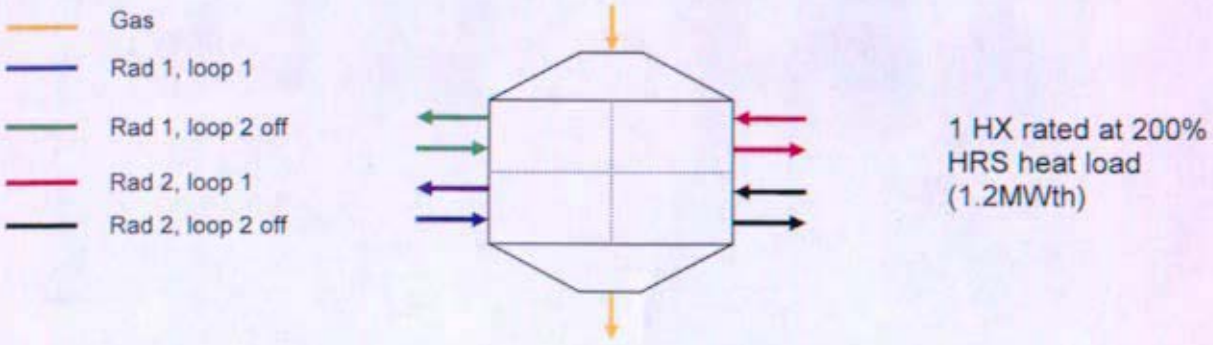
bring down only one radiator loop instead of multiple as seen in other configurations. Each radiator loop must be capable of dissipating 300 kWth. Each gas cooler has one radiator loop and is therefore rated at 300 kWth.

### 9.3.8.7 2-1-1 100 kWe Braytons (2 on) – Same gas cooler as 1-1-1



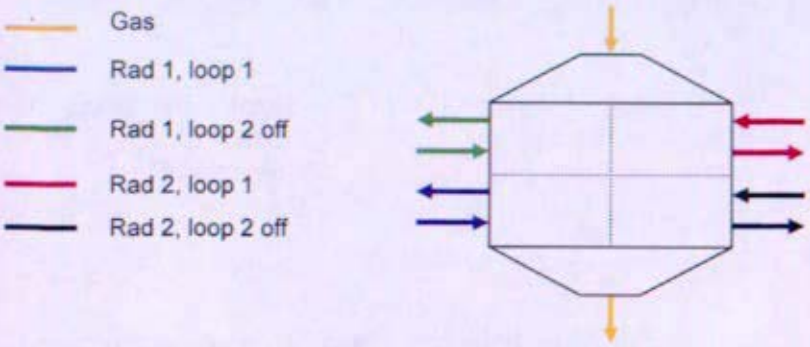

This 2-1-1 system architecture has two Brayton loops, one recuperator, and one gas cooler. Two of the radiator loops would operate, while two were off for redundancy. Therefore, each radiator loop would be capable of dissipating 300 kWth, resulting in a 1.2 MWth gas cooler. Redundancy of Brayton loops is provided in this configuration. While there is only one gas cooler, two Brayton loops are connected through valves to one gas cooler. Each Brayton is rated at 100 kWe and normal operation has both Brayton loops running.

### 9.3.8.8 2-1-1 200 kWe Braytons (1 on, 1 off) – Same gas cooler as 1-1-1



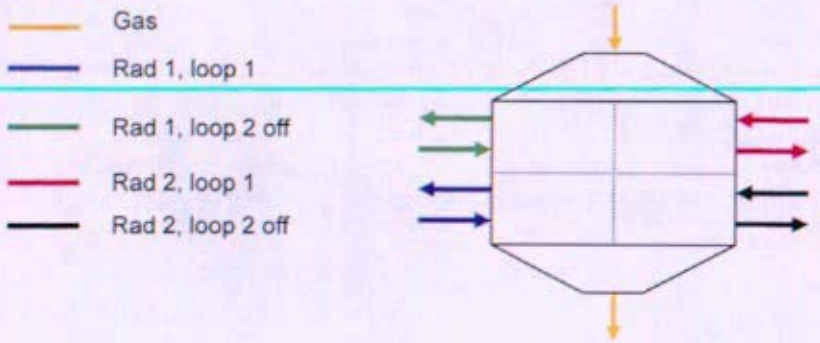

This 2-1-1 system architecture has two Brayton loops, one recuperator, and one gas cooler. Two of the radiator loops would operate, while two were off for redundancy. Therefore, each radiator loop would be capable of dissipating 300 kWth, resulting in a 1.2 MWth gas cooler. Redundancy of Brayton loops is provided in this configuration. While there is only one gas cooler, two Brayton loops are connected through valves to one gas cooler. Each Brayton is rated at 200 kWe and normal operation has one Brayton loop running with the other turned off as a spare.

### 9.3.8.9 2-1-1s Braytons rated at 200kWe (2 on at reduced capability)




This 2-1-1s system architecture has two Brayton loops, one recuperator, and one gas cooler. Two of the radiator loops would operate, while two were off for redundancy. Therefore, each radiator loop would be capable of dissipating 300 kWth, resulting in a 1.2 MWth gas cooler. Redundancy of Brayton loops is provided in this configuration. While there is only one gas cooler, two Brayton loops are connected through valves to one gas cooler. Each Brayton is rated at 200 kWe and normal operation has both Brayton loops running at reduced capacity (100 kWe). The gas cooler is the same as the 111 configuration, but may need to be sized 10-20% larger due to normal operating conditions being less efficient.

### 9.3.8.10 3-1-1 Braytons rated at 100kWe (2 on, 1 off) - Same as 1-1-1




The 3-1-1 system architecture has two Brayton loops, one recuperator, and one gas cooler. Two of the radiator loops would operate, while two were off for redundancy. Therefore, each radiator loop would be capable of dissipating 300 kWth, resulting in a 1.2 MWth gas cooler. Redundancy of Brayton loops is provided in this configuration. While there is only one gas cooler, three Brayton loops are connected through valves to one gas cooler. Each Brayton is rated at 100 kWe and normal operation has two Brayton loops running at full capacity (100 kWe) with one spare Brayton.

### 9.3.9 Mass Summary

A summary of mass estimates for the designs provided by each of the four vendors is as follows:

**Table 9-16 Mass Summary for a Water Coolant Design (Total Gas Cooler Dry Mass in kg)**

| Material | HS – Plate-fin/ Etched hybrid | Honeywell Shell and tube | Holtec Shell and Tube |
|---|---|---|---|
| Titanium alloy | 42.6 | 118.8 | NA |
| Stainless Steel | 57.2 | NA | NA |
| Nickel alloy | 60.3 | 217.5 | 407.3 |

Differences in weights by vendors are based on several factors. Mass estimate differences cannot be fully accounted for, but several differences have been found in the Scoping Phase final reports. The following are cited as potential mass discriminators:

- A chemically etched design will be higher mass than a plate-fin
- Shell and tube will be higher mass than the chemically etched
- Welds are heavier than brazes
- Assumed corrosion rates affect thickness, and therefore mass
- Followed structural design basis code application (ASME, TEMA, Aerospace Standards)

These mass estimates provided in Table 9-16 were based on the Scoping Phase requirements and heat balance shown in Figure 9-35. The vendor gas cooler mass estimates can be scaled to reflect work completed since the Scoping Phase.

Table 9-17 through Table 9-22 show the results of scaling Honeywell and Hamilton Sundstrand gas coolers to current projected component design specifications. Section 4 provides the closeout non-optimized heat balances that establish these current design parameters. The change in mass is due to increases in required heat transfer by the gas cooler from the primary loop to the heat rejection system, and increased water side temperatures and pressures of the heat rejection system.

**Table 9-17: Gas Cooler Mass Estimates Scaled from a Titanium Shell and Tube Design**

| |
|---|
| 1-1-1: 437.9 kg<br>2-1-1 (1on, 1 off): 437.9 kg |
| 2-2-2 (1on, 1off): 218.3 kg each, 436.7 kg total |
| 2-2-2 (2 at full capacity): 278.7 kg each, 557.3 kg total<br>3-3-3: 139.3 kg x 2 + 278.7 kg x 1, 557.3 kg total<br>3-2-2: 278.7 kg each, 557.3 kg total |
| 4-2-2: 302.2 kg each, 604.4 kg total<br>4-4-4: 151.1 kg each, 604.4 kg total |

**Table 9-18: Gas Cooler Mass Estimates Scaled from a Titanium Plate-fin/chemically etched Hybrid Design without a Barrier Layer**

| |
|---|
| 1-1-1: 157.1 kg<br>2-1-1 (1on, 1 off): 157.1 kg |
| 2-2-2 (1on, 1off): 78.3 kg each, 156.6 kg total |
| 2-2-2 (2 at full capacity): 100.0 kg each, 200.0 kg total<br>3-3-3: 50.0 kg x 2 + 100.0 kg x 1, 200.0 kg total<br>3-2-2: 100.0 kg each, 200.0 kg total |
| 4-2-2: 108.4 kg each, 216.8 kg total<br>4-4-4: 54.2 kg each, 216.8 kg total |

**Table 9-19: Gas Cooler Mass Estimates Scaled from a Titanium Plate-fin/chemically etched Hybrid Design with a Barrier Layer**

| |
|---|
| 1-1-1: 290.6 kg<br>2-1-1 (1on, 1 off): 290.6 kg |
| 2-2-2 (1on, 1off): 144.9 kg each, 289.7 kg total |
| 2-2-2 (2 at full capacity): 185.0 kg each, 370.0 kg total<br>3-3-3: 92.5 kg x 2 + 185.0 kg x 1, 370.0 kg total<br>3-2-2: 185.0 kg each, 370.0 kg total |
| 4-2-2: 200.5 kg each, 401.1 kg total<br>4-4-4: 100.3 kg each, 401.1 kg total |

**Table 9-20: Gas Cooler Mass Estimates Scaled from an Inconel Shell and Tube Design**

| |
|---|
| 1-1-1: 801.8 kg<br>2-1-1 (1on, 1 off): 801.8 kg |
| 2-2-2 (1on, 1off): 399.7 kg each, 799.7 kg total |
| 2-2-2 (2 at full capacity): 510.3 kg each, 1020.5 kg total<br>3-3-3: 255.1 kg x 2 + 510.3 kg x 1, 1020.5 kg total<br>3-2-2: 510.3 kg each, 1020.5 kg total |
| 4-2-2: 553.4 kg each, 1106.7 kg total<br>4-4-4: 276.7 kg each, 1106.7 kg total |

**Table 9-21: Gas Cooler Mass Estimates Scaled from an Inconel Plate-fin/chemically etched Hybrid Design without a Barrier Layer**

| |
|---|
| 1-1-1: 222.3 kg<br>2-1-1 (1on, 1 off): 222.3 kg |
| 2-2-2 (1on, 1off): 110.8 kg each, 221.6 kg total |
| 2-2-2 (2 at full capacity): 141.5 kg each, 283.0 kg total<br>3-3-3: 70.7 kg x 2 + 141.5 kg x 1, 283.0 kg total<br>3-2-2: 141.5 kg each, 283.0 kg total |
| 4-2-2: 153.4 kg each, 306.7 kg total<br>4-4-4: 76.7 kg each, 306.7 kg total |

**Table 9-22: Gas Cooler Mass Estimates Scaled from an Inconel Plate-fin/chemically etched Hybrid Design with a Barrier Layer**

| |
|---|
| 1-1-1: 411.3 kg<br>2-1-1 (1on, 1 off): 411.3 kg |
| 2-2-2 (1on, 1off): 205.0 kg each, 410.0 kg total |
| 2-2-2 (2 at full capacity): 261.8 kg each, 523.6 kg total<br>3-3-3: 131.0 kg x 2 + 261.6 kg x 1, 523.6 kg total<br>3-2-2: 261.8 kg each, 523.6 kg total |
| 4-2-2: 283.8 kg each, 567.6 kg total<br>4-4-4: 141.9 kg each, 567.6 kg total |

### 9.3.10 Future Work

A three phase gas cooler development plan had been envisioned to follow the Scoping Phase discussed. The next phase in the program would have been Phase I, a detailed gas cooler design. This design phase included initial design drawings with thermal, hydraulic, and structural analyses of the manifolds and internals. It would have been recommended that a minimum of two types of heat exchangers be included in Phase I. The two represented styles would have included a plate formed fin, chemically etched, or hybrid of the two, and a shell and tube design.

## 9.4 Piping

### 9.4.1 Summary and Conclusions

The baseline Space Nuclear Power Plant (SNPP) incorporates a piping system which circulates He-Xe coolant through the reactor and closed Brayton energy conversion system. Hydraulic analyses have been performed which calculated the percentage ΔP/P for various piping arrangements. When coupled with heat balance models, these analyses have shown that minimizing pressure drop is critical to maintaining the viability of the SNPP energy conversion cycle. The section of the piping between the reactor and the turbine required special design features to incorporate Ni-base superalloy pressure boundary. Due to the complexity of the hot leg piping design, further development efforts would have been required. The following sections discuss the methods used to calculate the system percentage ΔP/P as well as requirements of the hot leg piping development effort. The major development area with respect to piping includes:

- The section of the piping between the reactor and the turbine required special design features to incorporate a Ni-base superalloy metal pressure boundary. As a result, in Reference 9- 78, NR approved the Reference 9- 77 NRPCT hot leg piping recommendation, which recommended the development of internally insulated Ni-base superalloy hot leg piping. Due to the complexity of the hot leg piping design, further development efforts would have been required to overcome challenges in material selection, manufacturability, modeling, testing, and the turbine entrance temperature measurement.

### 9.4.2 Background

The SNPP design incorporates a piping system which circulates He-Xe coolant through the reactor and closed Brayton energy conversion system. The piping is comprised of high pressure (~2 MPa (290 psi)) and low pressure (~1 MPa (145 psi)) sections. The high pressure sections include piping from the reactor to the turbine inlet, piping from the compressor outlet to the recuperator, and piping from the recuperator to the reactor. The low pressure sections include piping from the turbine outlet to the recuperator, piping from the recuperator to the gas cooler, and piping from the gas cooler to the compressor inlet. The following heat balance, generated from the NASA-Glenn Excel spreadsheet, SRPS-opt, shown in Figure 9-37, depicts the nominal operating conditions for the plant piping used in calculations. A number of additional nominal heat balances have been created since the heat balance was established, but the heat balance below is still representative of the likely design.

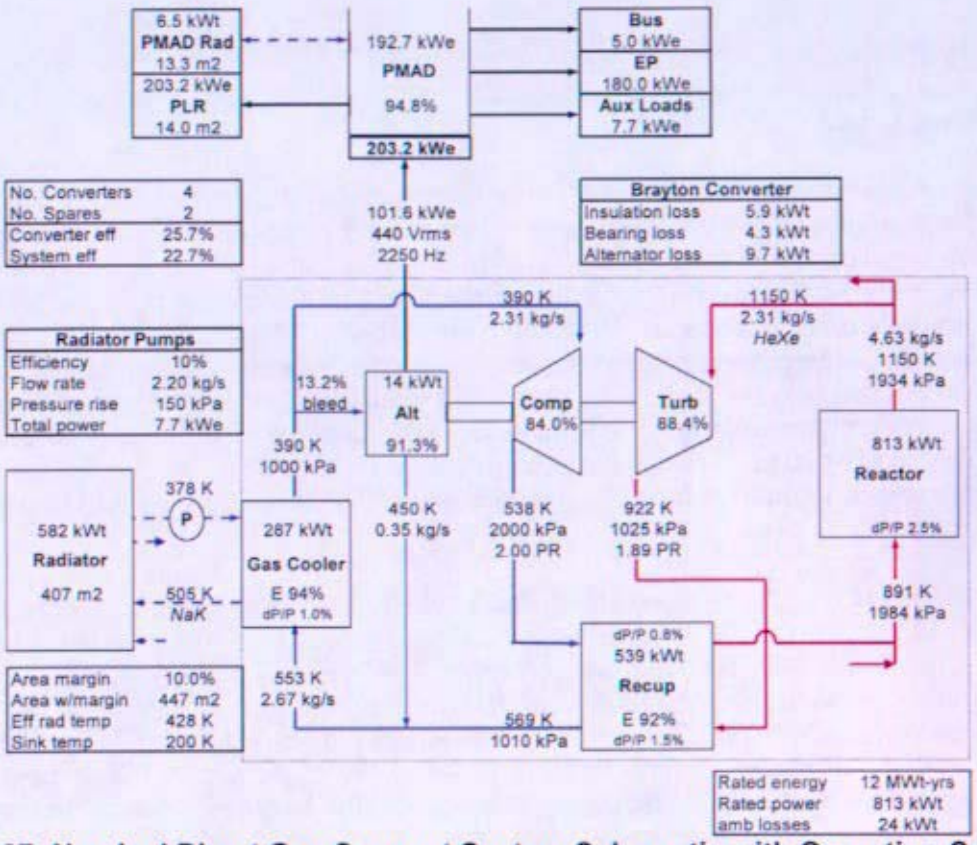



**Figure 9-37: Nominal Direct Gas Concept System Schematic with Operating Conditions**

These nominal values of operating pressure, temperature, and flow, shown in Table 9-23, were used in conjunction with the piping diameters from various arrangements presented in Section 8, to determine piping wall thicknesses as presented in Section 9.4.3. The resulting wall thicknesses were used in conjunction with these operating conditions to perform pressure drop calculations which are presented in Section 9.4.4.

**Table 9-23 – Nominal Piping Operating Parameters**

| Piping Run | | Pressure | | Gas Temperature | | Flow | |
|---|---|---|---|---|---|---|---|
| From | To | MPa | psi | K | °F | kg/s | lb/s |
| Reactor | Turbine | 1.934 | 281 | 1150 | 1610 | 4.63 | 10.21 |
| Turbine | Recuperator | 1.025 | 149 | 922 | 1200 | 2.315 | 5.10 |
| Recuperator | Cooler | 1.01 | 146 | 569 | 565 | 2.315 | 5.10 |
| Cooler | Compressor | 1 | 145 | 390 | 242 | 2.315 | 5.10 |
| Compressor | Recuperator | 2 | 290 | 538 | 509 | 2.315 | 5.10 |
| Recuperator | Reactor | 1.984 | 289 | 891 | 1144 | 4.63 | 10.21 |

The baseline material for the plant piping is Inconel 617, a Ni-base superalloy. The Ni-base superalloys Haynes 230 and Nimonic PE-16 were also under consideration. Ni-base superalloys are the primary piping material candidates due to their structural performance at high temperatures and compatibility with atmospheric constituents.

The piping from the reactor outlet to the turbine inlet, hereafter referred to as "the hot leg piping," would have contained the highest temperature gas and operated at high pressure. In the absence of a heat transfer barrier, the pipe metal temperature would approach the temperature of the coolant in contact with the piping. At temperatures above 900 K (1160 °F), Ni-base superalloys begin to significantly reduce their creep resistance and consequently lower material design strength. The reduced design strength can be be addressed by increasing ping wall thickness, but the mass of the system will increase. In addition, Ni-base superalloys may begin to decarburize at temperatures above 1050 K, leading to loss in creep strength and potentially contamination of refractory metal alloys exposed to the gas stream. As a result, the hot leg piping would have had distinctive design considerations which would not apply to the rest of the piping sections. The hot leg piping design is further discussed in Section 9.4.6. It should be noted that the turbine to recuperator piping section also contains gas at a temperature in excess of 900 K. However, the lower gas temperature and pressure (relative to the hot leg piping) and the ability to increase the wall thickness of this piping section likely preclude the need for additional control of pressure boundary temperature.

The hot leg piping, along with the reactor inlet piping, must travel around or through the reactor shielding. In order to minimize the impact of neutron and gamma streaming through the piping, the piping outer diameter has been limited to 16 cm (6.3 in.) for the preliminary arrangement studies. In the plant concepts with multiple Braytons, the energy conversion system piping is limited to 10 cm (3.9 in.) in diameter to facilitate arrangements. These sizes would have needed to be revisited and optimized as the design matured.

### 9.4.3 Pipe Sizing Calculations

Piping wall thickness calculations were performed for both straight piping and pipe bends to provide a preliminary estimate of acceptable pipe wall thicknesses. The wall thickness used in pressure drop calculations and mass estimates was conservatively based on the pipe wall thickness prior to bending, since these sections of piping require thicker walls to account for thinning due to bending (Reference 9- 69). Given a fixed outer pipe diameter, increased wall thickness decreases pipe inner diameter and increases pressure drop. Pipe sizing calculations were performed based on the ASME Boiler and Pressure Vessel (B&PV) Code for the straight sections of piping (Reference 9- 70). For pipe bends, wall thicknesses prior to bending were approximated by multiplying the thickness dictated the by the ASME B&PV Code by a bending ratio (Reference 9- 69).

The minimum thickness of a pipe wall ($t_m$), prior to bending, required for the system design pressure was calculated using the following equation:

**Equation 9-1**

$$t_m = \left[ \frac{P \cdot D_o}{2(S_{mt} + y \cdot P)} + C \right] \cdot Rat_B$$

where $P$ is the internal design pressure (operating pressure), $D_o$ is the outside diameter of the pipe, $S_{mt}$ is the maximum allowable stress intensity from the Space Structural Design Basis (SSDB) (Reference 9- 71), $y$ is a coefficient having a value of 0.4 (Reference 9- 70), $C$ , a corrosion factor, has a value of 0.1651 cm (0.065 in.) and is the additional thickness for plain

end pipe or tubes for diameters above one inch (Reference 9- 70), and $Rat_B$ is the bend ratio as defined in Equation 9-2 below from Reference 9- 69:

**Equation 9-2**

$$Rat_B = \frac{R + 0.5D_o}{R}$$

where $R$ is the bend radius of the pipe.

For the base case material, Inconel 617, the SSDB defines $S_{mt}$ for two separate temperature ranges as specified in Equation 9-3 and Equation 9-4 below:

**Equation 9-3**

$$S_{mt} = \min\left(10^{\left(\frac{25.19668T-40152}{2.48206T-8654.23}\right)} \cdot t_{EOL}^{\left(\frac{T}{2.48206T-8654.23}\right)},\quad 162.3 - 0.0078 \cdot T\right)(MPa)$$

$$for\ 294K \le T < 1002K$$

**Equation 9-4**

$$S_{mt} = \min\left(10^{\left(\frac{25.19668T-40152}{2.48206T-8654.23}\right)} \cdot t_{EOL}^{\left(\frac{T}{2.48206T-8654.23}\right)},\quad 634.4 - 0.479 \cdot T\right)(MPa)$$

$$for\ 1002K \le T \le 1200K$$

where $T$ is the pipe wall temperature in Kelvin and $t_{EOL}$ is the time at end of life in hours.

Table 9-24 below, presents several wall thickness values for varying bend radii and pipe operating parameters (temperature and pressure) which would have been experienced in the piping assembly for a mission lifetime of 15 yrs (~132,000 hrs). It should be noted that these values are minimum wall thicknesses and additional phenomenon may occur which would could have required the wall thicknesses to increase, such as creep-fatigue interactions, irradiation, and thermal ratcheting.

**Table 9-24 – Minimum Wall Thickness as a Function of Temperature, Pressure, and Bend Radius**

| T<br>K | P<br>MPa | $S_{mt}$<br>MPa | $D_o$<br>cm | R<br>cm | $t_{straight}$<br>cm | $Rat_B$ | $t_m$<br>cm |
|---|---|---|---|---|---|---|---|
| 390 | 1.00 | 159.26 | 10 | 10 | 0.20 | 1.50 | 0.29 |
| 390 | 1.00 | 159.26 | 10 | 20 | 0.20 | 1.25 | 0.25 |
| 390 | 1.00 | 159.26 | 10 | 30 | 0.20 | 1.17 | 0.23 |
| 538 | 2.00 | 158.10 | 10 | 10 | 0.23 | 1.50 | 0.34 |
| 538 | 2.00 | 158.10 | 10 | 20 | 0.23 | 1.25 | 0.29 |
| 538 | 2.00 | 158.10 | 10 | 30 | 0.23 | 1.17 | 0.27 |
| 891 | 1.98 | 109.50 | 16 | 16 | 0.31 | 1.50 | 0.46 |
| 891 | 1.98 | 109.50 | 16 | 32 | 0.31 | 1.25 | 0.39 |
| 891 | 1.98 | 109.50 | 16 | 64 | 0.31 | 1.13 | 0.35 |
| 922 | 1.03 | 82.49 | 10 | 10 | 0.23 | 1.50 | 0.34 |
| 922 | 1.03 | 82.49 | 10 | 20 | 0.23 | 1.25 | 0.28 |
| 922 | 1.03 | 82.49 | 10 | 30 | 0.23 | 1.17 | 0.26 |
| 1150 | 1.93 | 8.16 | 16 | 16 | 1.90 | 1.50 | 2.85 |
| 1150 | 1.93 | 8.16 | 16 | 32 | 1.90 | 1.25 | 2.37 |
| 1150 | 1.93 | 8.16 | 16 | 64 | 1.90 | 1.13 | 2.13 |
| 900 | 1.93 | 100.93 | 16 | 16 | 0.32 | 1.50 | 0.48 |
| 900 | 1.93 | 100.93 | 16 | 32 | 0.32 | 1.25 | 0.40 |
| 900 | 1.93 | 100.93 | 16 | 64 | 0.32 | 1.13 | 0.36 |

As temperature and pressure increase, the corresponding pipe wall thickness increases, while as the bend radius is increased, the required wall thickness decreases.

### 9.4.4 Pressure Drop Calculations

Pressure drop calculations were performed to provide a preliminary estimate of percentage ΔP/P for various piping arrangements. It should be noted that the arrangements analyzed are preliminary and unoptimized. Optimized piping arrangements would have required a balance between hydraulic and mechanical design considerations. The pressure drop in each section of piping was determined, using an Excel spreadsheet analysis, by combining the pressure drops due to friction, dividing and combining flows, pipe bends, and valves. The pressure drops in each section were then converted to a percentage ΔP/P which was summed to provide a total percentage ΔP/P for the entire piping arrangement. For a detailed description of the methods used for these pressure drop calculations, see Sections 9.4.4.1 through 9.4.4.6. Hydraulic analyses results are summarized in Section 9.4.5.1. Microsoft Excel is verified as part of the standard productivity suite for the NRPCT. The spreadsheets were created and tested for comparison to hand calculations for qualification. For hot leg piping pressure drop calculations, the internal insulation was assumed to be 1.5 cm thick, which is a conservative approximation based on Reference 9- 77.

#### 9.4.4.1 Pressure Losses Due to Friction

Pressure losses due to fluid flow were calculated utilizing formulas presented in Reference 9-72. Equation 9-5 was used to calculate the pressure drop though a straight length of piping ($\Delta P_p$):

**Equation 9-5**

$$\Delta P_p = \frac{4 f \rho v^2 \Delta L}{2D}$$

where $\rho$ is the fluid density (calculated using the ideal gas law), $v$ is the fluid velocity, $\Delta L$ is the length of the pipe segment, $D$ is the inner pipe diameter, and $f$ is the fanning friction factor (Equation 9-6). The friction factor was calculated using the Barenblatt formula (Equation 9-6 – Equation 9-8) which represents the friction factor presented in the Moody diagram for Reynolds numbers in the following range: $3.07 \times 10^3 < \mathrm{Re} < 3.23 \times 10^6$ (Reference 9- 73). The Barenblatt formula assumes a hydraulically smooth pipe, which is a reasonable assumption for the range of Reynolds numbers encountered, since the pipe would have been polished.

**Equation 9-6**

$$f = \frac{2}{\Psi^{2/(\alpha+1)}}$$

where

**Equation 9-7**

$$\Psi = \frac{e^{3/2}\left(\sqrt{3}+5\alpha\right)}{2^{\alpha}\alpha(\alpha+1)(\alpha+2)}$$

and

**Equation 9-8**

$$\alpha = 3/(2\ln \mathrm{Re})$$

such that *Re* is the Reynolds number as defined in Equation 9-9 below.

**Equation 9-9**

$$\mathrm{Re} = \frac{\rho v D}{\mu}$$

where $\mu$ is the viscosity of the He-Xe coolant, which is based on the first order Chapman and Enskog correlation for estimating mixture viscosity, see Section 9.3.

### 9.4.4.2 Pressure Losses Due to Dividing Flow Junctions

Pressure losses due to dividing flow junctions were calculated utilizing data provided in Section 73022 of Reference 9- 74. Equation 9-10 and Equation 9-11 were used to calculate the pressure drop for dividing flow junctions, with leg angle $\theta$, as shown in Figure 9-38 and Figure 9-39:

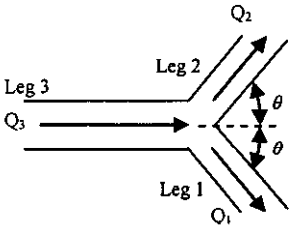



Figure 9-38: Dividing Y-Junction Schematic

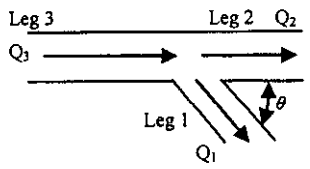



Figure 9-39: Dividing Angled-Junction Schematic

Data are presented for symmetrical Y-junctions as functions of flow ratio with the cross sectional areas in legs 1 and 2 being equal. The total pressure loss coefficient between leg 3 and leg 1 ($K_{31}$) is given in Figure 1 of Section 73022 of Reference 9- 74. The corresponding loss between leg 3 and leg 2 ($K_{32}$) can be found by reversing the labels on legs 1 and 2 and repeating the calculation.

In a dividing angled-junction, the total pressure loss coefficient for $Re_3 > 200{,}000$ between leg 3 and leg 1 ($K_{31}$) is given in Figures 2a to 2d of Section 73022 of Reference 9- 74 with the cross sectional areas in legs 2 and 3 being equal. The total pressure loss coefficient between leg 3 and leg 2 ($K_{32}$) can be assumed to be unaffected by the geometry of leg 1 and is given by Figure 3 in Section 73022 of Reference 9- 74 as a function of the flow ratio only.

After the appropriate total pressure loss coefficients were found for either dividing Y-junctions or dividing angled-junctions, the pressure losses in legs 1 and 2 were found using the following equations:

**Equation 9-10**

$$\Delta P_{d,leg1} = p_3 - p_1 = K_{31}\frac{1}{2}\rho v_3^{\,2}$$

and

**Equation 9-11**

$$\Delta P_{d,leg2} = p_3 - p_2 = K_{32}\frac{1}{2}\rho v_3^{\,2}$$

where $\Delta P_{d,leg1}$ is the pressure loss due to dividing flow in leg 1, $\Delta P_{d,leg2}$ is the pressure loss due to dividing flow in leg 2, and $v_3$ is the fluid velocity in leg 3. Additionally, for all dividing junctions, it was assumed that the junction corners were sharp.

### 9.4.4.3 Pressure Losses Due to Combining Flow Junctions

Pressure losses due to combining flow junctions were calculated utilizing data provided in Section 73023 of Reference 9- 74. Equation 9-12 and Equation 9-13 were used to calculate the pressure drop for a combining flow junction, with leg angle $\theta$, as shown in Figure 9-40 and Figure 9-41.

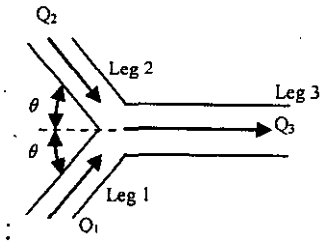



Figure 9-40: Combining Y-Junction Schematic

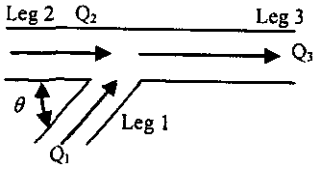



Figure 9-41: Combining Angled-Junction Schematic

Data are presented for symmetrical Y-junctions as functions of flow ratio with the cross sectional areas in legs 1 and 2 being equal. The total-pressure loss coefficient between leg 1 and leg 3 ($K_{13}$) is given in Figure 1 of Section 73023 of Reference 9- 74. The corresponding loss between leg 2 and leg 3 ($K_{23}$) can be found by reversing the labels on legs 1 and 2 and repeating the calculation.

In a combining angled-junction, the total-pressure loss coefficient for $Re_3 > 200{,}000$ between leg 1 and leg 3 ($K_{13}$) is given in Figure 2 of Section 73023 of Reference 9- 74 with the cross sectional areas in legs 2 and 3 being equal. The total pressure loss coefficient between leg 2 and leg 3 ($K_{23}$) can be assumed to be unaffected by the geometry of leg 1 and is given by Figure 3 in Section 73023 of Reference 9- 74 as a function of the flow ratio only.

After the appropriate total-pressure loss coefficients were found for either combining Y-junctions or combining angled-junctions, the pressure loss in legs 1 and 2 were found using the following equations.

**Equation 9-12**

$$\Delta P_{c,leg1} = p_1 - p_3 = K_{13}\frac{1}{2}\rho v_3^{\,2}$$

and

**Equation 9-13**

$$\Delta P_{c,leg2} = p_2 - p_3 = K_{23}\frac{1}{2}\rho v_3^{\,2}$$

where $\Delta P_{c,leg1}$ is the pressure loss due to combining flow in leg 1, $\Delta P_{c,leg2}$ is the pressure loss due to combining flow in leg 2, and $v_3$ is the fluid velocity in leg 3. Additionally, for all combining junctions it was assumed that the junction corners were sharp.

### 9.4.4.4 Pressure Losses Due to Pipe Bends

Pressure losses due to pipe bends ($\Delta P_b$) were calculated using data provided in Section 83037 of Reference 9- 74. Equation 9-14 through Equation 9-22 were used to calculate the pressure drop for bends in circular ducts with turbulent flow (Re ≥ 4000):

**Equation 9-14**

$$\Delta P_b = K_{S,G}\frac{1}{2}\rho v^2$$

where

**Equation 9-15**

$$K_{S,G} = K_b + K_c + K_d$$

such that $K_b$ is the friction loss in the piping, $K_c$ is the friction loss due to the curvature of the pipe, and $K_d$ is the loss due to reestablishment of fully established turbulent flow:

**Equation 9-16**

$$K_b = 0.07\theta(R/D)f$$

where $\theta$ is the bend angle in degrees.

**Equation 9-17**[1]

$$K_c = \frac{\theta}{90}\left(\frac{R}{D}\right)^{0.5}\left[0.03 + 1.3\left(\frac{\varepsilon}{D}\right)^{0.5}\right]$$

where $\varepsilon$ is the pipe roughness factor, which is assumed to be zero for a hydraulically smooth pipe.

For $R/D \geq 1$:

**Equation 9-18**

$$K_d = 0.2(R/D)^{-1.2}\phi_1\phi_2\phi_5$$

and for $R/D < 1$:

**Equation 9-19**

$$K_d = 0.2(R/D)^{-2}\phi_1\phi_2\phi_5$$

where $\Phi_1$ is the Reynolds number correction factor, $\Phi_2$ is the downstream tangent correction factor, and $\Phi_5$ is the bend angle correction factor.

**Equation 9-20**

$$\phi_1 = (1 + 10^4 / \mathrm{Re})$$

and

**Equation 9-21**

$$\phi_2 = 1 - \exp(-0.1L_d/D) + \frac{3[\exp(-L_d/D)]}{(R/D)^2}$$

such that $L_d$ is the distance to the next bend, tee, or component.

**Equation 9-22**

$$\phi_5 = 1.04 - \left[(110 - \theta)^2 / 10^4\right]$$

### 9.4.4.5 Pressure Losses Due to Valves

Pressure losses due to valves were calculated using data for *L/D* values provided in the Valve Section, Section 9.5. In the various arrangements analyzed, both isolation and check valves were used which have *L/D* values of 13 and 115 respectively. Equation 9-23 was used, derived from Equation 9-5, with the above *L/D* values to determine the pressure loss associated with the use of isolation and/or check valves ($\Delta P_v$):

**Equation 9-23**

$$\Delta P_v = \frac{4(L/D)f\rho v^2}{2}$$

### 9.4.4.6 Percentage ΔP/P Calculation

The pressure drops, described in the sections above, were used to calculate the percentage *ΔP/P* for the piping system, defined in Equation 9-24. This percentage *ΔP/P* was calculated for various piping arrangements in order to compare hydraulic performance.

**Equation 9-24**

$$Total\ \%\Delta P/P = 1.2 \sum_{piping\ section} \%\Delta P/P$$

[1] As mentioned in Section 9.4.4.1 the pipe is assumed to be smooth which sets ε in Equation 9-17 equal to zero.

where the total percentage $\Delta P/P$ is found by summing the individual percentage $\Delta P/P$ for each piping section and multiplying by 1.2 in order to add twenty percent margin to the percentage $\Delta P/P$ for conservatism. The percentage $\Delta P/P$ for each section is found using Equation 9-25:

**Equation 9-25**

$$\%\Delta P/P = 100 \cdot \left[ \frac{\Delta P_{p,leg3} + \Delta P_{b,leg3} + \Delta P_{v,leg3}}{P_{comp}} + \frac{\sum_{i=1}^{2} \left( \Delta P_{p,leg\ i} + \Delta P_{b,leg\ i} + \Delta P_{v,leg\ i} + \left( \Delta P_{c,leg\ i} \text{ or } \Delta P_{d,leg\ i} \right) \right)}{2P_{comp}} \right]$$

where $\Delta P_{p,leg3}$, $\Delta P_{b,leg3}$, and $\Delta P_{v,leg3}$ are the pressure drops in leg 3 for the straight piping, bends, and valves, respectively, and the second component of the equation is the average of the pressure drops in legs 1 and 2 since these are parallel legs. $\Delta P_{p,leg\ i}$, $\Delta P_{b,leg\ i}$, and $\Delta P_{v,leg\ i}$ are the total pressure drop in legs 1 or 2 for the straight piping, bends, and valves, respectively, and $\Delta P_{c,leg\ i}$ and $\Delta P_{d,leg\ i}$ are the pressure drops in legs 1 or 2 for either the combining or dividing flows, respectively, which is dependent upon the piping section being analyzed. $P_{comp}$ is either the compressor inlet or discharge pressure (1 or 2 MPa (145 or 290 psi)) depending on the piping section under analysis.
The model divides mass flow between parallel legs such that the total pressure drop from common point to common point is equal through the two legs. In general, mass flow is not equal in the two parallel legs because the piping configurations are not identical, i.e. parallel legs often have an unequal number of bends with different bend angles and radii as well as unequal piping lengths.

### 9.4.5 Piping Mass Estimates

Mass estimates were performed to provide a preliminary estimate of the plant piping mass for various piping arrangements. The mass estimates for each arrangement were calculated utilizing an Excel spreadsheet analysis, by combining the masses of the straight sections of piping and the pipe bends. Piping lengths and bend specifications were obtained directly from the piping arrangement drawings. The total plant piping length was determined by summing the straight piping lengths with the equivalent straight piping lengths of bends. The equivalent straight length of the pipe bends was found using Equation 9-26:

**Equation 9-26**

$$L_B = \sum_{Bends} \frac{\theta \cdot R \cdot \pi}{180}$$

where $\theta$ is the bend angle (in degrees) and $R$ is the bend radius. The mass of the piping was then determined using the following equation:

**Equation 9-27**

$$M_P = \rho_P \cdot \pi \cdot (L_B + L_S) \left( \frac{D_o}{2}^2 - \left( \frac{D_o}{2} - t_m \right)^2 \right)$$

where $\rho_P$ is the density of the piping, $L_S$ is the total straight piping section length, $D_o$ is the piping outer diameter, and $t_m$ is the pipe wall thickness from Section 9.4.3. The masses were calculated for each piping segment and then summed to provide the total mass for each arrangement. The mass of the insulating layer and liner were also calculated. For mass estimates, both the liner and insulation were assumed to be Inconel 617, with the density of the insulation being approximately 8.5% of that of the solid pipe.

### 9.4.5.1 Hydraulic Analysis and Mass Estimate – Results

Pressure drop calculations and mass estimates were performed for several piping arrangements used in the arrangements trade study, Section 8.4. Table 9-25 below summarizes the percentage *ΔP/P* and piping mass results for these arrangements. The arrangements are specified with an "x:y:z" nomenclature, where the first value is the number of turbines, the second is the number of recuperators, and the third is the number of gas coolers.

**Table 9-25- Hydraulic Results**

| Arrangement | Percentage ΔP/P | | | | | Mass |
|---|---|---|---|---|---|---|
| | Total | Piping | Bends | Tees | Valves | kg |
| 4:4:4-Revision 2a | 5.4 | 0.5 | 3.16 | 0.71 | 1.03 | 796 |
| 4:4:4-Revision 2b | 5.34 | 0.49 | 3.11 | 0.71 | 1.03 | 775 |
| 4:4:4-Revision 2c | 5.85 | 0.43 | 3.59 | 0.79 | 1.04 | 776 |
| 3:3:3-Revision 4 | 6.4 | 0.66 | 2.83 | 1.88 | 1.03 | 573 |
| 2:2:2-Revision 1 | 18.3 | 1.76 | 6.67 | 6.22 | 3.67 | 403 |
| 2:2:2-Revision 2b | 4.53 | 0.5 | 1.51 | 1.97 | 0.56 | 505 |
| 1:1:1 Revision 1 | 8.08 | 1.49 | 5.8 | 0.79 | NA | 244 |
| 1:1:1 Revision 2b | 2.17 | 0.36 | 1.7 | 0.11 | NA | 323 |

All arrangements, excluding the 2:2:2-Revision 2b and the 1:1:1-Revision 2b, had hot leg and cold leg (recuperator to reactor) piping with an outer diameter of 16 cm (6.3 in.), while the rest of the piping had an outer diameter of 10 cm (3.9 in.) with the exception of the alternator bleed flow line. The 2:2:2-Revision 2b and the 1:1:1-Revision 2b arrangements differed from the other arrangements in that all the piping, excluding the alternator bleed flow line, had an outer diameter of 16 cm (6.3 in.). Additional system complexity increases the pressure drop significantly, i.e. more bends, tees, and flow restriction. For a more detailed comparison of the various arrangements and the trade study conclusions, see Section 8.4.

### 9.4.5.2 Hydraulic Analysis and Mass Estimates – Diameter Sensitivity

For many of the piping and loop configurations, the percentage *ΔP/P* is higher than desired which negatively affects power generation, radiator area, and system mass. As a result, diameter sensitivity analyses were performed for all arrangements to compare percentage *ΔP/P* and piping mass to increases in piping outer diameters. The sensitivity analyses were performed by simultaneously varying the piping outer diameter for all sections of the piping with the baseline outer diameters being 16 cm (6.3 in.) for the hot and cold leg piping and 10 cm (3.9 in.) for the remaining piping, excluding the alternator bleed flow line. The system piping outer diameter was increased by ten centimeters in one centimeter increments. Figure 9-42 depicts the sensitivity of percentage *ΔP/P* and piping mass to outer diameter. The percentage *ΔP/P* of the 4:4:4 Revision 2b arrangement decreases from ~5.3% to ~0.6% and the piping mass increases from 775 kg (352 lb) to 2013 kg (1006 lb) as outer diameter is increased by 10 cm (3.94 in.).

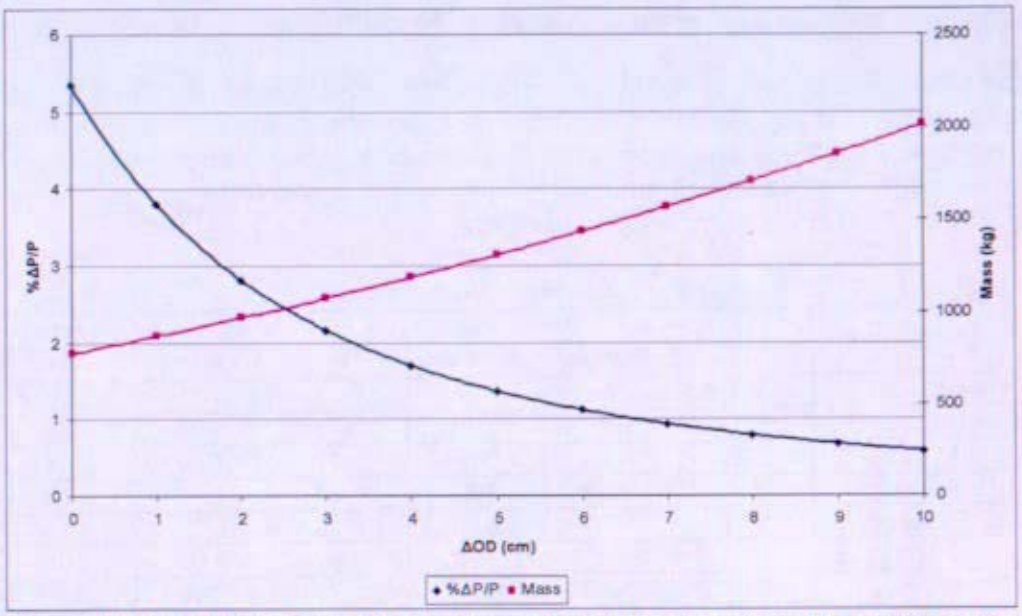



**Figure 9-42: %ΔP/P and Piping Mass Sensitivity to Pipe Outer Diameter Increases from Baseline for the 4:4:4 Revision 2b Configuration**

### 9.4.6 Hot Leg Piping

In Reference 9- 75, Naval Reactors (NR) approved the Reference 9- 76 Naval Reactors Prime Contractor Team (NRPCT) recommendation to develop a gas cooled reactor directly coupled to a Brayton power conversion system as the SNPP for Project Prometheus. The NRPCT has evaluated a variety of hot leg piping concepts for performance relative to the Reference 9- 76 system parameters, as well as for manufacturability and practicality. Reference 9- 77 presents the evaluation of the various hot leg piping concepts and recommended adopting an internally insulated Ni-base superalloy hot leg piping concept as the baseline. In Reference 9- 78, NR approved the Reference 9- 77 NRPCT hot leg piping recommendation in conjunction with the supplemental information provided in Reference 9- 79.

#### 9.4.6.1 Hot Leg Piping Requirements

The hot leg piping, from the reactor outlet to the turbine inlet, contains He-Xe gas at an operating temperature and pressure of approximately 1150K (1610 °F) and 1.93 MPa (281 psi)[2]. It is preferred that the piping material be a non-refractory metal in order to minimize material compatibility issues, cost, and uncertainties associated with the use and development of refractory metals. The challenges associated with a refractory metal hot leg pipe are summarized as follows:

- A controlled environment would be necessary for testing refractory metals (i.e. a high purity vacuum) at elevated temperature.
- There would be an increased risk of failure for long term operation of the ground test reactor due to the potential for loss of high purity vacuum (external to the primary pressure boundary).

[2] The range of the operating pressures for the hot leg piping is between 1.38 and 4 MPa (200 and 580 psi). The optimal pressure for the piping has not yet been determined, and it is recognized that the optimal value may have been higher or lower than the nominal operating pressure of 1.93 MPa (281 psi).

- There is a possibility of exposure to space-born chemical contamination from micrometeoroid impacts and gas particles in planetary orbits which are incompatible with refractory metals.
- Surface mission extensibility would be decreased since refractory metals could not be exposed to atmospheric constituents.
- A bimetallic pressure boundary joint would be required between the refractory outer pipe and the cast Ni-base superalloy turbine housing.
- Refractory piping requires either the reactor pressure vessel to be refractory metal or the addition of a second bimetallic pressure boundary joint at the reactor pressure vessel to the hot leg piping interface.

Three wrought high-temperature Ni-base superalloys were identified as candidate materials for the hot leg piping: Inconel 617, Haynes 230, and Nimonic PE-16. Throughout the evaluation presented in Reference 9- 77, Inconel 617 was used as a baseline to provide a common comparison. Although, all three Ni-base superalloys are considered equal candidates.

To maintain sufficient material strength and creep resistance with a reasonable wall thickness, analyses determined that the Ni-base superalloy pressure boundary should be maintained at a maximum of ~900K (1160 °F)[3], which is shown in the material breakpoint curve presented in Section 1.4 of Attachment B to Reference 9- 77. Reducing the pipe wall temperature from 1150K (1610 °F) to 900K (1160 °F) reduces the required pipe wall thickness from 2.9 cm (1.1 in.) to 0.5 cm (0.2 in.). In order to maintain the hot leg piping wall temperature at 900K (1160 °F), several concepts were developed which would reduce the wall temperature by adding additional paths of heat transfer resistance and/or cooling while protecting the pressure boundary from direct contact with the high temperature coolant. The hot leg piping concepts compared included four main variations termed *internally insulated*, *counter flow*, *bypass flow*, and *stagnant gas layer* which are described in Attachment A to Reference 9- 77. The remaining plant piping would have been below ~900K (1160 °F) and, therefore, this piping would not have required high temperature design features.

For the internally insulated piping concept, approximately 15 kW (14.2 BTU/s) total or 2 kW/m (0.6 BTU/s/ft) of heat must be removed from the hot leg piping to maintain an outer wall temperature of 900K (1160 °F), Attachment B to Reference 9- 77. As a result thermal management of the hot leg piping would have been developed as discussed in Section 10.3.

### 9.4.6.2 Baseline - Internally Insulated Hot Leg Piping Concept

In the internally insulated hot leg piping concept shown in Figure 9-43, the hot reactor outlet gas flows within a lined layer of ceramic or metallic insulation.

[3] This is a reference value which could have changes in the future as the design evolved and more materials data become available.

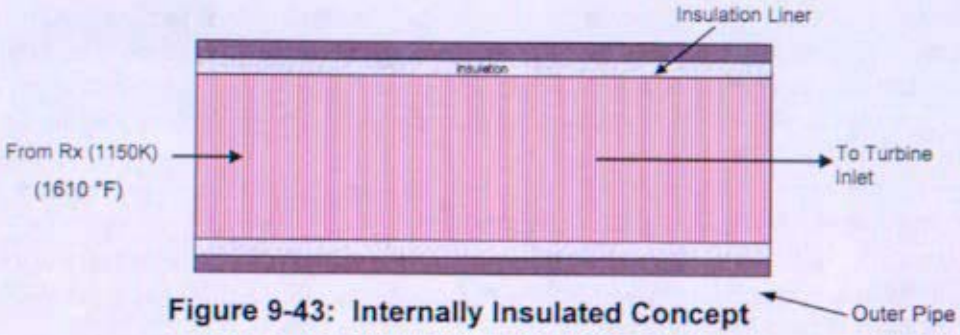



**Figure 9-43: Internally Insulated Concept**

Hydraulic performance, thermal performance, and manufacturability proved to have been the major concept discriminators between the four concepts under comparison. In the end, the internally insulated hot leg piping concept had significant hydraulic advantages over the majority of the other concepts considered. Hydraulic and thermal calculations, based on early arrangement studies, indicated that pressure losses within the SNPP piping systems were significant (see Attachment B to Reference 9- 77). Although the results were based on preliminary piping arrangements, the magnitude of the calculated losses indicate that piping pressure drops would continue to be a major driver in arrangements and system design. The internally insulated concept provided the largest design space, since it resulted in the lowest pressure drop while maintaining the required pressure boundary surface temperature of 900K (1160 °F). More detailed descriptions and performance comparisons of the concepts considered are presented in Attachment A to Reference 9- 77. In addition, Reference 9- 79 provides details on a number of concepts utilized in other high temperature gas reactors in industry which are comparable to the internally insulated, counter flow, bypass flow, and stagnant gas concepts discussed in Reference 9- 77 as well as NR Program experience with high temperature helium test loops.

### 9.4.6.3 Hot Leg Piping Development

The internally insulated Ni-base superalloy hot leg concept presented a number of significant development issues, including: material selection, manufacturability, modeling, testing, and the turbine entrance temperature measurement.

#### 9.4.6.3.1 Material Selection

In order for the internally insulated hot leg piping concept to have adequately performed, hydraulically, thermally, and structurally, appropriate materials must be selected. In addition, the chosen materials must meet all system requirements and constraints. The base case Ni-base superalloy and refractory metal materials proposed for use in the reactor plant were Inconel 617 and Mo-47.5Re, respectively. The final selection for the reactor plant materials would not have occurred for several years due to radiation testing and other long term materials testing; however, preliminary material selection would have been done in the near term to support conceptual design and proof of principal testing. The following sections outline the material development efforts which would have been required for the hot leg piping outer pipe, insulation, and liner.

##### 9.4.6.3.1.1 Outer Pipe

The outer pipe would have been designed to operate at a temperature of 900K (1160 °F) with an internal pressure of 1.93 MPa (280 psi). This restricts the outer pipe to a material that could withstand this temperature and pressure over the mission lifetime of 15 years without failure. The materials

which were being considered for the outer pipe were wrought high temperature Ni-base superalloys. Selection among the three wrought Ni-base superalloys considered (Inconel 617, Haynes 230, and Nimonic PE-16) would have been based on material strength at the expected temperature of 900K (1160 °F); material performance over time; compatibility with the reactor, turbine, and insulation materials; and manufacturability, specifically formability and weldability.

#### 9.4.6.3.1.2 Insulation

Insulation would have been required in the hot leg piping design to maintain the temperature of the pressure boundary (outer pipe). Material selection would have been based on thermal performance over the mission lifetime, corrosion reactions between dissimilar materials (reactor, turbine, outer pipe, liner), purity (the insulation must not significantly off-gas contaminants), manufacturability, and availability.

The maximum operating temperature of the insulation would have been approximately 1150 K (1610 °F). At this temperature, the most promising insulation materials for this application were ceramic or metallic foams. Figure 9-44 depicts Inconel 617 hollow sphere foam.

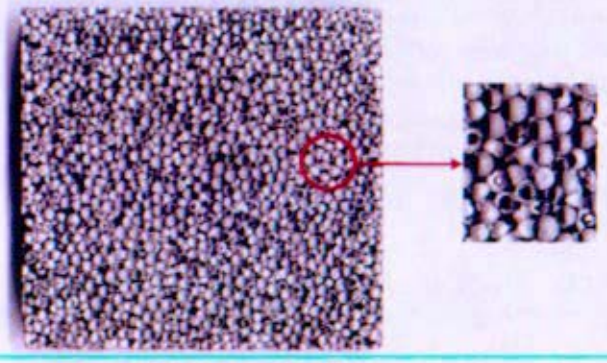


**Figure 9-44: Inconel 617 Hollow Sphere Foam**

Ceramic materials are lightweight and have low thermal conductivity. However, at elevated operating temperatures, radiation contributes significantly to the total heat transfer through the ceramic foam, because most ceramics are partially transparent to radiation. Thus, the heat transfer would be higher than expected based on ceramic foam's room temperature thermal conductivity alone. Cochran *et al* concluded that mullite and alumina foams made from spheres had low thermal conductivity values at low temperatures, see Reference 9- 80. Additional potential problems include material compatibility issues and mechanical properties.

Alternatively, metallic materials have potentially lower heat transfer at operating temperature, since metals are opaque at operating temperature. This opacity prevents thermal radiation from being as significant a factor as with the ceramic insulation. Moreover, metal foams have superior mechanical properties and could be made of similar materials with respect to the piping which may avoid potential compatibility issues.

Preliminary research indicated that foams made of hollow bonded microspheres, approximately three millimeters in diameter, would be a desirable morphology given their closed-cell structure and flexibility of fabrication. These microspheres have been successfully fabricated using a process

consisting of slurry coating. This process is composed of dipping or spraying uniformly sized polystyrene spheres using ceramic oxide or metal-precursor oxides (single element or alloy precursor mixtures), burning out the polystyrene beads, and subsequently sintering the microspheres in a reducing and/or a vacuum atmosphere to fully densify the sphere wall. This results in uniform sized, thin walled, hollow spheres whose interior contains the process gas or a vacuum. Other alternative foams and insulation materials would have been evaluated and tested to determine their suitability for this application. Given the complexity of the foam insulations under consideration, a research plan would have been developed.

#### 9.4.6.3.1.3 Liner

The purpose of the liner is to protect the insulation from the hot gas, which could possibly erode or break up the insulating structure, as well as minimize pressure drop by isolating the coolant from the rough insulation surface. The liner was not intended to act as a pressure boundary. Consequently, the material strength becomes less important, requiring only that the liner material can withstand 1150K (1610 °F) without deformation.

There were two different liner material classes under consideration: a refractory metal alloy and a Ni-base superalloy. The refractory options consist of niobium, tantalum, or molybdenum alloys. The Ni-base superalloy options are the same as those for the outer pipe: Inconel 617, Haynes 230, and Nimonic PE-16. Considerations that would have affected liner selection include the performance of the material at high temperatures, material compatibility with the insulation, reactor core materials, and turbine, as well as the interface with the reactor and turbine.

### 9.4.6.3.2 Manufacturability

The purpose of a manufacturability study would have been to determine the feasibility of acquiring and assembling the hot leg piping. Manufacturability issues for the internally insulated Ni-base superalloy hot leg piping include material availability, piping assembly, and component interfaces, including insulation containment and joining issues.

#### 9.4.6.3.2.1 Material Availability

The foremost concern for manufacturability would have been material availability; procurement of the piping materials would have been required prior to testing and analysis of the hot leg piping concept. After material selection, vendor searches would have commenced, in order to determine the supplier for the piping sections including the Ni-base superalloy outer pipe and either a Ni-base superalloy or refractory metal liner and insulation. Piping and liner thicknesses and diameters would have been selected based on preliminary strength and creep data. Insulation thickness would have been based on preliminary heat transfer and energy balance calculations. Additionally, the favored insulation, sintered hollow metal microspheres, has only been made in small quantities for research purposes. More material development would have been needed before this insulation could have been manufactured in its final form. However, a vendor search would still have been required to establish the lead time and manufacturability concerns for the chosen insulation.

#### 9.4.6.3.2.2 Piping Assembly

The piping assembly would have consisted of straight sections of piping with various bends and intersections as specified in the final SNPP arrangement. The outer pipe was intended to act as the pressure barrier for the hot leg piping. To ensure this, the annular insulation space between the outer

The next best configuration, with respect to response time, would have been thermal contact with a well in the gas stream as shown in Figure 9-48. This concept would not break the pressure boundary, but would still present a flow disruption. This sensor would track the gas temperature closely.

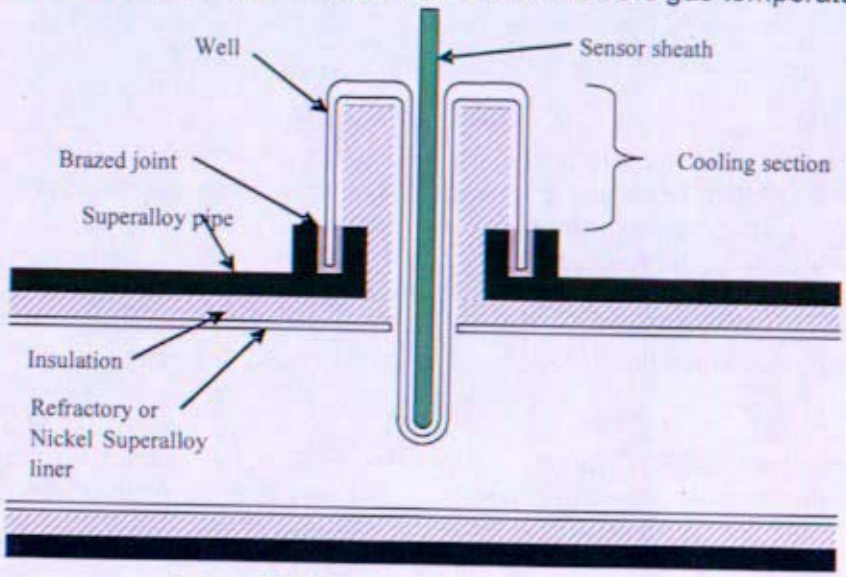



**Figure 9-48: Sensor in Well Concept**

From the standpoint of corrosion, the well material would not be an issue since an insert could be used to block interaction between the sheath and well. Since a superalloy well may not have enough strength in a full $T_{hot}$ well installation, a refractory metal well would have been called for. The well would have to be attached to the pipe in a way that does not transport excessive heat into the pipe. It would also have to penetrate the insulation in a way that does not result in a thermal hot spot on the outer pipe. If a refractory metal was used, it may become brittle at higher temperatures when in contact with oxygen. An advantage of FBG in this configuration would be that no isolation from the pipe or well metal would have been required.

For optical pyrometry, the well would serve as a blackbody hole 1 cm (0.39 in.) in diameter by 5 cm (1.97 in.) deep, the bottom of which would be in close thermal contact with the coolant stream. The minimum wall thickness at the bottom of the blackbody hole would have been set by pressure containment considerations. The exterior surfaces of the well would be refractory metal with a very low vapor pressure that does not form stable oxide layers, such as Mo, Re, or W. The surface could be textured or grown via chemical vapor deposition for increased emissivity. However, a simple polished metal surface likely would suffice. Some recalibration schemes, which require one to reflect a laser pulse off the measurement surface, would prefer a lower emissivity and likely would not benefit from a blackbody hole.

Any cavity with a 5:1 or greater depth to width ratio approaches blackbody emission behavior, especially if the walls have high intrinsic emissivity. However, unit emissivity would not be necessary and may even be disadvantageous due to recalibration options. The other advantage potentially provided by a well would be reduced thermal resistance between the radiating surface and the coolant, and thus, decreased response time in transients. The well would have a quartz window placed above it, in compensation for the weakening of the pressure boundary in that location.

A third option would have been to embed the sensor in the insulation between the two metal layers of the pipe, as shown in Figure 9-49. The sensor would have been attached to the outer wall of the liner in order to be as close to the gas temperature as possible. The advantages of this concept are that the liner remains intact, the flow remains undisturbed, and the sensor tracks the gas temperature closely.

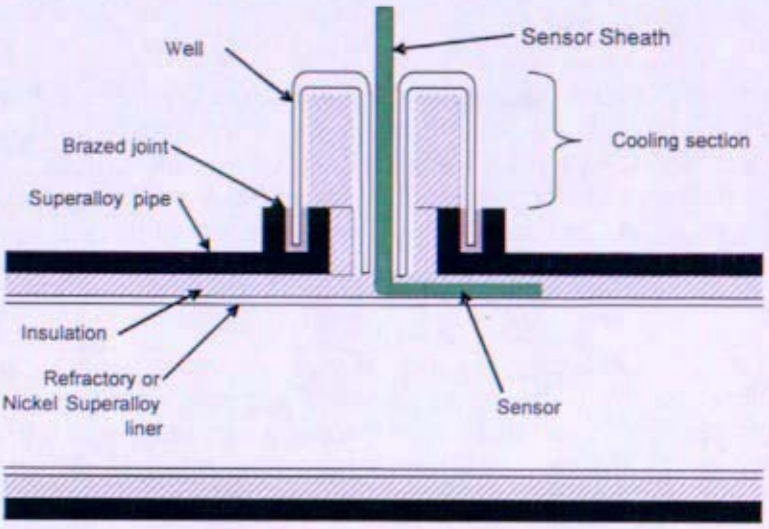



**Figure 9-49: Sensor Embedded in Insulation**

The solution providing the slowest response time but the least invasive configuration would have been attaching the sensor to the outer surface of the outer pipe. For this option, the sensor would be embedded in a material that is mechanically fixed or welded to the pipe, shown in Figure 9-50. If the attachment block was strapped or otherwise mechanically attached to the pipe, it would be made out of a barrier material to prevent interaction between the sensor sheath and pipe. If the block was welded (and thus made of similar material to the pipe) a separate barrier sleeve would be used around the sensor sheath to prevent interactions. The attachment block would be backed with thermal insulation to help it follow the pipe/gas temperature more accurately, but this presents the danger that the superalloy pipe under the block would become overheated.

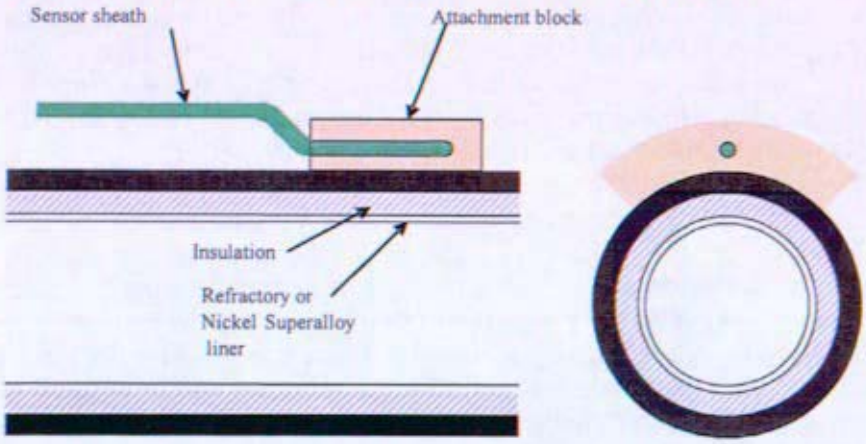



**Figure 9-50: Pipe Wall Attachment Concept**

Attaching the sensor in this way would require a known relationship between the temperature of the gas and the temperature of the outer pipe. The sensors need to see the temperature of the gas or an equivalent temperature from the pipe surface to make an accurate reading. The reason for the hot leg piping concept is to limit the amount of heat transferred between the inner and outer pipe. This would then reduce the amount of heat transported to the sensor causing the sensor temperature to lag behind the gas temperature significantly, see Section 9.4.6.3.5.1 for a quantification of the sensor delay time.

For ultrasonics, the attachment block would become the sensing element, and the wire waveguide would transition to the block with an acoustic horn. This presents an additional challenge in that the block must be attached with enough pressure to maintain good thermal contact with the pipe, but small enough pressure to limit acoustic coupling between the block and the pipe. Depending on the composition of the pipe, a coupling layer may be required which would have slowed the response time of the system. Depending on the system response time, this approach may not be acceptable for responding to changes in plant conditions.

Welding a RTD or thermocouple to the pipe would have been the least desirable option for attaching the sensor. Welding would require that the sheath be made of a material compatible with the pipe and would expose the sensing element to extremely high temperatures that could damage it. The weld joint would provide the lowest thermal time constant between the pipe and sensor but at a high cost. One related method, diffusion bonding the sheath to the attachment block and welding or fixturing that block to the pipe would be an alternative to welding if suitable materials could be identified.

The simplest, and perhaps the best, attachment technique for optical pyrometry would be to probe the infrared radiation directly from the pipe surface, if the time delay associated with transient response was judged to have been acceptable. The fiber optic waveguide would then be fixed to a part of the spacecraft support structure and not in direct contact with the pipe surface. In lieu of this arrangement, the optical fiber would have to have been fastened to the coolant pipe in such a manner as to maintain alignment but not conduct a significant amount of heat. The fixture would have been lightweight, as it would be neither load bearing nor intended to conduct heat; however, it would need to withstand vibration, resist sagging, and be chemically compatible with the pipe wall material for the life of the mission.

The analytical "surface" could be, but would not have been required to be a "blackbody cavity." It would be more advantageous to direct the fiber optic's collecting lens onto a flat surface a few centimeters in diameter. The acceptance angle of the lens would be set quite small, so as to allow for modest changes in alignment due to thermal expansion of components, vibration, or other causes. A small acceptance angle might also reduce concerns regarding stray reflected light, and/or sunlight. Alternatively, a more elaborate fixture would be made light-tight, or the fixture itself would serve as the shadow, preventing direct sunlight from being reflected into the pyrometer.

An additional concept under consideration for the ultrasonic temperature sensor would have been to transmit the ultrasonic signal from a wire waveguide, through an acoustic horn into the inlet wall, and through another acoustic horn into a refractory waveguide in the gas. Figure 9-51 is a diagram of this concept. The internal refractory waveguide is notched since it serves as the sensing element. Optimal performance would have been obtained if the ultrasonic signals transmit through the turbine inlet where no pipe insulation or inner liner would be present since the turbine casing would have been a cast Ni-base superalloy.

The refractory wire inside the pipe would be either centered in the flow stream or attached to the inner liner surface. The wire waveguide would remain acoustically isolated from all other components both inside and outside of the pipe. Materials would have been carefully chosen for the internal waveguide and horn that would allow attachment to the internal surface and would not diffuse into the gas stream at elevated temperatures. The horn and waveguide materials on both sides of the inlet should have similar acoustic impedances to the inlet material in order to minimize reflections at the interfaces.

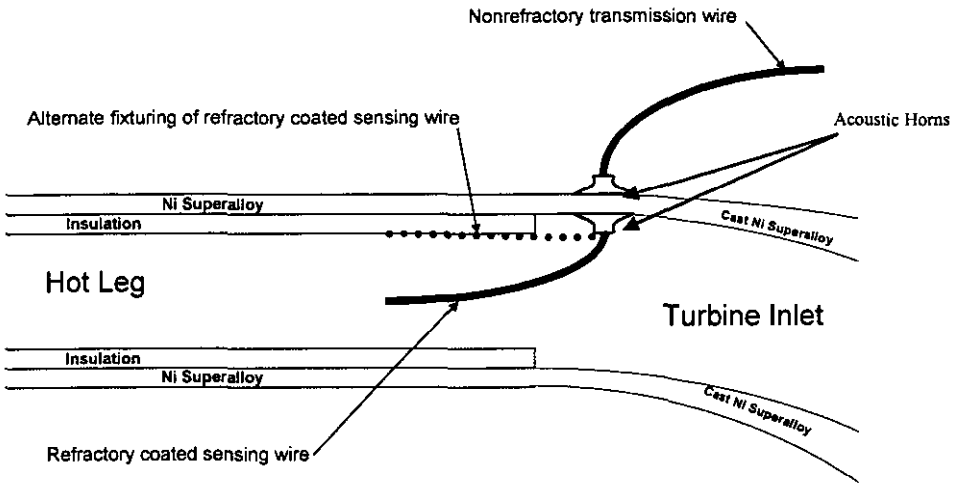



**Figure 9-51: Through Inlet Transmission of Ultrasonic Signal**

Again, the non-invasive requirement for the hot leg temperature sensor would have been balanced with the reactor control response time requirement in order to maximize sensor performance while minimizing the invasiveness of the sensor placement technique.

### 9.4.6.3.5.1 Quantification of Sensor Delay Time

A scoping analysis of the hot leg piping was performed in ABAQUS to quantify the delay time of external temperature measurement, This model made the same material property assumptions, thermal radiation parameters, and wall thicknesses provided in Reference 9- 77. Additionally, an inner wall convective heat transfer coefficient from the reactor plant transient model was assigned to provide the model conditions.

The thermal transient studied was a gas temperature increase from 900 K to 1150 K over a period of 1 second. A plot of the transient temperature response of the inner and outer walls is provided in Figure 9-52. As shown in the plot, there is a very large time lag in temperature response of the outer wall. It takes approximately 5000 seconds (~1.5 hr) for the outer wall to come within 2 degrees of its final steady state temperature. The inner wall responds more rapidly, coming to within 2 degrees of its final steady state value in 415 seconds.

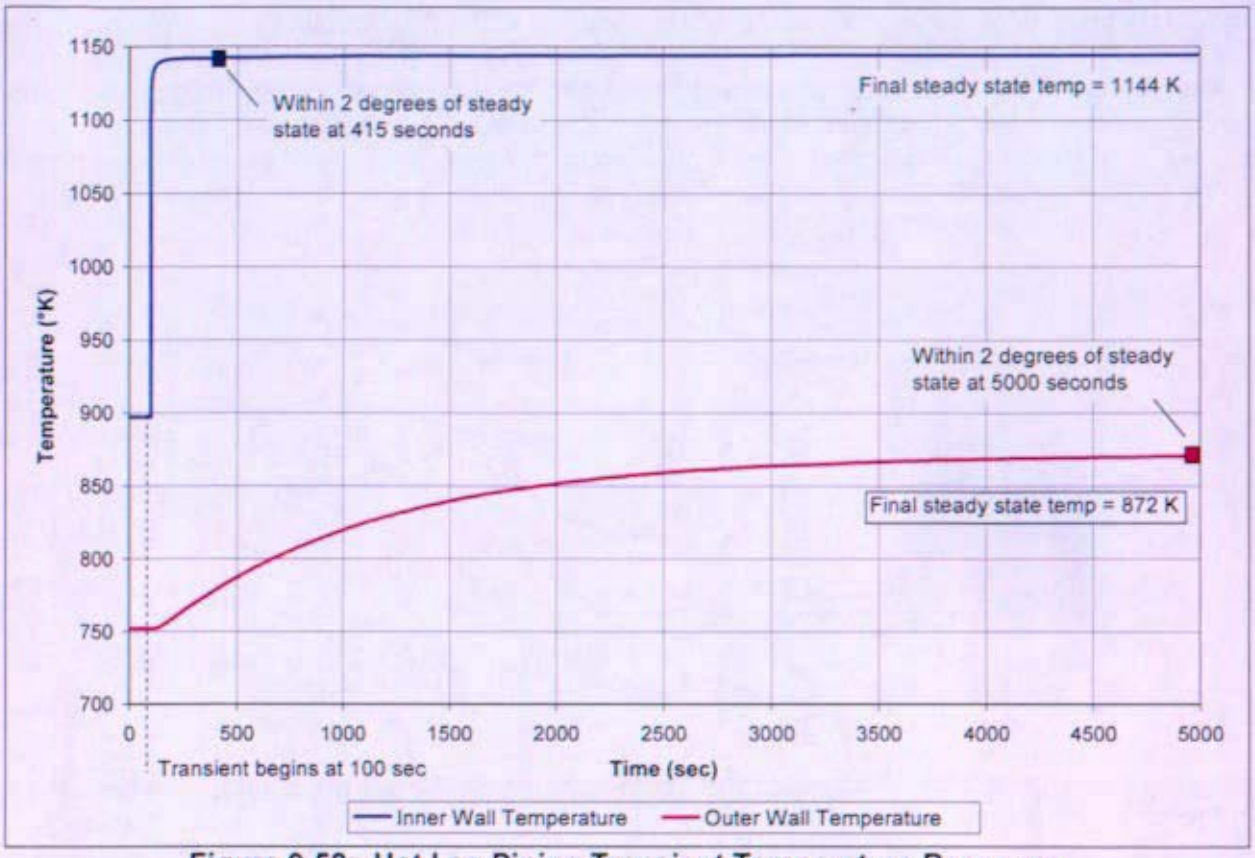



**Figure 9-52: Hot Leg Piping Transient Temperature Response**

The extensive lag time associated with the outer wall transient response demonstrates the infeasibility of using the outer wall temperature as part of the plant control system. Such slow thermal response would severely limit the control systems ability to react to rapidly changing conditions. It is conceivable that for a slow transient, a correlation could be created to account for the expected lag in response, allowing one to calculate the associated gas temperature. However, for fast transients, such as the loss of a Brayton or loss of coolant, the highly non-linear temperature difference between the inner and outer walls would make such a correlation impossible to establish. It is also difficult to conceive of a correlation that would work properly for all types of transients that may be encountered. This analysis would therefore indicate that a more direct gas temperature measurement of the hot leg would be required.

### 9.4.7 Future Development Needs

The internally insulated Ni-base superalloy hot leg concept presented a number of significant development issues including:

- In order for the internally insulated hot leg piping concept to have adequately performed hydraulically, thermally, and structurally, appropriate materials would need to have been selected. In addition, the chosen materials would need to have met all system requirements and constraints. Material development efforts would have been required for outer pipe, insulation, and liner.

- The purpose of a manufacturability study would have been to determine the feasibility of acquiring and assembling the hot leg piping. Manufacturability issues for the internally insulated nickel superalloy hot leg piping include material availability, piping assembly, and component interfaces which include insulation containment and issues associated with joining the hot leg piping to both the turbine inlet and reactor pressure vessel outlet.

- The temperature of the gas in the hot leg piping may have to have been monitored to supply feedback for reactor control. It was desired that the sensors making this measurement be as non-invasive as possible in order to minimize flow disruptions and discontinuities in the pressure boundary. The inherent response times of all sensors which were under consideration for measuring the coolant are on the order of several milliseconds. Placing them outside the gas stream would have introduced a finite delay time for the temperature at the sensor location to reach equilibrium during a transient. This delay time would have depended primarily on the heat transfer properties of the piping configuration and would dominate the response time of the hot leg temperature sensor. The non-invasive requirement for the hot leg temperature sensor must therefore be evaluated against impacts on reactor control response time.

(Intentionally Blank)

## 9.5 Valves

### 9.5.1 Summary and Key Conclusions

Isolation valves and valves that minimize reverse flow may be required if multiple Brayton units or shared heat exchangers are utilized in the Reactor Coolant segment of the Reactor module. During operations with an idle Brayton unit, valves are required to minimize reverse flow through the idle loop (to reduce the amount of gas bypassing the reactor) and to prevent counter rotation of the Brayton unit (a bearing concern). A Brayton unit bypass valve may be needed to terminate an over-speed Brayton unit transient caused by a complete loss of electrical load on an operating Brayton unit.

The number and location of valves will impact system reliability, performance and mass, and could increase system and operational complexity. Large diameter, high temperature, low pressure drop valves may need to be developed that will meet the functional requirements of the Reactor Coolant segment. The number of valves should be minimized (pressure drop concern), valves should be located in portions of the system with the lowest operating temperatures (reliability concerns). The following provides a summary of the main conclusions:

---

- Gas valves which meet the preliminary functional requirements (high temperature, long life, reliable, large diameter) are not available commercially. Testing is needed to better qualify actual requirements. If the preliminary functional requirements cannot be relaxed, the valves would have to be specifically designed, fabricated, and rigorously tested to demonstrate acceptability at the conditions identified for the space reactor coolant segment application.

- Pressure drops across currently available check valves are unacceptably high. A low pressure drop, high temperature gas check valve that operates independent of gravity is needed for this application. An isolation valve with an appropriate control scheme may meet the functional requirements of and be used in place of a check valve.

---

### 9.5.2 Valve Locations

The number, type, function, location, and size of required valves would have ultimately depended on the selected system architecture for the Reactor module Reactor Coolant segment (number of Brayton unit loops and shared components – see Section 3). As stated in Section 6, the current SNPP heat balance assumed a check valve and isolation valve would be included at the compressor outlet. Valve location and function is dependent on the specific plant configuration. Isolation valves may eliminate the need for check valves.

Section 3, System Archetecture, discusses the potential valve locations for several SNPP system architectures under consideration. The valve locations and combinations shown on the schematics do not depict all combinations of valves that could meet the segment functional requirements. Effects on overall system mass and pressure drop must be evaluated.

In general, for multi Brayton unit system architectures, an isolation valve and check valve would be located at the outlet of the compressor (see Figure 9-53). For system architectures that have a spare Brayton unit that can utilize the normally running Brayton unit's gas cooler and recuperator (Section 6.9; 3-2-2 or 2-1-1), then additional isolation valves are needed to isolate the cross strapping.

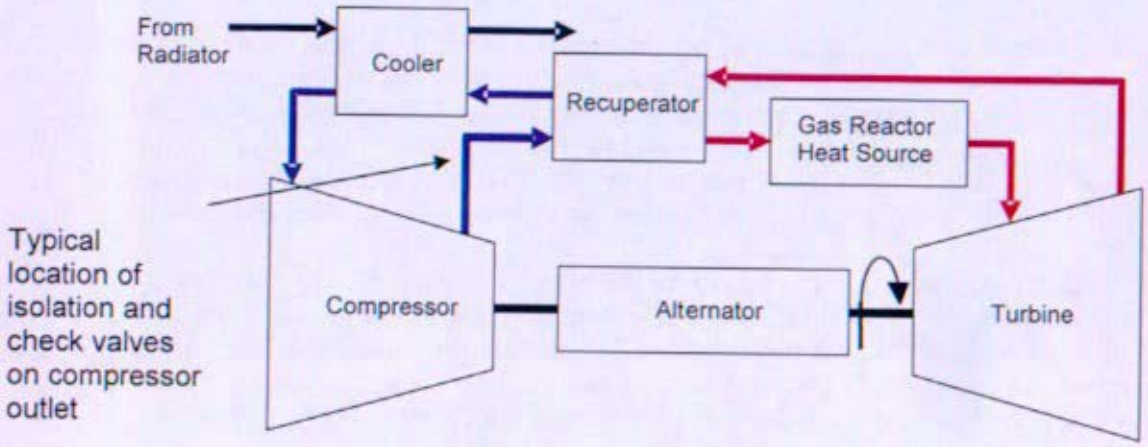



**Figure 9-53: Typical Location of isolation and Check Valves**

### 9.5.3 Valve Function

**Isolation Valves**

The primary function of the isolation valve is to prevent bypass flow through an idle loop or to shut off flow to shutdown an over speeding turbine. An isolation valve may also be utilized to replace a check valve, if the pressure drop across a check valve is detrimental to system performance. Seat leakage specifications have not been determined, but a small amount of bypass flow may be beneficial in maintaining an idle loop warm. A second normally open valve could be installed in series to increase system reliability depending on the criticality of valve operation. There is no intention of designing valves that are capable of "isolating" a gas leak. Carrying sufficient make-up coolant and energy storage to successfully identify a system leak (discern from other causes of pressure changes), shutdown the system (or shift operating components to isolate portions of the system), confirm leak location, un-isolate unaffected components and restart the system is not deemed practical.

Isolation valves being considered include gate valves, butterfly and ball valves. These valve types minimize system pressure drops when in the fully open position. The selected valve would need to be completely sealed from the space environment to prevent system leakage, with an external actuator to position the valve. A redundant actuator could be used to improve valve reliability and both actuators could be operated in parallel to free a sticking valve. The NRPCT does not have experience with solenoid operators on either the size valves proposed for the SNPP or at the temperatures proposed. Both valve performance, with respect to pressure drop (check valves), and valve actuation remain development challenges.

System valves range in sizes from 5 cm or 8 cm (outside diameter piping - the alternator cooling line) to 12 cm or 16 cm (outside diameter piping) for all other locations.

**Check Valves**

The primary function of a check valve is to prevent reverse flow to an idle Brayton unit. As discussed above, an isolation valve with the appropriate control scheme may be utilized to replace a check valve, if the pressure drop across a check valve is detrimental to system performance. Seat leakage specifications have not been determined, but a small amount of bypass flow may be beneficial in maintaining an idle loop warm. Bypass flow would need to be low enough not to overheat components in an idle loop.

Check valves being considered include ball check valves, traditional disc check valves and butterfly valves. These valves need to operate independent of gravity. A ball valve consist of a light ball in a cage that "seats" upon reverse flow.

System valves range in sizes from 12 cm to 16 cm (outside diameter piping).

### 9.5.4 Functional Requirements and Design Challenges

There were many demanding preliminary functional requirements and design issues identified for the various valve applications that would have challenged current commercial, aeronautical and space valve technology. Testing and further system analysis needed to establish minimum functional requirements for these valves.

#### 9.5.4.1 Key Design Goals

The key goals for the valve designs are listed below and discussed in more detail in the following sections.

Required Attributes

- Minimize mass and space envelope.
- Meet system requirements for pressure drop across valve and seat leakage.
- Valve sealed from the external environment to avoid gas leakage to space.
- Check and isolation valve stroke times meet system requirements.
- Construction materials are compatible with piping, system components and system temperature.
- Radiation hardened.
- Launch and operating load certified.

Desired Attributes

- Minimize amperage or power draw of operator.
- Minimize number of weld joints and joint length.
- Minimize seat leakage to the maximum extent practical.

### 9.5.4.2 Service Life

Contingent upon the final mission, the overall service life was identified as a minimum of 12 years to a maximum of 20 year of maintenance free operation while maintaining functional performance and mechanical integrity. Based on pipe size, operational environment, and ambient environment this is a challenging requirement. Typically, a spacecraft design would include redundant valves, operators or systems to ensure that critical functions could be performed for this duration. Redundancy must be balanced against mass and space considerations for the overall spaceship.

### 9.5.4.3 Valve Operational Pressure Drop

The lowest possible pressure drop across each valve is required. As the pressure drop induced by flow through a valve increases, the required reactor thermal rating would also increase. A preliminary design goal of a maximum pressure drop across each valve type was 5 kPa, including the check valve applications. Isolation valves could easily satisfy this requirement since current technical references (e.g. CRANE Technical Paper 410, 1988 Editions and later) cite that gate and ball type isolation valves result in resistances equivalent to equal lengths of pipe L/D ratio of ≤ 8, but it could be a challenge or limitation for check valves.

Preliminary concept and design efforts were terminated prior to obtaining formal vendor input on whether this value was practical or attainable for any or all valve applications. Initial values for valve loss coefficients, k-factors, were calculated in the following subsections. This work was performed in support of heat balance development, Section 6. For loss coefficient impact on plant heat balance, refer to the heat balance section.

#### 9.5.4.3.1 Check Valve Applications

Without gravity, most check valve designs require a mechanical means of closing (e.g., springs). The in-line check type considered viable for space application is designed to be fully opened (backseated) at the minimum flow requirements, and fully closed with sufficient force to achieve seat leakage goals (not yet determined) at all flows less than the minimum required. This is necessary to reduce cycles/fatigue of parts and maximize maintenance free service life. Hence the design is a balance between the spring load required to close versus the flow area of the disc required to fully open. The maximum area of the disc is dependent upon the maximum allowable pressure drop permitted for the application. Based on available vendor data, a minimum resistance value, equal to the length of pipe L/D ratios of around 115, seems achievable for larger diameters of pipe (16 cm and greater) but could be a challenge for the smaller diameter applications.

The optimization of the design most likely would have required further overall plant development and analysis refinement, and a better understanding of expected isolation valve performance in this regard, so that the maximum available pressure loss available for the check valve application is better known.

Other check valve designs were not evaluated.

#### 9.5.4.3.2 Isolation Valve Applications

Valve types with low K values or L/D ratios are required due to the need to minimize pressure drop losses to optimize and maintain system efficiency. Hence, standard globe-type valves, angle or in-line

are not feasible for the application. Gate, Ball and Butterfly valve-types were evaluated for viability in these applications.

#### 9.5.4.3.2.1 Gate Valves

Reference 9- 85 states that the flow resistance of a conventional gate valve will be approximately equal to a length of pipe 13 times the diameter of that pipe (L/D = 13). Reference 9- 85 cites page A-30 of reference 9- 87 for this information. An L/D ratio of 13 with friction factors of 0.0111 to 0.0127 results in a K value range of 0.14 to 0.165 for gate valves in the 4 to 6-inch (10 to 16 cm) sizes. Testing of Naval Nuclear Propulsion Program (NNPP) 4-inch and 6-inch gate valves in clean, smooth stainless steel pipe supports these values.

However, page A-27 of reference 9- 88 shows that $K = 8\ f_t$ for conventional Wedge Disc, Double Disc or Plug Type Gate valves where there is no venturi effect or reducers used ($\beta = 1$, $\theta = 0$) and where $f_t$ = the friction factor at fully turbulent flow. Assuming that $f_t = 0.0111$ to 0.0127 results in a K value range of 0.089 to 0.102 respectivly or a equilvant L/D ratio of 3.

Since reference 9- 88 is primarily based on empirical data, the reduction in hydraulic resistance between the 1965 edition and the 1988 edition must be a reflection of improved design and fabrication practices for conventional gate valves, but the Naval Reactors Prime Contractors Team (NRPCT) cannot substantiate this performance with NNPP data.

#### 9.5.4.3.2.2 Ball Valves

Reference 9- 88 shows that $K = 3\ f_t$ for a Ball Valve with no venturi effect or reducers ($\beta = 1$, $\theta = 0$), and with no shaft in the flow stream (L/D = 3). Reference 9- 84 shows that the typical $C_V$ performance of a 2-inch Full Port Ball Valve used in aerospace applications in the full open position is 440. This resulted in calculated L/D ratios between 6.5 and 8.

Accordingly, NRPCT concludes that an L/D ratio range from 3 to 8 seems practical and achievable for full open ball type Isolation valves in the 5 cm to 16 cm pipe sizes provided they have no shaft in the flow stream.

**Table 9-26: Ball, Butterfly and Check Valve K and L/D Evaluation for Space**

| Valve Type | Nom. Size (in.) | $C_V$ | D [OD(in)] | d [ID(in)] | K | L/D(min) | L/D(max) |
|---|---|---|---|---|---|---|---|
| Aerospace Ball Valve-Full Port | 2 | 440 | 2.375 | 2.067 | 0.084 | 6.6 | 7.6 |
| Aerospace Ball Valve-Reduced Trim | 2 | 131 | 2.375 | 2.067 | 0.948 | 74.6 | 85.4 |
| Aerospace Butterfly - 7% thick | 2 | 333 | 2.375 | 2.067 | 0.147 | 11.5 | 13.2 |
| Aerospace Butterfly - 35% thick | 2 | 154 | 2.375 | 2.067 | 0.686 | 54.0 | 61.8 |
| Aerospace Swing Check | 2 | 76 | 2.375 | 2.067 | 2.816 | 221.7 | 253.7 |
| Aerospace Recess Swing Check | 2 | 123 | 2.375 | 2.067 | 1.075 | 84.6 | 96.9 |
| Enertech DRV-Z Nozzlecheck | 2 | 74 | 2.375 | 1.939 | 2.300 | 181.1 | 207.2 |
| Enertech DRV-Z Nozzlecheck | 3 | 198 | 3.5 | 2.9 | 1.607 | 126.6 | 144.8 |
| Enertech DRV-Z Nozzlecheck | 4 | 237 | 4.5 | 3.826 | 3.399 | 267.6 | 306.2 |
| Enertech DRV-Z Nozzlecheck | 4 | 287 | 4.5 | 3.826 | 2.318 | 182.5 | 208.8 |
| Enertech DRV-Z Nozzlecheck | 6 | 772 | 6.625 | 5.761 | 1.647 | 129.7 | 148.4 |
| Enertech DRV-Z Nozzlecheck | 8 | 1694 | 8.625 | 7.625 | 1.050 | 82.6 | 94.6 |

Notes:

1. $C_V$ data for 2" aerospace valves obtained from Table 3.8.4.2c of Aerospace Fluid Component Designers' Handbook, Volume 1, Revion D; Technical Documentary Report No. RPL-TDR-64-25 dated February 1970.
2. Nominal Valve Size/$C_V$ Information for Enertech valves obtained from technical specification data available on internet for Model DRV-Z Nozzlecheck Valve.
3. Pipe OD data obtained from Table 1 of Machinery's Handbook, Twentieth Edition.
4. d = D - (2 x t) where t for the Enertech Nozzlecheck valves is for Schedule 80 5L, 5LX and XS pipe and for the aerospace valves is for Schedule 40 5L, 5LX, and STD pipe per Table 1 of Machinery's Handbook, Twentieth Edition.
5. $K = 891 \times d^4/C_V^2$; CRANE Technical Paper 410-1988, equation 3-16
6. L/D = K/f, where f = pipe friction factor; CRANE Technical Paper 410-1988, equation 3-15.
7. f = 0.0111 to 0.0127 (per E. Clementoni e-mail dated 10/19/05 2:38 PM).

### 9.5.4.3.2.3 Butterfly Valves

Butterfly valves generally have higher resistance than gate or ball valves due to the need to have the vane and stem in the flow stream. Reference 9- 88 shows $K = 45f_t$ for conventional butterfly valves in the 2-inch to 8-inch range (L/D = 45), which is significantly higher than the L/D ratios of gate and ball valves.

However, there are design features and techniques that can be implemented to lower butterfly valve resistance values. Reference 9- 84 shows that the typical $C_V$ performance for a 2-inch butterfly valve used in aerospace applications with a 7% thick vane is 333 and with a 35% thick vane it is 154, in the full open positions. This results in calculated L/D ratio ranges of 11 to 13 for the 7% thick vane valve and 54 to 62 for the 35% thick vane valve.

### 9.5.4.3.2.4 Summary – Isolation Valves

An L/D ratio of 8 for isolation valve resistance performance as identified in the later issues of CRANE Technical Paper 410 seems reasonable since both gate valve and ball valve current technology can support this level of performance. However, NRPCT cautions using this value as a design value since little-to-no margin will exist between operating performance and design criteria. Additionally, specifying an L/D ratio of 8 as design criteria would preclude the consideration of using butterfly valves in the application.

Accordingly, NRPCT concludes that an L/D ratio of 13 should be used for isolation valve resistance performance assessment because:

1. NRPCT experience supports this level of flow resistance performance for 4-inch and 6-inch gate valves.

2. It would potentially provide some margin between design criteria and operating performance, and, hence, margin to accommodate degradation of performance with time.

3. It may permit the use or consideration of butterfly valves for the application.

### 9.5.4.4 Fluid Leakage to Ambient

All valve applications must 100% hermetically seal the working fluid from the ambient. It was intended to test all valves for leakage-to-ambient using Helium gas as the test fluid and to certify them to the lowest detectable leakage rate capable by technology. Leakage from any component or piping to ambient decreases the amount of available working fluid and reduces system efficiency. Accounting for gross leakage to ambient with a fluid make-up system would add a significant amount of mass and complexity to the spacecraft.

### 9.5.4.5 Valve Seat Leakage

The allowable seat leakage and leakage testing methods for the isolation and check valves were given as preliminary constraints. These limitations were driven by the heat balance for the plant. Testing and additional analysis is needed to determine required seat leakage limits. Some backflow may be beneficial to maintain an idle loop warm.

#### 9.5.4.5.1 Isolation valve applications

Isolation valve seat leakage was required to be minimized to the lowest level practical. This preliminary requirement reduces the impact on the overall system efficiency.

Moreover, significant leakage past a shut isolation valve and check valve into an idle loop could cause reverse rotation of the Brayton unit, which could potentially damage the bearings. The amount of flow or bypass leakage to cause reverse rotation of an idle Brayton unit was not established, nor were means to "lock" the Brayton unit shaft to prevent rotation. However, "soft seat" materials most likely could not be used to accomplish this objective due to the operational and environmental conditions discussed in 9.5.4.6 and 9.5.4.7.

Testing and additional analysis is needed to determine required seat leakage limits.

#### 9.5.4.5.2 Preliminary Check valve Seat Leakage Specification

Check valve seat leakage was required to be minimized to the lowest level practical. A preliminary design goal of a maximum target value was set to no greater than 0.5% of the mass flow rate when tested with helium per an established test method when seated with the baseline system dp of 100 kPa. This requirement may be necessary to minimize the impact on overall system efficiency and prevent reverse rotation of a Brayton, although some allowable leakage may be desirable.

### 9.5.4.6 Operational Conditions/Environment

The valves were required to operate in a high temperature He-Xe inert gas environment where friction, galling and wear (tribophysics) of moving parts are critical concerns. With the current plant design, the fluid temperature for all potential locations except at the turbine outlet ranged from 350K to 600K. The temperature range for the turbine outlet location was identified as 875K to 950K, which posed serious challenges from the materials, operator, design analysis, and long term functionality viewpoints. Placing valves in the locations with the lowest possible operating temperature would help to negate the problem.

The operating pressure range for all locations except at the compressor outlet location ranged from 690 kPa to 2000 kPa. The pressure range for the compressor outlet location was identified as 1350 kPa to 4000 kPa. These operating pressure ranges were not considered to be a significant design challenge.

### 9.5.4.7 Environmental/Ambient Conditions

Some of the main challenges in designing valves for a non-isolated space plant were the ambient conditions. The space environment is harsh in both temperature and radiation. These variables became amplified and more complex when plant temperature fluctuations and reactor radiation were added to the design environment.

#### 9.5.4.7.1 Temperature

The plant design did not include a controlled environment or additional means of temperature control (e.g., cooling/heating jackets or coils) for valve operators. Employing either one of these features would have added mass and complexity to the spaceship. These valves will be housed within the reactor module. Prudent plant arrangement would be employed to minimize the extremes of the environmental temperature range to which the valves would be exposed. For all locations, except the turbine outlet, the ambient temperature range was identified as 200K to 500K. For the turbine outlet location the ambient temperature range was identified as 200K to 650K. These ambient temperature ranges posed challenges for valve operators and could preclude the use of solenoids as operators to actuate valve movement.

#### 9.5.4.7.2 Pressure

The ambient pressure range was identified as 0 to 1 atmosphere. This pressure range was not considered to be a significant design challenge for valves or operators.

#### 9.5.4.7.3 Radiation

It was not intended to include valves and operators in a shielded volume or space other than the reactor shield. Again, prudent plant arrangement would be used to attempt to provide some shielding for the valves and reduce the service life levels. However, preliminary maximum values of 0.833 giga rad ($1 \times 10^9$ rad) and $1 \times 10^{15}$ neutrons/cm$^2$ over a 20 year service life were initially identified for valve applications. Radiation levels of this magnitude would dictate material selections for construction of the valve and operator and mandate that operators and associated electronics be radiation hardened.

### 9.5.4.8 Valve Operators

Since the system would have to be an autonomous design and additional hydraulic or pneumatic subsystems where not planned to be incorporated, any actuation of isolation or throttling valves would have to be via an electromechanical operator from a primary power supply voltage of 28 VDC. As discussed in 9.5.4.7, the environmental/ambient temperature and radiation conditions posed serious challenges for the design and development of any type of operator. The temperature range potentially limited the types of operators that could be used (e.g. solenoids) and the radiation environment mandated that all operators and associated electronics be radiation hardened.

Additionally, for the turbine outlet location, the operational temperature of the fluid would necessitate that the operator be thermally isolated from the working fluid. Another design concern that existed for all types of electromechanical operators was the potting of electrical connections to the operator or the use of canned solenoids actuated across a pressure boundary.

### 9.5.4.9 Materials of Construction

Several challenges existed concerning selection of materials of construction for valves. To minimize corrosion and joining issues, the body/end connections of the valves should be designed and fabricated using the same material as its connecting pipe where practical. This limits the available valve vendors because many commercial vendors are not familiar with analyzing and machining equipment with the materials under consideration under consideration (i.e., titanium or ni-base superalloy).

Furthermore, due to the operational fluid environment, any material in contact with the working fluid must be compatible with the fluid and this environment due to concerns of material corrosion contamination in the fluid stream and the potential to deposit these materials to other parts of the plant and other components. Due to this concern, ambient radiation levels and the ambient and operational temperature ranges, the use of "soft-seat" materials for seating surfaces (non-metallics) to achieve leak tight goals most likely would not be possible, and "hard-seat" materials, such as Stellite or Colmonoy, would be used.

### 9.5.4.10 Design Basis

It was intended to impose Section 3, subsection NH of the ASME Pressure Vessel and Boiler Code (PVBC) for the design of valves and other components in the reactor plant. This design basis is consistent with commercial "N" stamp nuclear components and mandates a thicker wall and hence, heavier components. Hence, the space gas reactor valve applications were potentially a merging of requirements and technologies between commercial nuclear "N" stamp valves and aerospace/space valves.

As a result, the majority of vendors that typically provide valves for aerospace and space applications were not familiar with the design requirements and analysis techniques/codes required by Section 3 of the ASME PVBC. Additionally, not all of the materials considered for the fabrication of space plant components were covered by subsection NH, and for those that were, there was limited high temperature parameters and guidance available (i.e., long term creep).

### 9.5.4.11 Pipe Diameter

Valves used in relatively high temperature, light gas applications exist in the aerospace and space industries, but they are typically used in smaller and even fractional size piping systems (≤ 5 cm [2-inch] pipe diameter). The potential need for larger diameter pipe in the 10 cm to 16 cm outside diameter range was beyond the current commercial, aerospace, and space industrial gas valve applications.

Valve and operator mass increase significantly, and the ability to maintain leak tightness decreases, with increases in pipe and valve size. Use of reducers or venturi body designs to reduce valve/operator size was not considered practical from a hydraulic performance viewpoint.

Larger diameter valves have been used in land based High Temperature Gas Reactor applications, but these were one-of-kind designs where significant effort and cost was expended to design and qualify for the specific application. Additionally, the valves were relatively large and heavy designs with large electro-mechanical operators that could be maintained with periodic maintenance.

Discussions with space valve vendors indicated that the service life requirements combined with the size and performance requirements were a potential merging of satellite (small/fractional valves with long service life) and launch vehicle valve technologies (larger, high performance, but short life cycle valves).

Minimizing pipe size would allow use of existing valve technology, lowered valve design costs, and improved valve seat tightness performance.

### 9.5.4.12 Operational Cycles

Based on the latest operating schemes, it was not expected for any valve to exceed 200 cycles of operation over a 20 year service life. Some cycling may be needed to ensure proper valve operation and to prevent binding.

### 9.5.4.13 Thermal Cycles

The valves will be subjected to thermal cycles and stresses induced by heat-ups and cool-downs. It was anticipated that approximately less than 5 testing and additional analysis is needed to determine required seat leakage limits, 0 heat-up/cool-down cycles would be experienced between the temperature extremes identified in Section 9.5.4.6 for each potential valve application. At least one heat-up cycle will occur from the minimum temperature specified in Section 9.5.4.7.1 to the maximum temperature specified in Section 9.5.4.6 for each potential valve application.

### 9.5.4.14 Launch and Operating Loads

The valves will be subjected random high amplitude vibrations and the associated mechanical loads, and shock loads, during launch into space. They will also be subject to mechanical loads during transport and operation (normal, transient and vibration). All components must be certified to the load ratings as specified in the Environmental Requirements Document, Reference 9- 89.

### 9.5.4.15 Position Indication

Isolation valve applications will require remote position indication to monitor the full open and full closed status of the isolation valves. If throttle valves are needed, they will require remote position indication to monitor the full open, full closed and intermediate positions. The intermediate positions should be monitored to the nearest tenth of a percent. The required input and feedback electronics necessary to accommodate the proposed valve position indication instrumentation needs to be identified by valve vendors.

## 9.5.5 Potential Failure Modes

Additional and new failure modes are introduced with the use of valves that could impact plant performance and operation. Table 9-27 provides an outline of the most probable valve failure modes and potential causes for the SNPP application. Some of these items are discussed in more detail below. These have been accounted for in Section 7 reliability evaluation.

### 9.5.5.1 Seat Leakage

Leakage of fluid past valve seats into an idle Brayton loop could lower the plant efficiency. If significant, this would be accounted for by increased radiator size and mass. In addition, it could cause reverse rotation of an idle Brayton unit and cause damage to the gas foil bearings. Seat leakage specifications have not been determined, but a small amount of bypass flow may be beneficial in maintaining an idle loop warm. Valve body and seat design, valve body and seat materials, and operator load/thrust capability must be sufficient to last the service life in the operational and ambient environments identified. This is so that deformation or deterioration over time does not cause a significant impact to plant efficiency.

Additionally, particulates in the fluid stream must be minimized since it could cause accelerated seat erosion and interference between seating surfaces.

### 9.5.5.2 Leakage to Ambient

Leakage of cooling fluid impacts plant efficiency. Accounting for this leakage with a fluid make-up system adds mass and complexity to the spacecraft. Gross leakage could cause plant failure. The most probable locations for leaks are along valve stems. This can be minimized by utilizing welded valve caps with canned operators.

### 9.5.5.3 Sticking in the Shut Position/Failure to Open

If an isolation valve is stuck in the shut position it would prevent a standby Brayton unit from starting and would preclude bringing the loop on-line. If a check valve stuck in the closed position it would render that loop unusable.

Radiation hardening of the valve/operator and associated electronics, minimizing operator seating force, prudent selection of valve body and seating materials, and locating the valves in the regions of the plant with the lowest system and ambient temperatures would help mitigate this failure mode.

Also, periodically cycling the valves during the service life could help mitigate the mechanical failure mode of sticking between seating surfaces, and would provide assurance that the valve and operator are functioning, although this action would introduce a potential for failure.

### 9.5.5.4 Sticking in the Open Position/Failure to Close or Partial Closure

If an isolation valve stuck in the open position it would preclude the ability to isolate a loop. Also, if it partially closed, it would significantly increase system pressure drop thereby reducing system efficiency and could result in stalling an operating Brayton unit. If a check valve stuck open, it would lower plant efficiency. The potential causes and actions to mitigate this failure mode are consistent with those discussed in 9.5.5.3.

### 9.5.5.5 Wear Particles/Material Introduction to the Fluid

Material contamination into the fluid stream would cause a decrease in system efficiency, and because of the potential to be deposited to other surfaces and components, could increase the likelihood of overall system failure. Both wear of contacting parts and material deterioration due to the high temperature and radiation environment could cause material contamination into the fluid stream.

Prudent design, selection and qualification of materials and valves, radiation hardening of equipment, and locating the valves in the regions of the plant with the lowest system and ambient temperatures would help mitigate this concern. Additionally, minimizing the overall number of cycles of valve operation would minimize mechanical wear, but this action would have to be leveraged with the potential mitigating action discussed in 9.5.5.3 of occasionally cycling valves to assure they are functioning.

### 9.5.5.6 Electromechanical Operation

Failure of the electro-mechanical operator would render the isolation valve inoperable. Depending on the valve design and its position at time of the failure, this could cause the valve to stick shut and fail to open, stick open and fail to close, or stick somewhere in the mid-position. The consequences of these valve failure modes are discussed in 9.5.5.3 and 9.5.5.4.

Degradation of materials used for insulation, windings, coils and other electronic parts due to the radiation and temperature environments could cause electro-mechanical operator failure. Temperature variations also affect winding resistance and could affect operator function. Proper selection of materials, radiation hardening of all electronics, and testing to confirm the appropriate level of radiation hardening would be required to mitigate failure due to the radiation environment.

Proper selection of materials and operator type, and prototypic testing would be required to mitigate failure due to the ambient temperature environment. Prudent plant design and arrangement would provide shielding from radiation sources. Placing valves in locations with some degree of temperature control or reduced variation would also be required to mitigate electro-mechanical operator failure.

## 9.5.6 Summary

The preliminary functional requirements specified for the space gas valves were beyond the current state-of-the-art of commercialand aerospace valve technology. As such, the valves would have to be specifically designed, fabricated, and rigorously tested to demonstrate acceptability at the conditions identified for the space application. Including provisions to ensure that quality is designed and built into the valves, performing prototypic qualification test programs both independently on the valves and as part integrated testing with sub-systems, and prudent plant design and arrangements would all be required to mitigate potential failure modes and assure long-term valve functionality.

The valve equipment would be required to be NASA launch certified, but may also be required to be designed to Section 3, subsection NH of the ASME Pressure Vessel and Boiler Code, which is consistent with commercial nuclear "N" stamp component design requirements. This application also required a merging of space valve technology between that used on launch vehicles with that used in satellites. As such, the NRPCT considered solicitation of concepts from vendors who not only have a history of providing gas valves that have satisfied NASA requirements for launch vehicles and satellites, but who also have experience in supplying valves for commercial or Naval Nuclear applications. Capability to analyze and fabricate valves using the materials required for the SNPP application, in-house Quality Control standards satisfying a minimum of ISO 9000 standards and requirements, and familiarity with NNPP/DOD contracts terms and conditions were additional characteristics used as a criteria for vendor selection for the space gas valve conceptual study.

**Table 9-27: Failure Mode Summary**

| Failure Mode | Consequence | Potential Causes |
|---|---|---|
| Leakage Modes | | |
| -Across seats | -Lowers overall plant efficiency<br>-Could cause reverse rotation of Brayton unit | -Erosion<br>-Corrosion<br>-Scoring, spalling, fretting, wear, cracks<br>-Particle interference<br>-Valve seat distortion<br>-Improperly seating disc (misalignment)<br>-Improper contact or contact loads |
| -Through Wall | -Lowers overall plant output<br>-Could render a loop unusable or cause plant failure | -Erosion<br>-Corrosion<br>-Poor welds<br>-Rupture, cracking, structural failure (due to creep, fatigue, shock, meteorite impact, etc.) |
| Operational Modes | | |
| -Sticks in the Open, Closed or Mid-position. | -An isolation valve sticking open would preclude the ability to isolate a loop<br>-A check valve sticking open would lower overall plant efficiency<br>-An isolation valve sticking shut would prevent a standby Brayton unit from starting and bringing the loop on-line<br>-A check valve sticking shut would render that loop unusable<br>-If either type valve stuck partially open it would lower plant efficiency and could stall an operating Brayton unit | -Mechanical binding of contacting parts due to misalignments, corrosion, galling, chemical precipitation or thermal expansion in either the full open or full closed positions<br>-Differential thermal expansion of seating surfaces<br>-Overtorqued/loaded in the open or closed seats<br>-Operator failure |

| | | |
|---|---|---|
| - Disc/Ball/Vane detachment or stem/attachment part fracture. | -Render any valve type inoperable, and one of the Consequences for sticking open, closed or mid-position would occur | -Structural failure of retaining devices/parts<br>-Fatigue<br>-Overtorquing/Loading<br>-Corrosion |
| - Electro-mechanical Operator Failure | -Render any valve type inoperable, and one of the Consequences for sticking open, closed or mid-position would occur | -Degradation of insulation, coils or windings due to environmental temperatures and exposure to long-term, high levels of radiation<br>-Affect on resistance of coils/windings due to environmental temperature range |

## 9.6 Heat Rejection Segment

### 9.6.1 Summary and Conclusions

The heat rejection segment (HRS) couples with the gas coolers to reject the Brayton energy conversion cycle's waste heat. Northrop Grumman Space Technologies (NGST) was the Project Prometheus design agent for this system with government oversight and concurrence from NASA Glenn. The NRPCT also retained design concurrence for this system from our role as the space nuclear power plant design lead. Reference 9- 89 describes the NGST description of this system prior to project termination.

The heat rejection segment consists of a fluid loop that transports heat from the gas cooler to heat pipe radiator panels rejecting waste heat to the space environment. The base case heat rejection segment architecture at project termination consisted of:

- Two independent heat rejection assemblies
- An operating and redundant high temperature/high pressure heat transport water loops per heat rejection assembly
- Radiator panels consisting of gas loaded Ti/H20 heat pipes with Carbon/Carbon fins joined to the heat transport loops.

Several conclusions can be drawn from conceptual development and segment integration with the Reactor Module. They are:

---

- A large number of heat transport loop coolants were studied during Project Prometheus. Water and Sodium-Potasium alloys (NaK) were the only two coolants that met the functional requirements.

- The interface of this segment to the Reactor Module requires significant integration to resolve key tradroffs for reducing mass, spacecraft size, and project risk. Key integration items include the heat transport loop coolant and ducting materials that interface with the gas cooler, start-up and normal operational stragety, radiator mass versus temperature capability, heat load capability, and size.

- Continued research is required to understand high temperature water heat pipe performance and life capability needed for this application operating at relatively high power throughput and evaporator surface heat flux.

- The design requirements for this heat rejection system needed a significant amount of continued definition by analyzing the space nuclear power plant potential system design events. This would allow for whether protection actions were required to allow for recoverable credible design events scenarios.

---

### 9.6.2 Segment Description

The HRS is primarily constructed from two main assemblies: the heat transport loop assembly, and the radiator panel assembly. The main purpose of both of these assemblies is to transport heat to a high emissive surface that rejects this heat from the power system using thermal radiation to the space environment. Reference 9- 90 provides a comparison of heat rejection segment technologies for low (400-500K) and high (650-800K) heat rejection temperatures. The Brayton cycle integrates most effectively with a low temperature HRS. Figure 9-54 shows the layout and size of a NGST proposed Prometheus Baseline 1 (PB1) design. The heat rejection segment panels are shown as the blue panels on this drawing. This design has 4 deployable boom segments with deployable radiator panels that fold out from the fixed panel connected to the boom.

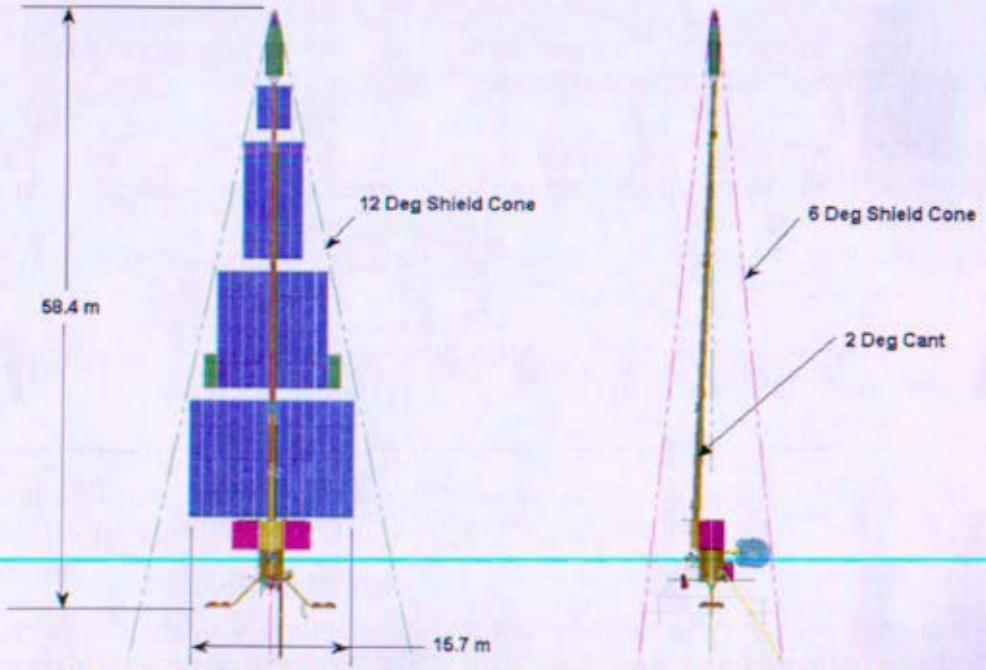



**Figure 9-54: Prometheus Baseline 1 Spacecraft (NGST drawing)**

Figure 9-55 shows a block diagram schematic of a HRS for a system architecture using four Brayton energy conversion loops that are each capable of generating 50% electrical power. This schematic shows the radiator panels as separated in two independent assemblies from the transport loops. The ability to integrate two fluid loops to each radiator panel was a key design element, allowing for redundantly transporting heat to the radiator panel area in the event that one radiator or energy conversion loop fails to continue to transport heat. The radiator panels are constructed of gas loaded water heat pipes and white painted carbon-carbon (C-C) radiator fins.

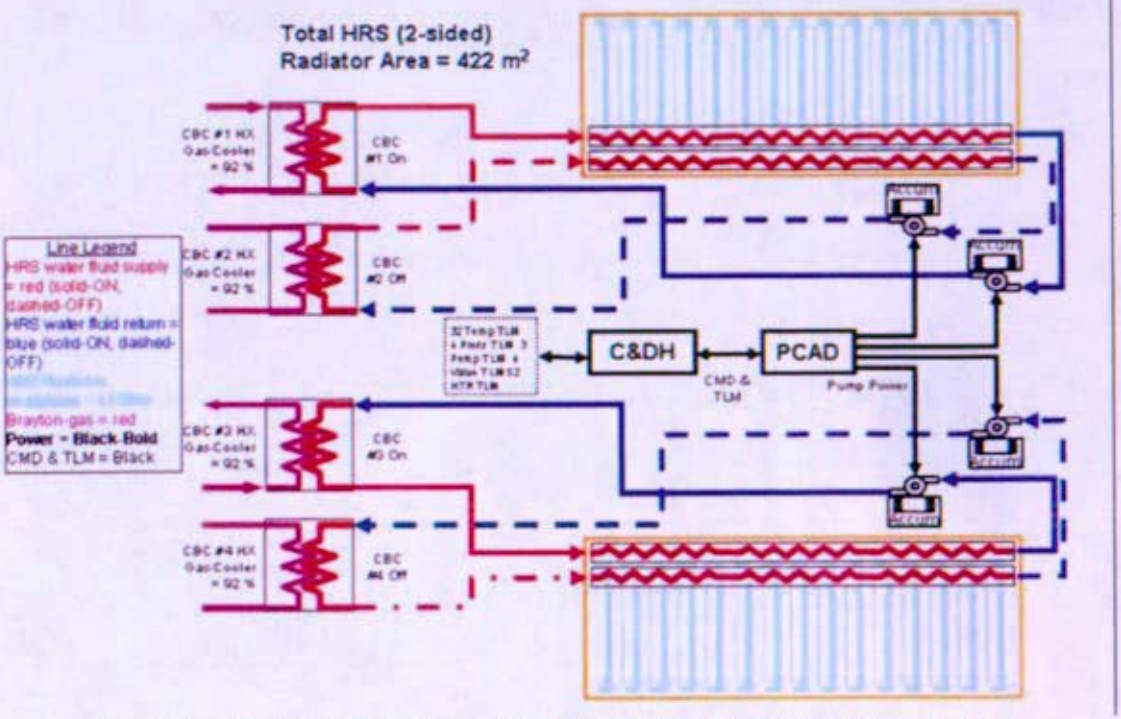



**Figure 9-55: Heat Rejection Segment Schematic (NGST drawing)**

A parameter list (Table 9-28) allows for comparison of heat rejection design parameters and performance variables. The current approach keeps with a 12 degree shield cone half angle and extends the spacecraft boom beyond the baseline of 49 meters when increased radiator area is needed. A rather simplistic method of establishing a fractional active heat rejecting area vs. trapezoidal active area behind the reactor coolant segment has been chosen to be 43 percent. Figure 9-56 shows the boom length for the various cases studied using the fractional method established from the prior PB1 NGST concept design.

Heat balance studies (Section 6) shows reductions in heat rejection segment radiator area with increasing radiator inlet temperature from 505K to 530K. Mass studies have not been performed to establish whether this trade would be an advantage from a mass perspective. Increasing radiator inlet temperature requires additional increases in loop operating pressure to keep the water subcooled, along with increases in the heat pipe diameter and potentially reduced heat pipe spacing to keep below their capillary limit power capability.

## Table 9-28: Heat Rejection Segment Parameter List for Non-Optimized System Arrangements/Heat Balances

| Case | | A | B | C | D | E | F | G | H |
|---|---|---|---|---|---|---|---|---|---|
| Case Description | | 1-1-1 (1 operating at 100% of its capacity) | 2-1-1 (1 operating / 1 BRU spare) | 2-2-2 (2 operating at 100% of their capacity / no BRU spare) | 2-2-2 (2 operating at 50% of their capacity) | 3-3-3 (3 operating at 66% of their capacity) | 3-2-2 ( 2 operating at 100% of their capacity / 1 BRU spare) | 4-2-2 (2 operating at 100% of their capacity / 2 BRU spares) | 4-4-4 (2 operating at 100% of their capacity / 2 BRU spares) |
| Thermal Power | kWth | 560 | 556 | 700 | 750 | 882 | 700 | 767 | 767 |
| Radiator Area w/Margin (required) | $m^2$ | 453 (395) | 449 (392) | 566 (494) | 606 (529) | 713 (623) | 566 (494) | 621 (542) | 621 (542) |
| Number of total loops | | 4 | 4 | 4 | 4 | 3 | 4 | 4 | 4 |
| Number of operating loops at design condition | | 2 | 2 | 2 | 2 | 2 | 2 | 2 | 2 |
| Number of loops in each radiator panel | | 2 | 2 | 2 | 2 | 3 | 2 | 2 | 2 |
| Radiator Inlet Temperature | K | 505 | 505 | 505 | 505 | 505 | 505 | 505 | 505 |
| Radiator Outlet Temperature | K | 379 | 379 | 379 | 379 | 379 | 379 | 379 | 379 |
| Mass Flow Rate (per loop) | kg/s | 0.51 | 0.51 | 0.64 | 0.69 | 0.81 | 0.64 | 0.70 | 0.70 |
| Operating Pressure (at design conditions) | MPa | 7.8 | 7.8 | 7.8 | 7.8 | 7.8 | 7.8 | 7.8 | 7.8 |
| Loop DP | kPa | 365 | 365 | 365 | 365 | 365 | 365 | 365 | 365 |
| Pump Efficiency | % | 30 | 30 | 30 | 30 | 30 | 30 | 30 | 30 |
| Pump Power (per operating loop) | kWe | 0.69 | 0.69 | 0.86 | 0.91 | 1.09 | 0.86 | 0.94 | 0.94 |
| Space Sink Temperature | K | 200 | 200 | 200 | 200 | 200 | 200 | 200 | 200 |
| Radiator Surface Emissivity | % | 90 | 90 | 90 | 90 | 90 | 90 | 90 | 90 |
| Fluid Film Avg. Drop | K | 5 | 5 | 5 | 5 | 5 | 5 | 5 | 5 |

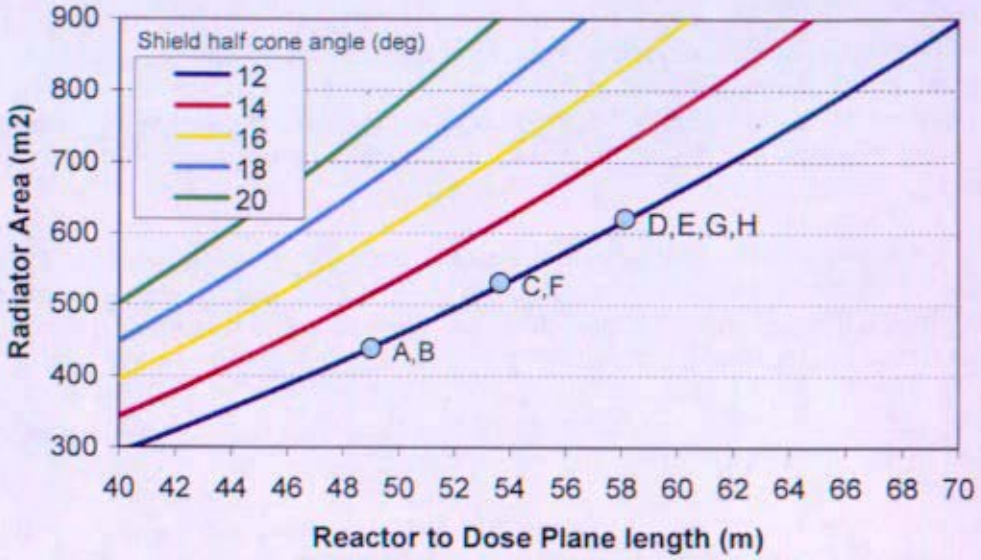



**Figure 9-56: Boom Length vs. Heat Rejection Radiator Area**

### 9.6.2.1 Heat Transport Loop Assembly

The heat transport loop assembly uses a fluid to transport heat from the gas cooler to the radiator panels. This assembly consists of the loop ducts, fluid, pumps, accumulator, valves, trace heaters, insulation, and attachment and deployment hardware that connect these ducts to the boom and radiator panels. A loop flow path through the radiator panels is shown on Figure 9-57. The NRPCT preliminary plant concept architecture has four independent loops, which does not vary with the number of energy conversion components selected, with the exception of the 3-3-3 concept operating all Braytons at part load power capability, which has 3 loops. The interface of the loops to the Brayton gas cooler heat exchanger(s) is presented in Section 9.3 with the failure combinations that would lead to mission success or failure for various failure scenarios.

The heat transport fluid selected for this conceptual design is water. Sodium potassium (NaK) eutectic and other organic fluids have been considered; they provide no clear advantage over water for the current temperatures selected for this system (505-379 K). Reference 9- 89 describes the tradeoff's that were considered in NGST's preliminary coolant decision. The NRPCT concurred with this recommendation with comment (Reference 9- 43). These comments include changes to the design basis for determining the design fluid overpressure, along with performing additional transient modeling simulations, and more detailed uncertainty analysis to better understand the system design. This letter also presented the need for continued technology development on heat pipe performance capability.

The pump complex is comprised of two centrifugal pump-motors with check valves, and a positive displacement accumulator. The design of the centrifugal pump is based on existing designs for the International Space Station (ISS) ammonia and water thermal control systems. The pump is a hermetic caned rotor with no electrical feedthough pressure boundary penetrations. This complex which includes redundant pumps per loop is the current assumption and would need better justification as to the affect on loop reliability prior to establishing this as the design reference.

The loop contains pressure relief valves or burst disks, to prevent over temperature and overpressure of the loop. Additional transient analyses with system control actions and testing would need to be performed to evaluate off nominal scenario's which may lead to needing or not needing pressure/temperature protection. Future testing and analysis would determine the acceptability of boiling within the gas cooler, and the method of integrating a temperature protection system for the heat pipe evaporators.

The heat transport fluid first flows through the radiator closest to the reactor to allow for high velocity flow for good heat transfer in the location transferring the largest quality of heat per unit flow length. Having low flow misdistribution in the parallel ducts of Sections 3 and 4 has been shown to be important to maximize the heat rejected per unit panel area.

The loop ducting current reference material is a titanium alloy construction. A materials trade has not been performed to study mass, corrosion, fouling, and cost.

Flexible ducts to facilitate deployment, multilayer insulation (MLI), survival heaters, and micrometeoroid shields around the ducts are other components of the heat transport loop assembly. The segment is planned to be launched with the loop filled and with survival heaters on to prevent water freezing prior to start-up of the Reactor Module. The survival heaters may need to be activated throughout the mission if a loop is isolated from the heat source (Brayton shutdown) for an extended period of time. The two redundant "idle" loops are envisioned to be heated above freezing by use of the trace heaters, or from a low speed pump operational mode. Another concept that has been considered includes holding the water in a fill tank prior to activation. The trade study results can be found in Reference 9- 89.

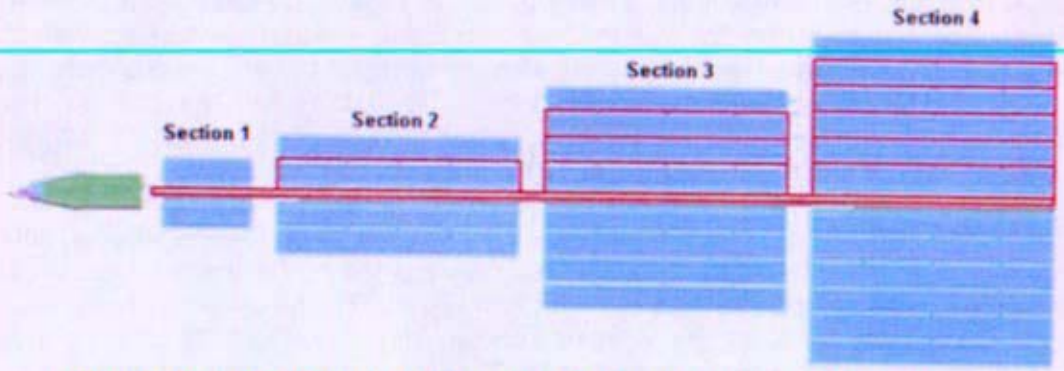



**Figure 9-57: Heat Transport Loop Assembly Layout (NGST drawing)**

### 9.6.2.2 Radiator Panel Assembly

The radiator panel assembly consists of Ti/H20 heat pipes that are connected to carbon-carbon fins through a layer of POCO graphite foam (Figure 9-58). These heat pipes are connected to the heat transport assembly ducts as shown in Figure 9-58 and Figure 9-59. This attachment concept of bending the heat pipes to join the evaporator parallel to the radiator duct while overlapping multiple heat pipes both increases the effective evaporator length thermally connected to the duct. This is another key design element that allows for increased heat pipe evaporator area to transport the heat

into the heat pipe for low maximum (~<10 W/cm$^2$) radial heat flux. The saddle (yellow structure on figures) is constructed of POCO graphite foam brazed to the heat pipes, heat transport loops, and C-C fins. NASA Glenn is working to define braze materials. The fluid in the heat pipes most likely need to be filled after the radiator panel is constructed due to these braze processes occurring at high temperatures. The capability of having a low temperature (<540K) bonding technique would be preferred over brazing if such a material existed that would be thermally stable at 500K for the mission life.

For start-up considerations, the current driving requirements are to keep the fluid in the ducts thawed with requiring less than ~1kWe of survival heater power. If assuming the full heat rejection segment with all radiator area is maintained at 300K (sufficient temp above freezing point 273K), the heater power required for a potential space sink temperature of 200K would be 20% of the normal heat rejected power, or 120kWe. This is clearly unacceptable. Heat pipes with a small amount of non condensable gas (Ar, Ne, Kr), referred to as a gas loaded heat pipes are used to effectively turn off the heat flow through the heat pipes at a determined temperature not allowing the heat rejection panels to be maintained at the loop temperature. This gas loaded heat pipe characteristic allows for low required survival power of ~1kWe needed to maintain the ducts thawed. At this cold "survival" condition, the non condensable gas expands due to the water vapor pressure being very low, preventing the water from being transported to the condenser. The current design allows for the heat pipe to effectively impede transporting heat below 313K, and is effectively fully operational over the entire condenser length above 343K.

The heat pipe technology currently being assumed is based on the NGST slab wick design with radial groves/threads in the evaporator to allow for a "boiling tolerant" wick. This technology has not been fully disclosed to NRPCT, though has been developed specifically for the Prometheus project under IRAD funding. Heat pipe power capability analysis has been performed at KAPL on the NGST heat pipe (Reference
9- 92). This analysis shows that the current 1cm OD heat pipe design barely supports initial normal steady state conditions. Later in the missions life, the radiator may degrade (heat pipe failures, decreases in emissivity) leading to the heat rejection segment operating at a higher temperature, while also needing to transport more power (heat flux) due to the system being less efficient to generate design electrical power. The current performance margin (power, temperature) of this design seems unacceptable.

Figure 9-60 and Figure 9-61 shows the geometry and estimated performance and operating curve of the NGST designed heat pipes. If the heat pipe operated above this capillary limit, the heat pipe evaporator would dry out, stopping heat transport and potentially freezing the water in the condenser of the heat pipe leading to an unrecoverable equipment failure. This could also cascade through the radiator failing all heat pipes. Further plant transient analysis with a detailed gas loaded heat pipe model developed from prototypic heat pipe testing is needed to evaluate this scenario.

The required radiator area is determined from the following key assumptions. The full design heat balance has been selected to have the capability of reaching full electrical power with 5% of the heat pipes failed, and a space effective sink temperature of 200K for the entire radiator surface area. Another 10% margin is built into the radiator to handle uncertainty of the heat load to the heat rejection segment from the energy conversion subsystem.

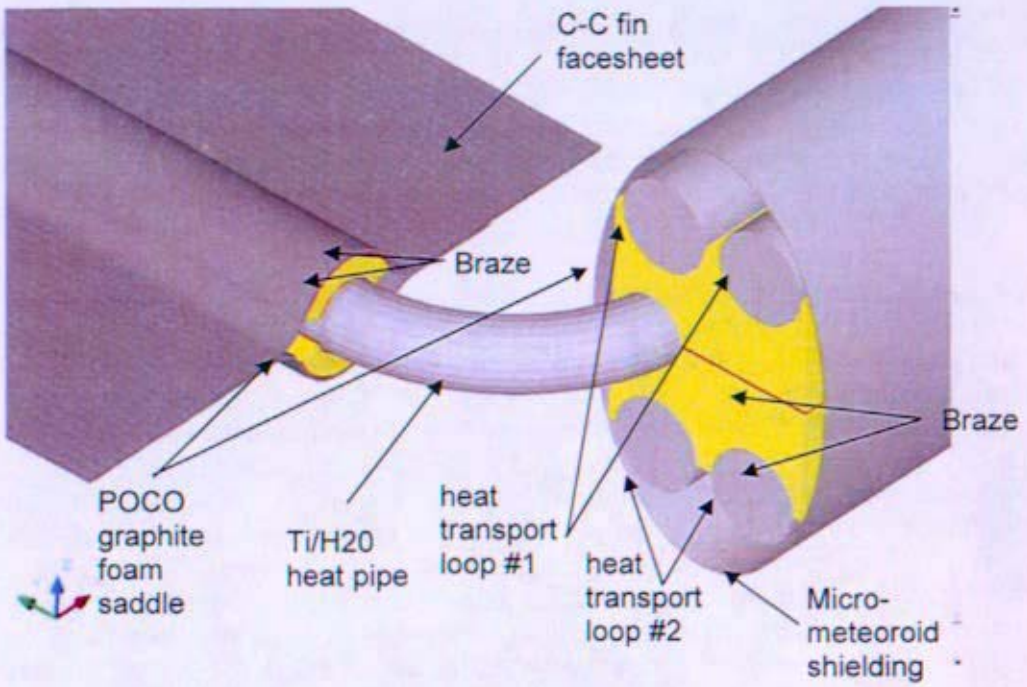



**Figure 9-58: Heat Pipe to Heat Transport Loop Assembly (NASA Glenn drawing)**

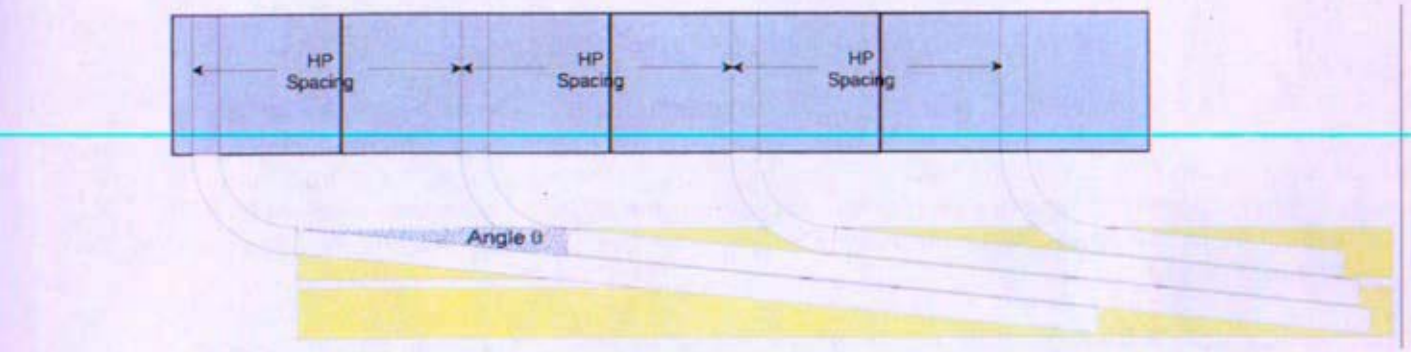



**Figure 9-59: Side View of the Heat Pipe to Heat Transport Loop Assembly (NASA Glenn drawing)**

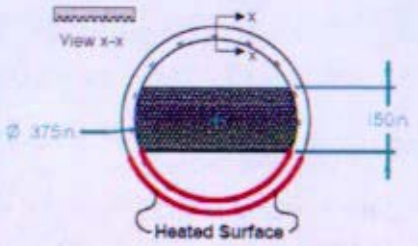



**Figure 9-60: NGST Heat Pipe Geometry**

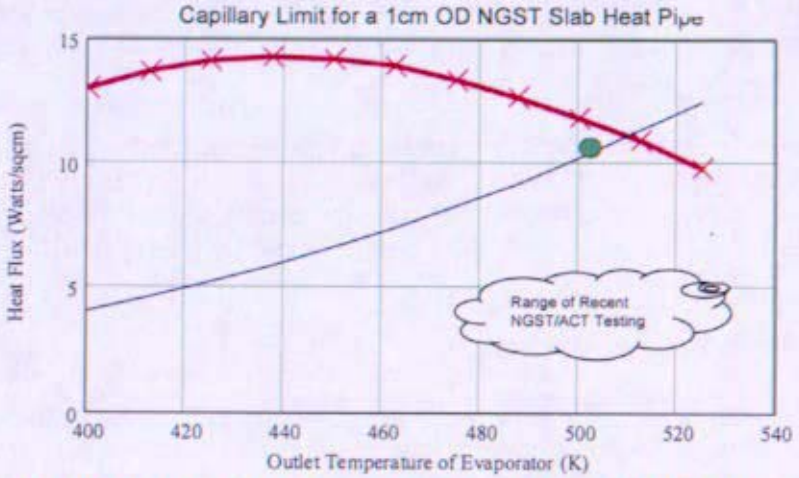



**Figure 9-61: H20 Heat Pipe Performance Capability for NGST Heat Pipe Design**

The C-C fins are designed with sufficient thickness to allow for low thermal resistance (high fin effectiveness) and acceptable structural rigidity. The fins are painted with an inorganic paint (Z93P) that is used to tailor the spectral radiative heat transfer properties of the surface. This paint has a high emissivity of ~90% over the majority of the infrared spectrum to reject heat at low temperatures (<600K) effectively. This paint also has very low absorbance for the solar incident spectrum, higher energy/low wavelength light. This paint prohibits the solar incidence from being absorbed, leading to heating the radiator panels if the spacecraft was perpendicular to the solar vector. Reference 9- 90 shows the effect if paint was not applied and having the radiator face the solar incident light. Applying this paint has a mass penalty, due to the C-C fins having a high normal emissivity over the entire spectrum. The standard application process results in a coating thickness of 0.127 mm (0.005 in), though NGST has applied this paint to large antennas with a coating thickness as thin as 0.051 mm (0.002 in) without impact to the normal emittance or solar absorptance. The current mass calculations assume a thickness of 0.076 mm (0.003 in) on each of the two sides of the radiator. NGST has been working to characterize the process of applying this paint to C-C material, with also including the property variations and bonding integrity over the missions' irradiation, thermal aging, and micrometeoroid damage.

### 9.6.3 Failure Modes

The following failure modes have been considered and are being used to mitigate mission failure.

#### 9.6.3.1 Launch / Deployment Failure Modes

***Launch loads*** – Launch loads could cause a fluid loop rupture if this fluid line was not supported effectively. Greater than two loop failures would lead to mission failure. The launch loads could also debond dissimilar material joints if the bond strength or process control was insufficient. This would lead to degradation of the radiator panel effective surface area, which has limited degradation margin.

***Survival heater failure*** – Loss of electrical power to the heaters, either by loss of the solar power, or energy storage would lead to all loops freezing, and likely mission failure. The survival heater circuits are currently redundant on each loop.

***Panel / Boom Deployment*** – The boom and heat rejection panel deployment is needed prior to reactor start-up. If there are deployment failures, the available heat rejection area would be affected, degrading the maximum heat rejection power capability. The deployment technology envisioned has not been reviewed by the NRPCT team, though had been studied by NGST IRAD funds prior to winning the JIMO Phase A contract.

#### 9.6.3.2 Normal Operation Failure Modes

***Loss of heat transport circulation*** – The loss of fluid circulation could occur from pump failure(s), check valve failure to open/shut on a pump switch, loss of the pump controller(s), fluid leak to space, or from a loss of pressure control (accumulator failure).

***Fluid leak to space*** – Losing fluid inventory to space is the most likely failure mode of the proposed system. Orbital debris and micrometeoroid (MM) damage could fail the relatively large projected area of ducting. The flexible joints are of concern due to the deployment, and added risk due of MM damage from the increased envisioned duct diameter and the potential unavailable use of standard MM shielding. Other sources include having a weld failure, or the pressure relief valves or burst disk failing.

***Accumulator Failure*** – The accumulator includes metal bellows to allow for coolant expansion and a gas charge to maintain system pressure in an appropriate banc. A gas or water leak to space or a gas leak to the fluid would be a failure of this component leading to a loop failure.

***Heat Pipe Failure*** – Failures of the heat pipes can occur from a variety of known modes, and unknown modes. The known failure scenarios for this application include micrometeoroids impacts leading to loss of fluid inventory, materials chemical stability including build up of non condensable gas and mass transport of corrosion products to the evaporator, and an over temperature (over power) leading to evaporator dry out from exceeding the heat pipes capillary limit.

***Over Power – Over Temperature*** - The over temperature scenario as discussed in the previous failure description could lead to a cascading effect that would fail all heat pipes on one side of the full radiator, leading to loss of mission. Heat pipe transient testing in a simulated environment is needed to examine the capability for the heat pipes to reprime once the coolant loop cools. Plant transient

simulations of credible casualty scenario would need to be evaluated to understand the over temperature capability needed to be built into the heat pipe design.

### 9.6.4 Future Development Needs

Continued research is required to understand high temperature water heat pipe performance capability needed for this application operating at relatively high power throughput and evaporator surface heat flux. The heat pipe design had no test data / operating experience that supported the proposed heat pipe design, only analytical performance modeling. A development program by NASA Glenn and NGST was in place to address the technology gaps and develop refined component and system designs that would have lead to a fully functional / reliable system architecture. The design requirements for the heat rejection segment needed a significant amount of continued definition by analyzing the space nuclear power plant potential system design events. This would allow for whether protection actions were required to allow for recoverable credible design events scenarios.

(Intentionally Blank)

## 9.7 Thermal Stress Analysis of Hot Leg Piping

### 9.7.1 Summary and Conclusions

Analyses have been performed of a pre-conceptual four Brayton hot pipe arrangement. The 4-4-4 (revision 2b) system arrangement which is discussed in Section 5.4.6 of this report was analyzed. These analyses assess the effects of piping wall thickness, primary support structure temperature and material, and the piping support flexibility on primary (pressure) and secondary (thermal) stress levels. Piping stress equations and limits are taken from ASME Boiler and Pressure Vessel (B&PV) Code Section III Div I – NB (Reference 9- 70). Inconel 617 was used for the piping material. The material design strength of this material are taken from the Space Structural Design Basis (SSDB) (Reference 9- 47).

A 3D beam element finite element model (FEM) was analyzed using the commercial code ABAQUS to obtain beam section moments at each point in the hot leg piping. These section moments have been used in spreadsheet calculations to determine the primary stress intensity and primary plus secondary stress intensity range values using the ASME NB pipe stress equations.

Important conlusions made from this analysis include:

---

- When the piping is assumed to be rigidly connected to the primary support structure the resulting primary plus secondary stresses are as high as eight times the ASME piping stress limits. In addition, the piping support flexibility study indicates that when the stiffness of the connectors are decreased to obtain a reasonable primary plus secondary stress level during operations, the result is an unsatisfactory low piping natural frequency for launch which is one fourth the acceptable level.

- The flexibility in the secondary support of the piping will not be sufficient in reducing thermal stresses in the hot pipe. The secondary supports are the the structural connections between the primary structure of the spaceship to the components of the reactor plant and energy conversion system. It is likely that the conclusions made in this analysis would be the same for a system with fewer Brayton energy conversion units. A smaller system would likely have shorter piping runs, but the differential thermal expansion between the piping and structure per length of piping would be the same if the operating temperatures are the same. Possible methods of designing around this issue are discussed below. The cold leg piping would have the same issues since the arrangement is similar and expected operating temperature is close to that of the hot pipe. The other piping sections have not been assessed in this analysis.

- The primary support sensitivity studies show that, high thermal stresses in the hot piping cannot be avoided solely through the use of a higher coefficient of thermal expansion (CTE) primary structure material and/or a higher primary support structure temperature.

- A number of stress relief methods could be considered as options but have not been explicitly evaluated, including:

- Floating/Sliding support at the Braytons and energy conversion components which are locked during launch and released during operation may be required. When they are released, the support will allow the approximately 3cm required by the piping expansion.
- Releaseable piping support collars along piping length.
- Use of more flexible piping elements such as Bellowed piping bends or increased numbers of expansion loops and bends in the piping.
- Pre-stressing the piping such that the stresses will be partially relieved during normal operations. This will reduce the stresses at the operating point of higher temperature and lower design strength.

It can be concluded that the structural design and analysis of the piping systems will be a significant effort. Balancing the competing factors of relief of thermal expansion stresses and providing sufficient structural support for launch would be a significant effort. This effort although challenging is not unlike the problems encountered during the design of other power piping systems.

---

### 9.7.2 Analysis Results

A number of sensitivity studies have been performed which investigate the effects of changing piping wall thickness, secondary support stiffness, and structure material and temperature on the ASME primary and primary plus secondary stress limits discussed above. A summary of the cases run is listed in Table 9-32. The primary stresses are only evaluated for the wall thickness study, because the primary stresses are not dependent on the other parameters studied. For all of the results tables, the minimum, average, and maximum stress values refer to the minimum, average, and maximum stress intensity values at all of the element nodes evaluated in the model. It is presented in this form to better comprehend the distribution of stress values.

The base case parameters listed in this table are taken from Reference 9- 93. The base case assumptions are: 900 K piping temperature, 400 K structure temperature, Titanium alloy structure material, piping 8 cm outer diameter (OD) and 0.8 cm wall thickness, and infinitely stiff secondary supports connecting piping to the primary structure. For these base case conditions, the primary stress intensity limit is met, but the primary plus secondary stress intensity range exceeds the the limit by about a factor of eight. The results are shown in Table 9-29, Figure 9-62, and Figure 9-63.

Table 9-29, Figure 9-62, and Figure 9-63 also include the results for the piping wall thickness study. The primary and primary plus secondary stresses decrease with increasing wall thickness. For this study the wall thickness is decreased from 8 cm to 3 cm. The primary stress limit is exceeded for the 3 mm case. The primary plus secondary stress limit is exceeded for all cases. Thinner walls were evaluated in this study because of mass concerns with the piping.

Table 9-30, Figure 9-64, and Figure 9-65 show the results from the primary structure temperature and material study. The base case structure temperature is increased from 400 K to 600 K. The primary plus secondary stresses were reduced to approximately six times the limit. This study was repeated to determine if designing the primary structure with a higher CTE material, Aluminum, improved stresses. Stresses are reduced to approximately three times the limit at a structure temperature of 600 K. The conclusion drawn from this study is that the piping stresses can't be sufficiently reduced

with the use of a high CTE structure material or high structure temperature, if a rigid secondary support is used to support the piping.

Table 9-31 and Figure 9-66 show the results of the secondary support stiffness study. The connector element stiffness supporting the piping is incrementaly decreased from the infinitely stiff (rigid) base case. A target goal of half of the primary + secondary stress limit is set to allow for the uncertainties with the stress ranges seen during the operational transients. These uncertainties in the stress levels are due to uncertainties in the operational transients at this time. To meet this target goal, the connector stiffness needs to be decreased to approximately 1E5 N/m (570 lb/in). Table 9-31 also includes the piping displacement magnitude at the Brayton furthest from the reactor.

**Table 9-29: Wall Thickness Sensitivity: Stress Intensity Results**

| Wall thickness (m) | | 0.003 | 0.004 | 0.006 | 0.008 (base case) |
|---|---|---|---|---|---|
| Primary Stress Intensity | Maximum Stress (Pa) | ***1.8E+08*** | 1.1E+08 | 5.1E+07 | 3.0E+07 |
| | Average Stress (Pa) | 3.6E+07 | 2.4E+07 | 1.3E+07 | 9.0E+06 |
| | Minimum Stress (Pa) | 4.8E+06 | 2.9E+06 | 1.4E+06 | 8.5E+05 |
| | Limit ($1.5S_{mt}$) Stress (Pa) | 1.51E+08 | | | |
| Primary + Secondary Stress Intensity Range | Maximum Stress (Pa) | ***4.8E+09*** | ***3.9E+09*** | ***2.9E+09*** | ***2.4E+09*** |
| | Average Stress (Pa) | ***8.6E+08*** | ***7.2E+08*** | ***5.5E+08*** | ***4.6E+08*** |
| | Minimum Stress (Pa) | 6.2E+07 | 4.8E+07 | 3.5E+07 | 2.8E+07 |
| | Limit ($3S_{mt}$) Stress (Pa) | 3.03E+08 | | | |

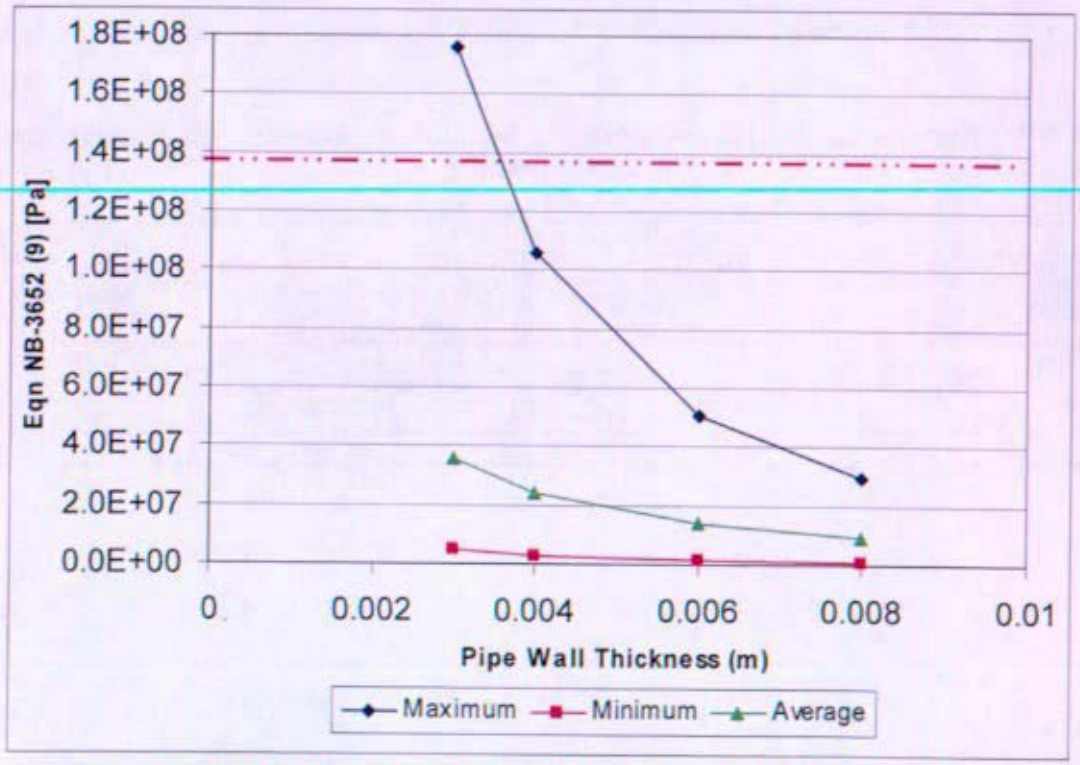



**Figure 9-62: Wall Thickness Sensitivity: Primary Stress Intensity**

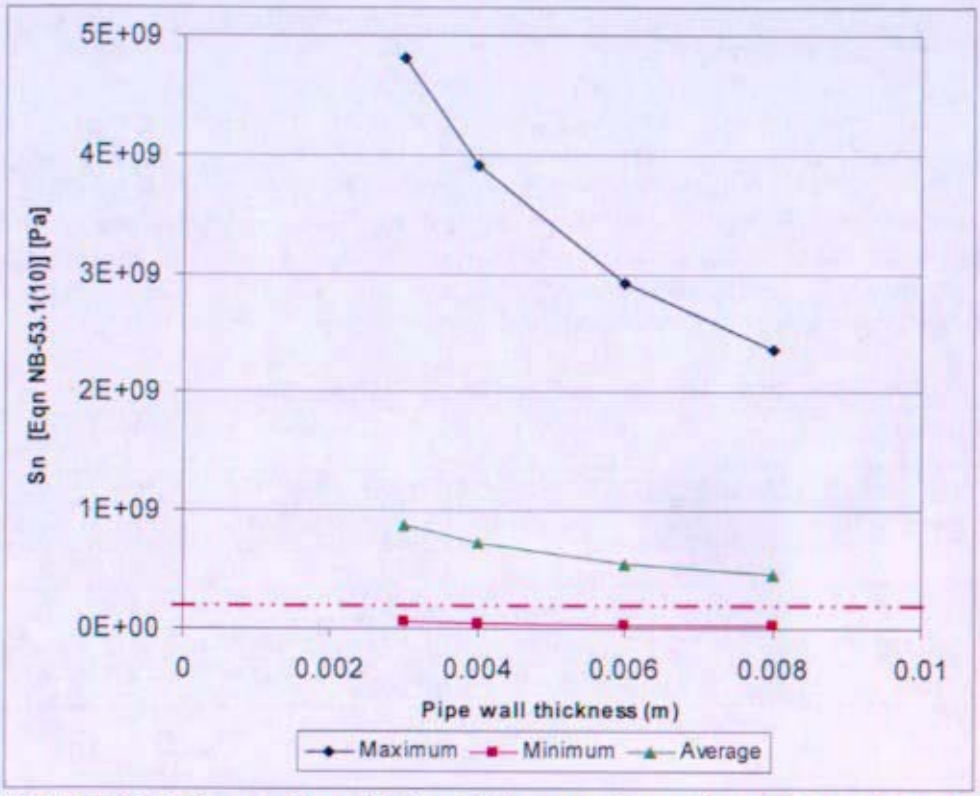



**Figure 9-63: Wall Thickness Sensitivity: Primary + Secondary Stress Intensity Range**

**Table 9-30: Structure Material & Temperature Sensitivity: Primary + Secondary Stress Intensity Results**

| | Structure Temperature (K) | 400 | 500 | 600 |
|---|---|---|---|---|
| Titanium Structure *Ti-6Al-2Sn-4Zr-2Mo-0.1S* | Maximum Stress (Pa) | **2.4E+09** | **2.1E+09** | **1.9E+09** |
| | Average Stress (Pa) | **4.6E+08** | **4.3E+08** | **3.9E+08** |
| | Minimum Stress (Pa) | 2.8E+07 | 2.8E+07 | 2.8E+07 |
| Aluminum Structure *T6-6061* | Maximum Stress (Pa) | ***2.0E+09*** | ***1.5E+09*** | ***9.5E+08*** |
| | Average Stress (Pa) | ***4.1E+08*** | ***3.3E+08*** | 2.5E+08 |
| | Minimum Stress (Pa) | 2.8E+07 | 2.8E+07 | 2.8E+07 |
| | Stress Limit ($3S_m$) (Pa) | 3.03E+08 | | |

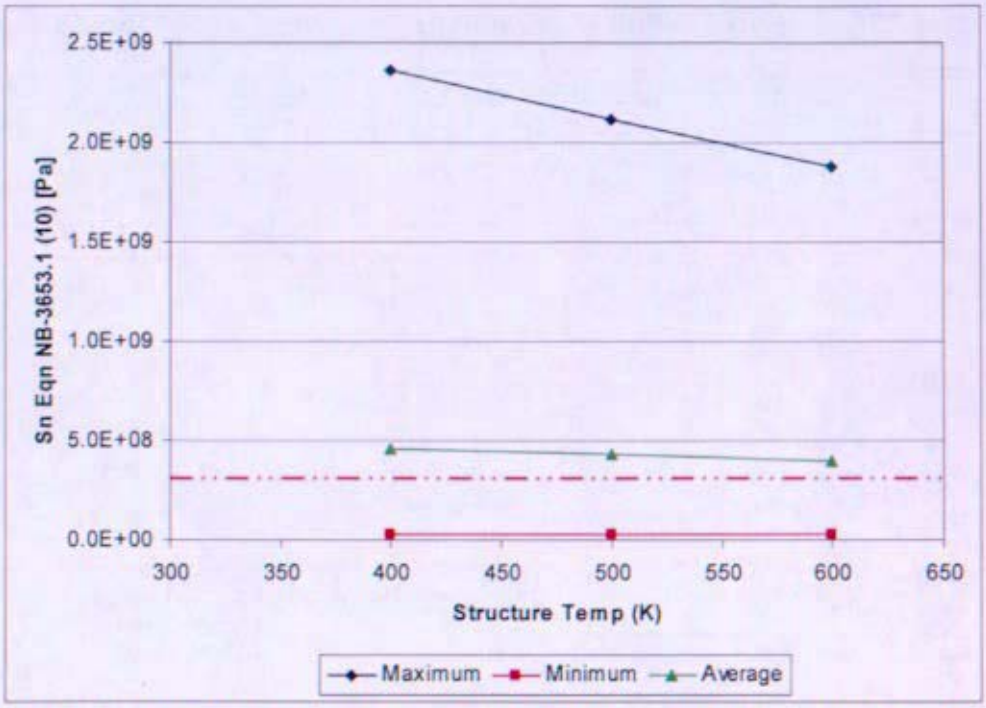



**Figure 9-64: Structure Temperature Sensitivity (Titanium): Primary + Secondary Stress Intensity Range**

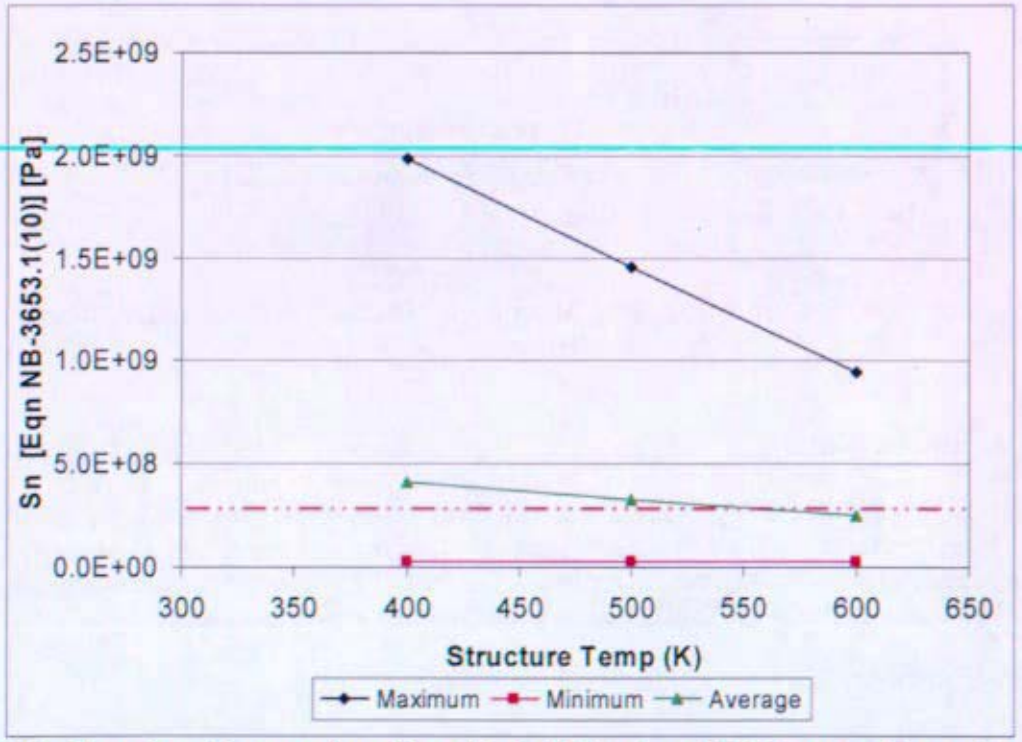



**Figure 9-65: Structure Temperature Sensitivity (Aluminum): Primary + Secondary Stress Intensity Range**

**Table 9-31: Secondary Support Stiffness Sensitivity: Primary + Secondary Stress Intensity Results**

| | Secondary Support Stiffness | Infinite | 1.00E+10 | 1.00E+06 | 1.00E+05 | 1.00E+04 | 1.00E+02 |
|---|---|---|---|---|---|---|---|
| Primary + Secondary Stress Intensity Range | Maximum Stress (Pa) | **2.4E+09** | **2.2E+09** | **8.7E+08** | 1.7E+08 | 7.4E+07 | 7.4E+07 |
| | Average Stress (Pa) | **4.6E+08** | **3.7E+08** | 1.5E+08 | 4.6E+07 | 3.1E+07 | 2.9E+07 |
| | Minimum Stress (Pa) | 2.8E+07 | 3.3E+07 | 2.7E+07 | 2.0E+07 | 2.0E+07 | 2.0E+07 |
| | Stress Limit ($3S_{mt}$) (Pa) | 3.03E+08 | | | | | |
| Piping Displacement At Last Brayton (cm) | | 0.3 | 1.0 | 2.4 | 3.1 | 3.2 | 3.2 |

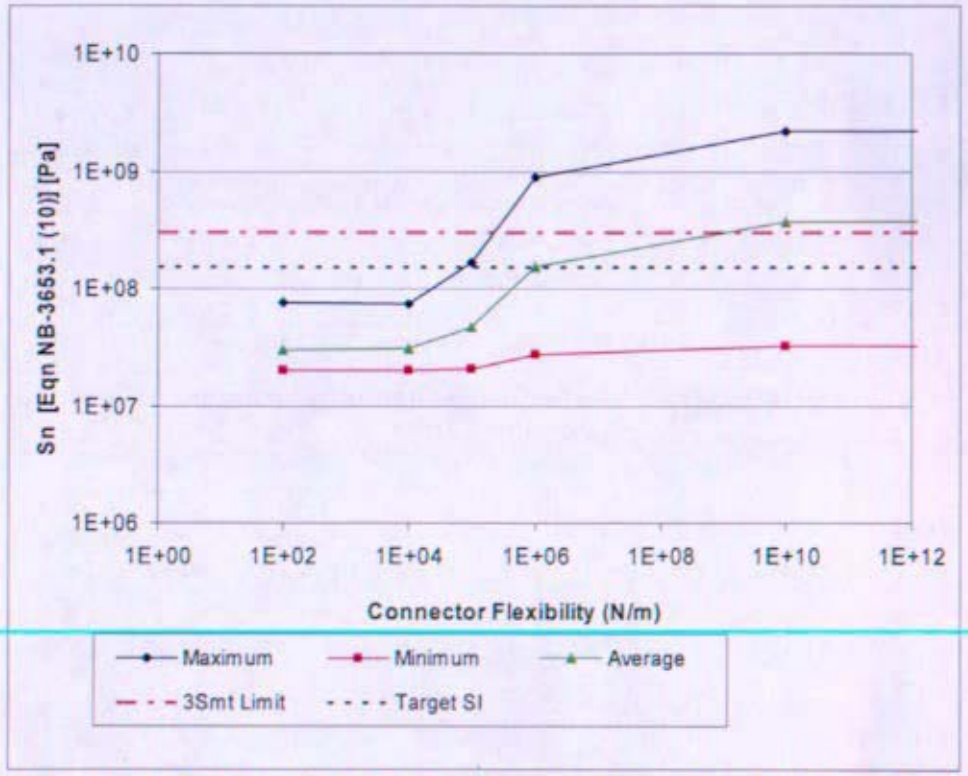



**Figure 9-66: Secondary Support Stiffness Sensitivity: Primary + Secondary Stress Intensity Range**

### 9.7.3 Thermal Stress Model

ABAQUS is used to model the hot leg piping for a four Brayton system. The model is used to determine the stresses due to thermal expansion during plant normal operation. The model is analyzed at the steady state normal operation point. The beam section moment results are used in spreadsheet calculations to perform ASME B&PV code piping stress calculations.

#### 9.7.3.1 Model Geometry

The geometry used for this analysis was taken from the 4:4:4 revision 2b system arrangement. This arrangement is discussed in Section 5.4.6 of this report. The hot leg piping is the only section of piping modeled in this analysis. Figure 9-67 and Figure 9-68 show the CAD representation of the hot leg piping which is modeled in this analysis. The bends and elbows in the arrangement are all 16cm

nominal bend radii. The reactor and Brayton units are shown to aid in the recognition of the arrangement. The model uses units of meters, kg, and seconds.

The stress results would be expected to vary to some extent with changes in the pipe layout or reduction in the quantity of Brayton energy converters. These effects have not been studied, but large reductions in stresses are not likely as a result of changing these parameters since the location of the connections of the piping and components to the structure would not change much and constraints on the routing and mass of the piping limit the layout of the piping.



**Figure 9-67: CAD Representation of Hot Leg Piping with Reactor and Four Brayton units (Side View)**

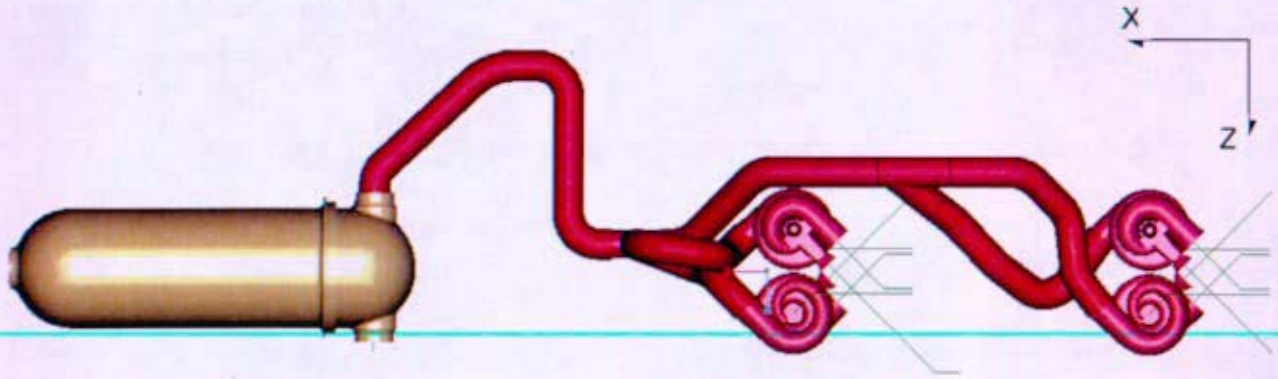



**Figure 9-68: CAD Representation of Hot Leg Piping with Reactor and Four Brayton units (Top View)**

The ABAQUS model utilizes beam elements in 3D space with piping cross sections. Figure 9-69 shows the ABAQUS model. The lines represent the centerline of the cross section of the piping. The piping has a 16 cm outer diameter and a base case of 0.8 cm thickness. Sensitivity studies which vary the thickness of the piping are discussed in section 0.

The ABAQUS model also includes a beam representation of the primary support structure. The general structure used is a square truss structure with four pipe sections. A sketch of the structure is shown in Figure 9-70. This structure is similar to what is discussed and analyzed in the dynamic analyses of the primary support structure in section 10.2.4 of this report.

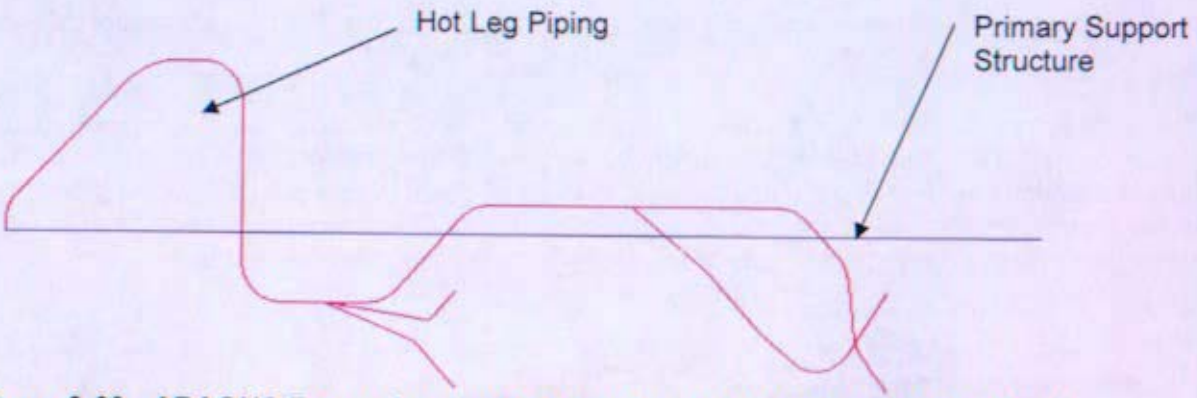



**Figure 9-69: ABAQUS Beam element Model with Primary Structure (Top View)**

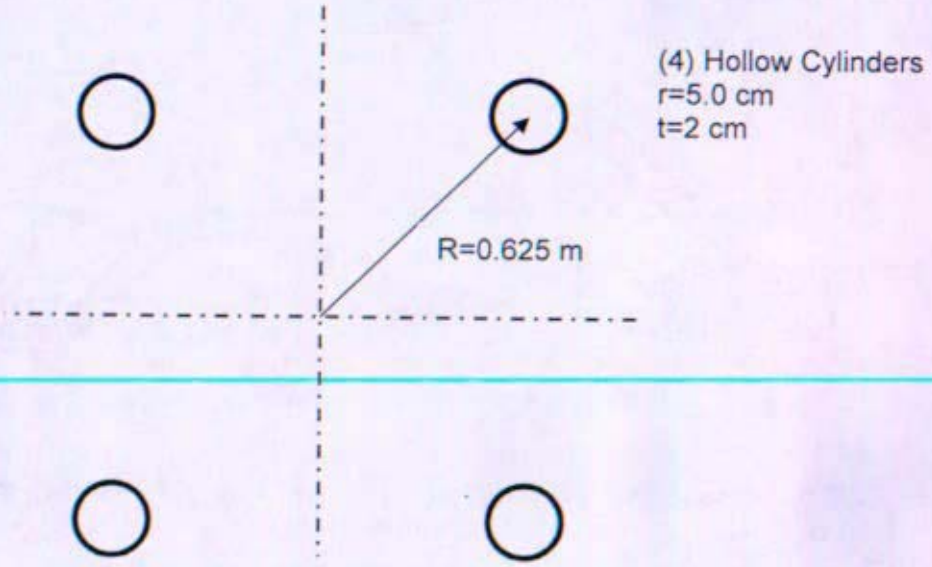



**Figure 9-70: Equivalent Representation of Cross Section of Primary Structure in ABAQUS Model**

### 9.7.3.2 Assumptions

The operating temperature of the piping is assumed to be a constant temperature of 900K. This temperature is the piping wall temperature as stated in Reference 9- 93. There will actually be a slight temperature drop along the length of the piping. This does not affect the conclusions made in this analysis, since the change in temperature is very small compared to the thermal expansion of the pipe from room temperature to 900K.

The stress state used for the evaluation of the primary plus secondary stress intensity range limit is: Stress State at (*Hot steady state normal operation*) – Stress State at (*ambient temperature (293 K) and zero gage pressure*)
The *ambient temperature and zero gage pressure* stress state has no residual stress, therefore this stress range is equivalent to the stress state at *Hot steady state normal operation*. It is known that this transient is not the most severe transient that the piping system will experience. A more extreme stress range would be experienced by the piping after launch but before plant heatup. At that time the temperature would be significantly lower than that assumed in this analysis. This stress state was not analyzed, because there is not enough known about the thermal behavior of the entire system during this time of inoperation. Thus the results in this analysis are considered unconservative, but they do not change the conclusions made in this in this analysis.

The actual piping will have more supports than what is modeled. The resulting stress ranges in this analysis are likely un-conservative because adding additional piping supports will likely increase the thermal expansion stresses. This does not change the conclusions made in this in this analysis.

### 9.7.3.3 Loads and Boundary Conditions

Two load cases are analyzed for each sensitivity study. The first load case is the primary stress case. In this case, a piping internal pressure is applied and no other mechanical or thermal loads are applied. The second load case is the primary plus secondary stress range. The pressure loads and thermal expansion loads result from the pressure and temperatures listed in Table 9-32.

The piping is assumed to have tied displacements and rotations to the structure at the point of connection to the reactor. A number of parameter studies varying the stiffness of these connectors have been performed as shown in Table 9-32. The four locations where the piping is connected to the turbine inlets are modeled using connector elements. This connector stiffness simulates the stiffness of the secondary support and Brayton. The base case assumes a tied connection to the structure (infinite stiffness). The values listed in this table represent the displacement stiffness in the x, y, and z directions in Newtons per meter. The support structure materials refered to in this table are typical support structure materials as discussed in section 10.2.3.3.

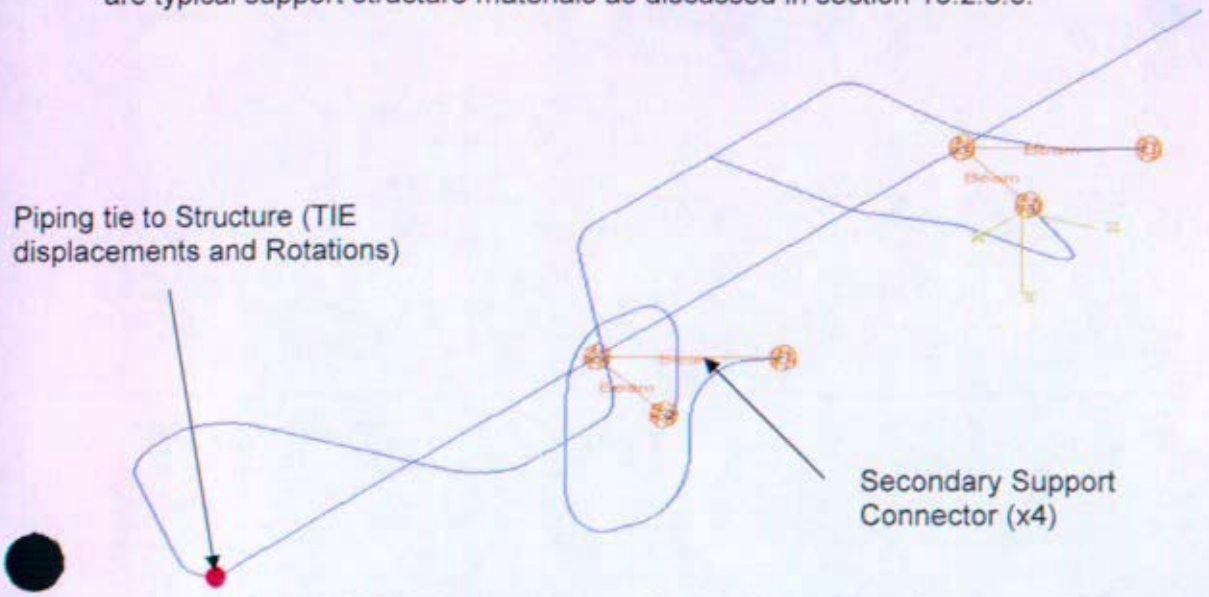



**Figure 9-71: ABAQUS Beam element Model: Secondary Support to Primary Structure Results**

## Table 9-32: Analysis Case Summary[4]

| Case Name | Piping Wall Thickness (mm) | Support Structure Material | Secondary Support Stiffness (N/m) | Load Case | | | | |
|---|---|---|---|---|---|---|---|---|
| | | | | Primary Stress Case | | Primary + Secondary Stress Case | | |
| | | | | Primary Pressure (MPa) | Piping and Structure Temp (K) | Primary Pressure (MPa) | Piping Temp (K) | Structure Temp (K) |
| 8mm (base case) | 8 | Ti-6Al-2Sn-4Zr-2Mo-0.1S | Infinite | 2.0 | 299 | 2.0 | 900 | 400 |
| 3mm | **3** | Ti-6Al-2Sn-4Zr-2Mo-0.1S | Infinite | 2.0 | 299 | 2.0 | 900 | 400 |
| 4mm | **4** | Ti-6Al-2Sn-4Zr-2Mo-0.1S | Infinite | 2.0 | 299 | 2.0 | 900 | 400 |
| 6mm | **6** | Ti-6Al-2Sn-4Zr-2Mo-0.1S | Infinite | 2.0 | 299 | 2.0 | 900 | 400 |
| 8mm 500K | 8 | Ti-6Al-2Sn-4Zr-2Mo-0.1S | Infinite | 2.0 | 299 | 2.0 | 900 | **500** |
| 8mm 600K | 8 | Ti-6Al-2Sn-4Zr-2Mo-0.1S | Infinite | 2.0 | 299 | 2.0 | 900 | **600** |
| 8mm 400K Al | 8 | **T6 Al** | Infinite | 2.0 | 299 | 2.0 | 900 | 400 |
| 8mm 500K Al | 8 | **T6 Al** | Infinite | 2.0 | 299 | 2.0 | 900 | **500** |
| 8mm 600K Al | 8 | **T6 Al** | Infinite | 2.0 | 299 | 2.0 | 900 | **600** |
| 8mm f10 | 8 | Ti-6Al-2Sn-4Zr-2Mo-0.1S | **1.0E10** | 2.0 | 299 | 2.0 | 900 | 400 |
| 8mm f6 | 8 | Ti-6Al-2Sn-4Zr-2Mo-0.1S | **1.0E6** | 2.0 | 299 | 2.0 | 900 | 400 |
| 8mm f5 | 8 | Ti-6Al-2Sn-4Zr-2Mo-0.1S | **1.0E5** | 2.0 | 299 | 2.0 | 900 | 400 |
| 8mm f4 | 8 | **(Ti-6Al-4V)** | **1.0E4** | 2.0 | 299 | 2.0 | 900 | 400 |
| 8mm f2 | 8 | **(Ti-6Al-4V)** | **1.0E2** | 2.0 | 299 | 2.0 | 900 | 400 |
| | | | | | | | | |

[4] Bold parameters are deviations from the base case.

### 9.7.3.4 Material Properties

The following Inconel 617 properties used for the piping analyses are obtained from Reference 9- 93.

| Temperature (K) | Poisson's Ratio | Elastic Modulus (Pa) |
|---|---|---|
| 273 | 0.2991 | 2.12E+11 |
| 373 | 0.2982 | 2.06E+11 |
| 473 | 0.2977 | 2.01E+11 |
| 573 | 0.2974 | 1.95E+11 |
| 673 | 0.2975 | 1.88E+11 |
| 773 | 0.2979 | 1.81E+11 |
| 873 | 0.2988 | 1.73E+11 |
| 973 | 0.3002 | 1.66E+11 |
| 1073 | 0.3022 | 1.57E+11 |
| 1173 | 0.3049 | 1.48E+11 |
| 1273 | 0.3089 | 1.39E+11 |
| 1373 | 0.3133 | 1.29E+11 |

| Density kg/m^3 |
|---|
| 8360 @ 293K |

| Temperature (K) | Coefficient of Thermal Expansion (m/m-K) |
|---|---|
| 373 | 1.16E-05 |
| 473 | 1.26E-05 |
| 573 | 1.31E-05 |
| 673 | 1.36E-05 |
| 773 | 1.39E-05 |
| 873 | 1.40E-05 |
| 973 | 1.48E-05 |
| 1073 | 1.54E-05 |
| 1173 | 1.58E-05 |
| 1273 | 1.63E-05 |

*(Reference Temperature=299K)*

| $S_{mt}$ (GPa) |
|---|
| 100.9 |

The following Ti-6Al-2Sn-4Zr-2Mo-0.1S properties from reference 9- 97 are used in the analyses. These properties are used for the structure material for the Titanium structure analysis cases.
Elastic Properties:

| Temperature (K) | Poisson's Ratio | Elastic Modulus (Pa) |
|---|---|---|
| 293 | 0.33 | 1.18E+11 |
| 922 | 0.33 | 7.4E+10 |

| Density kg/m^3 |
|---|
| 4430 |

| Coefficient of Thermal Expansion (m/m-K) |
|---|
| 9.0E-6 |

*(Reference Temperature=299K)*

The following T6 Aluminum properties have been used for the piping analyses from reference 9- 96. The elastic properties and geometry weren't changed for the T6 Aluminum cases, because the structure stiffness requirements will be independent of material. The only difference for the structure properties is the CTE used for the T6 Al analysis cases is actually that of T6 Aluminum. The CTE of Aluminum is higher than any other primary support structure material possibilities.
Elastic Properties:

| *Temperature (K)* | *Poisson's Ratio* | *Elastic Modulus (Pa)* |
|---|---|---|
| 293 | 0.33 | 1.18E+11 |
| 922 | 0.33 | 7.4E+10 |

| *Density kg/m^3* |
|---|
| 4430 |

| *Coefficient of Thermal Expansion (m/m-K)* |
|---|
| 22.9E-6 |

*(Reference Temperature=299K)*

### 9.7.3.5 Section Moment Calculation

An ABAQUS/Standard job has been run for each analysis case in Table 9-32. For each of these cases a pressure only steady state step and a case at operating temperature and pressure. These two steps correspond to the primary and the primary plus secondary stress cases respectively.

### 9.7.3.6 Method to Evaluate Piping Stress Limits

The SM1, SM2, and SM3 output parameters are section bending moments in the piping about the three local element axes (x, y, & z). These three output parameters are taken from the ABAQUS output and used in ASME B&PV Code Section III Div I – NB piping limit equations. The primary and the primary plus secondary stress range limits are evaluated for this analysis. The primary stress limit is evaluated for the pressure only load case for the cases listed in Table 9-32. The primary plus secondary stress limit is a limit on the stress intensity range. This requires a stress state at each end of the range. The range used to evaluate the limit is:
Stress State at (*Hot steady state normal operation*) - (*cold and zero pressure*)

The limits refer to a design stress intensity value ($S_m$). The time dependent stress intensity limit ($S_{mt}$) at 135,000 hours and 900K is used from reference 9- 94 for this value. The $S_{mt}$ value is 100.6 MPa which results in $1.5S_{mt}$= 151MPa and $3.0S_{mt}$=302MPa. The two limits evaluated from the piping design criteria in subsection NB-3600 are:

Primary stress intensity limit

$$B_1 \frac{PD_o}{2t} + B_2 \frac{D_o}{2I} M_i \le 1.5S_{mt}$$ Equation NB-3652 (9)

Primary plus Secondary Stress intensity Range Limit

$$C_1 \frac{PD_o}{2t} + C_2 \frac{D_o}{2I} M_i + C_3 E_{ab} \times \left| \alpha_a T_a - \alpha_b T_a \right| \le 3S_{mt}$$ Equation NB-3652.1 (10)

The third term of Equation NB-3652.1 (10) corresponds to the stress resulting from a temperature gradient across a gross structural discontinuity. As assumed, the temperature along the hot leg piping is constant with no temperature gradient. Since there are no structural discontinuities with temperature gradients in this segment of piping, the third term in the equation is neglected and then becomes:

$$C_1 \frac{PD_o}{2t} + C_2 \frac{D_o}{2I} M_i \leq 3S_m$$

The $B_1$, and $B_2$ terms are the primary stress indices. $C_1$, and $C_2$ terms are the secondary stress indices. As taken from Table NB-3681(a)-1 of Reference 9- 95, the values for straight sections of piping are as follows: $B_1$=0.5 and $B_2$=$C_1$=$C_2$=1.0. The values for these terms in the sections of curved pipe are calculated from the equations in section NB-3683.7 from Reference 9- 95. The equations are as follows:

$$B_1 = -0.1 + 0.4h \qquad \text{But not <0.0 nor > 0.5}$$

$$B_2 = 1.30 / h^{\frac{2}{3}} \qquad \text{But not <1.0}$$

$$C_1 = \frac{(2R - r_m)}{2(R - r_m)}$$

$$C_2 = 1.95 / h^{\frac{2}{3}} \qquad \text{But not <1.5}$$

Where:

$$h = \frac{t \cdot R}{r_m^{\,2}}$$

$$r_m = \frac{(D_o - t)}{2} \qquad \text{(Mean pipe radius)}$$

R=nominal bend radius

The resulting stress indices for the curved pipe and elbows is shown in Table 9-33.

**Table 9-33: Curved Pipe or Elbows Calculated Stress Indices**

| $D_o$ (cm) | Wall thickness (mm) | Bend Radius (cm) | Stress Indices | | | |
|---|---|---|---|---|---|---|
| | | | $B_1$ | $B_2$ | $C_1$ | $C_2$ |
| 16 | 3 | 16 | 0 | 7.13 | 1.48 | 10.7 |
| 16 | 4 | 16 | 0 | 5.83 | 1.48 | 8.75 |
| 16 | 6 | 16 | 0 | 4.38 | 1.46 | 6.56 |
| 16 | 8 | 16 | 0 | 3.55 | 1.45 | 5.32 |

The terms from the above equations are defined below.
Table 9-34 shows the moment of inertia values used in the calculations.

$$M_i = \sqrt{M_1^{\,2} + M_2^{\,2} + M_3^{\,2}}$$ (Resultant Moment)

$D_o$ = Outer Diameter
t = wall thickness
P = Pressure

$$I = \frac{\pi}{4}\left[\left(\frac{D_0}{2}\right)^4 - \left(\frac{D_0}{2} - t\right)^4\right]$$ (Moment of Inertia)

**Table 9-34: Moment of Inertia for Pipe Sections**

| $D_o$ (cm) | t: Wall thickness (mm) | I: Moment of Inertia (m^4) |
|---|---|---|
| 16 | 3 | 4.58E-06 |
| 16 | 4 | 5.97E-06 |
| 16 | 6 | 8.62E-06 |
| 16 | 8 | 1.11E-05 |

### 9.7.4 Piping Modal Analysis

A modal analysis with the 1E5 N/m connector stiffness case has been run. The model is the same as the *8mm f5* static stress analysis case, except that four 81 kg point masses are added to the ends of the pipe to simulate the mass of the Brayton engines and the analysis type is changed to a frequency extraction. The purpose of performing this calculation is to determine if flexible connectors which provide enough flexibility to make thermal stresses acceptable, can also provide sufficient support during launch.

A target goal of 20 Hz has been identified as a lower limit for the piping natural frequency in order to withstand launch dynamics. The 1st four modes from this analysis are at 5.0 Hz, 5.3 Hz, 13 Hz, and 15.6 Hz. This indicates that with the secondary support stiffness of 1.0E5 N/m, the piping is not sufficiently supported during launch.

Additional dynamic analysis has shown that a connector stiffness of 2.8E6 N/m is sufficient to increase the minimum frequency of the hot leg piping to greater than the 20 Hz threshold.

### 9.7.5 Checks

The displacements shown in Table 9-31 have been compared to the hand calculations in Figure 10-18 of this document. According to both calculations, the piping will expand about 3 cm if unconstrained. This serves an independent confirmation of proper application of the material properties in ABAQUS. Ryan Bechtel (KAPL) has performed an independent verification of the material properties used and the ASME B&PV spreadsheet calculations. Jay Schuren (Bettis) has reviewed the application of material properties, section properties, beam element cross sections, load amplitudes, and boundary conditions in the ABAQUS model.

## 9.8 References

9- 1 NGST Report 04.1F102.JM.006, "Task 2 Conceptual Design Summary Report, Jupiter Icy Moons Orbiter (JIMO) Phase A Study, JPL Contract N. 120530" dated 8/13/2004.

9- 2 Hamilton Sundstrand Letter HSPS2322190600, "Auxiliary and Ground Power Systems Reference Guide"

9- 3 AIResearch Letter APS-5334-R, "Final Report – The Design and Fabrication of the Brayton Rotating Unit (BRU)", dated 3/15/1971

9- 4 NASA TM X-52750, "Experimental Performance of a 2-15 Kilowatt Brayton Power System in the Space Power Facility Using Krypton", dated Jan. 1970

9- 5 NASA TM X-67841, "Post Test Inspection of Three Brayton Rotating Units", dated 8/3/1971

9- 6 NASA CR-159441, "Final Report – Analysis, Design, Fabrication, and Testing of the Mini-Brayton Rotating Unit (MINI-BRU)", dated 10/1978

9- 7 Capstone Letter 4100005, "Model C60 Performance", dated 5/2004

9- 8 AFRL-PR-WP-TR-2005-2018, "Integrated Power Unit (IPU) – Advanced Development Industry Version", dated 12/2004

9- 9 KAPL Letter SPP-67310-0010, "Decision to Competitively Bid Brayton Hardware Development, For NR Information", dated 7/20/2005

9- 10 KAPL Letter SPP-SEC-0033, "September 7th Glenn and Marshall Integration Meeting Minutes", dated 10/17/2005

9- 11 Barrett, M., Performance and Mass Modeling Subtleties in Closed-Brayton-Cycle Space Power Systems, Proc. of 2005 AIAA-IECEC conf.

9- 12 Wood, H. J., "Current Technology of Radial-Inflow Turbines for Compressible Fluids", J. of Eng. For Power. Trans. Am. Soc. Mech. Engrs., 85 (1963)

9- 13 NASA TN D-4384, Rohlik, H. E., "Analytical determination of Radial-Inflow Turbine Design Geometry for Maximum Efficiency", (1968)

9- 14 Kattus, J.R., "Ni-Base Alloys, MAR-M-247", in Aerospace Structural Metals Handbook, Purdue Research Foundation, West Lafayette, Indiana, 1999, Code 4218, pp 1-6

9- 15 NASA TM-2003-212734, Bowman, R., Ritzert, F., Freedman, M., "Evaluation of Candidate Materials for a High Temperature Stirling Converter Heater Head", Materials Division, NASA Glenn Research Center, Cleveland, OH, December 2003

9- 16 NASA TM-2005-214110, T. P. Gabb and J. Gayda, "Tensile and Creep Property Characterization of Potential Brayton Cycle Impeller and Duct Materials"

9- 17 KAPL Letter MDO-723-0051, "Initial Assessment of Joining Challenges for the Prometheus Project", 12/22/2005

9- 18 Bettis Letter B-MT(SPME)-14, "Dissimilar Metal Joining: Cast-to-Wrought Nickel-based Superalloys", dated 2/3/2006

9- 19 Wilson, D.G., "The Design of High-Efficiency Turbo-machinery and Gas Turbines", MIT Press, Cambridge, Massachusetts, 1984

9- 20 NASA TM X-73569, "Inspection of Two Brayton Rotating Units after Extensive Endurance Testing", dated December 1976

9- 21 Gayda, J., Gabb, T.P., "Two Dimensional Viscoelastic Stress Analysis of a Prototypical JIMO Turbine Wheel", NASA/TM-2005-213650, Washington, D.C., June, 2005

9- 22 Japikse, D., Centrifugal Compressor Design and Performance,1996, Concepts ETI Inc.

9- 23 KAPL Letter SPP-67110-005, "Space Nuclear Power Plant Concept Selection, For NR Approval" dated March 4, 2005

9- 24 Halsey, DG, Dolwing, RS, Nguyen, DC, Barrett, MJ, "Closed Brayton Cycle Engine Starter/Generator Cooling, AIAA 2005, IECEC

9- 25 KAPL Letter SPP-SRE-0026, Space Brayton Turboalternator Thermal Management, dated 1/26/06

9- 26 Bettis Letter B-MT(AMSI)-44, "Alternator Electrical Feedthrough Insulator Materials for Project Prometheus", dated January 4, 2006

9- 27 Allied Signal, Garrett Fluid Systems Division, "Space Power 1991 and Beyond" p.49, 1991

9- 28 IEEE Std 493-1997

9- 29 DellaCorte, C., et al. "Evaluation of Advanced Solid Lubricant Coatings for Foil Air Bearings Operating at 25 and 500 °C," NASA/TM-1998-206619, 1998

9- 30 Dellacorte, Christopher, et al. "Advanced Rotor Support Technologies for Closed Brayton Cycle Turbines." 3rd International Energy Conversion Conference. AIAA 2005-5513, Aug. 2005

9- 31 Dellacorte, Christopher and Mark J. Valco. "Load Capacity Estimation of Foil Air Journal Bearings for Oil-Free Turbomachinery Applications." NASA/TM-2000-209782, ARL-TR-2334, Oct. 2000

9- 32 KAPL Letter ARP-NT-0592-JCM, "Space Power Program - KAPL Rotordynamic Analyses of Proposed Closed Cycle Brayton Turboalternator; for Information/Use", dated 1/27/2006

9- 33 DOT/FAA Letter – Technical Standard Order (TSO) C77b, "Gas Turbine Auxiliary Units", dated Dec. 2000

9- 34 Mason, Lee and Barrett, Michael. "Preliminary Comments on Potential Brayton Turboalternator Failure Modes." Feb. 14, 2005

9- 35 KAPL Letter SPP-67210-0001/Bettis Letter B-SE-0037, "PROVIDE NR PROGRAM ASSESSMENT OF THE DESIGN SPACE FOR THE PROMETHEUS 1 PROJECT," Nov. 2004

9- 36 KAPL Letter SPP-SEC-0028, "Documentation of Proposed NASA Glenn Research Center FY06 Workscope," Sep. 2005

9- 37 NGST Report 04.1F102.JM.006, "Task 2 Conceptual Design Summary Report, Jupiter Icy Moons Orbiter (JIMO) Phase A Study, JPL Contract N. 120530" dated 8/13/2004.

9- 38 Bettis Letter B-SE(SPS)FMS-008, "Techincal Documentation in Support of Project Prometheus Plant Pre-Conceptual Design Report", dated 11/11/2005

9- 39 Hamilton Sundstrand, Windsor Locks, CT. "Evaluation of Gas Cooler Materials of Construction and Reliability, Scoping Phase Final Report." Bechtel Bettis Purchase Order #3007352, August 30, 2005

9- 40 Holtec International, Marlton, NJ. "Gas Cooler Materials of Construction and Reliability for Space Based Nuclear Power Plant." Bechtel Bettis Purchase Order, Holtec Report HI-2053418, Project 1489, September, 2005.

9- 41 Honeywell, Torrance, CA. "Nuclear Propulsion System Gas Cooler Scoping Phase Design Study." Bechtel Bettis Purchase Order #3007132, Honeywell Report 05-73670, October 18, 2005.

9- 42 Heatric, Dorset, UK "Design Study Phase I - Final Report" Heatric Report DR1-H1026, dated September 1, 2005

9- 43 SPP-67310-0009, "NRPCT Comments on the use of a Water Heat Rejection Loop", dated 6/17/2005

9- 44 Barrett, M. J. and Reid, B. M. "System mass variation and entropy generation in 100-kWe closed-Brayton-cycle space power systems", Proceedings of Space Technology and Applications International Forum (STAIF – 2004), pp. 445 – 452, 2004.

9- 45 KAPL letter MDO-723-0051, "Initial Assessment of Joining Challenges for the Prometheus Project/Specimen Matrix", TBI.

9- 46 Killackey, J. J. et al, "Brayton-Cycle Heat Exchanger Technology Program", prepared by AiResearch Manufacturing Company of California, NASA Contractor Report 135158, NASA Lewis Research Center, August 1976.

9- 47 KAPL Letter SPP-67320-0002, "Preliminary Space Structural Design Basis Development (SSDB), for NR Action", dated June 30, 2005.

9- 48 KAPL Letter SPP-67310-0010, "Decision to Competitively Bid Brayton Hardware Development, For NR Information", dated 7/20/2005

9- 49 Killackey, J. J. et. al, "Design and Fabrication of the Mini-Brayton Recuperator Final Report", prepared by AiResearch Manufacturing Company of California, NASA Contractor Report 159429, NASA Lewis Research Center, April 1978.

9- 50 Graham, L.W.; *Journal of Nuclear Materials*, vol. 171, pp. 76-83, 1990.

9- 51 Warren, M.R.; *High Temperature Technology*, vol. 4, pp. 119-130, 1986.

9- 52 Massalski, T.B., ed.; *Binary Alloy Phase Diagrams, 2nd ed.*, ASM International, 1990.

9- 53 Smithells, C.J.; *Metals Reference Book, 4th ed.*, Plenum Publishing Corporation, 1967.

9- 54 NGST Report 04.1F102.JM.006, "Task 2 Conceptual Design Summary Report, Jupiter Icy Moons Orbiter (JIMO) Phase A Study, JPL Contract N. 120530" dated 8/13/2004.

9- 55 Dunn, J. H. "Inspection of Two Brayton Rotating Units After Extensive Endurance Testing", NASA Technical Memorandum X-73569, NASA Glenn Research Center, December 1976.

9- 56 Taylor, M. F. et al., "Internal forced convection to low-Prandtl-number gas mixtures", International Journal of Heat and Mass Transfer, Vol. 31, pp. 13 – 25, 1988.

9- 57 Manglik, R. M. and Bergles, A. E. "Heat Transfer and Pressure Drop Correlations for the Rectangular Offset Strip Fin Compact Heat Exchanger", Experimental Thermal and Fluid Science, pp. 171 – 180.

9- 58 McEligot, D. M. et al. "Convective heat transfer and pressure drop in low-Prandtl-number gas mixtures" Idaho National Laboratory. DOE Office of Naval Reactors Contract DE-AC07-05ID14517, September 26, 2005.

9- 59 Von Arx, A. V. and Ceyhan, I. "Laminar Heat Transfer for Low Prandtl Number Gases", 8th Symposium Space Nuclear Power Systems, Albuquerque, AIP Conference Proceeding, pp. 719 – 722, 1991.

9- 60 Kays, W. M. and London, A. L. *Compact Heat Exchangers Third Edition*. New York, McGraw-Hill, 1984.

9- 61 SPP-SEC-0038, "Mini-Brayton Rotating Unit Recuperator Flow Maldistribution Study for Space Energy Conversion", TBI

9- 62 KAPL Letter SPP-67110-005, "Space Nuclear Power Plant Concept Selection, For NR Approval" dated March 4, 2005.

9- 63 R. K. Shah, R. K. and Sekulic, D. P., *Fundamentals of Heat Exchanger Design*. New York, John Wiley, 2003.

9- 64 Johnson, P. K. and Mason, L. S. "Design and Off-Design Performance of 100 kWe-Class Brayton Power Conversion Systems." Proceedings of Space Technology and Applications International Forum (STAIF – 2005), pp. 711 – 718, 2005.

9- 65 Hamilton Sundstrand, Windsor Locks, CT. "Evaluation of Gas Cooler Materials of Construction and Reliability." Bechtel Bettis Purchase Order #3007352, July 13, 2005.

9- 66 Staudt, J. E., "Design Study of an MGR Direct Brayton-Cycle Power Plant" PHD Thesis, Massachusetts Institute of Technology, May 1987.

9- 67 Garrett Fluid Systems, *Space Power 1991 and Beyond*, 1991.

9- 68 AiResearch Manufacturing Company of Arizona, "Executive Summary – Mini-BRU/BIPS 1300 $W_e$ Dynamic Power Conversion System Development", NASA Contractor Report 159440, NASA Glenn Research Center, Cleveland, OH, October 1978.

9- 69 Nayyar, Piping Handbook: Sixth Edition, McGraw-Hill, Inc. (1992)

9- 70 ASME Boiler and Pressure Vessel Code, Section III, Division I, Articles NB-3000 and NH-3000, (2004)

9- 71 Attachment (A) to SPP-67320-0002, Preliminary Space Structural Design Basis for Pre-Conceptual Design, dated June 30, 2005.

9- 72 Bird, Lightfoot, and Stewart, *Transport Phenomena: Second Edition*, John Wiley & Sons, Inc. (2002)

9- 73 Barenblatt, G.I., *Scaling, Self-Similarity, and Intermediate Asymptotics*, Cambridge University Press (1996), §10.2

9- 74 ESDU, Engineering Sciences Data, *Fluid Mechanics: Internal Flow Sub-Series Volume 2*, (1990)

9- 75 NR:RE:KHDonald l#05-01228, Space Nuclear Power- Reactor Coolant and Power Conversion System Concept – Approval of, Dated April 20, 2005.

9- 76 B-SE-077, Space Nuclear Power Plant Selection, For NR Approval, Dated March 4, 2005.

9- 77 B-SE-0124, Hot Leg Piping Concept for Further Development, For NR Approval, Dated June 30, 2005.

9- 78 NR:SSA:WEEvers E#05-03086, Space Power Program – Recommendation to Pursue Design Development of Internally Insulated Pipe for the Hot Leg Piping Portions of the Plant – Approval with Comments, Dated August 15, 2005.

9- 79 B-SE(SPS)-0001T, Telecon, Dated August 4, 2005.

9- 80 A.T. Chapman, J.K. Cochran, T.R. Ford, S.D. Furlong, and D.L. McElroy, "Reduction of High Temperature Thermal Conductivity of Thin-Wall Ceramic Spheres," Insulation Materials: Testing and Applications, 2, ASTM STP 1116, 464-475, (1991).

9- 81 B-MT(SRME)-45

9- 82 SM-7235-0006, "Initial Assessment of Joining Challenges for the Prometheus Project".

9- 83 Zheng Li, S. L. Gobbi, K. H. Richter, "Autogenous welding of Hastelloy X to Mar-M-247 by laser", J. Materials Processing Technology, vol. 70 (1997), 285-292.

9- 84 Aerospace Fluid Component Designers' Handbook, Volume 1, Revision D; Technical Documentary Report No. RPL-TDR-64-25 dated February 1970

9- 85 Engineering Practices for Large (4 Inches and Over) Gate, Globe and Check Valves in Water-Cooled Nuclear Reactor Systems; ORNL TM-3221 dated January 1971;

9- 86 Jet Propulsion Laboratory Prometheus Project Environmental Requirements Document, 982-00029

9- 87 Flow of Fluids Through Valves, Fittings, and Pipe; CRANE Technical Paper 410, 1965

9- 88 Flow of Fluids Through Valves, Fittings, and Pipe; CRANE Technical Paper 410, 1988

9- 89 NGST Report SDRL SE-002-001:D40224, " NGST Prometheus Spacecraft Module and Subcontractor-provided Reactor Module Segment Design Description – Draft", dated May 16, 2005

9- 90 KAPL Letter SPP-67210-0001/Bettis Letter B-SE-0037, "PROVIDE NR PROGRAM ASSESSMENT OF THE DESIGN SPACE FOR THE PROMETHEUS 1 PROJECT," Nov. 2004

9- 91 SPP-67310-0009, "NRPCT Comments on the use of a Water Heat Rejection Loop", dated 6/17/2005

9- 92 KAPL Letter SPP-SEC-0022, "Evaluation of the Capillary Limit for the Northrop-Grumman Water Heat Pipe", dated July 20, 2005

9- 93 KAPL Letter, SPP-67210-0007, "Hot Leg Piping Concept for Further Development - For NR Approval", dated June 30, 2005.

9- 94 KAPL Letter, SPP-67320-0002 Attachment A, "Preliminary Space Structural Design Basis for Pre-Conceptual Design", dated June 30, 2005.

9- 95 ASME Boiler and Pressure Vessel Code Section III, Division 1 Subsection NB, *Class 1 Components*; The American Society of Mechanical Engineers, dated July 1, 2004.

9- 96 Metals Handbook, Vol.2 - Properties and Selection: Nonferrous Alloys and Special-Purpose Materials, ASM International 10th Ed. 1990.

9- 97 DOT Report, DOT/FAA/AR-MMPDS-01, "Metallic Materials Properties Development and Standardization (MMPDS)", dated January 2003.

# Section 10
# Plant Structure and Environmental Protection

*PRE-DECISIONAL - For planning and discussion purposes only*

(Intentionally Blank)

# Plant Structure and Environmental Protection

## Table of Contents

10 Plant Structure and Environmental Protection ..... 6
10.1 Summary and Conclusions ..... 6
10.1.1 Description of Segment Elements ..... 8
10.1.2 Driving Requirements ..... 9
10.1.2.1 Performance Requirements ..... 9
10.1.2.2 Design Constraints ..... 10
10.1.2.3 Interface Requirements ..... 11
10.1.3 Overview of Environments ..... 12
10.1.3.1 Pre-Launch Environments ..... 12
10.1.3.2 Launch Environments ..... 12
10.1.3.3 Post-Launch Environments ..... 13
10.2 Structural Support Subsystem ..... 17
10.2.1 Introduction ..... 17
10.2.2 Requirements and Objectives ..... 17
10.2.2.1 Structural Requirements ..... 18
10.2.2.2 Objectives and Considerations ..... 19
10.2.3 Primary Support Structure Types ..... 20
10.2.3.2 Primary Support Structure Modeling Approach ..... 23
10.2.3.3 Structure Material Selection ..... 24
10.2.3.4 Primary Structure Development Approach ..... 24
10.2.4 Secondary Support Structure ..... 25
10.2.4.1 Preliminary Thermal Expansion Evaluation ..... 25
10.2.4.2 Dynamics and Thermal Response Model ..... 27
10.2.4.3 Secondary Support Structure Development Needs ..... 28
10.2.5 Summary ..... 29
10.3 Thermal Control Subsystem ..... 30
10.3.1 Introduction ..... 30
10.3.2 Summary of Conclusions ..... 30
10.3.3 Development Process ..... 32
10.3.4 Requirements and Goals ..... 33
10.3.5 Thermal Control Methods ..... 35
10.3.5.1 Passive Thermal Management Methods ..... 35
10.3.5.2 Active Thermal Management Techniques ..... 36
10.3.6 Thermal Management Zones ..... 38
10.3.6.1 Reactor Thermal Management ..... 38
10.3.6.2 Shield Thermal Management ..... 39
10.3.6.3 CDM Thermal Management ..... 40
10.3.6.4 Reactor Coolant and Plant Structure Thermal Management ..... 41
10.3.7 Power Plant Thermal Model ..... 43
10.3.7.1 Modeling Goals ..... 43
10.3.7.2 Modeling Approach ..... 43
10.3.7.3 Model Description ..... 44
10.3.7.4 Model Results ..... 44
10.3.7.5 Trade Studies ..... 46
10.3.7.6 Future Modeling Approach ..... 47
10.3.8 Summary ..... 48
10.4 Micrometeoroid and Orbital Debris ..... 49

10.4.1 Orbital Debris ..... 49
10.4.1.1 Orbital Debris Flux ..... 49
10.4.1.2 Orbital Debris Abatement ..... 51
10.4.2 Micrometeoroids ..... 51
10.4.2.1 Micrometeoroid Flux and Velocity ..... 52
10.4.2.2 Development of Protection Systems ..... 55
10.4.2.3 Historical Methods ..... 58
10.4.2.4 Current Methods ..... 59
10.4.2.5 Material Selection ..... 63
10.4.2.6 Impact Testing ..... 65
10.4.3 Summary ..... 66
10.5 Environmental Considerations for Instrumentation and Control ..... 67
10.5.1 Environmental Spacecraft Zones ..... 67
10.5.2 Radiation Environment ..... 68
10.5.2.1 Summary ..... 68
10.5.2.2 Transient and Trapped Particles ..... 68
10.5.2.3 Interaction of Radiation with Electronic Devices ..... 69
10.5.2.4 External Radiation Contribution from Space ..... 69
10.5.2.5 Internal Radiation Contribution from Reactor ..... 69
10.5.3 Thermal Environment ..... 70
10.5.3.1 Thermal Environment by Zones ..... 70
10.5.4 Summary ..... 73
10.6 References ..... 73

## List of Figures

Figure 10-1: Marshall Glenn Liquid Metal 4 Brayton PCS Concept ..... 21
Figure 10-2: Hexagonal Two Section Truss ..... 21
Figure 10-3: Stringer and Ring Cross Sections ..... 22
Figure 10-4: Northrop Grumman Sheet Stringer Concept ..... 22
Figure 10-5: Simple representation of the thermal expansion analysis geometry ..... 26
Figure 10-6: Primary Support Structure and RCS Thermal Expansion Comparison ..... 27
Figure 10-7: Schematic Cross Section of Typical Multilayer Insulation (MLI) Construction ..... 36
Figure 10-8: Example of Heat Pipe Configuration (Reference 10- 20) ..... 36
Figure 10-9: Available Heat Pipe Fluids in Low to Moderate Temperature Range ..... 37
Figure 10-10: Reactor Module and Related Environmental Zones ..... 38
Figure 10-11: Thermal model – Assembly of plant, shield back cap, and PSS shell ..... 44
Figure 10 - 12: Side view temperature profile ..... 45
Figure 10 - 13: Fore-aft thermal zoning ..... 46
Figure 10-14: Orbital Debris Flux Variation with Altitude (Reference 10- 5) ..... 50
Figure 10-15: Near Earth Micrometeoroid Flux – METEM ..... 53
Figure 10-16: Interplanetary Mission Phase Micrometeoroid Flux – METEM ..... 53
Figure 10-17: Jovian Mission Phase Micrometeoroid Flux – METEM ..... 54
Figure 10-18: Single Layer Protection ..... 60
Figure 10-19: Whipple Shield ..... 60
Figure 10-20: Critical Design Range ..... 60
Figure 10-21: Whipple Shield with Two Bumper Layers ..... 61
Figure 10-22: Titanium Multiwall Protection (Reference 10- 13) ..... 62
Figure 10-23: Stuffed Whipple Shield ..... 62
Figure 10-24: Modified Whipple Shield ..... 63

## List of Tables

Table 10-1: Prometheus Mission Fluence ..... 15
Table 10-2: Prometheus Mission Fluence ..... 16
Table 10-3: Description of Parameters Used in the Model ..... 26
Table 10-4: Number of Orbital Debris Impacts per Year (Reference 10- 6) ..... 51
Table 10-5: Number of Micrometeoroid Impacts per Year * ..... 54
Table 10-6: Average Speed of Micrometeoroids – METEM ..... 55
Table 10-7: Average Speed of Jovian Micrometeoroid Flux – METEM ..... 55
Table 10-8: Critical Penetration Thickness ..... 56
Table 10-9: Materials Evaluation Worksheet ..... 64
Table 10-10: Radiation Environment Induced by SNPP ..... 67
Table 10-11: Baseline Temperatures for I & C Component and System Design ..... 72

# 10 Plant Structure and Environmental Protection

## 10.1 Summary and Conclusions

This section presents results from efforts to describe the Plant Structure and Environmental Protection (PSEP) segment of the Reactor Module. The primary functions of this segment are to provide physical support for the various elements of the module, to control the thermal environment of the reactor module so that stress and temperature limits are not exceeded, and to protect the module from external environment effects, especially orbital debris and micrometeoroids. This section also considers the varying internal thermal and radiation environments for the instrumentation and control equipment. Internal environment considerations such as fission products and impurities in the helium/xenon working gas are not described in this Section.

Key conclusions are:

---

Structure:

- Accommodation of the differential thermal expansion between the primary structure and the piping of the reactor coolant system would be a significant design challenge. For nickel-base super-alloy piping at 900 K and titanium structure at 400 K, the differential expansion is near 3 cm. Further discussion of possible approaches to mitigate this concern is in Section 10.2.4.3 and 9.7. Use of a one or two Brayton system might partially alleviate this problem relative to a larger and longer three or four Brayton system.

- Three basic structure types need to be evaluated for the primary support structure. Each has strengths and weaknesses relative to the needs of the reactor module. An outline of the planned approach to evaluation is presented.

Thermal:

- The leading candidate for hot leg piping, internally insulated nickel-base super-alloy, requires specific external thermal management to reject heat in a controlled manner so that piping temperature remains within acceptable limits and heat loss is not excessive. Methods to transport the heat from the hot leg to an external radiator would need to be developed and would likely include a combination of radiation, conduction and possibly heat pipes. Isolation of the hot leg from internal components (probably via multi-layer blanketing) would be necessary to keep temperatures of other components outside the reactor coolant segment (primarily electronics and mechanisms) below 400 K. A balanced approach would be necessary to assure that beginning and end of life temperatures and heat loss are within desired ranges.

- Identification of thermal management materials is needed early in development phase so that testing can verify performance at high temperatures (around reactor and hot leg piping) and after extended exposure to high radiation levels (especially around reactor). The types of materials that need to be developed and/or demonstrated include high temperature blankets, high emissivity coatings or finishes for a variety of materials.

- Micrometeoroid protection and thermal management requirements are both realizable. However, where heat rejection to space is required, as may be the case for the reactor and portions of the shield, the number of protective layers may need to be limited to one or two.

Otherwise, heat rejection to space may be significantly reduced and undesirably high temperatures may result.

- The electric power needed to maintain all the reactor module external surfaces above 200 K prior to reactor start-up could be kept below approx 1500 Watts in the absence of solar illumination. This is below the anticipated start-up power. Orienting the radiator surfaces toward the sun would reduce required power and increase those external surface temperatures, although it would be necessary to determine if thermal cycling due to periodic absence of solar illumination would be detrimental. Although internal temperatures have not been calculated, maintaining external temperatures above 200 K would permit internal electrical component and sensor temperatures to be above 239 K (-34 C) which is a typical lower limit for widely available electronics.

Environmental:

- A detailed evaluation is needed to investigate the accumulated effect of the reactor upon charging of the spacecraft. Three major sources of charging include the reactor, the ion thrusters, and the external charged particle flux. The effects of the multiple charging sources needs to be studied, as well as possible interactions between spacecraft charging and electro-magnetic fields. As part of the mitigation for charging, it would be important to include electrical conductivity measurements as part of the material testing efforts.

- There are many different options available to provide a range of micrometeor protection levels. Multi-layer, special material options could provide protection from micrometeors up to 1 cm diameter, but the thickness of such a system may make it unsuitable for use near the reactor. Simpler, single or dual layer barriers may provide adequate protection for most of the reactor module. Another complication regarding protection near the reactor or shield is that the envelope of a protection system might be a source of radiation scattering which could impact on reactor shield design. Identification of candidate protection options is needed early in a development phase so that testing can be performed to verify effectiveness, especially for materials used near the high temperature, high radiation conditions around the reactor.

- The instrumentation and control (I&C) system components are distributed over a large portion of the spaceship, from the sensors and actuators located near the reactor (fore, in, and aft of the radiation shield) to the electronics located in the enclosure at the rear of the spaceship. To allow definition of the environmental requirements for the I&C components the thermal and radiation influences in different regions of the spacecraft must be evaluated including the thermal controls and radiation shielding affecting each zone.

---

The different subsystems within the PSEP segment are described below, and some of the important related requirements are discussed. These include both internal as well as external requirements, and some of the significant interface requirements.

Among the key external requirements are the environments that the spaceship will encounter before, during and after launch. The pre-launch environments are described in general, since these are rarely primary design drivers. The launch and post launch environments are discussed in more detail. Of special significance are radiation environments and considerations for instrumentation and control components, which are discussed in Section 10.5.

Each of the primary subsystems is described in detail, with particular focus on efforts to date and anticipated efforts that would follow, if continued.

### 10.1.1 Description of Segment Elements

1. Structural Support Subsystem – Supplies structural load paths necessary to maintain physical support and alignment of equipment and to accommodate all anticipated static, dynamic and thermally-induced loads. The system includes the primary support structure that provides overall support and connection of the Reactor Module to the Spacecraft Module, including the module portions of the separable interfaces. The system also includes the secondary support structure that provides structural connections among Reactor Module components and the primary support structure.

2. Micrometeoroid Protection Subsystem – Consists of material barriers around critical elements to protect the Reactor Module against impact damage, erosion and chemical contamination from micrometeoroids. This protection comes, in part, from existing structural elements and thermal control elements supplemented by other materials to provide the degree of protection desired.

3. Thermal Management Subsystem – Provides the heat rejection, thermal isolation, and supplemental heating needed to keep the different Reactor Module elements within temperature limits. The thermal management subsystem would include insulating materials (insulation, multi-layer blankets, spacers), surface thermo-optical materials (paints, coatings, treatments, etc), conductive and isolating materials, and probably more active elements such as heaters, temperature sensors and heat pipes.

## 10.1.2 Driving Requirements

Summarized below are some of the key requirements which apply to the Plant Structure and Environmental Protection (PSEP) segment of the reactor module. Some of the requirements come from higher level sources, such as Level 2 specifications which apply to the complete spaceship. Others are derived from the higher level requirements or have been recognized as important for the reactor module to satisfy mission requirements (such as rejection of internally generated heat). The requirements are listed in three categories:

- Performance Requirements, which address the primary functions of the PSEP segment
- Design Constraints, which are bounding limits on the PSEP characteristics or constraints on how the PSEP must be configured.
- Interface Requirements, which describe how the PSEP segment must interface with the space vehicle or with other elements of the reactor module.

These lists represent only some of the more important requirements identified to date, and are far from a complete listing.

### 10.1.2.1 Performance Requirements

| Requirement *(Source)* | Impact on Plant Structure and Environmental Protection Segment |
|---|---|
| The Space Nuclear Reactor design shall utilize technologies that facilitate extensibility to surface operations. *(Level 2 Requirement)* | Must consider compatibility of pressure boundaries, external surfaces, mechanisms, etc with surface environments. |
| The Project shall design the Deep Space Vehicle to have an operating lifetime greater than or equal to [20] years. *(Level 2 Requirement)* | Selected materials and segment design would have to satisfy performance requirements over long mission life. Key performance elements include providing radiation protection, accounting for radiation effects, and protecting from external environments such as micrometeoroids. |
| The Project shall assure that all Science System hardware in its deployed configuration, except approved science hardware, shall remain within the protected zone of the reactor radiation shield. *(Level 2 Requirement)* | Coordination between the shield and spaceship design is required to assure that maximum dose levels are not exceeded. This limits the envelope of the PSEP segment and could influence arrangements in order to maximize protection of critical components. |
| The Project shall obtain launch approval as specified in the Prometheus Launch Approval Plans. *(Level 2 Requirement)* | Safety assurance must be considered during design of PSEP elements. Influences could include design of the shield interfaces to separate from the reactor during a re-entry event, consideration of environmental impact when selecting materials, and preferential orientation of structure or components for safety considerations. |
| The Spaceship total dry mass at launch shall not exceed [25,000] kg. *(Level 2 Requirement)* | Minimum module mass would be a goal and a selection criteria for evaluation of different design options. |

Note: Values in brackets [XX] are preliminary or placeholder values and thus would be subject to change.

### 10.1.2.2 Design Constraints

| Requirement *(Source)* | Impact on Plant Structure and Environmental Protection Segment |
|---|---|
| The Project shall comply with the Prometheus Single Point Failure Policy as documented in the Prometheus Project Policies Document 982-00057. *(Level 2 Requirement)* | Structure and thermal management subsystems must be designed with fault tolerant capacity. This would include features such as ability to react flight loads in presence of element failure (with reduced margin) and redundant heaters and temperature sensors. Micrometeoroid and orbital debris protection reduce the risk in areas where single point failure can not be eliminated, such as the pressure boundaries. |
| The Spaceship launch configuration shall be compatible with a [5-m] launch vehicle payload fairing (dynamic envelope dimensions [4.5m] diameter & [26m] height), or smaller. *(Level 3 Requirement – Based on Boeing Delta IV Specification)* | Arrangements and overall sizing must fit within allocated space inside the fairing. This drives the overall dimensions of the plant structure, and bounds the volume within which all the components must be packaged. |
| The Prometheus flight hardware shall be designed and verified to meet applicable functional, performance, operation, and other design requirements without damage or degradation when exposed to the design environments specified herein {in ERD}. *(Level 3 Requirement)* | The module must withstand particle and radiation environments, launch loads, charging, and other space environments. |
| During no-thrust periods of Science Orbits, the Deep Space System shall continuously point a Spaceship-fixed vector to commanded directions in the target-centric reference frame to within 20, 20 and 20 mrad (3 sigma) about the reference frame X, Y and Z axes respectively... *(Level 3 Requirement)* | This requirement drives the need for positional stability of the spaceship. Counter-rotating Braytons, or alternate localized means to offset angular momentum, was anticipated to provide the needed stability. The need to eliminate dynamic coupling between the reactor and the mission module might have become a structural consideration. |
| The Prometheus Spaceship, cantilevered at the separation plane (i.e., with no compliance from the Payload Adaptor Fitting (PAF) or separation mechanism), shall have a minimum frequency of 30 Hz [TBR] in the thrust axis and 8 Hz [TBR] in the lateral axis. *(Level 2 Requirement, from Reference* 10-2*)* | In order to meet the spaceship requirement, the constituent elements of the vehicle must have higher frequencies. Based upon previous experience (and in the absence of detailed analyses), a minimum frequency of [10] Hz Lateral and [38] Hz Vertical are reasonable goals for the reactor module in the launch configuration, as measured from the vehicle interface of the vehicle to module support struts. |

Note: Values in brackets [XX] are preliminary or placeholder values and thus would be subject to change.

### 10.1.2.3 Interface Requirements

Collected below are requirements which need to be in place between the reactor module and the spacecraft module or between the PSEP and other reactor segments in order for the reactor module to meet performance requirements. Most of these represent requirements which were recognized as necessary during design efforts but which have not been captured in other released requirements collections.

| Requirement *(Source)* | Impact on Plant Structure and Environmental Protection Segment |
|---|---|
| The Spacecraft Module shall be capable of rejecting [682] kWt of heat from the Reactor Module. *(Level 3 Requirement)* | This is a place-holder requirement that captures the need to reject waste heat to the space environment via the radiators. The PSEP must accommodate the piping to and from the gas cooler and accommodate the differential expansions that will occur as the HRS and Brayton piping loops approach different temperatures, as well as the more moderate temperatures of any non-operating loops. |
| Structure shall provide attachment interfaces between space vehicle and reactor module which shall meet the following requirements:<br>Provide sufficient stiffness to meet overall stiffness goal<br>Be positioned inside shield cone angle (whether on front or back of shield) to avoid scattering<br>*(Derived from shield and dynamic requirements)* | Structural interface between boom and reactor module shall be controlled so that launch and deployed dynamic requirements are satisfied |
| The PSEP shall provide support for the module components that prevent excessive stresses or deflections in the components or the supporting structures. *(Derived from structural requirements)* | Structure and components must be designed to avoid amplification of dynamic excitation from the vehicle and from the energy conversion system. Structural supports must withstand launch loads and accommodate large temperature induced deflections. |
| Heat rejection from hot leg piping shall be controlled so that magnitude of heat transfer from piping is maintained at [2.1] kW/meter. *(Derived from hot leg piping analyses)* | Specific means to transport the heat from the hot leg piping to external radiating surfaces must be developed. Heat rejection approach must maintain the protection of the hot leg piping from the external threats of orbital debris and micrometeoroids |
| Temperatures shall be maintained above minimum acceptable levels using electrical heating power levels that are below those required for start-up. *(Derived from survival temperature and pre-start-up power availability limits)* | Most of the external surfaces of the module must be blanketed. Exceptions include the radiator surfaces for hot leg heat rejection, portions of the shield, and portions of the reactor. |
| Unless specified otherwise, temperatures of electronics and mechanisms (primarily including I & C electronics and CDM's) shall be maintained below [400] K, with target temperature goal of [300 K]. *(Derived from equipment temperature limits and goal of providing moderate temperature for electronics and mechanisms to improve performance and reliability)* | Isolation of the hot leg piping and hot components from the rest of the module is necessary. Blanketing of all components except the hot leg piping is anticipated. More detailed analyses would have indicated where further thermal isolation or coupling would be needed. |

Note: Values in brackets [XX] are preliminary or placeholder values and thus would be subject to change.

### 10.1.3 Overview of Environments

The Reactor Module would be subjected to a wide variety of environments during assembly, test and launch, and then throughout its mission in space. Most of these would be quantified based upon analyses and measurements of the launch and space characteristics. Some would be determined based upon existing knowledge and codes for handling and test of nuclear components. Still others, such as pre-launch temperature and humidity, are established within limits and then the local environment controlled to remain within these limits. In all cases, the environments must be fully characterized and the required testing and analyses performed to demonstrate that the module will perform as required during and after exposure to the various environments.

For convenience, the different sets of environments are grouped according to when they would occur: before launch, during launch, and after launch. Each of these is described below in more detail. Further details are available in Ref. 10- 9 or in other available literature.

#### 10.1.3.1 Pre-Launch Environments

The pre-launch environments primarily comprise the atmospheric and dynamic conditions to which a component or assembly will be exposed prior to launch. These do not include the simulated launch and flight environments to which hardware is subjected during test events. Generally, pre-launch environments are controlled so that they do not drive the design of flight hardware. These include,

- Dynamics – Vibration induced loads result primarily from handling and transportation of components and assemblies. Seismic loading must also be considered, especially in regions where such activity is frequent. The normal approach to pre-launch environments is to design handling equipment and containers to isolate the flight hardware from loads to an extent that resulting stresses are lower than those during or after launch.
- Temperature – Usually held within a nominal range. Preliminary JIMO range was 5 C to 40 C.
- Relative Humidity – Usually held between 30 % and 70 %. Lower limits are set to minimize risk of electrostatic discharge, while upper limits reduce oxidation and other interactions with atmosphere. When necessary, more narrow limits can be established.

In addition to utilizing facilities and equipment to limit pre-launch environmental effects to acceptable levels, it is important to also consider during the design phase what accommodations or protections need to be included in the flight hardware. A key example is the need to incorporate handling, lift and support locations into the structure early in the design phase. This allows for load paths, access, and manufacturing requirements for flight and non-flight to be addressed together. Another example is protection of sensitive finishes, such as high emissivity surfaces. It may be necessary to protect these surfaces during normal processing and to make accommodations for removal of these protective surfaces prior to testing or launch.

#### 10.1.3.2 Launch Environments

The most significant environment during launch is the collection of dynamic and load events which occur during the launch vehicle thrust stages. These include quasi-static loads due the combined accelerations, launch vehicle dynamic excitation and responses, and acoustic loading. There is also a high-frequency shock event resulting from the release of energy in the structural elements attaching the space vehicle to the launch vehicle. Other environments are the relatively rapid transition to

space vacuum conditions and localized heating of the fairing due to atmospheric friction. The latter is generally benign and is not discussed further here.

#### 10.1.3.2.1 Quasi-Static Loads

Accelerations associated with quasi-steady flight events are generated by engine-induced and external forces, which change slowly with time and for which the elastic responses are relatively small. Low frequency (<80 Hz) vibratory accelerations acting through the Spaceship c.g. induced by various launch vehicle dynamics events are added to the appropriate quasi-steady accelerations to produce worst-case quasi-static acceleration loads for Spaceship structural design purposes. Typical maximum accelerations are approximately 6 g's in the axial direction and 3 g's in the lateral direction. (Ref 10- 2, 10- 15)

#### 10.1.3.2.2 Dynamic Loading

The reactor module will experience random, periodic, and transient vibrations mechanically transmitted from the launch vehicle, as well as acoustically induced random vibrations mechanically transmitted from adjacent Spaceship elements. (Ref 10- 2) These environments are typically described by a random vibration spectrum for components which are not directly excited by the acoustic environment.

#### 10.1.3.2.3 Acoustic Environment

The acoustic environment occurs during the first minutes of launch, when the vehicle is exposed to the high noise levels from the rocket engines. Acoustic loading directly excites large surface areas, which can result in locally high loads as well as a dynamic response which would be reflected in the random vibration spectrums for different zones of the module.

#### 10.1.3.2.4 Shock

Shock within a space vehicle occurs as a result of separation events between the space and launch vehicles or at the restraint points of deployable assemblies. Shock results either from the explosive actuation frequently used to initiate a separation event or from the release of energy stored in the preloaded elements used to provide constraint prior to separation. These shock events are normally high frequency and primarily affect electronics, although brittle material such as ceramics could be affected.

#### 10.1.3.2.5 De-Pressurization

Pressure drop from sea-level atmospheric to near vacuum occurs soon after launch. Analysis is required to show that venting paths are sufficient to prevent differential pressures from exceeding limits for the equipment being evaluated. The rate of depressurization is typically defined in the applicable launch vehicle spec.

### 10.1.3.3 Post-Launch Environments

Post-launch environments can be described as falling into two categories – external and internal. External environments are predominantly described by the radiation, elemental, thermal, particle and electro-magnetic conditions that exist outside the Earth's protective atmosphere. The internal environment results from events and operational conditions within the space vehicle, often combined with interaction with the external environment. Examples of internal environments include dynamic

conditions due to equipment operational and vehicle response frequencies; radiation and charging due to reactor operation; deployment related shock loads (which are similar to those described in Section 10.1.3.2.4, Shock); internal heat generation (which is described in Section 10.3, Thermal Control Subsystem); and loads due to differential thermal expansion (which is discussed in Section10.2, Structural Support Subsystem).

### 10.1.3.3.1 Thermal Environments

The external thermal environment is described below and is characterized by the heat flux on the external surfaces and the deep space temperature to which the external surfaces radiate. Solar flux is largest, followed by reflected and emitted flux from the Earth. Above low-earth orbit (~10,000 kilometers), Earth reflected and emitted fluxes are minimal, and thus would have little influence upon the reactor module. When orbiting the Earth, there would probably be short periods of eclipse when solar and reflected flux would be blocked – however, these would have little effect upon the reactor module due to its high mass. An important characteristic of solar flux is the wavelength of the peak energy level, 0.5 μm. This value can be significant when evaluating external surface characteristics for effectiveness in either absorbing or reflecting solar energy.

Near-Earth Space Thermal Environment

- Direct solar flux
  - 1360 W/m$^2$ (average)
- Earth-reflected solar flux (Albedo) and Earth emitted Infra-Red flux
  - Albedo is 0.29 to 0.31 of direct solar flux
  - Earth emitted flux is 227 to 241 W/m2 at infra-red wavelength
- Deep Space Temperature
  - ~ 4 °K

Near-Jupiter Space Thermal Environment

- Direct solar flux
  - 50 W/m$^2$ (average)
- Albedo and emitted flux – Negligible for Reactor Module
- Deep Space Temperature
  - ~ 3 °K

### 10.1.3.3.2 Micrometeoroid and Orbital Debris

Micrometeoroids and orbital debris are space-borne particles ranging in size from very small ($10^{-12}$ g) to very large ($10^2$ g), and with velocities sometimes exceeding 20 km/s. Protection from these threats must be provided, especially for the critical pressure boundary components. A more detailed description of this environment, and a discussion of protection techniques, is located in Section 10.4, Micrometeoroid and Orbital Debris.

### 10.1.3.3.3 Radiation Environments

The external radiation environment is described in detail in the Environmental Requirements Document (982-00029). The internal radiation environment will be influenced by position relative to the reactor and shield, by local shielding, and by the external radiation levels. Solar, galactic and Jovian radiation sources, coupled with reactor radiation, must be considered during electronics selection, shielding trades and material evaluation. A detailed description of the internal radiation environments relative to the different zones of the reactor module can be found in Section 10.5,

Environmental Considerations for Instrumentation and Control. The significant effect radiation has upon many materials must be a central focus during the materials selection and testing phase of any future effort.

### 10.1.3.3.4 Charging and Electromagnetic Fields

The primary source of charged particles for space vehicles is usually the Sun. The total solar electron and proton fluence for the Prometheus mission is given in the table below, which is taken from the Environmental Requirements Document. However, significant energetic plasma exists around Jupiter which would have a significant influence on the spacecraft. Data on this environment was not yet available. A third source of charged particles would have been the reactor itself, which exposes the hardware to neutron fluence and gamma rays. A fourth source of charged particles would have been the ion thrusters, which emit charged xenon particles. The interaction among all the different charging fields and resulting electric currents and potential differences would require significant evaluation to quantify and to mitigate negative impacts.

**Table 10-1: Prometheus Mission Fluence.**

| Energy (MeV) | Electron Integral Fluence ($cm^{-2}$) | Proton Integral Fluence ($cm^{-2}$) |
|---|---|---|
| 0.1 | 5.84E15 | 8.50E16 |
| 0.2 | 3.07E15 | 1.70E16 |
| 0.3 | 1.93E15 | 6.60E15 |
| 0.5 | 1.07E15 | 2.21E15 |
| 1 | 5.28E14 | 4.91E14 |
| 2 | 2.46E14 | 1.02E14 |
| 3 | 1.48E14 | 4.48E13 |
| 5 | 7.23E13 | 1.50E13 |
| 10 | 2.34E13 | 3.31E12 |
| 20 | 6.34E12 | 6.27E11 |
| 30 | 2.77E12 | 2.36E11 |
| 50 | 9.23E11 | 9.57E10 |
| 100 | 1.96E11 | 4.37E10 |
| 200 | 4.18E10 | 1.31E10 |
| 300 | 1.69E10 | 4.70E09 |
| 500 | 5.44E09 | 2.88E04 |
| 1000 | 1.17E09 | 6.39E02 |

Some other related considerations which were to be addressed include:

- Reactor counter-acceleration due to neutron flow from reactor.
- Thrust imbalances due to reactor asymmetries and unbalanced flux of neutrons and charged particles from the reactor.
- Options to mitigate charge build-up
- Implementation of electrical conductivity testing to support evaluation of charge build-up and mitigation options.

Several high level environmental requirements regarding charging and electromagnetic fields appear in the Level 3 Key and Driving Requirements summary. Three which would directly affect the reactor module are listed in the following table.

**Table 10-2: Prometheus Mission Fluence.**

| Requirement | Typical Approaches to Meet Requirement |
|---|---|
| The Spaceship shall be designed to avoid spacecraft charging in the energetic plasma of Jupiter, as specified in the (ERD), or shall be designed to perform its mission in the event of resultant electrostatic discharge (ESD) events. | • Connect all internal and external conductive components with appropriate resistance to prevent ESD.<br>• Use ESD dissipative coatings on external dielectric materials.<br>• Use electrical interface surge protection. |
| The Spaceship design shall control possible high voltage breakdowns such as corona, multipaction, and secondary arcing anywhere during the mission, but especially in the Jovian plasma environment, as specified in the Environmental Requirements Document. | • Select and use high voltage insulators that will perform in high radiation, high temperature, charging environment.<br>• Use separation of high voltage components where practical.<br>• Verify performance with multi-environment testing. |
| The Spaceship design shall control low frequency electric and magnetic fields (LFE and LFH), as specified in the Environmental Requirements Document (ERD) | • Use twisted shielded pair cables and coaxial cables for power.<br>• Run power cables inside the boom.<br>• Design radiation and micrometeoroid shielding to also provide EMI shielding.<br>• Maximize separation of sensitive science instruments from interference sources. |

### 10.1.3.3.5 Vehicle Dynamics

After launch, the primary structural concerns of a space vehicle are accommodation of the thermal environment and management of the small vibration and acceleration forces. The thermal environment is discussed elsewhere, although one aspect, time variation, has not been discussed. In Earth orbiting vehicles, transitions from cold to hot, or the reverse, can force relative motions and cause low frequency vibrations. Design must account for these motions in order to assure that they are below certain levels and outside critical control frequencies. Although external induced transients for a vehicle in deep space would likely be small, there may be scenarios during transit to deep space or resulting from internal transients that must be considered.

Similarly, moving parts or fluids can create vibrations which must be considered during the design of the structure. Within the reactor module, the braytons and moving fluid are two clear sources of vibration which must be considered. Reactor control drive mechanisms will also create vibrations, although the relatively small associated mass and speed would likely make these vibrations low. Each of the potential vibration sources must be understood so that vehicle resonances are not excited and to assure that the attitude control system is able to handle any low level disturbances.

## 10.2 Structural Support Subsystem

### 10.2.1 Introduction

A multifunctional support structure that provides the load paths necessary to maintain physical support and alignment, as well as accommodates all anticipated static, dynamic, and thermally induced loads, is a fundamental requirement for all reactor module elements. This structure would include the Primary Support Structure and the Secondary Support Structure. The Primary Support Structure would support the reactor, shield, coolant, control and aero-thermal protection segments of the reactor module and supply attachment points for the Secondary Support Structure. The Primary Support Structure would provide the launch (support struts) and deployed (boom) interfaces between the spacecraft and reactor modules.

The Secondary Support Structure would interface between the Primary Support Structure mounting locations and component subassemblies, micrometeoroid shielding and thermal control subsystem elements such as radiators and thermal barriers. The Secondary Support Structure would provide thermal and mechanical isolation as required. Reactions in the Primary Support Structure depend partially on interactions with the Secondary Support Structure, which would require that development of both occur somewhat in parallel.

Efforts to date focused on capturing requirements and objectives for the structural support subsystem, identifying candidate structure types, and initiating efforts to model and perform sensitivity studies for different structure types. Creation of finite element models of the different structure types was underway when cancellation of the project was announced. Thus, significant results and conclusions are not available. Candidate structure types are described. An outline of the anticipated evaluation approach is presented, and important evaluation criteria are summarized.

### 10.2.2 Requirements and Objectives

There are numerous requirements and objectives which must be considered when identifying and evaluating the different structure options. Some requirements are descriptions of the primary functions. Others result from the fact that the structural support subsystem (hereafter referred to simply as structure subsystem) interfaces with each of the other segments and the space vehicle. Those items identified as requirements indicate that a minimum acceptable performance must be achieved, although that minimum value might not be identified yet. Objectives and considerations include secondary functions and characteristics which should be considered when evaluating candidate structure types.

The requirements and objectives in the following sections are not meant to be a complete listing – simply a presentation of requirements identified during development efforts as important to capture and consider during early phases of the structure development.

### 10.2.2.1 Structural Requirements

| Requirement *(Source)* | Discussion and Impact |
|---|---|
| Achieve minimum structural frequencies of [10] Hz lateral and [38] Hz axial. *(See Section 10.1.2.2)* | This requirement would have been driven the stiffness of the plant support structure. |
| Provide attachment interfaces between space vehicle and reactor module which:<br>Provides sufficient stiffness to meet overall stiffness goal<br>Is located inside shield cone angle (whether on front or back of shield) to avoid scattering<br>*(Derived from shield and dynamic requirements)* | A team including space vehicle vendor and NRPCT would have developed the structural interfaces. |
| Maintain structure mass below [TBD] kg *(Would be derived from mass budget)* | Mass budgets for the reactor module had not yet been developed but would have been a basic requirement and evaluation criteria for the different structure options. Working goal for ongoing efforts was to keep mass low enough to meet budget values once established. |
| Structure shall provide sufficient volume to house and protect reactor module elements aft of shield without exceeding volume allocation within launch vehicle fairing *(Derived from design constraints)* | This is a basic requirement of the plant support structure, and would have been one of the evaluation criteria for the different structure options. |
| Support the reactor module segments such that static and dynamic loads do not exceed limits for the different segments and components. *(Derived from component functional requirements)* | Coupled models would have been used to determine loads and response frequencies, and to develop a structure system that meets the requirements. |
| Maintain alignment of the different reactor module components within limits defined for each of those components. *(Derived from component functional requirements )* | It is anticipated that controlled movement of the CDMs relative to local structure and to the Reactor would have been an important and at times challenging requirement. Due to its effect on the vehicle and possible local dynamic effects, alignment control and knowledge for the moving parts of the module, especially the turbine/compressor assembly, would have been required. Alignment of piping and cabling would also need to be controlled. |
| Accommodate thermally-induced relative displacements *(Derived from functional requirements)* | Due to high temperatures that will be present in the module, significant relative displacement will occur between different module segments and within different segments. These relative displacements must be accommodated while still meeting other strength and stiffness requirements. |
| Provide thermal isolation (or coupling) at component mounting interfaces as determined necessary to meet component and thermal management requirements *(Derived from thermal control requirements)* | Because of high temperatures, it would sometimes be necessary to thermally isolate components from supports to prevent energy loss and to avoid exceeding temperature limits. In some cases, it will be desirable to minimize thermal isolation in order to reject heat or minimize thermal stresses. Both interface types will pose challenges and require materials with demonstrated performance characteristics. |
| Provide support for the thermal management subsystem *(Derived from segment functional requirements)* | The structure subsystem must provide radiative surfaces, or accommodate external radiators. Other thermal control elements such as heaters, temperature sensors and blankets must also be accommodated. |
| Provide support for the micrometeoroid protection *(Derived from segment functional requirements)* | At a minimum, the structure would need to support and be compatible with the micrometeoroid protection approach selected. It is possible that the structure itself could become an integral part of the protection. |

Note: Values in brackets [XX] are preliminary or placeholder values and thus would be subject to change.

### 10.2.2.2 Objectives and Considerations

In addition to the requirements which the support structure must meet, there are a variety of other functions and characteristics which should be considered when evaluating the different types of structure. Some of these are listed and briefly described below.

Point Interfaces vs Distributed / Line Interfaces – Some structures, most notably the truss, react (e.g., transition) loads at specific points, or nodes. This forces the interfacing components and structure to react loads at matching locations. This can be a benefit when there are only a discreet number of interfaces, such as support struts extending from the space vehicle to the reactor module interfaces. However, if loads and masses are distributed, or if support interfaces are large, then multiple interface points can be more efficient. How the support structure interfaces with other segments, with components in the reactor coolant segment, and with the space vehicle must all be considered when evaluating structure types. A hybrid structure, combining truss type characteristics near the point load locations and a more distributed structure away from these interfaces might have important advantages over a single structure type.

Secondary Attachment – Distributed structures, such as skin-stringer and especially honeycomb panels, provide large areas over which components can be attached. If the components are small, such as sensors, harness and piping supports, and heaters, then special local reinforcements would not typically be necessary. However, if items are large, special features may be necessary to provide sufficient distribution of the loads. With truss structures, secondary platforms are often necessary in order to provide sufficient mounting area for all the major and minor components. This can be burdensome if components are distributed throughout a region. However, if the components are concentrated in certain areas, this approach can provide advantages.

Radiation Protection – A distributed structure will generally provide some degree of radiation protection. If the materials are sufficiently dense, this protection may be important.

Micrometeoroid Protection – Distributed panel structures generally provide a significant degree of micrometeoroid protection. However, for deep space missions this protection may not be sufficient. Further investigation and probably test would be necessary to determine if additional protection would be required and whether an open or closed structure is preferable.

Heat Rejection – Distributed structures have large surface areas which can be used as radiative surfaces to reject heat. This can be advantageous when the temperature at which the heat is being rejected is within acceptable limits. However, if it is desirable to separate a higher temperature radiative surface from the rest of the structure, and / or to couple it with other components that are also at elevated temperature, a separate platform may be necessary and thus the advantage of available surface areas may not be realized.

Acoustic Excitation – Open truss structures generally experience less acoustic excitement than distributed structures. This generally results in lower vibration loads in the acoustic frequency range.

Shock Attenuation – Some structure types, such as welded assemblies, efficiently transmit shock. Others, such as bolted and distributed systems, tend to attenuate shock. This would be a consideration if components have parts which are sensitive to high shock levels.

Design flexibility – Generally, distributed structures offer more flexibility for placement of secondary structure and components. Changes after fabrication has begun are typically more difficult to make when working with the specific node points of a truss type structure.

Accessibility to Equipment – An open truss structure provide a high degree of access to the components mounted inside the truss assembly. Panel and skin type structures provide less access, and require specific design features (eg, removable access panels) to permit access to internal components.

Producibility – All structure types must be evaluated relative to how easy it will be to make and assemble the elements. Due to the elevated temperatures, high radiation levels, and need to minimize weight, it is difficult to characterize the relative advantages of the different options. Material and process development may be necessary for each option.

Cost – The relative cost of the different options will be closely coupled to the producibility. Cost must be a consideration from the beginning of the selection process through the detailed design process.

### 10.2.3 Primary Support Structure Types

Three construction types were considered most promising for the multiple requirements of the Primary Support Structure (PSS): truss/framework, sheet stringer, and skin-frame using honeycomb panels. Depending on the priority of technical and programmatic requirements, each structure provides a unique set of advantages and challenges. In order to design a PSS, the fundamental characteristics of each structural type should first be understood. Each is discussed in more detail in the following sections.

#### 10.2.3.1.1 Truss Structure

The truss is a basic engineering structure that provides a simple solution to many situations. A typical truss consists of straight members connected at joints, also known as truss nodes. Each member is connected at its extremities only, resulting in no continuous members through a joint. In general, the members of a truss are slender and can support little lateral load. Consequently all loads must be applied at the joints and not to the members themselves.

A common truss framework, the square truss, is shown in Figure 10-1 (From NASA Marshall Glen). This early concept contained a five section square truss structure with an adapter to connect to the back plate of the shield. Though not shown, each of the energy conversion units would need to be attached to the Primary Support Structure with individual mounting plates or adapters.

Another truss example provided is shown in Figure 10-2 (From NASA) and shows a hexagonal two section truss with adapters to the shield back plate and main boom of the reactor module. In this example the components are mounted inside the truss structure as opposed to the external mounting required in the square truss example of Figure 10-1. The two examples demonstrate two different options of truss configurations and highlights how they can be altered to meet mass, volume, or interface objectives.



**Figure 10-1: Marshall Glenn Liquid Metal 4 Brayton PCS Concept**



**Figure 10-2: Hexagonal Two Section Truss**

The truss is widely used in space applications due to its many benefits. For large structures, the truss supplies excellent strength, stiffness, shock attenuation, and numerous interfaces per truss node for primary to secondary connections. The main members of the truss are low surface area to mass items; therefore, they also have the benefit of not suffering from significant acoustic loading. Another advantage of the truss structure is that the members allow work to be easily performed within the structure after it is assembled or can be assembled around the components. The truss structure can also be assembled in different formations to accommodate component assembly requirements and provides convenient mounting locations for a protective sheet or micrometeoroid protection.

The truss structure presents several design challenges. The limited number of node points restricts the number of attachment options for the secondary structures and the components. Secondary mounting platforms or adapters would probably be necessary. These platforms could experience significant vibro-acoustic excitation if they have a large surface area to mass ratio. Due to the number of connections at each truss node, small design changes to the node locations of the PSS would result in large changes to the overall system. A possible disadvantage of the truss is its open nature; it provides little protection from the space environment or surface area for heat rejection to space, resulting in the need to independently provide these functions.

#### 10.2.3.1.2 Sheet Stringer

The sheet stringer design is used in the aerospace industry in many applications. The sheet stringer design contains three main structural members - the stringers, the rings, and the sheet - which are located at the perimeter of the supported volume. The individual members are relatively thin, resulting in the need for distributed loads or local reinforcement to prevent yielding of the members. The size, location, and cross section of the three members can be varied to obtain the desired strength and

stiffness characteristics. The stringers or rings can be mounted either internal or external to the sheet. Common profiles, or cross sections, are the "T" or "Z" for the stringer and either "J or "I" for the rings and are shown in Figure 10-3.

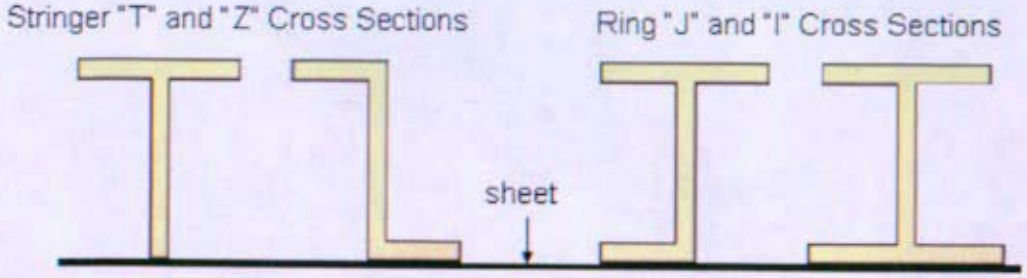



**Figure 10-3: Stringer and Ring Cross Sections**

Northrop Grumman Space Technology (NGST) generated a Prometheus concept, using internal stringers and rings, which provided adequate volume to accommodate the four Brayton PCS and its related piping. Figure 10-4 (Reference 10- 1) shows Northrop Grumman's rendition of a possible configuration for project Prometheus. The sheet has been removed from the figure to illustrate component placement within the stringers and rings.

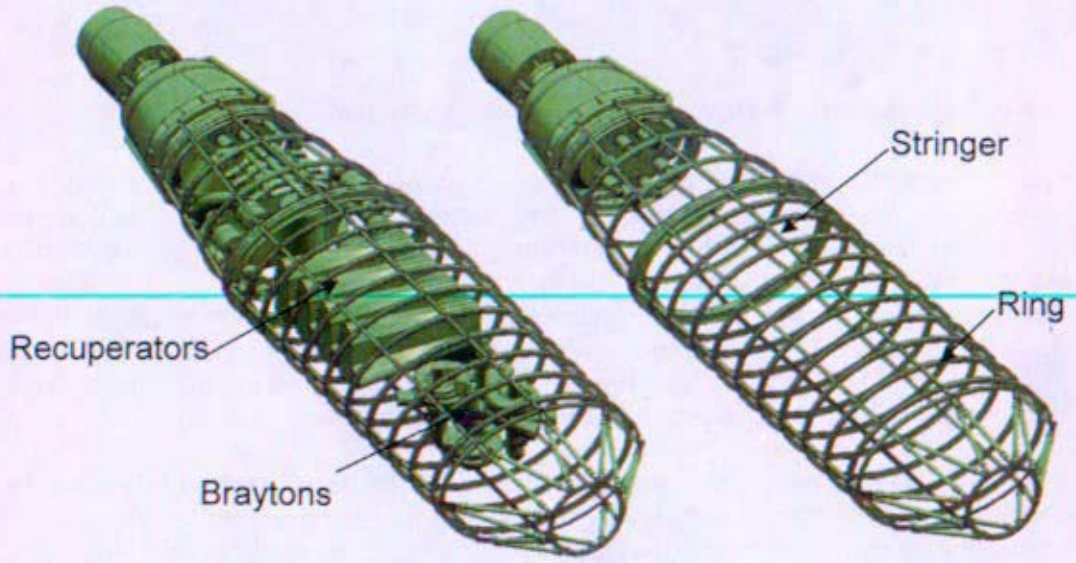



**Figure 10-4: Northrop Grumman Sheet Stringer Concept (Sheet Removed For Clarity)**

The sheet stringer has many advantages inherent to its basic design. By locating the main structural members at the volume's perimeter, the sheet stringer maximizes usable volume and provides protection from solar and galactic radiation and micrometeoroids. The use of relatively thin members around the perimeter increases the number of members used in the structure, thereby increasing the number of mounting interfaces for components and secondary structures. The large surface area could be beneficial for environmental protection and heat rejection.

The sheet stringer also has disadvantages. The large surface area to low mass ratio of the sheet makes the structure susceptible to vibro-acoustic excitation. The number of connections from the sheet to the stringers and rings complicates assembly work. Locating the main structural members at

the perimeter of the volume also requires the secondary structures to span larger distances to connect the components to the Primary Support Structure than the square truss design. The sheet-stringer design does not provide ready access to internal components, which would make installation of components difficult and require that special access features be designed into the structure.

#### 10.2.3.1.3 Honeycomb Panel / Frame Structure

A honeycomb structure consists of honeycomb sandwich panels attached either to a frame or in some instances to each other. The honeycomb panels consist of a honeycomb core sandwiched between metallic or composite face sheets. This arrangement permits use of stabilized, lightweight panels to carry most of the structural loads. Secondary supports would mount to inserts bonded within the honeycomb structure in various locations and orientations. Fittings or load spreaders are frequently required to transfer loads into and out of the honeycomb structure.

The honeycomb structure provides several advantages over the truss and sheet stringer designs. The honeycomb structure allows for placement of large quantities of equipment without predefined spatial locations. It provides a large proportion of useable volume and provides significant design flexibility. The honeycomb structure does not have the interruptions of stiffeners or rings, which allows for the removal of honeycomb panels for access once the structure is assembled. In addition to its spatial benefits, the honeycomb structure provides micrometeoroid protection and could provide additional area for heat rejection.

The construction of honeycomb structure presents several challenges that would need to be addressed during the design process. Materials that can withstand the elevated radiation and temperature environment would need to be demonstrated. If the components produce large point loads, additional structural elements to transmit loads to the panels would be required. Therefore, location, orientation, and load distribution for the components and secondary support structure needs to be evaluated early in the design. An additional concern is the large surface area of the honeycomb panels. The large surface area to mass ratio results in sensitivities to vibro-acoustic excitations.

### 10.2.3.2 Primary Support Structure Modeling Approach

Initial models were produced to investigate structure parameter sensitivities. The structures investigated were not optimized designs, but rather a tool for comparisons, within an individual structure, to understand the impact of variations such as support thickness or sheet material. This method would have lead to an optimization of the three structure types, and then a cross structure comparison would have been made, leading to a potential support structure candidate. It is important to understand that without optimization, cross structure conclusions can not be made.

Models were produced for two structure types: a square truss and a sheet-stringer assembly. A variation of the sheet stringer, referred to as the stringer ring, was also modeled, but it did not show advantage over the others. Sensitivity studies were established to determine stability of the model and the basic parameter effects on the natural frequencies for each structure. The structures could then have the secondary structure, piping, and micrometeoroid protection incorporated so they could be optimized for strength and mass requirements. The optimizations would also include variations to the foot print of the structures. Once optimized, the structures could be compared. The thermal requirements would be incorporated based on results of the preliminary studies.

The NRPCT determined Finite Element Analysis (FEA) models using ABAQUS 6.5-3, would help increase the familiarity with the behavior of the three Primary Support Structure configurations.

ABAQUS is the Naval Reactors program standard FEA code; it was verified with a suite of problems at the time of installation. Several simple models were created and tested for comparison to hand calculations for qualification. In addition, the class of problems analyzed is similar to the dynamic models used in the Naval Reactors program.

Details of the modeling effort can be found in Reference 10- 3. These details are not presented herein because the effort was still in the beginning stages when program termination started.

### 10.2.3.3 Structure Material Selection

Major considerations for the primary structure materials include stiffness, strength, mass, locally high temperatures and elevated radiation areas. Materials commonly used for space applications, where stiffness, strength and mass are primary considerations, include carbon composites, titanium, beryllium, and aluminum beryllium. Aluminum is also frequently used, especially where mass is less critical or where thermal spreading is desired.

Typically, if mass and stiffness are the primary drivers, composites and beryllium are the most effective, although each of these has drawbacks. Beryllium can be a hazardous material if dust is generated, such as during machining or during a casualty event. Carbon composites can be susceptible to radiation induced damage, and workmanship is more of a concern than with less labor intensive material systems. Thus, there is no clear choice for structural material. Due to potentially significant mass advantage, it would be advantageous to determine if carbon composites can withstand the radiation environment aft of the shield.

Since there is no clear choice for structural material, a number of candidate materials would need to be identified for both the primary and the secondary structures. Materials that can be used for multiple functions should be sought. For example, titanium can be used as a primary structure element, as a fastener, and as a moderately thermal isolating material due to it low conductivity compared to other metals. However, titanium would not be a good choice for an application requiring good thermal conduction, such as a heat spreader. Thus, a number of different materials will need to be identified and tested in order to assure that sufficient options are available for the different challenges.

### 10.2.3.4 *Primary Structure Development Approach*

Development of the reactor module primary structure would require several iterations to identify and evaluate different design options. The intended approach would have included the following steps and considerations. Many of the steps would necessarily be performed in parallel and repeated as necessary in order to achieve a realizable design.

- Develop structure designs which meet the key performance requirements such as stiffness, strength, volume, mass, etc.
- Initiate materials testing to demonstrate feasibility of using typical lightweight structure materials and systems (eg, graphite composite, aluminum beryllium, honeycomb panels). Identification of lightweight materials for use near the reactor and in the shield would also be needed so that testing can also be performed for these candidate materials.
- Perform analyses and design iterations of the different design candidates in order to progress the different design options to similar levels of maturity. During this process, the focus would be on achieving designs which best meet the different competing constraints such as mass,

stiffness, volume. Consideration would also be given to meeting other design objectives such as thermal control, micrometeoroid protection, design flexibility, cost, producibility, etc.

- Perform a trade study of the different design options in order to select the best option for detailed development. Each option would be assessed against the requirements and the objectives in order to identify a baseline design. It is possible that a baseline might combine aspects of the different construction types in order to best meet the competing requirements, and that alternate designs might be developed in order to accommodate different material sets and other variables that would still be under investigation.
- Further develop the baseline design, and alternates if available, using similar approach as described above.

### 10.2.4 Secondary Support Structure

Many components of the Reactor Module will be supported off the Primary Support Structure using Secondary Support Structure (hereafter referred to simply as secondary structure). Harness, sensor, radiator, blanket and control drive supports are examples of secondary structure.

A significant secondary structure challenge would be the structural connections between the Primary Support Structure and the Reactor Coolant Segment (RCS). These connections, which support the RCS throughout the duration of the mission, experience two distinctly different loading conditions. At launch, high strength and stiffness are required to withstand the launch loads, minimize deflections and prevent dynamic amplification of the structural vibrations. Upon start-up of the reactor, high temperatures and the resulting thermal expansion must be accommodated.

The dynamic loading during launch will be governed predominately by the Primary Support Structure, dynamic characteristics of the various components, and the number and type of connections between the Primary Support Structure and the components. Another consideration for support of the RCS is the need to avoid amplification, and if possible provide isolation, of the resonant frequencies within the operating brayton assemblies and the RCS.

Combined with the requirement to accommodate thermal expansion would be several other thermal considerations. Structural elements in contact with the high temperature components such as the piping, turbine, and recuperator would have to maintain structural adequacy at elevated temperatures. It is likely that RCS supports would have to provide thermal isolation in order to avoid locally elevated temperatures outside the RCS and the corresponding temperature decrease in the RCS component local to the support. In some cases, high thermal conductivity may be desirable, such as in the zones local to the hot leg piping where a significant amount of energy needs to be transported to external radiators for rejection to space.

Further development of the secondary structure would have addressed the challenges that both load conditions introduce, while also satisfying overall thermal management requirements.

#### 10.2.4.1 Preliminary Thermal Expansion Evaluation

The NRPCT performed analyses to compare the relative difference in expansion between a four meter section of hot leg pipe and a titanium alloy Primary Support Structure. The four meter length corresponds to the approximate length of a three or four Brayton RCS. The analysis focused on the difference in thermal expansion between candidate hot leg pipe materials at a uniform temperature of 900 K and the Primary Support Structure at a temperature of 400 K. This range of differences in

thermal expansion would have guided future designs of the secondary structure by providing limits for the amount of relative movement that must be accommodated.

### 10.2.4.1.1 Assumptions

Several simplifying assumptions were utilized in the thermal expansion analysis as follows:

- Fixed uniform hot leg pipe temperature and Primary Support Structure temperature of 900 K and 400 K, respectively. The actual temperatures would have slight variation and would not be uniform through the thickness or along length. Ignoring these variations tied to geometric factors and focusing on material comparisons was more useful, because it provided a potential range for the difference in thermal expansion.

- The total hot leg pipe length estimated as four meters from the back of the shield as approximated from the arrangement drawings for a three or four Brayton RCS. A simple representation of the geometry can be viewed in Figure 10-5.

- The Primary Support Structure was assumed to be made of Ti-6Al-2Sn-4Zr-2Mo-0.1Si; Duplex Annealed (To be referred to as 'Titanium Alloy'). The hot leg pipe material options reviewed were the nine different selections shown in Figure 10-6.

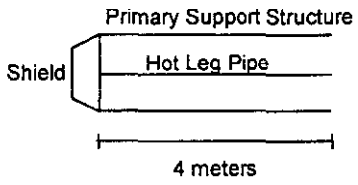



**Figure 10-5: Simple representation of the thermal expansion analysis geometry.**

### 10.2.4.1.2 Analysis Description

Analysis was performed using a Microsoft Excel spreadsheet based upon the following equation for thermal expansion:

$$Expansion = \alpha \Delta T L$$

**Equation 10-1: Expansion due to Thermal Strain**

**Table 10-3: Description of Parameters Used in the Model**

| | |
|---|---|
| $\alpha$ | Coefficient of Thermal Expansion between the target temperature and room temperature |
| $\Delta T$ | Temperature difference between room temperature and the current temperature |
| L | Length of Primary Support Structure and Hot Leg Pipe |

The value of thermal expansion for each candidate material was calculated using Equation 10-1. The difference in expansion between the pipe candidate materials and titanium Primary Support Structure is the relative movement between the two that secondary structure would need to accommodate.

Microsoft Excel is verified as part of the standard productivity suite for the NRPCT. The models were created and tested for comparison to hand calculations for qualification.

### 10.2.4.1.3 Spreadsheet Results

The secondary structure would need to account for a relative difference in thermal expansion ranging from 8 millimeters to 32 millimeters, depending on which hot leg pipe candidate was selected as shown in Figure 10-6.

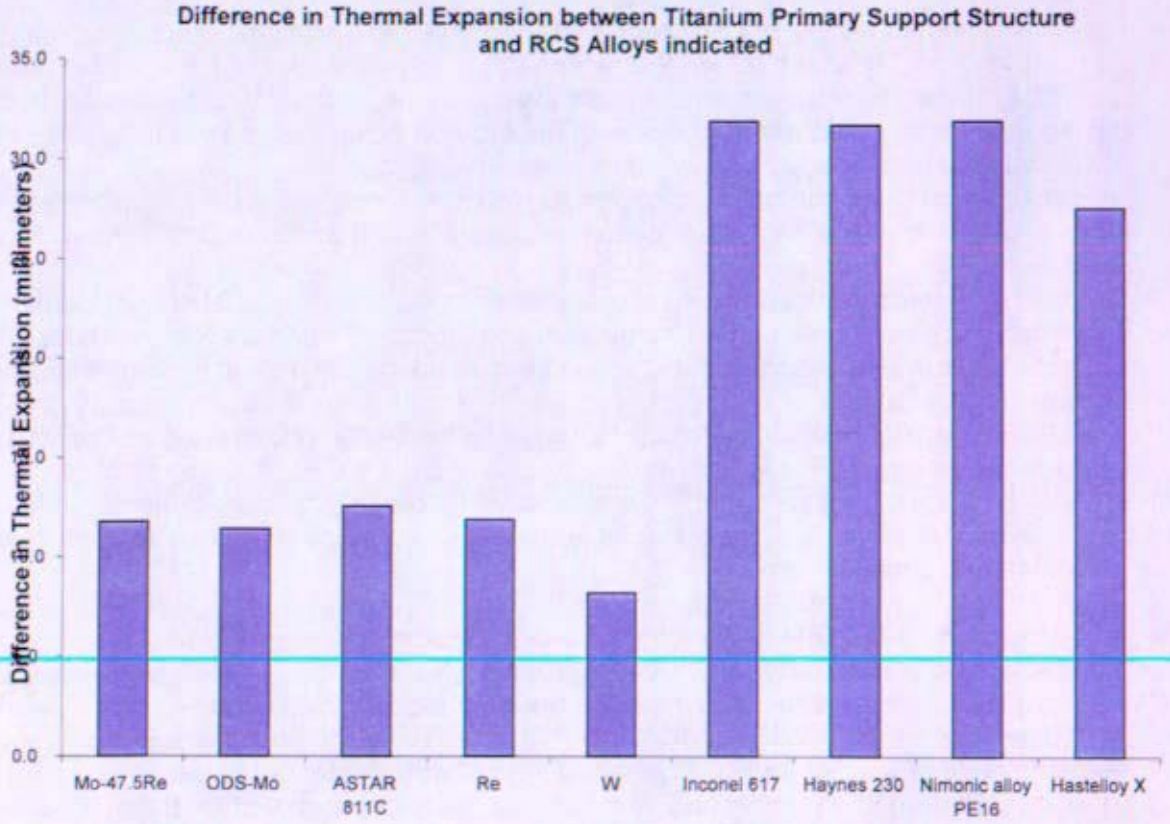



**Figure 10-6: Primary Support Structure and RCS Thermal Expansion Comparison**

### 10.2.4.2 Dynamics and Thermal Response Model

Analyses were performed of a pre-conceptual four Brayton hot pipe arrangement. The cold leg piping would have the same issues since the arrangement is similar and expected operating wall temperature is close to that of the hot pipe. The analyses assessed the effects of piping wall thickness, primary support structure temperature and material, and the piping support flexibility on primary (pressure) and secondary (thermal) stress levels. Section 9.7 of this report shows the details of this analysis.

The assessments with rigid piping supports showed high piping stresses (exceeding ASME allowable) due to the large linear thermal expansion difference between the piping and structure. Analysis indicated that the flexibility in the piping support needed to reduce thermal stresses would result in inadequately low piping system natural frequencies. These low frequencies would be excited during launch and probably result in excessive vibration loads. Alternatives to flexible piping supports are

necessary to provide for adequate piping system stiffness during launch and allow for sufficient differential thermal expansion of the piping to reduce stresses to an acceptable level.

### 10.2.4.3 Secondary Support Structure Development Needs

As identified previously, accommodation of thermal expansion would be a major function of the secondary structure. A number of stress relief methods may be considered as options but have not been explicitly evaluated, including:

- Floating/Sliding support at the Braytons and energy conversion components which are locked during launch and released during operation. When they are released, the support will allow the approximately 3cm movement required to accommodate the piping expansion. Use of this approach might also make grouping of the Brayton components advantageous so that the entire group can be allowed to move on a single platform.
- Releasable piping support collars along piping length. These releasable supports would react loads and assure adequate system dynamics during launch and then permit movement after reactor start-up.
- Materials with temperature dependent properties or with orientation dependent properties such that both sets of load conditions (launch and thermal) could be accommodated. Evaluation of material groups that better accommodate the differential movement would also warrant investigation.
- More flexible piping methods including Bellowed piping bends or more expansion loops and bends in the piping.
- Pre-stressing the piping such that the stresses will be partially relieved during normal operations. This will reduce the stresses at the operating point of higher temperature but reduce margin during launch.

An alternative to accommodate thermal expansion would be selection of materials which do not develop significant differential expansion induced stresses. For example, several materials shown in Figure 10-6 have lower relative expansion than the baseline nickel based super-alloys. However, these materials are not without other disadvantages, such as sensitivity to air, which make use difficult. With the materials within the RCS, particularly the hot leg pipe, not selected, there could have been an investigation into primary and secondary support structure and RCS materials that better accommodate thermal expansion on the basis of favorable coefficient of thermal expansion.

A combination of the above options might be desirable because not only must the hot and cold leg piping expansions be accommodated but also relative movement of the different components within the RCS as the system heats up (or cools down if switching to a backup Brayton or changing state points). As part of this hybrid accommodation approach, the use of more compliant materials for some of the supports might accommodate differential expansion as well as provide desirable vibration isolation and damping.

In addition to accommodation of thermal expansion, the secondary structure would need to perform other functions such as support other module components (cables, sensors, thermal control and micrometeor protection elements, etc), interface to hot components, provide dynamic isolation during operation, etc. Some of the challenges include:

- Provide thermal isolation of components while providing adequate strength and stiffness. This isolation would minimize temperature and thus stress gradients within the components being supported and the primary structure elements to which they would be attached. Testing would need to demonstrate performance and ability to withstand the elevated temperatures and radiation in the reactor module. A combination of different materials, joints and support configurations would need to be investigated.
- Withstand locally high temperatures, especially at joints. This is similar to the prior item, but focuses specifically at the need to withstand the high temperatures.
- Removal of heat away from the hot leg.
- Provide adequate stiffness, strength, and dynamic isolation during launch.
- Prevent transmission of dynamic excitations and prevent resonance amplification of vibrations during operation.

As component development continued, it would have been essential to include the dynamic response of each component and the connection to the secondary structure into an overall dynamic model. The component, secondary, and primary structures would be dynamically coupled, and a refined design would have been reached through parallel investigations.

### 10.2.5 Summary

A multi-functional support structure would be needed to satisfy the requirements of the reactor module throughout the life of the mission. The Primary Support Structure would supply strength and stiffness to the reactor module while providing mounting locations for the secondary structure and micrometeoroid protection. The Primary Support Structure would also need to account for thermal expansion and allow the components to radiate heat to space. The Secondary Support Structure would need to provide isolation and protection for the component subassemblies throughout the mission. It would also need to account for thermal expansion of the components relative to the Primary Support Structure while allowing heat to be radiated to space.

Successful development would require the Primary and Secondary support structures to work together, each performing specific tasks to support the overall objectives. Coordination of the support structure design with the design development of the piping, components, arrangements, and thermal management would be required to determine the best type of structure. As the reactor module design matured, each structural configuration would need to be optimized and compared to determine the best structure with respect to the mission requirements. The current support structure efforts do not indicate a clear solution, but rather a path for future investigations.

## 10.3 Thermal Control Subsystem

### 10.3.1 Introduction

The primary purpose of a thermal control subsystem is to maintain all the elements of a spacecraft system within minimum and maximum temperature limits for all mission phases. Another role of the Reactor Module thermal control subsystem is to minimize heat loss from the Reactor Coolant Segment (RCS) in order to prevent loss of usable energy. These goals are achieved through the use of thermal isolation between elements with different temperature limits, by thermal coupling of elements where applicable to minimize temperature differences and to transport heat energy as required, by addition of heat where necessary to maintain temperature above lower limits, and by rejection of heat to space via radiation.

The following sections summarize the pre-conceptual scoping efforts to develop an integrated thermal management approach for the reactor module. Several general conclusions are presented, based upon preliminary evaluation efforts. Subsequent sections also capture some of the important requirements and goals for a thermal control subsystem, describe basic thermal control approaches commonly used for space applications, describe the various environmental zones in the reactor module, summarize scoping calculations for several segments, and summarize the pre-conceptual thermal model efforts.

### 10.3.2 Summary of Conclusions

There are several competing thermal requirements within the reactor module. These include minimizing heat loss from some components; rejecting significant heat from some components; maintaining heat loss from the hot leg piping near a nominal level; maintaining sensitive components such as the alternator, the CDM's, sensors and other electronics at moderate temperatures; keeping pre-start-up temperatures and power demands within reasonable limits; and providing micrometeoroid protection. Scoping analysis and modeling were performed to assess the methods required to satisfy some of these requirements, to assess possible limitations on design options and to identify areas where more effort would be needed to develop and demonstrate materials or methods necessary to achieve the design goals.

One of the central thermal management requirements aft of the reactor is rejection of approximately 2.1 kW/meter of heat from the hot leg piping in order to maintain temperature within the pipe wall near 900 K. To meet this requirement, heat must be transferred away from the piping via radiation and/or conduction to surfaces with thermal properties selected and controlled to achieve the desired heat rejection flux. To maintain lower temperatures in the other portions of the reactor module, it is desirable to transport the heat to a radiative surface for rejection to space and to thermally isolate the hot leg from the rest of the plant. With this approach radiator area is kept small by rejecting heat during normal operation at an elevated temperature (assumed 500 K in the scoping calculations). Keeping the radiator area small permits a small amount of heat to maintain temperatures above lower limits before start-up. Non-uniform distribution of temperatures could pose an additional challenge in terms of distortion and stresses. Thermal and structural isolation of the heat rejection elements would help reduce impact of high temperature zones on other parts of the reactor module.

In order to implement effective rejection of heat from the hot leg piping, and isolate from the rest of the plant, several elements need to be demonstrated. These include:

A means to transport heat from hot leg piping to external radiator. Depending on the number of braytons, which would drive the amount of hot leg piping, the amount of heat to reject to space would likely be between 10 and 15 kW, which corresponds to a radiator area of approximately 4 to 7 $m^2$ assuming 500 K rejection temp. An effective means of transport will be needed to deliver this amount of heat to the radiator area. Further effort will likely be needed to demonstrate options such as a high conductive material, two-phase transport (heat pipe), or perhaps a light pipe for the needed temperature range.

Thermal coatings good to 500 – 600 K, (or higher near the reactor) with high emissivity, for the surfaces radiating to space. These need to be demonstrated for the radiation environment that will be encountered.

A complicating factor for both the structure and the thermal control subsystems would be the differential expansion between the primary support structure and the reactor coolant segment. Heat rejection elements would either need to be structurally un-coupled from the hot leg piping (eg, rely on radiative transfer) or move with the hot leg piping (eg, a floating platform that moves with the piping). These considerations would need to be a primary consideration as the structure and thermal control subsystems are developed.

Insulation is required to minimize the heat loss from most elements of the reactor coolant segment except the hot leg piping. A high temperature multi-layer insulation system was described in Reference 10- 4 which would provide an effective emissivity of .02. Scoping calculations using an effective emissivity of .03 (higher value to account for other parallel heat flow paths) for the hot components, except the hot-leg pipe and the turbine, show that heat loss is reduced by nearly half through the use of blankets (from approx 35 to 17 kWt).

The non-radiator portion of the reactor module envelope aft of the shield must be blanketed in order to keep pre-start-up temperatures above 200 – 250 K with a reasonable amount of heat input. However, excessive blanketing could result in excessive temperatures during normal operation. Preliminary calculations indicate that reducing the effective emissivity below ~ 0.1 to 0.2 could result in excessive temperatures during normal operation. Thus, a balance must be achieved between the normal and pre-start-up thermal requirements. It is possible that micrometeoroid protection could provide the degree of blanketing desired.

Power required to maintain pre-start-up temperatures above 200 K without solar illumination is estimated to be approximately 1500 Watts (see scoping calculations for plant support, shield, and reactor), which is below the power required for start-up. This assumes emissivity of 0.95 for the primary support radiator region (~4 - 7 $m^2$ as described previously), the shield, and the reactor envelope, and effective emissivity of 0.2 for the non-radiator regions of the primary support. If the radiator areas can be oriented toward the sun, the power to maintain temperature can be reduced significantly with proper selection of surface emissivities, and pre-start-up temperatures closer to room temperature.

It is highly likely that some sort of environmental shield would be desired to protect the reactor assembly from the detrimental effect of micrometeoroids, and a one or two layer shield is likely the best means to maintain modest heat rejection capability while providing significant protection. Scoping calculations indicate that a two layer micrometeoroid shield would result in effective

emissivity of approximately 0.3 (actual value would depend on thermal-optical properties of materials selected). It is likely that the leading surface (which would be located opposite the shield) would need to be more substantial to provide adequate protection. Preliminary analysis in Reference 10- 16 indicates that the effect on temperature of increased protection axially above and below the reflectors would be small. Efforts directed toward increasing emissivity of the reflector outer surfaces and reducing thermal coupling between the reflectors and the pressure vessel may help relieve the temperature increase caused by micrometeoroid shielding.

### 10.3.3 Development Process

The process to determine the thermal control measures needed for the reactor module would include the steps indicated below. An important effort that would need to happen in parallel with the process described would be the identification and testing of candidate materials and processes required to achieve the desired thermal control.

- Define requirements, acceptable temperatures and heat loss limits for each component
  - Depends mostly on the materials limits and operational constraints of each component
  - Most electronics perform better, and with greater reliability, at temperatures near 20 C, motivating efforts to reduce temperatures where possible.
  - Typically, minimum heat loss would be the goal except where temperature limits might be exceeded.
- Quantify heat sources
  - External Sources (Primarily solar)
  - Internal Sources (Includes Reactor, Reactor Coolant Segment, Radiation Heating, Energy Conversion and Transmission)
- Develop detailed mathematical models of the conductive and radiative heat transfer paths
  - Finite difference and finite element codes to handle the complex geometry and time varying conditions are available.
  - Correctly show interaction between the various reactor module segments, so that coupling and isolation can be captured.
- Implement required thermal isolation, thermal conduction, and thermal radiation control
  - Hot items are isolated from cooler items using low conductivity materials, blankets, and selective thermal coatings.
  - Excess heat is delivered to radiator surfaces using high thermal conductivity materials or heat transport systems.
- Test completed system to demonstrate control and update thermal model
  - Model correlation is performed in a thermal vacuum environment.
  - Design modification is sometimes required after test to achieve the desired temperature ranges and margins.

## 10.3.4 Requirements and Goals

Some important requirements which apply to the thermal control subsystem are listed below. For each, the source, a discussion of how it would affect the thermal control subsystem and possible impacts are given. The requirements and objectives which follow are not meant to be a complete listing – simply a presentation of requirements identified during development efforts as important to capture and consider during early phases of the design development.

| Requirements (Source) | Discussion and Impact |
|---|---|
| Heat rejection from hot leg piping shall be controlled so that magnitude of heat transfer from piping is maintained at [2.1] kW/meter. *(Derived from hot leg piping analyses)* | At 500 K, approximately 0.75 $m^2$ of radiator area is needed for each meter of pipe. Special accommodations must be made to transport the rejected heat to the radiator area, and minimize thermal and structural impact on nearby elements. Heat rejection approach must maintain the protection of the hot leg piping from the external threats of orbital debris and micrometeoroids. |
| Temperatures shall be maintained above minimum acceptable levels using electrical heating power levels below that required for start-up. *(Derived from survival temperature and pre-start-up power availability limits)* | By keeping outer surface temperatures above 200 K, internal temperatures will generally be well above 200 K. Goal is to keep stresses low, avoid temperatures outside the limits of widely available electrical components, and minimize temperature gradients during start-up without power levels exceeding those needed for start-up (thereby not increasing power demand for reactor module). Significant portions of the module aft of the shield must be blanketed to meet this requirement. |
| Temperatures and temperature induced stresses shall be maintained within the minimum and maximum allowable limits for materials and components *(Derived from environmental and performance requirements module)* | Temperature extremes and differential temperatures must be minimized to achieve this requirement. This will require thermal isolation of some components, blanketing of components and surfaces, and effective coupling to radiator surfaces, and other thermal control techniques. |
| Thermal performance requirements shall be met under the conditions of the external thermal environment as described in Section 10.1.3.3.1 *(Level 2 Requirement)* | Low space temperature and solar flux are the primary external thermal environments that would affect the module. Outer surface properties would be designed to provide the needed coupling to space. Solar flux would generally not be difficult to accommodate, and could provide desired heat prior to start-up. |
| Unless specified otherwise, temperatures of electronics and mechanisms (primarily including I & C electronics and CDM's) shall be maintained below [400] K, with target temperature goal of [300] K. *(Derived from equipment temperature limits and goal of providing moderate temperature for electronics and mechanisms to improve performance and reliability)* | Isolation of the hot leg piping and hot components from the rest of the module is necessary. Blanketing of all components except the hot leg piping is anticipated.<br><br>Note: The target temperatures which appear in brackets are placeholder values only. Actual values could differ and values for CDMs and other electronics could differ from each other. |

Note: Values in brackets [XX] are preliminary or placeholder values and thus would be subject to change.

In addition to the requirements listed above, there would have been a number of considerations which would have influenced the design of the thermal control subsystem. These include:

- Creation of thermal zones to meet the specific requirements of different components
- Changes in performance of components, thermal control materials, etc, over temperature and from beginning of life to end of life
- Interface heat transfer, which is often a limiting factor in heat transport
- Available power to provide supplemental heating during cyclic or transient events, and to make up for beginning vs end of life performance changes.
- Temperature effects on performance
  - Thermal gradient induced stresses
  - CTE Difference induced stresses
  - Reliability vs temperature
  - Performance vs temperature
  - Ability of heaters, temp sensors, etc to perform beginning of life functions and then withstand high temperatures
- Charge build up and conductive paths
  - All layers of a blanket system must be grounded to provide a means for charge dissipation.
  - Outer surfaces in general need to be treated to prevent charge build up, provide means for charge dissipation, and minimize SGEMP (system generated electro-magnetic pulse) due to impact of charged particles.
- Micrometeoroids
  - Blankets are generally the first layer of micrometeoroid protection. Goal would be to satisfy micrometeoroid protection needs using same materials used for thermal control.
  - Micrometeoroids erode and therefore compromise the effectiveness of external thermal surfaces. This effect must be taken into account in determining performance of the system near the end of the mission life.
  - Micrometeoroid protection around reactor could result in radiation scattering outside reactor envelope, which could cause shield size and mass to increase. Scattering and envelope considerations may also affect approach to orientation and selection of the CDM's to minimize impact on shield configuration.
- Radiation
  - Materials selected for thermal control must perform after exposure to long periods of radiation.
  - Solar ultraviolet light causes many thermal coatings to degrade over time. This degradation must be taken into account in determining performance of the system near the end of the mission life.
- Orientation and variation with time
  - Over time, the orientation of a system relative to the sun will change, and at times there will be no solar flux, requiring that the thermal control system account for this absence of external heating.
  - Different mission phases and operating modes will result in transient conditions which must be evaluated.
- Contamination
  - In low earth orbit, atomic oxygen has been found to severely erode and compromise performance of all thermal control surfaces.
  - Surface missions will have to account for performance reductions due to erosion, chemical interactions, and deposition onto reflective surfaces.
  - Thermal control materials must be selected that meet out-gassing requirements. Consideration must also be given to the fact that the outer surfaces and radiators, due to their relatively low temperatures, could be accumulation surfaces for outgassed materials.

### 10.3.5 Thermal Control Methods

Heat transfer is divided into three major categories:

*Conduction* is energy transfer through matter in the absence of fluid motion. In spacecraft components, conduction is primarily used within components and smaller assemblies.

*Convection* is energy transfer between a moving fluid and a solid interface. Convection requires the presence of a fluid, which in space only takes place in a closed system and so is not a major factor in most space systems.

*Radiation* is energy transfer via electromagnetic waves. Radiation is the only means of heat rejection to space (with exception of an open refrigerant cycle which is rarely used and very short-lived). Radiation is the means of heat transfer between different components which are not conductively coupled.

Thermal isolation through use of low conductivity materials and (or) radiation barriers is frequently required when hot components are located on or near components that can not tolerate high temperatures.

There are two categories of spacecraft thermal control – passive and active. A detailed discussion of each of these follows.

#### 10.3.5.1 Passive Thermal Management Methods

Passive methods maintain the component temperature within the desired range by control of conductive and radiative heat paths, through selection of the geometric configuration of surfaces and optical properties of materials. There are no moving parts or fluids.

- Thermal coatings - Typically used to minimize solar flux absorptance, maximize heat rejection, or control radiative coupling between components.
  - Commonly used coatings include chem-glaze and silicone paints.
  - Sometimes anodized surfaces are used, but non-conductive quality poses a charge build-up concern.
  - Reflective surfaces are frequently used to minimize solar heat flux while allowing heat rejection. Includes mirrors, aluminized tape, metallic coatings (Germanium, aluminum, etc).

- Blankets - Used to eliminate radiation coupling between hardware elements or between hardware and space environment.
  - Usually made from lightweight multiple layers of kapton or mylar with spacing material to eliminate conduction.
  - High temperature blanket materials include metal foils (e.g., nickel alloy, titanium) and glass fiber fabric.
  - See Figure 10-7 for example of typical blanket construction.

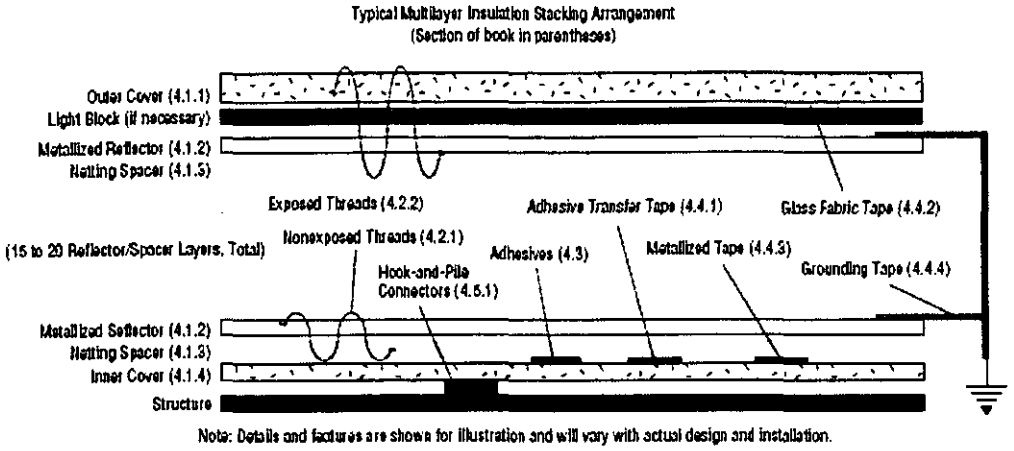



**Figure 10-7: Schematic Cross Section of Typical Multilayer Insulation (MLI) Construction (Not all elements need be present in every design) (Reference 10- 19)**

### 10.3.5.2 Active Thermal Management Techniques

Active thermal management techniques involve the use of moving elements or fluids, most commonly heat pipes, and the use of heaters which require active control and management. Other examples include moving louvers, which vary the amount of surface area exposed to space, and refrigeration cooling systems. Heat pipes and heaters are described below.

- Heat pipes are generally simple two phase fluid systems in which heat is removed from a source by evaporation, transported to the cooler end of the pipe, and then deposited into the sink by condensation, as shown in Figure 10-8. Some key characteristics of heat pipes include:
  - The fluid is transported by capillary action via external channels or through a wick.

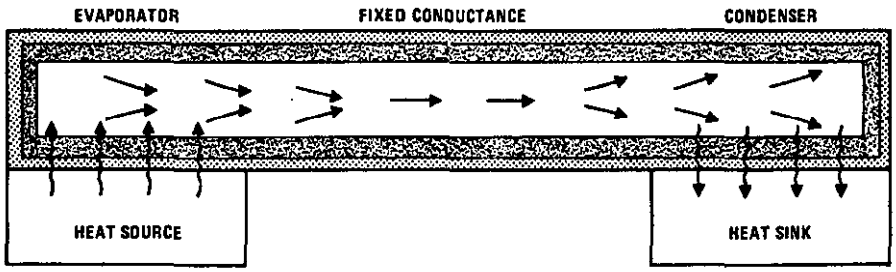



**Figure 10-8: Example of Heat Pipe Configuration (Reference 10- 20)**

- Heat pipes are used extensively in spacecraft as an effective means to transport heat from the point of generation to the point of removal to space.
- Different fluids are used in different temperature ranges. As indicated in the figure below, the capacity to transport heat near 300 K and above 500 K is somewhat limited. Further efforts to develop and fully demonstrate higher power heat transport near these temperatures, especially the range between 500 and 600 K, would increase design options for transport of the excess heat within the reactor module.

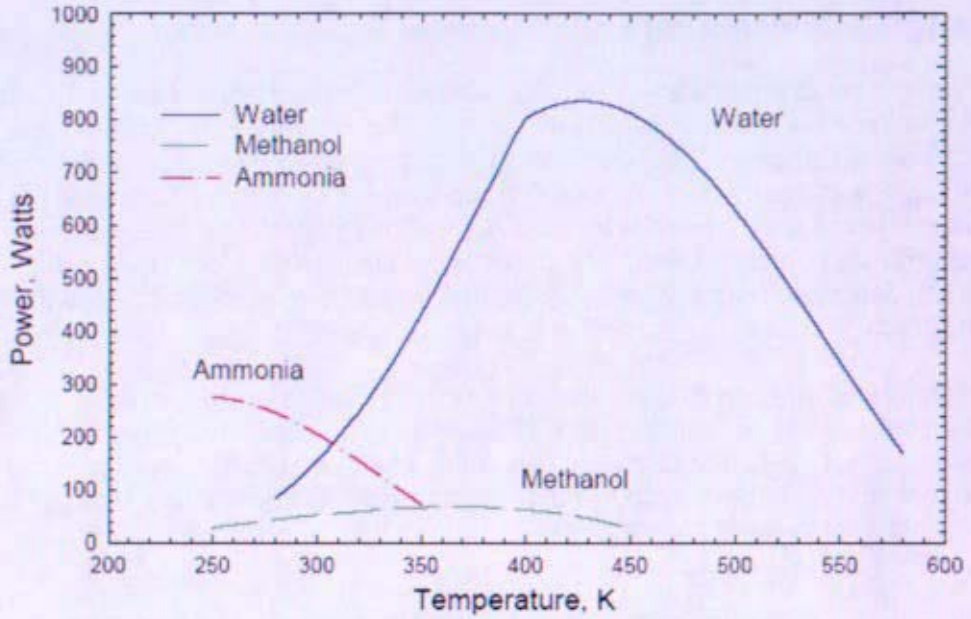



**Figure 10-9: Available Heat Pipe Fluids in Low to Moderate Temperature Range (Reference 10- 21)**

- Electric heaters are generally patch resistive elements mounted to surfaces with conductive adhesive. Temperature sensors near the heaters are required to indicate when supplemental heating is required. Control and power supply generally comes from the main space vehicle bus.

### 10.3.6 Thermal Management Zones

Different zones of the reactor module will require different thermal management solutions due to radiation, temperature, heat rejection requirements, configuration and other differences. The primary environmental zones are shown in the figure below. Scoping calculations for the reactor, shield and reactor coolant regions of the module were performed (Reference 10- 17) to provide rough estimates for thermal considerations such as pre-start-up power requirements, heat rejection levels, effect of micrometeoroid protection, radiator area, etc. In following sections, the primary thermal management considerations are described for the Reactor, Shield, Control Drive Mechanism (CDM), and Reactor Coolant / Plant Structure zones.

Considerations for the Signal and Power Transmission and Electronics zones are not explicitly discussed because these zones overlap with the space vehicle. However, it was assumed based upon communications with JPL that temperatures within the Signal and Power Transmission and Electronics zones would be controlled to remain within design and operational limits of the Instrumentation and Control components therein.

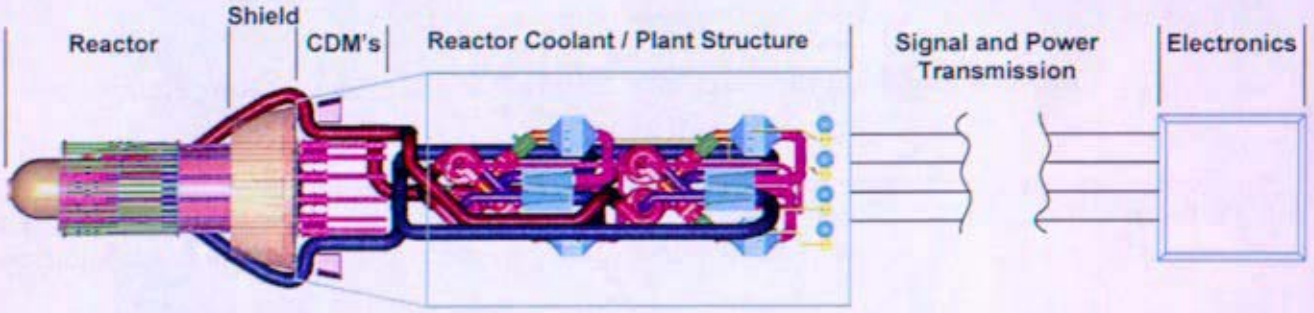



**Figure 10-10: Reactor Module and Related Environmental Zones**

#### 10.3.6.1 Reactor Thermal Management

This section looks briefly at the reactor segment thermal management from an external viewpoint – how does it interact with features such as the primary shield, micrometeoroid shielding, and hot leg piping and what significant concerns might be associated with thermal management of the reactor interfaces. Two thermal control concerns are impact of micrometeoroid shielding on reactor external temperatures and delivery of pre-start-up power to maintain the reactor at minimum acceptable temperatures prior to start-up. A scoping analysis (Reference 10- 17) assessed the degree to which micrometeoroid shielding would affect heat rejection and the maximum power needed to maintain the reactor envelope at 200 K before start-up.

The scoping analysis indicated that, given surfaces with typical thermo-optic properties, the effective emissivity is reduced from 0.8 to approximately 0.4 with a single layer cover and to approximately 0.3 with a two layer cover. Additional layers would further reduce heat rejection, thus increasing temperatures already estimated (Ref 10- 16) to be nearing material limits. Results from Reference 10- 16 indicate that reducing heat rejection at the ends of the reactor has less of an impact upon peak external temperatures than reducing heat rejection radially outward of the reflector zones. This could be significant because placement of micrometeoroid protection on the forward facing regions of the reactor would provide the most protection during forward travel of the vehicle with least thermal

impact on the reactor. Temperature increases due to micrometeoroid shielding might be lessened if the thermal coupling between the reactor pressure vessel and reflectors could be reduced and the thermal coupling could be increased between the micrometeoroid shielding and the reflectors, position controllers, etc.

There are several considerations regarding use of micrometeoroid protection around the reactor. Among the key advantages is protection of the vessel and the CDM's from the constant barrage of particulate it would experience during a long mission through different regions of the solar system. These materials would include a variety of elements, mostly carbon, hydrogen, oxygen and nitrogen. If unprotected, reactivity of exposed surfaces with these elements would need to be evaluated. Also, impact of micrometeoroids on CDM's may be a significant failure mechanism. It might be possible to provide a significant degree of protection by placing the majority of the protection forward of the reflectors, which would reduce the thermal impact on the reactor. A negative point would be the scattering that shielding outside the reactor envelope would create. If the shield is increased in size to protect against this scattering, a weight penalty could result. Another consideration when assessing the protection envelope is the position of the CDM's during launch. If the CDM's are full out away from the shield, the size of a protective envelope may be significantly larger, resulting in even further increases in shielding to protect from scattering. A final consideration is the selection and demonstration of protective material. Candidate materials would need to be tested for micrometeoroid protection effectiveness, for thermal properties, for radiation effects, and to assure that elements and compounds coming from the protective material, either in normal vacuum or following impact from micrometeoroids, does not have significant adverse effects on the reactor segment.

The scoping analysis indicated that the heat required to maintain the reactor outer surfaces above 200 K is around 400 Watts with no blanketing and conservatively assuming emissivity of 0.95. This represents an upper bound. Shielding, blanketing, lower emissivity and solar heating would all reduce this power level and/or increase the minimum temperature level.

The hot leg piping into the reactor poses two potential challenges – implementation of micrometeoroid protection and rejection of the heat necessary to keep the piping wall temperature at 900 K. An important option to consider would be thermally coupling the hot leg to the shield, thus using the shield area to reject the excess heat. A means to evenly transport the heat away from the piping and implement micrometeoroid protection would need to be worked out. Approaches to achieve these goals might use methods and materials similar to those used in the plant support area, but testing would be necessary to demonstrate these same methods can withstand the elevated radiation levels local to the reactor. Another constraint worth mentioning is the need to accommodate interface points for primary supports from the space vehicle and interface points for the aerothermal protection segment (aeroshell). These interfaces would need to be kept within the cone angle to avoid scattering and avoid interference with piping, reactor support, or other items.

### 10.3.6.2 Shield Thermal Management

The shield would comprise a large portion of the mass of the reactor module, and a significant surface area. This, combined with its location between the reactor and the rest of the reactor module, would make it an important element of the overall module thermal management. The target temperature of the shield would have to satisfy shield material requirements foremost – but other considerations would also be important. For example, shield temperatures mid-way between the reactor temperature and temperatures aft of the shield may help mitigate thermal stresses. The shield would need to reject heat from the hot leg piping (about 2.1 kW/meter of piping), which would necessitate that a portion of the shield be at elevated temperatures to effectively reject this heat. The shield might also need to reject heat near the reactor support locations to help moderate temperatures.

Several different shield options were being evaluated, and a discussion of these evaluations can be found in Reference 10- 18. With the exception of water, most materials considered for the shield can easily withstand the temperatures that would be expected. Extra measures would be required to isolate the water, if used, from higher temperature regions of the shield.

A scoping analysis for the shield was performed (Reference 10- 17) in order to describe the overall thermal behavior of the shield. A shield thermal model was created (Reference 10- 18) which provided some insight to how temperatures would be distributed within the shield, but this analysis was for early design configurations and does not match some boundary conditions. The scoping analysis characterized the average temperature and heat rejection characteristics of the shield, so that general feasibility can be evaluated and technical challenges identified. Specifically, sensitivity of the average temperature to blanketing and micrometeoroid shielding, and pre-start-up power requirements, were explored.

The following observations follow from the scoping analysis:
- The pre-start-up power required to maintain the shield outer surfaces (with emissivity of 0.95) at 200 K is about 300 Watts. This value could be up to 20 % higher for some of the larger shield sizes being considered. Solar energy would reduce this value somewhat, depending upon orientation and surface properties.
- Without blanketing or micrometeoroid protection, average temperature of the shield would be near 450 K. Addition of single or dual layer micrometeoroid shielding would result in significant increases in average temperature.
- Addition of a multi-layer insulating blanket over space-facing surfaces would result in significant heat retention, and unacceptable high temperatures.
- Thermal isolation of the shield from the module elements aft of the shield would probably be necessary to keep the non-RCS temperatures aft of the shield near target of 400 K.

Thermal management of the shield would need to consider the energy from the reactor and from the hot leg piping which passes through the shield. Energy from the reactor would be due to radiation induced heating inside the shield, as well as conductive and radiative transfer of thermal energy. The energy due to radiative heating is described in Reference 10- 18. The energy transfer due to thermal radiation and conduction are approximated in Reference 10- 17.

The latest concept for routing of hot leg piping through the shield has the pipe entering the shield top surface near one side, wrapping around the perimeter of the shield (just inside the outer surface), and exiting the opposite face up to 180 degrees from where it entered. As documented in the hot leg piping evaluations, approximately 2.1 kW/m of heat must be rejected form the hot leg to maintain acceptable temperature.

The combined energy input from the reactor and hot leg piping would need to be balanced primarily by heat rejection to space, with the resulting average temperature depending primarily upon the thermal optical properties of the space facing surfaces of the shield. Due to its elevated temperature, it is likely that the shield would need to be thermally isolated from the electronics and plant structure elements aft of the shield.

### 10.3.6.3 CDM Thermal Management

The region of the reactor module just aft of the shield houses the Control Drive Mechanisms (CDMs) The primary thermal goal in this region would be to maintain temperatures as near to room temperature as possible away from the reactor coolant piping. To achieve this goal, thermal isolation

from the coolant piping would be required. It would probably also be necessary to isolate from the shield. Multi-layer blankets could provide the degree of isolation desired, along with thermally isolating materials at the CDM and structure interfaces with the coolant piping and shield.

### 10.3.6.4 Reactor Coolant and Plant Structure Thermal Management

Thermal management concerns identified during the pre-conceptual efforts for the Reactor Coolant and Plant Structure segments include the following:

- Excess heat from the reactor coolant segment hot leg must be transported away from the hot leg piping and rejected to space. The amount of heat that must be transported away is approximately 2.1 kW per meter of pipe. The approach used would need to prevent large deviations from the targeted amount because too little heat removal would cause high temperatures and too much would force higher reactor power or temperatures to meet power demands.

- Heat loss from the reactor coolant segment must be minimized in order to minimize loss of power and to avoid excessive temperatures for nearby electronic components, cabling, mechanisms, and other components which would benefit from lower temperatures. In order to accomplish this, effective multi-layer insulation must be demonstrated to satisfy isolation requirements at high temperatures and elevated radiation levels. Further evaluation would be necessary to assess the degree of micrometeoroid protection provided by the multi-layer insulation.

- Related to the prior item is the need to provide thermal isolation of the reactor coolant segment components in order to minimize local heat transfer at interfaces. This would require identification and demonstration of insulating materials which can also meet structural requirements.

- Prior to start-up, temperatures within the plant must be maintained above minimum levels in order to prevent over-stressing electronics and structural elements. For the most readily available electronics, -34 C (239 K) is a minimum allowable temperature, and thus 239 K is a good goal for internal temperatures. If one assumes that there will be temperature gradients through exterior surfaces and blankets, and that zoning can be established to preferentially direct heat where desired, then a goal of 200 K for the outer plant surface appears reasonable. The heat input to achieve this goal is assessed.

- Protection from micrometeoroids typically requires multi-layer materials. These protective layers will reduce coupling to space of covered surfaces. The approaches to provide the necessary protection would need to be integrated with the thermal management efforts in order to satisfy both sets of requirements. The greatest challenge this would present would be meeting the micrometeoroid protection of the hot leg piping while simultaneously meeting the heat rejection requirements. Development of a heat rejection approach which transports the heat around the micrometeoroid protection might be necessary. This could be more difficult in the shield region, where envelope restrictions due to scattering restrict the available volume.

- Moderate temperatures for the electronic components aft of the shield would yield reliability and performance improvements over higher temperatures. For example, effective rejection of heat from the power transmission elements, especially near the alternator, will improve transmission efficiency. The CDM's would also benefit from moderate temperatures. In order to maximize transmission efficiency and avoid exceeding allowable insulation temperatures, similar heat rejection approaches used for the hot leg piping may be applicable.

### 10.3.6.4.1 Scoping Calculations for Reactor Coolant and Plant Support Segments

Scoping analyses for the Reactor Coolant and Plant Structure segments were performed. These analyses, which can be found in Reference 10- 17, are a simplified evaluation of the portion of the reactor module aft of the shield. A 2 brayton system was evaluated in order to match the thermal model effort described in the next section and capture an intermediate level of heat rejection.

The primary purpose of the analyses was to provide first order approximations for the amount of heat that must be rejected, the area needed to reject heat, the effect of blanketing, and the pre-start-up power needed to maintain external surface temperatures above 200 K. The latter evaluation was performed in order to determine if the power required to maintain moderate temperatures would be beyond the level which would be available prior to start-up.

In the scoping analyses, several global assumptions were made which are not defined elsewhere. These include:

- The ends of the plant support region are assumed to be adiabatic. (At shield and boom interfaces).
- No other module elements are included.
- Plant Support Segment dimensions are nominally those detailed in the Northrop -Grumman baseline configuration.

The following observations follow from the scoping analysis:

- Blanketing of the non-hot-leg components results in total of about 17 kW of heat that must be rejected, about 10 kW from the un-blanketed hot leg, 5 kW from the high temperature elements (turbine, turbine to recuperator piping, recuperator, and cold leg piping) and the balance from the other components. This result supports the observation during the modeling effort that grouping of higher temperature elements could establish easier to manage thermal zones.

- If assume that the excess heat from the hot leg piping, the turbine and the piping from the turbine to the recuperator (total of about 14 kW) is rejected via radiation to a 600 K sink, and then transported across a 100 K temperature delta to 500 K radiator surfaces, then the required radiator area to reject the excess heat is approximately 5 square meters, which is about 25% of the assumed plant outer envelope area. A more effective heat transport and distribution system that increases the heat rejection temperature would decrease radiator area. For example, an increase from 500 to 560 K would reduce area to almost 3 square meters.

- The average temperature for the remainder of the plant outer envelope is near 360 K, if assume that the effective emissivity for the non radiator area is 0.2. The effective emissivity of 0.2 is compatible with micrometeoroid protection. The value of 360 K is qualitative only, and there would be variation in the outer envelope temperatures. However, it does indicate that temperatures could be kept at moderate levels away from the reactor coolant segment components.

- The total power needed to maintain the radiator regions (effective emissivity 0.95) and non-radiator regions (effective emissivity 0.2) at 200 K before reactor start-up is approximately 700 Watts. Though only qualitative, this value indicates that modest power input will maintain pre-start-up temperatures above low extremes.

## 10.3.7 Power Plant Thermal Model

### 10.3.7.1 Modeling Goals

The overall goal of the plant thermal model was to quantify differences in heat fluxes, heat transfer within the plant, and global temperature fields for development of a thermal management strategy. During steady-state operation, thermal management strategy must balance component heat dissipation requirements and the need to thermally isolate hot components to prevent overheating of the support structure or loss of thermodynamic system efficiency. The initial modeling focused on the investigation of two thermal management concerns: development needs for passive strategies such as thermal coatings, blankets, isolation materials and the need for active heat dissipation during steady-state operation.

The expected use of the initial model was not to analyze a specific combination of arrangement geometry, heat balance state points, and thermal management strategy, but to use the arrangement and heat balance as the basis for running sensitivity studies.

### 10.3.7.2 Modeling Approach

The thermal modeling strategy explored appropriate use of flux or temperature boundary conditions as model inputs and the resulting model outputs. Due to the directional nature and the non-linearities inherent in the problem, prior spreadsheet calculations were of limited use for predicting local system temperatures. Use of system heat balance temperatures in the model ensured that an internally consistent set of temperature inputs was applied to the model. The model temperature outputs and heat balance temperatures were input into a spreadsheet calculation to predict model heat fluxes. This spreadsheet result was used to benchmark the model's estimate of system heat fluxes.

The model analysis code selected for the initial effort was ABAQUS version 6.5-3, because it was judged able to meet all of the stated requirements while also being the NR program standard finite element software. The 2:1:1 version 5 arrangement (Reference 10- 3) was selected for investigation to minimize the effort required to generate a layout and ensure some similarity between the thermal model and the state of the arrangements. Further details about the model, such as modeling assumptions, boundary conditions, modeling strategy, verification, qualification and sensitivity can be found in Reference 10- 17.

### 10.3.7.3 Model Description

Shown in Figure 10-11 is a view of the generated model of the energy conversion system inside the primary support structure shell. The energy conversion system was represented by simplified rectangular elements, and the shell as titanium sheet. The shell diameter was modeled at approximately 2.8 meters, which made conclusions about temperature distributions difficult.

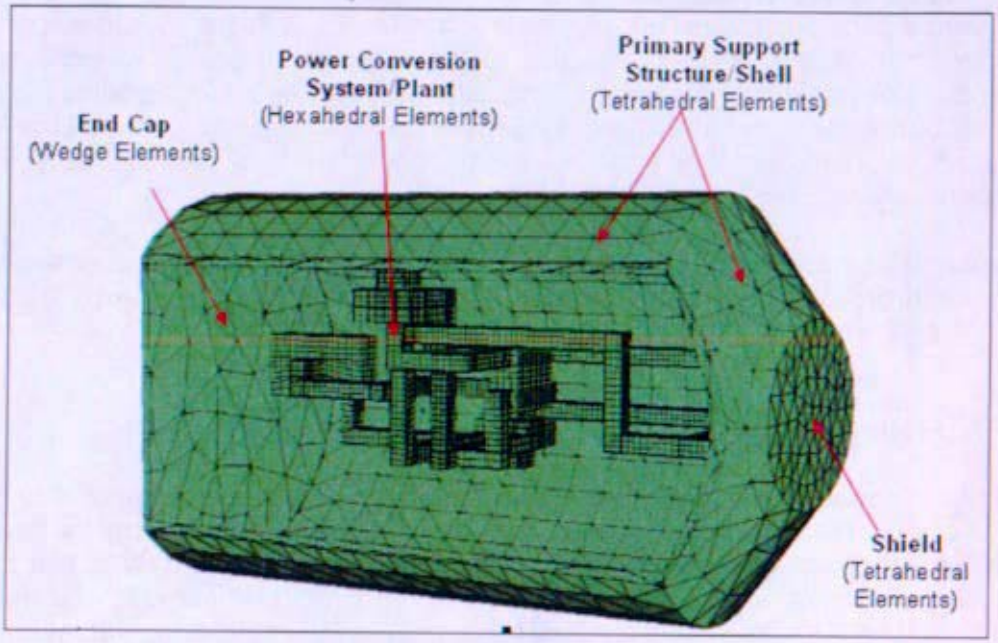



**Figure 10-11: Thermal model – Assembly of plant, shield back cap, and PSS shell**

### 10.3.7.4 Model Results

The baseline case was intended as a first-order, proof of concept model. The model had significantly greater capability than spreadsheet calculations and was capable of solving for local temperatures and fluxes in the shell and in components where no boundary conditions exist.

The outer structure temperature ranged from approximately 400K to 320K. Actual structure temperatures would be higher because the model radiation area of the outer shell is larger than a prototypic PSS would be, but the results provided a baseline for comparison. These results can be seen in Figure 10 - 12. The plant is shown directly below the shell in the same orientation for comparison. Note that in the left subfigure, the hot leg piping runs along the shell for a greater distance than in the right subfigure. This resulted in the hot spot along the centerline of the shell (indicated in lighter blue).

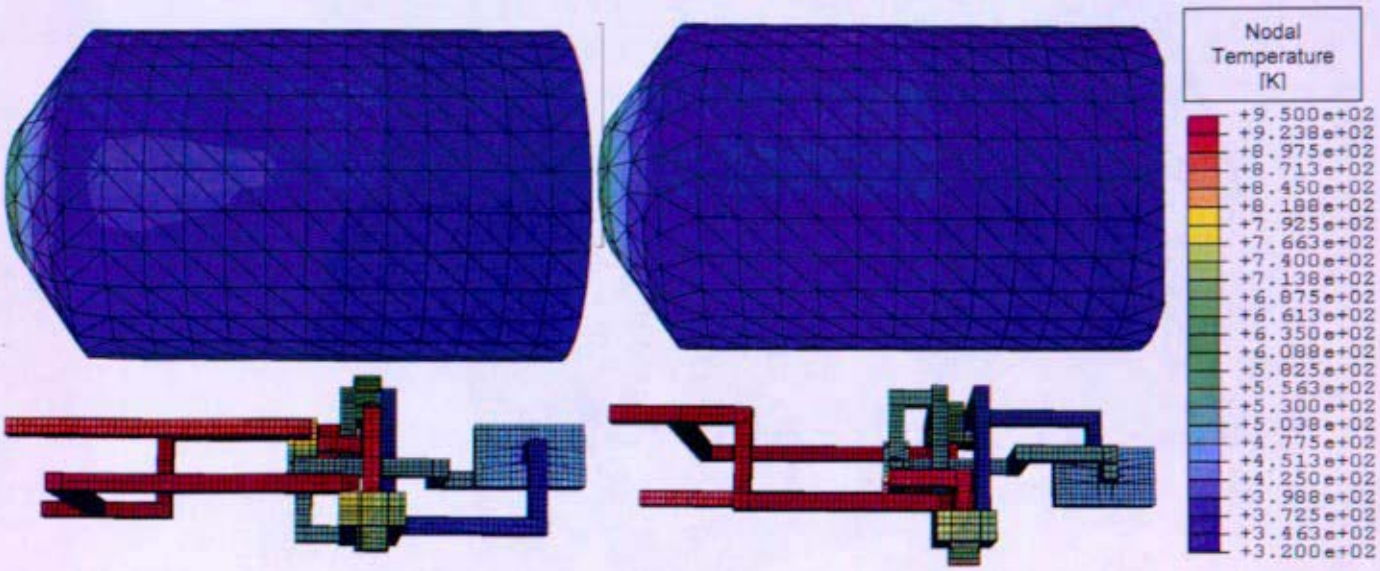



**Figure 10 - 12: Side view temperature profile**

The global heat transfer from the plant to the shell is estimated within ABAQUS as the sum of the radiation flux on the inner shell facets from the plant. This heat transfer was calculated to be 34.6 kWt for the *Baseline* case. This number serves as the figure of merit in any of the trade studies run off the *Baseline* case and will be discussed further in 10.3.7.5.

Minimizing heat loss can be accomplished in two fundamental ways: the thermal resistance can be increased by decreasing conductivity or emissivity, or the driving potential can be decreased by reducing the temperature difference. Reducing the temperature difference between a component and its environment can be accomplished by grouping components of like temperature into thermal zones.

Thermal zones are well defined in the fore-aft positioning of components in the model. Hotter components are grouped toward the front of the assembly, cooler components toward the rear. Figure 10 - 13 shows the result of the fore-aft thermal zoning. There is elevated temperature in the shell along the hot and cold legs but depressed temperature in the vicinity of the gas cooler and colder piping. The recuperator and Braytons are positioned centrally.

Further observations about thermal zoning within elements of the energy conversion system are presented in Reference 10- 17. The specific characteristics of the observations would be affected by many factors, including blanketing of elements, proximity to other elements and the outer shell, and presence of structural elements. Regardless of the specific observations from this model, the modeling of radiation interactions and thermal zoning is an important outcome of the modeling. Regardless of the global heat loss or material properties, the specifics of the arrangement geometry can create thermally isolated regions. These regions can be either advantageous or dis-advantageous depending upon the heat dissipation requirements of the component.

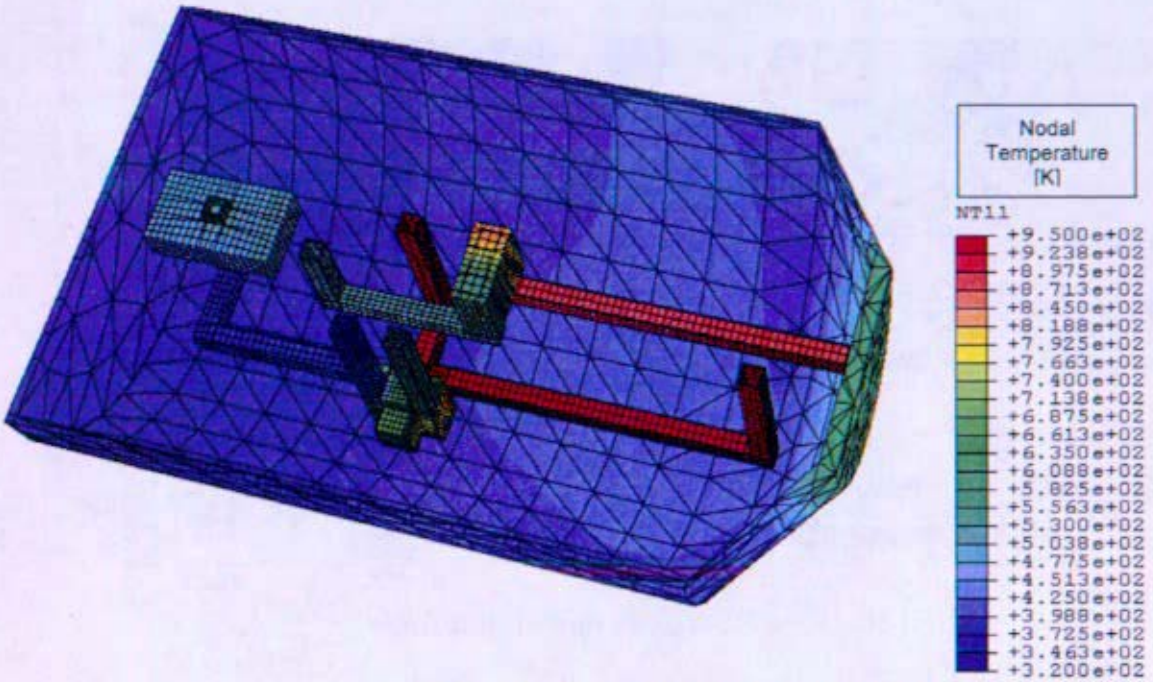



**Figure 10 - 13: Fore-aft thermal zoning**

### 10.3.7.5 Trade Studies

Four alternate cases were created to determine sensitivity of global heat loss to changes in different parameters. More details about the cases can be found in Reference 10- 17. The different cases and resulting observations are discussed below.

In one case, the shield temperature was reduced from 600 K (the baseline assumption) to 450 K to approximate the effect of thermally isolating the shield from the rest of the plant. This resulted in lower plant temperatures and a corresponding increase in heat rejection from 34.6 to 39.1 kW due to the lower shield and outer shell temperatures.

In the second case, insulation of the non-hotleg piping was represented by reducing the effective emissivity to .02. This case resulted in a nearly 30% decrease in heat rejection, from 34.6 to 24.7 kW. The pipe blanketing reduces heat loss as expected by isolating components from radiation interactions. Correlating this reduction to the blanketing strategy would be a priority of future work. This result indicates and confirms that, with the exception of the hot leg piping, the system must be thermally insulated throughout to minimize heat loss.

The third case used the NRPCT generated heat balance to generate energy conversion system boundary conditions, and contained a more reasonable estimate of hot leg pressure boundary temperatures and system state points that fully account for arrangement specific piping pressure drops. Details of the specific changes can be found in Reference 10- 17. Heat loss reduction of 8% resulted from the component temperature changes, indicating that the baseline was conservative and also that the modest changes do not have a large effect on predicted heat loss.

The fourth case took advantage of the off design capabilities of the NRPCT heat balance to investigate the difference in plant heat loss at different points during the mission lifetime. The heat balance incorporates a 14.5% margin in radiator area for the design point to account for damage to the radiator or radiator performance degradation (only 85.5% of the radiator would dissipate heat at end of life). The beginning of life cases assume that 100% of the radiator area (required area plus margin) is used resulting in increased system efficiency. This case resulted in a 2% decrease in plant heat loss. This change in heat loss is comparatively insignificant compared to the effects of thermal blanketing and change in shielding temperatures. Plant heat loss is a comparatively weak function of radiator margin within the operating range.

### 10.3.7.6 Future Modeling Approach

The next iteration of the model would have included a representation of the Secondary Structure. This inclusion would have provided a conduction path between the Reactor Coolant Segment and the Primary Support Structure. The addition of the Secondary Structure would likely create local hotspots on the Primary Structure, resulting in an increase in the overall amount of flux dissipated to space. The resulting temperature profile through the Secondary Structure could aid in the overall design of the Secondary Structure by means of providing an input to the thermal expansion analysis discussed in Section 10.2.4.

Future model development would be coupled to the Primary Support Structure discussed in Section 10.2. Currently the Primary Support Structure is represented as a sheet-stringer and a variation in this type to a truss, or honey-comb could cause great variation in the results. A model corresponding to each configuration would have been generated to ascertain which Primary Support Structure had the best thermal/system performance.

Future sensitivity studies would have focused on thermal blanketing, geometric dependences, variable boundary conditions, varying emissivities, and potential arrangement considerations like overall pipe layout optimization.

Component thermal models would have been incorporated into the second order model for future model iterations. Second order thermal models would have exceeded the current limitations of ABAQUS 6.5-3, leading to other modeling techniques being investigated. Future versions of ABAQUS will likely parallelize the calculation of the view factors and also allow the view factor matrix to be saved and reused in later calculations. These simple advancements would greatly reduce the run time, enabling more sensitivity studies to be run. It was further expected that nodal and memory limits would be raised in keeping with computational development. If ABAQUS were still found to have insufficient capability in the future, there are other aerospace thermal codes such as TRASYS and TSS that would warrant evaluation as the primary thermal modeling tool for the Reactor Module.

### 10.3.8 Summary

Several important observations resulted from the thermal control system efforts. These include the following:

Thermal control demands would be a significant driver for the arrangements. Placement of the hot leg piping away from the center and near the outer portions of the module would make isolation of the hot leg from other components easier and more importantly facilitate rejection of the excess heat to space. Isolation of hot and cold elements from each other, by a combination of blanketing and/or grouping into thermal zones, would be necessary to minimize heat loss and heat exchange between different plant components.

Technology development would be necessary to demonstrate the needed elements necessary to provide adequate thermal management. These include but are not limited to

- Demonstrate thermal coatings that can survive the temperatures and radiation levels within the *different zones*
- Demonstrate blanketing material options for different spacecraft zones
- Demonstrate thermal interface materials that can withstand the high temperature and radiation while providing the thermal conductivity or isolation required
- Demonstrate heat pipe or other heat transport performance for the needed heat input levels over the temperature range of 400 – 600 K

The non-radiator portion of the reactor module envelope aft of the shield must be blanketed in order to keep pre-start-up temperatures above 200 – 250 K with a reasonable amount of heat input. However, excessive blanketing could result in excessive temperatures during normal operation. Preliminary calculations indicate that reducing the effective emissivity below ~ 0.1 to 0.2 could result in excessive temperatures during normal operation. Thus, a balance must be achieved between the normal and pre-start-up thermal requirements. It is possible that micrometeoroid protection could provide the degree of blanketing desired.

The detail needed to provide complete thermal models would have exceeded the current limitations of ABAQUS 6.5-3, leading to other modeling techniques being investigated. Future efforts would need *to evaluate available analysis tools early in the design process, so that appropriate tools could be* made available when necessary.

It would be necessary to consider other requirements while developing the thermal control methodology. For example, micrometeoroid protection will serve as part of the thermal blanketing in some area. However, regions requiring both heat rejection to space and micrometeoroid protection might require special arrangements. For example, it might be necessary to place micrometeoroid protection between the radiator and the protected elements, and find methods to transport the heat to the radiative surfaces. Thermal protective surfaces would also need to mitigate charge build-up and minimize contamination.

## 10.4 Micrometeoroid and Orbital Debris

Micrometeoroids and orbital debris are space-borne particles ranging in size from very small ($10^{-12}$ g) to very large ($10^{2}$ g), and with velocities sometimes exceeding 20 km/s. Without adequate protection, there is an unacceptable chance that an impact by a micrometeoroid or orbital debris would result in a mission ending failure. To underscore this concern, the loss or termination of approximately eleven previous space missions is attributed to a micrometeoroid impact (Giotto, Image, ISEE-3, Mariner 4 and 7, MSTI 2, Olympus, SEDS 2, Vega, Voyager, and Wind), Reference 10- 6. Although unproven, several other missions are also thought to have been ended by a micrometeoroid impact.

The JIMO spacecraft would be much larger than most previous spacecraft. This fact, combined with the long mission duration and proven vulnerability of a spacecraft to mission ending damage, makes protection from micrometeoroids and orbital debris an important design consideration. To properly address this issue, it is important to understand the different protection methods and to incorporate them into the spacecraft design during the preliminary project efforts.

This section describes the nature of the micrometeoroid and orbital debris environments, methods for evaluating the threat to mission success, and approaches to design and testing of various mitigation systems. The goal of this section is to present the basic principles and to summarize how they could be applied to the reactor module design.

This section resulted from efforts to collect and organize the large amount of information regarding micrometeoroid and orbital debris protection. Most of the information in this section comes from other sources, mostly NASA. More detailed information can be found in the indicated references.

### 10.4.1 Orbital Debris

Orbital debris is classified as man-made debris in near Earth orbit with a mass typically greater than several grams. The orbital altitude for the majority of these objects ranges between 700 km and 2000 km, but it is possible for the debris to be in orbits higher and lower than those altitudes. Figure 10-14 is an example of the altitude dependence of the flux data.

There are approximately 100,000 objects in low Earth orbit greater than 1 cm in diameter, 12,000 of these are greater than 5 cm in diameter. Orbital debris can range from the microgram scale to kilograms. Aluminum is the predominant material due to prevalence of space junk, Reference 10- 14. The velocity profile for orbital debris is between 2 km/sec and 14 km/sec with the average velocity being around 10 km/sec.

The next two sections discuss data for orbital debris, how to apply it, and different methods that could be implemented to mitigate the possibility of mission ending failures due to orbital debris impact in low Earth orbit.

#### 10.4.1.1 Orbital Debris Flux

The flux of orbital debris, particles per square meter per year, for the JIMO mission was modeled using the Orbital Debris Engineering Model ORDEM2000 from the Johnson Space Center (JSC). This model provided flux data by specifying a combination of parameters. From these parameters, data can be obtained as a function of orbital altitude, velocity, inclination, and/or particle size. Tables were available from the NASA Jet Propulsion Laboratory (JPL) Prometheus Project Environmental Requirements Document (ERD), Reference 10- 9, and directly from JSC. JSC can also provide

predicted data for the number of hits by orbital debris per year at the different orbital altitudes. To provide this data, impact surface area, inclination, and the launch date must be supplied, as in Table 10-4.

Key information can be gathered from the collection of flux tables supplied by JPL and JSC. This includes flux data for the combination of particle size and velocity that is feasible to protect against. Above certain particle size and velocity combinations, depending on protection system mass constraints and design selections, the kinetic energy of particles would become too great to protect against. Section 10.4.2.2 discuses this in more detail. For high energy particles, alternative forms of problem mitigation could be developed.

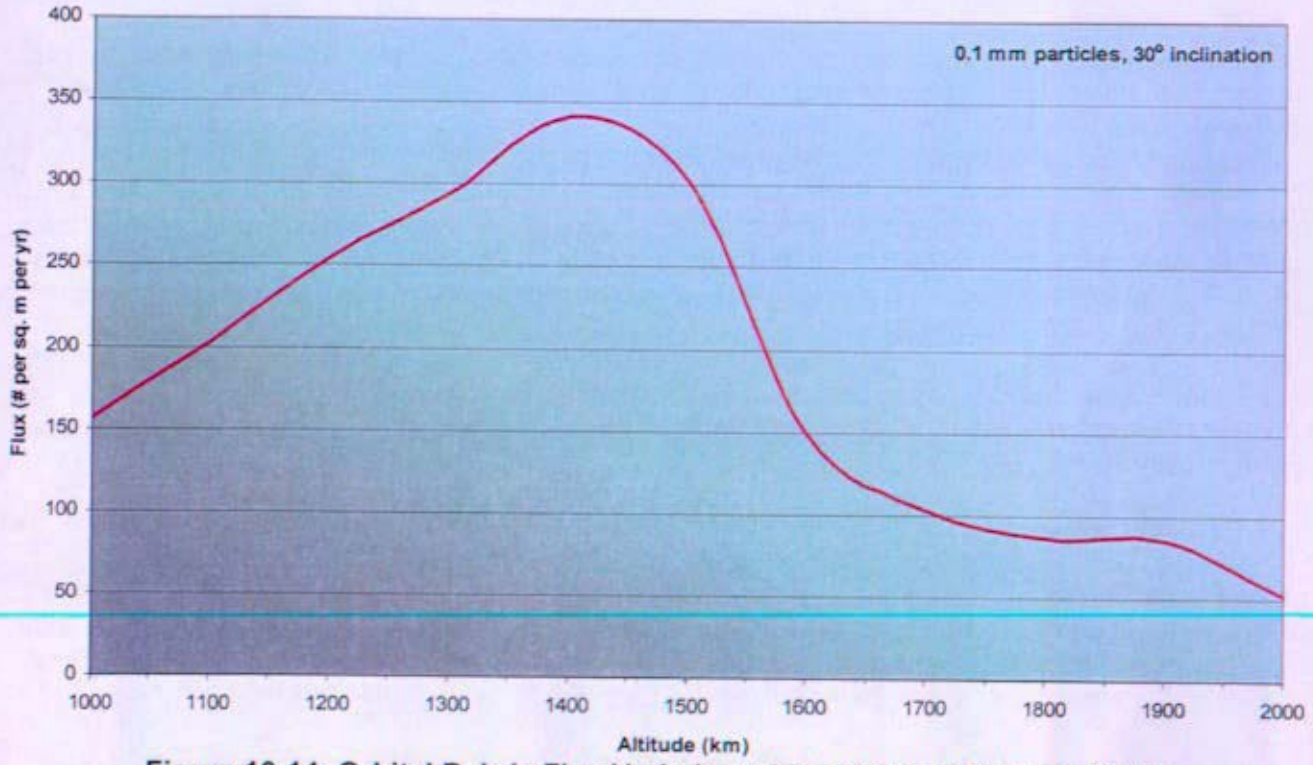



**Figure 10-14: Orbital Debris Flux Variation with Altitude** (Reference 10- 5)

**Table 10-4: Number of Orbital Debris Impacts per Year** (Reference 10- 6)

| Size / Alt. | ≥ 0.5 mm | ≥ 1 mm | ≥ 1 cm |
|---|---|---|---|
| 500 km | 60 | 6 | $8x10^{-4}$ |
| 1000 km | 207 | 19 | $4x10^{-3}$ |
| 2000 km | 104 | 8 | $3x10^{-4}$ |

Surface Area = 300 $m^2$, Spacecraft Inclination = 51.6°, Launch in 2012

### 10.4.1.2 Orbital Debris Abatement

Most orbital debris mitigation would come through the proper selection of the launch vector and spacecraft assembly altitude. If these are selected wisely, then the majority of the dangerous orbital debris could be avoided.

One potential method of protecting from orbital debris is designing a protection system for the reactor section of the spacecraft forward of the shield that could withstand much larger impacts than from micrometeoroids. This could include a combination of an ejectable aeroshell and the micrometeoroid protection for the reactor. In this case, the spacecraft could be oriented so that any impacts would be more likely to occur in the most heavily protected regions of the spacecraft.

Another possible way to mitigate the risk is to move the spaceship out of the way of large orbital debris using directional thrusters. This is most likely only feasible for larger objects on the kilogram scale.

### 10.4.2 Micrometeoroids

Micrometeoroids are very small, high velocity particles that are typically made up of silicates, iron, or CHON (Carbon, Hydrogen, Oxygen, and Nitrogen). Micrometeoroids range in size from the microgram scale, common, to the gram scale, uncommon. They travel at an average velocity of 20 km/sec near Earth, but can range in velocity from 10 km/sec to 70 km/sec depending on the location within the solar system, as referenced in Table 10-6 and Table 10-7.

Micrometeoroids pose several potential mission ending failure risks, including direct impact damage and chemical interaction. The choice of a protection system for the spaceship would be driven by the mission assurance requirements for each of the components and systems. Each component of the spaceship would be evaluated individually to determine what level of protection is necessary to meet the required mission success probability. This is usually the most mass effective method for developing a protection system. This means that different components and locations within the spaceship could employ different methods and materials for protection.

The following sections step through the different levels of data required and the methodology that would be used for selecting an appropriate protection system that would ensure mission completion. Most data can be obtained through the various NASA facilities as discussed below. Means to apply this data for preliminary sizing estimates and key factors in evaluating different protection systems are covered in Section 10.4.2.2. Historical examples of spacecraft protection systems are summarized in Section 10.4.2.3. Basic designs of various protection systems are described in Section 10.4.2.1. Analysis and selection of materials for micrometeoroid protection is covered in Section 10.4.2.5. Lastly, methods of testing and test performance are covered in Section 10.4.2.4. A summary of this information is available in Section 10.4.3.

### 10.4.2.1 Micrometeoroid Flux and Velocity

The micrometeoroid flux and velocity for each mission segment can be modeled using the Meteoroid Engineering Model METEM from JPL or the older Divine model from JSC as stated in Reference 10-7. The data for these models is based on previous satellite missions and ground-based radar. The models provide flux data at a specified location in the solar system for particle masses between 10-12g and 102 g. This data can be specified by particle velocity or local distance measurements depending on the selected output. Examples of the location dependant data are represented in Figure 10-15, Figure 10-16, Figure 10-17, and Table 10-5. Tables are available from the JPL Prometheus Project ERD, Reference 10- 9, and directly from JPL and JSC. Marshall Space Flight Center (MSFC) was working on a new and better model for micrometeoroid fluxes at the time of this report.

This data would be utilized after calculating the critical penetration thickness for a candidate protection system and the critical mass of a micrometeoroid that would cause penetration of the candidate protection system, Sections 10.4.2.2.1 and 10.4.2.2.2 respectively. The flux data could then be applied to the probability of component failure analysis, described in Section 10.4.2.2.3. Once the probability is calculated, an evaluation would take place to assess whether the calculated probability is within acceptable mission parameters. Iterations in the design of the protection system would occur until an acceptable probability of failure is reached.

For the JIMO mission, the primary micrometeoroid concerns would occur at the asteroid belt and at Jupiter. The moons of Callisto, Europa, and Ganymede would be the primary mission objective for JIMO, Reference 10- 8. The moons orbit at 26.33, 9.40, and 14.97 Jovian radii, respectively, which are beyond the range of the rings. Micrometeoroids velocities of 60 - 70 km/sec near Jupiter are possible, but velocities between 14 km/sec and 22 km/sec are more likely per Table 10-7. Table 10-6 and Figure 10-16 shows typical micrometeoroid velocities and flux distributions between Earth Orbit (1 AU) and Jupiter (5.2 AU).

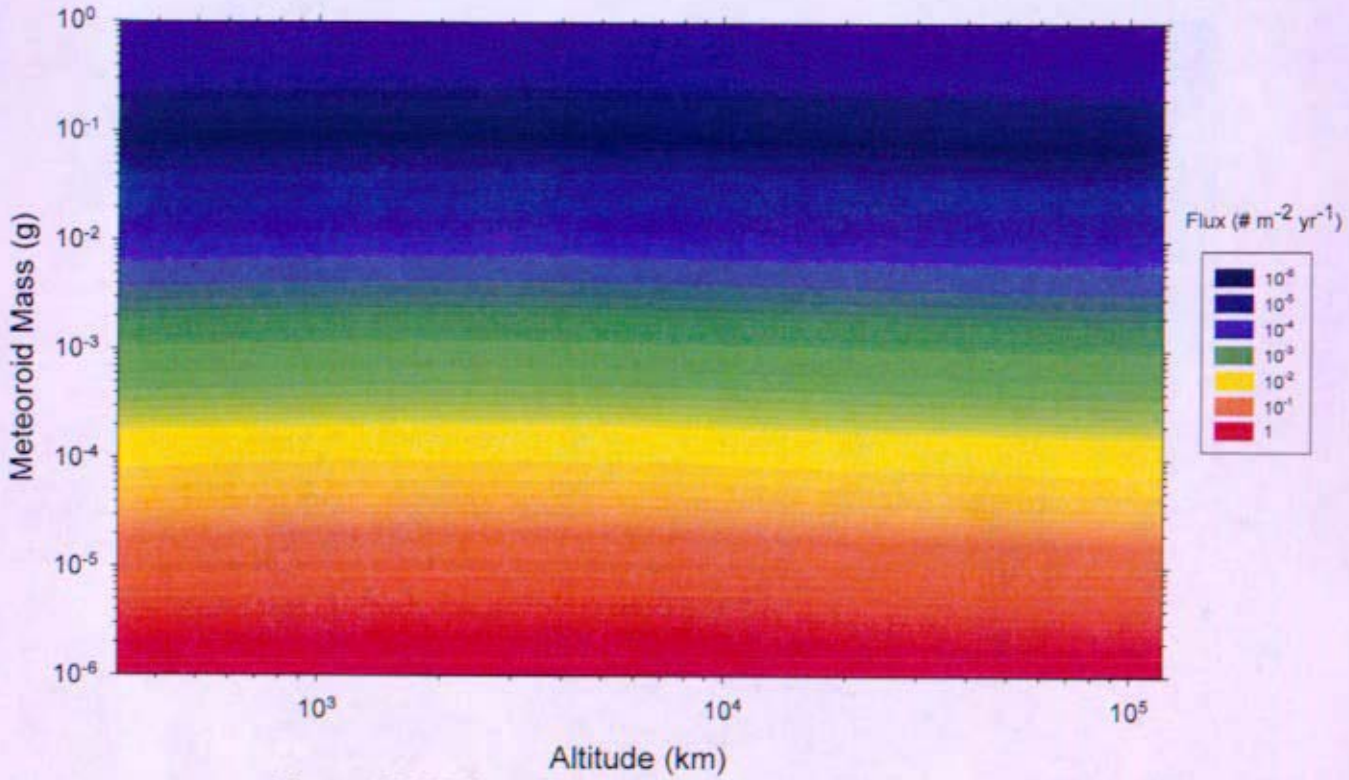



**Figure 10-15: Near Earth Micrometeoroid Flux – METEM**
(Reference 10- 5)

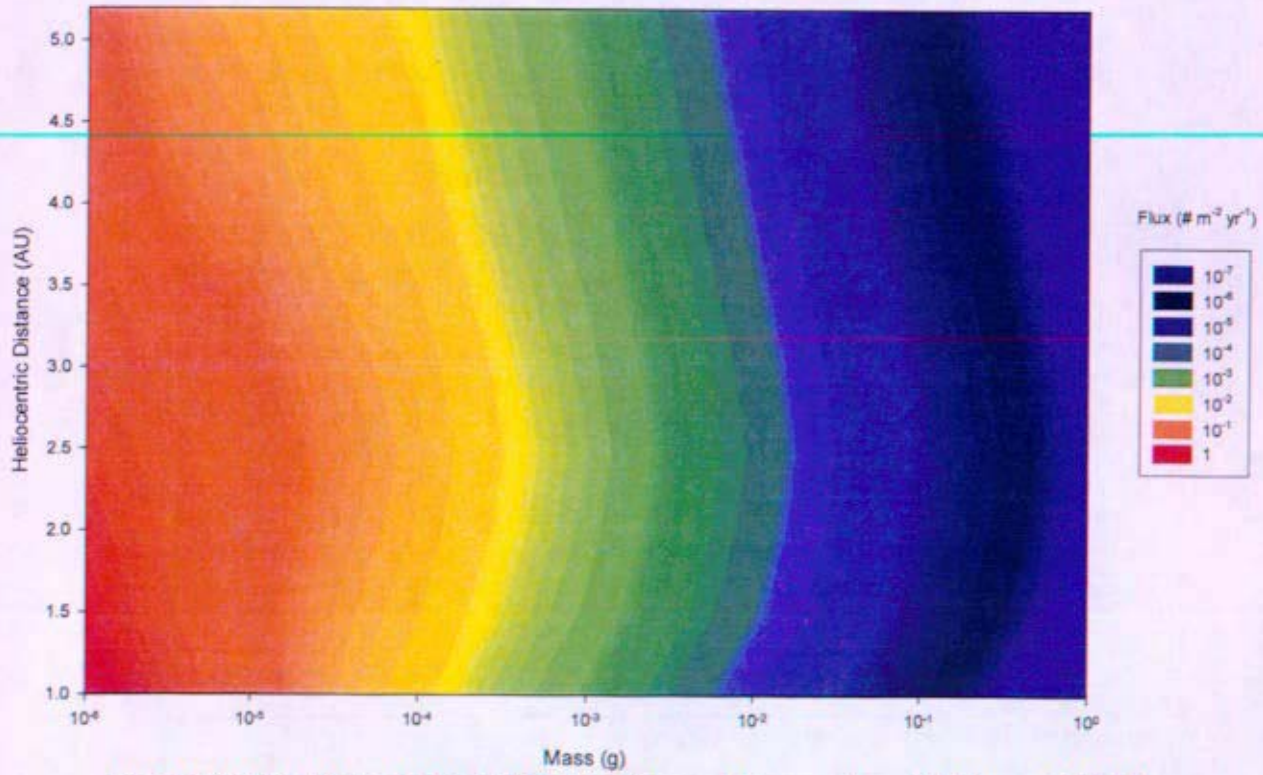



**Figure 10-16: Interplanetary Mission Phase Micrometeoroid Flux – METEM**
(Reference 10- 5)

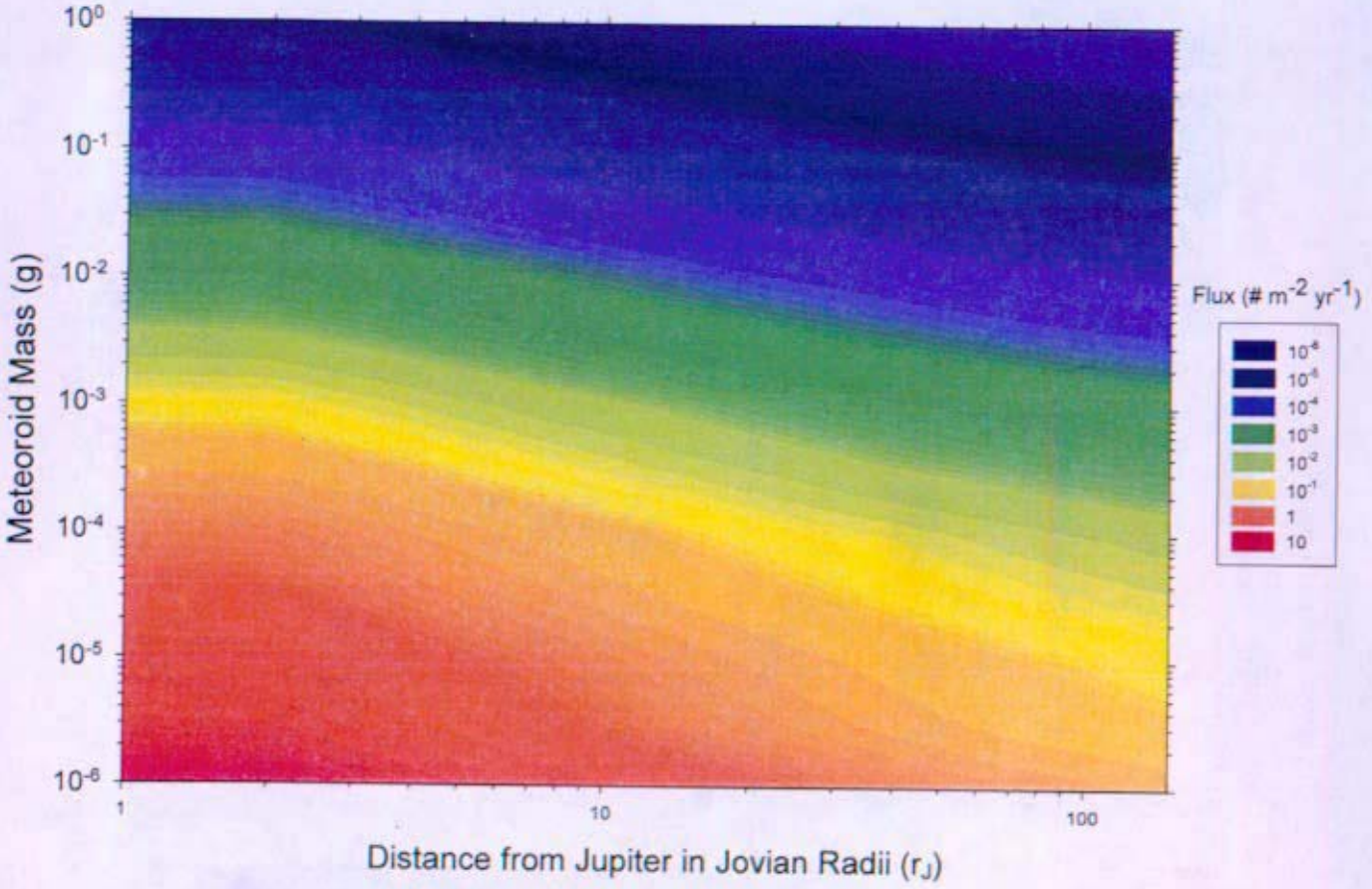



**Figure 10-17: Jovian Mission Phase Micrometeoroid Flux – METEM**
(Reference 10- 5)

**Table 10-5: Number of Micrometeoroid Impacts per Year ***
(Reference 10- 6)

| | ≥ 0.5 mm | ≥ 1 mm | ≥ 1 cm |
|---|---|---|---|
| 1 AU | 2.2[a] | 0.19 | 2.1 x10$^{-5}$ |
| 2 AU | 5.3 | 0.57 | 7.1 x10$^{-5}$ |
| 3 AU | 5.0 | 0.55 | 6.9 x10$^{-5}$ |
| 4 AU | 2.6 | 0.29 | 3.6 x10$^{-5}$ |
| 5 AU | 1.4 | 0.16 | 2 x10$^{-5}$ |

* Assuming a total surface area of 300 m$^2$
[a] Divine model, near ecliptic, circular orbit (M. Matney)

**Table 10-6: Average Speed of Micrometeoroids – METEM**
(Reference 10- 9)

| Heliocentric distance (AU) | Avg Speed (km/s) |
|---|---|
| 1 | 20.00 |
| 1.5 | 16.33 |
| 2 | 14.14 |
| 2.5 | 12.65 |
| 3 | 11.55 |
| 3.5 | 10.69 |
| 4 | 10.00 |
| 4.5 | 9.43 |
| 5 | 8.94 |
| 5.2 | 8.77 |

**Table 10-7: Average Speed of Jovian Micrometeoroid Flux – METEM**
(Reference 10- 9)

| Distance in Jovian radii | Avg Speed (km/s) |
|---|---|
| 1 | 60.18 |
| 2 | 43.00 |
| 3 | 35.47 |
| 4 | 31.03 |
| 5 | 28.03 |
| 6 | 25.84 |
| 7 | 24.15 |
| 8 | 22.80 |
| 9 | 21.70 |
| 10 | 20.77 |
| 20 | 15.94 |
| 30 | 13.97 |
| 40 | 12.87 |
| 50 | 12.16 |
| 60 | 11.66 |
| 70 | 11.29 |
| 80 | 11.01 |
| 90 | 10.78 |
| 100 | 10.60 |
| 110 | 10.45 |
| 120 | 10.32 |
| 130 | 10.21 |
| 140 | 10.11 |
| 150 | 10.03 |

### 10.4.2.2 Development of Protection Systems

A micrometeoroid protection system would be designed to protect against particles ranging from a few milligrams to a maximum of 3 - 4 grams, depending on the mission, risk evaluations, and other variables. Demonstration of protection for smaller particles would be difficult because they could not be accurately simulated in a test. More massive particles typically have high kinetic energy, making it difficult to design a mass efficient shield that would protect sufficient protection using current technologies. The details of the critical calculations that have to be made when designing a protection system to account for varying micrometeoroid types, sizes, and velocities are covered in the following three sections.

### 10.4.2.2.1 Critical Penetration Thickness

The critical penetration thickness, $t_{wall, critical}$, is the wall thickness of a sheet of metal that would be penetrated for a given type of particle of a certain size and velocity. This variable would have to be determined for each component based on the candidate protection system and level of protection that each component requires. Table 10-8 shows the calculated critical penetration thickness for single wall protection, as explained in Section 10.4.2.4.1, for a single sheet of Aluminum.

**Table 10-8: Critical Penetration Thickness**

| Particle | $\rho_p$ (g/cm$^3$) | $K_1$ | d (cm) | $m_p$ (gm) | $V_p$ (km/s) | KE (kJ) | $t_{wall, critical}$(cm) |
|---|---|---|---|---|---|---|---|
| Aluminum | 2.7 | 0.57 | 0.100 | 0.0014 | 10 | 7.07E-02 | 5.01E-01 |
| | | | 0.891 | 1.0000 | | 5.00E+01 | 5.05E+00 |
| | | | 1.000 | 1.4137 | | 7.07E+01 | 5.70E+00 |
| | | | 0.100 | 0.0014 | 14 | 1.39E-01 | 6.73E-01 |
| | | | 0.891 | 1.0000 | | 9.80E+01 | 6.77E+00 |
| | | | 1.000 | 1.4137 | | 1.39E+02 | 7.65E+00 |
| CHON | 3.5 | | 0.100 | 0.0018 | 20 | 3.67E-01 | 1.05E+00 |
| | | | 0.817 | 1.0000 | | 2.00E+02 | 9.66E+00 |
| | | | 1.000 | 1.8326 | | 3.67E+02 | 1.20E+01 |
| | | | 0.100 | 0.0018 | 70 | 4.49E+00 | 3.15E+00 |
| | | | 0.817 | 1.0000 | | 2.45E+03 | 2.89E+01 |
| | | | 1.000 | 1.8326 | | 4.49E+03 | 3.58E+01 |
| Iron | 8.5 | | 0.100 | 0.0045 | 20 | 8.90E-01 | 1.67E+00 |
| | | | 0.608 | 1.0000 | | 2.00E+02 | 1.12E+01 |
| | | | 1.000 | 4.4506 | | 8.90E+02 | 1.90E+01 |
| | | | 0.100 | 0.0045 | 70 | 1.09E+01 | 4.99E+00 |
| | | | 0.608 | 1.0000 | | 2.45E+03 | 3.35E+01 |
| | | | 1.000 | 4.4506 | | 1.09E+04 | 5.67E+01 |

The values chosen for the velocities are representative of the average and extreme cases for orbital debris (aluminum) and micrometeoroids (CHON and iron). Masses assume particle sizes ranging from 0.1 cm to 1.0 cm and are based on particle density. This table exemplifies the fact it will be very difficult to protect against impact using a single wall design for particle masses greater than 1.0 grams.

The row that is highlighted green is an example of the minimal protection required for the International Space Station (ISS). The diameter and velocity listed are the design parameters for its protection system, Section 10.4.2.3.5. The 5.7 cm thickness of aluminum required to mitigate the threat would require much more mass than the staged protection system described for the ISS in Section 10.4.2.3.5.

The row that is highlighted blue is a possible design case, and is similar to the 0.8 mm design size described for the Galileo mission in Section 10.4.2.3.3. Five cm thick aluminum is required for adequate protection using a single layer. However, this thickness is still too large for single wall protection schemes. Mission critical components for a JIMO mission would thus likely require a multi-layer protection system.

The thicknesses listed in Table 10-8 are computed using the Fish and Summers equation shown below, Reference 10- 12. Variations of this equation for different types of protection systems can be

found in References 10- 10 and 10- 11. Most of the multi-bumper (multi-layer) designs implement a form of the Cour-Palais equation also found in References 10- 10 and 10- 11. However, these formulas have only been demonstrated valid for velocities between 7 km/sec and 10 km/sec due to testing limitations as discussed in Section 10.4.2.4. Beyond these velocities, results would have to be extrapolated using assumptions and uncertainty factors of safety. This was not taken into account in Table 10-8

$$t_{wall,\,critical} = K_l m_p^{0.352} \rho_p^{0.167} \left(V_p \cos\beta\right)^{0.875}$$

where:
d: Particle Diameter; KE: Kinetic Energy
$K_l$: Material Constant, 0.57 for Aluminum
$m_p$: Particle Mass; $V_p$: particle velocity
β: Particle impact angle (direct impact assumes 0°)
$\rho_p$: Particle density

### 10.4.2.2.2 Critical Impact Mass

The critical particle impact mass, $m_{p,\,critical}$, is the mass of a micrometeoroid traveling at specified velocity that would penetrate through the protection system. This value should be calculated for each component during protection system design. This is to ensure that each component can function following a particle impact that is within the design parameters. The equation listed below is simply a rearrangement of the Fish and Summers equation listed in the previous section for single wall protection, Reference 10- 12. Different equations will have to be implemented for different types of protection systems. Many of these equations are available in References 10- 10 and 10- 11.

$$m_{p,\,critical} = \left( \frac{t_{wall}}{K_l \cdot \rho_p^{0.167} \cdot \left(V_p \cos\beta\right)^{0.875}} \right)^{1/0.352}$$

$K_l$: Material Constant, 0.57 for Aluminum
$t_{wall}$: Component Wall Thickness
$V_p$: Particle velocity
β: Particle impact angle
$\rho_p$: Particle density

### 10.4.2.2.3 Component Probability of Failure

A key to evaluating a protection system is to incorporate the orientation and location of a component within the spacecraft. This information would then be used to determine the probability that a critical component would fail due a micrometeoroid impact. This probability could be calculated per Reference 10- 10. Once the critical impact mass has been calculated, the appropriate flux data for each mission phase could be selected and translated into fluence data, impacts/$m^2$, over mission life. After this, appropriate components can be evaluated.

Critical spacecraft systems and components that would be evaluated include pressurized vessels and conduits such as the reactor and piping, electrical equipment, reactor control drive mechanisms and power cables essential to mission success. It is anticipated that reactor protection would be one of the more significant design challenges, due to the importance of the continuous reactor operation, the

presence of mechanisms around it, the interaction between the protection and the reactor, influence on shielding, and because the reactor would be oriented toward the forward (ram) facing direction for much of the mission.

After defining components requiring protection, the field of view (geometric factor corresponding to all visible surfaces on an object) and spacecraft attitude would be defined using information from NASA. The surface perpendicular to the velocity vector of the spacecraft would receive the highest fluence levels. Finally, the probability of failure for each component would be individually calculated.

The probability of failure would be calculated by multiplying the area of interest's impact surface area, fluence, geometric factor, and attitude factor for each mission phase to give the number of impacts in a certain area of the spaceship. A factor of 2 would typically be applied to any specified fluence data used for calculations to account for uncertainty. A Poisson distribution is then applied to the multiplied value to obtain the probability of failure. Using cumulative probability formulation, the overall probability of micrometeoroid induced failure for the reactor module could be calculated using the results from the individual area of interest calculations.

An alternative to this method is calculating the fluence level from the required probability of failure as specified by requirements documents. This would be performed by using the reverse of the previously stated probability analysis. Mass and velocity combinations could then be found at the required fluence level from the flux tables. The kinetic energy worst case combination of mass and velocity would then be taken from the accumulated data. After this, the protection system's thicknesses and standoff distance(s) could be designed to withstand the worst case mass and velocity combination. This should then meet the requirements for the probability of failure specified in mission assurance documents.

### 10.4.2.3 Historical Methods

When designing a micrometeoroid protection system, past designs should be evaluated for their relevance and scalability to the current project. The following are several different types of past and current spacecraft that have used varying forms and levels of micrometeoroid protection.

#### 10.4.2.3.1 Cassini

This spacecraft is a scientific probe that was sent to study Saturn, Saturn's rings, and its moons. To withstand the transit through the asteroid belt and the Saturn micrometeoroid environment, Mylar was used in a Whipple shield arrangement (Section 10.4.2.4.2). It served the dual purpose of micrometeoroid protection and multi-layer insulation (MLI). The standoff distance from the secondary shield varied from 2.5 inches to 18 inches. In some critical locations on the spacecraft, fuel tanks for example, two layers of beta cloth were added behind the Mylar.

#### 10,4.2.3.2 Contour

This probe was launched primarily to study two comets, Encke and Schwassmann-Wachmann. It employed five layers of Nextel and Kevlar to protect against impacts from the comet tail. The total thickness of the protections was 25 cm.

#### 10.4.2.3.3 Galileo

The primary mission for Galileo was the exploration of Jupiter. Its protection was designed to withstand particles up to 0.8 mm in diameter. The protection varied depending on the different

sections of the spacecraft. On the outside was a layer of 25.4 μm thick aluminized Kapton. Beneath the outer layer were two layers of 25.4 μm carbon filled polyester coating on 12.7 μm of Kapton. Lastly, there were 10 - 20 layers of 6.3 μm thick aluminized Mylar and Dacron net.

#### 10.4.2.3.4 Giotto

Researching Halley's Comet was the primary mission for Giotto. Its closest approach to the comet was 596 km. It employed a 1 mm thick bumper panel of aluminum with a standoff distance of 25 cm from 12 mm thick Kevlar arranged in a Whipple shield configuration. The protection was designed to withstand particle impacts up to one gram.

#### 10.4.2.3.5 International Space Station (ISS)

The protection system design for the ISS is multi-layered. The level of protection employed on the space station varies by location and criticality. The critical compartments and components have a 0.80 in aluminum bumper and a 0.188 in aluminum secondary protection wall. The spacing between the two is approximately 4.5 in. Between the two are 23 layers of multi-layer insulation, 6 layers of Nextel, and 6 Layers of Kevlar, Reference 10- 14. This is designed to withstand an impact of a 1 cm particle traveling at 10 km/sec.

#### 10.4.2.3.6 Stardust

The mission for this spacecraft was to collect dust and carbon-based samples from the comet Wild 2. It came within 240 km of the comet. It employed a double Whipple shield design to protect against the cometary coma. The bumper shields (Section 10.4.2.4.3) were made from composite panels. Beneath them were blankets of Nextel used to spread out the debris and dissipate the energy. It was designed to protect against particles up to 1 cm in diameter.

### 10.4.2.4 Current Methods

There are many different designs used to prevent against hypervelocity impacts. The following six methods are the most predominant designs that have been implemented in recent years and are being further developed.

#### 10.4.2.4.1 Single Layer Protection

For this design, the rear wall of the chosen protection material is in direct contact with the component it is protecting, Figure 10-18. The alternative is that the component wall thickness is made thick enough to withstand the design impact level. This is the simplest form of protection and thus more effective protection schemes exist.

The protective layer could be fastened to the component by wrapping the material directly over the component or being tied to the component. A single layer of protection is subject to pitting if it does not fail. The pitting could induce spalling of the component wall due to the shock wave created during pitting. This could be mitigated by keeping the material speed of sounds constant between the impacting material and the protection material.

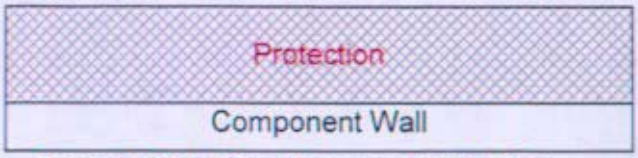



**Figure 10-18: Single Layer Protection**

### 10.4.2.4.2 Whipple Shield

This design consists of a bumper and a secondary layer of material, Figure 10-19. The bumper is designed with the intent to fail on impact. This could vaporize the impacting particle. If vaporization did not occur, typically a debris cloud would form. The cloud would cause less to no damage to the protected component. The secondary layer of material could be a second layer of protection in addition to the component's wall thickness or just the wall thickness of the protected component. This depends on the component's outer layer strength and the component's critically to the mission.

The distance between the bumper and secondary layer of protection is termed the standoff distance. An appropriate distance would be determined to avoid residual impact issues if this design is used. If the standoff distance is too little, the debris cloud would not disperse enough and its impact point on the second layer would be small, increasing the likelihood of failure. If the distance is too large, it would disperse the debris cloud too much; potentially sending parts of the cloud to components not rated at the same protection level which might cause penetration in those components.

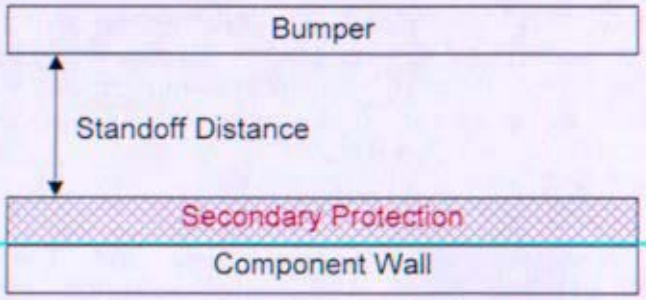



**Figure 10-19: Whipple Shield**

Ultimately the critical design range for protection thickness would have to be determined. Figure 10-20 characterizes the ratio of protection material thickness, t, to impact particle diameter, d, where V is the impact velocity of the particle. In the red section the micrometeoroid is vaporized. In the blue section the target material is vaporized. Where the two sections overlap, both the material and particle vaporize on impact. This is the optimum case. If the material is too thin, it would have no effect in lowering the impact energy. If it is too thick, there would be increased fragmentation impact on the secondary surface (or component wall) due to the bumper fragments.

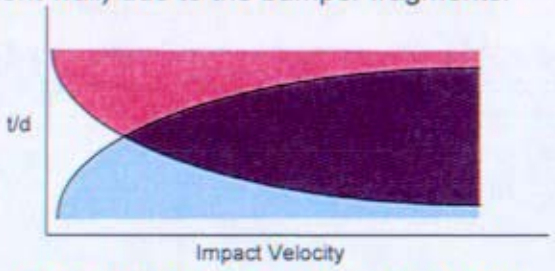



**Figure 10-20: Critical Design Range**

A significant challenge with this system is determining how to attach the bumper to the secondary layer. This could be done by attaching the bumper to an external structure or by having support hoops attached between the rear wall of the bumper and the outer wall of the secondary layer.

### 10.4.2.4.3 Multi Bumper Whipple Shield

This configuration is the same as the single Whipple shield with the addition a second, or more, bumper as seen in Figure 10-21. This increases the protection level but could add mass. The additional bumper(s) could be the same material as the primary bumper or different, such as multi-layer insulation.

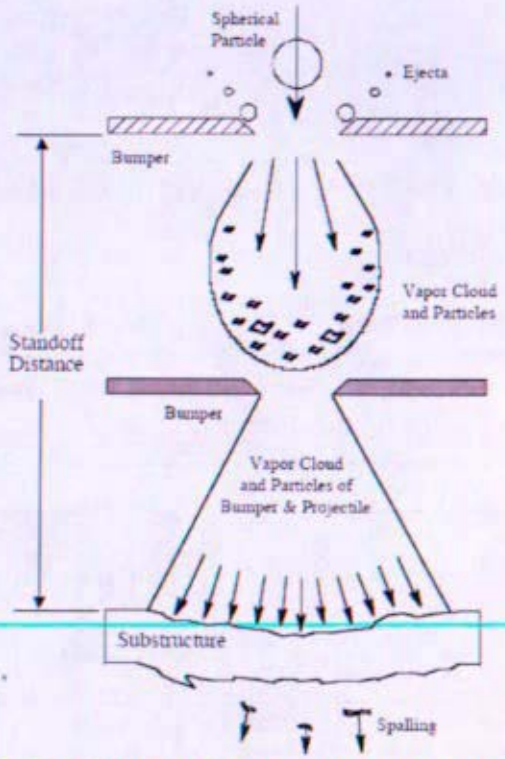



**Figure 10-21: Whipple Shield with Two Bumper Layers**
(Reference 10- 13)

### 10.4.2.4.4 Honeycombed Modification of Whipple Shield

Titanium, Inconel, and Aluminum have been used in the past as protection by having thin layers of the material spaced with ribbons made of the same material in a honeycomb or corrugated pattern, Figure 10-22. It serves three purposes: protection, thermal insulation, and structural support for components. The honeycomb design would increase the level of protection but the density of each material would increase protection mass greatly compared to blanketed material. This may be a good tradeoff if the component being protected is a component where a single point failure would end the mission.

Changing the cell size of the honeycombed structure will not decrease penetration chances. The amount of penetration is a stronger function of whether the particle impacts the center of the cell or on a ribbon, and therefore is considered highly random.

The honeycomb would also change the impact pattern on the main shield. A normal Whipple shield would have a symmetric debris dispersal cloud after impacting the bumper shield; this would not the case for the honeycomb cells. This may be due to the ribbons changing the directionality of various parts of the debris dispersal cloud.

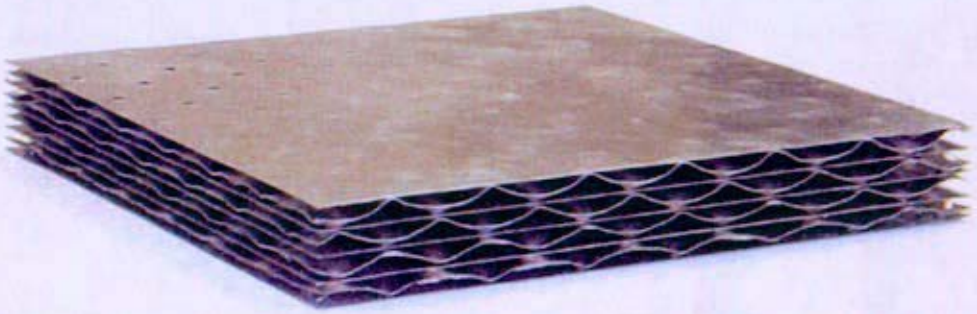


**Figure 10-22: Titanium Multiwall Protection** (Reference 10- 13)

### 10.4.2.4.5 Stuffed Whipple Shield

In this arrangement, the standoff distance between the bumper and the secondary layer of protection is filled with an energy absorbent material such as Kevlar or Nextel and possibly multi-layer insulation, Figure 10-23. This could decrease the standoff distance and the thickness of the bumper and secondary layer significantly while increasing the amount of protection.

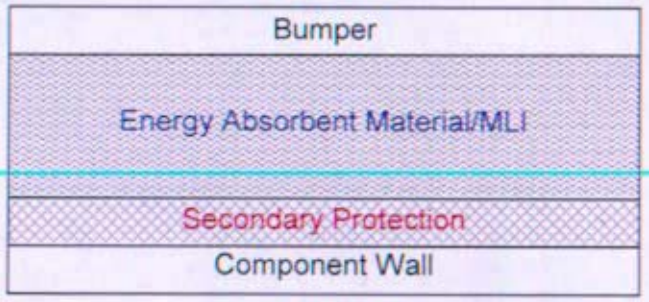



**Figure 10-23: Stuffed Whipple Shield**

### 10.4.2.4.6 Modified Whipple Shield

This is a new technology being developed similar to the stuffed Whipple shield. The difference between this design and the stuffed Whipple shield is that there is no bumper layer, Figure 10-24. Instead the first layer of protection is open-celled metallic foam which would be directly adhered to the secondary layer of protection. This eliminates the problem of how to create the standoff distance with the conventional Whipple shield.

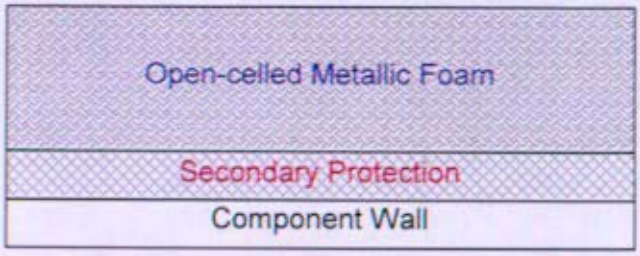



**Figure 10-24: Modified Whipple Shield**

### 10.4.2.5 Material Selection

The selection of materials for spacecraft protection is mission and component dependent. A mission to Jupiter would require a greater level of protection than a mission to the Moon or to Mars. This is because the gravity well of Jupiter and its rings create much faster micrometeoroids with higher fluence levels. Mars has an atmosphere that will filter out most micrometeoroids. A mission to the moon would most likely be placed on the Earth facing side of the moon and therefore it would be shielded from the majority of the micrometeoroid threat. Furthermore, a mission that requires a long near Earth orbit time for assembly and initial start-up may need a high level of protection to resist orbital debris damage.

For components that require a high level of protection, the materials could be modeled as a scaled down version of comet probes such as Contour, Giotto, and Stardust. The selection of materials would also be based on the location of the component with the spacecraft. If impacts could only occur at a direction perpendicular to the velocity vector of the spacecraft, then that component would receive a far lower fluence level compared to one that is exposed to impact from the front, in the direction of the spacecraft velocity vector. Preferential component location and orientation essentially shields the component from the particle flux and therefore reduces the scale of protection required.

Materials often considered for a protection system include Aerogel, aluminum, Astroquartz, Beta Cloth, Alloy 617, Kapton, Kevlar, Mylar, Nextel, and titanium. Each material has its own characteristics that could make it beneficial to use in a protection system. Furthermore, combinations of different materials could be used depending on component arrangement, thermal requirements, and level of protection required.

During the selection of the proper materials to be used for protection, several characteristics of each material would be rated to help narrow the decision. The minimum characteristics that should be evaluated for these materials are: ability to withstand environmental and plant produced radiation, coefficient of thermal expansion, density, electrical resistivity and conductance to control electrostatic discharge, material chemistry and composition, operational temperature range, resilience, specific heat, strength, stiffness, thermal conductivity, thermal radiation absorptivity, thermal radiation emissivity, the ability to fasten the material to the support structure and/or the components themselves, and the compatibility between the protecting material and material to which it would be fastened.

Table 10-9 represents the data that was being collected prior to mission cancellation and the method being implemented for quantifying the characteristics of each material. The ranking system would be subjectively dependant on the mission parameters. These qualities could not ultimately determine the proper protection materials. The final material selection would be based on the chosen protection configuration(s) and in-depth impact testing results.

## Table 10-9: Materials Evaluation Worksheet

| | | Material | | | | | | | | | | | | | | | | | | |
|---|---|---|---|---|---|---|---|---|---|---|---|---|---|---|---|---|---|---|---|---|
| | | Ti-6Al-4V | | | Inconel 617 | | | Aerogel | | | | Beta Cloth | Nextel 312 | Astro Quartz II | Kapton | | Kevlar | Mylar | |
| | | Honeycomb | Multilayer | 1 Layer | Honeycomb | Multilayer | 1 Layer | Berkeley | JPL | AR5101/5103 | AR3101/3103 | | | | Aluminized | Film | | Aluminized | Film |
| Temperature | % Weight | | | | | | | | | 5% | | | | | | | | | |
| | Range (K) | | | | | | | ? - 500 | | 260 - 473 | 260 - 473 | | ? - 1447 | ? - 500 | | | | | 23 - 473 |
| | *Rank* | | | | | | | | | | | | | | | | | | |
| Th. Conductivity | % Weight | | | | | | | | | 5% | | | | | | | | | |
| | λ (W/m·K) | | | 6.6 | | | 13.6 | 0.017 | 0.016 - 0.03 | 0.013 | 0.0141 - 0.0131 | | | | | | | | |
| | *Rank* | | | | | | | | | | | | | | | | | | |
| Coeff. Of Thermal Expansion | % Weight | | | | | | | | | 5% | | | | | | | | | |
| | $\alpha_e$ ($^oC^{-1}$) | | | 9 - 9.7x10$^{-6}$ | | | 11.6x10$^{-6}$ | 2 - 4x10$^{-6}$ | 2x10$^{-6}$ | | | | 3.00E-06 | | | | | | |
| | *Rank* | | | | | | | | | | | | | | | | | | |
| Specific Heat | % Weight | | | | | | | | | 5% | | | | | | | | | |
| | $C_p$ (J/g·K) | | | 0.586 | | | 0.419 | | | 1.046 | 1.046 | | 1.05 | | | | | | 1.17 |
| | *Rank* | | | | | | | | | | | | | | | | | | |
| Emissivity | % Weight | | | | | | | | | 5% | | | | | | | | | |
| | ε | | | | | | | | | 1 | | 0.32 | | | 0.55 - 0.86 | | | NA | |
| | *Rank* | | | | | | | | | | | | | | | | | | |
| Absorptivity | % Weight | | | | | | | | | 5% | | | | | | | | | |
| | $\alpha_r$ | | | | | | | | | | | 0.86 | | | 0.34 - 0.46 | | | 0.34 | |
| | *Rank* | | | | | | | | | | | | | | | | | | |
| Material Chemistry/ Composition | % Weight | | | | | | | | | 10% | | | | | | | | | |
| | Category | Metal | Metal | Metal | Metal | Metal | Metal | Porous Solid | Porous Solid | Porous Solid | Porous Solid | | Ceramic Fiber | Quartz Fiber | | Polyimide Film | | Polyester Film | |
| | Composition | | | AL, C, Fe, H, N, O, Ti, V | | | AL, B, C, Co, Cr, Cu, Fe, Mn, Mo, Ni, S, Si, Ti | | 99.8% Air, 0.2% $SiO_2$ | | | | $9AL_2O_3:2B_2O_3$ + amorph. $SiO_2$ | $SiO_2$, FEP, Al | | | | | |
| | *Rank* | | | | | | | | | | | | | | | | | | |
| Density | % Weight | | | | | | | | | 10% | | | | | | | | | |
| | ρ (g/cm$^3$) | | | 4.51 | | | 8.36 | 0.003 - 0.35 | 0.005 - 0.2 | 0.11 | 0.11 | | 2.7 | 0.0265 | | 1.42 | | | 1.39 |
| | *Rank* | | | | | | | | | | | | | | | | | | |
| Strength | % Weight | | | | | | | | | 5% | | | | | | | | | |
| | $\sigma_y$ (MPa) | | | 972 | | | 340 | 0.016 | | 0.083 | 0.088 | | 1700 | 3.45 | | 68.9 | | | 20 |
| | *Rank* | | | | | | | | | | | | | | | | | | |
| Stiffness | % Weight | | | | | | | | | 5% | | | | | | | | | |
| | E (GPa) | | | 105 | | | | 0.001 | | | | | 150 | 0.069 | | | | | 490 |
| | *Rank* | | | | | | | | | | | | | | | | | | |
| Resilience | % Weight | | | | | | | | | 10% | | | | | | | | | |
| | R (J/m$^3$) | #DIV/0! | #DIV/0! | 4498971 | #DIV/0! | #DIV/0! | #DIV/0! | 128 | #DIV/0! | #DIV/0! | #DIV/0! | #DIV/0! | 9633333 | 86310 | #DIV/0! | #DIV/0! | #DIV/0! | #DIV/0! | 408 |
| | *Rank* | | | | | | | | | | | | | | | | | | |
| Radiation | % Weight | | | | | | | | | 10% | | | | | | | | | |
| | Range (RAD) | | | | | | | | | | | | | | | | | | |
| | *Rank* | | | | | | | | | | | | | | | | | | |
| Electric Resistivity | % Weight | | | | | | | | | 10% | | | | | | | | | |
| | R (Ω-cm) | | | 1.68E-04 | | | 1.22E-04 | | 1.00E+18 | 1 | | 0.86 | | | 0.34 - 0.46 | | | 0.34 | |
| | *Rank* | | | | | | | | | | | | | | | | | | |
| Fastening | % Weight | | | | | | | | | 10% | | | | | | | | | |
| | *Rank* | | | | | | | | | | | | | | | | | | |
| **Overall Rating** | | 0 | 0 | 0 | 0 | 0 | 0 | 0 | 0 | 0 | 0 | 0 | 0 | 0 | 0 | 0 | 0 | 0 | 0 |
| | | Honeycomb | Multilayer | 1 Layer | Honeycomb | Multilayer | 1 Layer | Berkeley | JPL | AR5101/5103 | AR3101/3103 | Beta Cloth | Nextel | Astro Quartz II | Aluminized | Film | MLI | Aluminized | Film |
| | | Ti-6Al-4V | | | Inconel 617 | | | Aerogel | | | | | | | Kapton | | Kevlar | Mylar | |

Note: #DIV/0! in the resilience section is due to a mathematical computation based on the strength and stiffness.

### 10.4.2.6 Impact Testing

Impact testing is arguably the most important part of determining the proper protection system. Currently there are only limited mathematical models used to predict how different types of protection designs would react to a hypervelocity impact. This is because particle impact probability is a Gaussian distribution. This means the interaction with the protection system based on particle mass, size, and density cannot be accurately modeled since it is random. To account for this, multiple runs of testing for each evaluated protection system would have to be made. This is to determine the proper mathematical correlations of particle size and velocity to impact depth. The correlations could then be extrapolated out to higher velocities with the caveat of adding a margin of design safety into any probability and material thickness equations. This would account for the extrapolation uncertainty. As previously stated, this is typically done by increasing the fluence level by a factor of two. See References 10- 13 and 10- 22 for more information.

#### 10.4.2.6.1 Testing Material Simulation

Micrometeoroids have been most accurately simulated by using naturally occurring silica balls that are indigenous to Hawaii. The test specimens typically range in size from micrograms to milligrams and have a density between 2 g/cm$^3$ and 3 g/cm$^3$. Micrometeoroids could also be modeled using iron for iron micrometeoroids and polyethylene for CHON. Orbital debris could be modeled using aluminum balls of about the same density. The material chosen would have a large impact on test results since the chemical compatibility between the test particle and protection system material would be one of the factors that would determine the amount of damage sustained on impact. See References 10- 13 and 10- 22 for more information.

#### 10.4.2.6.2 Testing Facilities

There are multiple facilities at which hypervelocity impact testing could be performed including NASA facilities and national laboratories. Most of these facilities predominantly use one of the two testing methods listed below.

##### 10.4.2.6.2.1 Light Gas Gun

NASA Ames and MSFC both contain testing facilities with light gas guns. These guns are capable of accelerating small particles (0.1-1 mm in diameter) to velocities between 3 km/sec and 9 km/sec. Velocities greater than this are not recommended due to the potential for over-heating and damaging the light gas gun. Little testing data is thus available for higher hypervelocity impacts. The test chamber allowed for target samples up to 20 by 20 cm. Two guns have been shot at each other to achieve relative velocities of 20 km/sec.

##### 10.4.2.6.2.2 Electrostatic Gun

This form of testing could achieve velocities near 100 km/sec, but the particles would have to be electrically conductive. Since the best material to model micrometeoroids is silica, which is not conductive, this test would have limited applicability. Orbital debris rarely travels above 10 km/sec so this test would be considered overkill if aluminum were used for testing.

### 10.4.3 Summary

The threat of a mission ending failure due to micrometeoroids or orbital debris is real, but it is also manageable. Many different options exist to mitigate the risks and they will most likely increase in effectiveness as new technology is developed.

Options currently available include:

- Proper selection of launch vector and assembly altitude to avoid substantially large particles
- Inclusion of a ram shield over the reactor and reactor side of the hot-leg piping
- Use of protection system designs and materials for different components and regions within the spacecraft, such as
    - Single Wall
    - Whipple Shield
    - Multi-Bumper Whipple Shield
    - Honeycombed Modification of Whipple Shield
    - Stuffed Whipple Shield
    - Modified Whipple Shield

In order to complete a successful design, the following steps, extracted from NASA sources, would be recommended:

- Obtain mission specific orbital debris and micrometeoroid flux and velocity data from NASA.
- Select several combinations of particle mass and velocity that accurately represent the most likely and worst case design scenarios.
- Calculate the minimum component/system/region wall thickness for a single wall protection to obtain a reference point for starting the design process.
- Evaluate current and historical applicable protection system designs that have been effective.
- Learn current and state-of-the-art methods of protection.
- Quantitatively and subjectively rank different materials available for key attributes.
- Evaluate required level of protection for each spacecraft component/system/region per requirements documents.
- Calculate the probability of failure for each component/system/region and determine the overall reactor module probability of failure. Alternatively, use a target probability of failure to properly select a fluence, which will yield mass and velocity combinations to use for design.
- Design several protection systems for each component/system/region based on what level of protection is required, best suited materials, most applicable technology, and trade studies.
- Test the designs for:
    - Effects of reactor and environmental radiation on protection system.
    - Chemical compatibility between impacting particles and protection system.
    - Protection system material compatibility with nearby components and structures.
    - Simulation of hypervelocity particle impacts.
- Once impact testing is completed, determine test data correlations to extrapolate data to high velocities and different size masses.
- Evaluate each protection system.
- Iterate to completion.

These steps are deemed to be the most prudent way to design a mass conscious and highly effective protection system for the reactor design module. Much of the data, information, and facilities needed to complete this are available through NASA.

## 10.5 Environmental Considerations for Instrumentation and Control

Developing the instrumentation and control system of the reactor power plant would require understanding of the environments which affect its sensors, cables, and electronics. These components would be distributed throughout the Reactor Module and spacecraft in regions that vary strongly in their local radiation and thermal conditions. This section describes these environments at the pre-conceptual stage of the SNPP development.

### 10.5.1 Environmental Spacecraft Zones

The spaceship includes six distinct environmental zones in which the I & C equipment must function. These zones are shown in Figure 10-10. These consist of the reactor, shield, control drive mechanisms (CDM's), reactor coolant and plant structure, signal and power transmission, and the electronics vault regions. Radiation and thermal phenomena drive the I&C system component designs through the interaction of radiation with electronic devices and materials, and their sensitivity to temperature and heat. The selection of these devices would require a detailed understanding of the radiation and temperature sensitivities of each device. The internal radiation environment induced by the SNPP in these six zones is summarized in Table 10-10 with a listing of the reference radiation levels predicted for each region. The source and significance of these radiations for the I&C components is developed in Section 10.5.2. Similarly Table 10-11 presents the temperatures in the same regions and their significance is discussed in Section 10.5.3.

**Table 10-10: Radiation Environment Induced by SNPP**

| Region | | Radiation | |
|---|---|---|---|
| | | Total Ionized Dose (rads(Si)) | Displacement Damage Dose (n/cm$^2$) |
| Reactor | | $8.2\times10^9$ [Ref. 10- 26][a] | $6.6\times10^{19}$ [Ref. 10- 26][a] |
| Shield (centerline) | Fore | $4.5\times10^9$ [Ref.10- 26][a] | $3.8\times10^{19}$ [Ref. 10- 26][a] |
| | In | $5\times10^8$ [Ref.10- 26][a] | $5.2\times10^{16}$ [Ref. 10- 26][a] |
| | Aft | $2\times10^8$ [Ref. **10- 27**][b] | $6\times10^{14}$ [a] |
| Control Drive Mechanism | | $2\times10^8$ | $3.6\times10^{15}$[Ref. 10- 23][c] |
| Reactor Coolant and Plant Structure | | $2\times10^8$ [Ref. 10- 27][d] | $6\times10^{14}$ [Ref. 10- 27][d] |
| Signal and Power Transmission | | Approximate fall off as inverse square of distance plus shielding provided by the power conversion system [Ref. **10- 27**][e] | Approximate fall off as inverse square of distance plus shielding provided by the power conversion system [Ref. 10- 27][e] |
| Electronics Vault | | $25\times10^3$ [Ref.10- 9] | $5\times10^{10}$ [Ref.10- 9] |

[a] Assumes a 12 year mission.
[b] Assumes 15 full power year mission.
[c] Localized streaming around the control drive mechanisms.
[d] Maximum radiation for the power conversion system. Maximum radiation is located in region closest to the shield and CDM. The components will provide some shielding and the radiation will fall off as the inverse square of the distance.
[e] The radiation level will be reduced by shielding from components in the power conversion system.

## 10.5.2 Radiation Environment

### 10.5.2.1 Summary

The JIMO spacecraft would be subjected to radiations from two sources during its journey through space: the internal radiations generated by SNPP reactor and the external radiations generated by the stellar and planetary objects in space. The SNPP reactor would subject the remainder of the spacecraft to a continuous stream of neutron and gamma radiations at nearly constant levels for the duration of the mission, while space sources would impinge on the spacecraft in varying forms, rates, and intensities. It is the electrical and electronic systems aboard the spacecraft that would be particularly vulnerable to these radiations and that are the focus of the considerations herein.

The SNPP reactor induced radiations would subject the spacecraft and the I&C electrical and electronic components to radiation exposures larger than normally found in terrestrial nuclear applications, but they would be expected to be quite moderate compared to the Jovian radiation levels. In addition, the reactor gamma interactions at the outer surface of the reactor could knock electrons off the surface of the reactor to form an electron cloud that could travel around the shadow shield to the remainder of the spaceship. The existence of this electron radiation had not been confirmed, but needs to be evaluated for reactors which do not have significant amounts of gamma attenuation around the reactor, as would be the case with shadow shields as applied on the JIMO spaceship.

The JIMO spacecraft would be subjected to space radiation from a wide variety of sources while traveling through the radiation belts of Earth, interplanetary space, and the radiation belts of Jupiter. Moreover, the radiation exposure rate of the spacecraft would not be constant over the flight, but rather would vary from relatively low rates during the first years of flight to very large values near its termination. The Van Allen belts of Earth would initially subject the spacecraft to modest levels of electron and proton radiation. During the interplanetary journey to Jupiter, solar flares from the Sun and intergalactic cosmic rays would give rise to proton and heavy ion radiation at modest levels. As it traveled about the moons of Jupiter, the spacecraft would be exposed to intense electron, proton, and heavy ion radiation. The radiation in the Jovian environment was expected to be the most limiting source of radiation in so far as the spacecraft electronics and electrical components are concerned. At Jupiter, high electric field strengths and high electron energies would be expected.

### 10.5.2.2 Transient and Trapped Particles

There are two natural space radiations that are a particular concern for electronic components: transient particles such as high energy protons and heavy ions, and trapped particles consisting of protons, electrons, and heavy ions. Transient radiation consists of galactic cosmic rays and solar events including solar flares and solar coronal mass ejections. Galactic cosmic rays have omni-directional particles with low level fluxes and energies up to $10^{12}$eV. Solar eruptions consist of energetic protons, alpha particles, heavy ions, and electrons with energies in 100s of MeV Reference 10- 9.

Trapped particles, on the other hand, are found near the planetary environments of Earth and Jupiter. The environment near Jupiter contains high levels of energetic particles trapped by Jupiter's magnetic field. This radiation is similar to, but much more intense than that found within the Earth's Van Allen belts. Earth's trapped protons and heavier ions have energies exceeding 100 MeV and electrons with energies up to 10 MeV, whereas Jupiter's trapped particles have electrons with energies exceeding 100s MeV and protons with energies up to about 100 MeV.

### 10.5.2.3 Interaction of Radiation with Electronic Devices

Radiation interacts with materials and electronic devices through ionizing dose, displacement damage dose, and single electron effects. Ionizing dose and displacement damage dose are cumulative effects. The contributing environments are the Earth's Van Allen belts, the continuous irradiation due to gamma rays and neutrons from the reactor, and the intense radiation belts of Jupiter. Galactic cosmic rays and solar eruptions would contribute to the cumulative ionizing dose and displacement damage dose to a lesser degree than those environments stated earlier. Total ionizing dose (TID) and displacement damage dose (DDD) would degrade device performance and possibly render the device ineffective. Single electron effects are the result of impact into an electronic device from a single high energy particle. Transient radiation such as galactic cosmic rays particles and particles from solar events in space can cause single event upsets that complicate the reactor control function. Single event upsets can manifest themselves as noisy data or the upset can inadvertently trigger a bit flip at any point in time. The severity of the effect depends upon the criticality of the system in which the single event upset occurs. Galactic cosmic rays, solar eruptions, and high energy protons and heavy ions from the Earth's and Jupiter's radiation belts contribute to single electron effects.

The dominant sources for total ionizing dose and displacement damage dose are dependent upon the mission, as stated earlier, and the shielding capability. For the Jupiter Icy Moons Orbiter (JIMO) mission a shielding thickness of approximately 1000 mils (25mm) was being considered to satisfy the total ionizing dose and displacement damage dose requirements provided in the Parts Program Requirements Reference 10- 25. At 1000 mils the trapped Jovian electrons dominate the mission TID and DDD since most of the Earth's trapped electrons and protons and Jovian trapped protons would be effectively shielded.

### 10.5.2.4 External Radiation Contribution from Space

For the JIMO mission, the unshielded external total ionizing dose and displacement damage dose was specified as $1x10^9$ rads(Si) and $5.7x10^{15}$ 1-MeV equivalent neutrons per square centimeter, respectively (Reference 10- 9). The external environment would be dominated by charged particles, but it is described by a 1-MeV equivalent neutron. The radiation incident upon a component of interest is the sum of the external (shielded or unshielded) and internal radiation environment.

### 10.5.2.5 Internal Radiation Contribution from Reactor

The JIMO spacecraft would be subjected to radiation originating from the reactor throughout the mission. The estimated levels for the various regions of the spacecraft from the reactor are tabulated in Table 10-10. The region just aft of the reactor would experience high levels of radiation that would be subsequently attenuated through the shield. The radiation level throughout the shield would be high to modest and decrease to a minimum aft of the shield.

A design limit of $0.5x10^9$ rads(Si) TID was initially established for the I&C equipment immediately aft the reactor radiation shield based upon the most limiting elements in that region, i.e., electrical insulation materials for the cable, motors, and sensors. This design value $0.5x10^9$ rads(Si) TID incorporated a radiation design factor (RDF) of 2 and included contributions from the internal and external environment. The RDF is defined as the ratio of the device or material capability in the given application to the radiation environment at the device or material location. The internal and external contributions were assumed to be $2x10^8$ rads(Si) and $5x10^7$ rads(Si), respectively. It was found that the external radiation source could be easily attenuated by nearly an order of magnitude by as little as

10 to 20 mil of aluminum shielding (Reference 10- 9). This evaluation formed the basis for the estimate of internal radiation in the regions adjacent to the aft portion of the shield.

The control drive mechanisms would experience a highly localized spike in the radiation level due to streaming along the CDM rods through the shield. Aft of the shield the radiation level would fall off inversely with distance squared. The radiation level at a particular component would depend on shielding provided by other components in the plant along with the radiation level falling off as the inverse square of the distance.

The internal radiation falls off such that the TID and DDD at the electronic vault plane due to the reactor could be designed to be $25x10^3$ rads(Si) and $5x10^{10}$ 1-MeV equivalent neutrons per square centimeter (Reference 10- 9) based on an RDF of 2..

The TID and DDD requirements for the electronic components used in the JIMO mission are specified as $3x10^5$ rads(Si), preferably $1x10^6$ rads(Si), and $6x10^{11}$ 1-MeV equivalent neutrons per square centimeter as documented in the Parts Program Requirements, Reference 10- 25. Thus, the radiation environment inside the electronics vault would be shielded to a $1.5x10^5$ rads(Si) region and a $5x10^5$ rads(Si) and $3x10^{11}$ 1-MeV equivalent neutrons per square centimeter region. The external and internal radiation values along with the radiation hardened level for the components would determine the amount of shielding required for the electronic vault to achieve these desired dose levels.

### 10.5.3 Thermal Environment

As discussed earlier in this section, the spacecraft would be subject to a variety of external thermal environments during pre-launch activities, launch, orbital flight, and interplanetary flight to Jupiter. It would be exposed to a wide variation in temperature. To accommodate these extremes, the thermal management segments of the Reactor Module and of the spacecraft must provide the necessary thermal environments for the structures and components of the spacecraft to survive and operate reliably for the duration of the mission.

The reactor I&C equipment would be distributed over many regions of the spacecraft, such that interrelated elements of its subsystems would often be subjected to very different thermal conditions. An understanding of the thermal elements within each zone would guide the design and development of the I&C system components and the local thermal management subsystems to ensure that the I&C component thermal requirements would be met. This section presents the initial efforts to identify the thermal environments within the various regions of the spacecraft to allow the development of a rational set of requirements for the I&C equipment that reside within them.

#### 10.5.3.1 Thermal Environment by Zones

Table 10-11 summarizes the baseline temperatures in each of the six regions of concern to the design of the I & C Segment. This summary identifies the temperature of major thermal elements within each zone including fluids that may be measured, surfaces that may have I&C components attached to them, as well as sources that may radiate or conduct energy to a component. These temperatures represent a snapshot of the SNPP and spacecraft thermal environments during the pre-conceptual SNPP design process. The values were obtained from a wide variety of references that were undergoing constant revision as more became known of the reactor plant and spacecraft designs. These values would have eventually formed the basis for the system requirements for the I&C equipment.

#### 10.5.3.1.1 Aft of Reactor and Fore of Shield

In the internally insulated, nickel superalloy hot leg piping design, the temperature of the gas inside the hot leg is 1150 K (Section 2) with the outer surface insulated to 900 K (Reference 10- 28). The primary cold leg coolant return pipe is 891 K (Section 2).

#### 10.5.3.1.2 Interior of Shield

There were four shielding materials considered; lithium hydride (LiH), beryllium and boron tetrachloride (Be & $B_4C$), Boron, and water. The LiH material would require the interior neutron shield portion of the reactor shield operate between 600 K and 800 K for best material stability. The estimated thermal values for the Be & $B_4C$, Boron, and water assumed that the heat was radiated to space, while the LiH shield assumed heat was radiated to an insulated layer. If a micrometeoroid shield was determined necessary then the temperature of the Be & $B_4C$, Boron, and water shield would likely increase. Furthermore, the above values assumed that the hot leg travels a straight path through the shield. In order to reduce radiation streaming along the coolant pipes through the shield, other piping configurations, including a spiral path through the shield, would be considered and the longer path through the shield would likely increase the shield temperature (Reference 10- 18)

#### 10.5.3.1.3 Control Drive Mechanism and Aft of Shield

The goal of thermal control within the control drive mechanism region would be to limit CDM temperatures to 400 K maximum to satisfy the material requirements and to maximize the reliability of the CDMs. This goal may require the addition of thermal insulation or supplemental heat rejection. Insulation materials, if needed, would require development to insulate properly above 500 K. Near 600 K the permanent magnets may begin to degrade and would require further study.

#### 10.5.3.1.4 Reactor Coolant and Plant Structure

Similar to the control drive mechanism zone, there would be 300 K to 400 K regions within the Reactor Coolant and Plant Structure zone to satisfy the thermal requirements of the electronic components (primarily the cable and connectors). See Section 10.3.6.4. The temperature of the gas and surface pipes is provided to assist the design of the sensor and sensor fixture technology.

#### 10.5.3.1.5 Signal and Power Transmission

The region from the reactor coolant and plant structure zone to the electronics vault would be occupied by cabling and connectors for which temperatures from 200 K to 400 K would be targeted. After launch and prior to start up, the boom will be unfolded. In order to assure the cables unfold successfully at the hinge, heaters may be required to keep the temperature within the desired range. Thermal management is required to balance resistive heat generation with heat transfer external to the boom to maintain target temperatures.

#### 10.5.3.1.6 Electronics Vault

Thermal management would be needed to balance electronics heat generation with heat transfer external to the enclosure to maintain temperatures. Thermal control within the electronics vault would be designed to satisfy the 238 K to 348 K requirements for electronics.

**Table 10-11: Baseline Temperatures for I & C Component and System Design**

| | | Thermal (Internal) (K)<br>Snapshot Values | Current References |
|---|---|---|---|
| **Reactor** | | 1150 K Gas Hot Leg Interior<br>900 K Hot Leg Surface<br>889 K Cold Leg Surface | Section 10.3.6.1, Section 2 and Ref. 10- 28 |
| **Shield (centerline)** | **Fore** | 670 K ($Be/B_4C/LiH$)<br>405 K ($Be/B_4C$)<br>470 K (Boron)<br>535 K ($Be/B_4C/H_2O$) | Section 10.3.6.2<br>Ref. 10- 18 |
| | **In** | 665 K ($Be/B_4C/LiH$)<br>388 K ($Be/B_4C$)<br>400 K (Boron)<br>393 K ($Be/B_4C/H_2O$) | Section 10.3.6.2<br>Ref. 10- 18 |
| | **Aft** | 650 K ($Be/B_4C/LiH$)<br>379 K ($Be/B_4C$)<br>370 K (Boron)<br>350 K ($Be/B_4C/H_2O$) | Section 10.3.6.2<br>Ref. 10- 18 |
| **Control Drive Mechanism (CDM)** | | 1150 K Gas Hot Leg Interior<br>900 K Hot Leg Surface | Section 10.3.6.3<br>Ref. 10- 28 |
| | | 400K Ambient Temperature | Section 10.3.6.3 |
| | | 400 K CDM Temperature | Section 10.3.6.3 |
| **Reactor Coolant and Plant Structure** | | 300 K to 400 K ambient temperature | Section 10.3.6.4 |
| | | 900 K Hot Leg Surface<br>1150 K Gas Interior Hot Leg<br>1150 K Gas Turbine Inlet<br>927 K Gas Turbine Outlet<br>450 K Alternator Bleed Leg<br>556 K Gas Cooler Inlet Leg<br>390 K Compressor Inlet Leg<br>537 K Compressor Outlet Leg<br>891 K Reactor Inlet Leg<br>530 K Radiator Inlet Leg<br>379 K Radiator Outlet Leg | Section 10.3.6.4,<br>Section 2, Section 6, and<br>Ref. 10- 28 |
| **Signal and Power Transmission** | | Signal and Power Transmission:<br>218 K to 378 K<br>Radiator: 379 K to 530 K | Section 2 (radiator values)<br>Reference 10- 30 |
| **Electronics Vault** | | 238 K to 348 K | Reference 10- 29 |

### 10.5.4 Summary

The thermal and radiation requirements for the components making up the I&C system depend heavily on the ability to accurately describe the Reactor Module and spacecraft environment induced both the by the SNPP and the space environment. These requirements are crucial to the design, development, test and certification of the components. For this reason, the creation and development of quality models of the thermal and radiation environments for all the major regions of the SNPP and spacecraft is necessary.

## 10.6 References

10- 1: Prometheus Baseline 1 – Li/Brayton Concept, Northrop Grumman Space Technologies
10- 2: "Jupiter Icy Moons Orbiter (JIMO) Environmental Requirements Document - Preliminary", 982-00029, Rev. 0, July 6, 2005
10- 3: B-SE(SPS)FMS-008, "Technical Documentation in Support of Project Prometheus Plant Pre-Conceptual Design Report," November 11, 2005
10- 4: Haley, V.F., "Insulation for TEM Pump", General Electric Corporation, Sept. 23, 1987
10- 5:Cooke, Bill. "Jupiter Icy Moons Orbiter Meteoroids/Orbital Debris and JIMO" Presentation. MSFC/UNITeS. July 27, 2004.
10- 6: Garrett, Henry B. "Space Environment Interactions for JIMO" Presentation. JPL. August 4, 2004.
10- 7: JPL D-10178-3 Cassini Earth Swingby Plan Supplement
10- 8:JPL D-982-00001. Prometheus Nuclear Systems and Technology Program. Preliminary Prometheus Project Plan. NASA Unique Project Number: UPN # 982-00. Revision 1. May 2005
10- 9: JPL D-982-00029. Prometheus Project. Environmental Requirements Document. Revision 0. July 6, 2005.
10- 10: NASA Preferred Reliability Practice PD-EC-1107.
10- 11: NASA Contractor Report 4706 Structural Damage Prediction and Analysis for Hypervelocity Impacts- Handbook.
10- 12:NASA Conference Publication 3194-Part 2- LDEF-60 Months in Space.
10- 13: NASA/TM-2003-212440 Hypervelocity Impact Test Results for a Metallic Thermal Protection System.
10- 14: Williamsen, Joel. "Meteoroid and Orbital Debris Design Considerations for Space Operations." 2001 Core Technologies for Space Systems Conference. November 28, 2001.
10- 15 Larson, Wiley J. and Wertz, James R, Space Mission Analysis and Design, Mircocosm Inc and Kluwer Academic Publishers, 1992
10- 16 Bettis Letter B-SE(RE)THD-0007, "Pressure Vessel and Reflector Temperature Sensitivity Studies", Volk, David R., October 31, 2005
10- 17: KAPL Letter SPP-SPPS-0035 and Bettis Letter B-SE(SPS)FMS-012, Reactor Module Thermal Zone Scoping Analyses, For Information, To Be Issued
10- 18: KAPL Letter SPP-67210-0011, "Space Reactor Shield Design Summary, For Information", To Be Issued.
10- 19: NASA/TP-1999-209263, "Multilayer Insulation Material Guidelines," M.M. Finckenor, Marshall Space Flight Center, April 1999
10- 20: NASA SP-8105, Spacecraft Thermal Control, May 1973
10- 21: NASA/CR-1999-000000; Design, Fabrication and Test of a 6 kWt Space Radiator Demonstration Unit (RDU) – Phase I Final Report; September, 2004

10- 22: NASA/TP--2002-212076, Test and Analysis Capabilities of the Space Environment Effects Team at Marshall Space Flight Center
10- 23: KAPL letter FSO-64R00-05-096, Control Drive Mechanism Streaming Analysis for Space Reactor Shield, August 24, 2005
10- 24: JPL Systems Description 982-00051 Rev.0 August 6, 2004.
10- 25: Casani, J., Jet Propulsion Laboratory, "Parts Program Requirements" (982-00025), dated March 2004.
10- 26: ORNL/LTR/NR-JIMO/05-01, "JIMO Reactor Sensor Technology Development Plan," Holcomb, D. E., et al., ORNL report, January 2005.
10- 27: ORNL/LTR/NR-PROM1/05-21, "Radiation Transport Analyses to Support the Reactor Shield Materials Selection," Bucholz, J.A., et al., ORNL report, August 2005.
10- 28: KAPL letter SPP-67210-0007, "Hot leg Piping Concept for Future Development," dated June 30, 2005.
10- 29: JPL Document D-17868, Revision 2 "Design, Verification/Validation and Ops Principles for Flight Systems (Design Principles)", March 3, 2003.
10- 30: JPL Document D-8208, Revision 1, "Space Craft Design and Fabrication Requirements for Electronic Packaging and Cabling", January 14, 2002

# Section 11
# Potential Space Nuclear Power Plant Design Events

(Intentionally Blank)

# Potential Space Nuclear Power Plant Design Events

## Table of Contents

11 Potential Space Nuclear Power Plant (SNPP) Design Events ..... 5
11.1 Summary and Conclusions ..... 5
11.2 Normal Design Events ..... 6
11.2.1.1 System Pressure Test ..... 6
11.2.1.2 Initial System Fill ..... 6
11.2.1.3 Acceptance Testing ..... 6
11.2.1.4 Initial Criticality ..... 6
11.2.1.5 Launch ..... 6
11.2.1.6 Reactor Module Commissioning ..... 6
11.2.1.7 Temperature Adjustments over Life ..... 6
11.2.1.8 Transition from Full Power Mode to Reduced Power Mode ..... 7
11.2.1.9 Transition from Reduced Power Mode to Full Power Mode ..... 7
11.2.1.10 External Thermal Cycling ..... 7
11.2.2 Casualty Design Events ..... 7
11.2.2.1 Loss or Reduction of Reactor Coolant Flow ..... 7
11.2.2.2 Stuck Open Check Valve in an Idle Loop ..... 7
11.2.2.3 Partially Closed Check Valve or Control Valve in an Operating Loop ..... 8
11.2.2.4 Loss of Brayton Speed Control ..... 8
11.2.2.5 Startup of a Spare Brayton ..... 8
11.2.2.6 Increase in Reactor Coolant Flow ..... 8
11.2.2.7 Loss of Heat Rejection Segment (HRS) Flow in a HRS Loop ..... 9
11.2.2.8 Loss of Radiator Capability ..... 9
11.2.2.9 External Neutron Addition ..... 9
11.2.2.10 Stuck Reflector ..... 9
11.2.2.11 Inadvertent Reflector Motion ..... 9
11.2.2.12 Loss of Coolant (Gas leak) ..... 9
11.3 GTR Design Events ..... 10
11.3.1 Normal Design Events ..... 10
11.3.1.1 Normal Reactor Startup and Shutdown ..... 10
11.3.1.2 External Thermal Cycling ..... 11
11.3.1.3 Coolant Sampling ..... 11
11.3.2 Casualty Design Events ..... 11
11.3.2.1 Loss of Reactor Coolant Flow ..... 11
11.3.2.2 External Neutron Addition ..... 11
11.3.2.3 Inadvertent Reflector Motion ..... 11
11.3.2.4 Loss of Coolant (Gas leak) ..... 11
11.3.2.5 Emergency Shutdown ..... 12
11.3.2.6 Release of Cryogenic Fluid into Vacuum Chamber ..... 12
11.3.2.7 Air Contamination or Leakage into Vacuum Chamber ..... 12
11.3.2.8 Loss of HRS Flow ..... 12
11.3.2.9 Seismic Event ..... 12
11.3.2.10 Release of HRS Fluid into Vacuum Chamber ..... 12
11.4 References ..... 12

(Intentionally Blank)

# 11 Potential Space Nuclear Power Plant (SNPP) Design Events

## 11.1 Summary and Conclusions

This section describes potential design events for the Space Nuclear Power Plant (SNPP). Design events applicable specifically to the Ground Test Reactor (GTR) are listed in Section 11.3. A list of design events would have been finalized after the reactor module functional requirements were established and the system architecture selected.

Key Conclusions Regarding SNPP Design Events:

- The system architecture will determine how some design events affect the SNPP, and whether the design events are recoverable. For example, a permanent Brayton failure will be non-recoverable for a 1-1-1 architecture, but may be recoverable for a 2-2-2 architecture.
- Preliminary evaluations indicate that autonomous control action will be required for some transients to prevent a breach in the primary system. A significant loss of gas inventory would be mission-ending for the direct gas Brayton system regardless of system architecture.
- The location and differences in use of the GTR Facility will cause the GTR to have different design events from the SNPP.

Definition and characterization of design events are used to set design specifications for plant systems and components, as well as provide input for structural analyses such as fatigue and brittle fracture. A formal Design Events Document contains the list of events, the design number of cycles for each event expected during the lifetime of the SNPP, and a complete set of plant transient performance curves for all key plant parameters. The Design Events Document was not completed at the time of Prometheus Project termination; it would have been issued early in the Conceptual Design phase. This section provides a preliminary listing and qualitative description of each event. Section 12 provides transient analysis results for a subset of these events.

Reactor control commands would be issued from the Reactor Supervisory controller. Plant control commands (e.g., PCAD functions) would be issued from the PCAD controller. These commands would be programmed functions in the respective controllers and would be initiated autonomously in response to plant conditions, or initiated in response to commands from ground control and received by the controllers via the telecom and flight computer subsystems. Autonomous control is necessary because of the limited communication between the SNPP and ground control once the spaceship launched. Ground control commands are human issued commands that can be either a single command, a set of commands, or an initiator for a set of autonomous commands. For the SNPP, ground control commands travel through the Deep Space Network (DSN) and along the spaceship communication bus to the Reactor Supervisory controller.

The design events list was generated by reviewing historical references including the SP-100 Generic Flight System Duty Cycle Definitions (Reference 11- 1) and other applicable documents. Events that would create stress changes and that the SNPP would be designed to survive are considered design events. These events are then further divided into Normal Design Events and Casualty Design Events.

## 11.2 Normal Design Events

Normal design events encompass events that the SNPP would be expected to experience during the course of normal operation.

### 11.2.1.1 System Pressure Test

The SNPP will be pressurized to [Reserved] times the maximum operating pressure at [Reserved] temperature using inert gas to check for structural integrity and leak tightness.

### 11.2.1.2 Initial System Fill

The initial system fill will charge the SNPP with the proper amount and composition of gas to achieve normal conditions when operating. The method and procedures for filling the SNPP have not been established.

### 11.2.1.3 Acceptance Testing

Initial system level tests will be run to ensure that there are no gross manufacturing defects. This may include exercising the reflectors, motoring the Brayton units, exercising valves, and testing the reactor controller computers and software.

### 11.2.1.4 Initial Criticality

Initial reactor criticality will be part of a ground test program to verify that there are no gross manufacturing defects and to characterize the as-built reactivity characteristics of the SNPP reactor before launch. Reactor power and amount of time critical will be limited to prevent accumulation of fission products in excess of launch safety criteria.

### 11.2.1.5 Launch

Significant mechanical loads will be experienced by the SNPP during launch. Launch loads are dependent on the launch vehicle design, support ring, folded boom geometry, etc.

### 11.2.1.6 Reactor Module Commissioning

Reactor module commissioning occurs after launch and includes pre-critical checks, initiating primary coolant flow, bringing the reactor to criticality, heating up the plant and starting the Brayton units, starting (or increasing) the heat rejection segment (HRS) flow, bringing the spaceship to self-sustaining on nuclear power. See Sections 8.5.1 and 12.4.1.6 for details of the startup sequence.

### 11.2.1.7 Temperature Adjustments over Life

Primary coolant temperature would need to be adjusted over the life of the mission due to fuel burnup, aging of components and space environment changes (heat sink temperature). This will be accomplished by adding or removing core reactivity with the reactivity control devices.

### 11.2.1.8 Transition from Full Power Mode to Reduced Power Mode

Reduced Power Mode(s) could be used when the spaceship is entering a long period of decreased electrical demand. This potentially conserves fuel, minimizes fission product buildup, and reduces time-at-temperature and creep. More details on Reduced Power Mode options can be found in Sections 3.7 and 8.5.2.3.

### 11.2.1.9 Transition from Reduced Power Mode to Full Power Mode

The transition from Reduced Power Mode to Full Power Mode would occur when the spaceship is approaching a time of full electrical power demand (thrusting). More details on Reduced Power Mode options can be found in Sections 3.7 and 8.5.2.3.

### 11.2.1.10 External Thermal Cycling

The SNPP will experience thermal cycling as it orbits the Earth or a moon because it is alternately exposed to the Sun and in shadow.

## 11.2.2 Casualty Design Events

Casualty design events are unexpected events, usually resulting from a temporary or permanent failure of a system component, that the SNPP would be designed to survive without permanent loss of capability.

### 11.2.2.1 Loss or Reduction of Reactor Coolant Flow

The SNPP is assumed to be operating at full power when all or a portion of reactor coolant flow is lost (see Section 12). This could be caused by loss of a Brayton or an inadvertent valve closure. Preliminary modeling results have shown that both events are recoverable if negative reactivity is inserted and reactor coolant flow is maintained (multiple Brayton units running at the initiation of the casualty) or quickly reestablished (restarting a single Brayton unit or starting a standby unit). It may also be necessary to reduce HRS flow to minimize system cooldown. Restarting a Brayton with a cold HRS would produce a significant thermal transient in the gas cooler. See Section 12 for preliminary transient results of a partial loss of flow (Sections 12.4.1.3, 12.4.2.1, and 12.4.3.1) and a complete loss of flow (Section 12.4.3.6).

### 11.2.2.2 Stuck Open Check Valve in an Idle Loop

A check valve was placed in each of the Brayton loops to prevent reverse flow in an idle loop. If the valve fails to completely close, reverse flow through the idle loop will be driven by differential pressure across the reactor. [A backup isolation valve may be used to minimize the potential for this casualty.] This reverse flow can cause insufficient core cooling, overheating of idle loop components, or damage to the Brayton bearings. The reverse flow that bypasses the core causes reduced cooling flow through the reactor resulting in increases in temperatures. The amount of flow reduction will be dependent upon the flow resistance in the idle loop and the degree to which the valve remains open. Reverse flow is also a concern for the current design of the Brayton thrust bearing which is designed to operate in the forward direction only. The degree of reverse flow which could be permitted without overheating the reactor or idle loop components has not been determined. A small amount of backflow may be desirable in an idle loop to maintain temperature. It may also be necessary to include a Brayton shaft locking mechanism to prevent reverse rotation caused by reverse flow.

### 11.2.2.3 Partially Closed Check Valve or Control Valve in an Operating Loop

If the check valve or control valve fails to fully open in an operating loop, the valve will present a flow restriction in the loop. The overall system pressure drop will increase while reducing system mass flow rate, reducing the thermal efficiency of the system. A flow imbalance between the operating loops will exist because flow through the unrestricted loop will increase until its pressure drop equals that of the restricted loop. If the flow restriction is too severe, the reactor module may not be able to generate the required electrical power.

### 11.2.2.4 Loss of Brayton Speed Control

Brayton speed is controlled through the Parasitic Load Radiator (PLR). Each Brayton would have a PLR. If the PLR fails, Brayton speed control will be lost. The type of PLR failure will determine what load can be applied to the Brayton alternator. Insufficient load will result in an increase in Brayton shaft speed until a new balance between turbine and compressor work is achieved. See Section 12 for preliminary transient results of a complete loss of electrical load (Sections 12.4.1.4, 12.4.2.2, and 12.4.3.2) and a partial loss of electrical load (Section 12.4.3.3). The Section 12 results show system response with no action. The high shaft speeds reached during this casualty could result in exceeding mechanical stress limits in the affected Brayton. Another significant impact of this casualty is overheating in the HRS. Boiling in the HRS water coolant may overpressurize the system leading to an unrecoverable failure of the gas cooler. Control actions to prevent this may include Brayton control valve closure to stop primary gas flow and shut down the Brayton. Actions could also include increasing HRS flow to reduce or prevent boiling and overpressurization. If boiling is prevented, the additional heat load on the radiator heat pipes is also a concern. Multiple heat pipe failures could prevent the affected HRS loop from rejecting the necessary heat upon future restart. A gas cooler failure is likely to also cause a primary gas leak that would potentially be mission ending.

### 11.2.2.5 Startup of a Spare Brayton

A spare Brayton would be started when a component (Brayton, valve, HRS loop) renders an operating Brayton unit unable to produce the necessary electrical power or when directed by ground control. Depending upon the plant arrangement, this could require opening and shutting valves. The spare Brayton unit would be started by motoring it using power from an operating Brayton or an energy storage system. Starting a spare Brayton could cause a significant thermal transient for system components. System design would attempt to minimize coolant temperature differences prior to spare startup.

### 11.2.2.6 Increase in Reactor Coolant Flow

An increase in reactor coolant flow will result from either a spare Brayton inadvertently starting while the plant is operating at full power (and the associated loop valve(s) opening) or by an increase in the speed of an operating Brayton. If the increased flow is from a spuriously started spare Brayton, shutdown of that Brayton will return flow to normal levels. If it is caused by an increase in the speed of an operating Brayton, the PLR could be used to reduce speed or a control valve could be used to shut the Brayton down. Any increase in primary flow could also increase the HRS heat load. HRS flow control actions could also be required.

### 11.2.2.7 Loss of Heat Rejection Segment (HRS) Flow in a HRS Loop

Loss of HRS flow in a HRS loop can occur through loss of a pump or a breach in the secondary loop pressure boundary. This casualty will be mitigated by the HRS loop design (spare pumps and cross strapping). A breach in a HRS loop pressure boundary would lead to loss of fluid and an unrecoverable casualty for the affected HRS loop. See Section 12 for preliminary transient results of a loss of HRS flow (Sections 12.4.2.5, and 12.4.3.7). To prevent overheating in the primary loop it may be necessary to shut down the associated Brayton. This action would depend on the method and time required to restore HRS function.

### 11.2.2.8 Loss of Radiator Capability

Loss of radiator capability could be caused by heat pipe failure, reduction of radiator emissivity, and/or incident radiation. All three of these events will reduce the amount of heat rejected by the HRS and increase the HRS fluid temperature at the gas cooler inlet. This decreases the amount of heat transferred from the primary to the secondary coolant and increases the gas temperature at the compressor inlet, decreasing system efficiency. Margin would be built into the radiator area to offset this concern. Control action such as changes in HRS pump speed may also be used.

### 11.2.2.9 External Neutron Addition

Solar flares have the potential to add high energy neutrons to the core. This is of most concern during startup, where there may be the potential to add enough neutrons to affect the nuclear instrument indications.

### 11.2.2.10 Stuck Reflector

A control device may become stuck because of an electrical fault or a mechanical failure. The plant would be designed to perform all normal events with one stuck reflector.

### 11.2.2.11 Inadvertent Reflector Motion

A fault in the control drive mechanism (CDM) electronics or CDM controller could cause inadvertent motion of a reflector section, potentially driving it to its most reactive or least reactive position (although this is viewed as unlikely if the design utilizes stepping motors for reflector control). To maintain the desired power level, the control system would move the other reflector sections to counteract the reactivity change.

### 11.2.2.12 Loss of Coolant (Gas leak)

A slow loss of primary coolant would reduce the cycle efficiency which would require adjustments in other cycle parameters (e.g., turbine inlet temperature) to continue to produce rated power. Over time, the SNPP would be unable to generate rated power, crippling the spaceship and eventually leading to a loss of mission.

A large or sudden loss of primary coolant would result in a loss of the spaceship.

## 11.3 GTR Design Events

This section describes the differences between the design events for the GTR and the SNPP. Preliminary functional requirements[11.1] for the GTR Facility can be found in Reference 11- 2.

The GTR is designed to be as prototypic of the SNPP flight unit as possible; however, the dissimilar operating locations (deep space versus Earth's surface), the functional requirements (GTR is a test bed that will be highly instrumented), and use (GTR operations will result in many more cycles) drive differences. Based on location, different safeguards, containment, and auxiliary systems are required for the GTR. These systems may include a decay heat removal system, a fast shutdown protective system (this will likely need to be non-prototypical of the flight unit), some form of external and/or internal core cooling in the event of a loss of coolant or loss of flow casualty to remove decay heat, sampling, and containment. Also, dependent on materials, a loss of vacuum may be a casualty. With the ability of operators to monitor the GTR and to restart the plant manually and because of personnel safety concerns, the GTR can be shut down in casualties where the SNPP would attempt to maintain criticality; if the SNPP shuts down following commissioning, the spaceship could be lost. The GTR plant and reactor would probably be operated in a cryogenically cooled vacuum chamber to simulate the space environment. The GTR secondary cooling loop is not a prototypic radiator but a cooling tower or some other appropriate heat sink. The presence of gravity is another complication the GTR must address.

The GTR most likely would have two independent control and reactor safety systems; one simulating the SNPP (to support testing) and the other providing for manual operation of the GTR and rapid shutdown (scram) capability. Similar to the SNPP, the design events list was generated by looking at historical references including the SP-100 Generic Flight System Duty Cycle Definitions (Reference 11- 1) and other applicable documents. For this document, the plant arrangement was assumed to have no shared components. Events that would create stress changes and that the GTR would be designed to survive are considered design events. These events were then further divided into Normal Design Events and Casualty Design Events.

### 11.3.1 Normal Design Events

Normal design events encompass events that the GTR was expected to experience during the course of normal operation. All of the SNPP design events listed in Section 11.2 are applicable to the GTR, although the GTR most likely will experience many more cycles for each transient. Transients are only listed below if there is a significant difference between the GTR and SNPP design events or if the design event is unique to the GTR.

#### 11.3.1.1 Normal Reactor Startup and Shutdown

Normal startup and shutdown of the GTR may occur many times over the life of the unit for testing and maintenance. Normal shutdown will use power from the GTR Facility to drive the reflectors to their least reactive position and to maintain reactor flow (if required) to allow for decay heat removal.

[11.1] The functional requirements in the reference are preliminary, had not been reviewed against federal requirements, had not received any review, and had not been approved by Naval Reactors. They were a work in progress when the NRPCT participation in Project Prometheus was terminated.

#### 11.3.1.2 External Thermal Cycling

The GTR may simulate the SNPP exterior thermal cycling through thermal management of the vacuum chamber cryogenic shroud temperature (Reference 11- 2). However, shroud cooling would not be continued once heat balance testing had been completed (external cooling of the vacuum chamber to alleviate gamma heating of the vacuum chamber walls would continue throughout life)..

#### 11.3.1.3 Coolant Sampling

GTR primary coolant and HRS coolant sampling would be performed to study the coolant chemistry and composition. The method of sampling had not been defined.

### 11.3.2 Casualty Design Events

Casualty design events are casualties the GTR is designed to survive without permanent loss of capability. All of the design events listed in Section 11.2.2 are applicable to the GTR, and are only listed if there is a significant difference between the GTR and SNPP design events, or if the design event is unique to the GTR.

#### 11.3.2.1 Loss of Reactor Coolant Flow

In the event of a complete loss of flow casualty, the GTR may require supplementary cooling to ensure the reactor core is not damaged. External cooling of the GTR may be accomplished by direct gas injection into the vacuum chamber.

#### 11.3.2.2 External Neutron Addition

This may or may not be simulated on the GTR.

#### 11.3.2.3 Inadvertent Reflector Motion

A fault in the control drive mechanism (CDM) electronics or CDM controller could cause inadvertent motion of a reflector, potentially driving it to its most reactive or least reactive position (although this is viewed as unlikely if the design utilizes stepping motors for reflector control). To maintain the desired power level, the control system would move the other reflectors to counteract the reactivity change. The response to this may be to shut down the GTR.

#### 11.3.2.4 Loss of Coolant (Gas leak)

A slow loss of primary coolant would reduce the cycle efficiency which would require adjustments in other cycle parameters (e.g., turbine inlet temperature) to continue to produce rated power. Over time, the SNPP would be unable to generate rated power, requiring the GTR to shutdown or to makeup the gas losses.

A large or sudden loss of primary coolant would result in a shutdown of the GTR and potentially activation of engineered safeguards systems.

### 11.3.2.5 Emergency Shutdown

An emergency shutdown of the GTR would be initiated in the event of a severe reactor or facility casualty. This may include activating a fast shutdown protective system, initiating external core cooling and/or activating an engineered safeguards and containment systems to prevent core damage and fission product release. If the casualty involved loss of coolant, a gas makeup system could be used to remove decay heat from within the core.

### 11.3.2.6 Release of Cryogenic Fluid into Vacuum Chamber

The GTR vacuum chamber is partially cooled by a cryogenic shield on the interior of the vacuum chamber. The release of this cryogenic fluid into the vacuum chamber could have a thermal impact on the GTR and may introduce material contamination concerns.

### 11.3.2.7 Air Contamination or Leakage into Vacuum Chamber

Dependent on the materials used for the SNPP pressure boundary, this may or may not result in a casualty.

### 11.3.2.8 Loss of HRS Flow

Due to the non-prototypic nature of the HRS for the GTR, the GTR casualty may affect the cooling of additional components and impact the overall plant differently.

### 11.3.2.9 Seismic Event

The GTR will be designed to account for seismic loads for the area where the Facility is sited.

### 11.3.2.10 Release of HRS Fluid into Vacuum Chamber

The HRS fluid penetrates the vacuum chamber pressure boundary. A leak in the HRS piping inside the vacuum chamber would have a thermal impact on the GTR and may introduce material contamination concerns.

## 11.4 References

**11- 1:** SP-100 Generic Flight System Duty Cycle Definitions, PIR-1009 Rev. B, SP-100 Program Information Release, dated March 12, 1992

**11- 2:** B-SE(SPS)GT-005, "Space Nuclear Power Plant - Ground Test Reactor Facility Planning Closeout Report - For Information," dated December 13, 2005

# Section 12
# Transient Modeling

(Intentionally Blank)

# Transient Modeling

## Table of Contents

12 Transient Modeling ..... 11
12.1 Summary and Conclusions ..... 11
12.2 Description of Modeling Software ..... 13
12.2.1 MATLAB/Simulink ..... 13
12.2.2 TRACE and RELAP5-3D ..... 13
12.3 Scope of Modeling and Analysis ..... 15
12.3.1 Description of Plant Models ..... 15
12.3.2 Transients ..... 18
12.4 TRACE Model Description and Results ..... 21
12.4.1 TRACE Direct Gas Brayton Model Description ..... 21
12.4.1.1 Steady State Condition ..... 25
12.4.1.2 Reactor ..... 29
12.4.1.3 Turbomachinery ..... 37
12.4.1.4 Gas Cooler ..... 42
12.4.1.5 Recuperator ..... 43
12.4.1.6 Heat Rejection Segment (HRS) ..... 45
12.4.1.7 Reactor Coolant Piping ..... 49
12.4.2 TRACE Transient Results ..... 50
12.4.2.1 Mechanical Loss of One Brayton (TRACE) ..... 51
12.4.2.2 Complete Loss of Electrical Load for One Brayton (TRACE) ..... 53
12.4.2.3 Partial Loss of Electrical Load for One Brayton (TRACE) ..... 55
12.4.2.4 Positive Reactivity Addition (TRACE) ..... 57
12.4.2.5 Negative Reactivity Addition (TRACE) ..... 59
12.4.2.6 Complete Loss of Primary Flow (TRACE) ..... 61
12.4.2.7 Complete Loss of Flow in One HRS Loop (TRACE) ..... 62
12.5 RELAP5-3D Model Description and Results ..... 125
12.5.1 RELAP5-3D Direct Gas Brayton Model Description ..... 125
12.5.1.1 Steady State Condition Compared to Input Model Results ..... 126
12.5.1.2 Reactor Input Model ..... 128
12.5.1.3 Turbomachinery Input Model ..... 133
12.5.1.4 Gas Cooler ..... 135
12.5.1.5 Recuperator ..... 136
12.5.1.6 Heat Rejection Segment (HRS) ..... 137
12.5.2 RELAP5-3D Transient Results ..... 140
12.5.2.1 Mechanical Loss of One Brayton (RELAP5-3D) ..... 140
12.5.2.2 Complete Loss of Electrical Load for One Brayton (RELAP5-3D) ..... 141
12.5.2.3 Positive Reactivity Addition (RELAP5-3D) ..... 141
12.5.2.4 Negative Reactivity Addition (RELAP5-3D) ..... 142
12.5.2.5 Complete Loss of Flow in One HRS Loop (RELAP5-3D) ..... 142
12.5.2.6 Start-up (RELAP5-3D) ..... 142
12.6 References ..... 174

## List of Figures

Figure 12-1: Dual Loop Direct Gas Brayton System ..... 15
Figure 12-2: TRACE/SNAP Primary Plant Schematic View ..... 23
Figure 12-3: Design Point for TRACE Model (Heat Balance Case HB24) ..... 28
Figure 12-4: Reference Reactor Cross-section with Color Coded Pins for 6-Path TRACE Model ..... 29
Figure 12-5: SNAP View of TRACE Reactor Thermal Hydraulic Model ..... 30
Figure 12-6: Typical Arrangement for Reactor Vessel Downcomer Produced by Shroud ..... 31
Figure 12-7: TRACE/SNAP Geometry, Shim and $T_{ave}$ Controller View ..... 35
Figure 12-8: Typical Arrangement for a TCA Brayton ..... 39
Figure 12-9: TRACE/SNAP Brayton Loop One Shaft Torque Calc & Speed Controller View ..... 41
Figure 12-10: Shell-and-Tube-Fin Gas Cooler Model ..... 42
Figure 12-11: Plate-Fin Recuperator Model ..... 44
Figure 12-12: TRACE/SNAP Secondary Plant (HRS) Plant Schematic View ..... 47
Figure 12-13: TRACE/SNAP Animation View of Primary Plant Steady State Full Power Conditions .. 65
Figure 12-14: TRACE/SNAP Animation View of HRS Steady State ..... 67
Figure 12-15: Temperatures for Reactivity Feedback – Loss of Brayton (TRACE) ..... 69
Figure 12-16: Reactivity for Loss of Brayton (with CCEP maps) (TRACE) ..... 69
Figure 12-17: Reactor Power Resulting from Loss of One of Two Braytons (TRACE) ..... 70
Figure 12-18: Hot Spot Fuel Temperature Resulting from Loss of One of Two Braytons (TRACE) .... 70
Figure 12-19: Brayton 2 Pressures for Loss of Brayton 1 (TRACE) ..... 71
Figure 12-20: Brayton 2 Loop Flow for Loss of Brayton 1 (TRACE) ..... 71
Figure 12-21: Reactor Pressure Drop for Loss of Brayton 1 (TRACE) ..... 72
Figure 12-22: Brayton Component Power for Loss of Brayton 1 (TRACE) ..... 72
Figure 12-23: Reactor Inlet & Exit Temperatures for Loss of Brayton 1 (TRACE) ..... 73
Figure 12-24: Brayton 1 Loop Temperatures for Loss of Brayton 1 (TRACE) ..... 73
Figure 12-25: Brayton 2 Loop Temperatures for Loss of Brayton 1 (TRACE) ..... 74
Figure 12-26: Gas Cooler Water Temperatures for Loss of Brayton 1 (TRACE) ..... 74
Figure 12-27: Rx Power Following Loss of Brayton 1 – Reactivity Feedback Study (TRACE) ..... 75
Figure 12-28: Brayton Component Power for Brayton 1 Complete Loss of Load (TRACE) ..... 76
Figure 12-29: Brayton Shaft Speed for Brayton 1 Complete Loss of Load (TRACE) ..... 76
Figure 12-30: Brayton Loop Flow for Brayton 1 Complete Loss of Load (TRACE) ..... 77
Figure 12-31: Reactor Inlet & Exit Temps for Brayton 1 Complete Loss of Load (TRACE) ..... 77
Figure 12-32: Reactor Pressure Drop for Brayton 1 Complete Loss of Load (TRACE) ..... 78
Figure 12-33: Brayton 1 Loop Temperatures for Brayton 1 Complete Loss of Load (TRACE) ..... 78
Figure 12-34: Temps for Reactivity Feedback for Brayton 1 Complete Loss of Load (TRACE) ..... 79
Figure 12-35: Reactivity for Brayton 1 Complete Loss of Load (TRACE) ..... 79
Figure 12-36: Reactor Power for Brayton 1 Complete Loss of Load (TRACE) ..... 80
Figure 12-37: Hot Spot Fuel Temperature for Brayton 1 Complete Loss of Load (TRACE) ..... 80
Figure 12-38: Brayton Compressor Temp for Brayton 1 Complete Loss of Load (TRACE) ..... 81
Figure 12-39: Gas Cooler Water Temps for Brayton 1 Complete Loss of Load (TRACE) ..... 81
Figure 12-40: HRS Water Pressure for Brayton 1 Complete Loss of Load (TRACE) ..... 82
Figure 12-41: Brayton 2 Loop Temps for Brayton 1 Complete Loss of Load (TRACE) ..... 82
Figure 12-42: Primary Pressure for Brayton 1 Complete Loss of Load (TRACE) ..... 83
Figure 12-43: Brayton Component Power for Brayton 1 Partial Loss of Load (TRACE) ..... 84
Figure 12-44: Brayton Shaft Speed for Brayton 1 Partial Loss of Load (TRACE) ..... 84
Figure 12-45: Brayton Loop Flow for Brayton 1 Partial Loss of Load (TRACE) ..... 85
Figure 12-46: Reactor Inlet & Exit Temps for Brayton 1 Partial Loss of Load (TRACE) ..... 85
Figure 12-47: Reactor Pressure Drop for Brayton 1 Partial Loss of Load (TRACE) ..... 86

Figure 12-48: Brayton 1 Loop Temperatures for Brayton 1 Partial Loss of Load (TRACE)..... 86
Figure 12-49: Temps for Reactivity Feedback for Brayton 1 Partial Loss of Load (TRACE)..... 87
Figure 12-50: Reactivity for Brayton 1 Partial Loss of Load (TRACE)..... 87
Figure 12-51: Reactor Power for Brayton 1 Partial Loss of Load (TRACE)..... 88
Figure 12-52: Hot Spot Fuel Temperature for Brayton 1 Partial Loss of Load (TRACE)..... 88
Figure 12-53: Brayton Compressor Temp for Brayton 1 Partial Loss of Load (TRACE)..... 89
Figure 12-54: Gas Cooler Water Temps for Brayton 1 Partial Loss of Load (TRACE)..... 89
Figure 12-55: HRS Water Pressure for Brayton 1 Partial Loss of Load (TRACE)..... 90
Figure 12-56: Brayton 2 Loop Temps for Brayton 1 Partial Loss of Load (TRACE)..... 90
Figure 12-57: Primary Pressure for Brayton 1 Partial Loss of Load (TRACE)..... 91
Figure 12-58: Reactor Power Resulting from Positive Reactivity (TRACE)..... 92
Figure 12-59: Hot Spot Fuel Temperature Resulting from Positive Reactivity (TRACE)..... 92
Figure 12-60: Temps for Reactivity Feedback for Positive Reactivity without $T_{ave}$ Control (TRACE).. 93
Figure 12-61: Brayton Shaft Speed for Positive Reactivity (TRACE)..... 93
Figure 12-62: Reactor Reactivity Resulting from Positive Reactivity without $T_{ave}$ Control (TRACE).... 94
Figure 12-63: Reactor Reactivity Resulting from Positive Reactivity with $T_{ave}$ Control (TRACE)..... 94
Figure 12-64: Brayton Pressure for Positive Reactivity without $T_{ave}$ Control (TRACE)..... 95
Figure 12-65: Brayton Pressure for Positive Reactivity with $T_{ave}$ Control (TRACE)..... 95
Figure 12-66: Brayton Loop Flow for Positive Reactivity (TRACE)..... 96
Figure 12-67: Reactor Pressure Change for Positive Reactivity (TRACE)..... 96
Figure 12-68: Reactor Temperatures for Positive Reactivity Addition (TRACE)..... 97
Figure 12-69: Brayton Component Power for Positive Reactivity (TRACE)..... 97
Figure 12-70: Brayton Loop Temperatures for Positive Reactivity without $T_{ave}$ Control (TRACE)..... 98
Figure 12-71: Brayton Loop Temperatures for Positive Reactivity with $T_{ave}$ Control (TRACE)..... 98
Figure 12-72: Gas Cooler Water Temperatures for Positive Reactivity (TRACE)..... 99
Figure 12-73: Gas Cooler Water Pressure for Positive Reactivity without $T_{ave}$ Control (TRACE)..... 99
Figure 12-74: Reactor Power Resulting from Positive Reactivity – Sensitivity to Time (TRACE)..... 100
Figure 12-75: Reactor Power Resulting from Negative Reactivity (TRACE)..... 101
Figure 12-76: Hot Spot Fuel Temperature Resulting from Negative Reactivity (TRACE)..... 101
Figure 12-77: Temps for Reactivity Feedback for Negative Reactivity (TRACE)..... 102
Figure 12-78: Brayton Speed for Negative Reactivity (TRACE)..... 102
Figure 12-79: Reactor Reactivity Resulting from Negative Reactivity (TRACE)..... 103
Figure 12-80: Brayton Pressure for Negative Reactivity (TRACE)..... 103
Figure 12-81: Brayton Loop Flow for Negative Reactivity (TRACE)..... 104
Figure 12-82: Reactor Pressure Change for Negative Reactivity (TRACE)..... 104
Figure 12-83: Reactor Temperature for Negative Reactivity (TRACE)..... 105
Figure 12-84: Brayton Component Power for Negative Reactivity (TRACE)..... 105
Figure 12-85: Loop Temperatures for Negative Reactivity (TRACE)..... 106
Figure 12-86: Gas Cooler Water Temperatures for Negative Reactivity (TRACE)..... 106
Figure 12-87: Reactor Power for Complete Loss of Primary Flow (TRACE)..... 107
Figure 12-88: Hot Spot Fuel Temp for Complete Loss of Primary Flow (TRACE)..... 107
Figure 12-89: Reactivity Feedback Temps for Complete Loss of Primary Flow (TRACE)..... 108
Figure 12-90: Reactivity for Complete Loss of Primary Flow (TRACE)..... 108
Figure 12-91: Brayton Shaft Speed for Complete Loss of Primary Flow (TRACE)..... 109
Figure 12-92: Brayton Loop Flow for Complete Loss of Primary Flow (TRACE)..... 109
Figure 12-93: Primary Pressure for Complete Loss of Primary Flow (TRACE)..... 110
Figure 12-94: Gas Cooler Water Temps for Complete Loss of Primary Flow (TRACE)..... 110
Figure 12-95: Reactor Inlet & Exit Temps for Complete Loss of Primary Flow (TRACE)..... 111
Figure 12-96: Brayton Component Power for Complete Loss of Primary Flow (TRACE)..... 111
Figure 12-97: HRS Loop Flows for Complete Loss of Flow in HRS Loop 1 (TRACE)..... 112
Figure 12-98: Brayton Shaft Speeds for Complete Loss of Flow in HRS Loop 1 (TRACE)..... 112

Figure 12-99: Gas Cooler Water Temps for Complete Loss of Flow in HRS Loop 1 (TRACE)..... 113
Figure 12-100: HRS Pressure for Complete Loss of Flow in HRS Loop 1 (TRACE) ..... 113
Figure 12-101: Compressor Inlet Temps for Complete Loss of Flow in HRS Loop 1 (TRACE) ..... 114
Figure 12-102: Brayton Loop Flow for Complete Loss of Flow in HRS Loop 1 (TRACE) ..... 114
Figure 12-103: Brayton Loop 1 Temperatures for Complete Loss of Flow in HRS Loop 1 (TRACE) 115
Figure 12-104: Brayton Loop 2 Temperatures for Complete Loss of Flow in HRS Loop 1 (TRACE) 115
Figure 12-105: Brayton Component Torques for Complete Loss of Flow in HRS Loop 1 (TRACE).. 116
Figure 12-106: Thermal Power of Brayton Components for Complete Loss of Flow in HRS Loop 1 (TRACE)..... 116
Figure 12-107: Reactor Inlet & Exit Temps for Complete Loss of Flow in HRS Loop 1 (TRACE)..... 117
Figure 12-108: Temps for Reactivity Feedback for Complete Loss of Flow in HRS Loop 1 (TRACE) ..... 117
Figure 12-109: Reactivity for Complete Loss of Flow in HRS Loop 1 (TRACE)..... 118
Figure 12-110: Hot Spot Fuel Temperature for Complete Loss of Flow in HRS Loop 1 (TRACE).... 118
Figure 12-111: Reactor Power for Complete Loss of Flow in HRS Loop 1 (TRACE)..... 119
Figure 12-112: HRS Pressure with Action for Complete Loss of Flow in HRS Loop 1 (TRACE) ..... 119
Figure 12-113: HRS Pressure with Action for Complete Loss of Flow in HRS Loop 1 (TRACE) ..... 120
Figure 12-114: Gas Cooler Void Fraction at Water Exit for Complete Loss of Flow in HRS Loop 1 with Action (TRACE)..... 120
Figure 12-115: Brayton Loop 1 Compressor Inlet Temperature for Complete Loss of Flow in HRS Loop 1 with Action (TRACE)..... 121
Figure 12-116: Turbine Torques for Complete Loss of Flow in HRS Loop 1 with Action (TRACE)... 121
Figure 12-117: Compressor Torques for Complete Loss of Flow in HRS Loop 1 with Action (TRACE) ..... 122
Figure 12-118: Alternator Torques for Complete Loss of Flow in HRS Loop 1 with Action (TRACE) 122
Figure 12-119: Reactor Power for Complete Loss of Flow in HRS Loop 1 with Action (TRACE)..... 123
Figure 12-120: Hot Spot Fuel Temp for Complete Loss of Flow in HRS Loop 1 with Action (TRACE) ..... 123
Figure 12-121: HRS Pressure for Complete and Partial Loss of Flow in HRS Loop 1 (TRACE)..... 124
Figure 12-122: RELAP5-3D/SNAP Direct Gas Brayton Reactor Plant ..... 125
Figure 12-123: Design Point for RELAP5-3D Model ..... 126
Figure 12-124: RELAP5-3D Reactor Model..... 128
Figure 12-125: Notional Core Block for UN Core Design ..... 131
Figure 12-126: RELAP5-3D/SNAP Direct Gas Brayton Reactor Plant with Energy Conversion Loop 1 Highlighted ..... 133
Figure 12-127: RELAP5-3D/SNAP Direct Gas Brayton Reactor Plant Highlighting One Heat Rejection Loop..... 137
Figure 12-128: Reactor Power Resulting from Loss of One of Two Braytons (RELAP5-3D)..... 144
Figure 12-129: Hot Spot Fuel Temperature Resulting from Loss of One of Two Braytons (RELAP5-3D) ..... 144
Figure 12-130: Loop Temperatures Resulting from Loss of One of Two Braytons (RELAP5-3D)..... 145
Figure 12-131: Reactor Reactivity Resulting from Loss of One of Two Braytons (RELAP5-3D)..... 145
Figure 12-132: Mass Flow Rates Resulting from Loss of One of Two Braytons (RELAP5-3D) ..... 146
Figure 12-133: Shaft Speeds Resulting from Loss of One of Two Braytons (RELAP5-3D) ..... 146
Figure 12-134: First Brayton Loop Temperatures Resulting from Loss of One of Two Braytons (RELAP5-3D) ..... 147
Figure 12-135: Second Brayton Loop Temperatures Resulting from Loss of One of Two Braytons (RELAP5-3D) ..... 147
Figure 12-136: First Heat Rejection Loop Temperatures Resulting from Loss of One of Two Braytons (RELAP5-3D) ..... 148

Figure 12-137: Second Heat Rejection Loop Temperatures Resulting from Loss of 1 of 2 Braytons (RELAP5-3D) ..... 148
Figure 12-138: Reactor Power Resulting from Over speed of One of Two Braytons (RELAP5-3D) . 149
Figure 12-139: Hot Spot Fuel Temperature Resulting from Over speed of One of Two Braytons (RELAP5-3D) ..... 149
Figure 12-140: Loop Temperatures Resulting from Over speed of One of Two Braytons (RELAP5-3D) ..... 150
Figure 12-141: Reactor Reactivity Resulting from Over speed of One of Two Braytons (RELAP5-3D) ..... 150
Figure 12-142: Mass Flow Rates Resulting from Over speed of One of Two Braytons (RELAP5-3D) ..... 151
Figure 12-143: Shaft Speeds Resulting from Over speed of One of Two Braytons (RELAP5-3D) ... 151
Figure 12-144: First Brayton Loop Temperatures Resulting from Over speed of One of Two Braytons (RELAP5-3D) ..... 152
Figure 12-145: Second Brayton Loop Temperatures Resulting from Over speed of One of Two Braytons (RELAP5-3D) ..... 152
Figure 12-146: First Heat Rejection Loop Temperatures Resulting from Over speed of 1 of 2 Braytons (RELAP5-3D) ..... 153
Figure 12-147: Second Heat Rejection Loop Temperatures Resulting from Over speed of One of Two Braytons (RELAP5-3D) ..... 153
Figure 12-148: Reactor Power Resulting from Positive Reactivity (RELAP5-3D) ..... 154
Figure 12-149: Hot Spot Fuel Temperature Resulting from Positive Reactivity (RELAP5-3D) ..... 154
Figure 12-150: Loop Temperatures Resulting from Positive Reactivity (RELAP5-3D) ..... 155
Figure 12-151: Reactor Reactivity Resulting from Positive Reactivity (RELAP5-3D) ..... 155
Figure 12-152: Mass Flow Rates Resulting from Positive Reactivity (RELAP5-3D) ..... 156
Figure 12-153: Shaft Speeds Resulting from Positive Reactivity (RELAP5-3D) ..... 156
Figure 12-154: First Brayton Loop Temperatures Resulting from Positive Reactivity (RELAP5-3D) 157
Figure 12-155: Second Brayton Loop Temperatures Resulting from Positive Reactivity (RELAP5-3D) ..... 157
Figure 12-156: First Heat Rejection Loop Temperatures Resulting from Positive Reactivity (RELAP5-3D) ..... 158
Figure 12-157: Second Heat Rejection Loop Temperatures Resulting from Positive Reactivity (RELAP5-3D) ..... 158
Figure 12-158: Reactor Power Resulting from Negative Reactivity (RELAP5-3D) ..... 159
Figure 12-159: Hot Spot Fuel Temperature Resulting from Negative Reactivity (RELAP5-3D) ..... 159
Figure 12-160: Loop Temperatures Resulting from Negative Reactivity (RELAP5-3D) ..... 160
Figure 12-161: Reactor Reactivity Resulting from Negative Reactivity (RELAP5-3D) ..... 160
Figure 12-162: Mass Flow Rates Resulting from Negative Reactivity (RELAP5-3D) ..... 161
Figure 12-163: Shaft Speeds Resulting from Negative Reactivity (RELAP5-3D) ..... 161
Figure 12-164: First Brayton Loop Temperatures Resulting from Negative Reactivity (RELAP5-3D) 162
Figure 12-165: Second Brayton Loop Temperatures Resulting from Negative Reactivity (RELAP5-3D) ..... 162
Figure 12-166: First Heat Rejection Loop Temperatures Resulting from Negative Reactivity (RELAP5-3D) ..... 163
Figure 12-167: Second Heat Rejection Loop Temperatures Resulting from Negative Reactivity (RELAP5-3D) ..... 163
Figure 12-168: Reactor Power Resulting from Loss of Flow in One Heat Rejection Loop (RELAP5-3D) ..... 164
Figure 12-169: Hot Spot Fuel Temperature Resulting from Loss of Flow in One Heat Rejection Loop (RELAP5-3D) ..... 164

Figure 12-170: Loop Temperatures Resulting from Loss of Flow in One Heat Rejection Loop (RELAP5-3D) ..... 165
Figure 12-171: Reactor Reactivity Resulting from Loss of Flow in One Heat Rejection Loop (RELAP5-3D) ..... 165
Figure 12-172: Mass Flow Rates Resulting from Loss of Flow in One Heat Rejection Loop (RELAP5-3D) ..... 166
Figure 12-173: Shaft Speeds Resulting from Loss of Flow in One Heat Rejection Loop (RELAP5-3D) ..... 166
Figure 12-174: First Brayton Loop Temperatures Resulting from Loss of Flow in 1 Heat Rejection Loop (RELAP5-3D) ..... 167
Figure 12-175: Second Brayton Loop Temperatures Resulting from Loss of Flow in 1 HRS Loop (RELAP5-3D) ..... 167
Figure 12-176: First Heat Rejection Loop Temperatures Resulting from Loss of Flow in 1 HRS Loop (RELAP5-3D) ..... 168
Figure 12-177: Second Heat Rejection Loop Temperatures Resulting from Loss of Flow in 1 HRS Loop (RELAP5-3D) ..... 168
Figure 12-178: Reactor Power during a Plant Start-Up (RELAP5-3D) ..... 169
Figure 12-179: Loop Temperatures during a Plant Start-Up (RELAP5-3D) ..... 169
Figure 12-180: Reactor Reactivity during a Plant Start-Up (RELAP5-3D) ..... 170
Figure 12-181: Mass Flow Rates during a Plant Start-Up (RELAP5-3D) ..... 170
Figure 12-182: Shaft Speeds during a Plant Start-Up (RELAP5-3D) ..... 171
Figure 12-183: First Brayton Loop Temperatures during a Plant Start-Up (RELAP5-3D) ..... 171
Figure 12-184: Second Brayton Loop Temperatures during a Plant Start-Up (RELAP5-3D) ..... 172
Figure 12-185: First Heat Rejection Loop Temperatures during a Plant Start-Up (RELAP5-3D) ..... 172
Figure 12-186: Second Heat Rejection Loop Temperatures during a Plant Start-Up (RELAP5-3D). 173

## List of Tables

Table 12-1: Comparison of Direct Gas Brayton Model Parameters ..... 17
Table 12-2: Summary of Transients Analyzed during Pre-Conceptual Design ..... 18
Table 12-3: Comparison of Heat Balance Case 24 Design Point and TRACE Model State Points .... 27
Table 12-4: Concept Selection Reference UN Core Concept as Applied to TRACE Model ..... 33
Table 12-5: Comparison of CCEP and HB24 Design Points ..... 38
Table 12-6: TRACE Piping and Component Flow Parameters ..... 49
Table 12-7: Comparison of Design Point and RELAP5-3D Model State Points ..... 127
Table 12-8: Core Concept DS0-470 Parameters ..... 129
Table 12-9: Brayton Turbine Data ..... 134

(Intentionally Blank)

# 12 Transient Modeling

## 12.1 Summary and Conclusions

The NRPCT developed scoping models to provide preliminary information on the transient performance of the Space Nuclear Power Plant (SNPP). Three different modeling tools were used in these scoping evaluations. Preliminary system transients were evaluated with a point kinetics model developed using MATLAB/Simulink and RELAP5-3D. More detailed models were developed using TRACE and RELAP5-3D. Each model was used to study the integration of the gas reactor with dual Brayton loops and the heat rejection segment (HRS) during plant transients. Based on preliminary evaluations, the NRPCT has found the following:

---

- No inherent instability in plant response to planned and unplanned transients has been revealed, with either a single Brayton or multiple units, assuming the overall reactor temperature coefficient is negative and the Braytons are operating with active speed control. A negative temperature coefficient is predicted for the core designs under consideration, and active speed control using a Parasitic Load Radiator (PLR) is a baseline assumption for the plant.

- Preliminary results indicate that the Heat Rejection Segment (HRS) is more vulnerable to exceeding design limits than other components in the SNPP, including the reactor. The concern in a water-cooled HRS is coolant over-pressurization, leading to a potential gas cooler failure. In a Sodium-Potassium (NaK)-cooled HRS, the coolant is not over-pressurized, but the load-carrying capacity of the heat pipes may be exceeded. Further development of the SNPP would require a control system is needed to prohibit HRS damage.

- Accurate turbine and compressor performance maps are needed to fully characterize plant transients. Plant operations like startup and transients like complete loss of load have required extrapolating performance beyond available performance maps. SNPP model accuracy with extrapolated performance maps will have significant uncertainty until prototypical test data is obtained.

---

Transient results can be divided into two categories: 1) final plant conditions are stable and are within acceptable equipment operating limits; and 2) final plant conditions are not stable or equipment operating limits may be exceeded. The loss of flow in one of two operating Brayton loops falls into the first category. Reactor and plant response is stable, without any control system action. Transients such as a positive reactivity addition could fall into either category. For example, increased heat loads in the gas cooler can produce boiling in a water-cooled HRS, and depending on the size of the reactivity addition and the final plant design characteristics, could lead to an over-pressurization of the HRS. On the other hand, a NaK-cooled HRS has additional margin to boiling, and preliminary results do not indicate any issues with respect to over-pressurization. Future modeling efforts would have increased the detail in the HRS to include specific heat pipe models that would determine if their capacities were reached.

One of the limiting casualty design event transients in a multiple loop system is a complete loss of electrical load for a Brayton, which leads to an increase in reactor power and flow and potential for

overloading the HRS. Predictions indicate that with no control system response, the water in the gas cooler will heat up resulting in bulk boiling, which over-pressurizes the connected heat rejection loop. The likelihood of such a Brayton control system failure must be minimized through reliable electrical system design. Control system responses to the complete loss of load casualty could include closing an isolation valve in the applicable gas loop and/or increasing HRS flow rate. Figure 12-39 and Figure 12-40 show the response of the system to a loss of Brayton speed control with no control system response and with an increase in the HRS flow rate.

Another transient that may require control system response is the complete loss of heat rejection loop flow. This transient produces significantly different results depending on the HRS design and working fluid. When the gas cooler is water cooled (TRACE model) boiling occurs, potentially leading to system over-pressurization. Numerous control actions or design features are described in the TRACE analysis discussion. A key takeaway from these transient results is that multiple heat rejection loop pumps may be required. On the other hand, when flow in the NaK cooled HRS is lost the increased compressor inlet temperature appears to stall the Brayton before the HRS is overheated (RELAP5-3D model). Again, to prevent Brayton loop shutdown it may be advantageous to include a spare heat rejection loop pump. The heat rejection architecture proposed by Northrop Grumman Space Technologies (NGST) assumed an operating and idle HRS pump in parallel for each HRS loop (see Section 9.6).

## 12.2 Description of Modeling Software

### 12.2.1 MATLAB/Simulink

MATLAB/Simulink is a software package for modeling, simulating, and analyzing dynamic systems. It supports linear and nonlinear systems, modeled in continuous time, sampled time, or a hybrid of the two. For modeling, Simulink provides a graphical user interface (GUI) for building models as block diagrams, using click-and-drag mouse operations. Simulink includes differential equation solvers. Simulink includes a comprehensive block library of sinks, sources, linear and nonlinear components, and connectors, and provides the ability for user-defined custom blocks as well. The software includes many features to view the simulation results while the simulation is running. Simulation results can be used in the MATLAB workspace for post processing and visualization.

An advantage of using MATLAB/Simulink for early studies was that NASA contractors had already developed a MATLAB/Simulink model for one of the space reactor plant concepts, making development of the gas-cooled concept quicker. However, the MATLAB/Simulink model solves equations in terms of lumped-parameters. It is not practical to include all thermal-hydraulic calculations available in the special purpose RELAP5-3D and TRACE codes. In addition, there has been a long history of RELAP5-3D and TRACE code verification and qualification for nuclear plant analysis that does not exist for Simulink coding. The NRPCT program had experienced model builders and analysts knowledgeable in TRACE and RELAP5-3D, making these codes the best choice for more detailed modeling tasks.

### 12.2.2 TRACE and RELAP5-3D

TRACE and RELAP5-3D are used for safety analysis of land-based nuclear reactor power plants. TRACE was developed by the Nuclear Regulatory Commission, and RELAP5-3D was developed by the Idaho National Laboratory (INL). These codes use predominantly one-dimensional hydraulic components, though both have limited two and three dimensional hydraulic capability. The codes have similar functionality. They offer flexible component modeling capability in either open loop or multiple loop configurations. The primary system, secondary system, HRS, system controls, and reactor kinetics can be simulated. The code modeling capabilities include the simulation of large and small break loss-of-coolant casualties as well as operational transients such as anticipated transients without scram, loss of feed water, loss of power, loss of flow, and overcooling transients. The system behavior can be simulated up to the point of potential fuel damage and/or the validity of assumed coolant and material conditions (e.g., freeze-up of the coolants in a space environment and wall temperature melting limits). Hydrodynamic behavior is represented by a two-fluid, two-phase transient flow formulation in water loops and by a single-phase transient flow formulation in gas loops, with the ability to incorporate non-condensable gases in each loop type. Solution techniques replace the differential equations that enforce conservation of hydrodynamic mass, energy, and momentum with finite-difference equations that are partially implicit in time. Finite differences are used to advance the axial/radial heat conduction solutions. Reactor kinetics equations are solved using a Kaganove method in TRACE, and a modified Runge-Kutta method in RELAP5-3D. Although both codes have traditionally been utilized for analysis of two phase light water reactors, they have been generalized to include the use of a variety of coolants, including non-condensing/non-boiling gases and liquid metals, so as to permit the analysis of systems outside the range of traditional commercial nuclear reactor configurations.

Both TRACE and RELAP5-3D utilize a comprehensive model builder called Symbolic Nuclear Analysis Package (SNAP) that allows the analyst to model any hydrodynamic and heat transfer system by building it from a predefined set of components. For example, the hydraulic network of the reactor is modeled predominately from a combination of a variety of pipes, pumps, valves, and associated heat structures. Changing the geometric volume, area, length, and wall thickness allows a representation of the physical configuration of the plant. Additional operational details, such as pump/turbine/compressor operating characteristics, piping and valve loss factors, and heat transfer coefficient changes allow additional control in generating a model that better represents the intended physical system.

The heat transfer characteristics of the model are simulated via heat structures. Heat structures are one-dimensional abstract components used to represent the solid mass of the reactor plant. The one dimension is in the radial direction, perpendicular to the direction of fluid flow. Heat transfer in the axial direction (parallel to fluid flow) is represented by using several fluid volumes in the axial direction and connecting a heat structure to each. TRACE heat structures also permit two-dimensional conduction in Cartesian, cylindrical or spherical geometry. Conduction, convection, and radiation heat transfer modes can all be represented with heat structures. Heat structures, with their associated boundary conditions and neutron kinetics calculations, provide the ability to link thermal conditions among the plant structural, fuel (power components), coolant, and ambient environment (radiation enclosures).

Both TRACE and RELAP5-3D required modification to include compressor and turbine modeling capability. TRACE uses two specialized variations of the pump component to model the Brayton plant. The basic intent of a pump component in terms of its impact on the governing equations is to act as a source of momentum (pump head) and energy (frictional heating of the fluid). This characteristic is generalized to the compressor (which adds momentum and energy) and to the gas turbine (which extracts momentum and energy). The amount of momentum/energy addition/removal for the compressor/turbine is controlled either by supplying operational curves or via the definition of performance maps, depending on the level of modeling detail desired.

In RELAP5-3D, the compressor model is similar to the pump model. It performs the same function on a gas as the pump performs on fluids. It can be driven by a shaft or use the other capabilities available to a pump (speed table, motor torque table and/or the coastdown feature). The homologous head and torque curves required for a pump are replaced with compressor pressure ratio and efficiency appropriate for the compressor as a function of mass flow rate for up to 99 different shaft speeds. The compressor component consists of an inlet junction, a single volume and optionally an exit junction. Similar to TRACE, the turbine component in RELAP5-3D extracts momentum and energy.

## 12.3 Scope of Modeling and Analysis

### 12.3.1 Description of Plant Models

The NRPCT developed scoping models for many of the concepts under consideration to support concept selection in March 2005. MATLAB/Simulink and RELAP5-3D were used in these preliminary analyses and were documented in References 12-1 and 12-2. These models provided an important first look at the transient performance of the Lithium-Brayton, Heat Pipe-Brayton, and Direct Gas-Brayton plants.

After concept selection, modeling effort was largely shifted from Simulink to TRACE and RELAP5-3D. Simulink model results are documented in Reference 12-2 and 12-3. This report provides model descriptions and results for the TRACE (Section 12.4) and RELAP5-3D (Section 12.5) models. Detailed model descriptions can be found in References 12-4 and 12-5 for TRACE and RELAP5-3D, respectively.

At a high level, all three models depict dual loop Direct Gas Brayton plants, as shown in Figure 12-1. Because the pre-conceptual design phase was still underway, the three models share some similarities but also contain differences in the details. Table 12-1 compares the attributes of the three models. Each model matches a particular steady state condition; again, these are not consistent among the three models. Steady state model results are used to verify that the plant model is equivalent to a given power plant design, which is defined by a reference design heat balance.

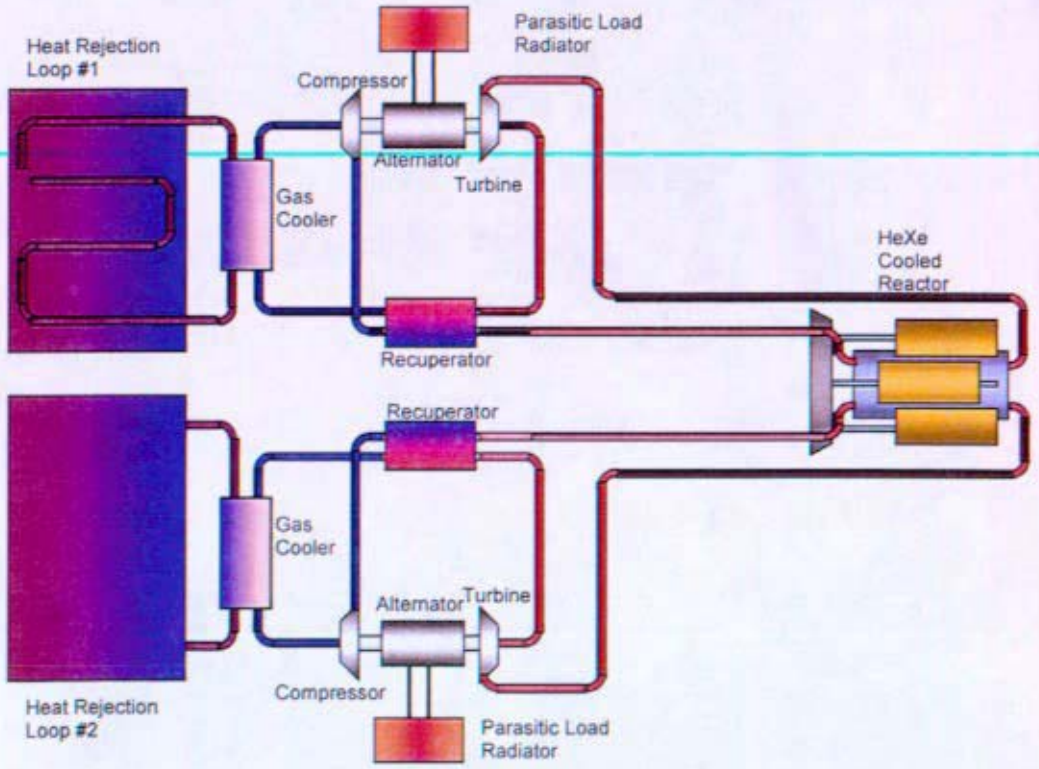



**Figure 12-1: Dual Loop Direct Gas Brayton System**

In all three models, two independent Brayton energy conversion systems are connected in parallel to a single reactor, each capable of supplying 50% of the full rated electrical power. Brayton performance for all three models is determined by Closed Cycle Engine Program (CCEP) maps provided by NASA Glenn Research Center (GRC) in Reference 12-8 (modified CCEP curves are also available in TRACE, as described in Section 12.4.1.3). Helium-Xenon gas is heated in the reactor and directed to the turbine inlet. As the gas passes the turbine blades, thermal hydraulic energy from the fluid is converted to mechanical energy, which spins the shaft of the turbine-alternator-compressor unit. The gas mixture is exhausted from the turbine at a lower temperature and pressure. The gas mixture is then passed through a regenerative heat exchanger, the recuperator, to transfer some of the heat of the exhaust gas into the cold leg to increase cycle efficiency. The gas mixture is then further cooled in the gas cooler before entering the compressor. The low pressure, low temperature gas mixture is compressed to a higher pressure increasing the temperature as a result. The compressor extracts its power from the spinning shaft, which is powered by the turbine. The high pressure gas is then heated in the recuperator before returning to the reactor inlet. Brayton shaft speed is controlled with a PLR, which applies the appropriate amount of electrical load to the alternator to maintain the shaft speed at the set point. This speed control function is included in each of the three plant models. A speed control system assures that the Brayton operates at a stable condition and prevents undesirable changes in reactor power caused by changes in plant electrical load. Without a speed or reactivity control system the reactor plants modeled show an inverse relationship between electrical load and reactor power. This relationship is called non-load following and results in increasing reactor power when alternator load is reduced. A detailed explanation of this behavior is provided in Section 12.4.2.3.

**Table 12-1: Comparison of Direct Gas Brayton Model Parameters**

| Location | RELAP5-3D | | TRACE | | MATLAB/Simulink | |
|---|---|---|---|---|---|---|
| | Temp (K) | Press (kPa) | Temp (K) | Press (kPa) | Temp (K) | Press (kPa) |
| Turbine Inlet | 1149 | 1933 | 1150 | 1902.8 | 1144.6 | 973.90 |
| Recuperator LP Side Exit | 565 | 1036 | 574 | 1024 | 563.7 | 510.71 |
| Gas Cooler Gas Inlet | 565 | 1037 | 559 | 1019 | 563.7 | 510.71 |
| Compressor Inlet | 393 | 1026 | 392.3 | 999 | 373.5 | 507.78 |
| Recuperator HP Side Exit | 894 | 1987 | 892 | 1979 | 879.7 | 993.1 |
| Gas Cooler HRS Inlet | 382 | 276 | 377 | 7744.0 | 363.1 | - |
| Gas Cooler HRS Exit | 521 | 273 | 510 | 7742.8 | 521.7 | - |
| **System Flows (kg/s)** | | | | | | |
| Brayton Loop Flow | 2.28 | | 2.47 | | 1.90 | |
| Alternator Cooling Flow | 0.0 (1) | | 0.34 | | 0.04 (gas), 0.07 (NaK) | |
| Gas Cooler Gas Flow | 2.28 (2) | | 2.81 | | 1.90 | |
| Gas Cooler HRS Flow | 2.36 | | 0.52 | | 1.453 | |
| **Reactor** | | | | | | |
| Reactor Thermal Rating | 1000 $kW_t$ | | 1000 $kW_t$ | | 533.2 $kW_t$ | |
| Core Configuration | Block | | Block | | Block | |
| Fuel Material | $UO_2$ | | UN | | UN | |
| Clad Material | MoRe | | Nb-1Zr | | NbZr | |
| Core Block Material | MoRe | | Nb-1Zr | | Re | |
| Number of Pins | 354 | | 192 | | 216 | |
| Reactor Power (- losses) | 796 $kW_t$ | | 899 $kW_t$ | | 533.17 $kW_t$ | |
| Reactor ($\Delta T$) | 255 K | | 273 K (fuel region) | | 270 K | |
| Reactor $\Delta P/P_{in}$ | 2.7% | | 2.43% | | 1.5% | |
| HeXe Mixture, mole fraction | 78.4% He | | 78.4% He | | 72% He | |
| **Brayton Loop** | | | | | | |
| Rating of Each Brayton | 100 $kW_e$ (2) | | 100 $kW_e$ | | 66 $kW_e$ | |
| Brayton (Configuration) | 2 (TAC) | | 2 (TCA) | | 2 (TAC) | |
| Loop Transport Time | 1.8 seconds | | 1.5 seconds | | 0.6 seconds | |
| Turbine PR ($\Delta T$) | 1.84 (228 K) | | 1.82 (216.6 K) | | 1.88 (224 K) | |
| Compressor PR ($\Delta T$) | 1.95 (147 K) | | 1.99 (148 K) | | 1.97 (142 K) | |
| Recuperator Effectiveness | 93% | | 91.5% | | 90% | |
| Recuperator $\Delta P/P_{in}$ LP (HP) | 1.46% (1.0%) | | 1.75% (0.73%) | | 1.5% (0.65%) | |
| Gas Cooler Effectiveness | 94% | | 91.2% | | 95% | |
| Gas Cooler Gas $\Delta P/P_{in}$ ($\Delta T$) | 0.9% (172 K) | | 1.4% (166 K) | | 0.37% (190 K) | |
| **HRS** | | | | | | |
| Coolant | NaK | | Water | | NaK | |
| HRS Loop Transport Time | 38 seconds | | 116 seconds | | 66 seconds | |
| Radiator Area Applied | 447 $m^2$ | | 447 $m^2$ | | 261 $m^2$ | |

Notes:
(1) Alternator cooling flow was not modeling in RELAP5-3D
(2) Bleed path was not modeled in RELAP5-3D

## 12.3.2 Transients

A summary of the transients analyzed is provided in Table 12-2. This compilation of transients provides initial insight into the SNPP design space that is the first step in specifying the specific design requirements of each power plant component. For some transients, numerous operating and/or protection strategies were modeled. Future transient analysis would involve model qualification and new model detail. Transients similar to those provided here would eventually become the Design Events Document (DED) that would be used for detailed equipment specifications, thermal-hydraulic and structural analysis, as discussed in Section 11.

**Table 12-2: Summary of Transients Analyzed during Pre-Conceptual Design**

| Transients | Simulink | RELAP5-3D | TRACE |
|---|---|---|---|
| Mechanical Loss of One Brayton | X | X | X |
| Mechanical Loss of One Brayton with reverse flow | X | | |
| Complete Loss of Electrical Load for One Brayton | X | X | X |
| Partial Loss of Electrical Load for One Brayton | | | X |
| Positive Reactivity Addition | X | X | X |
| Negative Reactivity Addition | X | X | X |
| Positive Reactivity Addition with Unbalanced Load | X | | |
| Complete Loss of Primary Flow | | | X |
| Complete Loss of Flow in One HRS Loop | | X | X |
| Reactor Startup | | X | |

All three models include two parallel direct gas Brayton loops connected to a gas cooled fast reactor. Each gas Brayton loop is cooled by a dedicated gas cooler and heat rejection loop. Differences between the models include power rating, fuel system, Brayton alternator cooling method, gas cooler design and HRS working fluid. There are also differences in reactor and Brayton control systems. While the differences in computer code and computer models do impact the results, similar conclusions regarding the operability and stability of the basic plant design have been confirmed by all three.

Most of the Simulink transients listed in Table 12-2 have been reproduced with both the TRACE and RELAP5-3D codes. The TRACE and RELAP5-3D models are more consistent with the most recent NRPCT SNPP concepts than the Simulink model. The Simulink results are not included in this report, and can be found in Reference 12-3. A few differences in the Simulink transients are noted here for completeness. The Simulink positive and negative reactivity addition transients used a much slower reactivity addition rate. In Simulink the reactivity was added over 180 seconds, vice 1 second for TRACE and RELAP5-3D. Simulink was also used to verify stability of two parallel operating Brayton systems (degraded turbine efficiency). Finally, the effect of reverse flow in a failed Brayton system was also investigated with Simulink.

Most of the Section 11 casualty design events are included in Table 16-2. Section 11 defines a casualty design event as a transient that the SNPP is designed to survive without permanent loss of capability. The transient results described in this section suggest that this requirement can be met. This conclusion is reached assuming that the SNPP will have a negative reactor temperature coefficient (as expected), a Brayton shaft speed control system and typical reactor protection features. Typical reactor protection may include a means to rapidly reduce reactivity (shim or scram). It may also be advantageous to use a reactivity control system based on Brayton coolant temperature. Other probable control features include a Brayton loop isolation valve that can be closed to rapidly stop loop flow. For example, the current SNPP design with a water-cooled HRS may be over-

pressurized during a complete loss of load event. For this and other transients the time it takes for the affected Brayton loop to stall on its own (no control actions) may overload the HRS.

While Section 11 discusses protecting the SNPP from permanent damage there may also be a distinction in casualties relative to continuity of power. In the final design the complete loss of load event may have been found to be sufficiently improbable that it may have been acceptable to quickly shutdown the affected Brayton. On the other hand, it may have been a system control requirement that a partial loss of load will not require the affected Brayton to be shut down. In other words, the more severe transients may require protective action that shuts down a Brayton, while system design and control features can maintain Brayton operation for a less severe event. Control system responses to the complete loss of load casualty could include closing an isolation valve in the applicable gas loop and/or increasing HRS flow rate. Depending on the final design, the control system may not require Brayton loop shutdown for a partial loss of load event. Transient results with and without control system action are discussed for the partial loss of load in Section 12.4.2.3. For the complete loss of load case Figure 12-39 and Figure 12-40 show HRS system response with and without a control system response. In this case that response is an increase in the HRS flow rate.

Brief descriptions of the TRACE and RELAP5-3D SNPP models are provided below. Following the TRACE model description a results section provides a summary of each transient. Many significant plant parameters are provided in the time-dependent plots after the results discussion. Similarly, RELAP5-3D results and plots are provided after the RELAP5-3D model description.

(Intentionally Blank)

## 12.4 TRACE Model Description and Results

### 12.4.1 TRACE Direct Gas Brayton Model Description

The TRACE executable is written in FORTRAN 90 and once compiled on a PC platform is run from the user's PC. The SNAP GUI provides a highly flexible and efficient way of building a complex thermal-hydraulic plant as well as complex control structures. Effective model building allowed for large models that could be quickly revised as the plant design evolved. The SNAP GUI also allows the input model to be quickly converted into an interactive animation tool. Monitoring the thermal-hydraulic and control system calculations interactively was an extremely valuable model building and debugging tool as well as a first cut at reviewing results. Results were also viewed using a plotting routine called ACGrace.

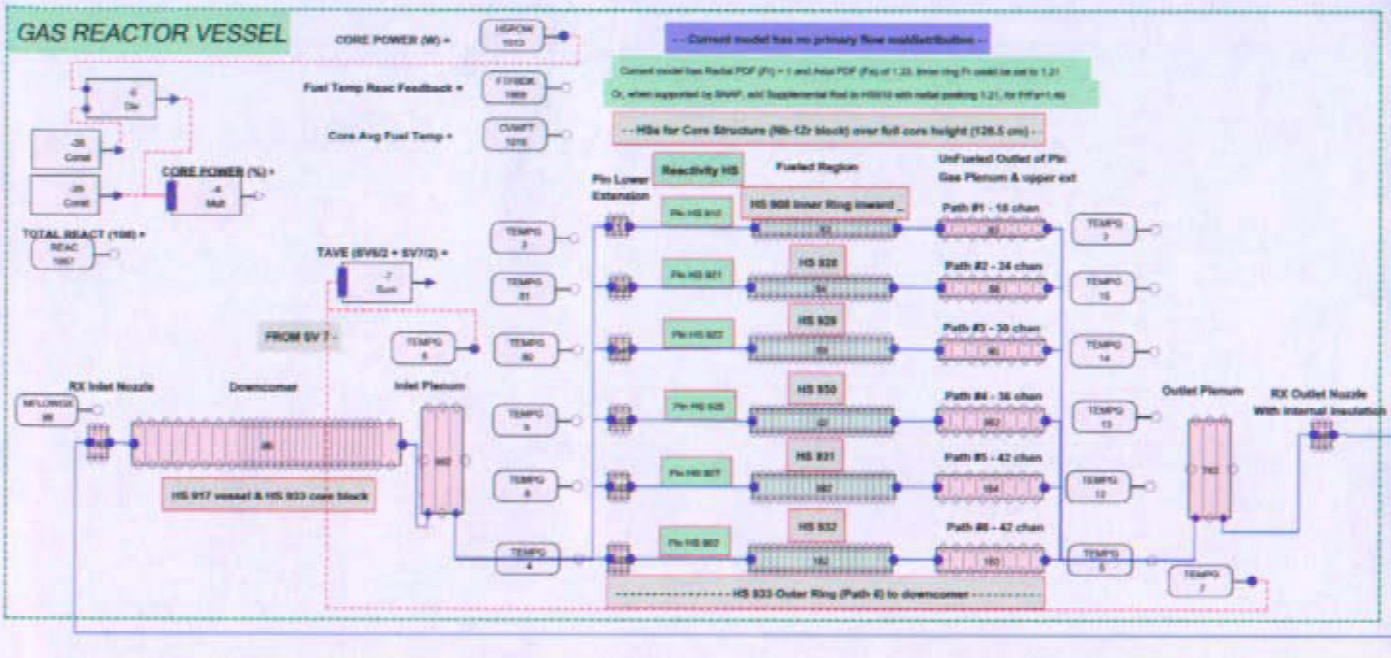
Using the TRACE/SNAP modeling tool, the SNPP model was developed in a modular fashion. Model builders built and tested stand alone versions of the reactor, HRS, recuperator, gas cooler, turbine and compressor. The SNAP GUI was effective in joining the pieces as well as duplicating large sections. For example, the second Brayton and heat rejection loops were copied and pasted within SNAP from the first loops. The TRACE plant model originally included component models that were developed during the concept selection phase. In order to provide the most current model, most of these sub-models were updated to post-concept selection versions.

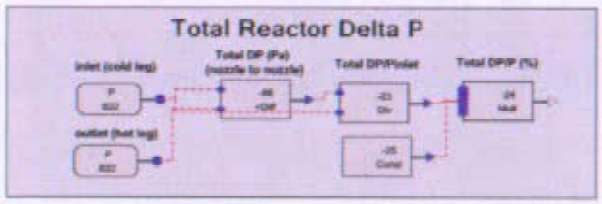
The SNPP TRACE model shown in Figure 12-2 represents two parallel Brayton loops directly coupled to a gas reactor, with a water coolant HRS loop dedicated to each Brayton. The TRACE model is built and edited with SNAP using four views. These include the primary hydraulic and instrumentation view shown in Figure 12-2 ; the HRS hydraulic view shown in Figure 12-12; the Brayton shaft and speed controller view in Figure 12-9; and the reactivity calculation and control view in Figure 12-7.

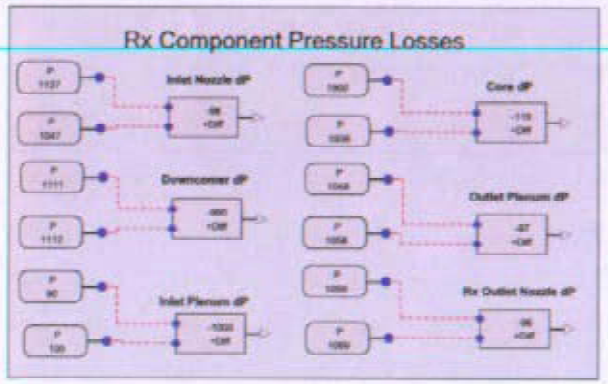
Overall the TRACE model represents a plant design consistent with interim heat balance case 24 (HB24). This heat balance was created in September 2005 and was based on an NRPCT-modified version of the GRC SRPS OPT spreadsheet (v. 29-NRv9-amg11). An important aspect of this heat balance is that it includes a detailed reactor coolant piping design that defines plant piping sizes and hydraulic resistances. This two-loop direct Brayton primary plant was combined with the most current HRS design available. The water-cooled HRS includes a detailed piping layout that models each radiator panel. The Brayton components match HB24 performance. The recuperator is a detailed model that was originally designed to match the concept selection heat balance. This design has been applied to the later heat balance with minimal impact on system performance. The TRACE gas cooler is a traditional shell-and-tube heat exchanger model. Gas cooler design had not progressed to the point that a detailed concept was available to connect a high pressure water HRS with direct gas Brayton primary plant. A shell-and-tube heat exchanger using relatively small tubes and external fins was selected for the TRACE model primary gas to water HRS interface. Smaller tubes would produce a more compact (lightweight) design but be more difficult to manufacture. Using this traditional design permitted the rapid development of a relatively high fidelity Mathcad and TRACE model for a design with a proven track record of reliable leak-free operation (in many industrial applications). The resulting gas cooler design has slightly lower effectiveness than the current heat balance design (91.2% vs. 94%).

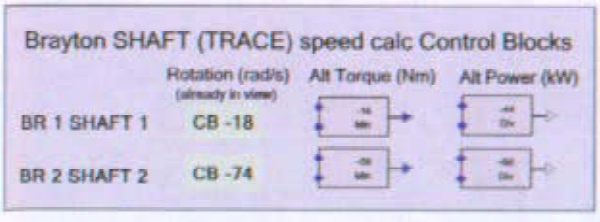
Finally, the TRACE reactor design is based on the reference reactor case defined in Enclosure 1 to Attachment D of the Reference 12-1 concept selection report. This annular flow block core uses UN fuel. The most recent NRPCT core concepts had switched to $UO_2$ fuel. The TRACE UN core model

results offer a useful comparison to the RELAP5-3D $UO_2$ model results. The RELAP5-3D model includes a $UO_2$ fuel system. The TRACE and RELAP core models produce similar overall plant transients. The largest difference is in the peak fuel temperature. $UO_2$ fuel designs generally have significantly higher temperature drops between the fuel and reactor coolant. Compared with $UO_2$ cores, UN cores have fewer but much longer (long gas plenums) fuel pins. With more fuel pins and the same primary flow rate, the $UO_2$ core pin spacing (pitch) can be closer together, reducing the hydraulic diameter. These core thermal/hydraulic differences would become more important when more detailed core performance and protection analysis was performed.



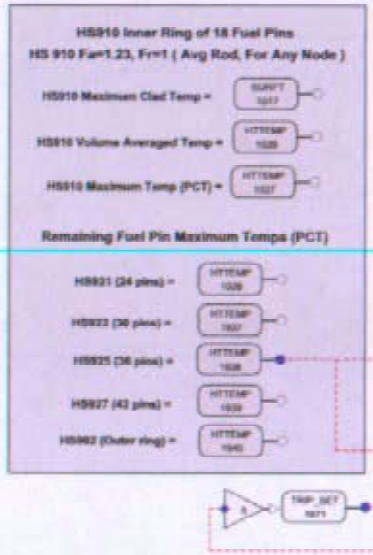



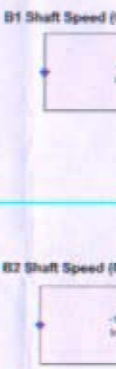









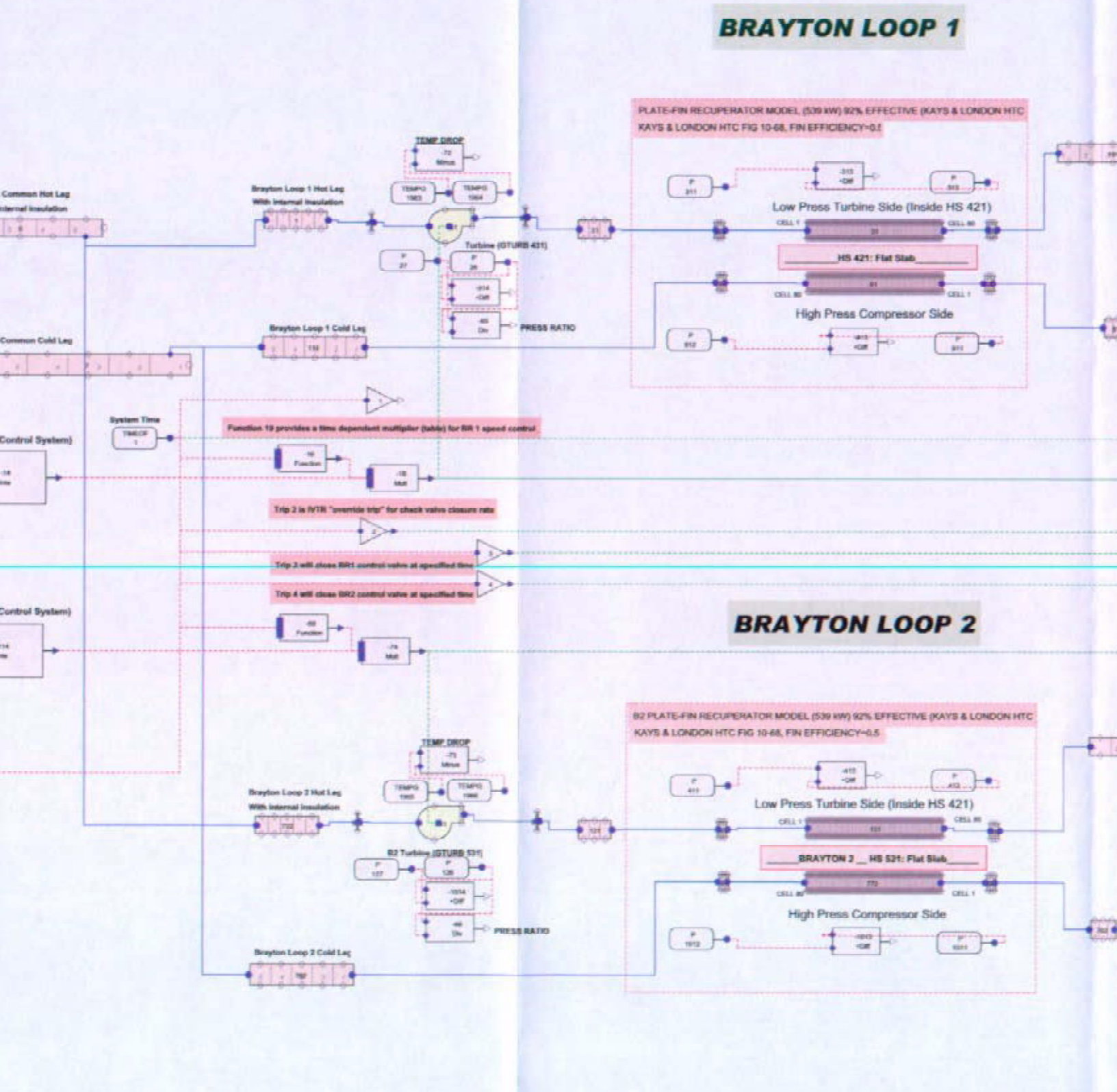







*PRE-DECISIONAL - For planning and discussion purposes only*

# TRACE Model of 2-Loop Direct Gas Brayton SNPP - SNAP Primary Hyd View - HeXe



**Coolant (78.4% Helium Mole Fraction)**

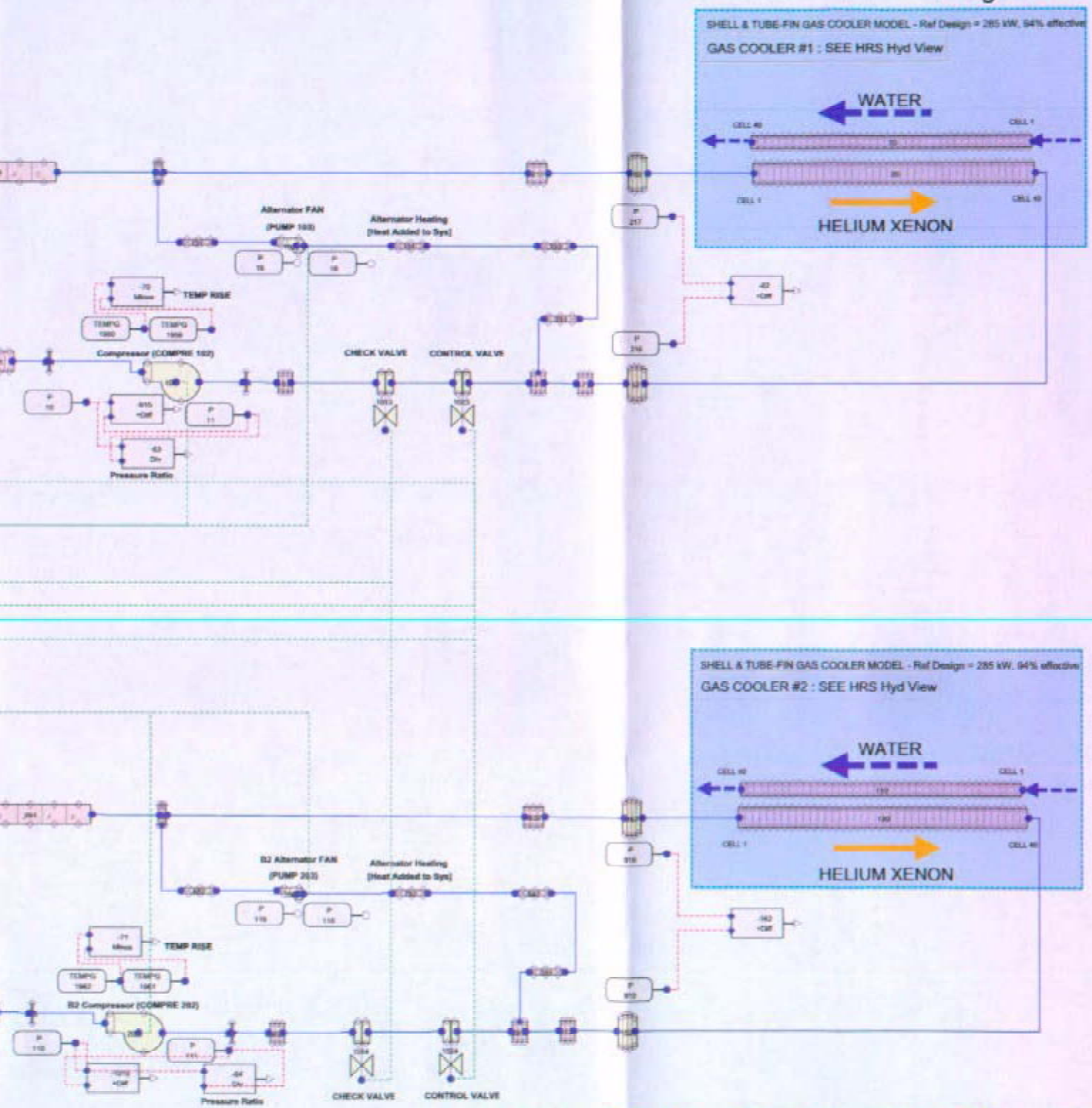



**Figure 12- 2: TRACE/SNAP Primary Plant Schematic View**

### 12.4.1.1 Steady State Condition

The heat balance for the space nuclear power plant direct Brayton concept is provided in Section 5. The heat balance methodology evolved throughout the Prometheus Project. A Space Reactor Power System program (SRPS-OPT) developed by GRC was initially revised by the NRPCT to perform heat balance calculations for two Brayton loop direct gas cooled reactor designs. In the concept selection report (Enclosure 1 to Attachment D of Reference 12-1) the SRPS-OPT program was used to produce an initial set of direct Brayton state points. As the design effort progressed, heat balance sensitivity studies were performed to account for design changes as well as variations in gas molecular weight, component efficiencies and primary plant pressure drops. Based on the timing to develop a full plant TRACE model, one of these interim heat balances was selected as a base case. This base case is referred to as Heat Balance 24 (HB24) and is provided in Figure 12-3. HB24 is similar to the concept selection heat balance, both using the same turbine (88.4%) and compressor (84.0%) efficiencies. One significant difference is that the HRS working fluid in HB24 was changed from NaK to water consistent with the NRPCT assessment in Reference 12-12. HB24 also had a companion piping design that included detailed pressure drop calculations. With a matching detailed piping design and water HRS, HB24 provided an effective reference for building the TRACE model.

The TRACE model was built in a modular fashion. Individual component models were built for the reactor, recuperator, gas cooler, turbine, compressor and HRS. Each of these "sub-models" was built and checked against the concept selection heat balance, HB24, and models built using other codes (such as Mathcad). For example, detailed Mathcad models of the recuperator and gas cooler were used to help determine TRACE code model inputs and verify steady state operating performance. This methodology was important to build robust, verified components that could later be connected to interact in a full plant model.

This full plant model captures some system thermal-hydraulic behavior that is not included in the heat balance spreadsheet programs. For example, the heat balance programs do not solve the momentum and energy equations to define the local working gas temperature and pressure. As shown in Figure 12-3, the gas temperature leaving the reactor (1150 K) is the same as that entering the turbine. In reality, and as modeled in TRACE, the gas temperature will be a function of the local pressure and velocity. Therefore, the TRACE results and heat balance spreadsheet calculations will never exactly match.

Table 12-3 compares the HB24 design point data with the TRACE model of the direct Brayton loop gas cooled reactor. Both results are based on a Xe mole fraction of 0.216 (the remainder is He), resulting in a working fluid molecular weight of 31.5 g/g-mole. As described above, TRACE model priority was given to individual component fidelity. The integrated TRACE model is allowed to find its own steady state condition. An average temperature controller is used to assist in finding a TRACE steady state that has about the same $T_{ave}$ as HB24 (1024 K). The TRACE $T_{ave}$ was defined as the average between reactor inlet and outlet plenum temperatures. TRACE reactor power is allowed to float to a new state point. For example, the HB24 reactor power is 851 $kW_t$, 25 $kW_t$ of which is assumed to be ambient losses and not included in the reactor temperature rise of 252 K ($\Delta T$). The HB24 power can be recalculated using the following equation:

$$Q = mdot \cdot c_p \cdot \Delta T = 4.97\ kg/s \cdot 659.9\ J/kg\text{-}K \cdot 252\ K = 826.5\ kW$$

However, the TRACE model calculates a different steady state power. Consistent with TRACE and SRPS-OPT power predictions, the codes also calculate slightly different gas velocities, pressures, and temperatures throughout the reactor and primary system. These differences result from higher fidelity thermal-hydraulic modeling (TRACE compared with spreadsheet calculations) as well as differences in individual component performance models. One way to compare the TRACE and heat balance power levels is to compare reactor $\Delta T$. It is important to clearly define where the TRACE reactor temperature rise is measured. By looking at the TRACE temperature rise across the fuel region the impact of velocity changes is minimized by eliminating flow area changes that occur outside the fuel region. Velocity changes are then limited to changes in gas density and momentum. The TRACE fuel temperature rise is about 273K (1162 K – 889 K). This is larger than the HB24 reactor temperature rise and consistent with a reactor power level of almost 900 $kW_t$. Although the HB24 and TRACE power levels are different, the components are operating at only slightly different points. As described above, it is not possible to exactly duplicate the HB24 conditions in a valid TRACE model.

While the TRACE and HB24 state points are not identical, most of the Table 12-3 parameters are very close. The TRACE results shown are based on selecting the CCEP direct option for both turbine and compressor models. This option is described in the turbomachinery section (Section 12.4.1.3). Both models show the same turbine inlet temperature of 1150 K. The largest differences are in the gas cooler water exit temperature and radiator flow rate. The TRACE gas cooler is somewhat less effective (91.2%) than HB24 shows (94%). The TRACE model and HB24 gas cooler designs are quite different. The SRPS-OPT spreadsheet gas cooler was originally a gas to NaK plate type heat exchanger. Additional gas cooler details are provided in Section 12.4.1.4.

TRACE temperature entries listed in Table 12-3 may require additional explanation. The TRACE program (like RELAP5-3D) solves energy and momentum equations throughout the hydraulics model. Flow paths are modeled with cylindrical representations (pipes) that are divided into control volumes. Velocity is defined at the interface between control volumes. Pressure and temperature are average properties of a control volume. With a compressible primary coolant, the coolant temperature in a control volume is a strong function of the pressure in that volume. The pressure will change due to changes in flow area (velocity) and hydraulic losses (form and friction). This behavior is responsible for what would otherwise appear to be inconsistent Table 12-3 temperatures. Examples include the difference between reactor $\Delta T$ (273 K) and recuperator high pressure (HP) exit to turbine inlet $\Delta T$ (258 K). Also note that the temperature changes on the two sides of the recuperator do not match (351 vs. 359 K). Two factors cause this difference. First, the recuperator low pressure (LP) side pressure drop is much smaller than on the HP side. The inlet plenum to core $\Delta P$ on the LP side is three times as large as the HP side. This corresponds to a higher plenum to core $\Delta T$ on the LP side. The other contributing factor is an error caused by the ratio of inlet to outlet $\Delta T$ (about 355 K) to local hot to cold side $\Delta T$ (30 to 40 K). The fewer nodes used between inlet and exit, the greater the error. This error is explained in greater detail in the recuperator description, Section 12.4.1.5.

Future TRACE model updates would have transitioned to an updated gas cooler design. Other future TRACE model updates would have included local assignment of ambient heat losses. TRACE heat structures were in place to distribute ambient losses throughout the plant. In addition, component test results for heat transfer and pressure drop would have been incorporated when available. For the TRACE Brayton components, additional detail was planned for bearing and windage losses (as a function of speed rather than a constant value), and more accurately modeling the alternator heat input (based on variable alternator efficiencies).

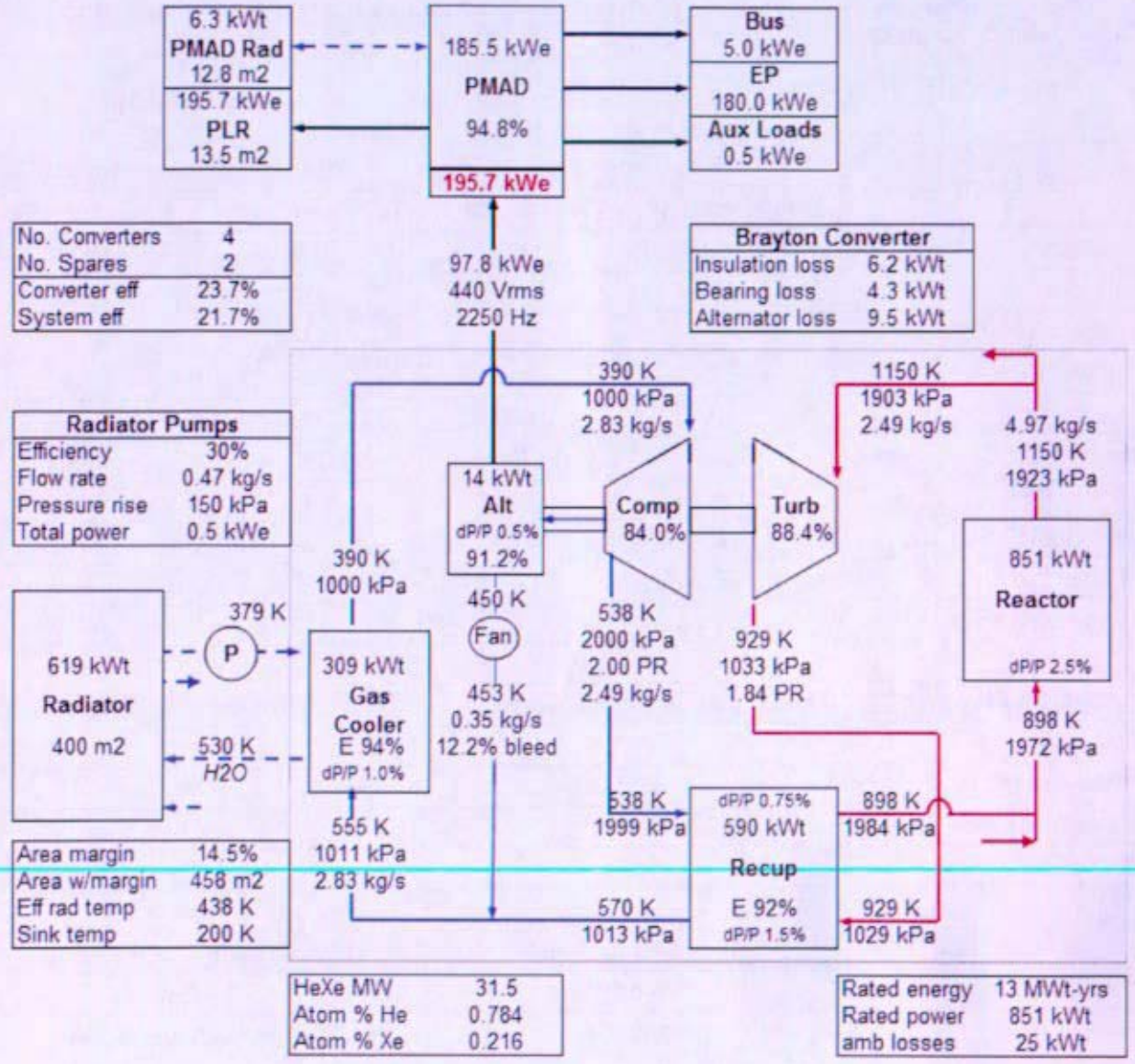
Overall, the TRACE model produces a steady state operating point that is in good agreement with separate heat balance calculations. This comparison is important as the first step in qualifying the TRACE code and model for a given plant design.

**Table 12-3: Comparison of Heat Balance Case 24 Design Point and TRACE Model State Points**

| Location | HB24 Design Point | | TRACE (with CCEP maps) | |
|---|---|---|---|---|
| | Temperature (K) | Pressure (kPa) | Temperature (K) | Pressure (kPa) |
| Turbine Inlet | 1150 | 1903 | 1150 | 1902.8 |
| Turbine Exit | 929 | 1033 | 933 | 1042 |
| Recuperator LP Side Exit | 570 | 1013 | 574 | 1024 |
| Gas Cooler Inlet | 555 | 1011 | 559 | 1019 |
| Gas Cooler Exit | 390 | 1000 | 393 | 1003 |
| Compressor Inlet | 390 | 1000 | 392 | 999 |
| Compressor Exit | 538 | 2000 | 541 | 1993 |
| Recuperator HP Side Exit | 898 | 1972 | 892 | 1979 |
| Gas Cooler H2O Inlet | 379 | - | 377 | 7744.0 |
| Gas Cooler H2O Exit | 530 | - | 510 | 7742.8 |

| System Flows | HB24 Design Point Flow (kg/s) | TRACE Flow (kg/s) |
|---|---|---|
| Brayton Loop Flow | 2.49 | 2.47 |
| Alternator Cooling Flow | 0.35 | 0.34 |
| Gas Cooler Gas Flow | 2.83 | 2.81 |
| Gas Cooler H2O Flow | 0.47 | 0.52 |

| Misc. | HB24 Design Point | TRACE (with CCEP maps) |
|---|---|---|
| Reactor Power (- losses) | 826.5 $kW_t$ | 899 $kW_t$ |
| Reactor ($\Delta T$) | 252 K | 273 K (through fuel region). |
| Reactor $\Delta P/P_{in}$ | 2.5% | 2.43% |
| Turbine PR ($\Delta T$) | 1.84 (221 K) | 1.82 (216.6 K) |
| Compressor PR ($\Delta T$) | 2.00 (148 K) | 1.99 (148 K) |
| Recuperator Effectiveness | 92% | 91.5% |
| Recuperator $\Delta P/P_{in}$ LP (HP) | 1.5% (0.75%) | 1.75% (0.73%) |
| Gas Cooler Effectiveness | 94% | 91.2% |
| Gas Cooler Gas $\Delta P/P_{in}$ | 1.0% | 1.4% |
| Radiator Area Applied | 400 $m^2$ (not including margin) | 447 $m^2$ (includes margin) |




*Piping System Pressure Drop = 39 kPa (2.3%)*
*Component Pressure Drop = 91 kPa (5.8%)*

**Figure 12-3: Design Point for TRACE Model (Heat Balance Case HB24)**

### 12.4.1.2 Reactor

The TRACE model includes a single fast spectrum gas cooled reactor. The model uses a single hot and cold leg nozzle. A point kinetics with reactivity feedback model is selected. The reactor design modeled with the TRACE code was taken from Table 2.2-1 of Enclosure 1 to Attachment D to the concept selection report (Reference 12-1). This table defined the reference design case parameters for a gas reactor using UN fuel and a block/pin, annular flow geometry. With a power rating of 1 MW thermal, the core was designed to use 72% helium and 28% xenon on a mole fraction basis. This coolant mixture is slightly different than the 78.4% helium mixture used in the reference heat balance and TRACE model. The higher helium concentration improves the gas heat transfer characteristics at the price of lower turbo-machinery efficiency.

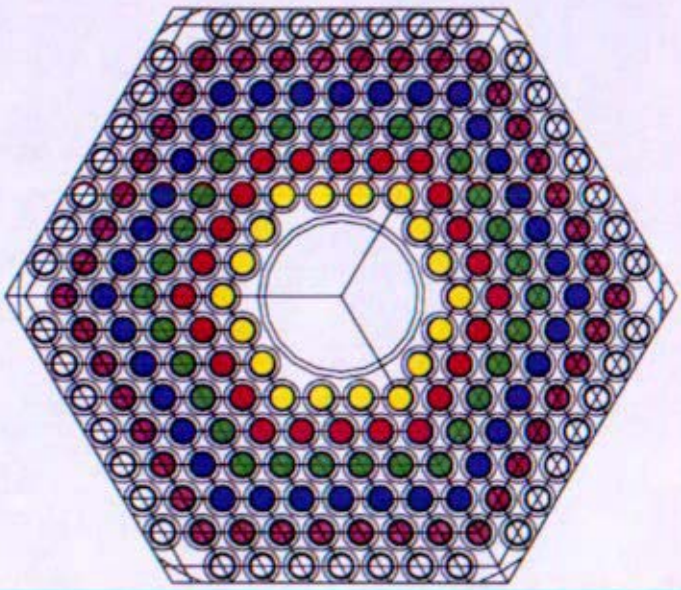


**Figure 12-4: Reference Reactor Cross-section with Color Coded Pins for 6-Path TRACE Model**

The TRACE reference reactor design contains a 192-pin layout in a triangular pitch of 3.035 cm. This produces a hexagonal layout with 6 rings of pins around a central annulus containing the shutdown safety rod, as shown in Figure 12-4. The fuel pins are centered in 192 cylindrical holes formed in a Niobium-1%Zirconium (Nb-1Zr) core block (128.5 cm in height). Annular flow passages are formed around each fuel pin, inside the core block hole. Each pin contains a center UN fuel region surrounded by a Rhenium (Re) liner and then a Nb-1Zr clad. A gap between the fuel and liner allows fission gasses to fill a large gas plenum at the cold end of the pin. The liner and clad are assumed to be bonded with no gap between them. Axial reflector material is installed at both ends of the fuel pin. TRACE heat structures are used to model each material in the fuel pin. Multiple radial nodes (10) are used in these heat structures to calculate a detailed temperature profile from the fuel center to the clad surface. Multiple (20) axial nodes are included in the fuel region to model an axial power profile and axial temperature distribution.

The TRACE reactor model (Figure 12-5) includes thermal-hydraulic representations of the reactor vessel inlet nozzle, inlet flow downcomer, inlet plenum, fuel pin lower extension (6), active fuel region (6), fuel pin gas plenum and upper extension (6), outlet plenum and outlet nozzle. The TRACE hydraulic core model includes six parallel flow paths, each representing one ring of fuel pins, as

shown in Figure 12-4. By having six paths in the core block region the model can represent radial primary flow maldistribution as well as a radial power profile. TRACE heat structures (7) are used to model the core block between each ring of annular flow passages. This heat structure detail allows the model to determine core structural temperature profiles in both the axial and radial directions. Heat transfer to the center and outside core block surfaces can also be calculated. At the outside of the core block the TRACE heat structure is tied to the downcomer, allowing for heat loss into the downcomer fluid ($T_{cold}$).

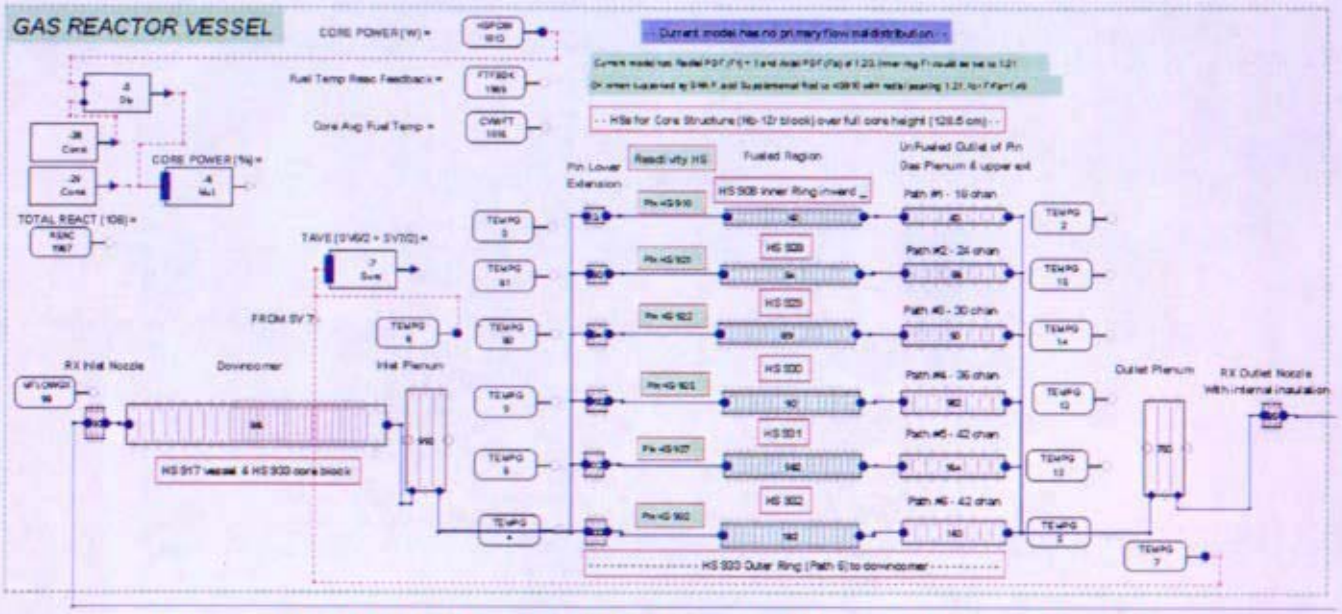



**Figure 12-5: SNAP View of TRACE Reactor Thermal Hydraulic Model**

The TRACE model shows the gas plenum at the hot end of the fuel. As the core mechanical design progressed, these features were moved to the cold end. The reactor vessel is designed to be made of Hastelloy X. To keep the reactor vessel temperatures low, the inlet cold leg gas flow is directed around a shroud that separates the hot core block and core exit gas from the reactor vessel (see Figure 12-6). This large annular flow region is hydraulically modeled in the TRACE downcomer.

The default TRACE heat transfer correlation for the working fluid is Dittus-Boelter. The helium-xenon binary gas mixture used as the reference coolant in this study has a much lower Prandtl number (0.2 to 0.7) than the air, steam and water fluids normally used in TRACE. Reference 12-7 describes a low Prandtl number literature search to determine what heat transfer correlation might be best for the reactor coolant. Consistent with this letter, the TRACE model invokes the Petukhov-Popov correlation in the fueled region. This special heat transfer correlation is referred to as the special gas fuel pin heat transfer package.

No special hydraulic resistance correlations have been applied in the TRACE reactor hydraulics. Instead, the standard TRACE modified Churchill equation is used with a surface roughness of 2.0E-6 meters. Hydraulic resistance flow factors are added to model non-recoverable form losses and to match the expected overall reactor pressure drop of 2.5% ($\Delta P$ / P inlet) defined in the heat balance.

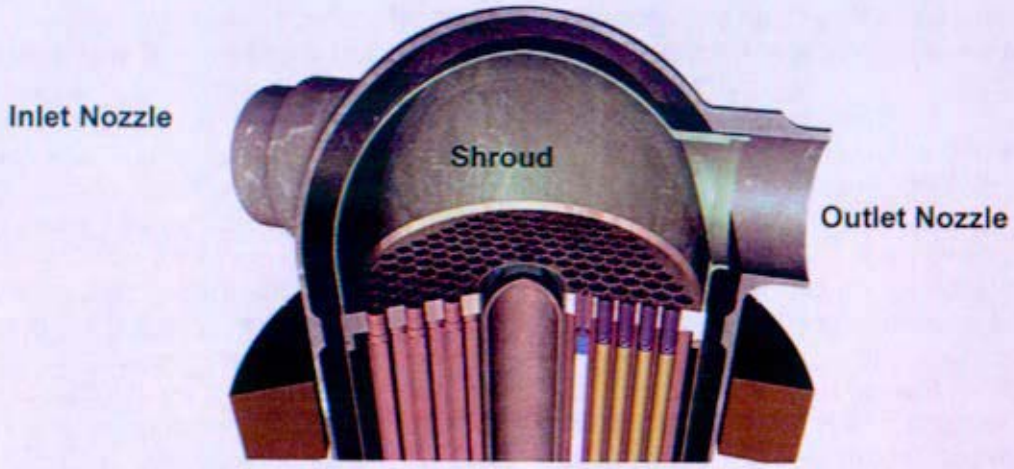



**Figure 12-6: Typical Arrangement for Reactor Vessel Downcomer Produced by Shroud**

The TRACE nuclear model uses built-in point kinetics calculations linked to the six fuel powered heat structures. A neutron lifetime of 1.0E-6 seconds is used along with a six group delayed neutron fraction. The code allows both axial and radial power profiles to be defined in the fuel region. A parabolic axial power profile has been applied with a peak power of 1.23 (consistent with the Reference 12-1 concept selection report Table 2.2-1). Currently, no radial power profile is modeled.

Negative reactivity feedback is modeled as equal contributions between fuel temperature feedback reactivity and geometric feedback reactivity. The fuel temperature reactivity coefficient is added as a constant -6.8E-6 $\delta\rho$/K over the entire operating temperature range. If desired, the coefficient can be added as a function of temperature. The geometry feedback coefficient (-6.8E-6 $\delta\rho$/K) is linked to the core block average temperature.

The TRACE model has a reactivity and temperature controller. Based on model setpoints the controller maintains plant temperature by changing the reactor reactivity. The TRACE control system uses average reactor temperature ($T_{ave}$) as the measured plant parameter to control on. The NRPCT has not down-selected to a single temperature control variable. The controller could be operated using $T_{hot}$, $T_{cold}$ or $T_{ave}$. $T_{hot}$ has the advantage of being related to equipment and system operating limits. For example the hot leg piping may have an operating temperature limit base on a maximum coolant temperature of 1150 K. The main problem with $T_{cold}$ is a much larger response time than $T_{hot}$. $T_{hot}$ will have the quickest response time to a perturbation by the controller. As $T_{ave}$ is an average of $T_{hot}$ and $T_{cold}$, it suffers from some of the problems with $T_{cold}$. $T_{ave}$, however, more accurately characterizes the behavior of the fuel temperature, and therefore has an advantage over $T_{hot}$ because the reactor power is partially based on fuel temperature.

The TRACE $T_{ave}$ controller is available to maintain a desired temperature or to change to a new average temperature, as shown in Figure 12-7. The controller may then be disabled if no active control is desired during the transient. A measured average temperature is compared to a desired average temperature using a PI controller. The PI controller determines the position of the sliders to accommodate for the change in temperature. The constants for the controller are k = -0.004 and $\Delta t_d$ = 80, where the equation is of the form:

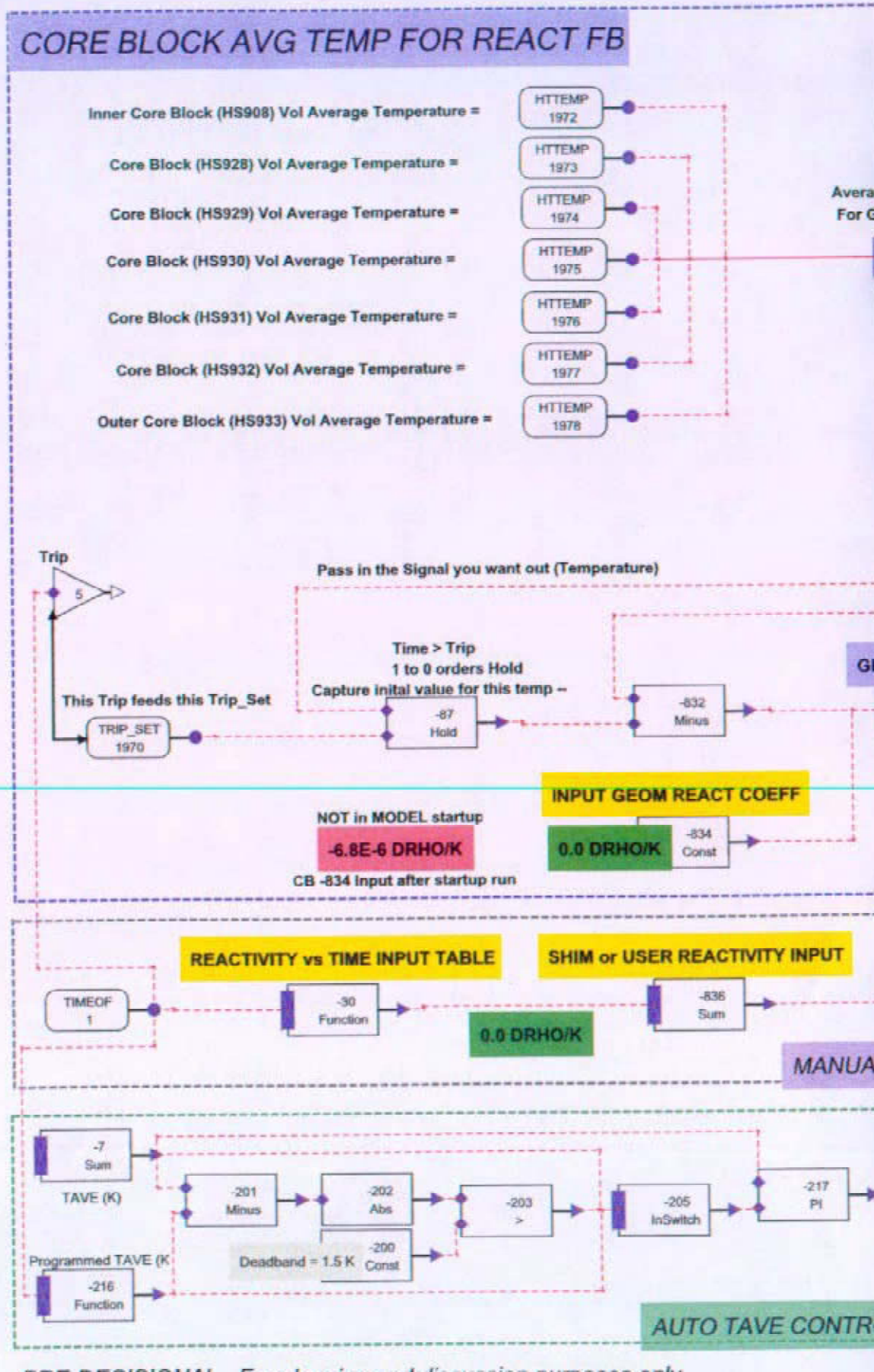
$$Position = k\,(\Delta F + 1/\Delta t_d \int \Delta F\, dt),$$

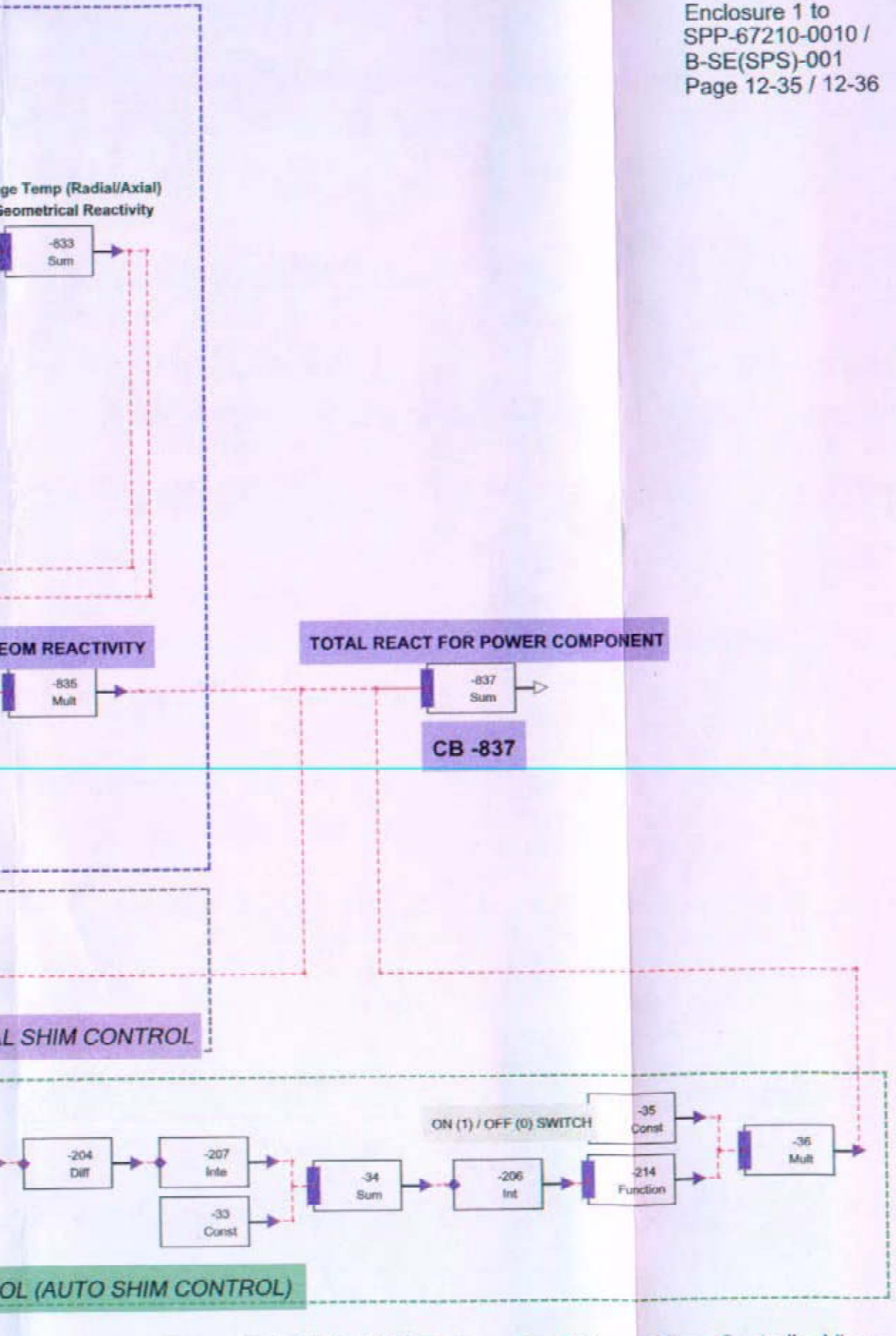
The term $\Delta F$ is the desired average temperature minus the measured average temperature. The control drive mechanisms (CDMs) have both discrete positions and a limitation on how often they can move. In the model, once the desired position is determined from the PI controller, it is then rate limited to one 1-mm step by a single slider each second. This is accomplished using a differentiation with a minimum and a maximum value and then integrating the result. After being rate limited, the position is then quantized to 1-mm steps per slider. The resulting position variable is input into a table of reactivity versus position. This table is a very rough approximation of typical slider worth for a typical center peaked parabolic axial power profile. At the steady state operating point, a single step of a single slider produces a temperature step of approximately 3 K in the average temperature. To prevent control system oscillations, there is a deadband around the desired average temperature of +/- 1.5 K. The controller is capable of maintaining the reactor at the desired operating temperature, but also capable of driving changes in temperature. The system has been demonstrated to make a step change in temperature or ramp through a range of temperatures. These changes are accomplished by making the desired average temperature a function of time.

**Table 12-4: Concept Selection Reference UN Core Concept as Applied to TRACE Model**

| Parameter | Value |
|---|---|
| Reference Case Coolant Mixture (from concept selection) | 72% He, 28% Xe |
| *TRACE model Coolant Mixture (to match current heat balance)* | *78.4% He, 21.6% Xe* |
| Fuel | UN |
| Rated Power ($MW_t$) *(TRACE model power)* | 1.0 *(0.9)* |
| Coolant flow rate (kg/s) *(TRACE model flow, w/TRACE 31.5 MW)* | 7.12 *(4.94)* |
| Neutron Spectrum | Fast |
| Core Geometry | Block/pin, annular flow |
| Pressure (MPa) *(TRACE model pressure)* | 1.38 *(2.0)* |
| # Safety Rods | 1 |
| Fuel liner material | Re |
| Clad material and core block structure material | Nb-1Zr |
| Vessel material | Hastelloy X |
| Number of fuel pins | 192 |
| Fuel diameter (cm) | 1.682 |
| Fuel height (cm) | 66.9 |
| BOL fuel-to-clad gap (cm) | 0.037 |
| Liner thickness (cm) | 0.079 |
| Clad thickness (cm) | 0.051 |
| Gas plenum height (cm) | 45 |
| Core diameter (cm) | 49.6 |
| Vessel thickness (cm) | 0.5 |
| Vessel OD (cm) | 55.7 |
| Safety rod material | Enr $B_4C$ |
| Safety rod OD (cm) | 11.7 |
| Radial reflector material/ percent TD (Theoretical Density) | BeO/95 |
| Radial reflector thickness (cm) | 11 |
| Channel thickness (cm) (radial gap in annular passage) | 0.384 |
| Pitch (cm) | 3.035 |
| Total channel flow area ($m^2$) | 0.0556 |
| Max FrFa (radial times axial power peaking factor) | 1.49 |
| Max Fr | 1.21 |
| Estimated Inlet and exit plenum height (cm) | 20 |
| Estimated pin lower extension length (cm) (including core plate) | 9.55 |
| Estimated pin upper extension length (cm) (including core plate) | 7 |
| Total hydraulic length (cm) | 128.5 |
| Downcomer ID (baffle OD) (cm) | 50.1 |
| Downcomer radial flow gap (cm) | 2.3 |

(Intentionally Blank)


CORE BLOCK AVG TEMP FOR REACT FB
Inner Core Block (HS908) Vol Average Temperature =
HTTEMP 1972
Core Block (HS928) Vol Average Temperature =
HTTEMP 1973
Core Block (HS929) Vol Average Temperature =
HTTEMP 1974
Core Block (HS930) Vol Average Temperature =
HTTEMP 1975
Core Block (HS931) Vol Average Temperature =
HTTEMP 1976
Core Block (HS932) Vol Average Temperature =
HTTEMP 1977
Outer Core Block (HS933) Vol Average Temperature =
HTTEMP 1978
Trip
5
This Trip feeds this Trip_Set
TRIP_SET 1970
Pass in the Signal you want out (Temperature)
Time > Trip
1 to 0 orders Hold
Capture inital value for this temp --
-87 Hold
-832 Minus
INPUT GEOM REACT COEFF
NOT in MODEL startup
-6.8E-6 DRHO/K
0.0 DRHO/K
-834 Const
CB -834 Input after startup run
REACTIVITY vs TIME INPUT TABLE
SHIM or USER REACTIVITY INPUT
TIMEOF 1
-30 Function
0.0 DRHO/K
-836 Sum
MANUA
-7 Sum
TAVE (K)
-201 Minus
-202 Abs
-203 >
-205 InSwitch
-217 PI
Programmed TAVE (K
-216 Function
Deadband = 1.5 K
-200 Const
AUTO TAVE CONTR


ge Temp (Radial/Axial)
Geometrical Reactivity
-833
Sum
EOM REACTIVITY
-835
Mult
TOTAL REACT FOR POWER COMPONENT
-837
Sum
CB -837
L SHIM CONTROL
ON (1) / OFF (0) SWITCH
-35
Const
-204
Diff
-207
Inte
-34
Sum
-206
Int
-214
Function
-36
Mult
-33
Const
OL (AUTO SHIM CONTROL)

### 12.4.1.3 Turbomachinery

The TRACE model has two parallel Brayton loops, each with a turbine and compressor. This configuration allows modeling multiple Brayton transients and confirming the stability of parallel loop systems. The TRACE code has been upgraded to include Brayton components. Specifically, a gas turbine (GTURB), compressor (COMPRE) and shaft (SHAFT) have been added to the available list of plant components available for power plant model building.

The GTURB component provides the capability to model the momentum and energy relationships for a single phase gas turbine. The unique GTURB input includes the following at rated conditions: turbine efficiency, head, mass flow rate and speed. For off-design conditions two dimensionless curves are available. The first table relates dimensionless turbine flow (function of ratios of actual and design mass flow and speed) to a dimensionless multiplier which is applied to the specified design pressure ratio. The second table relates dimensionless turbine flow to a dimensionless multiplier which is applied to the specified design efficiency.

The COMPRE component provides the capability to model the momentum and energy relationships for a single phase gas compressor. The unique COMPRE input includes the following design conditions: compressor dimensionless head, work input coefficient and flow coefficient. The blade tip diameter and rated rotational speed are also required. For off-design conditions two dimensionless curves are available. The first table relates dimensionless compressor flow (function of ratios of actual and design mass flow, speed, and density) to a dimensionless multiplier which is applied to the specified design head in the calculation of the actual head. The second table relates dimensionless compressor flow to a dimensionless multiplier applied to a design power which is used to calculate power.

The TRACE turbine and compressor off-design tables (maps) have been defined to approximate the GRC CCEP performance curves as applied in the CCEP off-design calculation worksheet documented in Reference 12-8. This off-design procedure was used to create three dimensional maps (pressure ratio, flow rate and efficiency as a function of corrected speed) for a particular Brayton design and fluid molecular weight. These design conditions have been redefined as the HB24 conditions. This translation is based on an assumption that new optimized Brayton equipment would behave in a similar manner as the original Reference 12-8 design. The original and extrapolated design values are shown in Table 12-5.

**Table 12-5: Comparison of CCEP and HB24 Design Points**

| | | CCEP | Heat Balance 24 |
|---|---|---|---|
| Compressor | Mdot | 2.21 kg/s | 2.49 kg/s |
| | PR | 2 | 2 |
| | $T_{in}$ | 426 K | 390 K |
| | $P_{in}$ | 0.5 MPa | 1 MPa |
| | EFF | 0.826 | 0.840 |
| | MW | 39.9 | 31.5 |
| Turbine | Mdot | 2.21 kg/s | 2.49 kg/s |
| | PR | 1.87 | 1.84 |
| | $T_{in}$ | 1144 K | 1150 K |
| | $P_{in}$ | 0.958 MPa | 1.903 MPa |
| | EFF | 0.855 | 0.884 |
| | MW | 39.9 | 31.5 |

The TRACE Brayton components have the option of acting in accordance with CCEP performance maps or in accordance with performance curves. The CCEP maps are three dimensional and represent the higher fidelity of the two options. The performance curves are two-dimensional (PR and efficiency), and the user has the ability to define these curves as part of the Brayton component definition. The curves offer a more robust behavior in dealing with conditions that would otherwise represent the components "running off of the map". The dependent variable on the performance curve (PR or efficiency) is a function of an independent variable parameter that combines the flow rate and rotational speed. The curves are characterized by a scale and a shape. For SNPP calculations, the scale of the performance curves was defined by matching the HB24 design point, and the shape of the performance curves was defined by matching CCEP performance map contours that run through the design point – i.e. the curves were generated by collapsing the maps about the design point. Therefore, when the performance curve option is invoked and the component is operating off the design point, the component behavior is only an approximation to the CCEP maps.

As described above an option was also added to TRACE to directly use the CCEP maps. When using this option the TRACE components are bypassed and the Brayton performance is fully defined by the CCEP maps. A limitation to this option is the restriction to remain on the curves. TRACE cannot extrapolate beyond the supplied curve performance. The TRACE curves and CCEP maps provide very similar results near the design point. As you move away from the design point both options produce qualitatively similar results. Quantitatively, the CCEP maps produce larger changes in mass flow rate for a given change in fluid conditions (density).

The Symbolic Nuclear Analysis Package (SNAP) version 23.17 was used as the input and output Graphical User Interface (GUI) for the TRACE model and executable. While the TRACE executable was updated to include Brayton components, time did not permit the supporting changes in SNAP. A simple workaround was used such that GTURB and COMPRE input could be passed through using the SNAP PUMP component. Therefore, the input model schematics show the SNAP PUMP component to locate both a turbine and compressor. Model option title cards were used to define those component numbers that would use SNAP PUMP input for a turbine or compressor. In a similar fashion, other TRACE options that are not currently supported in SNAP are input into TRACE using the model option title cards. These other options include special heat transfer correlations, CCEP map selection and input values, and SHAFT component data.

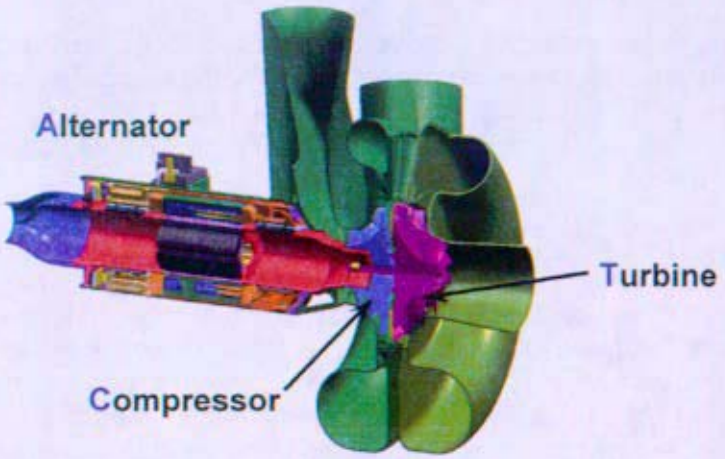



**Figure 12-8: Typical Arrangement for a TCA Brayton**

The TRACE model is based on the Turbine-Compressor-Alternator (TCA) Brayton configuration shown in Figure 12-8. This configuration bleeds off a fraction of the compressor inlet flow (the lowest temperature gas in the system) to cool the bearings and alternator. Since the compressor inlet is the lowest pressure point of the Brayton system, an internal fan provides the necessary head to circulate cooling gas. The fan is integral with the shaft at the opposite end from the turbine, pulling cooling gas through the Brayton and then pushing it back to the gas cooler inlet.

In the TRACE model, the bleed (cooling) path is fully modeled with a flow path that short-circuits the overall Brayton flow path. A pump is included in this path to model the momentum addition of the alternator fan. The pump (or compressor) is sized to produce the HB24 cooling (bleed) flow rate of about 0.35 kg/s. A TRACE bleed path heat structure is used to add the appropriate heat to the alternator and bearing cooling gas. The Brayton alternator is currently not explicitly modeled in TRACE. Instead, the alternator is defined by the appropriate torque for the shaft speed calculation. The turbine, alternator, and compressor are all connected to one shaft. Thus, these components all operate at identical shaft speeds. The shaft speed is determined by a balance of the torques on the shaft imposed by the components plus any parasitic losses. The equation for the load balance on the shaft is:

**Equation 12-1** $I\, d\omega/dt = \tau_T - \tau_C - \tau_A - \tau_P$

Where:
- $\tau_T$ = turbine torque = $\eta_T m \Delta P_T / \rho_T \omega$
- $\tau_C$ = compressor torque = $m \Delta P_C / \eta_C \rho_C \omega$
- $\tau_A$ = torque imposed by the alternator
- $\tau_P$ = torque imposed by parasitic losses
- $I$ = shaft moment of inertia
- $\eta_T$ = turbine efficiency
- $m$ = mass flow rate
- $\Delta P_T$ = turbine differential pressure
- $\rho_T$ = average fluid density in the turbine
- $\omega$ = shaft speed
- $\eta_C$ = compressor efficiency
- $\Delta P_C$ = compressor differential pressure
- $\rho_C$ = average fluid density in the compressor

TRACE alternator torque and power results provided in this report are based on the alternator mechanical or thermal performance. For example, at 110 $kW_t$, the alternator electrical output must be determined using the expected alternator efficiency. Using the HB24 alternator efficiency of 91.2%, the electrical output is 100 $kW_e$. A description of the TRACE model speed controller is provided below.

Prior to the development of the SNPP TRACE model, previous MATLAB/Simulink modeling work had shown that a direct gas, recuperated Brayton plant is "non-load following." The phrase "non-load following" refers to an inverse relationship between alternator electrical load and reactor power. This characteristic is once again illustrated in the partial loss of load transient described in this report. This transient models a load reduction that is not compensated for by the speed control system and is therefore a representation of plant response without speed control. In addition, for some plant conditions, a Brayton shaft load balance may be satisfied by more than one Brayton speed. In this case, only one of these operating points may be stable. The most common solution to the stability and load following characteristics is to use a Brayton speed control system (Reference 12-4). In order to regulate Brayton speed, two controllers are envisioned, one for each Brayton. The TRACE model controller detects operating speed, which is approximately proportional to bus frequency or voltage. The operating speed is then compared to a desired operating speed using a PI controller. The PI controller determines a combined Turbine-Compressor-Alternator (TCA) torque required to drive the Brayton to the desired operating speed. The TCA torque is equal to the turbine torque minus the sum of the compressor, alternator, and alternator cooling fan torque. The constants for the controller are k = 0.225 and $\Delta t_d$ = 10, where the equation is of the form:

$$TCA\ Torque = k\ (\Delta F + 1/\Delta t_d \int \Delta F\ dt)$$

The term $\Delta F$ is the desired operating speed minus the measured operating speed. These constants are tuned appropriately to provide a fast response while minimizing overshoot. The alternator torque is provided to the shaft component. The shaft component updates the shaft speed based on the net shaft torque, the Brayton inertia, and time integration.

This speed controller shown in Figure 12-9 is an approximation of a Power Conditioning and Distribution (PCAD) system with a PLR. In the actual system the controller would notionally measure current, load voltage, or load power and control to a compared desired value. This is done by switching on and off portions of the PLR resistors. An actual PCAD system would have limited alternator loading capability based on the PLR design maximum power. Therefore, the model has a power limitation on the alternator output of 120 kW as an approximation (based on a ~100 $kW_e$ alternator operating point). Similarly, an actual PCAD system could only accommodate a specific current in addition to the operating current. Based on the expected PCAD current limit (150% of normal current), a maximum model alternator torque is set at 32 Nm which was chosen as a reasonable starting point for the model. The TRACE speed controller also requires the alternator torque to be a zero or positive value. Finally, the model includes an input constant for the number of cables connecting the alternator and PCAD system. Three cables are modeled, corresponding to the number of power phases. This feature is used to approximate the alternator torque capability during partial loss of load casualties. The controller is capable of maintaining a Brayton at the desired operating speed, but also capable of driving changes in speed.

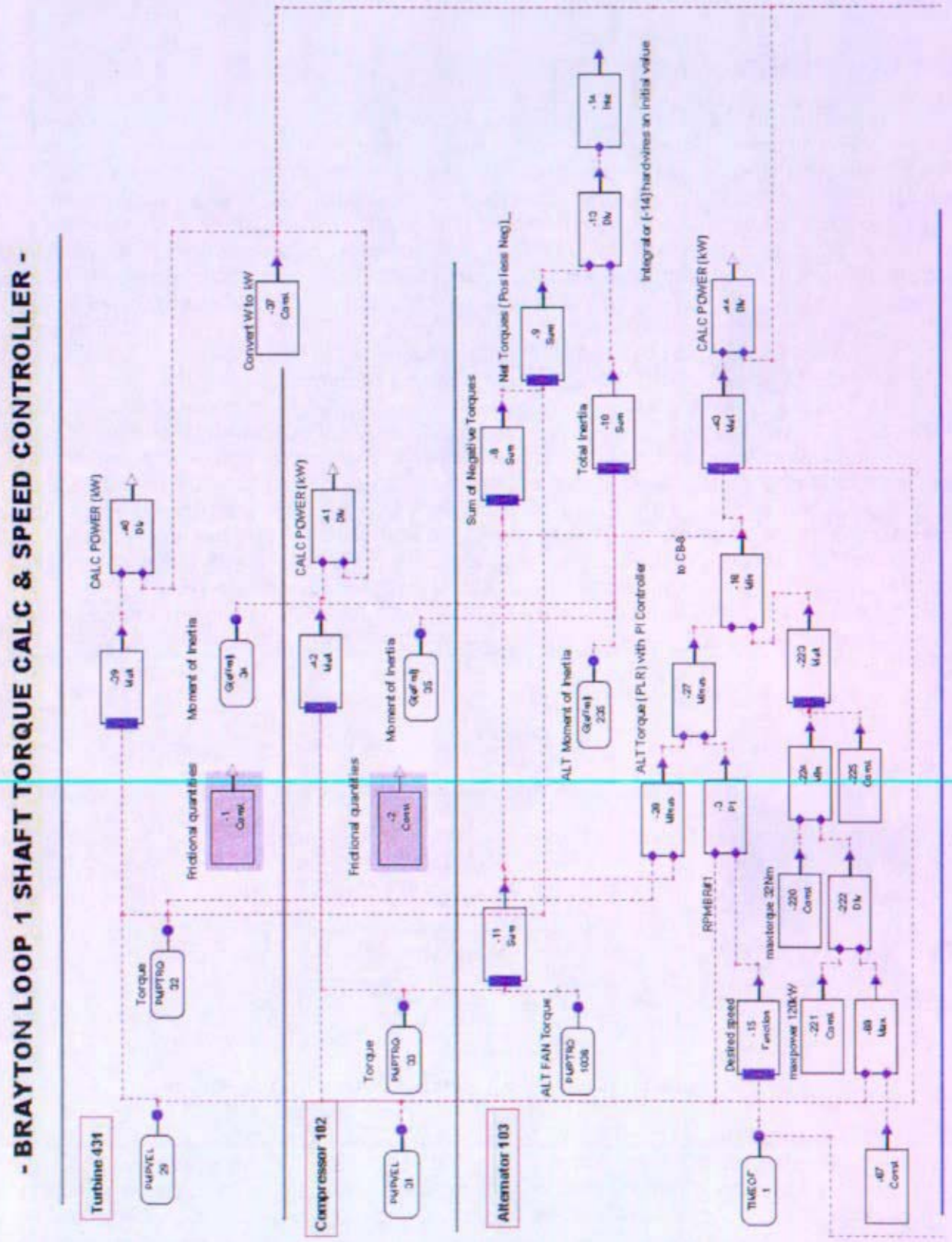



Figure 12-9: TRACE/SNAP Brayton Loop One Shaft Torque Calc & Speed Controller View

### 12.4.1.4 Gas Cooler

Each Brayton loop contains one gas cooler and dedicated HRS loop. The TRACE gas cooler model is significantly different than the RELAP5-3D models. The differences stem from two power plant design changes. The first was the selection of a direct Brayton system over other designs. For example, the SRPS-OPT Brayton plant sizing tool developed by GRC is an indirect Brayton system where the gas cooler does not contain primary coolant. Also, the original HRS loop coolant was low pressure NaK. The combination of low pressure HRS coolant and an intermediate Brayton loop coolant minimized the consequences of a gas cooler leak. To minimize size and weight, gas coolers were generally thought of as having a brazed plate configuration. With the transition to a direct Brayton design, the consequences of a gas cooler leak (even in a multiple Brayton plant) are mission ending. Therefore, a brazed plate design might pose a reliability issue. Secondly, when considering water as the HRS fluid, the HRS system design pressure becomes much higher.

Based on the higher operating pressures required to keep water subcooled, a different cooler design was adopted. Since more appropriate gas cooler designs were not available, a Mathcad model was built for a somewhat traditional shell-and-tube heat exchanger. This model became the steady state operating design case for a TRACE gas cooler model. To minimize weight, the high pressure water was assigned to the tube side and the gas flow to the shell side. To add gas side surface area, fins were added to the outside of the tubes. The size and weight of this TRACE gas cooler was not optimized. The NRPCT was investigating gas cooler designs in parallel to TRACE model development. Future TRACE model updates would have transitioned to an updated design.

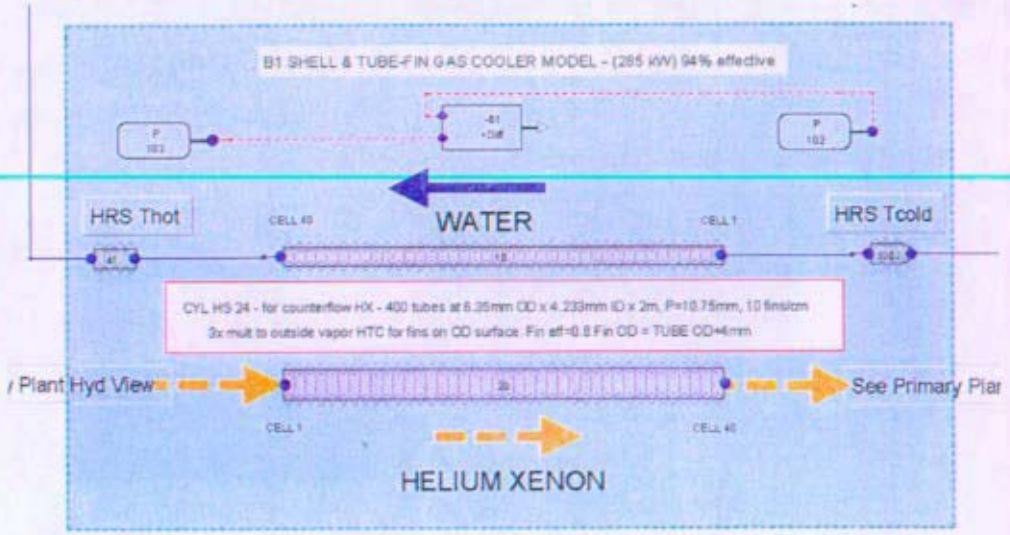



**Figure 12-10: Shell-and-Tube-Fin Gas Cooler Model**

The gas cooler model is shown in Figure 12-10. The gas cooler design was started using the concept selection heat balance and therefore was sized for about 285 kW. At this power level the cooler was 94% effective. At full power steady state conditions, the TRACE model calculates a gas cooler power level of about 303 kW. At these conditions the corresponding gas cooler effectiveness is about 91%. This difference does not have a significant impact on the overall TRACE model performance. The water side of the cooler is designed to operate at about 8 MPa. The gas cooler model is a counterflow design with 400 tubes at 6.35 mm OD and 1.058 mm tube wall thickness. The tube

length is about 2 meters. Including all fin area, the gas side heat transfer area is about 79 $m^2$. A relatively short and thin fin design is anticipated to provide moderately high fin efficiency. Using a fin efficiency of 0.6, the effective gas surface area is about 47 $m^2$. This fin efficiency is an approximation based on Figure 10-38, "Efficiencies for several longitudinal fin configurations" and Figure 10-39 "Efficiencies for annular fins of constant thickness," of Reference 12-13. These figures relate efficiency to the following relationship:

$$x = (r_e - r_b)\,[h_f / (k y_b)]$$

Where $(r_e - r_b)$ is the fin height and $y_b$ is the fin thickness. For the TRACE gas cooler design, the quantity "$x$" is about 1.5, resulting in a fin efficiency of about 0.6. The actual fin efficiency would be determined with a more detailed equipment design and subsequent testing. The TRACE model uses cylindrical geometry hydraulics and heat structures. The heat structure is nodalized at 40 axial and 5 radial nodes. Axial conduction is enabled. The material properties applied are for Alloy 600. The TRACE heat structure has the same dimensions as an individual tube. A multiplier is used to produce the correct total heat transfer area. The fin surfaces are not explicitly modeled in TRACE. Instead, a gas (outside tube) heat transfer coefficient multiplier is used to account for the additional effective area.

At steady state conditions the typical water temperatures entering and exiting the gas cooler are 375 K and 501 K respectively. This temperature drop is significantly less than the HB24 value of 151 K (530 – 395 K). The TRACE model $\Delta T$ is less because a higher water mass flow rate is used and the total cooler power is somewhat lower (303 vs. 309 kW). Later versions of the heat balance spreadsheet were updated with more consistent water based HRS design parameters and became more consistent with the TRACE results.

Currently the standard TRACE code heat transfer (Dittus-Boelter) and fluid pressure drop (Churchill and Moody) correlations are applied to the gas cooler. Use of the Churchill correlation and Moody curves, and mathematical representations of the curves, for calculation of the single-phase friction factor in a variety of flow-channel geometries is a common engineering practice. Information on the TRACE default correlations is available in the TRACE theory manual (Reference 12-9). A surface roughness of 2E-6 m is used with the TRACE single phase friction correlations. In order to match the HB24 pressure drop prediction, additional frictional flow factors are included in the hydraulic model. The TRACE model also includes plenums to provide a location to specify form loss factors for the gas cooler. The heat transfer and pressure drop correlations would have been updated as the cooler design was determined and as test data was collected.

### 12.4.1.5 Recuperator

Each Brayton loop contains one recuperator. The recuperator removes heat from the turbine discharge fluid and preheats the reactor inlet flow. System efficiency is improved because less heat must be rejected to space (through the gas cooler) in order to provide a low temperature compressor inlet flow. The recuperator model was based on a very detailed Mathcad model of a strip-fin plate-fin surface compact heat exchanger. The applicable design was defined in Figure 10-68 of Reference 12-10. This reference provides both measured heat transfer and pressure drop correlations. Based on the initial concept selection, the initial recuperator model was designed to transfer a power level of 539 kW. The HB24 power level was increased to 590 kW. At full power steady state conditions the TRACE recuperator model power is about 576 kW. The calculated TRACE recuperator effectiveness is about 91.5%, very close to the HB24 value.

The recuperator model is shown in Figure 12-11. The TRACE model uses the appropriate plate geometry hydraulic diameter of 1.8629E-3 m and a total hot and cold side flow area of 0.046 $m^2$ (each). The heated length is about 0.804 meters. Eighty axial fluid nodes are used to minimize the temperature error associated with this type of model. The model is based on 32 low pressure and 32 high pressure passages. The fin design is an offset rectangular double layer type. A TRACE flat slab heat structure is used to model the plates between flow paths. The heat structure nodalization is 80 length nodes by 5 thickness nodes. Axial conduction is enabled. The TRACE heat structure is based on the calculated effective plate and fin thickness of 1.315E-4 meters. When combined with the plate length of 0.804 m, the plate heat structure effective width of 85.87 m provides the total heat transfer area of 69 $m^2$. Alloy 600 material properties are used for the heat structure.

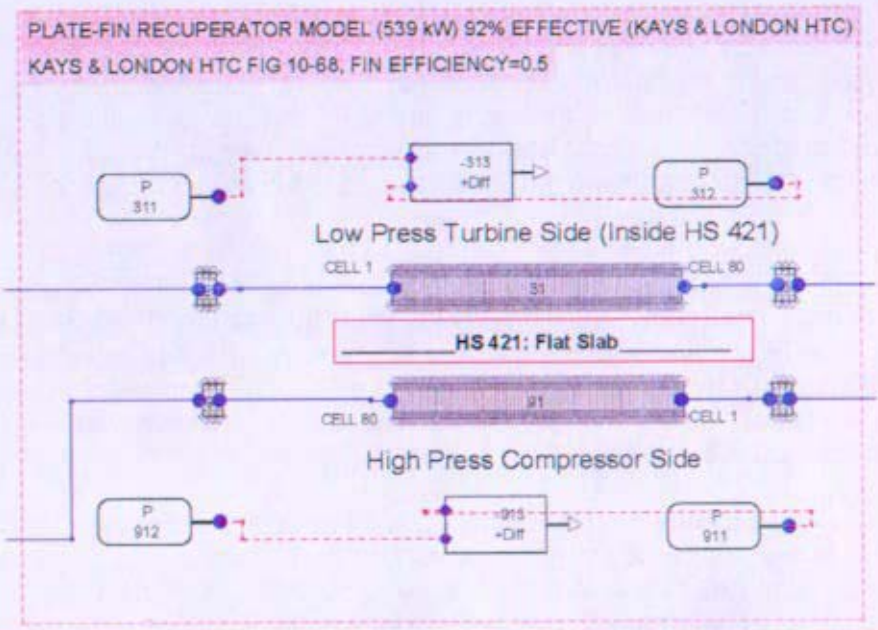



**Figure 12-11: Plate-Fin Recuperator Model**

The TRACE nodalized fluid-heat structure recuperator and gas cooler models were developed from Mathcad models. The temperature (power) errors associated with the TRACE nodalization were calculated and sensitivity studies were performed to select the number of nodes in the current model. The small errors that exist with the current nodalization are considered a reasonable compromise between model size and speed. For this application, the TRACE heat structure and fluid cell coupling has been significantly improved from the predecessor code, TRAC-P. TRAC model ROD/SLAB components use staggered heat structure cells. This aligned the heat structure cell with the fluid cell interface. That is, the heat structure cells were centered between hydraulic cells. This is consistent with the RELAP5-3D heat structure configuration. In TRACE the HTSTR (heat structure) component has been co-located with the fluid cell. This aligns the average cell fluid properties when a counterflow heat exchanger is modeled. This co-locating of fluid and heat structure cells reduces the number of nodes required to produce a reasonably small recuperator power error. The error associated with the full power steady state TRACE recuperator is less than 2%. Using the TRACE 80-node recuperator did not impact the time step selection of the TRACE code when running a stand alone or full plant model.

Kays & London (Reference 12-10) Figure 10-68 provides the heat transfer correlation that was added to the TRACE code and is invoked using the model option title cards. The correlation may be specified as:

$$Nusselt\ Number = 0.269\ (\ Re^{0.58} \cdot Pr^{1/3}\ )$$

This correlation is for the specific compact heat exchanger design modeled in Mathcad and TRACE for the space Brayton design. This offset strip-fin plate-fin design uses a double fin stack (0.255 inches) with 630 fins per meter. Currently the default TRACE single phase pressure drop correlation is applied with 2E-6 m surface roughness. In order to match the Kays & London pressure drop prediction, additional frictional flow factors are included in the hydraulic model. The total recuperator pressure drop is also verified to be close to the HB24 values. The TRACE model also includes plenums to provide a location to specify form loss factors for the recuperator model. The heat transfer and pressure drop correlations would have been updated as the recuperator design was further developed and as test data was collected.

### 12.4.1.6 Heat Rejection Segment (HRS)

The HRS in TRACE is modeled after the PB1 design described in Reference 12-11 and further discussed in Section 9.6. There are two water HRS loops in the TRACE model, one connected to each Brayton loop as shown in Figure 12-12. The gas cooler is the connection between the primary gas loop and the HRS water loop. The water flows out of the gas cooler after being heated and enters the heat transport loop assembly further discussed in Section 9.6.2.1. Each heat transport loop assembly consists of four sections of parallel circular water ducts that are connected to slab heat structures. These heat structures represent the radiator panel assemblies as described in Section 9.6.2.2. The four sections of pipes feed into a larger return duct that leads to a centrifugal pump and accumulator before returning to the inlet of the gas cooler.

As shown in Figure 12-12, the four sections of parallel hydraulic paths that are connected to radiator panels contain one, two, four, and six parallel pipe components stemming from a main path by 1.324 cm inner diameter pipes. Each parallel pipe in the TRACE model represents two coupled circular ducts with a hydraulic diameter of 1.024 cm and total flow area of 1.65 $cm^2$. With parallel paths of equal diameter, there was a large flow maldistribution in each section, so additive flow losses were included in the first few parallel pipes in order to achieve velocities among the parallel paths to within 25% of each other. The length of the parallel pipes is 11.45 m except for the pipe in the first section which is 4.2 m long. At the end of the fourth section, the water returns to a pump and accumulator through a 40.55 m long, 2 cm inner diameter pipe representing the length of pipe needed to bring the water from near the end of the boom to the energy conversion unit. For each loop, the total length of pipes is 212.5 meters.

There is one pump modeled per loop. The pump component is modeled after a generic compact single stage centrifugal pump, prototypic of what would be used in this water system. The pump head is 300 $m^2/s^2$ with a torque of 0.3 $Pa*m^3$ and speed of 356 rad/s (3400 RPM). At steady state conditions, the resulting pressure drop for the loop is 293 kPa with a flow rate of 0.52 kg/s. The electric power needed to run the pump is 0.530 $kW_e$ assuming the pump efficiency is 30%.

The accumulator is represented with a liquid-separator model. This represents an accumulator with metal bellows that allows for water expansion and a separate gas charge to control pressure changes from the normal operating system pressure of about 7.75 MPa. System pressure increases due to increased average water temperature (density) and a small amount of boiling are damped by the HRS

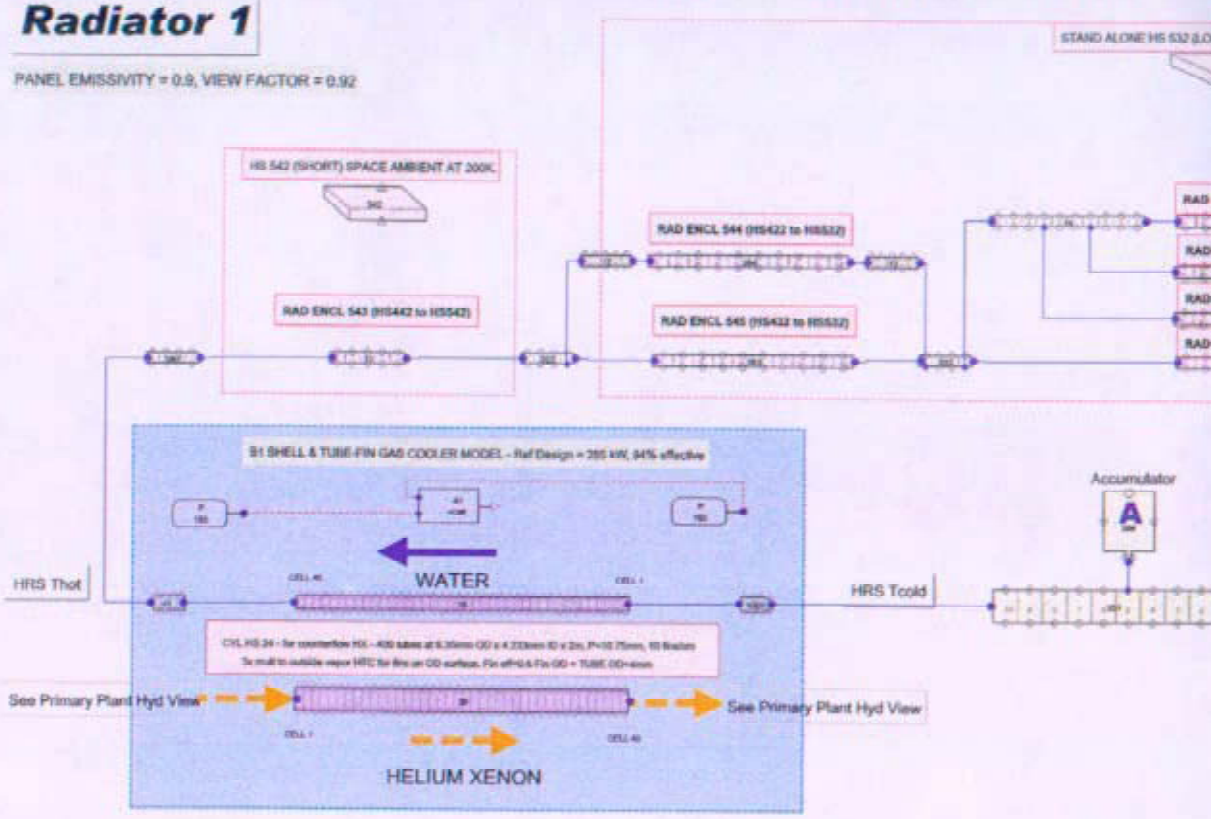
accumulator. The TRACE accumulator volume is 0.03535 $m^3$ and is assumed to be half gas (by volume) at nominal steady conditions. The accumulator is a built in TRACE component option that has been used without a heat structure. In other words adiabatic conditions apply for the enclosed volume.

The heat structure attached to each parallel pipe represents an assembly of material that is used in the radiator panel assembly. As described in Section 9.6.2.2, heat is transferred through the titanium water duct walls, the POCO foam saddle, the titanium wall of the heat pipe evaporator, the heat pipe, the titanium wall of the heat pipe condenser, and finally out into the carbon-carbon (C-C) radiator panels. This assembly of materials is modeled in TRACE using one slab heat structure per pipe which represents the associated assembly for that length of pipe. This was done by dividing the heat structure up into five radial sections consisting of titanium, POCO foam, titanium, titanium, and C-C material in series from the water pipe to the panels. The thickness of each section was determined so that the volume of material was conserved but fit to the area of the C-C radiator panels. An additional feature that was added was the modeling of the properties of a gas loaded heat pipe. As described in Section 9.6.2.2, the gas loaded heat pipe will be fully operational at 343 K and fully off at 313 K. This function was modeled in TRACE by revising the POCO foam thermal conductivity to be its normal value at 343 K and zero at 313 K, effectively stopping heat transfer to the radiator panels. The panel area for one loop is 223.7 $m^2$ making the total radiator area 447.4 $m^2$ which includes a 15% design margin for heat pipe failure and design uncertainties. The heat structures with an emissivity of 0.9 are coupled in a radiation enclosure with a view factor of 0.92 to a sink heat structure maintained at 200 K. In TRACE both the emissivity and view factor effectively reduce the surface area used in the radiation heat transfer calculation. The view factor was used to tune the HRS performance by approximating the HB24 gas cooler primary exit temperature. Future model development would have been based on matching certain aspects of detailed HRS models being developed by Northrup Grumman Space Technology.

TRACE Model of 2-Loop Direct Gas Brayton SNPF

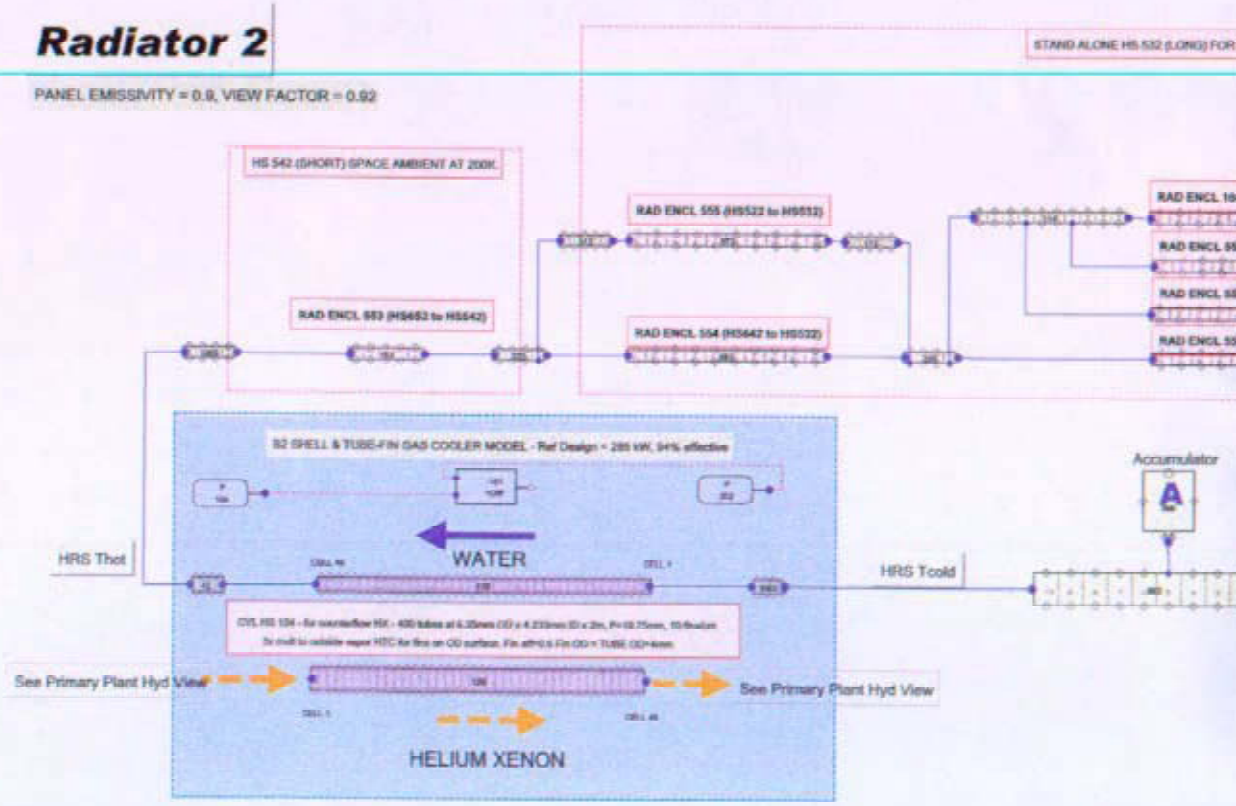
## Radiator 1

PANEL EMISSIVITY = 0.9, VIEW FACTOR = 0.92



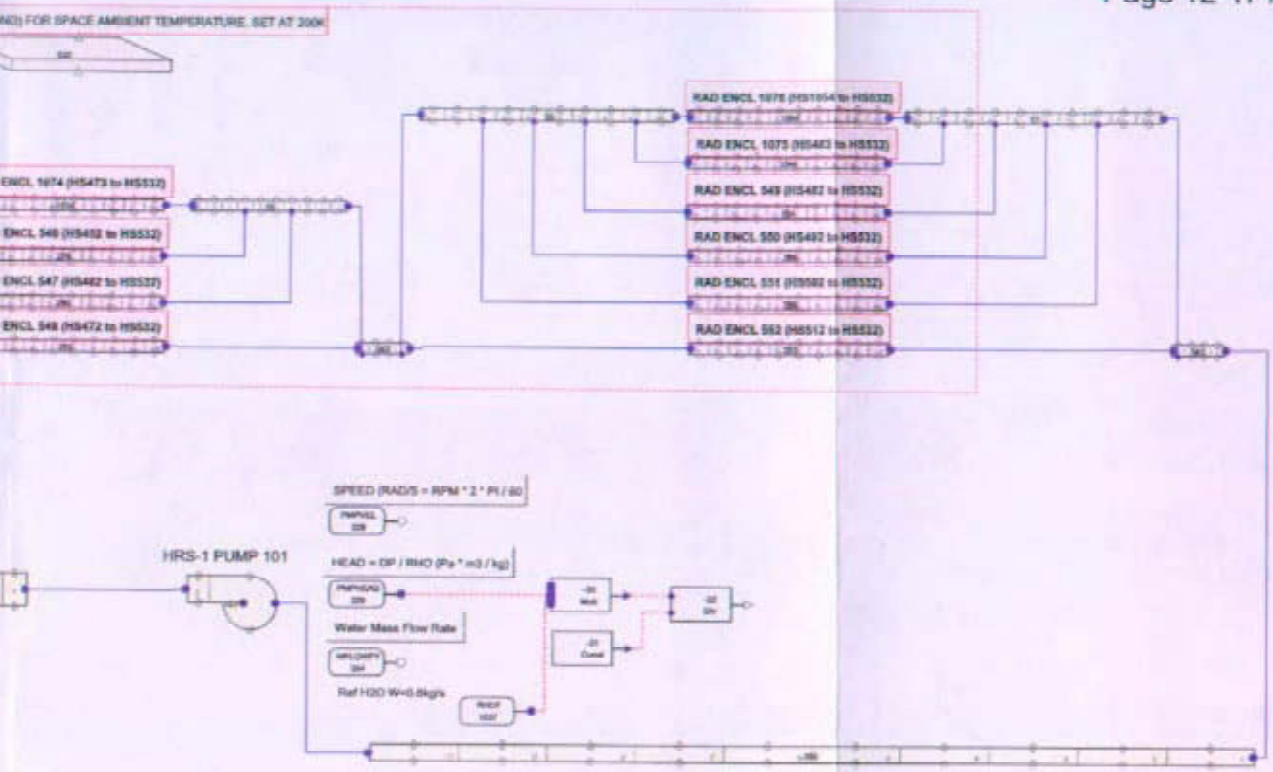

## Radiator 2

PANEL EMISSIVITY = 0.9, VIEW FACTOR = 0.92




*PRE-DECISIONAL – For planning and discussion purposes only*

P - SNAP Heat Rejection System (HRS) Hyd View - H2O Coolan



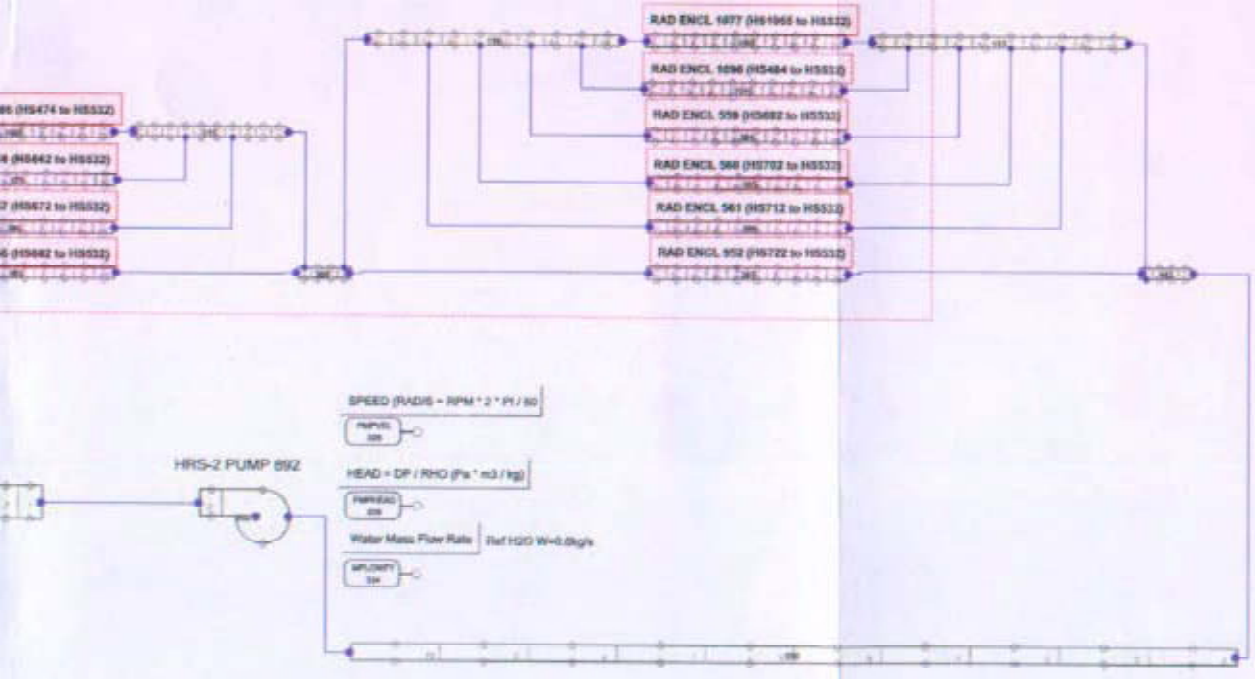




**Figure 12- 12: TRACE/SNAP Secondary Plant (HRS) Plant Schematic View**

### 12.4.1.7 Reactor Coolant Piping

An advantage of using HB24 for the TRACE model steady state design points was that HB24 was based on a detailed piping design. The HB24 and TRACE model piping design includes specific pipe diameters, lengths and hydraulic loss factors (for bends, tees and fittings). In addition to modeling the appropriate pipe diameters, the TRACE model includes insulated common and individual Brayton hot legs. The TRACE model includes the appropriate hot leg flow diameter, and a heat structure that includes a thin insulation liner, insulation, and thicker outer pipe wall. Total TRACE loop pressure drops were matched to those calculated with HB24. TRACE pipe and connected component flow parameters are provided in Table 12-6.

**Table 12-6: TRACE Piping and Component Flow Parameters**

| Description | Flow Area ($m^2$) | Length (m) | Thickness (cm) | ID (cm) | TRACE Loss Coefficient |
|---|---|---|---|---|---|
| Combined Hot Leg (HL) | 0.01227 | 3.9 | see below (*) | 12.5 | 0.07 |
| BR1 HL to Turbine | 0.01227 | 1.5 | see below (*) | 12.5 | 0 |
| TURB component | 0.01227 | 0.2 | n/a | 12.5 | 0 |
| BR1 Turbine to Recup | 0.01404 | 0.75 | 0.315 | 13.37 | 0.33 |
| RECUP (LP / hot side) | 0.046 | 0.924 | 0.01315 | 0.1863 (hyd) | 4.563 |
| BR1 Recup to Tee | 0.01423 | 2.7 | 0.27 | 13.46 | 0.08 |
| BR1 Tee (Alt cool return) | 0.01423 | 0.15 | 0.27 | 13.46 | 0 |
| BR1 Tee to Cooler | 0.01423 | 0.42 | 0.27 | 13.46 | 0 |
| COOLER | 0.015 | 2.32 | 0.1058 | 0.752 (hyd) | 0.20 |
| BR1 Cooler to Alt Tee | 0.01423 | 0.3 | 0.27 | 13.46 | 0 |
| BR1 Tee (Alt cool supply) | 0.01423 | 0.3 | 0.27 | 13.46 | 0 |
| BR1 Isolation Valve | 0.01327 | 0.1 | n/a | 13.0 | 0 |
| BR1 Check Valve | 0.01327 | 0.1 | n/a | 13.0 | 0 |
| BR1 Ck Valve to Comp | 0.01423 | 0.3 | 0.27 | 13.46 | 0 |
| COMP component | 0.01423 | 0.5 | n/a | 13.46 | 0 |
| BR1 Comp to Recup | 0.01406 | 0.6 | 0.31 | 13.38 | 0.30 |
| RECUP (HP / cold side) | 0.046 | 0.924 | 0.01315 | 0.1863 (hyd) | 7.96 |
| BR1 Recup to CL | 0.01824 | 2.5 | 0.38 | 15.24 | 0.10 |
| Common Cold Leg (CL) | 0.01824 | 5.0 | 0.38 | 15.24 | 0 |
| | | | | | |
| Alternator cooling (Tot) | 0.001257 | 6.5 | 0.3 | 4 | 0 |
| * Hot Leg Pipe = 16 cm OD: 0.37 cm outer wall, 1.28 cm insulation, plus 0.1 cm liner | | | | | |

All TRACE pipes include multiple fluid nodes and heat structures representing the pipe wall. Four radial nodes were used with thermal properties set as Alloy 600 (similar to A617 and other nickel superalloys). Currently the standard TRACE code heat transfer and fluid pressure drop correlations are applied to the piping. TRACE code options are available to modify the Dittus-Boelter heat transfer correlation exponents or use a completely different relationship. Currently the default TRACE single phase pressure drop correlation is applied with 2E-6 m surface roughness. In the current model the outside surface condition is set for adiabatic conditions. Some specialized future models may have included distributed heat losses to space.

## 12.4.2 TRACE Transient Results

In order to start a TRACE transient calculation the code is first run to reach a near steady state condition. A significant effort was made to individually model each individual component (reactor, recuperator, gas cooler, turbine, compressor and radiator). Each of these "sub-models" was built and checked against the concept selection heat balance, HB24 and models built using other codes (such as Mathcad). For example, detailed Mathcad models of the recuperator and gas cooler were used to help determine TRACE code model inputs and verify steady state operating performance. This methodology was important to build the best TRACE components that could later be connected to interact in a full plant model. A comparison between the TRACE steady state conditions and HB24 is provided in Section 12.3.1. This comparison includes some component inlet and outlet conditions but does not highlight many of the differences between the heat balance and TRACE steady state results. These differences are due to thermal-hydraulic modeling differences.

The TRACE full plant model captures system thermal-hydraulic behavior that is not included in the heat balance spreadsheet programs. For example, the heat balance spreadsheets do not solve the momentum and energy equations to define the local working gas temperature and pressure. The HB24 model in Figure 12-3 shows the gas temperature leaving the reactor (1150 K) is the *same* as that entering the turbine. In reality, and as modeled in TRACE, the gas temperature will be a function of the local pressure and velocity. Flow area changes that produce velocity changes, sometimes referred to as a recoverable $\Delta P$, as well as frictional or non-recoverable $\Delta P$ both produce coolant temperature changes. Section 12.4.1.1 provides additional discussion on these temperature changes. Therefore, the TRACE results and heat balance spreadsheet calculations will never exactly match.

Detailed TRACE steady state conditions are provided in Figure 12-13 and Figure 12-14. The first figure provides a SNAP animation view of the primary plant. The second figure provides detailed results for the TRACE model HRS. Each animation view can be interactively viewed while running the TRACE program. Comparing the steady state TRACE results with HB24 (Figure 12-3) illustrates some model and program differences. Both results are based on a He mole fraction of 0.784 (the remainder is Xe), resulting in a working fluid molecular weight of 31.5 g/g-mole. In order to converge at the desired operating temperature, TRACE is run with an average temperature controller that moves core reactivity until the desired average reactor temperature is achieved. This controller helps move the TRACE steady state to the HB24 average reactor temperature of 1024 K. To find the near steady state condition, the TRACE model is then allowed to run unperturbed for a long time interval.

The TRACE $T_{ave}$ was defined as the average between reactor inlet and outlet plenum temperatures. Once the TRACE model has been defined, the only constraints applied to the steady state run were the $T_{ave}$ (1024 ±1.5K), Brayton speed (4712.4 rad/s), and radiation heat transfer heat sink temperature (200 K). TRACE reactor power is allowed to float to a new state point. The TRACE fuel temperature rise is about 273K (1162 K – 889 K) at a reactor power level of almost 900 $kW_t$.

The TRACE model used in this study was a scoping tool that would have undergone many revisions and upgrades as the SNPP design progressed and as test data became available. Future TRACE model upgrades may have included new component models (new gas cooler, explicit heat pipe components, etc.), and additional energy management detail. However, current model fidelity should provide useful transient results. The TRACE transient evaluations can be used to determine operating strategy and equipment setpoints as well as identify and recommend potential plant design changes. The initial transients were intended to verify multiple Brayton plant stability during normal and abnormal operating conditions. The transients are discussed below. Seven different transients

were analyzed. Transients based on normal and casualty conditions were chosen to evaluate the response of the reactor and define the design space within which the reactor and the remainder of the plant would need to perform. For some transients, numerous operating and/or protection strategies were modeled. Each of those transients is discussed in the following sections.

### 12.4.2.1 Mechanical Loss of One Brayton (TRACE)

The TRACE power plant model (Section 12.4.1) includes two parallel identical Brayton loops. In this transient the first loop Brayton (B1) is assumed to fail (sudden stop) at time zero. The loss of Brayton is initiated using a TRACE code restart from the steady state condition defined in Table 12-3, Figure 12-13, and Figure 12-14. The loss of Brayton transient is initiated in TRACE by resetting the turbine and compressor head and torque to zero. This action effectively stops Brayton loop flow within one second. Other models have used a more gradual Brayton flow coastdown for this transient. A variety of events could cause a Brayton to shutdown or be isolated. These events may be control actions (e.g., valve closure) or mechanical failures in the turbine, compressor, or alternator. While some failures could result in a gradual coastdown, others could rapidly stop flow. The TRACE transient models the most rapid loss of flow.

When B1 flow stops, a check valve installed upstream of the compressor prevents gross back flow. A small leakage path in the check valve is modeled resulting in an idle loop reverse flow of about 0.007 kg/s. With the check valve feature, the reactor flow will initially decrease by about 50%. At 100% power and only 50% reactor flow, the fuel and core block (core structural) temperatures quickly increase (Figure 12-15). The TRACE model equally distributes temperature based reactivity feedback between the fuel and core block. The core block average temperature is used as a measure for the geometric reactivity coefficient. As the core block, reactor vessel, and slider (reflector) relative positions change with temperature, the core reactivity will change. The core structural temperature follows resulting in changes in the coolant temperature. This reactivity feedback will lag the more rapid fuel temperature feedback. Figure 12-16 illustrates the reactivity contribution and timing of the fuel and core block.

Future TRACE upgrades may have included a contribution of reactor vessel and reflector temperatures as well as redefining the reactivity split between fuel and geometry. Depending on the relative contributions between coolant temperature and direct power (gamma) heating of core structural materials, the TRACE model could be modified to include both effects. For the current TRACE model the contribution of gamma heating to changes in core block temperature was considered to be small.

The negative reactivity added by the fuel and geometry feedback mechanisms reduces the reactor power level (Figure 12-17). The reactor power level eventually approaches about 50% power. Figure 12-18 shows the predicted increase in fuel hot spot temperature during the loss of Brayton transient. Other plant operating changes are less obvious. For example, overall system pressure decreases when Brayton 1 is lost (Figure 12-19). This pressure reduction produces a reduction in the *operating* Brayton flow rate (Figure 12-20). The magnitude of Brayton 2 flow reduction is a function of the TRACE turbine and compressor maps selected (as discussed in Section 12.4.1.3). The reference CCEP performance maps show the largest change in Brayton 2 flow. This occurs because even though the TRACE component curves and CCEP maps are well matched at the heat balance operating point, they do not calculate the same off-design performance. Figure 12-20 illustrates this effect and the need for accurate Brayton performance maps and models. It is likely that both CCEP and TRACE performance curves would be replaced by future Brayton prototypic Brayton testing.

The reactor pressure drop is shown in Figure 12-21. Note that as flow decreases by about half, the pressure drop decreases to about one-fourth. The reactor flow path is shared by both Brayton loops. When B1 flow is lost, a small compensating effect occurs due to additional reactor flow area available for the remaining operating loop. The result is an effective decrease in reactor resistance.

Figure 12-22 shows the remaining operating Brayton component power levels. Compressor and turbine torque (and therefore power) initially drop, consistent with the predicted flow reduction. However, as the turbine inlet temperature increases, the turbine power increases. After the initial system pressure decrease, the constant speed and steady compressor inlet temperature produce a constant (lower) compressor power. At the new steady Brayton 2 conditions, the compressor power drops more than the turbine power. At the new Brayton torque (power) balance, the alternator load is increased by the speed control system to maintain constant shaft speed. The alternator power must increase from about 110 $kW_t$ to more than 125 $kW_t$. The increased Brayton 2 alternator load is assumed to be distributed by the PCAD system.

The plant temperatures throughout the primary loop are shown in Figure 12-23 through Figure 12-25. Reactor coolant exit temperature increases as flow decreases faster than power. Figure 12-26 shows the gas cooler water side (radiator) temperatures during the loss of Brayton transient. Other than operation of the Brayton speed controller, no control actions have been assumed during the transient. Therefore, the failed Brayton heat rejection loop water pump continues to run and cools the system to an isothermal temperature of about 315 K. At this temperature the radiator heat pipes are assumed to shutdown, limiting additional (rapid) cooling. If this HRS cool down is undesirable, the TRACE model could include HRS pump control to slow heat loss.

Finally, Figure 12-27 provides a sensitivity study showing the effect on power of moving all the negative reactivity feedback into the fuel temperature reactivity coefficient. Because the fuel temperature responds faster than the structural temperature, there is less power undershoot, and power more rapidly approaches 50% power.

The TRACE and RELAP5-3D transient results are generally very similar. One difference between the two transients is the initiating event. In RELAP, the loss of Brayton is gradual with a 20 second coastdown. The TRACE loss of Brayton is modeled as a step change at time zero. Reactor power behavior is very similar, both decreasing to about 40% and then recovering to near 50%. Because the TRACE transient is more rapid, the minimum power is reached in about 150 seconds while the RELAP minimum power is closer to 200 seconds. Other differences include the geometric reactivity feedback model, the HRS model (NaK vs. water), and the reactor core model ($UO_2$ vs. UN fuel). Consistent with a more rapid transient, the TRACE results show primary temperature ($T_{hot}$) increase somewhat larger (about 25 K) than in RELAP. The RELAP peak fuel temperature reduction (-190 K) is about twice as large as in TRACE (-75 K). A consistent difference (for all transients) is that the change in RELAP peak fuel temperature is larger than the corresponding TRACE value. The main reason for this difference is fuel pin materials and core design. At steady full power operation, the temperature drop between the coolant and peak fuel temperature is significantly larger for the $UO_2$ fuel core modeled in RELAP than the UN fuel TRACE core. Therefore, for a given change in power, the change in $UO_2$ peak temperature will be larger than for the UN fuel system.

Another small difference between the codes is the prediction of remaining Brayton flow rate. Using the CCEP performance maps, the TRACE model predicts Brayton 2 flow decreases with decreasing compressor inlet pressure (by about 15%) from about 2.5 to 2.2 kg/s. The predicted flow reduction is consistent with SIMULINK results. No similar flow reduction is shown in the RELAP5-3D results (or with the TRACE performance curve option selected). Later in the transient, differences between the TRACE and RELAP HRS system models can be seen. Since the TRACE transient uses a faster

Brayton coastdown, the gas cooler water exit temperature reaches the inlet temperature sooner than the RELAP NaK gas cooler. Once the TRACE water temperatures are equal it takes about one water loop transport time (roughly 2 minutes) for colder radiator return water to reach the gas cooler. In then takes an additional 400 seconds to reach the heat pipe shutdown temperature (about 315 K).

### 12.4.2.2 Complete Loss of Electrical Load for One Brayton (TRACE)

As stated in Section 12.4.1.3, the turbine, alternator, and compressor are all connected to one shaft and operate at identical shaft speeds. The shaft speed is determined by a balance of the torques on the shaft imposed by the components plus any parasitic losses, as given by Equation 12-1.

For a given Brayton and plant design, the shaft speed simply becomes a function of the working fluid density (temperature and pressure) and alternator torque. Alternator torque is a function of the electrical load on the alternator. In the TRACE model, a speed controller is used to match the actual Brayton speed with a desired (or programmed speed). The controller does this by adjusting the alternator load to balance the shaft torques at the desired speed. If shaft speed is high, the alternator load (torque) is increased to reduce speed. The available alternator loads are the spaceship hotel loads, the propulsion loads, the science loads, and the PLR. The PLR is sized to provide a full power electrical load (plus a design margin) even when other loads (like propulsion) are not available. The PLR is used to regulate the alternator torque to maintain constant speed. Some features of the TRACE speed control model include a representation of the maximum available PLR load (torque), and the major cable connections between the alternator and PLR. These speed control model features are important in the partial loss of load transient described in Section 12.4.2.3.

A loss of load transient occurs if there is a malfunction in the speed control system or related components. The most severe transient is a complete loss of load where the alternator torque decreases to zero. This casualty would likely be caused by an alternator failure, multiple PLR component failures, PCAD software failure, or micrometeoroid impact to the electrical cables between the alternator and PCAD. This severe casualty may be less credible than partial loss of load and may be caused by equipment failures that are not recoverable.

Complete loss of load results are illustrated in Figure 12-28 through Figure 12-42. The loss of load, initiated at time zero, is shown in Figure 12-28. Brayton 1 alternator power drops from about 110 $kW_t$ to 0 in less than one second. Since the alternator is used to control Brayton speed, complete loss of load results in a rapid increase in Brayton 1 shaft speed. Brayton 1 speed (Figure 12-29) increases until the turbine, compressor and parasitic mechanical loads reach a new equilibrium. Increasing shaft speed coincides with increasing Brayton 1 turbine and compressor power (Figure 12-28). The shaft stabilizes at a new speed where the magnitude of the compressor torque approaches that of the turbine torque. At higher shaft speeds, both the turbine and compressor efficiencies decrease. That tends to reduce the difference in the turbine and compressor torques as can be seen from Equation 12-1. In addition, while the temperature and pressure entering the turbine are fairly constant, the temperature entering the compressor increases (Figure 12-38) and the pressure decreases significantly as shaft speed increases because the turbine reduces pressure more and the recuperator removes less energy from the gas that flows toward the compressor. That causes the compressor density to decrease which also causes the difference between compressor and turbine torque to decrease.

As the compressor speed increases, the reactor coolant flow rate increases (Figure 12-30). The coolant flow rate is determined by TRACE using built in performance curves. These curves are used instead of the CCEP performance maps because the calculated speed increase moves off the CCEP

performance maps. Initially the reactor coolant flow rate increases by about 7%. This flow rate change is small compared with the increase in shaft speed (about 40%). The higher shaft speed is offset by decreasing compressor density. Figure 12-30 shows a number of different Brayton 1 flow curves. Three of these curves define the changes in Brayton 1 mass flow based on what actions are taken to reduce HRS temperature and pressure. These actions include maintaining HRS pump speed constant, increasing speed by 50% (1.5x) or doubling pump speed (2x). These actions are discussed further with the HRS results in Section 12.4.2.7. Two Figure 12-30 curves (in green) show the impact of performance map selection on Brayton 2 flow. Compared with using the TRACE curves, the CCEP maps result in a larger increase in Brayton 2 loop flow (2.6 vs. 2.5 kg/s). The two blue curves show that this difference in Brayton 2 flow does not significantly change the Brayton 1 flow.

The increased shaft speed causes the turbine to remove more energy from the gas coolant and the compressor to add more energy to the coolant. As a result, the compressor exit temperature increases (Figure 12-33). The resulting difference between the two recuperator inlet temperatures (turbine exit and compressor exit) is reduced by about half, as seen in Figure 12-33. That temperature difference is directly proportional to the heat transfer rate in the recuperator. Thus the recuperator transfers about half as much energy from the hot stream to the cooler stream. The reactor inlet temperature is lower as a result (Figure 12-31 and Figure 12-34), causing core reactivity (Figure 12-35) and reactor power to increase (Figure 12-36). The change in fuel peak temperature is shown in Figure 12-37. As stated above, this transient produces a modest increase in reactor flow rate. This would normally lead to an increase in reactor pressure drop. However, with the decrease in cold leg temperature shown in Figure 12-31, the net result is a reduction in reactor pressure drop as shown in Figure 12-32.

Figure 12-36 and Figure 12-37 show reactor power and core hot spot temperature. Depending on what actions are taken with HRS flow, the power peaks at between 111% and 116%. Hot spot temperature increases between 20 and 30 K.

Figure 12-39 shows the HRS water temperatures for the affected loop. The figure illustrates that the heat input into the HRS is increasing with increasing power and gas cooler gas inlet temperature. The increased heat load causes increasing HRS hot leg temperature. If no control actions are taken, bulk boiling in the gas cooler occurs in about 1 minute. This boiling produces a rapid pressure increase (Figure 12-40) that could exceed system design pressure. A protective action in the HRS system, such as a relief valve lift or rupture disk blow-off may be required to prevent structural failure of the gas cooler. The gas cooler must be protected so that the primary gas inventory is not lost. The exact pressure reached in this transient is somewhat uncertain. The TRACE code is executed using a zero gravity option. The accuracy of the boiling heat transfer correlations in TRACE for zero gravity is unknown at this time. Regardless, it is likely that large scale bulk boiling in the gas cooler would lead to loss of adequate heat transfer and system overpressurization.

Figure 12-39 also shows HRS water temperatures for two potential automatic control actions. The actions increase the HRS pump speed (or turn on an additional pump) to increase HRS flow. The first action is a 1.5 times pump speed increase 20 seconds after complete loss of load. The second action is a 2 times pump increase 30 seconds after the loss of load. These flow increases require a significant increase in pumping power (between 3 and 8 times). Figure 12-40 illustrates that both these control actions are effective in reducing the HRS loop water pressure. Therefore, to minimize the size and maximum power of the HRS pump the goal of an HRS control system should be to initiate speed change as soon as practical after the initiating transient. Of course, these actions may be irrelevant if an alternator load cannot be re-established for Brayton 1. Ultimately, if the load cannot be re-established it may be necessary to shut down Brayton 1 using a flow control valve. An analysis of this valve closure, including the indication used for valve closure and valve closing timing should be

performed to complete this transient analysis. The goal of this analysis would be to demonstrate HRS protection to prevent permanent system damage, preventing a loss of coolant and allowing an affected Brayton loop to be restarted.

The coolant flow rate discussion above noted that the Brayton 1 speed increase resulted in moving outside the CCEP performance maps. In general the same performance map or curve option is selected for both Braytons in the TRACE model. However, CCEP maps were applied to the Brayton 2 turbine and compressor. The impact of this change on the overall transient results is very small. The impact on Brayton 2 and Brayton 1 loop flows shown in Figure 12-30 was previously discussed. The difference can also be seen in the change in reactor exit temperature (Figure 12-41) and loop pressures (Figure 12-42).

Overall, the TRACE and RELAP5-3D results for the complete loss of alternator load transient are similar. RELAP results are presented in Section 12.5.2.2. Both transients produce a peak power increase of 110 to 117% as illustrated in Figure 12-36 and Figure 12-138. As expected, the change in peak fuel temperature for the RELAP $UO_2$ core is about twice that for the TRACE UN core. Relatively small differences are also seen in the calculated Brayton overspeed and resulting loop flow rates. The RELAP model predicts a peak Brayton speed of about 62,500 rpm while the peak TRACE speed is between 63,000 and 64,500 rpm (depending on actions taken with the HRS). This difference is considered small because these speeds move off the available CCEP performance maps. Therefore, the specific results depend on how performance characteristics are extrapolated and how the maps are incorporated into RELAP or TRACE. The RELAP and TRACE HRS system models respond in a similar manner, with the slower response of the NaK system evident in that it takes almost 600 seconds for the gas cooler NaK inlet temperature to increase. The TRACE gas/water cooler water inlet temperature begins increasing before 100 seconds.

### 12.4.2.3 Partial Loss of Electrical Load for One Brayton (TRACE)

While a complete loss of load transient is conservative in that it produces the highest overspeed condition, it may not be the most likely or relevant loss of load event. Failure mechanisms that might lead to a complete loss of load are also unlikely to allow system recovery. For example, an alternator failure might lead to a complete loss of load but also may result in a loss of Brayton. It is anticipated that PLR and PCAD hardware will be single fault tolerant. That is, they will be designed to maintain alternator load for most single equipment failures. When the electrical system architecture was established for the spaceship, the effects of component and connection failures would be further defined. Some failures may produce a partial loss of load. It is currently uncertain if a partial loss of load is a more likely event. For example, if power was routed through multiple paths or multiple circuit breakers were employed within the electrical distribution system, it is possible that the total load, including PLR, could decrease. If the speed control system is not able to maintain the required full power load (torque), a partial loss of load transient would occur. Both complete and partial losses of load transients have been analyzed with similar TRACE models. The primary difference between the TRACE models is the Brayton performance map or curve option selected. For the partial loss of load transient, the increase in Brayton speed is small enough to stay on the CCEP performance maps. Therefore, the CCEP option has been used for both Braytons in the TRACE partial loss of load analysis. TRACE results are illustrated in Figure 12-43 through Figure 12-57. In many cases the results include both Brayton performance map or curve options. These results provide sensitivity information for overall plant response.

The TRACE partial loss of load transient is modeled as the loss of one of three power cables between the alternator and the PLR. This represents a notional casualty that in the final system design may result in a complete loss of load. The PCAD architecture may not allow operating the speed control

system with less than three cables. The Brayton speed control system in TRACE provides the flexibility of specifying the number of intact cables. This feature provides a convenient modeling method to represent any partial loss of load event. At full power with three cables intact, the alternator power is about 110 $kW_t$. With only two cables available the alternator load drops to 80 $kW_t$. This difference is illustrated in Figure 12-43 between the alternator loads of Braytons 1 and 2. The alternator load imbalance is imposed on the steady state starting conditions at the beginning of this transient (time zero). Note that this drop is less than one-third of the initial power level. The decrease is smaller because the PLR attempts to compensate for the reduced load (and subsequent overspeed condition) by increasing the load with the remaining connections. The Brayton 1 turbine and compressor power increases until a new torque balance is achieved with the lower alternator torque. The new torque balance occurs at a higher shaft speed as shown in Figure 12-44. Brayton 1 speed increases from 4712 to about 5800 rad/s (or 56,000 rpm). This overspeed is significantly less than the 61,000 rpm reached in the *complete* loss of load casualty.

The plant response shown for this transient is similar to an alternator load reduction if the Brayton is operated without a speed control system. That is, without a speed control system, the Brayton speed will increase when electrical load is decreased. This speed increase produces a number of cascading effects that change the plant heat balance resulting in an increase in reactor power. Since the load reduction results in an increase in reactor power, the system is referred to as non-load following. This characteristic is a major reason that a Brayton shaft speed control system is employed. The following transient description explains what happens in the overall plant as alternator load decreases and Brayton shaft speed increases. The effects are shown based on a load reduction in one loop only. If the transient was not due to a casualty, it is likely that a load reduction would be shared by both (all) operating Brayton loops.

Since the partial loss of load transient can be run with either the TRACE performance curves or CCEP Brayton performance maps, a sensitivity study was performed to illustrate the differences. Figure 12-44 shows Brayton 1 overspeed for both Brayton map options. The CCEP option produces a higher shaft speed. Figure 12-45 shows an increase in Brayton 1 and 2 flow rates. Flow rate changes are larger when using the CCEP performance maps. Applying the CCEP maps, the Brayton 1 speed increases by about 23% and the flow rate increases 5.7% (reactor flow increases 4.5%). If the TRACE curves are applied, the flow increases are only 1.6% for Brayton 1 speed increase of 16% (1.2% reactor flow increase). These differences point out the importance of using accurate turbine and compressor off-design performance maps. For this study the CCEP maps are assumed to represent the most accurate data available. Prototypic test data would be needed to define actual Brayton performance. Loop 1 mass flow rate increases less than the shaft speed because of a significant reduction in compressor fluid inlet density. Compressor 1 inlet temperature increases (Figure 12-53) and pressure decreases (Figure 12-57) resulting in reduced working fluid density. Compressor inlet density drops from 9.65 to 7.96 $kg/m^3$.

The modest increase in reactor flow rate described above will tend to reduce the temperature drop across the reactor but have little impact on average reactor temperature. The more important system changes are related to the new Brayton 1 operating speed. As with the complete loss of load description, the recuperator heat transfer is reduced as the turbine exit temperature decreases with turbine power (Figure 12-48) and the compressor outlet temperature increases with compressor inlet temperature. At the higher speed, the turbine pressure ratio increases from 1.8 to 2.1 resulting in a corresponding decrease in turbine outlet temperature. Turbine $\Delta T$ changes from 217 to 262 K. The new turbine exit conditions mean that the recuperator low pressure inlet temperature is lower. Simultaneously, the compressor pressure ratio increases from 2.0 to 2.4 with a corresponding temperature increase in $\Delta T$ from 148 to 214 K. The increased compressor exit temperature means

that the recuperator high pressure inlet temperature is higher. The pressure ratio and temperature data described here is based on continuing the transient for 5000 seconds when conditions are very close to steady state.

The impact of the changes in recuperator inlet temperatures described above is a significant reduction in the amount of heat transferred between the two gas streams and a reduction in overall plant efficiency. The new recuperator high pressure exit temperature (reactor inlet temperature) of 865 K is significantly lower than the initial temperature of 889 K. It is this reduction in reactor inlet temperature, combined with increased flow rate that produce a lower average coolant temperature. The lower average coolant temperature results in a core block temperature change from the initial 1072 K to a final 1059 K. This temperature deficit produces the reactivity surplus that increases reactor power from 100% to a final value of about 110% (5000 sec).

As Brayton and reactor flow rate increases, the coolant pressure drop across the reactor increases. However, the increased pressure drop is somewhat offset by reduced reactor inlet temperature (Figure 12-46) and the resulting increase in density. The resulting balance between flow rate and fluid density (shown in Figure 12-47) is somewhat different depending on which Brayton performance maps are selected.

As reactor coolant temperature decreases the core block and fuel temperatures follow (Figure 12-49). This temperature reduction produces a reactivity addition shown in Figure 12-50. Consequently, the reactor power increases as shown in Figure 12-51. The transient is relatively slow resulting in little power overshoot. Depending on the Brayton performance option selected, the peak fuel temperature shown in Figure 12-52 increases by about 15 K (TRACE curves) or 23 K (CCEP maps).

The new system operating point results in increased gas temperature at the gas cooler inlet. This higher gas temperature results in higher HRS fluid temperature and higher HRS system heat load. Because the reactor power increases during the transient, more heat must be transferred to the HRS. In addition, the Brayton 1 alternator is removing less power (from 109.4 to 80 $kW_t$) than at the start of the transient. The new steady state plant heat balance results in a 27% increase in HRS heat transfer. Figure 12-54 shows the resulting increase in heat rejection fluid (water) temperature. At the higher temperatures a significant water pressure increase is predicted (Figure 12-55). Depending on the final system design and the actual PLR capacity, it may be necessary to increase HRS pump speed to maintain an acceptable HRS operating pressure.

### 12.4.2.4 Positive Reactivity Addition (TRACE)

Figure 12-58 through Figure 12-73 show the transient response to selected parameters for this transient. It is assumed that the reactivity is increased in the reactor an amount equivalent to about 50 K increase in temperature. Since the total temperature coefficient of the reactor for this analysis is assumed to be $-1.36 \times 10^{-5}$ $\delta\rho$/K, the reactivity change required for a 50 K temperature increase is 6.8E-4 $\delta\rho$. The transient is produced by adding this reactivity over a 1-second period. The reactivity increase of 6.8E-4 $\delta\rho$ was selected to be the same as used in RELAP5-3D transients, facilitating model comparison. The selection of a reactivity increase equivalent to 50 K was somewhat arbitrary. As a comparison, moving all sliders by about 1-mm will produce about the same reactivity change. The specific reactivity change is a function of time in life, slider position and core design. For example, the equivalent slider sensitivity in a $UO_2$ core might be less than a UN design. The TRACE transient resulted in a 48 K temperature increase. Figure 12-62 shows the reactivity contribution. Positive reactivity addition causes the reactor power and therefore reactor exit temperature to

increase as illustrated in Figure 12-58 and Figure 12-59. As the fuel and core block temperatures increase, negative reactivity feedback causes a reduction in power and reactor exit temperature (Figure 12-68). However, reactor power does not return to the initial power because the turbine removes more energy (Figure 12-69) at the increased turbine inlet temperature.

This transient was run with both the TRACE Brayton performance curves and the CCEP Brayton performance maps. Using the CCEP Brayton performance map fit option produced the most severe transient and is shown in the attached figures. Using the CCEP map option, the reactor power and exit temperature increase is large enough to raise the turbine power from about 350 $kW_t$ to almost 480 $kW_t$ (Figure 12-69). The compressor power (opposite in sign) also increases, but by a smaller amount. The result is an increase in available alternator power. If the alternator cannot supply the corresponding load, the shaft speed will increase until the Brayton component torques (powers) re-balance. The shaft speed control system used in TRACE has notional representations of the maximum torque and load that the PLR can provide. At the increased turbine power the available alternator load (based on the TRACE PLR model input of 120 $kW_t$) is too small to maintain constant Brayton shaft speed. Figure 12-61 illustrates the overspeed condition (over 5400 rad/s) that results. Unlike previous transients, the initiating event has a balanced impact on both Brayton loops. The Braytons respond identically and it is only necessary to show plots for one loop. This transient illustrates the kind of analysis that might go into sizing the PLR and providing the necessary system control. However, other control schemes may be adopted to control this transient. One such control system based on average reactor coolant temperature is discussed below.

Results are also shown with and without an automatic reactor temperature control system. This notional control system might be used to keep the reactor coolant temperature at (near) a desired operating point. The TRACE $T_{ave}$ control model uses a 1024 K set point with a 1.5 K dead band. Temperature adjustment is accomplished with small reactivity changes based on either a single slider (1 of 12) movement or bank slider motion at $1/12^{th}$ normal speed. $T_{ave}$ control would provide a reactivity correction to account for changes in core reactivity with time in life, changes in HRS surface emissivity and other gradual changes in system performance. The results with and without active $T_{ave}$ control are provided below. All results shown use the CCEP Brayton performance maps.

Without $T_{ave}$ Control

A maximum reactor power of almost 140% (Figure 12-58) is reached at approximately 20 seconds. The maximum Brayton alternator power (load) is reached at about 70 seconds and results in a shaft speed increase seen in Figure 12-61. Primary flow rate increases in the Brayton loops (Figure 12-66) and the reactor. Higher reactor flow and increasing reactor inlet temperature results in an increased reactor pressure drop (Figure 12-67). Increased reactor power results in an increase in the temperature and pressure for the HRS (Figure 12-72 and Figure 12-73).

With $T_{ave}$ Control

The transient was run again with an active $T_{ave}$ controller. Many of the plots provided show system parameters with and without $T_{ave}$ control. The $T_{ave}$ controller begins to affect the system at 30 seconds when the average temperature is more than 1.5 K above the $T_{ave}$ set point of 1024 K. $T_{ave}$ control reactivity change is clearly shown as small step changes in shim reactivity in Figure 12-63. Peak reactor power (Figure 12-58) is unchanged with $T_{ave}$ control active. However, power turns sooner and the resulting change in peak fuel temperature (Figure 12-59 in less than without $T_{ave}$ control). The effect of $T_{ave}$ control on primary coolant temperature is clearly seen in Figure 12-68, where maximum reactor exit temperature is reduced. Reduced reactor exit temperature results in reduced turbine power (Figure 12-69) and eliminates the Brayton 1 overspeed (Figure 12-61).

Figure 12-74 shows the results of a time step size sensitivity study. With decreasing the time step size, the results remain very close and do not increase the fidelity of the findings. The smaller time steps do show a smoothing of the curves due to decreasing numerical instabilities.

Positive Reactivity Transient TRACE/RELAP5-3D Comparisons

Figure 12-58 is a graph of reactor power for TRACE. The TRACE peak power of about 140% is close to the RELAP5-3D model result of about 145%. The RELAP discussion of the positive reactivity transient is contained in Section 12.5.2.3. Figure 12-59 is a graph of hot spot fuel temperature. When compared to the RELAP model, the TRACE model experiences a much smaller change in temperature. This difference is consistent with the two core designs modeled: the UN fuel modeling in TRACE has a smaller fuel to coolant temperature difference than the $UO_2$ fuel modeled in RELAP.

Figure 12-61 is a graph of Brayton shaft speeds. The TRACE model without $T_{ave}$ control experiences a change in shaft speed as explained earlier. The RELAP model does not experience a change in shaft speed as illustrated in Figure 12-153. The RELAP shaft speed controller does not include a maximum alternator load capacity and therefore functions to maintain constant shaft speed, regardless of turbine power.

Figure 12-62 and Figure 12-151 are graphs of reactor reactivity for TRACE and RELAP respectively. Since the TRACE model and RELAP5-3D model are adding the same amount of reactivity, the results look similar. Figure 12-66 shows Brayton loop mass flow rate. When comparing the increase in loop mass flow rate between TRACE and RELAP models, the TRACE model (without $T_{ave}$ control) show a significantly larger increase in flow rate. This difference is only seen when TRACE is run with the CCEP map option.

Figure 12-70 is a graph of the Brayton component and recuperator temperatures. The TRACE model has a change in Brayton shaft speed which results in new operating conditions for each turbine and compressor. With and without $T_{ave}$ control, all loop temperatures are affected. The TRACE results with $T_{ave}$ control active (Figure 12-71) produce a constant Brayton speed and temperature results that more closely match the RELAP5-3D model temperatures shown in Figure 12-154 and Figure 12-155.

Figure 12-72 is a graph of the gas cooler water temperatures. The TRACE model without $T_{ave}$ control shows an increase in the water temperatures leaving the gas cooler ($T_{hot}$). This is a result of the increased gas temperature entering the gas cooler (leaving the high pressure side of the recuperator) in the primary HeXe gas loops. The increase in gas cooler temperature was sufficient enough to start boiling in the gas cooler, so this transient should be further monitored with gas cooler boiling under consideration. The RELAP5-3D model shows only a small increase in temperature for the NaK in the HRS as illustrated in Figure 12-156 and Figure 12-157.

### 12.4.2.5 Negative Reactivity Addition (TRACE)

Figure 12-75 through Figure 12-86 show the transient response of selected parameters for the negative reactivity addition transient. The transient is produced by reducing the core reactivity by 6.8E-4 $\delta\rho$ between time zero and one second. (This is the same reactivity change modeled in RELAP5-3D, facilitating the comparison of model results.) This resulted in a 48 K temperature decrease. Figure 12-79 shows the reactivity contribution. This transient causes the reactor power and temperature to decrease rapidly, as seen in Figure 12-75 and Figure 12-76. As the fuel and core

block temperatures decrease, positive reactivity feedback causes an increase in power and fuel temperature (Figure 12-77). However, reactor power does not return to the initial power because the turbine removes less energy (Figure 12-84) at the reduced turbine inlet temperature.

Like the positive reactivity addition case, this transient was run with both the TRACE Brayton performance curves and the CCEP Brayton performance maps. Using the CCEP Brayton performance map fit option produced the most severe transient and is shown in the attached figures. Results are also shown with and without an automatic reactor temperature control system. The results with and without active $T_{ave}$ control are provided below.

Without $T_{ave}$ Control

Without $T_{ave}$ control, the reactor coolant temperature decreases by about 50 K (Figure 12-83). Unlike in the positive reactivity addition transient, the Brayton speed remains constant. The available power from each alternator drops from about 109 to 85 $kW_t$. The PLR is sized such that it has a design margin to accommodate an under power situation. However, after this design margin is exceeded, the speed controller would no longer be able to maintain speed, and the speed (and frequency) would begin to drop. In a reduced frequency situation, one of the propulsion units could trip off and allow the speed (and frequency) to recover. If all the propulsion power units are dropped and the system is still underpowered, the system will experience "brown-outs" because there is not enough power supplied. This behavior is not modeled because it requires a higher level of fidelity before such a system could be implemented.

With $T_{ave}$ Control

The transient was also run with a $T_{ave}$ controller which begins to affect the system at 30 seconds. After about 30 seconds, the controller begins adding reactivity to increase average reactor coolant temperature back to the 1024 K set point. As seen in Figure 12-75 the reactor power reduction is minimized with the controller activated. In fact, after the $T_{ave}$ controller turns reactor power, enough positive reactivity has been added (both shim and fuel/block cool down) that an overpower excursion is produced (up to about 120% power). This corrective overshoot would be an important feature to tune in an actual $T_{ave}$ control device. As seen in Figure 12-75, the $T_{ave}$ control case returns to 100% power, consistent with the initial average temperature. Figure 12-76 shows that the $T_{ave}$ controller also limits the drop in peak fuel temperature. The multiple graphs showing the results with and without $T_{ave}$ control are not shown for negative reactivity because the results are equal in magnitude and opposite in direction from the graphs for positive reactivity addition.

Negative Reactivity Transient TRACE/RELAP5-3D Comparisons

Figure 12-75 is a graph of reactor power for TRACE. The RELAP5-3D discussion of the negative reactivity transient is contained in Section 12.5.2.4. When compared to the RELAP model, both produce similar results with the TRACE model predicting a 5% smaller power excursion. Figure 12-76 is a graph of hot spot fuel temperature. When compared to the RELAP model (see Figure 12-159), the TRACE model experiences a much smaller change in temperature (~60K). This difference is consistent with the core designs modeled where the UN fuel model in TRACE has a smaller fuel to coolant temperature difference than the $UO_2$ fuel modeled in RELAP.

Figure 12-78 and Figure 12-163 are graphs of Brayton shaft speeds for TRACE and RELAP5-3D respectively. The TRACE and RELAP models predict constant shaft speed for negative reactivity addition. Figure 12-79 is a graph of the reactivity. Since the TRACE and RELAP models are adding the same amount of negative reactivity, the results look similar. Note that the TRACE plot uses

reactivity units in $\delta\rho$ while the RELAP plot uses $. (A reactivity change of 6.8e-4 $\delta\rho$ is equivalent to a change of about $0.106.) Figure 12-81 is a graph of mass flow rate. For TRACE, the mass flow rates in both loops are identical so only loop 2 is shown. Both TRACE and RELAP models predict a small reduction in mass flow rate. The reduction is caused by a slight drop in compressor inlet density (constant temperature and reduced pressure). Figure 12-83 is a graph for the reactor inlet, outlet, and average temperatures. The TRACE and RELAP models show similar results.

Figure 12-84 is a graph of Brayton component power. For TRACE, the Brayton component powers in both loops are identical so only loop 2 is shown. The TRACE model shows a decrease in power from the alternator (~80% of full power operating point). Figure 12-85 is a graph of loop Brayton and recuperator temperatures. For TRACE, the Brayton loop temperatures in both loops are identical so only loop 2 is shown. The results from TRACE and RELAP5-3D loop temperatures appear to be almost identical. Figure 12-86 is a graph of the gas cooler water temperature. Consistent with reduced power, the TRACE gas cooler water exit temperature slowly decreases during the transient. The RELAP model shows similar results.

### 12.4.2.6 Complete Loss of Primary Flow (TRACE)

Analysis of the complete loss of primary flow was performed to provide a rough estimate of the time available to re-establish flow and/or take protective action(s). The ability to either start or restart a Brayton, and time available to re-establish flow will also be a function of backup power reserves. Available backup power will depend on the plant configuration (spaceship vs. surface installation), mission, and time in life. This TRACE analysis is not an exhaustive protection analysis; rather, it is a scoping study to provide a first look at complete loss of flow.

The transient is initiated at time zero from the full power steady state conditions shown in Figure 12-13 and Figure 12-14. Unlike the TRACE loss of Brayton transient, a flow coast down is used instead of an initial zero speed condition. Complete loss of flow results are provided in Figure 12-87 through Figure 12-96, where Figure 12-91 shows the Brayton coast down (in 20 seconds). This Brayton coast down results in the loop flow rates shown in Figure 12-92. The time scale in Figure 12-92 is expanded to show only the first 25 seconds of the transient. Since the plotting resolution is one second, the expanded figure does not appear as a smooth curve. Figure 12-92 also illustrates a small numerical instability that occurs with the turbine calculation as the pressure ratio approaches 1.0 near 2000 rad/s (12 seconds into transient).

The loss of flow and therefore loss of core cooling results in rapid fuel temperature heatup (Figure 12-89). During the coast down phase, there is an initial increase in core structural temperature. However, once the flow reaches zero there is limited heat transfer into the core structural material. In-core radiation heat transfer and structural gamma heating are not modeled in this transient. In Figure 12-89 two curves are shown for the fuel temperature. The very rapid temperature increase curve corresponds to no protective action (no scram or shim other than a normal operating condition with a $T_{ave}$ controller). The $T_{ave}$ controller removes only one slider and inserts only a small amount of negative reactivity (Figure 12-90). On the other hand, Figure 12-89 also shows the effect of a protective bank slider high speed shim. The protective action is initiated at 11.5 seconds. The action is delayed 1.5 seconds after dropping below half normal operating Brayton speed. The 1.5 seconds is based on assumptions concerning I&C system and CDM delay times.

As the fuel heats up the resulting negative reactivity reduces power. As shown in Figure 12-87, the power decrease with no protective action significantly lags the flow decrease. This results in the

rapidly increasing peak temperatures shown in Figure 12-88. The peak temperature increases about 300 K in the first 100 seconds. With a protective action, a much more rapid power reduction (Figure 12-87) and gradual peak temperature increase (Figure 12-88) is predicted.

Other system parameters are shown in Figure 12-93 through Figure 12-96. The primary pressure (Figure 12-93), primary temperature (Figure 12-95), and Brayton power (Figure 12-96) graphs are expanded with a shorter time scale. The primary temperatures plotted represent the TRACE results in the common hot and cold leg piping (outside the reactor vessel). As in the actual plant, loop temperature is not a reliable indication once primary flow stops. For primary temperature plots, the information past 20 to 30 seconds may not be a reliable indication of nearby temperatures. The TRACE flow and heat transfer models are not qualified in a zero gravity environment with no forced flow. Once primary flow reaches zero the gas coolant temperature information will be highly dependent on the exact location in the plant. Without forced flow or gravity based natural convection, there will be large gas temperature gradients. The HRS water temperatures shown in Figure 12-94 are consistent with continued HRS pump operation. No action was taken to stop the HRS pump(s).

### 12.4.2.7 Complete Loss of Flow in One HRS Loop (TRACE)

These transient results are significantly different from those generated with the RELAP5-3D model (Section 12.5.2.5), due to the many differences in HRS models. The TRACE model utilizes pressurized water as the working fluid, while the RELAP model utilizes NaK. Water requires less pumping power than NaK; however, water has a larger film temperature drop. Descriptions of the TRACE and RELAP HRS models can be found in Sections 12.4.1.6 and 12.5.1.6.

The loss of flow in one of two HRS loops was initiated at time zero with the pump speed set to zero. Figure 12-97 through Figure 12-111 show the results of this transient with no corrective or protective action taken by the rest of the system. As shown in Figure 12-97, the flow in the HRS loop rapidly decreases to near zero in about 5 seconds. With the connected Brayton still rotating at the design speed of 4712.4 rad/s (45000 RPM) (Figure 12-98), the gas cooler is still transferring heat into the now idle water loop. This causes the temperature (Figure 12-99) and pressure (Figure 12-100) on the water side of the gas cooler to increase resulting in boiling, which commences 27 seconds after the HRS pump stopped, at pressure of about 8 MPa. From this point on, the pressure rapidly increases, surpassing the anticipated maximum pressure of 8.47 MPa (1.1 x steady state pressure), relief pressure of 9.32 MPa (1.1 x maximum pressure), and design pressure of 10.25 MPa (1.1 x relief pressure) for the HRS water loop taken from Reference 12-12. The relief pressure is the pressure that a burst disk in the HRS would rupture in order to prevent a structural failure or water to gas leak in the gas cooler which would compromise the connected Brayton loop. See Section 9.6 for additional discussion.

As gas cooler temperatures increase, there is a corresponding increase in compressor inlet temperature (Figure 12-101) and a slight decrease in the Brayton loop flow rate (Figure 12-102). Since this flow decrease is not sufficient to alleviate boiling in the gas cooler and increasing HRS pressure, corrective or protective action must be taken to prevent failure in the gas cooler and maintain primary gas loop integrity. To assess system response to potential actions, the complete loss of flow in the HRS was conducted with a corrective action initiated by three different indicators and two protective actions.

One corrective action would be to start a spare pump in the HRS loop that has lost flow. This is modeled with three different indicators to initiate the spare pump: pressure, temperature, and an electrical switch. The temperature sensor is tripped at the temperature that boiling first starts in the

gas cooler (569 K) with a 3 second delay until the pump is fully operational. The pressure sensor is tripped at a maximum pressure of 8.47 MPa (1.1 x nominal pressure) with a 3 second delay until the pump is fully operational. The third case utilizes an electrical switch activated 5 seconds after electrical indication of pump 1 shutdown. The two protective cases are instances where a spare pump is not available and the connected primary loop needs to be shut down. This is achieved in one case by adding a constant load to the alternator of 32 $Pa*m^3$ (maximum allowable alternator torque) and in the other case by closing an isolation valve in the Brayton loop. Both these actions are taken 2 seconds after the pressure in the HRS reaches 8.47 MPa. Figure 12-112 through Figure 12-120 show the comparative results for all of these actions.

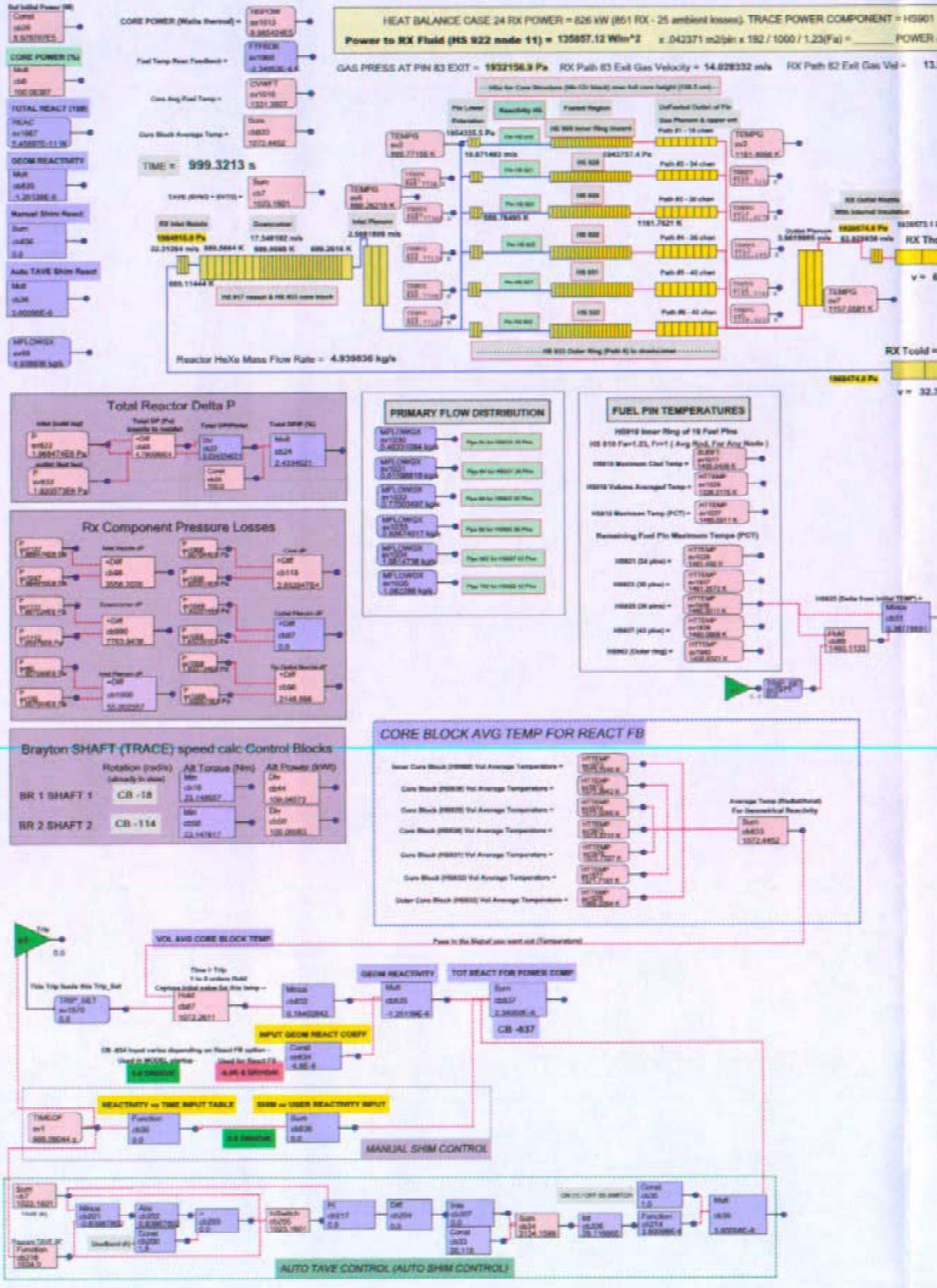
All three corrective actions that turn on a spare pump require approximately 600 seconds to return to steady state. They all have the same effect on the system, but are initiated at different times due to their triggering indicators. As seen in Figure 12-112, the corrective action that results in the earliest response is the electrical switch, followed by the temperature sensor, and finally the pressure sensor. Boiling does occur in the gas cooler for about 10 seconds with the temperature sensor and about 25 seconds with the pressure sensor (Figure 12-114) but not with the electrical switch case. All three return back to the same HRS pressure 100 seconds into the transient but continue to decrease to slightly different pressures before increasing to a slightly lower steady state pressure (Figure 12-112). All three maintain HRS pressure below the anticipated relief and design pressures. As seen from the results of these cases, turning the second pump on is an effective way of correcting this transient and results in little effect on the rest of the plant.

The two protective cases in which action is taken in the connected Brayton loop have much different results from the previously described corrective actions, since they behave more like loss of Brayton transients. As seen in Figure 12-113, closing an isolation valve occurs at the same time as the second pump being turned on with pressure indication. Closing the isolation valve, however, has a more gradual effect on reducing temperature and pressure in the HRS resulting in a longer period of boiling (Figure 12-114) in the gas cooler. The pressure exceeds the maximum pressure but does not reach the relief pressure. Although initiated at the same time as closing the isolation valve, the added torque load case does not stop flow in the Brayton loop fast enough to prevent pressure in the HRS from exceeding the anticipated relief pressure. Reaching this pressure would cause an unrecoverable failure in that HRS loop. Initial evaluations of these two protective actions suggest that closing an isolation valve in the Brayton loop may be required to protect the gas cooler and keep HRS loop from reaching a relief pressure. It is less likely that applying the maximum available alternator torque (load) will not stall the Brayton fast enough to protect the HRS loop from reaching the relief pressure.

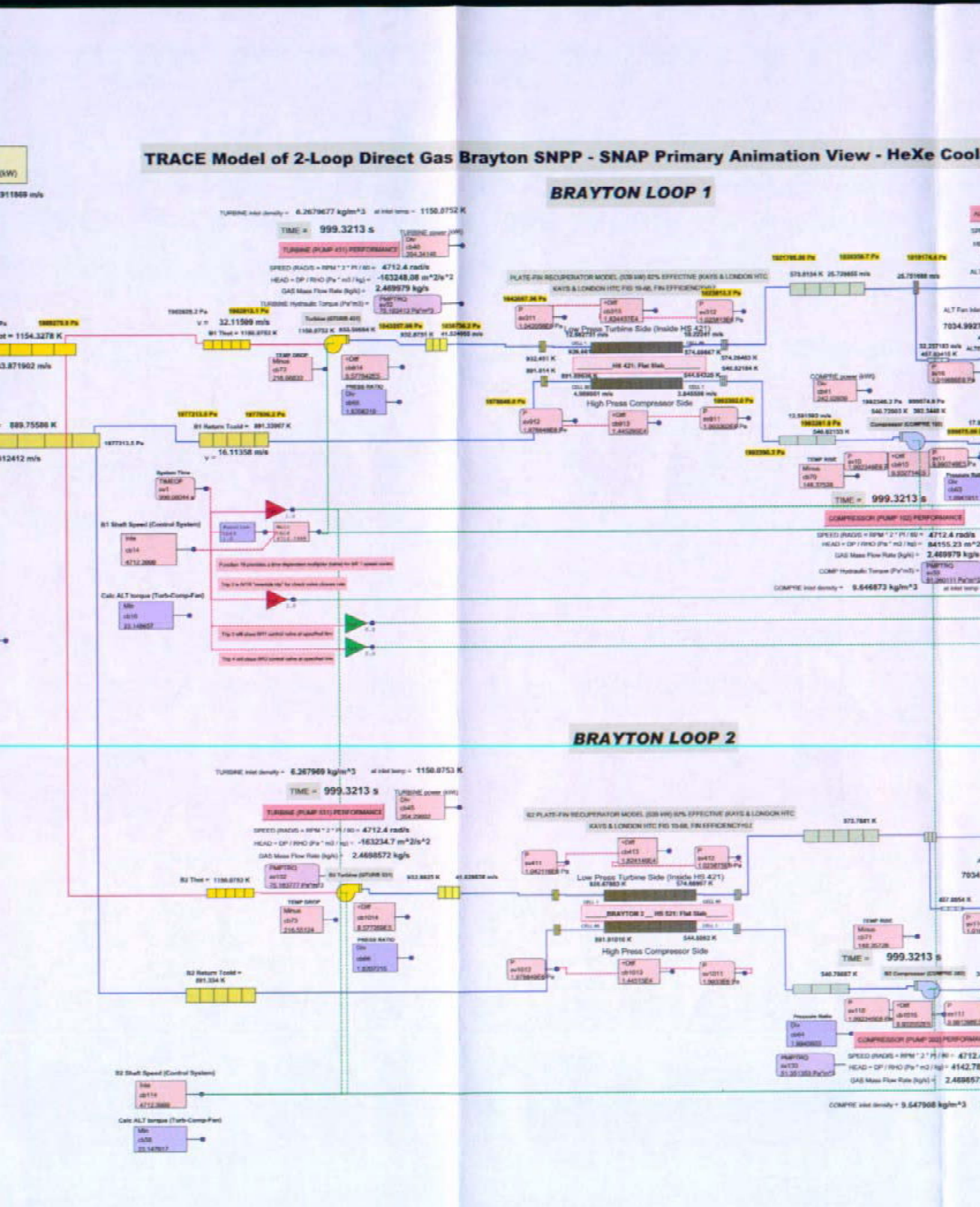
One design strategy to reduce the severity of a loss of HRS flow event is to operate two pumps in each loop. With two pumps normally operating, a single equipment failure would result in a partial loss of flow transient. A partial loss of HRS flow was evaluated in the TRACE model by reducing the operating speed of a single HRS pump. At time zero, the pump in the loop was set at half rotational speed (178 radians/s). The resulting flow rate is about half, delaying boiling in the gas cooler until 67 seconds after the partial loss of flow. HRS water coolant begins to boil in the partial loss of flow transient about 40 seconds after the complete loss of flow started boiling. As seen in Figure 12-121, the HRS loop 1 pressure eventually surpasses the relief and design pressures similar to the complete loss of HRS flow. It is apparent that the flow rate in the HRS needs to be appropriately controlled to prevent failure in the HRS loop. With a more detailed model of the HRS and a better certainty in the boiling calculations, it would be important to understand at what flow reduction boiling would occur in order to evaluate pump configurations and redundancy.

The results of all these transients are subject to uncertainties due to the boiling calculations being performed in the gas cooler. TRACE boiling correlations are qualified at gravity conditions on earth

while these calculations are being run at zero gravity. The behavior of boiling in the gas cooler in zero gravity conditions and its effects on heat transfer through the gas cooler need to be further understood and developed to best understand the results for this transient and its associated control actions.




*PRE-DECISIONAL - For planning and discussion purposes only*


TRACE Model of 2-Loop Direct Gas Brayton SNPP - SNAP Primary Animation View - HeXe Cool
BRAYTON LOOP 1
TIME = 999.3213 s
TURBINE (PUMP 451) PERFORMANCE
SPEED (RADS) = RPM * 2 * PI / 60 = 4712.4 rad/s
HEAD = DP / RHO (Pa * m3 / kg) = -163248.08 m^2/s^2
GAS Mass Flow Rate (kg/s) = 2.469979 kg/s
Low Press Turbine Side (Inside HS 421)
High Press Compressor Side
COMPRESSOR (PUMP 102) PERFORMANCE
SPEED (RADS) = RPM * 2 * PI / 60 = 4712.4 rad/s
HEAD = DP / RHO (Pa * m3 / kg) = 84155.23 m^2
GAS Mass Flow Rate (kg/s) = 2.469979 kg/s
COMPRESSOR inlet density = 9.646873 kg/m^3
B1 Shaft Speed (Control System)
Calc ALT torque (Turb-Comp-Fan)
BRAYTON LOOP 2
TIME = 999.3213 s
TURBINE (PUMP 551) PERFORMANCE
SPEED (RADS) = RPM * 2 * PI / 60 = 4712.4 rad/s
HEAD = DP / RHO (Pa * m3 / kg) = -163234.7 m^2/s^2
GAS Mass Flow Rate (kg/s) = 2.4698572 kg/s
Low Press Turbine Side (Inside HS 421)
High Press Compressor Side
TIME = 999.3213 s
B2 Shaft Speed (Control System)
Calc ALT torque (Turb-Comp-Fan)
COMPRESSOR inlet density = 9.647908 kg/m^3

ant (78.4% Helium Mole Fraction)

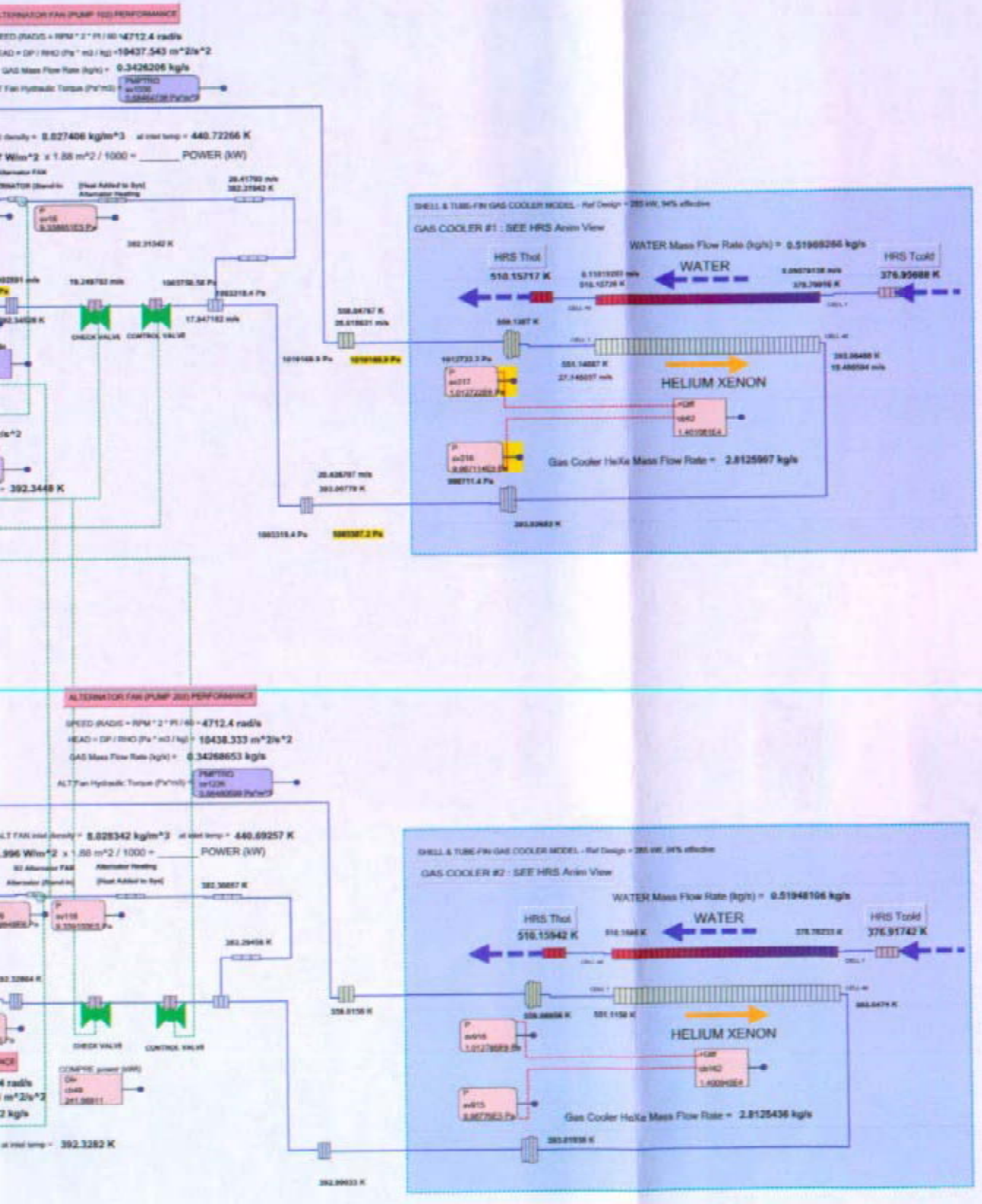
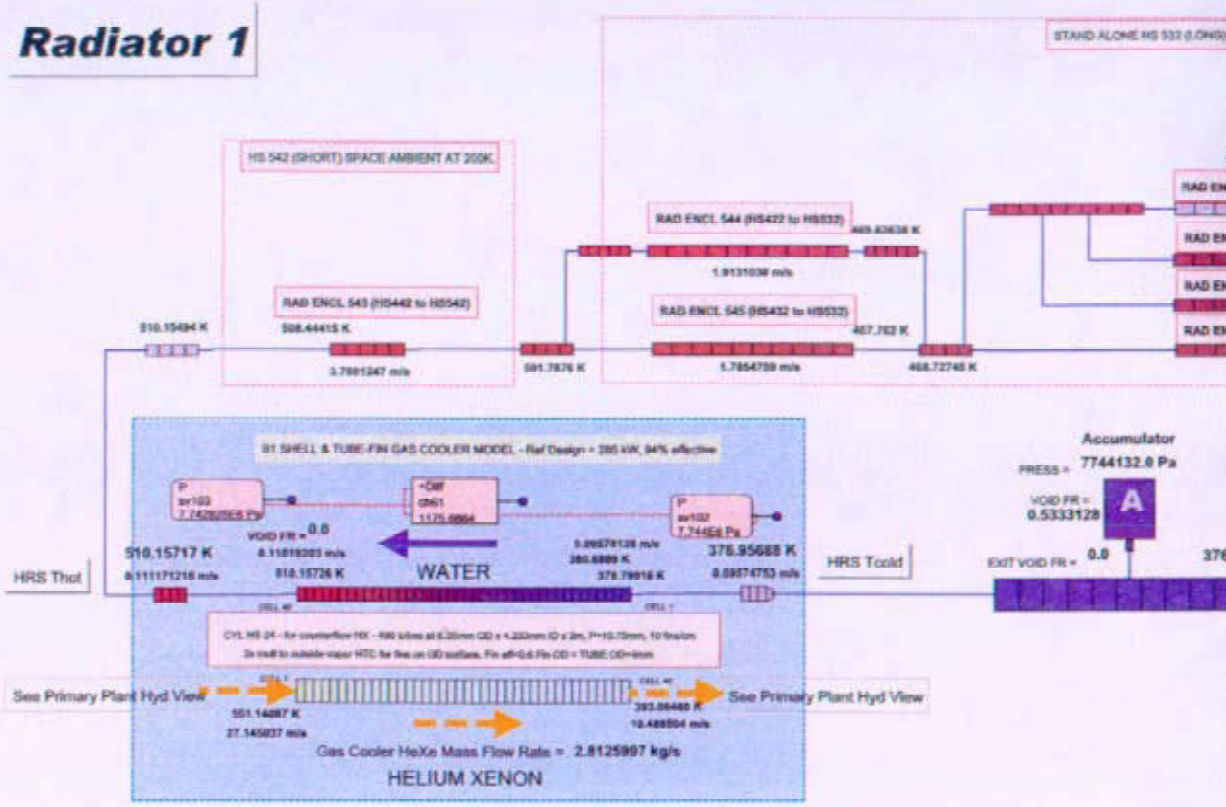


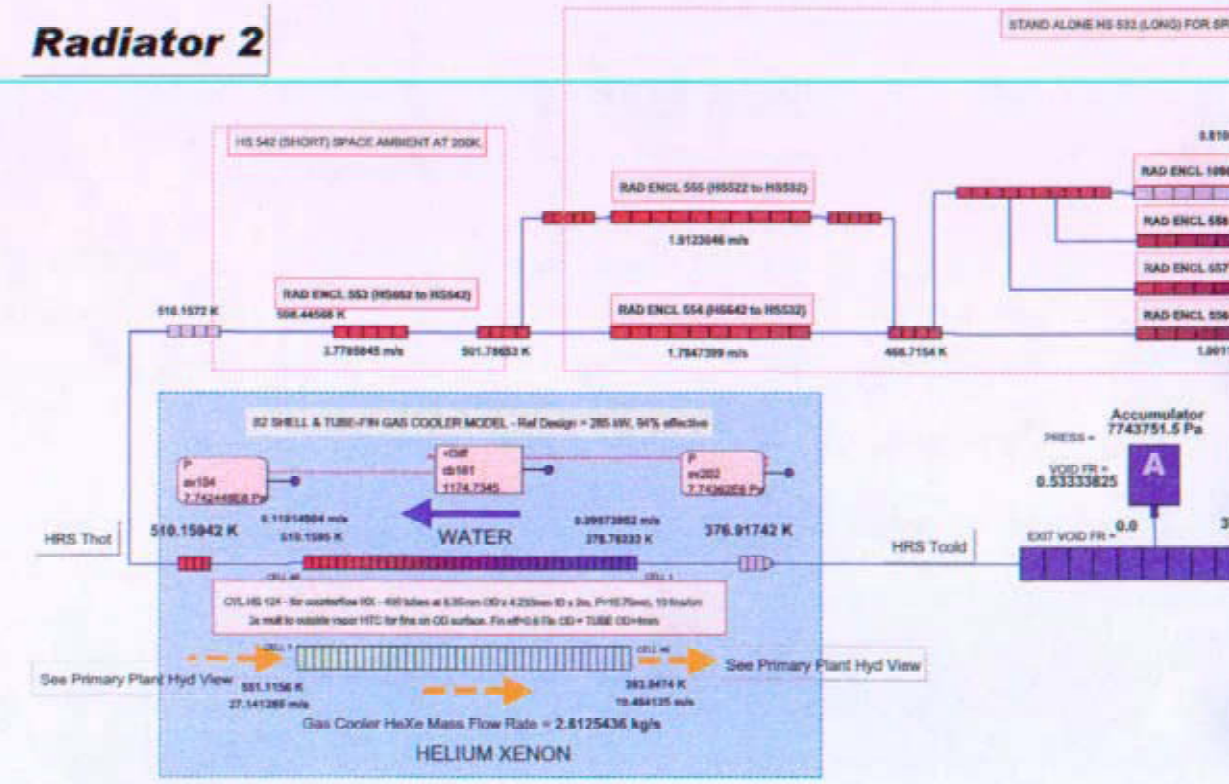

Figure 12- 13: TRACE/SNAP Animation View of Primary Plant Steady State Full Power Conditions

# TRACE Model of 2-Loop Direct Gas Brayton SNPP - SNAP

## Radiator 1




## Radiator 2




*PRE-DECISIONAL - For planning and discussion purposes only*

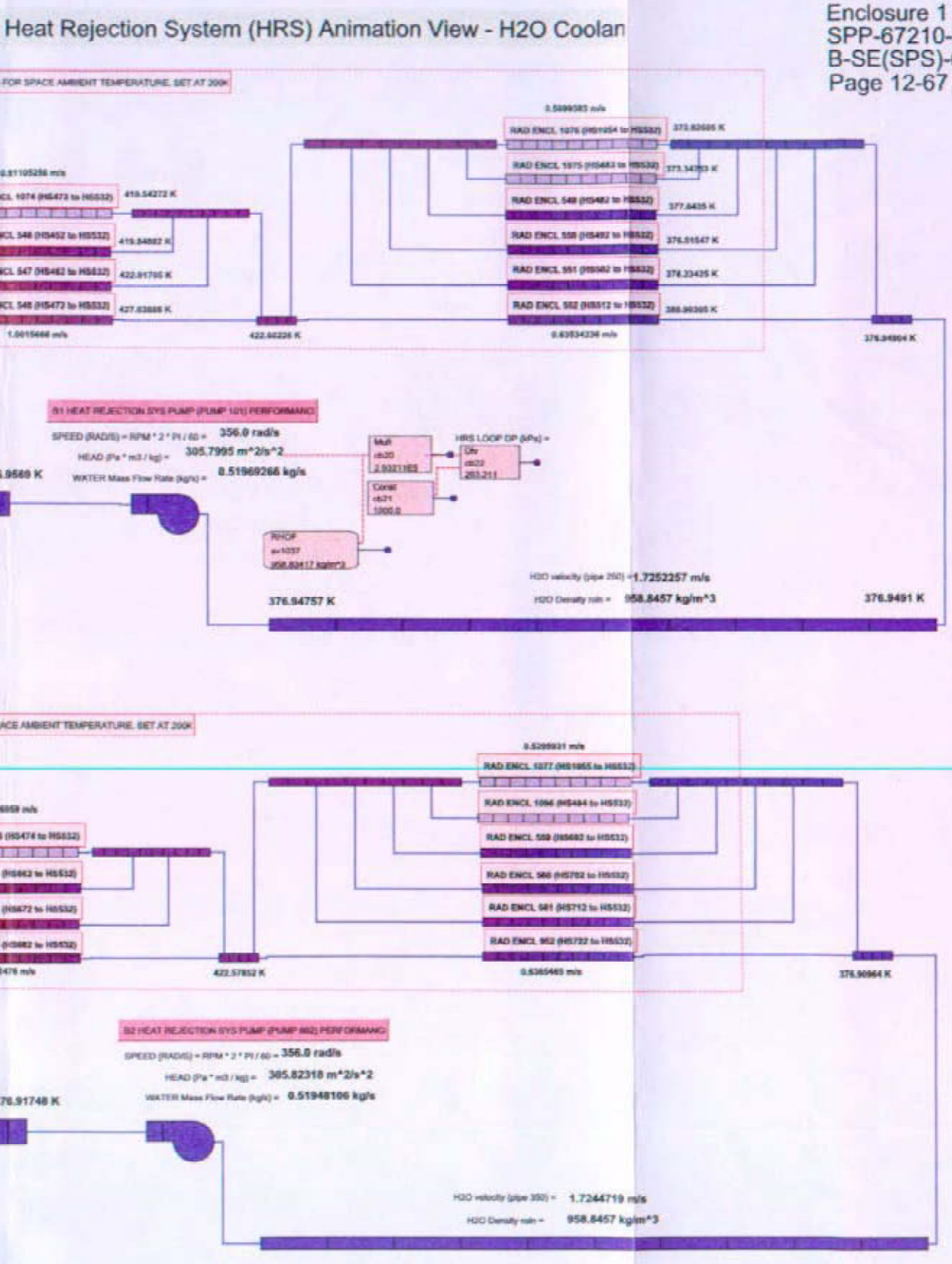



**Figure 12- 14: TRACE/SNAP Animation View of HRS Steady State Full Power Conditions**

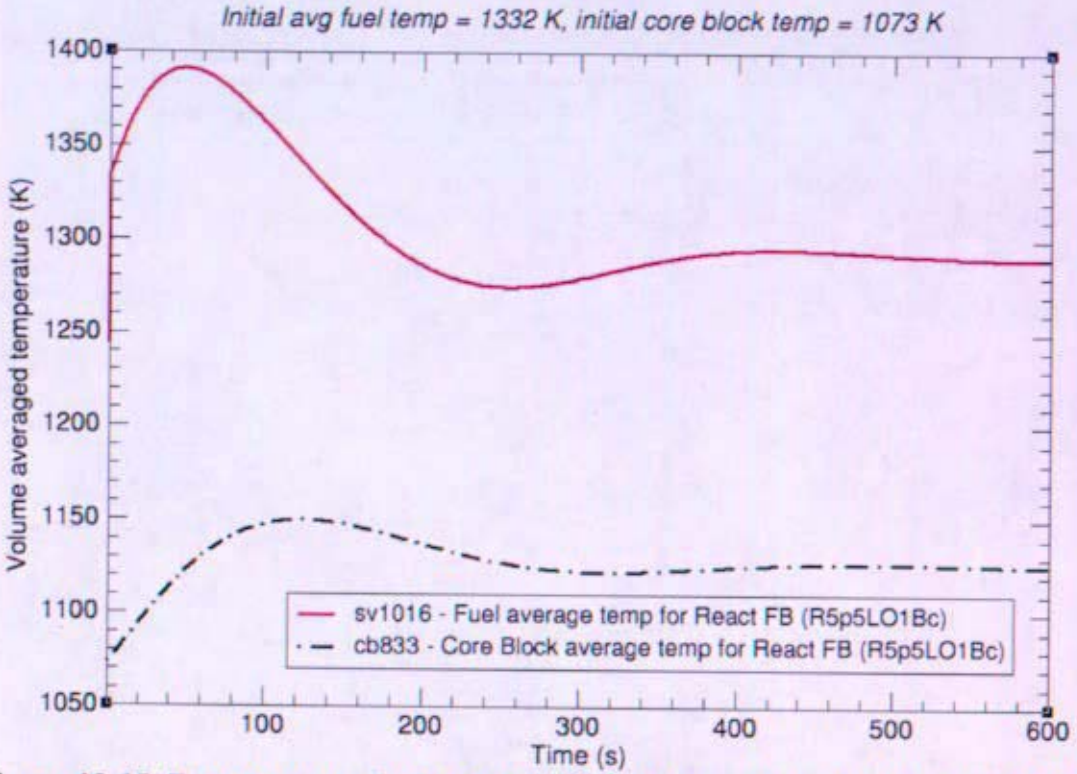



**Figure 12-15: Temperatures for Reactivity Feedback – Loss of Brayton (TRACE)**

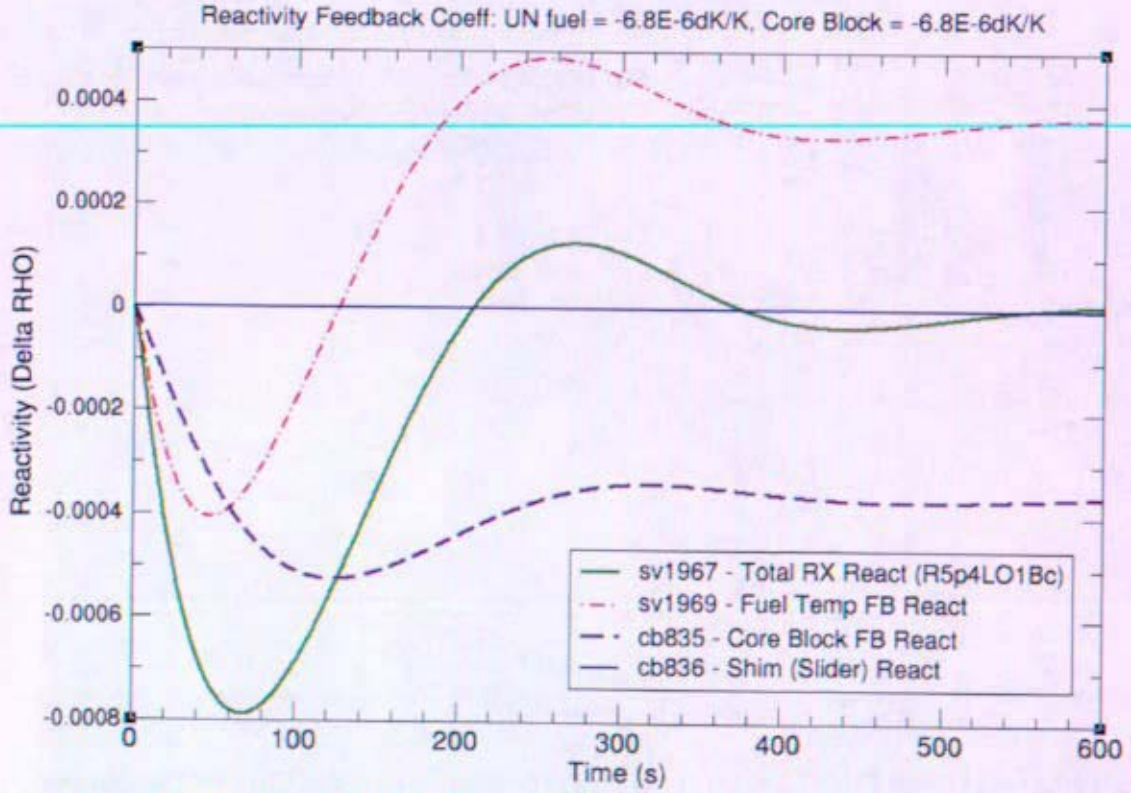



**Figure 12-16: Reactivity for Loss of Brayton (with CCEP maps) (TRACE)**

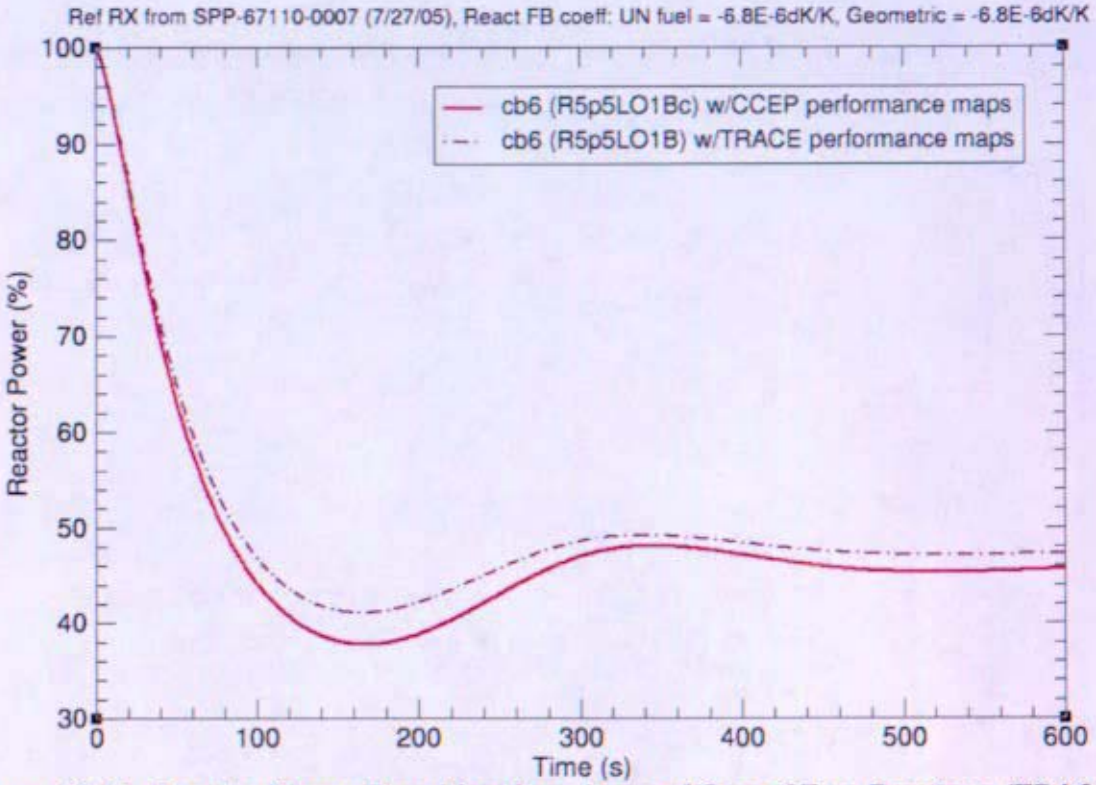



**Figure 12-17: Reactor Power Resulting from Loss of One of Two Braytons (TRACE)**

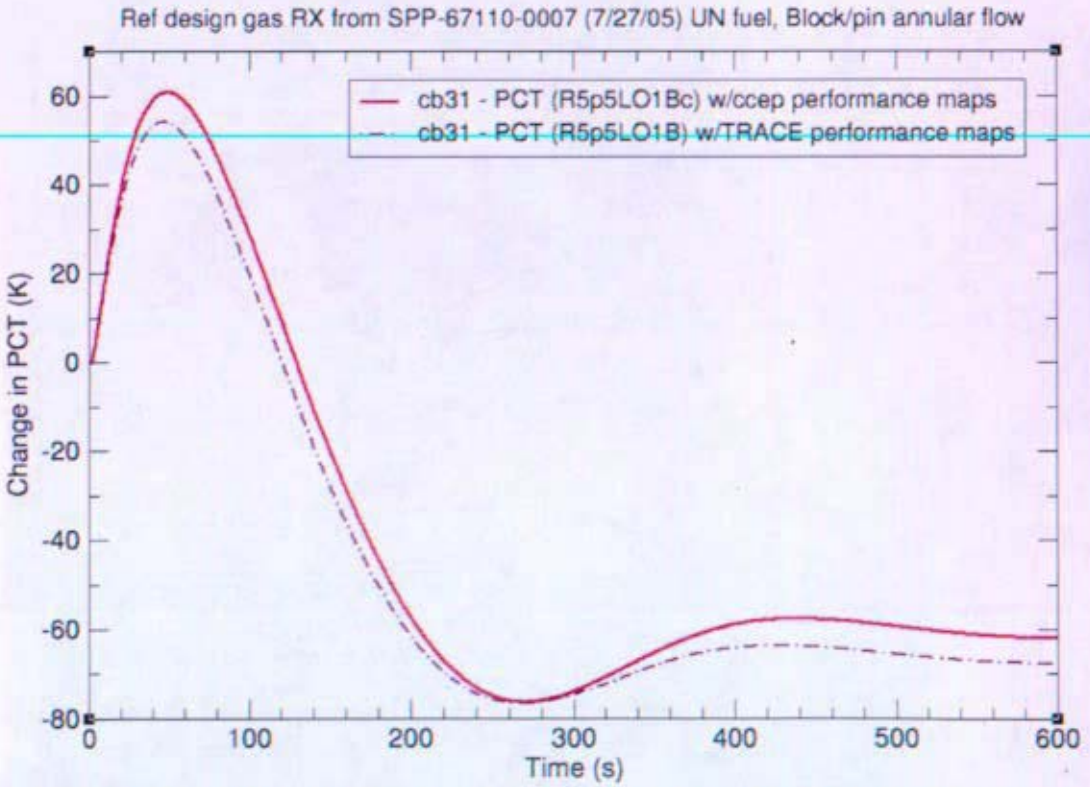



**Figure 12-18: Hot Spot Fuel Temperature Resulting from Loss of One of Two Braytons (TRACE)**

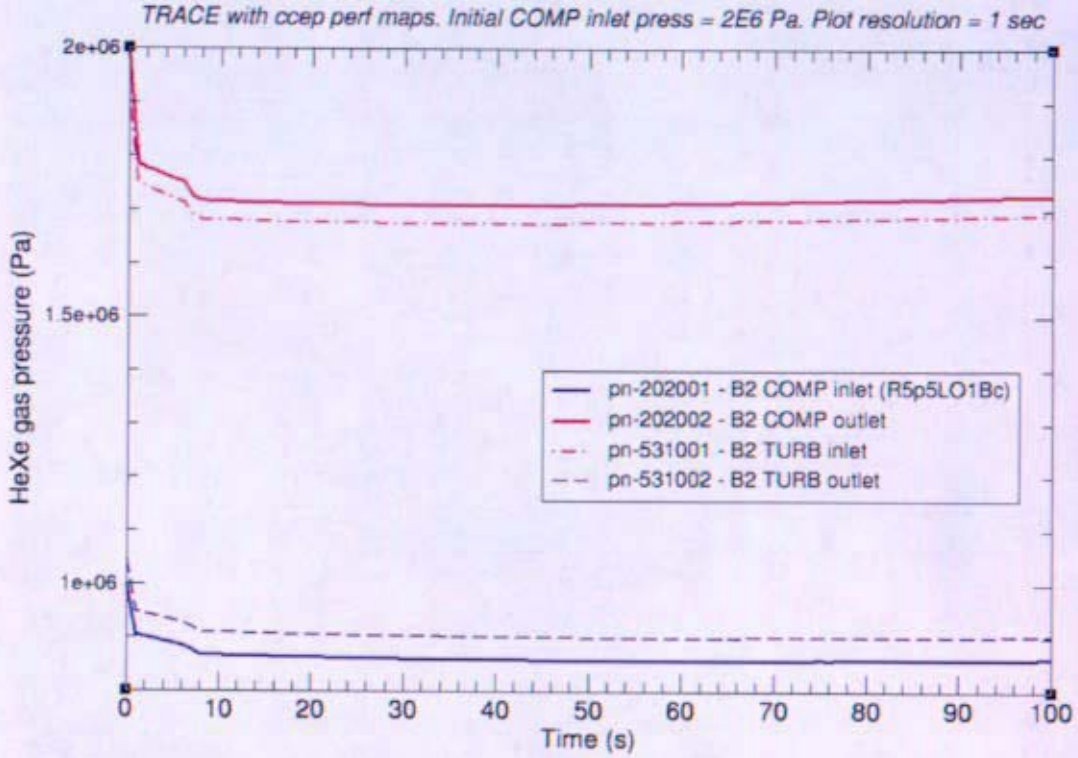



**Figure 12-19: Brayton 2 Pressures for Loss of Brayton 1 (TRACE)**

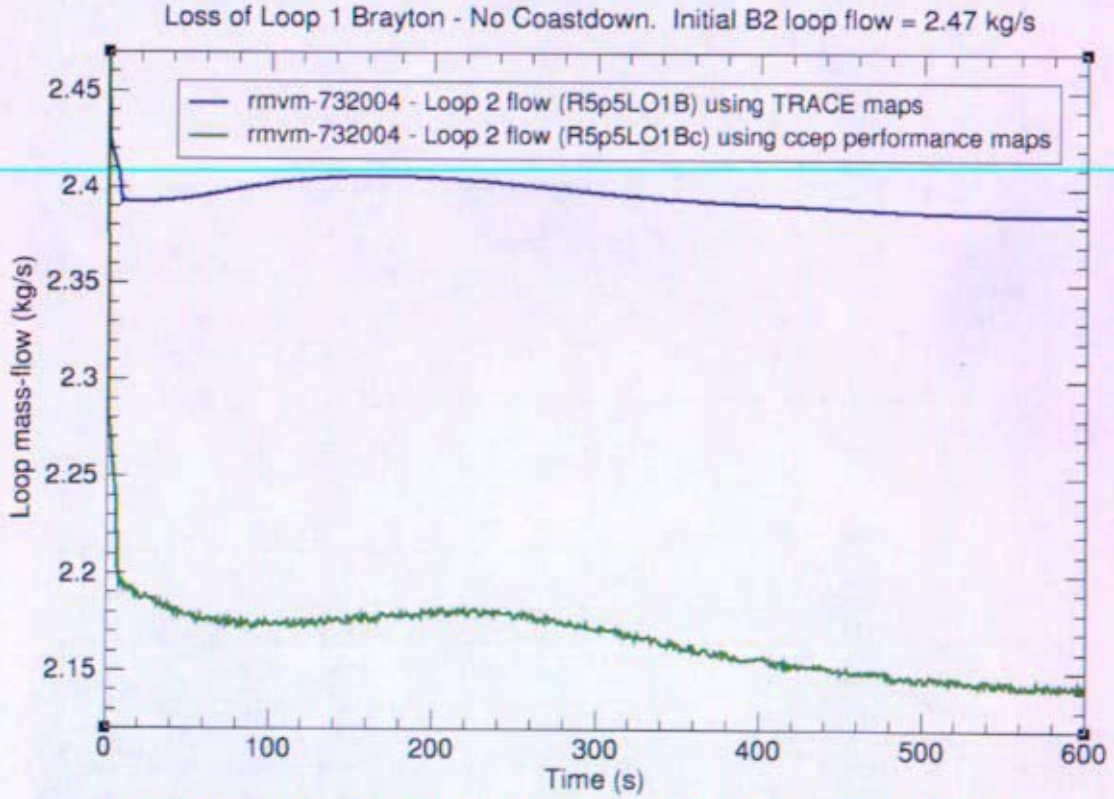



**Figure 12-20: Brayton 2 Loop Flow for Loss of Brayton 1 (TRACE)**

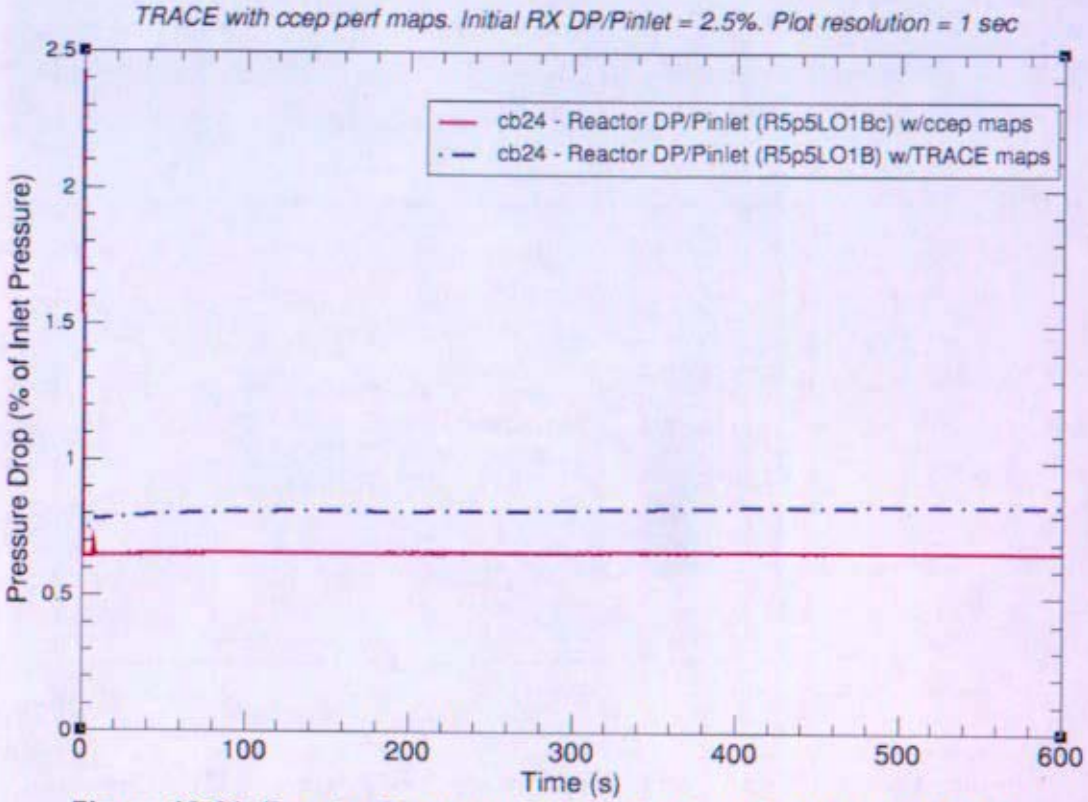



**Figure 12-21: Reactor Pressure Drop for Loss of Brayton 1 (TRACE)**

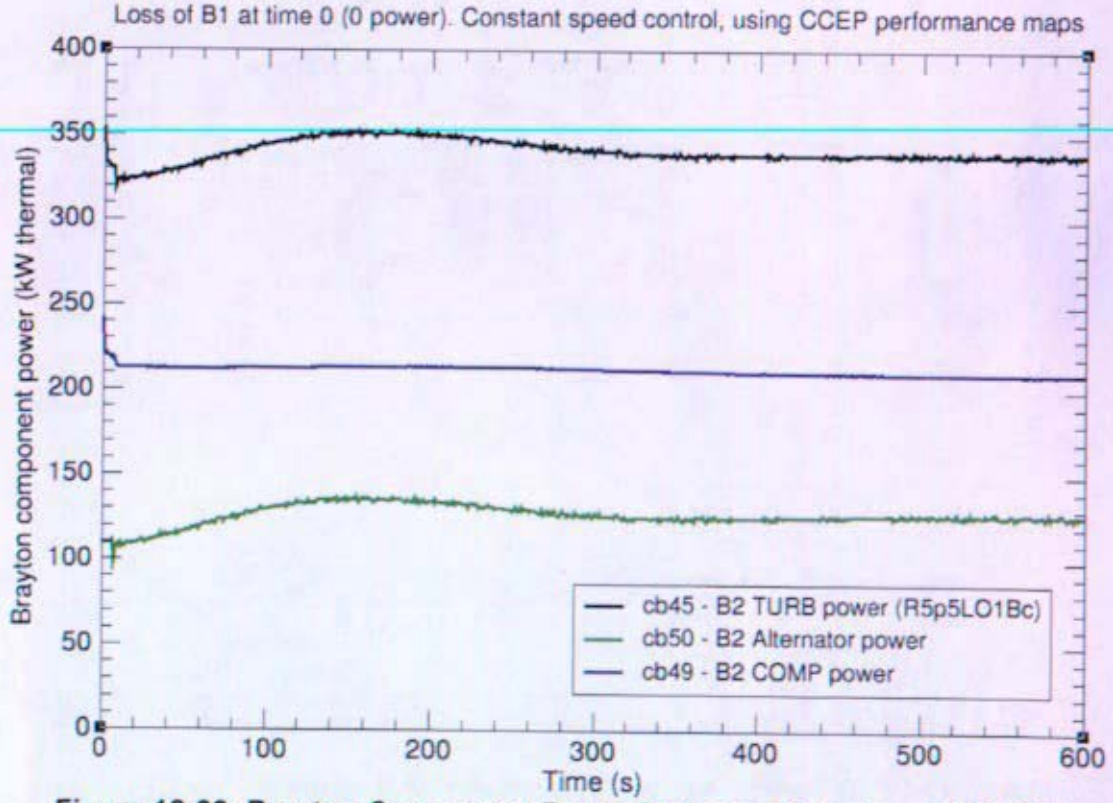



**Figure 12-22: Brayton Component Power for Loss of Brayton 1 (TRACE)**

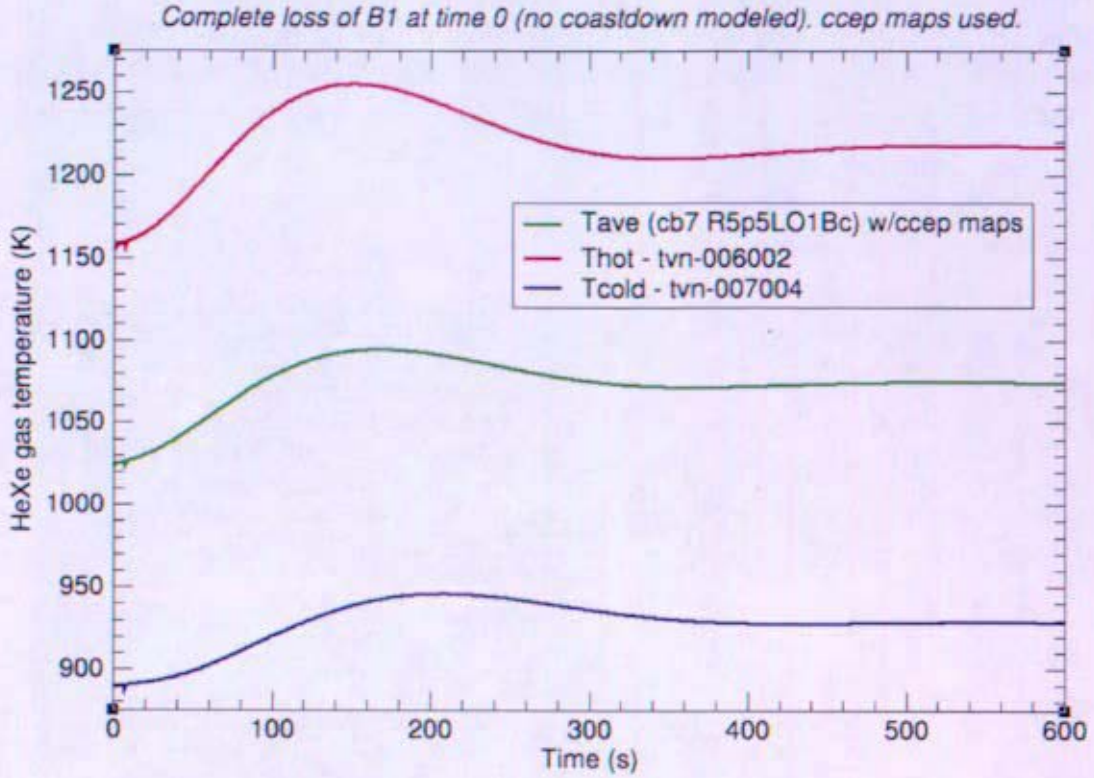



**Figure 12-23: Reactor Inlet & Exit Temperatures for Loss of Brayton 1 (TRACE)**

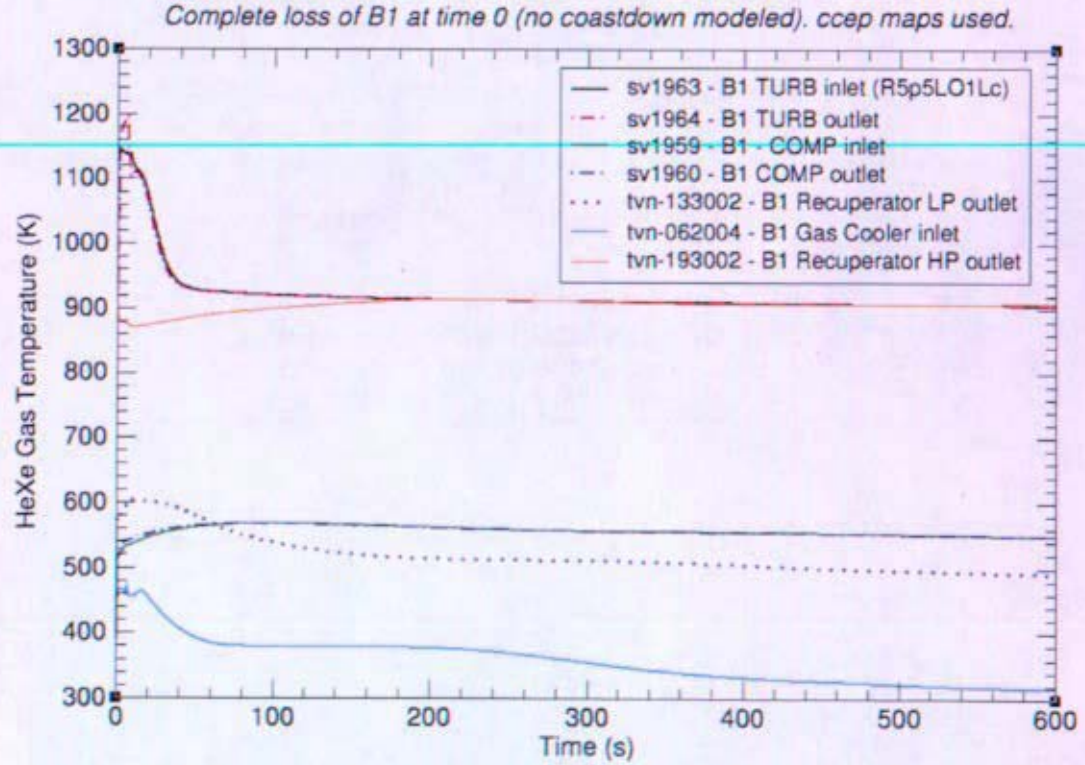



**Figure 12-24: Brayton 1 Loop Temperatures for Loss of Brayton 1 (TRACE)**

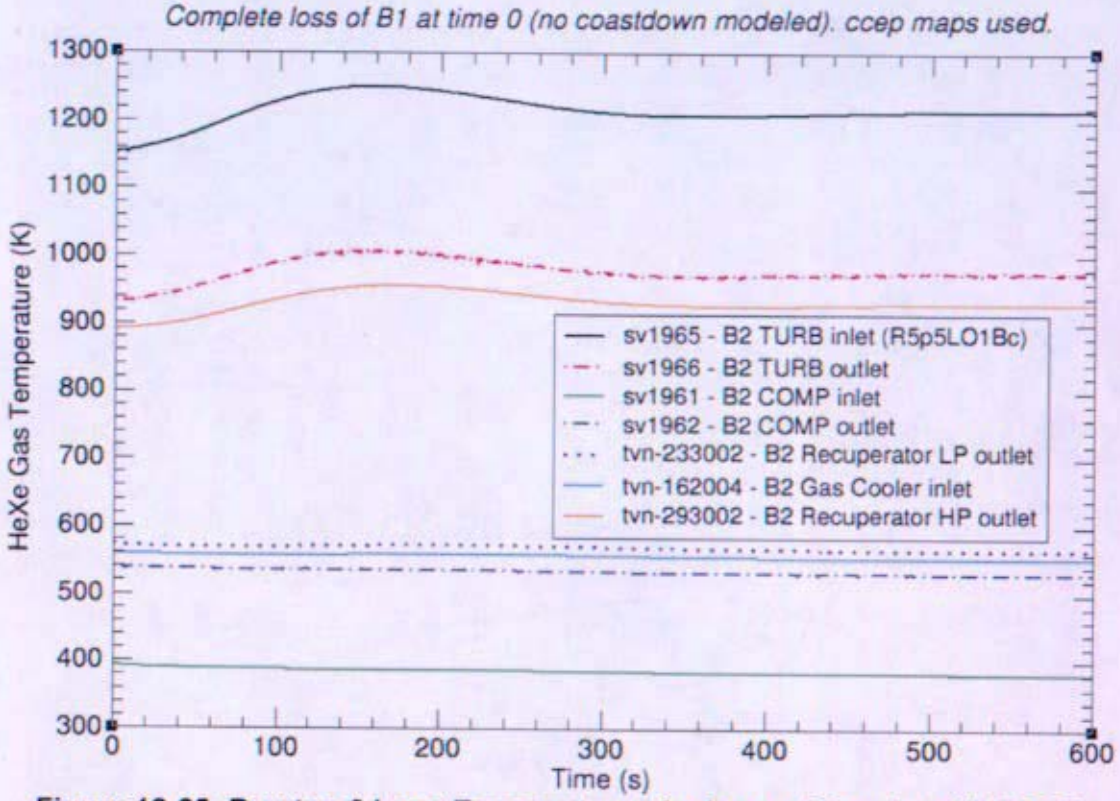



**Figure 12-25: Brayton 2 Loop Temperatures for Loss of Brayton 1 (TRACE)**

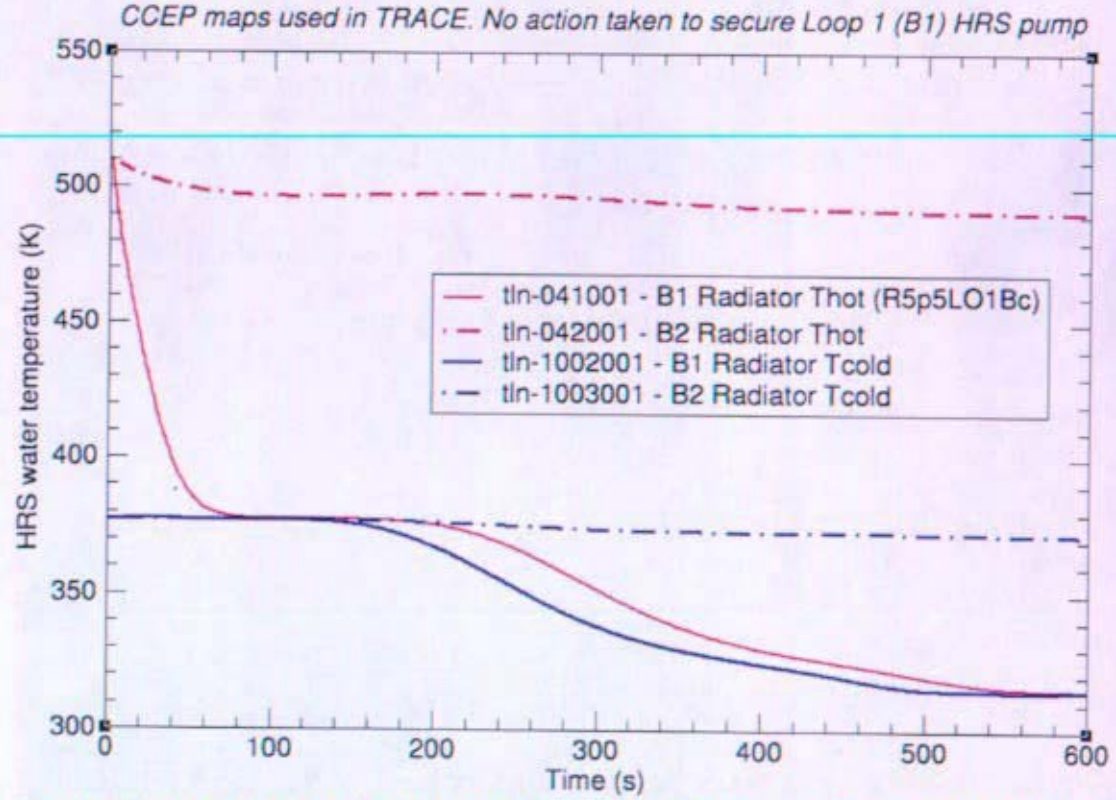



**Figure 12-26: Gas Cooler Water Temperatures for Loss of Brayton 1 (TRACE)**

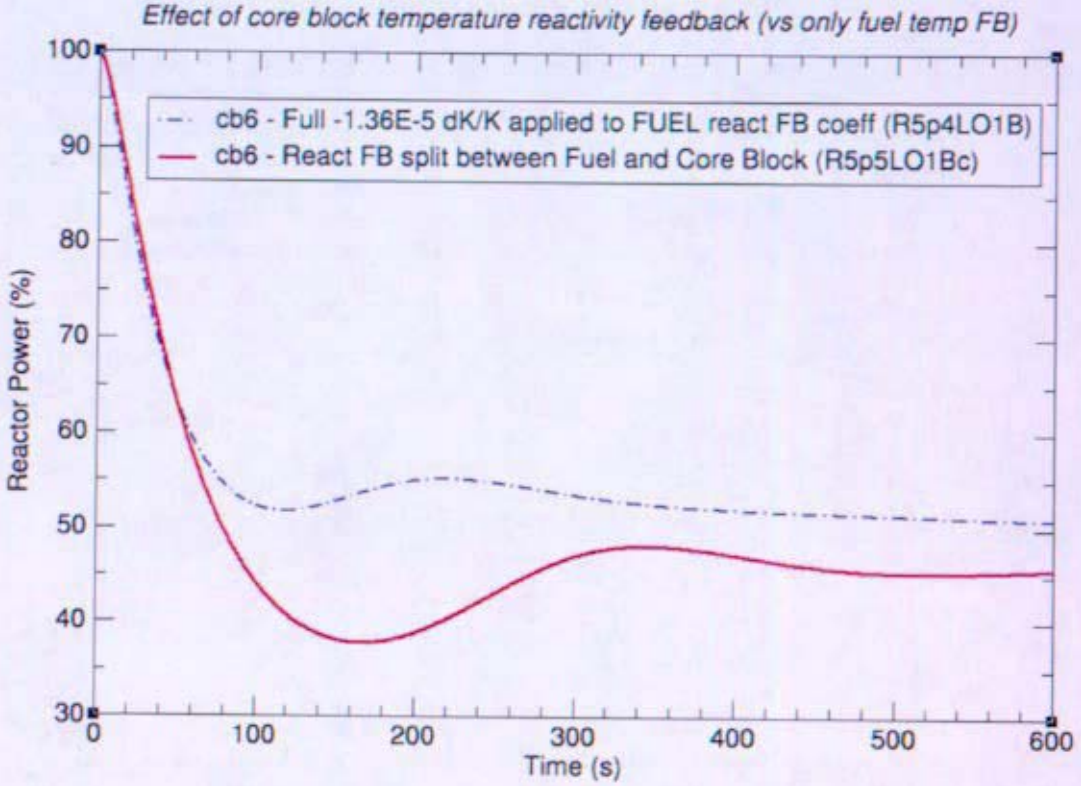



**Figure 12-27: Rx Power Following Loss of Brayton 1 – Reactivity Feedback Study (TRACE)**

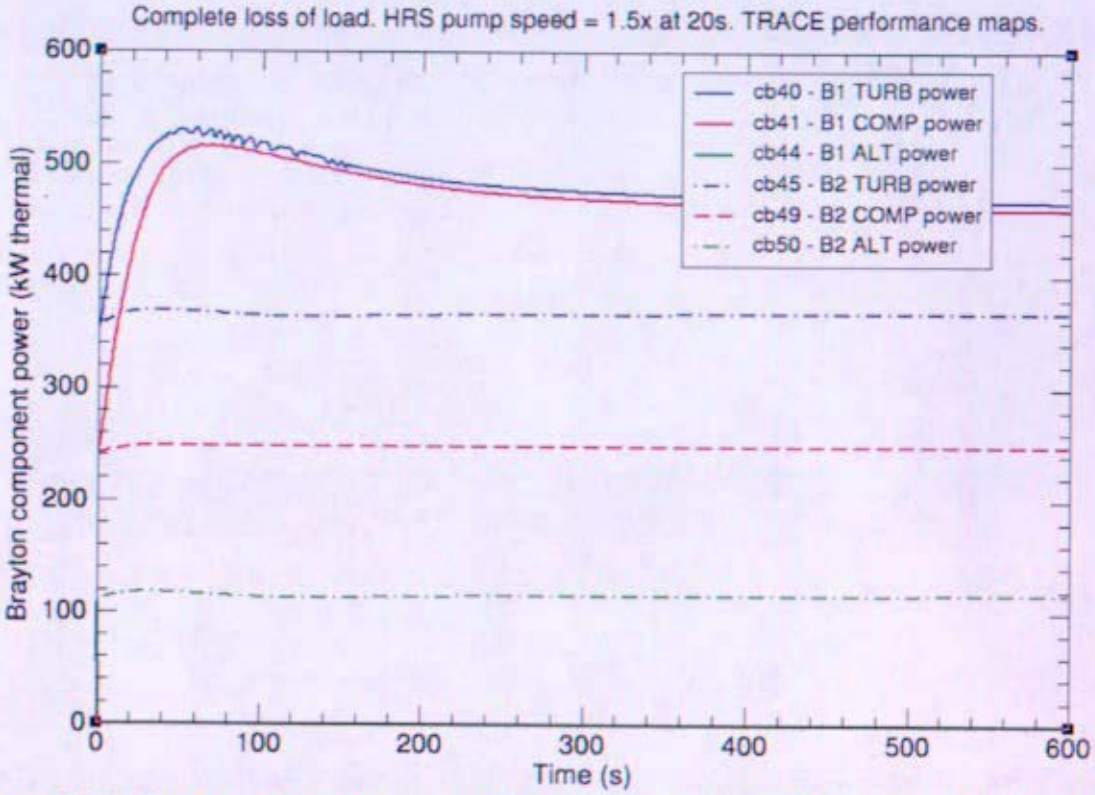



**Figure 12-28: Brayton Component Power for Brayton 1 Complete Loss of Load (TRACE)**

*R5p4LO1L2xPump doubles HRS-1 pump speed at 30s (61,150 rpm) & 1.5x at 20s (58,200 rpm)*

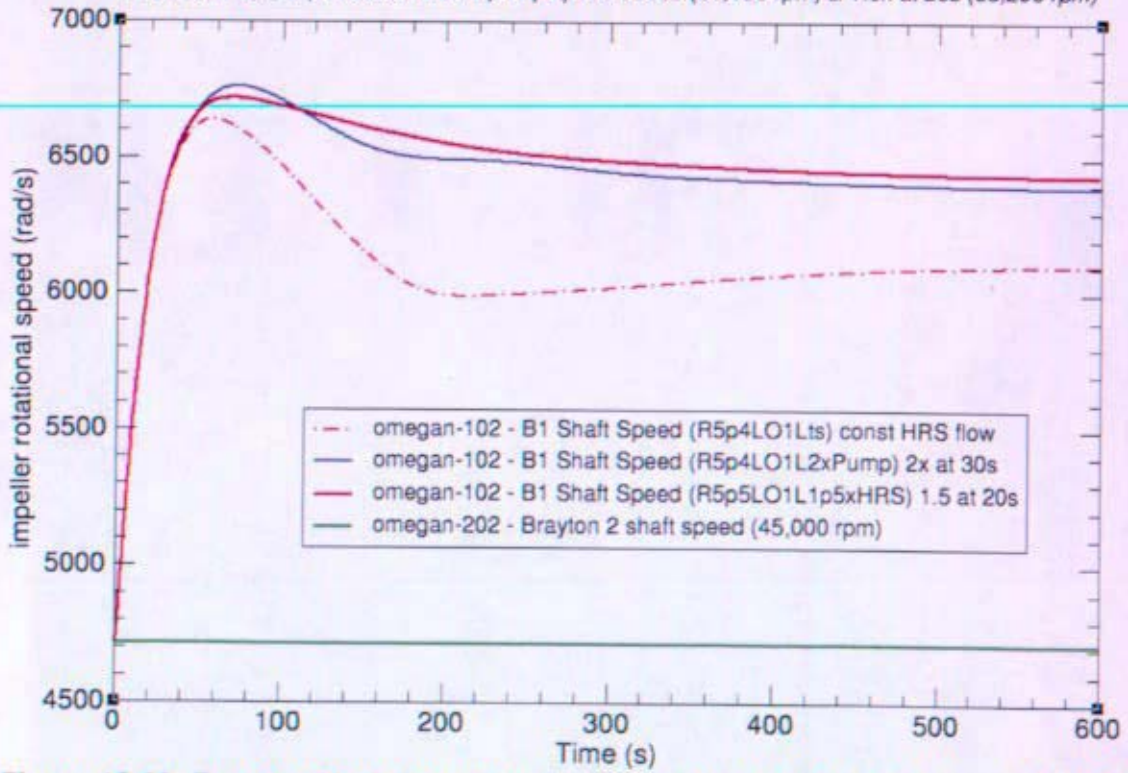



**Figure 12-29: Brayton Shaft Speed for Brayton 1 Complete Loss of Load (TRACE)**

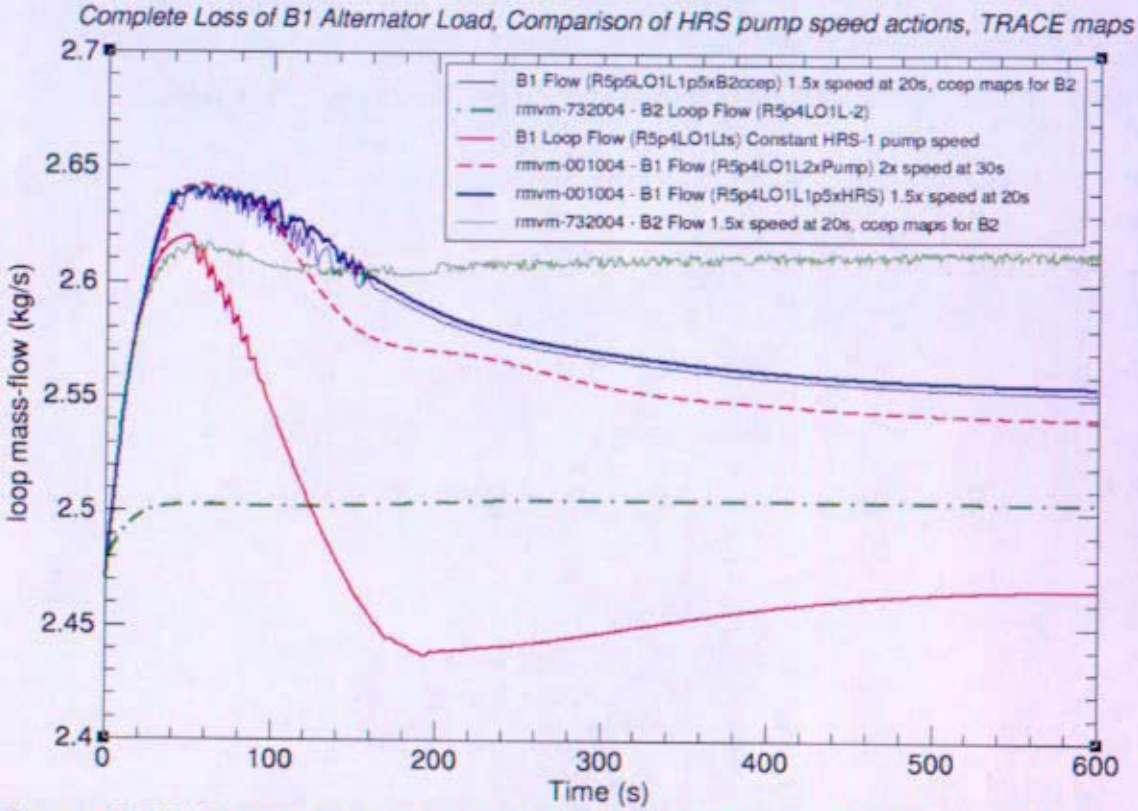



**Figure 12-30: Brayton Loop Flow for Brayton 1 Complete Loss of Load (TRACE)**

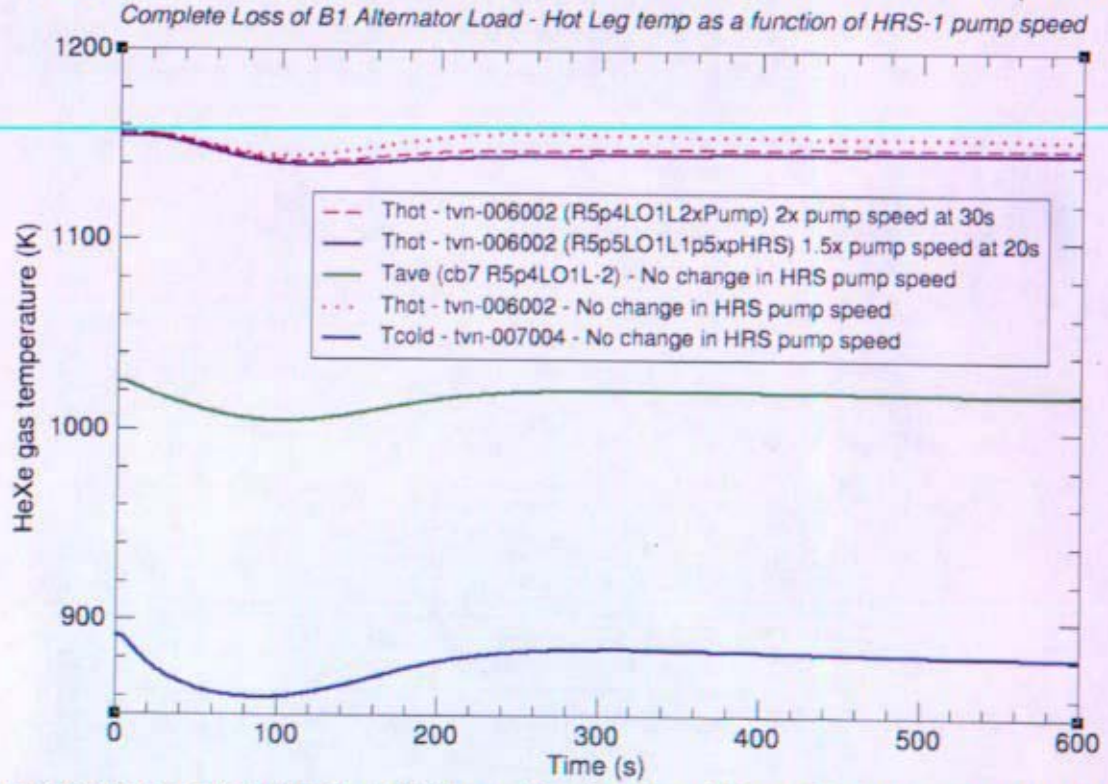



**Figure 12-31: Reactor Inlet & Exit Temps for Brayton 1 Complete Loss of Load (TRACE)**

*With TRACE performance maps. Complete loss of B1 alternator load.*

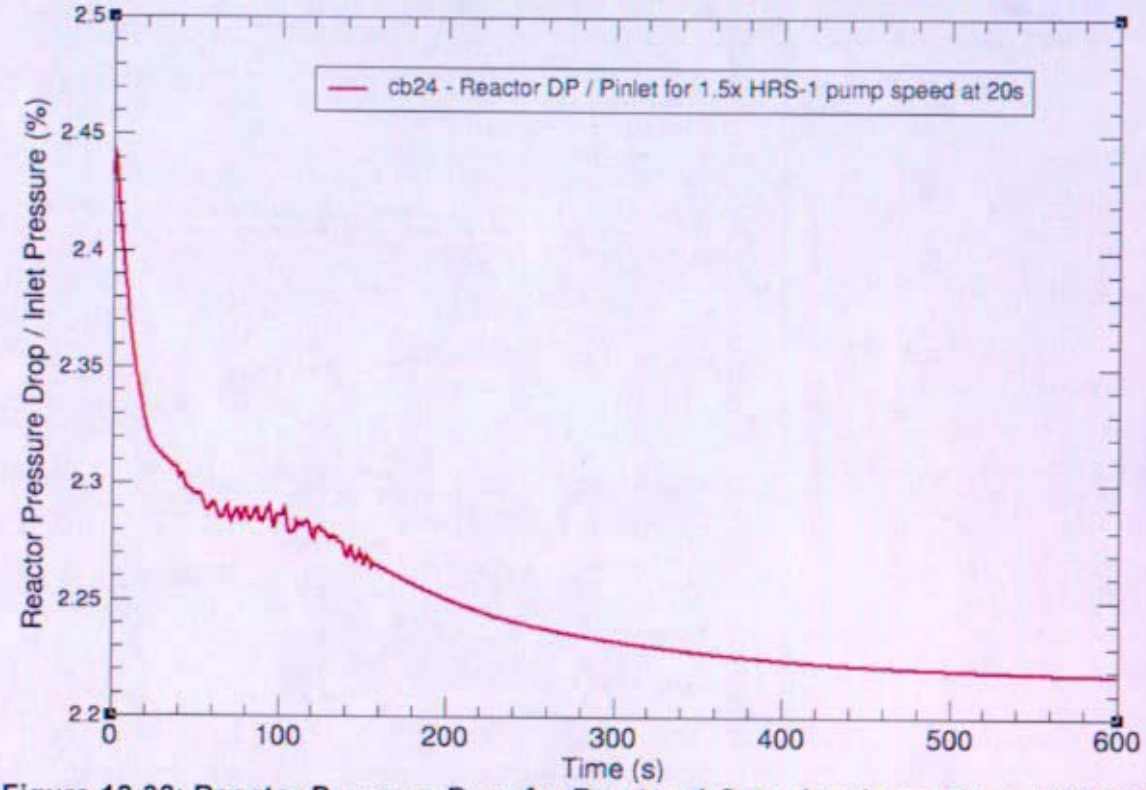



**Figure 12-32: Reactor Pressure Drop for Brayton 1 Complete Loss of Load (TRACE)**

*Complete loss of B1 Alt load at time 0. HRS flow = 1.5x at 20s. TRACE perf maps used.*

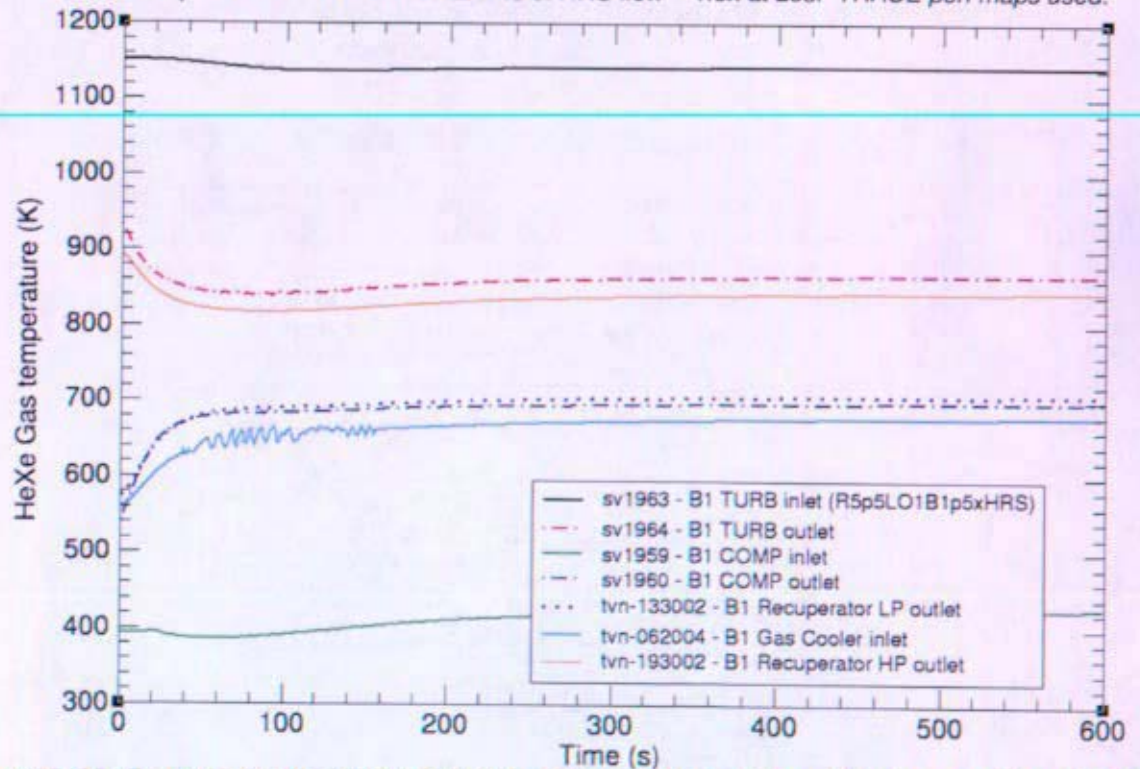



**Figure 12-33: Brayton 1 Loop Temperatures for Brayton 1 Complete Loss of Load (TRACE)**

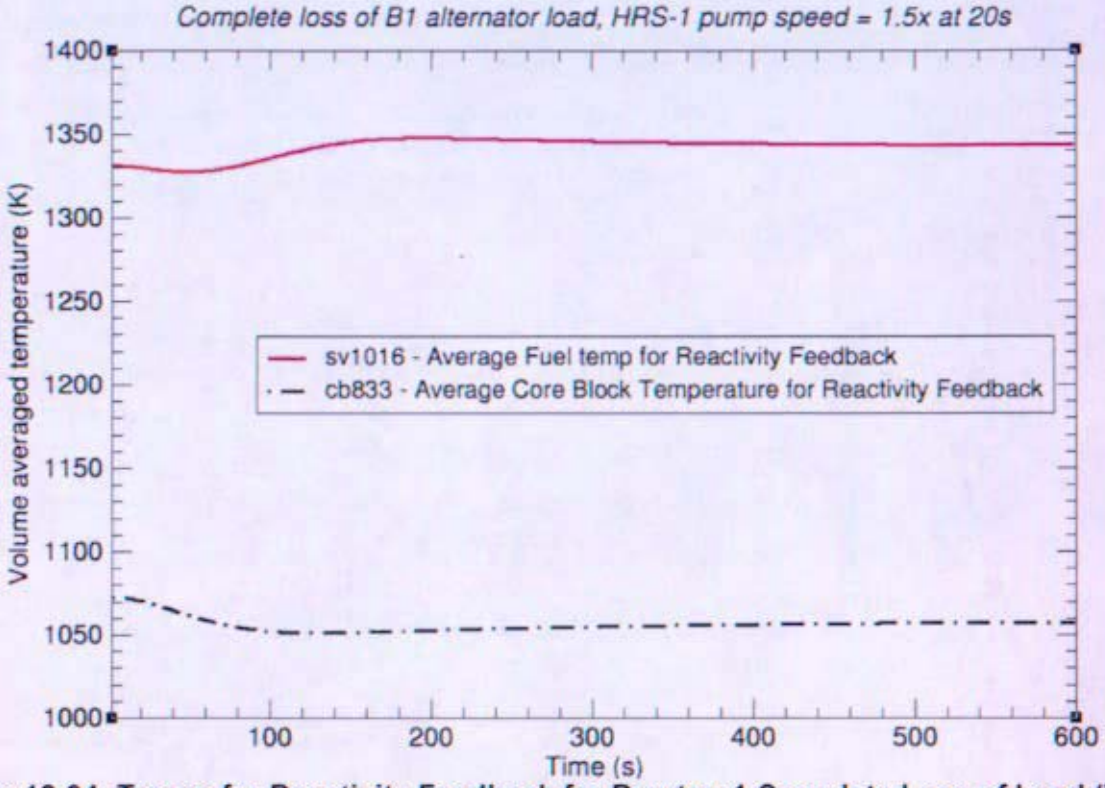



**Figure 12-34: Temps for Reactivity Feedback for Brayton 1 Complete Loss of Load (TRACE)**

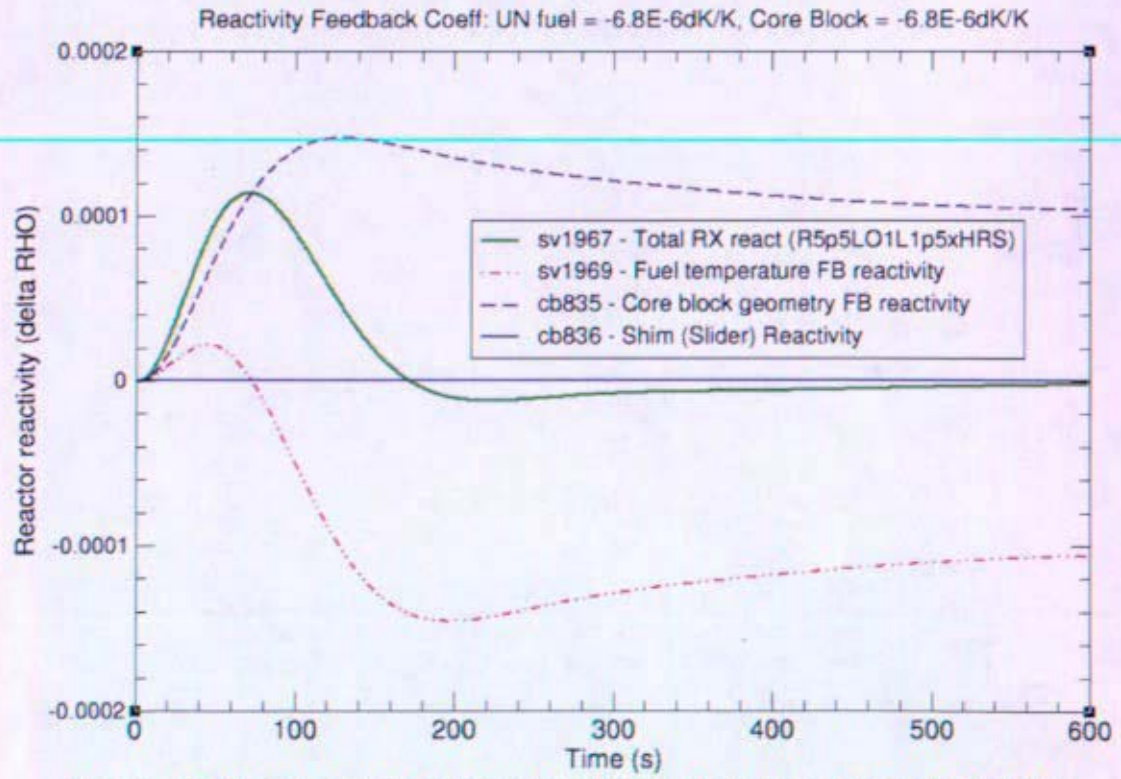



**Figure 12-35: Reactivity for Brayton 1 Complete Loss of Load (TRACE)**

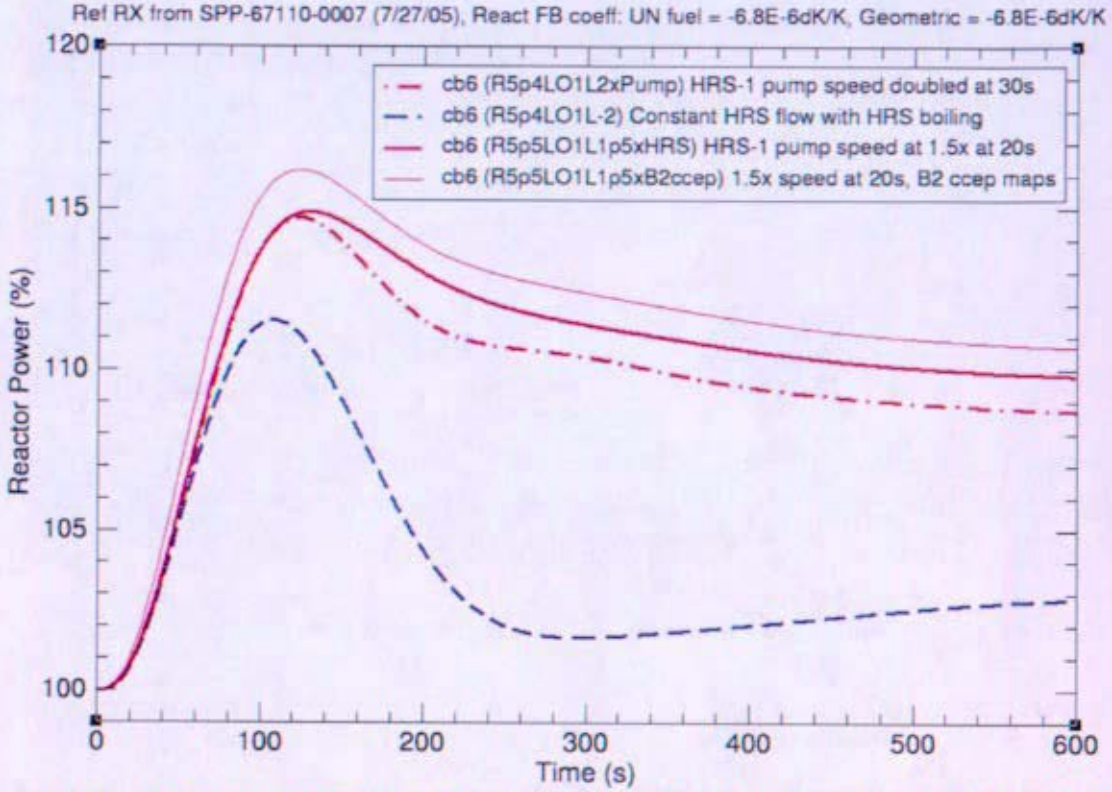



**Figure 12-36: Reactor Power for Brayton 1 Complete Loss of Load (TRACE)**

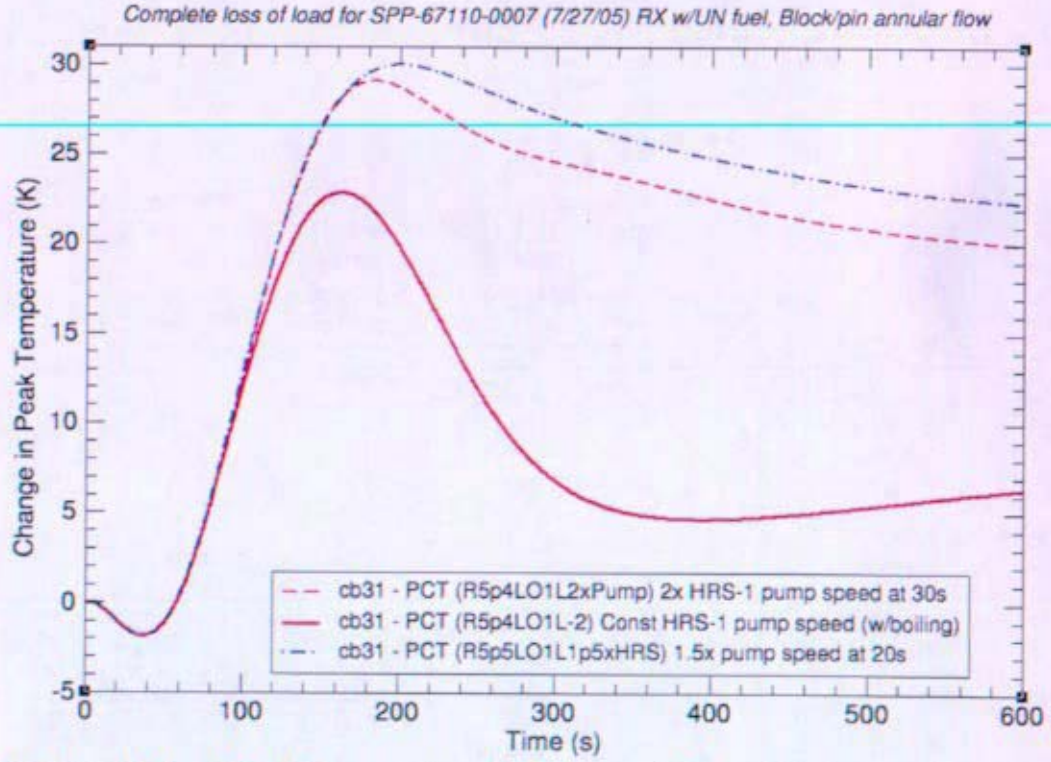



**Figure 12-37: Hot Spot Fuel Temperature for Brayton 1 Complete Loss of Load (TRACE)**

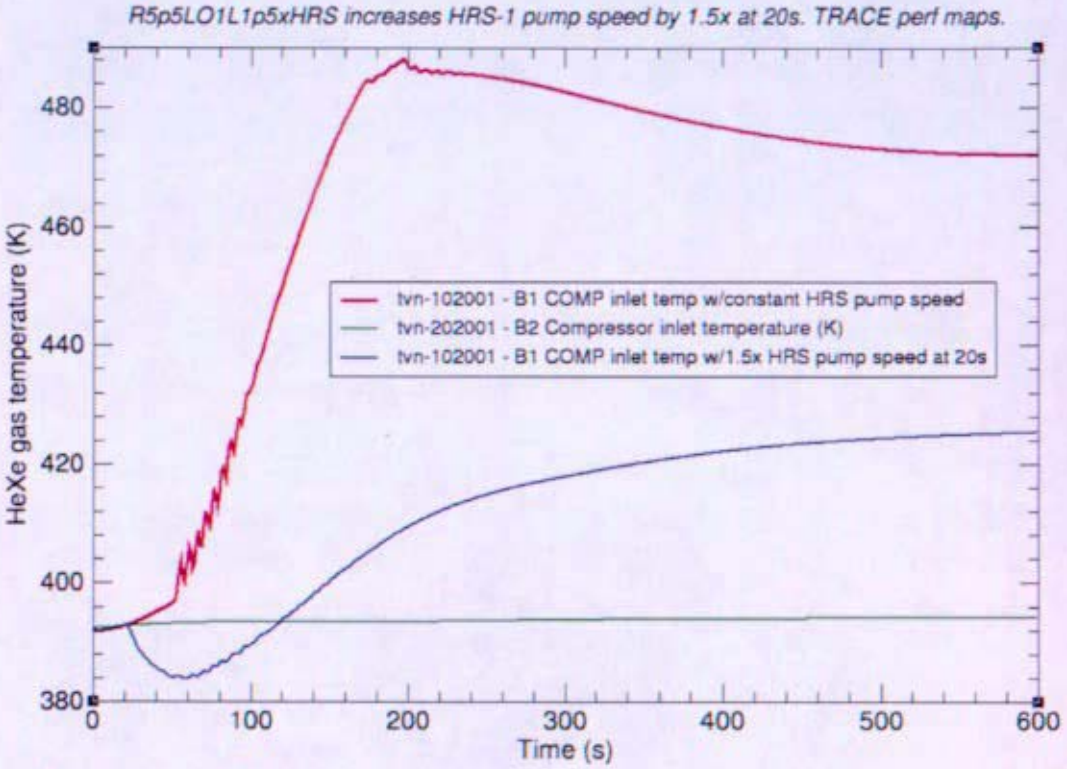



**Figure 12-38: Brayton Compressor Temp for Brayton 1 Complete Loss of Load (TRACE)**

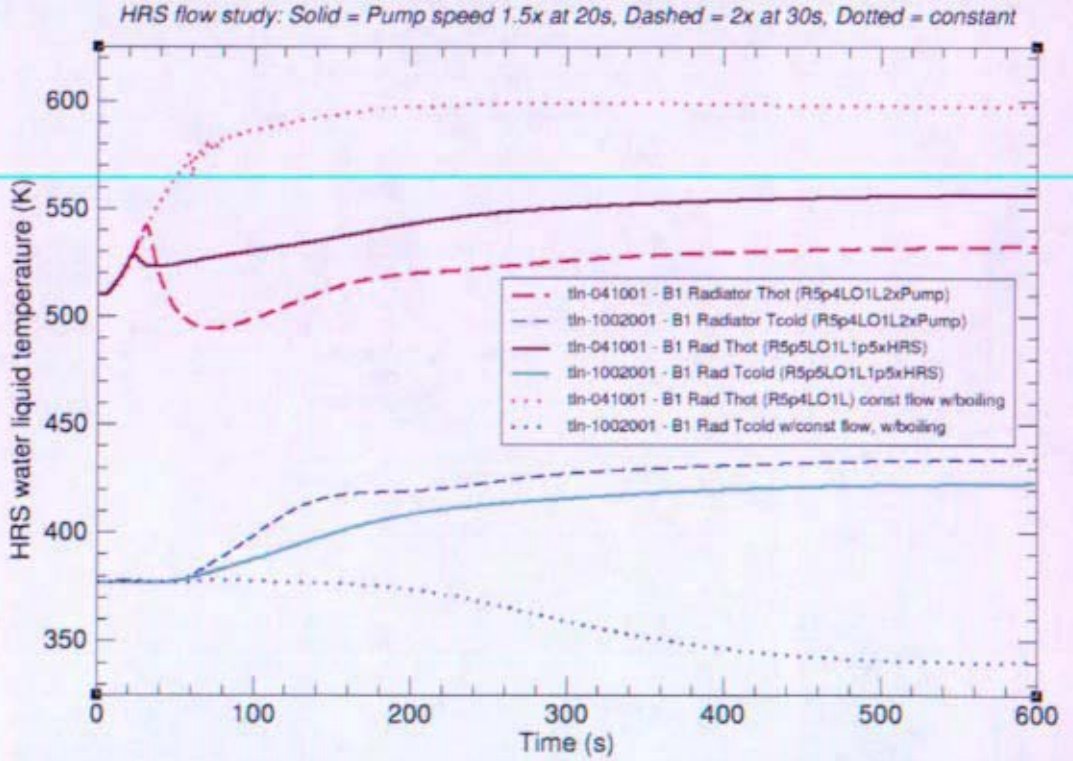



**Figure 12-39: Gas Cooler Water Temps for Brayton 1 Complete Loss of Load (TRACE)**

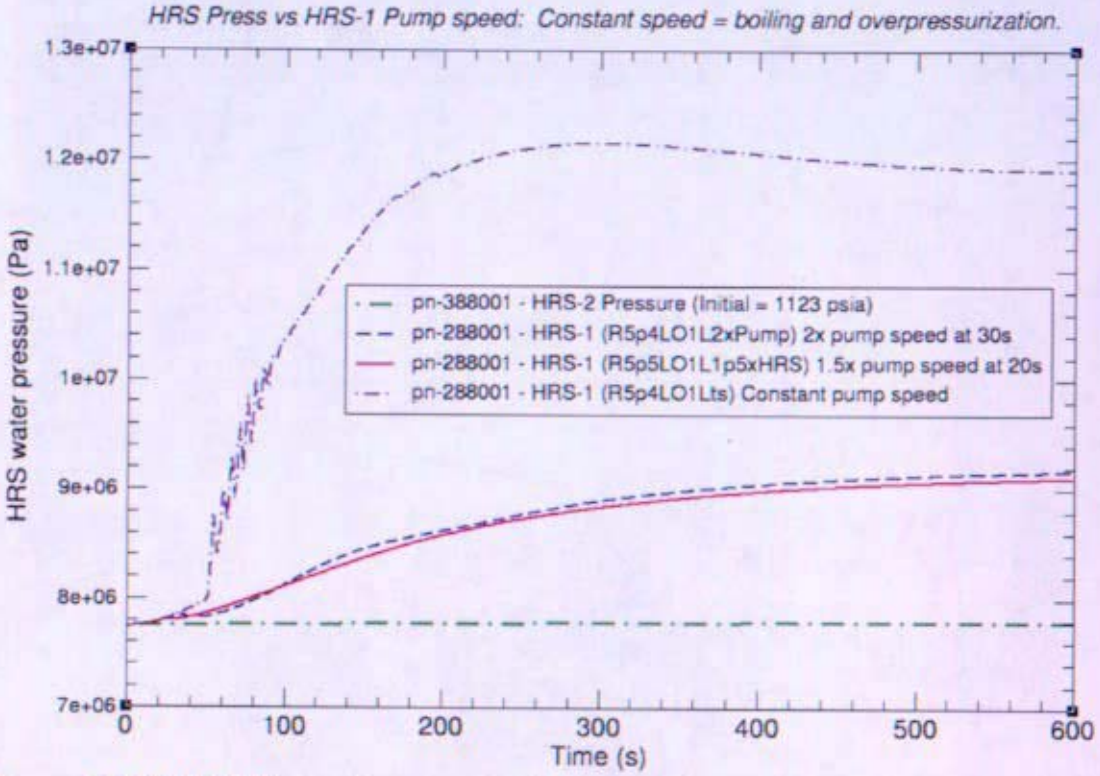



**Figure 12-40: HRS Water Pressure for Brayton 1 Complete Loss of Load (TRACE)**

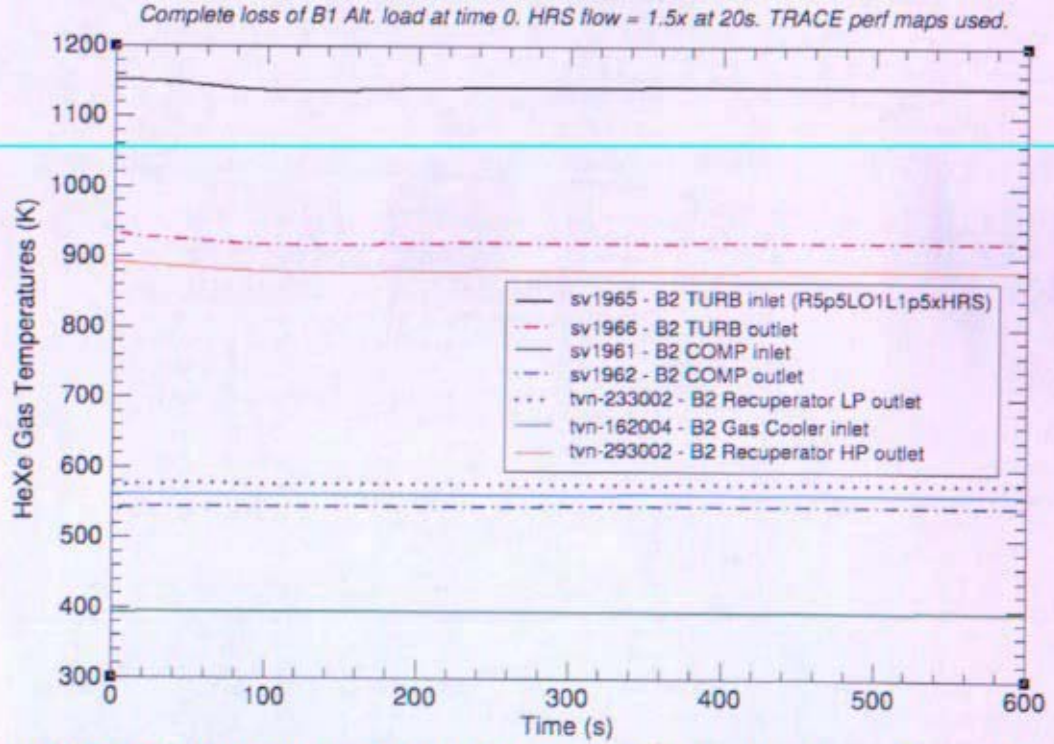



**Figure 12-41: Brayton 2 Loop Temps for Brayton 1 Complete Loss of Load (TRACE)**

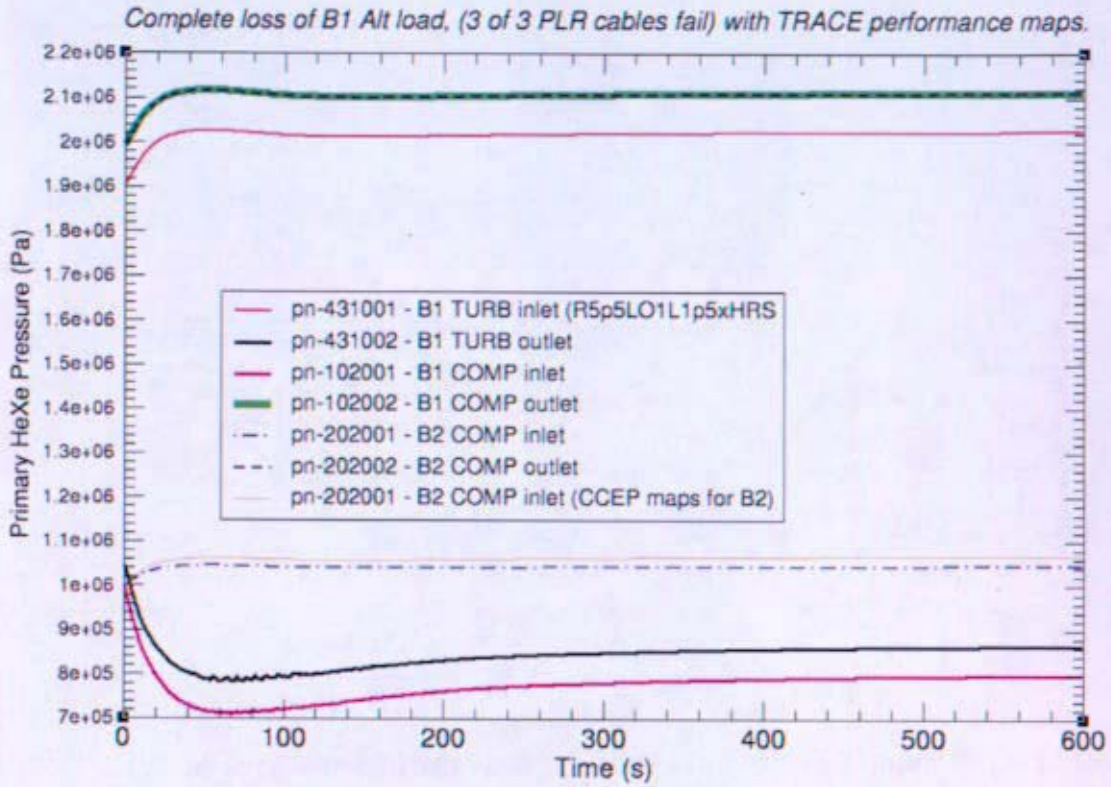



**Figure 12-42: Primary Pressure for Brayton 1 Complete Loss of Load (TRACE)**

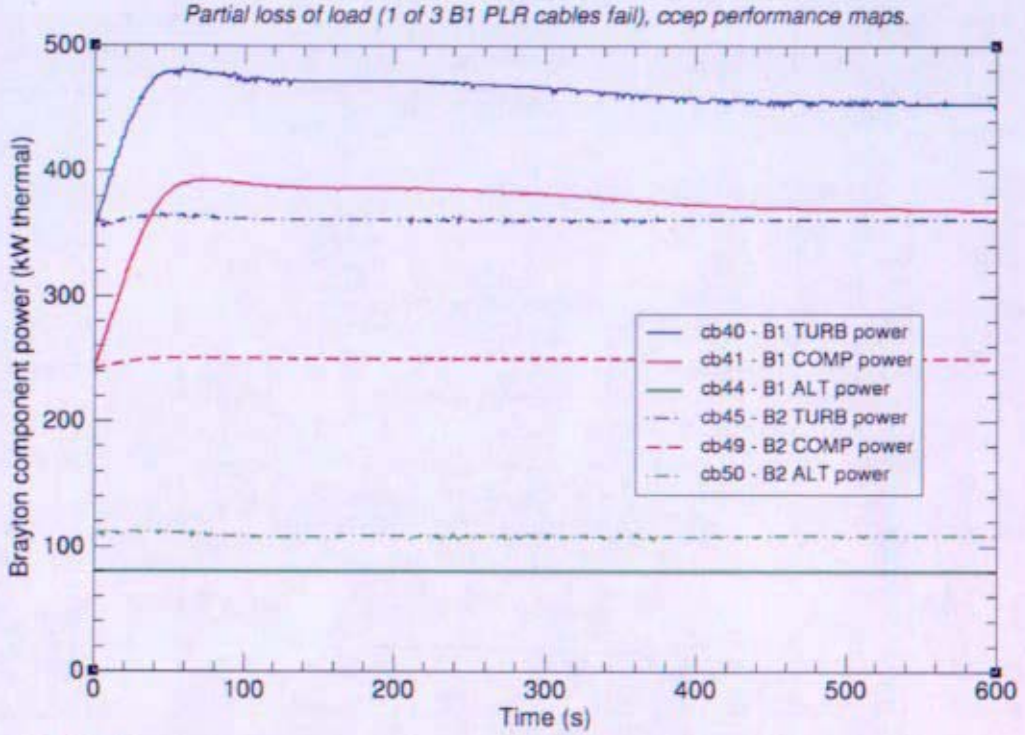



**Figure 12-43: Brayton Component Power for Brayton 1 Partial Loss of Load (TRACE)**

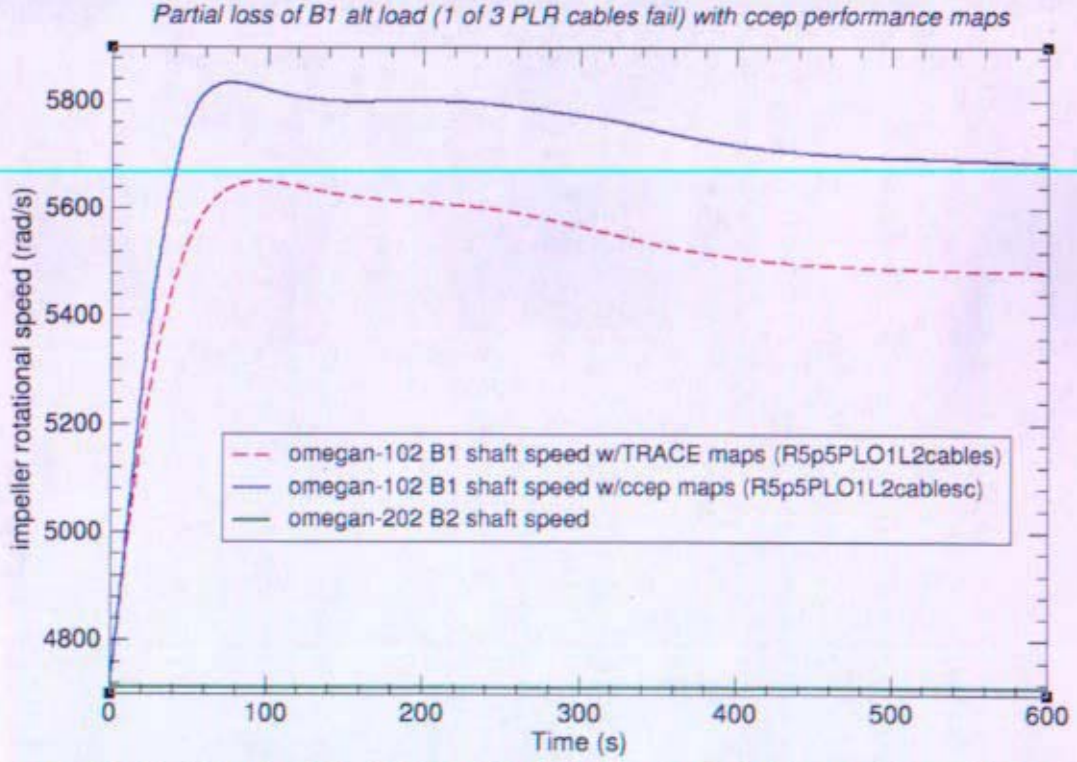



**Figure 12-44: Brayton Shaft Speed for Brayton 1 Partial Loss of Load (TRACE)**

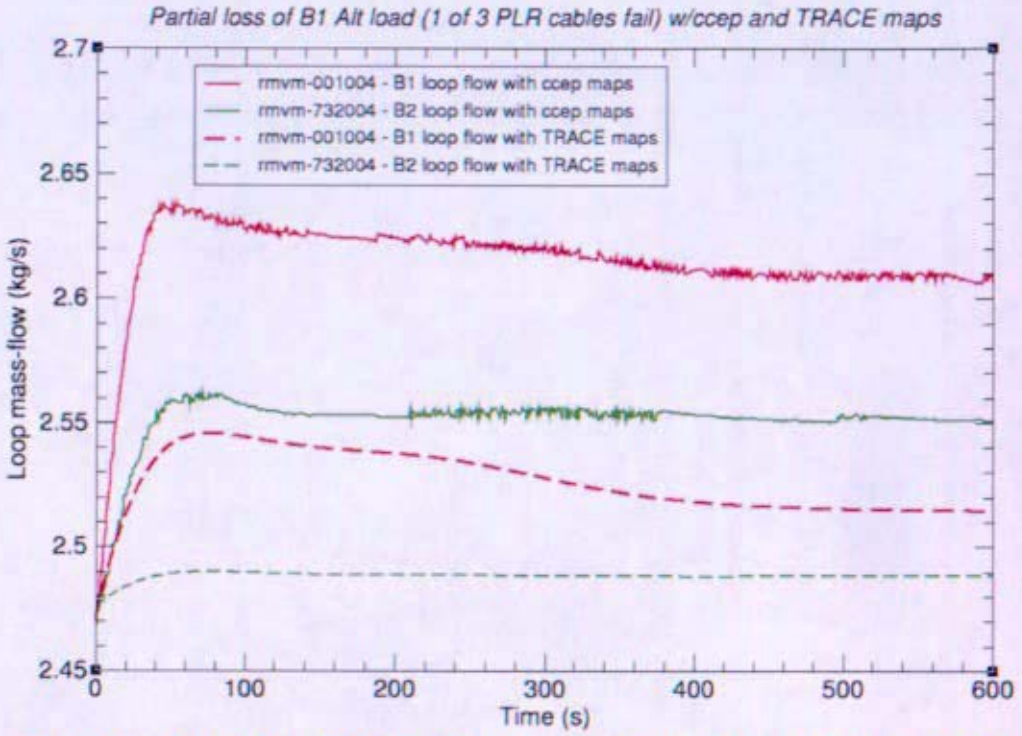



**Figure 12-45: Brayton Loop Flow for Brayton 1 Partial Loss of Load (TRACE)**

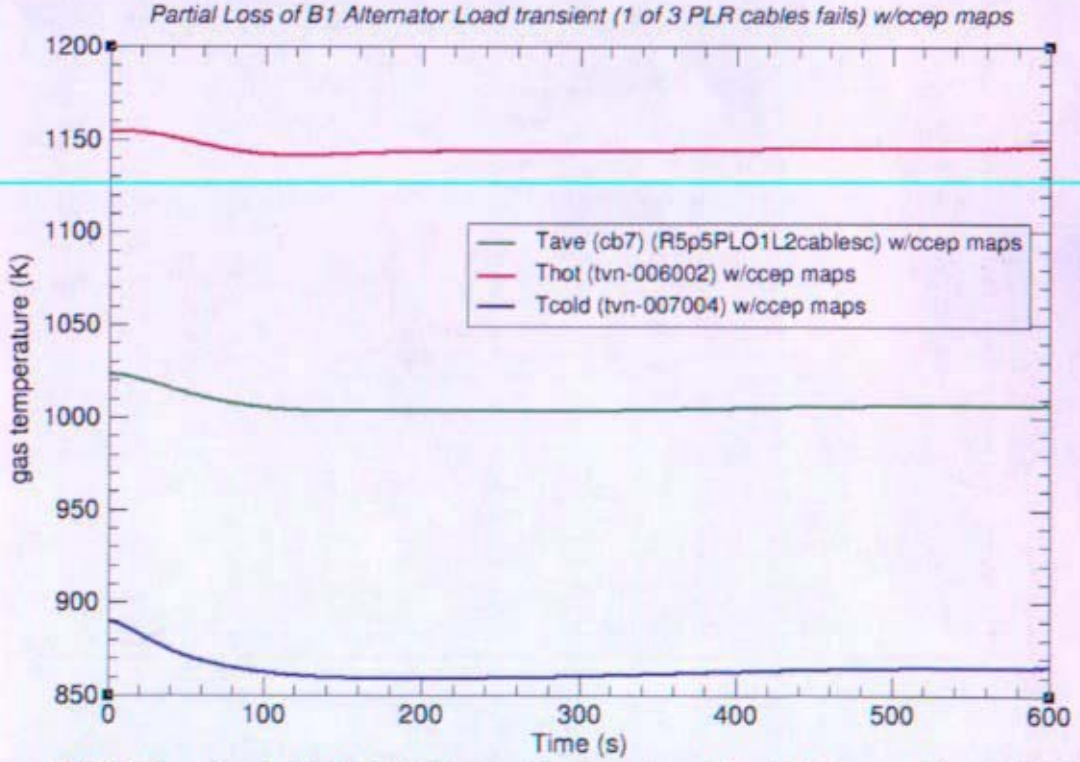



**Figure 12-46: Reactor Inlet & Exit Temps for Brayton 1 Partial Loss of Load (TRACE)**

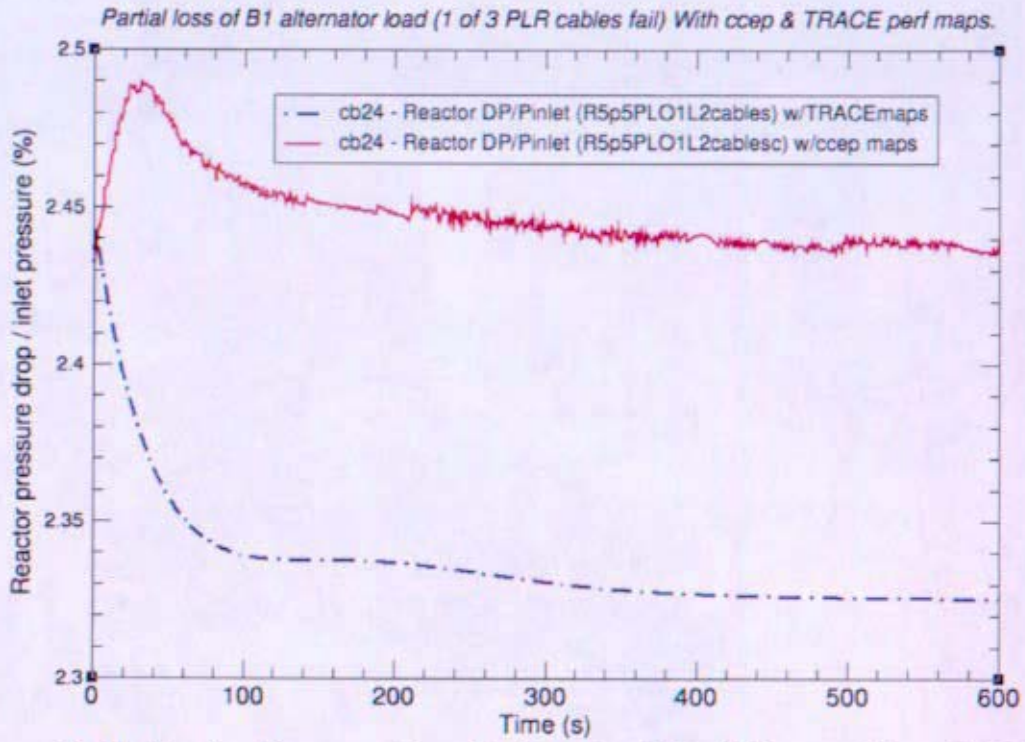



**Figure 12-47: Reactor Pressure Drop for Brayton 1 Partial Loss of Load (TRACE)**

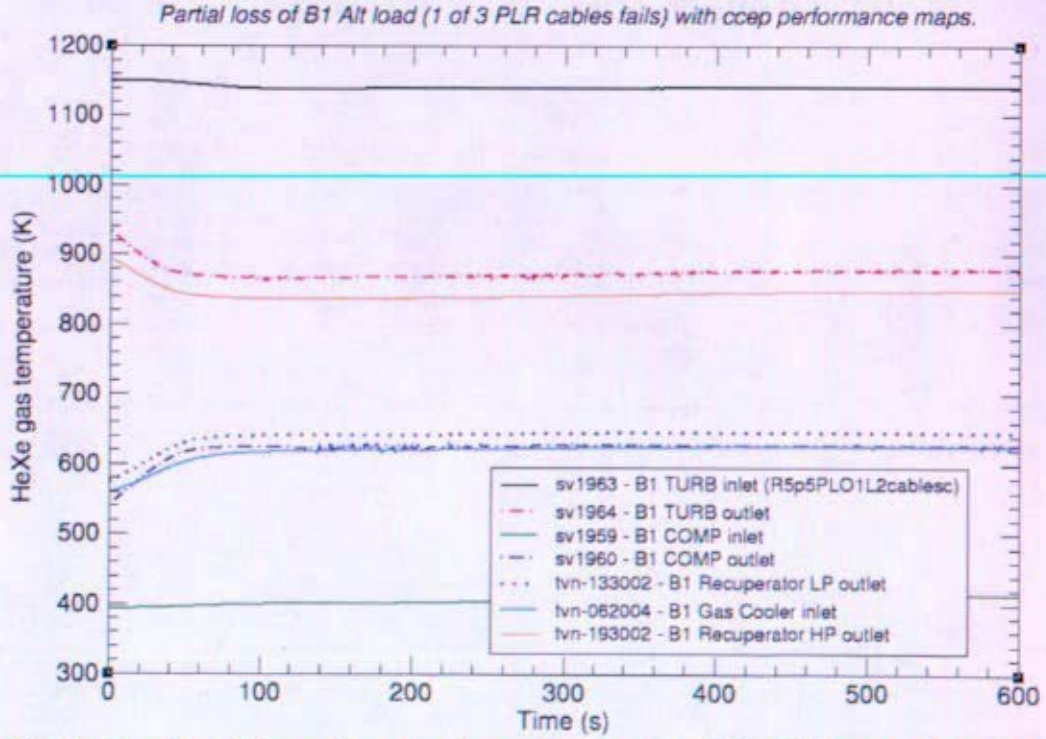



**Figure 12-48: Brayton 1 Loop Temperatures for Brayton 1 Partial Loss of Load (TRACE)**

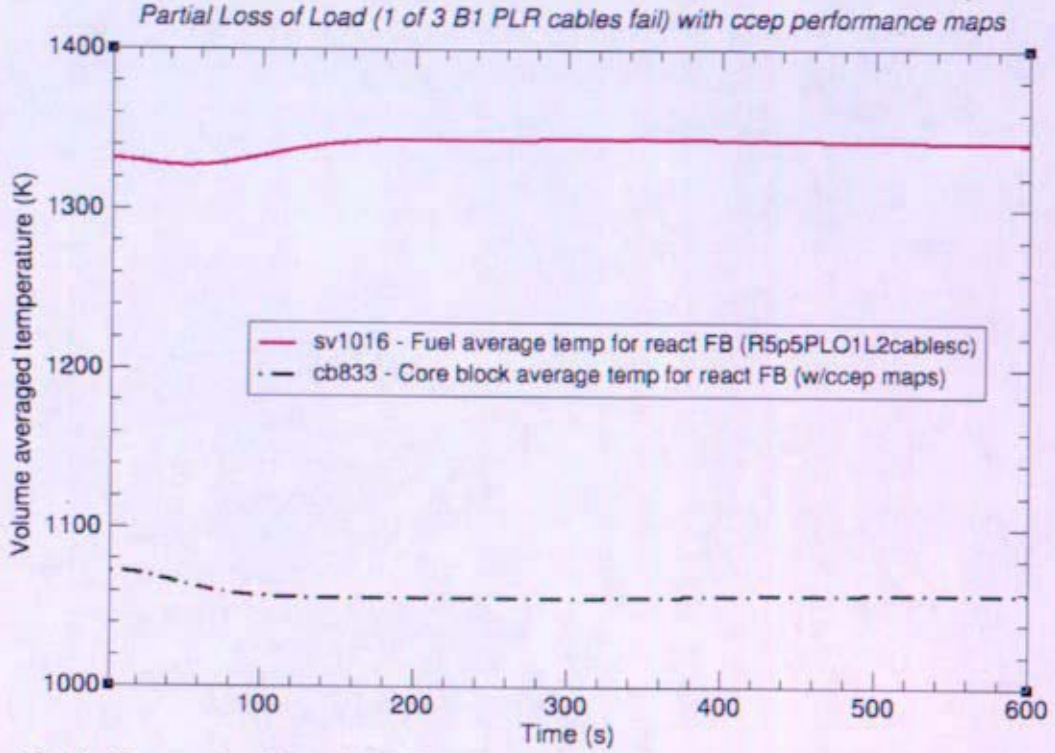



**Figure 12-49: Temps for Reactivity Feedback for Brayton 1 Partial Loss of Load (TRACE)**

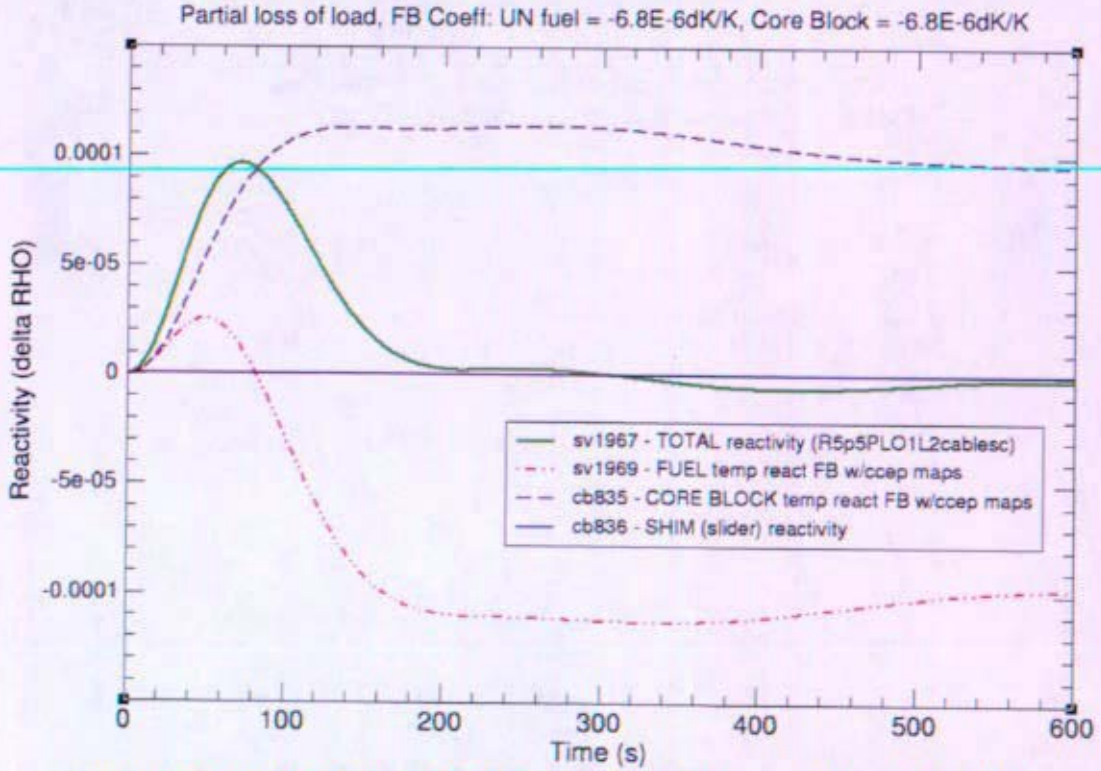



**Figure 12-50: Reactivity for Brayton 1 Partial Loss of Load (TRACE)**

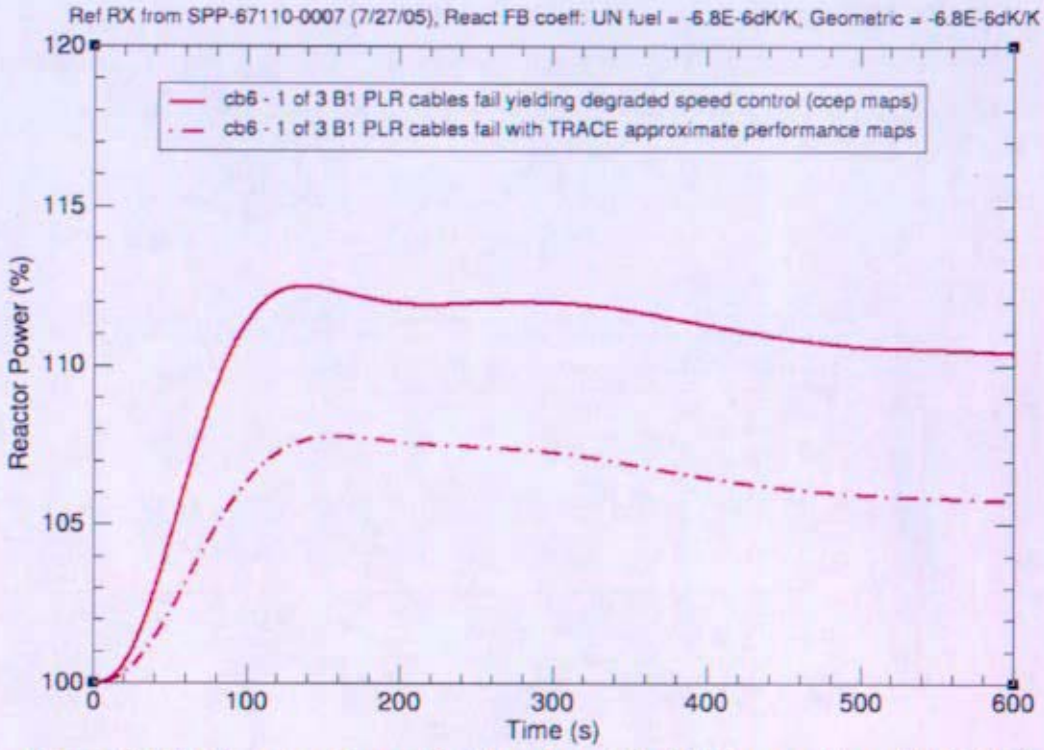



**Figure 12-51: Reactor Power for Brayton 1 Partial Loss of Load (TRACE)**

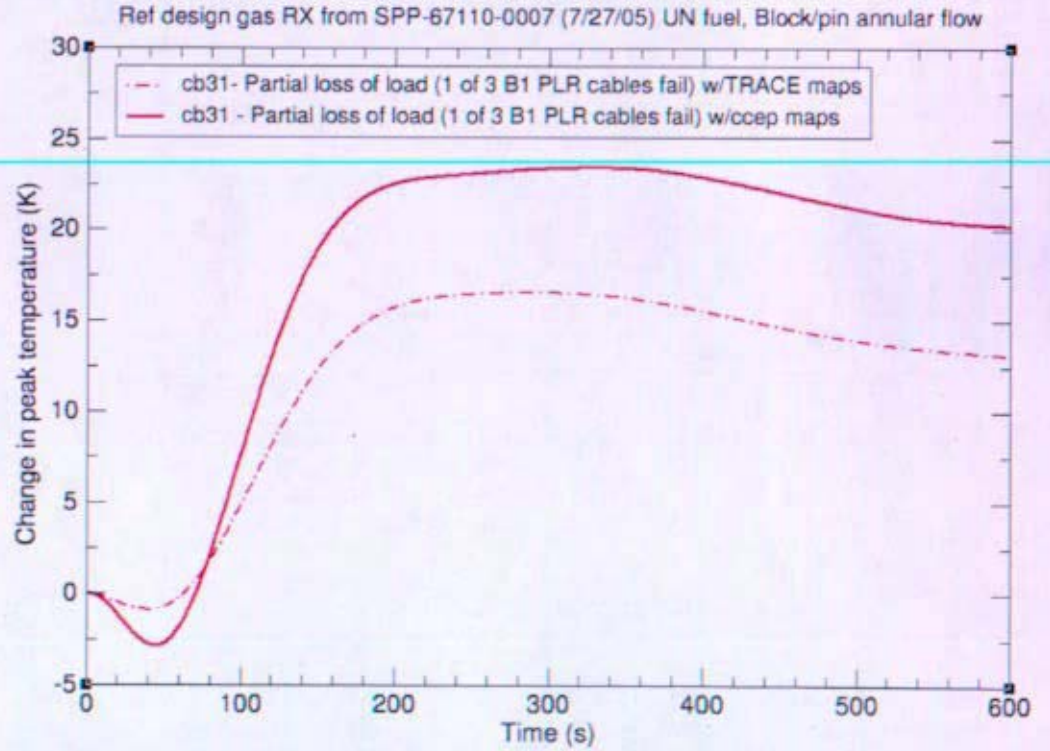



**Figure 12-52: Hot Spot Fuel Temperature for Brayton 1 Partial Loss of Load (TRACE)**

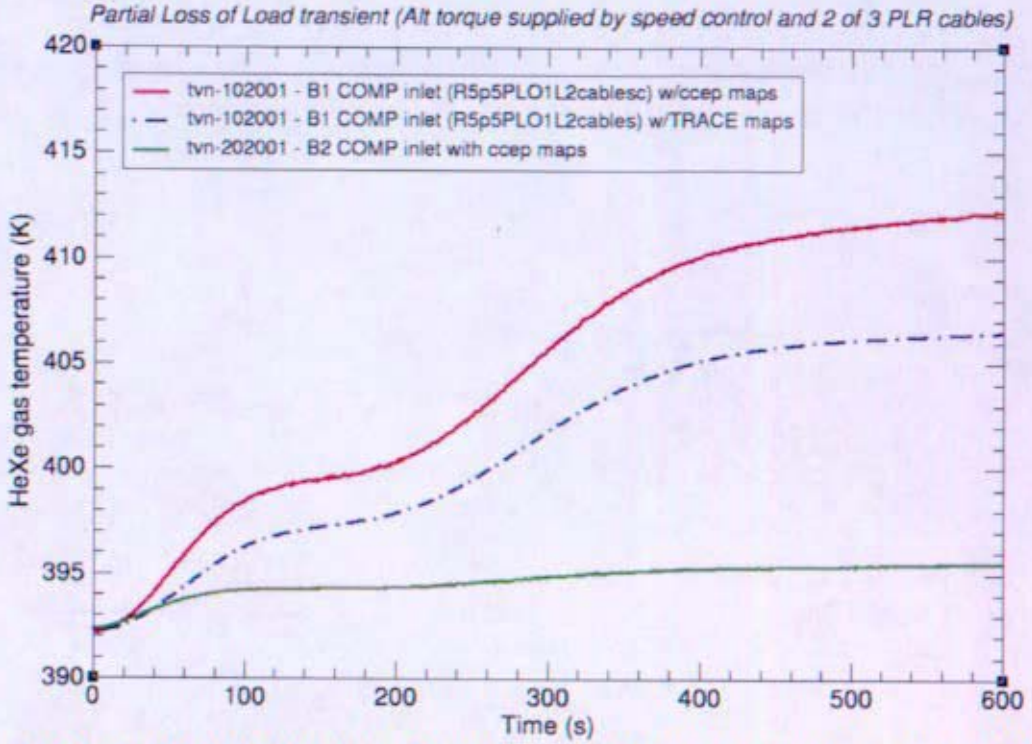



**Figure 12-53: Brayton Compressor Temp for Brayton 1 Partial Loss of Load (TRACE)**

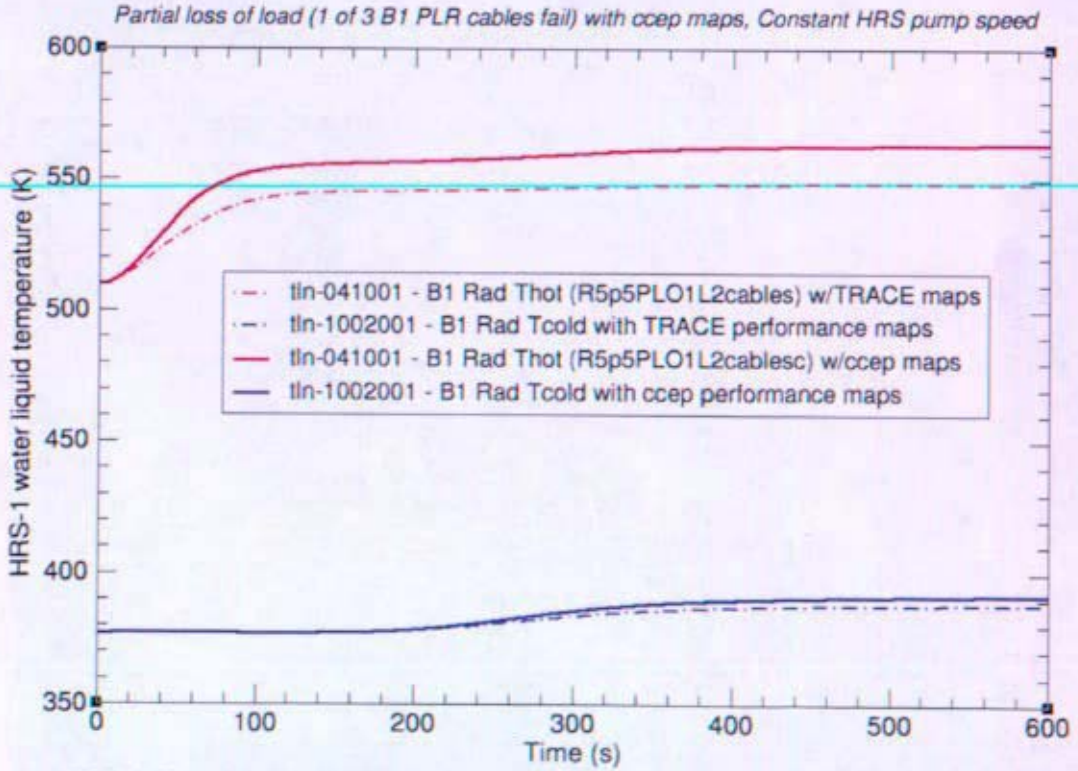



**Figure 12-54: Gas Cooler Water Temps for Brayton 1 Partial Loss of Load (TRACE)**

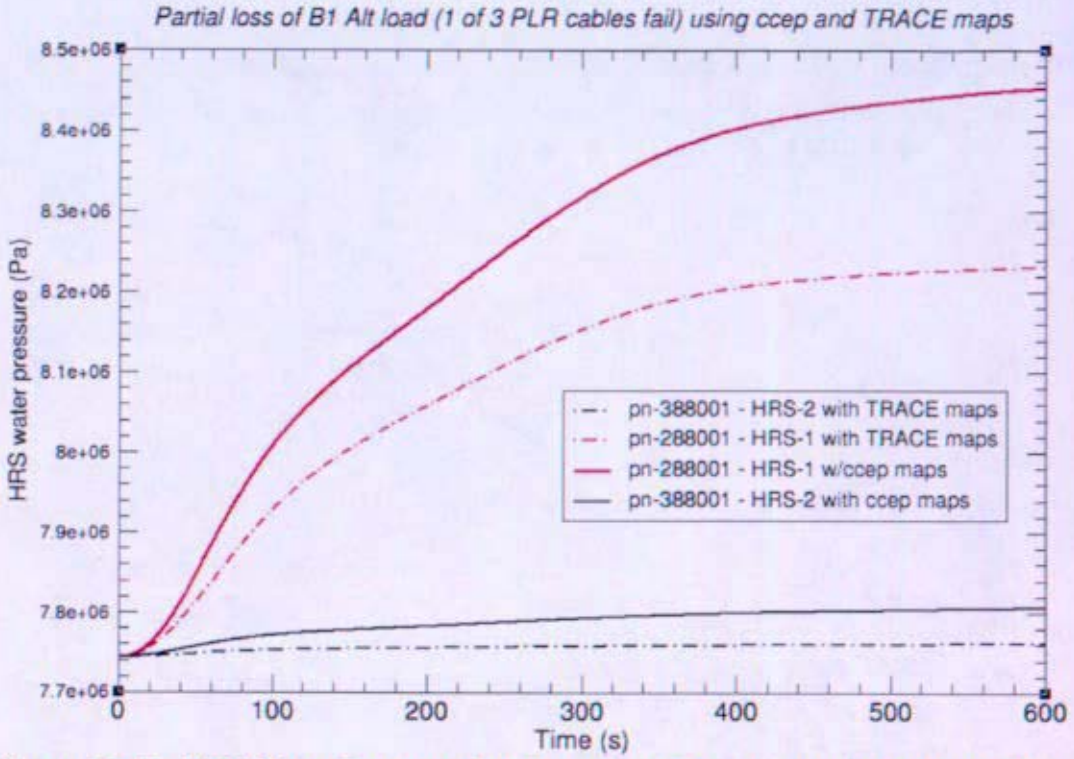



**Figure 12-55: HRS Water Pressure for Brayton 1 Partial Loss of Load (TRACE)**

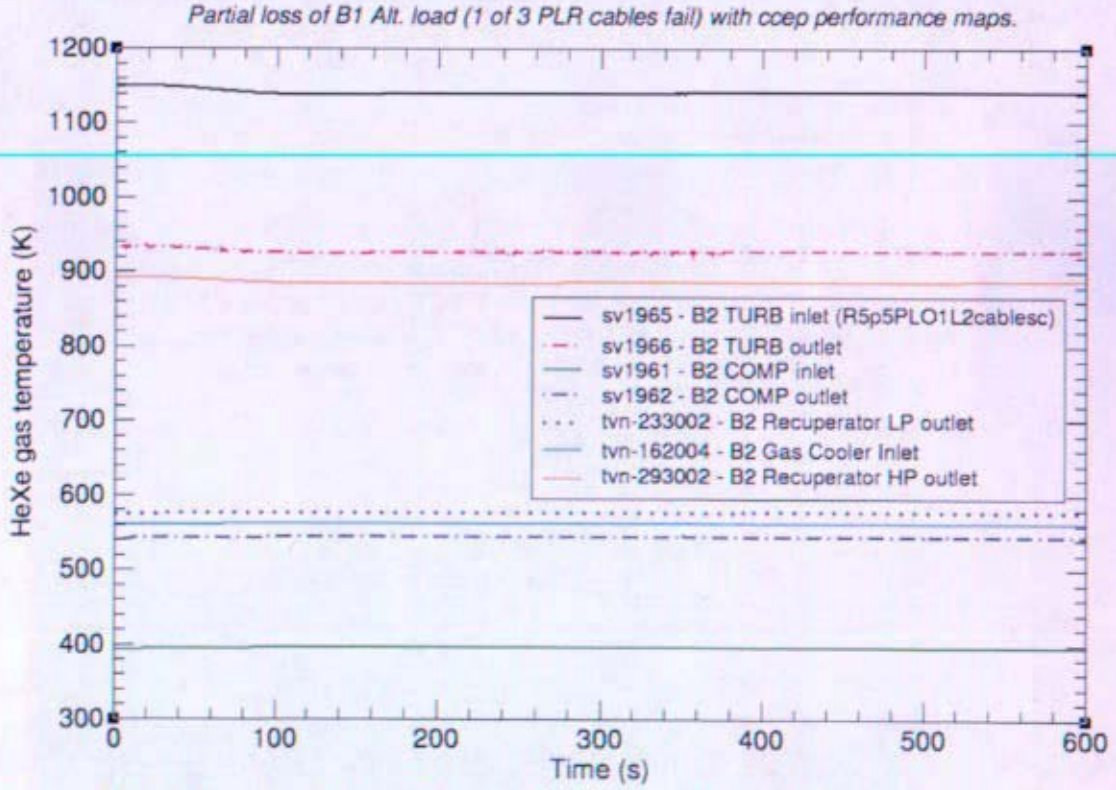



**Figure 12-56: Brayton 2 Loop Temps for Brayton 1 Partial Loss of Load (TRACE)**

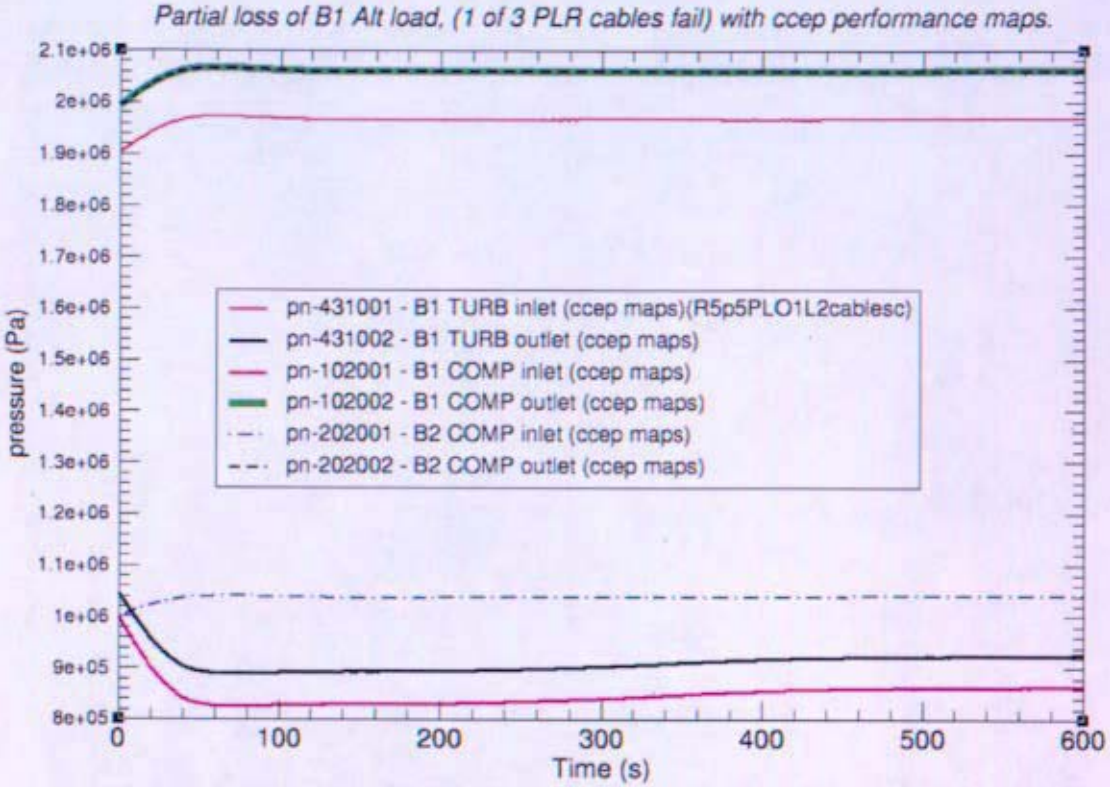



**Figure 12-57: Primary Pressure for Brayton 1 Partial Loss of Load (TRACE)**

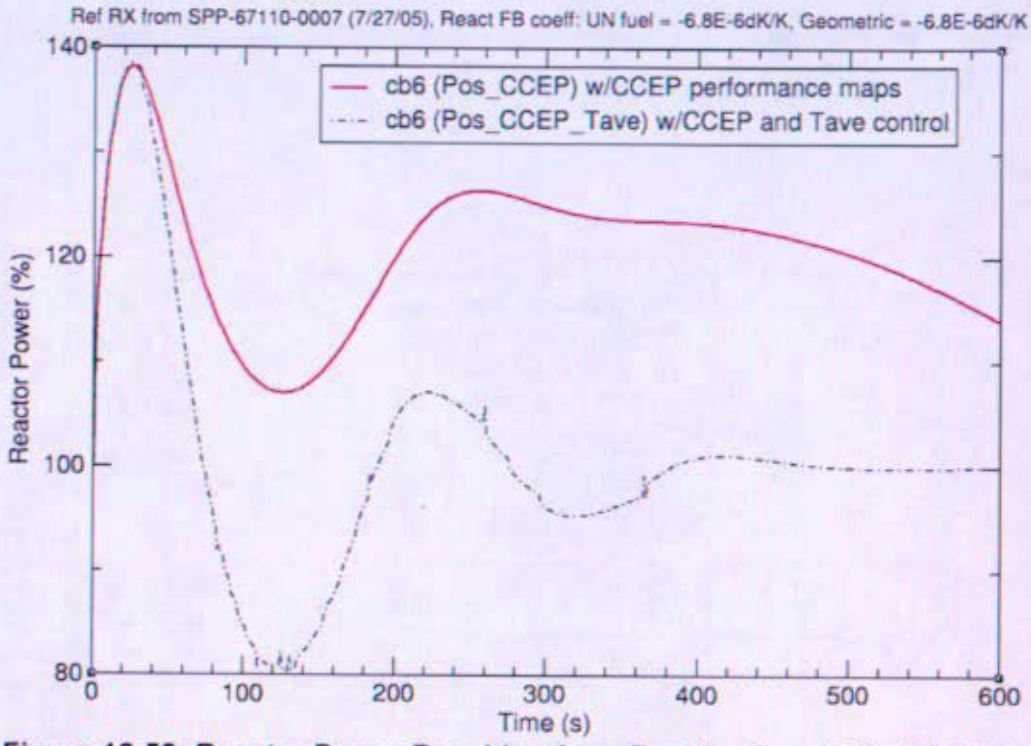



**Figure 12-58: Reactor Power Resulting from Positive Reactivity (TRACE)**

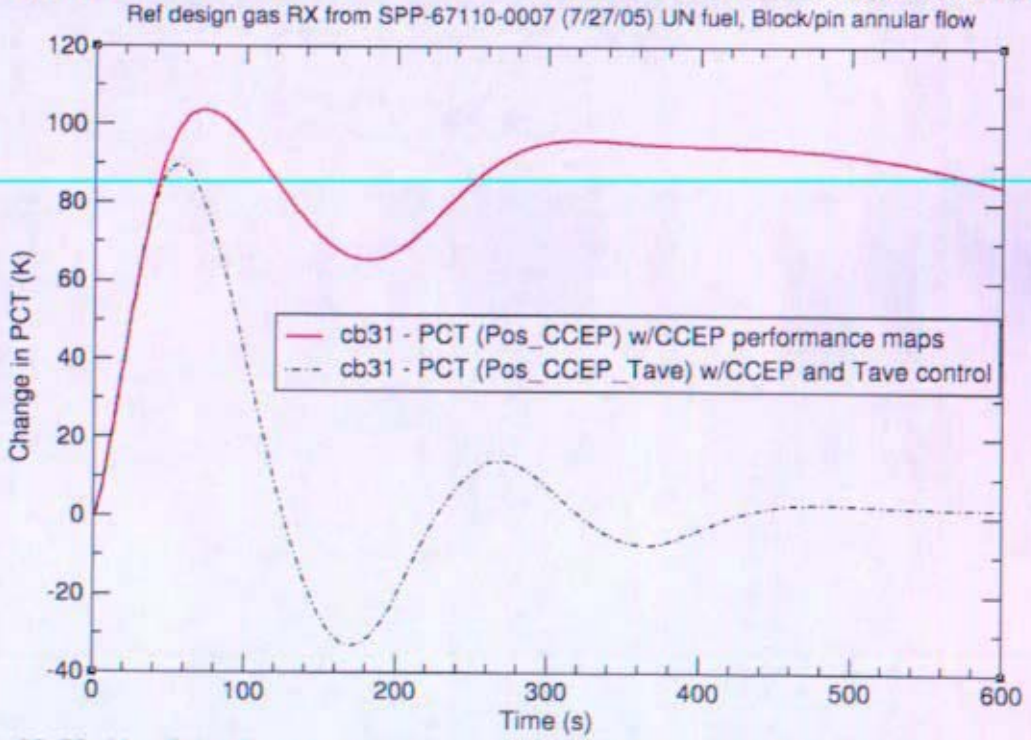



**Figure 12-59: Hot Spot Fuel Temperature Resulting from Positive Reactivity (TRACE)**

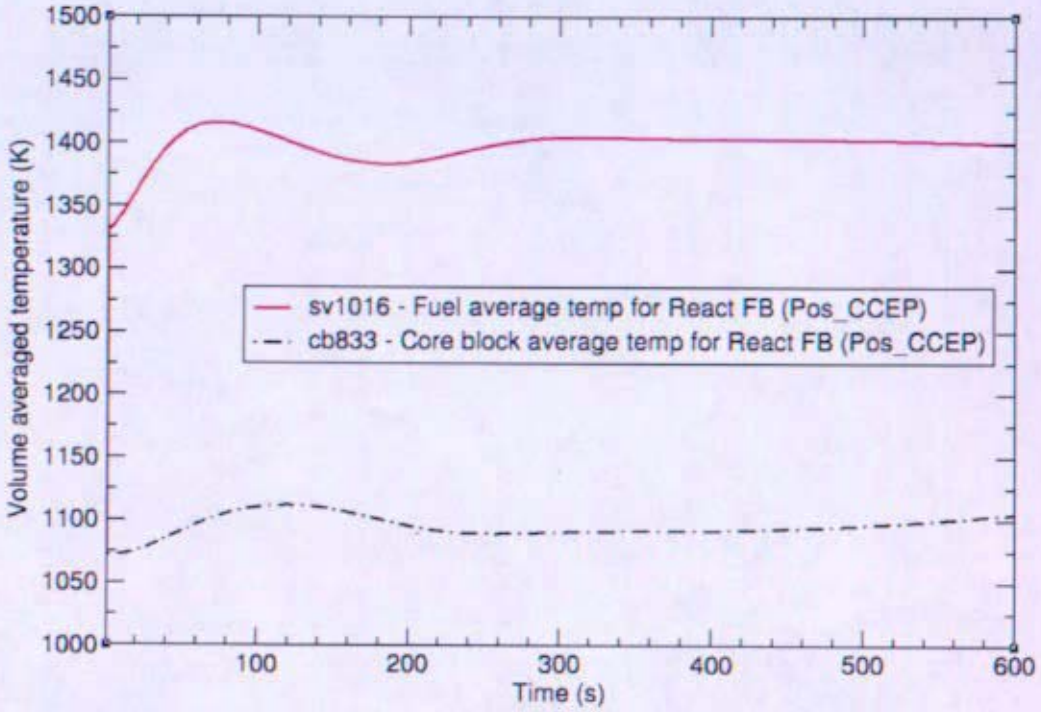



**Figure 12-60: Temps for Reactivity Feedback for Positive Reactivity without $T_{ave}$ Control (TRACE)**

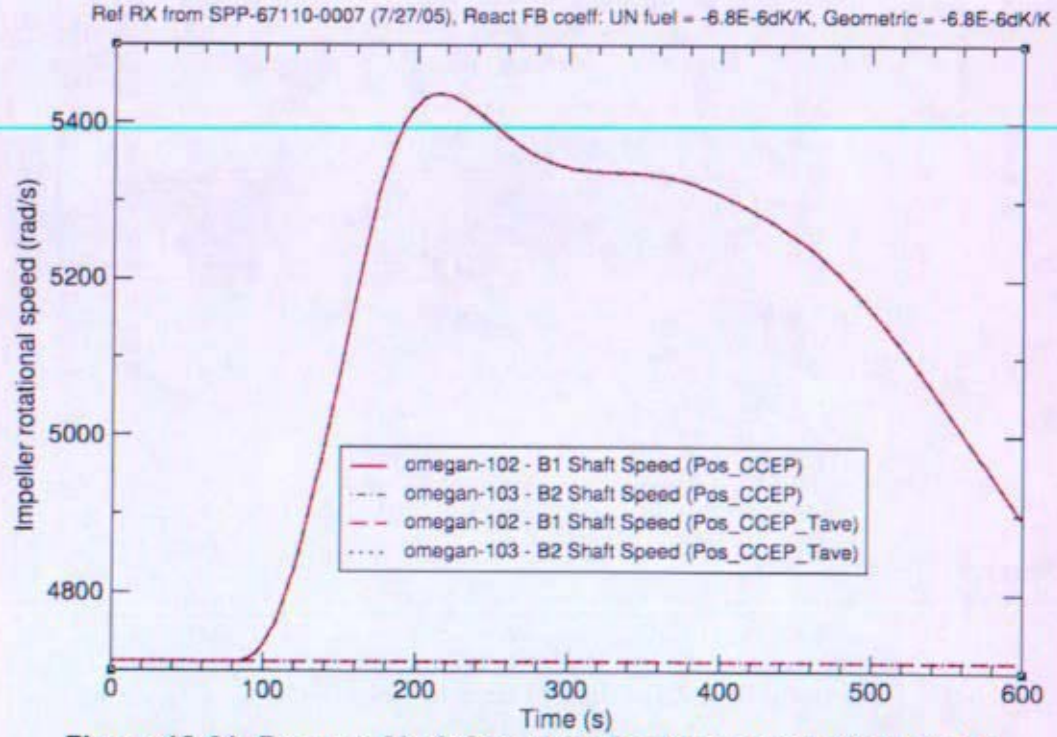



**Figure 12-61: Brayton Shaft Speed for Positive Reactivity (TRACE)**

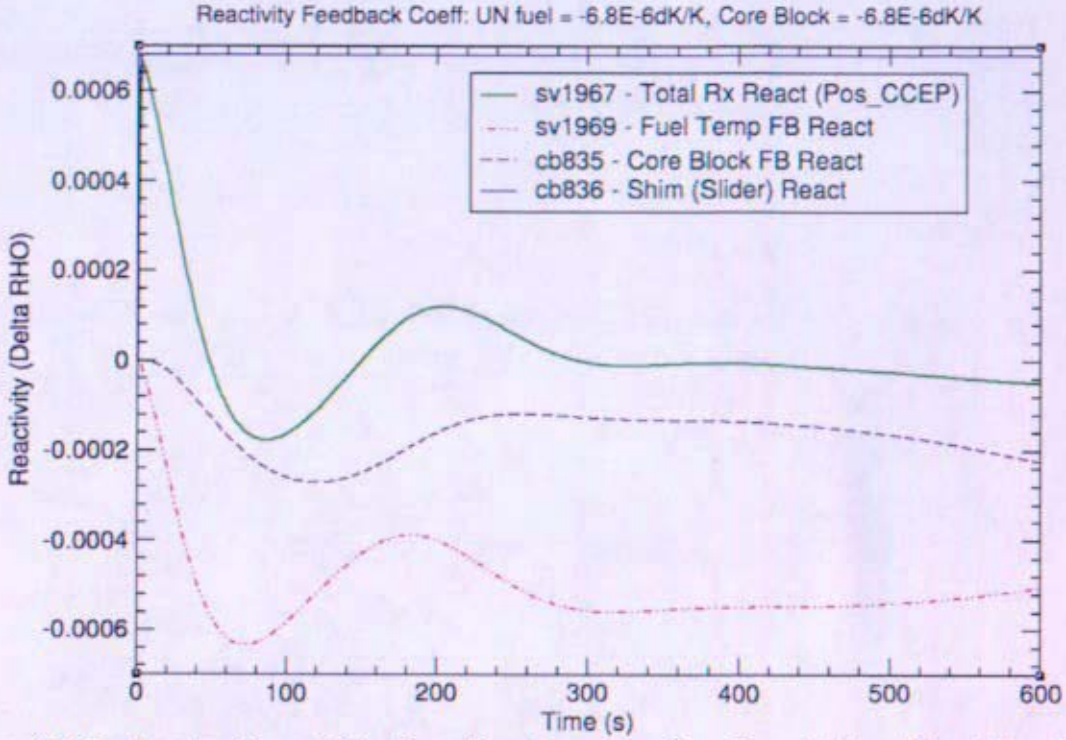



**Figure 12-62: Reactor Reactivity Resulting from Positive Reactivity without $T_{ave}$ Control (TRACE)**

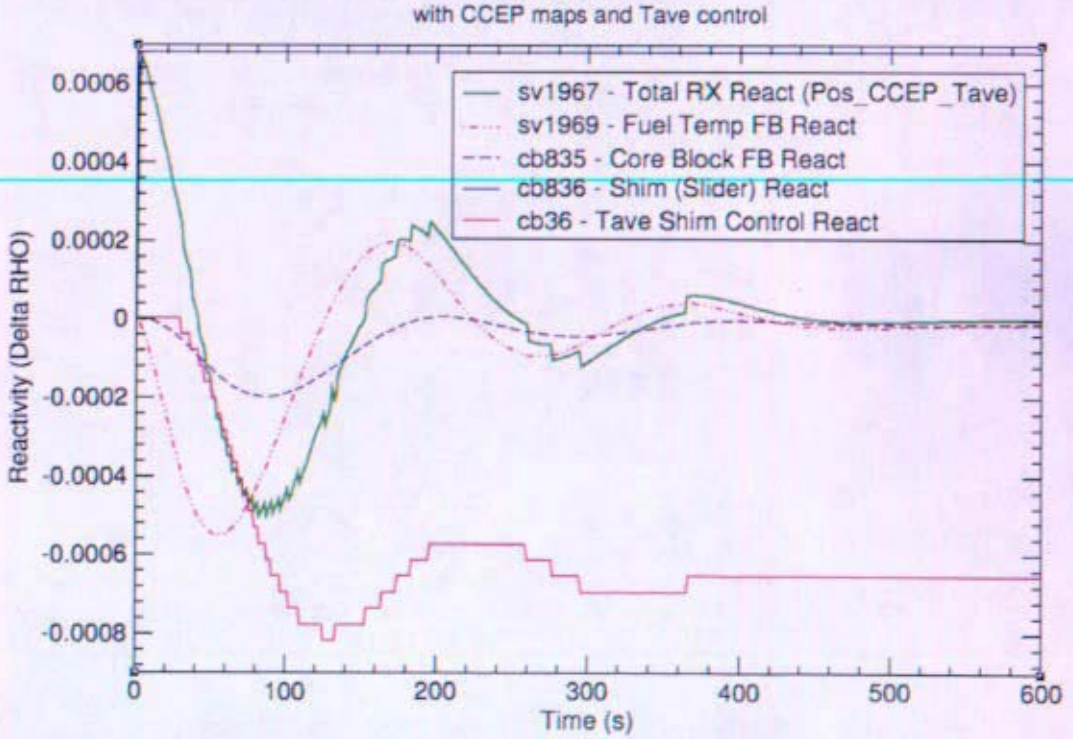



**Figure 12-63: Reactor Reactivity Resulting from Positive Reactivity with $T_{ave}$ Control (TRACE)**

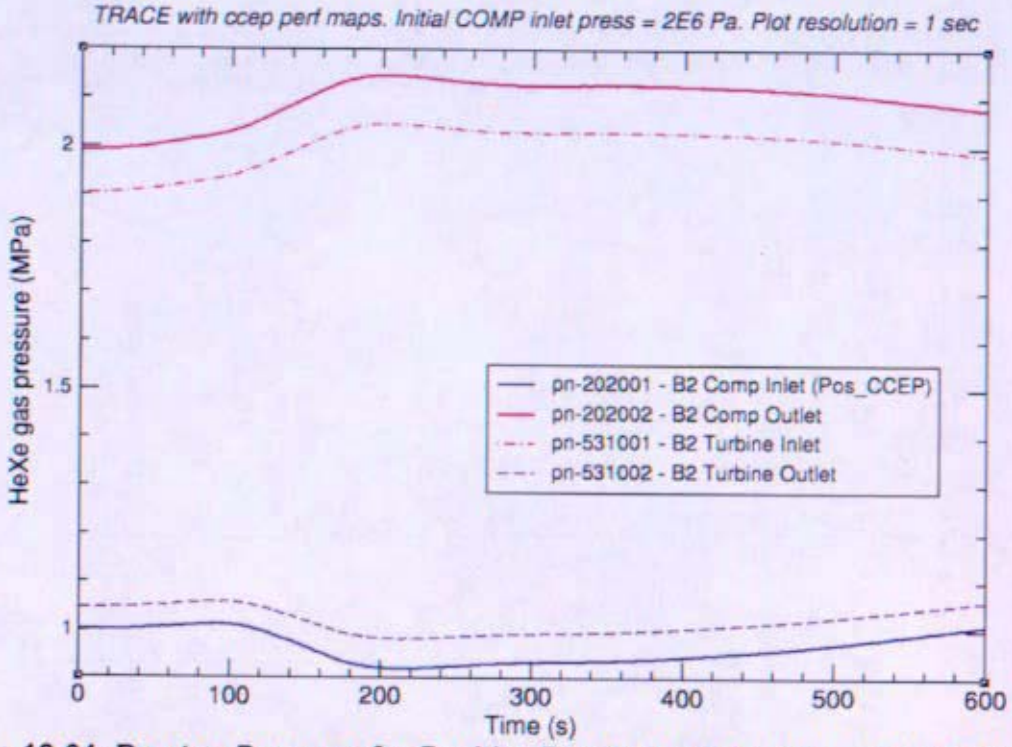



**Figure 12-64: Brayton Pressure for Positive Reactivity without $T_{ave}$ Control (TRACE)**

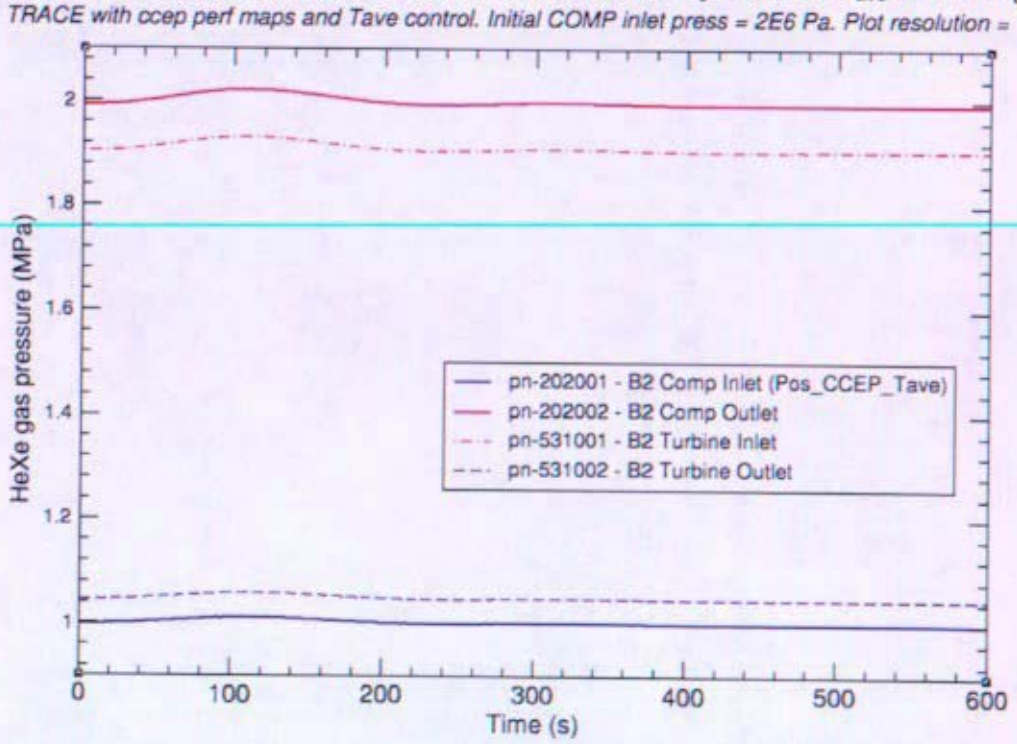



**Figure 12-65: Brayton Pressure for Positive Reactivity with $T_{ave}$ Control (TRACE)**

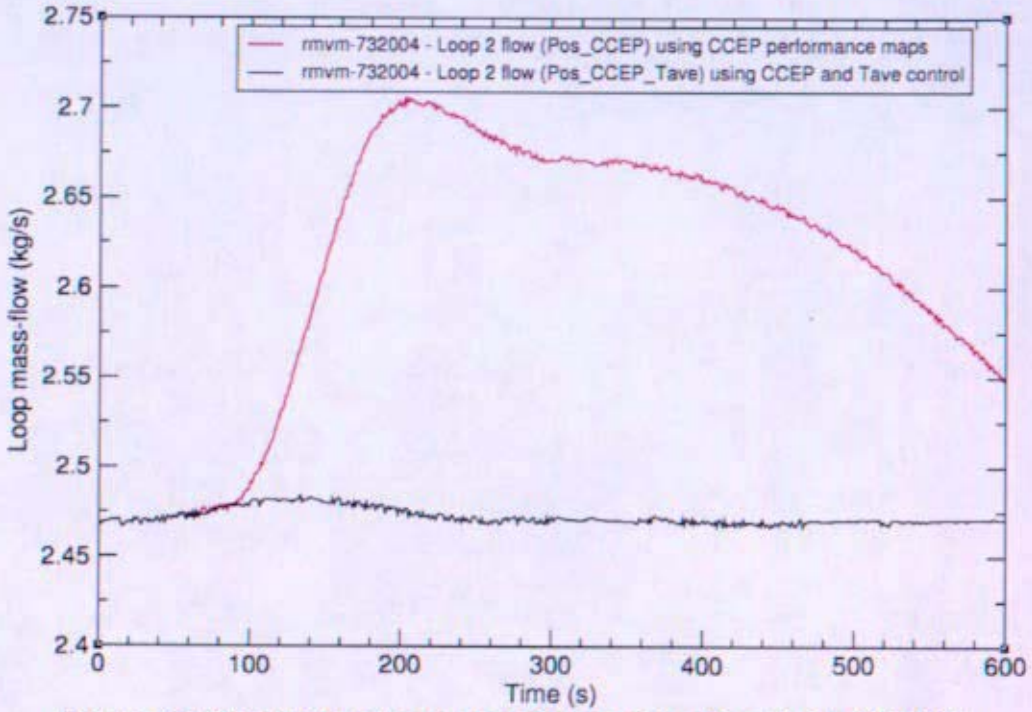



**Figure 12-66: Brayton Loop Flow for Positive Reactivity (TRACE)**

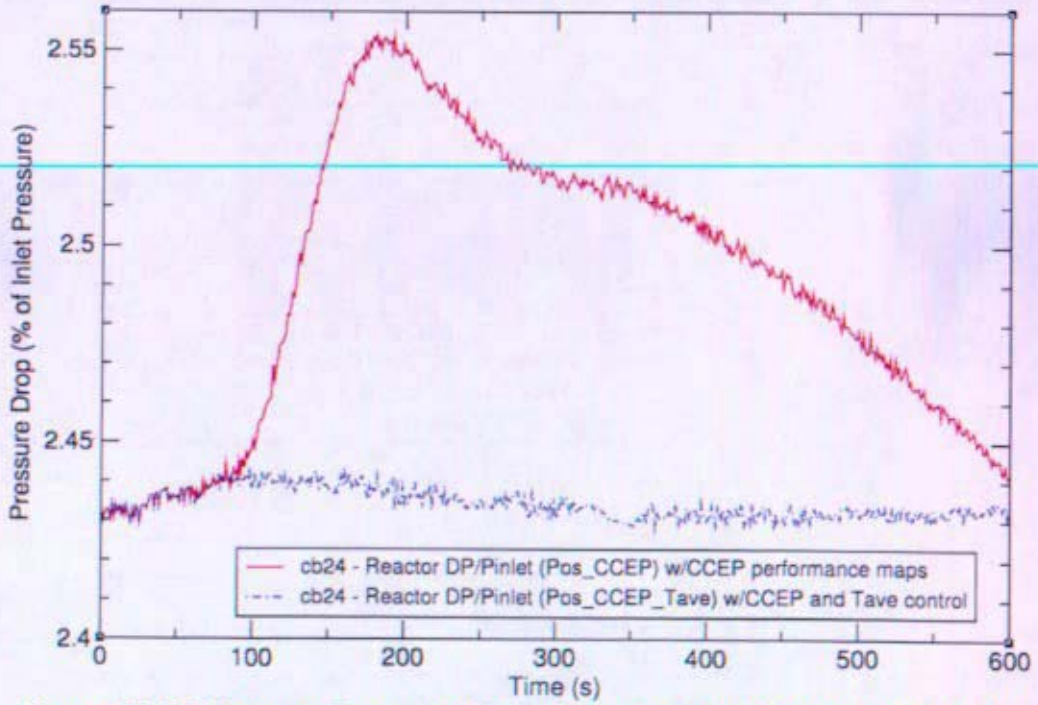



**Figure 12-67: Reactor Pressure Change for Positive Reactivity (TRACE)**

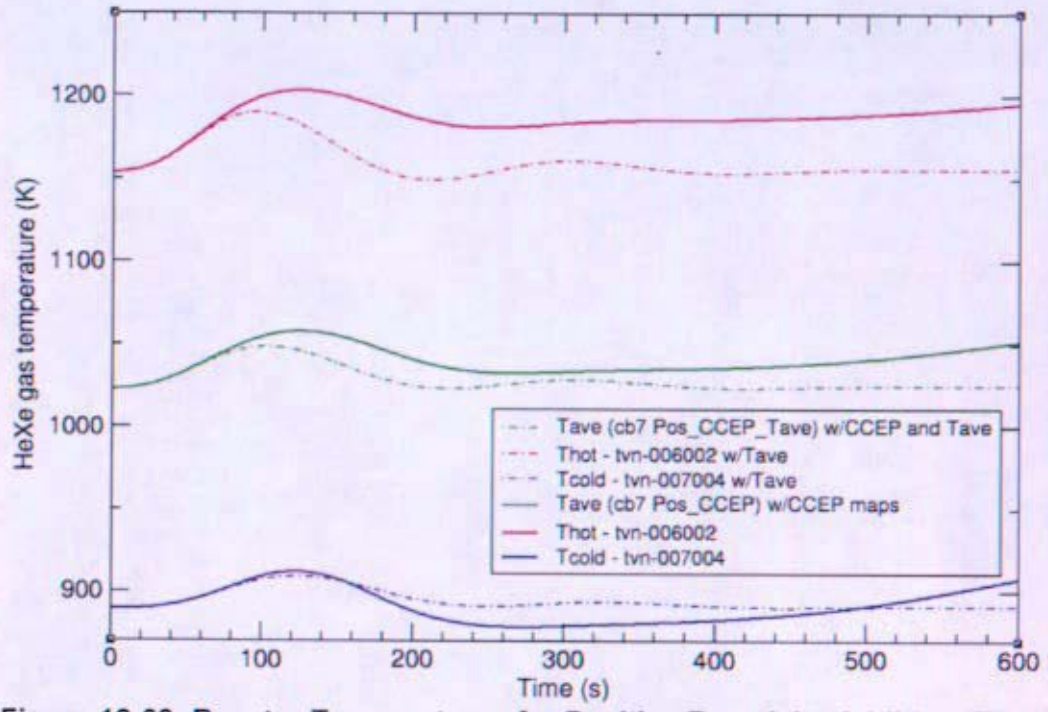



**Figure 12-68: Reactor Temperatures for Positive Reactivity Addition (TRACE)**

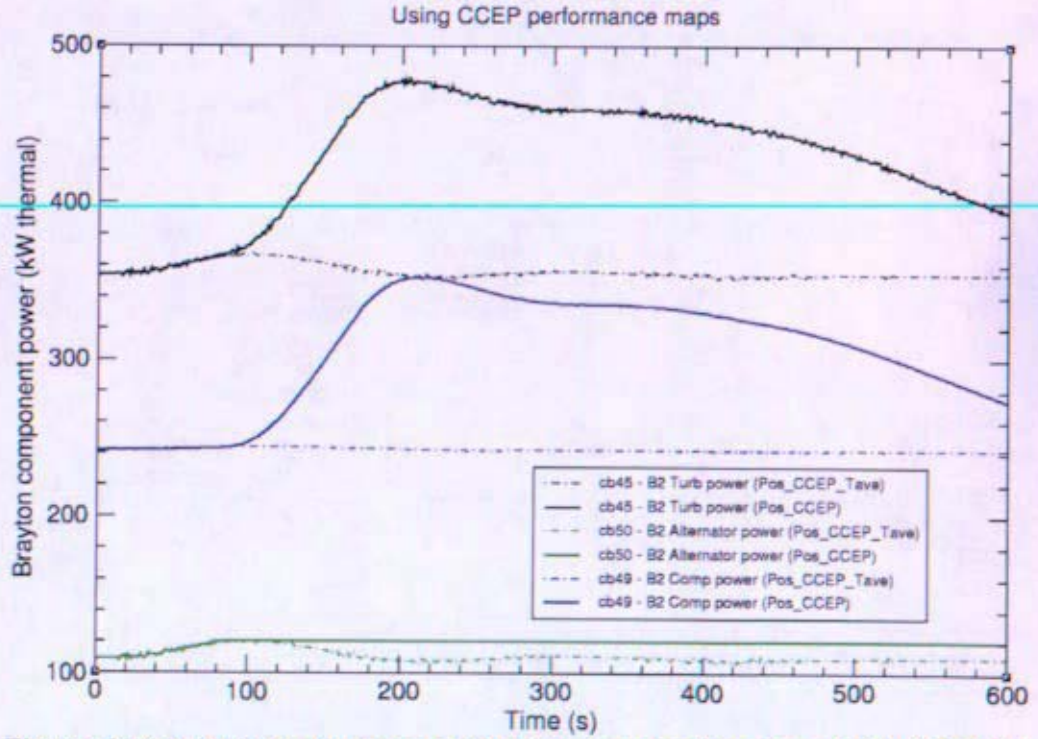



**Figure 12-69: Brayton Component Power for Positive Reactivity (TRACE)**

*ccep maps used.*

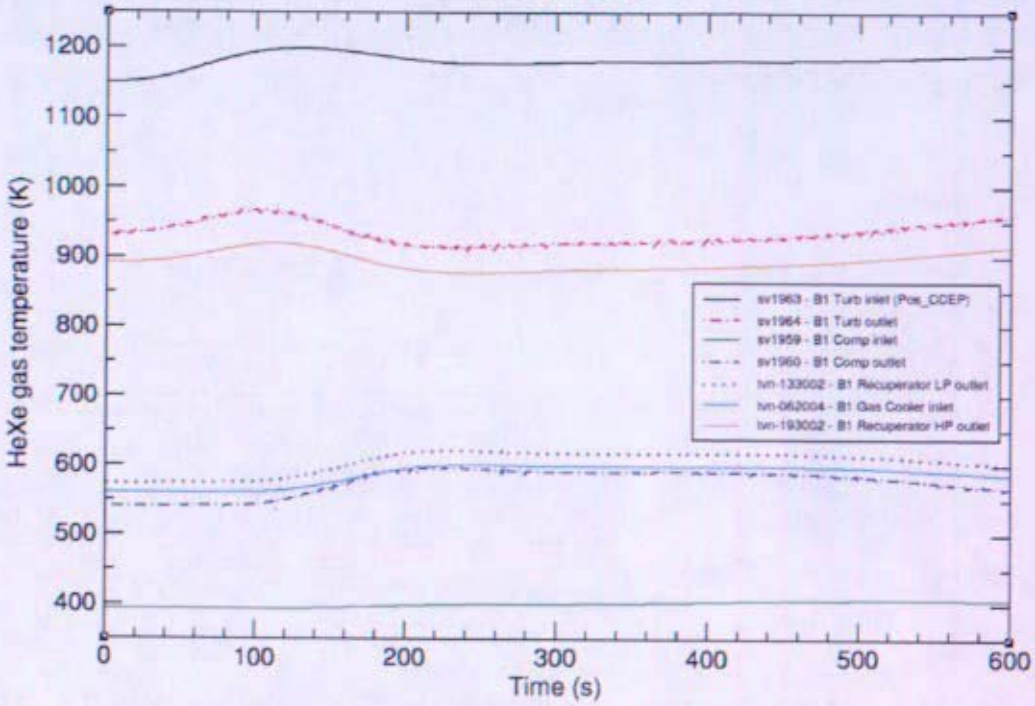



**Figure 12-70: Brayton Loop Temperatures for Positive Reactivity without $T_{ave}$ Control (TRACE)**

*Using CCEP maps and Tave control*

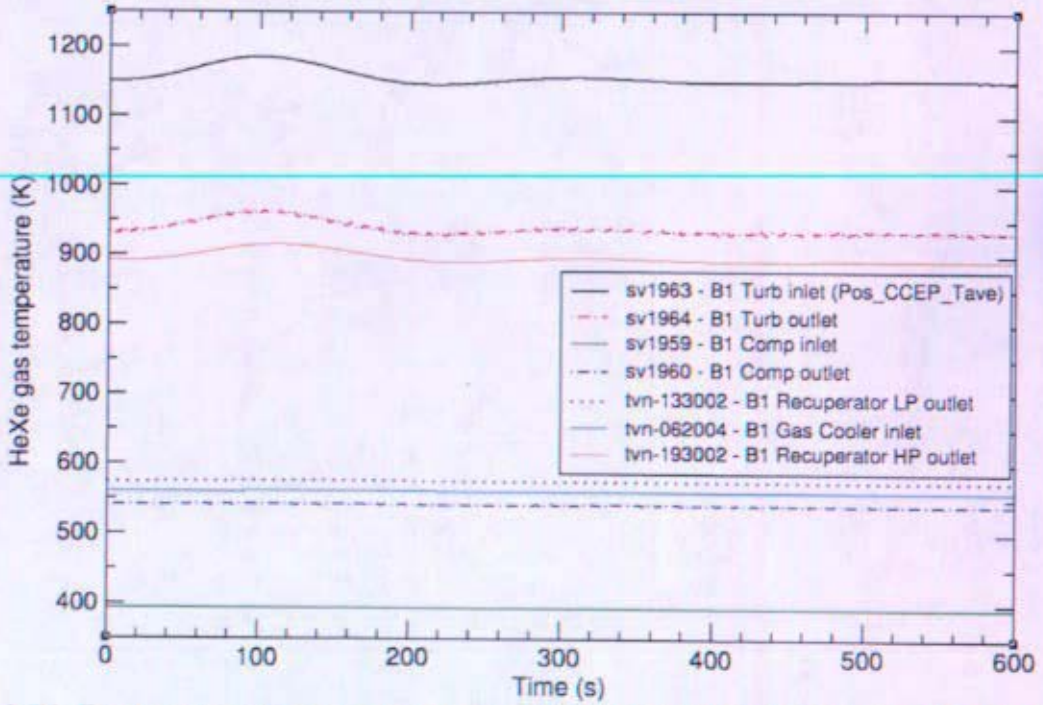



**Figure 12-71: Brayton Loop Temperatures for Positive Reactivity with $T_{ave}$ Control (TRACE)**

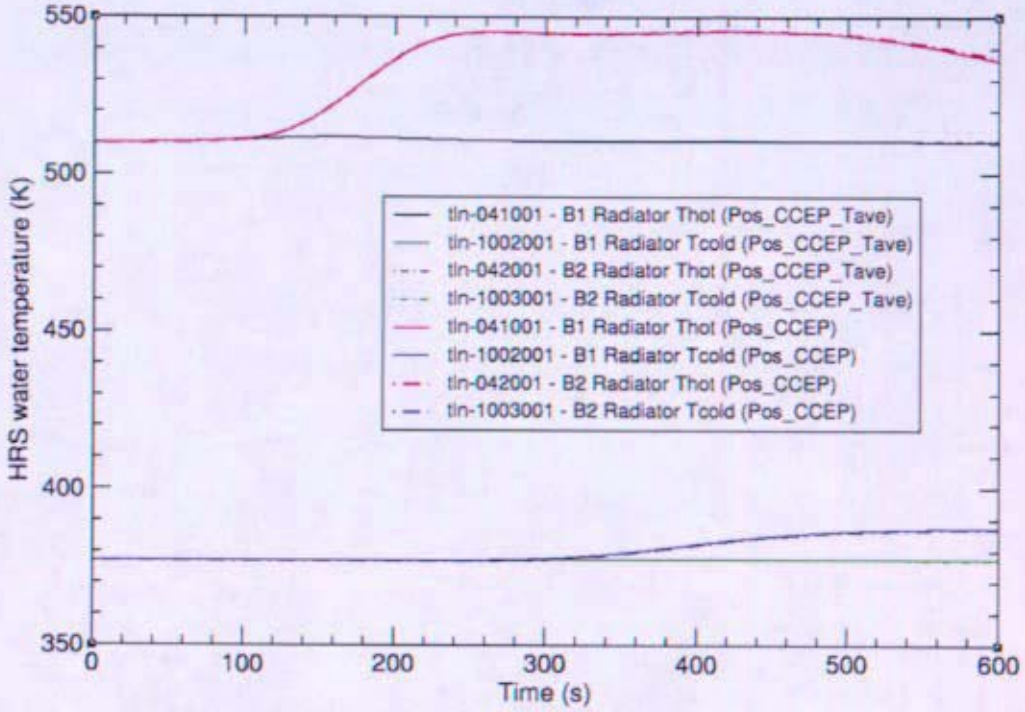



**Figure 12-72: Gas Cooler Water Temperatures for Positive Reactivity (TRACE)**

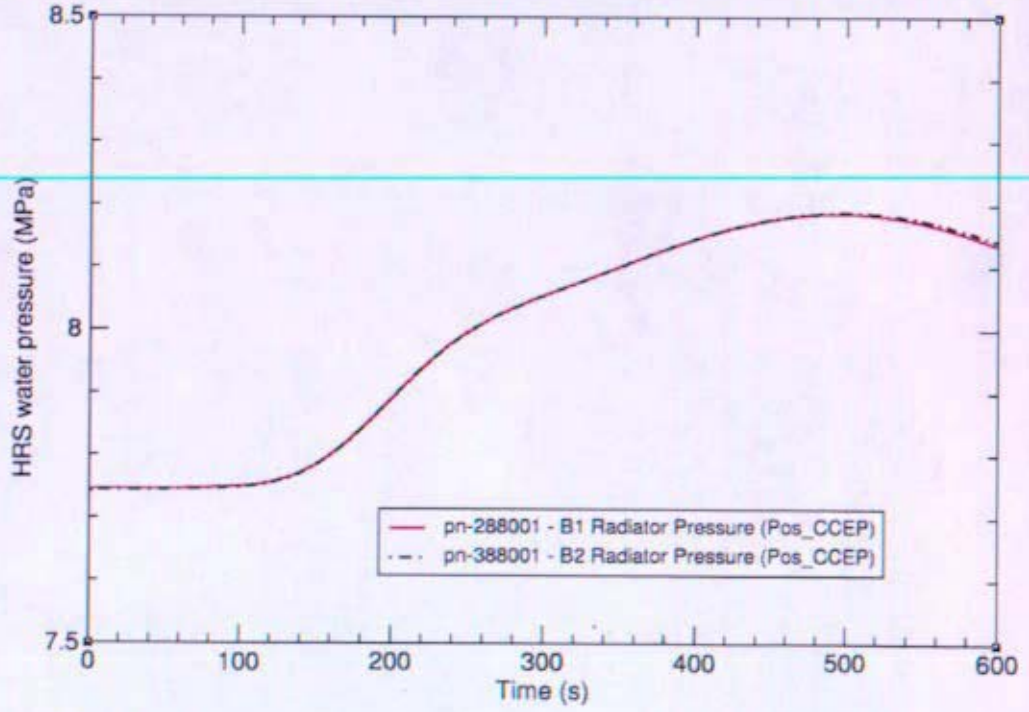



**Figure 12-73: Gas Cooler Water Pressure for Positive Reactivity without $T_{ave}$ Control (TRACE)**

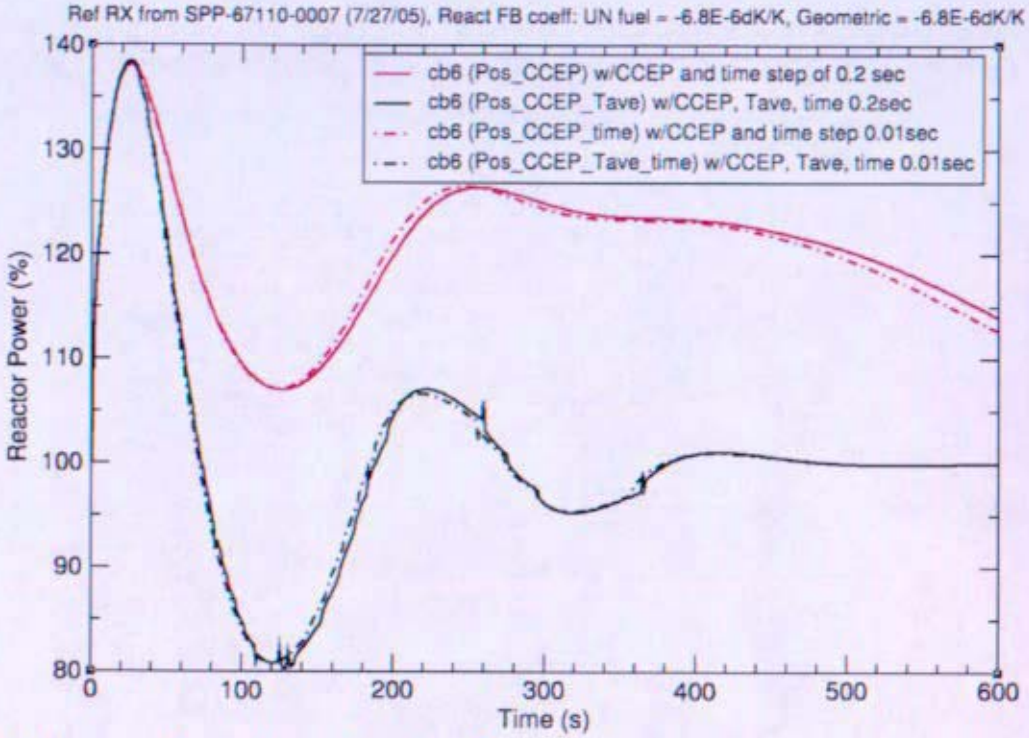



**Figure 12-74: Reactor Power Resulting from Positive Reactivity – Sensitivity to Time (TRACE)**

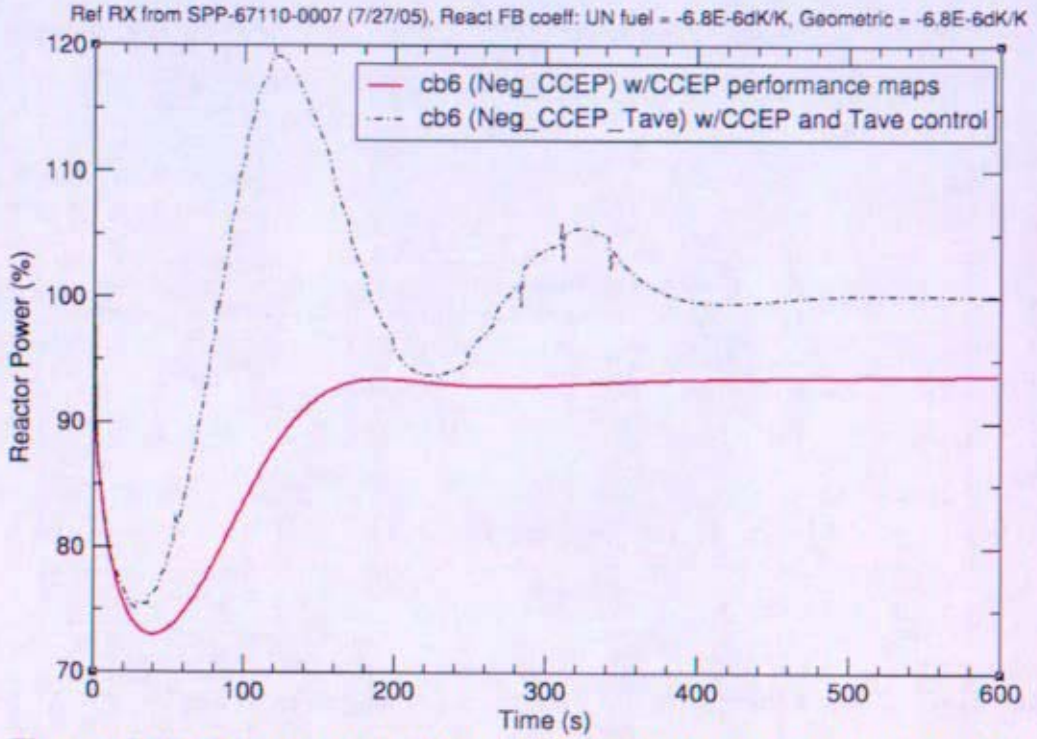



**Figure 12-75: Reactor Power Resulting from Negative Reactivity (TRACE)**

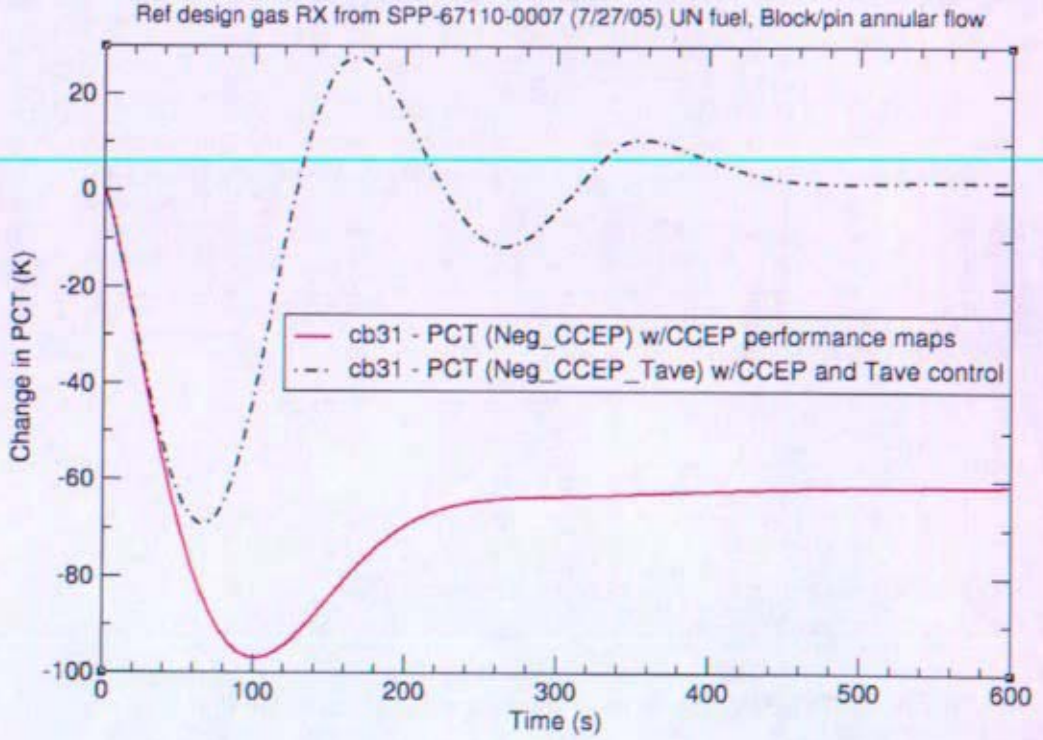



**Figure 12-76: Hot Spot Fuel Temperature Resulting from Negative Reactivity (TRACE)**

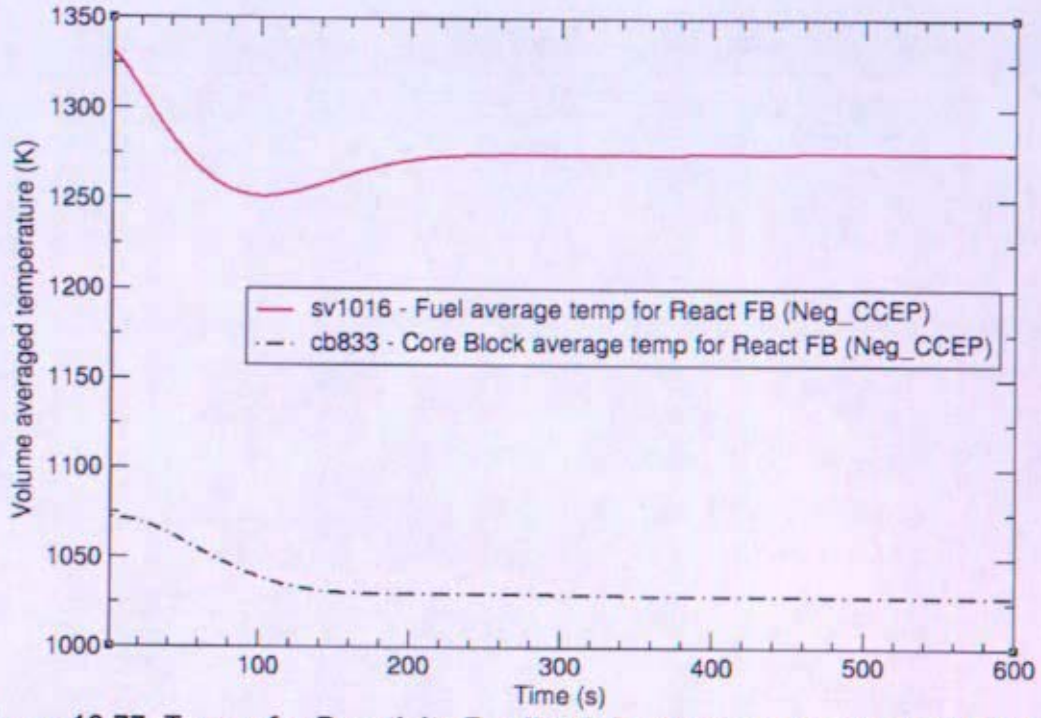



**Figure 12-77: Temps for Reactivity Feedback for Negative Reactivity (TRACE)**

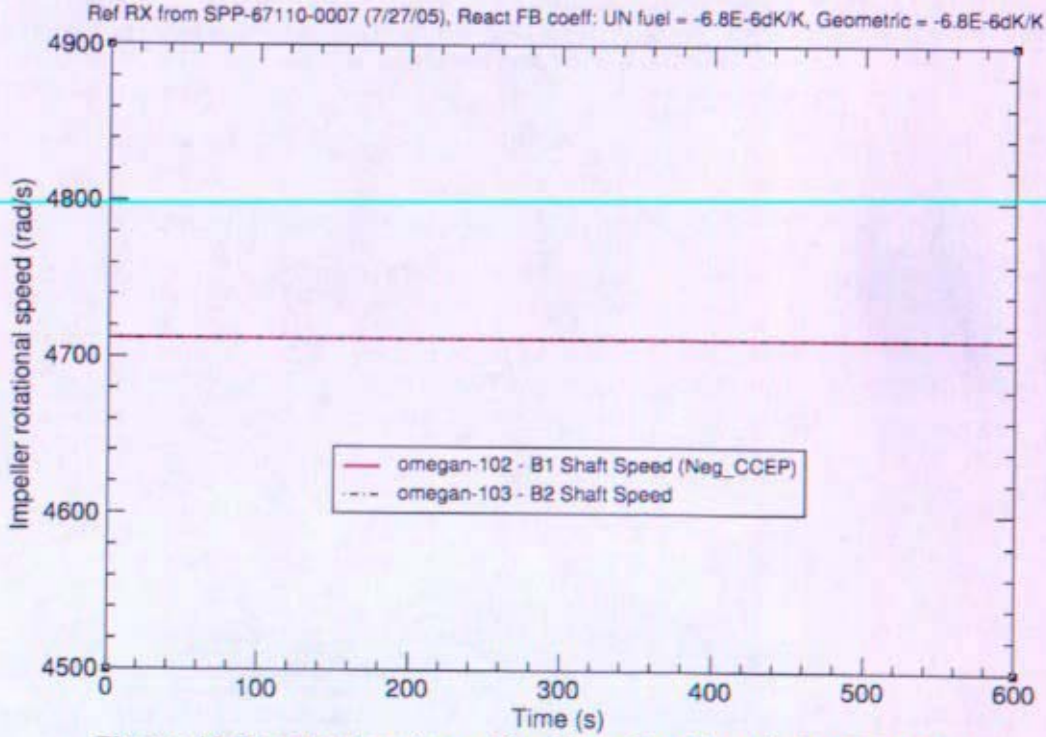



**Figure 12-78: Brayton Speed for Negative Reactivity (TRACE)**

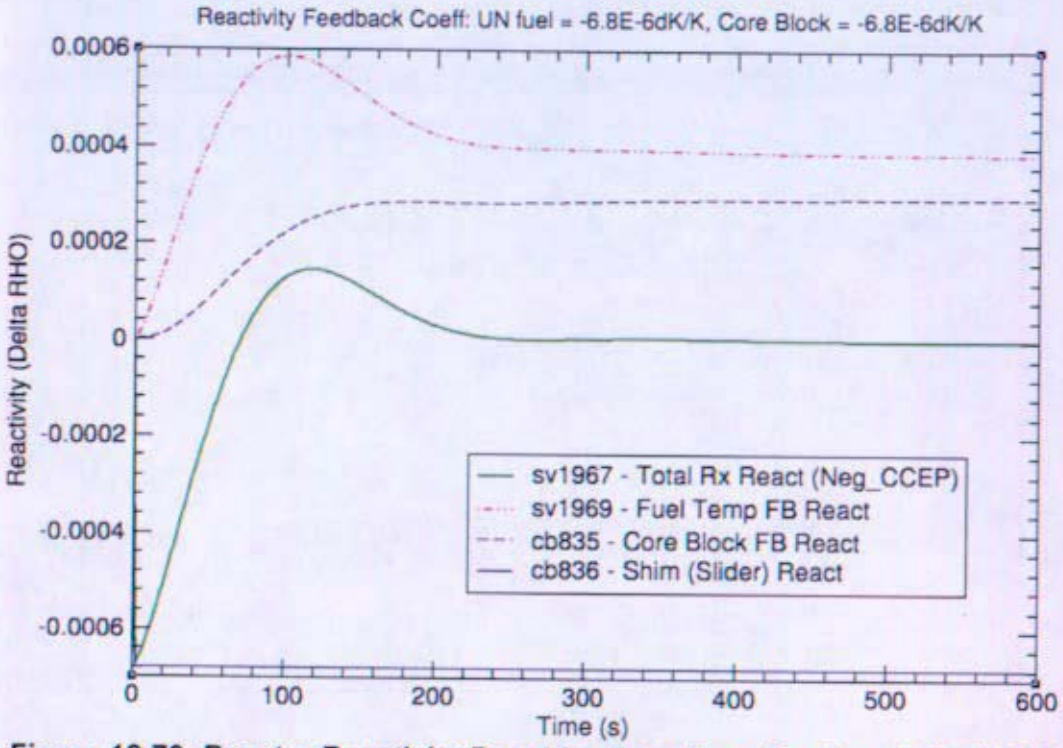



**Figure 12-79: Reactor Reactivity Resulting from Negative Reactivity (TRACE)**

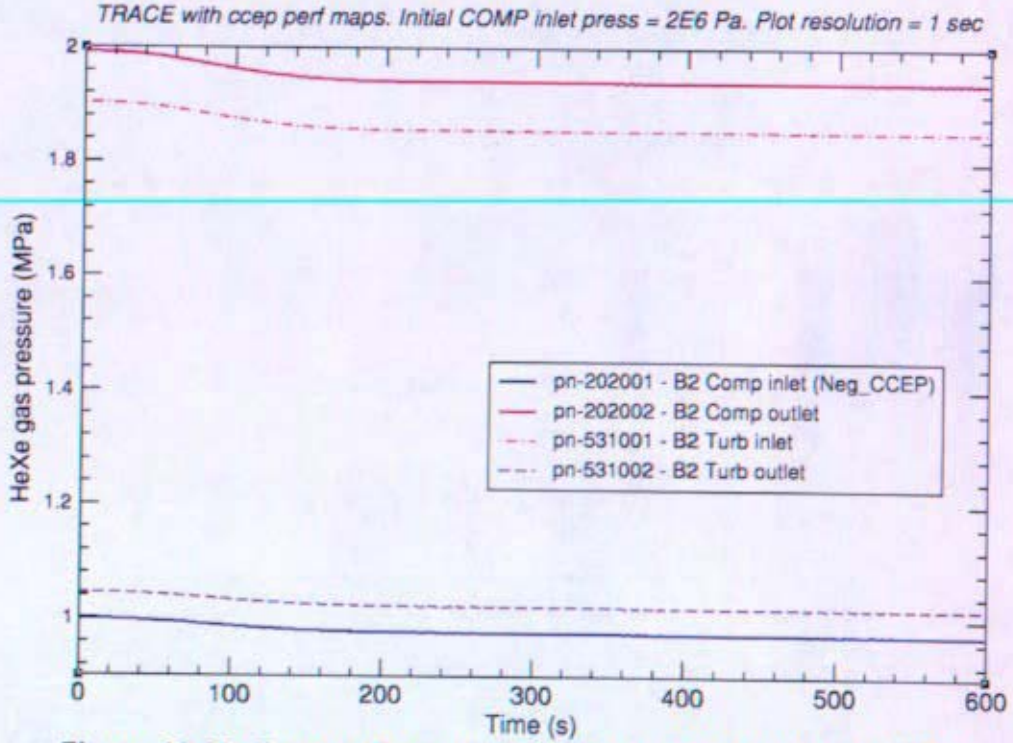



**Figure 12-80: Brayton Pressure for Negative Reactivity (TRACE)**

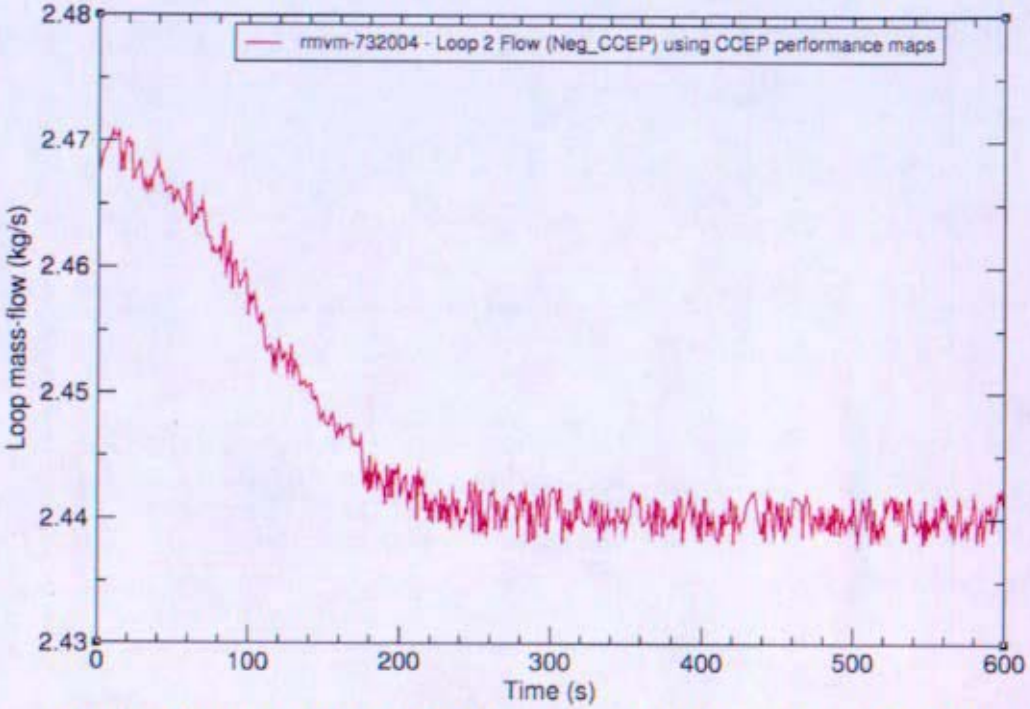



**Figure 12-81: Brayton Loop Flow for Negative Reactivity (TRACE)**

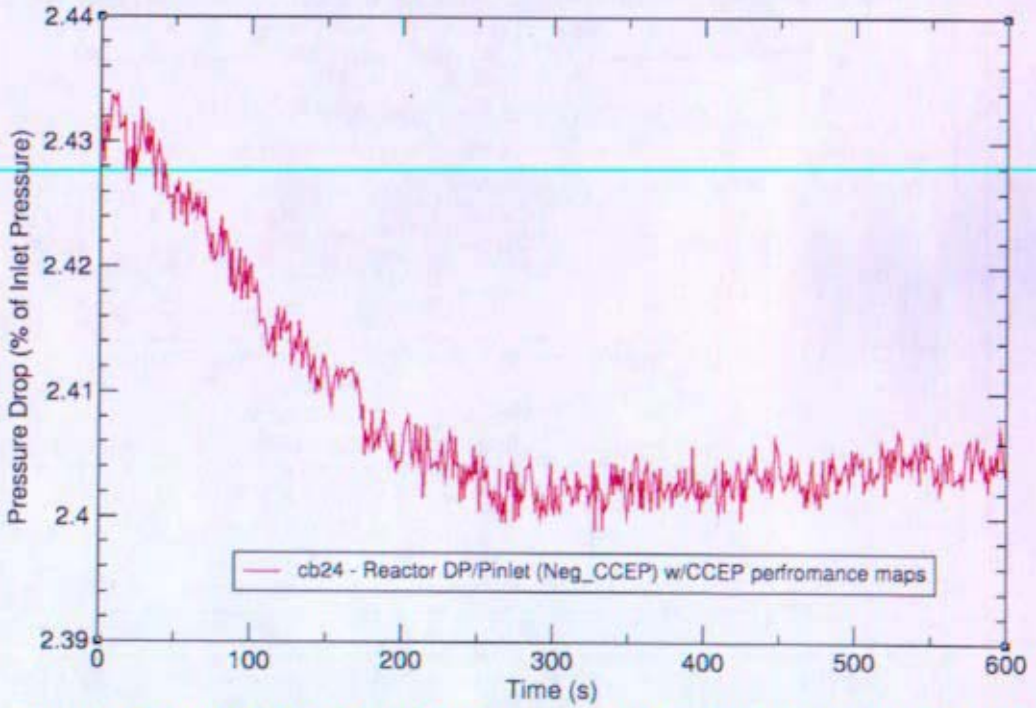



**Figure 12-82: Reactor Pressure Change for Negative Reactivity (TRACE)**

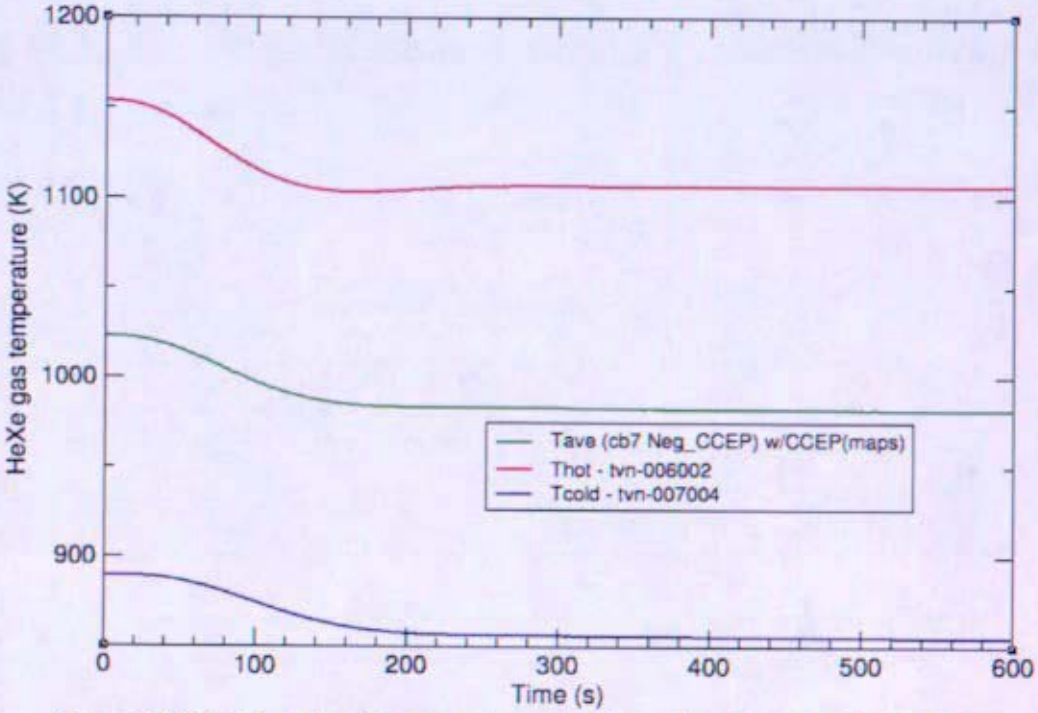



**Figure 12-83: Reactor Temperature for Negative Reactivity (TRACE)**

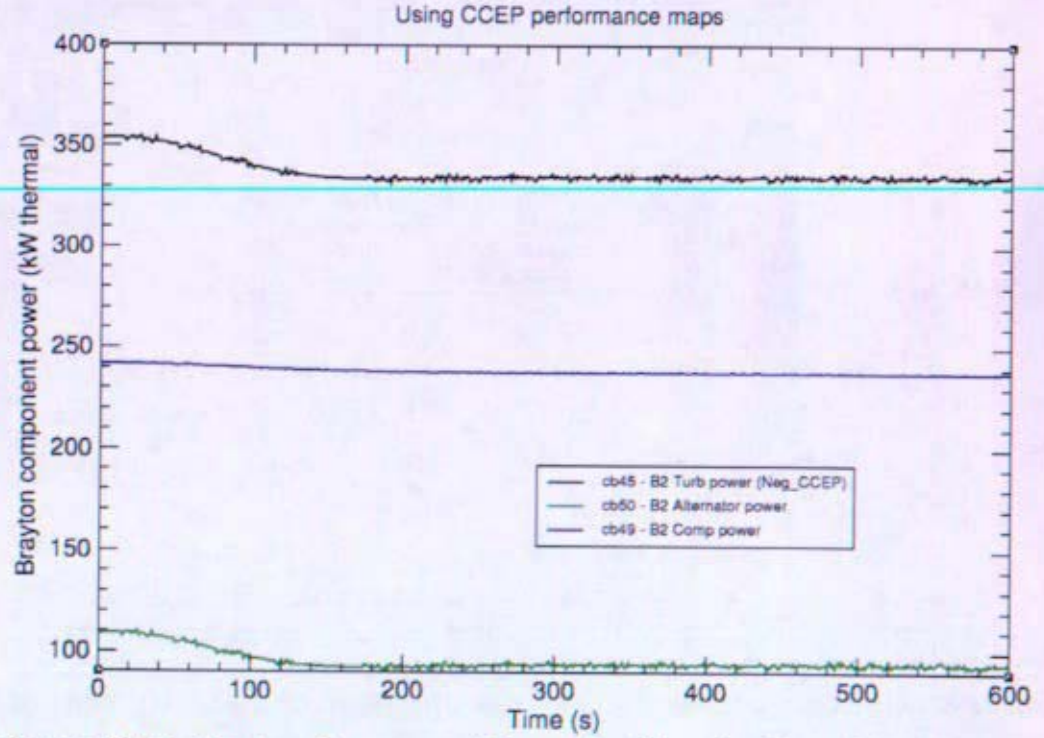



**Figure 12-84: Brayton Component Power for Negative Reactivity (TRACE)**

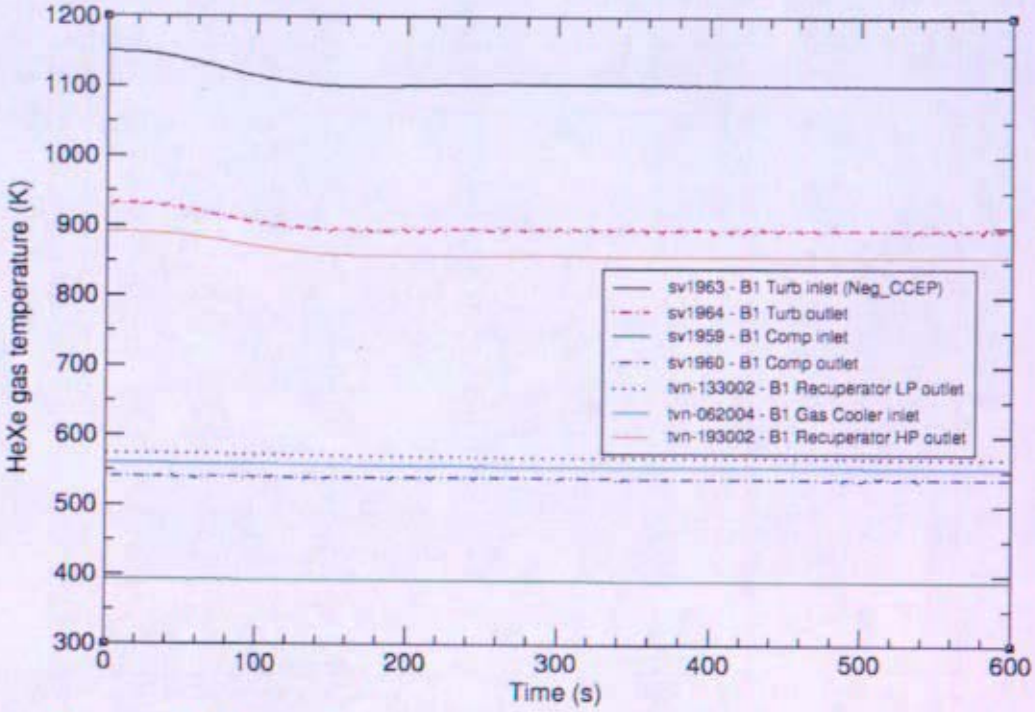



**Figure 12-85: Loop Temperatures for Negative Reactivity (TRACE)**

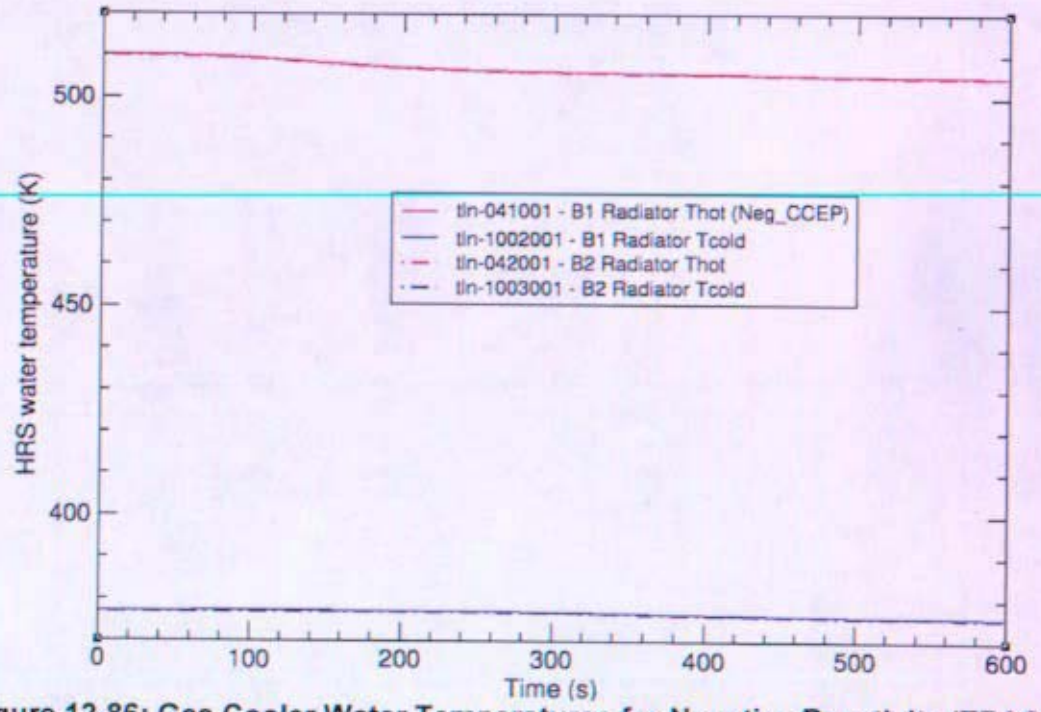



**Figure 12-86: Gas Cooler Water Temperatures for Negative Reactivity (TRACE)**

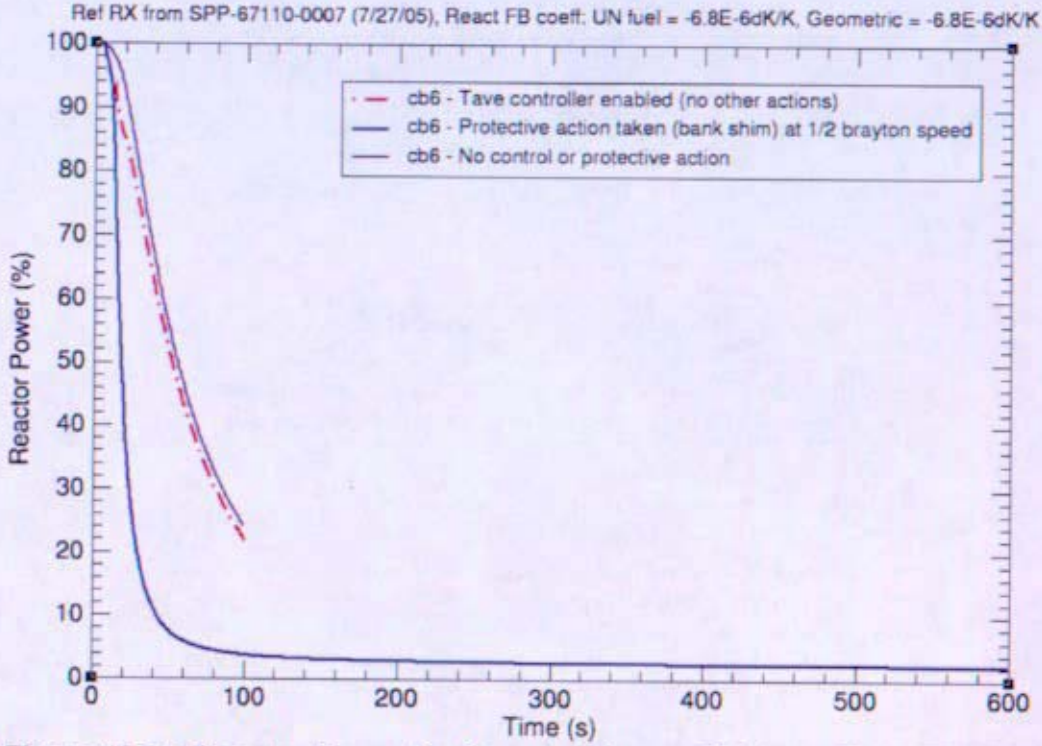



**Figure 12-87: Reactor Power for Complete Loss of Primary Flow (TRACE)**

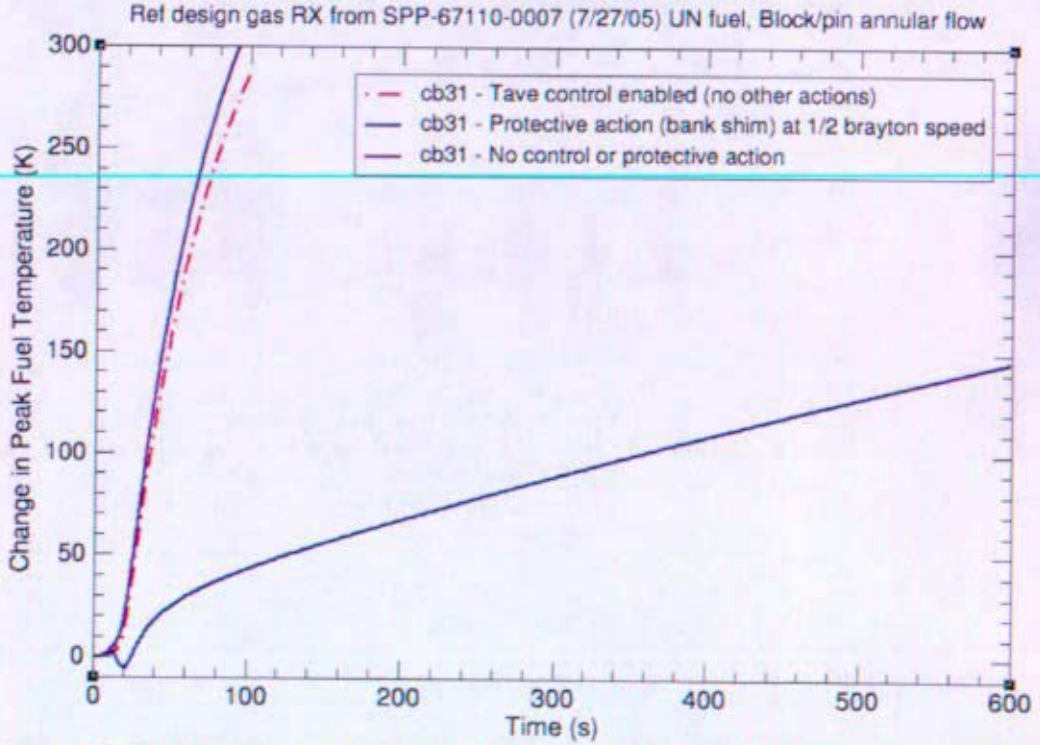



**Figure 12-88: Hot Spot Fuel Temp for Complete Loss of Primary Flow (TRACE)**

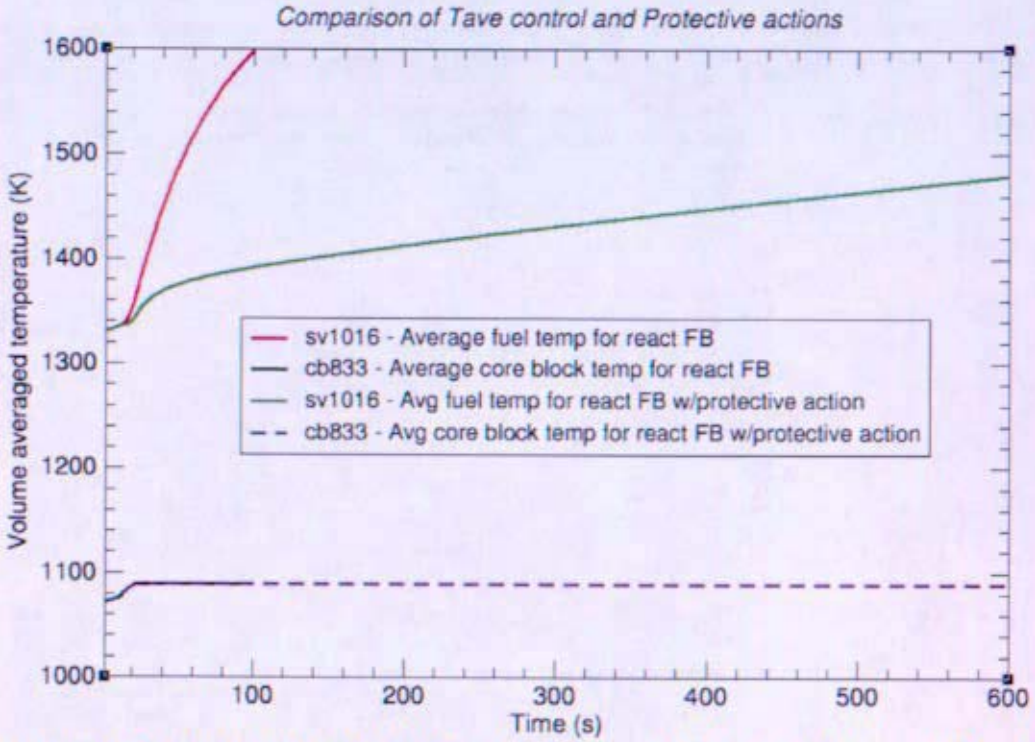



**Figure 12-89: Reactivity Feedback Temps for Complete Loss of Primary Flow (TRACE)**

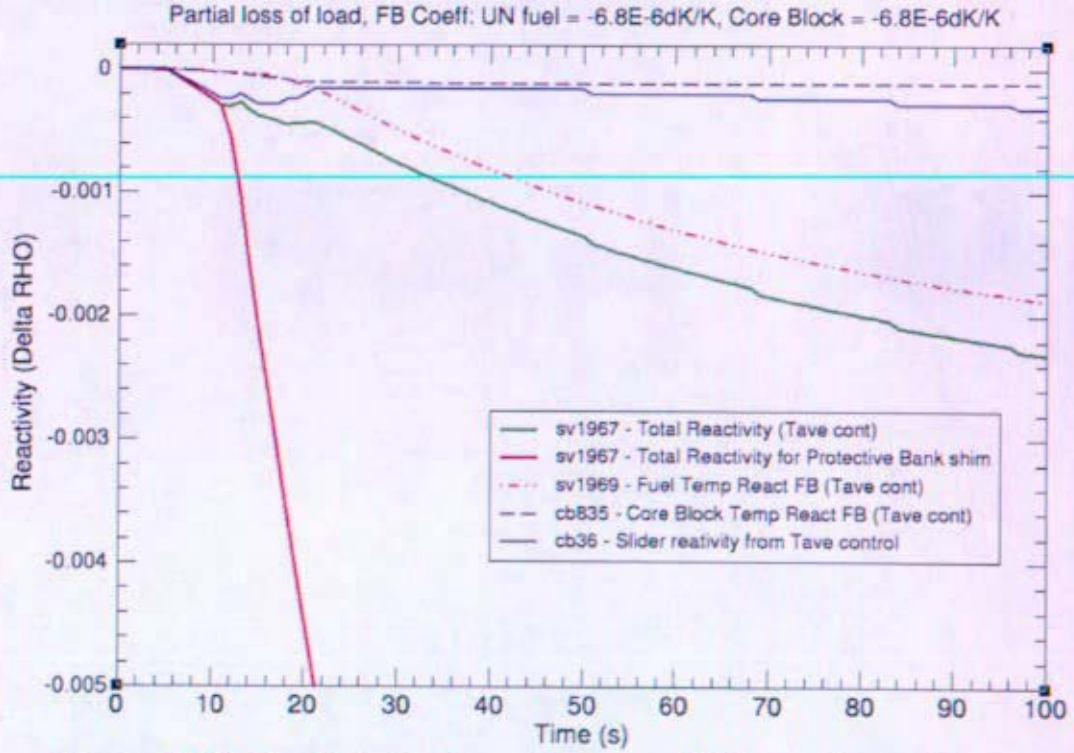



**Figure 12-90: Reactivity for Complete Loss of Primary Flow (TRACE)**

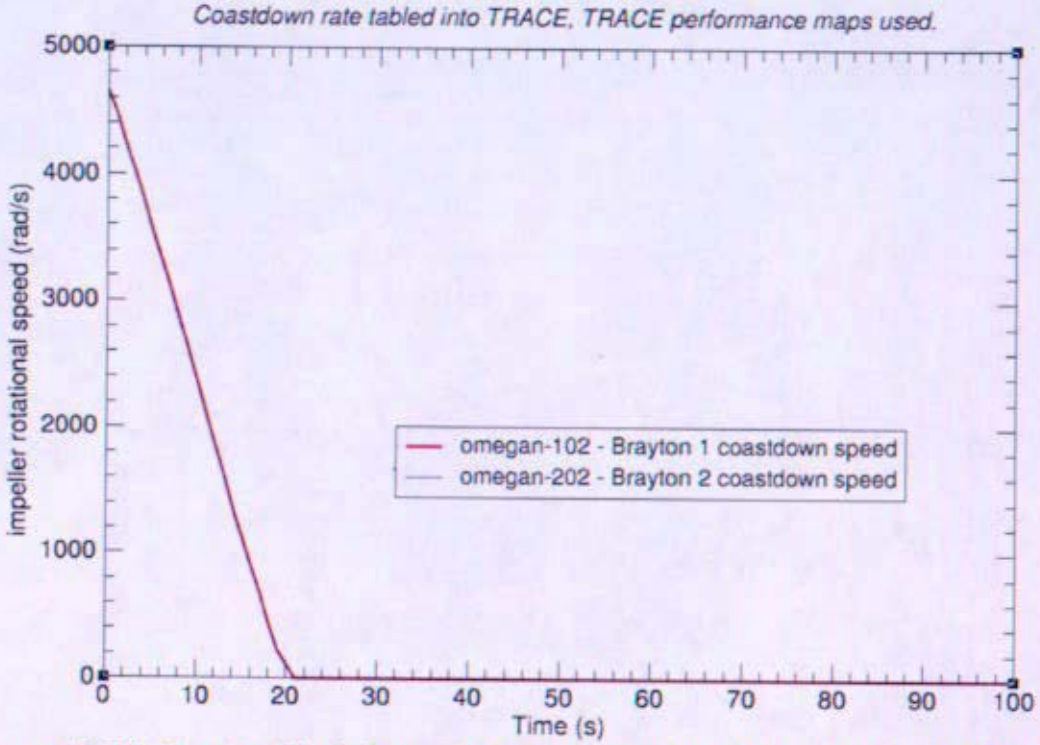



**Figure 12-91: Brayton Shaft Speed for Complete Loss of Primary Flow (TRACE)**

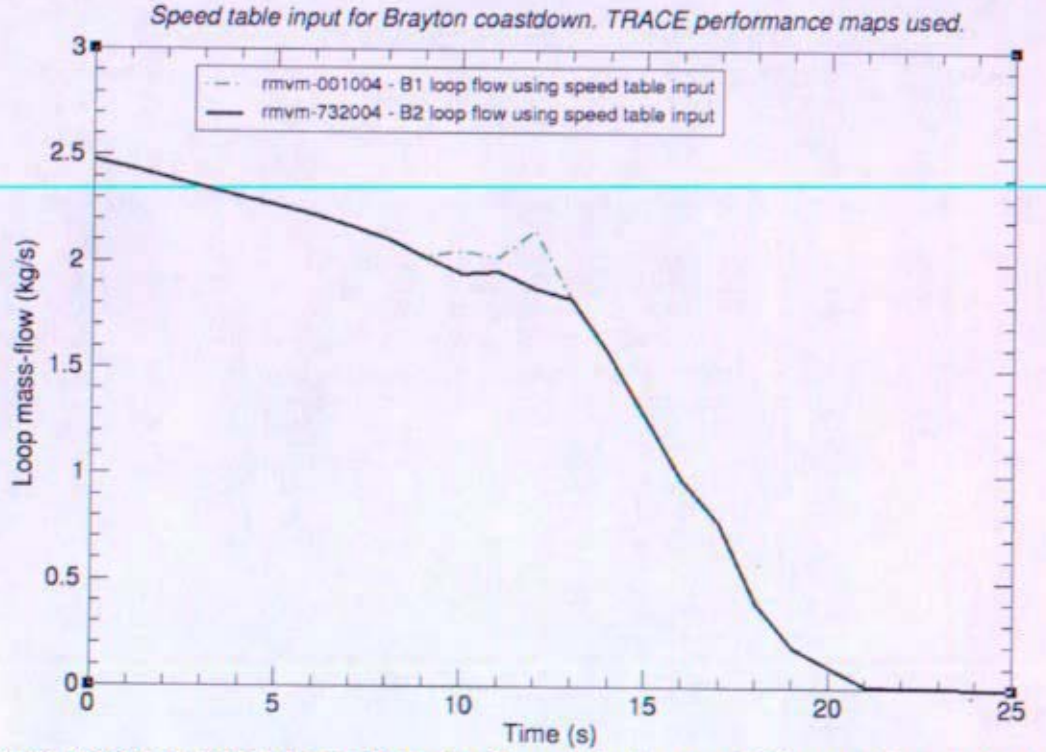



**Figure 12-92: Brayton Loop Flow for Complete Loss of Primary Flow (TRACE)**

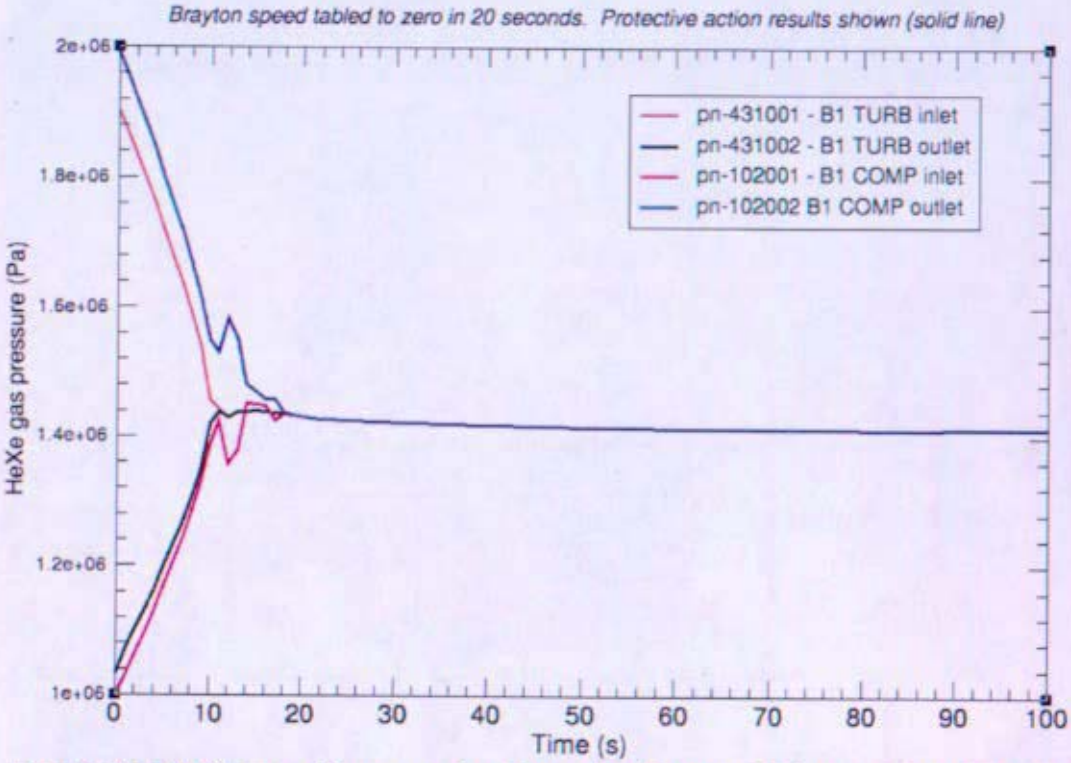



**Figure 12-93: Primary Pressure for Complete Loss of Primary Flow (TRACE)**

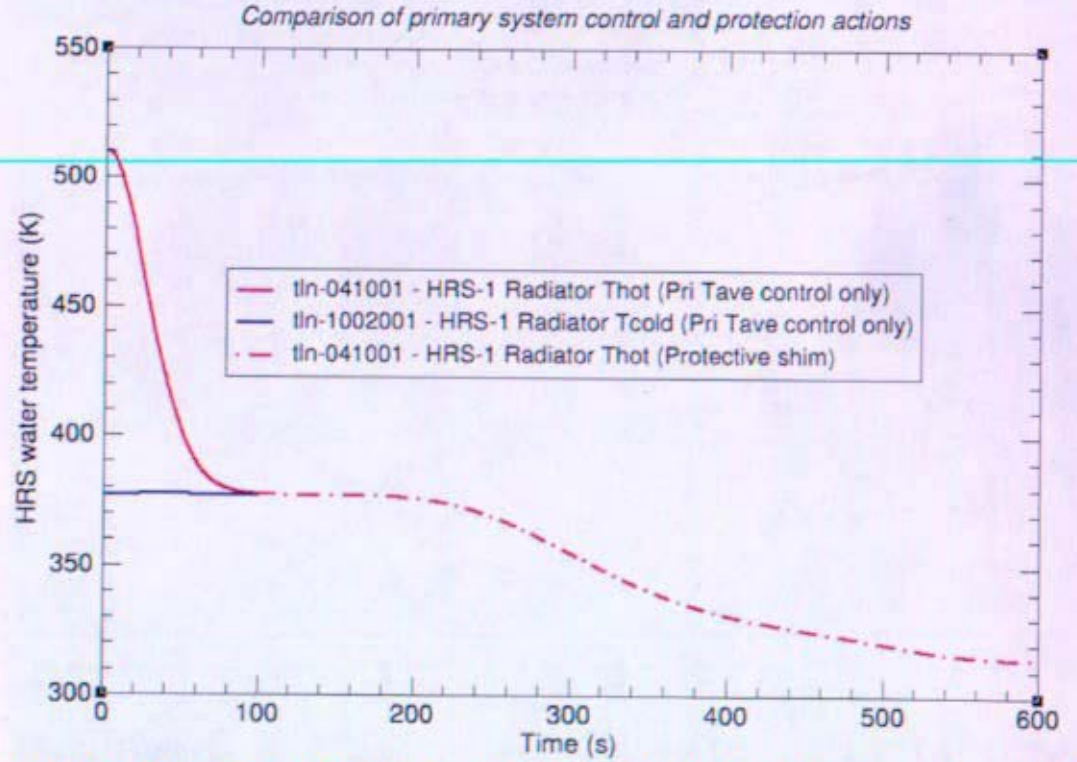



**Figure 12-94: Gas Cooler Water Temps for Complete Loss of Primary Flow (TRACE)**

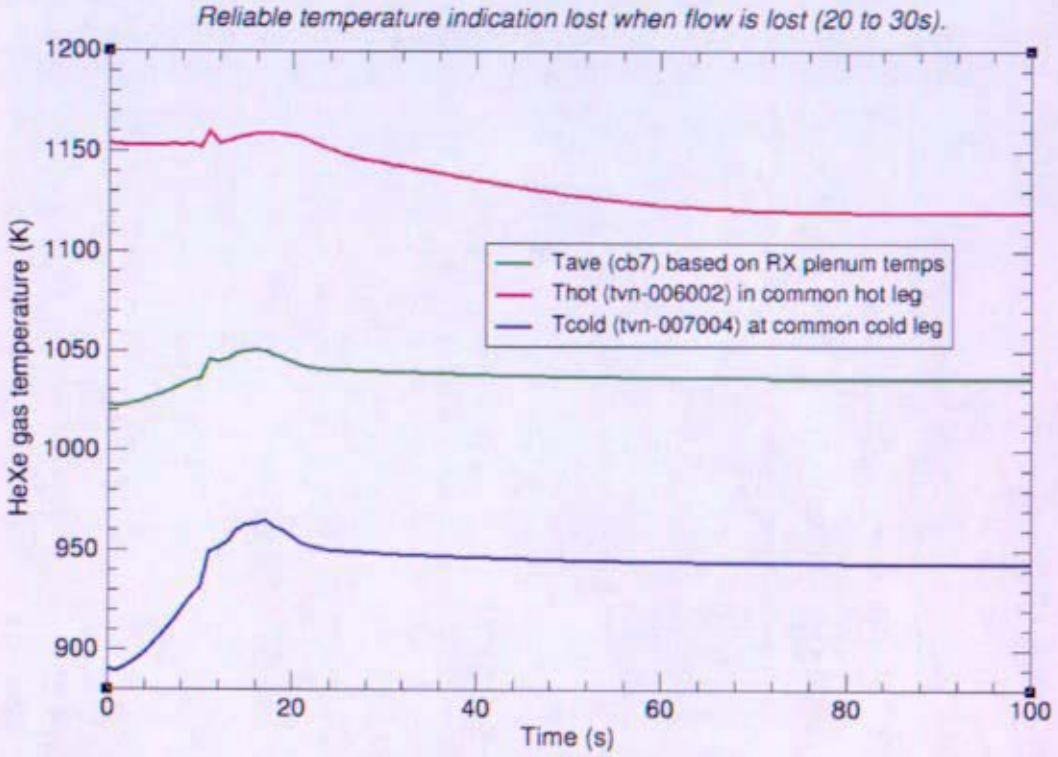



**Figure 12-95: Reactor Inlet & Exit Temps for Complete Loss of Primary Flow (TRACE)**

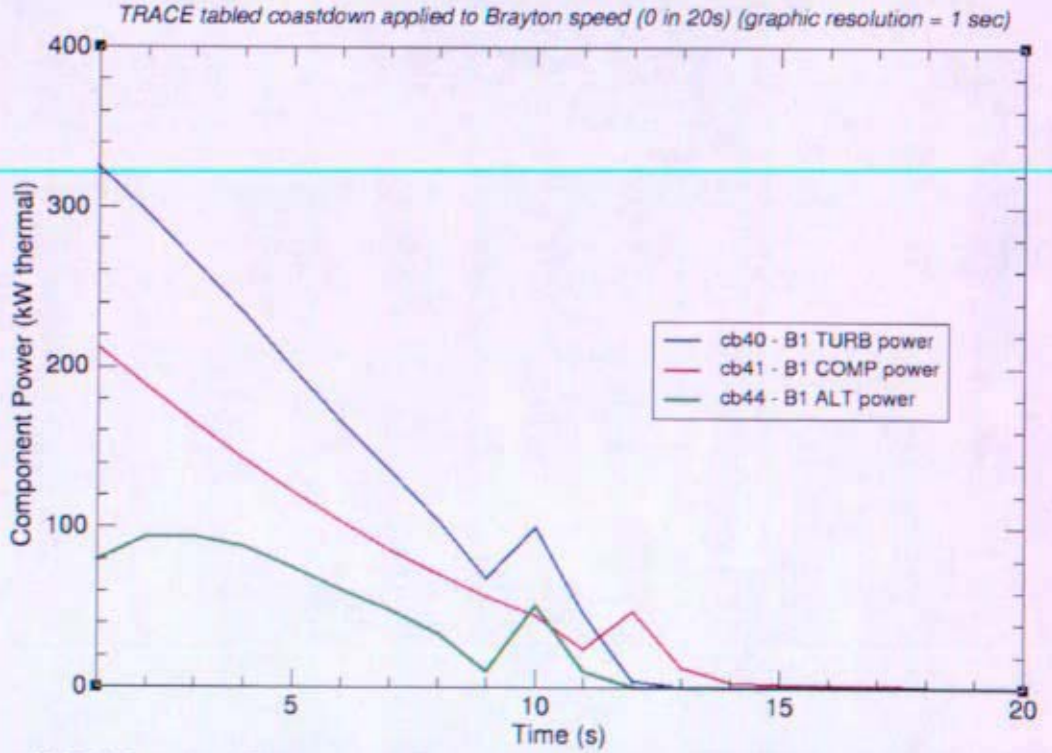



**Figure 12-96: Brayton Component Power for Complete Loss of Primary Flow (TRACE)**

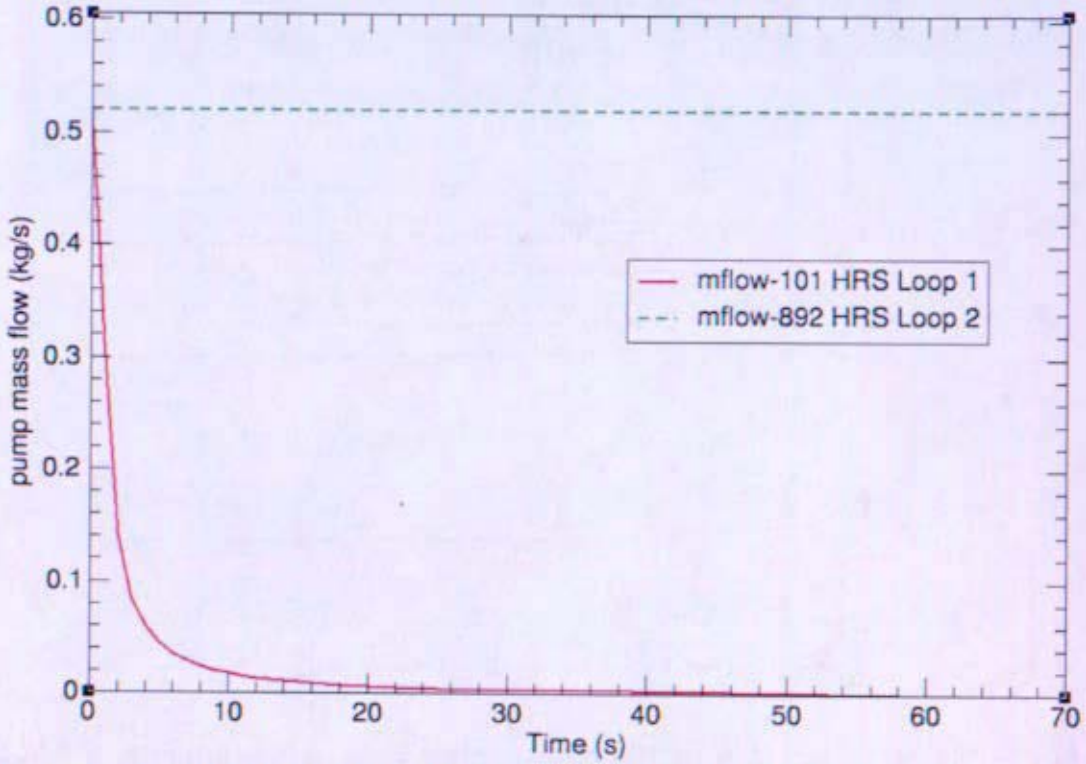



**Figure 12-97: HRS Loop Flows for Complete Loss of Flow in HRS Loop 1 (TRACE)**

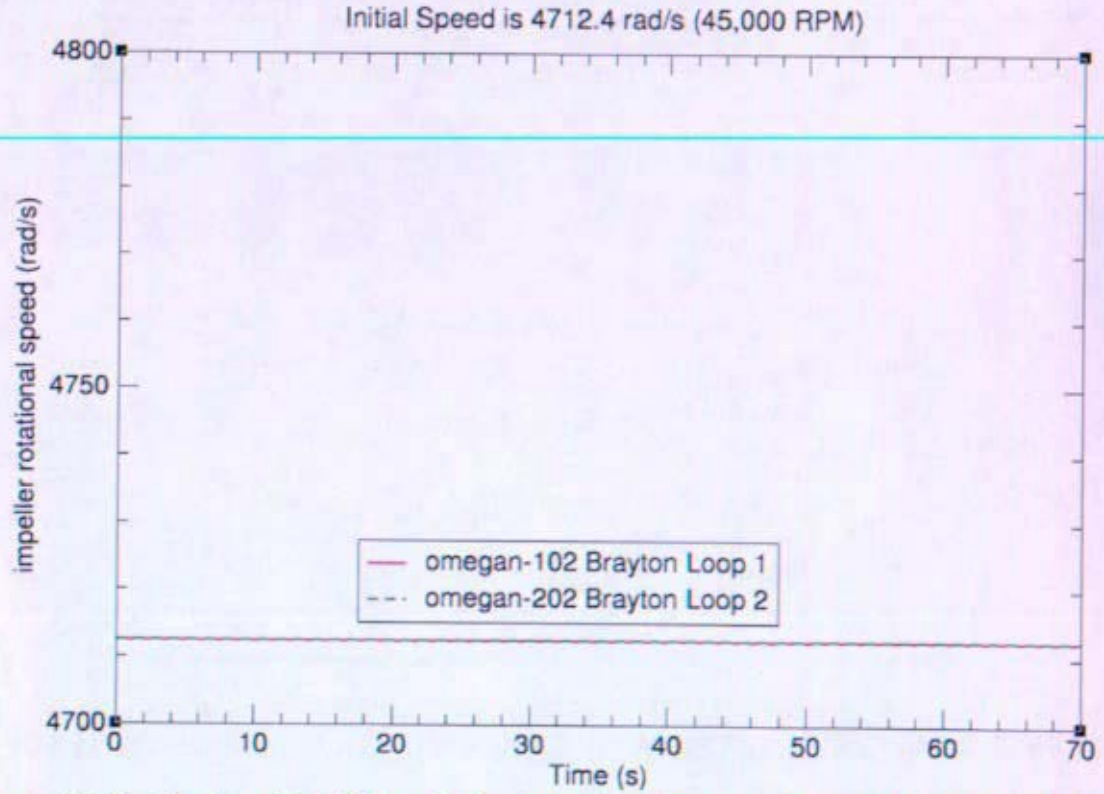



**Figure 12-98: Brayton Shaft Speeds for Complete Loss of Flow in HRS Loop 1 (TRACE)**

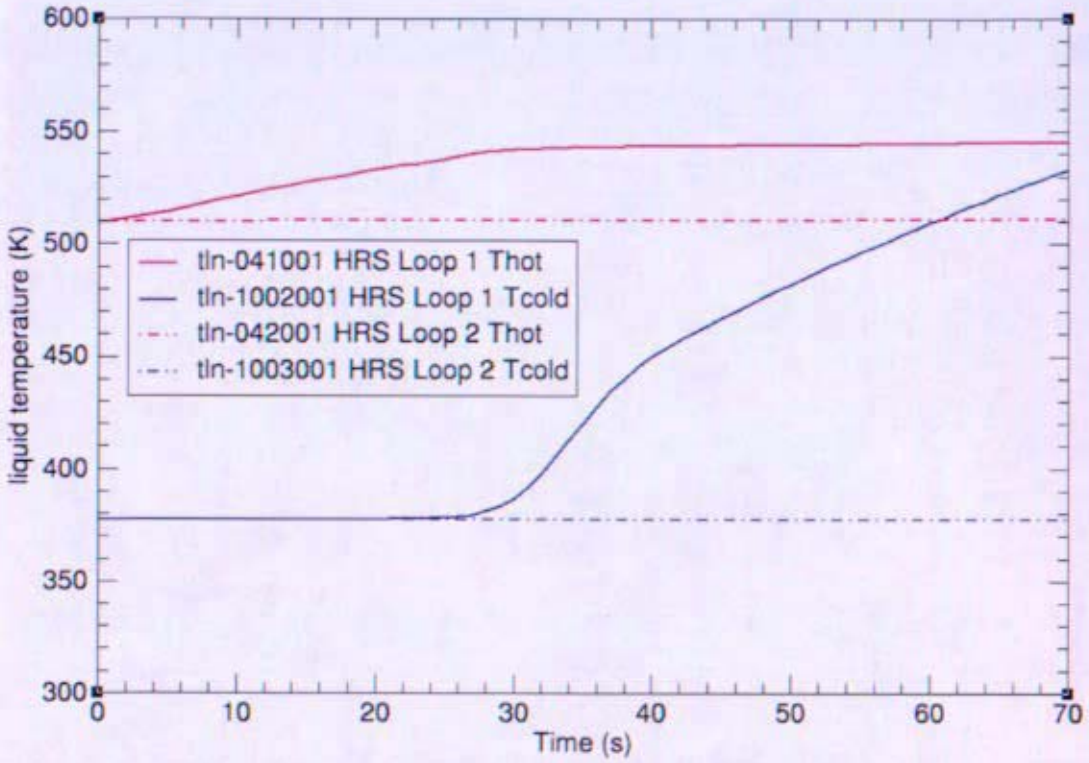



**Figure 12-99: Gas Cooler Water Temps for Complete Loss of Flow in HRS Loop 1 (TRACE)**

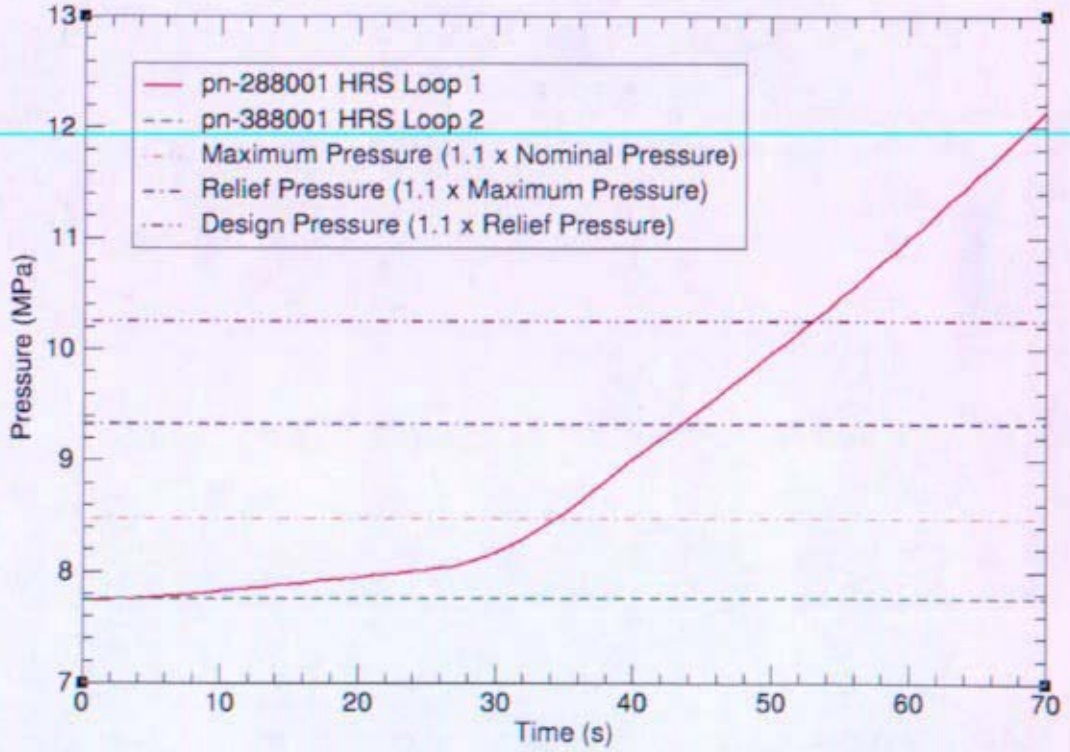



**Figure 12-100: HRS Pressure for Complete Loss of Flow in HRS Loop 1 (TRACE)**

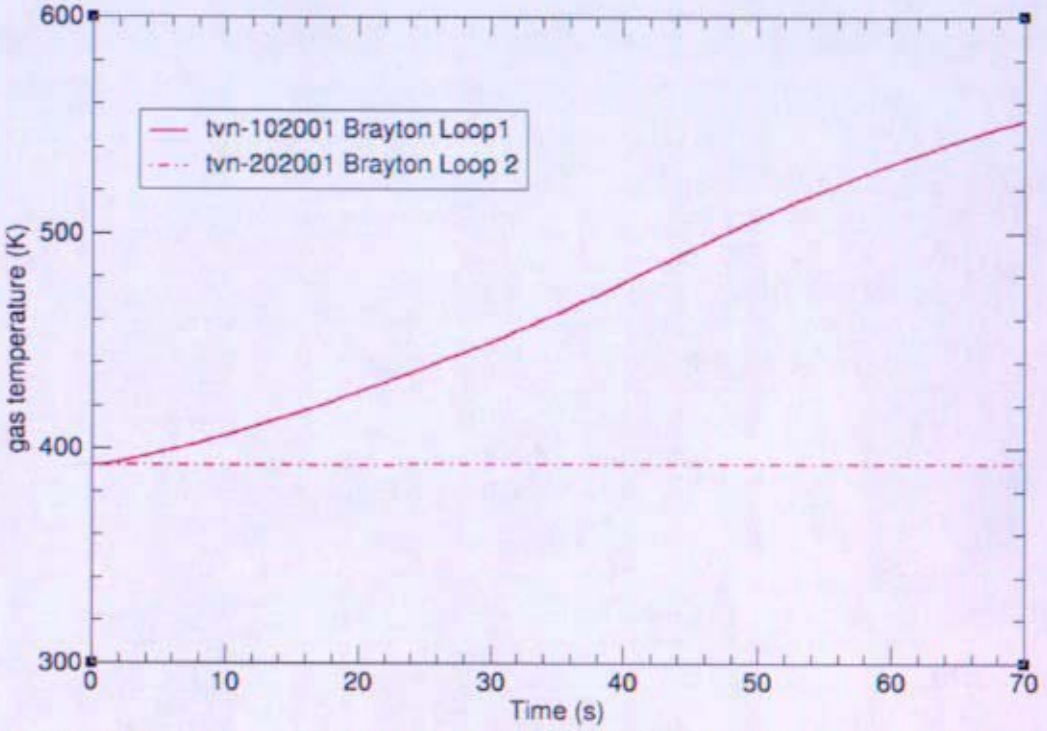



**Figure 12-101: Compressor Inlet Temps for Complete Loss of Flow in HRS Loop 1 (TRACE)**

Trace Maps Used

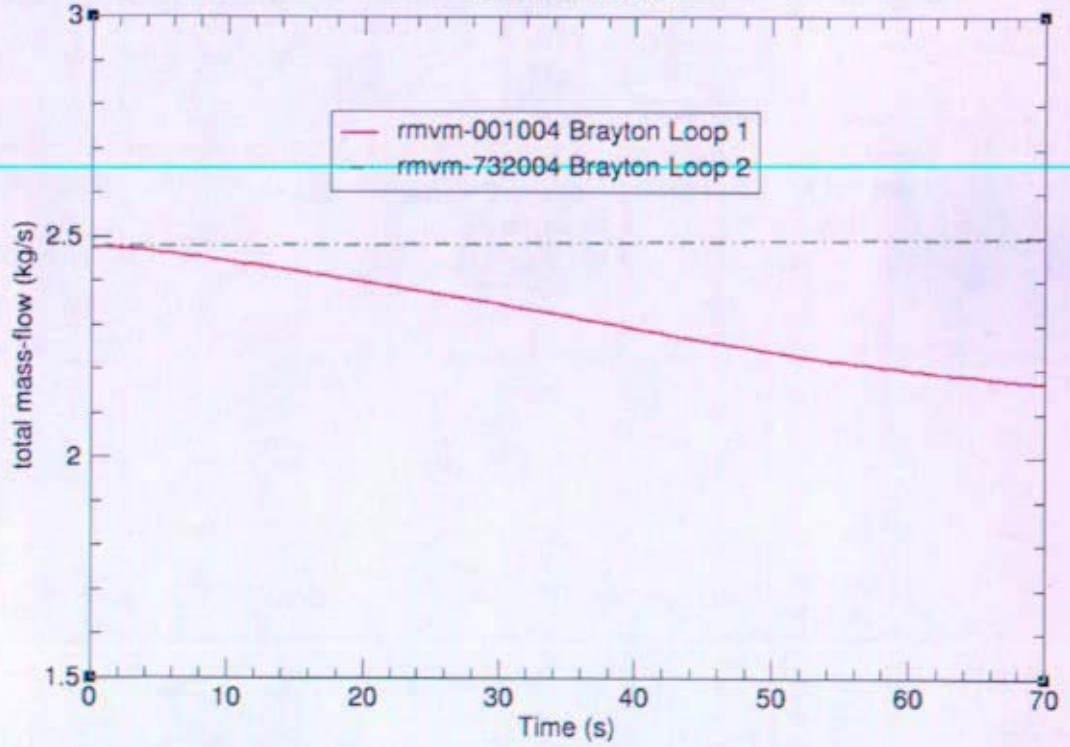



**Figure 12-102: Brayton Loop Flow for Complete Loss of Flow in HRS Loop 1 (TRACE)**

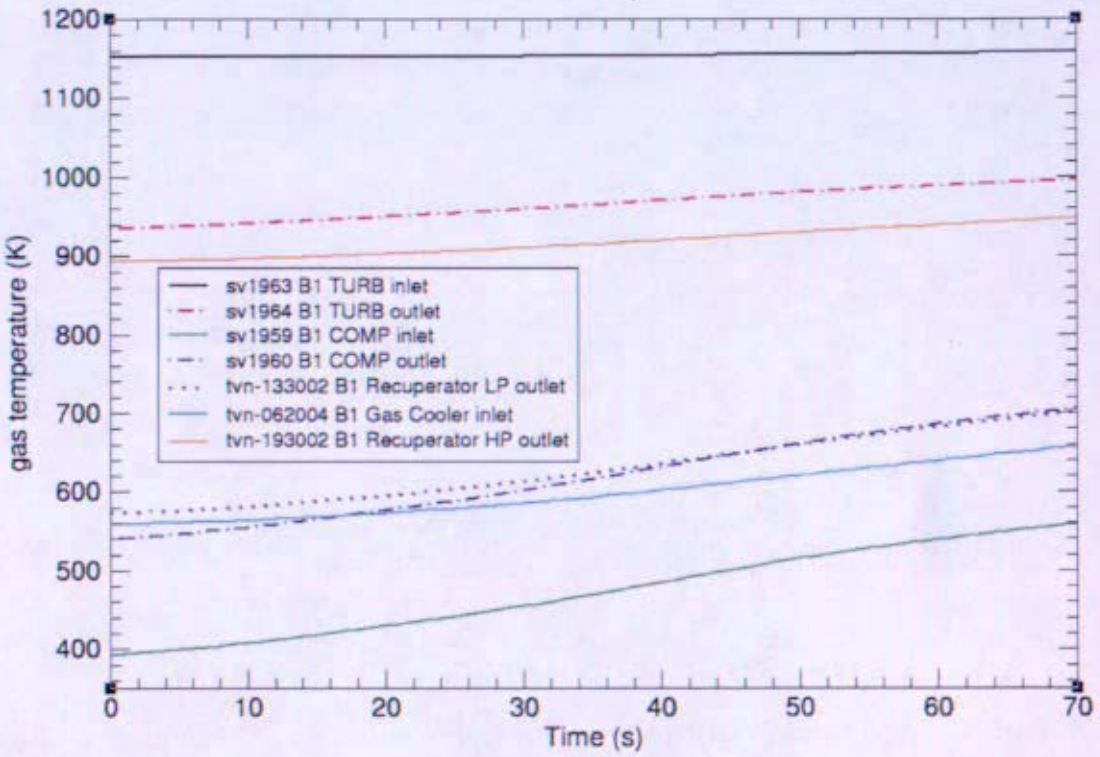



**Figure 12-103: Brayton Loop 1 Temperatures for Complete Loss of Flow in HRS Loop 1 (TRACE)**

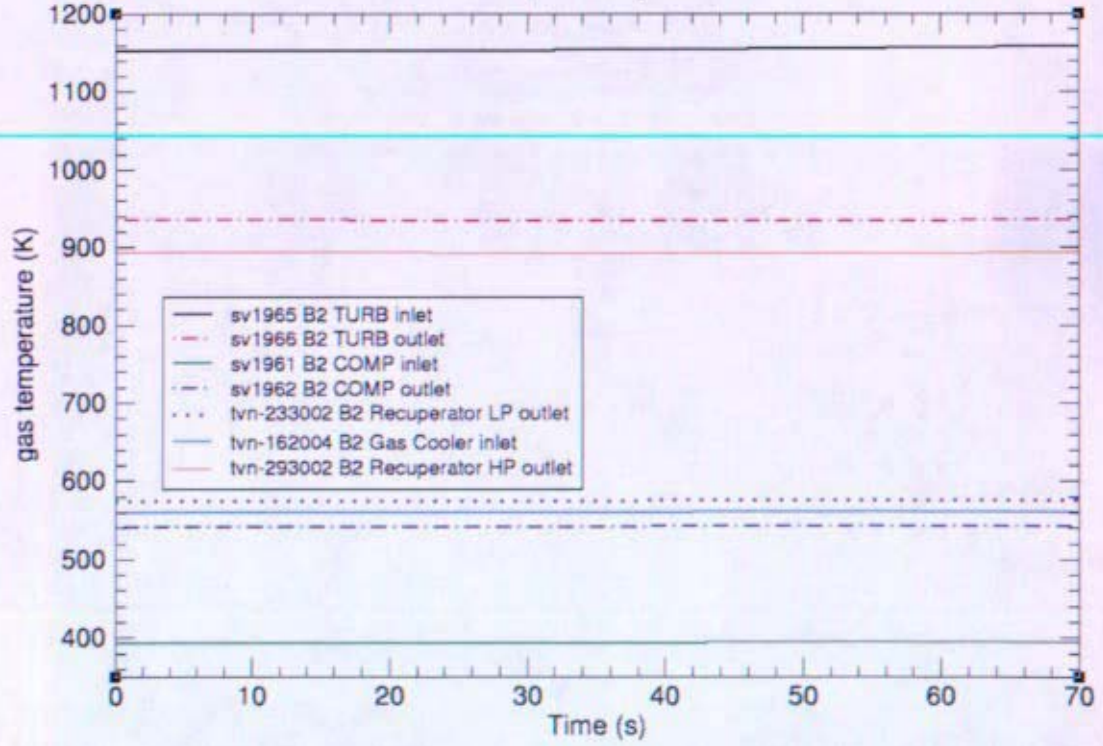



**Figure 12-104: Brayton Loop 2 Temperatures for Complete Loss of Flow in HRS Loop 1 (TRACE)**

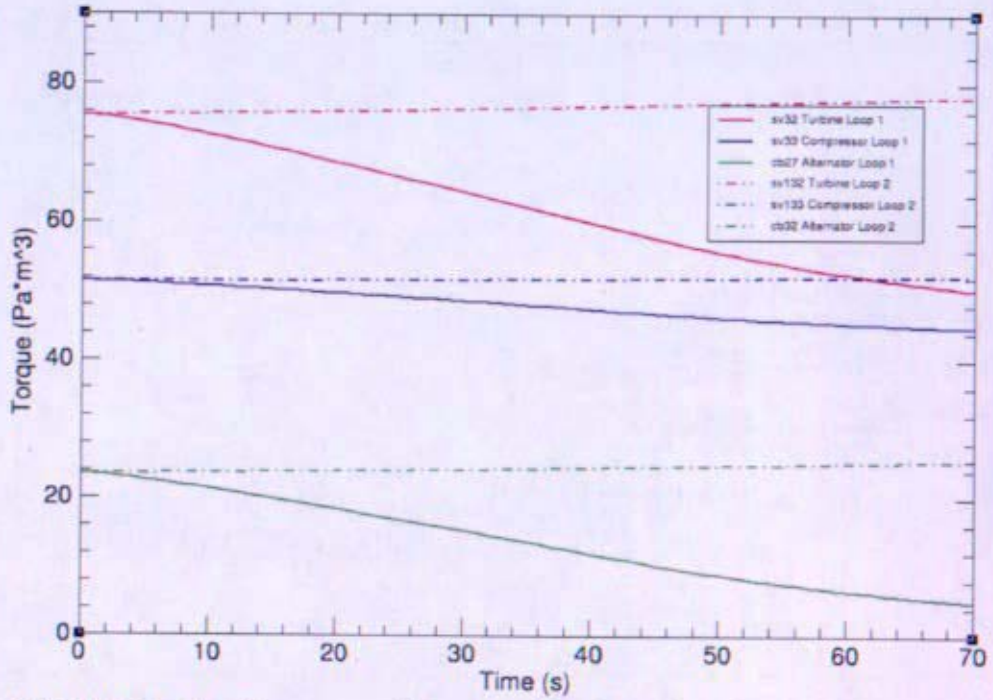



**Figure 12-105: Brayton Component Torques for Complete Loss of Flow in HRS Loop 1 (TRACE)**

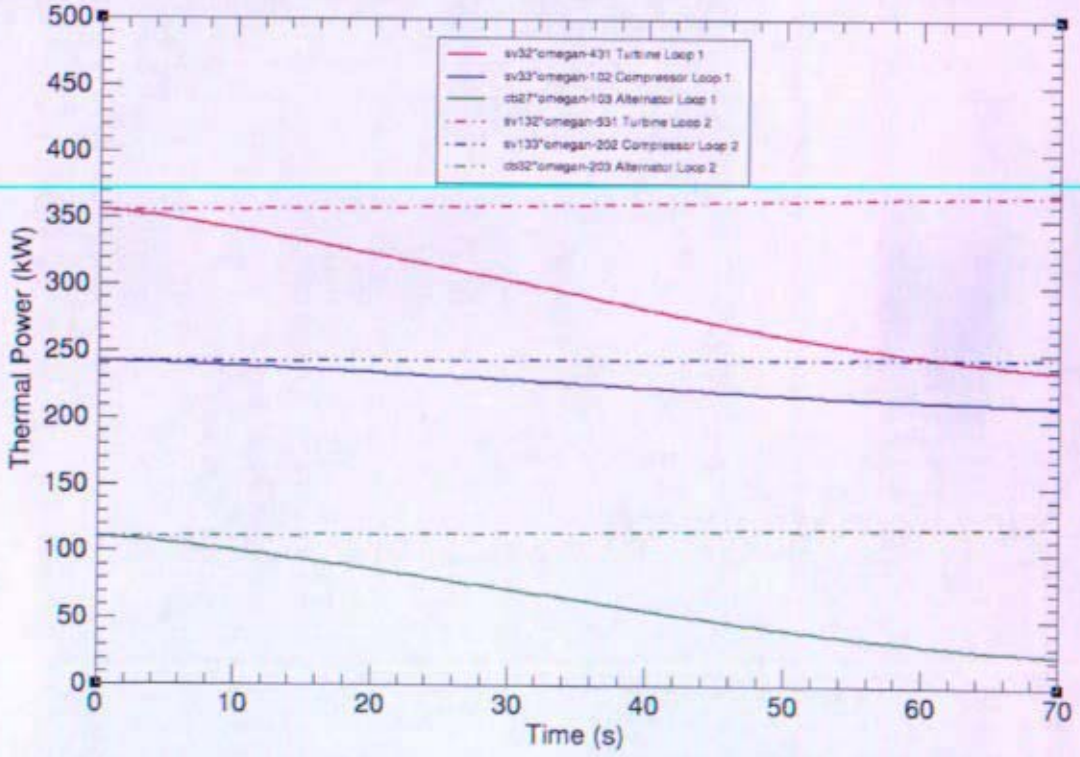



**Figure 12-106: Thermal Power of Brayton Components for Complete Loss of Flow in HRS Loop 1 (TRACE)**

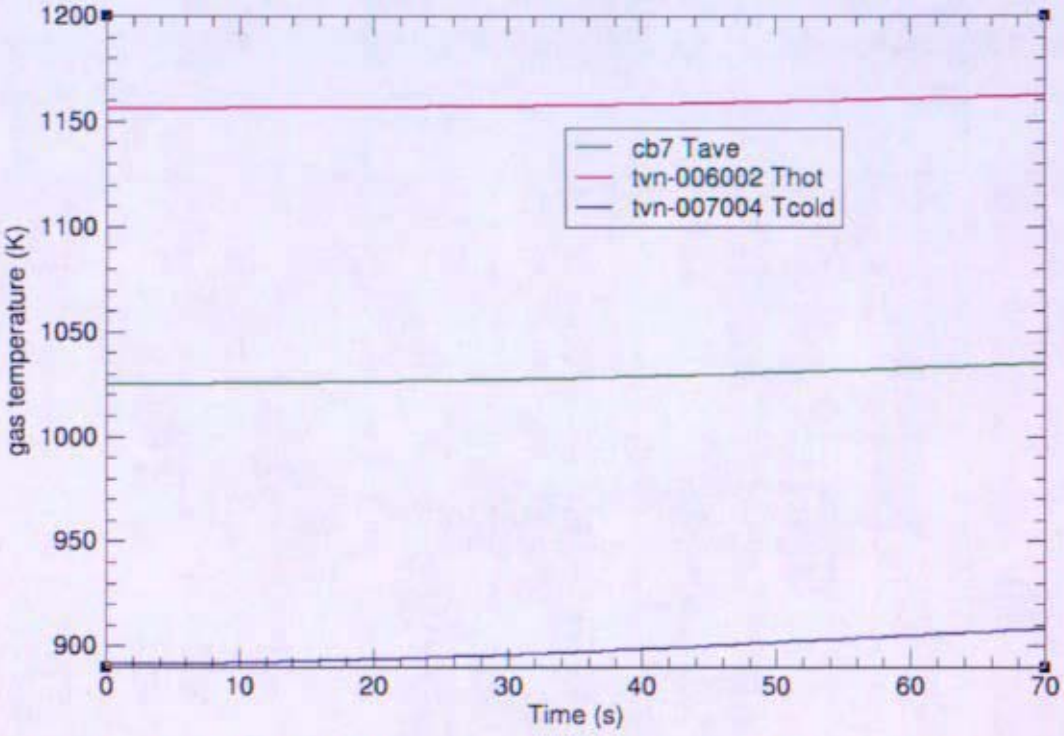



**Figure 12-107: Reactor Inlet & Exit Temps for Complete Loss of Flow in HRS Loop 1 (TRACE)**

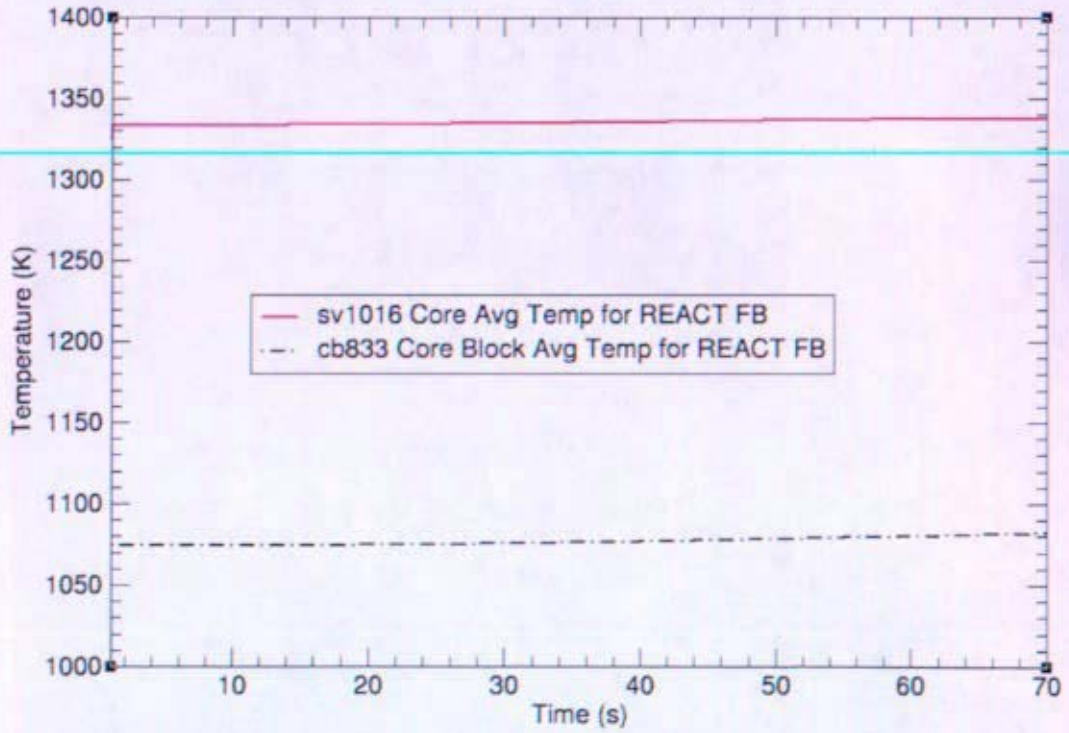



**Figure 12-108: Temps for Reactivity Feedback for Complete Loss of Flow in HRS Loop 1 (TRACE)**

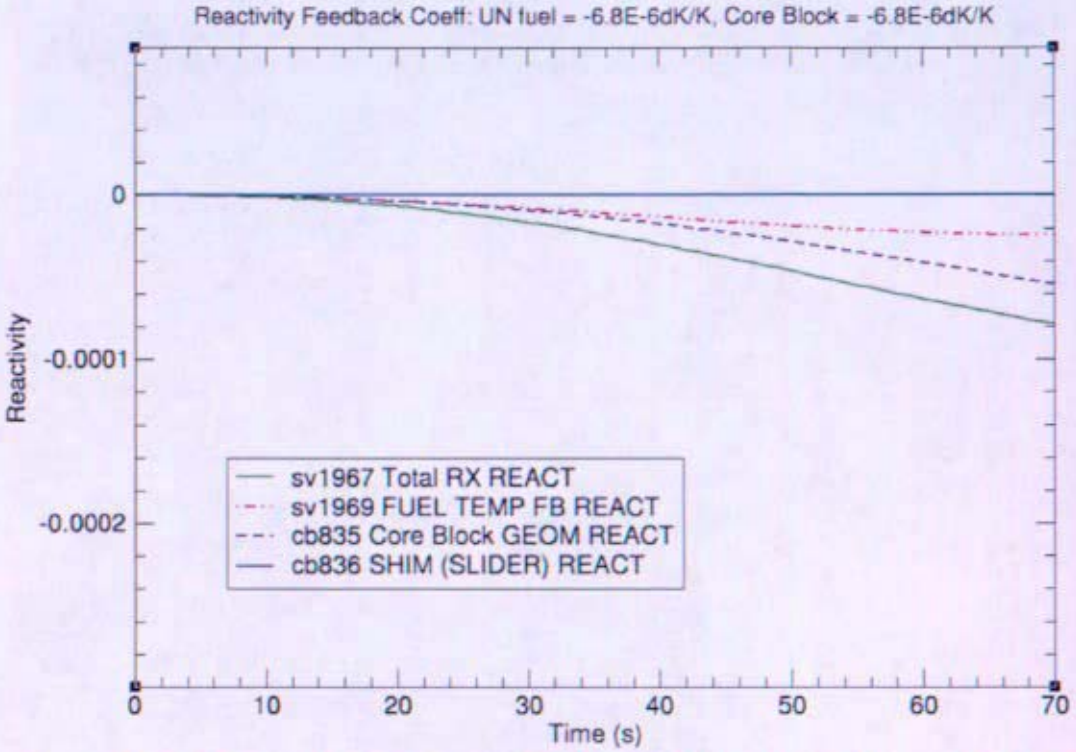



**Figure 12-109: Reactivity for Complete Loss of Flow in HRS Loop 1 (TRACE)**

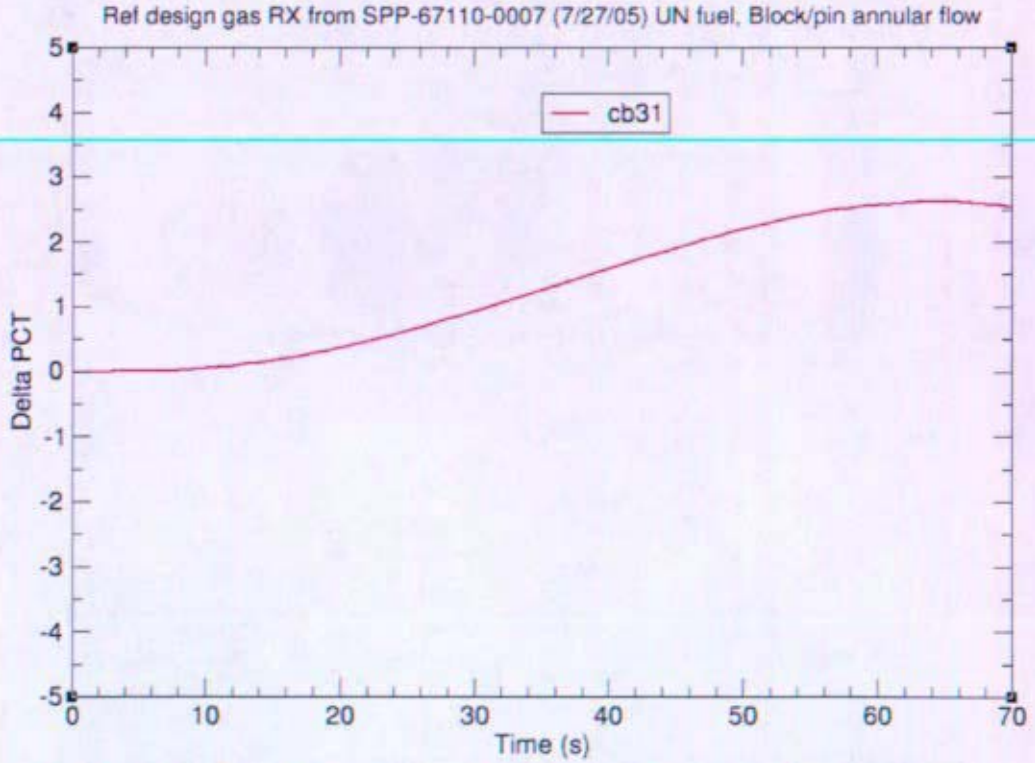



**Figure 12-110: Hot Spot Fuel Temperature for Complete Loss of Flow in HRS Loop 1 (TRACE)**

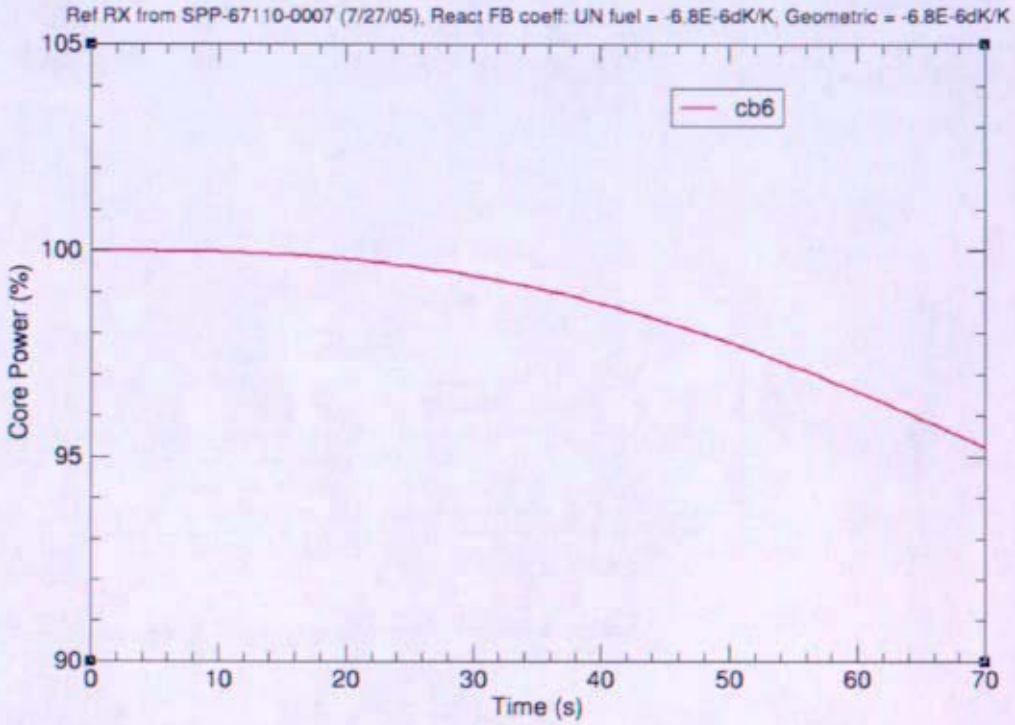



**Figure 12-111: Reactor Power for Complete Loss of Flow in HRS Loop 1 (TRACE)**

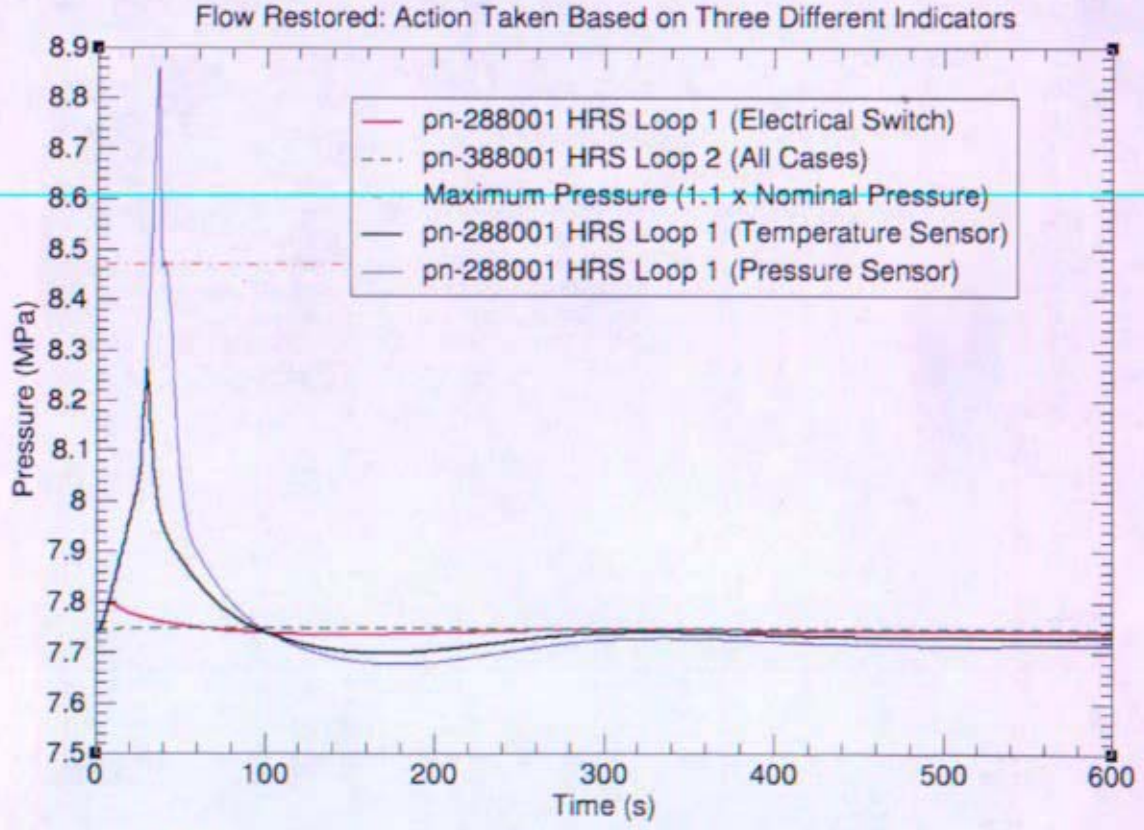



**Figure 12-112: HRS Pressure with Action for Complete Loss of Flow in HRS Loop 1 (TRACE)**

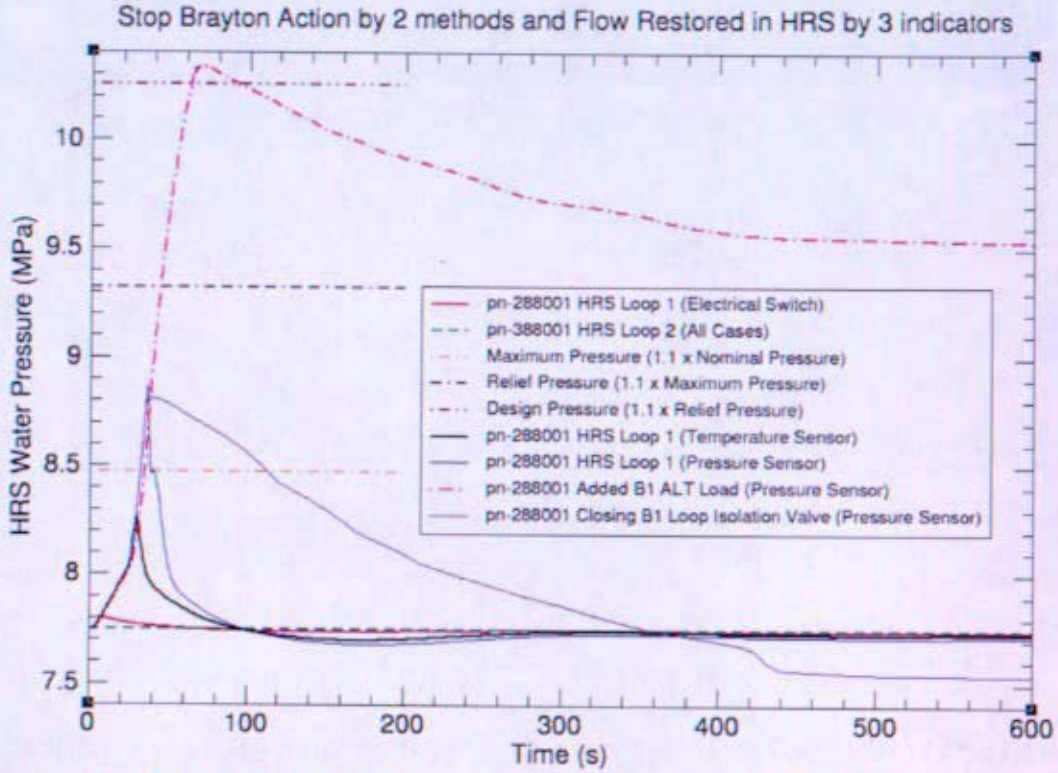



**Figure 12-113: HRS Pressure with Action for Complete Loss of Flow in HRS Loop 1 (TRACE)**

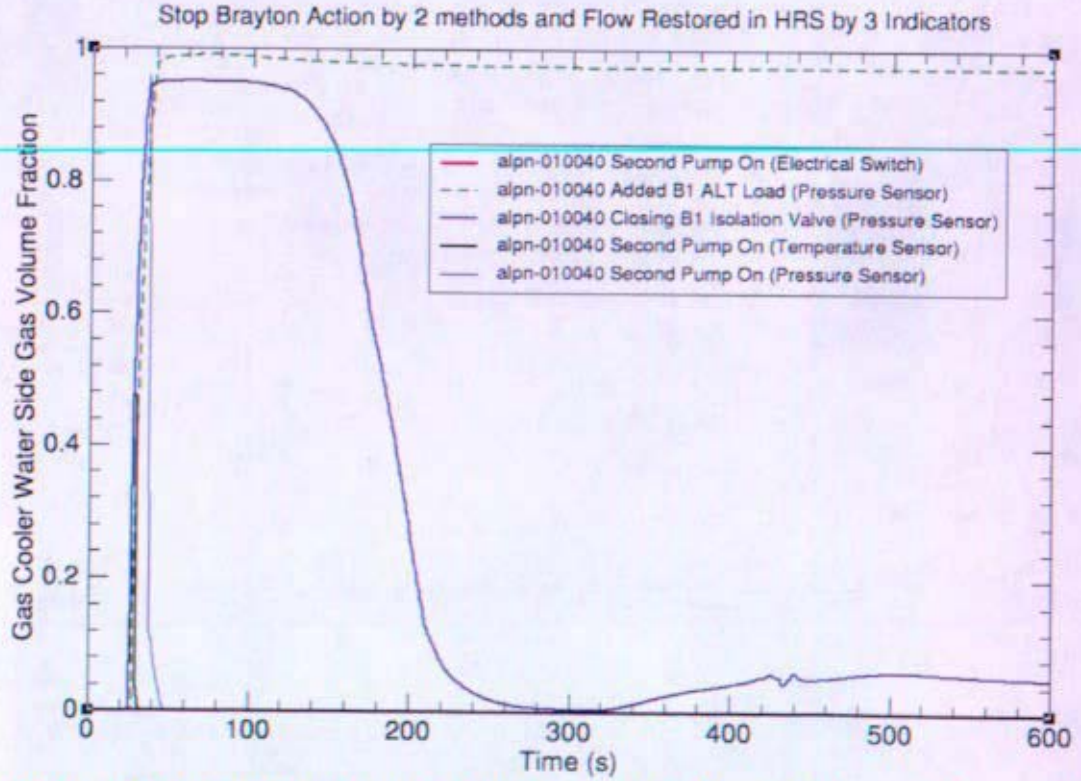



**Figure 12-114: Gas Cooler Void Fraction at Water Exit for Complete Loss of Flow in HRS Loop 1 with Action (TRACE)**

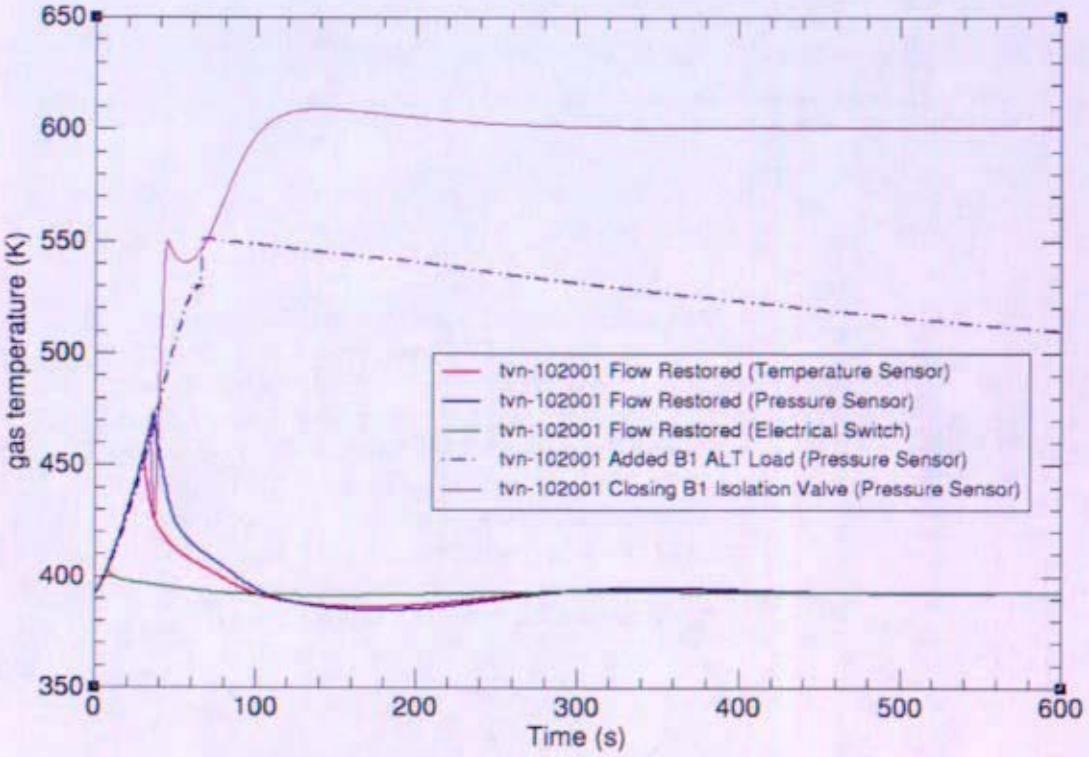



**Figure 12-115: Brayton Loop 1 Compressor Inlet Temperature for Complete Loss of Flow in HRS Loop 1 with Action (TRACE)**

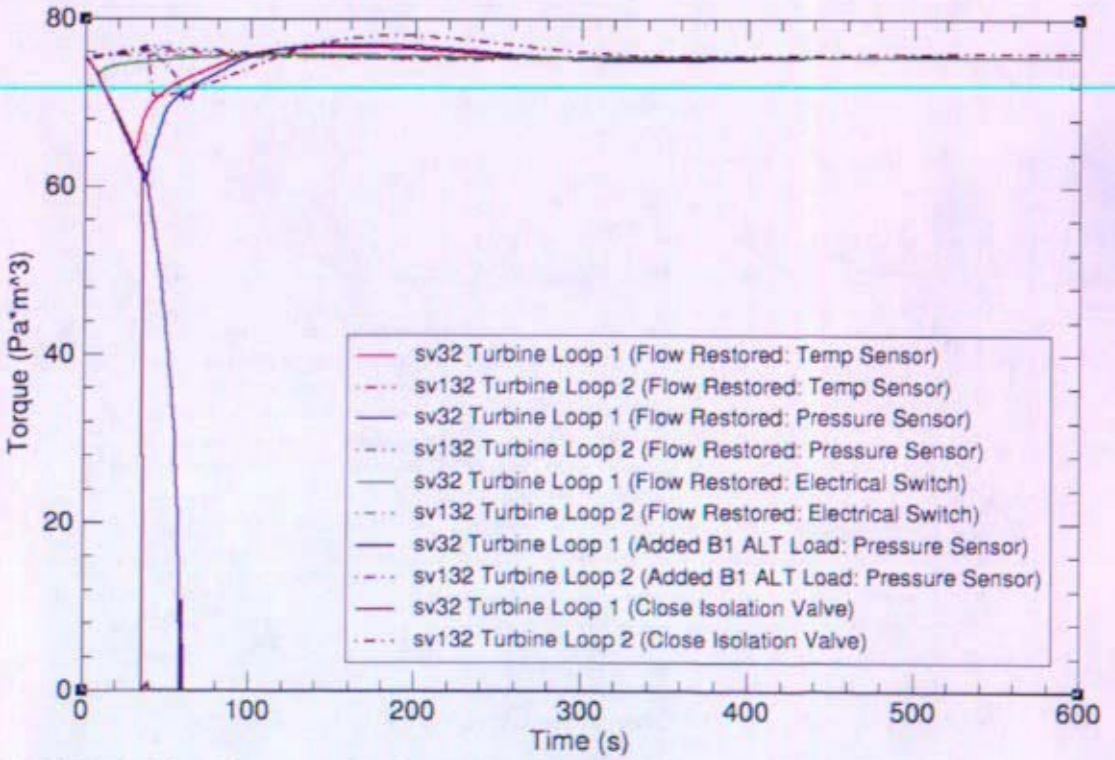



**Figure 12-116: Turbine Torques for Complete Loss of Flow in HRS Loop 1 with Action (TRACE)**

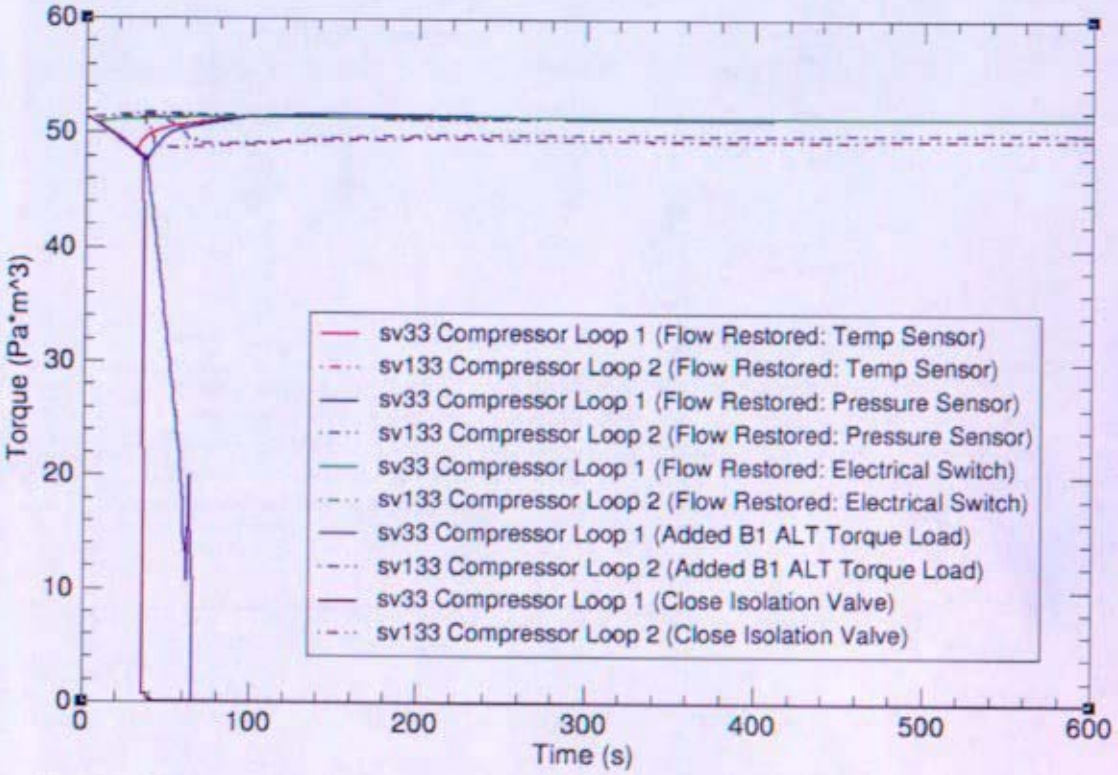



**Figure 12-117: Compressor Torques for Complete Loss of Flow in HRS Loop 1 with Action (TRACE)**

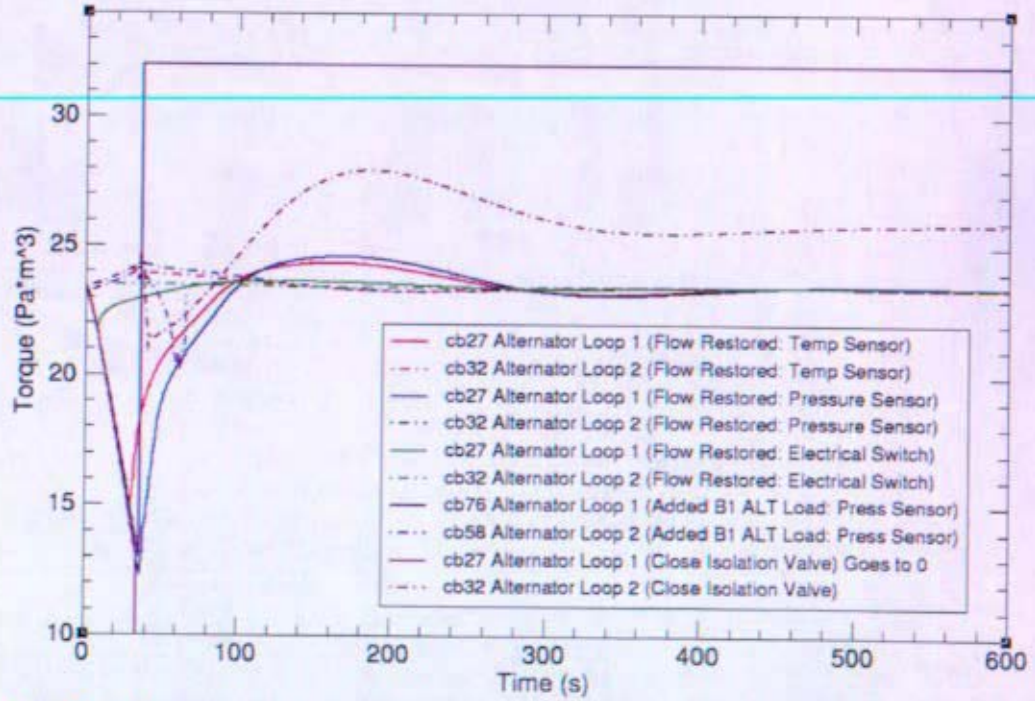



**Figure 12-118: Alternator Torques for Complete Loss of Flow in HRS Loop 1 with Action (TRACE)**

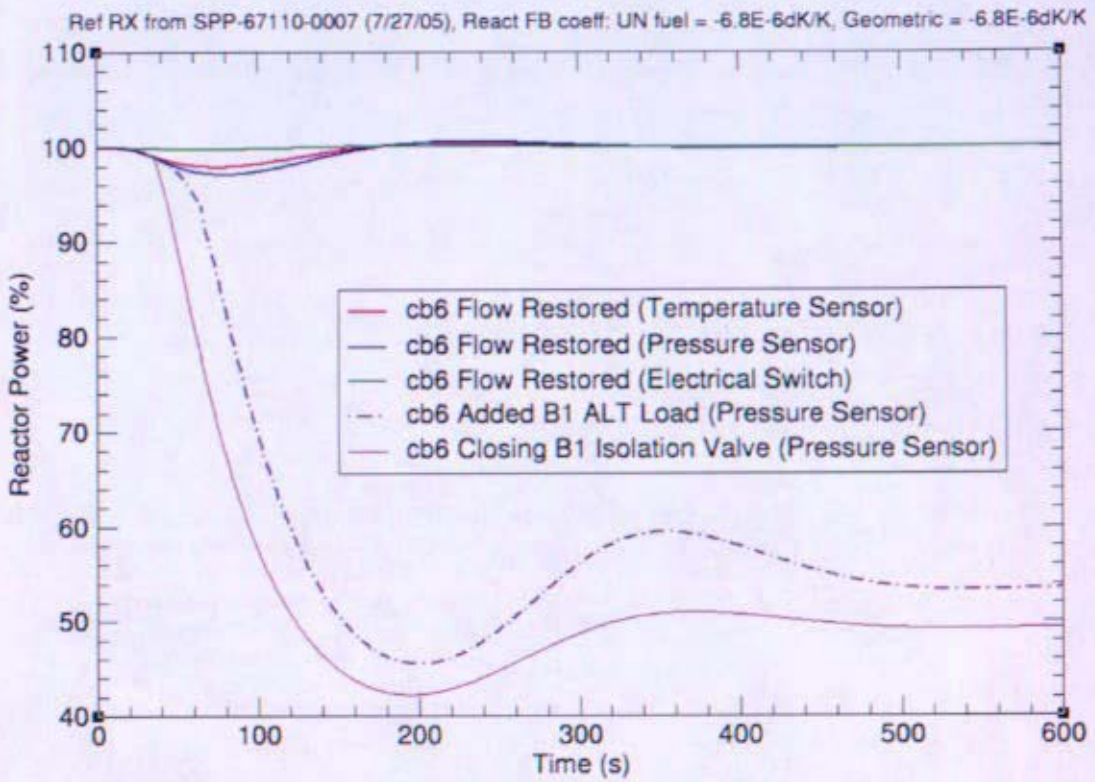



**Figure 12-119: Reactor Power for Complete Loss of Flow in HRS Loop 1 with Action (TRACE)**

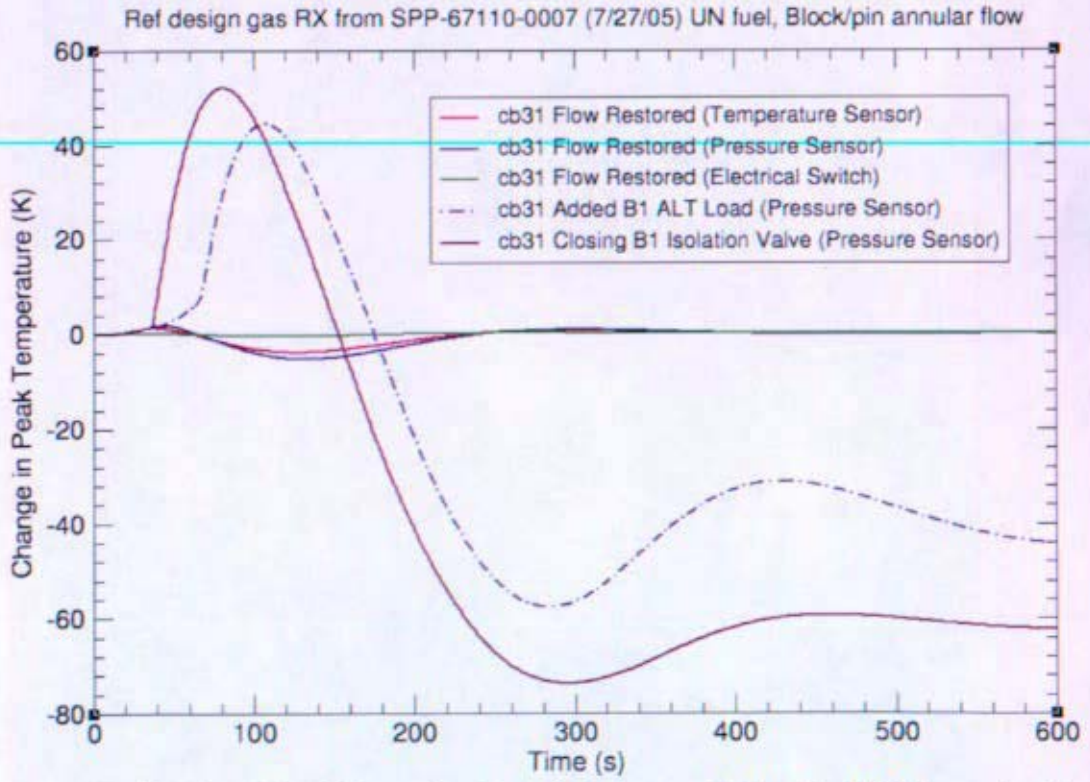



**Figure 12-120: Hot Spot Fuel Temp for Complete Loss of Flow in HRS Loop 1 with Action (TRACE)**

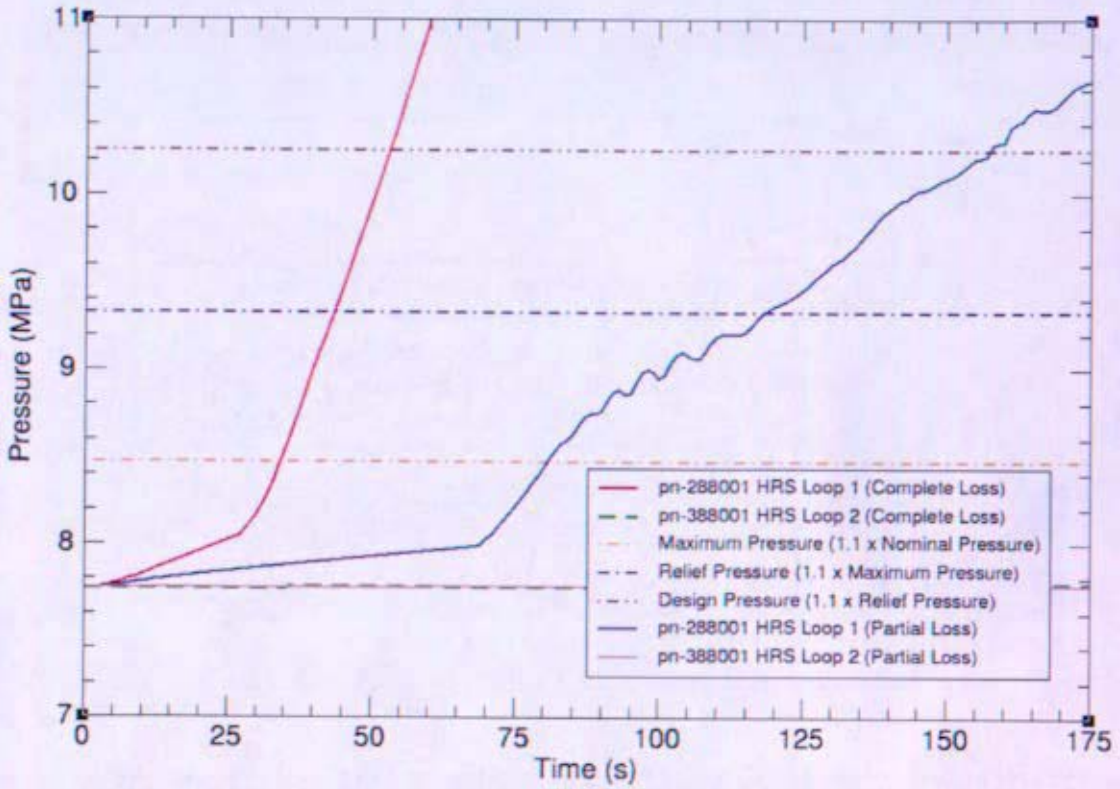



**Figure 12-121: HRS Pressure for Complete and Partial Loss of Flow in HRS Loop 1 (TRACE)**

## 12.5 RELAP5-3D Model Description and Results

### 12.5.1 RELAP5-3D Direct Gas Brayton Model Description

The RELAP5-3D direct gas Brayton model was developed from an initial RELAP5-3D scoping model created in parallel with the MATLAB/Simulink model in support of the Project Prometheus concept selection (Reference 12-1). The RELAP model employed two Brayton units operating in parallel with the reactor as the common heat source. The model uses a mixture of Helium (He) and Xenon (Xe) as the primary coolant with fluid properties based on National Institute of Standards and Testing data and mixture calculations performed by an external routine supplied by the INL. The energy conversion system employs a compressor model developed by INL for RELAP5-3D in support of Project Prometheus and the Massachusetts Institute of Technology Gas Fast Reactor efforts. The energy conversion system also employs the standard RELAP5-3D turbine model with an in-house modification to allow direct turbine performance map input.

There are three independent hydrodynamic systems contained in the model. The term "independent hydrodynamic systems" means that there is no way for fluid to flow from one system to the other (e.g., the gas coolant system and the two liquid metal HRS). Each of the hydrodynamic systems is assigned a reference component, a working fluid, and a name. As stated above, a mixture of He-Xe is used for the primary coolant. A mixture of liquid Sodium and Potassium (NaK) is used as the HRS fluid. Unless otherwise noted, all components are assumed to have a surface roughness of 0.0 triggering a smooth pipe Moody correlation consistent with the gas loop ducts for the GRC Brayton cycle studies (Reference 12-6).

Figure 12-122 is a depiction of the RELAP5-3D model created to simulate the transient behavior of the SNPP direct gas Brayton cycle reactor plant as seen in the SNAP user interface. The screen shot in Figure 12-122 has the gas cooled reactor portion of the model highlighted to indicate the demarcation point between the reactor fluid system and the Brayton cycle fluid system, since there is no physical separation between them.

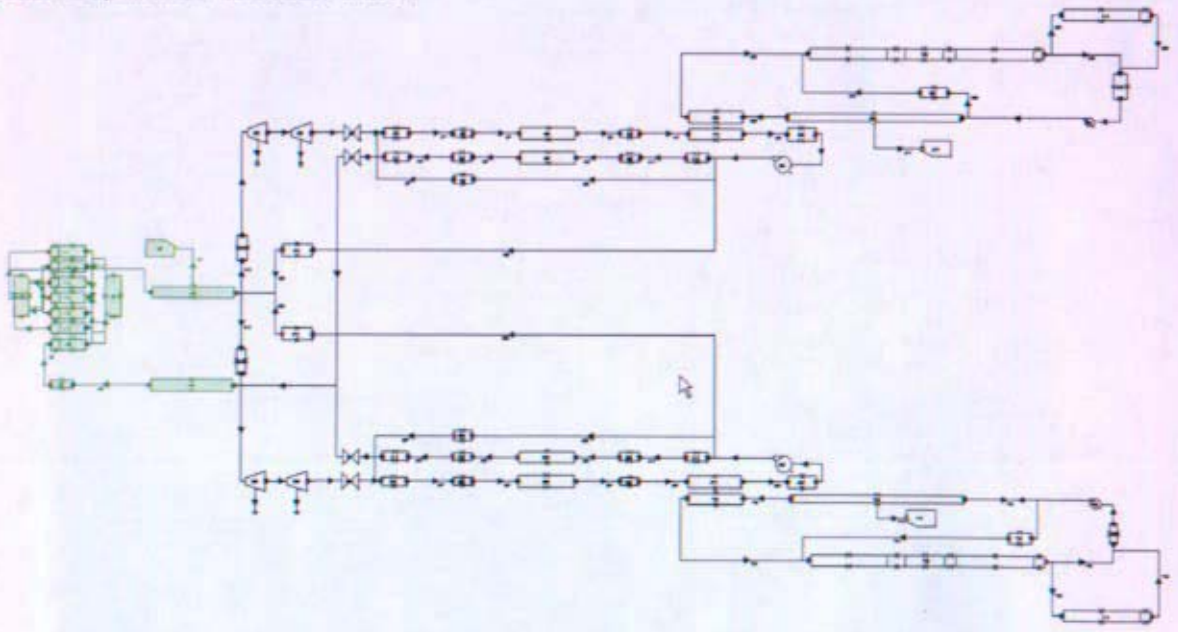


**Figure 12-122: RELAP5-3D/SNAP Direct Gas Brayton Reactor Plant**

### 12.5.1.1 Steady State Condition Compared to Input Model Results

Design points were established as the various Space Nuclear Power Plant reactor concepts evolved during the process to select one concept. Subsequent to the selection of the direct gas cooled reactor concept, a two Brayton loop direct gas cooled reactor RELAP5-3D model was developed. The design point for the model is shown in Figure 12-123, which is Figure 1.4-1 of Enclosure 1 to Attachment D of Reference 12-1 and based on a spreadsheet heat balance calculation. The He-Xe mixture in this design point has 21.6% Xe by mole-fraction.

Table 12-7 compares the design point data from the concept selection report with the RELAP5-3D model of the direct Brayton loop gas cooled reactor. Computer code improvements that were planned for future work included improved representation of temperature to more accurately represent the temperature gradient across heat exchangers. Even without that change the RELAP5-3D results are comparable to the calculated design point. The loop flow rate is 2.28 kg/s compared to the 2.31 kg/s design point flow rate. Also, the pressure drops across the components were adjusted to match the design point values more closely. Since the RELAP5-3D input model does not represent heat loss to the ambient (24 $kW_t$ in Figure 12-123), the reactor power is 801 kW compared to 813 kW in the state point. A future update to the model would have incorporated ambient heat losses and the bleed flow. With the same ambient heat loss, the predicted reactor power would be 825 kW. Overall, the model results are in good agreement with the state point with areas of improvement identified that could improve that agreement.

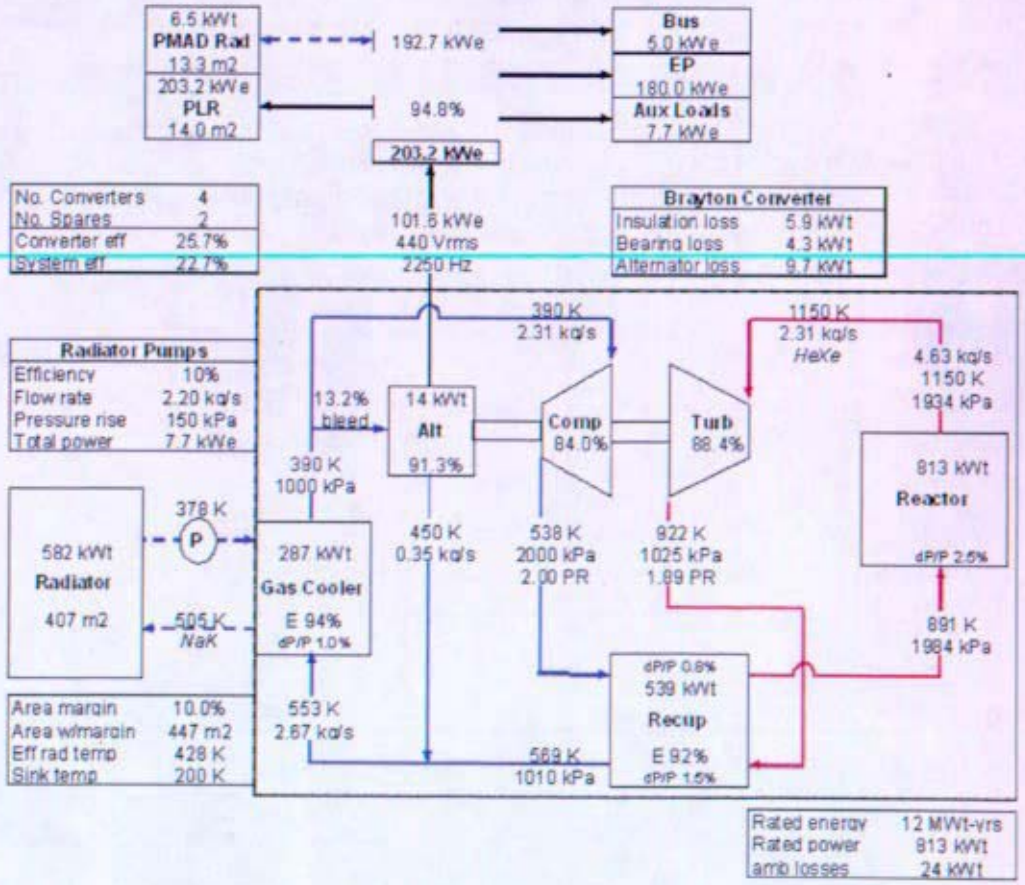



**Figure 12-123: Design Point for RELAP5-3D Model**

## Table 12-7: Comparison of Design Point and RELAP5-3D Model State Points

| Location | Design Point | | RELAP5-3D | |
|---|---|---|---|---|
| | Temperature (K) | Pressure (kPa) | Temperature (K) | Pressure (kPa) |
| Turbine Inlet | 1150 | 1934 | 1149 | 1933 |
| Turbine Exit | 922 | 1025 | 921 | 1051 |
| Recuperator Low Pressure Side Exit | 569 | 1010 | 565 | 1036 |
| Gas Cooler Inlet | 553 | 1010 | 565 | 1037 |
| Gas Cooler Exit | 390 | 1000 | 393 | 1028 |
| Compressor Inlet | 390 | 1000 | 393 | 1026 |
| Compressor Exit | 538 | 2000 | 540 | 2001 |
| Recuperator High Pressure Side Exit | 891 | 1984 | 894 | 1987 |
| Gas Cooler NaK Inlet | 378 | - | 382 | 276 |
| Gas Cooler NaK Exit | 505 | - | 521 | 273 |

| System Flows | Design Point (kg/s) | RELAP5-3D Flow (kg/s) |
|---|---|---|
| Brayton Loop Flow | 2.31 | 2.28 |
| Alternator Cooling Flow | 0.35 (gas) | 0.0(1) |
| Gas Cooler Gas Flow | 2.67 | 2.28 (2) |
| Gas Cooler NaK Flow | 2.20 | 2.36 |

| Misc. | Design Point | RELAP5-3D |
|---|---|---|
| Reactor Power (- losses) | 789 $kW_t$ | 796 $kW_t$ |
| Reactor ($\Delta T$) | 259 K | 255 K |
| Reactor $\Delta P/P_{in}$ | 2.5% | 2.7% |
| Turbine PR ($\Delta T$) | 1.89 (228 K) | 1.84 (228 K) |
| Compressor PR ($\Delta T$) | 2.00 (148 K) | 1.95 (147 K) |
| Recuperator Effectiveness | 92% | 93.4% |
| Recuperator $\Delta P/P_{in}$ LP (HP) | 1.5% (0.8%) | 1.46% (1.0%) |
| Gas Cooler Effectiveness | 94% | 94% |
| Gas Cooler Gas $\Delta P/P_{in}$ | 1.0% | 0.9% |
| Radiator Area Applied | 407 $m^2$ (not including margin) | 447$m^2$ (includes margin) |

Notes:
(1) Alternator cooling flow was not modeling in RELAP5-3D
(2) Bleed path was not modeled in RELAP5-3D

### 12.5.1.2 Reactor Input Model

The SNPP reactor model, shown in Figure 12-124, utilizes a single pass design where flow is piped to the aft of the reactor vessel (relative to the spaceship direction of travel), is directed to the front of the reactor by an internal downcomer annulus, travels aft through the heated portion of the reactor, is collected in the outlet plenum, and exits near the aft of the reactor vessel. Except where noted, all data used is from gas cooled reactor concept DS0-470 (Reference 12-14), which uses $UO_2$ fuel and has an annulus between each fuel pin and the core block for coolant flow. Table 12-8 lists pertinent parameters from this core concept. There are 354 fuel pins which are divided into five channels (three 72-pin channels, one 71-pin channel, and one 66-pin channel) plus one single channel "hot pin" for modeling purposes.

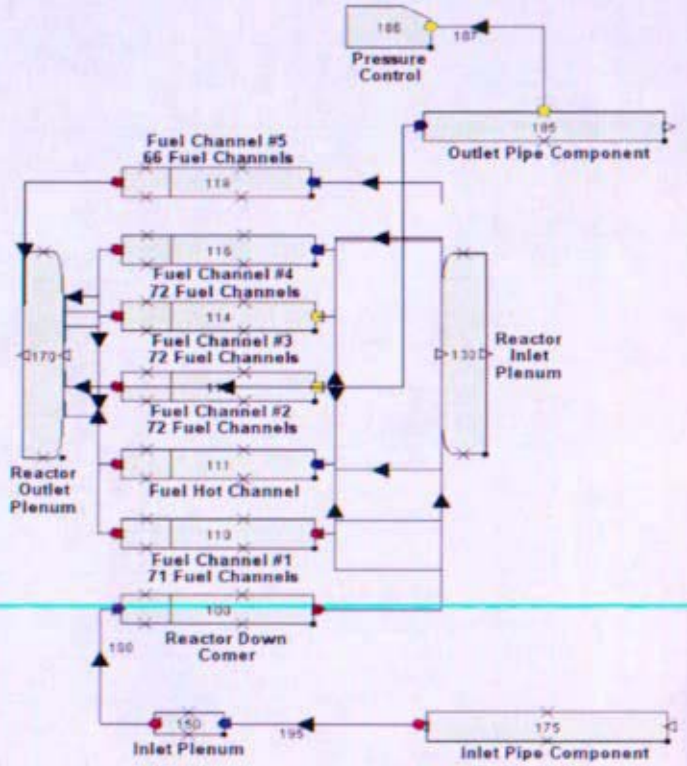



**Figure 12-124: RELAP5-3D Reactor Model**

The reactor inlet pipe directs the flow from the dual Brayton system to the reactor vessel inlet nozzle. The reactor outlet pipe directs the flow from the reactor vessel outlet nozzles to the dual Brayton systems. The reactor inlet and outlet piping should have been assumed to be twice the flow area as the outlet and inlet ducting respectively to a single Brayton system. However, previously considered plant configurations included a four-loop Brayton energy conversion system which would have resulted in twice the flow area of a two-loop configuration. This model inadvertently used the larger four-loop flow area with the two-loop hydraulic diameter. This oversight does not have any significant impact on transient model performance. The Brayton system outlet and inlet ducting is 0.007238 $m^2$ resulting in a reactor inlet and outlet pipe area of 0.028952 $m^2$ (four-times the flow area of one-loop configuration) with a hydraulic diameter of 0.13576 m in each pipe. Eight meters of pipe length are required to extend from the Brayton systems through the radiation shield to the reactor. Therefore, both the reactor inlet pipe and the reactor outlet pipe were assumed to be 8 m in length.

**Table 12-8: Core Concept DS0-470 Parameters**

| Parameter | Value |
|---|---|
| Pressure (MPa) | 1.38 |
| # Safety Rods | 1 |
| Fuel material | $UO_2$ |
| Fuel liner material | Re |
| Clad material | MoRe |
| Structure (core block) | MoRe |
| Vessel material | Hastelloy X |
| Number of fuel pins | 354 |
| Fuel diameter (cm) | 1.643 |
| Fuel height (cm) | 66.4 |
| BOL fuel-to-clad gap (cm) | 0.016 |
| Clad thickness (cm) | 0.051 |
| Gas plenum height (cm) | 14 |
| Core diameter (cm) | 57.5 |
| Vessel thickness (cm) | 0.5 |
| Vessel OD (cm) | 63.58 |
| Safety rod material | Enr $B_4C$ |
| Safety rod OD (cm) | 14.2 |
| Radial reflector material/ percent TD | BeO/95 |
| Radial reflector thickness (cm) | 11 |
| Channel thickness (cm) | 0.269 |
| Pitch (cm) | 2.569 |
| Pipe area - 4 times Brayton inlet duct area ($m^2$) | 0.028952 |
| Pipe hydraulic diameter $(4A/\pi)^{0.5}$ | 0.191997 |
| Pipe length, no basis, (m) | 8 |
| Forward outlet plenum exit K | 0.4442528 |
| Reverse outlet plenum exit K | 0.7894422 |

The reactor downcomer annulus surrounding the core block is modeled as a pipe component. Per Table 12-8, the downcomer flow area is based on the annulus thickness (0.0254 m) and the core block diameter (0.575 m) (Reference 12-15). Therefore, the downcomer flow area is 0.04791 $m^2$ with a hydraulic diameter of 0.0508 meters.

The reactor inlet plenum accepts flow from the downcomer and directs the flow to the fuel pins. The reactor outlet plenum accepts flow from each of the fuel pins and directs the flow to the outlet pipe. Reactor vessel height (1.335 m) and the fuel pin height (0.93 m) are taken from Reference 12-15. This leaves roughly 0.2 m on the top and bottom of the core for the inlet and outlet plenum respectively. Each plenum is modeled as a 0.2 m tall cylinder with the inlet plenum having the same diameter as the downcomer and the outlet plenum having the same diameter as the core block. The core block diameter is assumed to be 0.575 m and the downcomer is assumed to be a 0.0254 m annulus around the core block. These dimensions are also from Reference 12-15. Based on these assumptions, the inlet plenum cross-sectional area is 0.3076 $m^2$ with hydraulic diameter of 0.6258 meters. The outlet plenum cross-sectional area is 0.2597 $m^2$ with a hydraulic diameter equivalent to its diameter (0.575 m). The hydraulic diameter for the inlet and outlet plenum is based on the UN fuel system core block diameter (0.575 m) which is slightly different than the $UO_2$ core block diameter (0.496 m). The small difference between these entries has no effect on the transient model.

The reactor inlet and outlet plenum is modeled using a RELAP5-3D branch component to allow multiple connections to a single hydraulic component in a condensed input form. Form loss coefficients for the plenum connections are tuned to create a reactor pressure drop of approximately 2.5% of the inlet pressure as dictated by Reference 12-1. No exit flow losses are applied at the fuel pin exits; however, forward and reverse loss factors of 0.408 and 0.665 are applied between the outlet plenum and the outlet pipe.

There are 354 fuel pins in the core and each fuel pin has its own annular coolant channel. Taking into account the fuel pin diameter, the gap between fuel and clad, the clad thickness, and coolant channel thickness, the coolant annulus has an outer and inner radius of 1.1575 cm and 0.8885 cm respectively. The core fueled region is 0.664 m tall. The 354 fuel channels are modeled as six separate flow paths designed to represent radial variation in power although not utilized, since radial power variation has not been calculated. The coolant channel in contact with the fueled portion of the pin is represented with 10 equal height volumes to adequately model axial power profiles (plus space in the top volume for fission gas plenum).

One channel hydraulic diameter is equal to 0.00538 m, twice the annular thickness. The same hydraulic diameter is used for each channel regardless of how many pins it models. This allows the hydraulic combination of the fuel pins into lumped components to minimize computational requirements while maintaining the correct hydraulic characteristics.

There are 66 perimeter pins out of the total 354 pins that, because of their similar flux characteristics, are represented with one RELAP5-3D fuel channel. The remaining 288 fuel pins were initially divided into four coolant channels with 72 pins each. However, one pin was removed from the first channel and modeled explicitly as the "hot pin" for detailed thermal calculations leaving one channel with only 71 pins. The flow areas through each of the five RELAP5-3D fuel channels are based on multiples (66, 71, or 72) of the single pin flow area.

Based on standard empirical approximations, all of the channels have forward and reverse loss coefficients of 0.295 and 0.347 respectively between the first and second sub-volumes.

The core design for the RELAP5-3D model utilizes uranium dioxide ($UO_2$) fuel pellets supported inside a molybdenum-rhenium (MoRe) cladding sleeve. The fuel pellets and cladding are sized to nominally provide a 0.016 cm gap between the fuel and clad to allow for fuel swelling throughout core life. However, this gap was not positively maintained and the potential offset and fuel to clad contact was taken into account from both a nuclear and thermal limit perspective. Each cladding sleeve also includes a 14 cm gas plenum above the fuel in which the fission gases would accumulate. Several methods for maintaining this plenum including spring loading were under consideration. The core design consists of a cylindrical MoRe core block that would be gun drilled for each of the fuel pins and its attending coolant annulus.

Figure 12-125 depicts the core block for the uranium nitride (UN) fuel design, which uses less fuel pins than the $UO_2$ fueled core but has the same basic layout. The fuel pins are staggered on a 2.569 cm triangular pitch. The core block is surrounded by a 2.54 cm downcomer annulus between the core block and the reactor vessel. The vessel is made of Hastelloy X and is 0.5 cm thick.

The following assumptions are made for the reactor core heat structures.

- The heat transfer across the fuel to clad gap in the fuel pin is modeled as purely conduction/convection although minimal convection is expected (radiation heat transfer is neglected)
- Internal fuel pins and cooling channels are modeled as being surrounded by an adiabatic surface (the core block)
- Perimeter fuel pins and cooling channels are treated as partially adiabatic and partially convective to the downcomer depending on their specific location



**Figure 12-125: Notional Core Block for UN Core Design**

Using these assumptions, the reactor is modeled with five heat structures:

1. The fuel to coolant channel structure including heat generation inside the fuel, conduction across the fuel pin itself, conduction/convection across the fuel to clad gap, conduction through the cladding, and convection to the coolant channel.
2. The coolant channel to core block structure including convection from the coolant channel and conduction into the core block up to an adiabatic surface midway between the fuel pins.
3. The perimeter fuel pin coolant channel to downcomer structure including convection from the coolant channel, conduction across the core block, and convection into the downcomer annulus.
4. The downcomer to reactor vessel structure including convection from the downcomer annulus and conduction through the reactor vessel to an adiabatic (insulated) outside surface.
5. The fission gas plenum to coolant channel structure including conduction/convection from the gas plenum, conduction across the cladding, and convection to the coolant channel.

The coolant channels and downcomer are assigned to the appropriate heat structures, which are further sub-divided into ten axial segments per fuel pin. Nine of the axial segments are identical in length while the tenth includes an additional 14 cm for the gas plenum.

A heat structure is used to model the heat connection between each of the six fuel pin groups and their respective coolant channels. This heat structure represents the fission heat generated in the fuel pins and its subsequent transfer to the coolant channels. The heat structure uses cylindrical geometry, is composed of three separate regions (fuel, gap, and clad), and has an outside radius of 0.8885 cm, which is equivalent to the cladding radius. The heat structure has an adiabatic boundary at the fuel centerline.

Fission heat is generated in the fuel heat structure using the point kinetics option in RELAP5-3D and distributed, along with decay heat, axially over the heat structures using direct entry weighting factors. The fuel pins are grouped in a fashion to allow radial power distribution as well; however, no radial power shape information was available, so a flat profile is used. The fission heat is divided between the six fuel channels including the center channels, the perimeter channels, and the hot channel. The heat structure model in RELAP5-3D uses lumped parameters similar to the hydraulic model. This enables the combination of the heat structure from many components to couple their heat transfer to a similar representation of many channels.

Another heat structure is used to model the heat connection between each of the six coolant channels and the core block. The core block is divided into a hexagonal mesh with the same pitch as the fuel pins. Each individual hexagon in the mesh represents an adiabatic mass which can act as either a heat sink or source to the coolant channel. The adiabatic assumption is only strictly valid if all fuel cells are producing the same amount of heat. However, this assumption should not introduce any significant error even when the radial power shape is known and applied. The heat structure uses cylindrical geometry, is composed of a single MoRe region, and has an outside radius of 0.19132 cm, which is a cylindrical annulus of equivalent cross sectional area to the hexagonal mesh being modeled.

A portion of the core block is coupled to each of the six fuel channels based on the number of pins associated with each channel and their location. For the internal channels, the core block mass is connected adiabatically to the channel. For the perimeter channels, a portion of the surrounding core block is adiabatically connected to the channel as detailed in Reference 12-16. The remaining perimeter channel core block is modeled as a heat structure connecting the perimeter fuel channels to the downcomer. Since the core block extends above the fueled region of the core to encompass the fission gas plenum at the top of each fuel element, the top node of each core block heat structure is longer than the remaining nodes by 14 cm. The hot channel is a single channel making that component slightly different than the rest of the center channels. Since only a portion of the surrounding core block is treated as adiabatic for the 66 perimeter channels, their heat transfer area and length cannot be calculated as direct ratios of number of channels modeled.

The RELAP5-3D model simulates the fast gas reactor with a point kinetics model using separable feedback terms and standard fission product decay based on the 1979 American Nuclear Society standard for $^{235}U$. Separable feedback maintains the kinetics feedback due to fuel, moderator, and structure temperatures separately.

The reactor plant requires 660 kW to achieve the design point of a reactor gas outlet temperature of 1150K and a Brayton shaft speed of 45,000 rpm. This is achieved with a HeXe gas mixture of 72% He and 28% Xe by mole fraction. Neutron lifetime for the reactor is 1 μs (Reference 12-17) and a total delayed neutron fraction of 0.006339 (Reference 12-18). Fissions are modeled to produce the standard 200 $kW_e$ of usable energy. Delayed neutron production for the fast reactor is characterized with six delayed neutron precursor groups based on Reference 12-18.

An assumption is made that the reactivity feedback for the reactor is divided evenly between the fuel Doppler effect and feedback from the core structural materials. Doppler temperature feedback is a function of the square root of the volume average temperature of the volume to which the feedback is being applied. The overall temperature feedback is divided between two heat structures: the fuel pin structure for Doppler feedback and the core block structure for geometric feedback. Axial feedback coefficients are based on power squared weighting of the Doppler term calculated from the tabular input, and a geometric coefficient assumed to be half of the total temperature feedback. The

geometric coefficients are applied to the four internal core block heat structures, which does not include the hot cell or the perimeter cells.

### 12.5.1.3 Turbomachinery Input Model

The RELAP5-3D model includes two Brayton energy conversion loops directly coupled to the reactor. The energy from the hot gas exiting the reactor is converted to electrical power by expanding it through a turbo-alternator. In addition, a compressor coupled to the turbo-alternator shaft supplies the necessary motive force to circulate the gas through the reactor plant. Figure 12-126 has Brayton Loop 1 highlighted to indicate the demarcation points between both the directly coupled reactor and the parallel Brayton Loop 2. The physical dimensions for each component, flow length, flow area, and surface roughness, are drawn from Reference 12-19 unless otherwise noted.

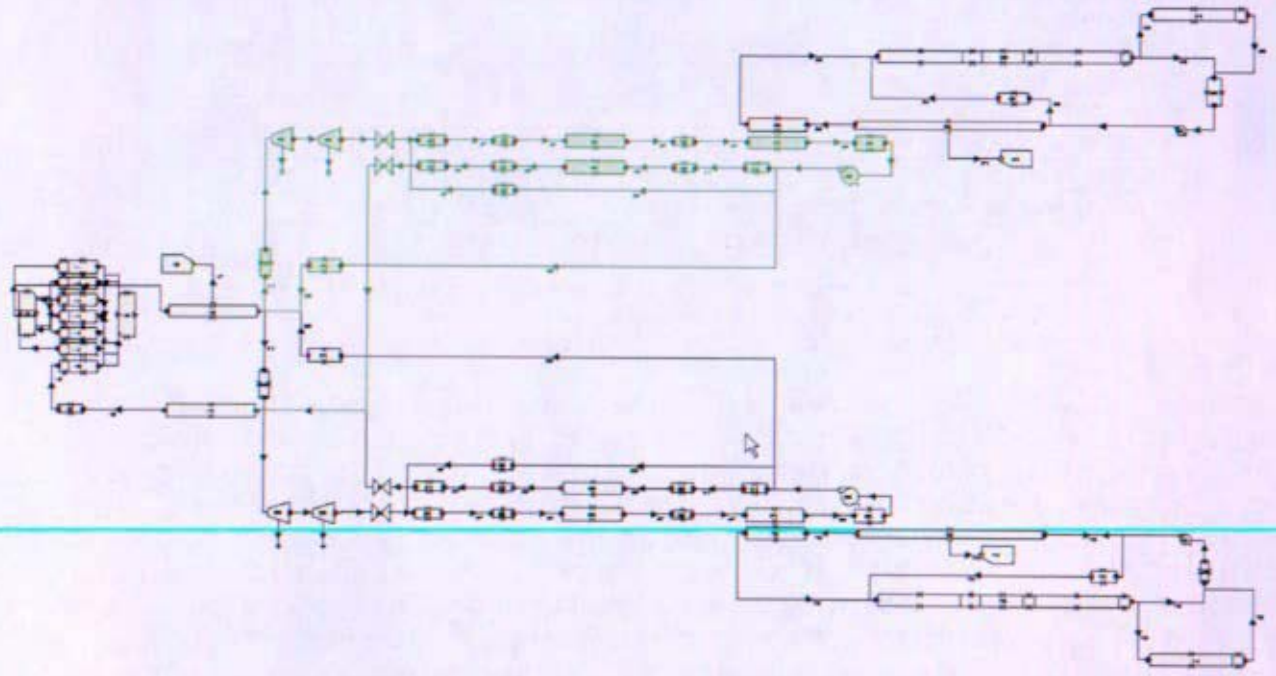


**Figure 12-126: RELAP5-3D/SNAP Direct Gas Brayton Reactor Plant with Energy Conversion Loop 1 Highlighted**

Each RELAP5-3D Brayton energy conversion loop employs a compressor model newly created by the INL for RELAP5-3D in support of Project Prometheus and the Massachusetts Institute of Technology Gas Fast Reactor efforts. Each loop also employs the standard RELAP5-3D turbine model with an in-house modification to allow direct turbine performance map input. Turbine components are a single volume representation of a steam or gas turbine that extracts energy from a fluid via a set of analyst specified performance maps. These maps dictate turbine efficiency and pressure drop as a function of shaft speed and mass flow rate. Compressor components are a single volume representation of a gas compressor that imparts flow energy to the fluid via a set of analyst specified curves derived from compressor performance maps. These curves define operating points for the compressor based on speed and mass flow rate

Turbine performance is based off of turbine maps which are input into the model as tables of efficiency vs. mass flow rate and pressure ratios vs. mass flow rates for given shaft speeds. Pressure ratio and efficiency are determined by linear interpolation based on mass flow and shaft speed. For shaft speeds and mass flow rates beyond the range of the turbine maps, linear extrapolation is performed based on the closest two data points. Additional control variables and trips are then used to calculate the form loss coefficient for the turbine at each time step. The turbine maps and discussion of the required calculations for off-design performance are provided in Reference 12-8.

The Brayton system turbine data is summarized below in Table 12-9. A loss coefficient multiplier is calculated as the problem runs based on turbine performance maps and provided to the turbine component via RELAP5-3D control variables.

**Table 12-9: Brayton Turbine Data**

| Component Name | Brayton |
|---|---|
| Component Type | Turbine |
| Flow Area ($m^2$) | 0.007854 |
| Flow Volume ($m^3$) | 0.011218 |
| Hydraulic Diameter (m) | 0.1 |
| Junction Area ($m^2$) | 0.007854 |
| Reynolds Number Independent Forward Flow Energy Loss Coefficient | 1 |
| Reynolds Number Independent Reverse Flow Energy Loss Coefficient | 1 |
| Inertia ($kg \cdot m^2$) | 0.068953 |
| Friction Coefficient | 0 |

The compressor is modeled with either the new RELAP5-3D compressor component or a pump component. The RELAP5-3D compressor component is used for all steady state and transient runs except for the complete loss of electrical load (overspeed) transient in which the pump component was used. The compressor component requires compressor data that covers the range of flow rates and shaft speeds that occur during a transient. Since the overspeed transient takes shaft speed well beyond the available compressor data, the necessary data extrapolation introduced too much error into the calculation and in many cases made the compressor unstable. The pump model, on the other hand, is able to calculate performance at the very high shaft speeds, and the pump performance curves were extrapolated to the necessary operating points. More compressor data would have been required to refine the analysis of the overspeed transient had the design continued.

For the compressor component, compressor maps are input directly. Pressure ratio and efficiency are provided as functions of relative corrected mass flow rate (CFLO) and corrected shaft speed (CORSPD). The compressor maps are further described in Reference 12-8. The compressor model uses the default junction control flags except no choking model is applied. The compressor performance is entirely described by the compressor maps. It was judged that if the choking model were used, choked flow might occur distorting the compressor performance.

For the pump component, compressor maps are input as pump homologous curve data in the form of non-dimensional pump head curves and pump torque curves. The homologous data for the compressor does not fall on a single curve as pump parameters normally do. So the data based on shaft speed at the design value are used when using the pump component approximation for the compressor. There is significant data scatter as shaft speed diverges from the design value. Therefore, the compressor component, which provides the ability to explicitly represent the pressure

ratio and efficiency as a function of shaft speed and mass flow rate, is used for transients other than overspeed as previously discussed.

The non-dimensional homologous curves are calculated based on the ratios of four normalized compressor parameters: head loss ($h$), torque ($\beta$), volume flow rate ($\nu$), and rotational shaft speed ($\alpha$). Each normalized quantity is computed by dividing the compressor off-design values by the design values. The performance parameters are converted to homologous form with independent variables of $\nu/\alpha$ or $\alpha/\nu$ and dependent variables of $h/\alpha^2$, $h/\nu^2$, $\beta/\alpha^2$, and $\beta/\nu^2$. The entire pump performance can be characterized with eight input regimes for head and eight for torque based on the relative values of $\alpha$ and $\nu$.

The shaft component in RELAP5-3D calculates shaft speed based on balancing the torques applied to it. The moment of inertia of the turbomachinery affects the transient response of the shaft speed. To control shaft speed, an additional torque is applied to the shaft. The required torque is calculated with RELAP5-3D control variables as the transient is run. The additional torque represents the total of the electrical load plus any losses in the turbomachinery. This also represents the power added during start-up

The turbine, alternator, and compressor are all connected to one shaft. Thus, these components all operate at identical shaft speeds. The shaft speed is determined by a balance of the torques on the shaft imposed by the components plus any parasitic losses. The equation for the load balance on the shaft is:

**Equation 12-2** $$I\, d\omega/dt = \tau_T - \tau_C - \tau_A - \tau_P$$

Where:
- $\tau_T$ = turbine torque = $\eta_T m \Delta P_T / \rho_T \omega$
- $\tau_C$ = compressor torque = $m \Delta P_C / \eta_C \rho_C \omega$
- $\tau_A$ = torque imposed by the alternator
- $\tau_P$ = torque imposed by parasitic losses
- $I$ = shaft moment of inertia
- $\eta_T$ = turbine efficiency
- $m$ = mass flow rate
- $\Delta P_T$ = turbine differential pressure
- $\rho_T$ = average fluid density in the turbine
- $\omega$ = shaft speed
- $\eta_C$ = compressor efficiency
- $\Delta P_C$ = compressor differential pressure
- $\rho_C$ = average fluid density in the compressor

### 12.5.1.4 Gas Cooler

The RELAP5-3D gas cooler is a counter flow heat exchanger that transfers heat from the HeXe working fluid in the Brayton loop to the NaK working fluid in the heat rejection loop. NaK was one of the working fluids considered for the heat rejection loop, although water was later selected for Project Prometheus. The heat structure utilizes a staggered coupling scheme developed specifically for counter flow heat exchangers that is fully described in Reference 12-20. This is accomplished using five separate heat structures: a staggered mesh connecting the two components, a gas side end

volume heat correction, a NaK side end volume heat correction, a gas side heat balance structure, and a NaK side heat balance structure as described in Reference 12-20.

The model of the gas cooler uses the default volume control flags except for the following: 1) the vertical stratification model is not used (since not relevant to single phase flow), 2) the ORNL ANS narrow channel model heat transfer correlation is applied, and 3) wall friction is not computed along the direction of flow. The ORNL ANS model provides the best approximation of experimental data for the low Prandtl number gas being used and the laminar flow regime. The Nusselt number from the ORNL ANS model is adjusted for both compact heat exchanger effects and Reynolds number dependency as described in Reference 12-20. Wall friction is not computed in favor of implementing the Kays and London correlation directly as a Reynolds number dependent form loss coefficient option.

The flow areas and hydraulic diameters are based on sizing studies performed by GRC and documented in Reference 12-6. For the gas side of the gas cooler, the relationship between the irrecoverable loss factor ( $K$ ) and Reynolds number are shown below. The irrecoverable loss factor is obtained as a function of Reynolds number per Reference 12-10 modified with a constant multiplier of 4712 in order to match the pressure drops supplied by GRC.

$$K = 4712 \times \mathrm{Re}^{-0.554177}$$

For both sides of the gas cooler, wall friction is turned off in order to provide direct control over the friction calculations. For the NaK side of the gas cooler, the Reynolds number dependent form loss coefficient option in RELAP5-3D is used to accurately represent the Kays and London compact heat exchanger 1/10-19.35 (Reference 12-10). The friction factor data is fit to the exponential format required by the code resulting in the following relation:

$$f = 2.08512\,\mathrm{Re}^{-0.554177}$$

This relation matches the desired friction factors to within +9/-15% over the entire range of data (Reynolds numbers of 200 to 4000). However, in order to match the state point pressure drop supplied by GRC, the constant (2.085) in the irrecoverable loss factor is increased to 95.56.

### 12.5.1.5 Recuperator

The recuperator uses heat from the turbine exhaust on the recuperator hot side to preheat the gas in the recuperator cold side returning to the reactor, increasing cycle efficiency. The hot and cold sides of the recuperator are each 20 sub-volume pipes that are coupled via a heat structure. The heat structure utilizes a staggered coupling scheme developed specifically for counter flow heat exchangers that is fully described in Reference 12-20. Five separate heat structures are used: a staggered mesh connecting the two components, a hot side end volume heat correction, a cold side end volume heat correction, a hot side heat balance structure, and a cold side heat balance structure as described in References 12-20 and 12-5.

The model of the recuperator uses the default volume control flags except for the following: 1) the vertical stratification model is not used (since not relevant to single phase flow), 2) the ORNL ANS narrow channel model heat transfer correlation is applied, and 3) wall friction is not computed along the direction of flow. The ORNL ANS model provides the best approximation of experimental data for the low Prandtl number gas being used and the laminar flow regime. The Nusselt number from the ORNL ANS model is adjusted for both compact heat exchanger effects and Reynolds number

dependency as described in Reference 12-20. Wall friction is not computed in favor of implementing the Kays and London correlation directly as a Reynolds number dependent form loss coefficient option.

The flow area and hydraulic diameter of the recuperator are based on sizing studies performed by GRC and documented in Reference 12-6. In the hot side of the recuperator, the relationship between the irrecoverable loss factor ( $K$ ) and Reynolds number are shown below. The irrecoverable loss factor is obtained as a function of Reynolds number per Reference 12-10 modified with a constant multiplier of 276.7 in order to match the pressure drops supplied by GRC.

$$K = 276.7 \times \mathrm{Re}^{-0.554177}$$

In the cold side of the recuperator, the relationship between the irrecoverable loss factor ( $K$ ) and Reynolds number are shown below. The irrecoverable loss factor is obtained as a function of Reynolds number per Reference 12-10 modified with a constant multiplier of 340.5 in order to match the pressure drops supplied by GRC.

$$K = 340.5 \times \mathrm{Re}^{-0.4662829}$$

### 12.5.1.6 Heat Rejection Segment (HRS)

The RELAP5-3D model includes two heat rejection loops that remove waste heat from the two Brayton loops. The heat is removed via a gas cooler that transfers the waste heat from the gas in the Brayton energy conversion loop to the liquid metal operating fluid composed of NaK in the HRS. Heat is then removed from the liquid metal by radiating it to space via several radiation panels. Motive force for the coolant is provided by one Annular Linear Induction Pump (ALIP) in each heat rejection loop. Since the heat rejection loops are identical, only one is highlighted in Figure 12-127.

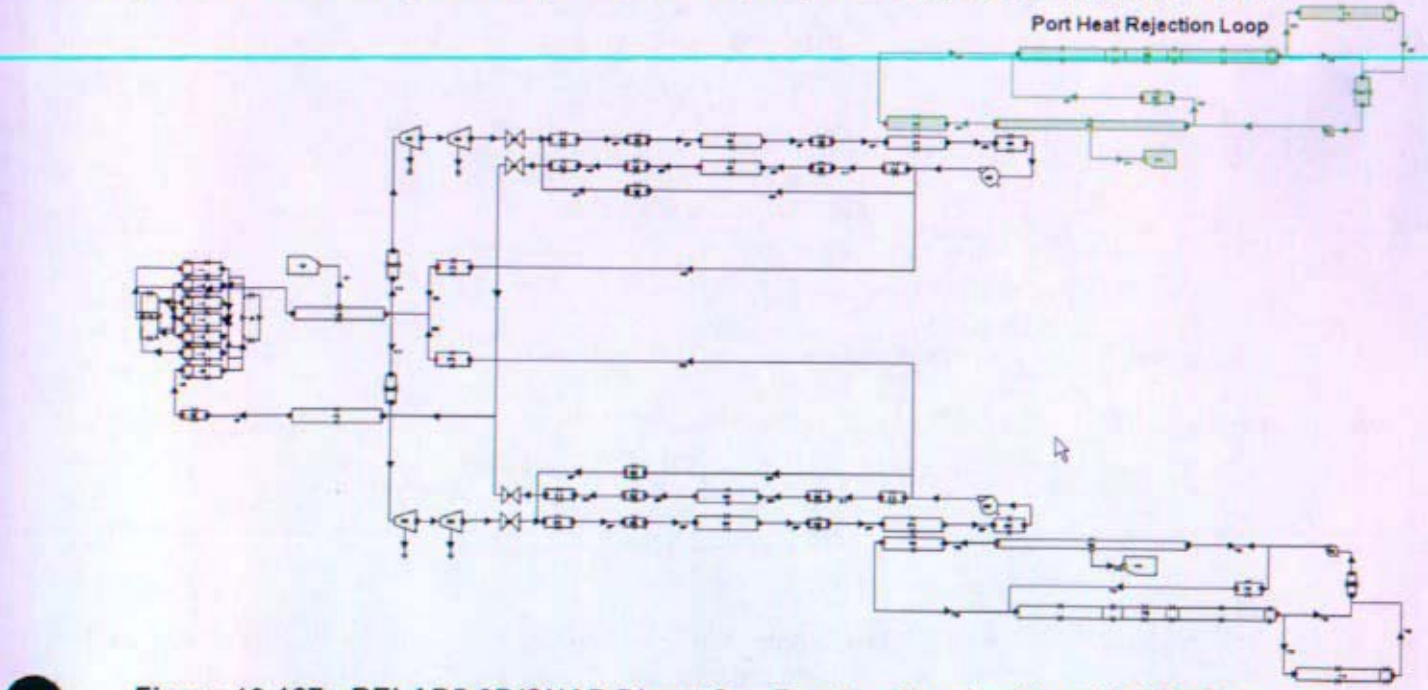



**Figure 12-127: RELAP5-3D/SNAP Direct Gas Brayton Reactor Plant Highlighting One Heat Rejection Loop**

For the HRS, all ducts have rectilinear cross sections and so the hydraulic diameter is calculated to be 0.0424 meters. In the calculation of the hydraulic diameter, the cross sectional area of 0.001824 $m^2$ and the wetted perimeter of 0.172m is based on 4-cm-by -5-cm ducts with a 0.1 cm thick inner sleeve (Reference 12-21). All duct lengths are determined from Reference 12-21.

Motive force for the HRS working fluid is provided by an ALIP. All rated pump conditions and performance curves are drawn from Reference 12-22. However, the rated torque, flow, and head are adjusted so that the pump performance reaches the conditions established in Reference 12-1. The ALIP is modeled as a normal canned motor pump because the code lacks a model specific to an ALIP. The design point for the ALIP modeled is based on state points developed by GRC (Reference 12-6). For that design point, the pump conditions are 100 kPa developed pump head while delivering 24.4 gpm at a temperature of 359K.

The ALIP characteristics for a range of pumps and conditions are discussed in Reference 12-22. Data for a pump whose rated conditions are 18 psi (124 kPa) developed pump head while delivering 28 gpm at a temperature of 400K are used in the model since this pump is the closest to the Reference 12-6 design point conditions. The data is converted to homologous pump curves as required for input to the RELAP5-3D pump model.

The radiator pipe is the structure through which heat is rejected to space. Wall friction is turned off in favor of representing the desired friction factor with the Reynolds number dependent form loss coefficient option in RELAP5-3D. Idel'chik (Reference 12-23) Section 8-2, paragraph 15, provides an empirical relation to determine the friction factor for flow past a bundle of vertically arranged tubes uniformly distributed over conduit cross sections. For a duct that is 3.8 cm wide with heat pipes in one row that have 12.5 cm between heat pipe centers and 2.2 cm outside diameters the equation for friction factor is:

$$friction\ factor = 1.52\left(\left(S_1 - d_{out}\right)/\left(S_2 - d_{out}\right)\right)^{-0.2}\left(S_1/d_{out} - 1\right)^{-0.5}\,\mathrm{Re}^{-0.2}\,z$$

$$friction\ factor = 1.52\left(\left(3.8 - 2.2\right)/\left(12.5 - 2.2\right)\right)^{-0.2}\left(3.8/2.2 - 1\right)^{-0.5}\,\mathrm{Re}^{-0.2}$$

$$friction\ factor = 2.5867\,\mathrm{Re}^{-0.2}$$

where: $S_1$ = duct width, 3.8 cm,
$d_{out}$ = heat pipe outside diameter, 2.2 cm,
$S_2$ = distance between heat pipe centers, 12.5 cm,
Re = Reynolds number, and
z = number of tube rows in parallel in the duct, 1.

Thus, from above:

$$form\ loss\ coefficient = 2.5867\,\mathrm{Re}^{-0.2}\left(L/D\right)$$

where: L = friction length of the sub-volume preceding the junction and
D = junction diameter.

Since the radiator sub-volumes are not constant length, the form loss coefficient varies over the length of the component. The form loss values were increased to match the pressure drops specified by the GRC state point calculations documented in Reference 12-6.

The primary heat structures for the HRS are the radiator panels used to reject the Brayton cycles waste heat to space. This is accomplished by building a heat structure that representative of the radiator panels and a heat structure that represents space and coupling the two using the RELAP5-3D Radiation/Conduction Enclosure Model. The heat structure for the radiator panel included 25 segments that directly corresponded to the 25 fluid volumes used to hydraulically model the components. Each of these segments is assigned an emissivity of 0.9 (Reference 12-21). None of the segments are coupled together so their internal view factors are set to 0.0. All of the segments have an unimpeded "view" of space so each segments view factor to space was set to 1.0. Heat is transferred between the radiator panels and space based on their relative temperature differences, emissivity, and the view factor.

Originally there were two types of heat structures that made up the radiator panels: one to represent the titanium heat pipes (Reference 12-21) and one to represent the face sheets. Each heat pipe has a 2.4 $cm^2$ cross section with a 1.0 cm inner radius. An equivalent volume cylindrical pipe is used in the heat structure to take advantage of the cylindrical geometry option in RELAP5-3D. The NaK boundary condition is set to convective. The heat pipe length and corresponding heat transfer area vary significantly throughout the panel. The face sheet heat structure has been taken out of this model because the Fourier number for the envisioned face sheet is calculated to be 930, which is three orders of magnitude too large. As a result, some non-physical results are obtained when the face sheet heat structure is included in the model. This thin sheet of carbon does not significantly affect the heat transfer rate in the model. Therefore, it is removed from the model and the heat pipes are assumed to radiate directly to space. The view factors are adjusted accordingly.

Another heat structure represents the constant heat sink of space at 200K to which the radiator radiates heat through the Radiation/Conduction Enclosure Model. The 200K deep space temperature is based on Reference 12-21.

## 12.5.2 RELAP5-3D Transient Results

Six different transients were analyzed with RELAP5-3D. Transients based on normal and casualty conditions were chosen to evaluate the response of the reactor and define the design space within which the reactor and the remainder of the plant would need to perform. Each of those transients is discussed in the following sections.

### 12.5.2.1 Mechanical Loss of One Brayton (RELAP5-3D)

The assumption in this transient is that one of two operating turbines stops suddenly. This is represented in the models by instantly disconnecting the turbine from the shaft that drives the alternator and compressor. When the turbine is disconnected from the shaft, the compressor and alternator coast to a stop. As a result, the flow to the reactor is reduced by about 50%. Some of the flow from the operating Brayton loops would flow backward through the idle Brayton loop if reverse flow were not prevented, reducing the reactor flow to less than 50%. Therefore, check valves are represented, one in each loop, in the input model.

Reactor power and core hot spot temperature are plotted for this transient in Figure 12-128 and Figure 12-129. Core structure and average fuel temperatures must increase to cause the reactor power to decrease. As flow decreases, less heat is being removed from the reactor so there is a power mismatch resulting in the core heating the fuel, coolant and core structures to higher temperatures. The temperature increase in the fuel and core structures is caused purely by reactor power and not by hotter coolant. Increased fuel and core structure temperatures cause reactor power to decrease. Since the heat up is driven by the fuel, the hot spot temperatures increase significantly before reactor power starts to decrease. The reactor power drops by about the same amount as the flow through the reactor, to about 50%, due to temperature feedback from the increasing core temperatures.

Figure 12-130 through Figure 12-137 show the responses of additional selected parameters during the loss of a Brayton. Loop temperatures immediately start to increase. The loop temperatures increase because the flow through the core decreases before power starts to decrease, heating the gas to a higher outlet temperature. The idle loop cold leg temperature also increases because less energy is removed from the gas in the idle loop as indicated in Figure 12-134. There is a slight increase followed by a reduction in reactor inlet temperature as flow in the idle Brayton loop coasts down. This temperature behavior is the result of hotter gas being supplied by the idle loop as it coasts down. Initially, the idled loop is supplying enough flow to increase the bulk reactor inlet temperature. However, as the idled loop flow decreases and the operating loop flow increases the reactor inlet temperature becomes dominated by the colder temperature of the operating loop. The shaft that drives the alternator and compressor in the idled loop coasts to a stop in about 30 seconds (Figure 12-133) after which time reactor inlet temperature is completely controlled by the operating loop.

HRS loop temperature in the affected loop, Figure 12-136, shows hot leg temperature dropping to equal cold leg temperature in about 100 seconds. After that, both temperatures decrease because there is no longer much energy supplied by the gas in the loop while the radiator is still removing energy.

### 12.5.2.2 Complete Loss of Electrical Load for One Brayton (RELAP5-3D)

As stated in Section 12.5.1.3, the turbine, alternator, and compressor are all connected to one shaft and operate at identical shaft speeds. The shaft speed is determined by a balance of the torques on the shaft imposed by the components plus any parasitic losses, as given by Equation 12-2. If the alternator load were suddenly removed there would be a net positive torque on the turbine shaft resulting in an increased rotational speed. Note that there is a control system to regulate shaft speed. If it is working properly, excess power would be transferred to a PLR by the shaft speed control system and the transient successfully averted. This transient assumes a failure in the shaft speed control system.

Figure 12-138 through Figure 12-147 show the transient response of some selected parameters. At the increased shaft speed the turbine removes more energy from the gas coolant as seen in Figure 12-144 and Figure 12-145. The higher shaft speed causes the compressor to add more energy to the fluid. As a result, the compressor exit temperature increases. The resulting difference between the two recuperator inlet temperatures (turbine exit and compressor exit) is reduced by about half. That temperature difference is directly proportional to the heat transfer rate in the recuperator. Thus the recuperator transfers about half as much energy from the hot stream to the cooler stream. The reactor inlet temperature is lower as a result, causing reactor power to increase.

The shaft speed stabilizes at a new higher speed where the compressor and any parasitic loads are balanced by the torque produced by the turbine, as shown in Figure 12-143. In order for the shaft to stabilize at a new speed, rather than increase indefinitely, the magnitude of the compressor torque must approach that of the turbine torque. At higher shaft speeds, both the turbine and compressor efficiencies decrease. That tends to reduce the difference in the turbine and compressor torques as can be seen from Equation 12-2. In addition, while the temperature and pressure entering the turbine are fairly constant, the temperature entering the compressor increases and the pressure decreases significantly as shaft speed increases because the turbine reduces pressure more and the recuperator removes less energy from the gas that flows toward the compressor. That causes the compressor density to decrease which also causes the difference between compressor and turbine torque to decrease.

Figure 12-142 shows that mass flow rate only briefly increases in the affected loop, even though shaft speed increases by nearly 40%. The mass flow rate is reduced by the decrease in compressor density described above; resulting in essentially the same mass flow rate as before the load was lost.

Figure 12-138 and Figure 12-139 show reactor power and core hot spot temperature. The power peaks at approximately 117% and hot spot temperature increases by about 75K before approaching steady state values of around 111% power and 60K above the starting temperatures.

Figure 12-146 and Figure 12-147 show HRS hot and cold leg temperatures. The hotter gas entering the gas cooler from the recuperator in the affected loop causes over 100K increase in hot leg temperature. The cold leg temperature eventually increases by about 25K.

### 12.5.2.3 Positive Reactivity Addition (RELAP5-3D)

Figure 12-148 through Figure 12-157 show the transient response of some selected parameters for this transient. It is assumed that the reactivity is instantly increased in the reactor an amount equivalent to a 50K increase in temperature. Since the total temperature coefficient of the reactor is -0.0021254 \$/K ($-1.36 \times 10^{-5}$ $\delta\rho$/K), the reactivity change required to change the temperature by 50 K is

$ 0.10627 (0.00068 δρ). Figure 12-151 shows the contributors to reactivity. This transient causes the reactor power and temperature to increase initially, and then reactor power decreases somewhat as reactor inlet temperature increases in response to the increased reactor outlet temperature. However, reactor power does not return back to the initial power because the turbine removes more energy from the gas with a higher inlet temperature causing the system power to increase. The power the turbine extracts from the fluid is defined by the following equation:

$$P = \eta m \Delta P / \rho$$

where: $\eta$ = turbine efficiency
$m$ = fluid mass flow rate
$\Delta P$ = pressure drop across the turbine
$\rho$ = average density in the turbine

For this transient, turbine efficiency, mass flow rate, and pressure drop are essentially constant. However, since the turbine inlet temperature increases, the density decreases both at the inlet and outlet of the turbine. Thus, the average density decreases by about 4%. This causes the power extracted by the turbine to increase by about 4%. At the same time, the torque required to operate the compressor is essentially unchanged resulting in an increase in the electric power produced.

### 12.5.2.4 Negative Reactivity Addition (RELAP5-3D)

Figure 12-158 through Figure 12-167 show the transient response of some selected parameters for this transient. This transient is the opposite of the positive reactivity addition casualty. In this case the reactivity is decreased instantaneously by $ 0.10627 (0.00068 δρ), as seen in Figure 12-161. Figure 12-158 shows that reactor power decreases then recovers somewhat but does not return to the initial power level because the turbine produces less power at lower temperature. This is the opposite effect as described in the positive reactivity transient previously. The changes in power and temperature are approximately equal in magnitude and in the opposite direction of the positive reactivity transient. All other parameters are fairly constant.

### 12.5.2.5 Complete Loss of Flow in One HRS Loop (RELAP5-3D)

Figure 12-168 through Figure 12-177 show the transient response of some selected parameters in this transient. This transient assumes the NaK pump stops operating in one loop. The NaK temperature increases slightly initially, as seen in Figure 12-176, causing the HeXe gas temperature exiting the gas cooler to get slightly hotter as well Figure 12-174.

Since the electric load is held constant in this transient, even small decreases in compressor density will cause the compressor torque to increase slowing the shaft speed (Equation 12-2). Figure 12-173 shows the shaft speeds. At slower shaft speeds the turbine produces less power resulting in further slowing of the shaft. At about 250 seconds the shaft stops due to the turbine stalling. If action were taken to reduce electric loads, the stall of the turbine could have been delayed.

### 12.5.2.6 Start-up (RELAP5-3D)

Figure 12-178 through Figure 12-186 show the transient response of some selected parameters during this scenario. The start-up transient is contingent on the assumptions made. For the start-up analyzed here it was assumed that the fluids all start at 400 K and the reactor is critical at the point of adding heat, 1% (8 $kW_t$) power. During start-up the HRS would be operated at reduced capacity, since it would overwhelm heat added to increase plant temperature. That is represented in this model

by holding the heat sink for the radiator (space) at 400K. Once operating temperature and shaft speed are reached, normal HRS capacity is restored in this model by reducing the radiator heat sink temperature to 200K. Although this is a non-physical method, the effect on the HRS is similar.

It is assumed that both turbines are initially motored at 25% shaft speed (11,250 rpm) to preclude damage to turbine bearings. The sliders are moved as required to heat the reactor outlet temperature to 1150 K in 2.5 hours (300 K/hr). In parallel, the motor speed of one turbine is increased at 13,500 rpm per hour until it is self-sustaining (the turbine torque exceeds compressor torque), then shaft speed is allowed to be dictated by the turbine and compressor torques until it reaches 45,000 rpm. Slider motion is simulated by moving the sliders at 0.5 cm/minute for 8 seconds then holding for 100 seconds. After the hold period the slider motion process is repeated if required in order to maintain reactor outlet temperature within 1 K of the heat up goal.

During the first 2.5 hours the reactor power increases to about 40% (Figure 12-178) and reactor outlet temperature increases to 1150 K (Figure 12-179), while shaft speed of the first Brayton increases to normal speed (Figure 12-182). After 2.5 hours the motor speed of the second turbine is increased at 13,500 rpm per hour until it is self-sustaining. At that point, since the temperature entering the Brayton loop is at 1150 K, the shaft speed quickly increases to the steady state speed of 45,000 rpm. The combination of increased coolant flow rate resulting from the second Brayton loop and the colder gas entering the reactor causes reactor power to peak at between 100% and then level off at around 83% power. Since the HRS capacity is reduced, the power does not reach 100%. Once normal HRS capacity is restored at about 5.4 hours, reactor power increases to 100%.

The oscillation in reactor power during heat-up is caused by the automatic slider motion described above. The reactivity caused by the slider motion is shown in Figure 12-180. The plant response to the slider motion causes the power oscillations. A person controlling the slider motion may be able to make the heat-up smoother. Adjustments to the timing for slider motion and holding the slider could also eliminate or reduce this oscillation.

This transient demonstrates the approximate response of this notional start-up and indicates that it is not an excessively severe transient. More careful control plus use of the shaft speed controller even after self-sustaining turbine conditions are reached could make the start-up even less severe. It is expected that start-up would occur over a much longer period which would reduce any power overshoot. The shaft speed would not likely increase simultaneously with temperature. Shaft speed and temperature would be increased alternately. The second loop would need to be brought up to speed before any temperature limits are violated in the loop components, which may require starting the loop before the first one reaches normal operating conditions. The electrical power required to motor the shaft indicted is approximately an order of magnitude larger than expected. This is because the compressor and turbine maps in the RELAP5-3D input model had to be extrapolated to perform this transient. If the JIMO program would have continued, compressor and turbine data would have been incorporated into the model to cover the range of all transients performed.

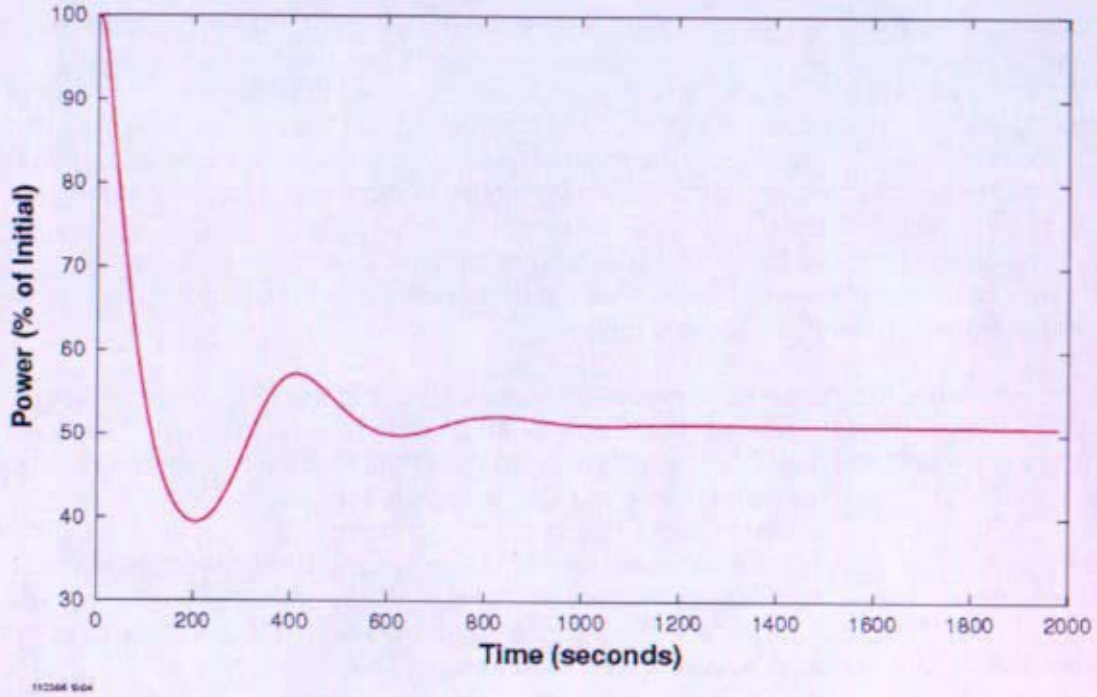



Figure 12-128: Reactor Power Resulting from Loss of One of Two Braytons (RELAP5-3D)

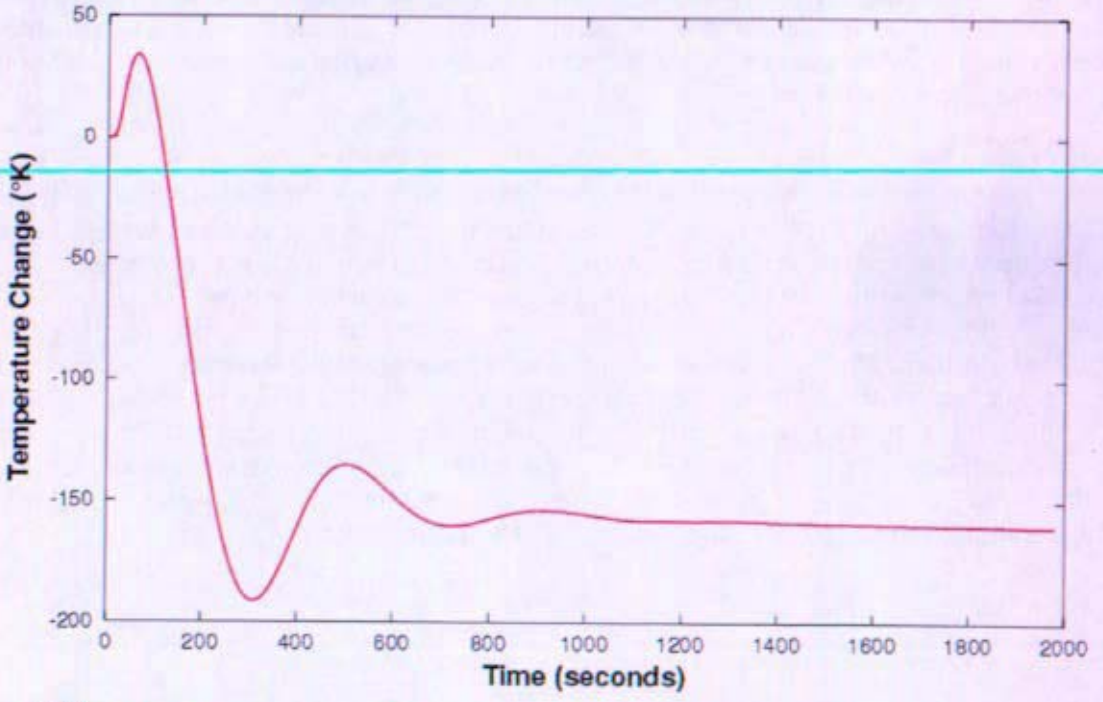



Figure 12-129: Hot Spot Fuel Temperature Resulting from Loss of One of Two Braytons (RELAP5-3D)

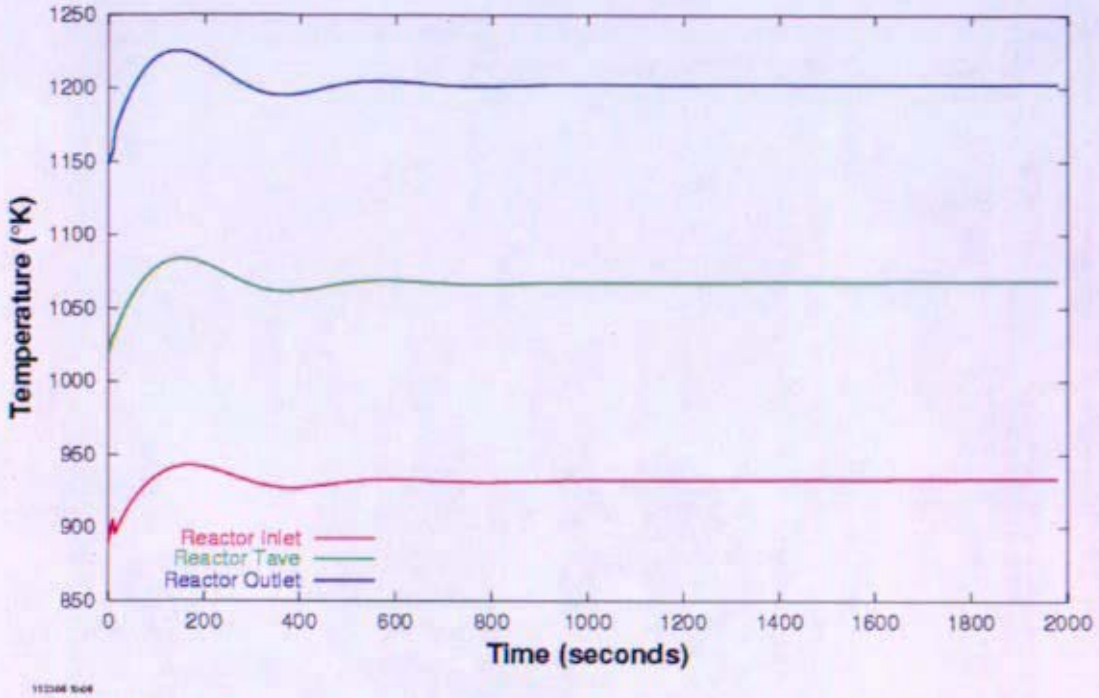



**Figure 12-130: Loop Temperatures Resulting from Loss of One of Two Braytons (RELAP5-3D)**

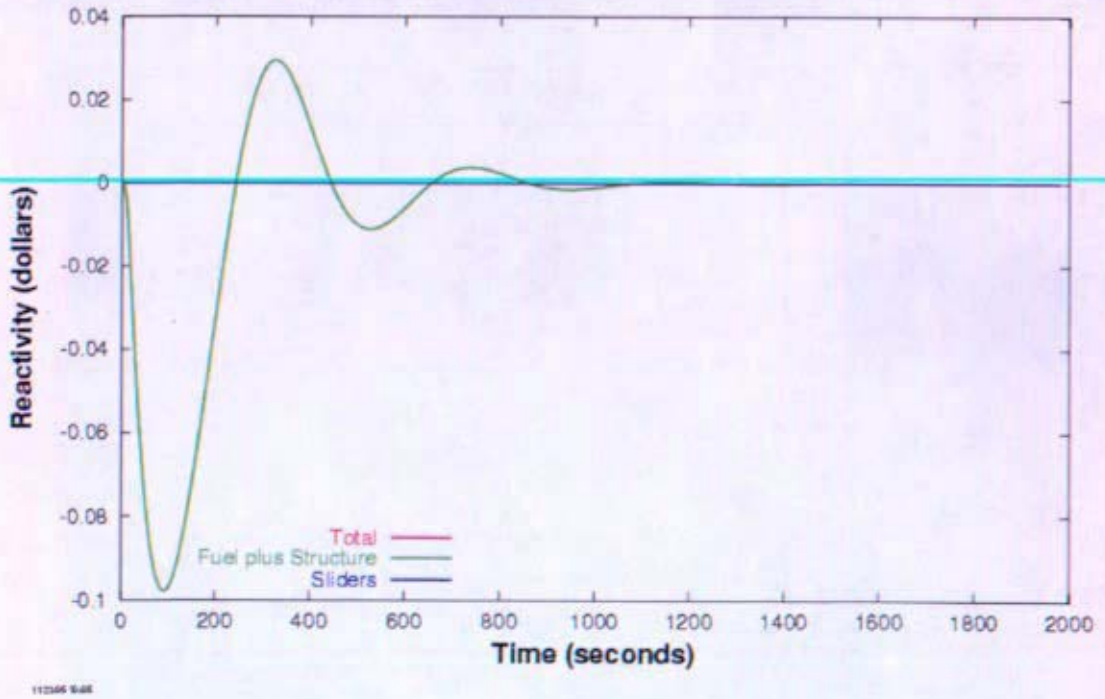



**Figure 12-131: Reactor Reactivity Resulting from Loss of One of Two Braytons (RELAP5-3D)**

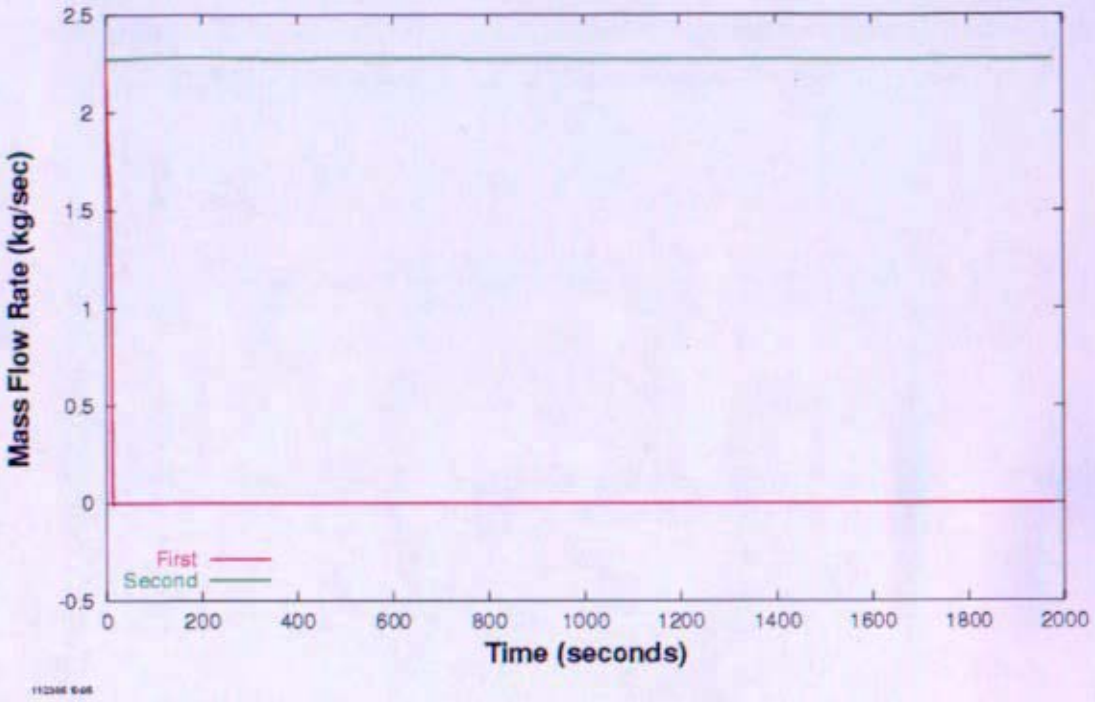



**Figure 12-132: Mass Flow Rates Resulting from Loss of One of Two Braytons (RELAP5-3D)**

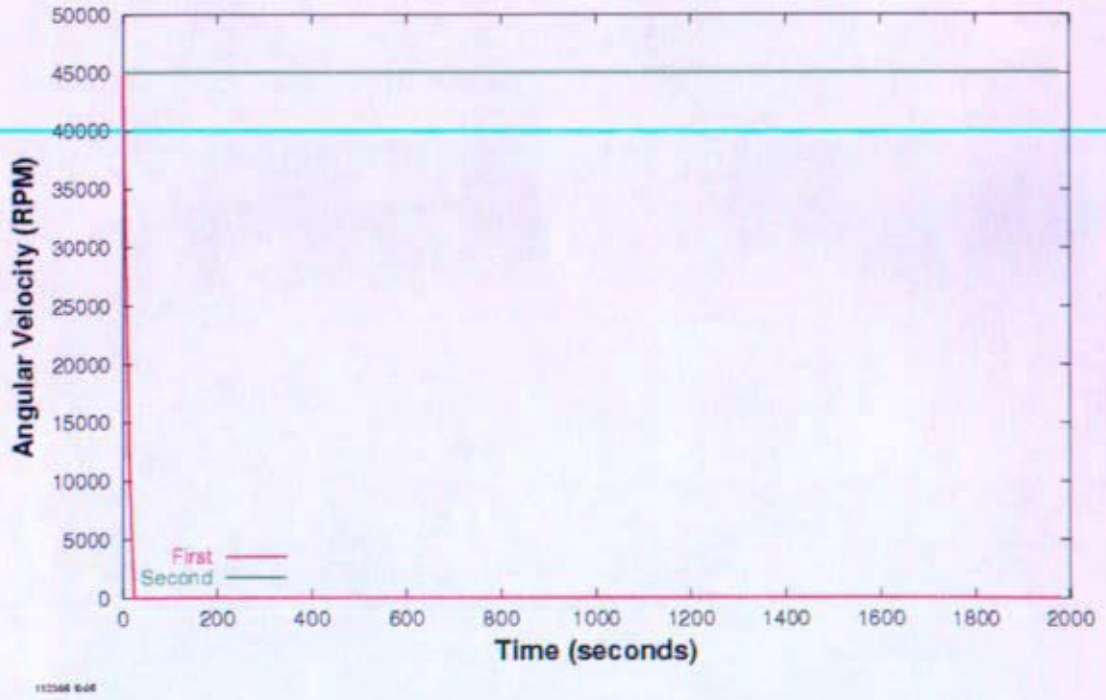



**Figure 12-133: Shaft Speeds Resulting from Loss of One of Two Braytons (RELAP5-3D)**

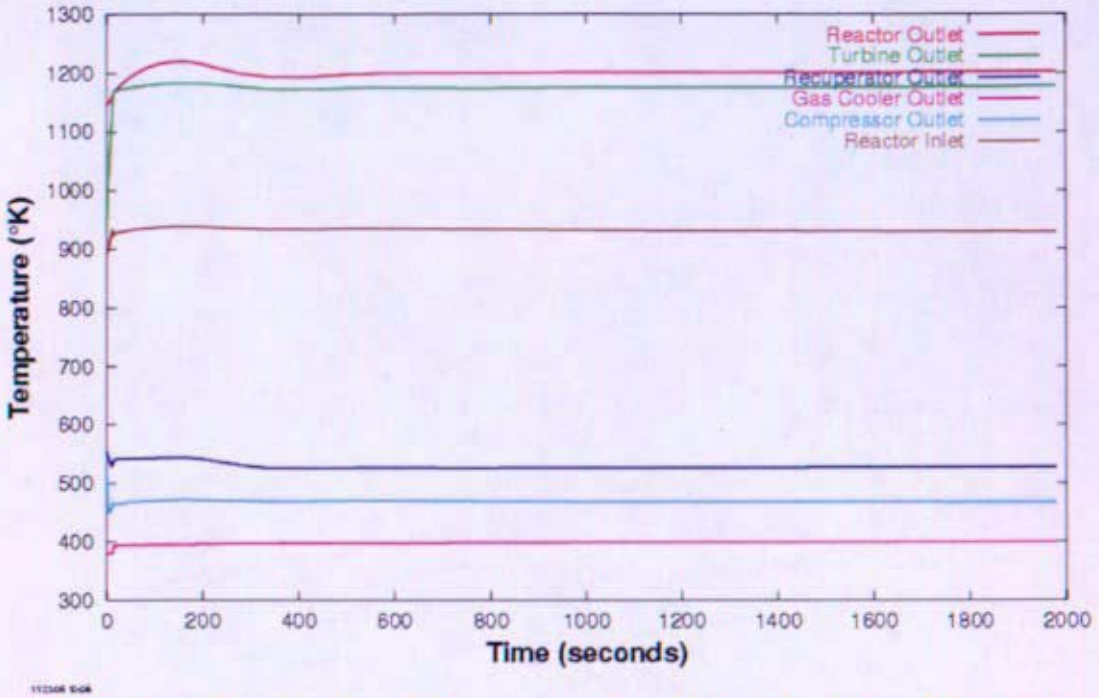



**Figure 12-134: First Brayton Loop Temperatures Resulting from Loss of One of Two Braytons (RELAP5-3D)**

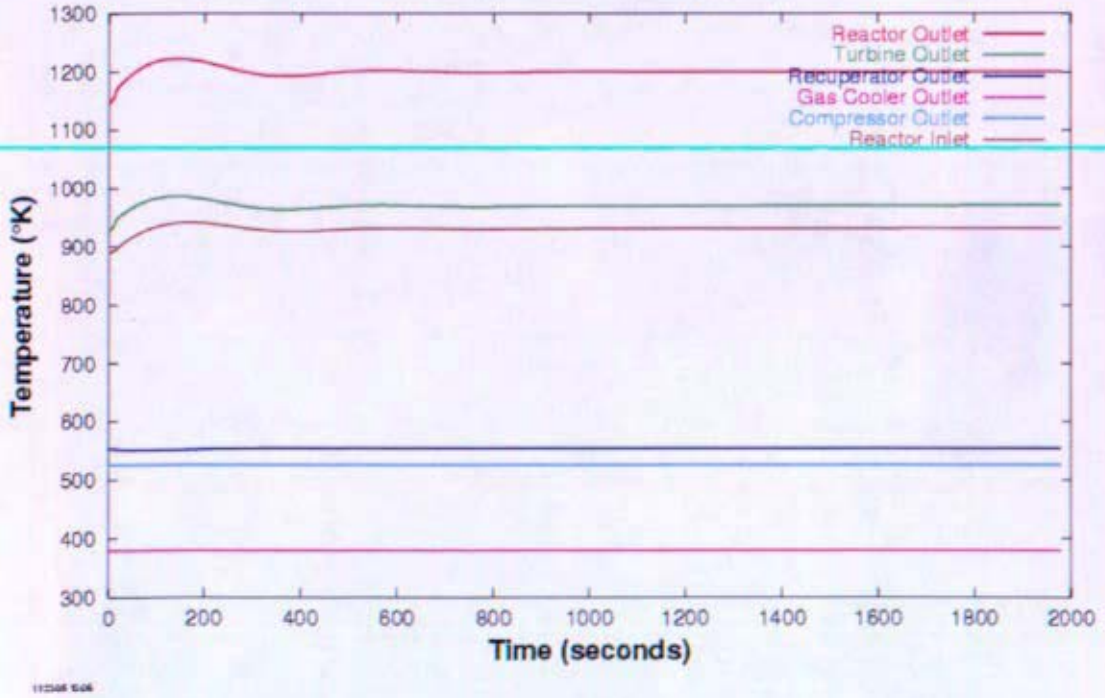



**Figure 12-135: Second Brayton Loop Temperatures Resulting from Loss of One of Two Braytons (RELAP5-3D)**

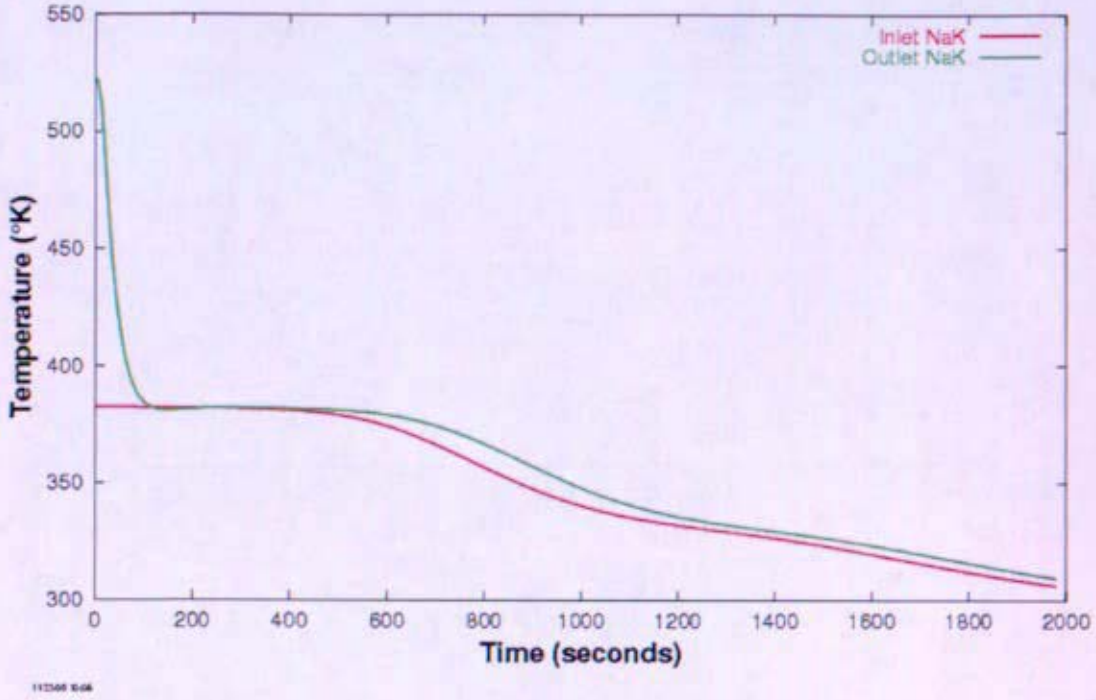



**Figure 12-136: First Heat Rejection Loop Temperatures Resulting from Loss of One of Two Braytons (RELAP5-3D)**

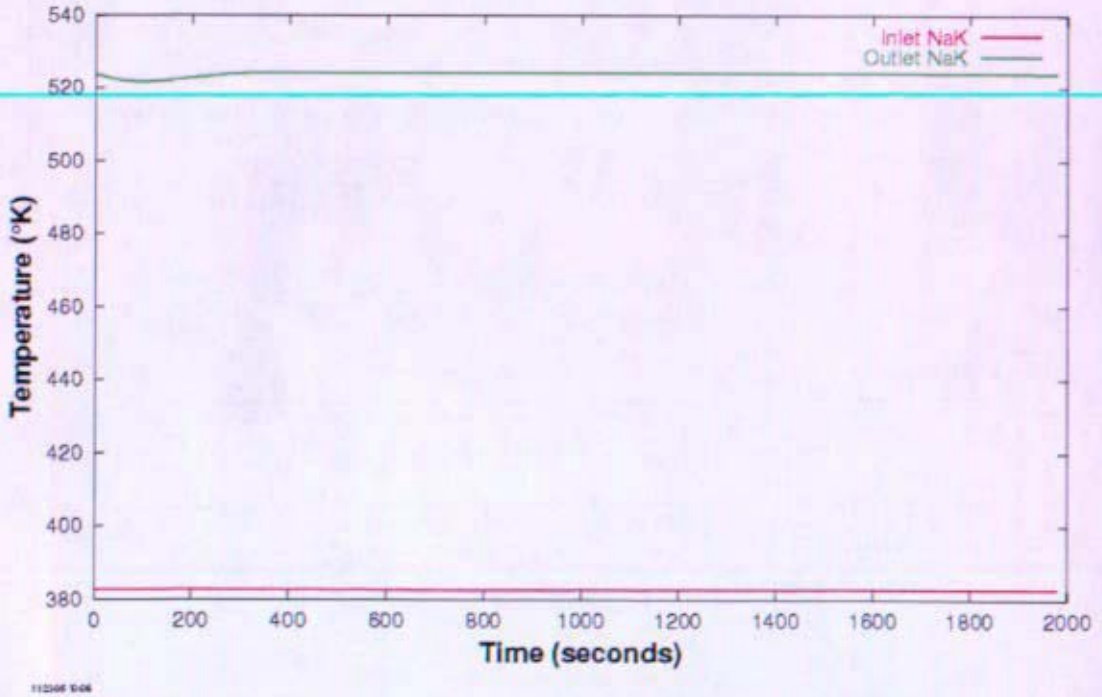



**Figure 12-137: Second Heat Rejection Loop Temperatures Resulting from Loss of 1 of 2 Braytons (RELAP5-3D)**

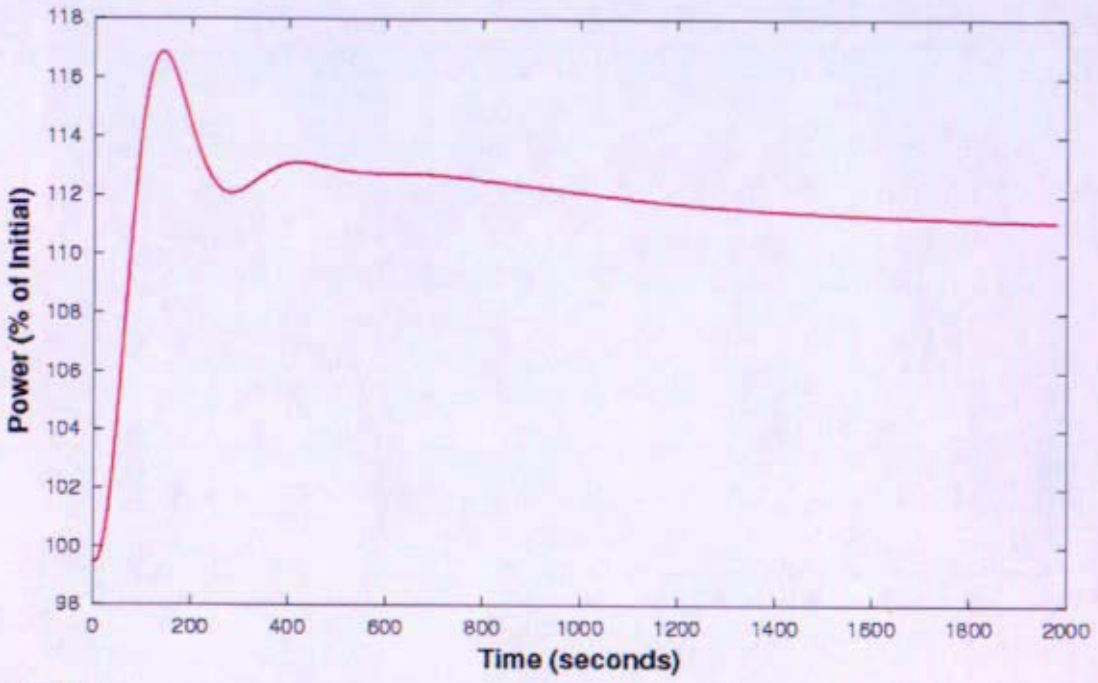



**Figure 12-138: Reactor Power Resulting from Over speed of One of Two Braytons (RELAP5-3D)**

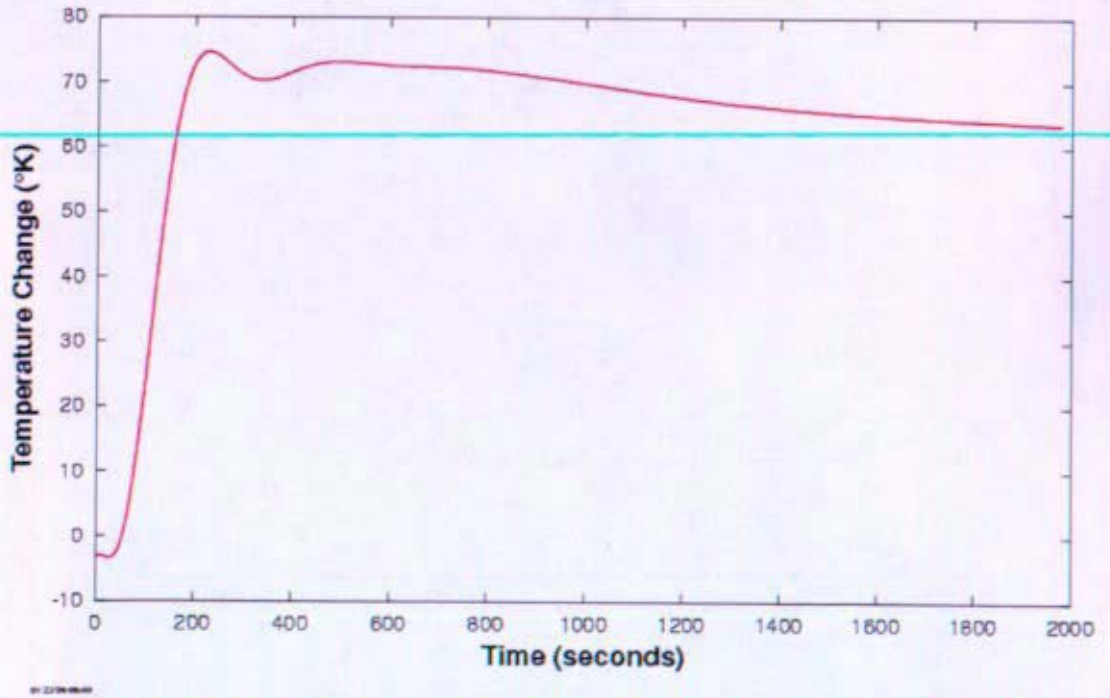



**Figure 12-139: Hot Spot Fuel Temperature Resulting from Over speed of One of Two Braytons (RELAP5-3D)**

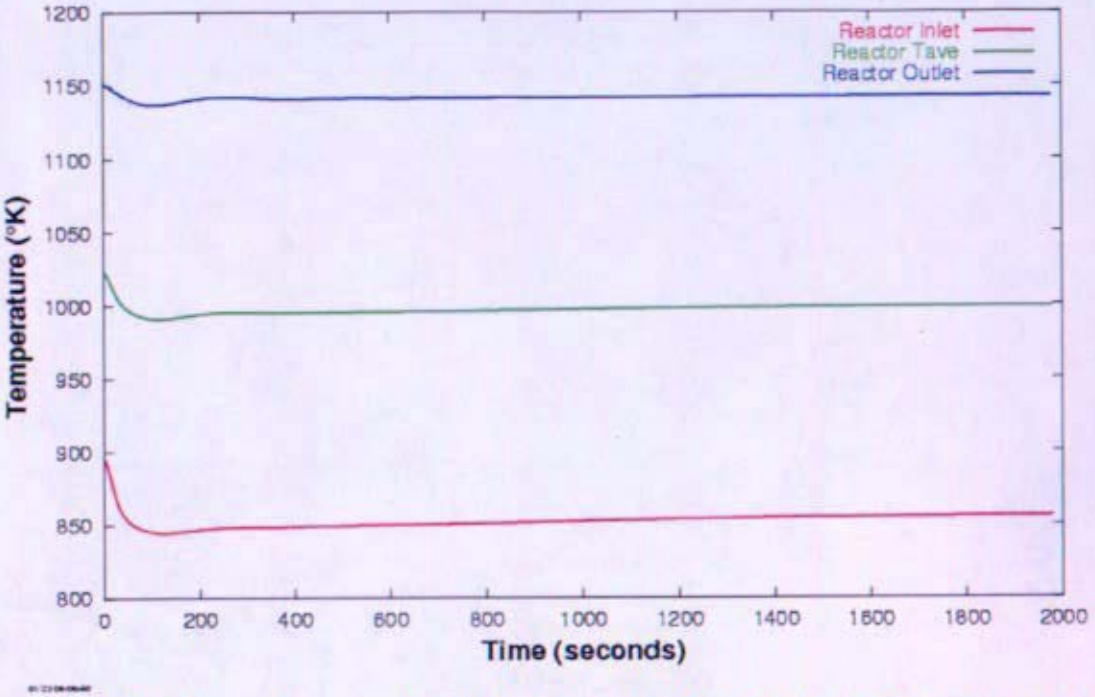



**Figure 12-140: Loop Temperatures Resulting from Over speed of One of Two Braytons (RELAP5-3D)**

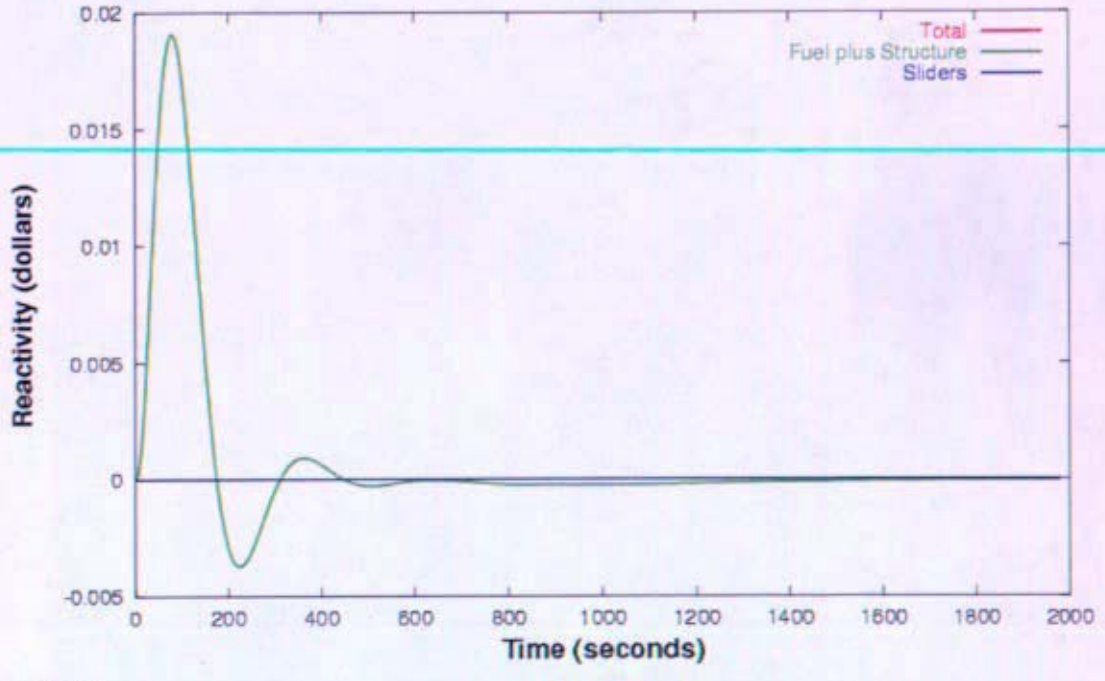



**Figure 12-141: Reactor Reactivity Resulting from Over speed of One of Two Braytons (RELAP5-3D)**

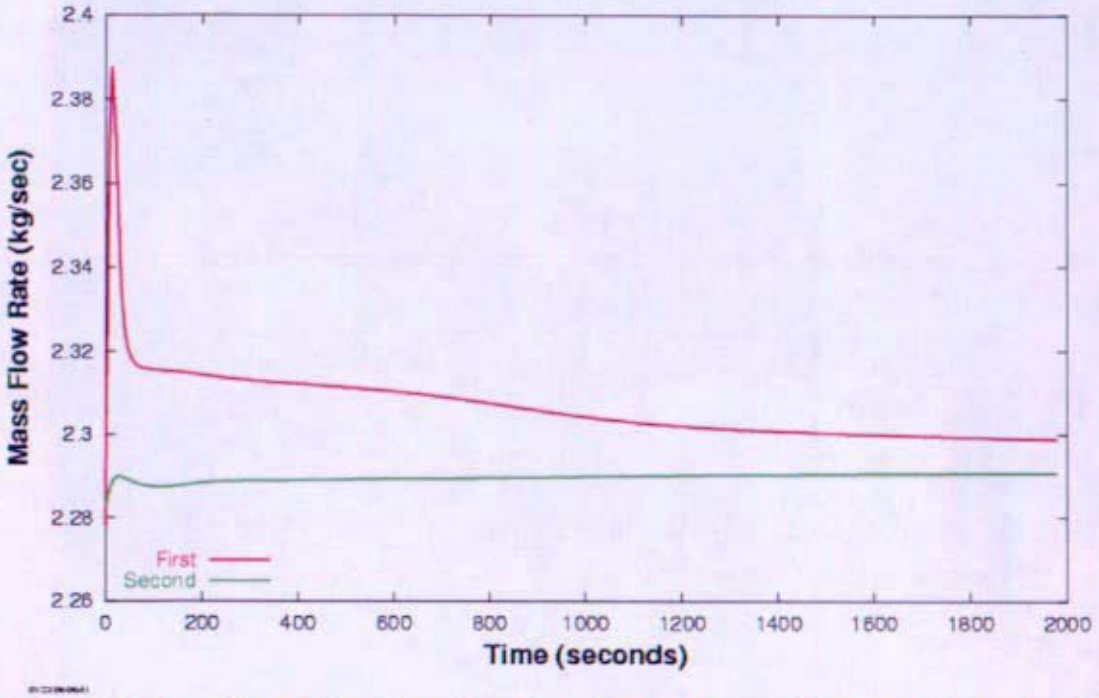



**Figure 12-142: Mass Flow Rates Resulting from Over speed of One of Two Braytons (RELAP5-3D)**

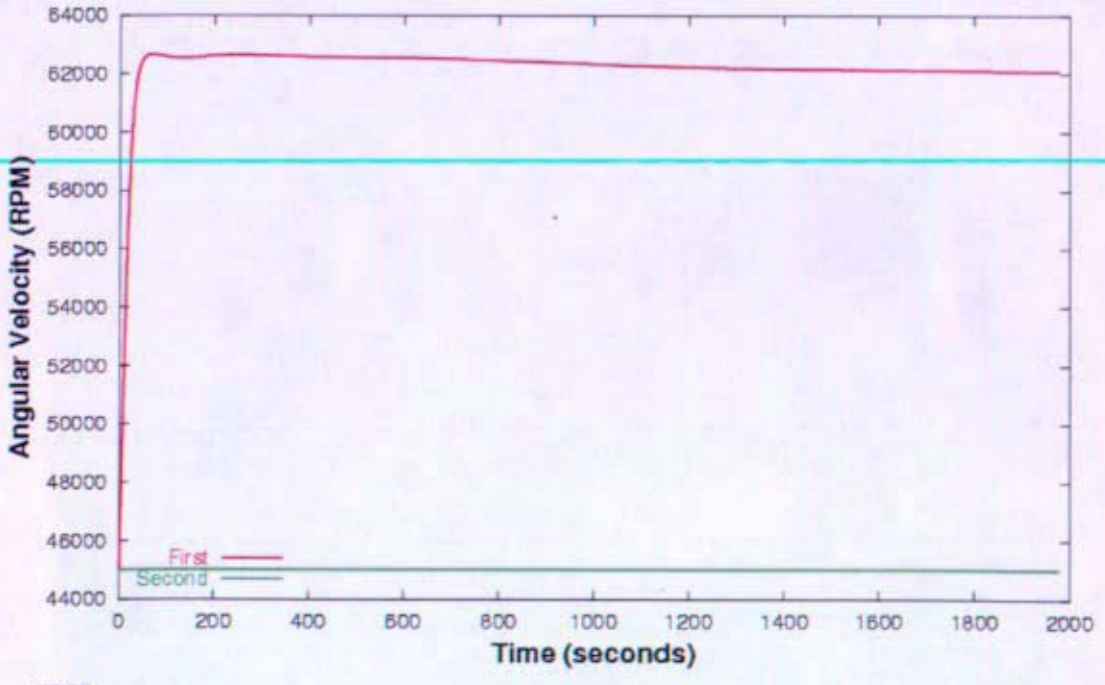



**Figure 12-143: Shaft Speeds Resulting from Over speed of One of Two Braytons (RELAP5-3D)**

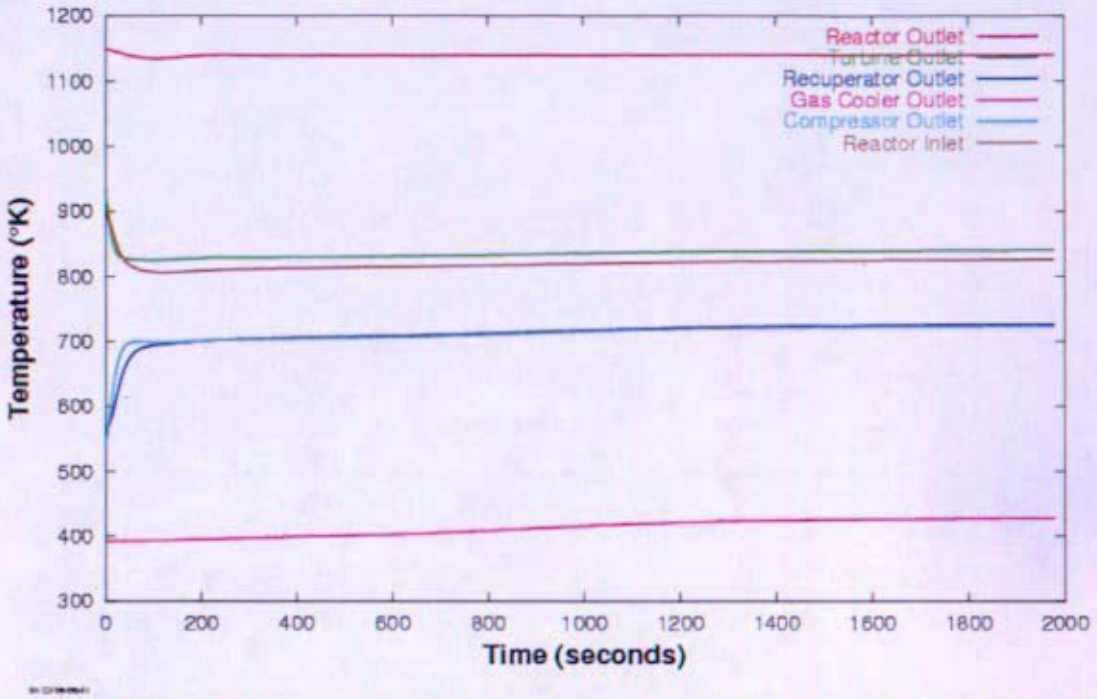



**Figure 12-144: First Brayton Loop Temperatures Resulting from Over speed of One of Two Braytons (RELAP5-3D)**

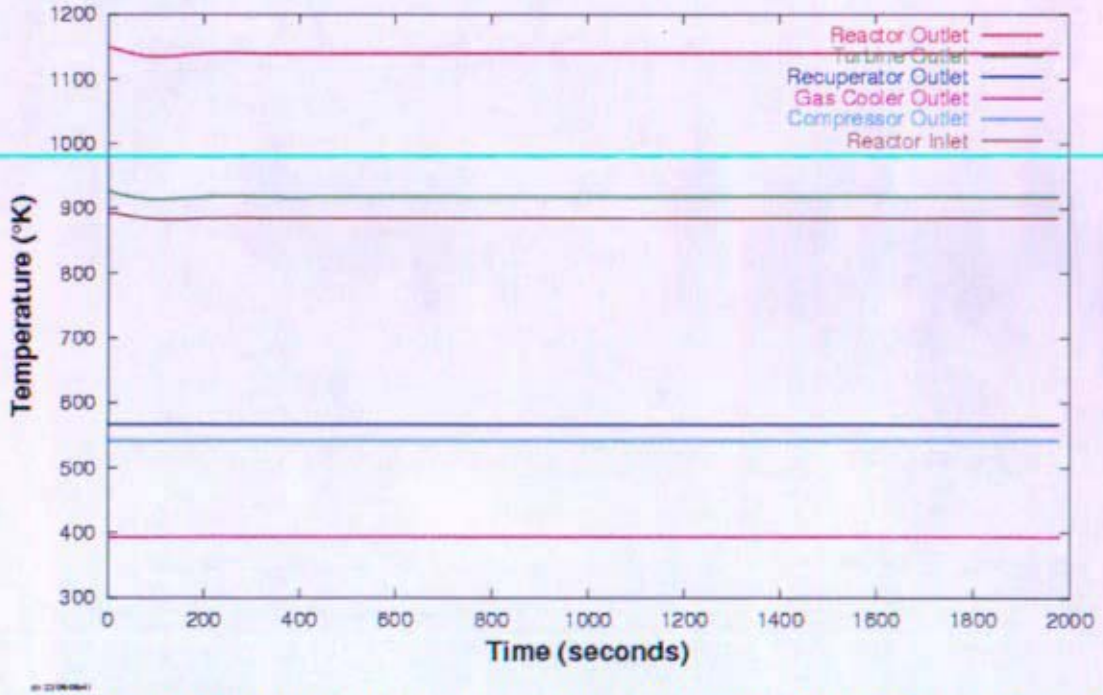



**Figure 12-145: Second Brayton Loop Temperatures Resulting from Over speed of One of Two Braytons (RELAP5-3D)**

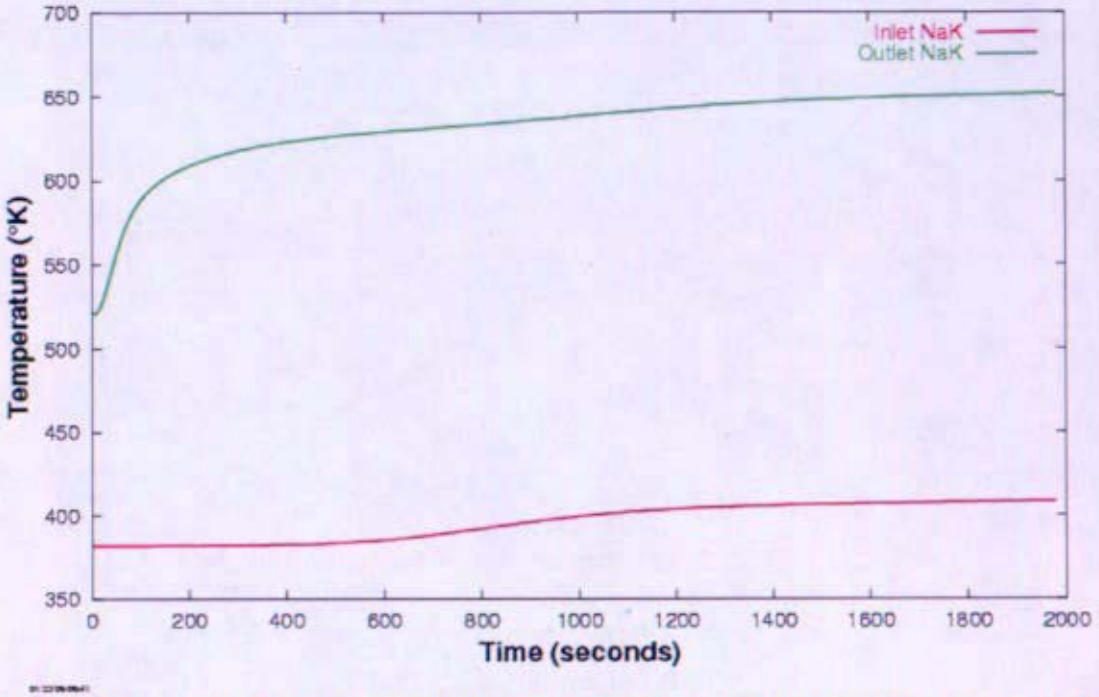



**Figure 12-146: First Heat Rejection Loop Temperatures Resulting from Over speed of 1 of 2 Braytons (RELAP5-3D)**

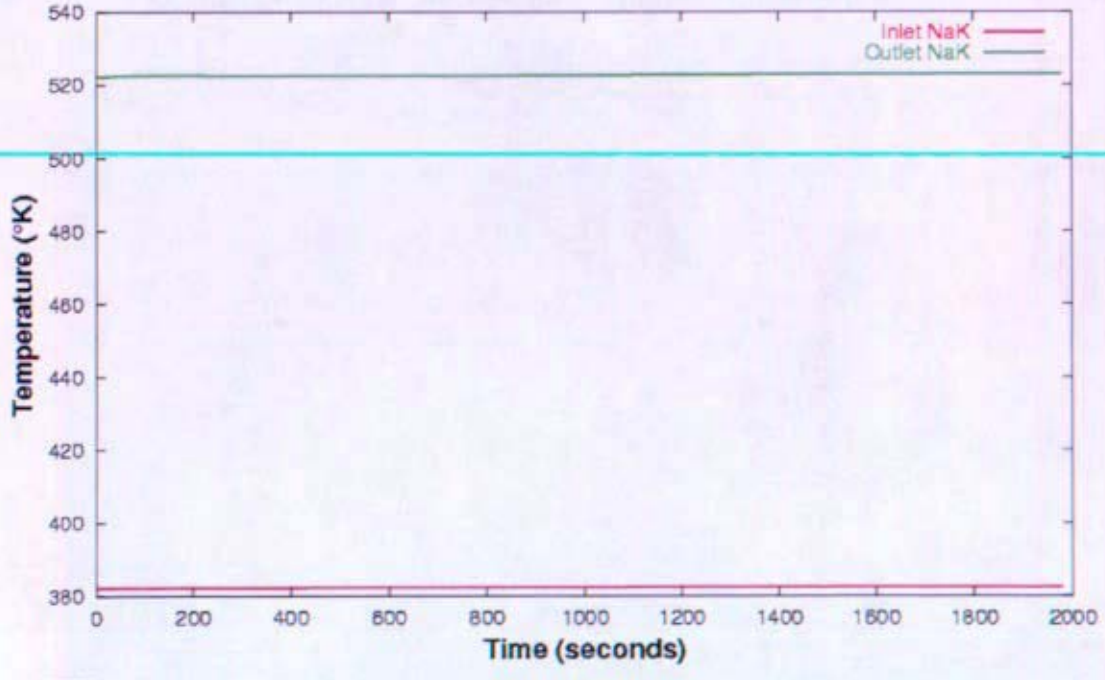



**Figure 12-147: Second Heat Rejection Loop Temperatures Resulting from Over speed of One of Two Braytons (RELAP5-3D)**

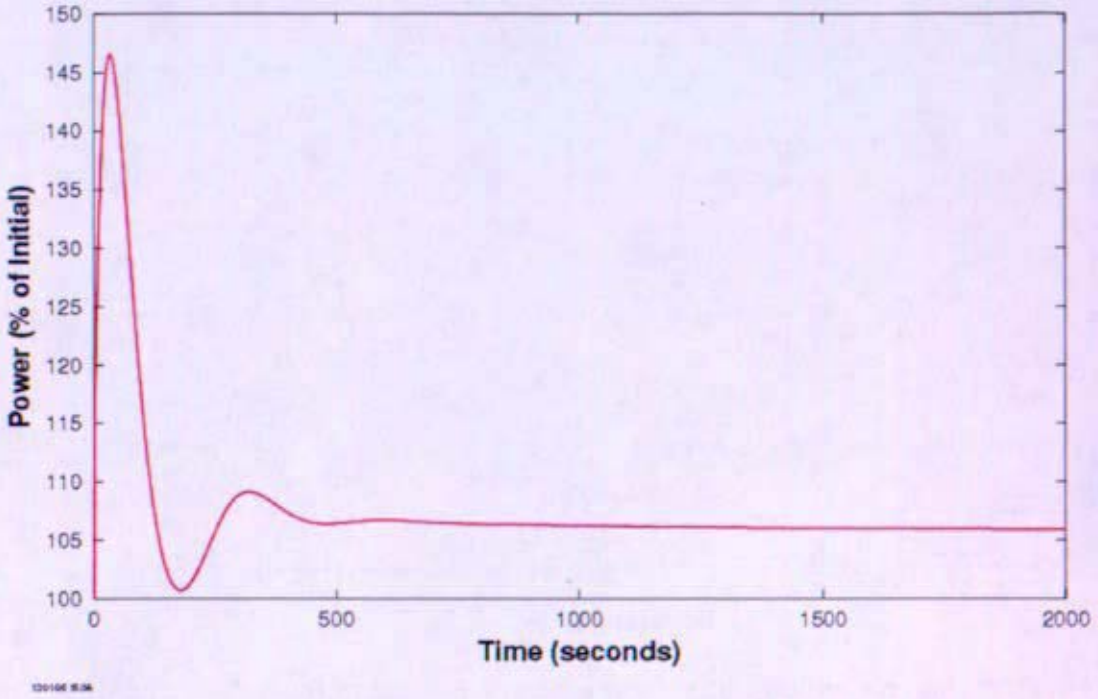



**Figure 12-148: Reactor Power Resulting from Positive Reactivity (RELAP5-3D)**

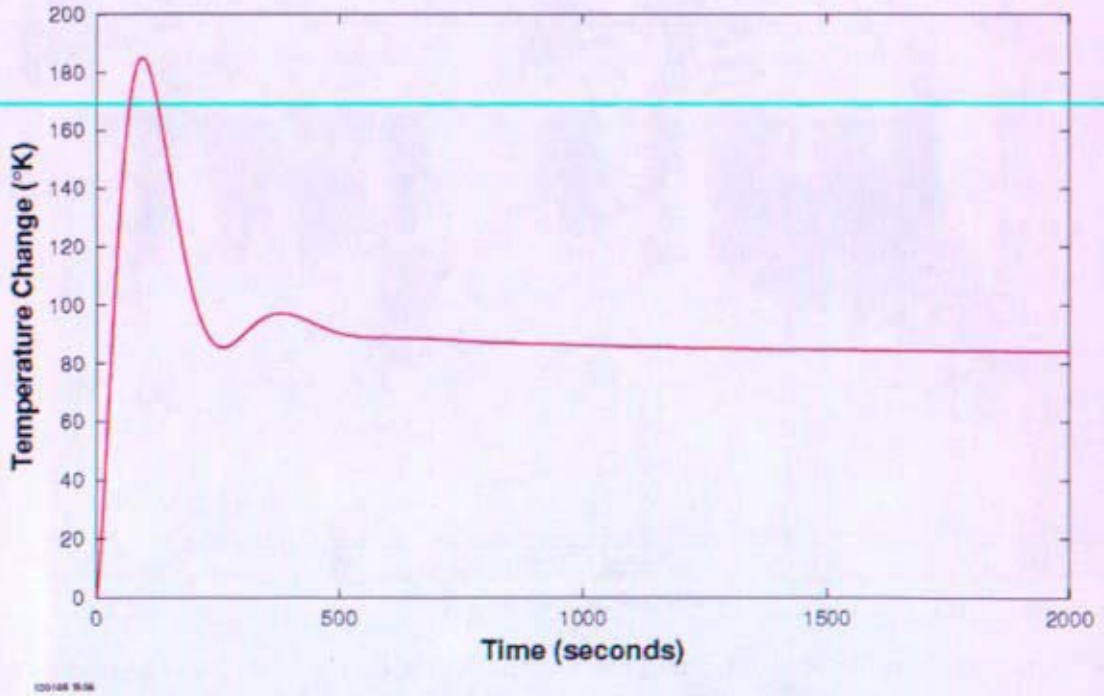



**Figure 12-149: Hot Spot Fuel Temperature Resulting from Positive Reactivity (RELAP5-3D)**

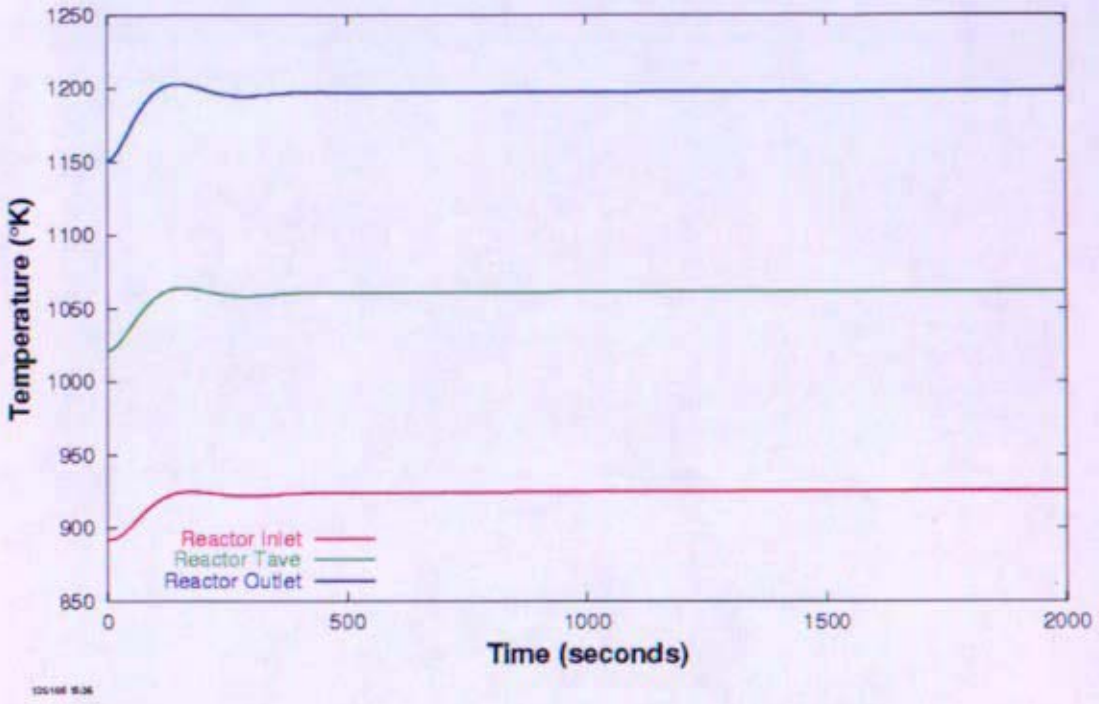



**Figure 12-150: Loop Temperatures Resulting from Positive Reactivity (RELAP5-3D)**

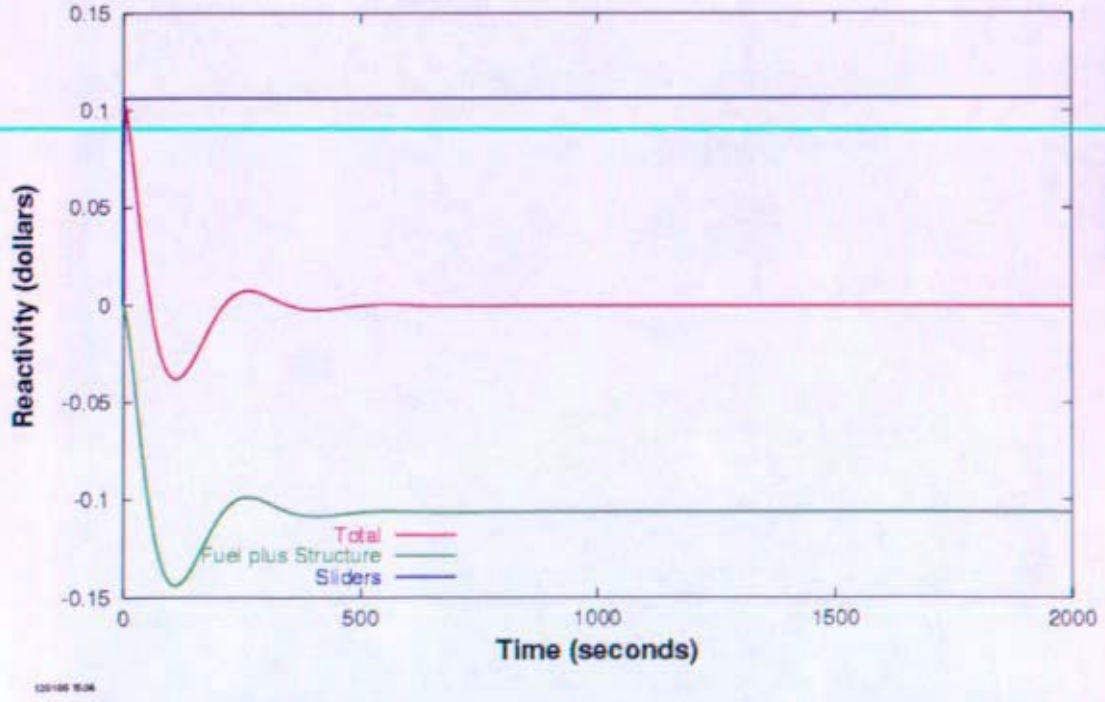



**Figure 12-151: Reactor Reactivity Resulting from Positive Reactivity (RELAP5-3D)**

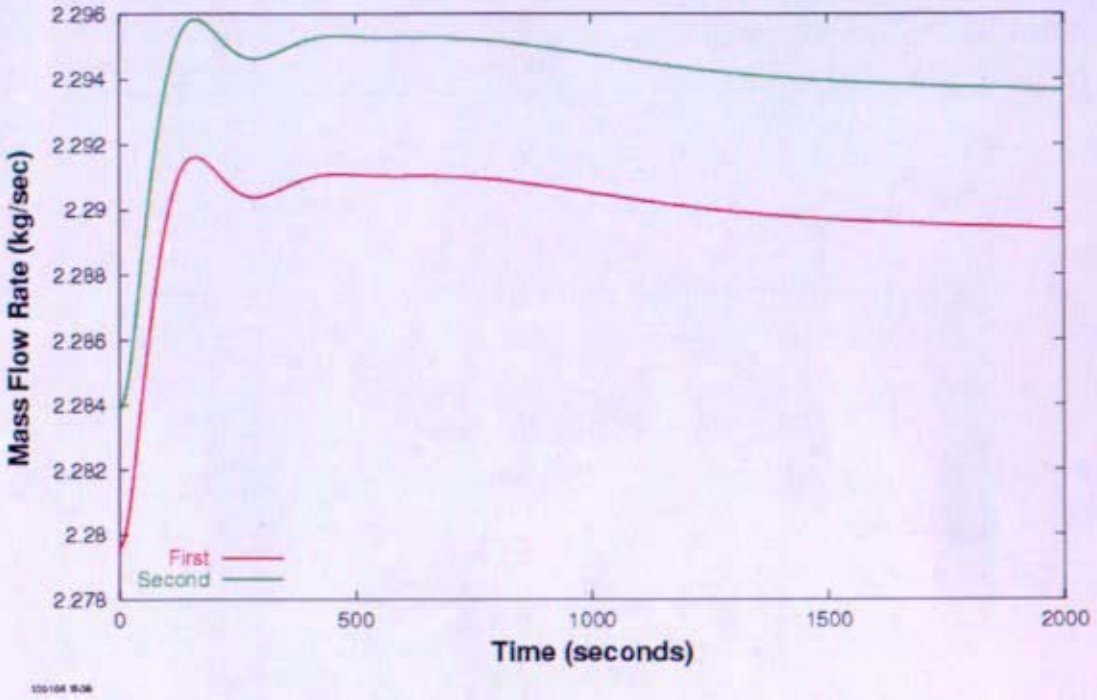



**Figure 12-152: Mass Flow Rates Resulting from Positive Reactivity (RELAP5-3D)**

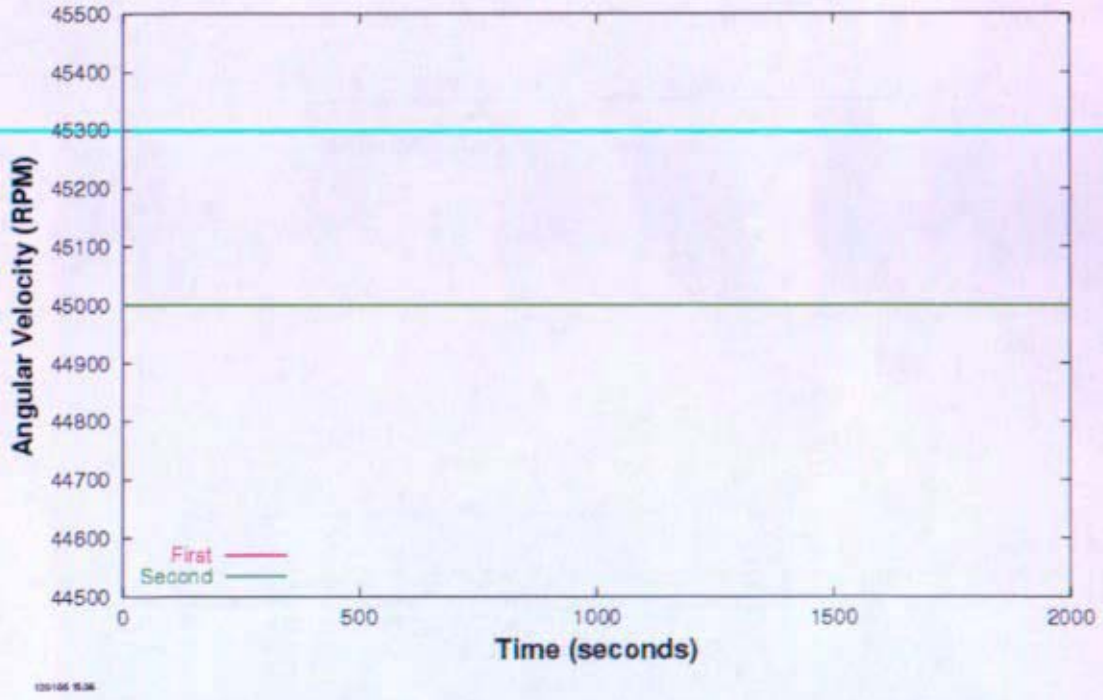



**Figure 12-153: Shaft Speeds Resulting from Positive Reactivity (RELAP5-3D)**

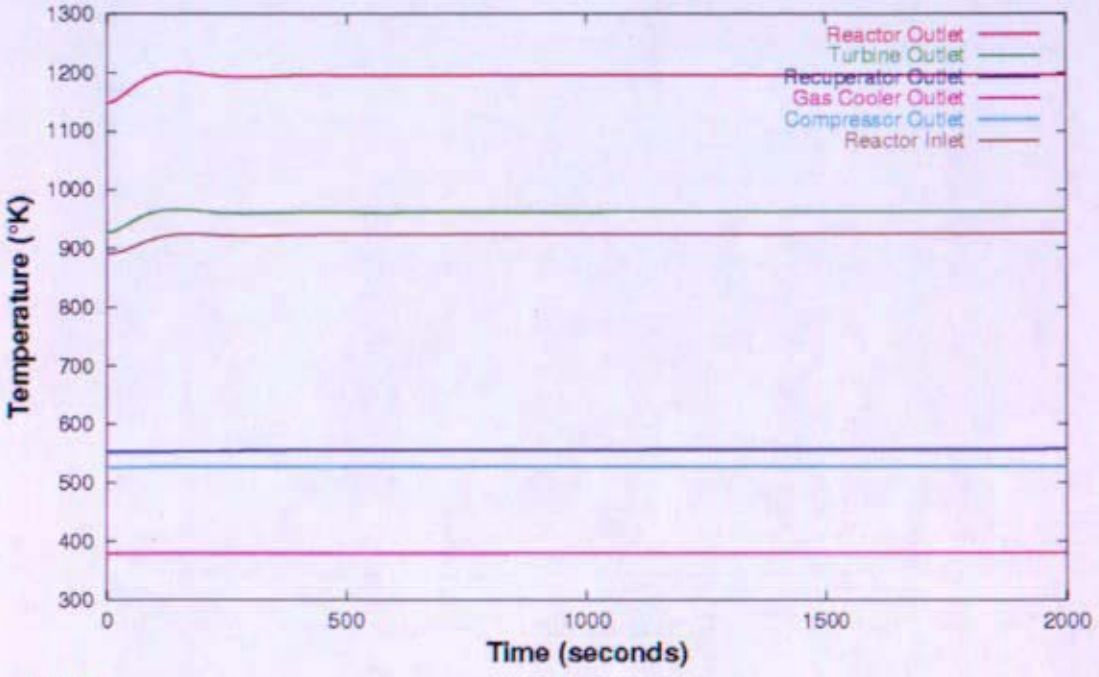



**Figure 12-154: First Brayton Loop Temperatures Resulting from Positive Reactivity (RELAP5-3D)**

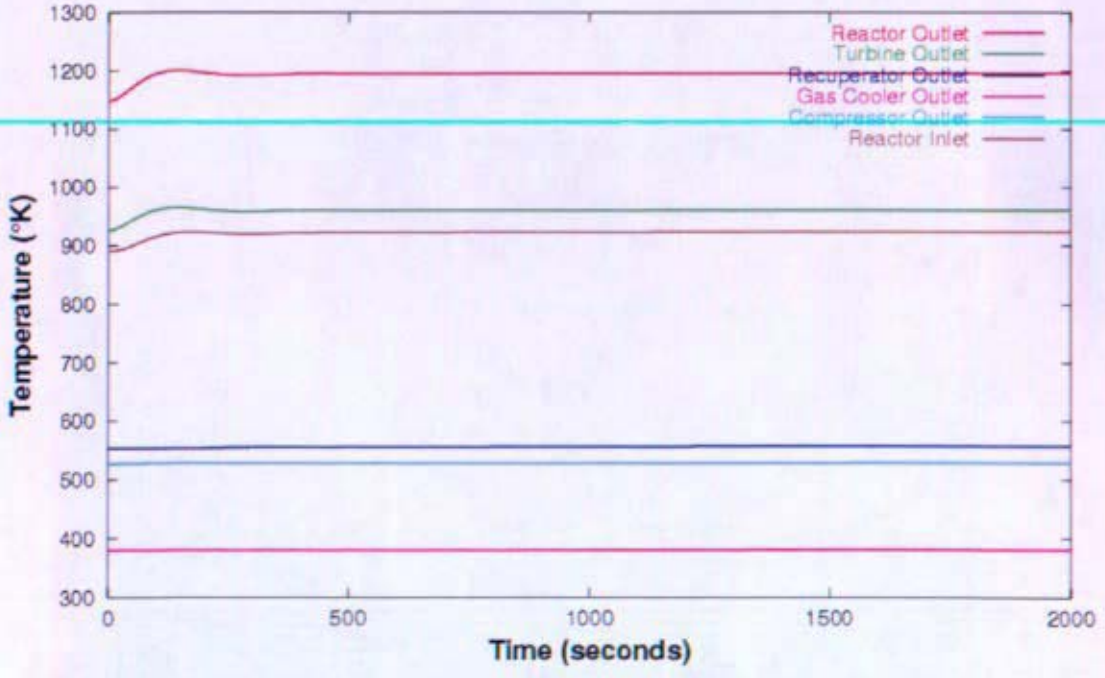



**Figure 12-155: Second Brayton Loop Temperatures Resulting from Positive Reactivity (RELAP5-3D)**

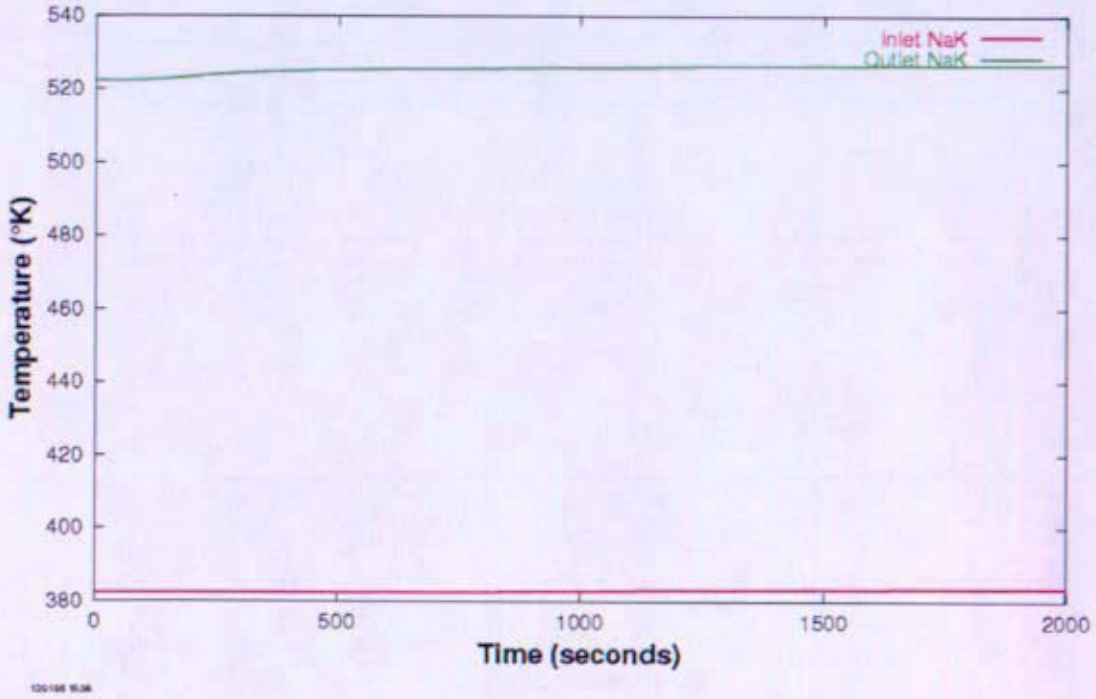



**Figure 12-156: First Heat Rejection Loop Temperatures Resulting from Positive Reactivity (RELAP5-3D)**

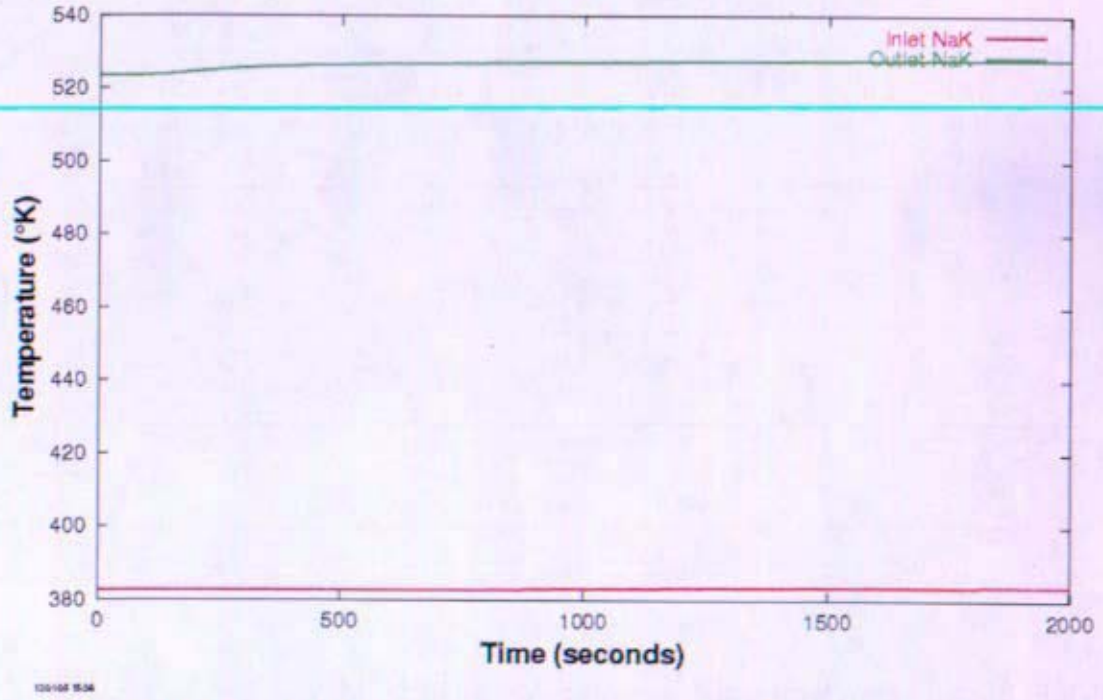



**Figure 12-157: Second Heat Rejection Loop Temperatures Resulting from Positive Reactivity (RELAP5-3D)**

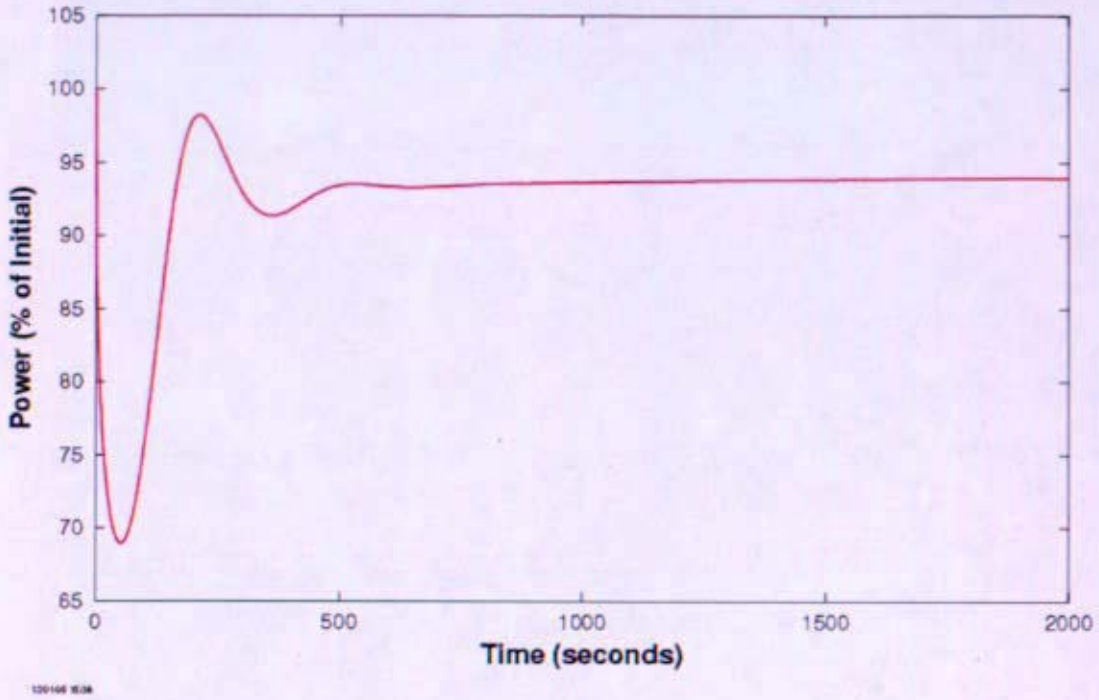



**Figure 12-158: Reactor Power Resulting from Negative Reactivity (RELAP5-3D)**

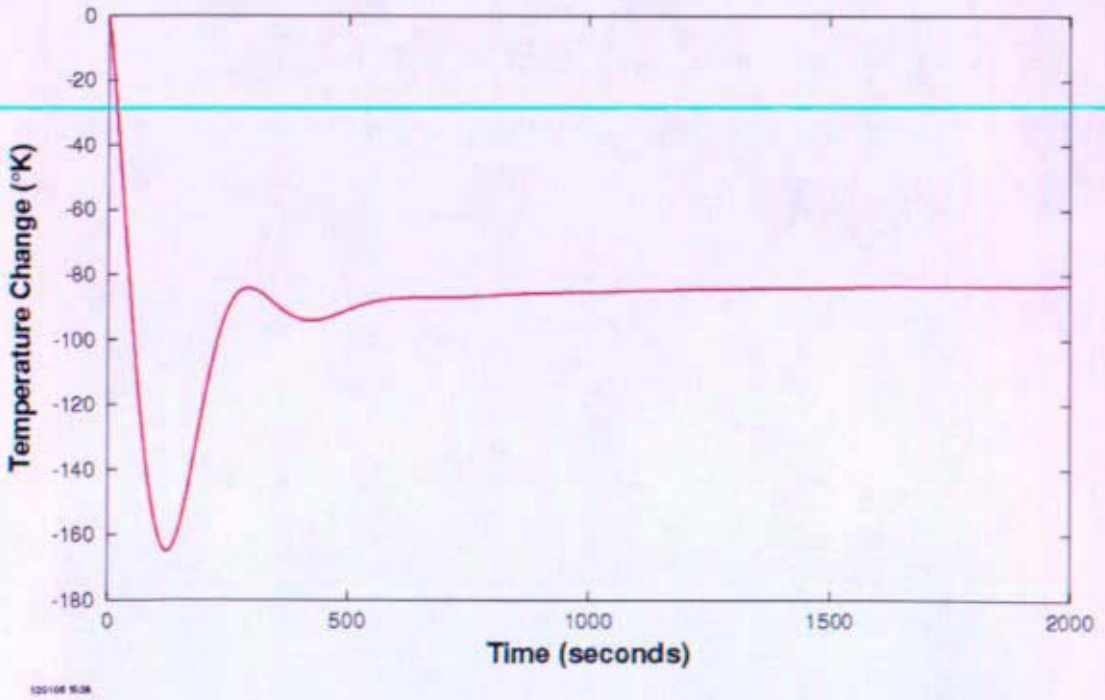



**Figure 12-159: Hot Spot Fuel Temperature Resulting from Negative Reactivity (RELAP5-3D)**

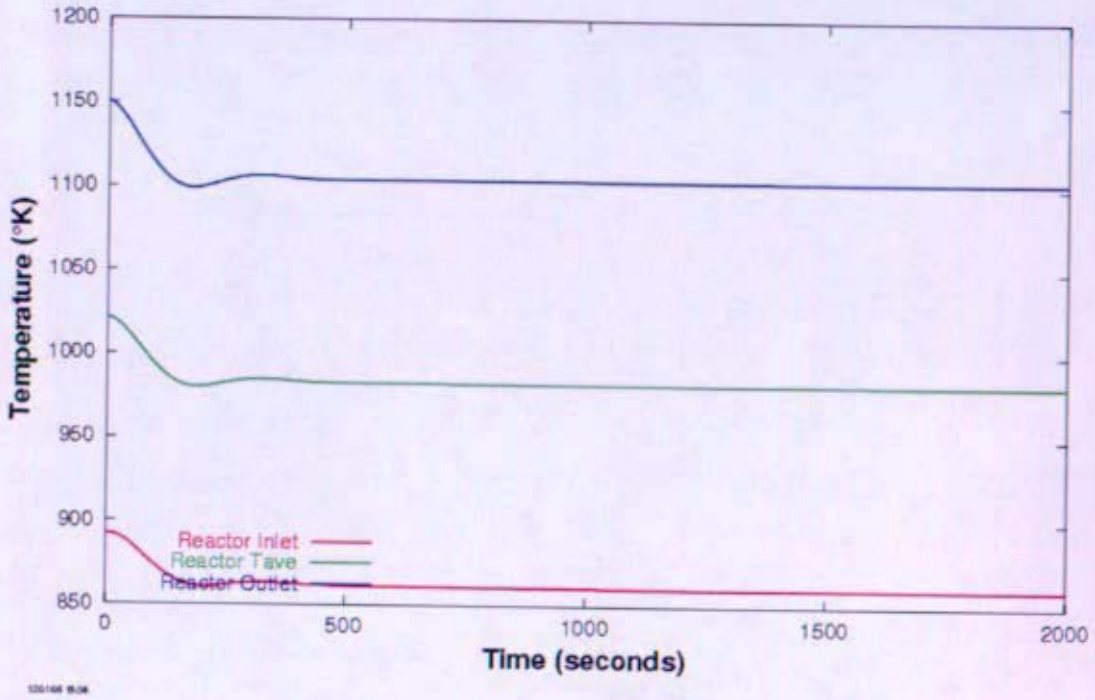



**Figure 12-160: Loop Temperatures Resulting from Negative Reactivity (RELAP5-3D)**

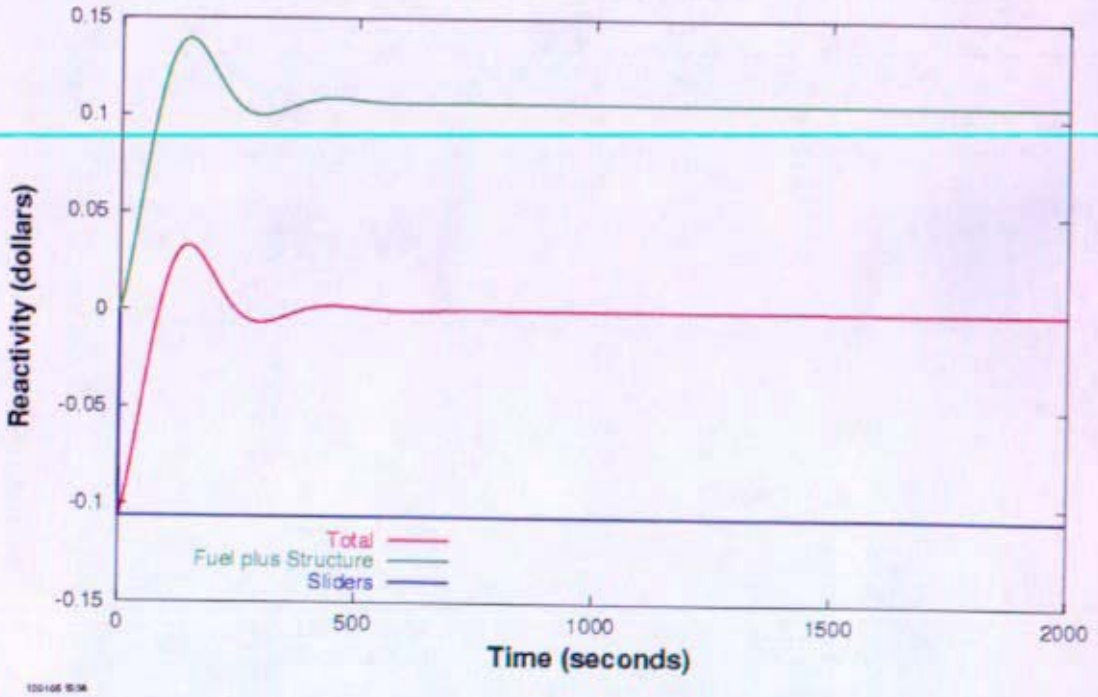



**Figure 12-161: Reactor Reactivity Resulting from Negative Reactivity (RELAP5-3D)**

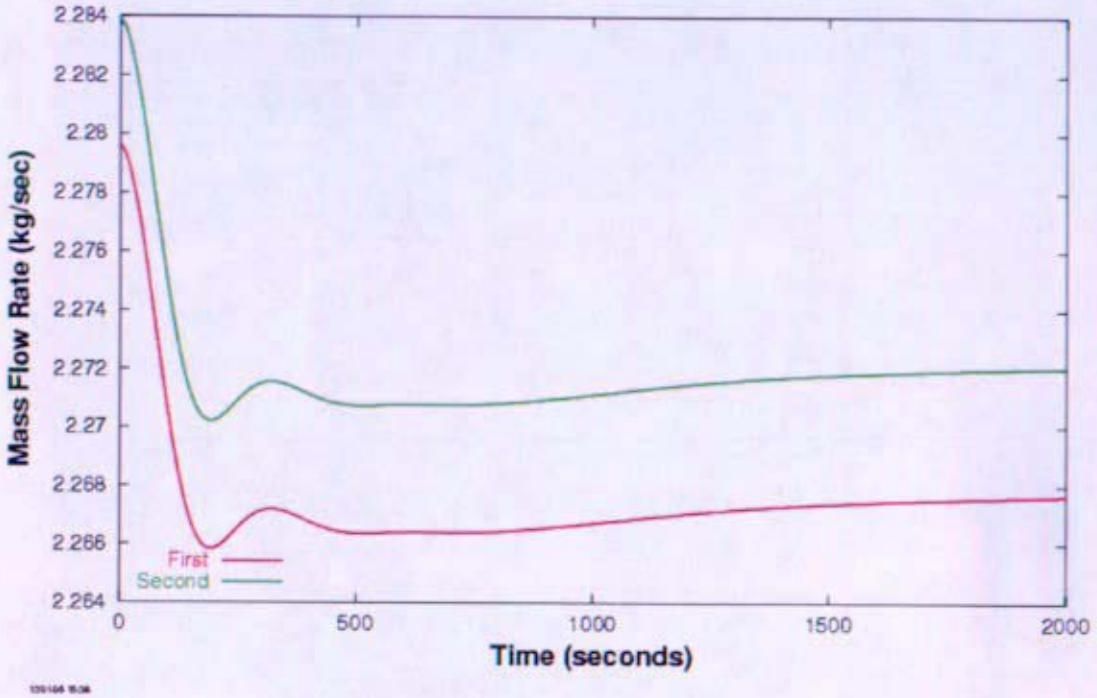



**Figure 12-162: Mass Flow Rates Resulting from Negative Reactivity (RELAP5-3D)**

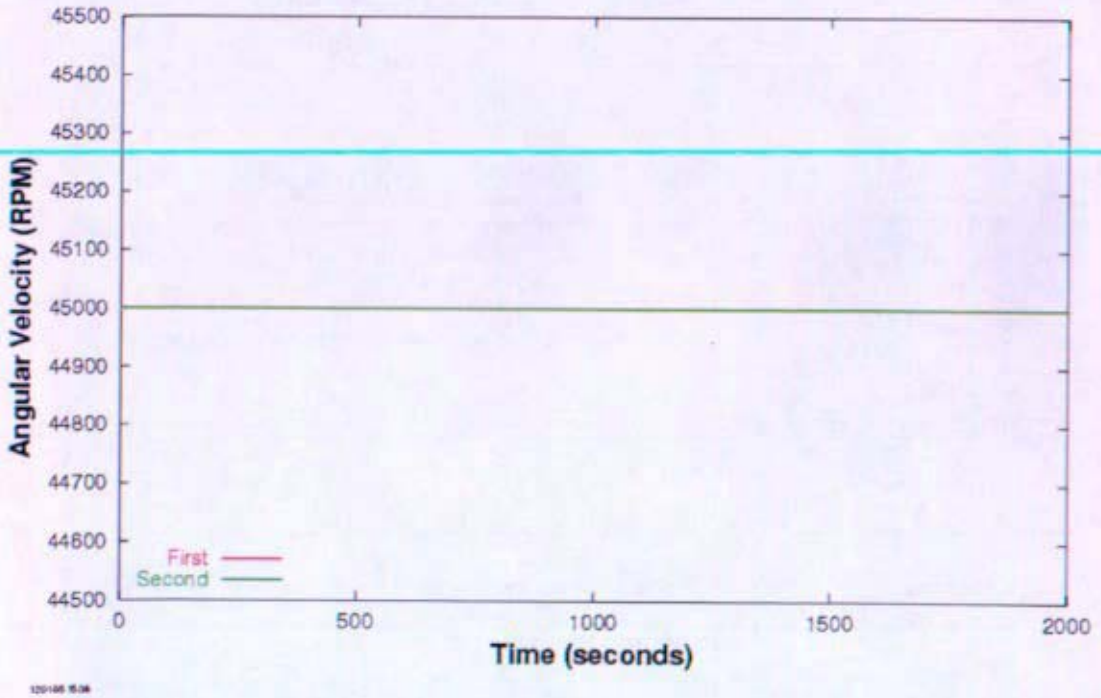



**Figure 12-163: Shaft Speeds Resulting from Negative Reactivity (RELAP5-3D)**

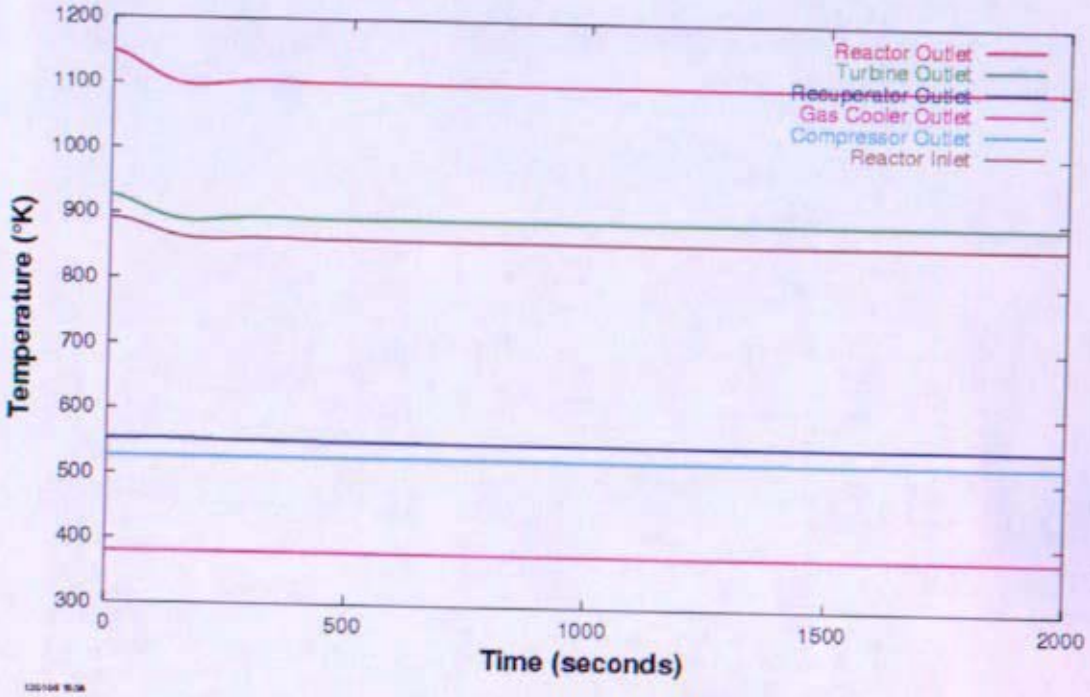



**Figure 12-164: First Brayton Loop Temperatures Resulting from Negative Reactivity (RELAP5-3D)**

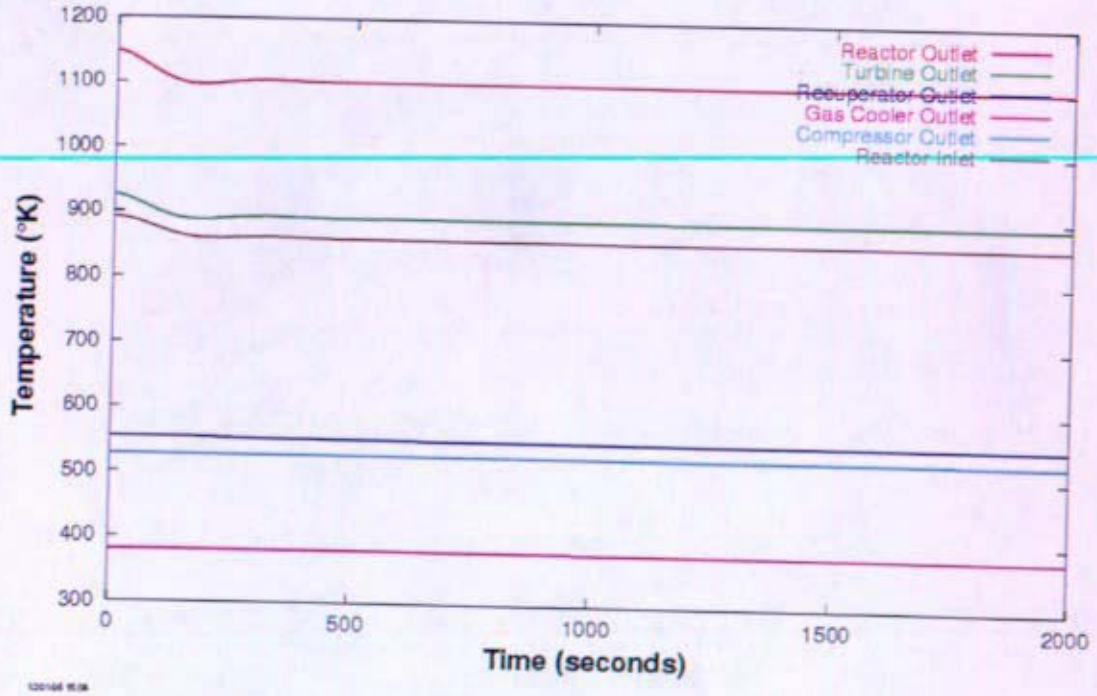



**Figure 12-165: Second Brayton Loop Temperatures Resulting from Negative Reactivity (RELAP5-3D)**

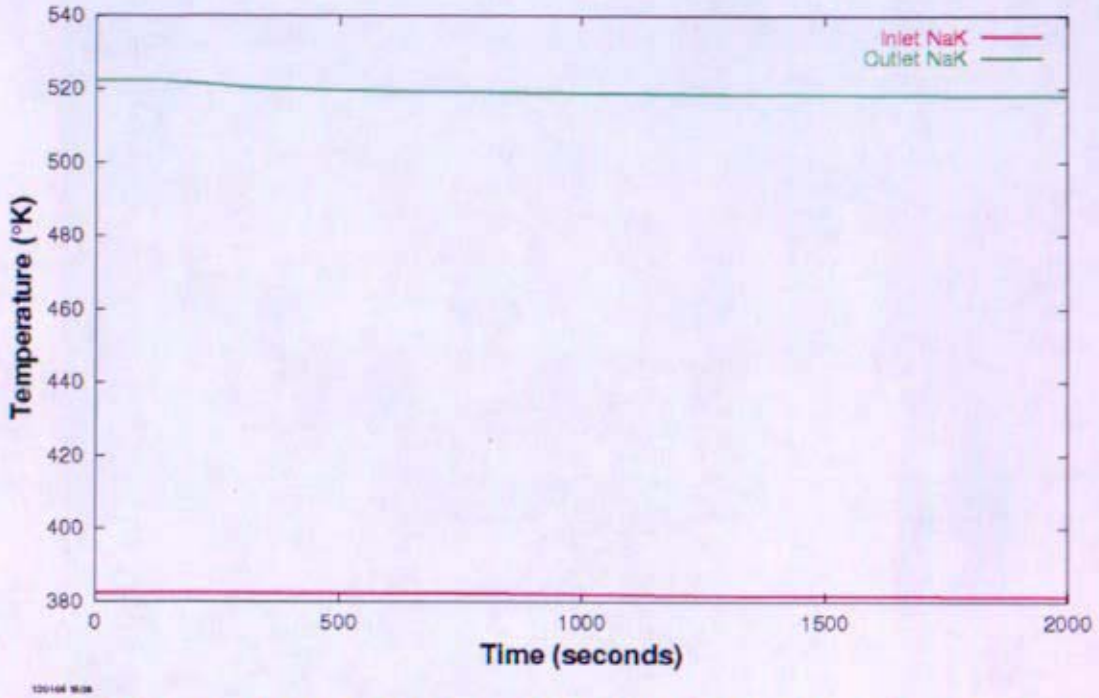



**Figure 12-166: First Heat Rejection Loop Temperatures Resulting from Negative Reactivity (RELAP5-3D)**

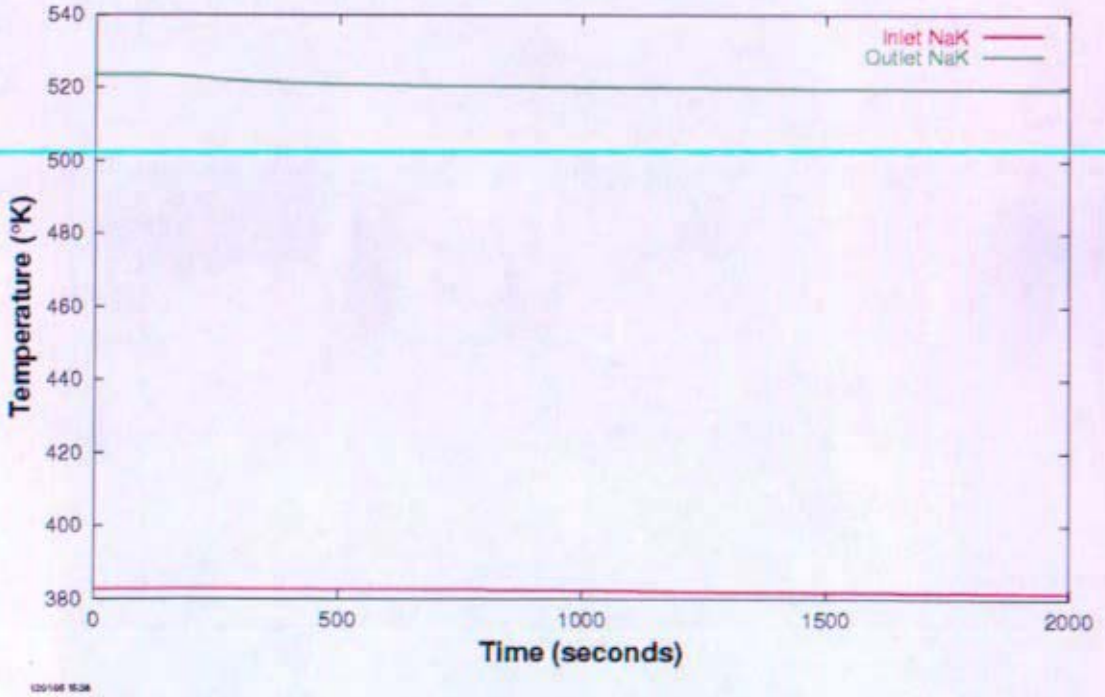



**Figure 12-167: Second Heat Rejection Loop Temperatures Resulting from Negative Reactivity (RELAP5-3D)**

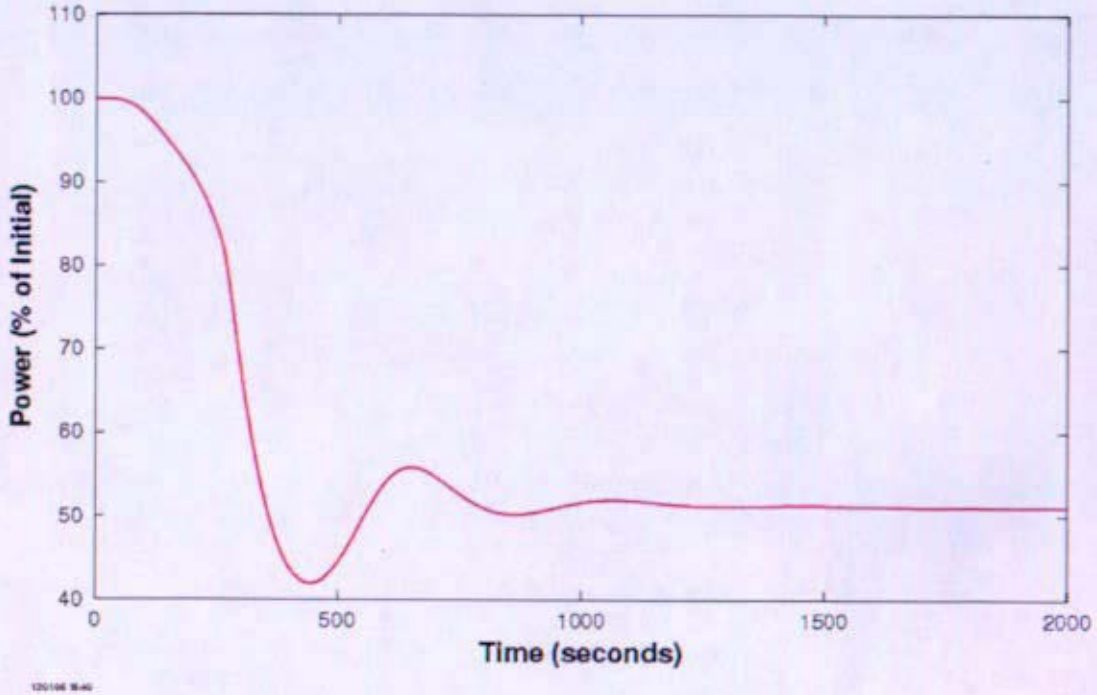



**Figure 12-168: Reactor Power Resulting from Loss of Flow in One Heat Rejection Loop (RELAP5-3D)**

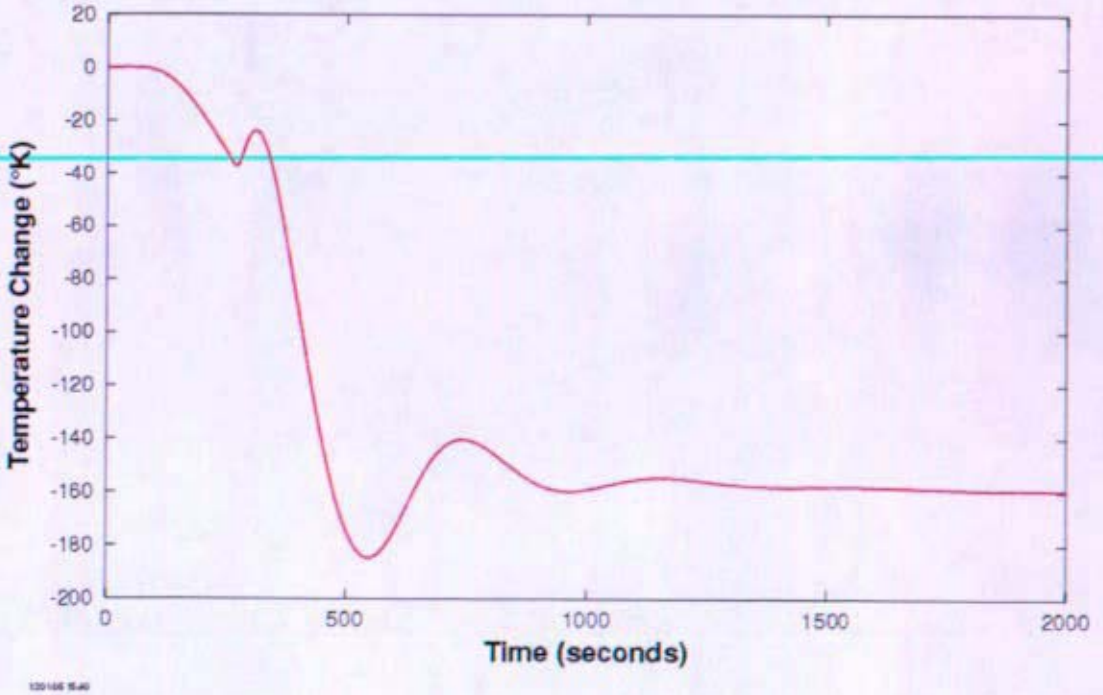



**Figure 12-169: Hot Spot Fuel Temperature Resulting from Loss of Flow in One Heat Rejection Loop (RELAP5-3D)**

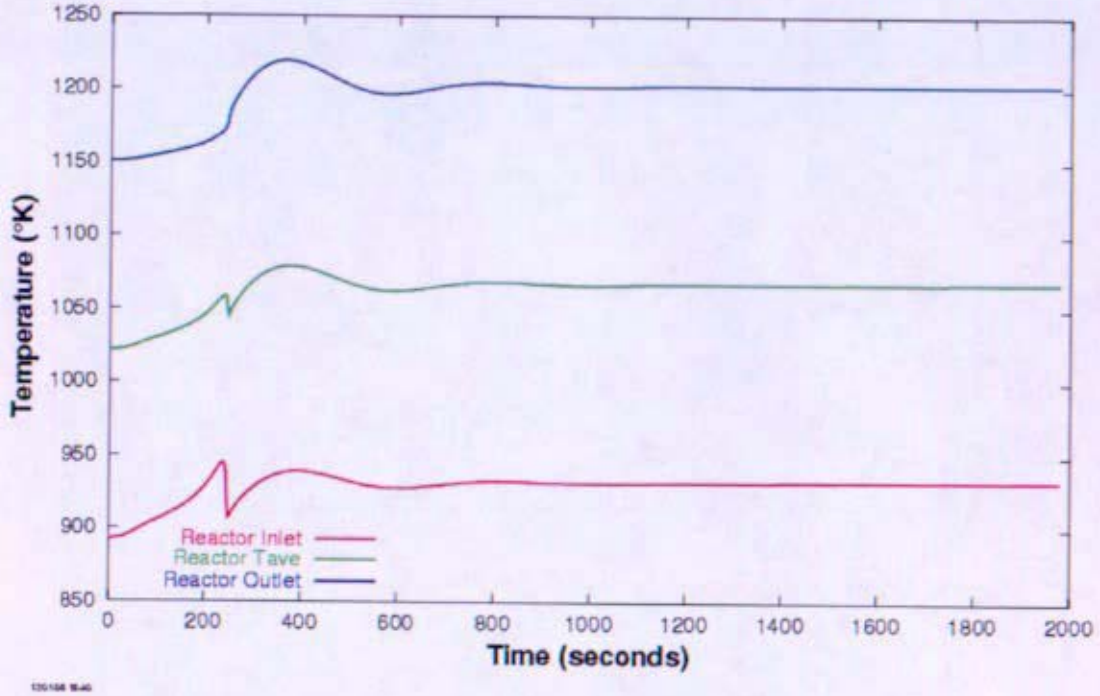



**Figure 12-170: Loop Temperatures Resulting from Loss of Flow in One Heat Rejection Loop (RELAP5-3D)**

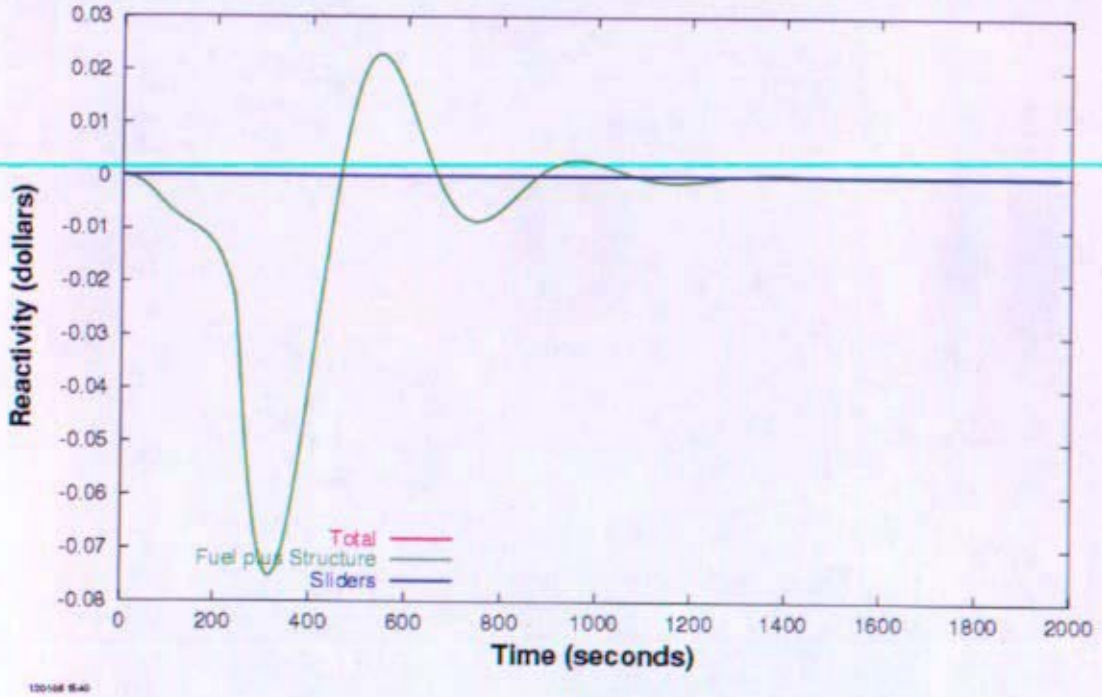



**Figure 12-171: Reactor Reactivity Resulting from Loss of Flow in One Heat Rejection Loop (RELAP5-3D)**

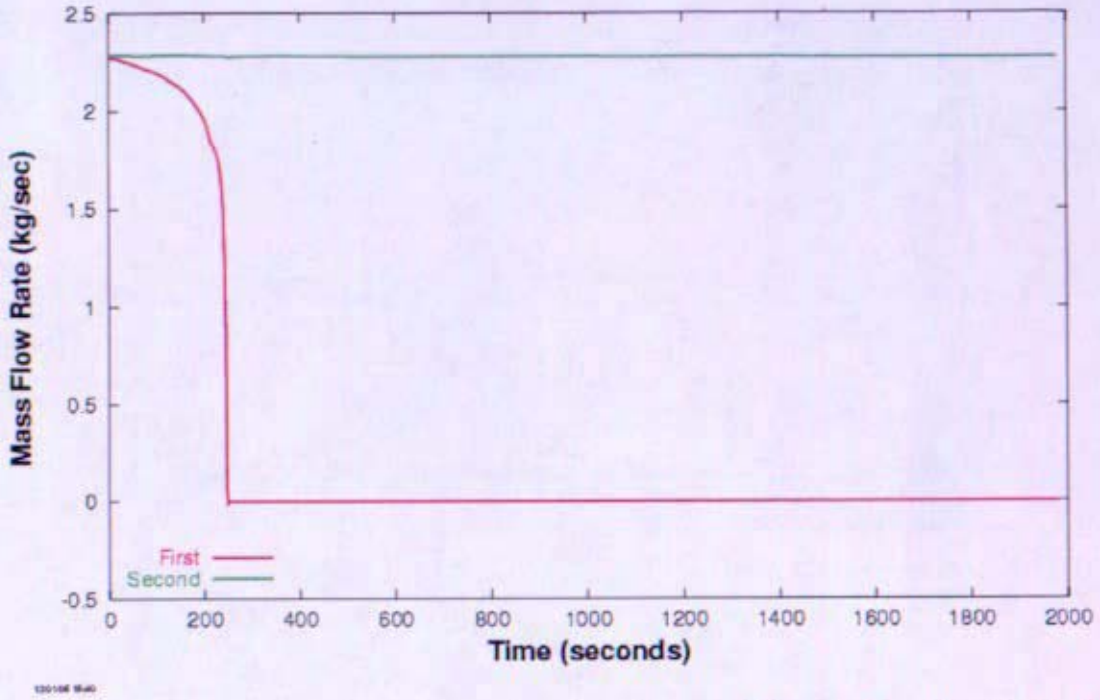



**Figure 12-172: Mass Flow Rates Resulting from Loss of Flow in One Heat Rejection Loop (RELAP5-3D)**

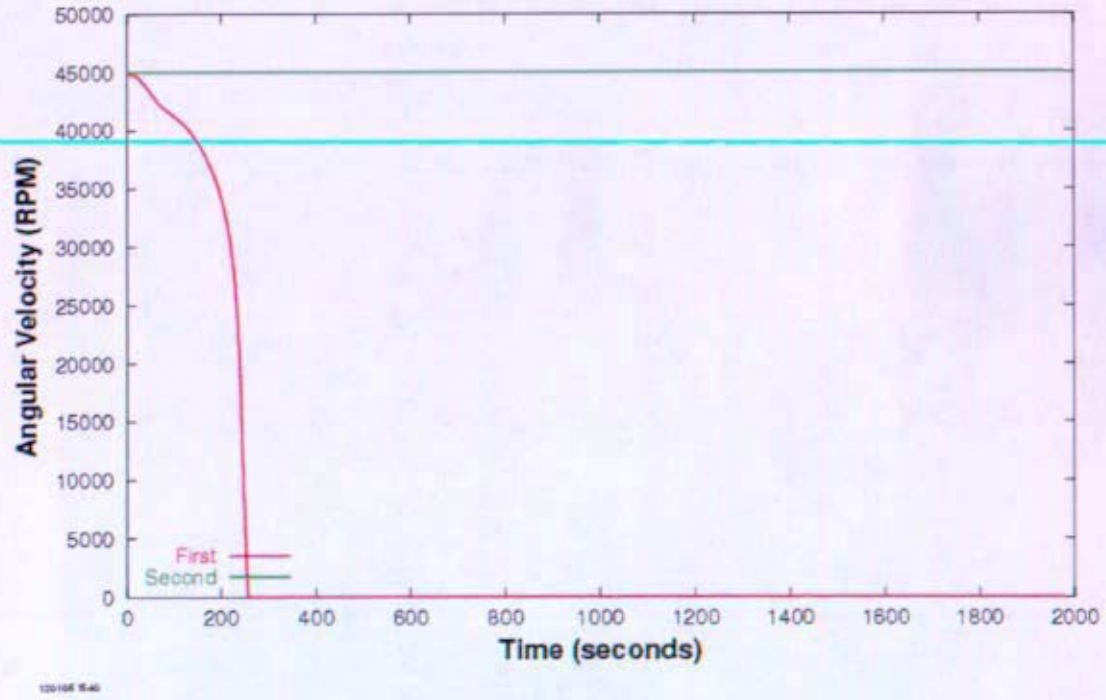



**Figure 12-173: Shaft Speeds Resulting from Loss of Flow in One Heat Rejection Loop (RELAP5-3D)**

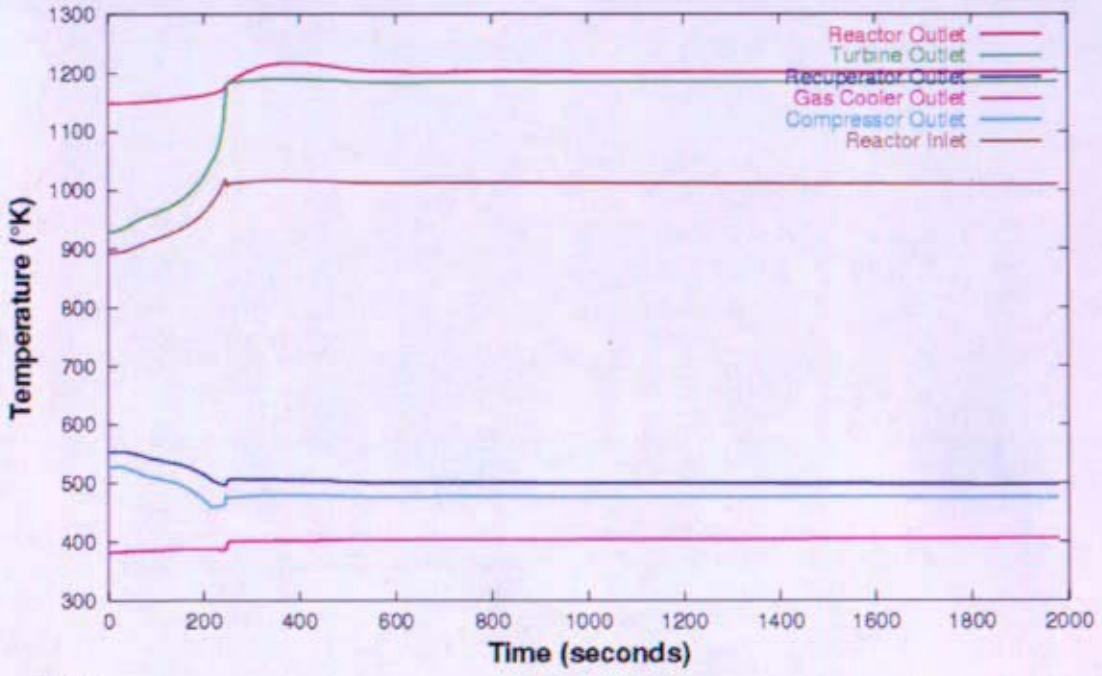



**Figure 12-174: First Brayton Loop Temperatures Resulting from Loss of Flow in 1 Heat Rejection Loop (RELAP5-3D)**

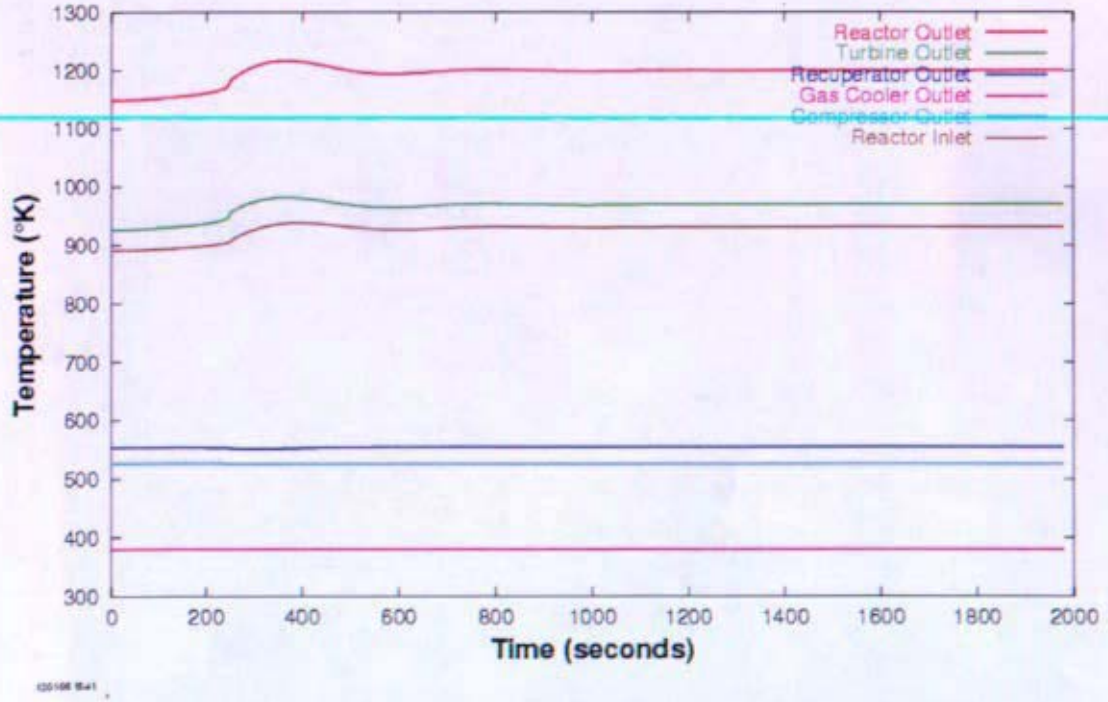



**Figure 12-175: Second Brayton Loop Temperatures Resulting from Loss of Flow in 1 HRS Loop (RELAP5-3D)**

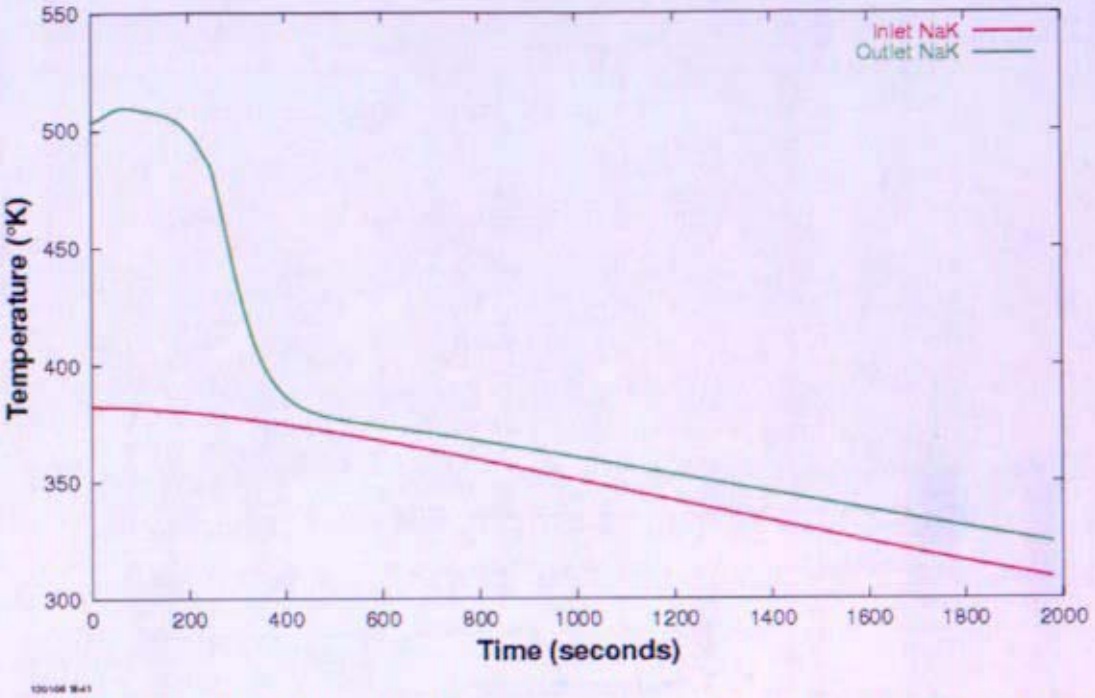



**Figure 12-176: First Heat Rejection Loop Temperatures Resulting from Loss of Flow in 1 HRS Loop (RELAP5-3D)**

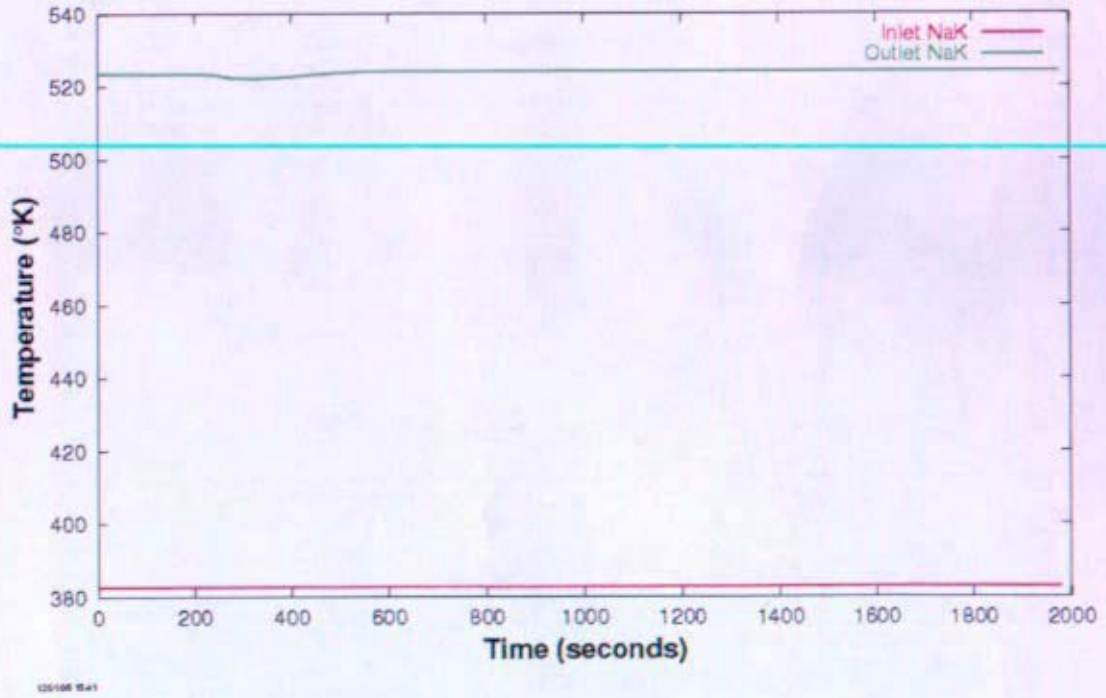



**Figure 12-177: Second Heat Rejection Loop Temperatures Resulting from Loss of Flow in 1 HRS Loop (RELAP5-3D)**

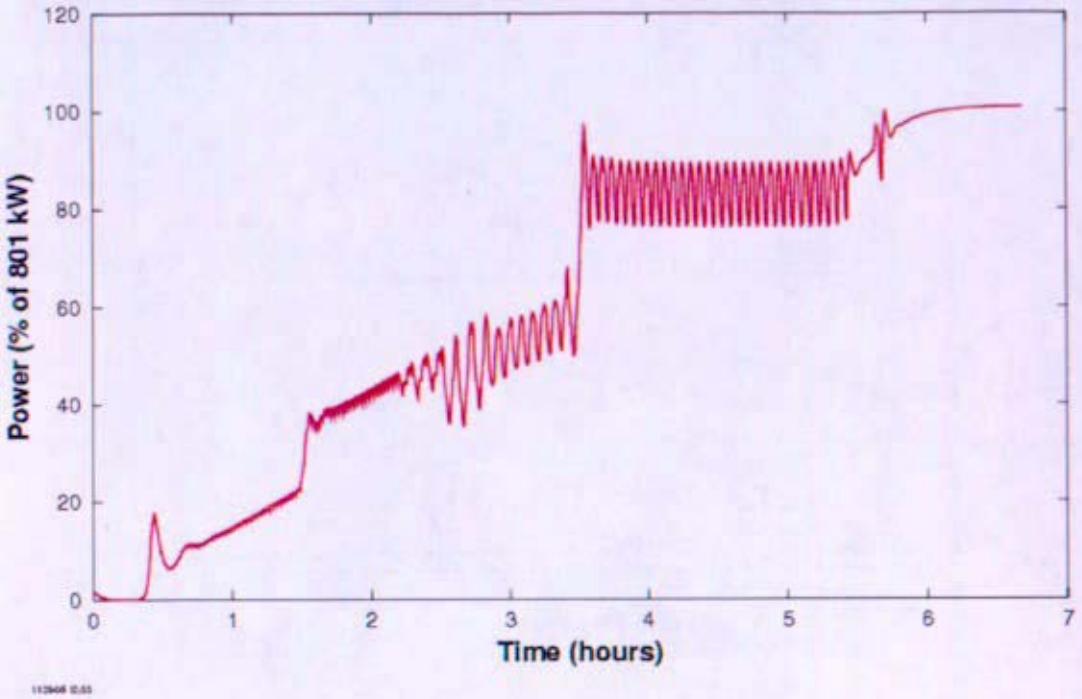



**Figure 12-178: Reactor Power during a Plant Start-Up (RELAP5-3D)**

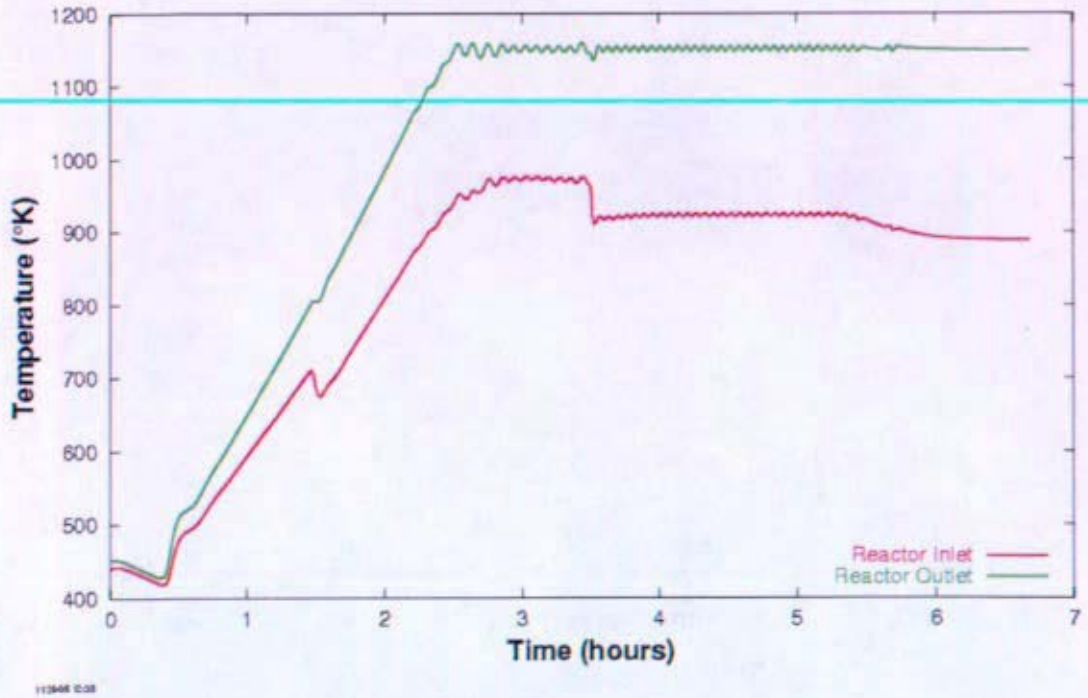



**Figure 12-179: Loop Temperatures during a Plant Start-Up (RELAP5-3D)**

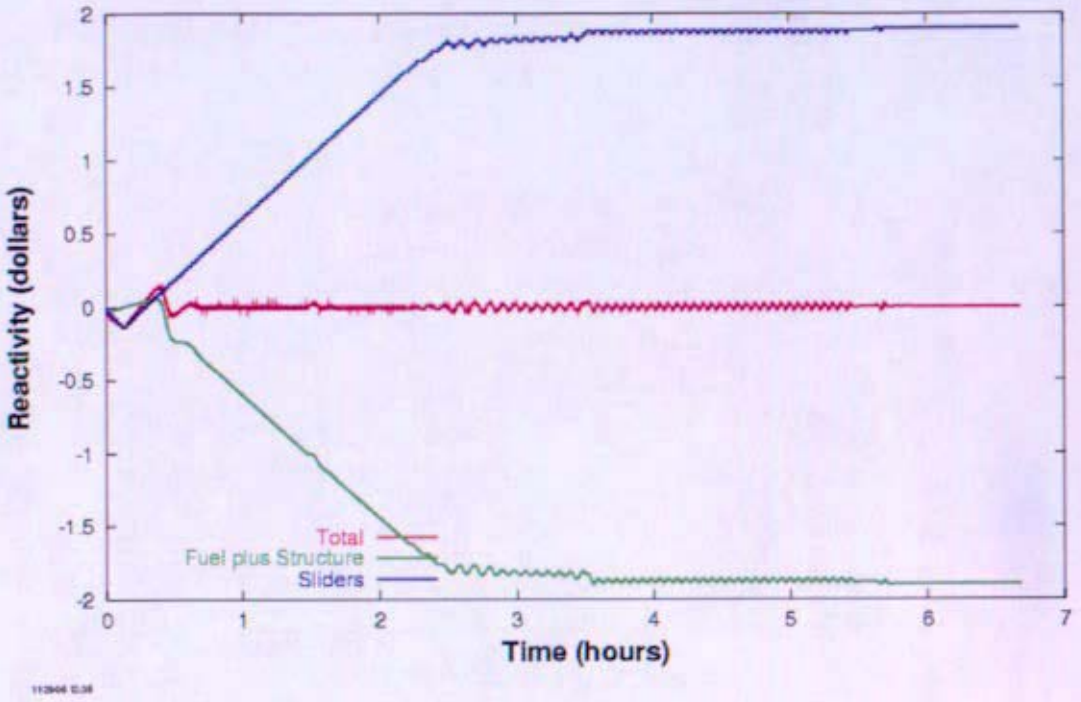



**Figure 12-180: Reactor Reactivity during a Plant Start-Up (RELAP5-3D)**

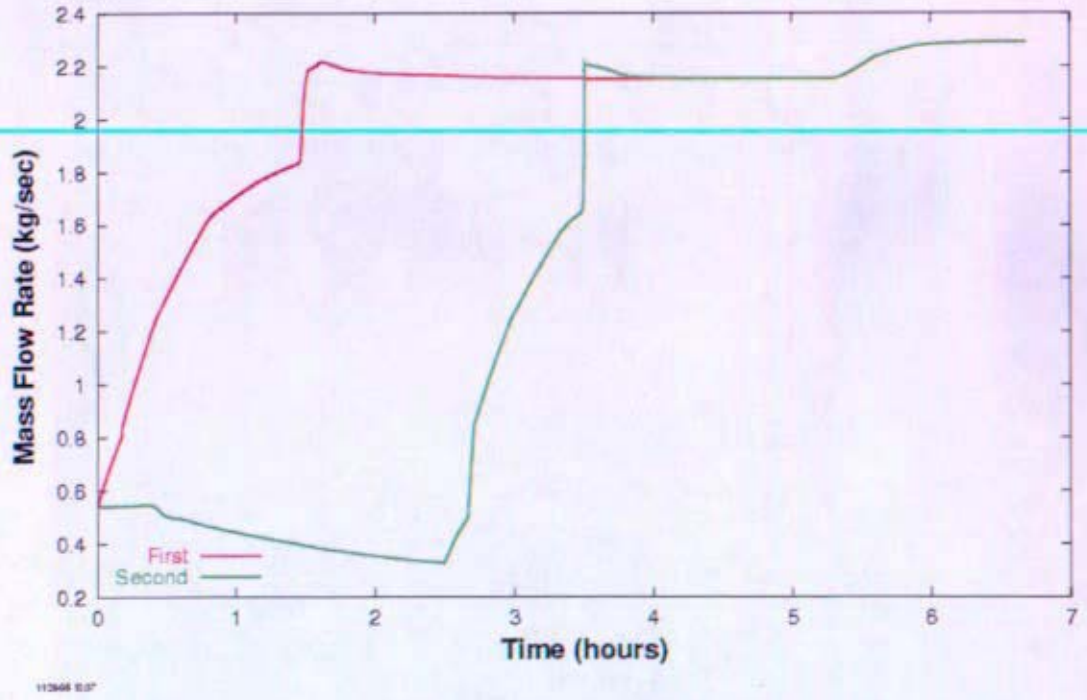



**Figure 12-181: Mass Flow Rates during a Plant Start-Up (RELAP5-3D)**

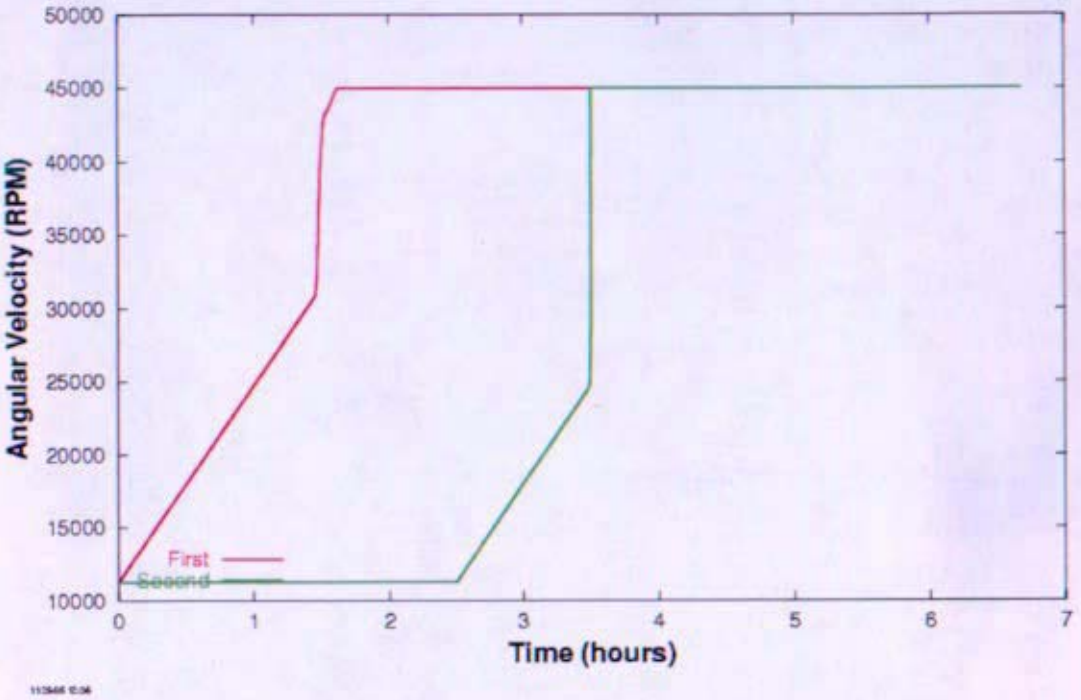



**Figure 12-182: Shaft Speeds during a Plant Start-Up (RELAP5-3D)**

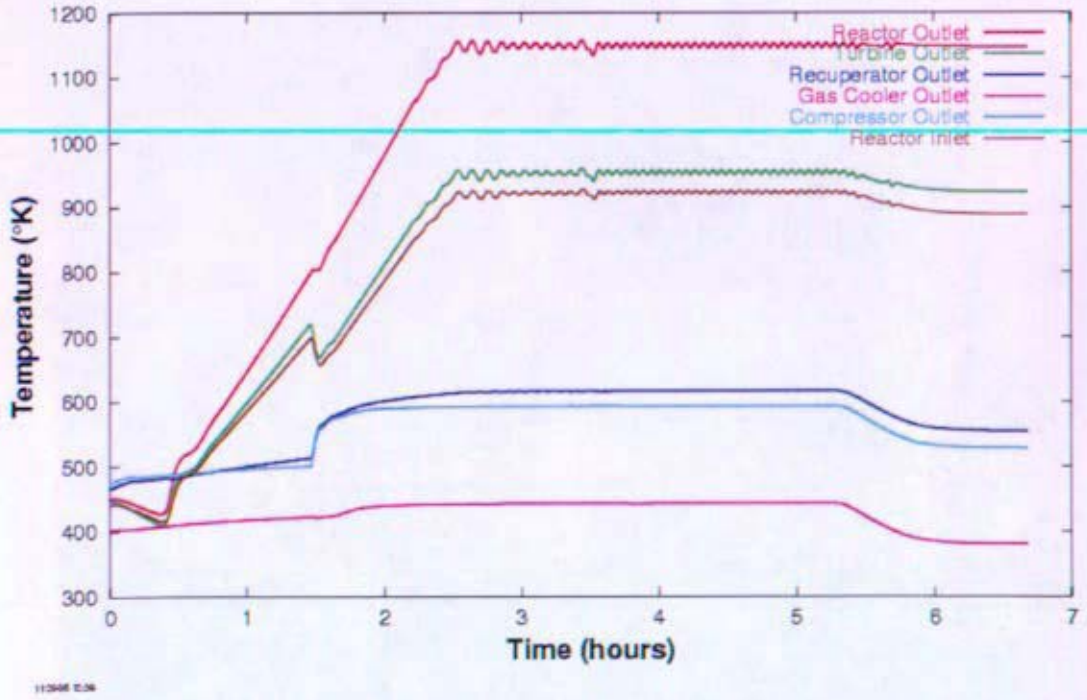



**Figure 12-183: First Brayton Loop Temperatures during a Plant Start-Up (RELAP5-3D)**

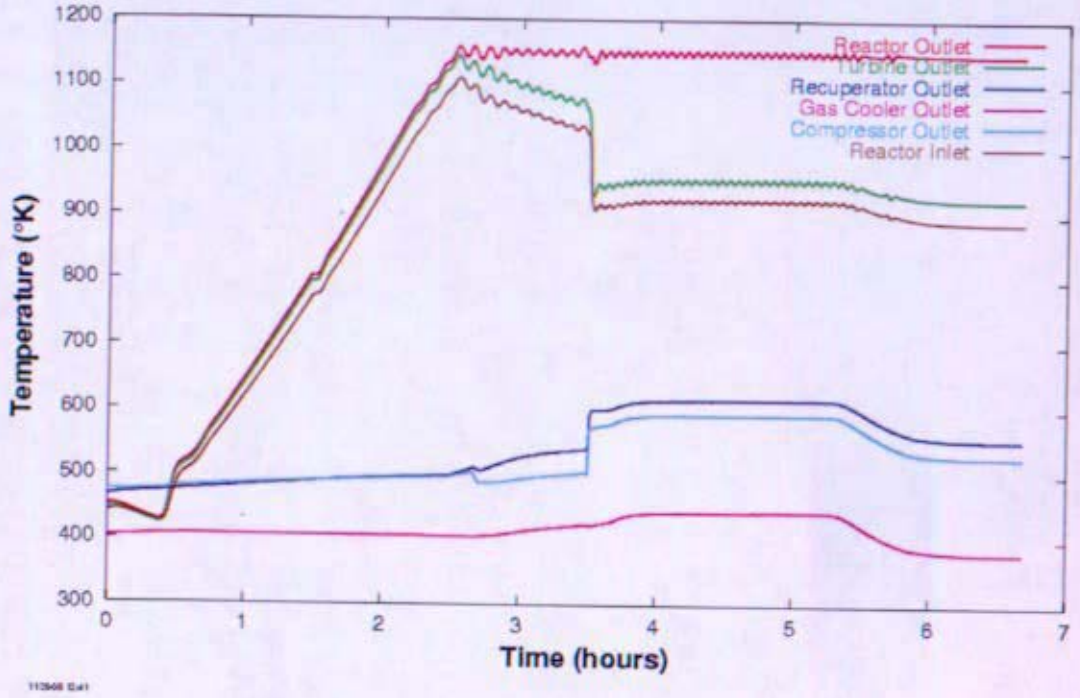



**Figure 12-184: Second Brayton Loop Temperatures during a Plant Start-Up (RELAP5-3D)**

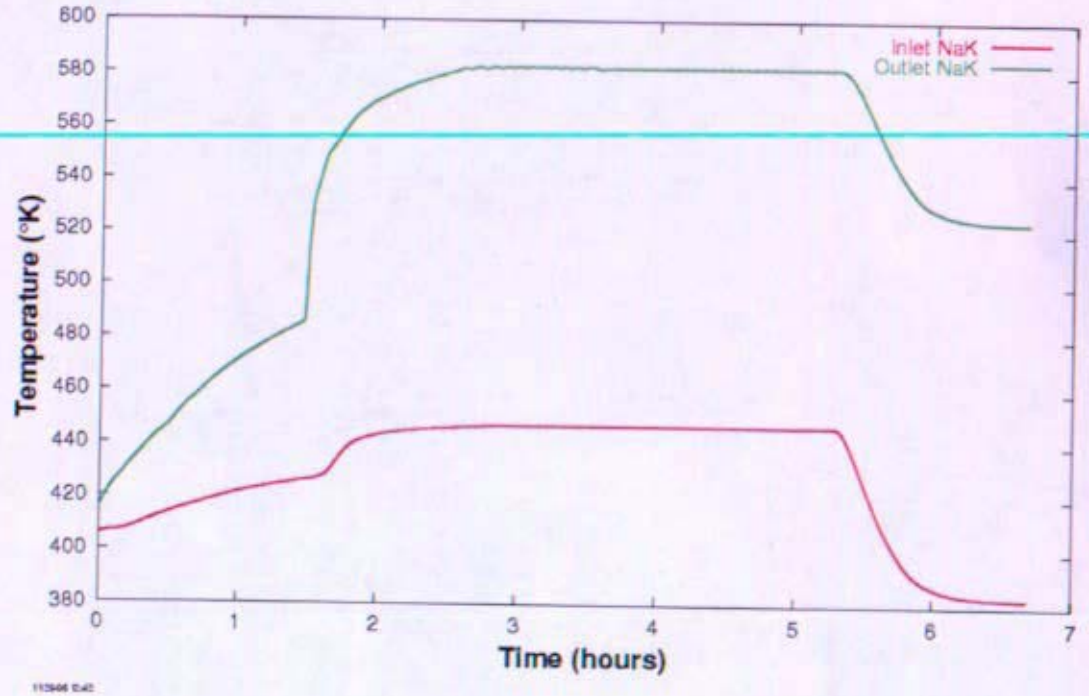



**Figure 12-185: First Heat Rejection Loop Temperatures during a Plant Start-Up (RELAP5-3D)**

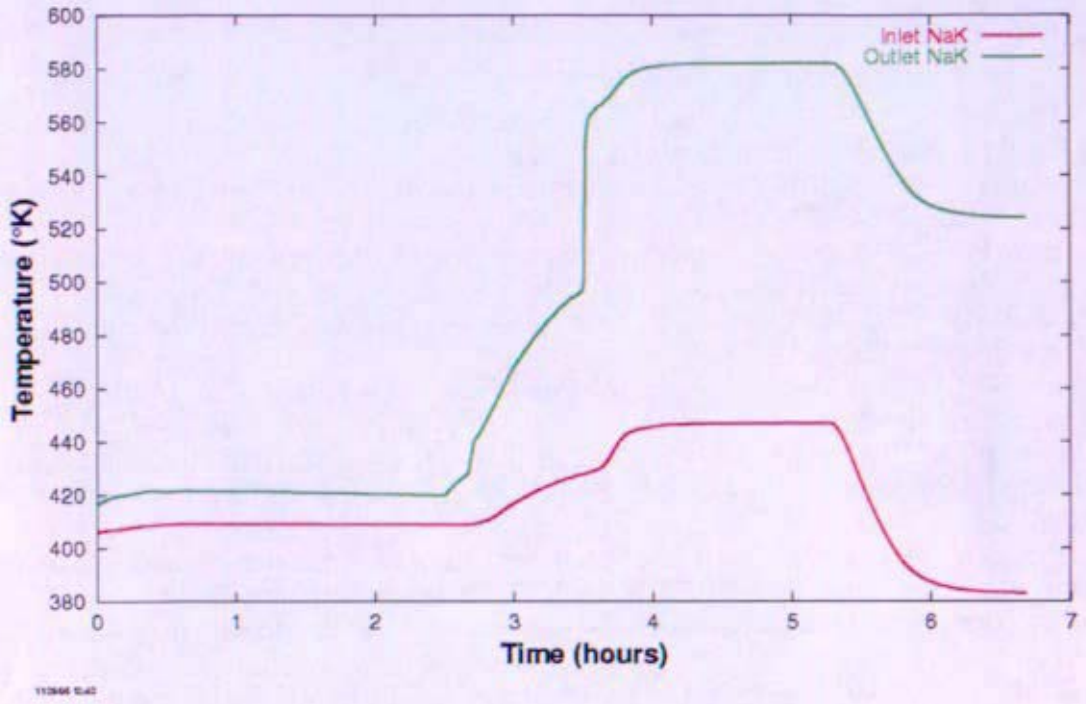



**Figure 12-186: Second Heat Rejection Loop Temperatures during a Plant Start-Up (RELAP5-3D)**

## 12.6 References

**12-1:** KAPL Letter SPP-67110-0007 / Bettis Letter #B-SE-0143, "Documentation of Space Nuclear Power Plant Concept Selection," dated 7/27/2005

**12-2:** KAPL Letter SPP-SPPS-0019, "Prometheus Space Nuclear Power Plant Dynamic Model Description," dated 8/30/2005

**12-3:** KAPL Letter SPP-SPPS-0031, "Prometheus Space Nuclear Power Plant Simulink Dynamic Model Plant Analysis," to be issued

**12-4:** KAPL Letter SPP-SEC-0036, "Space Nuclear Power Plant TRACE Model Description and Transient Results," to be issued

**12-5:** Bettis Letter B-SE(SPS)GT-007, "Space Nuclear Power Plant RELAP5-3D Model Description," to be issued

**12-6:** Attachment to KAPL Letter SPP-SPPS-0019, Johnson, Paul, "JIMO TB 2.5 Closed Brayton Cycle Design Point Physical Description," NASA Glenn Research Center, Cleveland, OH, 9/22/2004

**12-7:** KAPL letter SPP-SRE-0017, "Low Prandtl Number Literature Research," dated 8/29/2005

**12-8:** Attachment to KAPL Letter SPP-SPPS-0019, "CCEP Turbo-machinery Design and Off-Design Calculations," (Informal NASA/Glenn Research Center memo written by P. Johnson, undated)

**12-9:** KAPL Letter TIS-86B-0288, "Attainment of Production Status for KIPAC V6.0.3 on the PC Win32 Operating System – Modifications Supporting Project Prometheus," to be issued

**12-10:** Kays, W.M., London, A.L., "Compact Heat Exchangers," 3rd ed., McGraw-Hill Book Co., New York, 1984

**12-11:** NGST Report SDRL SE-002-001: D40224, "NGST Prometheus Spacecraft module and subcontractor-provided reactor module segment design description draft", dated May 16, 2005.

**12-12:** KAPL Letter SPP-67310-0009, "NRPCT Comments on the use of a Water Heat Rejection Loop", dated 6/17/2005

**12-13:** Chemical Engineer's Handbook, Fifth Edition, Perry and Chilton

**12-14:** Bettis Letter B-SE(RE)-0001, "Fuel Type Recommendation for the Project Prometheus Space Nuclear Reactors, For Naval Reactors Approval," 7/28/2005

**12-15:** Los Alamos Letter #LA-CP-04-0341, "Jupitor Icy Moons Orbitor Reactor Module Design and Development," Rev.1, April 2004

**12-16:** TWR #22426, "SE RELAP5-3D Modeling," Larry D. McCann

**12-17:** Wright, Steven A., "Preliminary Results of a Dynamic System Model for a Closed-Loop Brayton Cycle Coupled to a Nuclear Reactor," American Institute of Aeronautica and Astronautics, Sept 2003

**12-18:** G. R. Keepin, "Physics of Nuclear Kinetics," Addison-Wesley, 1965

**12-19:** Attachment to KAPL Letter SPP-SPPS-0019, "CCEP match attempt of Lee's JIMO TB 2.5 Brayton design point" (9/22/05)

**12-20:** Bettis letter B-SE(SPS)GT-006, Modeling Counter Flow Heat Exchangers with NUPAC, to be issued

**12-21:** Siamidis, John, Glenn Research Center report – "Jupiter Icy Moons Orbiter Heat Rejection System DRAFT"; Sept. 22, 2004

**12-22:** Atkins, Harold E., Pacific Northwest National Laboratory, #PNL-47163-1-1, "NaK(78) Annular Linear Induction Pump (ALIP) Design Study for Proposed Brayton Cycle Waste Heat Rejection System," Prepared for NASA GRC under contract JCN47163, June 2004

**12-23:** Idel'chik, I. E., "Handbook of Hydraulic Resistance," AEC-TR-6630, 1960 (Russian), 1966 (English)

# Section 13
# Testing

*PRE-DECISIONAL – For planning and discussion purposes only*

(Intentionally Blank)

# Testing

## Table of Contents

13 Testing ..... 5
13.1 Summary and Conclusions ..... 5
13.2 Assembly, Test and Launch Operation (ATLO) ..... 6
13.2.1 Overall Assembly, Integration and Test (AI&T) Strategy ..... 11
13.2.2 Integrated Test Plan ..... 11
13.2.3 Drivers / Issues ..... 20
13.2.4 Estimated Cost for AI&T Effort ..... 21
13.3 Description of Key Facilities ..... 23
13.3.1 Glenn Research Center (GRC) ..... 23
13.3.2 Marshall Space Flight Center (MSFC) ..... 24
13.3.3 Sandia National Laboratories (SNL) ..... 25
13.3.4 Plum Brook Station ..... 26
13.3.5 Johnson Space Center (JSC) ..... 27
13.4 NRPCT Component Development and Integrated Test Plan ..... 28
13.5 In-House Testing ..... 53
13.5.1 KAPL In-House Testing ..... 53
13.5.2 Bettis In-House Testing ..... 57
13.6 Marshall Space Flight Center (MSFC) Testing ..... 69
13.6.1 Liquid Metal Reactor ..... 69
13.6.2 Heat Pipe Reactor ..... 71
13.6.3 Gas Reactor ..... 73
13.6.4 Electric Heater Development (R-TH-1M) ..... 79
13.7 Glenn Research Center (GRC) Testing ..... 82
13.7.1 Bearing Testing ..... 82
13.7.2 Alternator Testing ..... 82
13.7.3 Brayton Transient Testing ..... 83
13.7.4 Materials Testing ..... 83
13.8 Final Perspectives ..... 84
13.9 References ..... 87

## List of Figures

Figure 13-1: Illustration of Reactor Module Terminology ..... 6
Figure 13-2: Prometheus Integrated Test Plan ..... 9
Figure 13-3: Notional ATLO Flowchart ..... 10
Figure 13-4: Options Considered for Extent of RM Replacement at Launch Site ..... 21
Figure 13-5: Two Illustrations of Vacuum Facility VF-5 at GRC ..... 23
Figure 13-6: VF-6 Chamber with Solar Simulator (Silver Dome) and the Solar Simulator ..... 24
Figure 13-7: MSFC EFF-TF Vacuum Chamber ..... 25
Figure 13-8: Plum Brook Station Space Power Facility ..... 26
Figure 13-9: Illustrations of JSC Vacuum Chamber A ..... 27
Figure 13-10: Test Flow Rates Needed to Model Gas Reactor ..... 54
Figure 13-11: Air-Water LDV Mean Velocity Data for Flow Across a 1-inch OD Cylinder Inside a 5.75-inch ID Pipe (Re based on cylinder is approximately 34,000) ..... 55
Figure 13-12: Air-Water LDV RMS Velocity Data for Flow Across a 1-inch OD Cylinder Inside a 5.75-inch ID Pipe (Re based on cylinder is approximately 34,000) ..... 56
Figure 13-13: Flow Visualization Test Apparatus of Gas-Cooled Reactor Concept ..... 59

Figure 13-14: Preliminary layout of DCBL ..... 60
Figure 13-15: Loop state points for the DCBL ..... 61
Figure 13-16: Prometheus Brayton Engine Concept Design ..... 63
Figure 13-17: Gas Leakage Pressure Vessel. ..... 65
Figure 13-18: Experimental Setup for the P-GL-1B Test at the Bettis Laboratory Fundamental Shock and Vibration Lab ..... 66
Figure 13-19: NASA GRC Experimental Setup for Gas Leakage Testing. ..... 67
Figure 13-20: Conax Multi-electrode Feedthrough. ..... 68
Figure 13-21: Stainless Steel Lithium Test Loop ..... 70
Figure 13-22: Heat Pipe Cross Section with Ancillary Test Systems ..... 72
Figure 13-23: DDG Assembly ..... 75
Figure 13-24: DDG Core View Showing 37 Electrical Heating Elements ..... 75
Figure 13-25: DDG Assembly in the EFF-TF Vacuum Chamber ..... 76
Figure 13-26: Single Channel Test Hardware ..... 77
Figure 13-27: Inlet Manifold ..... 78
Figure 13-28: Exit Manifold ..... 78
Figure 13-29: Graphite Rod Heater Element ..... 80
Figure 13-30: Wire Wrapped Mandrel Heater Element ..... 80
Figure 13-31: The High Pressure Foil Bearing Test Rig undergoing Shakedown Tests ..... 82
Figure 13-32: Hamilton Sundstrand Motor-Alternator Design Configuration ..... 83

## List of Tables

Table 13-1: ROM Cost Estimates for RMIF and Reactor Module AI&T ..... 22
Table 13-2: Description of Test Index Column Headings ..... 29
Table 13-3: Test Identification Numbering System ..... 30
Table 13-4: Project Prometheus Integrated Test Index ..... 31
Table 13-5: Design vs. Vendor / Testing Requirements ..... 64
Table 13-6: Random Vibration Force Limit Specifications ..... 65
Table 13-7: ROM Estimates for LM Loops Constructed of Refractory Metals ..... 71
Table 13-8: Estimated DDG Test Conditions ..... 74
Table 13-9: Nominal Flow Passage Dimensions for the Single Channel Test ..... 79

# 13 Testing

## 13.1 Summary and Conclusions

A few key observations regarding space nuclear power testing are:

- A minimum level of fundamental research and development must be maintained to provide long lead data (e.g., irradiation data, component lifetime, etc.) for space nuclear power.
- The NRPCT integrated testing strategy was to use the existing national infrastructure (NASA Centers, national DOE labs, etc.) whenever possible to minimize cost and lead time.
- The declining nuclear infrastructure in the United States is creating an increased challenge for performing nuclear development work in support of space reactors. This poses risks to meeting project timing and technical needs.

This section provides an overview of the Space Nuclear Power Plant (SNPP) integrated test plans for project Prometheus. While specific test plans were being developed by each technical community (e.g., material, physics, reactor safety, etc.), integration of all of these individual test plans was coordinated within the power plant organizations at KAPL and Bettis. In addition to this responsibility for integration of the various test programs, the power plant testing organizations at KAPL and Bettis were directly responsible for establishing the internal and external test facilities and programs for reactor plant (including energy conversion systems) thermal and hydraulic testing.

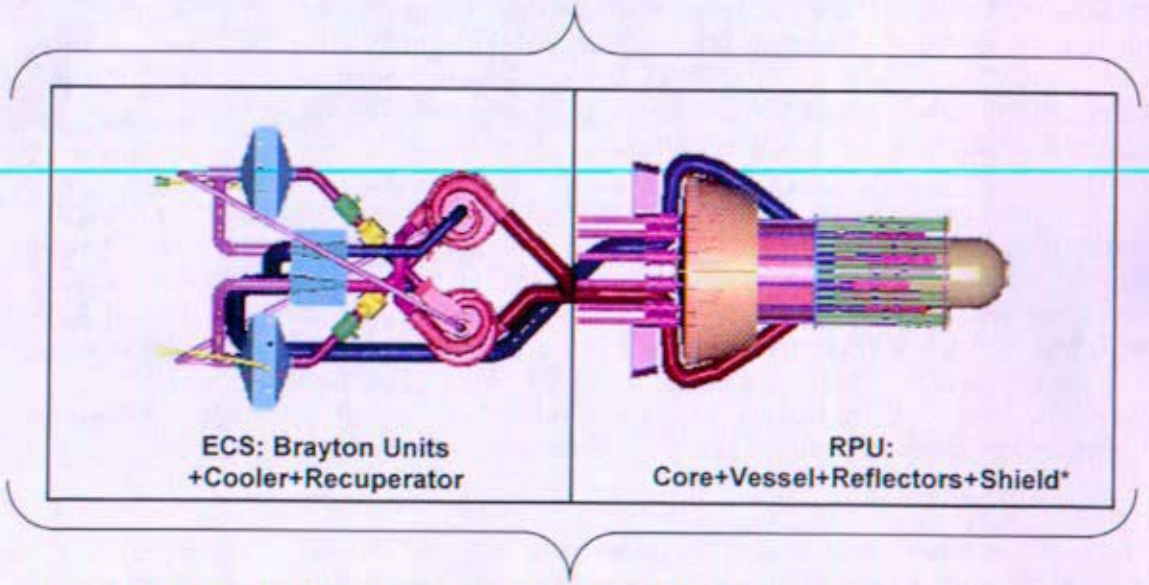
A key strategy in establishing the Prometheus test program was to use the existing national infrastructure (i.e., NASA facilities and national DOE labs) to the maximum extent practicable. This approach reduced the cost and start-up time necessary to meet the aggressive mission milestones originally planned for the Jupiter Icy Moons Orbiter (JIMO) mission. The Naval Reactors Prime Contractor Team (NRPCT) was in the process of reviewing the integrated test plan to assess extensibility for a lunar based type of mission at the time of project termination; however, no definitive test plans were established. Modifications to the baseline test plan were under consideration and they are discussed as appropriate in the specific sections.

At the start of the program, prior to concept down-selection, various reactor concepts (including heat pipe and liquid metal reactors) were being testing in parallel. Following selection of a direct gas cooled reactor with a Brayton energy conversion system, testing on heat pipe and liquid metal reactor concepts was terminated. No testing effort had yet begun on Stirling energy conversion systems for Prometheus prior to selection of a Brayton concept. Limited bench top testing of thermoelectrics was performed by the Jet Propulsion Laboratory (JPL) and this work was also discontinued as a part of Project Prometheus following concept selection.

While use of existing testing infrastructure was to be maximized as noted above, limited in-house testing at Bettis and KAPL was considered essential to the project. Specifically, in-house developmental testing focused on early concept designs, with low temperature and pressure testing of reactor element flow mockups already underway. These test programs were to guide the reactor design efforts and support the large scale, high temperature and pressure testing planned for external facilities. The new in-house test facilities that were planned are discussed in this section, as well as the limited test data obtained in existing test facilities prior to project termination. Test facility modifications for space work at KAPL and Bettis would have occurred in late 2006 or early 2007 had the project progressed.

## 13.2 Assembly, Test and Launch Operation (ATLO)

Figure 13-1 illustrates the terminology used in defining the reactor module (RM). The determination of how the reactor hardware would be assembled and tested was a key factor in the ATLO process and there were still significant open issues at the time of project termination. Figure 13-2 provides a notional flowchart of how the NRPCT envisioned the Prometheus 1 integrated test plan, from early developmental testing to launch. This figure represents a snapshot of a work-in-progress, at the time of project termination. It was developed using input from Oak Ridge National Laboratory (ORNL) and Northrop Grumman Space Technology (NGST) and assumed a 2015 launch date. Finally, Figure 13-3 provides a more detailed view of the envisioned ATLO process.




Reactor Module (RM) = Reactor Power Unit (RPU) + Energy Conversion System (ECS)

*(* Some concepts included the shield in reactor power unit, others considered the shield separate)*
(See Section 1 for definitions of individual segments)

**Figure 13-1: Illustration of Reactor Module Terminology**

**Acronyms used in Figure 13-2 Flowchart**

| | |
|---|---|
| ARR | ATLO Readiness Review (NGST Term) |
| ATLO | Assembly, Test and Launch Operations |
| BPMI | Bechtel Plant Machinery, Inc. – Operated by Bechtel Corp. |
| BWXT | BWX Technologies, Inc. in Lynchburg, VA – The Naval core vendor |
| CDBWXT | Conceptual Design BWX Technologies, Inc. in Lynchburg, VA – The Naval core vendor |
| CDR | Critical Design Review (NGST Term) |
| DM | Development Model: First-generation hardware |
| E2E | End-to-End |
| ECS | Energy Conversion System (the Brayton units) |
| EM | Engineering Model: Second-generation hardware |
| EP | Electric Propulsion System (ion thrusters) |
| ERD | Environmental Requirements Document (JPL document 982-00029) |
| FD | Final Design |
| FM | Flight Module |
| GRC | NASA – Glenn Research Center |
| GTR | Ground Test Reactor |
| HRS | Heat Rejection System (the solar array) |
| INSRP | Interagency Nuclear Safety Review Panel |
| JIMO | Jupiter Icy Moons Orbiter |
| JPL | Jet Propulsion Laboratory |
| JSC | NASA – Johnson Space Center |
| KSC | NASA – Kennedy Space Center |
| MRR | Mission Readiness Review (NGST Term) |
| MSFC | NASA – Marshall Space Flight Center |
| NGST | Northrop Grumman Space Technology – The spacecraft contractor |
| NRPCT | Naval Reactors Prime Contractor Team (Bettis, KAPL and BPMI) |
| ORR | Operational Readiness Review (NGST Term) |
| P1 | Prometheus 1 – The first flight unit. |
| PCD | Pre-Conceptual Design |
| PDR | Preliminary Design Review (NGST Term) |
| PSR | Pre-Ship Review (NGST Term) |
| QM | Qualification Model: Flight design hardware to be tested beyond mission requirements |
| RM | Reactor Module (RPU + ECS) |
| RMIF | Reactor Module Integration Facility |
| RPU | Reactor Power Unit (core, vessel, safety rod, reflectors, shield, CDMs, piping) |
| SM | Spacecraft Module |
| SNPP | Space Nuclear Propulsion Plant (RPU + ECS). Terminology is interchangeable with RM |
| STM | Structural Test Model aka Static Test Model |
| SVA | Shock, Vibration & Acoustic Test |
| TTM | Thermal Test Model |
| ZPC | Zero Power Critical test |

**This Page Intentionally Blank**

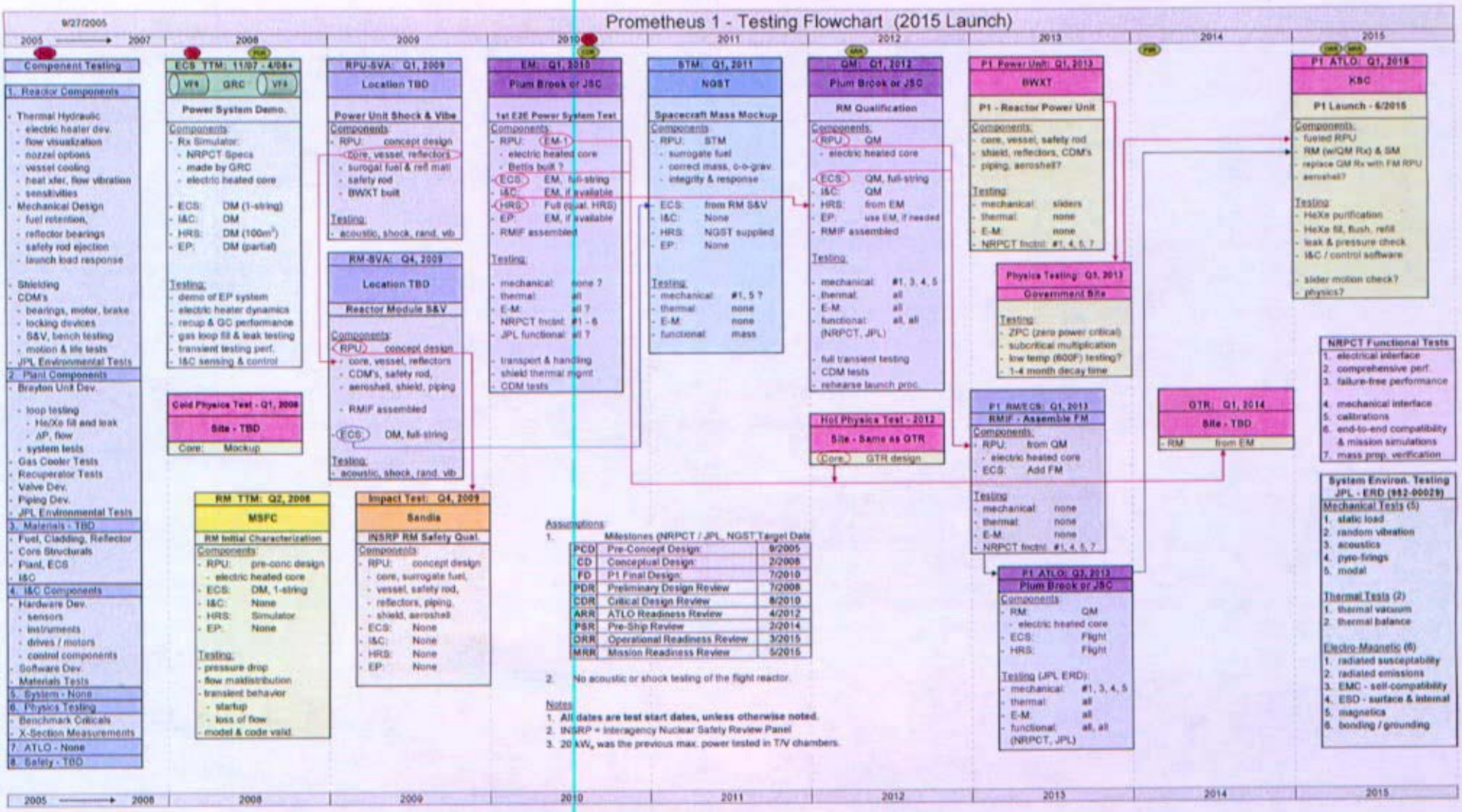



**Figure 13-2: Prometheus Integrated Test Plan**

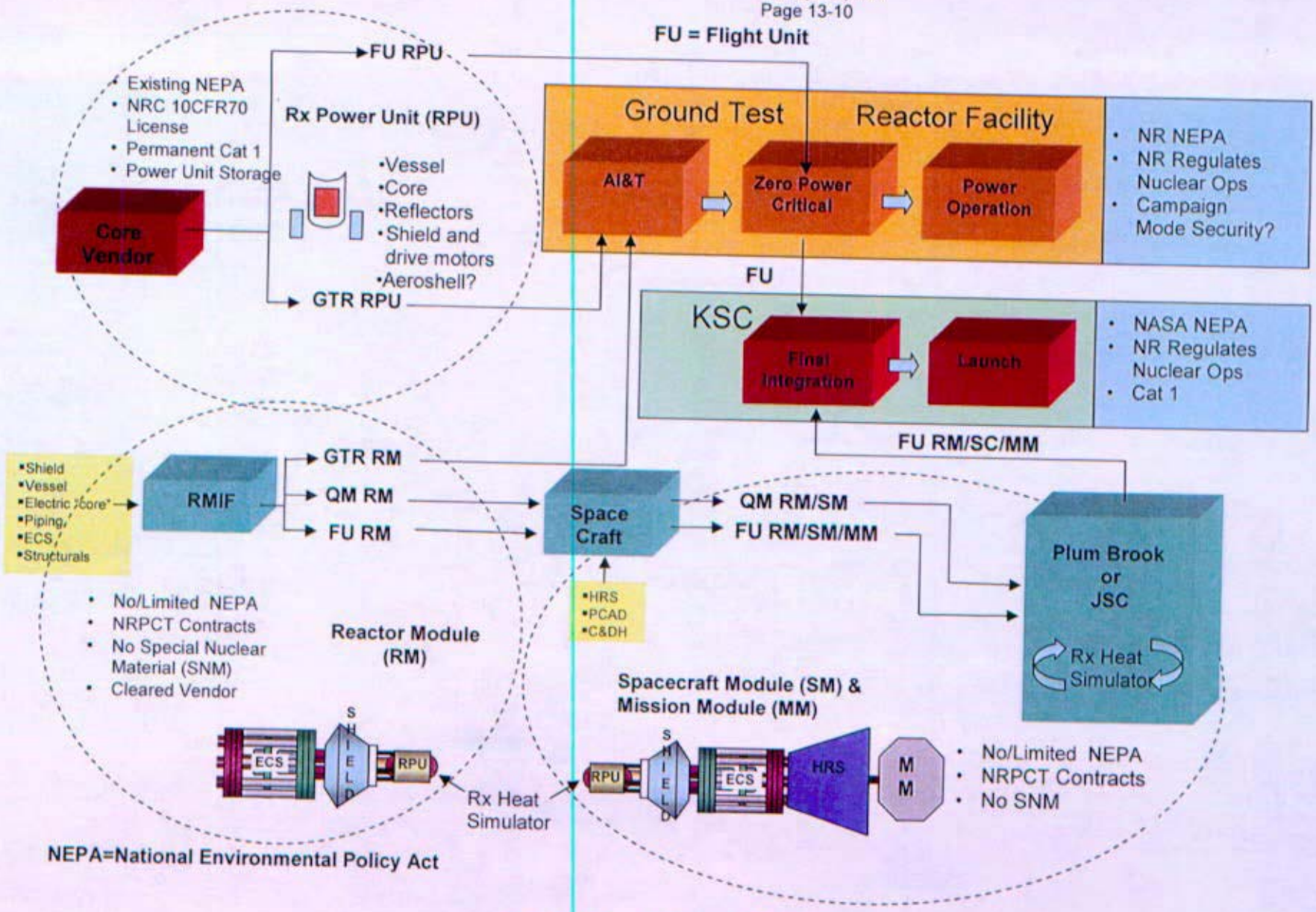



**Figure 13-3: Notional ATLO Flowchart**

### 13.2.1 Overall Assembly, Integration and Test (AI&T) Strategy

As the designated lead organization for Project Prometheus, the Jet Propulsion Laboratory introduced the use of their "test what you fly, fly what you test" philosophy that had provided them historical success. As the NRPCT testing plans evolved, it became clear that, although this JPL approach could be used on a number of components, testing the fueled flight reactor posed several problems. First, operating the flight unit reactor at power for any reasonable period of time would result in the build-up of a significant fission product inventory which was undesirable both in terms of handling requirements and safety concerns under inadvertent re-entry scenarios. Second, the NRPCT was unwilling to doubly expose the flight reactor to potentially damaging environments (the testing and the mission events). Finally, the large size of the spacecraft, combined with a significant quantity of special nuclear material, introduced burdensome logistical issues (facility licensing issues, security and safeguards, shipping, etc.) that would not allow integrated, fueled flight unit testing to proceed in an affordable, timely manner. Therefore, the NRPCT developed an AI&T and ATLO approach involving two paths – nuclear and non-nuclear. The paths merge as late in the assembly and test flow as possible to minimize the above concerns.

The non-nuclear path assumed that the RM would be assembled in a dedicated Reactor Module Integration Facility (RMIF). An electrically heated surrogate reactor power unit (RPU) would be mated to an energy conversion system (ECS) at this facility to form the RM. The successively more prototypical reactor modules would then be used for increasingly more "flight-like" development, qualification, and flight test programs. Since the fuel would not be present at this stage of the process, the selection of the location of the RMIF was relatively unrestricted. Also, the lack of special nuclear material for these activities would have minimized regulatory actions required to initiate construction.

The nuclear path assumed that the flight reactor and power unit would be assembled at the core vendor, shipped off-site for physics testing, and then shipped to the launch site for integration with the ECS / spacecraft. Acceptance of the flight reactor itself would rely on the qualification work performed on earlier test units rather than on direct full power, simulated space environment testing.

The integrated testing flowchart (Figure 13-2) presents a pictorial description of this approach for both the ATLO and earlier test phases. A detailed description of each flowchart step is presented below.

### 13.2.2 Integrated Test Plan

#### 13.2.2.1 Non-Nuclear Tests (no fuel)

##### 13.2.2.1.1 Component Testing

The ramp-up of Project Prometheus was to be dominated by a variety of individual component development tests, as summarized in the Space Reactor Program Test Index submitted in Reference 13-1 and included as Table 13-4. They are shown here only as a visual reminder of the component work required prior to integrated testing.

The purpose of the component tests was to:

- gather basic material property information
- test materials and components at prototypic operating conditions
- investigate fabrication and assembly approaches
- validate predictive models
- validate and refine designs

#### 13.2.2.1.2 Energy Conversion System Thermal Test Model (ECS-TTM)

This test was to provide an early demonstration that the electric propulsion system (ion thrusters) can actually be driven from a direct gas Brayton engine. The ECS-TTM was to be performed at Glenn Research Center (GRC), since they had both the lead for ion propulsion technology development and expertise on space energy conversion. A successful test at this early stage would help demonstrate the project's technical feasibility to stakeholders. The energy conversion hardware was to be based on the NRPCT pre-conceptual design planned for October 2005. The NGST supplied components were to be based on a first-generation development design.

The test components were to include:

- a heat source capable of generating one-half the design reactor power (100 $kW_e$). The heat source could be electric or gas and was not intended to be prototypical for this test.
- a single Brayton energy conversion unit
- a quarter-scale heat rejection system
- an ion thruster

The objectives of the test were to:

- demonstrate that thrust could be achieved using a gas driven Brayton unit
- characterize system response to normal / abnormal operating transients
- assess recuperator and gas cooler performance
- demonstrate gas loop fill and leak check procedures
- verify material strength and dimensions after exposure to temperature
- test I&C sensors and the software control package
- obtain test data to support plant model qualification

#### 13.2.2.1.3 Reactor Module Thermal Test Model (RM-TTM)

The RM-TTM was to be the initial test of the integrated reactor module (electrically heated power unit mockup + limited energy conversion system). It is the reactor counterpart to the energy conversion system thermal test model test. The RM-TTM test article would use "state-of-development" components (prototypic where possible) based on the NRPCT pre-conceptual design. This testing was planned for Marshall Space Flight Center (MSFC) since they were leading the reactor development (non-nuclear) testing for NRPCT and had experience working on electric mockups of space reactor designs with Los Alamos and Sandia National Laboratories.

The test components were to include:

- a one-half scale electrically heated reactor power unit (core, vessel, piping)
- a single Brayton energy conversion unit (development model generation)
- a simulated Heat Rejection System (HRS) to dump excess heat

The objectives of the test were to:

- validate electric heater element design for reactor simulation
- obtain pressure drop and flow distribution data for validation of analytical models
- characterize system response to controlled startup and loss-of-flow transient behaviors
- verify material strength and dimensions after exposure to temperature
- verify structural design margins
- validate computational fluid dynamics predictions

It is important to note that as the mission requirements changed, launch dates moved out in time and funding reductions for the first several years of the project were anticipated. At the time of project cancellation, a strategy to combine the EC-TTM and RM-TTM into a common test platform (called TTM) was initiated by the NRPCT. This approach would have reduced costs and enabled a comprehensive, system level demonstration of the proposed design to be built and tested relatively quickly.

#### 13.2.2.1.4 Reactor Power Unit Shock, Vibration, and Acoustic Test (RPU-SVA)

This test was to qualify the reactor for launch and mission loads. The reactor power unit was to be based on the NRPCT conceptual design.

The test components were to include:

- reactor core with surrogate fuel pellets of prototypic shape and mass
- reactor vessel
- reflectors (surrogate material of appropriate size and mass)
- safety rods – use of safety rods in this test was undecided at time of project termination

The objective of the test was to demonstrate that the reactor internals are not damaged when subjected to the vibration, shock and acoustic loads of launch and mission events. Although all components would have been evaluated for damage, the focus of the test was on the fuel pellets and reactor internals.

The core, vessel, and reflectors were to be re-used in the subsequent reactor module shock, vibration, and acoustic test (RM-SVA). Also, the power unit was to be fabricated in the core manufacturing facility using prototypic fabrication processes as part of manufacturing development.

### 13.2.2.1.5 Reactor Module Shock, Vibration, and Acoustic Test (RM-SVA)

This test was to qualify the integrated reactor module design for shipping, launch, and mission loads. The reactor module design was to be based on the NRPCT conceptual design.

The test components were to include the reactor power unit items described above, plus the following:

- coolant piping
- radiation shield
- reflector drive motors
- a full quantity of Brayton energy conversion units (development model generation)
- aeroshell – use of the aeroshell in this test was undecided at time of project termination

The objective of the test was to demonstrate that the reactor module met mission functional requirements after being subjected to the limiting shock, vibration and acoustic loads of shipping, launch and mission events.

It is noted that:

- The reactor power unit was to be re-used for reactor safety impact testing.
- The ECS was to be re-used as a mass mockup for the structural test model (STM).
- The RPU test unit was to be fabricated in the core manufacturing facility using prototypic fabrication processes as part of manufacturing development.

### 13.2.2.1.6 Impact Testing

This test was to help qualify the safety basis for the Interagency Nuclear Safety Review Panel (INSRP). The reactor power unit was to be the unit previously used in the RM-SVA test and was based on the NRPCT conceptual design. It contains non-hazardous surrogate fuel, reflector, and radiation shield materials. Testing was to include a series of drop tests from successively higher levels, culminating in a "rocket sled" test to simulate the impact from re-entry or an aborted launch. The test results were to be evaluated for impact resilience and to characterize the deformation.

### 13.2.2.1.7 Engineering Model (EM)

The engineering model was to be the first full-scale demonstration of the integrated power plant system, and was to make maximum use of prototypic materials and components. The reactor module was to be based on the NRPCT conceptual design, while the spacecraft module components were to be based on the NGST preliminary design review.

The test components were to include:

- a full scale, electrically heated reactor power unit
- a full quantity of ECS units (quantity yet to be determined)

- a suite of I&C instruments, sensors, and control software
- a full-scale heat rejection system (NGST supplied)
- an electrical propulsion system, if available (NGST supplied)

The test objectives were to:

- simulate reactor startup and full power and transient testing on the integrated system
- evaluate effectiveness of the reactor control software
- validate I&C system sensing and control methods
- demonstrate reactor feedback behavior and control with a high-fidelity ECS
- demonstrate the level of success of manufacturing and assembly techniques
- resolve transportation and handling issues associated with the assembled spacecraft
- develop procedural guidance for the qualification and flight reactor module tests
- qualify the HRS design (NGST objective)

It is noted that:

- The purpose of the radiation shield was to provide thermal and radiation protection to the components behind the shield. As this EM unit was to be non-nuclear, the radiation function of the shield could not be tested. Therefore, as a cost measure, a simulated shield using appropriate thermal materials may have been used.

- Due to the large size of the spacecraft, and NGST's desire to qualify the large heat rejection system, testing was envisioned to occur at the Plum Brook Station facility or at Johnson Space Center (JSC). The transportation and testing logistics of this EM test were not yet planned at the time of project termination.

- This RM would be assembled in the reactor module integration facility (RMIF), if available.

- Upon completion of EM testing, the energy conversion system components and possibly I&C hardware could be used in the Ground Test Reactor.

#### 13.2.2.1.8 Structural Test Model (STM)

This was to be a structural integrity and frequency response test of the spacecraft primary structure and was for NGST use only. Test results may have influenced the spacecraft design by showing whether additional structural strength was needed at critical acoustic and thrust frequencies. The STM would also be used by NGST as a pathfinder model to determine whether the movement, handling and processing operations on the full-scale spacecraft fit into the available envelope(s).

The reactor module components need only be represented by mockups of approximate shape, mass, and center of gravity. However, it was envisioned that the ECS portion of the RM would be represented by the full-string ECS previously used in the RM-SVA test since it would be available and would save the cost of fabricating mass mockups.

#### 13.2.2.1.9 Qualification Model (QM)

The qualification model was to be identical to the flight unit (i.e., uses flight quality hardware) except that it would use an electrically heated core mockup. The reactor module was to be based on the NRPCT final design, while the spacecraft module was to be based on the NGST critical design review (final design). The QM test would drive components to qualification level environmental testing, which would exceed mission requirements.

Test components were to include:

- an electrically heated reactor power unit
- a full quantity of ECS units (quantity yet to be determined)
- a suite of I&C instruments, sensors and control software
- a heat rejection system (re-used EM HRS)
- an electrical propulsion system, if needed (undetermined at time of project termination)

The test objectives were to:

- qualify the reactor module design (validate adequate design margin)
- demonstrate end-to-end mission operations capability
- rehearse assembly and pre-launch processing procedures

It is noted that:

- Thermal-vacuum testing of the QM would serve as the certification for the subsequent flight reactor. This was due to the risk associated with subjecting the flight reactor to environmental contaminants during the thermal-vacuum test with no subsequent means to verify the absence of material degradation.

- Upon completion of QM testing, the RPU was available for coupling to the flight ECS / spacecraft module assembly. This assembly was to be used to support ATLO testing of the spacecraft and mission modules.

- This RM would be assembled in the reactor module integration facility.

### 13.2.2.2 Nuclear Tests

#### 13.2.2.2.1 Cold Physics Test

This test would assess the adequacy of the physics design tools in calculating the cold physics characteristics for fuel configurations approximating the Prometheus reactor design. The test was to consist of a full-size fuel assembly with test specimens approximating the reactor geometric arrangement (fuel, structural, reflector, and poison material) and actual core loadings. Measurements were to include reflector critical configurations, reflector worth, safety rod worth, and neutron flux distributions. The test facility site was undetermined at the time of project cancellation. The cold physics testing is discussed in more detail in the Space Reactor Pre-Conceptual Report (Reference 13-28) under Mock-up Tests.

#### 13.2.2.2.2 Hot Physics Test

This test would assess the adequacy of the physics design tools in calculating the cold and hot physics characteristics of a manufactured Prometheus reactor, including the reactivity effects of core geometry changes as the reactor was heated from cold to normal operating temperature. Testing would have been performed at the Ground Test Reactor (GTR) site. Measurements were to include reflector critical configurations and differential worth as a function of temperature, static temperature coefficients of reactivity, and cold-to-hot temperature reactivity effect. If suitable, this core was to be used for the GTR.

#### 13.2.2.2.3 Ground Test Reactor (GTR)

The GTR is a comprehensive, nuclear, integrated test program (cold and hot, low and high power, and transients) to support mission assurance for P1. The GTR reactor module was to have been identical to the P1 core, subject to the terrestrial physics and regulatory requirements unique to ground testing (if suitable, the unit used for hot physics testing was to be re-used). Measurements were to include reflector critical positions and reactivity worth as a function of temperature, safety rod worth, static temperature coefficients of reactivity, power reactivity, kinetics parameters, transient response characteristics, nuclear detector response and neutron flux spatial distributions. Progress on the Ground Test Reactor Facility (GTRF) at the time of project termination is documented in Reference 13-22.

The test objectives were to:

- assess adequacy of physics design tools and dynamic response models in calculating physics characteristics and transient response of the reactor in the integrated plant
- assess the adequacy of procedures for reactor startup and plant transients (e.g., shimming to maintain temperature control, switching to coast mode, switching Brayton engine lineup, etc.)
- perform long term periodic testing to enable assessment of the lifetime trends of physics characteristics in advance of the flight unit cores

The GTR was to use reactor power unit components recovered from the EM test, as well as the EM full-string Brayton ECS.

### 13.2.2.3 Flight Unit ATLO Flow

A notional flight reactor flowchart is depicted in Figure 13-3. The NRPCT defined ATLO to begin with the assembly operations for the Prometheus flight unit. Fabrication of the fueled reactor power unit at the core manufacturing vendor would proceed in parallel with assembly of the unfueled reactor module at the RMIF. Appropriate acceptance testing was to be performed on each of these two segments. The two segments were then to be mated at the launch site, followed by the necessary fit, function, and performance testing.

#### 13.2.2.3.1 Fabricate Reactor Power Unit (fueled)

Fabrication of the reactor core and fueled power unit were assumed to take place at a qualified nuclear core manufacturer. A variety of options were considered as to how to best incorporate a fueled reactor core into the flight reactor module (RPU + ECS). The baseline assumption incorporated into the testing flowchart was that the core vendor would fabricate a complete flight power unit (core, vessel, safety rod, reflectors, shield, reflector drive motors, and piping). Only basic functional testing would be performed at the core vendor – a mechanical check of slider motion, mechanical and electrical interface checks, instrument calibrations, and a check of mass properties. The completed flight power unit would be shipped to the GTRF for physics testing.

#### 13.2.2.3.2 Physics Tests of Reactor Power Unit (fueled)

The completed flight power unit was to be received from the core vendor. Zero-power physics tests were to be performed to confirm that no significant manufacturing errors exist, and to obtain an initial physics characterization of the reactor. Measurements include reflector critical positions, differential and integral worth of reflectors, and integral worth of safety rod.

Upon completion of testing, the unit is stored at the GTRF to allow any activation products created by the physics testing to decay to a manageable level, and to minimize the amount of logistical support time required to safeguard special nuclear material at the launch site.

#### 13.2.2.3.3 Fabricate Reactor Module (no fuel)

The reactor module integration facility was to be responsible for assembly, integration, and testing of the non-fueled reactor modules. Under the baseline assumption for the P1 flight unit, the RMIF would assemble the flight ECS from the supplied parts (Braytons, recuperators, gas coolers, support cage, etc.), bend and attach (weld) the coolant piping, and attach the supplied QM electrically heated reactor power unit. Only very basic functional testing would be performed at the RMIF (e.g., system integrity verification, mechanical and electrical operational and interface checks, instrument calibrations, and a check of mass properties). This completed "flight" reactor module would be shipped to NGST for integration with the flight spacecraft, and then to Johnson Space Center or Plum Brook Station for environmental testing to acceptance levels.

### 13.2.2.3.4 Integrate & Acceptance Test RM / Spacecraft (no fuel)

The electrically heated "flight" reactor module was to be received by NGST and integrated into the flight spacecraft along with the scientific mission module. NGST would then subject the flight spacecraft to the mechanical, thermal, and electro-magnetic environmental tests required by the JPL Environmental Requirements Document (ERD). This testing was to occur at both the NGST integration facility and at an off-site thermal-vacuum facility (JSC or Plum Brook). The early preference was for JSC due to more favorable transportation logistics with a spacecraft of this size and mass. The flight spacecraft would then be shipped to Kennedy Space Center (KSC – the envisioned launch facility) to be mated with the fueled reactor module.

### 13.2.2.3.5 Mate Fueled RPU with RM / Spacecraft

The acceptance tested spacecraft and the certified fueled reactor module were to be received by KSC. The electrically heated power unit was to be replaced with the fueled power unit. Cutting and seal welding these joints was considered a critical, complex task, requiring extensive preparation and training. The HeXe coolant is purified, loaded, and sealed into the RM. Final functional, electrical, and software checks were to be performed. A preference existed to perform slider motion checks and zero-power critical tests at KSC prior to launch if this is appropriate from a regulatory standpoint (this issue had not been resolved at the time of project termination). The assembled spacecraft was to be mated to the launch vehicle and prepared for launch.

Launch Facility – KSC performed a conceptual study to inventory and evaluate existing facilities at both KSC and Cape Canaveral Air Force Station (CCAFS) for suitability to support the Project Prometheus spacecraft processing operations (Reference 13-21). The objective of the study also included the conceptual requirements and possible locations for a new spacecraft processing facility if no existing facilities were viable candidates. This study determined that no existing buildings were suitable and provided a recommendation for a new four-building facility.

The buildings were to include:

- a spacecraft processing facility large enough to accommodate an unfurled JIMO spacecraft
- a power unit processing facility to house the reactor prior to integration with the spacecraft
- a ground support equipment storage building
- an operations office building

Although the conceptual study was conducted with minimal input from the NRPCT, KSC recognized that the scope of requirements that would be invoked by NR, to support the presence of a nuclear reactor, would need to be developed and assessed for compatibility with existing KSC/CCAFS requirements. These requirements were expected to dictate some of the design attributes of the facility, and as such, they factored into the early phase of the spacecraft processing facility plan.

### 13.2.3 Drivers / Issues

#### 13.2.3.1 Definition of the Power Unit

One of the major aspects of the assembly and testing flow process that needed to be resolved was the definition of the power unit and the extent of reactor module assembly to be performed at the launch site. As discussed below, criticality safety questions still needed to be answered and trade studies had yet to be performed.

##### 13.2.3.1.1 Scope of Power Unit vs. Licensing Requirements

A concern existed regarding the extent to which the power unit could be assembled at a core vendor facility within the existing regulatory framework (10CFR70 license from the NRC). Consequently, a core vendor was requested to provide an assessment of the potential impact on the existing facility licensing requirements imposed by nuclear operations involving the fabrication, assembly, and limited pre-operational functional testing of a space reactor.

In Reference 13-25, BWX Technologies (BWXT) provided a reactor core and reactor module assembly sequence that ensured the system remained within the nuclear criticality safety license requirements during all phases of manufacture and test, including postulated accident conditions. This information had not been submitted to NR nor factored into the assembly and testing flow process at the time of project cancellation.

##### 13.2.3.1.2 Reactor Module Configuration Control after Zero Power Critical Testing

Ideally, the reactor power unit would not be disassembled following zero power critical testing. However, issues needed to be resolved regarding the configuration of the power unit during shipping which may have necessitated power unit disassembly. The open questions involved the criticality safety aspects of shipping the core with the reflectors installed and the cost of shipping containers large enough to accommodate the additional hardware required to maintain reactor-to-reflector relative positioning.

#### 13.2.3.2 Extent of Reactor Module Subjected to Testing

An electrically heated surrogate power unit (referred to as the "QM" reactor power unit) would be initially installed in the flight unit reactor module to support testing and then replaced by a fueled power unit. Related to the above question regarding the scope of the power unit was the question of how much of the RM would be replaced during the launch site fueling operation. A range of options were being considered from as little as a "core cartridge" to replacing everything from the ECS and forward (See Figure 13-4). The former option was attractive from the JPL "fly as you test, test as you fly" perspective but posed problems for reactor design and manufacturing and did not alleviate the configuration concerns discussed above. The latter option minimized the extent of the RM that would undergo flight testing and did not lessen the shipping container concerns but did alleviate the configuration concerns. The baseline case chosen for PMSR was the power unit (core, vessel, reflectors and some piping) without the shield. However, this was far from final and trade studies were to be performed for this issue, preferably early in the design cycle so that the disassembly logistics could be factored into plant arrangements studies.

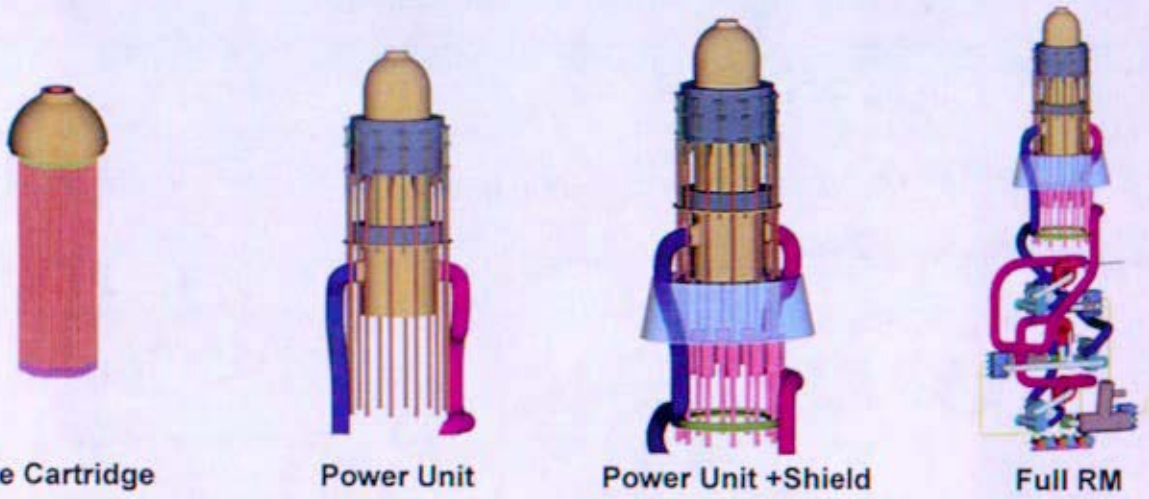



**Figure 13-4: Options Considered for Extent of RM Replacement at Launch Site**

### 13.2.3.3 Selection of Reactor Module Integration Contractor

The ATLO flow plan designated the contractor who would perform the assembly activities in the RMIF as the Reactor Module Integration Contractor (RMIC). It was also considered that a synergy could be gained by the RMIC also being a supporting contractor for the spacecraft integration activity and the performing contractor for the pre-launch fueling operation. The plan considered it advantageous to use a contractor with the proper skills mix but also one who was familiar with the NR culture. Commercial naval shipyards were being strongly considered for this role based on the familiarity aspect, but when partnered with aerospace sister companies, these contractors offered a comprehensive array of services not only in support of the assembly and test activities but also the pre-launch fueling evolution. As discussed below, the two shipyards that were engaged prior to project termination were General Dynamics Electric Boat and Northrop Grumman Newport News. These shipyards are affiliated with aerospace contractors General Dynamics Spectrum Astro and Northrop Grumman Space Technologies, respectively. Although the shipyard contractor concept was desirable, it was planned to execute a competitive bid process prior to selecting the RMIC.

## 13.2.4 Estimated Cost for AI&T Effort

Three contractors were engaged to provide rough order of magnitude (ROM) cost estimates for AI&T activities to support the Space Reactor Planning Estimate. The three contractors were BWXT, Northrop Grumman Newport News Shipbuilding (NGNN) and Electric Boat (EB). The ROM estimates generated (References 13-23, 13-24, and 13-25) are amalgamated into the Table 13-1 cost analysis discussed below.

**Table 13-1: ROM Cost Estimates for RMIF and Reactor Module AI&T**

| Item | Engineering Hours | Craft Hours | Subcontract & Materials | Comments |
|---|---|---|---|---|
| **Design & Provide RMIF** | 80,000 | 15,000 | $30 – 40M | |
| o maintain/upgrade RMIF (10 year cost) | 60,000 | 140,000 | $2.5M | 3 engineers, 7 crafts, AE per yr |
| o RMIF operational test procedures | 7,000 | 0 | | 35 procedures @ 200 hrs each |
| o operate/test RMIF prior to EM | 26,000 | 40,000 | | 13 engineers, 20 craft, 1 year |
| **RMIF Total** | **173,000** | **195,000** | **$32.5 - 42.5M** | |
| **Engineering Model (EM) at the RMIF** | 73,000 | 20,000 | $750,000 | |
| o planning | 40,000 | | | 8 engineers, 2.5 years |
| o assembly drawings | 13,000 | | | piping, electric, fastening, structural |
| o test procedures | 6,000 | | | 30 procedures @ 200 hrs each |
| o execution – assemble, weld & test | 14,000 | 20,000 | $750,000 | 7 engineers, 10 craft, 1 year |
| **Qualification Model (QM) at the RMIF** | 45,000 | 20,000 | $750,000 | |
| o planning | 24,000 | | | 8 engineers, 1.5 years |
| o assembly drawings | 5,000 | | | piping, electric, fastening, structural |
| o test procedures | 2,000 | | | update EM procedures |
| o execution – assemble, weld & test | 14,000 | 20,000 | $750,000 | 7 engineers, 10 craft, 1 year |
| **Flight Unit (FU) at the RMIF** | 51,000 | 22,500 | $750,000 | |
| Assemble QM RPU to flight ECS | | | | |
| o planning | 24,000 | | | 8 engineers, 1.5 years |
| o assembly drawings | 5,000 | | | piping, electric, fastening, structural |
| o test procedures | 2,500 | | | update QM procedures |
| o disassemble QM reactor module | 1,500 | 2,500 | | 3 engineers, 5 craft, 0.25 year |
| o execution – assemble, weld & test | 18,000 | 20,000 | $750,000 | 9 engineers, 10 craft, 1 year |
| **Flight Unit (FU) to SM at Test Site** | 16,700 | 6,400 | $460,000 | |
| o planning | 8,000 | | | 8 engineers, 0.5 years |
| o integration drawings | 800 | | | |
| o test procedures | 1,500 | | | |
| o execution – integrate, weld & test | 6,400 | 6,400 | $300,000 | 8 engineers, 8 craft, 0.4 year |
| o travel | | | $160,000 | $10K per person x 16 |
| **Fueled Reactor Power Unit at BWXT** | | | $18.4M | |
| BWXT estimate for RPU assembly | | | | Above price does not include:<br>o materials: $12 to $18M<br>o component fab: $5 to $10M |
| **FU/SM to Fueled Power Unit at KSC** | 44,000 | 18,000 | $440,000 | |
| o planning | 8,000 | | | 8 engineers for 0.5 year |
| o assembly drawings & procedures | 22,000 | 5,000 | | 25 drawings, 6 main procedures |
| o execution – integrate, monitor, test | 5,000 | 6,000 | $240,000 | 6 eng., 6 craft for 0.4 year |
| o radcon procedures & follow | 9,000 | 8,00<br>0 | | 3 eng. for 1.5y, 8 techs for 6m (24/7) |
| o travel | | | $200,000 | $10K per person x 20 |
| **Design Support** | 50,000 | 5,000 | $350,000 | |
| o AI&T planning, design planning | 48,000 | | | |
| o mockups, weld qualifications | 2,000 | 5,000 | $150,000 | |
| o drawing software, workstation rental | | | $200,000 | |
| **Program Management (EM - Launch)** | 250,000 | 0 | $110,000 | |
| o 5 managers for 10 years | 100,000 | | $110,000 | Office consumables |
| o various staff for 5 to 10 years | 150,000 | | | |
| **AI&T Totals – Excluding RMIF** | **530,000** | **92,000** | **$22M** | **(rounded)** |

## 13.3 Description of Key Facilities

### 13.3.1 Glenn Research Center (GRC)

NASA's Glenn Research Center is located in Cleveland, Ohio and is NASA's lead facility for developing space energy conversion systems, as well as the ion thrusters that were planned for the JIMO mission. GRC has significant experience in Brayton and Stirling energy conversion and power distribution systems for space applications. Two testing facilities were being considered for testing of JIMO components: Vacuum Facilities 5 and 6 (VF-5, VF-6). These vacuum facilities are optimal due to their vacuum capabilities ($10^{-6}$ torr), and the ability to configure the tanks to independently run separate components of a larger, integrated test (such as a reactor module in VF-6 connected to an ion propulsion system in VF-5).

VF-5 has a diameter of 4.6m (15 ft) and length of 18m (60 ft), and is uniquely suited to test ion thrusters due to its rapid vacuum pump-down speed. With a combination of oil diffusion pumps (ODP) and cryo-pumping, air can be expelled from the chamber at a rate of $3.5 \times 10^6$ l/sec. A 10-ton crane is available to handle prototypic components. Four test ports with a diameter range of 0.3 to 1.8m (1.0 to 5.9 ft) and length range of 0.3 to 2.4m (1.0 to 7.9 ft) are attached to the chamber. This facility allows for automated, unattended operation.

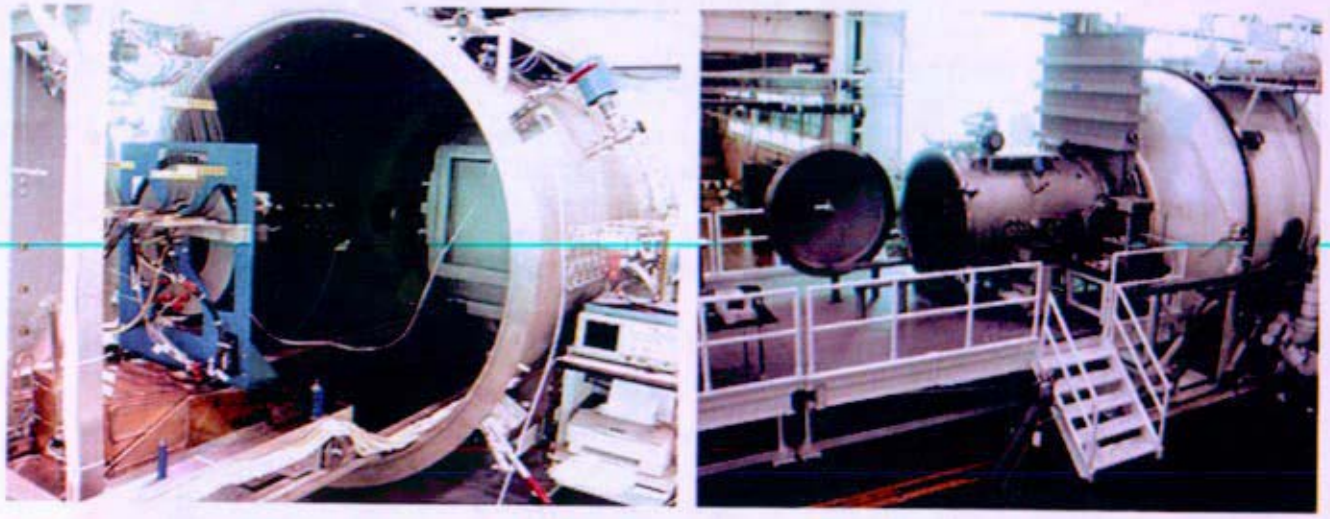


**Figure 13-5: Two Illustrations of Vacuum Facility VF-5 at GRC**

VF-6 has a diameter of 7.6m (24.9 ft) and length of 21m (68.9 ft), and is intended for power system testing and high power ion propulsion. This facility can simulate Earth and Mercury solar power concentrations and space thermal conditions (using a liquid nitrogen cooled shroud). The system is able to reject 2400 kW of thermal energy. As with VF-5, the facility allows for automated, unattended operation.

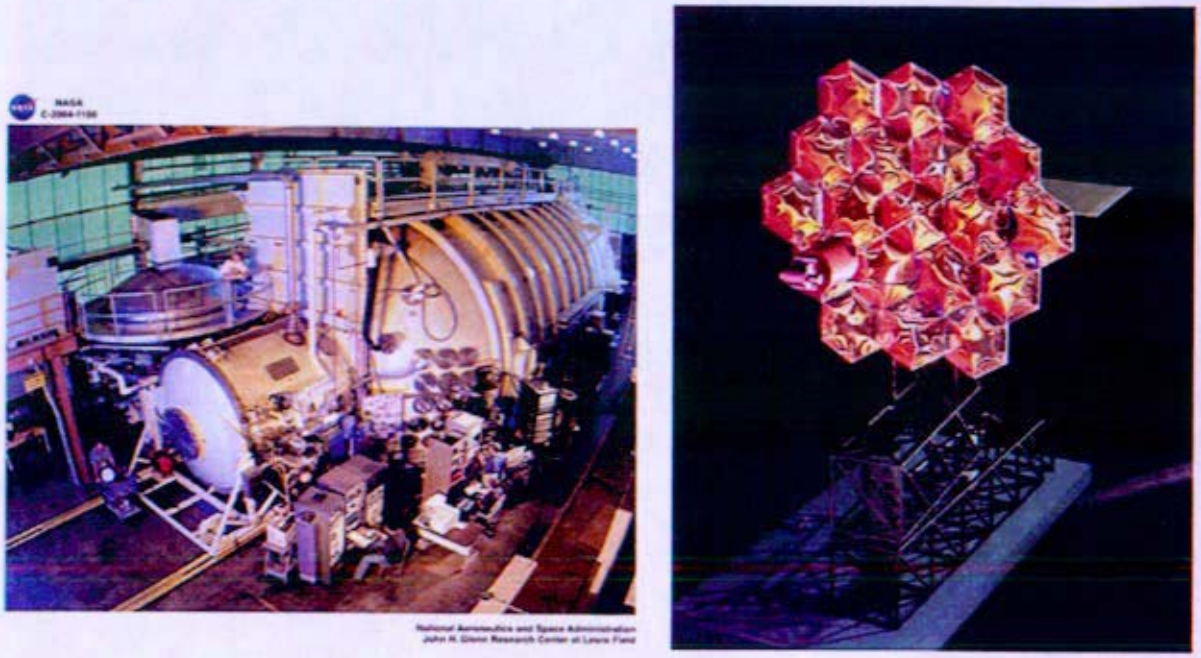


**Figure 13-6: VF-6 Chamber with Solar Simulator (Silver Dome) and the Solar Simulator**

Some limitations on this facility are:

1. Glenn Research Center does not have the necessary regulatory documentation to allow for testing of components containing special nuclear material.

2. There is no functional rail system to the VF-5/VF-6 test facilities, a potential issue for transportation of large parts; however, this is also an issue for other facilities as well.

### 13.3.2 Marshall Space Flight Center (MSFC)

NASA's Marshall Space Flight Center is located in Huntsville, Alabama and is a leading facility for developing and performing electrically heated (non-nuclear), thermal/hydraulic testing of space reactor mockups. MSFC had worked on various space reactor concepts prior to NRPCT involvement with Project Prometheus. The NRPCT took advantage of this experience to continue work on development of electrical heaters to simulate reactor fuel elements and initial studies of liquid metal and heat pipe reactor mockups. Effort was shifted to gas cooled reactor mockups following the concept selection. The specific work efforts performed by MSFC for NRPCT are described in Section 13.6. A brief description of the MSFC test facilities is provided here for information.

The majority of testing for project Prometheus was conducted in MSFC's Early Flight Fission Test Facility (EFF-TF) located in Building 4655. Limited work was also performed in glovebox setups outside of EFF-TF for liquid metal property studies, heat pipe filling, and manufacturing.

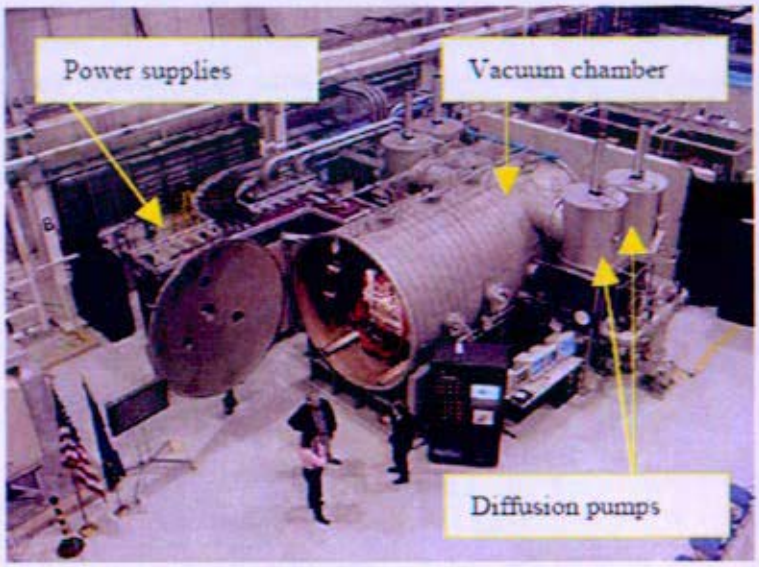



**Figure 13-7: MSFC EFF-TF Vacuum Chamber**

The EFF-TF vacuum chamber shown in Figure 13-7 has a diameter of 2.7m (9 ft) and a length of 6m (20 ft). It is capable of reaching a vacuum of $10^{-6}$ torr with the existing diffusion style pumps. Higher vacuum could be achieved, but would likely require cryogenic vacuum pumps ("cryo-pumps"), as well as tighter seals on the vacuum chamber penetrations. For most of the refractory materials under consideration, a vacuum on the order of $10^{-8}$ torr is required for test temperatures above 500°K due to material degradation caused by atmospheric impurities (primarily oxygen). Initial testing at EFF-TF used stainless steel pressure boundary materials at temperatures below 650°K to perform thermal/hydraulic simulation of the reactor concepts. As the design matured, prototypic materials and temperatures would be tested, and the need for higher vacuum capability would be addressed.

EFF-TF possesses a significant infrastructure for larger scale reactor mockup thermal/hydraulic testing. Electrical power capability on the order of a megawatt is available for electrically heating the reactor mockups. Nitrogen gas can be supplied from bottles or tank trucks, depending upon the needed volume. On past projects, closed loop testing was typically performed on reactor mockups using a compressor, while smaller scale tests used an open loop system. The ability to test with helium-xenon gas mixtures was not yet established since a leak tight, closed system would be needed (to minimize loss of expensive xenon gas).

### 13.3.3 Sandia National Laboratories (SNL)

Sandia National Laboratories is located near Albuquerque, New Mexico, and was under consideration for accident testing of the Prometheus reactor module mockups. This testing was intended to demonstrate how special nuclear material and any other environmentally hazardous materials (shield and/or reflector materials) would behave in the event of an unintended re-entry impact due to launch failure.

### 13.3.4 Plum Brook Station

Plum Brook Station, part of NASA Glenn Research Center, is located in Sandusky, Ohio, and houses the world's largest vacuum chamber in its Space Power Facility. The dome-topped cylinder is 30m (100 ft) in diameter and 37m (122 ft) tall. Accessible through two 15 by 15m (50 by 50 ft) access doors, the chamber is capable of handling a partially deployed, full-scale JIMO spacecraft. The chamber uses sixteen 1.2m (48-in) diffusion pumps and ten 1.3m (52-in) cryo-pumps, which can evacuate the chamber to $10^{-6}$ torr in eight hours. The chamber can also be configured to simulate solar radiation and the space thermal environment using a cryogenic cold wall. The chamber has a 20-ton polar crane and is pre-wired with pass-throughs for data acquisition and power, as well as ports for high pressure liquids and gasses. The chamber has a concrete enclosure for radiation shielding 1.8 to 2.4m (6 to 8 ft) in thickness since it was originally designed for nuclear testing for the NERVA nuclear rocket project.

The chamber has an adjacent experiment assembly area measuring 23 by 30m (75 by 150 ft) with clearance of 24m (80 ft). This area contains three sets of railroad tracks extending through the building to the east railroad spur. Access to the outside is through a 15 by 15m (50 by 50 ft) doorway.

On the other side of the chamber, there is an experiment disassembly area the same size as the assembly area. Rail tracks pass through this area and connect outside the building to the west rail spur. This area has extensive ventilation and contamination control and (like the vacuum chamber) has 1.8m (6 ft) thick concrete radiation shielding. Large capacity blowers are available for environmental control to create either positive or negative internal pressures.

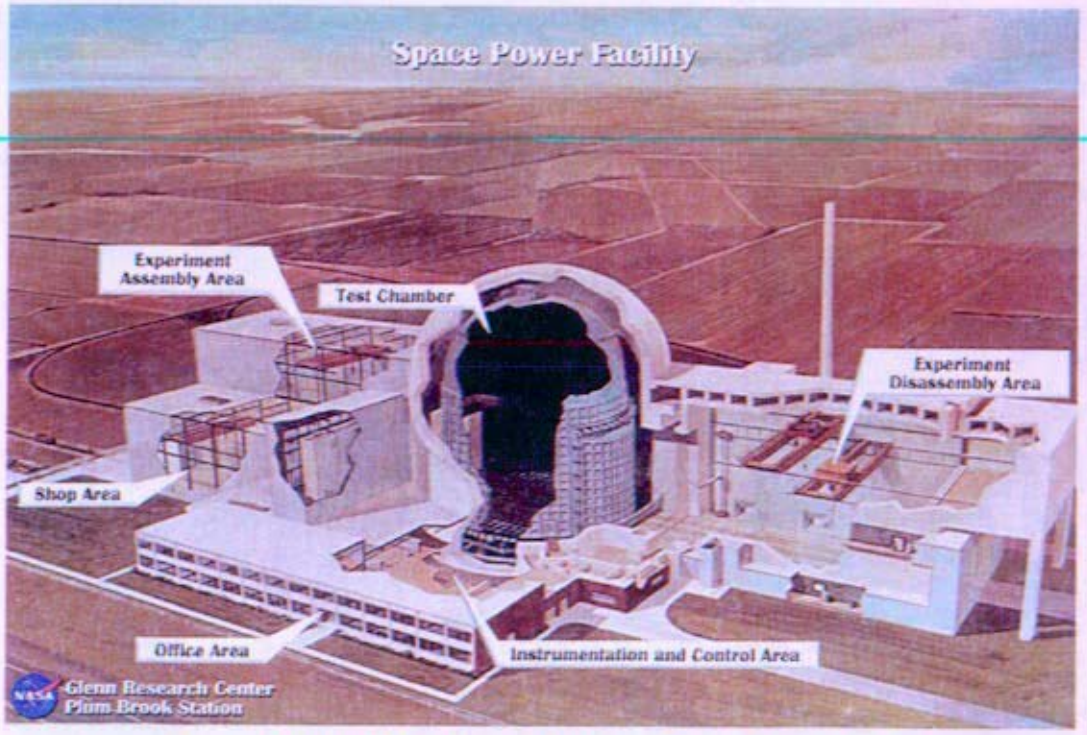
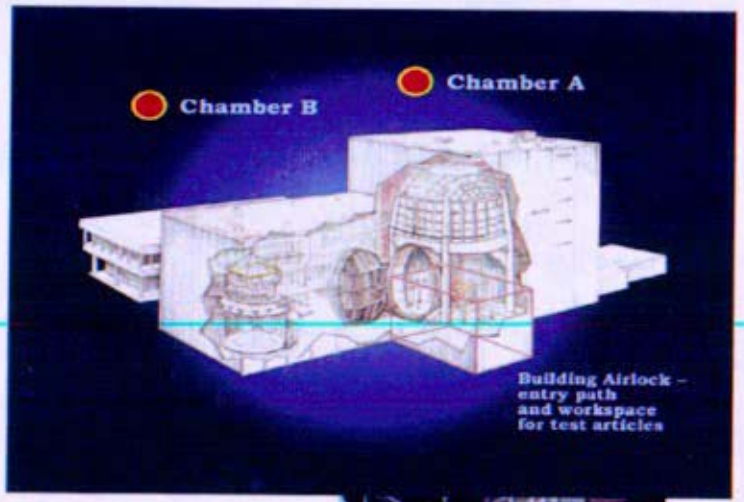


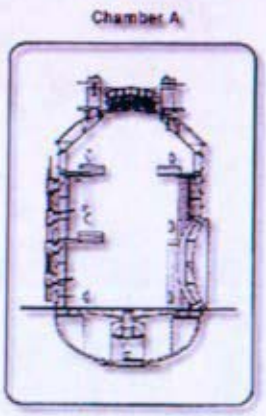

**Figure 13-8: Plum Brook Station Space Power Facility**

### 13.3.5 Johnson Space Center (JSC)

Johnson Space Center is located in Houston, Texas, and was under consideration as an alternative to Plum Brook for spacecraft vacuum tests. Preliminary investigations by NGST indicated that the logistics of transporting the full-scale spacecraft (size and mass issues) may favor JSC. Specific issues included the landing location for the C-5a aircraft (only vehicle capable of shipping the spacecraft), and subsequent movement from the airfield to the test facility. Initial studies indicated that a significant expense would be required to move overhead lines and provide adequate road support for transportation to Plum Brook. In addition, the cost of upgrading the clean room capability in the assembly and disassembly areas at Plum Brook would be significant, while JSC had already planned to undergo similar upgrades for the James Webb space telescope project.

There are two major vacuum chambers at JSC, Chamber A and Chamber B. Chamber A, shown in Figure 13-9, is the unit that was being considered as an alternative to Plum Brook Station. Chamber A has a working dimension of 16.7m (55 ft) in diameter and 27m (90 ft) tall, and it has a main access door 12m (40 ft) in diameter as seen in the illustrations. It can support a test article weight of 68,100 kg (150,000 lbs).






NASA JSC TV Chamber A

**Figure 13-9: Illustrations of JSC Vacuum Chamber A**

## 13.4 NRPCT Component Development and Integrated Test Plan

The Project Prometheus space reactor program required an extensive number of test programs for development and qualification of the reactor plant design. To track these test programs and monitor their progress towards qualification and delivery of the flight space reactor, a single, comprehensive test index was constructed. This index included all the technical disciplines (i.e., materials, plant, safety, I&C, etc.) required to deliver the final flight unit.

The NRPCT submitted the test index to Naval Reactors for approval of the format and content only, via Reference 13-1. Technical and funding approval of individual tests would be requested separately, as needed, to support specific Project Prometheus development and qualification efforts.

Table 13-4 provides the final version of the space reactor program test index. It incorporates NR comments provided in Reference 13-2, as well as NRPCT-initiated revisions made since the original document was issued. At the time of project termination, most of the test programs were still in the conceptual stage. Therefore, the test index should be viewed as a work-in-progress at the time of project termination. The index is organized into the following eight sections:

1. Reactor Component Development Testing (non-nuclear)
2. Plant Component Development Testing
3. Materials Development Testing
4. Instrumentation and Control System Development Testing
5. Integrated System Testing
6. Fueled Reactor Testing
7. Assembly, Test and Launch Operation (ATLO) Testing
8. Reactor Safety Testing

Additional background and testing details may be found in the individual test plan documents (References 13-1, 13-2, 13-3, 13-4, 13-5, 13-6, and 13-20).

Table 13-2 provides additional descriptions of the abbreviated test index column headings. Table 13-3 provides a test numbering system to uniquely identify and track each of the test programs. The system categorizes each test by its key discipline (sections 1-8 shown above), type of test, sequential test number, and test location.

**Table 13-2: Description of Test Index Column Headings**

| Column | Description |
|---|---|
| Test Program | Title of the test program. |
| Test ID | A descriptive test number to uniquely identify each test. The serialization format is provided in Table 13-3. |
| Objective | Self-explanatory. |
| Lead Test Sponsor | The lead NRPCT technical organization. |
| Test Location & Date | Test dates refer to either the test start date or an estimated start and completion date. |
| Test Specification Approval and Concurrence Authority | The organizations required to concur with and approve each test.<br>Concurrence – Agreement with the test concept.<br>Approval – Officially allowing the test to proceed. |
| NR Approval of Test Resume | Essentially all tests require NR technical and funding approval because of the magnitude or significance of the testing (with a few exceptions). The typical NRPCT method of obtaining test approval is by submittal of a test resume or test proposal. |
| Estimated Cost | The estimated costs for the tests were generally not well established. A few rough order-of-magnitude (ROM) cost estimates were included for information, but more formal estimates are recommended. Detailed cost estimates were to be included in the individual test program technical and funding approval requests. The ROM includes M&S charges for hardware and subcontracts to perform the work, but does not include:<br>• NRPCT labor costs.<br>• Facility costs to perform the tests, unless those costs are solely for the purpose of performing that specific test. |
| Comments / Design Basis | Self-explanatory. |

## Table 13-3: Test Identification Numbering System

| Section – Subsection – Number & Test Location (example: P-GC-1V) | | | | | | |
|---|---|---|---|---|---|---|
| Section | | Subsection | | Test Number | Test Location | |
| AT | ATLO | ACU | Acoustic | Sequential (as assigned) | A | Ames Research Center |
| F | Fueled | ALT | Alternator | | B | Bettis Laboratory |
| IC | I & C | BRY | Brayton Unit | | C | Kennedy Space Center |
| M | Materials | CDM | Control Drive Mechanism | | F | Foreign |
| P | Plant | CL | Cladding | | G | NASA Glenn Research Center |
| R | Reactor | CMP | Component | | H | Hamilton Sundstrand |
| S | Safety | EM | Engineering Model | | I | Idaho National Laboratory |
| SY | Integrated System | EMC | Electromagnetic Compatibility | | J | Jet Propulsion Laboratory |
| | | ENV | Environmental | | K | KAPL |
| | | FNC | Functional | | L | Los Alamos National Laboratory |
| | | FS | Fuel System | | M | NASA Marshall Space Flight Center |
| | | GC | Gas Cooler | | N | Northrop Grumman Space Park |
| | | GL | Gas Leakage | | O | Oak Ridge National Laboratory |
| | | GTR | Ground Test Reactor | | P | NASA Plum Brook Station |
| | | IMP | Impact | | R | Reactor Module Integration Facility |
| | | MD | Mechanical Design | | S | Sandia National Laboratories |
| | | PHY | Physics | | V | Vendor |
| | | PIP | Piping | | X | The core vendor |
| | | QM | Qualification Model | | Z | Physics Test Site |
| | | RCP | Recuperator | | | |
| | | SH | Shielding | | | |
| | | SHK | Shock | | | |
| | | STM | Static Test Model | | | |
| | | TH | Thermal Hydraulics | | | |
| | | TTM | Thermal Test Model | | | |
| | | TV | Thermal Vacuum | | | |
| | | VIB | Vibration | | | |
| | | VLV | Valves | | | |

Table 13-4: Project Prometheus Integrated Test Index

| 1. REACTOR COMPONENT DEVELOPMENT TESTING (NON-NUCLEAR) | | | | | | | | |
|---|---|---|---|---|---|---|---|---|
| **Test Program** | **Test ID** | **Objective** | **Lead Test Sponsor** | **Test Location & Dates** | **Test Spec. Appvl & Concur Authority** | **NR Approval of Test Resume** | **Estimated Cost** | **Comments / Design Basis** |
| **Reactor Thermal Hydraulic Tests** | | | | | | | | |
| REACTOR CORE MOCKUP HEATER DEVELOPMENT | R-TH-1M | • Develop high temperature heater elements to simulate nuclear fuel elements<br>• Assess heater element material compatibility with He/Xe<br>• Demonstrate heater capability | KAPL | MSFC<br>Q4, 2004 | Bettis Concur<br>MSFC Concur | Yes | $2.5M via NASA Funding | This test program extends previous MSFC work on electrical heater development. Key development issues include smaller diameter heaters, compatibility with refractory metal cladding, and axial profile simulation.<br>This test program was approved by l#04-03700 dated 11/4/04. |
| ACRYLIC VESSEL TEST | R-TH-2B | • Cold testing for qualitative flow visualization<br>• Evaluate flow stability in downcomer and inlet plenum<br>• Assess flow distribution at core inlet<br>• Assess sensitivities to vessel, nozzles, piping, downcomer, and plena geometry. | KAPL | Bettis<br>Q1-Q3, 2006 | TBD<br>Bettis Concur | Yes | $100K | Cold test designed with flexibility to accommodate various geometry changes. Air and potential water testing, dyes and tell-tales for visualization. |
| SINGLE CHANNEL HEAT TRANSFER TEST PHASE 1 | R-TH-3M | • Investigate Low Pr # affects on heat transfer correlations<br>• Investigate hydraulic diameter affects on heat transfer correlations<br>• Evaluate internal flow (annular tubes)<br>• Perform temperature, flow, gas mixture, and pressure sensitivities | KAPL | MSFC<br>Q4, 2005 | Bettis Concur<br>MSFC Concur | Yes | $550K via NASA Funding | Modification of a previous single channel test performed by MSFC. Heated test.<br>The initial test specification was provided in SPP-67410-0009, dated 7/7/2005. Phase 1 was to use some existing MSFC equipment (compressor, loop, etc.). If a new loop must be built, add<br>$200-400K to test cost. |
| SINGLE CHANNEL HEAT TRANSFER TEST PHASE 2 | R-TH-4V | • Continuation of R-TH-3M<br>• Evaluate pre-conceptual core geometry<br>• Support development of new heat transfer correlation<br>• He-Xe testing | KAPL | Vendor<br>Q3, 2005 to Q3, 2006 | TBD<br>Bettis Concur | Yes | TBD | Heated tests of various core geometries being considered for reactor applications. |
| ACRYLIC REACTOR MOCKUP #1 | R-TH-5 | • Evaluate geometry sensitivities for core (fueled region)<br>• Visualize flow distributions at inlet and outlet of core<br>• Measure inlet and outlet pressure drop loss coefficients<br>• Provide test data for analysis qualification<br>• Scoping to prepare for future core models | KAPL | KAPL<br>Q3, 2006 | TBD<br>Bettis Concur | Yes | TBD | Cold test. |
| ACRYLIC REACTOR MOCKUP #2 | R-TH-6 | • Evaluate geometry sensitivities for core (fueled region)<br>• Measure core flow distribution<br>• Measure inlet and outlet pressure drop loss coefficients<br>• Provide test data for analysis qualification | KAPL | KAPL<br>FY07 | TBD<br>Bettis Concur | Yes | TBD | Cold test. |
| NOZZLE TEST | R-TH-7 | • Evaluate nozzle options under consideration | KAPL | KAPL, Bettis or Vendor | TBD | Yes | TBD | Cold test. |

## 1. REACTOR COMPONENT DEVELOPMENT TESTING (NON-NUCLEAR)

| Test Program | Test ID | Objective | Lead Test Sponsor | Test Location & Dates | Test Spec. Appvl & Concur Authority | NR Approval of Test Resume | Estimated Cost | Comments / Design Basis |
|---|---|---|---|---|---|---|---|---|
| | | • Measure nozzle pressure drop loss coefficients<br>• Provide test data for CFD qualification | | FY07 | Bettis Concur | | | |
| VESSEL/THIMBLE COOLING TEST | R-TH-8V | • Evaluate mechanisms for ensuring proper cooling of vessel and thimble<br>• Measure flow past thimble<br>• Verify heat transfer coefficients on vessel and thimble walls | KAPL | KAPL, Bettis or Vendor<br>FY07 | TBD<br>Bettis Concur | Yes | TBD | Heated test using prototypic materials chosen during the pre-conceptual design phase. |
| ACRYLIC SINGLE CHANNEL/MODULE TEST | R-TH-9 | • Provide test data for hydraulic model qualification<br>• Evaluate alternatives for inlet and exit geometries<br>• Flow visualization of channel inlet and exit to ensure stable flow patterns | KAPL | KAPL | TBD<br>Bettis Concur | Yes | TBD | Cold test. |
| GAP HEAT TRANSFER TEST | R-TH-10 | • Obtain heat transfer data between the fuel pellet and the clad liner (heated test). | KAPL | KAPL, Bettis or Vendor<br>FY07 or later | TBD<br>Bettis Concur | Yes | TBD | Provides data for qualification of radiative heat transfer models used in fuel element design. |
| RIB AND WIRE WRAP TEST | R-TH-11V | • Evaluate impact of various rib and wire wrapping options on heat transfer, flow mixing, and pressure drop<br>• Test will be based on geometry from September 2005 downselect | KAPL | Vendor<br>FY07 | TBD<br>Bettis Concur | Yes | TBD | Heated tests. This test may be part of the Single Channel Test Program |
| SINGLE CHANNEL HEAT TRANSFER TEST PHASE 3 | R-TH-12V | • Continuation of R-TH-4V<br>• Final test data to support design heat transfer correlation<br>• Prototypic geometry<br>• Measure prototypic frictional pressure drop<br>• Off-nominal sensitivity studies (e.g., eccentricity)<br>• Investigate multiple power distributions | KAPL | Vendor<br>FY07 | TBD<br>Bettis Concur | Yes | TBD | Heated test. Work will be performed at University, National Lab, or NASA facility. |
| ORIFICE TEST | R-TH-13 | • Prototypic measurement of pressure drop loss coefficient<br>• Investigate different orifice designs | KAPL | KAPL or Bettis<br>FY07 or later | TBD<br>Bettis Concur | Yes | TBD | Heated test. |
| **Reactor Mechanical Design Tests** | | | | | | | | |
| **COMPONENT DEVELOPMENT TESTS – Provides data to support fabrication, function, and fit to demonstrate acceptability of the component** | | | | | | | | |
| REACTOR FUEL RETENTION TEST | R-MD-1B | Evaluate various concepts for maintaining compressive forces on the fuel pellets during launch and service loads. Thermal growth and swelling of the fuel pellets must be evaluated. | Bettis | Bettis<br>FY06 | TBD<br>KAPL Concur | Yes | TBD | Surrogate materials shall be used for fuel and refractory metals.<br>• launch loads (cold)<br>• operating conditions (hot) |
| REFLECTOR BEARING AND BEARING | R-MD-2G | Evaluate the friction and wear characteristics of candidate moveable reflectors (slider / rods, drums / bushings). Test various | Bettis | GRC | TBD | Yes | TBD | • friction forces (static and dynamic) |

| 1. REACTOR COMPONENT DEVELOPMENT TESTING (NON-NUCLEAR) | | | | | | | | |
|---|---|---|---|---|---|---|---|---|
| **Test Program** | **Test ID** | **Objective** | **Lead Test Sponsor** | **Test Location & Dates** | **Test Spec. Appvl & Concur Authority** | **NR Approval of Test Resume** | **Estimated Cost** | **Comments / Design Basis** |
| SURFACE LIFE TEST | | combinations of candidate materials. | | FY06-07 | KAPL Concur | | | • wear characteristics<br>• design life cycles<br>• metal diffusion |
| REFLECTOR BEARING AND LINKAGE TEST | R-MD-3B | Evaluate various concepts for bearings and linkages to develop a system capable of providing the required positioning accuracy. | Bettis | Bettis<br>FY06-07 | TBD<br>KAPL Concur | No | TBD | Smoothness of operation / backlash / springback |
| SAFETY ROD AND REFLECTOR LOCKING BLOCK EJECTION TEST | R-MD-4B | Evaluate various concepts for ejecting the safety rod and the reflector locking blocks. | Bettis | Bettis<br>FY06-07 | TBD<br>KAPL Concur | No | TBD | This test may be performed in conjunction with a CDM test. |
| REACTOR CORE SUBASSEMBLY FLOW INDUCED VIBRATION | R-MD-5B | Evaluate the flow induced vibrations of a reactor core subassembly when subjected to flow. As a minimum, a single module (one fuel pin/assembly and flow channel) shall be used. Measure strain & accelerations, and characterize mechanical interactions such as wear and scuffing. | Bettis | Bettis<br>FY07 | TBD<br>KAPL Concur | Yes | TBD | Surrogate materials shall be used for fuel and refractory metals. Significant thermal hydraulic support will be required. The dual Brayton loop from Test P-BRY-7B may be usable for this test. |
| REACTOR CORE SUBASSEMBLY DYNAMIC TEST | R-MD-6B | Evaluate the dynamic response of a reactor core subassembly when subjected to launch loads and service loads. As a minimum, a single fuel pin/assembly shall be used. Measure strain & accelerations, and characterize mechanical interactions such as wear and scuffing. | Bettis | Bettis<br>FY07 | TBD<br>KAPL Concur | Yes | TBD | Surrogate materials shall be used for fuel and refractory metals.<br>Hardware from R-MD-5B may be usable for this test. |
| REFLECTOR ASSEMBLY DYNAMIC TEST (SLIDER OR DRUM) | R-MD-7 | Evaluate the dynamic response of a reflector assembly when exposed to launch and service loads. | Bettis | Bettis/SNL<br>FY07 | TBD<br>KAPL Concur | Yes | TBD | • loads greater than design loads may be considered to evaluate margin<br>• pulverizing of reflector material<br>• cracking<br>• distortion |
| REACTOR VESSEL AND REFLECTOR DYNAMIC TEST | R-MD-8B | Evaluate the dynamic response of the reactor vessel and reflector assembly when subjected to launch loads and service loads. Measure strain & accelerations, and characterize mechanical interactions such as wear and scuffing. | Bettis | Bettis<br>FY07 | TBD<br>KAPL Concur | Yes | TBD | Surrogate materials shall be used for fuel, reflector material, and refractory metals.<br>• loads greater than design loads may be considered to evaluate margin<br>• cantilevered System<br>• distortion<br>• reflector movement / locking blocks |
| REACTOR ASSEMBLY THERMAL EXPANSION TEST | R-MD-9V | Evaluate the thermal response of the reactor assembly parts. Measure displacements and distortions and evaluate the effect on fit-up and function of all components. | Bettis | Vendor<br>FY09 | TBD<br>KAPL Concur | Yes | TBD | This test may be conducted using the hardware fabricated for the reactor module shock, vibration and acoustic test (SY-ENV-1V). |

| 1. REACTOR COMPONENT DEVELOPMENT TESTING (NON-NUCLEAR) | | | | | | | | |
|---|---|---|---|---|---|---|---|---|
| **Test Program** | **Test ID** | **Objective** | **Lead Test Sponsor** | **Test Location & Dates** | **Test Spec. Appvl & Concur Authority** | **NR Approval of Test Resume** | **Estimated Cost** | **Comments / Design Basis** |
| **COMPONENT QUALIFICATION TESTS – Demonstrate that the components meet specified req't's.** | | | | | | | | |
| REFLECTOR BEARING & LINKAGE FLEXIBILITY TEST | R-QM-1B | Demonstrate the suitability of the motion control in the mechanism (slider or drum) linkage and qualify the system. | Bettis | Bettis FY08 | TBD KAPL Concur | Yes | TBD | Smoothness of operation / Backlash / Spring back |
| AEROSHELL INTERFACE AND EJECTION TEST | R-QM-2V | Demonstrate that the reflector locking blocks, the safety rod, and the Aeroshell can be safely ejected and qualify the system design. | Bettis | Vendor FY07-08 | TBD KAPL Concur | Yes | TBD | |
| **Shielding** | | | | | | | | |
| BULK SHIELD BENCHMARK TEST | R-SH-1V | Measure integral and discrete (energy, scatter angle) neutron/gamma flux levels emanating from interactions with the candidate bulk shielding materials and shield stack-up configurations. Test data will also be obtained to benchmark the Genetic Algorithms currently being applied to derive the optimum bulk shield configuration. | Bettis | Vendor FY07 | TBD KAPL Concur | Yes | TBD | Perform testing to benchmark the method uncertainty factor(s) needed to cover uncertainties in the applied coupled neutron/gamma radiation transport computational tool and neutron cross section library. |
| RADIATION STREAMING BENCHMARK TEST | R-SH-2V | Measure integral and discrete neutron/gamma flux levels due to radiation streaming through expected shield penetration types. The performance of local shielding and/or shield caps will be included in the testing, where needed. | Bettis | Vendor FY07 | TBD KAPL Concur | Yes | TBD | ORNL was chartered to perform sensitivity analyses by August 2005 in evaluating importance of neutron cross-section uncertainty on shield design requirements. These results will be folded into the two tests described below. |
| NI RESPONSE TEST | R-SH-3V | Measure the absolute NI detector response for a representative shield configuration with the nuclear instrumentation system installed. Radiation transport predictions of the absolute NI response for the tested configuration will be performed prior to the test for overall planning purposes. | Bettis | Vendor FY07 | TBD KAPL Concur | Yes | TBD | Perform testing to benchmark the radiation transport computational tool being applied for predicting Nuclear Instrument Response. |
| NI RADIATION THRESHOLD TEST | R-SH-4V | Measure the threshold at which gamma and secondary radiation effects are important from a signal/noise standpoint with respect to NI detector response. | Bettis | Vendor FY07 | TBD KAPL Concur | Yes | TBD | |
| SPACE RADIATION ENVIRONMENT TEST | R-SH-5V | Measure the integral neutron flux levels due to heavy charged particle and electron interactions with the shield materials and/or support structure. The evaluation of the appropriate facility for this test would be a high priority item. | Bettis | Vendor FY07 | TBD KAPL Concur | Yes | TBD | Perform testing to benchmark computational predictions of neutron generation predictions due to interactions of high energy charged particles with the shield system. |
| PROTOTYPE SHIELD TEST | R-SH-6V | Perform gamma/neutron dose rate measurements outside the Prototype / GTR facility and compare test results to maximum allowed radiation levels. | Bettis | Vendor FY14 | TBD KAPL Concur | Yes | TBD | Perform shield testing on Prototype / Zero Ground Test Reactor facility to confirm all radiation level limits are satisfied for reactor |

## 1. REACTOR COMPONENT DEVELOPMENT TESTING (NON-NUCLEAR)

| Test Program | Test ID | Objective | Lead Test Sponsor | Test Location & Dates | Test Spec. Appvl & Concur Authority | NR Approval of Test Resume | Estimated Cost | Comments / Design Basis |
|---|---|---|---|---|---|---|---|---|
| SPACE SHIELD MOCK-UP TEST | R-SH-7V | Perform gamma/neutron integral measurements on a space reactor shield mock-up, to be installed with the GTR, to obtain a database to confirm computational model predictions of the Flight Reactor shield. | Bettis | Vendor<br>FY14 | TBD<br>KAPL Concur | Yes | TBD | operations and enhance the data base. |
| **Control Drive Mechanism Tests** | | | | | | | | |
| CDM COMPONENT DEVELOPMENT TESTS – Provide data to understand how each component functions, identify areas that do not meet requirements and require re-design, and in the end demonstrate acceptability of the component. | | | | | | | | |
| BEARING DEVELOPMENT TESTS | R-CDM-1 | Test rig testing of: rolling element bearings, ball nuts, and sliding bearings.<br>• Develop, test, and determine bearing designs capable of meeting the CDM requirements. | Bettis | TBD<br>Q1, 2006 to Q4, 2007 | TBD<br>KAPL Concur | Yes | $200K | The bearing test rig requires a high temperature vacuum chamber. If one is not available at a NASA center or national lab, one can be created at Bettis. |
| MOTOR DEVELOPMENT TESTS | R-CDM-2 | Test rig testing of rotating and linear stepper motors.<br>• Develop, characterize, test, and determine the motor type.<br>• Provide early data on torque or force output performance.<br>• Motor shock and vibration tests.<br>• Motor off-gassing tests. | Bettis | TBD<br>Q1-Q4, 2006 | TBD<br>KAPL Concur | Yes | $100K | Basic operating tests can be conducted in air.<br><br>Testing in a high temperature vacuum environment anticipated on the reactor is also required. |
| MOTOR QUALIFICATION TESTS | R-CDM-3 | A stand alone test of the motor in a test rig.<br>• Ensure motor meets requirements.<br>• Determine motor performance characteristics.<br>• Demonstrate acceptable torque or force output performance in the space environment.<br>• Determine motor shock and vibration capability. | Bettis | TBD<br>Q1, 2007 to Q4, 2008 | TBD<br>KAPL Concur | Yes | $200K | |
| BRAKE DEVELOPMENT TESTS | R-CDM-4 | Test rig testing<br>• Develop, test, and determine brake designs. | Bettis | TBD<br>Q1-Q4, 2006 | TBD<br>KAPL Concur | Yes | $100K | |
| CDM SCRAM OR FI DEVELOPMENT | R-CDM-5 | Bench testing and test rig testing<br>• The ground test CDM requires either a scram or FI capability for safety. The flight unit may require scram or FI capability if criticality is required before launch.<br>• Develop and test the scram or FI capability of the CDM. | Bettis | TBD<br>Q1-Q4, 2006 | TBD<br>KAPL Concur | Yes | $100K | |
| SAFETY ROD CDM COMPONENT DEVELOPMENT | R-CDM-6 | Bench testing and test rig testing<br>• Develop and test the features needed for the safety rod CDM.<br>• The ground test safety rod will be required to scram. | Bettis | TBD<br>Q1-Q4, 2006 | TBD<br>KAPL Concur | Yes | $100K | |

## 1. REACTOR COMPONENT DEVELOPMENT TESTING (NON-NUCLEAR)

| Test Program | Test ID | Objective | Lead Test Sponsor | Test Location & Dates | Test Spec. Appvl & Concur Authority | NR Approval of Test Resume | Estimated Cost | Comments / Design Basis |
|---|---|---|---|---|---|---|---|---|
| CONTROL ELEMENT SAFETY LOCK DEVELOPMENT | R-CDM-7 | Bench testing<br>• Locks and components may be required to prevent control element and safety rod movement until desired. | Bettis | TBD<br>Q1-Q4, 2006 | TBD<br>KAPL Concur | Yes | $100K | |
| FASTENER AND LOCKING DEVICE TESTS | R-CDM-8 | Bench testing<br>• Determine the preload for threaded fasteners.<br>• Demonstrate adequate holding capability of locking devices. | Bettis | TBD<br>Q1-Q2, 2007 | TBD<br>KAPL Concur | Yes | $50K | |
| CDM DEVELOPMENT UNIT TESTS – Provide early data on the performance of the CDM to identify areas requiring changes, understand performance, and develop testing methods. | | | | | | | | |
| GROUND TEST CDM DEVELOPMENT UNIT TESTS | R-CDM-9 | Test rig testing<br>• Measure performance in critical areas such as rod motion characteristics, force output, performance in air and in the space environment, and thermal performance.<br>• Mini-life test, as required<br>• Power supply compatibility, if required<br>• Position indicator performance, if required<br>• Shock and vibration tests<br>• Scram and/or safety locks, as required. | Bettis | TBD<br>Q3, 2006 to Q4, 2007 | TBD<br>KAPL Concur | Yes | $ 1.1M | Basic operating tests can be conducted in air.<br>Testing in a high temperature vacuum environment anticipated on the reactor is also required.<br>Bettis has shock and vibration test rigs that may be acceptable for transportation shock testing (in air). |
| GROUND TEST SAFETY ROD CDM DEVELOPMENT UNIT TESTS | R-CDM-10 | | Bettis | TBD<br>Q3, 2006 to Q4, 2007 | TBD<br>KAPL Concur | Yes | $ 1.5M | |
| FLIGHT UNIT CDM DEVELOPMENT UNIT TESTS | R-CDM-11 | | Bettis | TBD<br>Q1, 2007 to Q2, 2008 | TBD<br>KAPL Concur | Yes | $ 1.2M | |
| FLIGHT UNIT SAFETY ROD CDM DEVELOPMENT UNIT TESTS | R-CDM-12 | | Bettis | TBD<br>Q1, 2007 to Q2, 2008 | TBD<br>KAPL Concur | Yes | $600K | |
| CDM QUALIFICATION UNIT TESTS – Demonstrates that the CDM meets the specified requirements. Qualification testing is performed before any CDMs are assembled into a reactor or reactor test bed. | | | | | | | | |
| GROUND TEST CDM QUALIFICATION UNIT TESTS | R-CDM-13 | Test rig testing<br>• Demonstrate performance in critical areas such as rod motion characteristics, force output, performance in the space environment, and thermal performance.<br>• Demonstrate lifetime wear capability. N/A for safety rod.<br>• Demonstrate power supply compatibility, if required.<br>• Demonstrate acceptable position indicator performance, if required.<br>• Demonstrate acceptability under shock and vibration conditions.<br>• Demonstrate scram and/or safety locks as required. | Bettis | TBD<br>Q1-Q4, 2008 | TBD<br>KAPL Concur | Yes | $ 2.1M | Basic operating tests can be conducted in air. Testing in the space environment is also required.<br>These tests require a high temperature vacuum chamber. If one is not available at a NASA center or national lab, one can be created at Bettis.<br>Bettis has shock and vibration test rigs that may be acceptable for transportation shock testing (in air). |
| GROUND TEST SAFETY ROD CDM QUALIFICATION UNIT TESTS | R-CDM-14 | | Bettis | TBD<br>Q1-Q4, 2008 | TBD<br>KAPL Concur | Yes | $ 2.5M | |

| 1. REACTOR COMPONENT DEVELOPMENT TESTING (NON-NUCLEAR) | | | | | | | | |
|---|---|---|---|---|---|---|---|---|
| **Test Program** | **Test ID** | **Objective** | **Lead Test Sponsor** | **Test Location & Dates** | **Test Spec. Appvl & Concur Authority** | **NR Approval of Test Resume** | **Estimated Cost** | **Comments / Design Basis** |
| FLIGHT UNIT CDM QUALIFICATION UNIT TESTS | R-CDM-15 | | Bettis | TBD<br>Q2, 2008 to Q2, 2010 | TBD<br>KAPL Concur | Yes | $ 3.4M | |
| FLIGHT UNIT SAFETY ROD CDM QUALIFICATION UNIT TESTS | R-CDM-16 | | Bettis | TBD<br>Q2, 2008 to Q2, 2010 | TBD<br>KAPL Concur | Yes | $ 2.6M | |
| JPL SUBSYSTEM / ASSEMBLY ENVIRONMENTAL TESTING | | | | | | | | |
| ENVIRONMENTAL | Various | Validates that the QM and Flight hardware components can withstand the environments to which they will be subjected. Tests include:<br>• thermal vacuum<br>• random vibration<br>• pyro-shock<br>• structural loads<br>• magnetics<br>• radiated emisions<br>• conducted emissions<br>• grounding / isolation | Various | Various | NR Approval<br>JPL Approval<br>NRPCT Concur<br>NGST Concur<br>Test Site Concur | Yes | TBD | Refer to the test requirements in Table JPL 2.1-2a of Environmental Requirements Document |

## 2. PLANT COMPONENT DEVELOPMENT TESTING

| Test Program | Test ID | Objective | Lead Test Sponsor | Test Location & Dates | Test Spec. Appvl & Concur Authority | NR Approval of Test Resume | Estimated Cost | Comments / Design Basis |
|---|---|---|---|---|---|---|---|---|
| BRAYTON SYSTEM DEVELOPMENT | | | | | | | | |
| OPEN-LOOP BRAYTON SYSTEM | P-BRY-1K<br>P-BRY-1B | • increase design awareness and gain practical operating experience<br>• assess over-speed capabilities<br>• obtain a better understanding of failure mechanisms through destructive evaluation | KAPL | KAPL<br><br>Q4, 2005<br>to<br>Q4, 2006 | TBD<br><br>Bettis Concur | Yes | $200K | This test program uses commercially available Capstone C30 microturbines. The Capstone C30 is an open-loop, combustion fired Brayton system that has features common to the envisioned Prometheus energy conversion system. These 30-kW stand-alone units include turbine-compressor-alternators similar in configuration to the Hamilton Sundstrand conceptual design. They also have air foil bearings and a complete control system to regulate startup and operation.<br><br>This test program was approved by E#05-01782, dated 5/13/05. |
| DIRECT DRIVE GAS (DDG) REACTOR-MOCKUP + SINGLE BRAYTON CLOSED-LOOP SYSTEM | P-BRY-2M | • obtain test data to support plant model qualification<br>• characterize system response to normal / abnormal operating transients (e.g., startup, heatup, cooldown, shutdown)<br>• identify and resolve potential integration issues through hardware based testing<br>• assess reactivity feedback coefficients and their impact on system operation and flow<br>• develop and validate system sensing and control methods | Bettis | MSFC<br>DDG alone:<br>Q3-Q4, 2005<br><br>Integrated:<br>Q1, 2006<br>to<br>Q2, 2007 | KAPL Concur<br>MSFC Concur | Yes | $4M<br><br>(NASA Funding) | This test program couples the Direct Drive Gas (DDG) Reactor Mockup, previously tested as part of MSFC's earlier work on gas-cooled reactors, with the closed-loop modified Capstone Brayton system built by Barber-Nichols under contract with Sandia National Laboratories.<br><br>This test program was approved by E#05-01782, dated 5/13/05. |
| ALTERNATOR TEST UNIT (ATU) STAND WITH 100-kW, HAMILTON SUNDSTRAND ALTERNATOR | P-ALT-3G | • alternator loss modeling<br>• evaluate alternator scale-up and integration issues<br>• investigate overspeed accidents | KAPL | GRC<br><br>Q4, 2005<br>to<br>Q1, 2008 | TBD<br><br>Bettis Concur | Yes | $700K<br><br>(NASA Funding) | These tests are directly funded by NASA, with NRPCT guidance on scope and cost. |
| BEARING DEVELOPMENT | P-BRY-3G | • develop and verify bearing designs<br>• rotor dynamic analysis<br>• high pressure test rig<br>• mock rotor test rig<br>• capstone testing<br>• destructive and life testing | KAPL | GRC<br><br>Q3, 2006 | TBD<br><br>Bettis Concur | Yes | $1.3M<br><br>(NASA Funding) | |

## 2. PLANT COMPONENT DEVELOPMENT TESTING

| Test Program | Test ID | Objective | Lead Test Sponsor | Test Location & Dates | Test Spec. Appvl & Concur Authority | NR Approval of Test Resume | Estimated Cost | Comments / Design Basis |
|---|---|---|---|---|---|---|---|---|
| MINI-BRU | P-BRY-4G | • characterize system response to normal/abnormal operating transients (e.g., startup, heatup, cooldown, shutdown)<br>• assess Parasitic Load Radiator (PLR) response<br>• investigate failure mechanisms and nozzle/blade erosion | KAPL | GRC<br>Q1, 2005 to Q1, 2006 | TBD<br>Bettis Concur | Yes | $600K<br>(NASA Funding) | This test program is a continuation of ongoing GRC Brayton testing using the Mini-BRU unit originally developed in the 1970s. This testing will continue until the first generation Energy Conversion System (ECS) Thermal Test Model (TTM) is delivered. |
| HEAT EXCHANGER (RECUPERATOR MATERIAL TESTING) | P-RCP-1K | • lab preparation<br>• mini-BRU recuperator testing<br>• All comp recuperator testing | KAPL | GRC<br>Q3, 2007 | TBD<br>Bettis Concur | Yes | $600K<br>(NASA Funding) | |
| PROTOTYPIC BRAYTON ROTATING UNIT AND RECUPERATOR | P-BRY-6H | • evaluate selected design parameters for design improvements<br>• assess soundness of fabrication and compressor performance (pressure head, flow, efficiency) during startup, thermal cycling, and accelerated life testing<br>• perform leak checks (He/Xe)<br>• evaluate turbine wheel creep at operating temperature<br>• demonstrate reliable gas foil bearing design<br>• investigate failure mechanisms<br>• evaluate potential shock and vibration issues<br>• obtain test data to support plant model qualification<br>• determine flow distribution<br>• thermal/hydraulic performance (pressure drop and effectiveness) | KAPL | Vendor/GRC<br>Q3, 2007 to Q1, 2008 | Bettis Concur | Yes | $10M | This detailed design and development effort enables delivery of the first generation ECS-TTM (SY-TTM-1G) hardware.<br><br>This test program was approved by E#05-01782, dated 5/13/05. |
| | | • Phase 1 – Conceptual Design (no testing)<br>• Phase 2 – Final Design. Qualification testing of materials & sub-components. | | Vendor<br>Q2-Q3, 2006 | TBD<br>Bettis Concur | Yes | | |
| | | • Phase 3 - Fabrication / Assembly / Verification Testing | | Vendor<br>Q4, 2006 to Q1, 2007 | TBD<br>Bettis Concur | Yes | | |
| | | • Phase 4 - Performance Testing (normal, off-design) | | GRC<br>Q2, 2007 to Q1, 2008 | TBD<br>Bettis Concur | Yes | | |

## 2. PLANT COMPONENT DEVELOPMENT TESTING

| Test Program | Test ID | Objective | Lead Test Sponsor | Test Location & Dates | Test Spec. Appvl & Concur Authority | NR Approval of Test Resume | Estimated Cost | Comments / Design Basis |
|---|---|---|---|---|---|---|---|---|
| DUAL CLOSED BRAYTON LOOP | P-BRY-7B | Dual Closed Brayton Loop System<br>• increase design awareness & gain practical operating experience<br>• evaluate system response to normal / abnormal operating transients (startup, heat-up, cool down, shutdown, operating each unit at a different speed, simultaneously varying speed on both units, shutdown of one unit while other unit operates)<br>• develop and validate system sensing and control methods<br>• obtain test data to support plant model benchmarking<br>• evaluate proof-of-concept hardware and auxiliary equipment, including heat exchangers, valves, and pipe-in-pipe concepts | Bettis | Bettis<br>Q2, 2006 to Q1, 2009 | KAPL Concur | Yes | $820K | This test loop employs two Capstone C30 microturbines modified for closed-cycle use, similar to the single modified Capstone closed-loop built for Sandia National Laboratories and used in Test P-BRY-2M. The Braytons operate in parallel. Each loop contains a gas cooler and valve. A common heater with a common flow path is shared by both loops.<br><br>This test program was approved by E#05-01782 dated 5/13/05. The NRPCT contract has been canceled, but NASA Glenn intends to initiate a new contract with Barber-Nichols to complete the test loop. |
| GAS COOLER DEVELOPMENT (He/Xe to Water) | P-GC-1V | • Phase 2 – Stand alone testing<br>o Heat transfer testing<br>• Thermal cycling<br>• T&H performance vs. design requirements<br>• Pressure Drop<br>• Flow Distribution<br>o Mechanical testing<br>• Shock<br>• Vibration<br>o He/Xe leakage<br>o Component integration into system testing<br>• TTM Generation Testing | Bettis | Vendor or Bettis<br>Q1-Q3, 2007 | KAPL Concur<br>BPMI Concur | Yes | $500K | This test program was approved by E#05-01782 dated 5/13/05. |
| | | • Phase 3<br>o Testing of any design and/or fabrication modifications<br>o Component integration into system testing<br>• EM Generation Testing<br>• QM Generation Testing | | Vendor<br>Q3, 2007 to Q3, 2017 | KAPL Concur<br>BPMI Concur | Yes | $2M | |
| VALVE DEVELOPMENT | P-VLV-1 | Test valve actuator electrical components and control | BPMI | TBD | Bettis Concur<br>KAPL Concur | Yes | TBD | |
| PIPE DEVELOPMENT | P-PIP-1B | Hot leg piping test – This test evaluates the manufacturability and survivability of the recommended hot leg piping concept. The test evaluates issues such as incorporation of ceramic insulating material into pipe bends and the effects that thermal cycling will have on long term integrity. | Bettis | Bettis / KAPL<br>Q2, 2006 to Q3, 2006 | KAPL Concur | Yes | $100K | |

| 2. PLANT COMPONENT DEVELOPMENT TESTING | | | | | | | | |
|---|---|---|---|---|---|---|---|---|
| **Test Program** | **Test ID** | **Objective** | **Lead Test Sponsor** | **Test Location & Dates** | **Test Spec. Appvl & Concur Authority** | **NR Approval of Test Resume** | **Estimated Cost** | **Comments / Design Basis** |
| GAS LEAKAGE | P-GL-1B | Hot Testing<br>• characterize gas leakage (molecular diffusion and leakage through microcracks).<br>• assess integrity of potted joints to shock and vibration loads (launch and operating)<br>• heat potted connections to 400K at 1MPa to assess integrity | Bettis | GRC<br>Q3, 2006 to Q4, 2006 | KAPL Concur | Yes | $500K | |
| JPL SUBSYSTEM / ASSEMBLY ENVIRONMENTAL TESTING | | | | | | | | |
| ENVIRONMENTAL | Various | Validates that the QM and Flight hardware can withstand the environments to which they will be subjected. Tests include:<br>• thermal vacuum<br>• random vibration<br>• pyro-shock<br>• structural loads<br>• magnetics<br>• radiated emisions<br>• conducted emissions<br>• grounding / isolation | Various | Various | NR Approval<br>JPL Approval<br>NRPCT Concur<br>NGST Concur<br>Test Site Concur | Yes | TBD | Refer to the test requirements in Table JPL 2.1-2a |

## 3. MATERIALS DEVELOPMENT TESTING

| Test Program | Test ID | Objective | Lead Test Sponsor | Test Location & Dates | Test Spec. Appvl & Concur Authority | NR Approval of Test Resume | Estimated Cost | Comments / Design Basis |
|---|---|---|---|---|---|---|---|---|
| **Materials Development Tests** | | | | | | | | |
| TBD | TBD | The Materials test plan was submitted via B-MT(SMAT)-005 / MDO-723-0019, dated April 4, 2005. Those tests include:<br>• Fuel<br>• Cladding and Core Structural Materials<br>• Plant and Energy Conversion Material Development<br>• Shield Material Development<br>• Reflector Material Development<br>• Sensor Technologies<br>Conversion of those tests into this tabular format was not completed at the time of project termination. | See B-MT(SMAT)-005 MDO-723-0019 | See B-MT(SMAT)-005 MDO-723-0019 | TBD | TBD | TBD | |
| **Other Materials Tests** | | | | | | | | |
| CDM MATERIALS DEVELOPMENT | M-CDM-1 | Materials Testing of: motor insulation, motor magnets, motor windings, sliding and roller bearing materials, bearing coatings or lubricants, and CDM materials subjected to radiation.<br>Identify, develop, and qualify materials for the CDM. This will be a coordinated effort with Materials Testing. | Bettis | TBD<br>Q1, 2006 to Q3, 2010 | TBD | Yes | $300K | Glenn Research Center, as well as other NASA centers, and JPL have material test facilities and expertise in mechanism tribology. |

| 4. INSTRUMENTATION AND CONTROL SYSTEM DEVELOPMENT TESTING | | | | | | | | |
|---|---|---|---|---|---|---|---|---|
| **Test Program** | **Test ID** | **Objective** | **Lead Test Sponsor** | **Test Location & Dates** | **Test Spec. Appvl & Concur Authority** | **NR Approval of Test Resume** | **Estimated Cost** | **Comments / Design Basis** |
| COMPONENT TESTING | IC-CMP-1V | Perform hardware, software, and materials testing to support development of individual components including sensors, instruments, control drives/motors, and control system components. | Bettis<br>KAPL<br>BPMI | Bettis, KAPL, Vendors, National Labs<br>Q3, 2005 to Q4, 2012 | NR Approval<br>NRPCT Concur | Yes | TBD | Estimated effort represents manpower required by NRPCT to perform in-house testing and manage contracts with non-NRPCT organizations involved in testing. A large portion of the manpower is for sensor element and materials testing. |
| NRPCT FUNCTIONAL TESTING | | | | | | | | |
| HARDWARE & SOFTWARE INTEGRATION | Various | Perform hardware/software integration and compatibility testing for the I&C systems. This testing is required for each I&C system being delivered for the following (there will be four major HW/SW integration test programs in total):<br>1. EM Test<br>2. QM Test<br>3. GTR<br>4. Prometheus 1 | KAPL | KAPL<br>Q3, 2007 to Q3, 2014 | NR Approval<br>Bettis Concur | Yes | TBD | Estimated effort represents manpower required to develop and execute test programs. |
| INTEGRATED SYSTEM TESTING & QUALIFICATION | Various | Perform I&C system software verification & validation and integrated system testing and qualification. This testing is required for each I&C systems being delivered for the following (there will be four major SW V&V / integrated systems testing and qualification programs in total):<br>1. EM Test<br>2. QM Test<br>3. GTR<br>4. Prometheus 1 | Bettis | Bettis<br>Q1, 2008 to Q2, 2015 | NR Approval<br>KAPL Concur | Yes | TBD | Estimated effort represents manpower required to develop and execute test programs. |
| JPL ENVIRONMENTAL TESTING | | | | | | | | |
| ENVIRONMENTAL | Various | Validates that the QM and Flight hardware components can withstand the environments to which they will be subjected. Testing includes:<br>• t/v, thermal balance<br>• acoustic<br>• pyro-shock<br>• modal<br>• structural loads<br>• magnetics<br>• radiated susceptibility<br>• radiated emissions<br>• EMC & ESD<br>• bonding / grounding | Various | Various | NR Approval<br>JPL Approval<br>NRPCT Concur<br>Test Site Concur | Yes | TBD | Refer to the test requirements in Table JPL 2.1-2a of the JPL Environmental Requirements Document |

## 5. INTEGRATED SYSTEM TESTING

| Test Program | Test ID | Objective | Lead Test Sponser | Test Location & Date | Test SPEC. Appvl & Concur Authority | NR Approval of Test Resume | Estimated Cost | Comments / Design Basis |
|---|---|---|---|---|---|---|---|---|
| **Developmental Testing** | | | | | | | | |
| ENERGY CONVERSION SYSTEM THERMAL TEST MODEL | SY-TTM-1G | First demonstration of a Brayton PCS used to fire an EP system<br><br>Additional Goals:<br>• characterize system response to normal/abnormal operating transients (e.g., startup, heatup, cool down, shutdown)<br>• assess recuperator and gas cooler performance<br>• validate He/Xe loop fill procedures<br>• determine loop integrity (perform leak checks)<br>• perform preliminary testing of available breadboard sensors<br>• obtain test data to support plant model qualification | KAPL | GRC<br><br>Q4, 2007 | Battis Concur<br>NGST Concur<br>JPL Concur<br>GRC Concur | Yes | > $5M | This is a first-generation plant system test based on the pre-conceptual design.<br><br>Rx: Heat Source Simulator<br>ECS: DM (single-string)<br>I&C: DM<br>HRS: DM (partial)<br>EP: DM (partial) |
| REACTOR MODULE THERMAL TEST MODEL | SY-TTM-2M | Reactor Internal Flow Characterization<br><br>• measure pressure drop<br>• determine flow distribution<br>• characterize system response to controlled perturbations including loss of heat removal capability, variations in core power generation, and failure scenarios<br>• integrated system start-up and limited transient tests<br>• validate Computational Fluid Dynamics (CFD) results through analysis of test data and comparison with predicted results<br>• obtain test data to support plant model qualification | KAPL | MSFC<br><br>Q2, 2008 | Battis Concur<br>MSFC Concur | Yes | > $5M | This is a first-generation reactor system test based on the pre-conceptual reactor design, and is the reactor counterpart to SY-TTM-1G testing.<br><br>RM: Power Unit: elec. heated<br>Brayton: DM (single-string)<br>I&C: None (limited sensor breadboard testing)<br>HRS: None<br>EP: None |

## 5. INTEGRATED SYSTEM TESTING

| Test Program | Test ID | Objective | Lead Test Sponsor | Test Location & Date | Test SPEC. Appvl & Concur Authority | NR Approval of Test Resume | Estimated Cost | Comments / Design Basis |
|---|---|---|---|---|---|---|---|---|
| ENGINEERING MODEL | SY-EM-4V | First Full-Scale Demonstration of the Integrated Power Plant<br>• NRPCT mechanical & electrical functional testing<br>  • simulated reactor start-up, full power and transient testing on the integrated system<br>  • test reactor control software<br>  • initial test and validation of I&C system sensing and control methods<br>  • reactor feedback behavior & control with a high-fidelity ECS<br>  • demonstrate vendor mfg & assembly techniques and reproducibility<br>  • CDM testing?<br>  • shield thermal management test?<br>• JPL environmental testing (thermal, electro-magnetic)<br>• NGST – Potential full-size HRS testing/qualification | KAPL | JSC or Plum Brook<br>Q1, 2010 | NR Approval<br>JPL Approval<br>NGST Approval<br>Bettis Concur<br>Test Site Concur | Yes | > $25M | This is the first "full-up" test of the integrated power plant system. It uses second generation hardware based on the conceptual design.<br>This EM test will maximize the use of prototypic parts and materials. A thermal mockup of the shield will be used.<br>This PU and ECS may be re-used for the Ground Test Reactor (GTR).<br>RM: Power Unit: elec. heated<br>Brayton: EM (full-string)<br>I&C EM<br>HRS: EM<br>EP: EM (if available) |
| **Qualification Tests** | | | | | | | | |
| REACTOR<br>SHOCK, VIBRATION & ACOUSTIC | SY-ENV-1V | Qualify the Reactor for Launch Loads<br>• shock & pyro-shock testing<br>• random vibration testing<br>• acoustic testing<br>Components (conceptual design):<br>• core (surrogate fuel)<br>• vessel<br>• reflectors<br>• safety rod | Bettis | TBD<br>Q1, 2009 | NR Approval<br>JPL Approval<br>KAPL Concur<br>Test Site Concur | Yes | > $5M | Fabricated at the core vendor using prototypic processes as part of manufacturing development.<br>Prototypic materials for the reactor & vessel. Surrogate materials for the fuel and reflector. |

## 5. INTEGRATED SYSTEM TESTING

| Test Program | Test ID | Objective | Lead Test Sponsor | Test Location & Date | Test SPEC. Appvl & Concur Authority | NR Approval of Test Resume | Estimated Cost | Comments / Design Basis |
|---|---|---|---|---|---|---|---|---|
| REACTOR MODULE<br><br>SHOCK, VIBRATION & ACOUSTIC | SY-ENV-2V | Qualify Reactor Module Design & Mfg for Shipping & Launch Loads<br><br>• shock & pyro-shock testing<br>• random vibration testing<br>• acoustic testing<br><br>Components (conceptual design):<br>• core (surrogate fuel), vessel, reflectors & safety rod from SY-ENV-1V test<br>• loop piping<br>• shield<br>• CDMs<br>• aeroshell (DM or mass mockup)<br>• Brayton – DM units | Bettis | TBD<br><br>Q4, 2009 | NR Approval<br>JPL Approval<br><br>KAPL Concur<br>Test Site Concur | Yes | > $5M | Assembled at the RMIF (if ready), using prototypic processes as part of integration development.<br><br>Prototypic materials for the reactor & vessel. Surrogate materials for the fuel and reflector. Prototypic material for mass mockups, if practical, to support fabrication experience.<br><br>Incorporate test results into P1 Reference Design. |
| STATIC TEST MODEL | SY-STM-1N | Supports NGST Spacecraft Pathfinder and Load Testing<br><br>• pathfinder tests<br>• mechanical testing (load, modal)<br>• functional testing (mechanical compatibility, mass properties)<br><br>NRPCT Specific Goals:<br>• qualification of core vendor fabrication practices<br><br>PU: concept design mockup I&C: None<br>ECS: from SY-ENV-2V EP: None<br>HRS: NGST supplied | NGST<br><br>Bettis – QMA | NGST<br><br>Q1, 2011 | NR Approval (if power unit work serves to qualify the RMIC) | No | <$100,000 | STM supports NGST pathfinder and load tests.<br><br>STM is tested to qualification limits.<br><br>Surrogate materials used for the major components (correct mass, configuration, structural integrity).<br><br>Assembled at the RMIF, using non-prototypic processes. |

## 5. INTEGRATED SYSTEM TESTING

| Test Program | Test ID | Objective | Lead Test Sponsor | Test Location & Date | Test SPEC. Appvl & Concur Authority | NR Approval of Test Resume | Estimated Cost | Comments / Design Basis |
|---|---|---|---|---|---|---|---|---|
| QUALIFICATION MODEL | SY-QM-1V | Final Non-Nuclear Qualification Testing of the Flight Design Hardware<br><br>JPL Environmental Testing (see Table JPL 2.1-2a):<br>• thermal vacuum<br>• thermal balance<br>• acoustic<br>• pyro-shock<br>• modal<br>• structural loads<br>• magnetics<br>• radiated susceptibility<br>• radiated emissions<br>• EMC & ESD<br>• bonding/grounding<br><br>NR PCT Specific Goals:<br>• functional testing (performance, interfaces, calibrations, mass prop)<br>• reactor transient testing<br>• COM motion<br>• aeroshell separation?<br>• transport & handling<br>• rehearse launch procedures<br>o validate He/Xe loop fill procedures<br>o determine loop integrity (perform leak checks)<br>o validate I&C system sensing and control methods<br><br>Components:<br>• PU (electrically heated)<br>• ECS (full-string)<br>• I&C<br>• HRS (from EM test)<br>• EP (if essential) | KAPL | JSC or Plum Brook<br><br>Q1, 2012 | NR Approval<br>NGST Approval<br>JPL Approval<br><br>Bettis Concur<br>Test Site Concur | Yes | > $30M | The QM uses the final reactor design. It consists of fully qualified flight design components that are identical to the flight unit (except for use of electrically heated core). The RM will be subjected to qualification level environmental and functional testing.<br><br>All materials (other than fuel) are of flight design.<br><br>JPL environmental testing validates that the QM and Flight hardware components can withstand the environments to which they will be subjected. |

| 6. FUELED REACTOR TESTING | | | | | | | | |
|---|---|---|---|---|---|---|---|---|
| **Test Program** | **Test ID** | **Objective** | **Lead Test Sponsor** | **Test Location & Dates** | **Test Spec. Appvl & Concur Authority** | **NR Approval of Test Resume** | **Estimated Cost** | **Comments / Design Basis** |
| BENCHMARK CRITICALS | F-PHY-1L | Assess adequacy of neutron cross-sections for selected refractory metals. Simple geometry can be modeled in detail with as-built data, such that focus of experiment is on cross-section adequacy. | Bettis | LACEF<br><br>Q3, 2005 | KAPL Concur<br>LANL Concur | No | $1.4M | Vertical assembly arrangement of alternating layers of a refractory metal (Nb1Zr, Ta-2.5W, Mo, or Re), 93% High Enriched Uranium (HEU), and moderator materials in a partially reflected cylindrical configuration. Neutron spectra spans the normal operational range and flooded condition. Baseline test without refractory metal also planned.<br><br>Reference: B-SE-0116 |
| FUNDAMENTAL CROSS-SECTION MEASUREMENTS | F-PHY-2V | If the F-PHY-1L test program indicates a deficiency in neutron cross sections for Space Reactor materials, new cross section measurements may be recommended. | KAPL | LINAC facility at RPI<br><br>Q4, 2005 to Q4, 2006 | Bettis Concur<br>Test Site Concur | No | $520K | Material cross sections determined to be inadequate from the Benchmark Critical Tests will be selected for more accurate measurement.<br><br>Reference: B-SE-0116 |
| COLD PHYSICS EXPERIMENT | F-PHY-3V | Assess the adequacy of the physics design tools in calculating the cold physics characteristics for configurations approximating the geometry and loading of a Prometheus reactor design.<br><br>Based on the 9/2005 Pre-Conceptual Design. | KAPL | TBD<br><br>Q4, 2007 | NR Approval (if NRPCT provides fuel)<br><br>Bettis Concur<br>LANL/INL Concur (if vendor provides fuel)<br><br>Test Site Concur | Yes | $43M | Full-size critical assembly with test specimens approximating the reactor geometric arrangement (stacked fuel, structural, reflector, and poison material) and actual core loadings. Measurements to include: reflector critical configurations, reflector worth, safety rod worth, and potentially, neutron flux distributions.<br><br>Reference: B-SE-0116 |
| HOT PHYSICS EXPERIMENT | F-PHY-4Z | Assess the adequacy of the physics design tools in calculating the cold and hot physics characteristics of a manufactured Prometheus reactor, including the reactivity effects of core geometry changes as the reactor is heated from cold to normal operating temperature.<br><br>Based on the 2/2008 Conceptual Design. | KAPL | GTR Site<br><br>Q4, 2010 | NR Approval<br><br>Bettis Concur<br>Test Site Concur | Yes | TBD | Performed on the GTR prior to its installation in the Prototype plant, using a test rig and a connection to a heated coolant loop. Measurements to include reflector critical configurations and differential worth as a function of temperature, static temperature coefficients of reactivity, and cold-to-hot temperature reactivity effect.<br><br>Reference: B-SE-0116 |

| 6. FUELED REACTOR TESTING | | | | | | | | |
|---|---|---|---|---|---|---|---|---|
| **Test Program** | **Test ID** | **Objective** | **Lead Test Sponsor** | **Test Location & Dates** | **Test Spec. Appvl & Concur Authority** | **NR Approval of Test Resume** | **Estimated Cost** | **Comments / Design Basis** |
| GROUND TEST REACTOR | F-GTR-1Z | • Assess adequacy of physics design tools and dynamic response models in calculating physics characteristics and transient response of the Prometheus reactor in the integrated plant.<br>• Assess the adequacy of procedures for reactor startup and reactor plant transients, e.g., shimming to maintain temperature control, switching to coast mode, switching Brayton engine lineup, etc.<br>• Long term periodic testing will enable assessment of the lifetime trends of physics characteristics in advance of the flight unit cores.<br><br>Based on the 2/2008 Conceptual Design. | KAPL | TBD<br><br>Q1, 2014 | NR Approval<br><br>Bettis Concur<br>GTR Site Concur | Yes | TBD | The GTR is assumed to be identical to the P1 core, with the exception of safety features unique to ground testing.<br><br>The GTR is a comprehensive physics test program (cold and hot, low and high power, and transients) to support mission assurance for P1, and to form the basis for the final design of the Prometheus class reactors. Measurements to include: reflector critical positions and reactivity worth as a function of temperature, safety rod worth, static temperature coefficients of reactivity, power reactivity, kinetics parameters, transient response characteristics, nuclear detector response and neutron flux spatial distributions.<br><br>The EM Power Unit and ECS may be re-used for the GTR.<br><br>Reference: B-SE-0116 |

## 7. ATLO TESTING

| Test Program | Test ID | Objective | Lead Test Sponsor | Test Location & Dates | Test Spec. Appvl & Concur Authority | NR Approval of Test Resume | Estimated Cost | Comments / Design Basis |
|---|---|---|---|---|---|---|---|---|
| Prometheus 1 | AT-FNC-1X | Power Unit Tests<br>• thermal test (bakeout)<br>• functional tests<br>  • electrical interface<br>  • mechanical interface<br>  • calibrations<br>• mass properties | KAPL | The core vendor<br><br>Q1, 2013 | NR Approval<br><br>Bettis Concur<br>Core vendor Concur | Yes | TBD | Key Prometheus 1 assumptions include:<br>• The fueled power unit is assembled at the core vendor and then shipped to the GTR site for physics tests.<br>• Zero power physics tests are performed at the GTR site prior to delivery and assembly at the launch site. Measurements to include reflector critical positions, differential and integral worth of reflectors, and integral worth of safety rod.<br>• The P1 SNPP (using the QM electrically heated power unit) is assembled at the RMIF and shipped to NGST for integration with the spacecraft.<br>• The assembled spacecraft is shipped to JSC for environmental testing to acceptance levels.<br>• The tested spacecraft is shipped to KSC. The fueled power unit is shipped to KSC. The electrically heated power unit is replaced with the fueled power unit and final tested.<br>• The spacecraft is mated to the launch vehicle and prepared for launch at Cape Canaveral. |
| | AT-PHY-2Z | Physics Tests<br>• confirmation of the basic physics characteristics of the as-built Prometheus 1 flight unit reactor prior to shipment to KSC. | Bettis | GTR Site<br><br>Q3, 2013 | NR Approval<br><br>KAPL Concur<br>Test Site Concur | Yes | TBD | |
| | AT-FNC-3R | Prometheus 1 Plant Tests<br>• thermal test (bakeout)<br>• functional tests<br>  • electrical interface<br>  • mechanical interface<br>  • calibrations<br>• mass properties | KAPL | RMIF Site<br><br>Q1, 2013 | NR Approval<br><br>Bettis Concur<br>JPL Concur<br>NGST Concur<br>RMIF Concur | Yes | TBD | |
| | AT-ENV-4V | Final Spacecraft Assembly and Testing<br><br>• JPL Environment Requirements Document<br>  • mechanical tests (acoustic, vibration, pyro-shock, modal, structural load)<br>  • thermal tests (thermal vacuum, thermal balance)<br>  • electro-mechanical (radiated emissions & susceptibility, EMC, ESD, magnetics, bonding/grounding)<br>• NRPCT functional tests<br>  • electrical and mechanical interfaces<br>  • performance tests<br>  • calibrations<br>  • end-to-end compatibility & mission simulations<br>• mass properties | KAPL | NGST & JSC<br><br>Q3, 2013 | NR Approval<br>JPL Approval<br><br>Bettis Concur<br>NGST Concur<br>Test Site Concur | Yes | TBD | |

## 7. ATLO TESTING

| Test Program | Test ID | Objective | Lead Test Sponsor | Test Location & Dates | Test Spec. Appvl & Concur Authority | NR Approval of Test Resume | Estimated Cost | Comments / Design Basis |
|---|---|---|---|---|---|---|---|---|
| | AT-FNC-5C | Attach Fueled Power Unit, Test & Go<br>• He,Xe purification, fill, flush, refill<br>• leak & pressure checks<br>• functional tests<br>  • electrical and mechanical interfaces<br>  • performance tests<br>  • slider / safety rod motion | KAPL | KSC<br>Q2-Q3, 2014 | NR Approval<br>Bettis Concur<br>JPL Concur<br>KSC Concur | Yes | TBD | |

## 8. SAFETY TESTING

| Test Program | Test ID | Objective | Lead Test Sponsor | Test Location & Dates | Test Spec. Appvl & Concur Authority | NR Approval of Test Resume | Estimated Cost | Comments / Design Basis |
|---|---|---|---|---|---|---|---|---|
| P1 SAFETY | S- | The safety testing needs and an assessment of the testing capabilities of the national laboratories and NASA centers was not completed prior to project termination. Examples of potential tests included impact, aeroshell ablation, aeroshell aerodynamics and vacuum chamber heat transfer. | KAPL | TBD | Approvals TBD<br>Bettis Concur | TBD | TBD | |
| GTR SAFETY | S- | | Bettis | TBD | Approvals TBD<br>KAPL Concur | TBD | TBD | |

This Page Intentionally Blank

## 13.5 In-House Testing

A key strategy of the NRPCT test program for the Prometheus project was to use the available, national testing infrastructure to the maximum extent practical. This included NASA facilities and the national DOE laboratories as well as subcontractor facilities. The goal was to reduce costs and better meet the aggressive schedules originally set for the JIMO mission. However, limited in-house testing was necessary to support the reactor plant design efforts and help guide the larger test programs that would be performed at these outside facilities. The ability to rapidly test reactor concepts early in the design process and iterate on hardware changes with direct input from the Bettis and KAPL experimental communities were key drivers in this decision. In addition, providing NRPCT personnel with a first hand understanding of the behavior of these systems was an important consideration given NRPCT's general lack of familiarity with the closed Brayton cycle (CBC) and gas cooled reactors.

To effectively use the limited resources available for in-house testing and to avoid duplication of work, KAPL and Bettis divided the planned testing areas between the laboratories. Initial small scale, bench top testing would be completed by each laboratory, as needed, to support the local design organizations. Eventually, Bettis would lead the heated loop and gas leakage testing efforts while KAPL would lead the low temperature and pressure flow visualization testing.

The facilities and tests planned for in-house testing are described below. A joint KAPL/Bettis recommendation for the near term, in-house test facilities was submitted in Reference 13-5 and approved by Naval Reactors in Reference 13-6.

### 13.5.1 KAPL In-House Testing

KAPL's in-house test program for the reactor and plant areas was being performed in two facilities; the Fluid Mechanics Laboratory and Experimental Engineering. These facilities, and the work performed prior to project termination, are summarized below.

#### 13.5.1.1 Fluid Mechanics Laboratory

KAPL's Fluid Mechanics Laboratory specializes in low temperature and pressure mockups of reactor core and reactor plant components to guide design decisions through visualization and a fundamental understanding of flow behavior. The lab uses special instrumentation such as laser Doppler velocimetry (LDV), particle image velocimetry (PIV), high speed video (HSV), hot film anemometry (HFA), and other techniques to qualitatively and quantitatively map the flow field and provide information back to the hardware designers. Because of the lack of experience with compact gas reactors like the one being designed for Prometheus, this type of fundamental testing was considered essential in setting design features early in the process. These low temperature tests would provide direction and insight for the high temperature tests to be performed at outside facilities such as the NASA centers. Local flow field data would also support ongoing computation fluid dynamics (CFD) models of the reactor. Longer term, a prototypic, full scale plastic test of the reactor was envisioned to parallel these high temperature test programs to: 1) help diagnose any unexpected results during qualification and 2) provide detailed hydraulic data that could not be readily obtained in the high temperature test sections (velocities, individual channel flow distributions, etc.).

Reference 13-7 documents the work effort performed by KAPL's Fluids Mechanics Laboratory in support of Project Prometheus. Initial testing was focused in two areas: 1) understanding the ability to properly scale high temperature gas reactor systems with low temperature and pressure water and air test loops and 2) measurement techniques for obtaining accurate flow field data in a gas system using laser based systems. These efforts were necessary since most of the NR program's experience was with pressurized water reactors (PWRs) and the ability to hydraulically test scaled PWR reactor mockups with water is well understood.

Some key conclusions from the Fluid Mechanics Laboratory work are:

1. To avoid the need for a large and expensive air compressor, a combination of air and water testing would need to be performed in the Fluids Lab to effectively cover the range of Reynolds number (Re) for the gas reactor concept. Reactor core Reynolds numbers were on the order of 6000 for the annular flow design and 23,000 for the circular cooling passage design, so testing at reduced Reynolds numbers (i.e., flow rate) may not be possible because of the concern with entering into transitional flow regimes under test conditions.

2. Multiple blowers operating in parallel are required to properly scale the air flow rate and pressure head to reactor conditions. This is illustrated in Figure 13-10 as a function of the helium-xenon mole fraction selected for the plant design.

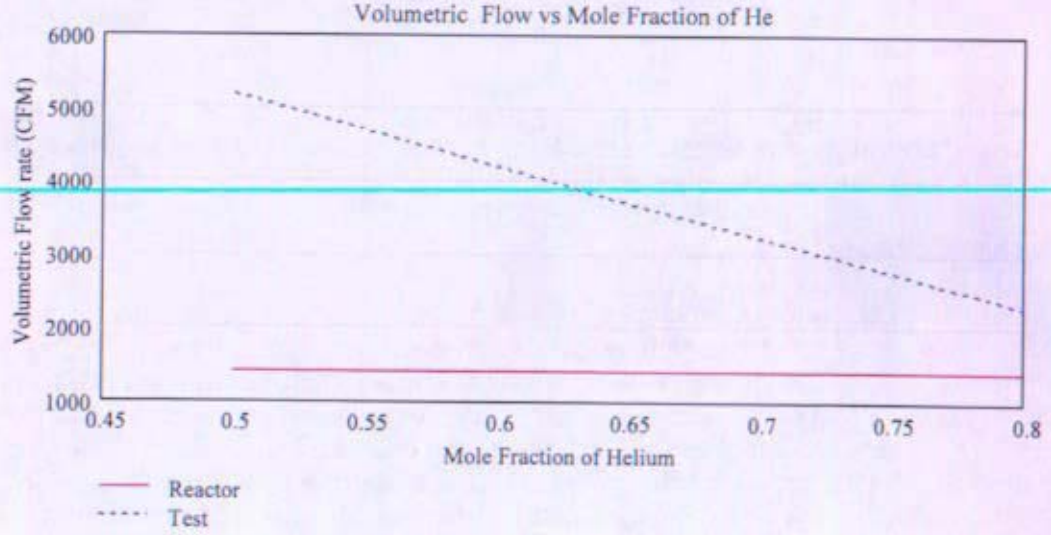



**Figure 13-10: Test Flow Rates Needed to Model Gas Reactor**

3. The existing Fluids Lab water loop could easily provide the necessary head and flow rate to match the range of Reynolds numbers for the gas reactor concept.

4. For mean flow velocity data, each of the seeding techniques used (i.e., atomized water droplets, fog generator using water-glycol mixture, and solid seed particles) provided consistent results in air testing (See Figure 13-11).

5. For turbulence intensity or Reynolds stress terms that require time accurate measurement of velocity fluctuations, a fog generator that better matches the ratio of seed/test fluid inertial and viscous characteristics is recommended. This ensures the seed particles more accurately follow the detailed fluid behavior (See Figure 13-12).

6. Water based testing to dynamically simulate a gas system at equivalent Re is acceptable for unheated testing. However, the specific test conditions need to be examined to validate no additional effects outside of Re similarity when using water to simulate a gas system.

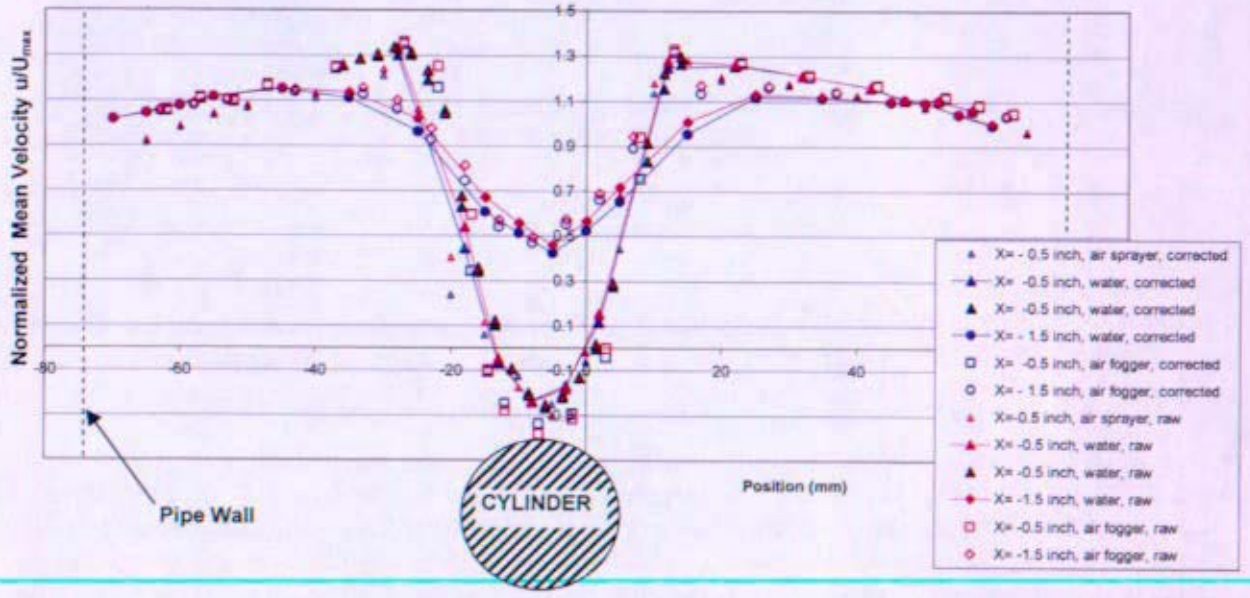



**Figure 13-11: Air-Water LDV Mean Velocity Data for Flow Across a 1-inch OD Cylinder Inside a 5.75-inch ID Pipe (Re based on cylinder is approximately 34,000)**

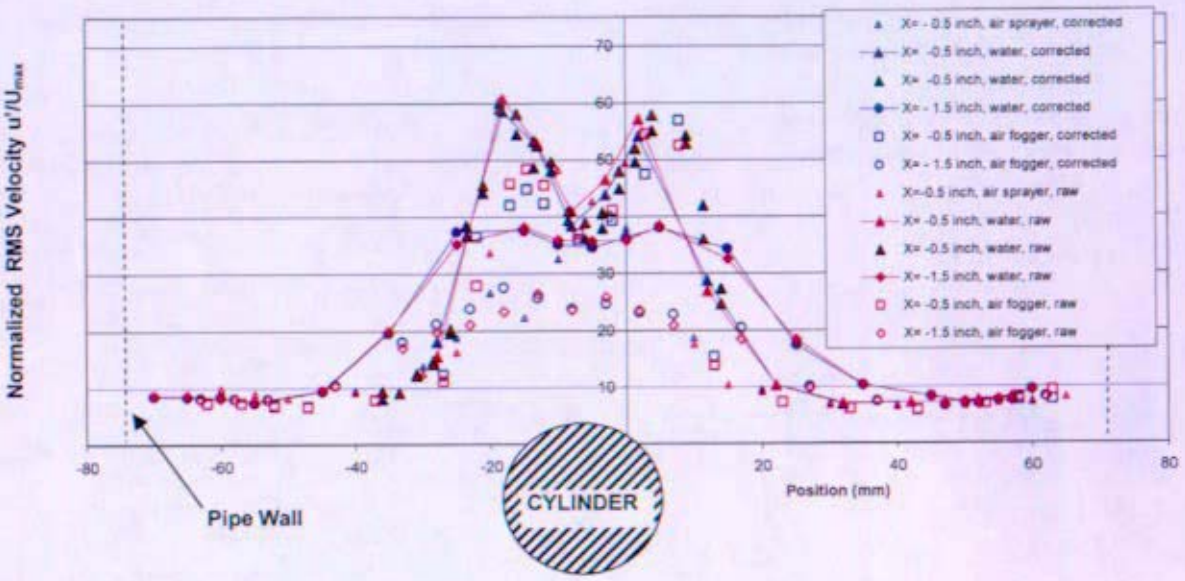



**Figure 13-12: Air-Water LDV RMS Velocity Data for Flow Across a 1-inch OD Cylinder Inside a 5.75-inch ID Pipe (Re based on cylinder is approximately 34,000)**

Plans were underway to construct a new water and air test loop in addition to KAPL's Fluids Mechanics Laboratory that would be largely dedicated to the Space Power Program. These loops would provide the necessary flow capacity to match gas reactor Reynolds number and ensure dedicated testing could occur without impacting other programs. A concept design for the new test facility was completed prior to termination of the project and details are provided in Reference 13-7.

### 13.5.1.2 Experimental Engineering

KAPL's Experimental Engineering facility supported early Brayton engine testing. The NR program was interested in quickly learning how Brayton engines (i.e., turbine, alternator, and compressor units) perform and specifically how such an engine would behave in conjunction with a gas cooled reactor. Besides understanding the fundamental operation and behavior of the system, failure modes and the consequence of a Brayton failure to the reactor plant were of particular concern. It was also considered important to have designers gain familiarity with hardware operation, particularly for a key component such as the Brayton engine. Since experienced plant operators at NRPCT were unavailable for a closed Brayton cycle reactor, this was an effort to provide some early level of experience for the staff.

KAPL's initial work in Experimental Engineering was focused on testing an open cycle Capstone C30 Microturbine unit. The use of a commercially available, open cycle Capstone turbine provided a quick and cost effective approach to obtaining a basic understanding of Brayton hardware and performance characteristics. The C30 was the same model modified for use in Sandia's closed Capstone loop and also the same model that was being modified for Bettis' dual, closed loop

system (see Section 13.5.2.2 below). In this regard, it provided an opportunity to compare the various data obtained in these facilities under different design and operating conditions. Another factor in this selection was that GRC had extensive experience in operating the C30 units and had provided Capstone with support on the gas bearing design.

Two C30 units were purchased for a total of $89,000 which included 1 year of technical support from the vendor. The plan was to first operate the unit in accordance with its normal operation to gain a basic understanding of the unit and allow the engineers to become trained on operating procedures. This would provide limited data since the units are designed for emergency or auxiliary power and are generally intended to be turned on and off as needed. Next, the unit would be operated outside of its normal operating procedures but within the design of the hardware to obtain data on performance and behavior during off-normal and transient conditions. This testing would require more direct control of the unit. KAPL was in the process of investigating what types of testing would be possible with the Capstone control system. SNL and Barber-Nichols, who modified the C30 units for SNL's closed loop (Reference 13-8), had extensive experience in this regard and were assisting with the NRPCT's understanding the control systems of the unit. Finally, the Capstone unit may have been subjected to design basis types of testing such as ingestion of debris or over-speeding casualties where a high risk of unit failure would exist. This risk was the reason for procurement of two units; one to serve as a backup should failure occur early in the testing.

At the time the project was cancelled, the two C30 units were delivered to KAPL and one unit was installed in the TF-139 test chamber. The second unit was stored. Since termination of the project, both units were returned to Capstone for a refund. No testing was ever performed with the Capstone units at KAPL.

### 13.5.2 Bettis In-House Testing

Bettis planned to perform the following in-house testing of reactor and plant components (facility upgrades were necessary to accommodate these tests):

#### 13.5.2.1 Acrylic Vessel Test (R-TH-2B)

**Objective**

The objective was to construct and test a half-scale acrylic model of the gas cooled reactor concept to qualitatively assess flow distribution and stability. Areas of interest for flow visualization were the inlet nozzle, the inlet plenum, the downcomer, and the lower plenum. Pressure measurements were to be taken to estimate the parasitic losses in the reactor inlet regions. The model was not a prototypical mock-up of the fueled core geometry. Instead, it included a perforated plate that simulated the pressure drop across the fuel region of the reactor. Flow fields in the outlet plenum and outlet nozzle were not to be evaluated in this test.

**Functional Requirements**

The focus of the test was to obtain and observe even flow distributions throughout the specified regions of interest. Clear acrylic components were planned for the inlet plenum, downcomer, and lower plenum regions to allow flow visualization. The test would attempt to match the targeted prototypic Reynolds number of 680,000 (based on a 17.8 cm (7 in) inlet nozzle diameter with a gas inlet temperature of 880°K (1124.6°F), and molecular mixture weight of 31.5 g/mol (.06945 $lb_m$/mol)). Simplified core geometries were to be used to mock-up the resistance of fueled core region. To achieve the objectives of the test, the following areas of modularity were to be considered:

- Inlet nozzle designs
  - Varying diameters
  - Sharp-edged or tapered geometry
  - Side, top, and angled entry
  - Multiple inlets used simultaneously
- Bottom plenum shapes
  - Hemispherical
  - Elliptical
  - Smooth or finned
- Downcomer width - changing outer or inner diameter
- Upper and lower vent geometries

**Testing and Facility Requirements**

Testing was to include two phases:

- Phase I was to be an air test to obtain baseline qualitative behavior of flow at low Reynolds number. Patterns were to be observed with "tell tales" (sewing thread) within the test section.
- Phase II was to be a water test to more easily achieve the prototypic Reynolds number of 680,000. A flow rate of 0.0315 $m^3/s$ (500 gpm) and operating temperature of 311K (100°F) are necessary to obtain the value. The test loop was to produce up to 0.0631 $m^3/s$ (1000 gpm) with a maximum operating pressure of 689.5 $kN/m^2$ (100 psi). The test section design was to accommodate temperatures and pressures up to 316K (109°F) and 344.75 $kN/m^2$ (50 psi) respectively. Flow visualization in the water experiment could be achieved in a variety of ways, including the use of polystyrene beads, nitrogen bubble injection, and blue dye injection. Pressure was to be monitored during testing at specific locations in the vessel to ensure that the model accurately depicted the prototypic conditions. Water temperature measurements were to be controlled to ensure the acrylic vessel did not exceed its design conditions

**Test Hardware**

As stated, the main areas of interest were the upper and lower plenums, the downcomer and the inlet nozzles. In these specified regions of interest, the hardware would be manufactured from acrylic. Figure 13-13 shows the test apparatus hardware. There were four separate inlet nozzles that could be used to vary the angle of entry into the inlet plenum. Aluminum inserts designed to

plug the unused inlets could also be used to vary the inlet nozzle diameter and inlet geometries. The model allowed for two inlets to be used at one time. Only one outlet nozzle was included since no evaluation of the outlet region was planned.

The bottom plenum was flanged and could be easily replaced to test other designs for that region. For example, an ellipsoidal shaped plenum could be used with the same flange dimensions. The vent plate and orifice plate could also be easily exchanged with those having different geometries, and the colander plate could be removed. The downcomer width could be changed by using another acrylic outer shell (changing O.D.) or a different core barrel (changing I.D.).

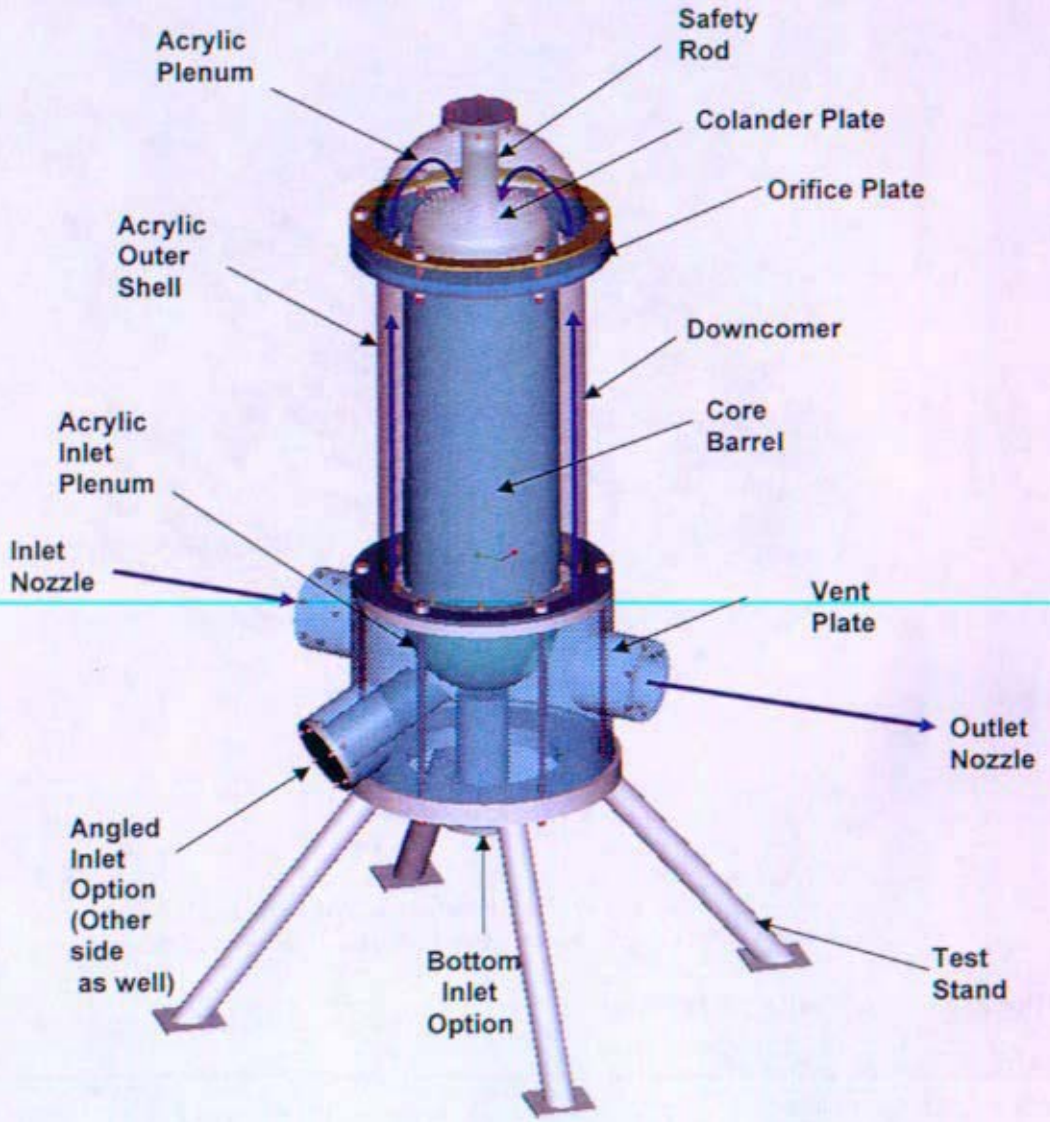



Figure 13-13: Flow Visualization Test Apparatus of Gas-Cooled Reactor Concept

### 13.5.2.2 Dual Closed Brayton Loop (DCBL) Test (P-BRY-7B)

#### Objectives

The objectives of this test were to design and build a first-of-a-kind dual closed Brayton test loop to gain operations and control experience with two Brayton engines operating in parallel. This would be the only dual closed loop test available until the prototypic Engineering Model testing started in 2010. Of particular interest were the interactions of the Brayton engines during transient evolutions and steady state operation. The loop was also to be a test bed for operational strategies, sensor technologies, and benchmarking of modeling methods. A representation of the loop is shown in Figure 13-14, where the white arrows indicate the flow direction.

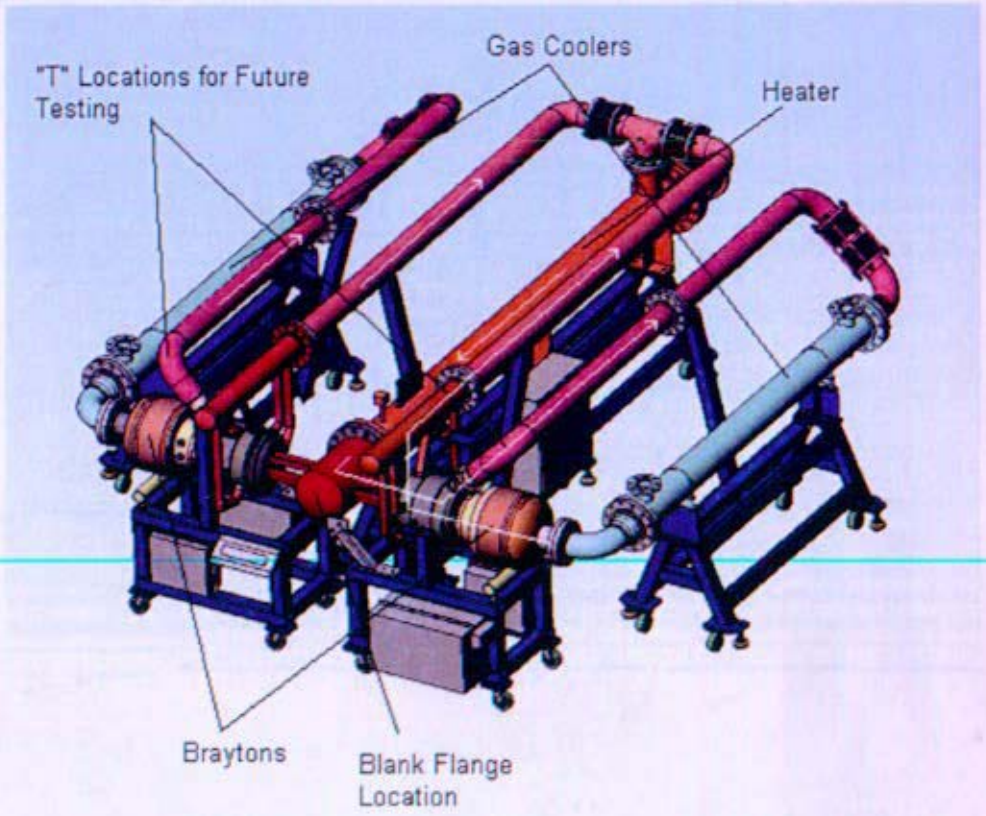



**Figure 13-14: Preliminary layout of DCBL (check valves and removable flanged pieces not shown)**

#### Functional Requirements and Design

The DCBL was to be a first-of-a-kind test loop that connected two Brayton engines in parallel with a common electric resistance heater. The Brayton engines to be used were modified versions of commercially available Capstone C30 microturbines. The C30s have gas foil thrust and journal bearings and integral recuperators. They were to be modified from open-cycle to closed-cycle engines with nitrogen as the working fluid. Each loop contains a water-to-nitrogen gas cooler for heat rejection and a check valve at the compressor inlet to prevent reverse flow when only one loop was operating. Each loop also had a removable flanged piece between the gas cooler outlet

and the compressor inlet, and another removable flanged piece between the low pressure recuperator outlet and the gas cooler inlet. A blank flange at the heater outlet and a tee at each low pressure recuperator outlet were to be used for future testing of proof-of-concept hardware and flow testing. The locations of the blank flange and tees are indicated in Figure 13-14.

Full power design parameters for one loop are shown in Figure 13-15. The Brayton engines were estimated to produce 15 $kW_e$ each with a turbine inlet temperature of 1000K (1340°F) and a compressor inlet temperature no higher than 315K (107°F). The power generated by the Brayton engines was to be dissipated by an air cooled resistive load bank. Piping for the loop was to be made out of 304H stainless steel in accordance with ASME specification number SA-312.

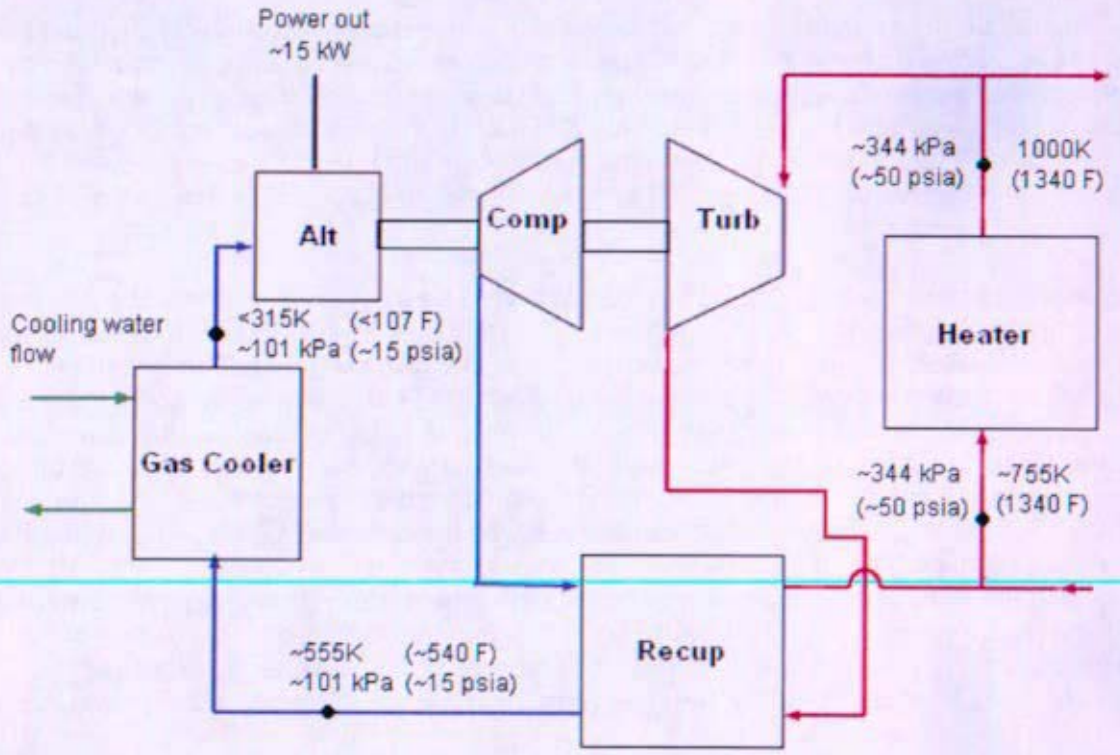



**Figure 13-15: Loop state points for the DCBL**

A National Instruments (NI) control and data acquisition system was to be investigated for use in the loop. This system was to interface with the Capstone controllers supplied with the C30 units. System controls were to be Brayton speed and either heater power or turbine inlet temperature. Brayton speed would be controlled by issuing a command to the NI system which would then command the Capstone controller to that speed. The user would select heater power or turbine inlet temperature to control the heat input.

The loop was required to perform the following transients:

- Operate one Brayton at full power and start up the second Brayton
- With both Brayton engines operating at full power, shut down one Brayton

To support model benchmarking and operational evaluation, other tests under consideration were:

- Operate each Brayton at a different steady state speed
- Change the speed of one Brayton while the other Brayton operates at a constant speed
- Change the speed of each Brayton simultaneously

Safety features on the loop included burst disks for over-pressure protection on the gas side and pressure relief valves on the water side. An emergency shutdown could be commanded by the user, or triggered automatically in the event a safety device was activated. The emergency shutdown would command the turbines to shut down and turn off all heater power. A safety barrier to provide noise reduction and to protect against debris (in the event of a catastrophic failure) was considered. The requirements for the barrier had not been finalized at the time the project was canceled.

Two areas of concern during the design of the loop were addressed. The first issue involved the gas foil thrust bearings on the Brayton engines. The bearings on the C30 were designed for steady state operation in ambient air. Because of this, the gas foil thrust bearing had less load carrying capacity than prototypic bearings would have. This led to a concern about the ability of the DCBL to undergo rapid transient evolutions. Resolution of this issue was to add a monitor to the control system to evaluate the thrust load the bearings were carrying and compare the results to a maximum allowable thrust load. This monitor would then be used to determine how rapidly transient evolutions could occur. The second issue was the potential for a non-operating Brayton to experience damaging temperatures while the other Brayton was in operation. It was postulated that exposing the aluminum compressor wheel to high temperature gas would overheat the journal bearing coatings through conduction down the turbine/compressor shaft. Resolution of this issue was to place sensors in key locations to ensure temperature limits were not exceeded. If temperature limits were approached, the non-operating loop would be started to provide cooling flow.

The contract to design and build the DCBL was awarded to Barber-Nichols, Inc. (BNI) of Arvada, CO. BNI had recent experience building a similar single closed Brayton loop for Sandia National Laboratories (see Reference 13-8), thus most of the design and development work was already completed. BNI was to assemble the loop and perform acceptance testing at their facilities. Following acceptance testing, the loop was to be disassembled and shipped to Bettis for installation in an on-site test facility. The loop was to be fully operational at Bettis in June 2006. Upon project cancellation, this contract was terminated. NASA Glenn Research Center planned to initiate a new contract with BNI to complete the DCBL.

**Testing and Facility Requirements**

Bettis Facility requirements for the loop were:

- Heater
  - 480 VAC, 3 phase, 220 amp, 180 kWe
- Gas Cooler (one for each Brayton)
  - 190 L/min (50 gpm) water flow for each of two gas coolers
  - 6K (10F) maximum temperature delta
  - 4-inch, 150 lb flange interface in/out
  - 300K (80F) inlet water for a 315K (107F) compressor inlet temperature at maximum condition
- Control/Data Acquisition System: approx. 1 kW @ 120 VAC
- Nitrogen supply
- Sound/Debris Barrier
- Room Cooling/Ventilation
  - load bank of 30 kW heat + 10 kW Loop Heat
- Preliminary Loop Footprint: 6.7 x 5.5 x 2.1m tall (22 x 18 x 7 feet)

**17.4.2.3 Gas Leakage Test (P-GL-1B)**

**Objective**

The Brayton engine, shown conceptually in Figure 13-16, contains electrical feedthroughs to facilitate transfer of the generated electricity from within the alternator housing to the external Power Conditioning and Distribution (PCAD) system. Both constituents of the gas coolant, helium and xenon, are expected to permeate through the feedthrough sealant materials during the life of the mission. The objective of this test was to create a bench-top test to determine the leakage modes and rates through various electric feedthrough materials (such as Grafoil, ceramics, and glass).

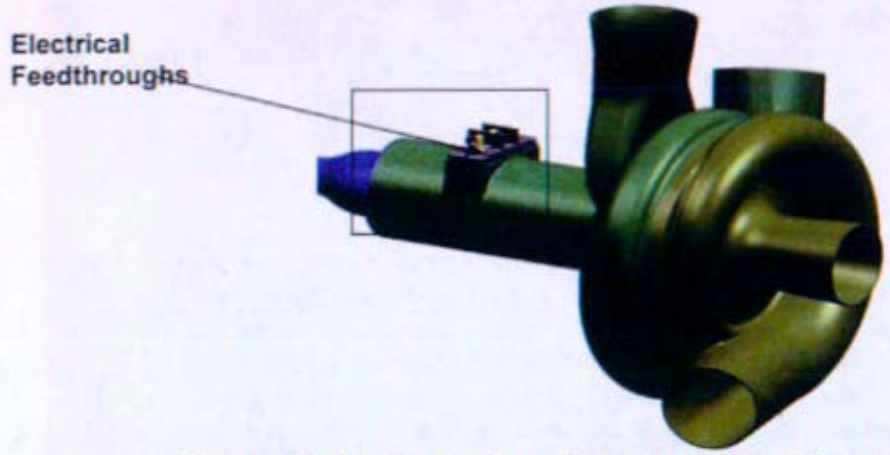



**Figure 13-16: Prometheus Brayton Engine Concept Design**

**Functional Requirements**

The purpose of this test was to determine the gas leakage rates of vendor supplied developmental electrical feedthroughs to determine if they met mission requirements. A list of design and test requirements are listed below, but a more detailed description of the electrical feedthrough design is provided in Section 9.

During initial discussions with the electrical feedthrough vendor community, the NRPCT learned that the vendors were unable to supply production feedthroughs that met every design specification. While vendors were capable of meeting individual requirements, the combination of specifications involved significant feedthrough engineering efforts. Of particular vendor concern was predicting and assuring feedthrough lifetime at the elevated temperature and pressure requirements. Therefore, the NRPCT provided design requirements on a "best efforts" basis. Vendors were allowed to specify a maintenance-free lifetime rather than design to meet a contractually specified limit. Feedthrough performance was evaluated by one metric, the maximum gas leakage rate.. A comparison of the design and vendor requirements is shown in Table 13-5.

**Table 13-5: Design vs. Vendor / Testing Requirements**

| Item | Design | Vendor / Testing |
|---|---|---|
| Gas composition: | 78.4 %v He / 21.6 %v Xe | 100% He |
| Maximum gas temperature: | 500K (440°F) | 500K (440°F) |
| Bleedflow maximum gas pressure : | 4000 kPa (588 psig) | 2000 kPa (~300 psig) |
| Maximum permitted gas leakage rate: | $1x10^{-9}$ std cc/s | $1x10^{-9}$ std cc/s |
| External vacuum: | $1x10^{-14}$ torr | $1x10^{-5}$ torr |
| Housing material: | TBD | Inconel 625 |
| Maintenance free lifetime: | 15 yrs | Vendor specified |
| Alternator output: | 3 phase AC | 3 phase AC |
| Alternator voltage: | 440 Vrms line to line | 440 Vrms line to line |
| Alternator power: | 100 kWe | 100 kWe |
| Alternator electrical frequency: | 2250 Hz | 2250 Hz |
| Vibratory Loading: | Launch loads per JPL | Launch loads per JPL |
| | | |

**Testing and Facility Requirements**

Testing was to consist of two phases. Phase 1 was to be vendor development and Phase 2 was to be thermal and vibratory validation and gas leakage testing of the feedthroughs.

Phase 1 was to consist of validation testing of developmental feedthroughs provided by selected vendors. Three vendors would be selected based on their ability to design and construct a feedthrough that met most requirements. Validation testing was to consist of a random frequency vibratory test to simulate launch conditions. The test would be conducted at ambient temperature and pressure. Table 13-6 provides the random vibratory frequencies requirements established by Jet Propulsion Laboratory Environmental Requirements Document (ERD).

**Table 13-6: Random Vibration Force Limit Specifications .**

| Frequency, Hz | Force Spectral Density Level |
|---|---|
| $20 - f_o$ | $(384 \times F)$ $N^2/Hz$ |
| $f_o - 1000$ | -6 dB / octave |

Notes:

$f_o$ = the first predominant resonance frequency in the axis of test.

F = the product of the acceleration spectrum times the square of the total mass of the assembly in kg.

N = Newtons

dB = decibels

After Phase 1 testing, an approximate leakage rate was to be determined using a gas sniffer wand (to an order of magnitude uncertainty). If minimal gross gas leakage was detected, then the test specimens would be sent to Phase 2. What constitutes "minimal" has not yet been determined at time of project termination. Figure 13-17 is an illustration of a test specimen that would be used during Phase 1 testing.

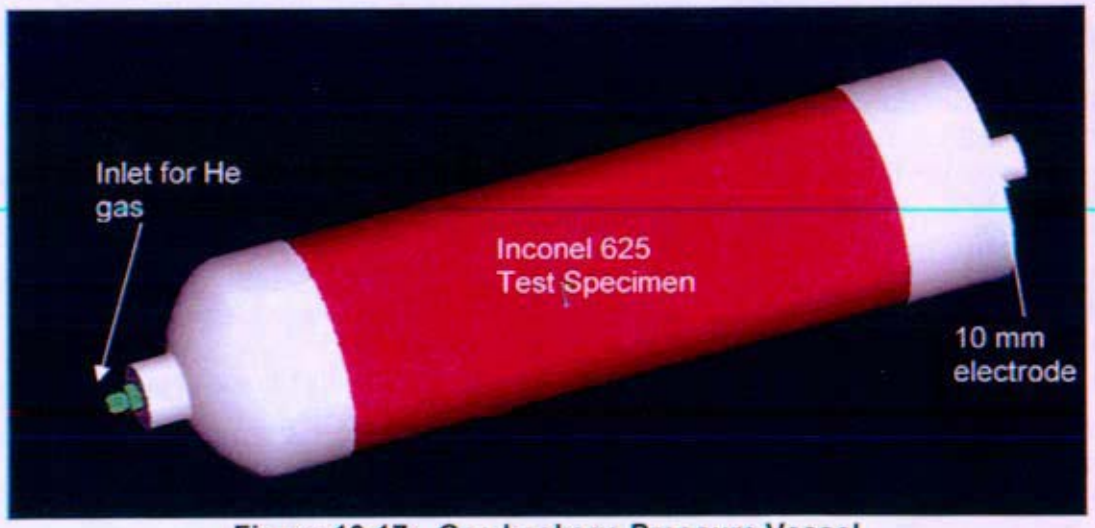



**Figure 13-17: Gas Leakage Pressure Vessel**

Figure 13-18 shows the Phase 1 vibratory test experimental setup. A vibration-rated flex hose allows for isolation of the test specimen from the external helium tank. A pressure relief valve prevents over-pressurization of the test specimen in the event of failure of the pressure regulator.

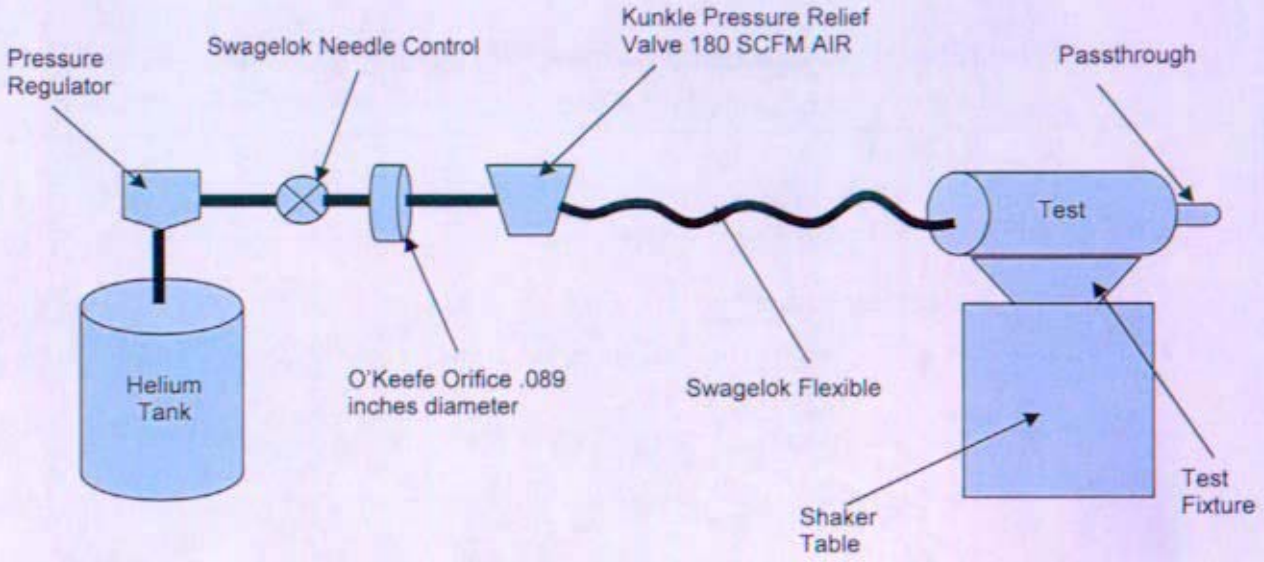



**Figure 13-18: Experimental Setup for the P-GL-1B Test at the Bettis Laboratory Fundamental Shock and Vibration Lab**

Phase 2 was to consist of more aggressive testing on those feed throughs that passed Phase 1. In this phase, the test specimen would be thermally cycled from 310 to 500K (98 to 440°F) at constant pressure of 2000 kPa (290 psig) in a vacuum chamber. The thermal cycling would test the expansion and contraction behavior of the potted material. A cylindrical silicon carbide resistance heater inserted inside the test specimen would provide the heating. A pressure regulator maintains constant pressure during the test. Figure 13-19 provides an illustration of the experimental setup. The leakage rates were to be monitored using a mass spectrometer before, during, and after the thermal cycling. The mass spectrometer measurements are highly accurate, and are used to confirm the leak rates measured at Bettis. All test specimens would be thermally cycled at NASA GRC.

Following the thermal cycling testing, half of the specimens were to undergo random vibration testing at Bettis per the JPL ERD. The leak rates of these specimens would be compared to the leak rates of the non-vibration tested control specimens to quantify the leakage due to vibration.

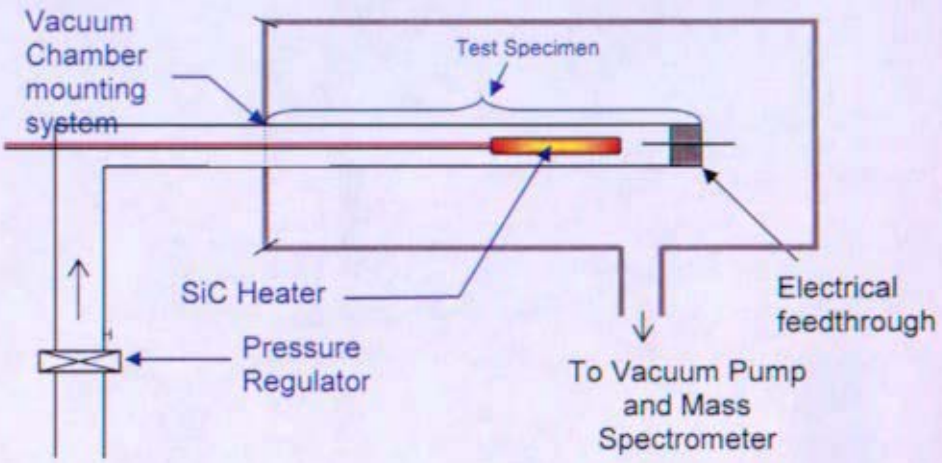



**Figure 13-19: NASA GRC Experimental Setup for Gas Leakage Testing**

Note – Both phases of the gas leakage test were to be conducted with a non-energized electrode. An energized electrode would likely add heat to the feedthrough, possibly creating a thermal expansion difference between the electrode and feedthrough housing. Thermal expansion issues could also exist if different materials were used for the electrode and feedthrough housing. The magnitude and effect of the thermal expansion issue when using energized electrodes was to be further investigated in a subsequent test program.

**Test Hardware**

The initial list of vendors evaluated for the alternator electrical feedthroughs included: CeramTec Corp. (Ceramaseal® products), Conax Buffalo Technologies, Hermetic Seal Company, and Morgan Advanced Ceramics (Alberox products).

- CeramTec North America Corporation produces ceramic-to-metal hermetically-sealed feedthroughs for ultra-high vacuum or high-pressure environments (172 MPa, 25,000 psig) over a wide range of temperatures.

- Conax Buffalo Technologies specializes in mechanical insulator/conductor seals. Conax specializes in polymer and plastic sealing glands. Figure 13-20 shows the layout for a typical Conax feedthrough that uses a follower to apply axial compression on the sealing gland, producing compressive radial stresses that hermetically seal the electrode. The feedthrough shown is designed to have multiple electrodes that pass through the pressure boundary.

- Hermetic Seal Corporation (HSC) specializes in glass-to-metal seals and is the preferred vendor for Hamilton Sunstrand. The thermal compression mismatch of the insulator and conductor is utilized, along with reaction bonding of the joint, to produce hermetic seals.

- Alberox Products (Morgan Advanced Ceramics, New Bedford, MA) produces custom ceramic-to-metal seals and assemblies. Claimed benefits of their seals compared to glass-to-metal seals in terms of stability at high temperatures, durability, and strength.

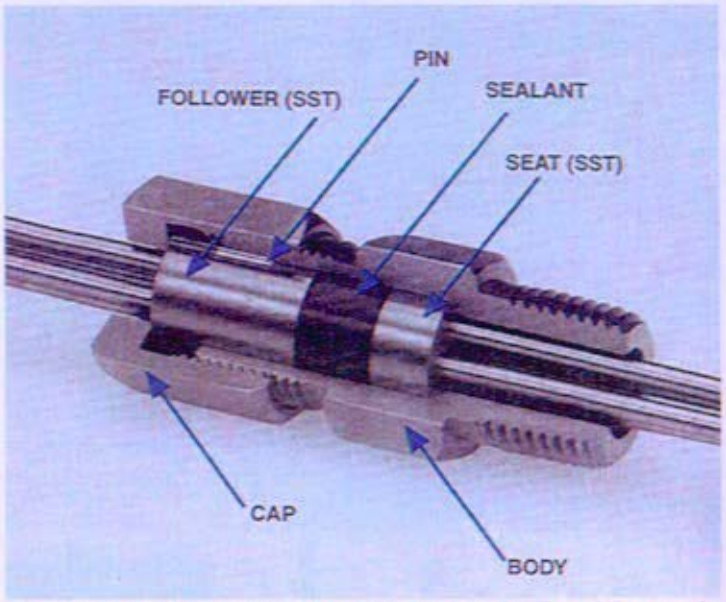



**Figure 13-20: Conax Multi-electrode Feedthrough**

### Conclusions

A final evaluation of the various vendors and designs was not completed and additional vendors may also be available. Electrical feedthroughs were considered a key issue to ensure gas inventory integrity so multiple options would likely be pursued early in the program to maximize the likelihood of success. The list of vendors in this report should provide a good starting point should this work resume in the future.

## 13.6 Marshall Space Flight Center (MSFC) Testing

Prior to the concept down-select, the NRPCT was conducting parallel-path investigations of several competing reactor module technologies, including liquid metal cooled reactors, heat pipe based reactors and gas-Brayton systems. MSFC was tasked with several studies, based on their past experience in these areas prior to NRPCT involvement in Project Prometheus. Upon selection of the Direct Drive Gas – Brayton system, MSFC work was re-directed to focus on selected issues associated with that reactor module concept. The following sections provide a summary of the testing, completed and in-progress, performed by MSFC. More detailed descriptions of the tests are provided in the referenced MSFC final reports.

### 13.6.1 Liquid Metal Reactor

The purpose of the liquid metal test was to provide NRPCT experience with a lithium liquid metal system and to understand the nature of liquid lithium, freeze/thaw issues, and operational issues. The NRPCT directed MSFC to modify an existing stainless steel sodium/potassium (NaK) circuit to allow it to be operated with lithium. Basic circuit components included a simulated reactor segment (a 37 pin core block, outer pressure shell, inlet plenum, outlet plenum), lithium to gas heat exchanger, electromagnetic (EM) liquid metal pump, load/drain reservoir, expansion reservoir, instrumentation, and trace heaters, as shown in Figure 13-21. Testing was to occur in the Early Flight Fission Test Facility (EFF-TF) vacuum chamber described in Section 13.3.2.

The lithium circuit was modeled using a MSFC developed Generalized Fluid System Simulation Program (GFSSP) code. In order to begin to validate the code with lithium properties and behavior (freeze/thaw) before the entire loop was assembled and tested, small test programs were conducted. The GFSSP analysis results provide the numerical predictions of pressure and temperature at various locations in the flow circuit.

Additional small-scale tests were also conducted to gain familiarity with liquid lithium handling. Information gained from these tests include:

- Solid lithium out-gases when melted.
- Wetting can be accomplished at the test temperatures.
- The technique for introducing lithium was verified.
- Thermocouples on the outside of the tubes normalize to the lithium temperature.

Upon concept down-select to a gas-Brayton system, work on the lithium test loop project was cancelled prior to commencement of any loop testing. The test loop circuit was removed from the EFF-TF vacuum test chamber and put into storage. The final MSFC close-out report for the lithium test loop is provided in Reference 13-9.

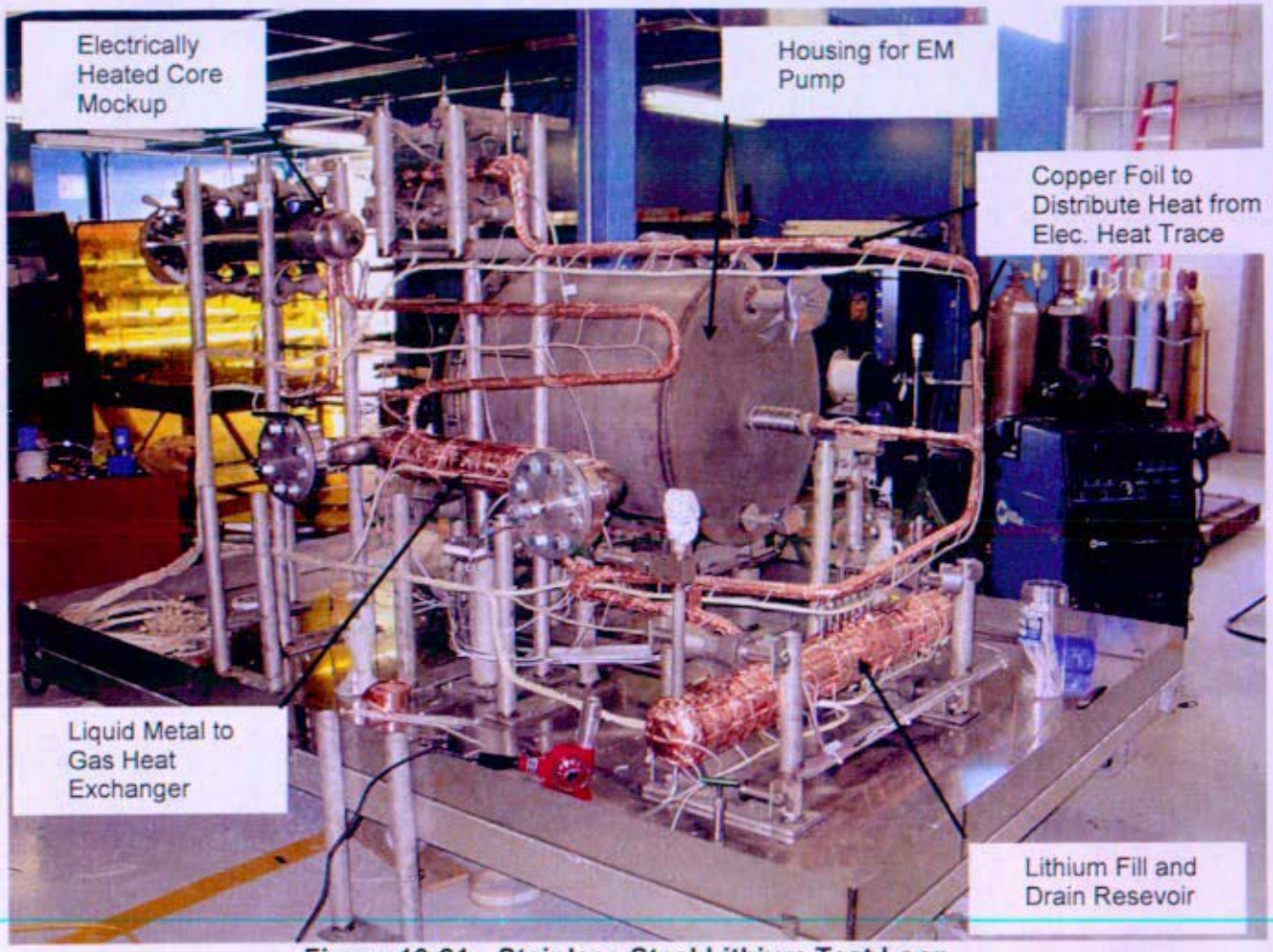



**Figure 13-21: Stainless Steel Lithium Test Loop**

### Refractory Metal Loop Cost Estimates

MSFC was to provide a rough order of magnitude (ROM) estimate for delivery a liquid lithium loop constructed from refractory metals. Four candidate materials were identified by the NRPCT: Mo-47.5%Re, T-111, ASTAR-811C, and Nb-1%Zr. The ROM cost estimates for Mo-47.5%Re and T-111 are shown in Table 13-7. This work was cancelled prior to completion of the estimates for the other two materials. The MSFC ROM reports are provided in References 13-17 and 13-18.

**Table 13-7: ROM Estimates for LM Loops Constructed of Refractory Metals**

| Description | Mo-47.5%Re | | Tantalum (T-111) | |
|---|---|---|---|---|
| | Cost (millions) | Delivery (months) | Cost (millions) | Delivery (months) |
| Basic Materials | | | | |
| ○ PM – Shapes (tubes, rod, sheet) | $1.50 | 9 | $3.00 | 16 |
| ○ Arc Cast – Shapes | $1.80 | 12 | | |
| Fabrication Equipment / Hardware | $1.75 | 12 | $1.75 | 12 |
| ○ Welding Monitoring (Chambers / Portable / NDE) | | | | |
| ○ Heat Treat Furnaces (Vacuum / Hydrogen) | | | | |
| Fabrication Design / Development | $2.00 | 12 | $3.00 | 12 |
| ○ Fabrication Processes / Procedures | | | | |
| ○ Experimental Material Evaluations | | | | |
| Component Fabrication (Core / HX / Tanks) | $1.00 | 12 | $1.50 | 12 |
| Assembly of Major Circuit Components | $1.00 | 9 | $1.00 | 12 |
| Integration Design/Development | $0.75 | 9 | $0.75 | 9 |
| ○ Layout / Geometry / Interfaces in Test Chamber | | | | |
| ○ Ancillary Systems (Heaters, Pump, Ins. etc.) | | | | |
| Test Chamber Integration / Ancillary Sys. Fabrication | $1.00 | 12 | $1.00 | 12 |
| ○ Dev. Procedures & Facility Modifications | | | | |
| ○ Acquire and Fabricate (Pump, Supports etc.) | | | | |
| **Total** (assuming PM material) | **$9.00** | **30** | **$12.00** | **36** |

### 13.6.2 Heat Pipe Reactor

Considerable historical life test data exists for sodium / refractory metal heat pipes at temperatures consistent with those needed for the JIMO design. Previous investigators had demonstrated heat pipe longevity of up to 50,000 hours, but documentation was seldom available on how temperature, material impurity levels, and mass fluence affected the corrosion behavior of the heat pipes. In addition, few post-test forensic examinations had been conducted. The purposes of this program were to verify that heat pipes built with current procedures met the historical longevity database and to then extend the database to other materials of interest (such as Nb1%Zr and T-111).

Since running 50,000 hour life tests was not a practical method of obtaining timely data, a key objective of this program was to establish an effective test method to provide both near term physical test results, as well as insight to allow extrapolation of life-limiting effects. The planned evaluation activity required around-the-clock operation of the heat pipes with the goal of accumulating up to three years of test time (approximately 25,000 hours). Data was expected to be produced early in the program. The first heat pipe would be removed after six months and examined by a combination of non-destructive and destructive methods to assess the effects of aging. This process would be repeated every six months to build confidence in extrapolations and provide insight into possible random manufacturing and processing defects.

The test hardware included sixteen heat pipes constructed of Mo-44.5%Re material (formed using the powder metallurgy method). The proposed wick structure was an annular crescent design fabricated from seven layers of 400x400 mesh cloth made from Mo-5%Re. The wick tube was to be equipped with a bonded plug at the evaporator end while the condenser end remained open (sealed by the excess liquid sodium which pools at the end of the condenser section). The evaporator end plugs were equipped with a zirconium-based getter pack to irreversibly trap impurities collected in the evaporator pool during normal operation. Power transfer into and out of the heat pipe was provided by non-contact methods to minimize the potential for introducing impurities. Power was to be supplied using a radio frequency induction coil on the evaporator section and removed from the condenser using a low pressure static gas (helium argon mixture) gap coupled water calorimeter. Each heat pipe temperature was to be monitored with a single non-contact optical pyrometer sighted at the evaporator exit, (just upstream of the calorimeter assembly).

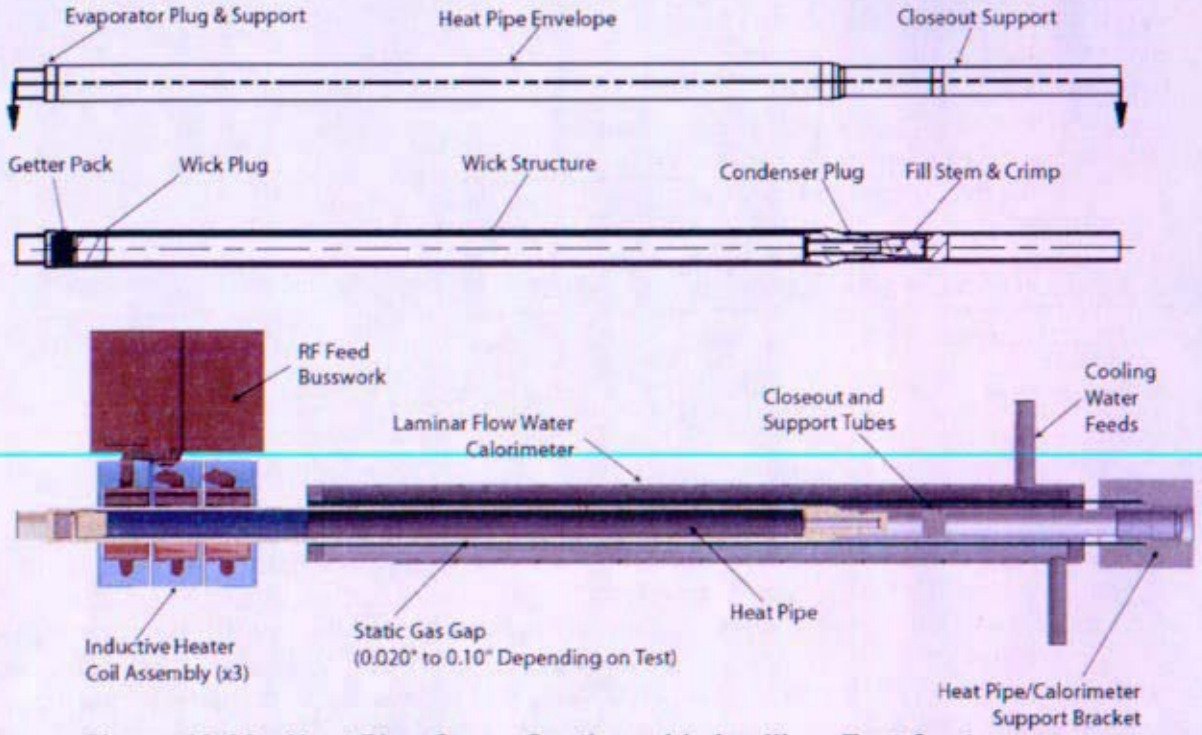



**Figure 13-22: Heat Pipe Cross Section with Ancillary Test Systems**

The accelerated heat pipe life test project was cancelled due to a shift in program direction with the selection of a gas cooled reactor concept to support nuclear electric propulsion. During execution of the project, a heat pipe design was established, a majority of the laboratory test equipment systems were specified, and operating and test procedures were developed. Procurements for the heat pipe units and all major test components were underway at the time the stop work order was issued. No technical issues had been identified which would have prevented testing as planned. The final MSFC close-out report is provided in Reference 13-16.

### 13.6.3 Gas Reactor

Upon concept down-selection, MSFC work was re-directed to focus on the following areas associated with the Direct Drive Gas – Brayton reactor module concept.

#### 13.6.3.1 Direct Drive Gas (DDG) Cooled Reactor Testing (P-BRY-2M)

The purpose of this effort was to focus on reactor core thermal-hydraulics and initial system integration issues using a non-nuclear, electrically heated reactor core that accurately simulated a direct gas cooled nuclear system. Specific work was to include: steady-state and transient testing, and development of dynamic models of the system heater controls to simulate reactivity feedback (neutronic response) in a non-nuclear test unit. Data from this testing was needed to guide development efforts for gas reactor modeling (i.e., heat transfer and pressure drop correlations). The testing was also to provide operational experience with testing a gas reactor at relatively high temperatures. The DDG reactor mockup was one previously developed jointly by SNL, LANL, and MSFC. Its design, annular flow around pins within a monolithic core block, was one being considered for Prometheus. As such, it provided a convenient test bed while more prototypical gas reactor mockups were designed and built. The DDG reactor mockup was to be refurbished and integrated into the EFF-TF vacuum chamber.

As this workscope was placed with MSFC only three months prior to project termination, no testing had occurred. Planned efforts included:

- Steady-state operation at various system pressures, power levels and flow rates to obtain baseline thermal/hydraulic data for core design models and comparison to transient conditions. Specific issues of interest included the pressure drop and temperature distribution with this type of annular design.

- Transient testing to understand reactor thermal-hydraulic performance during normal system startup and shutdown, as well as off-normal or casualty conditions (loss of flow, overpower, loss of coolant, etc.). Initial steady-state and transient testing was to be performed with pure nitrogen to validate system integrity and performance but the ability to use pure helium, helium/argon or helium xenon mixture was required to more accurately represent prototypical fluid properties.

- Incorporation of a closed Brayton component (a modified Capstone unit) into the MSFC test loop. Evaluation was to include:

    - Determination of the test conditions that could be achieved with DDG core and the existing system (i.e., pressure, temperature, power, etc.)

    - Determination of the ability to operate the Brayton unit with He/Xe or He/Ar working fluid

    - Recommendation of modifications to better incorporate a Brayton unit in a closed system.

- An engineering assessment of two options for integration of a Brayton cycle to the existing DDG cycle. Option 1 was a Sandia National Laboratories developed closed-loop brayton cycle using a modified, commercially available open-loop 30-$kW_e$ gas turbine. Option 2 was to buy a commercially available Brayton cycle and modify it consistent with the modifications performed by Barber-Nichols for the SNL funded unit. Analysis, layout drawings, and cost

estimates were to be generated for both options. This assessment was subsequently provided in Reference 13-13.

- Incorporation of high-fidelity neutronic models to provide simulated reactivity feedback. This approach allows a better understanding of system integration issues, system response times and response characteristics, potentially allowing for design improvements prior to large fiscal and staffing investments in a nuclear test program. The implementation of the DDG reactor operations was to be on a phased basis as follows (see Reference 13-15):

  - Phase 1: Initial integration of DDG with feedback control system. This phase was to use the DDG in a loop, with a compressor (for flow) and pre-heater located external to test chamber. No Brayton engine was to be installed. The purpose of this phase was to directly examine core responses (uncoupled and controlled) to various feedback signals.

  - Phase 2: Investigation of the DDG start-up, shutdown, and transient responses (nominal and off-nominal / off-design conditions). System response testing was to be carried out by studying the interaction between the DDG and the compressor and pre-heater.

  - Phase 3: Incorporation of a Brayton engine into the DDG loop. The Brayton engine was to be a closed Capstone unit. The Phase 2 tests would be repeated using this more prototypic system. Additional testing included a detailed analysis of the Capstone air bearings (using a Glenn Research Center algorithm), an assessment of Capstone turbine and compressor for other gas mixtures, and an assessment of how the system would respond to changes in applied electrical load.

Figure 13-23 shows the DDG unit assembly. The DDG unit contained an array of electric heaters to simulate fuel pins in 37 annular flow channels located within a solid matrix core (see Figure 13-24). Figure 13-25 illustrates how the DDG unit would be incorporated into MSFC's EFF-TF vacuum facility (Reference 13-12). The DDG vessel was capable of operating at the following maximum conditions: 0.37 MPa (53 psi), 1144K (1600°F) for up to 1000 hours using nitrogen as both the coolant gas and the surrounding ambient environment. Strain gauges were to measure thermal deformations at various locations on the unit. Locations were selected to measure growth in both radial and axial directions. This data was to be used in the thermal expansion finite element model and would eventually be used to provide thermal growth feedback for reactivity simulation. Thermocouples within the core block were to provide core temperature data in both the axial and radial directions. Steady-state and transient thermal and hydraulic gas data were required for the specified test points.

The maximum electrical power that could be generated using nitrogen gas was 24.0 $kW_e$. This yielded the estimated test conditions shown in Table 13-8.

**Table 13-8: Estimated DDG Test Conditions**

| Turbine speed (RPM) | Turbine inlet temp. | Flow rate | Thermal input ($kW_t$) | Maximum DDG temp. | Compressor inlet pressure | Compressor discharge pressure | DP across DDG | Overall system efficiency |
|---|---|---|---|---|---|---|---|---|
| 96,300 | 1044 K (1420°F) | 0.30 kg/sec (0.66 lb/sec) | 99.4 | 1144°K (1600°F) | 0.1 Mpa (14.7 psia) | 0.37 Mpa (53 psia) | 0.38 MPa (5.54 psia) | 24.10% |

Thermal and structural analyses showed that the DDG and Brayton systems, when combined, could operate at acceptable and satisfactory power levels and temperatures. Although pressure

drops across the DDG were slightly higher than desired, they were viewed as acceptable. Minor modifications would allow higher thermal input to support this testing.

The final MSFC close-out report for the DDG gas reactor effort is provided in Reference 13-14.

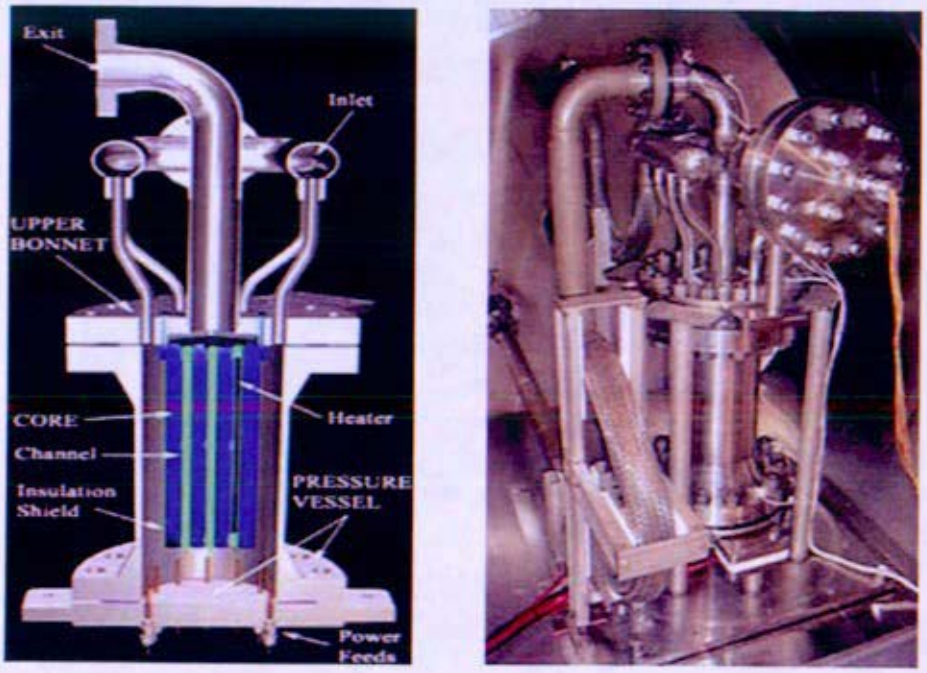



**Figure 13-23: DDG Assembly**

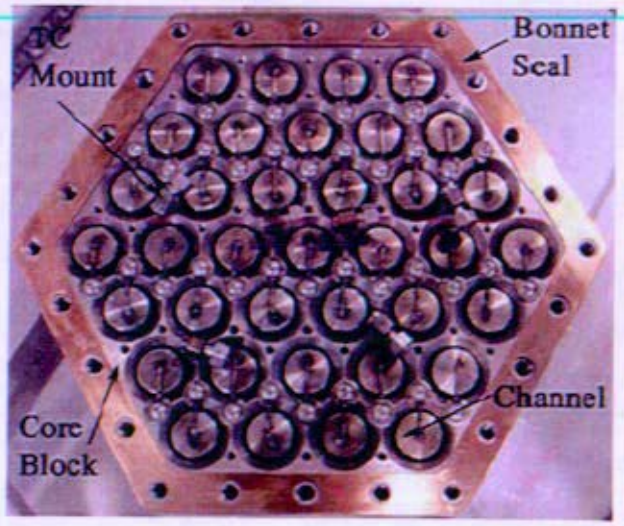
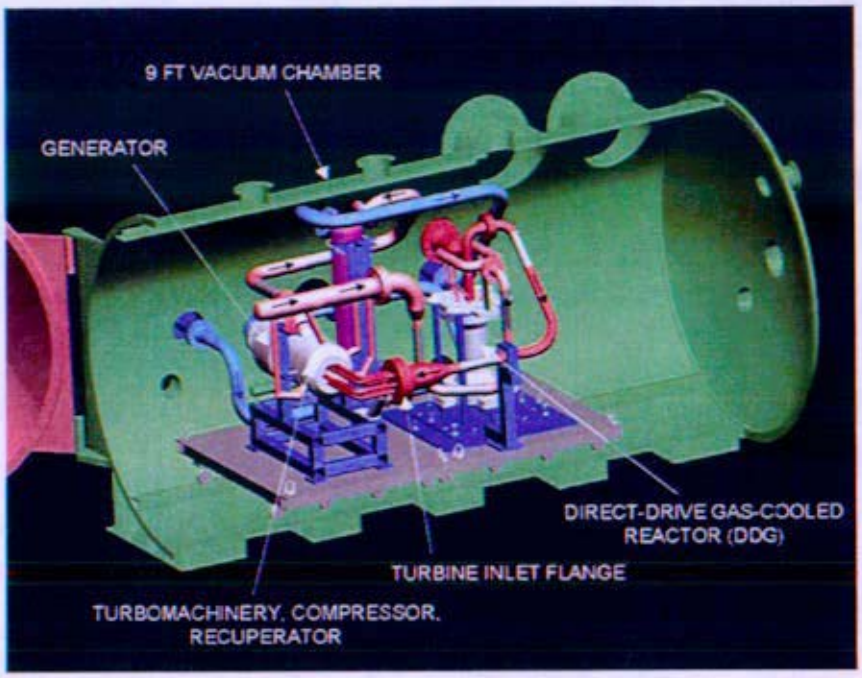



**Figure 13-24: DDG Core View Showing 37 Electrical Heating Elements**



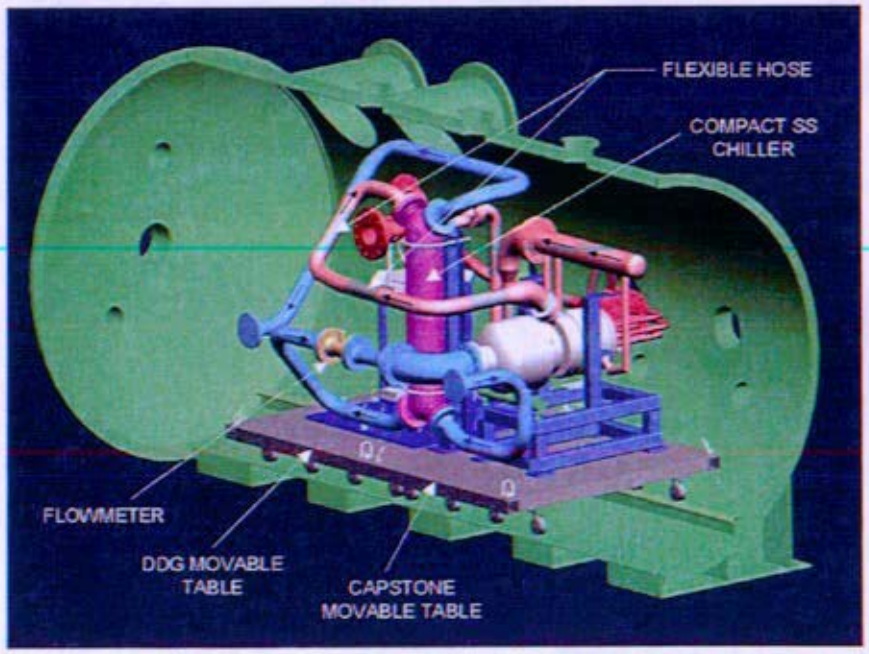




**Figure 13-25: DDG Assembly in the EFF-TF Vacuum Chamber**

### 13.6.3.2 Single Channel Testing (R-TH-3M)

Reactor design work supporting Project Prometheus focused on a gas-cooled reactor using a HeXe coolant mixture. Prototypic thermal hydraulic data was required to support the sizing effort for the core and Brayton heat exchangers. This data included pressure drop and heat transfer characteristics for the geometries and system conditions under consideration. Two reactor design issues arose that prompted the need for this test – a lack of heat transfer correlations for gas mixtures with Prandtl numbers of approximately 0.2, and potential inaccuracies in published correlations used in the evaluation of these gases in annular pin geometries. The goal of the single channel test was to obtain heat transfer correlations for low Prandtl number gas mixtures flowing through annular fuel pin geometries, and to compare this data to analytical codes and existing correlations to guide the core design process. The test hardware is depicted in Figure 13-26 through Figure 13-28.

Gas enters the inlet manifold, passes through a flow straightener (not depicted), and flows through the annulus region between the simulated fuel pin and the jacket (simulated core wall). Flow measurements were to be acquired by using a turbine flow meter. Temperature measurements were to be provided by K-type thermocouples placed along the length of the channel. Pressure measurements were made at the pressure taps along the channel length. Test data was to be acquired from a range of low power, low flow conditions to high power, high flow conditions.

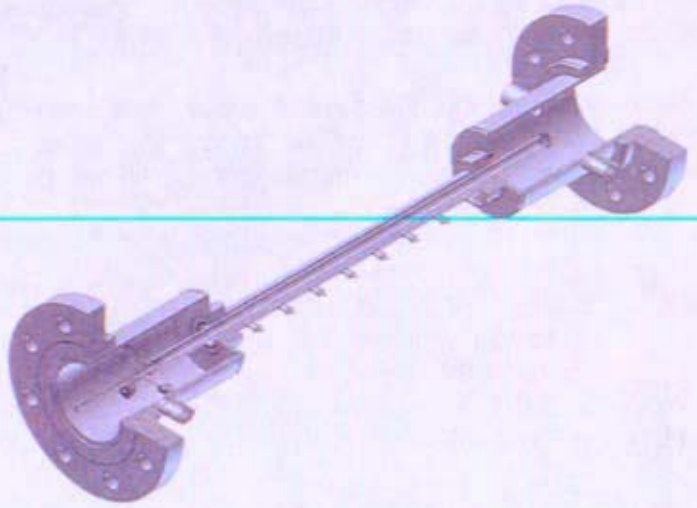


**Figure 13-26: Single Channel Test Hardware**

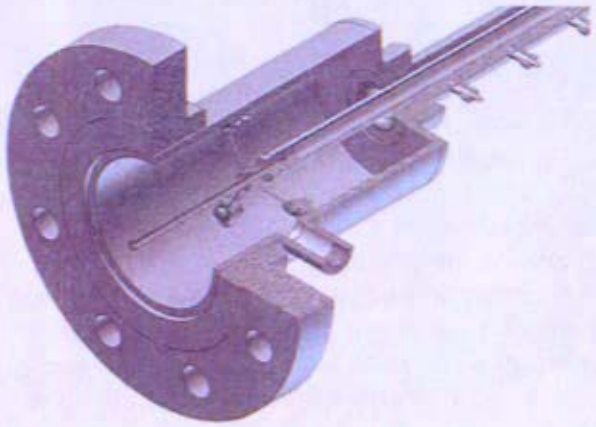


**Figure 13-27: Inlet Manifold**

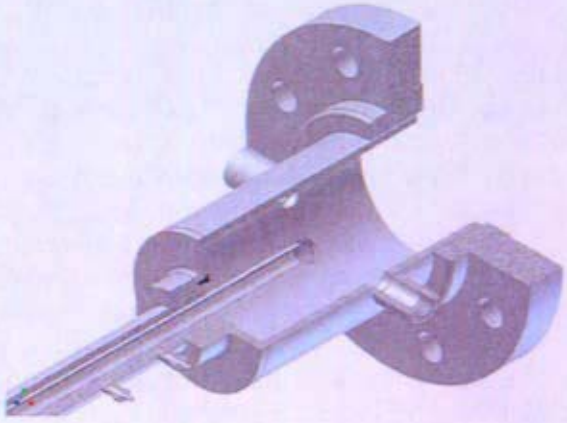


**Figure 13-28: Exit Manifold**

There were two phases of testing initially planned:

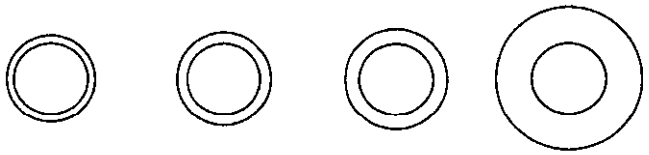
- Phase 1 testing would use a constant flow of pure gas (nitrogen or argon) at ambient temperature to obtain baseline heat transfer data.
- Phase 2 testing would use the appropriate HeXe gas mixture and be operated at prototypical conditions (see below). An electrically powered graphite heater located within the fuel tube provides the heat source, with the goal of matching the axial temperature rise expected for the reactor core.

  - Pressure: 1.38 to 4.0 MPa (200 to 580 psi)
  - GasTemperature: 800 to 1150 K (980 to 1610°F)
  - HeXe Mixture: 50 to 100% helium
  - Power: up to 6000W
  - Prandtl Number: 0.22 to 0.7
  - Reynolds Number: up to 30,000

Several annular geometries were to be included in both phases of these tests as detailed in Table 13-9. The MSFC close-out report for the single channel testing is provided in Reference 13-11.

**Table 13-9: Nominal Flow Passage Dimensions for the Single Channel Test**

| Test Section ID# | Geometry Type | Tube OD (in) | Jacket ID (in) | Annular Ratio (tube OD/Jacket ID) |
|---|---|---|---|---|
| AF1 | Annular Duct | 0.625 | 0.750 | 0.833 |
| AF2 | Annular Duct | 0.625 | 0.815 | 0.767 |
| AF3 | Annular Duct | 0.625 | 0.875 | 0.714 |
| AF4 | Annular Duct | 0.625 | 1.25 | 0.500 |




### 13.6.4 Electric Heater Development (R-TH-1M)

Operational testing of reactor module concepts and components requires a heat source to simulate the heat generated by the nuclear fuel. The focus of this effort was to develop and provide electrical heater elements that were as prototypic of the nuclear fuel geometry as practical (i.e., matching the performance characteristics of the core, not just the fuel temperatures). The possible use of refractory metals for the core design introduced material compatibility and contamination concerns, thus necessitating a sealed (sheathed) heating element design to prevent contamination of the reactor mockup or other loop components.

MSFC has extensive test experience with un-sheathed solid graphite heating elements. These heaters are robust, dependable, and can be machined to provide an axial power profile, if desired. They were the heater-of-choice for the DDG testing effort. A graphite rod is split down the middle of its axis, and acts like a large resistor (see Figure 13-29). Power is input at one end of the graphite, with the current flowing along one side of the rod and returned along the opposite half. Alumina shims inserted within the graphite split prevent contact which would short the heater. Additional alumina insulator rings place on the outside diameter of the element electrically isolate the heater from the test article. Total operating hours for these simulators (combined time of all individual simulators in all tests) was in excess of 20,000 hours and hundreds of thermal cycles with no heater rod failures.

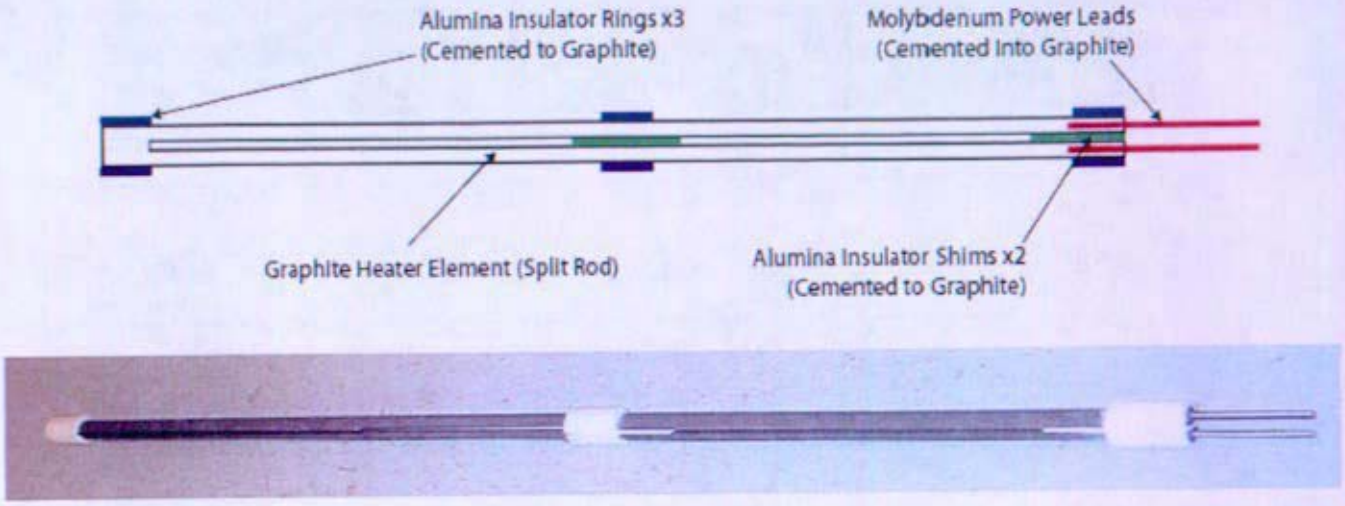



**Figure 13-29: Graphite Rod Heater Element**

However, these graphite heaters become fragile at small fuel pin diameters and they introduce contaminants detrimental to refractory metal core materials. In addition, they offer less flexibility in terms of providing specific axial heat flux profiles (although the desired profiles tended to be a relatively simple cosine shape). Liquid metal reactor designs being considered early in the project included those with small fuel pin diameters of 0.5 to 0.75 cm (0.2 to 0.3 in) in a refractory metal core. Therefore, early FY2005 development efforts were refocused on the use of alumina mandrels wrapped with various refractory metal wires or with carbon fiber rope (Figure 13-30).

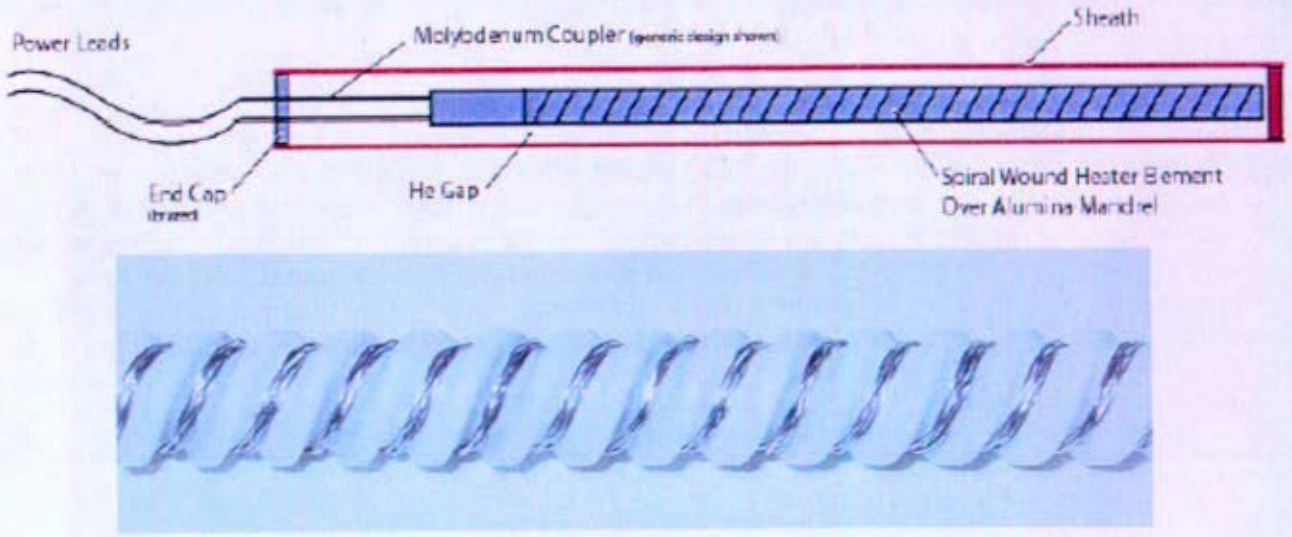



**Figure 13-30: Wire Wrapped Mandrel Heater Element**

The alumina mandrel provides the necessary structural strength and electrical insulation while the refractory wire wrap provides material compatibility with the core materials. The wires were wrapped in either a single pass or double pass fashion around a spiral groove etched along an alumina mandrel. Axial power profiling can be more accurately controlled than on solid graphite heaters by varying the helical pitch along the axis. The wire materials included rhenium, tantalum, niobium, tungsten, hafnium, and carbon fiber, and testing included both single and braided wires. Materials recommended for continued development include tantalum and tungsten braid. All successfully ran for over 100 hours at 1200 watts (the acceptance criteria) with no failures. Disadvantages of the alumina/wire wrap heaters include assembly difficulties (maintaining a tight wrapping of refractory wire around the mandrel), interactions between the alumina and wire, and higher material and fabrication costs (at least five times higher).

Future thermal simulator work was to extend testing on the current materials and assembly designs. Recommended work included:

- incorporation of diagnostic instrumentation within the structure of the heater assembly, and within the test chamber
- development of an automated control system
- adoption of more rigorous cleaning and chamber preparation procedures
- conduction of tests in both vacuum and high purity inert gas environments
- incorporation of a heat removal method to better mimic the assembly boundary conditions in the full test article
- development of advanced thermal simulator designs to better match key performance properties of nuclear fuel elements

Just prior to project termination, the reactor core design requiring smaller diameter fuel pin designs was losing favor (although the final decision had not yet been made). In addition, MSFC was developing refractory metal sheathing to use on all heater designs, including the solid graphite rods. The sheathing isolates any heating element contaminants from the core materials. It was believed that the best use of restricted funds may be to re-direct MSFC efforts to return to the approach judged most achievable in the short term – development of robust, larger diameter, solid graphite heaters, sheathed in refractory metal.

Reference 13-10 provides a thorough review of the work done by MSFC on heater development through March 2005. A final closeout report of this work was provided in Reference 13-19.

## 13.7 Glenn Research Center (GRC) Testing

The NASA Glenn Research Center was involved in various testing activities related to the Prometheus project prior to and during the NRPCT involvement. The NRPCT had not yet entered into any formal contractual agreements to direct the testing at GRC, and therefore, no formal reports were provided. However, GRC did keep the NRPCT aware of the pertinent testing activities and provided periodic informal summaries. A number of conference papers were also generated from these efforts. This testing activity is summarized below.

### 13.7.1 Bearing Testing

Gas foil bearings were identified as a key technology requiring extensive testing during the evolution of the Prometheus spacecraft. Testing activities related to the bearing development involved the upgrading and acquisition of various test rigs and the actual testing of bearings on existing rigs. In order to test at the high pressures envisioned for the Prometheus spacecraft, a high-pressure test rig was being developed from an existing rig. This modified test rig will be capable of testing up to 700 psig. It is shown below in Figure 13-31.

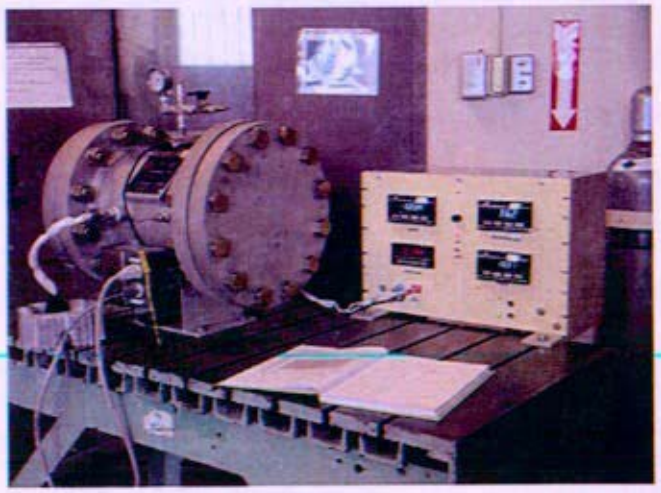


**Figure 13-31: The High Pressure Foil Bearing Test Rig undergoing Shakedown Tests**

Additional bearing testing took place to investigate the performance of the gas foil bearings in gases other than air. GRC completed a small amount of preliminary testing in helium, air, and argon over a pressure range of 0.05 to 0.255 MPa (7 to 37 psi). This test data suggested that the load capacity of the bearing increased slightly with pressure and molecular weight, as was expected. A further description of this testing is provided in Reference 13-26. Bearing testing in He-Xe at higher pressures was in the planning stage.

### 13.7.2 Alternator Testing

Ongoing work was being conducted at GRC in the area of high power alternator testing. The main objective of this work was to procure an alternator test unit and associated test support equipment to conduct tests that would aid the design of the Prometheus alternator. The alternator test unit would therefore be representative of the envisioned design, being of similar power level, materials, and operating frequency. The development of the alternator test unit was taking place at Hamilton

Sundstrand under contract by GRC. At the end of NRPCT involvement in the project, GRC had been overseeing design reviews at Hamilton Sundstrand. The delivery of the test unit was planned for February 2006 with testing to begin later in the year. Figure 13-32 below shows the Hamilton Sundstrand design configuration.

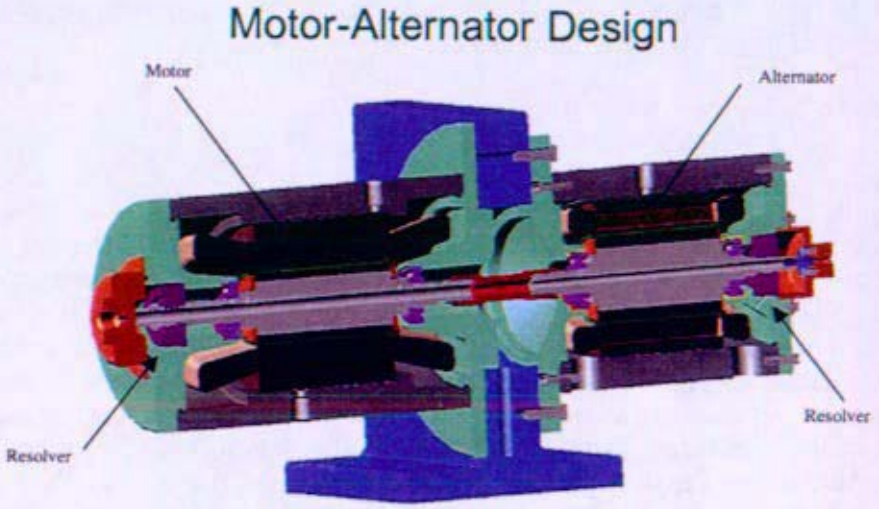



**Figure 13-32: Hamilton Sundstrand Motor-Alternator Design Configuration**

### 13.7.3 Brayton Transient Testing

GRC has had a long history of testing Brayton units starting in the 1960s. This work primarily involved the 10.5-kW Brayton Rotating Unit (BRU) and the 2-kW mini-BRU. More recently in support of the Prometheus Project, the mini-BRU was returned to operating condition and placed in the Vacuum Facility #6 for thermal transient testing. A draft test plan matrix is provided in Reference 13-27. The primary objective of this testing was to support the various closed cycle Brayton modeling efforts that were underway. Due to the existing instrumentation system, this testing would be focused on the slowest characteristic thermal time scales. Plans were in place to upgrade the instrumentation in FY06 to allow better definition of rapid transients, such as those seen during start-up. Although testing began prior to NRPCT's devolvement in the project, no formal test results had been published to date.

### 13.7.4 Materials Testing

GRC was performing various materials tests focused on joining techniques. In particular, joining options for dissimilar materials were being evaluated since it was likely that such joints would be required somewhere in the plant. Two of the key transitions being evaluated were: 1) refractory to non-refractory joint to transition from high temperature reactor to lower temperature energy conversion system, and 2) titanium to carbon-carbon brazing in the heat exchanger region. In addition to these joining tests, GRC was performing creep testing of MAR-M247 superalloy for turbine wheel applications. Formal documentation of this work was not yet issued at the time of this report.

## 13.8 Final Perspectives

Because significant test programs had not yet commenced for the project prior to termination, there are few lessons learned regarding testing. However, some general testing perspective gained in the sixteen months of the project is warranted.

### "Test as You Fly, Fly as You Test" Philosophy

NASA/JPL discussed with NRPCT their philosophy of "test as you fly, fly as you test." This was based upon significant lessons learned from previous missions and the need to do everything practical to exercise the actual flight system on the ground, since repair after launch would not be possible. The ideal would be to fully test the complete system on the ground in a prototypical manner to provide greater certainty of success and help eliminate unknown issues that may not have surfaced in more isolated, separate effects test programs. While this approach makes sense, it was recognized and accepted early on that the presence of a nuclear reactor would present significant limitations in the ability to meet this principle. All plans formulated assumed that the fueled reactor would be integrated with the spacecraft after integrated system testing was completed. It would not be feasible to launch a reactor that had run at significant enough power to produce a fission product inventory that would make the impact of a reentry accident unacceptable. Therefore, truly prototypical integrated testing would never quite be achieved. To address this limitation, the test strategy relied upon multiple test programs, including ground test reactors, to achieve a similar result. For a mission of this type (i.e., space nuclear power), this will always be a challenge.

### Test Early and Often

A major benefit of the gas Brayton concept was that it was viewed as more "testable" than the liquid metal systems. This is particularly true when non-refractory materials are used for the pressure boundary. The need to commence testing early in the program and to continually iterate between testing and design was recognized because of the lack of significant experience with the reactor plant concepts being considered for space applications. While this issue is related to the "test as you fly..." perspective above, it is different in that it drove the desire for early, fundamental testing to gain insight into the design, even when the hardware being tested was not prototypical in many ways. The value in early testing using commercially available hardware was not universally accepted and a source of much debate. This early, fundamental testing was intended to quickly lead to testing of first generation hardware, culminating in testing of final flight hardware. The need for 3 key test programs (TTM, EM, and QM) was also debated because of time and cost constraints. It was also unclear how much the hardware would evolve between these successive designs to warrant new testing. Throughout these debates, the philosophy of testing early and often weighed heavily, and the decision to reduce the number of test programs would be only made later in the project if confidence was gained to provide adequate mission assurance without additional data.

**United States Nuclear Testing Infrastructure**

The selection of a fast reactor with the possibility of refractory alloy or ceramic core materials led to the need for significant nuclear and materials test programs that could not be entirely accommodated in the United States because of the decline of nuclear energy research facilities in this country since the 1980s. Specifically, no adequate fast flux reactors were available to perform fuel and materials irradiation testing. For this reason, the Japanese JOYO reactor was being pursued to perform the key materials irradiation testing. Other options, including Russian reactors were also being considered to address the lack of facilities in the United States. However, both of these options faced significant risk of not being executed in a timely manner due to political and security issues.

The SNAP programs of the 1960s and 1970s had a significant nuclear testing infrastructure available and a great deal of data was obtained during those programs. SP-100 had considerably less nuclear testing infrastructure available. This was a significant issue with SP-100 and some people familiar with that project considered the expense and difficulty of constructing a ground based prototype one reason for the project's cancellation. Project Prometheus had even less nuclear testing infrastructure available and as a result, performance of critical and power range testing (i.e., ground test reactor) were significant issues to meeting the aggressive project milestones. A decision to seriously pursue space nuclear power will require an adequate nuclear testing infrastructure to provide key data and longer term research and development support. Such an infrastructure will likely rely upon a multinational approach unless nuclear power research resumes in earnest in the U.S. However, complete reliance on foreign research reactors will pose concerns from a security aspect and will significantly reduce the flexibility in the type and timing of testing that can be accomplished.

**Loss of Space Nuclear Power Expertise**

At the start of NR Program participation in the Prometheus program and throughout the sixteen months of effort, NRPCT solicited input from a variety of individuals who worked on the SNAP and SP-100 space nuclear power programs. In addition, personnel who worked on some of the liquid metal and gas reactor programs at Oak Ridge National Laboratory (ORNL) in the 1960s and 1970s discussed their experience in establishing and running these challenging test programs. These individuals provided valuable insight into the successes and failures of these prior programs. These personal meetings were particularly beneficial since the documentation of these prior programs was not always complete and the first-hand accounts of the work provided greater perspective than would be gained simply by reading the formal reports. One observation is that this expertise is being lost as the number of the engineers and scientists from the 1960s, 70s and 80s are declining. The SNAP program of the 1960s had the most direct knowledge of space nuclear power, since a significant amount of reactor testing was performed and it is the only U.S. program to actually launch and deploy a space reactor. SP-100, while also a key program in the 1980s, never performed nuclear testing and never delivered flight hardware, so less direct design and testing experience is available from this program. Prometheus accomplished a great deal during the short time period it was in existence, but this program matured even less than SP-100 and no significant testing started prior to its termination, so little testing experience is available from this effort.

Space nuclear power poses many testing challenges and the ability to use the expertise (and infrastructure) from prior programs is a significant enabler to quickly and efficiently meet the many needs of such an effort. As pursuit of space nuclear power moves further beyond the peak research efforts in the 1960s, delivering space nuclear power becomes increasingly difficult.

## 13.9 References

**13-1** KAPL / Bettis Letter SPP-67210-0006 / B-SE-0128, "Space Reactor Program Test Index-For Approval," June 30, 2005

**13-2** NR Letter E#05-03014, "Space Reactor Program-Scope and Format for Space Reactor Program Test Index; Approval With Comments," August 5, 2005

**13-3** Bettis / KAPL Letter B-MT(SMAT)-005 / MDO-723-0019, "Space Materials Plan – For Technical Approval," April 4, 2005

**13-4** NR Letter S#05-02607, "Space Materials Plan – Approval With Comment," August 5, 2005

**13-5** KAPL Letter SPP-67210-0003/Bettis Letter B-SE-0088, "Space Nuclear Power Plant (SNPP) Integrated Near Term Test Plan and Procurement Strategies-For Naval Reactors Technical and Funding Approval," April 12, 2005

**13-6** NR Letter E#05-01782, "Space Reactor Program-Near Term Test Plan and Procurement Strategies to Support Concept Development of Primary Plant Systems and Components; Partial Approval," May 13, 2005

**13-7** KAPL Letter SPP-SPPS-0029, "KAPL Space Power Program Fluid Mechanics Laboratory Test Program Closeout Report," November 15, 2005

**13-8** Wright, S.A., Fuller, R., Lipinski, R.J., Nichols, K., Brown, N., "Operational Results of a Closed Brayton Cycle Test Loop," Space Technology and Applications International Forum – STAIF 2005, CP746, February 2005

**13-9** MSFC Report ER11-05-WI4a-001, dated 24 June 2005, "Final Report – Documentation of Stainless Steel, Lithium Circuit Test Section Design," T.J. Godfroy

**13-10** MSFC Report ER11-05-WI1-001, dated 30 Mar 2005, "Heater Development, Fabrication and Testing: Analysis of Fabricated Heaters," S. Bragg-Sitton, R. Dickens, J. Farmer, J. Davis, and M. Adams

**13-11** MSFC Report ER11-05-WI4d-001, dated 28 October 2005, "Heat Transfer and Pressure Drop in Concentric Annular Flows of Binary Inert Gas Mixtures," R. Reid, J. Martin, D. Yocum, E. Stewart

**13-12** MSFC Report ER11-05-WI4C3-001, dated 12 August 2005, "Evaluation of an Integrated Direct Drive Gas-Cooled Reactor Simulator and Brayton Cycle, Interim Report," D. Andy Hissam, Eric Stewart

**13-13** MSFC Report ER11-05-WI4C3-002, dated 30 September 2005, "Evaluation of an Integrated Direct-Drive Gas-Cooled Reactor Simulator and Brayton Cycle, Final Report," D. Andy Hissam, Eric Stewart

**13-14** MSFC Report ER11-05-WI4C1-001, dated 15 October 2005, "Final Report-Documentation of Status of Direct Drive Gas Cooled Reactor Simulator," T.J. Godfroy, A. Garber, S. Bragg-Sitton

**13-15** MSFC Report ER11-05-WI4c4-001, dated 14 October 2005, "Application of Simulated Reactivity Feedback in Non-Nuclear Testing of a Direct Drive Gas Cooled Reactor", S. Bragg-Sitton, K. Webster

**13-16** MSFC Report ER11-05-WI2-004, dated 16 June 2005, "Closeout Report for the Refractory Metal Accelerated Heat Pipe Life Test Activity," J. Martin, R. Reid, E. Stewart, R. Hickman and O. Mireles

**13-17** MSFC Report ER11-05-WI4B-001.0, dated 10 March 2005, "Cost Estimate for a Mo-47.5% Re Refractory Metal Flow Circuit Concept Based on a Stainless Steel Lithium Circuit," R.R. Hickman, A.J. Bryhan, G. Schmidt, J.J. Martin, T.J. Godfroy

**13-18** MSFC Report ER11-05-WI4B-003, dated 10 May 2005, "Cost Estimate for a Tantalum Alloy Refractory Metal Flow Circuit Concept Based on a Stainless Steel Lithium Circuit," A.J. Bryhan, R.R. Hickman, J.J. Martin, T.J. Godfroy

**13-19** MSFC Report ER11-05-WI1-002, dated 15 October 2005, "Heater Development, Fabrication and Testing: Update", S. Bragg-Sitton, R. Dickens, J. Farmer, J. Martin, K. Webster, M. Adams and J. Davis

**13-20** KAPL / Bettis Letter SPP-67410-0006 / B-SE-0116, "Space Reactor Physics Test Plan; for Information", May 25, 2005

**13-21** NASA Kennedy Space Center Letter, KS-VA-7384, 6/17/05

**13-22** Bettis Letter B-SE(SPS)GT-005, "Space Nuclear Power Plant - Ground Test Reactor Facility Planning Closeout Report - For Information," December 13, 2005

**13-23** EB Letter 472-SPP-4389/JHC/7.1.3, "Space Nuclear Power Plant (SNPP), Rough Order of Magnitude (ROM) Budgetary Cost Estimate for Reactor Module Integration Contractor (RMIC) Effort," 9/30/05

**13-24** NGNN Letter 1143T-0052, "Rough Order of Magnitude (ROM) Estimate for Space Reactor Program; Bechtel Bettis Reactor Plant Planning Yard (RPPY) Purchase Order 2101506 (NGNN Job Order 1143T)," 8/31/05

**13-25** BWXT Letter CP-054-233, "ROM Cost Estimate for Space Reactor Assembly and Facility Modifications," 8/19/05

**13-26** Dellacorte, C., et al. "Advanced Rotor Support Technologies for Closed Brayton Cycle Turbines," 3rd International Energy Conversion Conference, AIAA 2005-5513, August 2005.

**13-27** Hervol, D., "Closed Cycle Brayton Power Conversion Unit Thermal Transients Test Plan (DRAFT)."

**13-28** SPP-67410-0013 / B-SE(RE)-0003, "Prometheus Reactor Pre-Conceptual Design Report", dated 01/27/2006

# Section 14
# Plant Materials Summary

*PRE-DECISIONAL - For planning and discussion purposes only*

(Intentionally Blank)

# Plant Materials Summary

## Table of Contents

14 Plant Materials Summary ..... 5
14.1 Summary and Conclusions ..... 5
14.2 Discussion ..... 6
14.3 Material Cases ..... 7
14.3.1 Material Case 1 – Refractory metal alloy core with Ni-base superalloy vessel piping and equipment ..... 7
14.3.2 Material Case 2 – Refractory metal alloy core and vessel with Ni-base superalloy piping and equipment ..... 8
14.3.3 Material Case 3 – Refractory metal alloy core, vessel and hot leg pipe with Ni-base superalloy cold leg piping and equipment ..... 9
14.3.4 Material Case 4 – Silicon carbide core with Ni-base superalloy vessel piping and equipment ..... 10
14.4 References ..... 11

## List of Figures

Figure 14-1 Material Case 1 ..... 8
Figure 14-2 Material Case 2 ..... 9
Figure 14-3 Material Case 3 ..... 10
Figure 14-4 Material Case 4 ..... 11

(Intentionally Blank)

# 14 Plant Materials Summary

## 14.1 Summary and Conclusions

Two primary concerns for the Reactor Module are the materials capability and longevity. To address these concerns the NRPCT established a plan for materials development efforts that concentrated on specific materials and manufacturing issues associated with the Reactor Module focusing on the pressure boundary and components within. The plant materials portion of this plan is summarized herein. Some general conclusions can be drawn from the research and work that was done to date. These are:

- Potential pressure boundary materials identified for Reactor Module use were Ni-base superalloys and refractory metal alloys.
- Potential pressure boundary Ni-base superalloys were Nimonic PE-16, Alloy 617 and Alloy 230. Ni-base alloys have a well-developed commercial fabrication infrastructure, and their long-term thermal creep behavior is reasonably well known.
- Niobium, tantalum and molybdenum-base refractory metal alloys were under consideration for core and pressure boundary materials due to their high thermal creep resistance (FS-85, ASTAR-811C, T-111, PWC-11, MoRe, and Ta-10W).
- Silicon carbide maintains excellent high temperature strength and resistance to creep and radiation damage but suffers from difficulty in retaining fission products in its composite form and poor ductility in its monolithic form.
- Oxide dispersion strengthened (ODS) materials have promising creep behavior, but were eliminated due to very poor weldability.
- Use of refractory metal alloys in conjunction with Ni-base superalloys would possibly require the use of coatings to prevent the mass transport of impurities such as carbon from the Ni-base materials from being adsorbed by the refractory metal alloys and promoting embrittlement.
- Candidate pressure vessel materials of Ni-base and refractory metal alloys are susceptible to radiation embrittlement at relevant space reactor conditions. Nuclear grade Ni-base alloys and cobalt-base alloys may be viable options, but require testing and development.
- Development of passive methods (e.g., getter) for controlling the oxidation and carburization potentials in the Reactor Module working gas may be necessary to maintain the mechanical properties of any selected structural materials.
- Titanium was being considered for components up to a temperature of 600 K.
- Austenitic and ferritic / martensitic steels were not considered for the pressure vessel as they do not have sufficient thermal creep resistance.

Reference 14-1 documented a materials assessment for Prometheus that focused on reactor outlet temperatures up to 1350 K. The purpose of the assessment was to narrow the number of space reactor plant concepts being considered to support the Prometheus SNPP development schedule. In February 2005, Naval Reactors Prime Contractor Team (NRPCT) decision teams reviewed the compiled technical information and analyses and recommended a gas-cooled reactor with a directly coupled Brayton energy conversion system to provide space nuclear power in support of Project Prometheus.

The Reference 14-2 Space Materials Plan was submitted for NR approval which presented a strategy that was developed to specifically support the delivery of a direct gas Brayton nuclear power plant system for the Prometheus JIMO mission. In this plan the NRPCT outlined the following approaches:

- Recommend the most promising materials for all major systems in FY-05 based upon limited performance data.
- Carry fuel system options through irradiation testing, but focus the limited fuel development resources and national infrastructure of the effort on a primary candidate system and a limited effort on backup approaches.
- Use modeling and bench-top testing, to close gaps in the data, at a level well beyond historical experience.
- Perform simultaneous separate effects and integrated testing activities.
- Utilize DOE, NASA, commercial and international infrastructure, experience and expertise.

The Space Materials Plan was approved with comment by Reference 14-3.

## 14.2 Discussion

While plant material selections were not finalized, the NRPCT worked toward narrowing the list of possible material systems. The Direct Gas Brayton system uses a common reactor coolant and Brayton working fluid where materials selected for the fuel, clad, reactor vessel, core structure, piping, and energy conversion equipment will be exposed to the same gas in a recirculating loop. This design creates the potential for impurity transfer between the loop materials that can significantly impact the mechanical properties of the structural materials in contact with the gas. Reference 14-2 identified material categories on which work continued until the termination of NRPCT involvement. These material categories were chosen based on temperature, anticipated stresses and neutron fluence for different portions of the reactor module. Refractory metal alloys and silicon carbide were identified for the reactor core, refractory metal alloys and Ni-base superalloys for the reactor vessel and hot leg piping (piping between the reactor outlet nozzle and the turbine inlet) and Ni-base superalloys for the energy conversion equipment (turbine, piping and coolers). In addition, early work with Northrop Grumman indicated that Ti alloys would be considered for use in the Heat Rejection Segment.

Results from a thermochemical analysis between core and plant structural materials showed a strong driving force for the mass transport of impurities, such as carbon, from nickel-base superalloys to refractory metal alloys that would promote interstitial embrittlement of the latter. Mitigation of this effect may require lower operating temperatures, the development of protective coatings, or the use of alternate materials of construction. Further details of this work and the results can be found in Reference 14-6.

High temperatures anticipated for portions of the energy conversion system pushed materials selection to Ni-base superalloys for the plant ducting and hot-section components of the

turboalternator. All materials exposed to the working fluid gas stream need to be considered as possible contributors to environmental degradation of the system, but lower temperature regions in the recuperator, aft piping, and gas cooler may allow for other material options. Component development programs were in progress with various vendors doing scoping studies and evaluations for the turboalternators and heat exchangers with each vendor recommending alloys of construction for their specific component.

Two solid solution strengthened Ni-base alloys (Alloys 617 and 230) and one precipitation hardened Ni-base alloy (Nimonic PE-16) were selected for the JOYO (Japanese reactor) test program (Reference 14-4). Hastelloy X was also considered for use as a pressure boundary material, as this material was investigated in previous space reactor programs. However, it was not included in the JOYO testing because of inferior elevated temperature properties compared to Alloys 617 and 230 as well as the limited amount of test space in the JOYO fast reactor.

Diffusion of Helium through Ni-base alloys was considered during the material evaluation process. Reference 14-8 discusses the permeability of helium through Ni-base alloys and microcracks and concludes that diffusion is not a concern and that well constructed and tested systems would have no problems with porosity and microcrack leakage.

## 14.3 Material Cases

The combinations of the candidate pressure boundary and core materials comprised a material system. The material systems considered were:

1. A refractory metal alloy core coupled to a Ni-base superalloy vessel and plant equipment, with some titanium plant components (cooler tubing).
2. A refractory metal alloy core coupled to a refractory metal alloy vessel and Ni-base superalloy plant system, with some titanium plant components (cooler tubing).
3. A refractory metal alloy core coupled to a refractory metal alloy vessel with a refractory metal alloy hot plant system and a Silicon Nitride turbine, perhaps with Ni-base superalloy and some titanium plant components (cooler tubing) in the cooler parts of the system.
4. A SiC core coupled to a Ni-base superalloy vessel and plant systems, with some titanium plant components (cooler tubing).

Each of these systems was examined for strengths and weaknesses compared to the other cases. These are summarized in the following sections.

### 14.3.1 Material Case 1 – Refractory metal alloy core with Ni-base superalloy vessel piping and equipment

Figure 14-1 shows a representation of the material options for Material Case 1. This case shows the refractory metal alloy core completely contained within a Ni-base superalloy vessel. Refractory metal alloys suffer from interstitial embrittlement after adsorption of impurities such as oxygen, carbon and nitrogen, so precluding their exposure to external environmental conditions was a major goal of the NRPCT. Protection of the refractory metal core from both micrometeoroids for the flight unit and Earth's atmosphere for the Ground Test Reactor (GTR) is provided by the He-Xe coolant within the Ni-base superalloy vessel. However, due to their sensitivity to interstitial impurities likely to be present in the coolant, core refractory metal alloy components would likely need to be coated for protection.

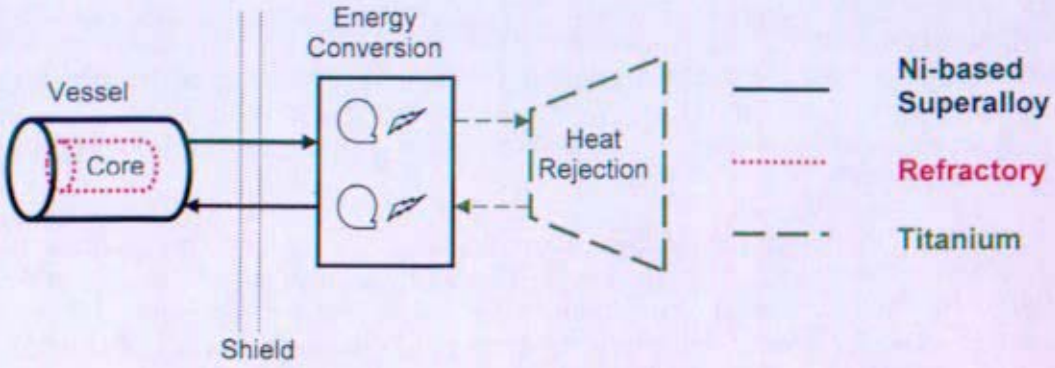



**Figure 14-1 Material Case 1**

| Strengths | Weaknesses |
|---|---|
| Refractory metal alloy core has very robust elevated temperature strength and creep resistance. | Nickel-base alloys are susceptible to radiation-induced embrittlement and may not allow adequate life. |
| Refractory metal alloy core is protected from impurities in the external environment for simplified ground based testing. | Refractory metal alloys are susceptible to radiation hardening and embrittlement at low temperatures, limiting thermal cycling. |
| Ni-base superalloy pressure vessel is more robust to chemical interactions from the coolant and external environment. | Refractory metal alloys are likely susceptible to radiation-induced phase stability at elevated temperatures. |
| No dissimilar metal joints. | Both Ni-base and refractory metal alloys may require coatings or controlled coolant chemistry to prevent impurity transport and adsorption. |

### 14.3.2 Material Case 2 – Refractory metal alloy core and vessel with Ni-base superalloy piping and equipment

Figure 14-2 shows a representation of the material options for Material Case 2. This case may be necessary if testing found that the Ni-base superalloy pressure vessel could not provide the lifetime necessary in the high radiation environment near the reactor core. This case would provide some significant challenges in building and testing a GTR because of the exposed high temperature refractory material. It also presents challenges in making a strong dissimilar metal joint between the Ni-base superalloy plant components and the refractory metal alloy reactor vessel.

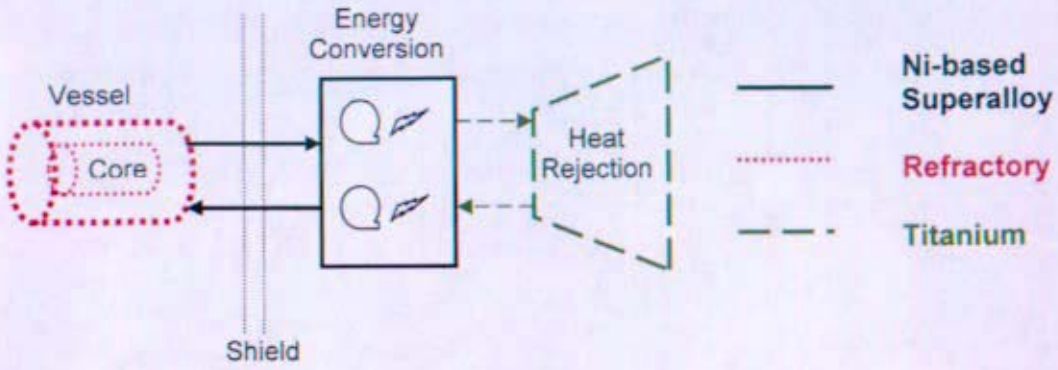



**Figure 14-2 Material Case 2**

| Strengths | Weaknesses |
|---|---|
| A refractory metal alloy vessel would permit operation to higher temperatures with increased efficiency. | Dissimilar metal joint required, which is a potential pressure boundary weakness. |
| Refractory metal alloy core has very robust elevated temperature strength and creep resistance. | Refractory metal alloys are susceptible to radiation hardening and embrittlement at low temperatures, limiting thermal cycling. |
| Refractory metal alloy core is protected from impurities in the external environment for simplified ground based testing. | Refractory metal alloys are likely susceptible to radiation-induced phase stability at elevated temperatures. |
| | Both Ni-base and refractory metal alloys may require coatings or controlled coolant chemistry to prevent impurity transport and adsorption. |
| | Exterior surface of the refractory metal alloy pressure vessel would need a very robust coating and/or ground-based testing is a vacuum chamber. |

### 14.3.3 Material Case 3 – Refractory metal alloy core, vessel and hot leg pipe with Ni-base superalloy cold leg piping and equipment

Figure 14-3 shows a representation of the material options for Material Case 3. This case is very similar to Case 2 except the refractory metal to Ni-base superalloy joint is located farther away from the reactor vessel, perhaps the entire hot leg would be refractory metal alloy and even the turbine casing. The dissimilar joint would still be required on the return piping (cold leg). This case was broken out separately to demonstrate that flexibility exists in determining the location of the dissimilar metal joint and that the location was never finalized.

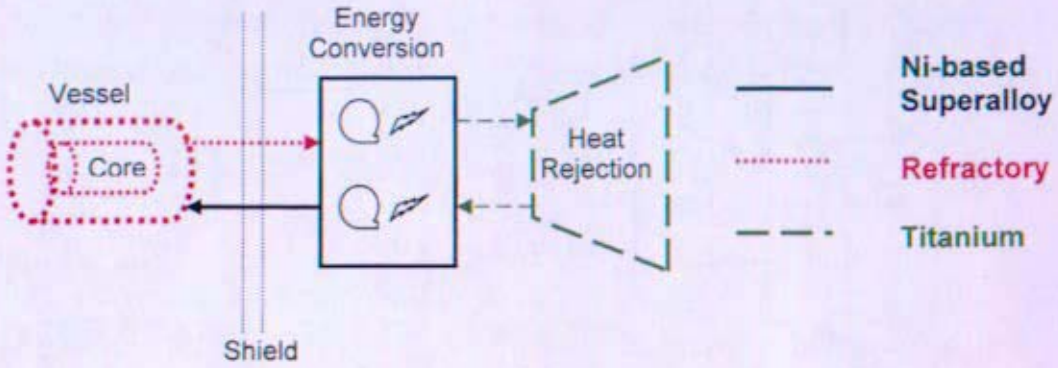



**Figure 14-3 Material Case 3**

| Strengths | Weaknesses |
|---|---|
| A refractory metal alloy vessel would permit operation to higher temperatures with increased efficiency. | Dissimilar metal joint required, which is a potential pressure boundary weakness. |
| Flexibility in design to allow the location of the dissimilar metal joint to be located in a cooler section, minimizing microstructural phase instability and the degradation of joint integrity. | Refractory metal alloys are susceptible to radiation hardening and embrittlement at low temperatures, limiting thermal cycling. |
| Refractory metal alloy core has very robust elevated temperature strength and creep resistance. | Refractory metal alloys are likely susceptible to radiation-induced phase stability at elevated temperatures. |
| Refractory metal alloy core is protected from impurities in the external environment for simplified ground based testing. | Both Ni-base and refractory metal alloys may require coatings or controlled coolant chemistry to prevent impurity transport and adsorption. |
| | Exterior surface of the refractory metal alloy pressure vessel would need a very robust coating and/or ground-based testing is a vacuum chamber. |
| | Extensibility to surface missions may be limited based on development of a robust environmental barrier coating. |

### 14.3.4 Material Case 4 – Silicon carbide core with Ni-base superalloy vessel piping and equipment

Figure 14-4 shows a representation of the material options for Material Case 4. This case is similar to Case 1 but has a SiC core and structure. It is also highly desirable from the standpoint of ease of building and testing a GTR since there are no exposed refractory metal alloy components.

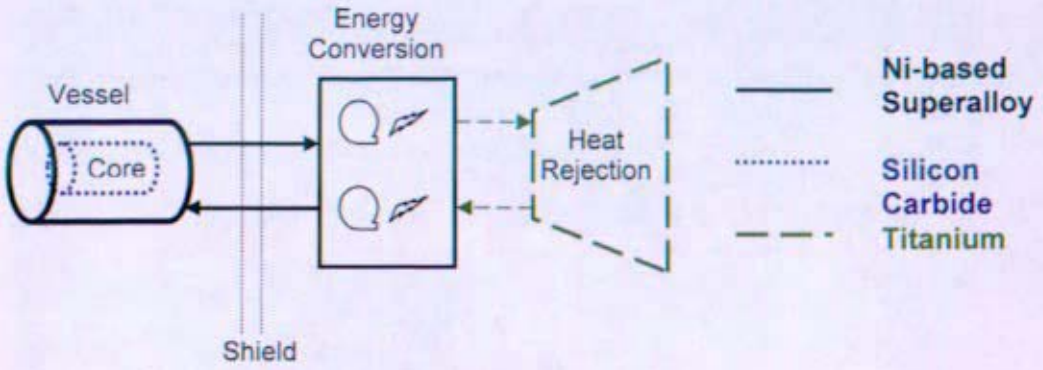



**Figure 14-4 Material Case 4**

| Strengths | Weaknesses |
|---|---|
| Ni-base superalloys and SiC are more resistant to chemical interactions by a coolant that is slightly oxidizing. | Monolithic SiC is inherently brittle, potentially compromising fuel structure geometry and the retention of fission products. |
| No dissimilar metal joints. | Composite SiC is more flaw tolerant, but less hermetic. Fission products would more likely be released to the coolant and impact the plant materials. |
| | Nickel-base alloys are susceptible to radiation-induced embrittlement and may not allow adequate life. |
| | SiC is damaged by radiation, but the effects become saturated at relatively low fluence. |
| | Both Ni-base alloys and SiC may require coatings or controlled coolant chemistry to prevent corrosion in impure coolant. |

Further information on plant material suitability and compatibility can be found in References 14-4 through 14-7.

## 14.4 References

**14-1** NRPCT joint letter SPP-67110-0004/B-SE-0037, "Provide NR Program Assessment of the Design Space for the Prometheus 1 Project" dated November 2, 2004

**14-2** NRPCT joint letter B-MT(SMAT)-005/MDO-723-0019, "Space Materials Plan, for Technical Approval" April 4, 2005

**14-3** NR letter S#05-02607, "Space Materials Plan; Approval with Comment", dated 08/05/2005

**14-4** NRPCT joint letter MDO-723-0021/B-MT(SRME)-21, "Request for Technical and Funding Approval of the Test Matrix and Associated Changes for the JOYO-1 Irradiation Test of Structural Materials in the JOYO Experimental Fast Reactor to Support Space Reactor Development", dated April 18, 2005

**14-5** Bettis letter, B-MT(SPME)-4, "Compatibility of Space Nuclear Power Plant Materials in an Inert He/Xe Working Gas Containing Reactive Impurities (U)", dated 10/18/2005

**14-6** KAPL letter MDO-723-0018, "Initial Assessment of Environmental Barrier Coatings for the Prometheus Project", dated 12/15/2005

**14-7** KAPL letter MDO-723-0010, "Summary of Structural Materials Considered for the Prometheus Space Nuclear Power Plant (SNPP)

**14-8** Attachment to KAPL letter SPP-SEC-0018, "Permeability of Helium Coolant in Space Reactor Systems", dated 9/2005

# Section 15
# Structural Design Basis Summary

*PRE-DECISIONAL - For planning and discussion purposes only*

(Intentionally Blank)

# Structural Design Basis Summary

## Table of Contents

15 Space Structural Design Basis (SSDB) Summary ..... 5
15.1 Summary and Conclusions ..... 5
15.2 SSDB Scope ..... 5
15.3 SSDB Development Strategy ..... 6
15.4 Required Contents of SSDB ..... 8
15.5 Preliminary SSDB to Support Pre-conceptual Design ..... 9
15.6 Future Work ..... 9
15.7 References ..... 9

## List of Tables

Table 15-1: Notional assignment of existing procedures to structural failure modes ..... 6
Table 15-2: Environmental effects for Reactor Module components ..... 7
Table 15-3: Required Contents of SSDB ..... 8

(Intentionally Blank)

# 15 Space Structural Design Basis (SSDB) Summary

## 15.1 Summary and Conclusions

The main focus of the SSDB effort prior to project termination had been on the identification of potential structural failure modes for the Reactor Module, the development of high level required contents of the SSDB, and the establishment of a preliminary SSDB to support component sizing in the pre-conceptual design of the Reactor Module, an early milestone of the Prometheus project.

Based on the experience gained in the SSDB development effort, NRPCT recommends the following considerations for future projects.

- A balanced approach among analysis, component or sub-component testing to qualify design procedures, and component proof tests should be pursued to ascertain the structural integrity of the Reactor Module design.

- Early material testing to characterize structural property degradation due to environmental effects such as irradiation, thermal aging, gas corrosion, fission product release, and material sublimation in vacuum should be pursued to reduce uncertainty in concept designs.

- *Creep-fatigue interaction was not a significant structural concern* for the planned flight profile of the Prometheus deep space missions with few temperature transients. However, creep-fatigue interaction is a very limiting high temperature failure mode that could potentially drive the structural design for applications with a wide range of operating transients. This would have been assessed for the Ground Test Reactor.

- The Preliminary SSDB was based on high temperature design bases developed for land-based nuclear reactors. Structural design methodologies employed in various weight/mass critical applications such as aircrafts and space vehicles would have been assessed to explore ways to reduce the degree of conservatism in the SSDB.

## 15.2 SSDB Scope

The role of a structural design basis is to provide designers with design procedures, design limits, design curves, design data, and design analysis methods to ensure the structural adequacy of a design, with margin as deemed appropriate for the intended application.

The SSDB would cover all Reactor Module structural components, including the reactor vessel, core structures, control drive mechanism, plant piping, energy conversion components, shield structure, primary support structure, and connection of Reactor Module to the main structure of the spacecraft. These components would be subject to various temperature environments, from low temperatures where the development of structural design procedures and design analysis methods was quite mature, to high temperatures where the effect of creep would be significant and structural design bases were less well developed. The structural response of these Reactor Module components could be broadly grouped into three regimes: transportation and launch, reactor startup, and operating mode. Thus a variety of load sources, e.g., acoustic, vibratory, acceleration, shock, pressure, thermal, rotary, micrometeoroid impact, interaction, etc., would need to be considered.

The Ground Test Reactor and electrically heated integrated system tests were planned to support the design and test of the Reactor Module. Relevant Reactor Module structural components employed in these tests would also need to be covered by the SSDB.

## 15.3 SSDB Development Strategy

The high-tier SSDB development strategy was developed in Reference 15- 1. It identified potential failure modes and environmental effects that could impact the structural performance of the Reactor Module components. Based on a technical assessment of various high temperature structural design bases and guidelines for land-based nuclear reactor components, it was concluded in Reference 15-1 that no single source of design procedures would fully meet the needs of the Reactor Module design. All of the design codes and guidelines reviewed had some common basis with the ASME Boiler and Pressure Vessel (B&PV) high temperature code. It was recommended that the ASME B&PV high temperature code be used as a foundation for the SSDB. This would be supplemented by other existing procedures, either directly or with modifications, as well as NRPCT in-house efforts in the development of the SSDB.

The design methodology for the SSDB would be based on the design-by-analysis approach of the ASME B&PV Code, Section III, Division 1. This means that stress analysis results would be required to demonstrate conformance with the design limits. The SSDB was envisioned as a single design document that would serve as the repository for structural design procedures, design limits, design curves, design data, and design analysis methods that would be required to demonstrate structural integrity of the Reactor Module structural components.

A notional assignment of existing procedures to the potential Reactor Module structural failure modes was developed in Reference 15- 1 and is shown in Table 15-1.

**Table 15-1: Notional assignment of existing procedures to structural failure modes**

| Structural Failure Mode | Load Type/Load Duration | Temp. (%) | Procedure (*) |
|---|---|---|---|
| Ductile failures: burst, pure shear | Single, short term | All | NH |
| Gross deformation | Single, short term | All | NH |
| Incremental collapse (ratcheting) | Cyclic | L | NB/NRPCT |
| Structural instabilities: column buckling, external pressure collapse | Single, short term | All | NH |
| Ductile void growth failure (tri-axial stressing/straining) | Single, short term | All | NH |
| Deformation/functional limits | Single, short term | All | NH/NRPCT |
| Fatigue | Cyclic | L | NB/NRPCT |
| Brittle fracture | Single, short term | L | XI/NRPCT |
| Fatigue crack growth | Cyclic | L | XI/NRPCT |
| Ductile tearing | Single, short term | All | RCC-RM/NRPCT |
| Incremental collapse (ratcheting) | Cyclic | H | NH |
| Structural instabilities: column creep buckling, external pressure creep collapse | Single, long term | H | NH |
| Creep rupture | Single, long term | H | NH |

| Structural Failure Mode | Load Type/Load Duration | Temp. (%) | Procedure (*) |
|---|---|---|---|
| Fatigue | Cyclic | H | NH |
| Creep/fatigue interaction | Cyclic plus long term dwell | H | NH |
| Creep crack growth | Single, long term | H | R5/NRPCT |
| Fatigue crack growth | Cyclic | H | R5/NRPCT |
| Creep/fatigue crack growth | Cyclic plus long term dwell | H | R5/NRPCT |
| Micrometeoroid impact (flight units) | Single, short term | All | SP100/NRPCT |

Footnotes to Table 15-1:

(%) Temperature: High (H), Low (L) or All
(*) Procedure:

- NH – ASME B&PV Code, Section III, Subsection NH
- NB/NRPCT – NRPCT to modify the ASME B&PV Code Section III, Subsection NB procedure and to meld it to SSDB
- XI/NRPCT – NRPCT to modify the ASME B&PV Code Section XI procedure and to meld it to SSDB
- RCC-RM/ NRPCT – NRPCT to qualify the French RCC-RM procedure (Design and Construction Rules for Mechanical Components of Fast Breeder Reactor Nuclear Islands) and meld it to SSDB
- NH/NRPCT – NH provides the structural deformation limits and NRPCT to specify the functional deformation limits
- R5/NRPCT – NRPCT to qualify the applicable British R5 procedure (Assessment Procedure for the High Temperature Response of Structures) and to meld it to SSDB
- SP100/NRPCT – NRPCT to qualify the applicable SP100 criteria (Structural Design Criteria for the SP100 Space Reactor Power System) or to develop new procedure, and to meld it to SSDB

Potential structural performance degradation due to internal and external environmental effects had to be accounted for in the Table 15-1 procedures in order to ensure an adequate structural design for the Reactor Module. The recognized environmental effects from Reference 15- 1 are summarized in Table 15-2.

**Table 15-2: Environmental effects for Reactor Module components**

| Environmental Effects | Potential Structural Performance Impact |
|---|---|
| Irradiation | Reduction in strength, ductility, fracture toughness, ductile tearing resistance, creep ductility and creep life |
| Thermal ageing | |
| Material incompatibility due to coolant impurities and/or materials transport in the primary coolant loop (gas corrosion) | |
| Fission product release | |
| Sublimation of materials in vacuum | Loss of structural strength |

## 15.4 Required Contents of SSDB

The required contents of the SSDB were presented in Reference 15- 2. They were grouped as shown in Table 15-3.

**Table 15-3: Required Contents of SSDB**

1. Design Requirements and Stress and Deformation Limits
    a. Transportation and Launch
    b. Pressure Boundary Components
    c. Core Support Structures
    d. Metallic Fuel Clad and Bonded Liners (pending on the fuel down-select decision)
    e. Support Structures
2. Material Properties
3. Design Techniques and Structural Evaluation Methods
4. High Temperature Inelastic Finite Element Analysis Design Guide

Item 1 would correspond to the design requirements and stress and deformation limits. Five parts were envisioned for Item 1. Part a would be related to low temperature design requirements and limits to guard against structural failure of the Reactor Module during transportation and launch, and structural damage induced during transportation and launch that would affect the structural performance of the Reactor Module during subsequent operation. Parts b through d would correspond to the high temperature design requirements and limits for pressure boundary components, core support structures, and metallic fuel clad and bonded liners, respectively. The contents from Part d would only be required if metallic fuel clad with bonded liners were to be chosen in the fuel down-selection. Part e was for support structures (shield structure, supports for Reactor Module components, primary support structure, and supports/foundations for the ground test reactor).

Item 2 would correspond to the necessary physical properties, design limits, design curves, and design data that would be required in Item 1. It would also include material parameters for inelastic constitutive equations that were to be specified in Item 4 to support inelastic finite element design analyses.

Item 3 would correspond to design techniques and structural evaluation methods. These would include evaluation methods for brittle fracture, ductile tearing, fatigue crack growth, creep crack growth, and buckling.

Item 4 would correspond to the high temperature finite element analysis design guide. This would provide guidance and requirements for acceptable methods, models and assumptions necessary for design analyses of Reactor Module components using inelastic finite element methods. Qualified inelastic constitutive equations for Reactor Module materials would be provided in Item 4. Results from these design analyses were to be used to demonstrate compliance of the deformation limits of Part I. This would be necessary when elastic results fail to meet the screening criteria for the deformation limits and more detailed inelastic stress analysis is required. Specification for the development of finite element post-processing tools would also be established to streamline the structural design process.

It was understood in Reference 15- 2 that the required contents of the SSDB were evolving and revisions would be made, when needed, in the updates of the SSDB.

## 15.5 Preliminary SSDB to Support Pre-conceptual Design

Many required contents of the SSDB as outlined above were yet to be developed. Reference 15- 2 contained a preliminary version of the SSDB that provided sufficient guidance for the pre-conceptual structural design of the Reactor Module components with a Nickel-base superalloy, Alloy 617. This involved the specification of Alloy 617 primary stress limits that would allow the designers to determine the component wall thicknesses and basic dimensions. Inelastic strain limits, buckling limits and simplified screening procedure were also provided in the Preliminary SSDB for use in component scoping analyses. Although the plant structural materials have not yet been selected, only Alloy 617 was included in Reference 15- 2 because all the material property test programs for the Prometheus project were only at the initiation stage and no test data were as yet available. NRPCT was able to obtain a commercial database on the tensile and creep strength of Alloy 617. Subsequent to the issuance of Reference 15- 2, a tensile and creep strength database for another Nickel-base superalloy, Haynes 230, was obtained by NRPCT from commercial source. Primary stress limits similar to those developed for Alloy 617 had been developed in Reference 15- 3 for Haynes 230.

## 15.6 Future Work

The primary objective of the Reference 15- 2 Preliminary SSDB was to support component sizing in the pre-conceptual design of the Reactor Module, an early milestone of the Prometheus project. Thus many of the failure modes identified in Table 15-1 as well as property degradation due to environmental effects were not addressed in the Preliminary SSDB. They included ratcheting, creep ratcheting, creep instabilities, fatigue, creep/fatigue interaction, brittle fracture, ductile tearing instability, fatigue and creep/fatigue crack growth, and micrometeoroid impact. Development of design procedures to address these issues in any future space reactor efforts would contribute to Item 1 - Design Requirements and Stress and Deformation Limits of Table 15-3. Work on the development of Items 2, 3, and 4 of Table 15-3, would also be required so that designers would have the necessary design procedures, design methods and design analysis tools to ensure the structural adequacy of a successful space reactor power plant design in any future space reactor project.

## 15.7 References

15- 1: KAPL Letter SPP-67320-0001, "Space Structural Design Basis Development (SSDB) Plan, for NR Information," dated 5/16/05
15- 2: KAPL Letter SPP-67320-0002, "Preliminary Space Structural Design Basis Development (SSDB), for NR Action," dated 6/30/05
15- 3: KAPL Letter SPP-SEC-0032, "Development of Interim Physical Properties and Primary Stress Limits for Haynes 230," dated 12/15/05

(Intentionally Blank)

# Section 16
# Extensibility

(Intentionally Blank)

# Extensibility

## Table of Contents

16 Extensibility ..... 5
16.1 Summary and Conclusions ..... 5
16.2 Requirements for Extensibility ..... 6
16.3 Summary of Differences in Other Mission Requirements ..... 7
16.3.1 Extensibility to Other Deep Space Missions ..... 7
16.3.2 Extensibility to Moon and Mars Surface Missions ..... 8
16.3.2.1 Power Rating and Lifetime ..... 9
16.3.2.2 Environmental Conditions ..... 10
16.3.2.3 Reactor Safety ..... 11
16.3.2.4 Shielding ..... 11
16.3.2.5 Continuity of Power ..... 12
16.4 References ..... 12

## List of Figures

Figure 16-1: Illustration of Possible Deep Space Missions (NASA) ..... 8

## List of Tables

Table 16-1: Power Rating and Plant Lifetime for JIMO and a Notional Surface Mission ..... 9
Table 16-2: Environmental Conditions for JIMO and Lunar Missions ..... 10

(Intentionally Blank)

# 16 Extensibility

## 16.1 Summary and Conclusions

The Naval Reactors program was specifically chartered to work on a deep space nuclear power system for the Jupiter Icy Moons Orbiter (JIMO) mission. The requirements for the Deep Space Vehicle (which includes the Reactor Module) included multi-mission capability for other civilian deep space exploration missions. The high level requirements of the Prometheus project also included that the nuclear power technologies developed be "extensible" to Moon/Mars surface exploration missions. This requirement of extensibility was implemented by NASA through Level 1 and Level 2 requirements as discussed below.

Key conclusions are:

- The selection of a gas-cooled reactor directly coupled to a Brayton energy conversion system for the JIMO mission provides key technologies that would be extensible to both surface missions and other deep space missions.
- Significant system design changes would likely be required to support a manned, surface mission compared to an unmanned, deep space mission.
- While extensibility was one of many factors in the reactor concept selection, it did drive selecting a system with the potential to avoid refractory materials in the reactor module pressure boundary that are not compatible with the surface environment.

The selection of a direct gas cooled reactor coupled to a Brayton energy conversion system would best support the envisioned JIMO mission, as well as be extensible to other deep space missions and surface missions on the Moon or Mars. Although some features of the nuclear power plant would likely be the same, significant modifications to the heat rejection segment (HRS) and shielding would have been required for a manned surface mission vs. a deep space mission. Despite these anticipated design changes, the underlying technologies (material development, fuel, etc.) would have been extensible to a surface mission. The direct gas Brayton concept remains mass competitive with other reactor concepts over a range of powers between 25 kWe and 300 kWe.

Extensibility was one of many factors that influenced selection of the gas Brayton system. The reactor operating temperatures at JIMO power levels are several hundred degrees Kelvin lower in the direct gas Brayton system than in liquid metal or heatpipe cooled reactors. The Brayton system operating temperature offers the potential to allow using more conventional materials, such as nickel-based alloys, for the entire system boundary. Use of refractory materials in the pressure boundary could be avoided. While refractory materials may survive the high reactor temperatures in the deep vacuum of space, they would not easily endure the Lunar or Martian atmospheres without additional protection (vacuum chamber, canning, or coating). At JIMO reactor operating temperatures refractory metals are extremely susceptible to property changes, corrosion, and degradation when exposed to elements commonly found in a lunar or Mars surface environment , specifically oxygen and carbon. Such protection would significantly complicate the design and operation, and would make the deep space reactor much less extensible to surface missions. Nickel-base superalloys were primarily being considered for the reactor and energy conversion pressure boundary, but no final material selections were made at the time of project termination.

This section discusses some of the alternative mission requirements and how they differ from the deep space requirements in place for the JIMO mission. While some aspects of surface missions might make the design easier (lower power, shorter lifetime, available manning for operation or repair, possible backup solar/battery power for restart, etc.), the additional requirements for personnel and environmental safety associated with a manned mission would be significant and would require a major redesign of the shielding, control system, and potentially the core.

## 16.2 Requirements for Extensibility

Requirements for extensibility were formally included in the overall project requirements. The Level 1 JIMO Requirements established by NASA included the Development Technology requirements, which describe 1) the primary technical goals required to enable a deep space mission, and 2) the mission and science requirements, which describe delivery of the space vehicle to the Jovian system and operation during the science phase. The Level 1 requirements formed the central starting point for development of project requirements and conceptual design efforts.

The specific Level 1 Development Technology requirement that discussed extensibility to surface missions was as follows:

> ***"The following Space Nuclear Reactor technologies shall be developed for Lunar and Mars surface power reactors: 1) Nuclear fuel, 2) Reactor core materials and coolants, and 3) Instrumentation and Control."*** (This item was indicated as an objective – minimum requirement not yet defined.)

At the time of project termination, this Level 1 requirement was further incorporated into a Level 2 requirement:

| Key Level 2 Requirement | Impact on Reactor Module | Implementation |
|---|---|---|
| *The Space Nuclear Reactor design shall utilize technologies that facilitate extensibility to surface operations.* | Drives selection of design and materials compatible with Lunar and Mars missions. | Must consider compatibility of pressure boundaries and external surfaces with surface environments. |

It would not have been practicable to design a single reactor plant that could work equally well for both deep space and surface missions because of the significantly different requirements and drivers for such missions (manning, power level, lifetime, etc.). Such a "generic" reactor would have been a significant compromise for either application because of the tight mass constraints and the need to only include hardware and functionality required for a specific mission. However, the goal was to leverage key technology development so that future missions would require less resources and less lead time to deliver a reactor module. Also, depending upon the actual mission requirements, it is possible the core design would require few modifications but that is not clear since alternative missions were not defined. These general requirements on extensibility were factored into the nuclear power plant selection process.

## 16.3 Summary of Differences in Other Mission Requirements

Extensibility can be broken into two broad categories:

1. Other deep space, nuclear electric propulsion missions
2. Surface missions, specifically the Moon and Mars

NASA was also evaluating missions that require nuclear thermal propulsion (NTP) technology. However, NTP was never evaluated by the Naval Reactors Prime Contractor Team (NRPCT) as part of this project and it would likely require a significantly different design and may require some different technologies than the space nuclear power plant designs for electrical power generation.

### 16.3.1 Extensibility to Other Deep Space Missions

Some of the overall Prometheus program requirements already factored in extensibility to other deep space missions beyond JIMO. As described in Section 1, some of the Level 2 requirements were established specifically for the JIMO mission and some were multi-mission, meaning that they would meet the expected requirements for all the deep space missions for the deep space vehicle. For example, a target mission lifetime of 20 years was based upon supporting projected follow-on missions, even though the JIMO mission was only expected to last 10 to 12 years. Future missions that were studied by NASA include:

- Saturn and its moons
- Neptune and its moons
- Kuiper Belt rendezvous
- Comet and multi-asteroid sample return

While these possible mission concepts were only preliminary in scope, they were all estimated to be achievable within a 20 year lifetime and the power requirements established for JIMO (i.e., ~200 kWe). Other possible missions such as an "interstellar precursor" to the Heliopause (200 AU from the sun) were beyond the 20 year mission life of Prometheus requirements and not truly extensible from the JIMO design. Figure 16-1 illustrates the location of these missions relative to earth. In several ways, the JIMO mission was more challenging than other envisioned deep space missions because of the high radiation fields around Jupiter and the high propulsion power needed to navigate the gravity wells of Jupiter's moons. An initial design lifetime requirement of 15 years was established with the idea that a 20 year lifetime might be achievable with operating experience and further technology maturation.

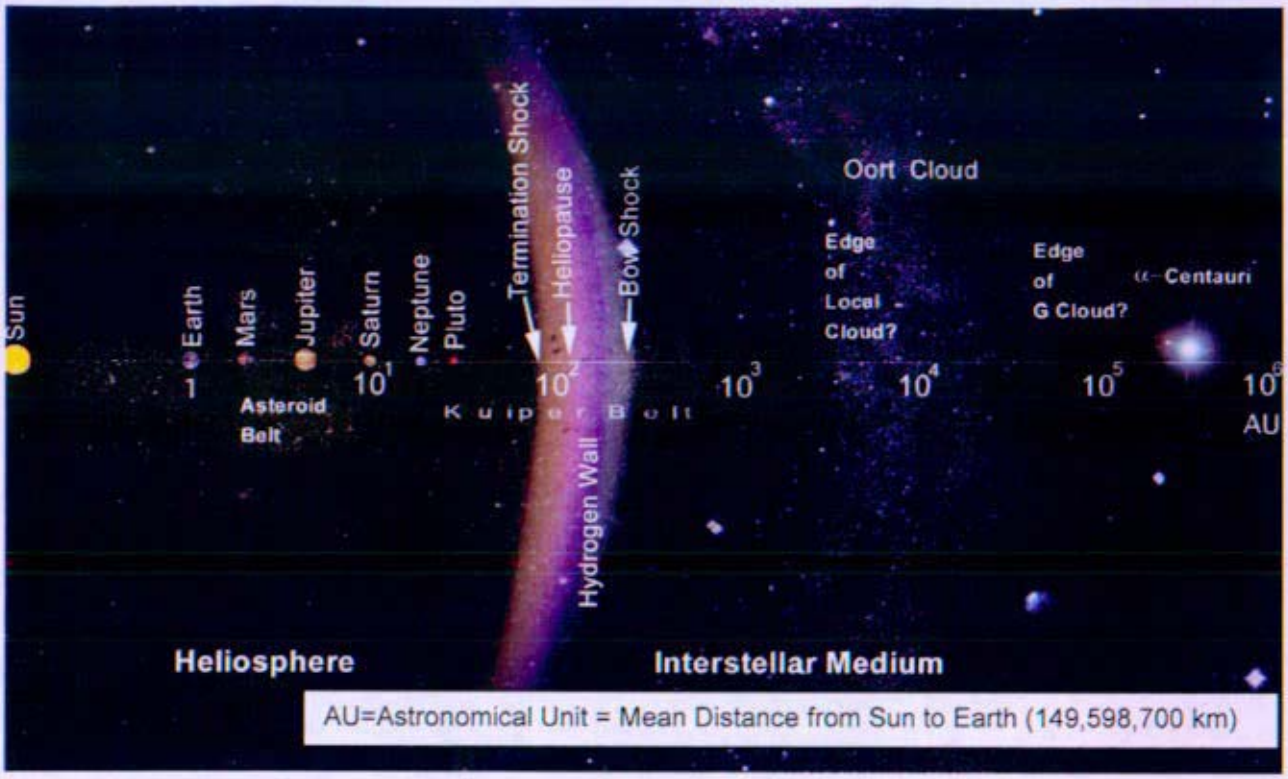



**Figure 16-1: Illustration of Possible Deep Space Missions (NASA)**

The 10 years of full power operation required for JIMO were expected to encompass these longer missions as well. This was because despite the longer mission lives, there would also be longer reduced power periods between thrusting (approximately 50% for a 20 year mission) such that the number of full power years was no greater than for JIMO. In contrast, JIMO would only have 2 or 3 years of reduced power in its 12 year mission, 5 years of reduced power mode assumed for a design life of 15 years.

Specific mission and environmental requirements for these other deep space missions were not well defined and no effort was expended by the Naval Reactors program in evaluating specific issues with these other deep space missions. However, in general, it was judged that the JIMO reactor design would be relatively extensible to these types of missions. One key issue would be system reliability as mission life approached 20 years. As noted above, it was considered that the ability to design a system for 20 years of operation may become feasible as the JIMO technology matured and test and flight system data were obtained and factored into subsequent designs.

### 16.3.2 Extensibility to Moon and Mars Surface Missions

Extensibility to surface missions posed significantly greater challenges for the nuclear power plant design, particularly since planned missions to the moon and Mars were to be manned. Specific surface missions under consideration by NASA at the time of project termination included establishment of a base camp on the moon and an eventual manned mission to Mars. Because of the major differences between these types of surface missions and the planned JIMO mission, extensibility to surface missions was a more significant factor in the design than extensibility issues with other deep space missions. As noted above, a clear example of this was the decision to

eliminate refractory materials in the pressure boundary if possible. While there were concerns with refractory metals in the pressure boundary for even a deep space mission, the difficulty foreseen in such a design for a surface mission became a strong influence in selecting non-refractory pressure boundary materials as the initial reference case.

A comparison of some of the key requirements for the JIMO mission vs. a notional surface mission is provided below.

### 16.3.2.1 Power Rating and Lifetime

The plant power ratings and lifetimes for JIMO and a notional surface mission (Reference 16- 2) are shown in Table 16-1.

**Table 16-1: Power Rating and Plant Lifetime for JIMO and a Notional Surface Mission**

| | JIMO Mission | Surface Mission |
|---|---|---|
| Plant Lifetime (Years) | 10-12 (15 design) | ~10 |
| Full Power Years | 10 | 5-10 |
| Electrical Rating (kWe) | 200 | ~50 |

In terms of these parameters, the JIMO mission was more limiting and the design could be relatively easily extended to a surface mission in terms of power and lifetime. Because of the lower electrical power rating for a surface mission, there would be greater design and operational flexibility in terms of the number of Brayton engines and possibly lower operating temperatures for a surface mission. Lower operating temperatures could be used to reduce thermal stresses, corrosion and creep if needed, but given the relatively short plant life for a surface mission, this may not be a key driver unless environmental conditions on the moon significantly shortened material lifetime. Instead, a smaller reactor could be designed to reduce mass and still meet the power and lifetime requirements.

A significant difference for surface missions was the lower required power levels as compared to deep space missions. At power levels closer to 25 kWe, some alternatives to the Direct Gas Brayton concept (such as the liquid-metal Stirling concept) become more competitive, but they still pose issues. Further information about other concepts, their design issues, and trends can be found in references (16- 3), (16- 4), and (16- 5).

Late in the project, the NRPCT began considering a neutronically moderated gas reactor for a surface mission with relatively low power levels. A description of this concept is provided in reference (16- 6). The primary motivation for considering a moderated gas reactor was to reduce fuel loading and enable use of a commercially based fuel system, which has a better experience base for high temperature operation than the notional fuels considered for JIMO. This reactor has considerable mechanical and thermal design challenges and would require detailed concept development based on firm mission requirements to better judge feasibility.

### 16.3.2.2 Environmental Conditions

A detailed set of space environmental conditions was being prepared for the JIMO mission (Reference 16-1). While not finalized, factors such as radiation levels, micrometeorites, temperature, and pressure were to be included in JPL's Environmental Requirements Document. For the JIMO mission, environmental requirements were divided into separate phases for launch, earth orbit, outbound cruise and Jovian atmosphere because of the significantly different conditions for each phase of the mission. For a lunar mission, conditions will be similar to earth orbit conditions in many cases. The key differences would be between deep space transit and Jovian orbit compared to a lunar surface mission. A comparison of some of the key environmental factors for JIMO vs. a lunar mission is provided in Table 16-2.

**Table 16-2: Environmental Conditions for JIMO and Lunar Missions**

| | JIMO Mission | Lunar Mission |
|---|---|---|
| Direct Solar Flux ($W/m^2$)<br>*[Values approach 0 during eclipses]* | Near Earth: 1368<br>Outbound: 1368 to 50<br>Jovian: 50 | 1368 |
| Albedo | Near Earth: 0.3<br>Outbound: Negligible<br>Jovian: 0.13 to 0.58 | 0.3 |
| Pressure (torr) | Near Earth: $10^{-5}$<br>Outbound: $10^{-14}$<br>Jovian: TBD | $10^{-5}$ |
| Deep Space Temperature (K) | Near Earth: 4<br>Outbound: 3<br>Jovian: 2.7 | 4 |
| Effective Radiator Heat Sink Temperature (K) | 70 – 200<br>(depends upon proximity to other bodies) | 180 (night) -314(day) |
| Gravity | Zero | 0.166 g |
| Radiation (Full Mission)*<br>Total Ionizing Dose (TID)<br>Displacement Damage Dose (DDD)<br>**Values for design factor of 1 and excludes reactor radiation* | $1x10^9$ rads (Si)<br>$5.7x10^{15}$ 1-MeV equiv. $n/cm^2$ | Levels not yet defined but considered to be less than JIMO mission |
| Contamination | Micrometeorites and atomic oxygen but relatively clean environment. | Regolith[1] on lunar surface that becomes airborne and will coat surfaces. |

[1] Regolith composition varies by location but the following composition by wt. percent was used by JPL in a study for lunar mission (Reference 16- 2)

| Element | O | Si | Al | Fe | Ca | Mn | Ti |
|---|---|---|---|---|---|---|---|
| Weight Fraction | 0.422 | 0.193 | 0.073 | 0.123 | 0.089 | 0.048 | 0.045 |

There are many other environmental factors for these missions but some key observations are:

1. Surface missions have significant solar flux available to supply an energy storage system for backup power. Deep space missions do not have a similar capability once the spacecraft travels much beyond the earth's orbit. This availability of solar power provides greater flexibility for a moon or Mars mission in terms of backup power and may affect the number of components and operating strategy compared to a deep space mission.
2. The issue of material cleanliness is significantly greater for a lunar mission than a deep space mission and makes extensibility more challenging if materials are sensitive to this contamination. This was a concern with refractory materials in the pressure boundary. This is also a concern relative to coating heat transfer surfaces such as the radiator, as well as coating electronics and mechanisms. Similar concerns would exist for Mars which has a $CO_2$ atmosphere and dusty conditions.

It is unclear whether the net effect of these differences would make the envisioned lunar mission easier or harder to achieve. However, if pressure boundary materials were chosen that could withstand the atmospheric conditions on the moon, then the radiation conditions seem more favorable for a lunar mission. The HRS would likely be more problematic on a surface mission due to environmental contaminates that would tend to reduce heat transfer effectiveness. Also, the higher effective reject temperature on a lunar mission would result in a larger required radiator area than for an equivalent power deep space mission.

### 16.3.2.3 Reactor Safety

Reactor safety for a surface mission, particularly for a manned mission, poses significantly greater challenges relative to extensibility. For unmanned, deep space missions, reactor safety focused on ensuring the reactor remained safe during postulated re-entry scenarios during launch and earth orbit (if any) prior to starting the reactor. As a result, there were no reactor safety issues once the reactor was out of earth's orbit. In this case, a reactor casualty or shutdown would result in the end of the mission. While this is clearly undesirable, it would not pose reactor safety concerns that require redundant safety features that complicate the system design. However, the lack of such features also limits the opportunity to recover from a casualty so operational flexibility is reduced. For a manned mission, reactor controls from a safety aspect would become similar to the Ground Test Reactor (GTR) so testing and system design at the GTR would more closely simulate mission operation. The specific constraints on a lunar reactor were not yet defined relative to contamination boundaries and protecting the lunar surface. However, it is clear that the reactor would need to incorporate safety features that would not be present on the JIMO reactor. The extent of these differences was not evaluated in detail.

### 16.3.2.4 Shielding

Shielding represents another area where there would be significant differences between the JIMO mission and a surface mission. This is due to the additional requirement to provide adequate shielding for human habitability, as well as the ability to locate equipment further away from the reactor than possible on a spacecraft. A reactor shield, similar to that designed for a deep space mission would still be needed for a surface mission to reduce radiation damage to key components close to the reactor. Since some of the electronics could be moved away from the reactor after landing, and the surface mission was expected to be shorter than the JIMO mission, if the local terrain

or surface materials could be used for personnel shielding the as-launched reactor shield could possibly be less massive. No trades were done by NRPCT to evaluate shield designs for a surface mission.

A NASA evaluation of options for shielding a lunar surface reactor for support manned operation can be found in Reference 16-2.

### 16.3.2.5 Continuity of Power

Because lives depend on reliable operation of the power plant for a manned surface application, greater emphasis in the design would be placed on reliability and the ability to recover from a fault. While the JIMO mission posed many challenges, one easier aspect of this mission was the relatively simple operation of the system once it was started. The reactor plant would either operate at full power for the entire mission and shed load to a parasitic load radiator (PLR) as needed or there could be some lower power coast and science gathering periods totaling several years during the mission. This type of operation minimized the complexity of operating modes and transients on the system. However, because repair of any failures during flight would not be possible (except for possible software errors), system reliability became a particular concern (see Section 7).

For a surface mission, the system must still be highly reliable and safe, but the possibility of repair exists and provides greater flexibility in the plant design and operation. Also, solar power and energy storage could be available for backup power so a restart capability of the reactor becomes much more feasible. Also, having astronauts or ground controllers available to perform troubleshooting or take adaptive actions if necessary provides additional flexibility. However, the system would still likely be designed for autonomous operation to minimize the need for operator involvement.

## 16.4 References

**16- 1:** JPL Document 982-00029, Rev. 0, "Prometheus Project Environmental Requirements Document, Preliminary," dated July 6, 2005

**16- 2:** JPL Report 982-R66153, "Lunar Fission Surface Power System Study Report," dated August 17, 2005

**16- 3:** NRPCT letter SPP-67110-0005, B-SE-0077 "Space Nuclear Power Plant (SNPP) Concept Recommendation for Prometheus 1 Space Craft for NR Action (U)", dated March 4, 2005

**16- 4:** SPP-67210-0001 / B-SE-0037, "Provide NR Program Assessment of the Design Space for the Prometheus 1 Project", dated November 2, 2004

**16- 5:** KAPL letter SPP-67310-0011, "Documentation of Naval Reactors Papers and Presentations for the Space Technology and International Forum (STAIF) 2006", to be issued

**16- 6:** SPP-67410-0013 / B-SE(RE)-0003, "Prometheus Reactor Pre-Conceptual Design Report", dated January 27, 2006

CONCURRENCE/DESIGN CHECK FORM FOR DOCUMENT NO. SPP-67210-0010 / B-SE(SPS)-001 Date: January 27, 2006

DOCUMENT TITLE: Space Nuclear Power Plant Pre-Conceptual Design Report; for Information

REFERENCES: ENCLOSURES:

1. ADSARS: PERMANENT RECORD: Yes X No ___ Repository MFLIB Corporate Author: K NR PROGRAM ___

Key Words: Prometheus, Heat Balance, Model, SNPP, final report, plant, system, JIMO, NRPCT

| | | | | | | | | | | |
|---|---|---|---|---|---|---|---|---|---|---|
| Need to Know Categories | SGN | REC | REP | | | | | | | |
| Available Sites: | PRNR | | | | | | | | | |
| Design File Location(s) | | | | | | | | | | |

## 2. DESIGN CHECK

| Type of Check | Signature(s) | Comments: (Including Reference to Check Document If Appropriate) |
|---|---|---|
| A. No check considered necessary | | |
| B. Check vs. previous results/issues | | |
| C. Checked calculations made | | |
| D. Checked computer input and/or output | | |
| E. Computer Programs approved/qualified | | |
| F. Performed independent audit | | |
| G. Spot checked significant points | | |
| H. Reviewed methods used | | |
| I. Reviewed results for reasonableness | | |
| J. Comparison with test data | | |
| K. Reviewed vs. drawings | | |
| L. Verified procedures | | |
| M. Technical content reviewed | | |
| N. Management verification of adequate review by others | | |
| O. Performed Lessons Learned Search | | |
| P. Used Measurement Uncertainty Methods | | |
| Q. Other Checks (Describe) | | |

## 3. CONCURRENCE REQUIREMENTS: Indicate signatures required by X:

| | | | | | |
|---|---|---|---|---|---|
| ___ | SPP MANAGER | ___ | ADVANCED CONCEPTS | ___ | FLUID DYNAM |
| ___ | NUCLEAR ENGINEERING | ___ | SHIELDING | ___ | STRUC. ENGRG |
| ___ | REACTOR TH/MECH DESIGN | ___ | REACTOR SAFETY | ___ | DRAFTING |
| X | SPP REACTOR ENG. | ___ | TO | ___ | QA |
| per telecon 1-26-06 | SPP MECHANICAL | ___ | RSO | ___ | OTHER |
| X | SPP ELECTRICAL | ___ | FSO | X per telecon 1-26-06 | BETTIS SPS/FMS |
| ___ | FINANCE | X | MDO 1/26/06 | ___ | BPMI |
| ___ | PROJECT OFFICE | ___ | ARP | X DES | ADMIN REVIEW |
| X | ENERGY CONVERSION | | | | |

Cognizant Manager ___

(Must Be Subsection or Higher for External Letters)

4. AUTHORIZED CLASSIFIER: Reviewed By: Wayne B. Broome CLASSIFICATION: (U)

5. RELATED SUBJECTS:

| | | | | | |
|---|---|---|---|---|---|
| | | Commitment Made (Y/N) | N | Commitment Complete (Y/N) | Y |
| UTRS Implication (Y/N) | N | Design Basis Info. (Y/N) | N | UTRS Doc. # | |
| Safety Council Review (Y/N) | N | Design Review (Y/N) | N | | |

## 6. Distribution:

| | |
|---|---|
| TN Rodehaver | NR 08I |
| SJ Rodgers | NR 08E |
| WJ Pollock | NR 08S |
| ST Bell | NR 08I |
| JP Mosquera | NR 08C |
| WE Evers | NR 08E |
| D. Potts | SNR |
| JA Andes | PNR |

| | |
|---|---|
| M Wollman | KAPL |
| MJ Zika | Bettis |
| JM Ashcroft | KAPL |
| H. Schwartzman | KAPL |
| CD Eshelman | Bettis |
| D McCoy | KAPL |
| K Loomis | KAPL |
| DP Hagerty | Bettis |
| GM Brewer | Bettis |
| SA Simonson | KAPL |
| WS Niznik Jr | Bettis |
| KM Poczynek | BPMI |
| FJ Barilla | BPMI |
| RF Hanson | BPMI |